IMMUNITY IN COMPROMISED NEWBORNS

EDITED BY: Per T. Sangild, Duc Ninh Nguyen, Andrew Currie and Tobias Strunk

PUBLISHED IN: Frontiers in Immunology

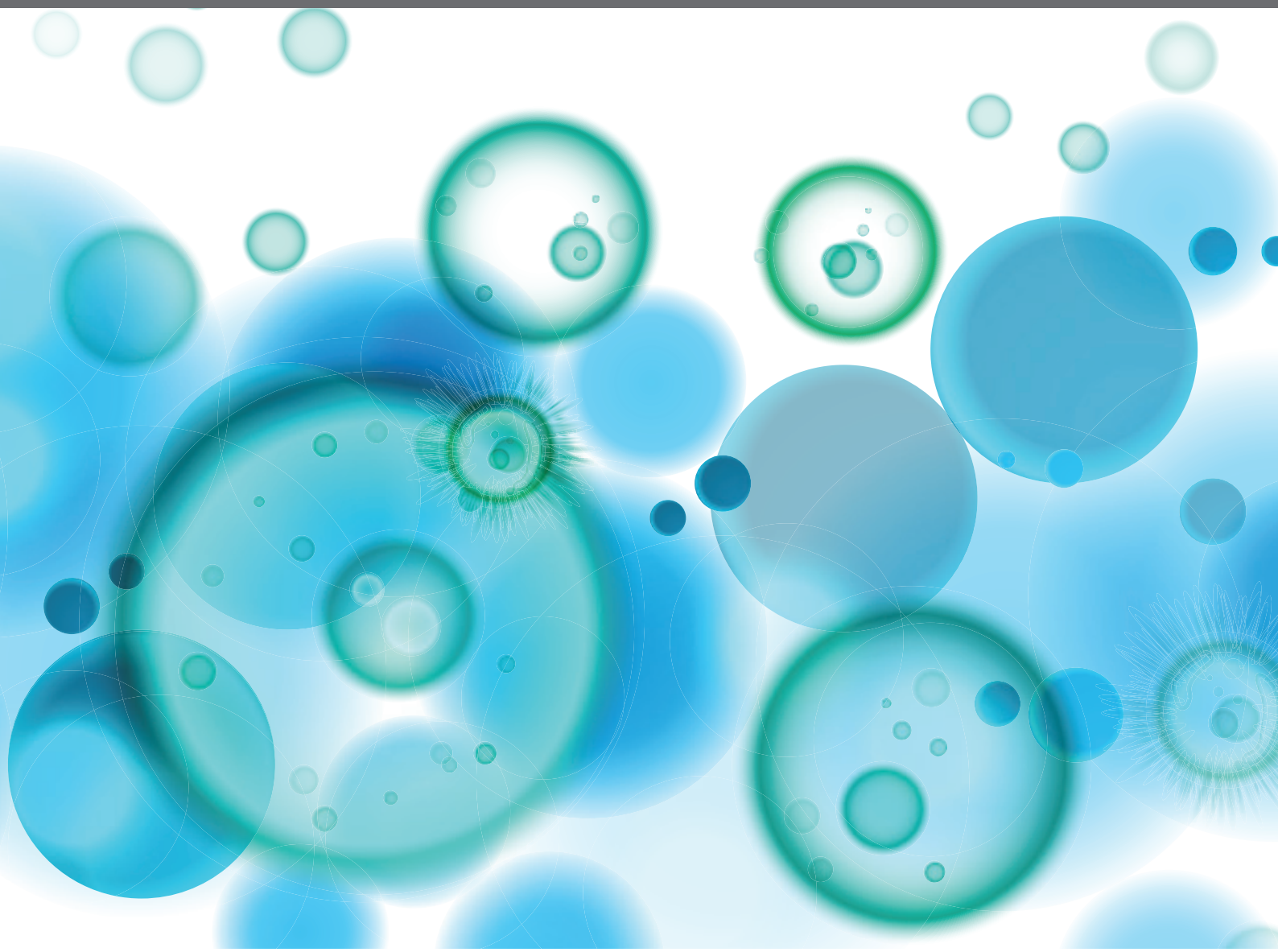

frontiers Research Topics

frontiers

ISSN 1664-8714
ISBN 978-2-88971-314-1
DOI 10.3389/978-2-88971-314-1

About Frontiers

Frontiers is more than just an open-access publisher of scholarly articles: it is a pioneering approach to the world of academia, radically improving the way scholarly research is managed. The grand vision of Frontiers is a world where all people have an equal opportunity to seek, share and generate knowledge. Frontiers provides immediate and permanent online open access to all its publications, but this alone is not enough to realize our grand goals.

Frontiers Journal Series

The Frontiers Journal Series is a multi-tier and interdisciplinary set of open-access, online journals, promising a paradigm shift from the current review, selection and dissemination processes in academic publishing. All Frontiers journals are driven by researchers for researchers; therefore, they constitute a service to the scholarly community. At the same time, the Frontiers Journal Series operates on a revolutionary invention, the tiered publishing system, initially addressing specific communities of scholars, and gradually climbing up to broader public understanding, thus serving the interests of the lay society, too.

Dedication to Quality

Each Frontiers article is a landmark of the highest quality, thanks to genuinely collaborative interactions between authors and review editors, who include some of the world's best academicians. Research must be certified by peers before entering a stream of knowledge that may eventually reach the public - and shape society; therefore, Frontiers only applies the most rigorous and unbiased reviews.
Frontiers revolutionizes research publishing by freely delivering the most outstanding research, evaluated with no bias from both the academic and social point of view. By applying the most advanced information technologies, Frontiers is catapulting scholarly publishing into a new generation.

What are Frontiers Research Topics?

Frontiers Research Topics are very popular trademarks of the Frontiers Journals Series: they are collections of at least ten articles, all centered on a particular subject. With their unique mix of varied contributions from Original Research to Review Articles, Frontiers Research Topics unify the most influential researchers, the latest key findings and historical advances in a hot research area! Find out more on how to host your own Frontiers Research Topic or contribute to one as an author by contacting the Frontiers Editorial Office: frontiersin.org/about/contact

IMMUNITY IN COMPROMISED NEWBORNS

Topic Editors:
Per T. Sangild, University of Copenhagen, Denmark
Duc Ninh Nguyen, University of Copenhagen, Denmark
Andrew Currie, Murdoch University, Australia
Tobias Strunk, King Edward Memorial Hospital, Australia

Citation: Sangild, P. T., Nguyen, D. N., Currie, A., Strunk, T., eds. (2021). Immunity in Compromised Newborns. Lausanne: Frontiers Media SA.
doi: 10.3389/978-2-88971-314-1

Table of Contents

frontiers in Immunology

EDITORIAL
published: 26 July 2021
doi: 10.3389/fimmu.2021.732332

Editorial: Immunity in Compromised Newborns

Per T. Sangild[1,2,3]*, *Tobias Strunk*[4,5,6]*, *Andrew J. Currie*[6,7]* and *Duc Ninh Nguyen*[1]*

[1] Comparative Pediatrics and Nutrition, Department of Veterinary and Animal Sciences, University of Copenhagen, Frederiksberg, Denmark, [2] Department of Neonatology, Rigshospitalet, Copenhagen, Denmark, [3] Department of Pediatrics, Odense University Hospital, Odense, Denmark, [4] Centre for Molecular Medicine & Innovative Therapeutics, Murdoch University, Perth, WA, Australia, [5] Wesfarmers Centre for Vaccines and Infectious Diseases, Telethon Kids Institute, Perth, WA, Australia, [6] Neonatal Directorate, Child and Adolescent Health Service, Western, Australia, [7] Centre for Neonatal Research and Education, The University of Western Australia, Perth, WA, Australia

Keywords: immune development, inflammation, antibiotics, preterm, birth, milk, sepsis, necrotizing enterocolitis

Editorial on the Research Topic

Immunity in Compromised Newborns

OPEN ACCESS

Edited and reviewed by:
Willem Van Eden,
Utrecht University, Netherlands

***Correspondence:**
Per T. Sangild
pts@sund.ku.dk
Tobias Strunk
tobiasstrunk@yahoo.de
Andrew J. Currie
A.Currie@murdoch.edu.au
Duc Ninh Nguyen
dnn@sund.ku.dk

Specialty section:
This article was submitted to Nutritional Immunology, a section of the journal Frontiers in Immunology

Received: *28 June 2021*
Accepted: *30 June 2021*
Published: *26 July 2021*

Citation:
Sangild PT, Strunk T, Currie AJ and Nguyen DN (2021) Editorial: Immunity in Compromised Newborns. Front. Immunol. 12:732332. doi: 10.3389/fimmu.2021.732332

The risk of infection-related morbidities and mortality is particularly high in the newborn period. Before birth, the mammalian fetus is protected from adverse effects of exogenous pathogenic microbes and can normally develop its immune system in a near-sterile environment with limited need for immune responses. This condition changes dramatically at birth when rapid adaptations of the innate and adaptive immune systems are required to tolerate and respond to commensal and pathogenic bacteria at epithelial surfaces (e.g. gut, lungs, skin) and fight microbes penetrating to blood and internal organs. Carefully balanced responses of the systemic, organ-related and epithelial immune systems are required to avoid bacterial overgrowth, translocation across immature barriers, and excessive inflammation. The many arms of the mammalian immune system develop differently in different species but comparative studies facilitate insights into mechanisms of perinatal immune development and help identify prophylactic and therapeutic opportunities. Interventions to support neonatal immunity are most critical for those born preterm, growth-restricted, hypoxic, infected or otherwise compromised at birth.

This Research Topic presents a collection of 29 original research articles and reviews on perinatal immunology, aimed to understand the special challenges of compromised newborns. The Research Topic collection is connected with the completion of the international NEOMUNE research consortium, led by University of Copenhagen (www.neomune.ku.dk, 2013-20), having a focus on milk and microbiota influences on gut, immunity and brain development. The Research Topic and this editorial combine knowledge obtained in the NEOMUNE consortium with a series of complementary articles. We encourage studies into the mechanisms of systemic and mucosal immune development, and how dietary, microbial and pharmacological interventions support immune maturation assessed by both classical immune markers and exploratory omics techniques. The latter methods have recently emerged as novel tools to better understand immune development and prepare the way for a new precision medicine approach to the prevention, diagnosis and treatment of neonatal immune disorders (1, 2).

TRANSITION AT BIRTH AND POSTNATAL IMMUNE DEVELOPMENT

Before birth, the uterus and fetal membranes protect the mammalian fetus from exposure to environmental bacteria, viruses and fungi, and the mother is kept in a state of relative immunosuppression to avoid immunological rejection of the fetus. At this time, placental integrity, a near-sterile environment (particularly in the first two trimesters of pregnancy) and maternal immunity protect the developing fetus against infections. After birth, the protective and immunomodulatory properties of colostrum and milk provide continued support, concomitant with a gradual development of both the innate and adaptive arms of the newborn immune system. The innate immune system and the epithelial barriers are the first line of defense against infections and immune cells can react rapidly, non-specifically and pre-programmed to combat infectious stimuli before more adaptive immunity develops. The cellular, structural and functional elements of the immune system may remain distinct from those in older individuals for days, weeks or months after birth, yet this special early life immune status may also confer certain survival benefits for the host. Thus, a relatively 'dormant' immune system may support a physiologic and metabolic state that helps to dampen hyper-inflammatory responses following the sudden exposure of the newborn host to a world of microbes (3, 4).

What then if newborns are born too early and/or too small? Annually, an estimated 20 million infants (10-20% of all infants) are born preterm (< 37 weeks gestational age, GA) and/or growth-restricted (< 10% growth percentile). Their health complications account for up to half of all infant deaths (5, 6). Preterm birth is associated with short- and long-term health consequences, including increased infection rate, even until adulthood (7). On the other hand, the immunological adaptation of such compromised newborns in early life is remarkable. Across several papers, this Research Topic demonstrates that mammals have a surprising capacity to adapt their immune systems postnatally, even after serious prenatal insults.

In humans, spontaneous preterm birth is related to one of two overlapping disease etiologies: Fetal infection/inflammation, leading to placental dysfunction, or placental vascular dysfunction, causing hypertensive disorders and fetal growth restriction (with/without preterm birth). Dramatic advances in neonatal medicine, including ventilator management, nutrition and medical therapies now allow good survival rates of extremely preterm infants from 60% GA (of total 40 weeks). Yet, the immature state of many organs at birth predisposes to later complications, many of which have a clear immunological or inflammatory component (e.g. LOS, late-onset sepsis; BPD, bronchopulmonary dysplasia; NEC, necrotizing enterocolitis; WMD, white matter damage; PNALD, liver parenteral nutrition associated liver disease; AKI, acute kidney injury). Understanding the complexity of all these interacting diseases in early life of preterm infants demands a multi-organ research approach and appropriate animal models of immune-related disease in early life.

Successful perinatal immune adaptation is a delicate balance between tolerance and resistance of the immune system to pathogens and/or inflammatory factors, with bacterial colonization along host epithelial surfaces and diet playing important roles. Many endogenous host factors may support the development of balanced immune responses. In this Research Topic, Viemann reviewed how alarmins, e.g., S100A8/9, are crucial factors for perinatal immune regulation. Based on a large cohort of Gambian children, Odumade et al. indicated that developmental changes in adenosine deaminase (ADA) levels may also play a role for this immunological transition. In therapeutic settings, adjunct therapies to antibiotics, such as the phosphodiestarease inhibitor pentoxifylline (PTX), may help to dampen damaging pro-inflammatory responses, without limiting bacterial clearance, as shown by Speer et al. in newborn mice infected with Gram-negative *E. coli*. Similar anti-inflammatory effects in newborns are shown after Gram-positive infection of newborn mice (8), and as shown in this Research Topic by Gravina et al. The size of such pups (1-2 g) makes longitudinal clinical assessment and blood/organ sampling difficult. In this regard, preterm piglets may be more suitable models for recording multi-organ effects of systemic infections and sepsis in compromised infants, as shown previously (8, 9) and in this Research Topic by Bæk et al. Muk et al. showed how serial blood and cerebrospinal fluid (CSF) collections from preterm piglets can be used to reveal new proteome biomarkers of neonatal Gram-positive infection, potentially affecting both systemic and brain compartments, and how responses are modulated by milk diets.

Preterm infants have a T cell population adapted to life in utero, in part explaining their reduced Th1 response and higher susceptibility to infections, but with more systemic Treg cell activity to help protect them from excessive inflammation. In this Research Topic, the reviews by Sampah and Hackam and Sproat et al. add important information to existing reviews on immune ontogeny in infants and include description of the various cellular components (4, 10). The reviews focus on how immature infants show deficient capacity to respond to bacterial and viral infections in blood, organs and/or along surface epithelia.

Neutrophils are a vital component of innate immunity since they are often the first cells to be recruited to fight bacterial, viral, and fungal infections. Neonatal neutropenia is a common phenomenon after preterm birth (11) but neutrophils also have a remarkable capacity to proliferate, adapt and respond to infectious challenges in the days and weeks after preterm birth, as shown in preterm pigs (8, 12, 13). Notable phenotypic and functional disparities exist between neonatal and adult neutrophils with regards to cell membrane receptors and functions. Depressed neutrophil phagocytic function in newborns may function to allow establishment of a healthy microbiome (14). Neutrophils are also essential components for proper B and T cell function, antigen presentation, and tissue repair and regeneration and these neutrophil functions are reduced in preterm neonates with high risk of LOS and NEC (14), similar to many other immune cell types and functions (Sampah and Hackam). Across preterm infants, pigs and newborn mice, there is up-regulation of circulating cell-free DNA and neutrophil-associated proteins at or shortly before LOS

and/or NEC (8). However, not all immune cell populations and functions are immature in preterm neonates as discussed in the Research Topic reviews by Sampah and Hackam, and Sproat et al., supporting the observed similar reponses to pathogens by preterm and term blood monocytes (15).

In the intestine, the mucosal innate immunity and repair mechanisms rely on numerous interacting components from the environment (diet, microbiota) and specialized cell types support immune tolerance and sensitivity to inflammatory insults. The review by Leushcow and McElroy provides an example from the perspective of the relatively late-developing intestinal Paneth cells, secreting important antimicrobial peptides. Thus, ablation of murine Paneth cells in growing mice results in greater sensitivity to NEC lesions, and infants with NEC have reduced Paneth cell numbers in their intestinal tissues. Such mucosal effects may have long-term consequences for the immature gut via epigenetic regulation of gene transcription. A study by Pan et al. in this Research Topic shows that the immature intestine has a remarkable capacity to adapt its immune gene expressions soon after preterm birth in pigs. This multi-level control of postnatal innate immunity is critical to avoid excessive gut inflammation to colonizing bacteria after birth, leading to NEC, and its interaction with inflammatory responses at other epithelia or distant organs. On this background, it is not surprising that 10-30% of very preterm infants develop immune-related disorders such as NEC and LOS and that many organ complications in preterm infants are partly related to dysregulated local host immune responses to infection/inflammation. Hyper-inflammatory conditions like NEC and LOS may also induce immunosuppression, predisposing to secondary infection risks, as indicated by infant studies (16) and blood cell transcriptome and immune studies in preterm pigs with NEC (17, 18).

ADAPTIVE IMMUNITY AND IMMUNIZATION IN COMPROMISED NEWBORNS

Systemic immunoglobulin G produced by B cells is the most abundant antibody type in the body, binds to cell surface receptors on many cell types to stimulate immune cell phagocytosis, cytotoxicity and activates complement cascades. Thus, systemic transfer of immunoglobulins from mother to offspring during the fetal and/or neonatal period helps to expose naïve immune cells to antigens in a controlled fashion, regulate their pathogen responses and stimulate maturation of the immune system, facilitate tolerogenic responses and prevent excessive inflammatory responses. Distinct differences exist among mammals in the time and mode of transmission of this passive immunity. In newborn ungulates (e.g. large farm animals) this occurs mainly via uptake of colostrum via the gut while for infants this occurs in utero across the placenta in the last third of pregnancy. The Research Topic review by Westrøm et al. provides an updated review on the knowledge of the immature gut barrier and the transfer of immunoglobulins from mother to young across species, and its role in immune maturation. Such passive immunoglobulin transfer may have effects beyond immune protection in gut and blood, potentially affecting more distant organs such as the immature brain, as reviewed by Pierzynowska et al.

At birth, very preterm infants have <50% of serum immunoglobulin G levels, compared with term infants (19), contributing to their high infection sensitivity. Conversely, preterm newborn pigs or other husbandry animals are completely devoid of blood immunoglobulins making them even more sensitive to systemic infections, even by low-virulent pathogens, if not fed mother's colostrum, as demonstrated by Bæk et al. In preterm newborns, such infections may lead to inflammatory lesions in various organs, including the immature brain (9). Supplemental systemic immunoglobulin has limited LOS- and NEC-preventive effects in pigs or infants (20, 21). Conversely, protective effects of oral IgG, and especially IgA, are possible (22), particularly for formula-fed preterm infants. Such effects may occur via local gut immune responses to colonizing bacteria, highlighting the importance of fresh maternal milk for compromised newborns (see later section).

Active immunization against specific pathogens in early life is often hampered by impaired initiation, immunogenicity, antibody production and cell-mediated response, requiring highly species-, age- and patient-specific vaccine approaches (23). These concerns of inadequate vaccine responses in newborns may be particularly relevant for preterm infants and Kulkarni-Munje et al. showed that although Indian preterm infants mounted adequate systemic immune responses to the majority of antigens of a pentavalent vaccine, diminished immunological memory remained a concern, relative to term infants. Local tissue environments and mediators from non-immune cells may determine the degree to which individual tissues respond effectively to infections and vaccinations, as shown by Bonney et al. for lung epithelial production of IL-6, supporting immune responses in influenza-challenged young mice. Similarly, in vitro work by Sharma et al. on isolated APC cell lines from mouse lungs, demonstrated how co-stimulants, including a ligand of the viral TLR5 receptor, flagellin, are effective to support cellular responses to viral infections or nasal vaccination in early life. Along such body epithelia, the virome may be critical for early life innate immune 'training' of the newborn host. In fetuses and preterm newborns, relatively harmless viral exposures, such as those of cytomegaloviruses (CMVs), may cause serious organ injury, including in the CNS. The tissue- and age-specific interaction between CMV and host cells depends critically on macrophages and monocytes, facilitating the balance between 'longer-term immune benefits or immunopathology', as elegantly reviewed by Baasch et al. in this Research Topic. Possibly, diet-dependent effects of the developing gut virome and bacteriome determine later-life mucosal immunity via cell-specific epigenetic changes (24).

Locally in the gut, toll-like receptors are important to recognize pathogen-associated molecular patterns (PAMPs) in early life and could trigger innate immune responses not only in the gut, but also in distant organs, such as the lung and brain, by signaling the recruitment of immune cells to these organs and

facilitate secondary immune responses, as reviewed by Sampah and Hackam. Experimentally, this is well demonstrated in mouse pups where NEC-related activation of TLR4 leads not only to systemic immune responses, but also to homing of gut-derived IFN-γ releasing CD4+ T cells to the brain, activation of inflammatory responses in microglial cells (25), or corresponding homing of proinflammatory Th17-secreting cells to lungs, activating local TLR4-dependent pathways (Sampah and Hackam). Consistent with this, brain inflammatory responses were also demonstrated after development of severe NEC lesions in preterm pigs (26, 27). In this Research Topic, Wedgwood et al. showed in young rat pups that the inflammatory effect of postnatal growth restriction on the developing lung may occur partly via changes to the gut microbiota with excessive activation of Gram-negative (TLR4-mediated) pathways. This helps to explain the commonly observed association between gut bacterial dysbiosis and NEC, growth restriction and later lung BPD development in preterm infants.

FETAL INSULTS AFFECTING NEWBORN IMMUNE DEVELOPMENT

Inter-organ immune communication and inflammatory insults may occur even before birth, preterm or term, and affect postnatal immune development. Chorioamnionitis (CA, inflammation of fetal membranes) is a key predisposing factor for preterm birth and adverse postnatal outcomes in CA infants (e.g. EOS, NEC, WMD, BPD) are well known but responses are highly time-, GA-, age-, organ- and pathogen-specific. There are reports of reduced LOS risk following CA in preterm infants (28), and fetal inflammation may under certain circumstances induce immune maturation. The systematic review by Villamor-Martinez et al. shows that the overall moderate CA-associated increase in later infections (LOS, 1-1.5 fold) partly relates to CA infants being born at lower GA while the CA effect on infant infections at birth is clear (EOS, 3-5 fold increases). By transcriptomic analyses on cord blood, Golubinskaya et al. showed high expression of S100A alarmins in cord blood monocytes of CA-exposed preterm infants, potentially helping to diagnose and treat CA effects after birth. Such associations show the need to do well-controlled studies in animals, allowing separation of the effects of preterm birth from its fetal and maternal predisposing factors, and thereby understand mechanisms across species and organs.

Following their previous works on the developing brain and lung, showing highly dose- and time-dependent effects of intra-amniotic inflammation (29), Heymans et al. demonstrated in cohorts of fetal lambs that fetal inflammation induces marked structural changes to the immature gut, including its enteric system and immune-regulatory glial cells. From lamb studies, it remains unclear if such effects predispose to later development of NEC lesions because preterm lambs are difficult to rear postnatally. In preterm pigs, few days of intra-amniotic exposure with LPS (reflecting Gram-negative infection) had limited or no effects on later NEC sensitivity (30, 31), or on gut microbiota or mucosal transcriptome, as observed by Pan et al. in this Research Topic. In this study, any postnatal gut influence of fetal inflammation appeared overshadowed by the immune-modulating effects of enteral feeding and microbial colonization just after birth. On the other hand, Muk et al. showed that kidneys, in contrast to gut, lungs and liver (30), showed more robust and longer-term inflammatory reactions after prenatal Gram-negative infection in preterm pigs, confirming the postnatal systemic immune suppression assessed by blood transcriptome analyses (32). It remains that the immune effects of fetal inflammation are highly species-, time-, age-, pathogen- and organ-specific. While animal studies help to verify mechanisms, it remains challenging to apply this to interventions preventing infections in complex clinical settings.

Another large proportion of compromised newborns, both preterm and term, are those exposed to placental dysfunction, with or without infection/inflammation, leading to gestational hypertension, fetal hypoxia and intra-uterine growth restriction (IUGR), with differential effects on immune development. Independently of predisposing factors, IUGR infants show increased infection susceptibility, probably due to low blood leukocyte, lymphocyte and macrophage counts just after birth, while specific effects on gut and lung inflammatory disorders (NEC, BPD) are more limited (33, 34). Yet, infants being born both preterm and IUGR are at highest risk for adverse outcomes, especially when combined with perinatal inflammation. In preterm pigs, moderate growth restriction at birth has limited NEC effects (35) but induces immune suppression in the first week, as shown in another study by Bæk et al. but with limited effects later, as shown in another study by Bæk et al. The studies in preterm pigs confirm the remarkable immunological adaptive capacity of immature and compromised newborns (12, 13, 36).

The synergistic effect of inflammation and dysregulated blood and oxygen supply around birth has been used to establish term animal models of perinatal gut, lung and brain damages (37, 38). Gravina et al. demonstrated in mice that the brain-damaging effects of hypoxia were most pronounced in male pups and during the acute phase of systemic infection with gram-positive bacteria. Male-specific higher mortality and immune defects were also demonstrated in the immediate postnatal period of preterm pigs (36).

DIET AND POSTNATAL IMMUNE DEVELOPMENT

The host immune system undergoes the most rapid changes in the perinatal period, together with profound changes in two central immune-modulating environmental factors, diet and microbiota. It is therefore not surprising that even small perturbations in this co-development can have profound consequences, especially for those with an underdeveloped immune system. A critical window of diet-microbiota susceptibility may exist shortly after birth and early life (dietary) interventions may have most pronounced effect on immune development in the first days and weeks of life, especially when birth occurs preterm. Initially, these infants are often

nourished parenterally but lack of luminal gut stimulation may in itself lead to impaired mucosal and systemic immune development via deficient gut trophic and immunomodulatory effects (e.g. immunoglobulins, lactoferrin, growth factors) and disturbed bacterial colonization. Further support for early enteral nutrition is related to the risk that excessive supply of parenteral metabolic substrates (glucose, amino acids) may create hyperinflammatory responses in immature immune cells (4).

Breast-feeding associates with fewer infections in infants, but effect sizes vary greatly (39) and are most pronounced within the first year of life (40) and for preterm infants. In this Research Topic, Sproat et al. summarized the factors in milk (immunoglobulins, milk immune cells, oligosaccharides, lactoferrin, growth factor peptides) that may affect innate and adaptive immunity in immature newborns. The first milk, colostrum, is particularly rich in immune-regulating factors and these may act to enhance immune defense in both species-specific and species-unspecific ways. Recently, bovine colostrum was investigated as a supplementary diet for mother´s own milk, formula or donor human milk for preterm infants (41, 42), based on preterm pig studies (9, 35, 43–48). In this Research Topic, Li et al. and Bæk et al. showed that bovine colostrum feeding before or after formula feeding had greatest effects on both mucosal and systemic immunity in preterm pigs when provided immediately after birth (e.g. blood neutrophils, Treg cells, gut IL8 response). Further, Pan et al. demonstrated epigenetic programming and NEC-protective effects of early colostrum supplementation on gut mucosal immunity and gene expression in newborn preterm pigs on parenteral nutrition (44, 49). In either case, the effects may be mediated by local species-unspecific immunoglobulin binding of pathogens and modulation of local mucosal immune responses (50, 51). The potential to use bovine colostrum as supplemental immunological protection in compromised preterm infants and other sensitive pediatric groups, is currently being investigated (41, 42, 50, 52).

MICROBIOTA, ANTIBIOTICS AND NEWBORN IMMUNE DEVELOPMENT

A wealth of information has recently emerged on the role of the developing gut, lung and skin microbiota on immune development in compromised newborns. While many studies in infants report only associations, not cause-effect relationships, direct effects of pre-, pro and antibiotics (AB) on the developing immune system via changes to the gut microbiota are demonstrated across many studies. However, due to wide individual variation in gut microbiota composition, type of pre- and probiotic products, and their interactions with milk diet and the non-bacterial gut microbiota (viruses, fungi), many questions remain unresolved. Across trials and products tested, dietary pre- and probiotics reduce NEC, and to a lesser degree, LOS in preterm infants (53, 54). Increased local and systemic immune competence after pre- and probiotic exposures may occur via competitive exclusion of pathogens, production of antimicrobial products and activation of mucosal immune cells with subsequent systemic effects. Finally, benefits may also occur by enhancing gut barrier properties, especially considering that a large proportion of LOS cases result from translocation of dominating gut bacterial species across an immature gut (55, 56). Similar barrier mechanisms may explain why rectal (not oral) transplantation of a mature fecal microbiota protects against NEC and mucosal bacterial adherence in preterm pigs, while stimulating systemic immune cell populations (57).

Due to the risk of systemic infections at or shortly after birth, empiric use of broad-spectrum AB is common for newborn very preterm infants [50-100% of infants (58),]. At population levels, long-term use of AB is clearly associated with adverse immune outcomes, gut microbiota turbulence, and increased antimicrobial resistance (4). The study by Oosterloo et al. in this Research Topic shows that immune-related markers in plasma of term infants may be affected up to 1 year after neonatal exposure to AB. In piglets, Hu et al. showed that low-dose, longer-term AB treatment reduced Th1-related blood immune responses while intestinal innate immunity-related genes were enriched, together with reduced IFN-γ and IL-6 expression. Together these studies indicate that AB-treated hospitalized infants could be more sensitive to later gut and systemic infections, especially if treated for longer periods (59). Importantly, 'confounding by disease' often complicates interpretation from such studies, and effects may vary according to time, dose, duration and route of AB administration. In very preterm infants, short-term (< 3 days) neonatal systemic AB treatment was associated with less (not more) NEC, but effects on systemic immunity or gut microbiota were unknown (60). In this Research Topic, Jiang et al. showed by plasma proteomics that NEC progression in preterm pigs affected many systemic immune markers, while short-term systemic AB treatment (< 5 days) had limited effects. On the other hand, neonatal AB treatment by the oral route seemed to delay gut colonization, improve gut immune gene expressions, plasma proteins and metabolites, indicating immune maturation and reduced systemic inflammation (56, 61–64). In immature, compromised newborns, an initial delay in gut bacterial colonization may allow better control of immune development but these initial benefits may later reduce both mucosal and systemic immune defense in both preterm pigs and infants (4, 59, 65). More research is required to demonstrate both benefits and possible harm of early life microbiota interventions for various subgroups of compromised newborns.

CONCLUSIONS

Birth is a dramatic, yet miraculous event. Rapid adaptations are required throughout the body to survive the transition from a stable life in utero to the microbe-dense outside world. These adaptations include tolerance to billions of colonizing and invading bacteria, viruses and fungi along the outer surfaces (gut, lung, skin), together with completely new modes of nutrition, respiration, metabolism and excretion. Via 29 reviews and original research articles this Research Topic has shown how perinatal immunity develops in compromised newborns.

Dysregulated immune development in newborns born preterm, growth-restricted, infected or subjected to placental dysfunction or birth asphyxia - is not a surprise. Rather, it is surprising how well these infants survive, adapt and thrive, despite their increased susceptibility to infections and inflammation in early life. Due to the age-, cell–, organ- and species-specificity of the developing immune systems, only a few interventions enhancing bacterial protection and immunity have become universally accepted for sensitive infants (e.g. breast-feeding, hygiene, certain antibiotics, vaccines). Novel dietary, microbiota and pharmacological interventions still require better documentation and evidence of mechanisms. Cross-species studies and omics-based analyses may help to understand mechanisms and ensure healthy development without side effects. Newborns that are compromised by fetal growth restriction, inflammation, infection, preterm birth and/or delivery complications often experience immunological deficits in the immediate postnatal period. Yet, their adaptive capacity is remarkable, making immune modulation of compromised newborns a difficult balance between potential benefits and possible harm.

AUTHOR CONTRIBUTIONS

PS, TS, AC and DN served as Guest Editors in the Research Topic. PS wrote the outline of this manuscript. TS, DN and AC reviewed and edited the manuscript. All authors contributed to the article and approved the submitted version.

FUNDING

The work was funded in part by grants from Innovation Fund Denmark (NEOMUNE and NEOCOL grants).

REFERENCES

1. Ng S, Strunk T, Jiang P, Muk T, Sangild PT, Currie A. Precision Medicine for Neonatal Sepsis. *Front Mol Biosci* (2018) 5:70. doi: 10.3389/fmolb.2018.00070
2. Lee AH, Shannon CP, Amenyogbe N, Bennike TB, Diray-Arce J, Idoko OT, et al. Dynamic Molecular Changes During the First Week of Human Life Follow a Robust Developmental Trajectory. *Nat Commun* (2019) 10(1):1092. doi: 10.1038/s41467-019-08794-x
3. Conti MG, Angelidou A, Diray-Arce J, Smolen KK, Lasky-Su J, De Curtis M, et al. Immunometabolic Approaches to Prevent, Detect, and Treat Neonatal Sepsis. *Pediatr Res* (2020) 87(2):399–405. doi: 10.1038/s41390-019-0647-6
4. Kollmann TR, Kampmann B, Mazmanian SK, Marchant A, Levy O. Protecting the Newborn and Young Infant From Infectious Diseases: Lessons From Immune Ontogeny. *Immunity* (2017) 46(3):350–63. doi: 10.1016/j.immuni.2017.03.009
5. Taylor AW, Blau DM, Bassat Q, Onyango D, Kotloff KL, Arifeen SE, et al. Initial Findings From a Novel Population-Based Child Mortality Surveillance Approach: A Descriptive Study. *Lancet Global Health* (2020) 8(7):e909–19. doi: 10.1016/s2214-109x(20)30205-9
6. Easter SR, Eckert LO, Boghossian N, Spencer R, Oteng-Ntim E, Ioannou C, et al. Fetal Growth Restriction: Case Definition & Guidelines for Data Collection, Analysis, and Presentation of Immunization Safety Data. *Vaccine* (2017) 35(48 Pt A):6546–54. doi: 10.1016/j.vaccine.2017.01.042
7. Miller JE, Hammond GC, Strunk T, Moore HC, Leonard H, Carter KW, et al. Association of Gestational Age and Growth Measures at Birth With Infection-Related Admissions to Hospital Throughout Childhood: A Population-Based, Data-Linkage Study From Western Australia. *Lancet Infect Dis* (2016) 16 (8):952–61. doi: 10.1016/s1473-3099(16)00150-x
8. Nguyen DN, Stensballe A, Lai JC, Jiang P, Brunse A, Li Y, et al. Elevated Levels of Circulating Cell-Free DNA and Neutrophil Proteins Are Associated With Neonatal Sepsis and Necrotizing Enterocolitis in Immature Mice, Pigs and Infants. *Innate Immun* (2017) 23(6):524–36. doi: 10.1177/1753425917719995
9. Brunse A, Worsøe P, Pors SE, Skovgaard K, Sangild PT. Oral Supplementation With Bovine Colostrum Prevents Septic Shock and Brain Barrier Disruption During Bloodstream Infection in Preterm Newborn Pigs. *Shock (Augusta Ga)* (2019) 51(3):337–47. doi: 10.1097/shk.0000000000001131
10. Sharma AA, Jen R, Butler A, Lavoie PM. The Developing Human Preterm Neonatal Immune System: A Case for More Research in This Area. *Clin Immunol (Orlando Fla)* (2012) 145(1):61–8. doi: 10.1016/j.clim.2012.08.006
11. Shah J, Balasubramaniam T, Yang J, Shah PS. Leukopenia and Neutropenia at Birth and Sepsis in Preterm Neonates of <32 Weeks' Gestation. *Am J Perinatol* (2020). doi: 10.1055/s-0040-1721133
12. Ren S, Hui Y, Obelitz-Ryom K, Brandt AB, Kot W, Nielsen DS, et al. Neonatal Gut and Immune Maturation Is Determined More by Postnatal Age Than by Postconceptional Age in Moderately Preterm Pigs. *Am J Physiol Gastrointest liver Physiol* (2018) 315(5):G855–67. doi: 10.1152/ajpgi.00169.2018
13. Nguyen DN, Jiang P, Frøkiær H, Heegaard PM, Thymann T, Sangild PT. Delayed Development of Systemic Immunity in Preterm Pigs as a Model for Preterm Infants. *Sci Rep* (2016) 6:36816. doi: 10.1038/srep36816
14. Lawrence SM, Corriden R, Nizet V. How Neutrophils Meet Their End. *Trends Immunol* (2020) 41(6):531–44. doi: 10.1016/j.it.2020.03.008
15. de Jong E, Hancock DG, Hibbert J, Wells C, Richmond P, Simmer K, et al. Identification of Generic and Pathogen-Specific Cord Blood Monocyte Transcriptomes Reveals a Largely Conserved Response in Preterm and Term Newborn Infants. *J Mol Med (Berlin Germany)* (2018) 96(2):147–57. doi: 10.1007/s00109-017-1609-2
16. Strunk T, Hibbert J, Doherty D, Nathan E, Simmer K, Richmond P, et al. Impaired Cytokine Responses to Live Staphylococcus Epidermidis in Preterm Infants Precede Gram-Positive, Late-Onset Sepsis. *Clin Infect Diseases: an Off Publ Infect Dis Soc America* (2021) 72(2):271–8. doi: 10.1093/cid/ciaa063
17. Ren S, Pan X, Hui Y, Kot W, Gao F, Sangild PT, et al. Sub-Clinical Necrotizing Enterocolitis-Induced Systemic Immune Suppression in Neonatal Preterm Pigs. *Am J Physiol Gastrointest Liver Physiol* (2021) 321(1):G18–28. doi: 10.1152/ajpgi.00408.2020
18. Pan X, Muk T, Ren S, Nguyen DN, Shen RL, Gao F, et al. Blood Transcriptomic Markers of Necrotizing Enterocolitis in Preterm Pigs. *Pediatr Res* (2021). doi: 10.1038/s41390-021-01605-4
19. Palmeira P, Quinello C, Silveira-Lessa AL, Zago CA, Carneiro-Sampaio M. IgG Placental Transfer in Healthy and Pathological Pregnancies. *Clin Dev Immunol* (2012) 2012:985646. doi: 10.1155/2012/985646
20. Sangild PT, Thymann T, Schmidt M, Stoll B, Burrin DG, Buddington RK. Invited Review: The Preterm Pig as a Model in Pediatric Gastroenterology. *J Anim Sci* (2013) 91(10):4713–29. doi: 10.2527/jas.2013-6359
21. Ohlsson A, Lacy JB. Intravenous Immunoglobulin for Preventing Infection in Preterm and/or Low Birth Weight Infants. *Cochrane Database System Rev* (2020) 1(1):Cd000361. doi: 10.1002/14651858.CD000361.pub4
22. Foster JP, Seth R, Cole MJ. Oral Immunoglobulin for Preventing Necrotizing Enterocolitis in Preterm and Low Birth Weight Neonates. *Cochrane Database System Rev* (2016) 4(4):Cd001816. doi: 10.1002/14651858.CD001816.pub3
23. Soni D, Van Haren SD, Idoko OT, Evans JT, Diray-Arce J, Dowling DJ, et al. Towards Precision Vaccines: Lessons From the Second International Precision Vaccines Conference. *Front Immunol* (2020) 11:590373. doi: 10.3389/fimmu.2020.590373
24. Liang G, Zhao C, Zhang H, Mattei L, Sherrill-Mix S, Bittinger K, et al. The Stepwise Assembly of the Neonatal Virome Is Modulated by Breastfeeding. *Nature* (2020) 581(7809):470–4. doi: 10.1038/s41586-020-2192-1
25. Zhou Q, Niño DF, Yamaguchi Y, Wang S, Fulton WB, Jia H, et al. Necrotizing Enterocolitis Induces T Lymphocyte-Mediated Injury in the Developing Mammalian Brain. *Sci Trans Med* (2021) 13(575). doi: 10.1126/scitranslmed.aay6621
26. Sun J, Pan X, Christiansen LI, Yuan XL, Skovgaard K, Chatterton DEW, et al. Necrotizing Enterocolitis Is Associated With Acute Brain Responses in

Preterm Pigs. *J Neuroinflamm* (2018) 15(1):180. doi: 10.1186/s12974-018-1201-x
27. Brunse A, Abbaspour A, Sangild PT. Brain Barrier Disruption and Region-Specific Neuronal Degeneration During Necrotizing Enterocolitis in Preterm Pigs. *Dev Neurosci* (2018) 40(3):198–208. doi: 10.1159/000488979
28. Strunk T, Doherty D, Jacques A, Simmer K, Richmond P, Kohan R, et al. Histologic Chorioamnionitis Is Associated With Reduced Risk of Late-Onset Sepsis in Preterm Infants. *Pediatrics* (2012) 129(1):e134–41. doi: 10.1542/peds.2010-3493
29. Gussenhoven R, Westerlaken RJJ, Ophelders D, Jobe AH, Kemp MW, Kallapur SG, et al. Chorioamnionitis, Neuroinflammation, and Injury: Timing Is Key in the Preterm Ovine Fetus. *J Neuroinflamm* (2018) 15 (1):113. doi: 10.1186/s12974-018-1149-x
30. Nguyen DN, Thymann T, Goericke-Pesch SK, Ren S, Wei W, Skovgaard K, et al. Prenatal Intra-Amniotic Endotoxin Induces Fetal Gut and Lung Immune Responses and Postnatal Systemic Inflammation in Preterm Pigs. *Am J Pathol* (2018) 188(11):2629–43. doi: 10.1016/j.ajpath.2018.07.020
31. Cilieborg MS, Schmidt M, Skovgaard K, Boye M, Weber NR, Heegaard PM, et al. Fetal Lipopolysaccharide Exposure Modulates Diet-Dependent Gut Maturation and Sensitivity to Necrotising Enterocolitis in Pre-Term Pigs. *Br J Nutr* (2011) 106(6):852–61. doi: 10.1017/s000711451100047x
32. Ren S, Pan X, Gao F, Sangild PT, Nguyen DN. Prenatal Inflammation Suppresses Blood Th1 Polarization and Gene Clusters Related to Cellular Energy Metabolism in Preterm Newborns. *FASEB J: Off Publ Fed Am Societies Exp Biol* (2020) 34(2):2896–911. doi: 10.1096/fj.201902629R
33. Hodzic Z, Bolock AM, Good M. The Role of Mucosal Immunity in the Pathogenesis of Necrotizing Enterocolitis. *Front Pediatr* (2017) 5:40. doi: 10.3389/fped.2017.00040
34. Wirbelauer J, Thomas W, Rieger L, Speer CP. Intrauterine Growth Retardation in Preterm Infants ≤32 Weeks of Gestation Is Associated With Low White Blood Cell Counts. *Am J Perinatol* (2010) 27(10):819–24. doi: 10.1055/s-0030-1254547
35. Che L, Thymann T, Bering SB, LEH-L I, D'Inca R, Zhang K, et al. IUGR Does Not Predispose to Necrotizing Enterocolitis or Compromise Postnatal Intestinal Adaptation in Preterm Pigs. *Pediatr Res* (2010) 67(1):54–9. doi: 10.1203/PDR.0b013e3181c1b15e
36. Bæk OCM, Nguyen DN, Bering S, Thymann T, Sangild PT. Sex-Specific Survival, Growth, Immunity and Organ Development in Preterm Pigs as Models for Immature Newborns. *Front Pediatr* (2021) 9:626101. doi: 10.3389/fped.2021.626101
37. D'Angio CT, Ryan RM. Animal Models of Bronchopulmonary Dysplasia. The Preterm and Term Rabbit Models. *Am J Physiol Lung Cell Mol Physiol* (2014) 307(12):L959–69. doi: 10.1152/ajplung.00228.2014
38. Nolan LS, Wynn JL, Good M. Exploring Clinically-Relevant Experimental Models of Neonatal Shock and Necrotizing Enterocolitis. *Shock (Augusta Ga)* (2020) 53(5):596–604. doi: 10.1097/shk.0000000000001507
39. Quigley MA, Carson C, Sacker A, Kelly Y. Exclusive Breastfeeding Duration and Infant Infection. *Eur J Clin Nutr* (2016) 70(12):1420–7. doi: 10.1038/ejcn.2016.135
40. Christensen N, Bruun S, Søndergaard J, Christesen HT, Fisker N, Zachariassen G, et al. Breastfeeding and Infections in Early Childhood: A Cohort Study. *Pediatrics* (2020) 146(5). doi: 10.1542/peds.2019-1892
41. Ahnfeldt AM, Hyldig N, Li Y, Kappel SS, Aunsholdt L, Sangild PT, et al. FortiColos - A Multicentre Study Using Bovine Colostrum as a Fortifier to Human Milk in Very Preterm Infants: Study Protocol for a Randomised Controlled Pilot Trial. *Trials* (2019) 20(1):279. doi: 10.1186/s13063-019-3367-7
42. Juhl SM, Ye X, Zhou P, Li Y, Iyore EO, Zhang L, et al. Bovine Colostrum for Preterm Infants in the First Days of Life: A Randomized Controlled Pilot Trial. *J Pediatr Gastroenterol Nutr* (2018) 66(3):471–8. doi: 10.1097/mpg.0000000000001774
43. Ahnfeldt AM, Bæk O, Hui Y, Nielsen CH, Obelitz-Ryom K, Busk-Anderson T, et al. Nutrient Restriction Has Limited Short-Term Effects on Gut, Immunity, and Brain Development in Preterm Pigs. *J Nutr* (2020) 150 (5):1196–207. doi: 10.1093/jn/nxaa030
44. Pan X, Gong D, Gao F, Sangild PT. Diet-Dependent Changes in the Intestinal DNA Methylome After Introduction of Enteral Feeding in Preterm Pigs. *Epigenomics* (2018) 10(4):395–408. doi: 10.2217/epi-2017-0122
45. Rasmussen SO, Martin L, Østergaard MV, Rudloff S, Li Y, Roggenbuck M, et al. Bovine Colostrum Improves Neonatal Growth, Digestive Function, and Gut Immunity Relative to Donor Human Milk and Infant Formula in Preterm Pigs. *Am J Physiol Gastrointest liver Physiol* (2016) 311(3):G480–91. doi: 10.1152/ajpgi.00139.2016
46. Shen RL, Thymann T, Østergaard MV, Støy AC, Krych Ł, Nielsen DS, et al. Early Gradual Feeding With Bovine Colostrum Improves Gut Function and NEC Resistance Relative to Infant Formula in Preterm Pigs. *Am J Physiol Gastrointest liver Physiol* (2015) 309(5):G310–23. doi: 10.1152/ajpgi.00163.2015
47. Sty AC, Sangild PT, Skovgaard K, Thymann T, Bjerre M, Chatterton DE, et al. Spray Dried, Pasteurised Bovine Colostrum Protects Against Gut Dysfunction and Inflammation in Preterm Pigs. *J Pediatr Gastroenterol Nutr* (2016) 63 (2):280–7. doi: 10.1097/mpg.0000000000001056
48. Sun J, Li Y, Pan X, Nguyen DN, Brunse A, Bojesen AM, et al. Human Milk Fortification With Bovine Colostrum Is Superior to Formula-Based Fortifiers to Prevent Gut Dysfunction, Necrotizing Enterocolitis, and Systemic Infection in Preterm Pigs. *JPEN J Parenteral Enteral Nutr* (2019) 43(2):252–62. doi: 10.1002/jpen.1422
49. Yan X, Sangild PT, Peng Y, Li Y, Bering SB, Pan X. Supplementary Bovine Colostrum Feedings to Formula-Fed Preterm Pigs Improve Gut Function and Reduce Necrotizing Enterocolitis. *J Pediatr Gastroenterol Nutr* (2021). doi: 10.1097/mpg.0000000000003147
50. Sangild PT, Vonderohe C, Hebib VM, Burrin DG. Potential Benefits of Bovine Colostrum in Pediatric Nutrition and Health. *Nutrients* (2021).
51. Ulfman LH, Leusen JHW, Savelkoul HFJ, Warner JO, van Neerven RJJ. Effects of Bovine Immunoglobulins on Immune Function, Allergy, and Infection. *Front Nutr* (2018) 5:52. doi: 10.3389/fnut.2018.00052
52. Li Y, Juhl SM, Ye X, Shen RL, Iyore EO, Dai Y, et al. A Stepwise, Pilot Study of Bovine Colostrum to Supplement the First Enteral Feeding in Preterm Infants (Precolos): Study Protocol and Initial Results. *Front Pediatr* (2017) 5:42. doi: 10.3389/fped.2017.00042
53. Morgan RL, Preidis GA, Kashyap PC, Weizman AV, Sadeghirad B. Probiotics Reduce Mortality and Morbidity in Preterm, Low-Birth-Weight Infants: A Systematic Review and Network Meta-Analysis of Randomized Trials. *Gastroenterology* (2020) 159(2):467–80. doi: 10.1053/j.gastro.2020.05.096
54. Johnson-Henry KC, Abrahamsson TR, Wu RY, Sherman PM. Probiotics, Prebiotics, and Synbiotics for the Prevention of Necrotizing Enterocolitis. *Adv Nutr (Bethesda Md)* (2016) 7(5):928–37. doi: 10.3945/an.116.012237
55. Stewart CJ, Embleton ND, Marrs ECL, Smith DP, Fofanova T, Nelson A, et al. Longitudinal Development of the Gut Microbiome and Metabolome in Preterm Neonates With Late Onset Sepsis and Healthy Controls. *Microbiome* (2017) 5(1):75. doi: 10.1186/s40168-017-0295-1
56. Nguyen DN, Fuglsang E, Jiang P, Birck MM, Pan X, Kamal SB, et al. Oral Antibiotics Increase Blood Neutrophil Maturation and Reduce Bacteremia and Necrotizing Enterocolitis in the Immediate Postnatal Period of Preterm Pigs. *Innate Immun* (2016) 22(1):51–62. doi: 10.1177/1753425915615195
57. Brunse A, Martin L, Rasmussen TS, Christensen L, Skovsted Cilieborg M, Wiese M, et al. Effect of Fecal Microbiota Transplantation Route of Administration on Gut Colonization and Host Response in Preterm Pigs. *ISME J* (2019) 13(3):720–33. doi: 10.1038/s41396-018-0301-z
58. de Waard M, Li Y, Zhu Y, Ayede AI, Berrington J, Bloomfield FH, et al. Time to Full Enteral Feeding for Very Low-Birth-Weight Infants Varies Markedly Among Hospitals Worldwide But May Not Be Associated With Incidence of Necrotizing Enterocolitis: The NEOMUNE-NeoNutriNet Cohort Study. *JPEN J Parenteral Enteral Nutr* (2019) 43(5):658–67. doi: 10.1002/jpen.1466
59. Ting JY, Synnes A, Roberts A, Deshpandey A, Dow K, Yoon EW, et al. Association Between Antibiotic Use and Neonatal Mortality and Morbidities in Very Low-Birth-Weight Infants Without Culture-Proven Sepsis or Necrotizing Enterocolitis. *JAMA Pediatr* (2016) 170(12):1181–7. doi: 10.1001/jamapediatrics.2016.2132
60. Li Y, Shen RL, Ayede AI, Berrington J, Bloomfield FH, Busari OO, et al. Early Use of Antibiotics Is Associated With a Lower Incidence of Necrotizing Enterocolitis in Preterm, Very Low Birth Weight Infants: The NEOMUNE-NeoNutriNet Cohort Study. *J Pediatr* (2020) 227:128–34. doi: 10.1016/j.jpeds.2020.06.032
61. Birck MM, Nguyen DN, Cilieborg MS, Kamal SS, Nielsen DS, Damborg P, et al. Enteral But Not Parenteral Antibiotics Enhance Gut Function and Prevent

Necrotizing Enterocolitis in Formula-Fed Newborn Preterm Pigs. *Am J Physiol Gastrointest liver Physiol* (2016) 310(5):G323–33. doi: 10.1152/ajpgi.00392.2015
62. Jiang P, Jensen ML, Cilieborg MS, Thymann T, Wan JM, Sit WH, et al. Antibiotics Increase Gut Metabolism and Antioxidant Proteins and Decrease Acute Phase Response and Necrotizing Enterocolitis in Preterm Neonates. *PloS One* (2012) 7(9):e44929. doi: 10.1371/journal.pone.0044929
63. Pan X, Gong D, Nguyen DN, Zhang X, Hu Q, Lu H, et al. Early Microbial Colonization Affects DNA Methylation of Genes Related to Intestinal Immunity and Metabolism in Preterm Pigs. *DNA Res: An Int J Rapid Publ Rep Genes Genomes* (2018) 25(3):287–96. doi: 10.1093/dnares/dsy001
64. Jiang P, Trimigno A, Stanstrup J, Khakimov B, Viereck N, Engelsen SB, et al. Antibiotic Treatment Preventing Necrotising Enterocolitis Alters Urinary and Plasma Metabolomes in Preterm Pigs. *J Proteome Res* (2017) 16(10):3547–57. doi: 10.1021/acs.jproteome.7b00263
65. Brunse A, Offersen SM, Mosegaard JJ, Deng L, Damborg P, Nielsen DS, et al. Enteral Broad-Spectrum Antibiotics Antagonize the Effect of Fecal Microbiota Transplantation in Preterm Pigs. *Gut Microbes* (2021) 13(1):1–16. doi: 10.1080/19490976.2020.1849997

Conflict of Interest: The authors declare that the research was conducted in the absence of any commercial or financial relationships that could be construed as a potential conflict of interest.

Publisher's Note: All claims expressed in this article are solely those of the authors and do not necessarily represent those of their affiliated organizations, or those of the publisher, the editors and the reviewers. Any product that may be evaluated in this article, or claim that may be made by its manufacturer, is not guaranteed or endorsed by the publisher.

frontiers in Immunology

ORIGINAL RESEARCH
published: 10 October 2019
doi: 10.3389/fimmu.2019.02402

Growth Restriction and Systemic Immune Development in Preterm Piglets

*Ole Bæk, Per Torp Sangild, Thomas Thymann and Duc Ninh Nguyen**

Section for Comparative Pediatrics and Nutrition, Faculty of Health and Medical Sciences, University of Copenhagen, Frederiksberg, Denmark

Background: Many preterm infants are born with growth restriction (GR) following maternal or fetal complications before birth. Such infants may continue to grow slowly after birth, regardless of birth weight (BW), due to morbidities related to their immature organs. Severe GR increases the susceptibility to infections, but it is not clear if this is a consequence of impaired systemic immunity or other factors, such as prolonged hospital stay or poor mucosal barrier function. Using preterm pigs as models for preterm infants, we hypothesized that moderate GR, exerting limited clinical effects, does not influence systemic immune development.

Methods: Preterm pigs were delivered by cesarean section and fed bovine milk diets until 19 d. Piglets with fetal growth restriction (F-GR, the lowest 25% of BW, $n = 27$, excluding those with BW <350 g) and postnatal growth restriction (P-GR, the lowest 25% of postnatal growth rate, $n = 24$) were compared with their corresponding controls (F-CON, $n = 92$, and P-CON, $n = 85$, respectively). Organ weights were determined and blood collected for assessment of clinical status (blood chemistry and hematology). For a subgroup ($n = 58$), in depth analyses of neutrophil function, T cell counts, plasma cytokine levels, and leucocyte gene expression were performed.

Results: For F-GR pigs, adrenal gland weight was increased and bone mineral content decreased at 19 d. Total leucocyte levels were lower at birth and interleukin-10 levels increased at d 8–10. In P-GR pigs, total leucocyte, neutrophil, monocyte, and eosinophil counts along with helper T cell fractions were elevated at 8–19 d of age, while the fraction of neutrophils with phagocytic capacity was reduced. Diarrhea and all remaining organ weights, blood chemistry, and immune variables were not affected by F-GR or P-GR.

Conclusion: Moderate GR before and after preterm birth has limited effect on systemic immune development in preterm pigs, despite marginal effects on immune cell populations, adrenocortical function, and body composition. Similar responses may be observed for preterm infants with moderate fetal and postnatal growth restriction.

Keywords: growth restriction, intrauterine, extrauterine, immune system, development, immunity, preterm, infant

OPEN ACCESS

Edited by:
Xin Zhao,
McGill University, Canada

Reviewed by:
Daiwen Chen,
Sichuan Agricultural University, China
Niel Karrow,
University of Guelph, Canada
Sarah Comstock,
Michigan State University, United States

****Correspondence:***
Duc Ninh Nguyen
dnn@sund.ku.dk

Specialty section:
This article was submitted to Nutritional Immunology, a section of the journal Frontiers in Immunology

Received: *01 July 2019*
Accepted: *25 September 2019*
Published: *10 October 2019*

Citation:
Bæk O, Sangild PT, Thymann T and Nguyen DN (2019) Growth Restriction and Systemic Immune Development in Preterm Piglets. Front. Immunol. 10:2402. doi: 10.3389/fimmu.2019.02402

BACKGROUND

Preterm infants (<37 weeks of gestation) have an increased risk of developing life-threatening infections and up to 40% develop sepsis in the neonatal period (1). This may be related to an underdeveloped immune system, inadequate transfer of maternal antibodies, but also to iatrogenic interventions, such as mechanical ventilation and vascular catheterization (1, 2). Antenatal factors, leading to slow fetal growth, may also play a role in increasing the risk of postnatal infection (3). Severely impeded fetal growth, resulting in intra uterine growth restriction (IUGR, defined as <10% of the body weight percentile), is a consequence of placental insufficiency or medical conditions, such as preeclampsia, uterine complications, or maternal/fetal infections (4). These infants show reduced leukocyte, lymphocyte, and neutrophil counts at birth (5, 6) and leukocytes exhibited reduced capacity to be activated by lipopolysaccharide following *ex vivo* whole blood challenge (3). Likewise, newborn infants show higher tolerable bacterial loads than adults during bacteremia, possibly as a result of energy constraints (7), which may be exacerbated after IUGR. Together this may be a cause for their increased risk of neonatal sepsis and later mortality, compared with infants born with a normal body weight for their gestational age (1, 8–10). IUGR infants have also been shown to have reduced thymus size at birth, a prognostic factor for later sepsis risk (11, 12). Adolescents born IUGR have lower levels of plasma thymopoietin (13), indicating long term effects of IUGR on thymus function, while any IUGR related reduction in plasma immunoglobulin levels at birth may disappear within the first year (14). Despite these results, the immune effects of different degrees of fetal growth restriction after preterm birth remain poorly understood. Even without IUGR, preterm birth is associated with low blood cell counts and immature blood cell functions (2), and the "double hit" of IUGR and preterm birth may either increase or decrease the immune deficits documented for IUGR infants born at full term.

In addition to poor prenatal growth, a major proportion of preterm infants experience postnatal growth restriction (15). After birth, preterm infants have higher nutritional requirements than term infants and have a high risk of feeding intolerance due to an immature gut, leading to difficulties in achieving growth rates that resemble those *in utero* (15, 16). Alleviating or preventing this extra uterine growth restriction (EUGR) may be critical for later neurodevelopment (17), but it is not clear if EUGR is associated with defects in other critical functions, such as immunity. Children have higher baseline levels of inflammatory cytokines, if exposed to EUGR in infancy (18), and malnutrition induced EUGR may affect immunity in children in low-income countries (19). For preterm infants, fortification of mother's own milk may be required to provide adequate amounts of nutrients, but even with adequate nutrient intake, preterm infants may experience slow growth, indicating that multiple factors lead to EUGR (15), not only low nutrient intake, low birth weight, and shortened gestation (20, 21).

Studies in full term piglets have contributed important information about the postnatal consequences of IUGR on physiological functions, including immunity (22–25). Much less is known for preterm pigs or infants, and especially for more moderate growth restriction before or after birth. The immature status of such newborns may render them more or less susceptible to the consequences (metabolic, endocrinological, inflammatory, or other) of moderate growth restriction. Using preterm pigs as a model for preterm infants, we hypothesized that moderate fetal and postnatal growth restriction, represented by individuals with the lowest 25% birth weight or postnatal growth rates, and excluding any pigs with extremely low birth weight, would not show deficient organ growth or immune development, relative to remaining litter-mate controls. Growth restricted pigs were selected from a cohort of 71 of preterm pigs reared for 19 days for recording of body composition, hematological, biochemical, and immune parameters.

METHODS

Animals and Experimental Design

Using three separate animal experiments with similar design, we identified a cohort of preterm piglets to investigate the impact of fetal and postnatal growth restriction. The experiments were all performed in accordance to the principals of the Basel Declaration and approved by the Danish National Committee of Animal Experimentation (2009/561-1731). A total of 125 piglets from 7 litters (Landrace × Yorkshire × Duroc, Gadbjerg, Denmark) were born prematurely by cesarean section at day 106 (90% gestation, term at 117 ± 2 days). Immediately after birth, piglets were individually housed in heated incubators (37–38°C) and resuscitated with mechanical ventilation, if required. Four piglets died of respiratory failure before randomization, leaving 121 (54% male) piglets for the cohort study. While still anesthetized from the cesarean section, each animal was prepared with an orogastric catheter for enteral feeding and an umbilical arterial catheter for parenteral nutrition and blood sampling. All piglets were passively immunized by systemic infusion of maternal plasma (total of 25 mL/kg, in three boluses within the first 24 h).

Piglets were fed increasing amounts (16–180 ml/kg/day) of bovine milk fortified with bovine colostrum (Biofiber Damino, Gesten, Denmark), whey protein concentrate and/or human milk oligosaccharide fractions (all products from Arla foods ingredients, Viby, Denmark) until postnatal day 19. All pigs

Abbreviations: IUGR, Intrauterine growth restriction; EUGR, Extrauterine growth restriction; PN, Parenteral nutrition; F-GR, Fetal growth restriction (Group name); F-CON, Fetal growth restriction control (Group name); P-GR, Postnatal growth restriction (Group name); P-CON, Postnatal growth restriction control (Group name); MFI, Median fluorescent index; qPCR, Quantitative polymerase chain reaction; *TNFA*, Tumor necrosis factor alpha (gene); IL4, Interleukin-4 (gene); *IL6*, Interleukin-6 (gene); *IL10*, Interleukin-10 (gene); *IFNG*, Interferon gamma (gene); *GATA*, GATA binding protein-3 (gene); *TBET*, T-box transcription factor TBX21 (gene); *TLR2*, Toll-like receptor 2 (gene); *TLR4*, Toll-like receptor 4 (gene); *HPRT1*, Hypoxanthine Phosphoribosyltransferase 1 (gene); IL-2, Interleukin-2; IL-6, Interleukin-6; IL-10, Interleukin-10; TNF-α, Tumor necrosis factor alpha; CRP, C reactive protein; ELISA, Enzyme linked immune assay; MCHC, Mean cellular hemoglobin concentration; MCV, Mean cellular volume; MPV, Mean platelet volume; MPC, Mean platelet component, BUN, Blood urea nitrogen; ALAT, Alanine aminotransferase; AST, Aspartate aminotransferase; GGT, Gamma glutaminyl transferase.

TABLE 1 | Study overview.

Study characteristics				Feeding volumes (ml/kg/day)									
Litters	***N***	**Blood sample (days)**	**Immune subgroup***	**Day 1**	**Day 2**	**Day 3**	**Day 4**	**Day 5**	**Day 6**	**Day 7-8**	**Day 9**	**Day 10–15**	**Day 16–19**
1	10	1◇, 8° & 19□	Yes	32	48	64	96	96	112	128	144	160	180
2	10	1◇, 8° & 19□	Yes	32	48	64	96	96	112	128	144	160	180
3	23	1◇, 8° & 19□	Yes	32	48	64	96	96	112	128	144	160	180
4	17	1◇, 8° & 19□	Yes	32	48	64	96	96	112	128	144	160	180
5	21	1◇, 10□ & 19•	No	16	32	48	64	96	112	128	144	160	180
6	24	1◇, 10□ & 19•	No	16	32	48	64	96	112	128	144	160	180
7	20	1◇, 10□ & 19•	No	16	32	48	64	96	112	128	144	160	180

**Blood samples used for T cell characterization, neutrophil phagocytic capacity, lymphocyte gene expression, and plasma cytokine levels. ◇, Cord blood; ○, Umbilical catheter; □, Jugular vein puncture; •, Cardiac puncture.*

were fed the same relative amounts of diet according to their body weight. The macronutrient levels in enteral diets were 33–43 g/L of carbohydrate, 38–52 g/L of fat, and 27–55 g/L of protein, resulting in 2.6–3.6 MJ/L. An overview of the different dietary regimens are shown in **Table 1**. To prevent diarrhea all animals were given oral antibiotics within the first 10 days of life. A combination of antibiotics were used consisting of: amoxicillin with clavulanic acid (Bioclavid, Sandoz GmbH, Kundl, Austria), gentamicin (Gentocin Vet, ScanVet, Fredensborg, Denmark) and metronidazole (Flagyl, Sanofi-aventis, Hørsholm, Denmark), given as 2 doses/day on day 9 and 10 (litters 1–4) or 2 doses/day on day 1–5 (litter 5–7).

Parenteral nutrition (PN, Kabiven and Vitalipid, Fresenius Kabi, Uppsala, Sweden) was optimized to preterm piglets and contained 2.8 MJ/L of energy, 72 g/L of glucose, 31 g/L of lipid, and 22 g/L of amino acids. PN was provided from birth until day 7 (decreasing from 120 to 48 ml/kg/day) at which time PN nutrition was stopped. For litters 1–4, the PN was replaced with a saline solution to maintain the catheters until blood sampling on day 8. For litters 5–7 the umbilical catheters were removed after secession of PN on day 7. The same TPN formulation was used for all animals, regardless of dietary regimen. On day 10, piglets were moved to larger individual cages, still with adequate heating and free access to drinking water (tap water) until euthanasia on day 19.

Within each litter, fetal growth restricted preterm pigs were defined as pigs with the lowest 25% birth weight (F-GR, $n = 27$), excluding extremely growth restricted piglets below 5% of mean birth weight (corresponding to ∼350 g, $n = 2$, due to mortality shortly after birth) and compared with the remaining pigs in each litter (F-CON, $n = 92$). For the evaluation of postnatal growth restriction until day 19, animals that survived at least until day 14 were included ($n = 109$). Within each litter, piglets with the 25% lowest growth rate, as in relative body weight increase per day (g/kg/day), from birth to 14 days were defined as postnatally growth restricted (P-GR, $n = 24$) and compared with the remaining pigs in each litter (P-CON, $n = 85$). Given the study design, there was an overlap between the fetal and postnatal growth restricted groups, as illustrated in **Table 2**.

TABLE 2 | Distribution of pig numbers in groups.

	P-GR	**P-CON**	**Total**
F-GR	6	14	20
F-CON	18	71	89
Total	24	85	109

Number of fetal growth restricted preterm pigs and controls (F-GR, F-CON) and, postnatally growth restricted preterm pigs and controls (P-GR, P-CON).

TABLE 3 | Primers used for qPCR analyses.

Gene	**Forward primer**	**Reverse primer**
TNFA	ATTCAGGGATGTGTGGCCTG	CCAGATGTCCCAGGTTGCAT
IL2	AAGCTCTGGAGGGAGTGCTA	CAACAGCAGTTACTGTCTCATCA
IL4	GTACCAGCAACTTCGTCCAC	CCTTCTCCGTCGTGTTCTCT
IL6	TGCCACCTCAGACAAAATGC	AGGTTCAGGTTGTTTTCTGCC
IL10	GTCCGACTCAACGAAGAAGG	GCCAGGAAGATCAGGCAATA
IFNG	AGCTTTGCGTGACTTTGTGT	ATGCTCCTTTGAATGGCCTG
TBET	CTGAGAGTCGCGCTCAACAA	ACCCGGCCACAGTAAATGAC
GATA3	ACCCCTTATTAAGCCCAAGC	TCCAGAGAGTCGTCGTTGTG
HPRT1	TATGGACAGGACTGAACGGC	ACACAGAGGGCTACGATGTG

Blood Sampling, Body Composition, and Tissue Collection

Blood samples (∼1.5 mL) were collected at different time points, including cord blood from birth (all litters), in the morning of day 8 from umbilical catheter (litter 1–4), in the morning of day 10 from jugular vein puncture (litter 5–7) and day 19, either by jugular vein puncture, in the morning before euthanasia (litter 1–4) or by cardiac puncture at euthanasia (litter 5–7). EDTA stabilized blood samples were used for hematology, T cell subset phenotyping, analysis of neutrophil phagocytosis functions and whole blood gene expressions. EDTA stabilized plasma was used for cytokine assays and serum for biochemical analyses. On day 19, before euthanasia, animals were anesthetized and subjected to a full body dual energy X ray absorptiometry (Lunar Prodigy

scanner, GE Healthcare, Little Chalfont, UK) to determine body composition. Afterwards all animals were euthanized by an intracardial injection of pentobarbital (60 mg/kg) after which the weight of all internal organs was recorded.

Hematology, Blood Biochemistry, and Systemic Immune Parameters

Hematology and serum biochemistry were performed using an Advia 2120 hematology system and an Advia 1800 Chemistry System, respectively (Siemens Healthcare Diagnostics, Tarrytown, NY, USA). For a subgroup of 58 animals (F-GR = 11, F-CON = 47, P-GR = 11, P-CON = 39), additional evaluation of systemic immune maturation was performed. T cell characterization, neutrophil phagocytic function, leucocyte gene expression, and plasma cytokine levels were determined using EDTA stabilized blood samples from day 1, 8, and 19. For T cell subset characterization, erythrocytes from blood samples were lysed (BD lysing solution, BD Biosciences, USA) and leucocytes were washed and incubated with fluorescent antibodies against porcine CD3 (PerCP-Cy5.5-conjugated mouse anti-CD3, IgG2a isotype, BD Bioscience), CD4 (FITC-conjugated mouse anti-pig CD4, IgG2b isotype, Biorad, Copenhagen, Denmark), and CD8 (PE-conjugated mouse anti-pig CD8, IgG2a isotype, Biorad). Negative controls included PerCP-Cy5.5-conjugated mouse IgG2a isotype control (BD Bioscience), PE-conjugated mouse IgG2a negative control, and FITC-conjugated mouse IgG2b negative control antibodies (Biorad). Leukocytes were analyzed by flow cytometry using BD Accuri C6 flow cytometer (BD Biosciences, USA). Lymphocyte population was gated using the forward scatter (FSC) and side scatter (SSC) dot plots, and the lymphocyte subsets were defined as follows: T cells ($CD3^+$ lymphocytes), helper T cells ($CD3^+CD4^+CD8^-$ lymphocytes), cytotoxic T cells ($CD3^+CD4^-CD8^+$ lymphocytes). Median fluorescent index (MFI) was used to estimate surface expression levels of CD4 and CD8.

Blood neutrophil phagocytosis function was tested by *ex vivo* whole blood stimulation with fluorescent marked *Escherichia coli* (pHrodo Red *E. coli* (560/585 nm), using bioparticles phagocytosis kit for flow cytometry (Thermofisher) for 30 min, followed by FACS analysis, as described previously (26). This determined the fraction of neutrophils with internalized bacteria (phagocytic rate) and average load of ingested bacteria per cell (MFI of $pHrodo^+$ neutrophil population, phagocytic capacity).

Leucocyte gene expression was evaluated by quantitative polymerase chain reaction (qPCR) of whole blood mRNA from 39 blood samples on day 8 (F-GR = 6, F-CON = 33, P-GR = 9, P-CON = 30) and 37 on day 19 (F-GR = 6, F-CON = 31, P-GR = 9, P-CON = 28). Briefly, fresh blood was fixed by addition of a lysis binding solution (Thermofisher) to fresh whole blood and frozen (−80°C) for later processing, as previously described (27). Later, RNA was extracted (MagMAX 96 Blood RNA Isolation Kit, Thermofisher) and converted to cDNA according to the manufacturer's instructions (High capacity cDNA reverse transcription kit, Applied Biosystems, USA). We failed to extract RNA from one sample on day 8 (in F-CON and P-CON groups) and excluded this from analysis. Using a LightCycler 480 system (Roche, Switzerland) with a commercial qPCR kit (QuantiTect SYBR Green PCR Kit, Qiagen, Netherlands), gene expressions were determined for tumor necrosis factor alpha (*TNFA*), interleukin-4 (*IL4*), interleukin-6 (*IL6*), interleukin-10 (*IL10*), Interferon gamma (*IFNG*), GATA binding protein-3 (*GATA3*), T-box transcription factor TBX21 (*TBET*), toll-like receptor 2 (*TLR2*), toll-like receptor 4 (*TLR4*), and using hypoxanthine

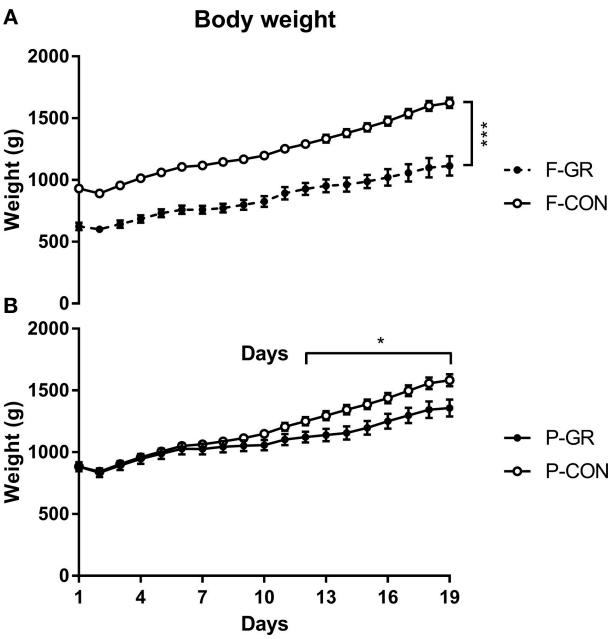

FIGURE 1 | Body weight across the study period in fetal growth restricted preterm pigs and controls (F-GR, $n = 27$; F-CON, $n = 92$, **A**) and postnatally growth restricted preterm pigs and controls (P-GR, $n = 24$; P-CON, $n = 85$, **B**). Values are means with corresponding standard error of the mean. $^*p < 0.05$, $^{***}p < 0.001$.

TABLE 4 | Relative weight (g per kg body weight) of internal organs on day 19.

	F-GR, $n = 19$	F-CON, $n = 86$	P-GR, $n = 24$	P-CON, $n = 81$
Heart	6.8 ± 0.4	6.5 ± 0.1	6.6 ± 0.2	6.5 ± 0.1
Lung	19.1 ± 1.5	18.6 ± 0.6	20.4 ± 1.6$^{(*)}$	17.8 ± 0.6
Kidney	8.2 ± 0.4$^{(*)}$	7.2 ± 0.1	7.9 ± 0.3**	7.1 ± 0.1
Adrenals	0.40 ± 0.02***	0.29 ± 0.01	0.31 ± 0.02	0.30 ± 0.01
Spleen	2.6 ± 0.3	2.8 ± 0.1	2.7 ± 0.3	2.8 ± 0.1
Liver	23.4 ± 1.3	25 ± 0.6	23.5 ± 1.3	24.5 ± 0.6
Stomach	7.7 ± 0.4	6.8 ± 0.1	7 ± 0.3	6.8 ± 0.1
Intestine	40.9 ± 1.8	41.7 ± 0.9	42.6 ± 1.9	42.0 ± 0.9
Colon	17.9 ± 1.8	20 ± 1.2	22.1 ± 2.4	19.4 ± 1.1

*Data is presented as means ± SEM. **$p < 0.01$, ***$p < 0.001$, $^{(*)}p < 0.10$ for F-GR vs. F-CON or P-GR vs. P-CON comparisons, respectively. Data shown for fetal growth restricted preterm pigs and controls (F-GR, F-CON) and postnatally growth restricted preterm pigs and controls (P-GR, P-CON). SEM, Standard error of the mean.*

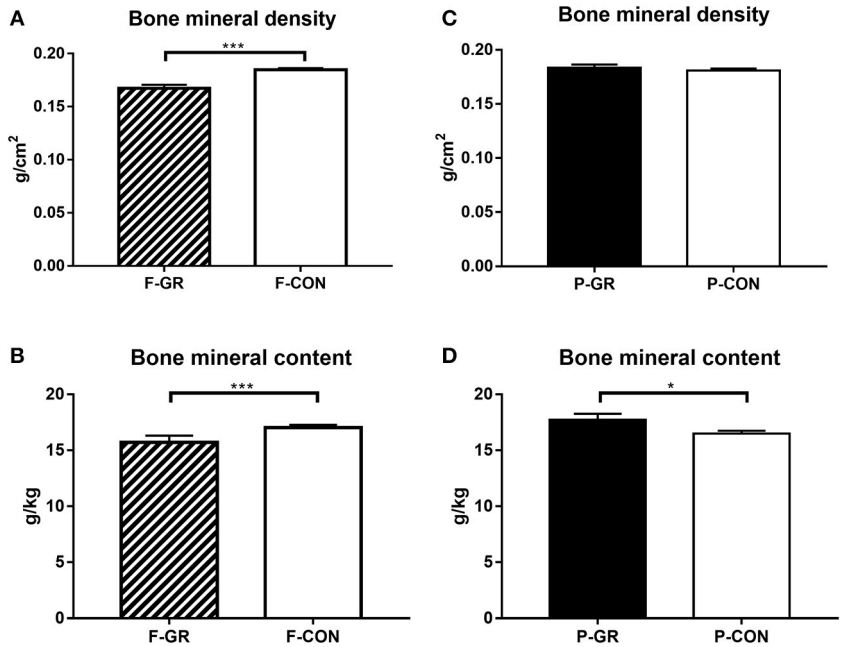

FIGURE 2 | Bone mineral density and bone mineral content (relative to body weight) at euthanasia in fetal growth restricted preterm pigs and controls (F-GR, $n = 16$; F-CON, $n = 70$, **A,B**) and in postnatally growth restricted preterm pigs and controls (P-GR, $n = 20$; P-CON, $n = 66$, **C,D**). Values are means with corresponding standard error of the mean. $^{*}p < 0.05$, $^{***}p < 0.001$.

phosphoribosyltransferase 1 (*HPRT1*) as a housekeeping gene. Primers were designed using the *Genes* database and Primer-BLAST software (both National Center for Biotechnology Information, USA). All primers used are listed in **Table 3**. Samples were run in duplicates with expected 2.5% of variation of Cq values. For all samples, *HPRT1* was quantified within this variation limit. For the remaining genes, data were excluded if the variation of Cq values were higher than 2.5%. For information on the number of censored samples, please see **Supplementary Table 1**. Results were presented as fold changes, relative to expression levels of *HPRT1*. Ratios of *TBET*/*GATA3*, *IL2*/*IL4*, *IFNG*/*IL4,* and *TNFA*/*IL6* were used for indication of type 1 or type 2 T cell polarization (Th1 and Th2, respectively). The ratio of TNF-α to IL-6 is especially relevant in newborn infants (28, 29).

Plasma levels of interleukins 2, 6, and 10 (IL-2, IL-6, and IL-10), C reactive protein (CRP), cortisol and tumor necrosis factor alpha (TNF-α) were determined using ELISA (porcine specific duoset kits, R&D Systems). Samples below the detection were assigned an arbitrary value of half of the detection limit for statistical analyses.

Statistics

Statistical analyses were performed using Stata 14.2 (StataCorp, Texas, USA). All data were evaluated for each time point separately, using linear regression models, with pig group (F-GR vs. F-CON or P-GR vs. P-CON) and litter as fixed effects. Data were logarithmically transformed, if necessary. Data without normal distribution were evaluated by Kruskal–Wallis' test. Mortality and group distribution were compared by Chi^2 test. Means and corresponding standard error of means (SEMs) were reported. *P*-values <0.05 were considered statistically significant, and *p*-values < 0.1 was reported as a tendency to a difference.

RESULTS

Effects of Fetal Growth Restriction on Clinical Variables and Organ Development

Birth weight of F-GR piglets were 648 ± 26 vs. 930 ± 17 g in F-CON pigs ($p < 0.001$), but the subsequent relative daily weight gain until day 14 did not differ between the groups (27 ± 1 vs. 29 ± 1 g/kg/day). Body weight differed between F-GR and F-CON piglets for all time points (**Figure 1A**). Days with diarrhea (mean 6 days in both groups) and CRP levels (3.2 ± 1.1 vs. 7.2 ± 2.0 μg/mL on day 19 for F-GR and F-CON) did not differ, but mortality was higher in the F-GR group (7 of 27 before day 14 vs. 6 of 95 for F-CON pigs, $p < 0.01$). On day 19, surviving F-GR pigs had lower body weight (1,113 ± 80 vs. 1,624 ± 41 g, $p < 0.001$), while relative adrenal gland and kidney weight was higher (**Table 4**, $p < 0.001$ and $p = 0.07$, respectively) than in F-CON pigs. Plasma cortisol levels at day 19 did not differ between F-GR and F-CON pigs (23 ± 4 vs. 33 ± 8 ng/mL). For body composition, F-GR pigs had lower bone mineral density and relative bone mineral content than F-CON pigs (**Figures 2A,B**, both $p < 0.001$). Lean body mass (95.3 ± 0.3 vs. 95.4 ± 0.2%) and fat mass (3.9 ± 0.3 vs. 3.7 ± 0.2%) were similar.

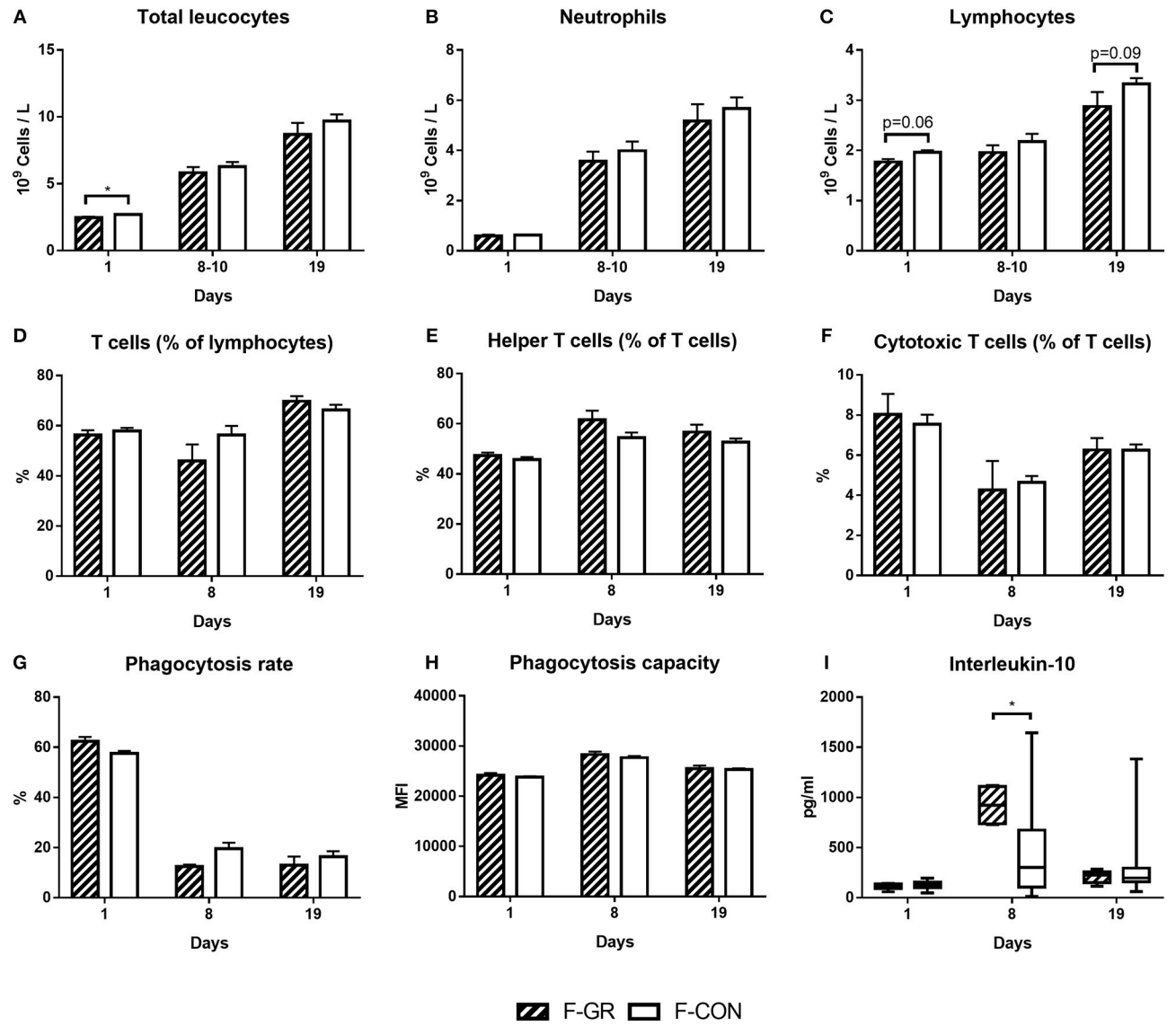

FIGURE 3 | Development of systemic immune parameters in fetal growth restricted preterm pigs and controls (F-GR, $n = 19$–24 for **A–C** and $n = 6$–10 for **D–I**; F-CON, $n = 71$–89 for **A–C** and $n = 34$–37 for **D–I**), day 1 (cord blood) to day 19. **(A–C)** leucocyte cell counts, **(D–F)** fractions of T cell subsets, **(G,H)** neutrophil phagocytosis function, I: interleukin-10 levels in plasma (two samples were below detection limit on day 8, both in F-CON group). Values in **(A–H)** are presented as means with corresponding standard error of the mean. Values in I are presented as range plots with corresponding means, all analyzed by Kruskal–Wallis' test. *$p < 0.05$.

Effects of Fetal Growth Restriction on Blood Hematology, Biochemistry, and Immune Development

F-GR pigs had lower total blood leucocyte counts (**Figure 3A**, $p < 0.05$) at birth, mainly driven by lower lymphocyte counts (**Figure 3C**, $p = 0.06$). Cytotoxic T cell MFI tended to be higher in F-GR animals (847 ± 120 vs. 768 ± 133, $p = 0.06$). No other blood immune cell counts, T cell fractions, T cell MFI, plasma cytokine levels or markers for blood neutrophil phagocytic function differed at birth (**Figures 3B,D–H**). By day 8, only plasma IL-10 levels were higher in F-GR vs. F-CON pigs (**Figure 3I**, $p < 0.05$), whereas all other leucocyte counts (**Figures 3A–C**), T cell subsets (**Figures 3D–F**), neutrophil phagocytic function (**Figures 3G,H**) and plasma cytokine levels and T cell MFI (data not shown) were similar between the two groups, both at day 8–10 and day 19. Ratios of TNFα/IL-10 did not differ at any time points.

For all tested leucocyte gene expressions, no differences at day 8 were observed (**Figures 4A,C**), apart from a tendency to higher *IL10* expression in F-GR, relative to F-CON pigs (**Figure 4B**, $p = 0.06$). By day 19, *IL10* expression was lower (**Figure 4E**, $p < 0.05$) and there was a tendency to an increased *TBET*/*GATA3*

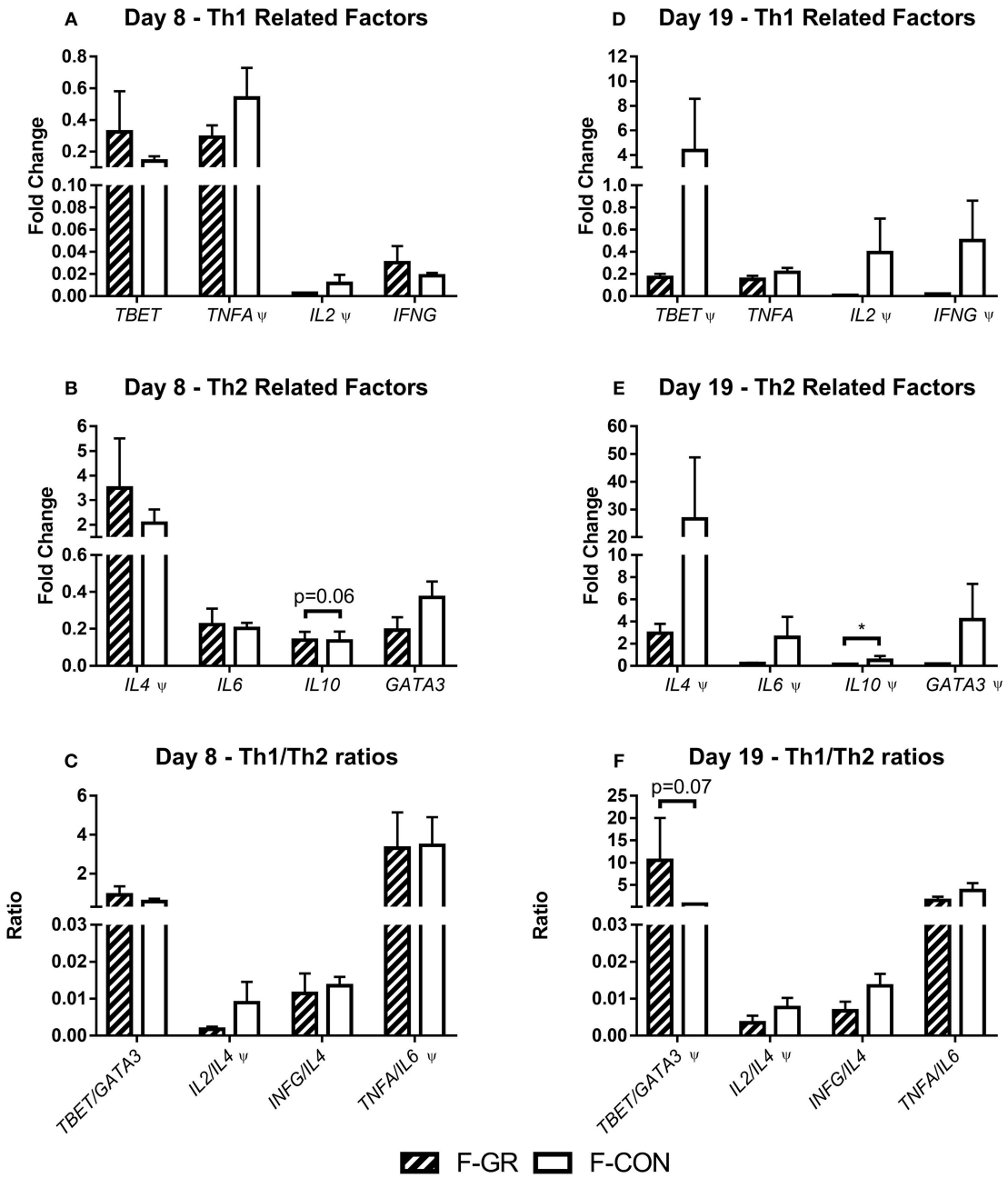

FIGURE 4 | Leucocyte gene expression in fetal growth restricted preterm pigs and controls on day 8 (**A–C**, F-GR, $n = 5$–6; F-CON, $n = 26$–32) and 19 (**D–F**, F-GR, $n = 5$–6; F-CON, $n = 27$–31). **(A,D)** type 1 helper T cell related genes, **(B,E)** type 2 helper T cell related genes, **(C,F)** ratios of type 1 and type 2 helper T cell related genes. Results presented as mean fold changes in relation to housekeeping gene with corresponding standard error of the mean **(A,B,D,E)** or as ratios between fold changes **(C,F)**. *$p < 0.05$, Ψ, analyzed by Kruskal–Wallis' test.

ratio in F-GR pigs (**Figure 4F**, $p = 0.07$). Likewise, there was a tendency toward a lower *TNFA/IL10* ratio in F-GR pigs at day 19 (2.9 ± 1.0 vs. 3.8 ± 0.9, $p = 0.09$)

For non-immunological parameters, F-GR pigs showed higher values of mean platelet volume than F-CON pigs at birth and day 8–10 (MPV, **Table 5**, both $p < 0.05$) but no serum biochemical values at day 19 showed any differences between F-GR and F-CON pigs.

Effects of Postnatal Growth Restriction on Clinical Variables and Organ Development

Birth weight did not differ between P-GR and P-CON pigs (883 ± 37 vs. 883 ± 21 g). P-GR pigs had reduced postnatal relative weight gain (20 ± 1 vs. 31 ± 1 g/kg/day in P-CON pigs, $p < 0.001$), and lower body weight at day 19 ($1{,}357 \pm 68$ vs. $1{,}583 \pm 48$ g in P-CON pigs, $p < 0.05$). Body weight started to differ after day 12 (**Figure 1B**). Days with diarrhea

TABLE 5 | Hematological parameters at day 1, 8–10, and 19.

	Day	F-GR $n = 19–24$	F-CON $n = 71–89$	P-GR $n = 18–23$	P-CON $n = 67–80$
Erythrocytes (10^{12} cells/L)	1†	4.1 ± 0.1	4.0 ± 0.0	4.0 ± 0.1	4.1 ± 0.0
	8–10	4.1 ± 0.2	4.0 ± 0.1	4.0 ± 0.2	4.1 ± 0.1
	19	4.5 ± 0.2	4.5 ± 0.1	4.5 ± 0.1	4.5 ± 0.1
Hemoglobin (mmol/L)	1†	5.5 ± 0.1	5.4 ± 0.0	5.4 ± 0.1	5.5 ± 0.1
	8–10	4.8 ± 0.3	4.7 ± 0.1	4.8 ± 0.2	4.8 ± 0.1
	19	4.7 ± 0.2	4.7 ± 0.1	4.6 ± 0.2	4.8 ± 0.1
Hematocrit (%)	1†	29.9 ± 0.4	29.5 ± 0.3	29.2 ± 0.4	29.6 ± 0.3
	8–10	25.9 ± 1.5	25.1 ± 0.5	25.5 ± 1.1	25.5 ± 0.5
	19	25.6 ± 1	26.0 ± 0.5	26.0 ± 1.0	25.9 ± 0.5
MCHC (mmol/L)	1†	18.4 ± 0.3	18.2 ± 0.2	17.7 ± 0.8	18.5 ± 0.1
	8–10	18.7 ± 0.4	18.7 ± 0.1	18.7 ± 0.3	18.8 ± 0.1
	19	18.6 ± 0.4	18.3 ± 0.3	17.9 ± 0.8	18.5 ± 0.2
MCV (fL)	1†	72.3 ± 1.0	73.5 ± 0.7	72.5 ± 1.1	72.9 ± 0.7
	8–10	62.4 ± 1.4	63.2 ± 0.7	63.6 ± 1.2	62.9 ± 0.7
	19	57.5 ± 1.2	58.2 ± 0.6	57.5 ± 1.0	58.2 ± 0.7
Platelets (10^9 cells/L)	1†	187 ± 23	210 ± 11	191 ± 23	201 ± 11
	8–10	343 ± 41	359 ± 22	456 ± 56(*)	341 ± 18
	19	432 ± 60	487 ± 28	528 ± 65	460 ± 27
MPV (fL)	1†	10.5 ± 0.3*	10.1 ± 0.1	10.2 ± 0.2	10.1 ± 0.1
	8–10	13.1 ± 1.3**	10.6 ± 0.4	11.9 ± 1.2	10.5 ± 0.3
	19	9.7 ± 0.6	9.6 ± 0.3	9.6 ± 0.6	9.6 ± 0.3
MPC (g/L)	1†	220 ± 2	220 ± 1	219 ± 2	220 ± 1
	8–10	224 ± 5	224 ± 2	228 ± 5	223 ± 2
	19	228 ± 4	231 ± 2	230 ± 3	230 ± 2

*Data is presented as means ± SEM. †Cord blood sample; (*)$p < 0.1$, *$p < 0.05$, and **$p < 0.01$ for F-GR vs. F-CON or P-GR vs. P-CON comparisons, respectively. Data shown for fetal growth restricted preterm pigs and controls (F-GR; F-CON) and postnatally growth restricted preterm pigs and controls (P-GR, P-CON). MCHC, Mean cellular hemoglobin concentration; MCV, Mean cellular volume; MPV, Mean platelet volume; MPC, Mean platelet component; SEM, Standard error of the mean.*

(6–7 days in both groups) and CRP levels (12.1 ± 4.7 vs. 5.2 ± 1.7 μg/mL) were similar between P-GR and P-CON pigs. Among the 20 surviving F-GR pigs, six of them were categorized as P-GR, thus the incidence of P-GR did not differ significantly between F-GR and F-CON pigs ($p > 0.1$). Relative kidney weight was increased in P-GR animals (**Table 4**, $p < 0.05$) with a tendency toward increased relative lung weight (**Table 4**, $p = 0.06$). For body composition, bone mineral content was increased in P-GR pigs (**Figure 2D**, $p < 0.05$), while values for bone mineral density (**Figure 2C**), lean mass (95.7 ± 0.4 vs. 95.3 ± 0.2%) and fat mass (3.5 ± 0.3 vs. 3.8 ± 0.2%) were similar.

Effects of Postnatal Growth Restriction on Blood Hematology, Biochemistry, and Immune Development

At birth, no differences in blood immune cell parameters, neutrophil phagocytic function, T cell fractions, T cell MFI or plasma cytokine levels were found between P-GR and P-CON pigs (**Figures 5A–I**). By day 8–10, there was higher total blood leucocyte counts in the P-GR group (**Figure 5A**, $p < 0.05$), mainly driven by increased neutrophil counts (**Figure 5B**, $p < 0.01$). In addition, the neutrophil phagocytic rate (**Figure 5G**, $p < 0.01$) was reduced, with a tendency to improved phagocytic capacity (**Figure 5H**, $p = 0.05$) in P-GR pigs. At day 19, total leucocyte and neutrophil counts remained higher in P-GR pigs (**Figures 5A,B**, both $p < 0.05$), with a tendency to lower neutrophil phagocytic rate (**Figure 5G**, $p = 0.08$). In addition, monocyte (0.50 ± 0.09 vs. 0.34 ± 0.03 × 10^9 cells/L, $p < 0.05$) and eosinophil (0.16 ± 0.03 vs. 0.09 ± 0.01 × 10^9 cells/L, $p < 0.05$) counts, as well as the fraction of helper T cells (**Figure 5E**, $p < 0.01$), were increased in P-GR animals. Plasma levels of IL-10 (**Figure 5I**) or other cytokines, as well as T cell MFI (data not shown) did not differ at day 8 or 19 between P-GR and P-CON pigs. Likewise, ratios of TNFα/IL-10 did not vary at any time point. The P-GR animals tended to have lower platelet counts (**Table 5**, $p = 0.05$) at day 8–10, relative to P-CON pigs. Other than lower alkaline phosphatase levels in P-GR pigs at day 19, no biochemical variables or plasma cortisol level differed between groups (**Table 6**, $p < 0.05$).

Leucocyte gene expression at day 8 showed reduced expression of *IL2* (**Figure 6A**, $p < 0.05$) and *GATA3* (**Figure 6B**, $p < 0.05$), together with a tendency toward an increased ratio of *TNFA* to *IL6* (**Figure 6C**, $p = 0.08$) in P-GR pigs. By day 19 several genes were expressed at numerically lower levels in P-GR animals, but only *TBET* (**Figure 6D**, $p < 0.05$) expression was

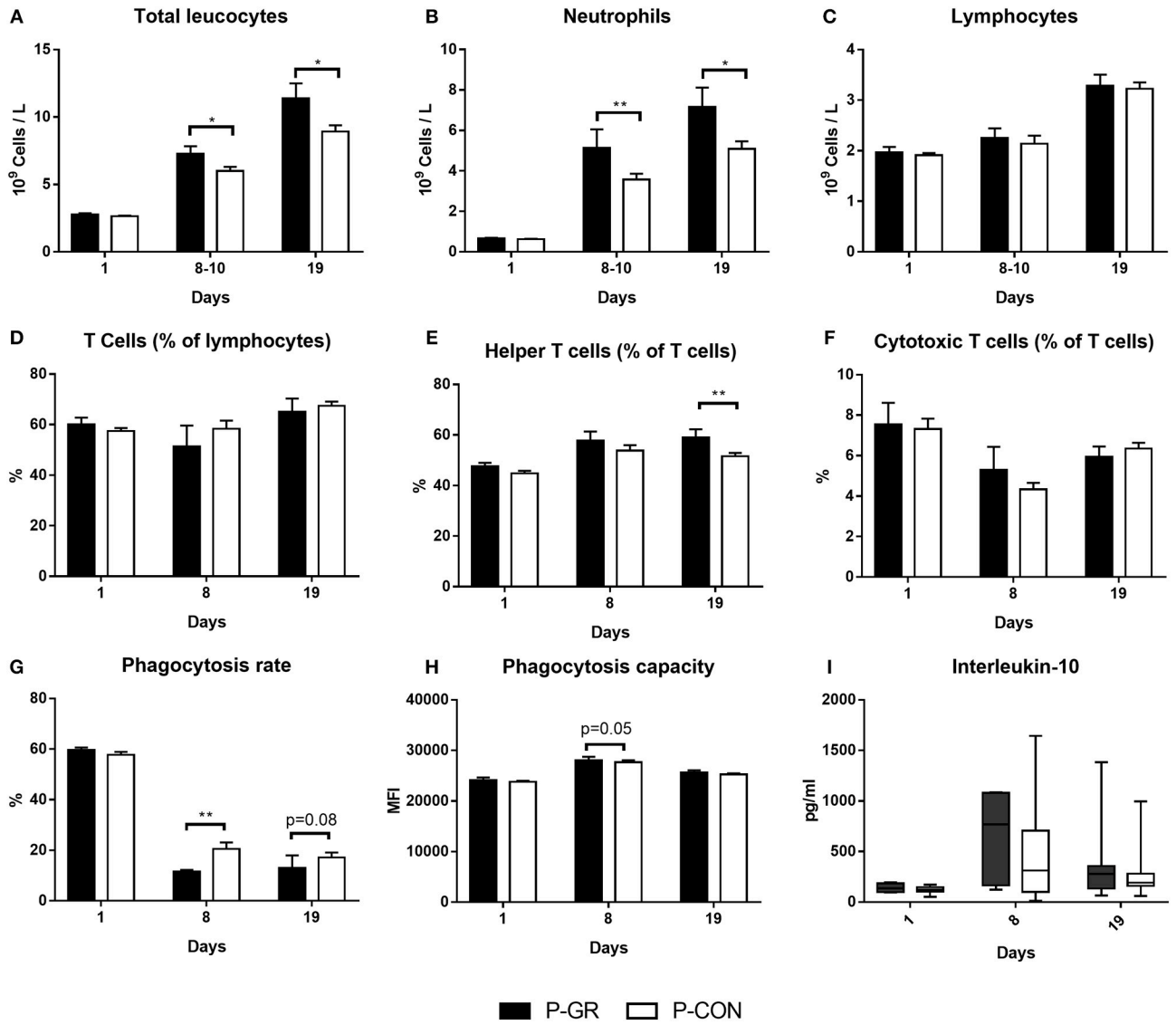

FIGURE 5 | Development of systemic immune parameters in postnatally growth restricted preterm pigs and controls (P-GR, $n = 18$–23 for A–C and $n = 9$–10 for **D–I**; P-CON, $n = 67$–80 for **A–C** and $n = 29$–34 for **D–I**) from day 1 (cord blood) to day 19. **(A–C)** leucocyte cell counts, **(D–F)** fractions of T cell subsets, **(G,H)** neutrophil phagocytosis function, I: interleukin-10 levels in plasma (two samples were below detection limit on day 8, both in P-CON group). In **(A–H)**, values are presented as means with corresponding standard error of the mean. In **(I)**, values are presented as range plots with corresponding means, all analyzed by Kruskal–Wallis' test. $^*p < 0.05$, $^{**}p < 0.01$.

significantly down regulated in the P-GR piglets. No differences were observed for Th2 related factors (**Figure 6E**). Ratios of TNFA/IL10 did not differ at any time point between P-GR and P-CON (data not shown).

DISCUSSION

Preterm infants, especially those born extremely preterm (<28 weeks gestation), show a high sensitivity to infections in the postnatal period. A large proportion of these are born growth restricted and show growth deficits after birth due to multiple maternal, fetal, and postnatal factors (4, 30). It is important to know if low growth rates are associated with impaired immune development because this would call for special clinical interventions to avoid infections. Using preterm pigs as a model for preterm infants, we show that a moderate growth restriction at birth, excluding extremely low birth weight preterm pigs, was associated with increased adrenal gland weight, reduced bone mineralization, and a transient change in circulating IL-10 levels. Conversely, slow postnatal growth rates were associated with modest increases in bone mineralization, blood neutrophil, monocyte, and eosinophil counts, and a transiently higher helper T cell fraction. Taken together, surprisingly few

TABLE 6 | Blood biochemistry at day 19.

	F-GR $n = 22$	F-CON $n = 81$	P-GR $n = 22$	P-CON $n = 77$
Albumin (g/L)	16.6 ± 0.9	17.6 ± 0.4	17.3 ± 1	17.4 ± 0.4
Total protein (g/L)	27.9 ± 1.2	29.5 ± 0.7	29.4 ± 1.7	29.1 ± 0.6
BUN (mmol/L)$^{\Psi}$	7.4 ± 0.9	6.8 ± 0.5	8.1 ± 1.0	6.5 ± 0.5
ALAT (U/L)	34 ± 3	32 ± 1	33 ± 2	32 ± 1
AST (U/L)$^{\Psi}$	50 ± 8	35 ± 2	40 ± 5	37 ± 2
Alkaline phosphatase (U/L)	1,085 ± 122	1,080 ± 63	956 ± 116*	1,117 ± 63
Bilirubin (μmol/L)$^{\Psi}$	1.3 ± 0.2	1.6 ± 0.2	1.5 ± 0.3	1.6 ± 0.2
GGT (U/L)$^{\Psi}$	20.1 ± 1.6	22.4 ± 1	21.9 ± 2.3	22.0 ± 0.9
Cholesterol (mmol/L)$^{\Psi}$	2.5 ± 0.1	2.7 ± 0.1	2.6 ± 0.1	2.6 ± 0.1
Creatine (mmol/L)$^{\Psi}$	62.5 ± 10.3	53.2 ± 1.4	65.1 ± 9.0	52.1 ± 1.4
Creatine kinase (mmol/L)$^{\Psi}$	375 ± 145	213 ± 25	223 ± 48	250 ± 43
Glucose (mmol/L)$^{\Psi}$	4.6 ± 0.5	5.2 ± 0.2	4.8 ± 0.4	5.1 ± 0.2
Lactate (mmol/L)$^{\Psi}$	4.6 ± 1.0	4.9 ± 0.4	5.1 ± 1.0	4.8 ± 0.4
Sodium (mmol/L)$^{\Psi}$	140 ± 2	143 ± 2	142 ± 4	143 ± 2
Potassium (mmol/L)	4.4 ± 0.3	4.7 ± 0.1	4.6 ± 0.3	4.6 ± 0.1
Phosphate (mmol/L)	2.3 ± 0.1	2.5 ± 0.1	2.4 ± 0.1	2.5 ± 0.1
Calcium (mmol/L)	2.5 ± 0.1	2.6 ± 0.0	2.5 ± 0.1	2.6 ± 0.0
Magnesium (mmol/L)	0.9 ± 0.0	0.9 ± 0.0	1.0 ± 0.1	0.9 ± 0.0
Iron (mmol/L)$^{\Psi}$	10.2 ± 1.3	9.1 ± 0.7	9.4 ± 1.2	9.3 ± 0.7

*Data is presented as means ± SEM. *$p < 0.05$ for P-GR vs. P-CON comparison. Ψ, comparison done by Kruskal–Wallis' test. Data shown for fetal growth restricted preterm pigs and controls (F-GR, F-CON) and postnatally growth restricted preterm pigs and controls (P-GR, P-CON). ALAT, alanine aminotransferase; AST, aspartate aminotransferase; BUN, blood urea nitrogen; GGT, gamma glutaminyl transferase; SEM, standard error of the mean.*

parameters differed between F-GR/P-GR and control littermate pigs, suggesting that moderate growth restriction before or after preterm birth is not associated with major developmental defects in the systemic immune system. In addition, postnatal growth restriction was in fact associated with an increase in several immune cell types, possibly indicating accelerated immune cell maturation. However, it remains elusive whether those changes related to growth restriction may lead to altered immune competence against infectious challenges. Further studies with *in vivo* infection challenges are required to allow conclusion about mechanisms possibly causing increased risk of infection in growth restricted infants as previously documented (1, 8–10). Nevertheless, our data indicate that with appropriate clinical care and nutrition, moderately growth restricted preterm infants may show great capacity for short term systemic immune adaptation, although long term effects are unknown.

Following fetal growth restriction, we found a lower total leucocyte and lymphocyte counts at birth in F-GR pigs, but with no differences in T cell subsets or plasma cytokine levels. By day 8, plasma levels and whole blood gene expressions of IL-10 were elevated in F-GR pigs. By day 19 however, the expression of *IL10* was reduced in the F-GR animals and the *TBET/GATA3* ratio tended to be increased, possibly indicating higher Th1 activity. Overall, the leucocyte gene expressions on day 19 showed lower expressions of most genes. IL-10 has been considered as an anti inflammatory cytokine produced by Th2 and regulatory T cells (31), but is also expressed by many other adaptive and innate immune cells (32). However, IL-10 production in innate cells is driven primarily by microbial activation of macrophages and dendritic cells (32, 33). The lack of clinical, CRP or immune cell responses suggest that the IL-10 changes observed may be derived from regulatory T or Th2 cells. Any systemic immune suppressive state shortly after preterm birth may disappear after 19 days. Such effects may relate to increased adrenocortical activity after fetal growth restriction, as indicated by increased relative adrenal gland weight in F-GR pigs, despite the unaffected basal cortisol levels detected at day 19. Apparently, the catabolic effects of increased adrenocortical activity in F-GR piglets did not induce notable postnatal growth restriction as F-GR pigs were not subject to more frequent postnatal growth restriction than F-CON pigs. Likewise, biochemical indices at day 19 were unaffected by the slow fetal growth rate.

During postnatal growth restriction, bone growth may be prioritized, supported by the lower levels of alkaline phosphatase, possibly indicating reduced osteoblastic activity (34). Likewise, the kidneys appeared to be a prioritized organ in postnatal growth restricted animals, as indicated by elevated relative weight on day 19. More importantly, postnatal growth restriction was associated with changes in immune cell populations. On day 8–10 P-GR animals had higher neutrophil counts, but lower fractions of neutrophils with phagocytic capacity, suggesting increased recruitment of immature neutrophils (35, 36). Neutrophils mature in the bone marrow over a period of 30 days and are under normal homoeostatic circumstances kept in the bone marrow as a reserve and slowly released to the circulation, a process regulated by granulocyte colony stimulation factor (37). During immunological reactions, these mature neutrophils

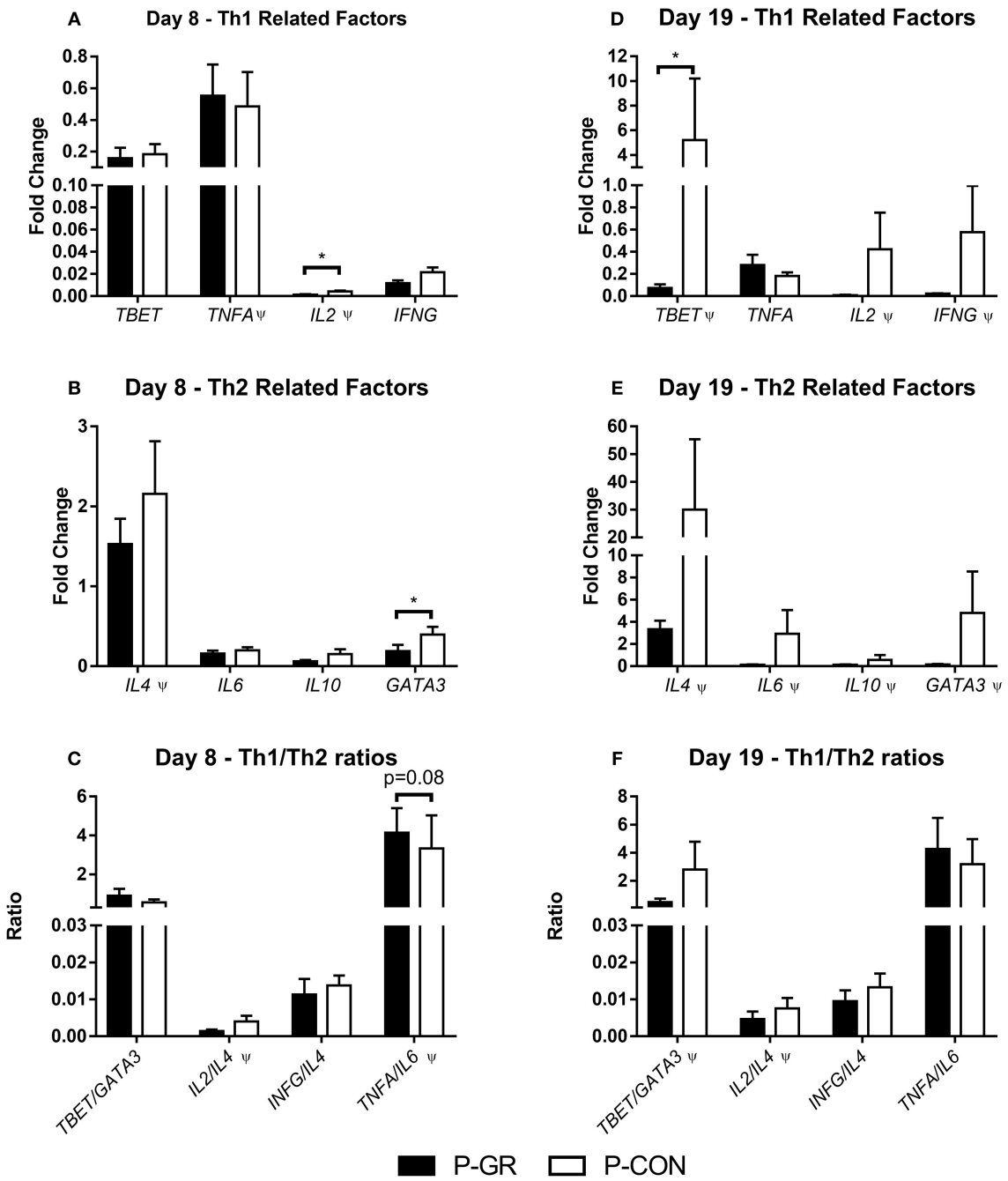

FIGURE 6 | Leucocyte gene expression in postnatally growth restricted preterm pigs and controls, on day 8 (**A–C**, P-GR, $n = 8$–9; P-CON, $n = 24$–29) and 19 (**D–F**, P-GR, $n = 7$–9; P-CON, $n = 25$–28). **(A,D)** type 1 helper T cell related genes, **(B,E)** type 2 helper T cell-related genes, **(C,F)** ratios of type 1 and type 2 helper T cell related genes. Results presented as mean fold changes in relation to housekeeping gene with corresponding standard error of the mean **(A,B,D,E)**, or as ratios between fold changes **(C,F)**. *$p < 0.05$, Ψ, analyzed by Kruskal–Wallis' test.

can be recruited to the circulation under the influence of other chemotactic agents (38). A higher level of immature neutrophils in P-GR pigs could indicate a smaller reservoir of mature neutrophils or an accelerated granulopoiesis. Apart from neutrophils, monocytes, basophils, eosinophil counts as well as helper T cell fractions were all elevated in P-GR pigs at day 19. However, plasma cytokine levels and leucocyte gene expression were not affected, or even tended to be down regulated at day 19 in P-GR vs. P-CON pigs. In the absence of clinical symptoms of infections, as well as few changes in organ weights and biochemical parameters, the slow growing preterm pigs managed to support and even increase proliferation of innate

immune cells. Leucocyte gene expressions on day 8 showed reduced expression of *IL2*, a key Th1 cytokine, and *GATA3* a Th2 transcription factor. Thus, it seems that both Th1- and Th2-related factors were down regulated, while Th1/Th2 ratios were largely unaffected, apart from a tendency to an increased *TNFA/IL6* ratio. At day 19, a similar pattern of gene expressions was observed between P-GR and P-CON pigs. Similar to the trends in F-GR animals, most of the measured genes showed low mean expressions in the P-GR group. The similarity in leucocyte gene expression may be partly explained by the overlap of pigs included into both the P-CON and F-CON groups. On the other hand, the higher proportion of neutrophils observed in the P-GR group could also play a role in decreased the expression of the investigated lymphocyte related genes.

In conclusion, we observed limited effects of moderate fetal and postnatal growth restriction on organ growth, blood biochemistry and immune cell development during the first 3 weeks after birth in preterm pigs. We excluded preterm pigs with extreme growth restriction (<350 g, lowest 5%) due to mortality shortly after birth, hence our results may be translationally most relevant for preterm infants without serious complications and GR in the immediate neonatal period. Our experimental conditions may have influenced GR effects on some immune parameters, such as the use of antibiotics, which are known to influence immune system development (27). Further, the higher mortality of F-GR piglets during the first weeks may have differentially affected various immune parameters as recorded on day 19. Likewise, other than neutrophil phagocytic capacity, we did not perform *ex vivo* challenges to immune cells, so the impact of growth restriction on some immune cell functions (e.g., cytokine response) is unknown. Finally, given the overlap in groups and the wide variability in the leucocyte gene expressions, these data should be interpreted with caution. Nevertheless, the factors leading to moderate growth restriction (genetic or environmental influences before or after birth) did not prevent surviving preterm pigs from following a near normal immune developmental trajectory, compared to control animals in the early postnatal period. While extreme growth restriction (<10% growth percentile) and prematurity (<28 weeks gestation) may compromise immunity at many levels, our results indicate that neonates subjected to moderate growth restriction and immaturity have a remarkable capacity to adapt their systemic immune system during the first weeks after birth. The long term effects on cell population, immune function and susceptibility to infections remain to be elucidated in future studies.

DATA AVAILABILITY STATEMENT

The datasets generated for this study are available on request to the first and corresponding author.

ETHICS STATEMENT

The animal study was reviewed and approved by Danish National Committee of Animal Experimentation.

AUTHOR CONTRIBUTIONS

OB, DN, and PS planned the research. TT supervised the experiments. OB and DN did data analysis and interpretation of results. OB wrote the manuscript. PS and DN had primary responsibility for the final content. All authors read and approved the final paper.

FUNDING

The work was supported by NEOCOL grant from Innovation Foundation Denmark.

ACKNOWLEDGMENTS

We would like to thank Agnethe M. Ahnfeldt, Charlotte H. Nielsen, Karina Obelitz-Ryom, Jane Povlsen, Kristina Møller, and Elin Skytte for technical support on animal procedures and laboratory analyses.

SUPPLEMENTARY MATERIAL

The Supplementary Material for this article can be found online at: https://www.frontiersin.org/articles/10.3389/fimmu.2019.02402/full#supplementary-material

REFERENCES

1. Stoll BJ, Hansen N, Fanaroff AA, Wright LL, Carlo WA, Ehrenkranz RA, et al. Late-onset sepsis in very low birth weight neonates: the experience of the NICHD Neonatal Research Network. *Pediatrics.* (2002) 110:285–91. doi: 10.1542/peds.110.2.285
2. Strunk T, Currie A, Richmond P, Simmer K, Burgner D. Innate immunity in human newborn infants: prematurity means more than immaturity. *J Matern Neonatal Med.* (2011) 24:25–31. doi: 10.3109/14767058.2010.482605
3. Tröger B, Müller T, Faust K, Bendiks M, Bohlmann MK, Thonnissen S, et al. Intrauterine growth restriction and the innate immune system in preterm infants of ≤32 weeks gestation. *Neonatology.* (2013) 103:199–204. doi: 10.1159/000343260
4. Gilbert WM, Danielsen B. Pregnancy outcomes associated with intrauterine growth restriction. *Am J Obstet Gynecol.* (2003) 188:1596–601. doi: 10.1067/mob.2003.384
5. Wirbelauer J, Thomas W, Rieger L, Speer CP. Intrauterine growth retardation in preterm infants ≤32 weeks of gestation is associated with low white blood cell counts. *Am J Perinatol.* (2010) 27:819–24. doi: 10.1055/s-0030-1254547
6. Ferguson AC. Prolonged impairment of cellular immunity in children with intrauterine growth retardation. *J Pediatr.* (1978) 93:52–6. doi: 10.1016/S0022-3476(78)80599-X
7. Harbeson D, Francis F, Bao W, Amenyogbe NA, Kollmann TR. Energy demands of early life drive a disease tolerant phenotype and dictate outcome in neonatal bacterial sepsis. *Front Immunol.* (2018) 9:1918. doi: 10.3389/fimmu.2018.01918
8. Tröger B, Göpel W, Faust K, Müller T, Jorch G, Felderhoff-Müser U, et al. Risk for late-onset blood-culture proven sepsis in very-low-birth weight infants born small for gestational age: a large multicenter study from the German Neonatal Network. *Pediatr Infect Dis J.* (2014) 33:238–43. doi: 10.1097/INF.0000000000000031

9. Simchen MJ, Beiner ME, Strauss-Liviathan N, Dulitzky M, Kuint J, Mashiach S, et al. Neonatal outcome in growth-restricted versus appropriately grown preterm infants. *Am J Perinatol.* (2000) 17:187–92. doi: 10.1055/s-2000-9423
10. Weisz B, Hogen L, Yinon Y, Gindes L, Shrim A, Simchen M, et al. Perinatal outcome of monochorionic twins with selective IUGR compared with uncomplicated monochorionic twins. *Twin Res Hum Genet.* (2011) 14:457–62. doi: 10.1375/twin.14.5.457
11. Cromi A, Ghezzi F, Raffaelli R, Bergamini V, Siesto G, Bolis P. Ultrasonographic measurement of thymus size in IUGR fetuses: a marker of the fetal immunoendocrine response to malnutrition. *Ultrasound Obstet Gynecol.* (2009) 33:421–6. doi: 10.1002/uog.6320
12. Ekin A, Gezer C, Taner CE, Solmaz U, Gezer NS, Ozeren M. Prognostic value of fetal thymus size in intrauterine growth restriction. *J Ultrasound Med.* (2016) 35:511–7. doi: 10.7863/ultra.15.05039
13. McDade TW, Beck MA, Kuzawa CW, Adair LS. Prenatal undernutrition and postnatal growth are associated with adolescent thymic function. *J Nutr.* (2001) 131:1225–31. doi: 10.1093/jn/131.4.1225
14. Ballow M, Cates KL, Rowe JC, Goetz C, Desbonnet C. Development of the immune system in very low birth weight (less than 1500 g) premature infants: concentrations of plasma immunoglobulins and patterns of infections. *Pediatr Res.* (1986) 20:899–904. doi: 10.1203/00006450-198609000-00019
15. Embleton NE, Pang N, Cooke RJ. Postnatal malnutrition and growth retardation: an inevitable consequence of current recommendations in preterm infants? *Pediatrics.* (2001) 107:270–3. doi: 10.1542/peds.107.2.270
16. Vlaardingerbroek H, van Goudoever JB, van den Akker CHP. Initial nutritional management of the preterm infant. *Early Hum Dev.* (2009) 85:691–5. doi: 10.1016/j.earlhumdev.2009.08.052
17. Hsiao C-C, Tsai M-L, Chen C-C, Lin H-C. Early optimal nutrition improves neurodevelopmental outcomes for very preterm infants. *Nutr Rev.* (2014) 72:532–40. doi: 10.1111/nure.12110
18. Ortiz-Espejo M, Pérez-Navero JL, Olza-Meneses J, Muñoz-Villanueva MC, Aguilera-García CM, Gil-Campos M. Prepubertal children with a history of extra-uterine growth restriction exhibit low-grade inflammation. *Br J Nutr.* (2014) 112:338–46. doi: 10.1017/S0007114514000920
19. Rytter MJH, Kolte L, Briend A, Friis H, Christensen VB. The immune system in children with malnutrition—a systematic review. *PLoS ONE.* (2014) 9:e105017. doi: 10.1371/journal.pone.0105017
20. Clark RH, Thomas P, Peabody J. Extrauterine growth restriction remains a serious problem in prematurely born neonates. *Pediatrics.* (2003) 111:986–90. doi: 10.1542/peds.111.5.986
21. Ehrenkranz RA, Younes N, Lemons JA, Fanaroff AA, Donovan EF, Wright LL, et al. Longitudinal growth of hospitalized very low birth weight infants. *Pediatrics.* (1999) 104:280–9. doi: 10.1542/peds.104.2.280
22. Han F, Hu L, Xuan Y, Ding X, Luo Y, Bai S, et al. Effects of high nutrient intake on the growth performance, intestinal morphology and immune function of neonatal intra-uterine growth-retarded pigs. *Br J Nutr.* (2013) 110:1819–27. doi: 10.1017/S0007114513001232
23. Hu L, Liu Y, Yan C, Peng X, Xu Q, Xuan Y, et al. Postnatal nutritional restriction affects growth and immune function of piglets with intra-uterine growth restriction. *Br J Nutr.* (2015) 114:53–62. doi: 10.1017/S0007114515001579
24. Che L, Thymann T, Bering SB, Le Huërou-Luron I, D'Inca R, Zhang K, et al. IUGR does not predispose to necrotizing enterocolitis or compromise postnatal intestinal adaptation in preterm pigs. *Pediatr Res.* (2010) 67:54–9. doi: 10.1203/PDR.0b013e3181c1b15e
25. D'Inca R, Gras-Le Guen C, Che L, Sangild PT, Le Huërou-Luron I. Intrauterine growth restriction delays feeding-induced gut adaptation in term newborn pigs. *Neonatology.* (2011) 99:208–16. doi: 10.1159/000314919
26. Nguyen DN, Jiang P, Frøkiær H, Heegaard PMH, Thymann T, Sangild PT. Delayed development of systemic immunity in preterm pigs as a model for preterm infants. *Sci Rep.* (2016) 6:36816. doi: 10.1038/srep36816
27. Mærkedahl RB, Frøkiær H, Lauritzen L, Metzdorff SB. Evaluation of a low-cost procedure for sampling, long-term storage, and extraction of RNA from blood for qPCR analyses. *Clin Chem Lab Med.* (2015) 53:1181–8. doi: 10.1515/cclm-2014-1054
28. Levy O. Innate immunity of the newborn: basic mechanisms and clinical correlates. *Nat Rev Immunol.* (2007) 7:379–90. doi: 10.1038/nri2075
29. Angelone DF, Wessels MR, Coughlin M, Suter EE, Valentini P, Kalish LA, et al. Innate immunity of the human newborn is polarized toward a high ratio of IL-6/TNF-alpha production *in vitro* and *in vivo*. *Pediatr Res.* (2006) 60:205–9. doi: 10.1203/01.pdr.0000228319.10481.ea
30. Radmacher PG, Looney SW, Rafail ST, Adamkin DH. Prediction of extrauterine growth retardation (EUGR) in VVLBW infants. *J Perinatol.* (2003) 23:392–5. doi: 10.1038/sj.jp.7210947
31. Grazia Roncarolo M, Gregori S, Battaglia M, Bacchetta R, Fleischhauer K, Levings MK. Interleukin-10-secreting type 1 regulatory T cells in rodents and humans. *Immunol Rev.* (2006) 212:28–50. doi: 10.1111/j.0105-2896.2006.00420.x
32. Siewe L, Bollati–Fogolin M, Wickenhauser C, Krieg T, Müller W, Roers A. Interleukin-10 derived from macrophages and/or neutrophils regulates the inflammatory response to LPS but not the response to CpG DNA. *Eur J Immunol.* (2006) 36:3248–55. doi: 10.1002/eji.200636012
33. Akbari O, DeKruyff RH, Umetsu DT. Pulmonary dendritic cells producing IL-10 mediate tolerance induced by respiratory exposure to antigen. *Nat Immunol.* (2001) 2:725–31. doi: 10.1038/90667
34. Leung KS, Fung KP, Sher AH, Li CK, Lee KM. Plasma bone-specific alkaline phosphatase as an indicator of osteoblastic activity. *J Bone Joint Surg Br.* (1993) 75:288–92. doi: 10.1302/0301-620X.75B2.8444951
35. Drifte G, Dunn-Siegrist I, Tissières P, Pugin J. Innate immune functions of immature neutrophils in patients with sepsis and severe systemic inflammatory response syndrome*. *Crit Care Med.* (2013) 41:820–32. doi: 10.1097/CCM.0b013e318274647d
36. Taneja R, Sharma AP, Hallett MB, Findlay GP, Morris MR. Immature circulating neutrophils in sepsis have impaired phagocytosis and calcium signaling. *Shock.* (2008) 30:618–22. doi: 10.1097/SHK.0b013e318173ef9c
37. Lieschke G, Grail D, Hodgson G, Metcalf D, Stanley E, Cheers C, et al. Mice lacking granulocyte colony-stimulating factor have chronic neutropenia, granulocyte and macrophage progenitor cell deficiency, and impaired neutrophil mobilization. *Blood.* (1994) 84:1737–46.
38. Furze RC, Rankin SM. Neutrophil mobilization and clearance in the bone marrow. *Immunology.* (2008) 125:281–8. doi: 10.1111/j.1365-2567.2008.02950.x

Conflict of Interest: The authors declare that the research was conducted in the absence of any commercial or financial relationships that could be construed as a potential conflict of interest.

frontiers in Immunology

ORIGINAL RESEARCH
published: 15 November 2019
doi: 10.3389/fimmu.2019.02651

Rapid Proteome Changes in Plasma and Cerebrospinal Fluid Following Bacterial Infection in Preterm Newborn Pigs

*Tik Muk[1], Allan Stensballe[2], Stanislava Pankratova[1,3,4], Duc Ninh Nguyen[1], Anders Brunse[1], Per Torp Sangild[1,4,5] and Ping-Ping Jiang[1,6]**

[1] Section for Comparative Paediatrics and Nutrition, Department of Veterinary and Animal Sciences, University of Copenhagen, Copenhagen, Denmark, [2] Department of Health Science and Technology, Aalborg University, Aalborg, Denmark, [3] Department of Neuroscience, University of Copenhagen, Copenhagen, Denmark, [4] Department of Neonatology, Rigshospitalet, Copenhagen University Hospital, Copenhagen, Denmark, [5] Department of Paediatrics, Odense University Hospital, Odense, Denmark, [6] School of Public Health, Sun Yat-sen University, Guangzhou, China

Background: Neonatal infection and sepsis are common for preterm infants due to their immature immune system. Early diagnosis is important for effective treatment, but few early markers of systemic and neuro-inflammatory responses in neonates are known. We hypothesised that systemic infection with *Staphylococcus epidermidis* (SE), a Gram-positive bacteria, induces acute changes to proteins in the plasma and cerebrospinal fluid (CSF), potentially affecting the immature brain of preterm neonates.

Methods: Using preterm pigs as a model for preterm infants, plasma and CSF samples were collected up to 24 h after SE infection and investigated by untargeted mass spectrometry (MS)-based proteomics. Multiple differentially expressed proteins were further studied *in vitro*.

Results: The clinical signs of sepsis and neuroinflammation in SE-infected piglets were associated with changes of multiple CSF and plasma proteins. Eight plasma proteins, including APOA4, haptoglobin, MBL1, vWF, LBP, and sCD14, were affected 6 h after infection. Acute phase reactants, including complement components, showed a time-dependent activation pattern after infection. Feeding bovine colostrum reduced the sepsis-related changes in clinical indices and plasma proteins. Neuroinflammation-related neuropeptide Y (NPY), IL-18, and MMP-14 showed distinct changes in the CSF and several brain regions (the prefrontal cortex, PVWM, and hippocampus) 24 h after infection. These changes were verified in TLR2 agonist-challenged primary microglia cells, where exogenous NPY suppressed the inflammatory response.

Conclusion: Systemic infection with SE induces inflammation with rapid proteome changes in the plasma and CSF in preterm newborn pigs. The observed early markers of sepsis and neuroinflammation in preterm pigs may serve as novel biomarkers for sepsis in preterm infants.

Keywords: Gram-positive infection, proteomics, CSF, plasma, neuroinflammation, sepsis, enteral feeding

OPEN ACCESS

Edited by:
Fabrizio Ceciliani, University of Milan, Italy

Reviewed by:
Anna Bassols, Autonomous University of Barcelona, Spain
Mark McLaughlin, University of Glasgow, United Kingdom

***Correspondence:**
Ping-Ping Jiang
jiangpp3@mail.sysu.edu.cn

Specialty section:
This article was submitted to Comparative Immunology, a section of the journal Frontiers in Immunology

Received: *07 July 2019*
Accepted: *25 October 2019*
Published: *15 November 2019*

Citation:
Muk T, Stensballe A, Pankratova S, Nguyen DN, Brunse A, Sangild PT and Jiang P-P (2019) Rapid Proteome Changes in Plasma and Cerebrospinal Fluid Following Bacterial Infection in Preterm Newborn Pigs. Front. Immunol. 10:2651. doi: 10.3389/fimmu.2019.02651

INTRODUCTION

Preterm infants are at a high risk of bacterial infection in the neonatal period and systemic infections, leading to sepsis, are important for the overall mortality and morbidity of these infants (1, 2). The risk of infection increases with decreasing birth weight and gestational age (GA) (3) and 25–60% of extremely preterm infants (GA <28 weeks) experience at least one infection period in the neonatal period (1). Infections also sensitise preterm infants to non-inflammatory insults, such as hypoxia-ischaemia, and may damage many organs, including the immature brain (1). Infants surviving neonatal sepsis may therefore show increased morbidity related to the respiratory, gastrointestinal, and nervous systems (1, 4–6). Increased susceptibility to infection in preterm infants in the neonatal period can be partly explained by delayed development of the immune system, which may persist into childhood and even adulthood (1, 7). The use of invasive procedures and parenteral nutrition during hospitalisation further predispose preterm infants to systemic infection and inflammation (8).

In neonatal intensive care units, Gram-positive bacteria, such as coagulase-negative staphylococci (CoNS), are often observed as causative pathogens in neonatal infection (3). In surveillance data from the UK, Gram-positive bacteria were causative in 70% of late-onset sepsis (LOS) cases, with 42% due to CoNS (8). *Staphylococcus epidermidis* (SE), a skin commensal bacteria, has been reported to be responsible for up to 50% of LOS cases (9). Unlike Gram-negative bacteria, which triggers the immune response of the host via a lipopolysaccharide (LPS) to activate Toll-like receptor 4 (TLR4), SE triggers the host response mainly via TLR2 (10). In our previous study, bloodstream infection with live *S. epidermidis* caused multiple signs of sepsis in preterm neonatal pigs, such as lethargy, hypotension, respiratory acidosis, internal organ haemorrhage, and neuroinflammation (11). Even without the entry of bacteria into the central nervous system (CNS), Gram-positive infections can cause cerebral inflammation via the activation of TLR2 and are associated with white matter injury and impaired neurodevelopment (10). The systemic administration of a synthetic TLR2 agonist, Pam3CSK4, adversely affects brain development in newborn mice (12), suggesting TLR2 activation has a key role in brain injury associated with Gram-positive infection in neonates.

Prompt diagnosis of infection in preterm infants is difficult as the clinical manifestation is often variable, subtle, and further complicated by non-infectious conditions (13), resulting in delayed or suboptimal treatment. Moreover, antibiotic treatment for treating sepsis alone does not decrease the risk of sepsis-associated cerebral injury (1). Early enteral feeding has been recommended to prevent infections, and antimicrobial proteins and peptides (APPs, e.g., lactoferrin) have been suggested as adjunctive therapies (8). Our previous report showed that early oral feeding of bovine colostrum, rich in bioactive components, can dampen the systemic inflammation caused by Gram-positive infections in preterm pigs (11). In this study, we hypothesised that a Gram-positive infection rapidly alters the inflammatory proteome in the plasma and cerebrospinal fluid (CSF), and enteral feeding mitigates these changes. Sequential plasma collections (6, 12, and 24 h after infection) were used to search for early systemic proteome responses that may provide new targets for more timely sepsis diagnosis and treatment. CSF proteins were profiled to reveal changes pertaining to neuroinflammation in the surrounding CNS. The potential inflammatory effect of selected brain proteins, including NPY, a neuroimmune messenger (14–16) and memory and learning regulator (16, 17), and IL-18, a pro-inflammatory cytokine related to inflammation and blood–CSF barrier integrity (18–20), were further investigated using *in vitro* cell culture systems.

METHODS

Animal Procedure

The delivery, rearing, inoculation, and euthanasia of the premature piglets were carried out as previously described (11) and are schematically presented in **Figure 1A**. Briefly, preterm piglets ($n = 40$) delivered from two sows (Danish Landrace × Large White × Duroc) via caesarean section at 91% gestation age (107 ± 1 d) were individually incubated with heating (37–38°C) and an oxygen supply. Each piglet was fitted with one vascular catheter (4F, Portex, Kent, UK) into the dorsal aorta via the umbilical cord and an orogastric tube (6F, Portex). Pareteral nutrition and eternal nutrition for each piglet, if applicable, started immediately after the catheterisation. A group of piglets was intra-arterially inoculated with live *Staphylococcus epidermidis* (SE) re-suspended in sterile saline (1.0×10^9 CFU/kg bw; bw, body weight) over 3 min. Fourteen inoculated piglets received enteral feeding of bovine colostrum (10 mL/kg bw/3 h, Biofiber-Damino, Gesten, Denmark) via the orogastric tube and parenteral nutrition (3 mL/kg bw/h) via the umbilical catheter (SE+ENT, $n = 14$). The remaining inoculated pigs received parental nutrition (6 mL/kg bw/h, SE, $n = 15$) only. Piglets that were not inoculated and only received parenteral nutrition (6 mL/kg bw/h) served as controls (Control, $n = 11$). The parenteral nutrition was formulated, as previously described, based on Kabiven (Fresenius-Kabi, Bad Homburg, Germany) and modified to meet the requirement of preterm pigs with

Abbreviations: APOA4, apolipoprotein A-IV; APPs, antimicrobial proteins and peptides; aSOFA, SOFA score adapted to preterm piglets; BCB, blood-CSF barrier; C1QA, complement C1q A chain; C1R, complement C1r; C5, complement C5; CFU, colony-forming units; CNS, central nervous system; CoNS, coagulase-negative staphylococci; CRP, C-reactive protein; CSF, cerebrospinal fluid; ECM, extracellular matrix; FDR, false discovery rate; GA, gestational age; HP, haptoglobin; HPX, hemopexin; IgG, immunoglobulin G; IHC, immunohistochemistry; IL-18 BP, IL-18 binding protein; IL-18, interleukin 18; LBP, LPS-binding protein; LOS, late-onset sepsis; LPS, lipopolysaccharide; LTA-SA, lipoteichoic acid from *S. aureus*; MBL1, mannose-binding lectin (protein A) 1; MMP-14, matrix metalloproteinases 14; MS, mass spectrometry; MT-MMPs, membrane-type matrix metalloproteinases; NPY 1R, neuropeptide Y receptor type 1; NPY, neuropeptide Y; Pref cortex, prefrontal cortex; PVWM, paraventricular white matter; SAA, serum amyloid A; sCD14, soluble CD14; SE, *Staphylococcus epidermidis*; SEM, standard error of the mean; SOFA, sequential organ failure assessment; TLR, toll-like receptor; TLR2, toll-like receptor 2; TLR4, toll-like receptor 4; TNF-α, tumour necrosis factor-α; VCAM1, vascular cell adhesion protein 1; vWF, von Willebrand factor.

A

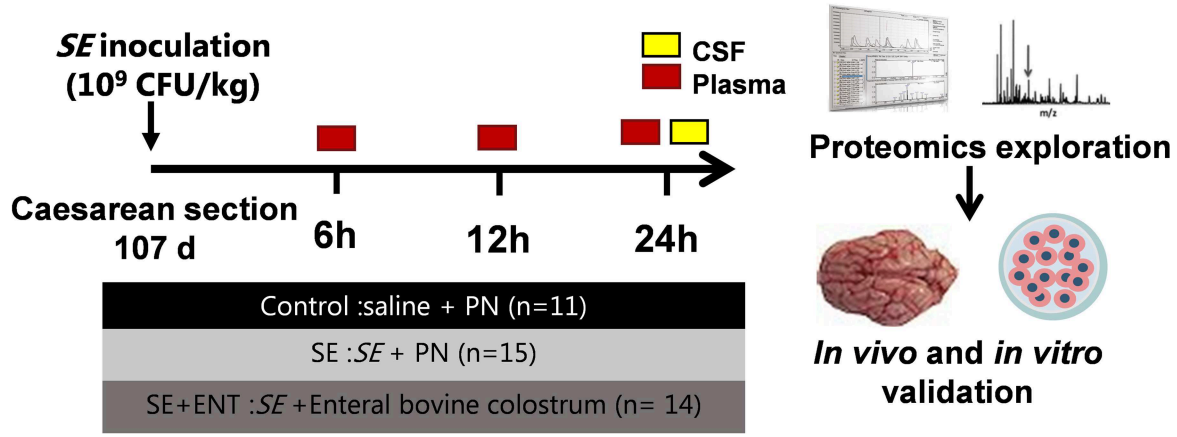

B

	SE vs. Control	SE+ENT vs. Control	SE+ENT vs. SE
CSF	**83**	**27**	**0**
24 h plasma	**80**	**16**	**65**
12 h plasma	**38**	**3**	**19**
6 h plasma	**8**	**0**	**5**

C

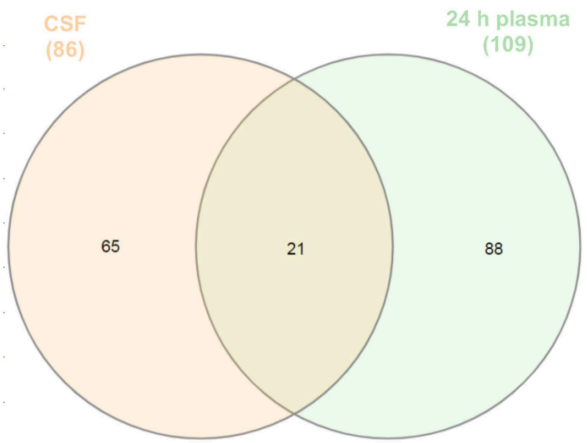

D

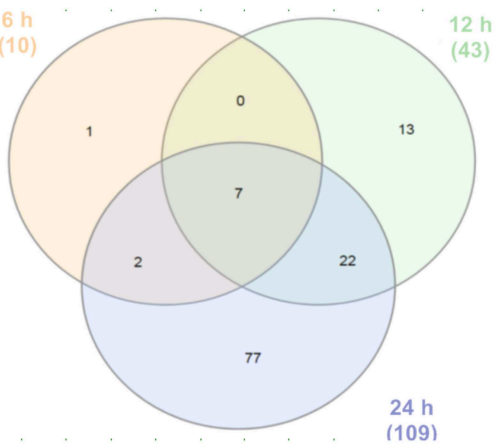

FIGURE 1 | Overview of the animal procedure and the proteomic analysis. **(A)** Animal procedure; **(B)** numbers of samples adopted in the proteomic analysis; **(C)** numbers of proteins with differential abundance in both the CSF and plasma (24 h); **(D)** numbers of plasma proteins with differential abundance at 6, 12, and 24 h post-infection. Numbers in **(C,D)** are numbers of proteins showing difference in any comparison between the treatment groups and are different from those in **(B)** and **Table S2** specifying difference between treatment groups.

added vitamins and minerals (Soluvit, Vitalipid, and Peditrace, Fresenius-Kabi) (11).

At 6, 12, and 24 h post-inoculation, blood was obtained from the umbilical arterial catheter from each piglet for bacteriological, haematological, and blood gas analyses, and EDTA-treated plasma was separated and saved at −80°C for proteomic analysis. Sodium fluorescein (2%, 5 mL/kg bw, Sigma-Aldrich, Brøndby, Denmark) was administered via the umbilical catheter 30 min

before the scheduled euthanasia for assessment of blood–CSF barrier permeability. Under anaesthesia, piglets were euthanised with a lethal intracardial injection of sodium barbital (Apotek, Glostrup, Denmark). CSF was directly collected by sub-occipital puncture from each piglet and save at −80°C for proteomic analysis. CSF samples with possible blood contamination, examined by oxyhemoglobin absorbance ($\lambda = 414$ nm), were discarded. The number of CSF and plasma samples applied to the proteomic analysis are shown in **Figure 1B**.

The right hemisphere of the brain was fixed in ice-cold 4% paraformaldehyde for immunohistochemistry (IHC), and different brain parts, including the prefrontal cortex, paraventricular white matter (PVWM), and hippocampus, of the left hemisphere were dissected, snap-frozen, and saved at −80°C for later analysis. Animals were treated in compliance with the Animal Experimentation Act of Denmark, which is in accordance with the Council of Europe Convention ETS 123. The study was approved by the Danish National Committee on Animal Experimentation (2014-15-0201-00418).

Mass Spectrometry (MS)-Based Proteomics

The preparation of protein samples was performed using a filter-aided protocol, as previously described (21). Protein concentration was determined by the absorbance at 280 nm on a NanoDrop Spectrophotometer (Thermo Scientific, Waltham, MA, USA) with bovine serum albumin (BSA) as a standard. CSF or a plasma sample containing 100 μg protein was transferred onto an Amicon Ultra centrifugal filter (10 kDa, 0.5 mL, Millipore, Søborg, Denmark) and mixed with a buffer containing sodium deoxycholate (5%) and triethylammonium bicarbonate (50 mmol/L, pH 8.0). The protein was reduced by TCEP solution [0.5 mol/L, 1:50 (v/v)], alkylated by chloroacetamide [0.5 mol/L, 1:50 (v/v)], and digested by trypsin (Promega, 1 μg/100 μg protein, 37 °C overnight) inside the spin filter with a centrifuge step (14,000 × g for 15 min) in between. Tryptic peptides were recovered by another step of centrifugation and purified by phase extraction using ethyl acetate acidified by trifluoroacetic acid (1%, v/v). Vacuum-dried peptides were suspended in a solution of 2% acetonitrile, 0.1% Formic acid, and 0.1% trifluoroacetic acid and applied onto a Dionex RSLC UPLC System (Thermo Scientific) coupled to a Q-Exactive HF Hybrid Quadrupole-Orbitrap Mass Spectrometer (Thermo Scientific) for analysis. A total of 5 μg of peptide was injected onto a 2 cm reverse-phase C18 material trapping column and separated on a 50 cm analytical column (Acclaim PepMap100, 75 μm ID, 100 Å, Thermo Scientific) with both columns kept at 40°C. The elution gradient was set at a constant flow rate of 300 nL/min and started with a mixture of water (96%) and acetonitrile (4%) containing 0.1% formic acid; it was then increased to 30% acetonitrile over 225 min. Mass spectrometric data were obtained in positive ionisation mode in a data-dependent acquisition fashion with survey spectra and isolation/fragmentation spectra alternating using a top 12 method. Selected peptides were excluded from re-analysis for 30 s. All samples were analyzed in duplicates in a random order.

Protein annotation and quantification based on mass spectra of peptides were carried out using a MaxQuant (version 1.5.2.8) (22) against the UniProt reference database with isoforms (*Sus scrofa,* UP000008227, last modified 2016-08-02) (23). Raw data was searched using an internal re-calibration at 4.5 ppm using two missed cleavages. Cysteine carbamethylation was set as fixed modification and methionine oxidation as variable modification. Allowable missed cleavages were set as 1. The detection of at least two unique peptides per protein and a protein being present in at least 70% of samples in each group were required criteria for protein annotation and quantification. Common contaminants and reverse decoy matches were removed from the annotated protein list. Using the Perseus software (version 1.2.0.17) (24), protein abundance data were normalised and the two-based logarithm transformed to conform to normal distribution and to reduce variability from data acquisition, which was aligned with protein identities and grouping information, such as the treatment and the litter (sow). Aligned data were exported into R (version 3.4.1) (25) and integrated with R Studio (version 3.1.18) (26) for data analysis. The MS proteomic data are available at the ProteomeXchange Consortium (http://www.proteomexchange.org/) with the data set identifier PXD016013.

Primary Culture of Microglial Cells

The primary culture of microglial cells was prepared as previously described (27) with minor modifications. In brief, hippocampi obtained from preterm piglets from another litter were chopped in ice-cold Krebs-Ringer modified buffer and digested with trypsin for 10 min at 37°C (all from Sigma-Aldrich). Pelleted cells were then washed in the presence of DNase and trypsin inhibitor, re-suspended in Dulbecco's modified Eagle's medium (DMEM) supplemented with 100 μg/mL penicillin, 100 U/mL streptomycin, and 10% heat-inactivated foetal bovine serum (FBS; all from Gibco, Taastrup, Denmark), and kept in cell culture flasks (NUNC, Roskilde, Denmark) to reach confluence. Microglial cells were collected from the supernatant by shaking the culture flask at 250 RPM at 37°C for 4 h. Isolated microglial cells were re-seeded into either 6-well-plates at the density of 25,000 cells/cm^2 for gene expression analysis or 96-well-plates at the density of 250,000 cells/cm^2 for ELISA. After overnight rest and growing in serum-free medium for 8–12 h, microglial cells were treated, in duplicates, with either 2.5 μg/mL LTA-SA (from *S. aureus*, InVivoGen, Toulouse, France) or 20 ng/mL Pam3CSK4 (InVivoGen) alone or in the presence of 0.5 μM exogenous NPY peptide (synthetic human NPY, Schafer-N, Copenhagen, Denmark) for 24 h. The level of tumour necrosis factor-α (TNF-α) in the culture was determined in triplicates using porcine DuoSetELISA kits (R&D Systems, Minneapolis, MN, USA).

To estimate the purity of the culture, microglial cells, isolated as described above, were plated into PLL-coated 8-well-Lab-Tek® Permanox chamber slides (NUNC), allowed to grow for 24 h, fixed with 3.7% (v/v) formaldehyde and 1% (v/v) methanol in PBS, and stained with anti-Iba1 antibody (1:2,000, rabbit, ab5076, Abcam, Cambridge, UK) followed by secondary Alexa Fluor 488-conjugated antibody (1:1,000, goat anti-rabbit, Molecular Probes). Cell nuclei were counterstained by DAPI using mounting media (Molecular Probes). Images

were recorded using an Axiovert 100 microscope (Zeiss, Jena, Germany) equipped with an AxioCam MRm camera (Zeiss) and ZEN 2012 software (Zeiss). The enriched microglia culture was 90% pure, as determined by the ratio of Iba-1-positive cells to total cells (**Figure S1**).

Immunohistochemistry (IHC)

To localise the cerebral neuropeptide Y (NPY) in the brain tissue, brain sagittal sections (5 μm) were probed with primary antibody against NPY (rabbit, 1:3,000, ab30914, Abcam) and a biotin-conjugated secondary antibody (goat-anti-rabbit, 1:500, Vector Labs, Peterborough, UK) after standard deparaffinisation, rehydration, antigen retrieval, and blocking procedure. Staining was visualised with 0.04% 3,3′-diaminobenzidine (DAB, Sigma-Aldrich) using an ABC Peroxidase Staining Kit (Thermo Scientific). For the quantification of NPY expression in brain, whole sections were scanned at a 10 × objective magnification on a Zeiss Axio Scan Z1 (Zeiss). The region of interest was selected in similar anatomical regions across samples, and the number of NPY-positive cells was counted in the defined frames. Representative images were acquired with a BX-51 microscope (Olympus, Ballerup, Denmark) using Integrator System software (Visiopharm).

ELISA

The concentration of IL-18 in CSF and plasma samples was measured with a porcine IL-18 ELISA kit (RayBiotech, Norcross, Georgia, USA). The frozen tissue of two brain regions, the prefrontal cortex and PVWM, was homogenised and lysed for protein extraction. Total protein concentration was determined by a Pierce™ BCA kit (Thermo Scientific, Waltham, Massachusetts, U.S) for total protein adjustment later. The concentration of NPY in two brain regions was measured with a porcine Neuropeptide Y (NPY) ELISA kit (Phoenix Pharmaceuticals, Burlingame, CA, USA), and the final concentration was adjusted to total protein concentration.

Gene Expression by Real-Time qPCR

Transcription of selected genes in the prefrontal cortex, PVWM, and hippocampus was determined by real-time qPCR, using predesigned primers (sequences listed in **Table S5**). Briefly, total RNA in tissue homogenate was isolated with RNeasy Lipid Tissue Mini Kit (Qiagen, Copenhagen, Denmark). RT-qPCR was performed using a QuantiTect SYBR Green PCR Kit (Qiagen) on a LightCycler 480 (Roche, Hvidovre, Denmark). The relative level of target genes was normalised to the housekeeping gene *HPRT1* (28).

Data Analysis and Statistics

Before analysis, the mean protein abundance of three technical replicates of each sample in the proteomic analysis were combined into one as previously described (29). An univariate analysis was applied to proteomics data in each sample type (CSF or plasma) at each sampling time-point in R. Briefly, a linear mixed-effect model was fitted to each protein with treatment as the fixed-effect factor and litter as a random-effect factor using the lme4 package (30). A Tukey *post-hoc* test (package multcomp) on this model was adopted to compare the effect between three treatment groups, i.e., Control, SE, and SE+ENT, in a pairwise fashion (31). To control the type I error, p-values were further adjusted by false discovery rate (FDR, $\alpha = 0.2$) into q values within each comparison of each sample type (plasma or CSF) at each time-point using the multtest package (32). Proteins with a $q \leq 0.10$ in any comparisons were chosen for functional assignment, which is generally accepted for this kind of explorative proteomic analysis. Dunn's Kruskal-Wallis Multiple Comparisons test of various clinical data and Pearson's correlation test were conducted in R. Results from RT-qPCR and ELISA were analyzed using a Student's t-test and a two-tailed $p < 0.05$ was considered as statistically significant. Data were presented as mean ± SEM unless otherwise stated.

RESULTS

Clinical Data

As shown in our previous report, preterm piglets inoculated with live SE developed sepsis and blood–CSF barrier disruption, and enteral feeding ameliorated these damages (11). The clinical variables of the piglets included for proteomic analysis, namely the aSOFA score, leucocyte count in the CSF and blood, platelet count in blood, and CSF–blood fluorescein ratio, are presented in **Table S1**. Similar to our previous report, the SOFA score adapted to preterm piglets (aSOFA), CSF leukocyte count, blood levels of C-reactive protein (CRP), and fibrinogen at 24 h were elevated after SE infection (all $p < 0.05$), indicating sepsis and elevated systemic and intracranial immune response in the SE piglets. Blood–CSF barrier permeability was higher in SE piglets, as shown by the higher CSF-serum fluorescein ratio ($p < 0.05$) relative to the controls. The blood leukocyte number decreased after birth ($p < 0.05$) in Control, while SE infection maintained the leukocyte count over time ($p = 0.91$), although generally lower than in Controls. The blood leukocyte number in SE + ENT piglets tended to decrease over time ($p = 0.08$), similar to Control, but at a lower level. The platelet number increased over time in all three treatment groups, while the value in SE piglets was lower than that in Control and SE+ENT pigs ($p < 0.05$ for all comparisons between treatment groups, except SE vs. Control at 24 h). The values in SE+ENT pigs were similar to those in Control.

CSF and Plasma Proteomics

No significant difference in the protein concentration of CSF samples was observed among the three groups ($P = 0.17$) as tested by a linear model including factors such as treatment, sex, and litter. In CSF and plasma samples, 1,960 and 735 proteins were annotated (as shown in **Data Sheets S1** and **S2**), respectively, and 86 CSF proteins and 114 plasma proteins that met the selection criterion ($q \leq 0.1$ in at least one treatment comparison) were selected for functional assignment (**Figure 1C**). The numbers of differential proteins in any comparison in the CSF and plasma at the different time-points are listed in **Figures 1B–D** and **Table S2**. Among the selected CSF proteins, 83 showed differential expression between SE vs. Control, while 27 showed differential expression for SE+ENT

vs. Control and 1 for SE + ENT vs. SE. In plasma, the number of differential proteins (SE vs. Controls) increased over time, 10, 43, and 109 at 6, 12, and 24 h, respectively (**Figure 1D**). Twenty-one proteins with differential abundance appeared in both the CSF and 24 h plasma, and proteins, such as serpin G1, von Willebrand factor (vWF), LPS-binding protein (LBP), haptoglobin, hemopexin (HPX), MRC1, and VCAM1, changed similarly in the CSF and 24 h plasma (**Figure 2**). Seven plasma proteins, including haptoglobin, vWF, serpin a3-8, serpin a3-6, sCD14, LBP, and apolipoprotein A-IV, maintained their differential abundance pattern across three time-points, although at different significance levels (**Figure 1D**).

According to their major physiological functions, listed in the Uniprot database and publications, differential proteins were categorised into groups including "neurodevelopment (development)," "immune response," "protein processing," "metabolism," and "others." Observed acute phase reactants were categorised as a separate group. The protein groups may show overlap and are not mutually exclusive. Information on proteins with differential abundance, including UniProt ID, gene name, protein name, and abundance in each group, is shown in **Tables S3**, **S4**.

Immune Response Proteins

In the CSF, 38 differential proteins were related to immune response (45% of all regulated proteins, **Table S3**), whereas 48 (44%) immune-related proteins were detected in plasma at 24 h, 24 (56%) at 12 h, and 8 (80%) at 6 h (**Table S4**). All differential immune response proteins, including acute phase reactants, in the CSF were affected by the SE infection (SE vs. Control). None of these proteins, except IL-18 BP, were affected by enteral feeding (SE+ENT vs. SE). Fifteen of 21 proteins present in both the CSF and 24 h plasma were associated with immune response, including A2M, BF, C1R, C5, CPN2, HP, HPX, ITIH1, ITIH4, KNG1, LBP, Serpin A3-8, MRC1, SAA2, and APOB (**Figure 2** and **Tables S3, S4**). Among them, A2M, ITIH1, KNG1, and APOB were elevated in the CSF of SE pigs relative to the Control, but decreased in 24 h plasma. The remaining proteins showed elevated abundance in both types of samples after SE infection (**Figure 2**). At 24 h, 45 of the 62 differentially regulated proteins in plasma by SE were also affected by the enteral feeding (SE+ENT vs. SE, $q < 0.1$), 16 proteins were affected at 12 h, but only 5 proteins at 6 h.

Neuropeptide Y (NPY)

Neuropeptide Y (NPY) was only detected in the CSF samples and not in plasma samples, and it was detected at a lower level in the SE pigs relative to the Control (**Figure 3A**). In the brain tissue, *NPY* transcription is lower in the prefrontal cortex and PVWM in SE piglets relative to the Control, while enteral feeding increased the transcription of *NPY* and one of its key receptors, *NPY 1R*, in the prefrontal cortex (**Figures 3B,C**). Unlike that in the prefrontal cortex, transcription of *NPY* ($p < 0.05$) and *NPY 1R* ($p = 0.08$) in the hippocampus increased after SE infection, but no effect of enteral feeding was observed. The protein level of NPY in two brain regions, the prefrontal cortex and PVWM, was significantly lower in SE piglets, which was consistent with the transcription and proteomic data (**Figure 3D**). Immunohistochemical staining for NPY in selected brains confirmed its presence within the same brain regions (**Figure 3G**).

In a previous study, the immuno-positive brain area against Iba-1, a marker for microglial cells, significantly increased in the SE group compared with the controls, but it was not significantly affected by the colostrum feeding (11). Therefore, to investigate the direct response of microglial cells to acute SE stimulation, a primary porcine cell culture was employed. In this culture, stimulation for 24 h with TLR2 agonists (LTA-SA, Pam3CSK4) decreased *NPY* transcription ($p < 0.01$, **Figure 3E**) but increased the transcription of *NPY 1R* (only by Pam3CSK, $p < 0.05$, **Figure S1B**). Treatment with exogenous *NPY* upregulated the transcription of *NPY* (vs. LTA-SA alone, $p < 0.01$, **Figure 3E**) and *NPY 1R* (vs. Pam3CSK4 alone, $p < 0.05$, **Figure S1B**). Further, exogenous NPY (0.01, 0.10, 0.50, and 1.00 μmol/L) dose-dependently suppressed the production of TNF-α triggered by TLR2 agonists (**Figure 3F**).

IL-18, IL-18 BP, and MMP-14

In the CSF, IL-18 binding protein (IL-18 BP) was only detected in the SE and SE + ENT groups, with the highest level being in SE pigs ($q < 0.05$, **Figure 4A**). Levels of IL-18 in the CSF and plasma (24 h) of SE piglets, determined by ELISA, were elevated when compared with the Control (both $p < 0.05$, **Figures 4B,C**), but enteral feeding decreased IL-18 levels (both $p < 0.05$, **Figures 4B,C**). In the hippocampus and PVWM, *IL-18* transcriptions were higher in the SE than in the Control and SE+ENT pigs (all $p < 0.05$, **Figure 4D**). In the primary microglial culture, *IL-18* expression was upregulated by TLR2 agonists ($p < 0.01$, **Figure 4E**).

The CSF level of MMP-14 was higher in SE piglets than that in Control ($q < 0.05$), while no significant difference was observed between SE+ENT and SE piglets (**Figure 4F**). Similarly, *MMP-14* transcription increased relative to the Control in the brain of SE piglets as well as in TLR2 agonist-challenged primary microglial cells (all $p < 0.05$, **Figures 4G,H**).

Acute Phase Reactants

Multiple acute phase reactants were detected in the CSF and plasma after SE infection, including those related to opsonisation (CRP, SAP, C1q), SAA, coagulation factors (fibrinogens, factor VIII and vWF), α-2-macroglobulin, microbial iron uptake-inhibiting haptoglobin, and complement components and various serpins including α-1-antitrypsin (**Table S4**). These "positive" acute phase reactants increased post-SE infection, while multiple 'negative' acute phase reactants decreased, including albumin, transferrin, transthyretin, and retinol-binding protein 4 (**Table S4**).

Multiple immune response proteins, including Serpin A3-6, Serpin A3-8, MBL1, vWF, haptoglobin, LBP, and sCD14, increased in abundance as early as 6 h post-SE infection. Most proteins, including LBP, vWF, Serpin A3-6, and Serpin A3-8, maintained this change until 24 h (all $p < 0.05$, **Figure 5**). In 24 h plasma, C1QA, C1R, C2, C5, C6, C8B, and C4BPA increased in SE piglets relative to the Controls. Increases in

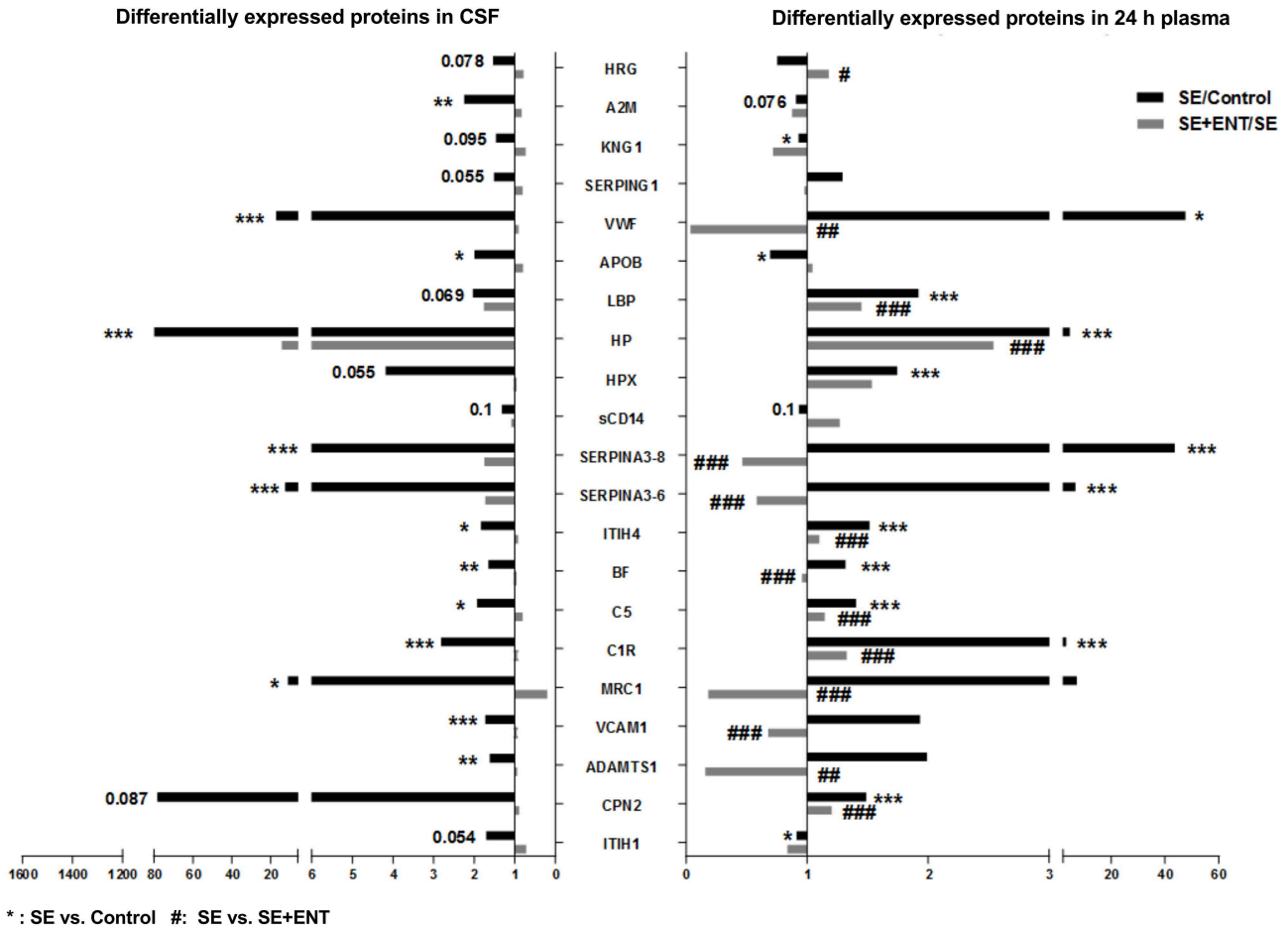

FIGURE 2 | Twenty-one differentially expressed proteins present in the CSF and plasma 24 h post-infection. A majority of these proteins, 15 of 21, present in both the CSF and 24 h plasma were associated with immune response, most of which changed in the same direction. Fold changes of SE/Control and SE+ENT/SE of specific proteins are displayed in bars. *SE vs. Control; #SE vs. SE+ENT; * or #, q, or $p < 0.05$; ** or ##, q, or $p < 0.01$; *** or ###, q, or $p < 0.01$.

C1R, C1QA, and C5 levels were observed in 12 h plasma as well (all $p < 0.05$, **Figure 6**). However, no C3 and C4 were observed with differential abundance in plasma within 24 h. ApoA4 increased significantly in the SE+ENT group from 6 h to 24 h when compared with the Control and SE groups (all $p < 0.001$, **Figure 5**).

DISCUSSION

In this study of systemic infection with SE-induced sepsis and neuroinflammation, preterm pigs were used as a model for preterm infants. Within 24 h of SE infection, a large number of proteins related to the immune response were affected in the CSF and plasma, and a number of proteins (genes) had their expression affected in various brain regions. Enteral feeding with bovine colostrum modified the proteome response in plasma within 24 h, while less CSF proteins were affected within this time frame. Collectively, these results suggest that plasma and CSF proteins may be a rich source of early biomarkers for sepsis and neuroinflammation in preterm neonates. Furthermore, they show that early enteral feeding may be important in dampening the systemic and brain inflammatory response to infection.

Besides activating leukocytes, the systemic immune system may enlist proteins supporting immune response to enter the CNS. In the current study, 15 immune response-related proteins changed in abundance in both the CSF and plasma following SE infection, and most of them changed in the same direction. The majority of these proteins were related to immune defence, for example, KNG1 was involved in blood coagulation and platelet degranulation. Other proteins were involved in acute phase response, such as A2M, properdin, C1R, C5, CPN2, haptoglobin (inhibition of microbial iron uptake), serpins (inter-α-trypsin inhibitors), and SAA (immune cell recruitment). LBP and sCD14 (presepsin), involved in TLR4 activation, were also stimulated by SE infection (**Table S4**), confirming results from newborn infants (33); a Gram-negative infection, however, may induce even a higher level of sCD14 than a Gram-positive infection (34). The SE-elevated proteins found in the CSF may partly originate from the systemic circulation and travelled through a more permeable blood–CSF barrier in these preterm pigs. Of many proteins,

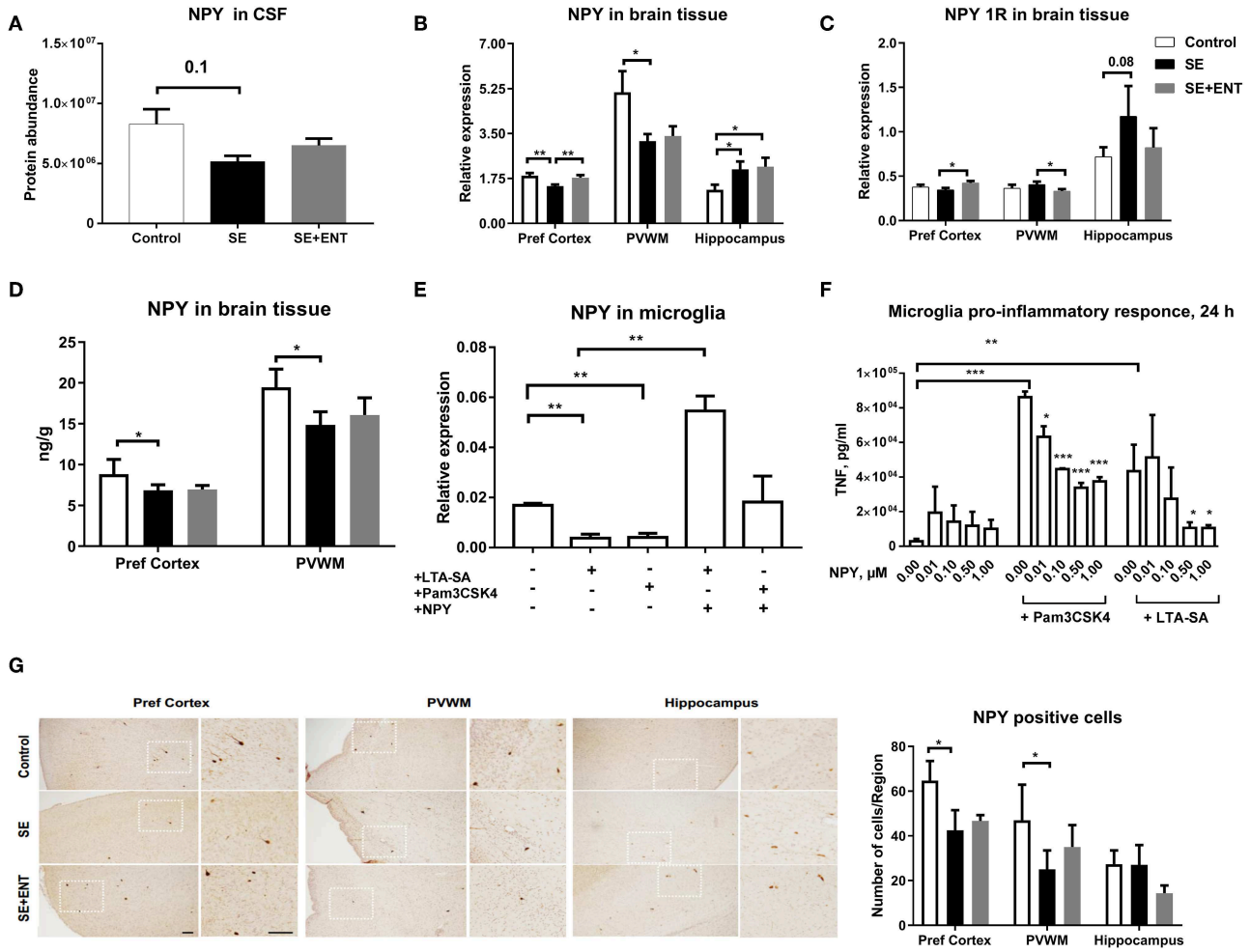

FIGURE 3 | Proteomics, brain transcription, and *in vitro* analyses of NPY. **(A)** Protein level of NPY in CSF decreased post-infection; **(B)** transcription of NPY decreased by SE infection in two brain regions, the prefrontal cortex and PVWM, but increased in the hippocampus; **(C)** transcription of NPY 1R increased by colostrum feeding in prefrontal cortex and PVWM; **(D)** protein level of NPY in significantly down-regulated by SE infection; **(E)** transcription of NPY in cultured primary microglia cells challenged by TLR2 agonists alone and in combination with NPY (0.5 μM); **(F)** secreted TNFα level in primary microglia culture co-treated with LTA-SA, Pam3CSK4, and NPY for 24 h. The TNFα level was decreased by exogenous NPY; **(G)** NPY-positive cells in prefrontal cortex, PVWM, and hippocampus. All data are presented as mean ± SEM. White squares are magnified inserts. Scale bar, 100 μm. *, *q*, or $p < 0.05$; **, *q*, or $p < 0.01$; ***, *q*, or $p < 0.001$.

enteral feeding of bovine colostrum only affected the plasma level (**Tables S3, S4**), suggesting that enteral feeding, at least with bovine colostrum, mainly affected the systemic inflammation and had a limited effect inside the CNS, at least in this short term.

The brain inflammatory response was demonstrated by the SE-induced change in abundance of 38 CSF proteins that were related to neuroinflammation and 23 proteins related to neurodevelopment, including glial cell differentiation, astrocyte migration, and synaptic adhesion (**Table S3**). Among these proteins, neuropeptide Y (NPY), a neuropeptide in the CNS with pleiotropic roles in neurogenesis, neuroprotection, and neuroinflammation (35), showed decreased abundance in the CSF after SE infection. NPY mediates the interaction between the nervous and immune systems (35) and may be involved in the activation of resident immune cells; microglia and its upregulation may counteract inflammatory processes (36). In the current study, differential expression of *NPY* in three brain regions of SE-infected pigs (the prefrontal cortex, PVWM, and hippocampus) indicates that brain-derived NPY, at least in part, contributes to the altered NPY level in SE-infected CSF. On the other hand, circulating NPY may also have contributed to the NPY levels in the CSF, especially in the light of the elevated blood–CSF permeability post-SE infection. Unlike that in the prefrontal cortex and PVWM, the hippocampal expression of *NPY* was elevated in the SE group. Besides, elevated transcription of *NPY 1R*, one key receptor of *NPY*, was only found in the hippocampus of SE piglets, supporting other studies (37). Our results suggest that SE infection triggers highly distinct responses in different brain regions of preterm neonates.

Microglial cells, the resident macrophages in the brain, provide an immune defence that involves TLRs and are a key source of NPY production (35). Primary porcine microglial

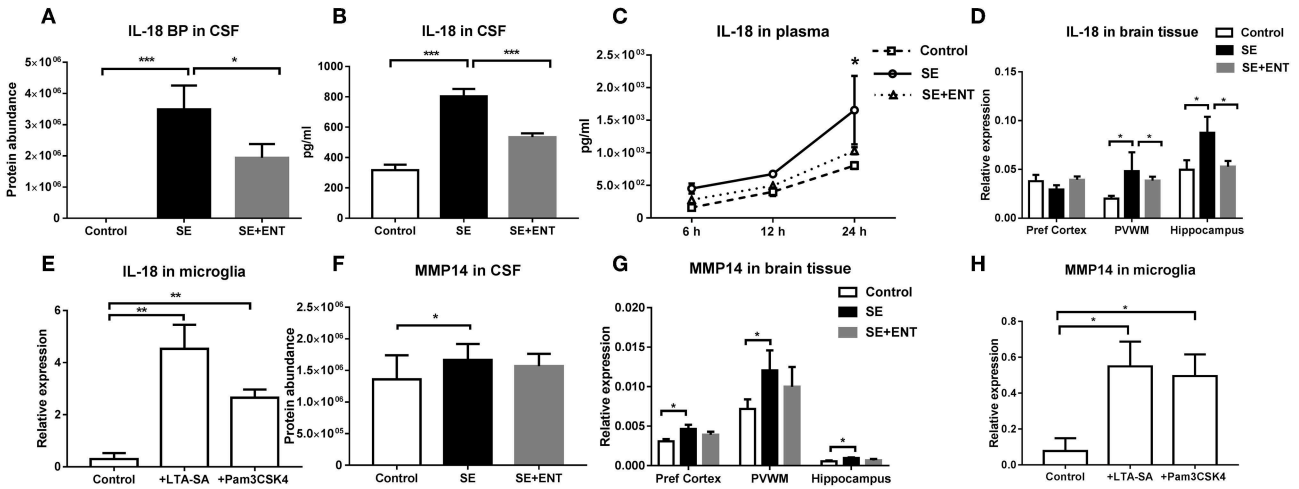

FIGURE 4 | IL-18 BP, IL-18, and MMP-14 in CSF, plasma, brain tissue, and cultured microglia. **(A)** IL-18 BP level in the CSF detected only in SE and SE+ENT piglets; **(B,C)** IL-18 levels in the CSF and plasma, both significantly upregulated by SE infection; **(D)** transcription of IL-18, significantly increased in the SE group in three brain regions and decreased by enteral feeding of colostrum in the PVWM and hippocampus; **(E)** transcription level of IL-18 in primary microglia, significantly increased by the treatment of TLR2 agonists; **(F)** protein level of MMP-14 in the CSF, increased in SE pigs; **(G)** transcription level of MMP-14 in three brain regions, increased by SE infection; **(H)** transcription level of MMP-14 in primary microglia, increased by the treatment of TLR2 agonists. Data are presented as mean ± SEM. *, *q*, or $p < 0.05$; **, *q*, or $p < 0.01$; ***, *q*, or $p < 0.001$.

cells decrease their expression of *NPY* when treated with TLR2 agonists, indicating that microglial cells are involved in the altered expression of *NPY* after SE infection. Surely this does not exclude the potential contribution of other neuronal cells to NPY level in the CNS. NPY works in an autocrine fashion via its receptor, NPY 1R, to control the microglia neuroinflammatory response (35). This is consistent with our observation that exogenous NPY reduced the TNF-α related inflammatory response in TLR2-challenged microglial cells, similar to its previously documented effects on LPS-induced microglial production of IL-1β (38). Enteral feeding with colostrum dampened the neuroinflammation (reduced leukocyte count and CRP levels), but did not affect the NPY level in the CSF, suggesting that dietary modulation of neuroinflammation did not affect cerebral NPY production. Nevertheless, our data suggest that exogenous NPY may have the potential to suppress neuroinflammation in preterm neonates.

IL-18 is a pro-inflammatory cytokine, and the levels of it in CSF and plasma increase during bacterial meningitis (39) and sepsis (40). In our study, the CSF and plasma levels of IL-18 increased in SE piglets relative to Controls, as did the physiological inhibitor, IL-18 BP (34), in the CSF. The *IL-18* transcription level increased only in PVWM and the hippocampus of SE piglets, not in the prefrontal cortex. In isolated preterm pig microglial cells, *IL-18* transcription increased following TLR2 stimulation. Together, these confirm the cerebral contribution to the elevated IL-18 level in the CSF during SE infection. The elevated IL-18 BP level in CSF, probably recruited from the systemic circulation, may exacerbate the intracranial inflammation, as IL-18 BP can neutralise the action of IL-18 in counteracting invading bacteria. Enteral feeding reduced the infection-induced IL-18 response, as shown by lowered abundance of IL-18 and IL-18 BP in CSF and plasma and decreased *IL-18* transcription in brain tissues.

Neuroinflammation involving IL-18 affects membrane-type matrix metalloproteinases (MT-MMPs) (18). CSF abundance of MMP-14, a MT-MMP, and its transcription in the brain tissues increased in SE-infected piglets relative to the Controls, in accordance with other studies (41). Being a proteinase-cleaving extracellular matrix (ECM) protein, MMP-14 inreases its level to digest the tight junction of the blood–CSF barrier and basement membrane to allow immune cells to enter the brain parenchyma to attack invading bacteria (42); increased levels of leukocytes and platelets were also observed in this study. Our results suggested that this MMP-14 regulation in the CNS involved the activation of microglia cells via TLR2. Furthermore, no clear effect of the enteral feeding on MMP-14 abundance in the CSF or its transcription in brain tissues was observed. Together with the limited effects of enteral feeding of colostrum on other proteins in the CSF, this suggests that early enteral feeding mainly has an impact on systemic inflammation but not on neuroinflammation.

Among the early response proteins in plasma, eight showed differential abundance as early as 6 h post-infection, and these included haptoglobin, Serpin A3-6, Serpin A3-8, vWF, LBP, sCD14, MBL1, and APOA4 (**Table S4**). Haptoglobin, LBP, and the serpins in particular responded with a clear linear increase in plasma levels over the first 24 h after SE infection, suggesting their high relevance as early markers of sepsis and bacterial infection. On the other hand, enteral feeding increased, rather than reduced, the levels of these proteins (plus sCD14 and ApoA4) in plasma. Thus, the immune-dampening effect of enteral feeding is not mediated by a reduction in haptoglobin, LBP, serpins, sCD14, and ApoA4 in plasma, and colostrum

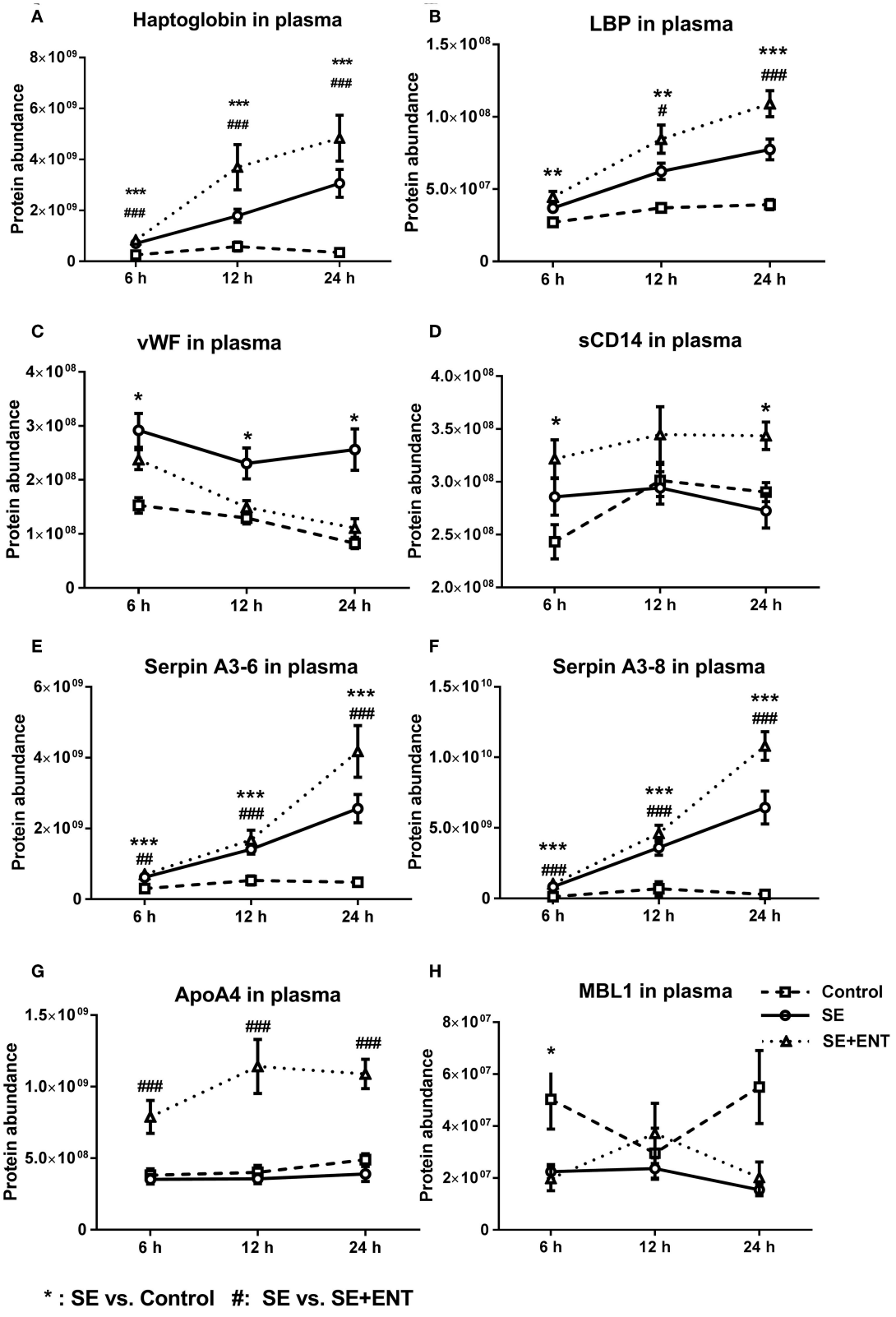

FIGURE 5 | Abundance change of plasma proteins over time. **(A)** haptoglobin, **(B)** LBP, **(C)** vWF, **(D)** sCD14, **(E)** Serpin A3-6, **(F)** Serpin A3-8, **(G)** ApoA4, and **(H)** MBL1. Immune response proteins increased in abundance as early as 6 h post-SE infection, and most of those proteins maintained this change until 24 h. Data are presented as mean ± SEM. *SE vs. Control; #SE+ENT vs. SE; * or #, *q*, or $p < 0.05$; ** or ##, *q*, or $p < 0.01$, *** or ###, *q*, or $p < 0.01$.

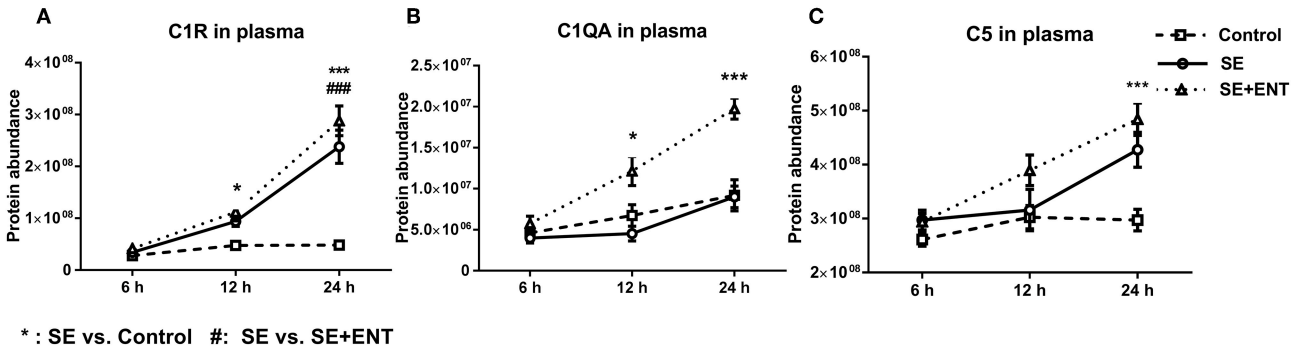

FIGURE 6 | Plasma level of complement components. **(A)** C1R, **(B)** C1QA, **(C)** C5, C1QA, C1R, and C5 showed change 12 h after SE infection, and C2, C4BPA, C5, and C8B showed changes 24 h after infection. Data are presented as mean ± SEM. *SE compared to Control; #SE+ENT compared to SE; *or #$q < 0.05$; ** or ##$q < 0.01$, *** or ###$q < 0.01$.

may even stimulate their synthesis, independently of any direct effect on inflammation. By contrast, enteral feeding reduced the level of vWF, a coagulation factor, as early as 6 h after infection. The level of vWF was negatively correlated with mean platelet counts, confirming that vWF localises platelets to the endothelial surface in sepsis (43). Plasma vWF is reported to be more active in infants than in adults, and vWF can be the first haematological sign of sepsis (44). Collectively, the results suggest that the plasma vWF level may serve as an early indicator of sepsis as well as the immunomodulatory effects of early colostrum feeding.

Among the plasma proteins related to development, metabolism, and protein processing, 14 proteins were affected at 12 h, with 13 affected by SE and only three by enteral feeding with colostrum. At 24 h, 33 of 46 proteins were affected by SE infection and 21 by enteral feeding. None of the 46 CSF proteins, except IL-18, were affected by enteral feeding. Combined with the observation of immune response proteins, this supports that enteral feeding for 24 h had limited short term effects on protein levels in the CSF after SE infection. During sepsis, multiple complement proteins may enter the CNS and engage in neuroinflammation (45). It was not until 12 h after SE infection that plasma complement factors (e.g., C1QA, C1R, and C5) changed in concentration and other complement factors (C2, C4BPA, C5, and C8B) were affected at 24 h. The small activation fragments affected by SE infection, such as C3, C4a, and C5a, increase the permeability of blood vessels and attract leukocytes (8, 20, 21). The complement system also plays a role in eliminating invading bacteria and regulating the immune response to CNS infection by another Gram-positive bacteria, *Streptococcus pneumonia* (46). C1q, MBL1, and properdin may play a role in initiating the lectin and alternative complement pathways. Considering that MBL1 showed a difference already at 6 h, while C1q and properdin showed differences at 12 and 24 h, it is possible that there is a time-dependent activation of the three complement pathways in sepsis.

Many of the proteins that responded to SE infection and enteral feeding with colostrum warrant further investigation, including NPY, IL-18, and MMP-14, due to their roles in neuroinflammation, microglia activation, and blood–CSF barrier disruption. It is possible that exogenous NPY may be used to dampen neuroinflammation in newborns. Two of the detected proteins in plasma, IL-18 and sCD14, show a differential response to Gram-positive and Gram-negative sepsis, with IL-18 levels being highest in Gram-positive sepsis (47) and sCD14 highest in Gram-negative sepsis (34). Combining these two proteins could render us a tool for early differentiation between Gram-positive and Gram-negative sepsis. Compared with classical blood biomarkers of systemic inflammation (e.g., CRP), the proteins detected in this study, including haptoglobin, vWF, MBL1, MRC1, sCD14, and LBP, showed a very early response to infection, indicating their potential in serving as new early markers of infection or sepsis.

The preterm pig is the only model of sepsis in preterm neonates that incorporates all the normal clinical signs of prematurity, such as impaired immunity, respiratory distress, and metabolic dysfunctions. It is highly relevant to study piglet response to bacterial infection during the immediate postnatal adaptation phase, which represents a highly sensitive period for infections and maladaptation in preterm infants. However, it cannot be excluded that the brain-related response to SE and enteral feeding with bovind colsotrum would have been more pronounced after longer exposure (beyond the first 24 h) to SE and enteral feeding. Due to the extremely high technical demand of this pig model, a non-inoculated but colostrum-fed group was skipped. It remains to be investigated whether the effect of colostrum feeding observed in this study is specific to the highly bioactive bovine colostrum or if it is a general effect of enteral feeding, independent of the diet type. Cerebral and systemic responses may also vary according to gestational age at birth, postnatal age, type of pathogen, and infection intensity. Clearly, both pre-clinical and clinical studies are required to clarify the several variables that affect the pathological response to systemic bacterial infection and sepsis in preterm neonates. Combined with proteomic analyses of plasma and CSF, our animal model has shown a new path to investigate both mechanisms and clinically relevant markers of sepsis in preterm neonates.

CONCLUSION

Our findings in this study may reflect how systemic infection by Gram-positive bacteria soon after birth may affect brain development and neuroinflammation in preterm infants. *S. epidermidis* infection induced rapid changes in inflammation-related CSF and the plasma proteome, and early enteral feeding dampened the SE-induced changes in the plasma proteome, but with limited effect in the CSF. The affected plasma proteins may serve as new early biomarkers of Gram-positive systemic infection in newborns, which may also affect central aspects of neuroinflammation, such as microglia activation and blood–CSF barrier disruption.

DATA AVAILABILITY STATEMENT

The mass spectrometry proteomics data have been deposited to the ProteomeXchange Consortium via the PRIDE partner repository with the dataset identifier PXD016013.

ETHICS STATEMENT

All experimental animal protocols were performed in accordance with the Danish Animal Welfare Act and this study was approved by the Danish Committee for Animal Research.

AUTHOR CONTRIBUTIONS

TM conceived the study, analyzed the proteomic data, performed qPCR and ELISA experiments, and prepared the manuscript. AS performed the proteomics analysis and protein annotation. SP performed the primary cell culture. AB and DN performed the animal experiment, sample collection, and assisted in interpreting the data. PS conceived the study, interpreted the data, and prepared the manuscript. P-PJ conceived the study, analyzed and interpreted the data, and prepared the manuscript. All authors drafted the work, revised it critically for important intellectual content, and approved the final version.

FUNDING

This study was supported by Arla Center for Health (STIMMUNE), Innovation Fund Denmark (NEOCOL), and a scholarship from Oversea Study Program of Guangzhou Elite Project (TM).

ACKNOWLEDGMENTS

We thank Dr. Xiaoyang Wang at the University of Gothenburg, Sweden, for the kind donation of the culture of *Staphylococcus epidermidis* used in this study. We would also like to thank Ms. Yan-Nan Jiang at Sun Yat-sen University for assistance in preparing the supplementary tables.

SUPPLEMENTARY MATERIAL

The Supplementary Material for this article can be found online at: https://www.frontiersin.org/articles/10.3389/fimmu.2019.02651/full#supplementary-material

Figure S1 | Microglia purity and NPY 1R response.

Table S1 | Clinical data of piglets included in the proteomics analysis.

Table S2 | Number of proteins with differential abundance in CSF and plasma.

Table S3 | Proteins with differential abundance in CSF.

Table S4 | Proteins with differential abundance in plasma.

Table S5 | Primer sequence of selected genes.

Data Sheets S1 and S2 | Proteomics information for identification.

REFERENCES

1. Strunk T, Inder T, Wang X, Burgner D, Mallard C, Levy O. Infection-induced inflammation and cerebral injury in preterm infants. *Lancet Infect Dis.* (2014) 14:751–62. doi: 10.1016/s1473-3099(14)70710-8
2. Strunk T, Currie A, Richmond P, Simmer K, Burgner D. Innate immunity in human newborn infants: prematurity means more than immaturity. *J Matern Fetal Neonatal Med.* (2011) 24:25–31. doi: 10.3109/14767058.2010.482605
3. Stoll BJ, Hansen N. Infections in VLBW infants: studies from the NICHD neonatal research network. *Semin Perinatol.* (2003) 27:293–301. doi: 10.1016/S0146-0005(03)00046-6
4. Saigal S, Doyle LW. An overview of mortality and sequelae of preterm birth from infancy to adulthood. *Lancet.* (2008) 371:261–9. doi: 10.1016/s0140-6736(08)60136-1
5. Mwaniki MK, Atieno M, Lawn JE, Newton CR. Long-term neurodevelopmental outcomes after intrauterine and neonatal insults: a systematic review. *Lancet.* (2012) 379:445–52. doi: 10.1016/s0140-6736(11)61577-8
6. Stoll BJ. Early-onset neonatal sepsis: a continuing problem in need of novel prevention strategies. *Pediatrics.* (2016) 138:e20163038. doi: 10.1542/peds.2016-3038
7. Miller JE, Hammond GC, Strunk T, Moore HC, Leonard H, Carter KW, et al. Association of gestational age and growth measures at birth with infection-related admissions to hospital throughout childhood: a population-based, data-linkage study from Western Australia. *Lancet Infect Dis.* (2016) 16:952–61. doi: 10.1016/S1473-3099(16)00150-X
8. Shane AL, Stoll BJ. Neonatal sepsis: progress towards improved outcomes. *J Infect.* (2014) 68:S24–32. doi: 10.1016/j.jinf.2013.09.011
9. Vergnano S, Menson E, Kennea N, Embleton N, Russell AB, Watts T, et al. Neonatal infections in England: the NeonIN surveillance network. *Arch Dis Childhood Fetal Neonatal Ed.* (2011) 96:F9–14. doi: 10.1136/adc.2009.178798
10. Bi D, Qiao L, Bergelson I, Ek CJ, Duan L, Zhang X, et al. *Staphylococcus epidermidis* bacteremia induces brain injury in neonatal mice via toll-like receptor 2-dependent and -independent pathways. *J Infect Dis.* (2015) 212:1480–90. doi: 10.1093/infdis/jiv231
11. Brunse A, Worsoe P, Pors SE, Skovgaard K, Sangild PT. Oral supplementation with bovine colostrum prevents septic shock and brain barrier disruption during bloodstream infection in preterm newborn pigs. *Shock.* (2019) 51:337–47. doi: 10.1097/shk.0000000000001131
12. Du X, Fleiss B, Li H, D'Angelo B, Sun Y, Zhu C, et al. Systemic stimulation of TLR2 impairs neonatal mouse brain development. *PLoS ONE.* (2011) 6:e19583. doi: 10.1371/journal.pone.0019583
13. Ng PC. Diagnostic markers of infection in neonates. *Arch Dis Child Fetal Neonatal Ed.* (2004) 89:F229–35. doi: 10.1136/adc.2002.023838

14. Farzi A, Reichmann F, Holzer P. The homeostatic role of neuropeptide Y in immune function and its impact on mood and behaviour. *Acta Physiol.* (2015) 213:603–27. doi: 10.1111/apha.12445
15. Gonzalez-Stegmaier R, Villarroel-Espindola F, Manriquez R, Lopez M, Monras M, Figueroa J, et al. New immunomodulatory role of neuropeptide Y (NPY) in *Salmo salar* leucocytes. *Develop Comp Immunol*. (2017) 76:303–9. doi: 10.1016/j.dci.2017.06.018
16. Borbely E, Scheich B, Helyes Z. Neuropeptides in learning and memory. *Neuropeptides*. (2013) 47:439–50. doi: 10.1016/j.npep.2013.10.012
17. Gotzsche CR, Woldbye DP. The role of NPY in learning and memory. *Neuropeptides*. (2016) 55:79–89. doi: 10.1016/j.npep.2015.09.010
18. Ojala JO, Sutinen EM. The role of interleukin-18, oxidative stress and metabolic syndrome in Alzheimer's disease. *J Clin Med.* (2017) 6:E55. doi: 10.3390/jcm6050055
19. Jung HK, Ryu HJ, Kim MJ, Kim WI, Choi HK, Choi HC, et al. Interleukin-18 attenuates disruption of brain-blood barrier induced by status epilepticus within the rat piriform cortex in interferon-gamma independent pathway. *Brain Res*. (2012) 1447:126–34. doi: 10.1016/j.brainres.2012.01.057
20. Rashad S, Niizuma K, Sato-Maeda M, Fujimura M, Mansour A, Endo H, et al. Early BBB breakdown and subacute inflammasome activation and pyroptosis as a result of cerebral venous thrombosis. *Brain Res*. (2018) 1699:54–68. doi: 10.1016/j.brainres.2018.06.029
21. León IR, Schwämmle V, Jensen ON, Sprenger RR. Quantitative assessment of in-solution digestion efficiency identifies optimal protocols for unbiased protein analysis. *Mol Cell Proteomics*. (2013) 12:2992–3005. doi: 10.1074/mcp.M112.025585
22. Cox J, Mann M. MaxQuant enables high peptide identification rates, individualized p.p.b.-range mass accuracies and proteome-wide protein quantification. *Nat Biotechnol.* (2008) 26:1367–72. doi: 10.1038/nbt.1511
23. Brenner BM, Garcia DL, Anderson S. Glomeruli and blood pressure. Less of one, more the other? *Am J Hypert.* (1988) 1:335–47. doi: 10.1093/ajh/1.4.335
24. Tyanova S, Temu T, Sinitcyn P, Carlson A, Hein MY, Geiger T, et al. The Perseus computational platform for comprehensive analysis of (prote)omics data. *Nat Methods*. (2016) 13:731–40. doi: 10.1038/nmeth.3901
25. RCoreTeam. *R: A Language and Environment for Statistical Computing*. Vienna: R Foundation for Statistical Computing (2013).
26. RStudioTeam. *R Studio: Integrated development for R*. Boston, MA: RStudio, Inc. (2012).
27. Tambuyzer BR, Nouwen EJ. Inhibition of microglia multinucleated giant cell formation and induction of differentiation by GM-CSF using a porcine in vitro model. *Cytokine*. (2005) 31:270–9. doi: 10.1016/j.cyto.2005.05.006
28. Barber RD, Harmer DW, Coleman RA, Clark BJ. GAPDH as a housekeeping gene: analysis of GAPDH mRNA expression in a panel of 72 human tissues. *Physiol Genomics*. (2005) 21:389–95. doi: 10.1152/physiolgenomics.00025.2005
29. Bijlsma S, Bobeldijk I, Verheij ER, Ramaker R, Kochhar S, Macdonald IA, et al. Large-scale human metabolomics studies: a strategy for data (pre-) processing and validation. *Analyt Chem*. (2006) 78:567–74. doi: 10.1021/ac051495j
30. Bates D, Maechler M, Bolker B, Walker S. Fitting linear mixed-effects models using lme4. *J Stat Softw*. (2015). 67:1–48. doi: 10.18637/jss.v067.i01
31. Hothorn T, Bretz F, Westfall P. Simultaneous inference in general parametric models. *Biom J.* (2008) 50:346–63. doi: 10.1002/bimj.200810425
32. Pollard KS, Gilbert HN, Ge Y, Taylor S, Dudoit S. *multtest: Resampling-Based Multiple Hypothesis Testing*. R version: 2.42.0 (2005). Available online at: https://git.bioconductor.org/packages/multtest
33. Berner R, Fürll B, Stelter F, Dröse J, Müller H-P, Schütt C. Elevated levels of lipopolysaccharide-binding protein and soluble CD14 in plasma in neonatal early-onset sepsis. *Clin Diagn Lab Immunol*. (2002) 9:440–5. doi: 10.1128/cdli.9.2.440-445.2002
34. Blanco A, Solis G, Arranz E, Coto G, Ramos A, Telleria J. Serum levels of CD14 in neonatal sepsis by Gram-positive and Gram-negative bacteria. *Acta Paediatr*. (1996) 85:728–32.doi: 10.1111/j.1651-2227.1996.tb14135.x
35. Malva JO, Xapelli S, Baptista S, Valero J, Agasse F, Ferreira R, et al. Multifaces of neuropeptide Y in the brain–neuroprotection, neurogenesis and neuroinflammation. *Neuropeptides*. (2012) 46:299–308. doi: 10.1016/j.npep.2012.09.001
36. Duarte-Neves J, Pereira de Almeida L, Cavadas C. Neuropeptide Y (NPY) as a therapeutic target for neurodegenerative diseases. *Neurobiol Dis.* (2016) 95:210–24. doi: 10.1016/j.nbd.2016.07.022
37. Kim Y-W, Kim K-H, Ahn D-K, Kim H-S, Kim J-Y, Lee DC, et al. Time-course changes of hormones and cytokines by lipopolysaccharide and its relation with anorexia. *J Physiol Sci*. (2007) 57:159–65. doi: 10.2170/physiolsci.RP003407
38. Ferreira R, Xapelli S, Santos T, Silva AP, Cristovao A, Cortes L, et al. Neuropeptide Y modulation of interleukin-1{beta} (IL-1{beta})-induced nitric oxide production in microglia. *J Biol Chem*. (2010) 285:41921–34. doi: 10.1074/jbc.M110.164020
39. Fassbender K, Mielke O, Bertsch T, Muehlhauser F, Hennerici M, Kurimoto M, et al. Interferon-γ-inducing factor. (IL-18) and interferon-γ in inflammatory CNS diseases. *Neurology*. (1999) 53:1104–1104. doi: 10.1212/wnl.53.5.1104
40. Novick D, Schwartsburd B, Pinkus R, Suissa D, Belzer I, Sthoeger Z, et al. A novel IL-18BP ELISA shows elevated serum IL-18BP In sepsis and extensive decrease of free IL-18. *Cytokine.* (2001) 14:334–2. doi: 10.1006/cyto.2001.0914
41. Bar-Or A, Nuttall RK, Duddy M, Alter A, Kim HJ, fergan I, et al. Analyses of all matrix metalloproteinase members in leukocytes emphasize monocytes as major inflammatory mediators in multiple sclerosis. *Brain.* (2003) 126:2738–49. doi: 10.1093/brain/awg285
42. Candelario-Jalil E, Yang Y, Rosenberg GA. Diverse roles of matrix metalloproteinases and tissue inhibitors of metalloproteinases in neuroinflammation and cerebral ischemia. *Neuroscience*. (2009) 158:983–94. doi: 10.1016/j.neuroscience.2008.06.025
43. Hyseni A, Kemperman H, de Lange DW, Kesecioglu J, de Groot PG, Roest M. Active von Willebrand factor predicts 28-day mortality in patients with systemic inflammatory response syndrome. *Blood*. (2014) 123:2153–6. doi: 10.1182/blood-2013-08-508093
44. Finkelstein Y, Shenkman B, Sirota L, Vishne TH, Dardik R, Varon D, et al. Whole blood platelet deposition on extracellular matrix under flow conditions in preterm neonatal sepsis. *Eur J Pediatr*. (2002) 161:270–4. doi: 10.1007/s00431-002-0938-4
45. Brennan FH, Anderson AJ, Taylor SM, Woodruff TM, Ruitenberg MJ. Complement activation in the injured central nervous system: another dual-edged sword? *J Neuroinflamm*. (2012) 9:137. doi: 10.1186/1742-2094-9-137
46. Rupprecht TA, Angele B, Klein M, Heesemann J, Pfister HW, Botto M, et al. Complement C1q and C3 Are critical for the innate immune response to *Streptococcus pneumoniae* in the central nervous system. *J Immunol*. (2007) 178:1861–9. doi: 10.4049/jimmunol.178.3.1861
47. Tschoeke SK, Poberholzer A, Molfawer LL. Interleukin-18: a novel prognostic cytokine in bacteria-induced sepsis. *Crit Care Med.* (2006) 34:1225–33. doi: 10.1097/01.CCM.0000208356.05575.16

Conflict of Interest: The authors declare that the research was conducted in the absence of any commercial or financial relationships that could be construed as a potential conflict of interest.

frontiers in Immunology

ORIGINAL RESEARCH
published: 10 January 2020
doi: 10.3389/fimmu.2019.02939

Neonatal Antibiotic Treatment Is Associated With an Altered Circulating Immune Marker Profile at 1 Year of Age

*Berthe C. Oosterloo[1], Belinda van't Land[2,3], Wilco de Jager[2], Nicole B. Rutten[4], Margot Klöpping[2], Johan Garssen[3,5], Arine M. Vlieger[4] and Ruurd M. van Elburg[1]**

[1] Department of Pediatrics, Emma Children's Hospital, Amsterdam UMC, University of Amsterdam, Amsterdam, Netherlands, [2] Center for Translational Immunology, University Medical Centre Utrecht, Utrecht, Netherlands, [3] Danone Nutricia Research, Utrecht, Netherlands, [4] St. Antonius Hospital, Department of Pediatrics, Nieuwegein, Netherlands, [5] Utrecht Institute for Pharmaceutical Sciences (UIPS), Utrecht University, Utrecht, Netherlands

OPEN ACCESS

Edited by:
Tobias Strunk,
University of Western Australia, Australia

Reviewed by:
Zhuoran Yin,
Brigham and Women's Hospital and Harvard Medical School, United States
Yanfei Zhang,
Geisinger Health System, United States

***Correspondence:**
Ruurd M. van Elburg
rm.vanelburg@amsterdamumc.nl

Specialty section:
This article was submitted to Nutritional Immunology, a section of the journal Frontiers in Immunology

Received: 10 July 2019
Accepted: 29 November 2019
Published: 10 January 2020

Citation:
Oosterloo BC, van't Land B, de Jager W, Rutten NB, Klöpping M, Garssen J, Vlieger AM and van Elburg RM (2020) Neonatal Antibiotic Treatment Is Associated With an Altered Circulating Immune Marker Profile at 1 Year of Age. Front. Immunol. 10:2939. doi: 10.3389/fimmu.2019.02939

Background: Neonatal antibiotics disturb the developing gut microbiome and are therefore thought to influence the developing immune system, but exact mechanisms and health consequences in later life still need to be elucidated. Therefore, we investigated whether neonatal antibiotics influence inflammatory markers at 1 year of age. In addition, we determined whether health problems during the first year of life, e.g., allergic disorders (eczema and wheezing) or infantile colics, were associated with changes in the circulating immune marker profile at 1 year of age.

Methods: In a subgroup ($N = 149$) of the INCA-study, a prospective birth-cohort study, a blood sample was drawn from term born infants at 1 year of age and analyzed for 84 immune related markers using Luminex. Associations of antibiotic treatment, eczema, wheezing, and infantile colics with immune marker concentrations were investigated using a linear regression model. The trial is registered as NCT02536560.

Results: The use of broad-spectrum antibiotics in the first week of life, was significantly associated with different levels of inflammatory markers including sVCAM-1, sCD14, sCD19, sCD27, IL-1RII, sVEGF-R1, and HSP70 at 1 year of age. Eczema was associated with decreased concentrations of IFNα, IFNγ, TSLP, CXCL9, and CXCL13, but increased concentrations of CCL18 and Galectin-3. Wheezing, independent of antibiotic treatment, was positively associated to TNF-R2 and resistin. Infantile colics were positively associated to IL-31, LIGHT, YKL-40, CXCL13, sPD1, IL1RI, sIL-7Ra, Gal-1, Gal-9, and S100A8 at 1 year of age, independent of early life antibiotic treatment.

Conclusion: In this explorative study, we identified that neonatal antibiotics are associated with immunological alterations at 1 year of age and that, independent of the antibiotic treatment, infantile colics were associated with alterations within gut associated markers. These findings support the importance of the first host microbe interaction in early life immune development.

Keywords: biomarkers, immune development, infant, antibiotics, infantile colic, eczema

INTRODUCTION

Early immune development is influenced by many different pre- and post-natal factors (1). Delivery mode, infant feeding, exposure to the environment, and antibiotic treatment are all early life exposures known to influence the developing immune system (2–6). One of the mechanisms by which these early life factors can influence the immune system is probably through their impact on the developing gut microbiome (1). The microbiome development starts right after birth, and is very dynamic during the early life period (7). When the microbiome development is disrupted, this may impact immune development, with long term health effects such as development of asthma and/or allergies but also of inflammatory bowel disease (IBD), type 1 diabetes (6). One of the most important and well-known factors that disturbs the normal microbiome development is antibiotic treatment in early life (5, 6). Antibiotics are nevertheless the most frequently prescribed drug for neonates (8).

The INCA study, a prospective birth-cohort study, was designed to investigate the long-term clinical, immunological and microbial effects of antibiotic treatment in the first week of life. The primary hypothesis was that children treated with antibiotics in the first week of life would have eczema more often (9). In this cohort, we previously demonstrated an increased risk for infantile colic and wheezing in the first year of life in children treated with antibiotics during the first week of life, but not for eczema (10). Although epidemiologic studies show a direct association between the use of antibiotics during the first year of life and the risk for development of asthma and other diseases later in life (6, 11), the analysis of inflammatory biomarkers in these otherwise healthy infants remains rather limited.

We hypothesized that antibiotic treatment in the first week of life may induce certain levels of immunological misbalance, resulting in alteration of circulating immune marker profile at 1 year of age. Aim of this explorative study was to measure the circulating immune marker profile at 1 year of age in a subgroup of the INCA study, with or without antibiotic treatment in the first week of life. In addition, we explored whether health problems such as allergic disorders (eczema or wheezing) or infantile colics in the first year of life were associated with changes in this circulating immune marker profile in children at 1 year of age.

METHODS

Study Design

The INCA (INtestinal microbiota Composition after Antibiotic treatment in early life) study is a prospective birth-cohort study. Design, inclusion and exclusion criteria of this cohort have been published previously (9). Between August 2012 and January 2015, term-born infants (≥36 weeks of gestation) were recruited from the maternity and neonatal wards of four teaching hospitals in the Netherlands. Antibiotic treatment was started at the pediatrician's discretion, according to hospital protocol for suspected early onset neonatal infection and based on the Dutch guideline for early onset sepsis (12). In general, infants with suspicion of infection received broad-spectrum antibiotics (a combination of gentamycin and a penicillin-derivative), after a blood culture was taken. In case of a negative blood culture, combined with a low clinical suspicion of infection and low c-reactive protein, antibiotics were discontinued after 2–3 days, otherwise antibiotics were continued for 7 days. All term born infants staying in the hospital for at least 24 h were eligible for inclusion. Exclusion criteria were severe congenital malformations, severe infection needing transfer to a neonatal intensive care unit, and insufficient knowledge of the Dutch language. Around the age of 1 year, children visited the outpatient clinic for follow-up. During this visit, a blood sample was obtained if the parents had given additional informed consent. After centrifugation, serum samples were aliquoted and stored at −80°C until further use. Informed consent was obtained from both parents at inclusion. The study was approved by the ethical board of the St. Antonius Hospital in Nieuwegein. The study was registered as NCT02536560.

Data Collection

Atopic diagnoses were recorded as published previously (10). In short, parents kept a diary and reported symptoms of atopic disorders and crying for more than 3 h per day. Doctor diagnosed eczema (DDE) in this study was defined as eczema confirmed by the general practitioner, investigated via the General Practitioner electronic medical database using the International Classification of Primary Care (ICPC) (13). An episode of wheezing was defined as wheezing present for at least two consecutive days. Infantile colics were defined according to the Rome III criteria with parent-reported crying for ≥3 h of crying per day, ≥3 days within a week, within the first 3 months of life (14).

Cytokine Measurements

Measurements of immune-related markers ($n = 84$) (**Supplementary Table 1**) were performed using an in-house developed and validated multiplex immunoassay based on Luminex technology (xMAP, Luminex Austin, TX, USA). The assay was performed as described by Scholman et al. (15). In short, a-specific heterophilic immunoglobulins were pre-absorbed from all samples with heteroblock (Omega Biologicals, Bozeman MT, USA). Next, samples were incubated with antibody-conjugated MagPlex microspheres for 1 h at room temperature with continuous shaking, followed by 1 h incubation with biotinylated antibodies, and 10 min incubation with phycoerythrin-conjugated streptavidin diluted in high performance ELISA buffer (HPE, Sanquin, the Netherlands). Acquisition was performed with the Biorad FlexMAP3D (Biorad laboratories, Hercules, USA) in combination with xPONENT software version 4.2 (Luminex). Data was analyzed by 5-parametric curve fitting using Bio-Plex Manager software, version 6.1.1 (Biorad). Potential cross-reactive samples were identified using a negative control (15) and were excluded from analysis. After determining the cytokine/chemokine serum levels, the out of range (OOR) data have been imputed with the lower limit of quantification (LLOQ) in lower OOR threshold or the upper limit of quantification (ULOQ) in the upper OOR threshold by using assay characteristics (LLOQ and ULOQ) as

previously published (15). If ≥40% of the data was imputed for the same biomarker, and equally divided over the compared outcome, the biomarker was excluded from further analysis.

Statistical Analyses

Basic descriptive statistics (Mann Whitney U- or X-squared tests) were used to describe the patient population. As described previously, an unsupervised hierarchal clustering analysis, with min-max normalization per protein, was performed to investigate the discriminative potential of a single or a combination of proteins (16).

Not-normally distributed cytokines and chemokines were log-transformed to achieve a Gaussian distribution. With a linear regression the association between (log-transformed) cytokines and chemokines and an antibiotic course in the first week of life was investigated. Next, we investigated the association of the cytokines and chemokines and doctor's diagnosed eczema, wheezing and infantile colic. Wheezing and infantile colic analyses were additionally adjusted for antibiotic treatment in the first week of life as this was shown before to be associated. Doctor's diagnosed eczema was not associated to the antibiotic course in the first week of life and therefore these analyses were not adjusted for antibiotic treatment in the first week of life. Back -transformed βs are shown for the log-transformed variables.

As we consider this study an exploratory, hypothesis-generating study, $p < 0.05$ were considered significant. We do acknowledge, however, the problem of multiple testing in this study, therefore we focus mainly on the associations with a $p < 0.01$.

Statistical analyses were performed using either IBM SPSS Statistics 24, R statistics version 3.5.1, Omniviz 6.1.2, or Graphpad Prism 7.

RESULTS

Baseline Characteristics

Baseline characteristics were comparable between the complete INCA-cohort ($n = 436$) and the subpopulation analyzed in this study of which a sufficient serum sample was obtained ($n = 167$, **Table 1**). Of these 167 samples, 18 were excluded from further analysis due to cross reactivity, leaving 149 samples from 149 infants suitable for analysis (Luminex-group). Of all markers, 14 were excluded as they were ≥40% below the LLOQ (**Supplementary Table 1**). No significant differences were found in describing characteristics of the children with and without antibiotics (**Table 1**).

Neonatal Antibiotic Treatment and Circulating Immune Profile at 1 Year of Age

Antibiotic treatment in the first week of life was significantly associated with higher or lower concentrations of IL-12 (β 0.63, 95% CI 0.45, 0.89), CCL2 (β −10.14, 95%CI −19.35, −0.92), CXCL4 (β 0.80, 95% CI 0.67, 0.94), sVCAM-1 (β −0.66, 95% CI −1.27, −0.06), sCD14 (β 1.09, 95% CI 1.02, 1.16), sCD19 (β 0.20, 95% CI 0.09, 0.46), sCD27 (β 0.44, 95% CI 0.28, 0.69), TNF-R1 (β 0.62, 95% CI 0.42, 0.93), sVEGF-R1 (β 0.74, 95% CI 0.58, 0.94), E-selectin (β −11.52, 95% CI −23.01, −0.03), and HSP70 (β 0.36, 95% CI 0.21, 0.62) (**Table 2**).

Moreover, the concentrations of sVCAM-1, sCD14, sCD19, sCD27, IL-1RII, sVEGF-R1, and HSP70 were significantly ($p < 0.05$) associated with neonatal antibiotic treatment in a differentiating cluster (**Figures 1A,B**). Overall, some of inflammatory markers measured showed significant differences between the AB+ and AB− groups (**Table 3**).

Health Problems in the First Year and Circulating Immune Profile at 1 Year

The incidence of DDE in the infants in the subgroup was comparable to the incidence of DDE in the total INCA clinical cohort (13.4 vs. 13.3%, respectively, **Table 1**). DDE was significantly associated with lower concentrations of IFNα (β 0.44, 95% CI 0.23, 0.83), IFNγ (β 0.50, 95% CI 0.25, 0.99), TSLP (β 0.47, 95% CI 0.25, 0.91), CXCL9 (β 0.64, 95% CI 0.45, 0.91), and CXCL13 (β 0.76, 95% CI 0.59, 0.98). In children with DDE there was a positive association with CCL18 (β 1.26, 95% CI 1.01, 1.56) and Galectin-3 (β 1.34, 95% CI 1.02, 1.75) (**Table 2**).

Incidence of wheezing in the subgroup was comparable to the incidence of wheezing in the total INCA clinical cohort (36.2 vs. 34.2%). In children that wheezed both TNF-R2 (β 1.54, 95% CI 1.04, 2.28) and resistin (β 1.20, 95% CI 1.00, 1.43) were positively associated (**Table 2**).

TABLE 1 | Participant characteristics of samples analyzed with luminex compared to the whole cohort.

		Luminex cohort (*N* = 149)	AB− (*N* = 95)	AB+ (*N* = 54)	INCA clinical cohort (*N* = 436)
Gender	Male (%)	90 (60.4%)	56 (58.9)	34 (63.0)	237 (54.4%)
Gestational age	(SD)	39.7 (1.5)	39.4 (1.5)	40.0 (1.2)	39.7 (1.5)
Birthweight	(SD)	3,552 (544)	3,465 (557)	3,707 (489)	3,526 (546)
Delivery mode	Vaginal (%)	111 (74.5%)	68 (71.6)	43 (79.6)	599 (68.6%)
Breastfed exclusive	0 months (%)	33 (22.1%)	42 (44.2)	31 (57.4)	99 (22.7%)
	1–3 months	63 (42.3%)	26 (27.4)	7 (13.0)	181 (41.5%)
	>3 months	53 (35.6%)	27 (28.4)	16 (29.7)	156 (35.8%)
Antibiotics (<day 7)	(%)	54 (36.2%)			151 (34.6%)
Infantile colic	(%)	26 (17.4%)	14 (14.7)	12 (22.2)	74 (17.0%)
Eczema	(%)	20 (13.4%)	15 (15.8)	5 (9.3)	58 (13.3%)

TABLE 2 | The significantly altered immune marker concentrations in one of the associations.

Immune marker		AB+ vs AB–				Doctors diagnosed eczema				Wheezing (adjusted for AB)				Infantile colics (adjusted for AB)			
			95%CI				95%CI				95%CI				95%CI		
Unit	Marker	β	Low	Up	*p*-value	β	Low	Up	*p*-value	β	Low	Up	*p*-value	β	Low	Up	*p*-value
pg/ml	IL-12	0.63	0.45	0.89	0.010	1.09	0.66	1.81	n.s.	1.27	0.89	1.80	n.s.	1.34	0.86	2.09	n.s.
pg/ml	IL-17	0.83	0.67	1.03	n.s.	0.83	0.61	1.13	0.01	0.81	0.65	1.01	n.s.	1.04	0.79	1.38	n.s.
pg/ml	IL-17F	0.87	0.68	1.10	n.s.	0.87	0.62	1.22	n.s.	1.30	1.02	1.65	n.s.	1.52	1.13	2.04	0.006
pg/ml	IL-22	0.73	0.50	1.07	n.s.	1.43	0.83	2.46	n.s.	1.04	0.71	1.53	n.s.	1.62	1.00	2.62	0.050
pg/ml	IL-31	0.92	0.65	1.30	n.s.	0.58	0.36	0.94	0.027	1.03	0.72	1.45	n.s.	1.72	1.11	2.65	0.015
pg/ml	IL-33	0.71	0.54	0.92	n.s.	0.92	0.62	1.36	n.s.	1.05	0.80	1.38	n.s.	1.61	1.15	2.25	0.006
pg/ml	IFNa	0.97	0.61	1.55	n.s.	0.44	0.23	0.83	0.012	0.81	0.51	1.29	n.s.	1.26	0.70	2.27	n.s.
pg/ml	IFNg	1.30	0.80	2.13	n.s.	0.50	0.25	0.99	0.048	0.76	0.47	1.25	n.s.	1.37	0.73	2.57	n.s.
pg/ml	TSLP	1.19	0.75	1.90	n.s.	0.47	0.25	0.91	0.025	0.74	0.46	1.18	n.s.	1.44	0.80	2.62	n.s.
pg/ml	LIGHT	0.94	0.64	1.37	n.s.	0.91	0.54	1.56	n.s.	1.13	0.77	1.65	n.s.	1.70	1.06	2.74	0.028
ng/ml	YKL-40	0.96	0.81	1.14	n.s.	0.97	0.76	1.24	n.s.	1.06	0.89	1.26	n.s.	1.25	1.01	1.55	0.044
pg/ml	*CCL2	−10.14	−19.35	−0.92	0.031	−5.24	−18.42	7.93	n.s.	7.70	−1.51	16.91	n.s.	6.92	−4.79	18.63	n.s.
ng/ml	CCL18	1.03	0.88	1.21	n.s.	1.26	1.01	1.56	0.040	1.08	0.92	1.27	n.s.	1.03	0.85	1.26	n.s.
μg/ml	CXCL4	0.80	0.67	0.94	0.009	0.98	0.77	1.25	n.s.	0.94	0.80	1.12	n.s.	0.97	0.79	1.21	n.s.
pg/ml	CXCL9	1.11	0.86	1.42	n.s.	0.64	0.45	0.91	0.014	1.03	0.80	1.33	n.s.	1.02	0.74	1.40	n.s.
pg/ml	CXCL13	1.09	0.91	1.30	n.s.	0.76	0.59	0.98	0.034	1.09	0.91	1.31	n.s.	1.28	1.02	1.61	0.034
pg/ml	*sPD1	−81.83	−197.41	33.75	n.s.	−70.59	−234.25	93.06	n.s.	61.96	−54.15	178.08	n.s.	185.17	40.75	329.59	0.012
ng/ml	sCD19	0.20	0.09	0.46	0.000	0.86	0.25	2.91	n.s.	1.33	0.58	3.06	n.s.	1.34	0.47	3.87	n.s.
pg/ml	sCD27	0.44	0.28	0.69	0.000	0.61	0.31	1.17	n.s.	1.01	0.64	1.60	n.s.	1.44	0.81	2.56	n.s.
pg/ml	TNF-R1	0.62	0.42	0.93	0.020	0.67	0.38	1.18	n.s.	1.54	1.04	2.28	0.033	1.31	0.79	2.17	n.s.
ng/ml	*TNF-R2	−0.13	−0.30	0.05	n.s.	−0.11	−0.35	0.14	n.s.	0.14	−0.04	0.31	n.s.	0.23	0.01	0.45	0.037
ng/ml	sIL-7Ra	0.76	0.52	1.11	n.s.	1.03	0.60	1.77	n.s.	1.04	0.71	1.52	n.s.	1.74	1.08	2.80	0.023
ng/ml	sVEGF-R1	0.74	0.58	0.94	0.014	0.94	0.66	1.32	n.s.	1.18	0.93	1.50	n.s.	1.21	0.89	1.64	n.s.
ng/ml	*Gal-1	−1.57	−3.53	0.39	n.s.	−0.31	−3.10	2.48	n.s.	1.07	−0.90	3.04	n.s.	3.92	1.50	6.34	0.002
ng/ml	Gal-3	0.86	0.71	1.04	n.s.	1.34	1.02	1.75	0.038	1.06	0.87	1.29	n.s.	1.19	0.93	1.52	n.s.
ng/ml	Gal-9	0.91	0.76	1.09	n.s.	0.96	0.75	1.24	n.s.	1.19	1.00	1.42	n.s.	1.31	1.05	1.63	0.018
ng/ml	*E-selectin	−11.52	−23.01	−0.03	0.049	5.98	−10.40	22.37	n.s.	5.56	−5.99	17.11	n.s.	6.38	−8.24	21.01	n.s.
ng/ml	S100A8	0.96	0.71	1.30	n.s.	1.06	0.69	1.61	n.s.	1.16	0.86	1.57	n.s.	1.51	1.03	2.20	0.034
ng/ml	HSP70	0.36	0.21	0.62	0.000	0.95	0.43	2.11	n.s.	1.25	0.73	2.16	n.s.	1.38	0.69	2.75	n.s.
ng/ml	Resistin	1.00	0.83	1.19	n.s.	0.99	0.77	1.28	n.s.	1.20	1.00	1.43	0.048	0.65	−1.16	2.46	n.s.

*n.s. is non-significant. *Reflects the values that were not log-transformed.*

Incidence of infantile colics within the subgroup was comparable to the total INCA clinical cohort (17.0 vs. 17.4%, respectively). Interestingly, the positively significantly associated markers are known as inflammatory and gut associated immune markers (**Table 2**); Il-22 (β 1.62, 95% CI 1.00, 2.62), LIGHT (β 1.70, 95% CI 1.06, 2.74), YKL-40 (β 1.25, 95% CI 1.01, 1.55), CXCL13 (β 1.28, 95% CI 1.02, 1.61), sPD1 (β 185.17, 95% CI 40.75, 329.59), sIL-7ra (β 1.74, 95% CI 1.08, 2.80), Gal-1 (β 3.92, 95% CI 1.50, 6.34), Gal-9 (β 1.31, 95% CI 1.05, 1.63), S100A8 (β 1.51, 95% CI 1.03, 2.20). The only negatively associated marker was TNF-R2 (β 0.23, 95% CI 0.01, 0.45).

DISCUSSION

In this INCA-cohort, we found that children treated with neonatal antibiotics (in the first week of life) have a different circulating immune marker profile at 1 year of age compared to children not exposed to neonatal antibiotics. In addition, children who suffered from infantile colics during the first 3 months of their life, had increased (gut-associated) inflammatory markers (like IL-33 and S100A8 and Galectin 1) at 1 year of age. Moreover, we found that children with doctor's diagnosed eczema had limited capacity to induce Th1 cytokines (like IFN-gamma and CXCL9) and more eczema/skin related marker CCL18 (PARC). To our knowledge, this is the first study that explored the impact of antibiotic treatment in the first week of life in term-born infants on the circulating immune marker profile at 1 year of age.

Diversity of the early developing gut microbiota and repeated exposure to new bacterial antigens seems to be more important for normal immune maturation than the distribution of specific species (17). Aberrant immune maturation in early infancy has been linked to limited intensity and reduced diversity of microbial stimulation (18). Consequently, antibiotic treatment can be seen as a risk factor for development of altered microbial

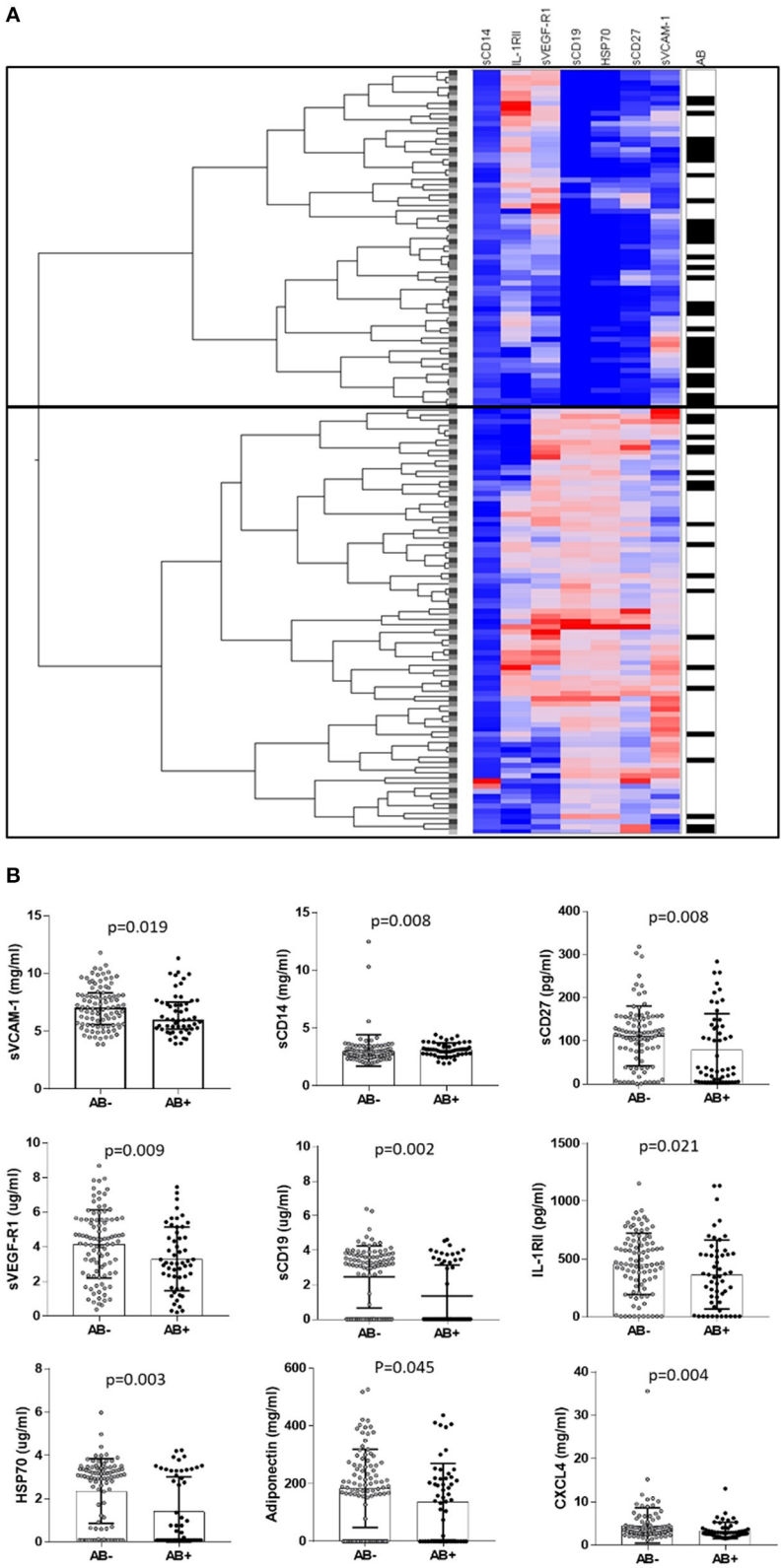

FIGURE 1 | (A) Hierarchical differentiating clustering, differentiating factor is Antibiotic treatment in first week of life; markers associated are sVCAM-1, sCD14, sCD19, sCD27, IL-1RII, sVEGF-R1, and HSP70. **(B)** Distribution of immune markers appearing in the hierarchical cluster between the children treated with antibiotics in the first week of life compared to those who were not.

TABLE 3 | Absolute values of the markers significantly differing in children treated without (AB–) and with (AB+) antibiotics in the first week of life, given in median [inter quartile range (IQR)].

		AB– $n = 95$			AB+ $n = 54$			
/ml		Median	IQR		Median	IQR		*p*-value
pg	IL-22	3.7	3.7	7.7	3.7	1.5	4.0	<0.05
pg	CCL2	55	38	81	44	31	71	<0.05
µg	CXCL4	3.5	2.8	4.5	2.9	2.3	3.9	<0.01
µg	sVCAM-1	7.1	5.6	8.3	6.0	5.2	7.5	<0.05
µg	sCD14	2.8	2.5	3.2	3.1	2.8	3.6	<0.01
ng	sCD19	3.2	0.0	3.7	0.0	0.0	3.5	<0.01
pg	sCD27	114	75	154	36	5.4	135	<0.01
pg	IL-1RII	461	266	649	346	115	543	<0.05
pg	TNF-R1	99	47	196	83	30	134	<0.05
ng	sVEGF-R1	4.4	2.5	5.6	3.1	2.1	4.6	<0.01
ng	HSP70	3.0	0.6	3.4	0.5	0.1	3.3	<0.01
µg	Adiponectin	190	0.2	265	142	0.2	219	<0.05

diversity in early life, with the potential of altered immune development (5). Neonatal nutritional status is one of the important environmental factors in this process of immune maturation. However, no association between the duration of breastfeeding and clinical characteristics or immune markers could be detected between AB+ and AB– study groups. Due to the explorative nature of the study, it is difficult to determine the role of changes in individual cytokines. However, some interesting markers could be related to an altered microbial management capacity of the immune system in infants receiving antibiotics. For instance, changes in the levels of both sCD14 and CXCL4 concentrations suggest higher levels of microbial components within circulation (19, 20). Moreover, whereas CD19 and CD27 are linked to B-cell development, known to be involved in the dynamic immune maturation period in children, the concentrations of sCD19 and sCD27 were lower in infants receiving antibiotics compared to healthy controls. This might be a reflection of an altered B-cell development, suggesting a link between the sIgA development and early life microbiome establishment (21). Subsequently, the presence of reduced levels of individual circulating inflammation related receptors (like IL1-RII, TNF-R1, and sVEGF-R1) are indicative for an altered immune development in infants receiving early life antibiotics. Clustering of these markers showed a different immune development at 1 year of age in infants who received antibiotic treatment in the first week of life. This in turn is illustrative for the importance and understanding of the long-lasting effects of several environmental factors which occur early in life and are known to be associated with changes later in life.

One of the features of an altered immune development or immune dysbiosis in early life is the development of allergic disorders. Although, within the INCA study, no increased risk was shown for doctor's diagnosed eczema after neonatal antibiotic treatment at 1 year of age (10), increased concentrations of Gal-3, CCL17 (TARC), and CCL18 (PARC) were detected within the infants with DDE. These markers are associated with either skin inflammation, Gal-3 (22), or eczema severity, TARC, and PARC (23). It is interesting to note that characteristic eczema severity markers like TARC and PARC, were not associated with the parental reported eczema (data not shown). Parental reported eczema (PRE) is considered to be less specific for the (real) presence of eczema. Increased concentrations of Gal-3 in children with PRE may reflect another form of skin inflammation. Non-specific eczema-like symptoms can be caused by a wide range of factors, all associated with their own immune marker profile.

One additional atopy-related outcome evaluated within the INCA study was wheezing. Infants treated with neonatal antibiotics had an increased risk for wheezing in the first year of life (10). Wheezing is, however, a non-specific outcome, as many young children suffer from an episode of wheezing, often due to viral infections. Yet, it is used as a predictor for the development of asthma. Its non-specific nature (i.e., can both represent a respiratory infection as well as an allergic response), might be an explanation for the absence of clear differences in circulating immune marker profile between children who suffered from wheezing and those who did not.

We previously showed that neonatal antibiotic treatment is a contributing risk factor for development of infantile colics in the first year of life (10). The etiology of infantile colics is largely unknown, but may be related to gut function immaturity, low grade inflammation, gut dysmotility, food allergy and, similarly to parental stress, anxiety, and exhaustion (24–26). Moreover, gut microbiota alterations, associated with intestinal barrier dysfunction, are reported in colicky infants (27). The effect of neonatal antibiotics on the circulating immune marker profile in children with infantile colics was not investigated due to the small size of the subgroup. However, we additionally accounted for neonatal antibiotic treatment in the analyses. Because infantile colics usually resolved without specific treatment around 3 months of age, it is very interesting that at 1 year of age gut associated inflammatory markers such as IL-31, Gal-1, Gal-9, S100A8 were increased in children that previously had infantile colics compared to those who had not. These markers are reported to be both gut associated and allergy associated (28–31). Given this finding, it is interesting that recent studies have focused on the association between infantile colics and gastrointestinal disorders later in life, suggesting that infantile colics may have long term consequences (32, 33).

Very limited information is available regarding the levels of inflammatory markers within healthy infants. However, some of the markers are associated with increased inflammation status, specifically acting as marker for disease activity. Regarding the marker profile associated with infantile antibiotics use, only associations can be made. i.e., it is known that after exposure to bacterial endotoxin, monocytes release sCD14 and plasma levels are altered in conditions associated with microbial translocation such as insulin resistance, liver inflammation, and cardiovascular disease (34–36). A marker such as Heat Shock Protein 70 (HSP) is a stress-responsive protein (37). In addition, sCD27 may act to differentiate activated memory or recently antigen-experienced B cells (38). In addition, eczema was associated with decreased concentrations of IFNα, IFNγ,

TSLP, CXCL9, and CXCL13, but with increased concentrations of CCL18 and Galectin-3. Most of the potential biomarkers described thus far in the literature for the development of eczema related disorders, like atopic dermatitis, are more or less related to the issue of severity and their changes during the therapeutic regimen. Among these, thymus and activation-regulated chemokine (CCL17), macrophage derived chemokine (CCL22), cutaneous T-cell-attracting chemokine (CCL27), IL-31, IL-33, IL-22, LL37, IL-18, IL-16, pulmonary and activation-regulated chemokine (CCL18), periostin, and the soluble IL-2 receptor are describing different phenotypes of disease (39). Although the very initial stage of infantile atopic dermatitis is very difficult to diagnose, the typical eczematous lesions on respective localizations emerge around the second month of life and may or may not develop into an allergic phenotype (40). Limited information is available regarding the levels of these individual markers within infants and their link to eczema. Moreover, regarding Infantile colics which were positively associated to IL-31, LIGHT, YKL-40, CXCL13, sPD1, IL1RI, sIL-7Ra, Gal-1, Gal-9, and S100A8 at 1 year of age, the impairment of the intestinal mucosal immunity significantly increases the risk of acute and chronic diseases. Within gastrointestinal diseases, a galectin-specific signature in the gut delineates Crohn's disease and ulcerative colitis from other human inflammatory intestinal disorders (41). Moreover, IL-31 is a Th2 type cytokine, which may be involved in the immune and inflammatory responses of the intestinal mucosa. During inflammation, S100A8/A9 is released actively and exerts a critical role in modulating the inflammatory response by stimulating leukocyte recruitment and inducing cytokine secretion (42). Lymphoid chemokines, such as CCL19, CCL21, and CXCL13, have an important role in the formation of secondary lymphoid organs and Peyers Patches (43, 44) These associations collectively warrant the notification within our study that the inflammatory cytokine profile has been altered, which is indicative for possible change in immune balance development.

A limitation of this study is the cross-sectional design. Ideally, more sampling time points would have given us the possibility to analyze time-dependent changes in immune marker development. Additionally, due to the sample size and cross-sectional design, no additional confounder adjustments were made, such as for the mode of delivery, which is known to contribute to an altered gut microbiome composition in the first weeks and months after birth (45). We are aware that many factors could influence the development of the immune marker profile during the first year of life other than "only" neonatal antibiotic treatment, e.g., other antibiotic courses in the first year of life. Nevertheless, this study does provide novel insights regarding the immune marker profile of a relatively healthy 1 year old population. While this is one of the largest groups of young children described in literature so far, the design of the study and sample size do not allow for determination of causal associations. However, it may help in elucidating the consequences of neonatal antibiotic treatment for the risk of developing infantile colics and atopic disorders. Although our biomarker study does show alterations within inflammatory biomarkers associated with the early life use of antibiotics, it has not been designed for development of predictive biomarker profiles. The impact of antibiotic use on clinical features has been demonstrated, which now seems reflected in small but significant alteration of biomarker profiles. However, due to the fact that a diversity of markers are changing, as not a single one stands out, combined with the small sample size, we have to conclude that our understanding of the impact of early life antibiotics use remains limited. Aforementioned factors refrain us from developing a predictive biomarker set in this regard.

In conclusion, this explorative study shows that the circulating immune marker profile at 1 year of age is affected by antibiotic treatment during the first week of life. Furthermore, infants who suffered from infantile colics in the first 3 months of life show increased gut-associated immune markers at 1 year of age. Follow-up of this cohort can elucidate whether these increased gut associated markers predispose them for gastro-intestinal disorders later in life. The results of this explorative study imply the existence of long-term negative consequences of antibiotic treatment on immune development, possibly resulting in negative health effects later in life.

DATA AVAILABILITY STATEMENT

The dataset generated to support the findings of this study are available from the corresponding author, upon reasonable request.

ETHICS STATEMENT

The studies involving human participants were reviewed and approved by the ethical board of the St. Antonius Hospital in Nieuwegein. Written informed consent to participate in this study was provided by the participants' legal guardian/next of kin.

AUTHOR CONTRIBUTIONS

BO, BL, and RE: data analysis and writing the manuscript. WJ and MK: sample analysis and critical reading of the manuscript. NR and AV: conception of the study, data collection, and critical reading of the manuscript. JG: critical reading the manuscript.

FUNDING

This work was supported by the Nutricia Research Foundation (Grant No. NRF 2016-74).

ACKNOWLEDGMENTS

We would like to thank Carin Bunkers for her help with the data collection and Ger Rijkers for his input during the design of the study. Furthermore, we would like to thank the staff of the contributing hospitals.

SUPPLEMENTARY MATERIAL

The Supplementary Material for this article can be found online at: https://www.frontiersin.org/articles/10.3389/fimmu.2019.02939/full#supplementary-material

REFERENCES

1. Gollwitzer ES, Marsland BJ. Impact of early-life exposures on immune maturation and susceptibility to disease. *Trends Immunol*. (2015) 36:684–96. doi: 10.1016/j.it.2015.09.009
2. Dominguez-Bello MG, Costello EK, Contreras M, Magris M, Hidalgo G, Fierer N, et al. Delivery mode shapes the acquisition and structure of the initial microbiota across multiple body habitats in newborns. *Proc Natl Acad Sci USA*. (2010) 107:11971–5. doi: 10.1073/pnas.1002601107
3. Guaraldi F, Salvatori G. Effect of breast and formula feeding on gut microbiota shaping in newborns. *Front Cell Infect Microbiol*. (2012) 2:94. doi: 10.3389/fcimb.2012.00094
4. Thompson AL, Monteagudo-Mera A, Cadenas MB, Lampl ML, Azcarate-Peril MA. Milk- and solid-feeding practices and daycare attendance are associated with differences in bacterial diversity, predominant communities, and metabolic and immune function of the infant gut microbiome. *Front Cell Infect Microbiol*. (2015) 5:3. doi: 10.3389/fcimb.2015.00003
5. Tanaka S, Kobayashi T, Songjinda P, Tateyama A, Tsubouchi M, Kiyohara C, et al. Influence of antibiotic exposure in the early postnatal period on the development of intestinal microbiota. *FEMS Immunol Med Microbiol*. (2009) 56:80–7. doi: 10.1111/j.1574-695X.2009.00553.x
6. Zeissig S, Blumberg RS. Life at the beginning: perturbation of the microbiota by antibiotics in early life and its role in health and disease. *Nat Immunol*. (2014) 15:307–10. doi: 10.1038/ni.2847
7. Arrieta MC, Stiemsma LT, Dimitriu PA, Thorson L, Russell S, Yurist-Doutsch S, et al. Early infancy microbial and metabolic alterations affect risk of childhood asthma. *Sci Transl Med*. (2015) 7:307ra152. doi: 10.1126/scitranslmed.aab2271
8. Rosli R, Dali AF, Abd Aziz N, Abdullah AH, Ming LC, Manan MM. Drug utilization on neonatal wards: a systematic review of observational studies. *Front Pharmacol*. (2017) 8:27. doi: 10.3389/fphar.2017.00027
9. Rutten NB, Rijkers GT, Meijssen CB, Crijns CE, Oudshoorn JH, van der Ent CK, et al. Intestinal microbiota composition after antibiotic treatment in early life: the INCA study. *BMC Pediatr*. (2015) 15:204. doi: 10.1186/s12887-015-0519-0
10. Oosterloo BC, van Elburg RM, Rutten NB, Bunkers CM, Crijns CE, Meijssen CB, et al. Wheezing and infantile colic are associated with neonatal antibiotic treatment. *Pediatr Allergy Immunol*. (2018) 29:151–8. doi: 10.1111/pai.12857
11. Marra F, Marra CA, Richardson K, Lynd LD, Kozyrskyj A, Patrick DM, et al. Antibiotic use in children is associated with increased risk of asthma. *Pediatrics*. (2009) 123:1003–10. doi: 10.1542/peds.2008-1146
12. Guideline. *Perinatal Group B-Streptococcal (GBS) Disease*. Dutch Society for Obstetrics and Gyneacology (Utrecht: NVOG) (2008).
13. Verbeke M, Schrans D, Deroose S, De Maeseneer J. The International Classification of Primary Care (ICPC-2): an essential tool in the EPR of the GP. *Stud Health Technol Inform*. (2006) 124:809–14. doi: 10.3233/978-1-58603-647-8-809
14. Benninga MA, Faure C, Hyman PE, St James Roberts I, Schechter NL, Nurko S. Childhood functional gastrointestinal disorders: neonate/toddler. *Gastroenterology*. (2016) 150:1443–55.e2. doi: 10.1053/j.gastro.2016.02.016
15. Scholman RC, Giovannone B, Hiddingh S, Meerding JM, Malvar Fernandez B, van Dijk MEA, et al. Effect of anticoagulants on 162 circulating immune related proteins in healthy subjects. *Cytokine*. (2018) 106:114–24. doi: 10.1016/j.cyto.2017.10.021
16. van den Ham HJ, de Jager W, Bijlsma JW, Prakken BJ, de Boer RJ. Differential cytokine profiles in juvenile idiopathic arthritis subtypes revealed by cluster analysis. *Rheumatology*. (2009) 48:899–905. doi: 10.1093/rheumatology/kep125
17. Rodriguez JM, Murphy K, Stanton C, Ross RP, Kober OI, Juge N, et al. The composition of the gut microbiota throughout life, with an emphasis on early life. *Microb Ecol Health Dis.* (2015) 26:26050. doi: 10.3402/mehd.v26.26050
18. Renz H, Brandtzaeg P, Hornef M. The impact of perinatal immune development on mucosal homeostasis and chronic inflammation. *Nat Rev Immunol*. (2011) 12:9–23. doi: 10.1038/nri3112
19. Marcos V, Latzin P, Hector A, Sonanini S, Hoffmann F, Lacher M, et al. Expression, regulation and clinical significance of soluble and membrane CD14 receptors in pediatric inflammatory lung diseases. *Respir Res*. (2010) 11:32. doi: 10.1186/1465-9921-11-32
20. Jin Z, Cha SH, Choi YS, Kim YI, Choi SA, Yeo SG. Expression of CXCL4 and aquaporin 3 and 10 mRNAs in patients with otitis media with effusion. *Int J Pediatr Otorhinolaryngol*. (2016) 81:33–7. doi: 10.1016/j.ijporl.2015.11.035
21. Kaetzel CS. Cooperativity among secretory IgA, the polymeric immunoglobulin receptor, and the gut microbiota promotes host-microbial mutualism. *Immunol Lett*. (2014) 162(2 Pt A):10–21. doi: 10.1016/j.imlet.2014.05.008
22. Larsen L, Chen HY, Saegusa J, Liu FT. Galectin-3 and the skin. *J Dermatol Sci*. (2011) 64:85–91. doi: 10.1016/j.jdermsci.2011.07.008
23. Gros E, Bussmann C, Bieber T, Forster I, Novak N. Expression of chemokines and chemokine receptors in lesional and nonlesional upper skin of patients with atopic dermatitis. *J Allergy Clin Immunol*. (2009) 124:753–60.e1. doi: 10.1016/j.jaci.2009.07.004
24. Milidou I, Sondergaard C, Jensen MS, Olsen J, Henriksen TB. Gestational age, small for gestational age, and infantile colic. *Paediatr Perinat Epidemiol*. (2014) 28:138–45. doi: 10.1111/ppe.12095
25. Zeevenhooven J, Koppen IJ, Benninga MA. The New Rome IV criteria for functional gastrointestinal disorders in infants and toddlers. *Pediatr Gastroenterol Hepatol Nutr*. (2017) 20:1–13. doi: 10.5223/pghn.2017.20.1.1
26. Partty A, Kalliomaki M, Salminen S, Isolauri E. Infantile colic is associated with low-grade systemic inflammation. *J Pediatr Gastroenterol Nutr*. (2017) 64:691–5. doi: 10.1097/MPG.0000000000001340
27. de Weerth C, Fuentes S, de Vos WM. Crying in infants: on the possible role of intestinal microbiota in the development of colic. *Gut Microbes*. (2013) 4:416–21. doi: 10.4161/gmic.26041
28. Chen X, Song CH, Liu ZQ, Feng BS, Zheng PY, Li P, et al. Intestinal epithelial cells express galectin-9 in patients with food allergy that plays a critical role in sustaining allergic status in mouse intestine. *Allergy*. (2011) 66:1038–46. doi: 10.1111/j.1398-9995.2011.02585.x
29. Cornelissen C, Luscher-Firzlaff J, Baron JM, Luscher B. Signaling by IL-31 and functional consequences. *Eur J Cell Biol*. (2012) 91:552–66. doi: 10.1016/j.ejcb.2011.07.006
30. Sands BE. Biomarkers of inflammation in inflammatory bowel disease. *Gastroenterology*. (2015) 149:1275–85.e2. doi: 10.1053/j.gastro.2015.07.003
31. Sundblad V, Quintar AA, Morosi LG, Niveloni SI, Cabanne A, Smecuol E, et al. Galectins in intestinal inflammation: galectin-1 expression delineates response to treatment in celiac disease patients. *Front Immunol*. (2018) 9:379. doi: 10.3389/fimmu.2018.00379
32. Camilleri M, Park SY, Scarpato E, Staiano A. Exploring hypotheses and rationale for causes of infantile colic. *Neurogastroenterol Motil.* (2017) 29:e12943. doi: 10.1111/nmo.12943
33. Vandenplas Y, Ludwig T, Bouritius H, Alliet P, Forde D, Peeters S, et al. Randomised controlled trial demonstrates that fermented infant formula with short-chain galacto-oligosaccharides and long-chain fructo-oligosaccharides reduces the incidence of infantile colic. *Acta Paediatr*. (2017) 106:1150–8. doi: 10.1111/apa.13844
34. Durieux JJ, Vita N, Popescu O, Guette F, Calzada-Wack J, Munker R, et al. The two soluble forms of the lipopolysaccharide receptor, CD14: characterization and release by normal human monocytes. *Eur J Immunol*. (1994) 24:2006–12. doi: 10.1002/eji.1830240911
35. Oesterreicher C, Pfeffel F, Petermann D, Muller C. Increased *in vitro* production and serum levels of the soluble lipopolysaccharide receptor sCD14 in liver disease. *J Hepatol*. (1995) 23:396–402. doi: 10.1016/0168-8278(95)80197-9

36. Su GL, Dorko K, Strom SC, Nussler AK, Wang SC. CD14 expression and production by human hepatocytes. *J Hepatol*. (1999) 31:435–42. doi: 10.1016/S0168-8278(99)80034-8
37. Qu B, Jia Y, Liu Y, Wang H, Ren G, Wang H. The detection and role of heat shock protein 70 in various nondisease conditions and disease conditions: a literature review. *Cell Stress Chaperones*. (2015) 20:885–92. doi: 10.1007/s12192-015-0618-8
38. Dang LV, Nilsson A, Ingelman-Sundberg H, Cagigi A, Gelinck LB, Titanji K, et al. Soluble CD27 induces IgG production through activation of antigen-primed B cells. *J Intern Med*. (2012) 271:282–93. doi: 10.1111/j.1365-2796.2011.02444.x
39. Thijs JL, van Seggelen W, Bruijnzeel-Koomen C, de Bruin-Weller M, Hijnen D. New developments in biomarkers for atopic dermatitis. *J Clin Med*. (2015) 4:479–87. doi: 10.3390/jcm4030479
40. Thijs J, Krastev T, Weidinger S, Buckens CF, de Bruin-Weller M, Bruijnzeel-Koomen C, et al. Biomarkers for atopic dermatitis: a systematic review and meta-analysis. *Curr Opin Allergy Clin Immunol*. (2015) 15:453–60. doi: 10.1097/ACI.0000000000000198
41. Papa Gobbi R, De Francesco N, Bondar C, Muglia C, Chirdo F, Rumbo M, et al. A galectin-specific signature in the gut delineates Crohn's disease and ulcerative colitis from other human inflammatory intestinal disorders. *Biofactors*. (2016) 42:93–105. doi: 10.1002/biof.1252
42. Wang S, Song R, Wang Z, Jing Z, Wang S, Ma J. S100A8/A9 in inflammation. *Front Immunol*. (2018) 9:1298. doi: 10.3389/fimmu.2018.01298
43. Mebius RE. Organogenesis of lymphoid tissues. *Nat Rev Immunol*. (2003) 3:292–303. doi: 10.1038/nri1054
44. Okada T, Ngo VN, Ekland EH, Forster R, Lipp M, Littman DR, et al. Chemokine requirements for B cell entry to lymph nodes and Peyer's patches. *J Exp Med*. (2002) 196:65–75. doi: 10.1084/jem.20020201
45. Sbihi H, Boutin RC, Cutler C, Suen M, Finlay BB, Turvey SE. Thinking bigger: how early-life environmental exposures shape the gut microbiome and influence the development of asthma and allergic disease. *Allergy*. (2019) 74:2103–15. doi: 10.1111/all.13812

Conflict of Interest: JG is head of the Division of Pharmacology, Utrecht Institute for Pharmaceutical Sciences, Faculty of Science at the Utrecht University, and partly employed by Nutricia Research. BL is employed by Nutricia Research and as indicated by the affiliations, leading a strategic alliance between Nutricia Research and University Medical Center Utrecht/Wilhelmina Children's Hospital.

The remaining authors declare that the research was conducted in the absence of any commercial or financial relationships that could be construed as a potential conflict of interest.

The handling editor declared a past co-authorship with one of the authors RE.

frontiers in Immunology

ORIGINAL RESEARCH
published: 30 January 2020
doi: 10.3389/fimmu.2019.03062

Bovine Colostrum Before or After Formula Feeding Improves Systemic Immune Protection and Gut Function in Newborn Preterm Pigs

Yanqi Li[1*†], *Xiaoyu Pan*[1†], *Duc Ninh Nguyen*[1], *Shuqiang Ren*[1], *Arshnee Moodley*[2] *and Per Torp Sangild*[1,3,4]

[1] Comparative Pediatrics and Nutrition, Department of Veterinary and Animal Sciences, University of Copenhagen, Copenhagen, Denmark, [2] Veterinary Clinical Microbiology, Department of Veterinary and Animal Sciences, University of Copenhagen, Copenhagen, Denmark, [3] Department of Pediatrics and Adolescent Medicine, Rigshospitalet, Copenhagen, Denmark, [4] Department of Paediatrics, Odense University Hospital, Odense, Denmark

OPEN ACCESS

Edited by:
Lijuan Yuan,
Virginia Tech, United States

Reviewed by:
Viviana Parreño,
Instituto Nacional de Tecnología Agropecuaria, Argentina
Francisco José Pérez-Cano,
University of Barcelona, Spain

***Correspondence:**
Yanqi Li
yli@sund.ku.dk

[†]*These authors share first authorship*

Specialty section:
This article was submitted to Nutritional Immunology, a section of the journal Frontiers in Immunology

Received: *11 October 2019*
Accepted: *16 December 2019*
Published: *30 January 2020*

Citation:
Li Y, Pan X, Nguyen DN, Ren S, Moodley A and Sangild PT (2020) Bovine Colostrum Before or After Formula Feeding Improves Systemic Immune Protection and Gut Function in Newborn Preterm Pigs. Front. Immunol. 10:3062. doi: 10.3389/fimmu.2019.03062

Objectives: Maternal milk is often absent or in limited supply just after preterm birth. Many preterm infants are therefore fed infant formula as their first enteral feed despite an increased risk of feeding intolerance, necrotizing enterocolitis (NEC), and infection. Using preterm pigs as a model for preterm infants, we hypothesized that bovine colostrum given before or after formula feeding would alleviate formula-induced detrimental effects during the first days after preterm birth.

Methods: A total of 74 preterm pigs received gradually increasing volumes of formula (F) or bovine colostrum (C) until day 5, when they were euthanized or transitioned to either C or F for another 4 days, resulting in six groups: C or F until day 5 (C5, F5, $n = 11$ each), C or F until day 9 (CC, FF $n = 12$–13 each), C followed by F (CF, $n = 14$), and F followed by C (FC, $n = 13$).

Results: Systemically, colostrum feeding stimulated circulating neutrophil recruitment on day 5 (C5 vs. F5, $P < 0.05$). Relative to initial formula feeding, initial colostrum feeding promoted the development of systemic immune protection as indicated by a decreased T-helper cell population and an increased regulatory T-cell population (CC + CF vs. FC + FF, $P < 0.01$). In the gut, colostrum feeding improved intestinal parameters such as villus heights, enzymes, hexose absorption, colonic goblet cell density, and decreased the incidence of severe NEC (27 vs. 64%), diarrhea (16 vs. 49%), and gut permeability on day 5, coupled with lowered expression of *LBP*, *MYD88*, *IL8*, *HIF1A*, and *CASP3* (C5 vs. F5, all $P < 0.05$). On day 9, the incidence of severe NEC was similarly low across groups (15–21%), but diarrhea resistance and intestinal parameters were further improved by colostrum feeding, relative to exclusive formula feeding (CC, CF, or FC vs. FF, respectively, all $P < 0.05$). The expression of *MYD88* and *CASP3* remained

downregulated by exclusive colostrum feeding (CC vs. FF, $P < 0.01$) and colostrum before or after formula feeding down regulated *HIF1A* and *CASP3* expression marginally.

Conclusion: Colostrum feeding ameliorated detrimental effects of formula feeding on systemic immunity and gut health in preterm newborns, especially when given immediately after birth.

Keywords: bovine colostrum, formula feeding, preterm infants, systemic immunity, gut health, necrotizing enterocolitis

INTRODUCTION

Optimal nutrition supply is an essential aspect of clinical care for very preterm infants (gestational age < 32 weeks). Clinical nutrition guidelines recommend initiation of enteral feeding within a few hours, and the goal is to minimize time to full enteral feeding (TFF) without inducing feeding intolerance and other intestinal complications, such as necrotizing enterocolitis (NEC) (1–4). This goal is better achieved when maternal milk (MM) is available. Unfortunately, it is often seen that MM is in short supply immediately after very preterm birth, and preterm infant formula (indicated as formula below), which is designed to mimic MM, is therefore used as the first milk, particularly in hospitals with limited resources (e.g., space for mothers, personnel and freezers to receive expressed MM, and donor milk banks). However, formula remains associated with longer TFF, increased risk of feeding intolerance and NEC (5), and impaired systemic immunity (e.g., more sepsis) (6, 7). This may be due to the fact that formula lacks many bioactive components that are present in MM and beneficial to immune defense (e.g., alpha-lactalbumin, lactoferrin, osteopontin) (8). Natural MM also contains various sugars (e.g., lactose, glucose, and oligosaccharides), while formula contains high levels of plant-derived carbohydrates (e.g., maltodextrin), which may impair antibacterial responses (9). In addition, milk fat is replaced by vegetable oil during formula processing, and therefore, formula also lacks milk fat globule membrane, which consists of numerous lipids and proteins that have functions on immune-related pathways (10, 11).

Early feeding of formula, even with small volumes for a short period, has showed detrimental effects in the gut (12, 13). Hence, it is crucial to find an alternative to formula as the first milk especially in the resource-limited hospitals. Bovine colostrum (indicated as colostrum below), the first milk from cows postpartum, contains high levels of trophic, antimicrobial, and immune-modulatory factors, such as insulin-like growth factor-I (IGF-I), immunoglobulins, lysozymes, transforming growth factor-β (TGF-β), and lactoferrin, similar to the bioactive components found in MM (14). It has been repeatedly shown that, in preterm pigs, a model for preterm infants, colostrum improves digestive and absorptive functions, dampens inflammation, protects against NEC, and improves systemic immunity, relative to formula (12, 13, 15–19). Therefore, we investigated whether initial colostrum feeding protects against later suboptimal formula feeding and whether colostrum has any therapeutic effects on an impaired intestine caused by initial formula feeding. We hypothesized that colostrum provided either before or after formula feeding just after preterm birth protected against formula-induced detrimental effects on systemic immunity and gut health. Using preterm pigs as a model for preterm infants, we fed different combinations of colostrum and isocaloric formula for 9 days and measured clinical variables, blood biochemistry and cell counts, gut functions and NEC incidence, systemic immunity, and gut immune gene expressions.

METHODS

Pigs, Experimental Design, and Nutrition

All animal procedures were approved by the Danish National Committee on Animal Experimentation. Seventy-four preterm pigs were delivered from four sows by cesarean section at 106 days gestation (Large White Danish × Landrace × Duroc, Askelygaard Farm; term = 117 ± 2 days; male/female, 36/38). Surgical procedures were performed with an orogastric feeding tube and an umbilical catheter for parental nutrition and sow's plasma (for passive immunization), as described previously (20). The pigs were stratified according to birth weight and gender and allocated randomly into two groups: one group receiving colostrum and the other group receiving formula, both for 4 days until day 5 of the experiment. On day 4, pigs in each group were further stratified according to body weight and gender and allocated randomly into three groups: euthanasia on day 5, continuation with the same feeding for another 4 days, and shift to the other diet for an additional 4 days. For pigs euthanized on day 5, there were two groups: colostrum feeding until day 5 (C5, $n = 11$) and formula feeding until day 5 (F5, $n = 11$). For pigs euthanized on day 9, there were four feeding groups: colostrum feeding until day 9 (CC, $n = 12$), colostrum feeding for 4 days followed by formula until day 9 (CF, $n = 14$), formula feeding for 4 days followed by colostrum until day 9 (FC, $n = 13$), and formula feeding until day 9 (FF, $n = 13$). For repeated variables measured before euthanasia on day 5, pigs fed colostrum and formula were termed as C and F, respectively ($n = 37$ each). A sample size of 10–15 piglets per group is often used in this model to detect a ∼50% reduction in NEC incidence ($\alpha = 0.05$, $\beta = 80\%$), and this reduction is expected when comparing bovine colostrum and infant formula feeding according to our previous studies (21).

Pigs received gradually increasing volumes of enteral nutrition from 16 ml kg^{-1} day^{-1} at birth to 64 ml kg^{-1} day^{-1} on day 4 (increasing by 16 ml kg^{-1} day^{-1}) and volumes were kept at this level on day 5 and increased gradually again

to 112 ml kg^{-1} day^{-1} on day 8 (increasing by 16 ml kg^{-1} day^{-1}). The colostrum diet was freshly prepared each day by reconstitution of 170 g colostrum powder (ColoDan, Biofiber Damino, Gesten, Denmark) into 1 L water and stored at 4°C. The formula diet was prepared by blending the following commercially available ingredients, providing protein (whey, DI-9224 whey protein isolate; casein, Miprodan 40; both from Arla Foods Ingredients, Århus, Denmark), carbohydrate (Fantomalt, from Nutricia, Allerøde, Denmark), lipids (Liquigen, Calogen; Nutricia), and vitamins and minerals (SHS Seravit; Nutricia). The amounts of each ingredient were adjusted to ensure the same macronutrient composition and energy levels for the colostrum and formula diets (**Table 1**). Before each feeding, diets were warmed in a water bath not exceeding 40°C. Parental nutrition was given to maintain sufficient amount of fluid and nutrients. The rate was 96 ml kg^{-1} day^{-1} for the first 4 days and 84 ml kg^{-1} day^{-1} for the remaining days. If the catheters dislocated before euthanasia, enteral nutrition was accordingly increased. A commercially available parenteral nutrition product (Kabiven, Fresenius Kabi, Bad Homburg, Germany) was used after adjustments, as earlier described (22). The experimental design is illustrated in **Figure 1**.

Clinical Evaluation and Sample Collection

Pigs were continually monitored and were euthanized with an intracardiac injection of pentobarbitone sodium (60 mg/kg) upon clinical indications (e.g., severe pain) or at the end of the study for sample collection. Clinical conditions, fecal characters (e.g., firm, pasty, diarrhea, bloody diarrhea), and degree of dehydration were recorded twice daily according to predefined scoring systems (18). Body weights were measured once a day, and daily weight gain was calculated. Time to motor skill acquisition was monitored every 3 h until the pigs were able to open at least one eye, to stand without support, or to walk without support. The physical activity of each pig was recorded by infrared video surveillance cameras placed over each incubator to analyze the proportion of active time using a motion-detection software (PigLWin, Ellegaard Systems, Faaborg, Denmark).

At euthanasia, organ weights of lungs, heart, liver, spleen, kidneys, adrenals, stomach, small intestine (SI), and colon were measured. The entire SI was evenly divided into three regions, proximal (Prox), middle (Mid), and distal (Dist), and the length was measured. Macroscopic lesion scores (1–6) were given to stomach, Prox, Mid, Dist, and colon, respectively, depending on the extent and severity of pathological changes such as hyperemia, edema, hemorrhage, pneumatosis, and necrosis as previously described (18). Pigs with a score of ≥3 in any of the four intestinal regions were diagnosed as "NEC," while pigs with a score of ≥4 were identified as "severe NEC." Intestinal whole-wall and mucosal tissue samples were collected from each region and immediately snap frozen in liquid nitrogen and stored at −80°C or fixed in paraformaldehyde solution for further analyses. The intact left thigh of each pig was dislocated, without breaking any bones for subsequent bacterial analysis of the bone marrow. Bacteria were cultured from aseptically collected bone marrow samples from the left femur and cerebrospinal fluid (CSF) on 5% blood agar and colonies were enumerated, isolated, and identified using matrix-assisted laser desorption/ionization time-of-flight mass spectrometry as previously described (23).

TABLE 1 | Nutrient composition of experimental diets.

Constituent L	Colostrum	Formula
SHS Seravit (g)		12
SHS Liquigen (100 ml)		43
Nutricia Calogen (100 ml)		30
Nutricia Fantomalt (g)		18
Whey protein isolate DI-9224 (g)		70
Casein Miprodan 40 (g)		35
Colondan colostrum powder (g)	170	
Energy (kJ/L)	3,405	3,398
Protein (g/L)	92.2	92.4
Whey (g/L)	62	62
Casein (g/L)	30	30
Fat (g/L)	37.4	37.1
Carbohydrate (g/L)	26.7	26.5
Maltodextrin		24
Lactose (g/L)	26.7	
Others (g/L)		2
Minerals (g/L)		
Calcium	1.70	0.41
Phosphorus	1.53	0.35
Iron (mg/L)	0	8
Sodium	0.51	0.79
Magnesium	0.34	0.04
Potassium	1.02	0.91

Blood Biochemistry, Blood Cell Count, and Systemic Immunity

Blood samples were collected at the time of euthanasia from cardiac blood, and plasma was obtained for the analysis of biochemistry and inflammatory mediators. Blood biochemistry was analyzed by the Advia 1800 Chemistry System (Siemens, Erlangen, Germany). Plasma inflammatory mediators, such as C-reactive protein, interleukin (IL)-1β, and IL-6 at euthanasia were analyzed by commercial porcine DuoSet ELISA kits according to the manufacturer's protocols (R&D Systems Denmark, Abingdon, United Kingdom). On days 5 and 9, arterial blood from the umbilical catheter was collected before euthanasia for the characterization of immune cell subsets and functions, including blood cell count by an automatic cell counter (Advia 2120i Hematology System, Siemens, Germany), T-cell profiling, and *ex vivo* neutrophil phagocytosis function by flow cytometry, as previously described (24, 25). Neutrophil phagocytosis function was measured as the proportion of phagocytic neutrophils using pHrodo Red *Escherichia coli* bioparticles phagocytosis kit for flow cytometry (Thermofisher). Briefly, whole blood was incubated with pHrodo Red-conjugated *E. coli* at ∼10:1 particle/phagocyte ratio at 37°C and 5% CO_2 for 30 min. After removing erythrocytes by the lysis buffer, leukocytes were washed and analyzed on a BD Accuri C6 flow cytometer (BD Biosciences). The proportion of phagocytic

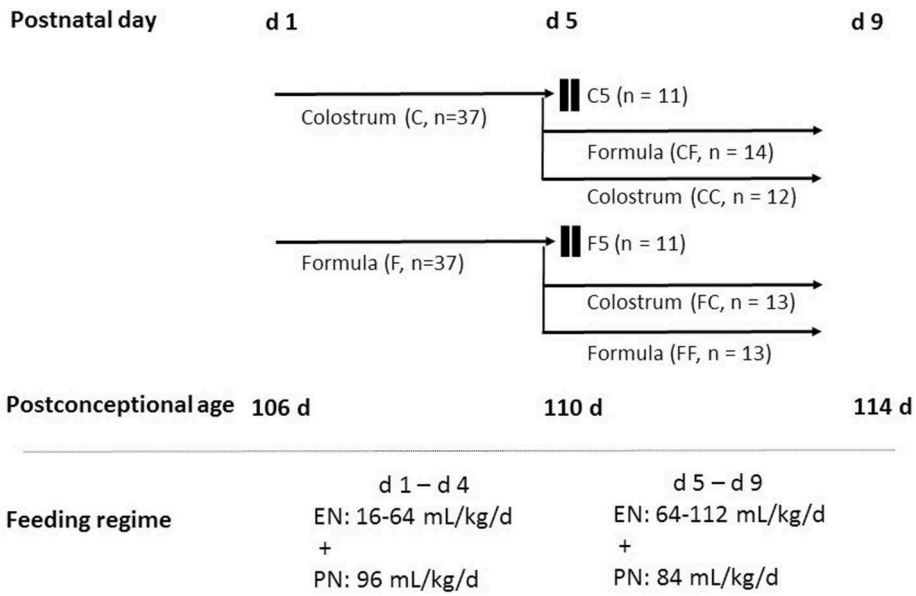

FIGURE 1 | Schematic overview of the animal experimental design. Seventy-four preterm pigs from four sows were delivered at 106 days gestation. The pigs were stratified according to birth weight and gender and allocated randomly into two groups: one group receiving colostrum (C, $n = 37$) and the other group receiving formula (F, $n = 37$) for 4 days until day 5 of the experiment. On day 4, pigs in each group were further stratified into three groups to be euthanized on day 5, fed the same feeding for another 4 days, and fed the other diet for another 4 days resulting in six groups: colostrum feeding until day 5 (C5, $n = 11$), formula feeding until day 5 (F5, $n = 11$), colostrum feeding for 4 days followed by formula until day 9 (CF, $n = 14$), colostrum feeding until day 9 (CC, $n = 12$), formula feeding for 4 days followed by colostrum until day 9 (FC, $n = 13$), and formula feeding until day 9 (FF, $n = 13$). Pigs received gradually increasing volumes of enteral nutrition 16–64 ml kg^{-1} day^{-1} on days 1–4 and 64–112 ml kg^{-1} day^{-1} on days 5–8. Parenteral nutrition was given at decreasing rates of 96–84 ml kg^{-1} day^{-1}. C, colostrum; EN, enteral nutrition; F, formula; PN, parenteral nutrition.

neutrophils was calculated as the proportion of $pHrodo^+$ neutrophils in the total neutrophil population (%).

For T-cell subset profiling, erythrocytes from whole blood were lysed by BD FACS lysing solution (BD Biosciences, Lyngby, Denmark), and the remaining leukocytes were then washed and permeabilized in fixation/permeabilization buffer (eBioscience, San Diego, CA, USA) for 30 min at 4°C in the dark. Thereafter, Fc receptors were blocked by porcine serum (10 min, 4°C in the dark), and the cells were stained with a mixture of four antibodies: PerCP-Cy5.5 conjugated anti-pig CD3 antibody (IgG2a isotype, BD Biosciences), fluorescein isothiocyanate-conjugated anti-pig CD4 antibody (IgG2b isotype, BioRad, Copenhagen, Denmark), phycoerythrin-conjugated mouse anti-pig CD8 antibody (IgG2a, isotype, Bio-Rad), and allophycocyanin-conjugated antimouse/rat Foxp3 antibody (IgG2a isotype, eBioscience). T-cell subsets were then identified by their markers using a BD Accuri C6 flow cytometer (BD Biosciences), including helper T cells (T_h, $CD3^+CD4^+CD8^-$ lymphocytes), cytotoxic T cells (T_c, $CD3^+CD4^-CD8^+$ lymphocytes), double-negative T cells (DN, $CD3^+CD4^-CD8^-$ lymphocytes), and regulatory T cells (T_{reg}, $CD3^+CD4^+Foxp3^+$ lymphocytes).

Gut Histology, Brush Border Enzyme Activities, and *in vivo* Functions

Villus height and crypt depth of three small intestinal regions (proximal, middle, and distal) were measured on light microscopy images using the Image J processing and analysis software program on HE-stained paraformaldehyde-fixed histology slices (22). Mucin-containing goblet cell density in the distal SI and colon was quantified by Alcian blue and periodic acid–Shiff staining as previously described (26). Activities of six brush border enzymes, lactase, maltase, sucrase, aminopeptidase N (ApN), aminopeptidase A (ApA), dipeptidylpeptidase IV (DPPIV) were analyzed in tissue homogenates (12). Intestinal absorptive function was assessed *in vivo* by measuring the concentration of plasma galactose after an oral bolus of 10% galactose (15 ml/kg) on days 4 and 8. Intestinal permeability was tested *in vivo* by giving an oral bolus (15 ml/kg) containing 5% lactulose and 5% mannitol 3 h before urine collection at euthanasia and measuring its lactulose to mannitol ratio. Detailed methods of these *in vivo* tests have been described earlier (22).

Intestinal Mucosal Gene Expression

Eleven genes related to gut immunity, hypoxia, apoptosis, angiogenesis, and integrity and a house keeping gene (hypoxanthine-guanine phosphoribosyltransferase, HPRT1) were selected and measured by quantitative PCR. Primers spanning the exon–exon junctions (**Table 2**) were designed using Primer3 version 0.4.0 (bioinfo.ut.ee/primer3-0.4.0) or Primer-BLAST (https://www.ncbi.nlm.nih.gov/tools/primer-blast/). In brief, frozen distal SI mucosa was homogenized, and total RNA was isolated with RNeasy Mini Kit (Qiagen, Hilden, Germany). The RNA concentration was measured using a NanoDrop 2000

TABLE 2 | List of primer sequences used for quantitative PCR (qPCR).

Gene	Forward primer	Reverse primer
HPRT1	5′–TATGGACAGGACTGAACGGC–3′	5′–ATCCAGCAGGTCAGCAAAGA–3′
MYD88	5′–GCAGCATCCCTTGGATGTCA–3′	5′–ATCCGACGGCACCTCTTTTC–3′
LBP	5′–CCCAAGGTCAATGATAAGTTGG–3′	5′–ATCTGGAGAACAGGGTCGTG–3′
IL8	5′–CTGTGAGGCTGCAGTTCTGG–3′	5′—CCAGGCAGACCTCTTTTCCAT–3′
C3	5′–ATCAAATCAGGCTCCGATGA–3′	5′–GGGCTTCTCTGCATTTGATG–3′
MPO	5′–CCCGAGTTGCTTTCCTCACT–3′	5'—AAGAAGGGGATGCAGTCACG–3′
TLR4	5′–TGGTGTCCCAGCACTTCATA–3′	5′–CAACTTCTGCAGGACGATGA–3'
HIF1A	5′–TGTGTTATCTGTCGCTTTGAGTC–3′	5′–TTTCGCTTTCTCTGAGCATTC–3′
OCLN	5′–GACGAGCTGGAGGAAGACTG–3′	5′–GTACTCCTGCAGGCCACTGT–3′
CASP3	5′–ATTGAGACGGACAGTGGGAC–3′	5′–GCTGCACAAAGTGACTGGAT–3′
VEGF	5′–ATGCGGATCAAACCTCACCA–3′	5′–TTTCGCTTTCTCTGAGCATTC–3′
OLFM4	5′–CGAATCCCAGTCGGTTTCCA–3′	5′–TGATTTCCAAGCGCTCCACT–3′

spectrophotometer (Thermo Scientific), and 2 μg of isolated RNA was converted to single-stranded complementary DNA (cDNA) using High-Capacity cDNA Reverse Transcription Kit (Cat. No. 4368814, Applied Biosystems). For quantitative PCR, 10 μl of reaction mix consisting of 1.5 μl of cDNA, 200 nM of each primer, and 5 μl of 2× concentrated master mix (LightCycler 480 SYBR Green I Master, Cat. No. 04 887352001, Roche, Mannheim, Germany) were run under the following conditions: initial denaturation at 95°C for 10 min, 45 cycles of 15 s at 95°C, 30 s at 57°C, 30 s at 72°C for the signal detection. All samples were run in duplicates in 384-well reaction plates (LightCycler 480, Roche). The relative expression of target gene was calculated by $2^{-\Delta\Delta CT}$ method and normalized to the expression level of housekeeping gene. The purity of PCR products was verified by melting curve analysis.

Statistical Analysis

Repeated measurements (e.g., physical activity) were analyzed using the linear mixed effects model followed by group comparisons using the *lsmeans* package in the software package R (version 3.2.2). Binary outcomes, such as NEC incidence, were evaluated by multiple logistic regression models, and other continuous outcome measures (e.g., weight gain) were analyzed using linear models. Time-to-event data, such as motor skill acquisition, was analyzed using cox proportional hazard model. Ordered categorical outcomes (NEC severity score) were analyzed using a proportional odds logistic regression model. The abovementioned models were all adjusted for potential confounders, including birth weight, sex, litter, and life time. *Post-hoc* Dunnett's test with FF as the control group was performed to correct for the multiple comparisons for the four groups of 9-day pigs. The normality and homoscedasticity of the residuals and fitted values were performed for model validation, and data were transformed when required. Non-parametric analysis was applied when data could not be transformed properly. Data are presented as raw arithmetic means and SEM, unless otherwise stated. $P < 0.05$ was considered as statistically significant, and $P \leq 0.15$ was discussed as a tendency to an effect.

RESULTS

Clinical Outcomes and Organ Dimensions

Three pigs in the F5 group and none in the C5 group were euthanized before the scheduled date due to severe pain. Birth weights and lifetime did not differ between C5 and F5 groups, but C5 pigs had greater daily weight gain ($P < 0.05$, **Table 3**). In the 9-day pigs, birth weights, weights at euthanasia, daily weight gain, and lifetime did not differ among groups (**Table 3**). Pigs that received exclusive or initial colostrum feeding had less diarrhea on day 4 (C vs. F, $P < 0.001$) and day 8 (CC or CF vs. FF, respectively, both $P < 0.05$, **Table 3**). At day 5, NEC incidence was reduced in C5 pigs, especially concerning severe NEC lesions (NEC score ≥ 4, $P < 0.05$), and the lesions mainly differed between groups in the colon ($P < 0.05$, **Table 3**). In the 9-day pigs, the incidences of both overall and severe NEC were similar among groups (**Table 3**). Systemic infection indicated by bacterial counts in bone marrow or CSF did not differ significantly among groups (**Table 3**). *Enterococcus* and *Staphylococcus* were the two genera identified in bone marrow tissues. Motor skill acquisition monitored by the time to first eye opening, standing, and walking did not differ among groups (**Figure 2**). The proportion of physical activity (a marker of well-being) was greater in colostrum- than formula-fed pigs on days 3 and 4 ($P < 0.05$ on both days), but was similar among groups for the remaining days (**Figure 2**).

On day 5, the relative weights of the stomach, liver, and spleen were all lower in the C5 vs. F5 pigs (all $P < 0.05$, **Table 3**), while on day 9, these and other organ weights were similar among groups. However, at this time point, stomach content weight tended to be less in FC vs. FF pigs ($P = 0.067$, **Table 3**), and likewise, the relative weight of the colon (including its contents) tended to be lower in the pigs fed colostrum exclusively or for the last days, relative to pigs fed exclusive formula ($P < 0.08$ for CC vs. FF and FC vs. FF, **Table 3**).

Blood Biochemistry

Blood biochemistry parameters (**Table 4**) showed that, despite similar protein intake, C5 pigs had lower albumin concentrations than F5 pigs on day 5 ($P < 0.05$), although these were similar among groups on day 9. In terms of liver functions, γ-glutamyltransferase was elevated, and total bilirubin was lowered in C5 vs. F5 pigs (both $P < 0.05$) but similar among groups on day 9. Conversely, cholesterol levels were highest in 9-day-old pigs fed colostrum exclusively or for the last 4 days (CC or FC vs. FF, respectively, both $P < 0.05$), while there was only a tendency to an effect at 5 days ($P = 0.122$ for C5 vs. F5).

TABLE 3 | Clinical outcomes and organ dimensions[a].

	C5	F5	P_1	CC	CF	FC	FF	P_2
N	10–11	10–11		11–12	13–14	11–13	13	
Birth weight (g)	1,104 ± 65	1,086 ± 91	0.684	1,135 ± 51	1,032 ± 80	976 ± 88	986 ± 84	0.643
Kill weight (g)	1,190 ± 72	1,119 ± 94	<0.05	1,437 ± 59	1,251 ± 103	1,120 ± 107	1,206 ± 108	0.757
Weight gain (g/day)	21 ± 3	8 ± 3	<0.05	33 ± 4	28 ± 4	25 ± 4	27 ± 4	0.789
Life time (h)	96 ± 0.2	90 ± 3.0	0.355	193 ± 0.5	188 ± 4.5	189 ± 2.4	190 ± 2.1	0.524
Diarrhea incidence on day 4, *n* (%)[b]	6 (16)	18 (49)	<0.001	–	–	–	–	–
Diarrhea incidence on day 8, *n* (%)	–	–	–	3 (25)**	6 (43)*	9 (69)	11 (85)	<0.001
NEC incidence, *n* (%)	5 (45)	8 (73)	0.097	8 (67)	10 (71)	8 (62)	10 (77)	0.798
Severe NEC incidence, *n* (%)	3 (27)	7 (64)	<0.05	2 (17)	3 (21)	2 (15)	2 (15)	0.988
SI lesion score	2.00 ± 0.43	2.36 ± 0.51	0.216	1.83 ± 0.34	2.07 ± 0.27	1.31 ± 0.17	1.38 ± 0.24	0.165
Colon lesion score	1.64 ± 0.34	3.00 ± 0.49	<0.01	2.50 ± 0.36	2.50 ± 0.27	2.62 ± 0.33	2.85 ± 0.22	0.780
Bacteria in bone marrow/CSF, *n* (%)	6 (55)	7 (78)	0.290	5 (42)	7 (54)	9 (69)	10 (83)	0.288
Bacterial load in bone marrow, cfu/g, median (IQR) × 10^4	0.3 (0–0.5)	1.3 (0–1.9)	0.239	0 (0–4.7)	1.0 (0–2.6)	0.3 (0–11)	0.6 (0.2–4.4)	0.695
Organ dimensions, relative to kill weight								
Stomach (g/kg)	5.8 ± 0.4	6.6 ± 0.5	<0.05	7.6 ± 1.0	6.0 ± 0.3	8.7 ± 1.5	6.5 ± 0.3	0.225
Stomach content (g/kg)	12.5 ± 1.7	11.1 ± 2.1	0.986	14.1 ± 2.4	15.2 ± 1.2	9.8 ± 2.4[c]	16.0 ± 2.2	0.084
Small intestine (g/kg)	29.2 ± 1.1	27.7 ± 1.0	0.466	34.7 ± 1.6	34.7 ± 1.5	31.3 ± 1.0	32.2 ± 1.2	0.167
Small intestinal length (cm/kg)	276 ± 11	286 ± 13	0.404	267 ± 12	298 ± 17	300 ± 20	318 ± 21	0.360
Colon (g/kg)	12.8 ± 0.8	13.3 ± 1.1	0.221	16.1 ± 1.1*	21.6 ± 1.6	16.5 ± 1.1[d]	20.4 ± 1.5	<0.01
Liver (g/kg)	22.5 ± 0.8	26.1 ± 1.4	<0.05	25.2 ± 1.2	25.8 ± 0.8	26.4 ± 1.8	27.6 ± 2.0	0.948
Spleen (g/kg)	1.85 ± 0.13	2.67 ± 0.36	<0.001	2.96 ± 0.22	2.68 ± 0.18	2.56 ± 0.17	2.71 ± 0.16	0.342
Heart (g/kg)	7.3 ± 0.2	7.3 ± 0.2	0.412	6.9 ± 0.3	7.0 ± 0.2	7.3 ± 0.2	6.8 ± 0.2	0.251
Lungs (g/kg)	23.6 ± 1.7	25.5 ± 2.2	0.286	26.5 ± 1.9	26.1 ± 0.9	24.5 ± 1.0	24.2 ± 1.2	0.627
Kidneys (g/kg)	9.1 ± 0.9	9.6 ± 0.6	0.961	8.8 ± 0.4	8.7 ± 0.3	9.2 ± 0.6	9.5 ± 0.5	0.499
Adrenal glands (g/kg)	0.19 ± 0.01	0.19 ± 0.01	0.561	0.17 ± 0.02	0.18 ± 0.01	0.16 ± 0.02	0.18 ± 0.02	0.705

[a] *Values are means ± SEMs unless otherwise noted; P_1 indicates the P value comparing the two 5-day groups, i.e., C5 and F5; P_2 indicates the P-value comparing the four 9-day groups, i.e., CC, CF, FC, and FF; The post-hoc comparison between the respective three groups and the control group (FF) was performed by Dunnett's test, and significance was indicated by superscript asterisks: $^*P < 0.05$, $^{**}P < 0.01$.*

[b] *Values are diarrhea incidence on day 4 in all pigs fed colostrum or formula. N = 37 in each group.*

[c] *FC vs. FF, P = 0.067.*

[d] *FC vs. FF, P = 0.078.*

C5, colostrum feeding until day 5; CC, colostrum feeding until day 9; CF, 4 days colostrum feeding followed by formula feeding until day 9; CSF, cerebrospinal fluid; F5, formula feeding until day 5; FC, 4 days formula feeding followed by colostrum feeding until day 9; FF, formula feeding until day 9; NEC, necrotizing enterocolitis.

The creatinine concentration was similar on day 5 but decreased significantly thereafter in the FF group compared with the CC group ($P < 0.05$). The last 4 days of colostrum feeding in the FC group tended to increase creatinine levels compared with FF pigs ($P = 0.094$). For blood glucose, iron, and calcium, the pigs fed colostrum exclusively or for the last 4 days (CC, FC), but not for the first 4 days (CF), had lower values than FF pigs (CC or FC vs. FF, respectively, both $P < 0.1$). For magnesium and ionized phosphate levels, colostrum-fed pigs had higher values on day 5 (C5 vs. F5, both $P < 0.01$). On day 9, ionized phosphate levels were increased by colostrum fed exclusively or for the last days (CC or FC vs. FF, respectively, both $P < 0.001$), and the increase was to a less degree for magnesium levels, both $P < 0.1$, **Table 3**).

Blood Cell Count, Neutrophil Phagocytosis, T-Cell Profiling, and Plasma Mediators

Blood cell count results are shown in **Table 5**, and a few parameters differed among groups at both time points. On day 5, the neutrophil counts and proportions were higher in the C group, whereas the proportion of lymphocytes and large unstained cells (reflecting activated lymphocytes and peroxidase-negative cells) were less than in the F group (all $P < 0.05$). Interestingly, both neutrophil count and proportion increased on day 9 in all pigs, but the increment was to a lesser degree in CF pigs (CF vs. FF, both $P < 0.05$). Accordingly, the proportions of lymphocyte and monocyte decreased from day 5 to 9, in general, but the decline in lymphocyte proportion was smaller and the monocyte proportion did not decrease in the CF group (CF vs. FF, both $P < 0.05$). The proportion of eosinophils was similar on day 5 between the groups and tended to be lower in CC vs. FF pigs on day 9 ($P = 0.065$).

The proportion of phagocytic neutrophils ($pHrodo^+$ neutrophils) was lower in the colostrum-fed pigs compared with formula-fed pigs (C vs. F, $P < 0.05$) on day 5 and decreased to ∼10% across groups by day 9 (**Figure 3A**). The frequency of blood T cells ($CD3^+$ lymphocytes) in the lymphocyte population did not differ among groups on both days (59 ± 2% in both 5-day and 9-day pigs). The frequency of cytotoxic

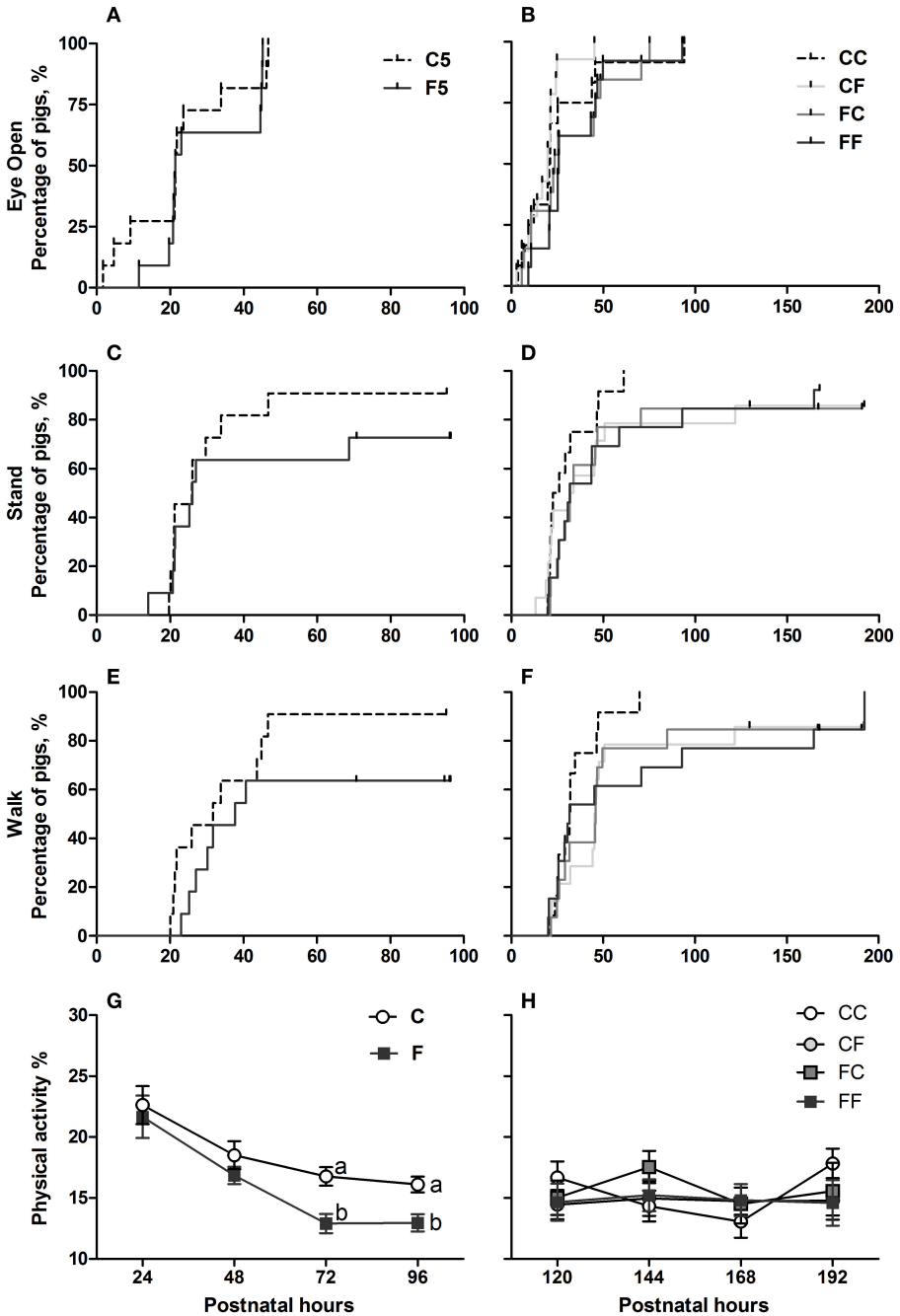

FIGURE 2 | Time to acquisition of basic motor skills and home cage activity. Kaplan–Meier plots of time to first eyelid opening **(A,B)**, first stand **(C,D)**, and first walk **(E,F)** expressed as percentage of pigs. Home cage activity percentage over postnatal hours 24–48 **(G)** and 120–192 **(H)** expressed as means ± SEM. Means marked with different letters on the same day are significantly different, $P < 0.05$. $n = 11$ for C5 and F5 groups, $n = 37$ each for C and F groups, and $n = 12$–14 for CC, CF, FC, and FF groups. C, colostrum feeding for the first 4 days; CC, colostrum feeding until day 9; CF, 4 days colostrum feeding followed by formula feeding until day 9; F, formula feeding for the first 4 days; FC, 4 days formula feeding followed by colostrum feeding until day 9; FF, formula feeding until day 9.

T cells (T_c, $CD3^+CD4^-CD8^+$) in the T-cell population was similar among groups on both days (9.9 ± 0.7% on day 5 and 13.0 ± 0.5% on day 9). The frequency of helper T cells (T_h, $CD3^+CD4^+CD8^-$) in the T-cell population was similar between the C and F groups, and on day 9, the frequency tended to be lower in the CC and CF groups compared with the FF group ($P = 0.064$ and 0.131, respectively, **Figure 3B**). Accordingly, the frequency of DN ($CD3^+CD4^-CD8^-$) in total T cell was higher or tended to be higher in the CC and CF groups compared with the FF group ($P = 0.082$ and <0.05, respectively, **Figure 3C**).

TABLE 4 | Blood biochemistry parameters[a].

	C5	F5	P_1	CC	CF	FC	FF	P_2
N	11	11		12	14	13	13	
Total protein (g/L)	26.1 ± 0.3	26.5 ± 0.9	0.132	28.4 ± 0.9	27.5 ± 0.7	29.3 ± 1.6	28.2 ± 0.8	0.692
Albumin (g/L)	9.9 ± 0.3	10.6 ± 0.4	<0.05	12.7 ± 0.6	12.2 ± 0.4	13.6 ± 1.0	13.2 ± 0.4	0.527
ALP (U/L)	2,506 ± 328	2,145 ± 311	0.175	1,447 ± 102	1,883 ± 77	1,698 ± 285	1,700 ± 180	0.190
ALT (U/L)	16.0 ± 0.9	16.1 ± 0.6	0.451	16.2 ± 0.8	16.1 ± 0.7	17.5 ± 1.2	16.9 ± 0.6	0.549
AST (U/L)	31.5 ± 9.3	34.0 ± 10.0	0.785	20.7 ± 1.6	33.5 ± 5.4	57.9 ± 12.4	27.6 ± 1.9	<0.05
GGT (U/L)	46.9 ± 5.9	26.3 ± 3.5	<0.05	34.8 ± 3.5	33.9 ± 3.0	26.2 ± 2.5	32.5 ± 3.9	0.364
Total bilirubin (μmol/L)	1.7 ± 0.4	3.2 ± 0.6	<0.05	1.1 ± 0.3	1.1 ± 0.2	2.1 ± 0.4	1.5 ± 0.3	0.350
Cholesterol (mmol/L)	2.2 ± 0.2	1.8 ± 0.2	0.122	2.4 ± 0.2**	2.0 ± 0.1	2.2 ± 0.2*	1.6 ± 0.1	<0.05
Creatinine (μmol/L)	48.8 ± 2.4	47.7 ± 1.5	0.194	48.0 ± 1.8*	43.1 ± 1.7	44.8 ± 2.5[b]	38.9 ± 2.4	0.054
Creatine kinase (U/L)	81 ± 11	80 ± 11	0.797	71 ± 5	117 ± 21	170 ± 32	96 ± 6	<0.05
BUN (mmol/L)	5.0 ± 0.7	5.8 ± 0.6	0.893	10.0 ± 1.1	10.3 ± 0.9	9.5 ± 1.0	10.4 ± 0.9	0.736
Lactate (mmol/L)	1.4 ± 0.3	1.5 ± 0.2	0.585	1.9 ± 0.3	1.6 ± 0.2	2.2 ± 0.3	2.1 ± 0.5	0.572
Glucose (mmol/L)	2.2 ± 0.3	2.5 ± 0.3	0.580	2.8 ± 0.2[c]	3.4 ± 0.3	3.0 ± 0.4	3.8 ± 0.3	0.114
Iron (μmol/L)	4.8 ± 1.0	4.0 ± 0.7	0.205	3.2 ± 0.6	4.0 ± 0.5	2.9 ± 0.5	3.9 ± 0.7	0.140
Calcium (mmol/L)	2.5 ± 0.0	2.5 ± 0.1	0.723	2.37 ± 0.03*	2.54 ± 0.03	2.39 ± 0.08[d]	2.52 ± 0.04	<0.01
Magnesium (mmol/L)	0.87 ± 0.05	0.71 ± 0.02	<0.001	0.91 ± 0.05**	0.71 ± 0.02	0.83 ± 0.03[e]	0.73 ± 0.02	<0.001
Ionized phosphate (mmol/L)	1.5 ± 0.0	1.3 ± 0.1	<0.01	1.7 ± 0.1***	1.2 ± 0.1	1.9 ± 0.1***	1.1 ± 0.1	<0.0001
Sodium (mmol/L)	144 ± 1	146 ± 1	0.983	140 ± 1	143 ± 1	145 ± 3	144 ± 1	0.560
Potassium (mmol/L)	4.1 ± 0.1	4.0 ± 0.2	0.342	4.0 ± 0.2	3.8 ± 0.1	4.1 ± 0.2	4.0 ± 0.2	0.655

[a] *Values are means ± SEMs; P_1 indicates the P-value comparing the two 5-day groups, i.e., C5 and F5; P_2 indicates the P-value comparing the four 9-day groups, i.e., CC, CF, FC, and FF; the post-hoc comparison between the respective three groups and the control group (FF) was performed by Dunnett's test, and significance was indicated by superscript asterisks: $^{*}P < 0.05$, $^{**}P < 0.01$, $^{***}P < 0.001$.*

[b] *FC vs. FF, P = 0.094.*

[c] *CC vs. FF, P = 0.078.*

[d] *FC vs. FF, P = 0.099.*

[e] *FC vs. FF, P = 0.091.*

ALP, alkaline phosphatase; ALT, alanine aminotransferase; AST, aspartate aminotransferase; GGT, gamma-glutamyltransferase; BUN, blood urea nitrogen; C5, colostrum feeding until day 5; CC, colostrum feeding until day 9; CF, 4 days colostrum feeding followed by formula feeding until day 9; CSF, cerebrospinal fluid; F5, formula feeding until day 5; FC, 4 days formula feeding followed by colostrum feeding until day 9; FF, formula feeding until day 9.

The frequency of T_{reg} cells ($CD3^+CD4^+Foxp3^+$) in the T_h population did not differ on day 5, but was higher in CC and CF pigs, relative to FF pigs with either a statistical significance or a tendency ($P = 0.089$ and <0.05, respectively, **Figure 3D**). The ratio of helper/cytotoxic T cells was similar for both diet and age (6.7 ± 0.7 on day 5 and 4.1 ± 0.2 on day 9 across groups).

Collectively, relative to initial formula feeding (pooled FF and FC pigs), initial colostrum feeding (pooled CC and CF pigs) decreased the frequency of T_h (CC + CF vs. FC + FF, 48 ± 1 vs. 55 ± 1%) and increased the frequencies of DN (39 ± 1 vs. 31 ± 2%) and T_{reg} (6 ± 0.3 vs. 4 ± 0.3%) in the T-cell population (all $P < 0.05$). Finally, plasma IL1-β was below the detection limit, and the levels of C-reactive protein and IL-6 were similar among groups on day 5 (2.69 ± 0.52 mg/L and 0.53 ± 0.10 ng/ml across groups) and on day 9 (5.09 ± 0.43 mg/L and 0.37 ± 0.02 ng/ml across groups).

Gut Histology, *in vivo* Intestinal Function, and Brush Border Enzyme Activities

Colostrum feeding increased the villus height relative to formula feeding in the proximal region of the SI on both day 5 and 9 (both $P < 0.001$, **Figure 4A**), and in the middle SI, the increment was only seen on day 9 ($P < 0.05$, **Figure 4B**). In the proximal SI, both CF and FC groups had increased villus height either significantly or with a tendency, relative to the FF group ($P < 0.001$ and $P = 0.114$, respectively, **Figure 4A**). When it comes to the crypt depth and villus/crypt ratio, any colostrum feeding (i.e., C5, CC, CF, and FC) could decrease the depth or increase the ratio, relative to formula feeding for either 4 days (i.e., F5) or 8 days (i.e., FF, all $P < 0.05$, **Figures 4D,G**). In the middle region, crypt depth was decreased in the colostrum-fed pigs on day 5 (C5 vs. F5, $P < 0.05$), and villus/crypt ratio was increased in colostrum-fed pigs both on day 5 (C5 vs. F5, $P < 0.05$) and on day 9 (CC vs. FF, $P < 0.05$, **Figures 4E,H**). In the distal region, only tendencies of increased villus height and villus/crypt ratio were observed in the CC vs. FF groups ($P = 0.143$ and $P = 0.061$, respectively, **Figures 4C,I**), and no difference was observed on crypt depth in this region (**Figure 4F**). Mucin-containing goblet cell density in the colon was also increased by colostrum feeding on day 5 (C5 vs. F5, $P < 0.05$), and on day 9, formula-fed pigs start to have similar density to the colostrum-fed pigs (**Figure 5A**).

In vivo intestinal functions such as hexose uptake and intestinal permeability were all improved in the colostrum-fed compared with the formula-fed group on day 5 (all $P < 0.001$, **Figures 5B,C**). On day 9, hexose absorption was increased in

TABLE 5 | Blood cell count parameters[a].

	C	F	P_1	CC	CF	FC	FF	P_2
N	24	24		9	10	5	8	
Total leukocyte count (10^9/L)	2.70 ± 0.18	2.44 ± 0.28	0.192	8.35 ± 1.92	6.22 ± 0.89*	6.22 ± 0.54	9.06 ± 1.86	0.105
Total erythrocyte count (10^9/L)	3.90 ± 0.09	3.71 ± 0.11	0.283	2.69 ± 0.46	3.85 ± 0.42	3.17 ± 0.39	3.29 ± 0.17	0.403
Hemoglobin	4.95 ± 0.10	4.55 ± 0.23	0.162	3.19 ± 0.56	4.58 ± 0.42	3.76 ± 0.42	3.89 ± 0.22	0.354
Hematocrit	0.28 ± 0.01	0.27 ± 0.01	0.490	0.19 ± 0.03	0.26 ± 0.02	0.22 ± 0.03	0.23 ± 0.01	0.351
MCV	72.6 ± 0.7	73.4 ± 0.8	0.583	69.4 ± 1.0	69.4 ± 0.84	70.0 ± 1.0	69.5 ± 0.8	0.993
MCHC	17.5 ± 0.1	16.7 ± 0.7	0.279	16.3 ± 0.8	17.3 ± 0.1	16.8 ± 0.4	17.0 ± 0.1	0.661
Platelets	101 ± 21	86 ± 18	0.685	464 ± 96	496 ± 53	557 ± 97	426 ± 56	0.497
MPV	13.7 ± 0.9	15.1 ± 0.7	0.280	12.3 ± 1.1	12.3 ± 0.8	15.3 ± 2.8	14.7 ± 1.3	0.980
MPC	236 ± 2	236 ± 2	0.928	242 ± 6	245 ± 4	236 ± 8	244 ± 6	0.155
Neutrophil count (10^9/L)	1.43 ± 0.13	1.17 ± 0.23	<0.05	5.97 ± 1.65	3.89 ± 0.79*	3.97 ± 0.48	6.86 ± 1.83	<0.05
Neutrophil proportion (%)	52.3 ± 2.1	43.8 ± 2.8	<0.01	65.1 ± 4.0	57.7 ± 5.2*	64.0 ± 5.7	69.9 ± 4.8	<0.05
Lymphocyte count (10^9/L)	1.08 ± 0.07	1.06 ± 0.07	0.943	1.88 ± 0.23	1.93 ± 0.16	2.01 ± 0.38	1.76 ± 0.20	0.899
Lymphocyte proportion (%)	41.3 ± 2.0	47.8 ± 2.7	<0.05	28.7 ± 3.7	35.4 ± 4.8*	32.0 ± 5.5	25.2 ± 4.5	0.065
Monocyte count (10^9/L)	0.12 ± 0.02	0.12 ± 0.02	0.830	0.29 ± 0.09	0.27 ± 0.04	0.14 ± 0.02	0.20 ± 0.04	0.729
Monocyte proportion (%)	4.3 ± 0.5	4.9 ± 0.5	0.228	3.3 ± 0.4	4.5 ± 0.5*	2.2 ± 0.5	2.5 ± 0.6	<0.05
Eosinophil count (10^8/L)	0.11 ± 0.02	0.09 ± 0.02	0.249	0.36 ± 0.11	0.32 ± 0.04	0.42 ± 0.10	0.95 ± 0.50	0.262
Eosinophil proportion (%)	0.4 ± 0.1	0.4 ± 0.1	0.718	0.4 ± 0.1[b]	0.6 ± 0.1	0.7 ± 0.2	0.9 ± 0.3	0.106
Basophil count (10^8/L)	0.04 ± 0.01	0.05 ± 0.01	0.717	0.08 ± 0.03	0.09 ± 0.01	0.14 ± 0.06	0.11 ± 0.04	0.975
Basophil proportion (%)	0.2 ± 0.02	0.2 ± 0.03	0.546	0.2 ± 0.05	0.2 ± 0.02	0.2 ± 0.08	0.2 ± 0.04	0.769
LUC count (10^8/L)	0.45 ± 0.09	0.72 ± 0.15	0.066	1.56 ± 0.38	0.94 ± 0.15	0.54 ± 0.14	1.29 ± 0.41	0.421
LUC proportion (%)	1.5 ± 0.3	2.8 ± 0.3	<0.001	2.2 ± 0.5	1.7 ± 0.3	0.9 ± 0.02	1.5 ± 0.3	0.355

[a] *Values are means ± SEMs; P_1 indicates the P-value comparing the two groups fed colostrum or formula on day 5, i.e., C and F; P_2 indicates the P-value comparing the four 9-day groups, i.e., CC, CF, FC, and FF; the post-hoc comparison between the respective three groups and the control group (FF) was performed by Dunnett's test and significance was indicated by superscript asterisks: *$P < 0.05$.*

[b] *CC vs. FF, $P = 0.063$.*

C, colostrum feeding; CC, colostrum feeding until day 9; CF, 4 days colostrum feeding followed by formula feeding until day 9; CSF, cerebrospinal fluid; F, formula feeding; FC, 4 days formula feeding followed by colostrum feeding until day 9; FF, formula feeding until day 9; LUC, large unstained cells; MCHC, mean corpuscular hemoglobin concentration; MCV, mean corpuscular volume; MPC, mean platelet component; MPV, mean platelet volume.

CC and CF groups, and the permeability was decreased in CC, CF, and FC groups, relative to the FF group (all $P < 0.05$, **Figures 5B,C**). Compared with the F5 group, the activity of brush border sucrose was similar, while maltase was lower in the C5 group in all SI regions (all $P < 0.01$, **Figures 6A,C**), whereas the other enzyme activities were all increased in the C5 group in the proximal region and in one of the middle and distal regions (all $P < 0.05$, **Figures 6E,G,I,K**). On day 9, all colostrum-feeding groups, i.e., CC, CF, and FC, had higher enzyme activities than the FF group (all $P < 0.01$, **Figures 6B,D,F,H,J,L**). The activities of lactase, ApA, and DPPIV in the middle SI were also increased by any colostrum feeding (CC, CF, and FC vs. FF, respectively, all $P < 0.05$, **Figures 6B,F,J,L**). The maltase activity was decreased and ApN activity was increased in CC vs. FF groups in the middle region (both $P < 0.05$, **Figures 6D,H**). Distal enzyme activities were not influenced by feeding in general on day 9, except for the lactase activity being marginally higher in CC and CF groups compared with FF group ($P = 0.068$ and $P < 0.05$, respectively, **Figure 6F**). Collectively, the results indicate that any colostrum feeding (provided to CC, CF, or FC pigs) reduced the damaging effects of a period of formula feeding (provided to FF pigs) in the intestinal structure, function, and integrity.

Gene Expression Related to Inflammation, Proliferation, and Tight Junctions

The genes related to gut innate immune response, such as lipopolysaccharide (LPS) binding protein (*LBP*), myeloid differentiation primary response 88 (*MYD88*), interleukin-8 (*IL8*), and complement C3 (*C3*) were all upregulated in F5 compared with C5 pigs on day 5 (all $P < 0.01$, except for *C3*, $P = 0.053$, **Figures 7A–D**). The genes related to tissue hypoxia, integrity, and apoptosis, namely, hypoxia inducible factor 1 subunit alpha (*HIF1A*), occludin (*OCLN*), and caspase-3 (*CASP3*), were also upregulated in the F5 group (all $P < 0.05$, **Figures 7G–I**). The genes related to immune defense, myeloperoxidase (MPO) and toll-like receptor 4 (TLR4), angiogenesis, vascular endothelial growth factor (*VEGF*), and an intestinal stem cell marker, olfactomedin 4 (*OLFM4*), did not differ between C5 and F5 groups (**Figures 7E,F,J,K**). On day 9, the expression of *MYD88* ($P < 0.01$, **Figure 7B**), *HIF1A* ($P = 0.117$, **Figure 7G**), *OCLN* ($P = 0.059$, **Figure 7H**), and *CASP3* ($P < 0.01$, **Figure 7I**) remained higher in the formula-fed pigs (FF group), relative to pigs fed with only colostrum (CC group). Feeding colostrum before or after a period of formula feeding (CF or FC) did not modulate the expression of analyzed genes except for some tendencies in *HIF1A* (CF vs. FF, $P = 0.091$, **Figure 7G**)

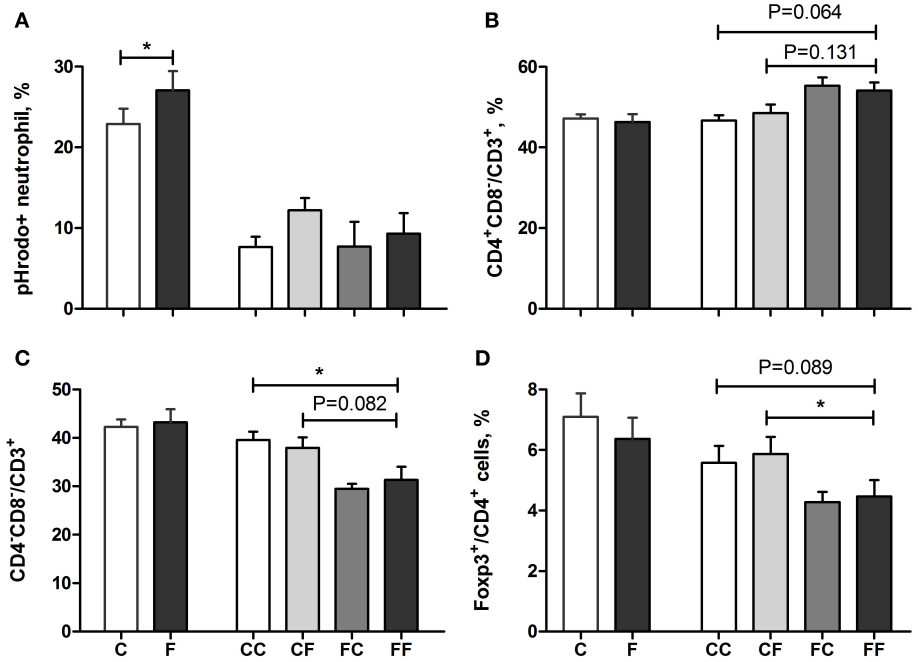

FIGURE 3 | Systemic immunity, including neutrophil function and blood T-cell subsets. Neutrophil phagocytic rate **(A)**, T_h frequency **(B)**, DN frequency **(C)**, and T_{reg} frequency **(D)**. $n = 21$–27 for C and F groups and $n = 4$–8 for CC, CF, FC, and FF groups. Values (means ± SEM) designated with asterisks are significantly different, $^*P < 0.05$; T_h, helper T cells. DN, double-negative T cells; T_{reg}, regulatory T cells; C, colostrum feeding for the first 4 days; CC, colostrum feeding until day 9; CF, 4 days colostrum feeding followed by formula feeding until day 9; F, formula feeding for the first 4 days; FC, 4 days formula feeding followed by colostrum feeding until day 9; FF, formula feeding until day 9.

and *CASP3* (CF and FC vs. FF, $P = 0.079$ and 0.065, respectively, **Figure 7I**). Collectively, proinflammatory response was mainly dampened by colostrum feeding during the first 5 days, whereas hypoxia and apoptosis response was downregulated by initial or any period of colostrum feeding.

DISCUSSION

We have previously shown the effects of colostrum feeding on systemic immunity, gut function and immunity, and NEC protection in this preterm pig model. Systemically, early colostrum feeding prevented septic shock and ameliorated neuroinflammation in preterm piglets that received intra-arterial *Staphylococcus epidermidis* (15). In the gut, piglets fed with colostrum as minimal enteral nutrition (12), full enteral nutrition (16), or supplementation to donor milk (17, 19) showed improved digestive functions, integrity, anti-inflammatory responses, and NEC resistance. Several clinical trials are being performed in very preterm infants to document this for its clinical application (14, 27, 28). A pilot study has demonstrated the feasibility and tolerability of initial colostrum feeding (27, 28), which has led to an ongoing randomized clinical trial powered for TFF as the primary outcome in very preterm infants (ClinicalTrials.gov Identifier: NCT03085277). How colostrum feeding before or after suboptimal formula feeding protects or restores formula-induced intestinal impairment still remains unclear. Similar to previous short-term studies (5 days), our results show that colostrum feeding improved weight gain and protected against NEC and diarrhea. The intestinal structure, digestive and absorptive functions, and barrier function were all improved by colostrum feeding, accompanied by lower expression of genes related to innate immune activation, apoptosis, and hypoxia in the gut tissue. Meanwhile, colostrum feeding increased total blood neutrophil count/proportion, indicating the maturational effect of colostrum in innate immunity. Newly recruited neutrophils may not be fully functional, explaining the higher portion of non-phagocytic neutrophils in colostrum- vs. formula-fed pigs.

In a longer term study when following the pigs for 9 days, diet-dependent NEC sensitivity decreased with age and weight gain increased to the similar levels in both colostrum- and formula-fed pigs, whereas the diarrhea incidence remained higher in the formula-fed pigs. The intestinal structure, functions, and integrity remained superior in the colostrum pigs, and apoptosis and hypoxia-related genes were still expressed at a lower level. Colostrum feeding for 8 days decreased the frequency of T_h and increased the frequencies of double-genitive T_c and T_{reg}. Initial 4 days colostrum feeding was able to prevent later formula-induced diarrhea and gut structural and functional impairment. In addition, the frequencies of T_h, double-genitive T_c and T_{reg}, and apoptosis/hypoxia-related genes were similarly regulated by first 4 days colostrum feeding as exclusive colostrum feeding. Later 4 days colostrum feeding could restore formula-induced gut impairment and the upregulation of an apoptosis gene.

In this study, NEC lesions were more subclinical and primarily contained to the colon region, similar to our previous studies using gradual advancement of enteral feeding (12). More severe NEC cases were observed in formula-fed pigs on day 5, but the

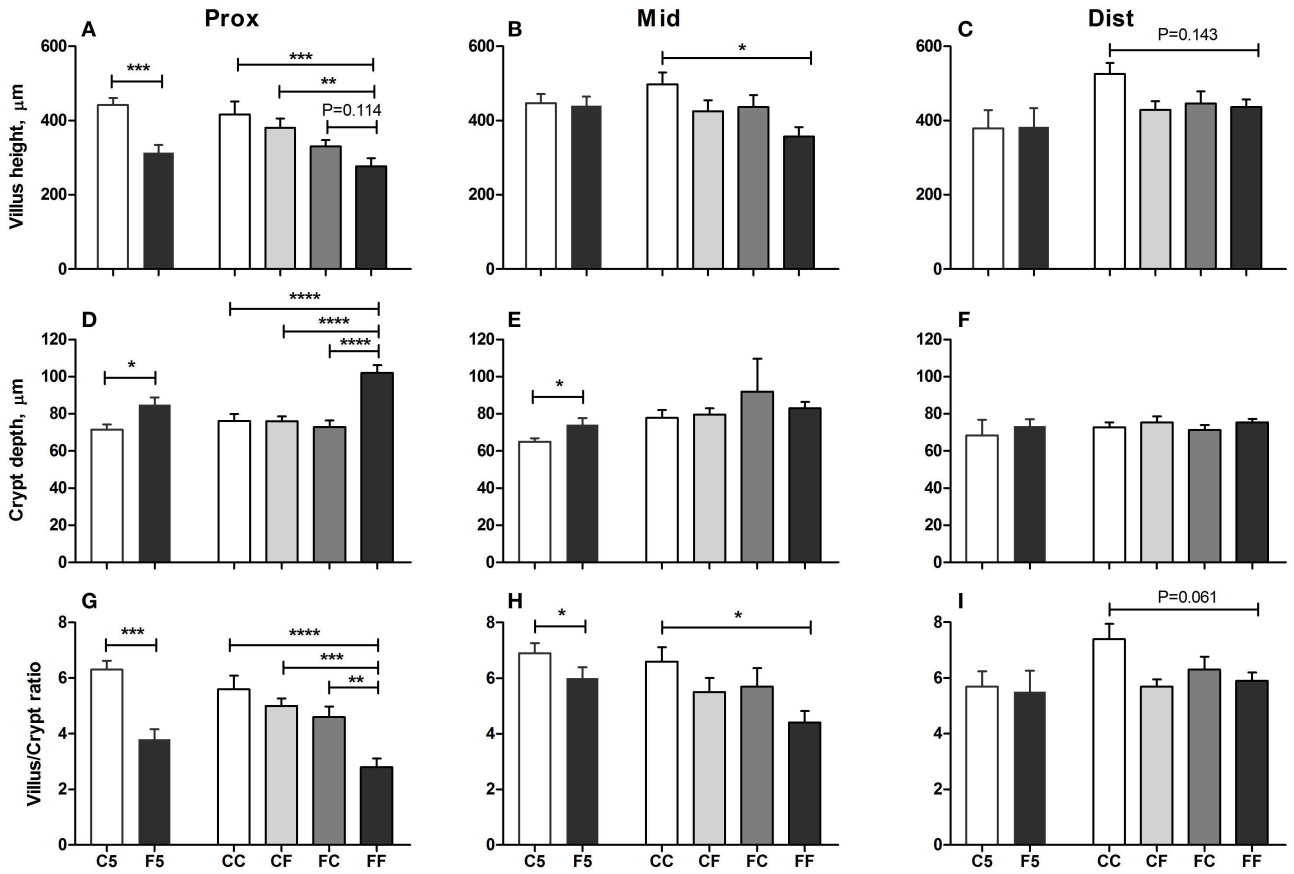

FIGURE 4 | Mucosal morphology. Villus heights in the proximal, middle, and distal small intestine **(A–C)**, crypt depth in the proximal, middle, and distal small intestine **(D–F)**, villus/crypt ratio in the proximal, middle, and distal small intestine **(G–I)**. Values (means ± SEM) designated with asterisks are significantly different, $^{*}P < 0.05$, $^{**}P < 0.01$, $^{***}P < 0.001$, $^{****}P < 0.0001$. $n = 11$ for C5 and F5 groups and $n = 12$–14 for CC, CF, FC, and FF groups. C5, colostrum feeding until day 5; CC, colostrum feeding until day 9; CF, 4 days colostrum feeding followed by formula feeding until day 9; F5, formula feeding until day 5; FC, 4 days formula feeding followed by colostrum feeding until day 9; FF, formula feeding until day 9.

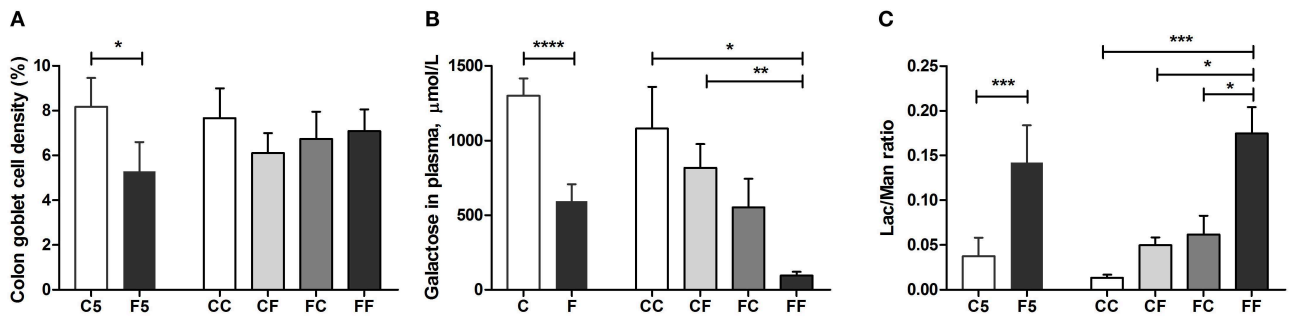

FIGURE 5 | Goblet cell density and *in vivo* intestinal functions. Goblet cell density in the colon **(A)**, intestinal hexose absorptive capacity on days 4 and 8 **(B)**, and intestinal permeability measure before euthanasia **(C)**. Values (means ± SEM) designated with asterisks are significantly different, $^{*}P < 0.05$, $^{**}P < 0.01$, $^{***}P < 0.001$, $^{****}P < 0.0001$. $n = 8$–11 for C5 and F5 groups, $n = 33$ each for C and F groups, and $n = 7$–14 for CC, CF, FC, and FF groups. C, colostrum feeding for the first 4 days; C5, colostrum feeding until day 5; CC, colostrum feeding until day 9; CF, 4 days colostrum feeding followed by formula feeding until day 9; F, formula feeding for the first 4 days; F5, formula feeding until day 5; FC, 4 days formula feeding followed by colostrum feeding until day 9; FF, formula feeding until day 9.

severity decreased over time in the 9-day-old pigs. This differed from our earlier studies where formula feeding increased NEC severity relative to colostrum both on day 5 (12) and in longer term studies [57% severe NEC on day 11 (18)]. Maldigestion of maltodextrin, the common carbohydrate source in preterm formula (29), is considered to induce NEC, at least in preterm pigs (30). Maltodextrin was used in the current study to induce NEC, but the concentration was low to match the carbohydrate

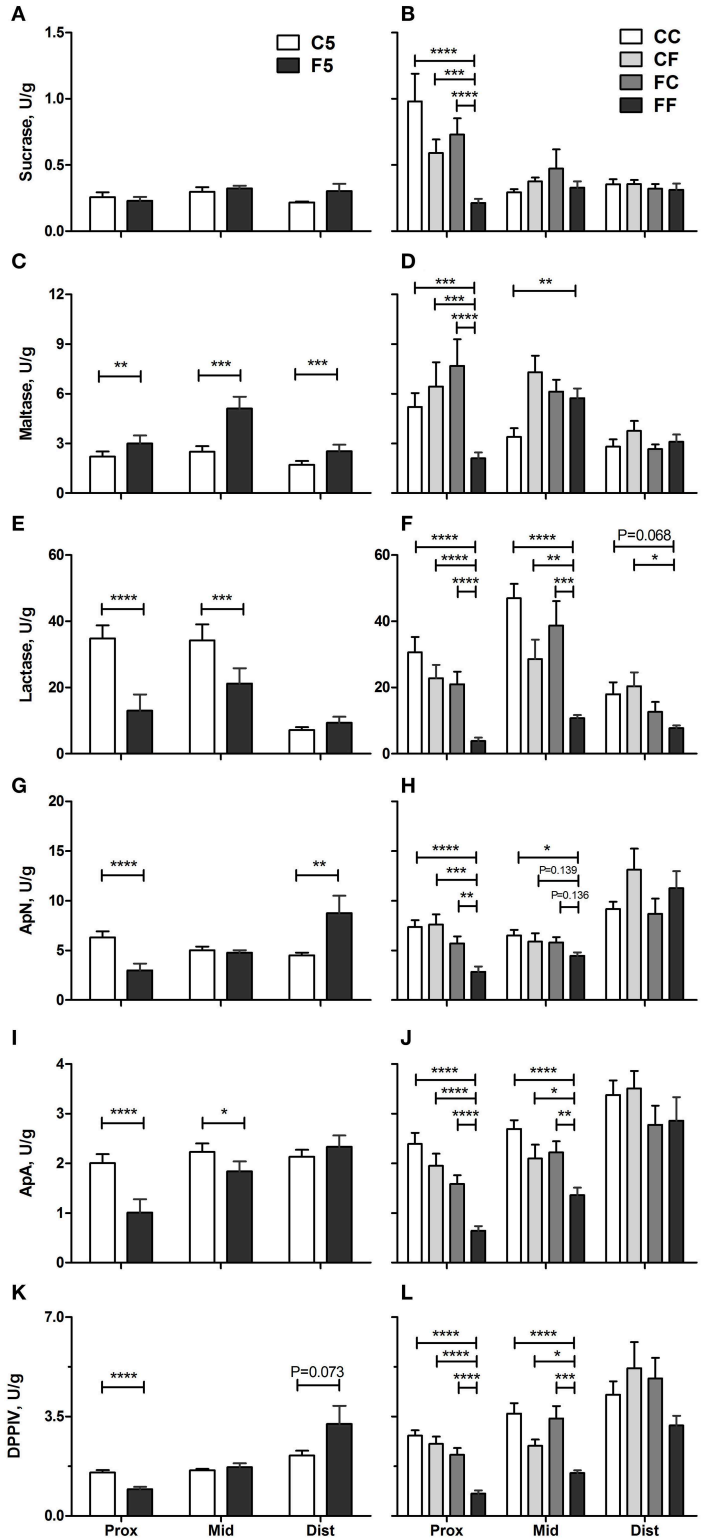

FIGURE 6 | Brush border enzyme activities. Sucrase **(A,B)**, maltase **(C,D)**, lactase **(E,F)**, ApN **(G,H)**, ApA **(I,J)**, and DPPIV **(K,L)** in the proximal, middle, and distal small intestine. Values (means ± SEM) designated with asterisks are significantly different, $^{*}P < 0.05$, $^{**}P < 0.01$, $^{***}P < 0.001$, $^{****}P < 0.0001$. $n = 11$ each for C5 and F5 groups, and $n = 12$–14 for CC, CF, FC, and FF groups. ApA, aminopeptidase A; ApN, aminopeptidase N; C5, colostrum feeding until day 5; CC, colostrum feeding until day 9; CF, 4 days colostrum feeding followed by formula feeding until day 9; DPPIV, dipeptidylpeptidase IV; F5, formula feeding until day 5; FC, 4 days formula feeding followed by colostrum feeding until day 9; FF, formula feeding until day 9.

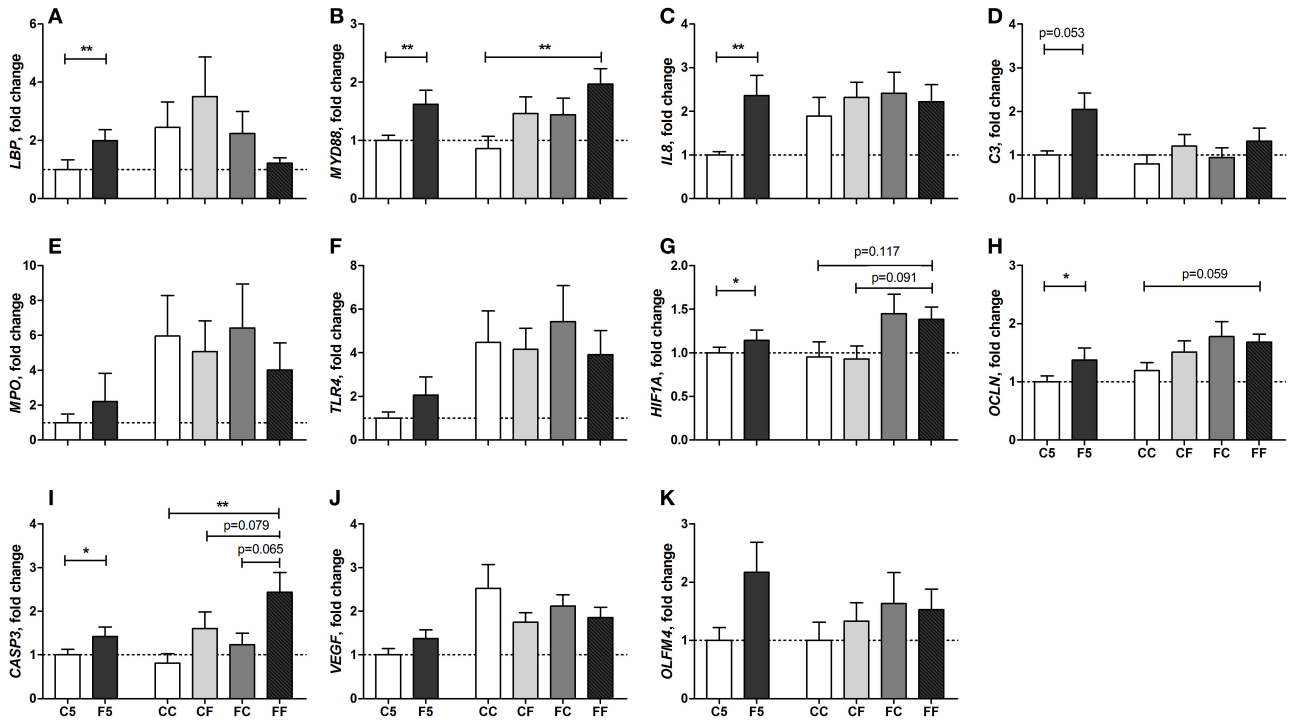

FIGURE 7 | Fold change of intestinal gene expression levels relative to the C5 group. *LBP* **(A)**, *MYD88* **(B)**, *IL8* **(C)**, *C3* **(D)**, *MPO* **(E)**, *TLR4* **(F)**, *HIF1A* **(G)**, *OCLN* **(H)**, *CASP3* **(I)**, *VEGF* **(J)**, *OLFM4* **(K)** in the distal small intestine. Values (means ± SEM) designated with asterisks are significantly different, $^{*}P < 0.05$, $^{**}P < 0.01$. $n = 8$ each for C5 and F5 groups, and $n = 9$–13 for CC, CF, FC, and FF groups. C5, colostrum feeding until day 5; CC, colostrum feeding until day 9; CF, 4 days colostrum feeding followed by formula feeding until day 9; F5, formula feeding until day 5; FC, 4 days formula feeding followed by colostrum feeding until day 9; FF, formula feeding until day 9.

level in colostrum (27 g/L), which may partly explain the lower NEC severity in formula-fed pigs compared with the previous study [84 g/L (18)]. Moreover, colon barrier function indicated by the density of mucin-containing goblet cells was initially reduced by formula feeding and restored over time, which may also be related to the decline of NEC severity over time. Genes related to immune defense (TLR4, MPO), barrier function (OCLN), and angiogenesis (VEGF) were generally higher on day 9 than on day 5 disregarding feeding. In addition, gut microbiota also play important role in NEC development. A systemic review reported microbial dysbiosis before NEC onset as increased *Proteobacteria* and decreased *Firmicutes* and *Bacteroidetes* in preterm infants (31). In the same model, rectal transplantation with fecal microbiota from healthy term piglet donors decreased the NEC incidence in formula-fed preterm piglets, indicating important microbial effects in NEC pathogenesis (32). When it comes to feeding, colonic microbiota did not differ between colostrum- and formula-fed 5-day-old pigs (12), while the diversity was increased and *Campylobacter* was decreased in colostrum-fed 11-day-old pigs (18). Whether the beneficial effects of colostrum attribute (or partly) to gut microbiota remains to be investigated.

Despite the minimal effects on macroscopic NEC lesions in the SI region, structural, and functional parameters were largely impaired by formula feeding both in short- and longer-term studies. Similar to our previous results, formula feeding, irrespective if given in large volumes in a rapid advancing manner or small volumes in a slow advancing manner, induces villus atrophy (decreased villus height and increased crypt depth), digestive dysfunction, and increased permeability (12, 16, 22). In a previous study, we showed that formula-induced villus atrophy in preterm pigs may be due to increased enterocyte apoptosis (33), which is supported by the upregulation of an apoptosis gene, *CASP3* in the formula-fed pigs in this study. Bioactive factors found in high amounts in colostrum, such as lactoferrin, TGF-β2, and IGF-I, have been shown to attenuate epithelial apoptosis in cell and animal models (34–36). In this study, colostrum feeding was able to prevent and restore formula-induced impairment in terms of villus atrophy, digestive and absorptive functions, and permeability, which may relate to its apoptosis-suppressed effects supported by the similarly downregulation of CASP3 in the CF and FC groups, relative to the FF group.

Furthermore, the impaired gut structure and increased permeability may allow bacteria and/or toxins to adhere to mucosae and translocate, leading to local inflammation or even systemic immune stimulation. Fluorescence *in situ* hybridization staining showed that colostrum-fed pigs had less bacterial adhesion to SI mucosa relative to the formula-fed ones (18, 19). The close contact with bacteria and its toxins induces mucosal inflammation and further deteriorate gut integrity. In the current study, gut innate immunity- and hypoxia-related genes such as *LBP, MYD88, IL8*, and *C3* were upregulated in formula-fed pigs

as shown in previous studies (12, 17, 18, 37). *LBP* regulates the transcription of LPS binding proteins in enterocytes, which binds and deactivates LPS during the acute phase response to endotoxin (38). The upregulation of MYD88 (an adaptor protein activates the transcription of NF-κB), IL8 (a key neutrophil chemoattractant and activator), and C3 (a key component in complement system facilitating phagocytosis or direct lysis of targeted cells) designated the activation of Toll-like receptor pathways and enhanced neutrophil recruitment and phagocytosis in response to the inflammatory challenge (18, 39). These genes were less affected by diets in 9-day-old pigs, which may reflect a reduction in inflammatory challenge to the mucosa over time.

Mucosal inflammation limits the oxygen availability and may lead to secondary hypoxia in the epithelial cells and subsequent inflammatory lesions (40). Upregulated HIF1A (the master transcriptional regulator of hypoxia stress) has been observed in human NEC tissues (41), and its downregulation by colostrum feeding might be an important strategy in preventing inflammatory lesions in the gut. Our results showed that the initial downregulation of HIF1A by colostrum feeding persisted on day 9 even when switched to formula feeding for the last 4 days. These gut effects of colostrum may attribute to the high levels of bioactive compounds that neutralize bacteria and toxins (e.g., lysozyme, lactoferrin, Igs), stimulate intestinal function and integrity (e.g., IGF-I, TGF-β, lactoferrin), or attenuate inflammation, apoptosis, and oxidative and hypoxic stress (e.g., lactoferrin, TGF-β) (33, 42, 43).

Relative to exclusive formula feeding, initial feeding of colostrum for 4 days influenced the development of T-cell subpopulation on day 9, even when switched to formula feeding, including lowered T_h and increased T_{reg} and DN frequencies. Lowered T_h frequency has also been observed in breast-fed infants compared with formula-fed ones, suggesting less systemic immune activation in MM-fed infants (44). The corresponding increase in T_{reg} reflected the development of immune tolerance toward excessive inflammatory response in the circulation. This effect of colostrum on systemic immune regulation may function via the gut by dampening mucosal proinflammatory response immediately after birth and potentially reducing gut translocation of bacteria and toxins. It is noteworthy that the flow cytometer used in this study can maximally detect four colors, which limited our choice to staining for CD3, CD4, CD8, and Foxp3. Although $CD4^+CD25^+Foxp3^+$ are often used as T_{reg} markers, it has been reported that T_{reg} can be present in both $CD25^+$ and $CD25^-$ forms with similar capacity of producing anti-inflammatory cytokines (IL-10 and TGF-β) in pigs (45). Therefore, it is considered sufficient, at least in pigs, to use $CD3^+CD4^+Foxp3^+$ as markers for T_{reg}. Similarly, NK cells in pigs are $CD3^-$ (46, 47) and therefore are not categorized as T_c cells (stained as $CD3^+CD4^-CD8^+$) in this study. However, some subsets of NKT cells in pigs may express CD8, so the T_c cells in this study may contain some NKT cells, although with very low frequency [0.01–1% of total $CD3^+$ T cells (48)].

In the current study, we aimed to investigate the effects of intact colostrum as a food matrix, rather than investigating individual bioactive components separately. In a recent large randomized controlled trial with 2,203 preterm infants, oral supplementation of bovine lactoferrin (the most promising single bioactive milk compound) failed to reduce the risk of late-onset infection and other morbidities (49). Possibly, these bioactive factors found in milk may function in synergy, and an isolated factor may not be effective. Nevertheless, unmodified colostrum should not be used as the sole food for infants, as it contains unbalanced nutrient composition relative to human milk. For example, colostrum contains high proteins, low carbohydrates, and different levels of vitamins and minerals compared with MM and formula (14). On the other hand, severely modified colostrum will lose its bioactivity and may exert detrimental effect in preterm infants (50). In conclusion, our study underlines the importance of initial enteral feeding and how initial feeding shapes the developmental trajectory of intestinal health and systemic immunity in preterm neonates. Although colostrum also had some therapeutic effects to repair the detrimental effects induced by formula feeding, it was more restricted in the digestive system with less strength. Thus, bovine colostrum is suggested to be used as the initial feeding to prepare the digestive and immune systems in very preterm infants for the later consumption of formula in resource-limited hospitals, when MM is not available immediately after birth.

DATA AVAILABILITY STATEMENT

The datasets generated for this study are available on request to the corresponding author.

ETHICS STATEMENT

The animal study was reviewed and approved by Danish National Committee on Animal Experimentation.

AUTHOR CONTRIBUTIONS

YL, XP, DN, and PS designed research and interpreted the data. YL and XP conducted the animal experiments. XP, SR, and AM conducted lab analyses. YL analyzed data and wrote the paper. All authors critically revised and approved the final manuscript.

FUNDING

The study was funded by the Innovation Fund Denmark (NEOCOL, grant number 6150-00004B) and Biofiber Damino, Denmark. The funding bodies were not involved in the study design, collection, analysis, interpretation of data, the writing of this article or the decision to submit it for publication.

ACKNOWLEDGMENTS

We thank Elin Skytte, Kristina Møller, Jane Povlsen, Jing Sun, Tik Muk, Tine Røngaard Stange Jensen, Wenchao Chen, Charlotte Holme Nielsen, Line Møller, and Anders Brunse for their technical support with animal procedures and/or laboratory analyses.

REFERENCES

1. Agostoni C, Buonocore G, Carnielli VP, De Curtis M, Darmaun D, Decsi T, et al. Enteral nutrient supply for preterm infants: Commentary from the european society of paediatric gastroenterology, hepatology and nutrition committee on nutrition. *J Pediatr Gastroenterol Nutr*. (2010) 50:85–91. doi: 10.1097/MPG.0b013e3181adaee0
2. Fallon EM, Nehra D, Potemkin AK, Gura KM, Simpser E, Compher C, et al. A.S.P.E.N. clinical guidelines: nutrition support of neonatal patients at risk for necrotizing enterocolitis. *J Parenter Enter Nutr*. (2012) 36:506–23. doi: 10.1177/0148607112449651
3. Dutta S, Singh B, Chessell L, Wilson J, Janes M, McDonald K, et al. Guidelines for feeding very low birthweight infants. *Nutrients*. (2015) 7:423–42. doi: 10.3390/nu7010423
4. Cai W. CSPEN guidelines for nutrition support in neonates. *Asia Pac J Clin Nutr*. (2013) 22:655–63. doi: 10.6133/apjcn.2013.22.4.21
5. Menon G, Williams TC. Human milk for preterm infants: why, what, when and how? *Arch Dis Child Fetal Neonatal Ed*. (2013) 98:559–63. doi: 10.1136/archdischild-2012-303582
6. Patel AL, Johnson TJ, Engstrom JL, Fogg LF, Jegier BJ, Bigger HR, et al. Impact of early human milk on sepsis and health-care costs in very low birth weight infants. *J Perinatol*. (2013) 33:514–9. doi: 10.1038/jp.2013.2
7. Corpeleijn WE, Kouwenhoven SMP, Paap MC, Van Vliet I, Scheerder I, Muizer Y, et al. Intake of own Mother's milk during the first days of life is associated with decreased morbidity and mortality in very low birth weight infants during the first 60 days of life. *Neonatology*. (2012) 102:276–81. doi: 10.1159/000341335
8. Lönnerdal B. Infant formula and infant nutrition: bioactive proteins of human milk and implications for composition of infant formulas. *Am J Clin Nutr*. (2014) 99:712–7. doi: 10.3945/ajcn.113.071993
9. Nickerson KP, Chanin R, McDonald C. Deregulation of intestinal anti-microbial defense by the dietary additive, maltodextrin. *Gut Microbes*. (2015) 6:78–83. doi: 10.1080/19490976.2015.1005477
10. Yang M, Cong M, Peng X, Wu J, Wu R, Liu B, et al. Quantitative proteomic analysis of milk fat globule membrane (MFGM) proteins in human and bovine colostrum and mature milk samples through iTRAQ labeling. *Food Funct*. (2016) 7:2438–50. doi: 10.1039/C6FO00083E
11. Timby N, Domellöf M, Lönnerdal B, Hernell O. Supplementation of infant formula with bovine milk fat globule membranes. *Adv Nutr*. (2017) 8:351–5. doi: 10.3945/an.116.014142
12. Shen RL, Thymann T, Østergaard MV, Støy ACF, Krych Ł, Nielsen DS, et al. Early gradual feeding with bovine colostrum improves gut function and NEC resistance relative to infant formula in preterm pigs. *Am J Physiol Gastrointest Liver Physiol*. (2015) 309:G310–23. doi: 10.1152/ajpgi.00163.2015
13. Støy ACF, Heegaard PMH, Thymann T, Bjerre M, Skovgaard K, Boye M, et al. Bovine colostrum improves intestinal function following formula-induced gut inflammation in preterm pigs. *Clin Nutr*. (2014) 33:322–9. doi: 10.1016/j.clnu.2013.05.013
14. Ahnfeldt AM, Hyldig N, Li Y, Kappel SS, Aunsholdt L, Sangild PT, et al. FortiColos - a multicentre study using bovine colostrum as a fortifier to human milk in very preterm infants: study protocol for a randomised controlled pilot trial. *Trials*. (2019) 20:1–9. doi: 10.1186/s13063-019-3367-7
15. Brunse A, Worsøe P, Pors SE, Skovgaard K, Sangild PT. Oral supplementation with bovine colostrum prevents septic shock and brain barrier disruption during bloodstream infection in preterm newborn pigs. *Shock*. (2019) 51:337–47. doi: 10.1097/SHK.0000000000001131
16. Jensen ML, Sangild PT, Lykke M, Schmidt M, Boye M, Jensen BB, et al. Similar efficacy of human banked milk and bovine colostrum to decrease incidence of necrotizing enterocolitis in preterm piglets. *Am J Physiol Integr Comp Physiol*. (2013) 305:R4–12. doi: 10.1152/ajpregu.00094.2013
17. Sun J, Li Y, Pan X, Nguyen DN, Brunse A, Bojesen AM, et al. Human milk fortification with bovine colostrum is superior to formula-based fortifiers to prevent gut dysfunction, necrotizing enterocolitis, and systemic infection in preterm pigs. *JPEN J Parenter Enteral Nutr*. (2019) 43:252–62. doi: 10.1002/jpen.1422
18. Rasmussen SO, Martin L, Østergaard MV, Rudloff S, Li Y, Roggenbuck M, et al. Bovine colostrum improves neonatal growth, digestive function, and gut immunity relative to donor human milk and infant formula in preterm pigs. *Am J Physiol Gastrointest Liver Physiol*. (2016) 311:G480–91. doi: 10.1152/ajpgi.00139.2016
19. Sun J, Li Y, Nguyen DN, Mortensen MS, van den Akker CHP, Skeath T, et al. Nutrient fortification of human donor milk affects intestinal function and protein metabolism in preterm pigs. *J Nutr*. (2018) 148:336–47. doi: 10.1093/jn/nxx033
20. Sangild PT, Thymann T, Schmidt M, Stoll B, Burrin DG, Buddington RK. Invited review: the preterm pig as a model in pediatric gastroenterology. *J Anim Sci*. (2013) 91:4713–29. doi: 10.2527/jas.2013-6359
21. Siggers RH, Siggers J, Thymann T, Boye M, Sangild PT. Nutritional modulation of the gut microbiota and immune system in preterm neonates susceptible to necrotizing enterocolitis. *J Nutr Biochem*. (2011) 22:511–21. doi: 10.1016/j.jnutbio.2010.08.002
22. Li Y, Jensen ML, Chatterton DEW, Jensen BB, Thymann T, Kvistgaard AS, et al. Raw bovine milk improves gut responses to feeding relative to infant formula in preterm piglets. *Am J Physiol Gastrointest Liver Physiol*. (2014) 306:G81–90. doi: 10.1152/ajpgi.00255.2013
23. Chen JHK, Ho PL, Kwan GSW, She KKK, Siu GKH, Cheng VCC, et al. Direct bacterial identification in positive blood cultures by use of two commercial matrix-assisted laser desorption ionization-time of flight mass spectrometry systems. *J Clin Microbiol*. (2013) 51:1733–9. doi: 10.1128/JCM.03259-12
24. Nguyen DN, Thymann T, Goericke-pesch SK, Ren S, Wei W, Skovgaard K, et al. Prenatal intra-amniotic endotoxin induces fetal gut and lung immune responses and postnatal systemic in fl ammation in preterm pigs. *Am J Pathol*. (2018) 188:2629–43. doi: 10.1016/j.ajpath.2018.07.020
25. Ren S, Hui Y, Obelitz-ryom K, Brandt AB, Kot W, Nielsen DS, et al. Neonatal gut and immune maturation is determined more by postnatal age than by postconceptional age in moderately preterm pigs. *Am J Physiol Gastrointest Liver Physiol*. (2019) 315:G855–67. doi: 10.1152/ajpgi.00169.2018
26. Li Y, Nguyen DN, Obelitz-Ryom K, Andersen AD, Thymann T, Chatterton DEW, et al. Bioactive whey protein concentrate and lactose stimulate gut function in formula-fed preterm pigs. *J Pediatr Gastroenterol Nutr*. (2018) 66:128–34. doi: 10.1097/MPG.0000000000001699
27. Juhl SM, Ye X, Zhou P, Li Y, Iyore EO, Zhang L, et al. Bovine colostrum for preterm infants in the first days of life : a randomized controlled pilot trial. *J Pediatr Gastroenterol Nutr*. (2018) 66:471–8. doi: 10.1097/MPG.0000000000001774
28. Li Y, Juhl SM, Ye X, Shen RL, Iyore EO, Dai Y, et al. A stepwise, pilot study of bovine colostrum to supplement the first enteral feeding in preterm infants (precolos): study protocol and initial results. *Front Pediatr*. (2017) 5:42. doi: 10.3389/fped.2017.00042
29. Hay WW, Hendrickson KC. Preterm formula use in the preterm very low birth weight infant. *Semin Fetal Neonatal Med*. (2017) 22:15–22. doi: 10.1016/j.siny.2016.08.005
30. Thymann T, Møller HK, Stoll B, Støy ACF, Buddington RK, Bering SB, et al. Carbohydrate maldigestion induces necrotizing enterocolitis in preterm pigs. *Am J Physiol Gastrointest Liver Physiol*. (2009) 297:G1115–25. doi: 10.1152/ajpgi.00261.2009
31. Pammi M, Cope J, Tarr PI, Warner BB, Morrow AL, Mai V, et al. Intestinal dysbiosis in preterm infants preceding necrotizing enterocolitis: a systematic review and meta-analysis. *Microbiome*. (2017) 5:1–15. doi: 10.1186/s40168-017-0248-8
32. Brunse A, Martin L, Rasmussen TS, Christensen L, Skovsted Cilieborg M, Wiese M, et al. Effect of fecal microbiota transplantation route of administration on gut colonization and host response in preterm pigs. *ISME J*. (2019) 13:720–33. doi: 10.1038/s41396-018-0301-z
33. Li Y, Østergaard MV, Jiang P, Chatterton DEW, Thymann T, Kvistgaard AS, et al. Whey protein processing influences formula-induced gut maturation in preterm pigs. *J Nutr*. (2013) 143:1934–42. doi: 10.3945/jn.113.182931
34. Ozen S, Akisu M, Baka M, Yalaz M, Sozmen EY, Berdeli A, et al. Insulin-like growth factor attenuates apoptosis and mucosal damage in hypoxia/reoxygenation-induced intestinal injury. *Biol Neonate*. (2005) 87:91–6. doi: 10.1159/000081897
35. Ben-Lulu S, Pollak Y, Mogilner J, Bejar J, Coran AG, Sukhotnik I. Dietary transforming growth factor-beta 2 (TGF-β2) supplementation reduces methotrexate-induced intestinal mucosal injury in a rat. *PLoS ONE*. (2012) 7:e45221. doi: 10.1371/journal.pone.0045221

36. Zhang T, Wang Y, Ban R, Tong L, Qiao H, Lao H, et al. Oral administration of lactoferrin attenuates intestinal ischemia-reperfusion injury in rats. *Eur Surg Res*. (2012) 49:99–106. doi: 10.1159/000342633
37. Pan X, Gong D, Gao F, Sangild PT. Diet-dependent changes in the intestinal DNA methylome after introduction of enteral feeding in preterm pigs. *Epigenomics*. (2018) 10:395–408. doi: 10.2217/epi-2017-0122
38. Vreugdenhil AC, Dentener MA, Snoek AM, Greve JW, Buurman WA. Lipopolysaccharide binding protein and serum amyloid A secretion by human intestinal epithelial cells during the acute phase response. *J Immunol*. (1999) 163:2792–8.
39. Sünderhauf A, Skibbe K, Preisker S, Ebbert K, Verschoor A, Karsten CM, et al. Regulation of epithelial cell expressed C3 in the intestine – relevance for the pathophysiology of inflammatory bowel disease? *Mol Immunol*. (2017) 90:227–38. doi: 10.1016/j.molimm.2017.08.003
40. Colgan SP, Taylor CT. Hypoxia: an alarm signal during intestinal inflammation. *Nat Rev Gastroenterol Hepatol*. (2010) 7:281–7. doi: 10.1038/nrgastro.2010.39
41. Chan KYY, Leung KT, Tam YH, Lam HS, Cheung HM, Ma TPY, et al. Genome-wide expression profiles of necrotizing enterocolitis versus spontaneous intestinal perforation in human intestinal tissues: dysregulation of functional pathways. *Ann Surg*. (2014) 260:1128–37. doi: 10.1097/SLA.0000000000000374
42. Lönnerdal B. Bioactive proteins in human milk—potential benefits for preterm infants. *Clin Perinatol*. (2017) 44:179–91. doi: 10.1016/j.clp.2016.11.013
43. Corpeleijn WE, van Vliet I, de Gast-Bakker D-AH, van der Schoor SRD, Alles MS, Hoijer M, et al. Effect of enteral IGF-1 supplementation on feeding tolerance, growth, and gut permeability in enterally fed premature neonates. *J Pediatr Gastroenterol Nutr*. (2008) 46:184–90. doi: 10.1097/MPG.0b013e31815affec
44. Hawkes JS, Neumann MA, Gibson RA. The effect of breast feeding on lymphocyte subpopulations in healthy term infants at 6 months of age. *Pediatr Res*. (1999) 45:648–51. doi: 10.1203/00006450-199905010-00006
45. Wen K, Li G, Bui T, Liu F, Li Y, Kocher J, et al. High dose and low dose *Lactobacillus acidophilus* exerted differential immune modulating effects on T cell immune responses induced by an oral human rotavirus vaccine in gnotobiotic pigs. *Vaccine*. (2012) 30:1198–207. doi: 10.1016/j.vaccine.2011.11.107
46. Gerner W, Käser T, Saalmüller A. Porcine T lymphocytes and NK cells - an update. *Dev Comp Immunol*. (2009) 33:310–20. doi: 10.1016/j.dci.2008.06.003
47. Piriou-Guzylack L, Salmon H. Membrane markers of the immune cells in swine: an update. *Vet Res*. (2008) 39:54. doi: 10.1051/vetres:2008030
48. Schäfer A, Hühr J, Schwaiger T, Dorhoi A, Mettenleiter TC, Blome S, et al. Porcine invariant natural killer T cells: functional profiling and dynamics in steady state and viral infections. *Front Immunol*. (2019) 10:1380. doi: 10.3389/fimmu.2019.01380
49. ELFIN Trial Investigators Group. Enteral lactoferrin supplementation for very preterm infants: a randomised placebo-controlled trial. *Lancet*. (2019) 393:423–33. doi: 10.1016/S0140-6736(18)32221-9
50. Balachandran B, Dutta S, Singh R, Prasad R, Kumar P. Bovine colostrum in prevention of necrotizing enterocolitis and sepsis in very low birth weight neonates: a randomized, double-blind, placebo-controlled pilot trial. *J Trop Pediatr*. (2017) 63:10–7. doi: 10.1093/tropej/fmw029

Conflict of Interest: The University of Copenhagen holds a patent on the use of colostrum for pediatric patients. PS is listed as a sole inventor but has declined any share of potential revenue arising from commercial exploitation of such a patent.

The remaining authors declare that the research was conducted in the absence of any commercial or financial relationships that could be construed as a potential conflict of interest.

frontiers in Immunology

ORIGINAL RESEARCH
published: 18 February 2020
doi: 10.3389/fimmu.2020.00171

The TLR5 Agonist Flagellin Shapes Phenotypical and Functional Activation of Lung Mucosal Antigen Presenting Cells in Neonatal Mice

Pankaj Sharma[1,2], *Ofer Levy*[1,2,3*†] *and David J. Dowling*[1,2*†]

[1] Precision Vaccines Program, Division of Infectious Diseases, Boston Children's Hospital, Boston, MA, United States, [2] Harvard Medical School, Boston, MA, United States, [3] Broad Institute of MIT and Harvard, Cambridge, MA, United States

Intranasal mucosal vaccines are an attractive approach to induce protective mucosal immune responses. Activation of lung antigen presenting cells (APCs), a phenotypically and functionally heterogeneous cell population located at distinct mucosal sites, may be key to the immunogenicity of such vaccines. Understanding responsiveness of newborn lung APCs to adjuvants may the inform design of efficacious intranasal vaccines for early life, when most infections occur. Here, we characterized and phenotyped APCs from neonatal (7 days of life) and adult (6–8 weeks of age) mice. Neonatal mice demonstrated a relatively high abundance of alveolar macrophages (AMs), with lower percentages of plasmacytoid dendritic cells (pDCs), CD103$^+$ (cDC1), and CD11b$^+$ (cDC2) DCs. Furthermore, neonatal CD103$^+$ and CD11b$^+$ DC subsets demonstrated a significantly lower expression of maturation markers (CD40, CD80, and CD86) as compared to adult mice. Upon stimulation of lung APC subsets with a panel of pattern recognition receptor (PRR) agonists, including those engaging TLRs or STING, CD11c$^+$ enriched cells from neonatal and adult mice lungs demonstrated distinct maturation profiles. Of the agonists tested, the TLR5 ligand, flagellin, was most effective at activating neonatal lung APCs, inducing significantly higher expression of maturation markers on CD103$^+$ (cDC1) and CD11b$^+$ (cDC2) subsets. Intranasal administration of flagellin induced a distinct migration of CD103$^+$ and CD11b$^+$ DC subsets to the mediastinal lymph nodes (mLNs) of neonatal mice. Overall, these findings highlight age-specific differences in the maturation and responsiveness of lung APC subsets to different PRR agonists. The unique efficacy of flagellin in enhancing lung APC activity suggests that it may serve as an effective adjuvant for early life mucosal vaccines.

Keywords: early life immunization, newborn, dendritic cells, mucosal immunity, cross presentation, TLR5, flagellin

OPEN ACCESS

Edited by:
Andrew Currie, Murdoch University, Australia

Reviewed by:
Sofia A. Casares, Naval Medical Research Center, United States
Carmen Alvarez-Dominguez, Marqués de Valdecilla Health Research Institute (IDIVAL), Spain

***Correspondence:**
Ofer Levy
ofer.levy@childrens.harvard.edu
David J. Dowling
david.dowling@childrens.harvard.edu

†These authors share senior authorship

Specialty section:
This article was submitted to Vaccines and Molecular Therapeutics, a section of the journal Frontiers in Immunology

Received: *30 July 2019*
Accepted: *22 January 2020*
Published: *18 February 2020*

Citation:
Sharma P, Levy O and Dowling DJ (2020) The TLR5 Agonist Flagellin Shapes Phenotypical and Functional Activation of Lung Mucosal Antigen Presenting Cells in Neonatal Mice. Front. Immunol. 11:171. doi: 10.3389/fimmu.2020.00171

INTRODUCTION

The persistently high global burden of infections in the very young provides a compelling rationale for developing additional safe and effective early life vaccines (1). Most childhood pathogens access the body through mucosal membranes (2). Additionally, viral infections including respiratory syncytial virus (RSV) and influenza virus are often more severe and/or prolonged in early life as compared to adult life (3). Parenteral vaccines, such as those delivered intramuscularly, are

often poor inducers of protective immunity at mucosal surfaces (4). While, effective immunization against mucosal infections usually requires topical-mucosal vaccine administration, which could neutralize the pathogen on the mucosal surface before it can cause infection, only a few human vaccines are oral-e.g., those against cholera, typhoid, polio, and rotavirus, and only one, an influenza vaccine, is administered intranasally (5). Moreover, vaccines delivered via different routes interact with different APCs that activate distinct arms of immunity (6). Tissue distribution and migratory properties of APCs, such as alveolar macrophages (AMs), plasmacytoid DCs (pDCs), and conventional DCs (cDCs) contribute to the generation of distinct immune responses (7). In mice, cDCs have been classified into two major subsets, cDC1, which express CD103 (CD8α) and specialize in cross-presentation to $CD8^+$ T cells critical for immunity against intracellular pathogens, viruses, and cancer; and cDC2, which express CD11b and promote $CD4^+$ T cell differentiation into subsets specializing in anti-viral, -fungal, or -helminth immunity (8). Immune cells in the neonatal lung differ in quantity and quality from adults and, hence, react differently to environmental, microbial, and vaccine exposures (9). Mucosal administration of antigen may drive a more effective mucosal response to respiratory infections (10, 11), potentially reflecting activation of antigen-specific secretory IgA responses and development of lung resident memory T cells (12–14).

Generation of mucosal immunity may be achieved via various routes including oral, intranasal (pulmonary), rectal, and vaginal (4). The intranasal route is attractive considering injection-free delivery (15), and ease of clinical administration (16) in early life. However, the challenge to early life intranasal vaccination can be the induction of non-specific inflammation and/or the generation of tolerance to unknown or novel antigens (17). Such challenges may be a particular concern in early life, where the T-helper response is biased toward type-2 immunity, exacerbation of which may predispose individuals to eosinophilia and pulmonary disorders (18). Nevertheless, solutions to such challenges may be found in the use of precision adjuvants (19) which drive the appropriate activation of APCs and help in shaping the immune system (20, 21). Adjuvantation is a key tool to enhance vaccine-induced immunity (22). Adjuvants can enhance, prolong, and modulate immune responses to vaccine antigens to maximize protective immunity (21, 22), and may potentially enable more effective immunization in the very young and the elderly (23). Despite evidence suggesting ontological differences in the innate response in the mucosal APCs, there are gaps in the understanding of basic mechanisms and whether adjuvants could drive mature and enhance the functions of lung APC subsets in diverse age groups such as infant and neonates (24). A deeper understanding of mucosal APCs in early life may inform the design of effective mucosal vaccines for the very young.

In the present study, we examined the phenotypic and functional differences in mucosal APC subsets isolated from newborn and adult murine lungs and characterized their responsiveness to different PRR agonists/adjuvants. We found that DC subsets from neonate mice lungs are phenotypically and functionally distinct from those of the adult mice, as they exhibit a different activation pattern to various PRR agonists. The TLR5 agonist flagellin, a globular protein that arranges itself in a hollow cylinder to form the filament in a bacterial flagellum, strongly activated lung migratory DC (migDCs) subsets and upregulated their expression of CD40, CD80, CD86, and CCR7. Also, when used as an adjuvant during intranasal vaccination, flagellin regulated the migration of DC subsets to the draining lymph nodes, and potentiated the phagosome maturation in $CD103^+$ DC subset, correlating with their ability to mount a robust antigen cross presentation phenontype. These findings suggest that TLR5 may play an important role in the maturation and activation of lung migratory DCs in neonates and could be an empirically promising target for intranasal mucosal vaccines delivered in early life.

Abbreviations: MTT, 3-(4,5-dimethylthiazol-2-yl)-2,5-diphenyltetrazolium bromide; AMs, alveolar macrophages; ANOVA, Analysis of variance; Kb, anti-mouse MHC class I molecule; Abs, antibodies; APCs, antigen presenting cells; BCH, Boston Children's Hospital; CD, cluster of differentiation; cDCs, conventional DCs; 2′3′-cGAMP, cyclic [G(2′,5′)pA(3′,5′)p]; DOL, day of life; DQ-OVA, DQ^{TM} ovalbumin; EU, endotoxin units; EDTA, ethylenediaminetetraacetic acid; Ig, immunoglobulin; MACS, magnetic activated cell sorting; MHC, major histocompatibility complex; mLNs, mediastinal lymph nodes; migDCs, migratory DC; mAb, monoclonal Ab; MPLA, monophosphoryl Lipid A; ODNs, oligonucleotides; PAM2CSK4, Pam2CysSerLys4; PAM3CSK4, Pam3CysSerLys4; PRR, pattern recognition receptor; Kb-SIINFEKL, peptide SIINFEKL Abs; PBS, phosphate-Buffered Saline; pDCs, plasmacytoid DCs; PDCA-1, plasmacytoid dendritic cell antigen-1; RBC, red blood cell; RSV, respiratory syncytial virus; FLA-ST, *Salmonella typhimurium* flagellin; TLR, Toll-like receptor.

MATERIALS AND METHODS

Animals

All experiments involving animals were approved by the Animal Care and Use Committee of Boston Children's Hospital and Harvard Medical School (protocol numbers 15-11-3011 and 16-02-3130). C57BL/6 mice were obtained from Taconic Biosciences or Charles River Laboratories and housed in specific pathogen-free conditions in the animal research facilities at Boston Children's Hospital. For breeding purposes, mice were housed in couples, and cages checked daily to assess pregnancy status of dams and/or the presence of pups. When a new litter was discovered, that day was recorded as day of life (DOL) 0. Both male and female pups were used for experiments. CO_2 was used as the primary euthanization method, with cervical dislocation as a secondary physical method to ensure death.

Reagents

Collagenase-1, DNase-1, 3-(4,5- dimethylthiazol-2-yl)-2,5-diphenyltetrazolium bromide (MTT), Griess reagent, FITC-dextran, and Concanavalin-A were all purchased from Sigma Aldrich (St. Louis, MO). CD11c magnetic cell separation kit (MACS) were purchased from Miltenyi Biotec (Bergisch-Gladbach, Germany). All monoclonal antibodies (Abs) were purchased from eBioscience (San Diego, CA), while all the PRR agonists were purchased from *InvivoGen* (San Diego, CA). For all *in vivo* studies, ultrapure *Salmonella typhimurium* flagellin (FLA-ST) from *InvivoGen* (endotoxin level < 0.05 endotoxin units (EU)/mg) and was employed. FLA-ST is purified by acid

hydrolysis, heating and ultrafiltration to obtain an estimated at 10% purity, before an additional purification step using monoclonal anti-flagellin affinity chromatography to obtain purity >95%.

Preparation of Single Cell Suspension From Murine Lungs and Isolation of Lung APCs

To prepare single cell suspensions, neonates and adult mice were euthanized and the lungs were exposed by dissecting through the thorax by raising the sternum to avoid any injury to the lung. Mice lungs were perfused through the right ventricle by adding ice cold Phosphate-Buffered Saline (PBS) [containing 2 mM ethylenediaminetetraacetic acid (EDTA)] and the lung lobes were carefully isolated and manually minced into small pieces in petri dishes. Next, these minced pieces were incubated at 37°C for 30 min in a digestion medium containing 2 mg/ml of collagenase and 80 U/ml of DNase-1. Digested lung tissue was subsequently passed through a 40 μM cell strainer and centrifuged at 300 g for 10 min at 4°C. Red blood cell (RBC) lysis was carried out in the cell pellet using BD Pharm Lyse following instructions of the manufacturer (*BD Biosciences*). For multicolor immunophenotyping and *in vitro* stimulation assay, lung APCs were enriched using CD11c based magnetic activated cell sorting (MACS) following the manufacturer's instructions.

In vitro Stimulation Assay

All PRR agonists employed in the study were verified endotoxin-free as indicated by the manufacturers (*InvivoGen*). For stimulation experiments, isolated lung $CD11c^+$ cells from newborn and adult mice were plated in round bottom 96-wells non-tissue culture-treated plates at the density of 10^5 cells/well in 200 μl of fresh complete culture medium and stimulated for 24 h with 100 ng/ml of Pam3CysSerLys4 (PAM3CSK4), PAM2CSK4, Poly I:C, Monophosphoryl Lipid A (MPLA), *S. typhimurium* flagellin, 5′ppp-dsRNA; 0.1 μM of CL075, CpG class C—oligonucleotides (ODN) 2,395 or 100 μg/ml of cyclic [G(2′,5′)pA(3′,5′)p] (2′3′-cGAMP, hereto referred to as cGAMP). Stimulation concentrations were chosen based on optimal maturation responses achieved (cytokine production, upregulation of co-stimulatory markers) in murine neonatal and adult bone-marrow dendritic cell assays, as previously described by the authors (25, 26). Cultured DCs demonstrated no obvious signs of spontaneous maturation in the control conditions.

Flow Cytometry

CD11c enriched cells from mice lungs were stained with the monoclonal Abs directed against CD11c, CD11b, CD103, F4/80, and plasmacytoid dendritic cell antigen-1 [PDCA-1 (also known as CD317)] to identify the five major APC populations in the lung. To monitor the expression of co-stimulatory molecules, *in vitro* stimulated $CD11c^+$ cells were washed with ice cold PBS once and stained with Ab cocktail containing monoclonal Abs for CD40, CD80, and CD86 along with APC surface markers. Data were acquired on BD Fortessa flow cytometer and was analyzed using Flowjo (Treestar). All Abs used for flow cytometry are listed in **Table S1**.

Analysis of Phagocytosis and Antigen Processing Capacity of Lung APCs

Isolated $CD11c^+$ cells were incubated with either FITC-dextran (1 mg/ml) or with DQ™ ovalbumin (DQ-OVA) (0.5 mg/ml) for 45 min in a CO_2 incubator at 37°C. The fluorescence of gated cells was measured using BD Fortessa as described recently (27).

Intranasal Administration of DQ-OVA

Fifty microliters of PBS, DQ-OVA (50 μg), and flagellin (3 μg total) adjuvanted DQ-OVA (50 μg) were applied *via* the nostrils as recently described (28). DQ-OVA was used for degradation and accumulation assays as it consists of OVA bound to a self-quenching fluorescent dye, which upon intracellular degradation releases specific fluorescence (excitation at 505 nm, emission at 515 nm). Accumulated DQ-OVA forming dimers emit fluorescence in a different channel (excitation at 488 nm, emission at 613 nm). Animals were euthanized 4 or 24 h after intranasal administration and lung and or lung draining lymph nodes were harvested to determine the uptake, trafficking, phenotype, and antigen degradation (28). Tracking the quantity and localization of specific APC *in vivo* was achieved via the use of a SIINFEKL monoclonal Ab (mAb), which specifically reacts with ovalbumin-derived peptide SIINFEKL bound to H-2Kb of major histocompatibility complex (MHC) class I. To enumerate the antigen cross presentation, DCs from the draining lymph nodes were stained with PE anti-mouse MHC class I molecule (Kb) bound to the peptide SIINFEKL Abs (Kb-SIINFEKL) (*BioLegend*; San Diego, CA). Data was acquired on BD Fortessa flow cytometer.

Statistical Analysis

Statistical significance and graphs were generated using Prism v. 7.0a (GraphPad Software, La Jolla, CA, USA) and Microsoft Excel (Microsoft Corporation, Redmond, WA). For data analyzed by normalization to control values (vehicle), column statistics were conducted using the two-tailed Wilcoxon Signed Rank Test or unpaired Mann-Whitney test as appropriate. Group comparisons employed two-way Analysis of variance (ANOVA) with Sidak multiple comparison post-test. Results were considered significant at $p < 0.05$, and indicated as follows: $^{*}p < 0.05$, $^{**}p < 0.01$, $^{***}p < 0.001$, $^{****}p < 0.001$.

RESULTS

Neonate Murine Lung Antigen Presenting Cells and Their Precursors Demonstrate Distinct Percentages and Co-stimulatory Molecule Expression

To prepare single cell suspensions, neonates and adult mice were euthanized and the lungs were isolated, digested, and enriched for $CD11c^+$ cell fractions (**Figure 1A**). A panel of cell surface makers were used in combination to identify heterogeneous populations of lung APCs studied in this article (**Figures 1B,C**). As mucosal APCs are heterogeneous, we employed a stringent gating strategy to distinguish the different subsets and their progenitors. By using the combination of different surface

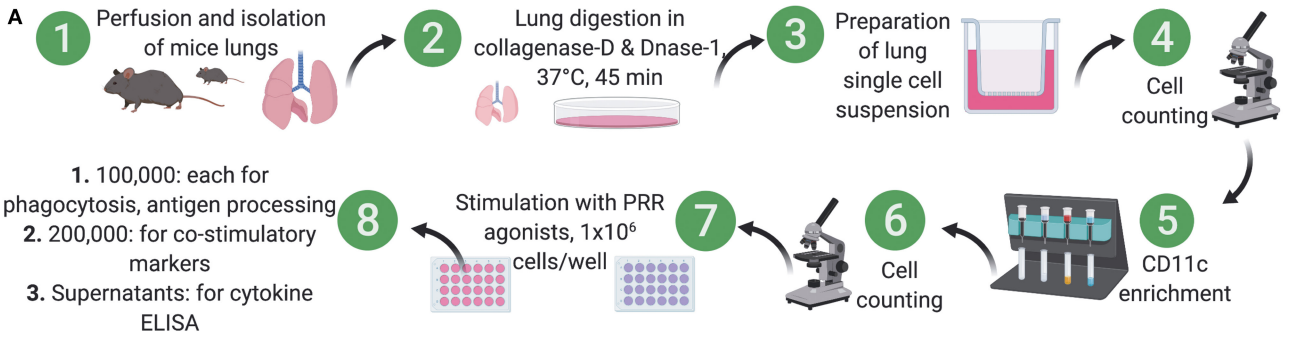

B

Table 1. Gating strategy to encompassed heterogeneity of lung APCs

APC subsets	AMs	moDCs	CD103⁺ DCs	CD11b⁺ DCs	pDCs
F4/80	+++	++	-	+/-	-
CD11c	+	+	+	+	+
CD103	-	-	++	+/-	-
MHCII	+	+	+	+	low
PDCA-1	-	-	-	-	++
Precursors markers					
Ly6c	High	High	Mid	-	-
CD11b	+	+	+	-	-

AMs: Alveolar macrophages; APC: antigen presenting cell; DC: dendritic cell; MHC: major histocompatibility complex; moDCs: monocyte DCs; pDC: Plasmacytoid DCs; PDCA-1: plasmacytoid dendritic cell antigen-1.

C

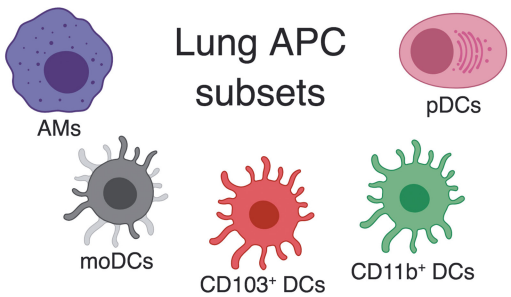

FIGURE 1 | Preparation of single cell suspensions from neonatal and adult murine lungs for isolation of APCs. **(A)** To prepare single cell suspensions, neonatal and adult mice were euthanized and the lungs were exposed by dissecting through the thorax by raising the sternum to avoid any injury to the lung, perfused through right ventricle by adding ice cold PBS (containing 2 mM EDTA) and lung lobes were carefully isolated and were manually minced into small pieces in Petri dishes. Minced pieces were digested and digested lung tissue was subsequently passed through a cell strainer. For multicolor immunophenotyping and *in vitro* stimulation assay, lung APCs were enriched using CD11c- based magnetic beads for use in *in vitro* stimulation assays. **(B)** List of known pan- and precursor- markers used in combination to identify heterogeneous populations of lung APCs. **(C)** Overview of the lung APCs studied in this study.

markers and a hierarchal gating strategy, we identified alveolar macrophages (AMs), moDCs, CD103$^+$ DCs, CD11b$^+$ DCs, and pDCs (**Figure 2A**). While the percentage of Ly6C$^+$ cells was significantly higher in neonatal vs. adult mice (**Figure 2B**), and AMs and moDCs subsets were similar between both age groups, neonates demonstrated a significanly lower percentage of lung DC subsets CD103$^+$ DCs ($n = 12$, $P < 0.001$), CD11b$^+$ DCs ($P < 0.001$), and pDCs ($P < 0.05$) (**Figure 2C**). Remarkably, while both adult and neonatal antigen uptake capability was similar for all the major APC subsets (**Figure 3A**), CD103$^+$ and CD11b$^+$ DCs from neonates demonstrated relatively lower expression of basal co-stimulatory molecules CD40 [CD11b$^+$ ($n = 12$, $P < 0.001$) and CD103$^+$ ($P < 0.01$) DCs], CD80 ($P < 0.001$), and CD86 ($P < 0.001$) (**Figures 3B–D**). These observations demonstrated that neonatal murine lung APCs contain a greater proportion of phenotypically distinct immature DC precursor cells, including CD103$^+$ and CD11b$^+$ DCs, relative to their adult counterparts.

Neonatal Murine Lung APCs Demonstrate Distinct Functional Responses to PRR Agonists

Our observations regarding the phenotype of DC subsets in neonatal murine lungs indicated an intrinsic age-specific difference in the percentages and maturation status of migratory APC subsets, raising the possibility that functional responses of migDCs subsets to stimuli such as PRR agonist adjuvants may also be distinct. To test this hypothesis, we stimulated CD11c$^+$ cells isolated from the lungs of different aged mice and stimulated them with different classes of PRR receptor agonists at a concentrations reported most active for bone marrow DC activation (25, 26). We then summarized the combined flow cytometry all APCs maturation data collected following *ex vivo* stimulation, and graphed the data as volumetric dot sizes indicating the relative fold change (ranging from <1 to >4.5) for CD40, CD80 and CD86, per F4/80, CD11b, CD103, PDCA-1 APC subsets, as compared with un-stimulated controls per age group. Overall, unique activation and maturation patterns were observed by stimuli, age, marker, and APC subset (**Figure 4**). Ranking by sum fold-change activation, CpG ODN ranked first in adult mice. Flagellin ranked first in the ability to mature neonatal lung APCs (**Figure 4**). PRR agonists TLR1 (PAM3CSK4), TLR2 (PAM2CSK4), and TLR3 (Poly I:C), NOD1 (C12-iE-DAP) and NOD2 (and L18-MDP) moderately activated APCs from neonatal adult mice lungs. Contrary to these ligands, the TLR5 agonist flagellin and STING agonist 2′3′-cGAMP specifically and strongly activated the neonatal CD103$^+$ and CD11b$^+$ DC subsets, while the TLR4 (MPLA), TLR8/7 (CL075), TLR9 (CpG), and RIG-I (5′ppp-dsRNA) showed comparable

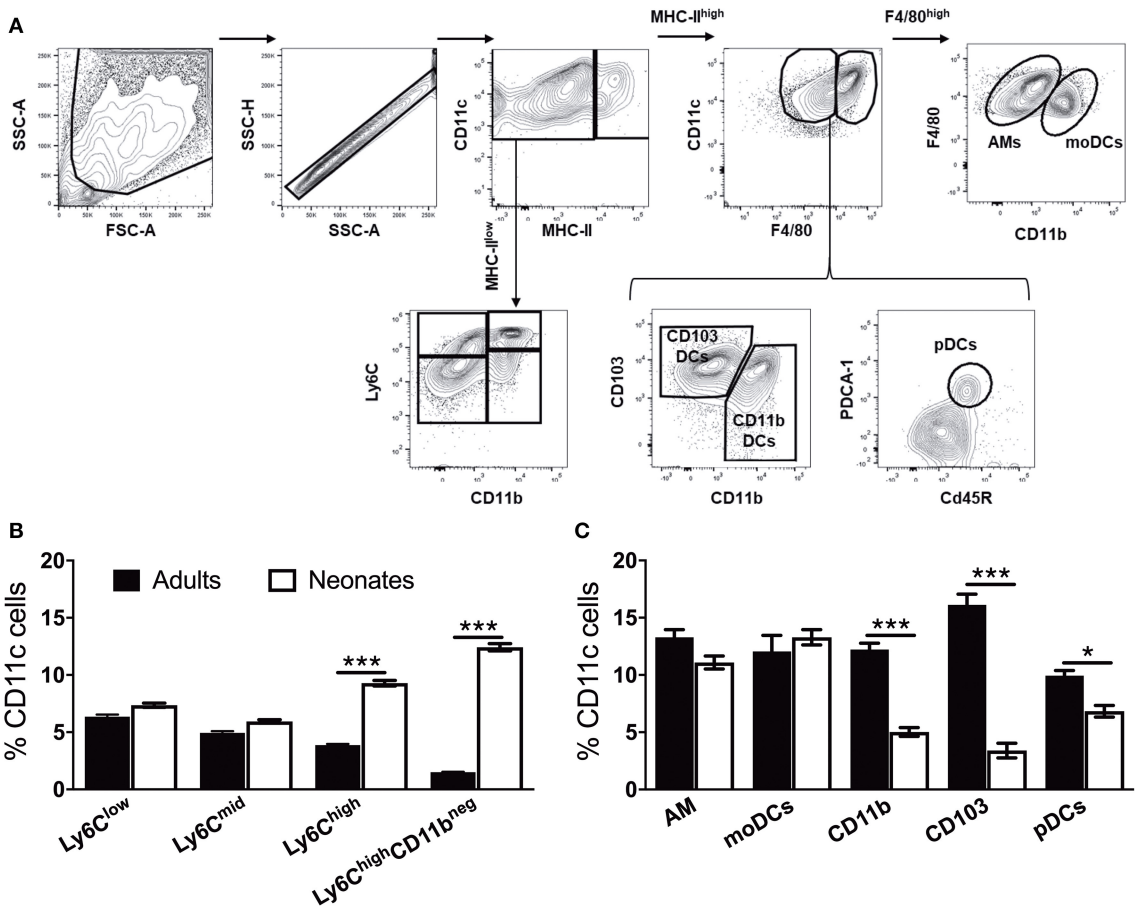

FIGURE 2 | Neonate murine lung antigen presenting cells and their precursors demonstrate distinct subset percentages. **(A)** An overview of the flow cytometry gating strategy used for the identification of murine APC precursors and subsets in both adult and neonatal lungs. **(B)** The percentage of APC precursors, as defined by CD11c, Ly6C, and CD11b cell expression. **(C)** The percentage of APC subsets, as defined by CD11c, F4/80, CD11b, CD103 PDCA-1, and CD45R cell expression in mice lungs. Results are expressed as mean ± SEM of $n = 12$ per age group. $^{*}p < 0.05$, $^{***}p < 0.001$ determined by repeated measures two-way ANOVA with Sidak *post-hoc* test.

activity for all the DC subsets from the neonates and adult mice. We also assessed cytokine production by lung CD11c enriched cells after stimulation. As compared to adults, APCs from neonatal mice produced lower IL-12p70, IL-6, TNF, and IL-1β in responses to NOD1, TLR2/6, 3, 4, 8/7, and 9 stimulation, while TLR5 (flagellin), RIG-I (5′ppp-dsRNA) and STING (2′3′-cGAMP) stimulation mounted a comparable cytokine response from neonatal and adult APCs (**Figure S1**). These observations demonstrate functional differences in the major APC subsets of murine lungs and highlight flagellin and 2′3′-cGAMP as potential activators of mucosal immunity in early life.

Flagellin Upregulates the Expression of CCR7 on Neonatal CD11c Enriched Cells and Drives the Lymph Node Homing of migDC Subsets

As different stimuli induce distinct activation of lung APC subsets, we characterized the expression of lymph node homing receptor CCR7 on lung CD11c^{+} cells isolated from the neonatal and adult mice. CCR7 and CCR9 are both chemokine receptors that regulate homing of immune cells. Specifically, up-regulation of CCR7 on mature DCs is required for migration to draining/secondary lymphoid organs (29, 30). Conversely, immature DCs express high levels of CCR9, as an indication of lower migration potential (31). Consistent with the *in vitro* co-stimulatory molecule stimulation data, and when ranked by MFI, MPLA, CL075, CpG-ODN, and STING demonstrated moderate upregulation of CCR7 on neonates as well as on the adult APCs (**Figure 5A**), while as compared to unstimulated controls, flagellin most strongly upregulated the expression of CCR7 on neonatal APCs (**Figure 5B**, $P < 0.001$) and to a significant but lesser level in adults ($P < 0.01$). Conversely, as compared to adults ($P < 0.05$), neonatal lung CD11c^{+} DCs CCR9 expression was not significantly increased (**Figure 5C**). We also noted that the APCs from the neonates and adults responded similarly to the NOD1 and NOD2 agonists studied (C12-iE-DAP and L18-MDP) (**Figures 4**, **5A**). These findings suggest that TLR5 might drive

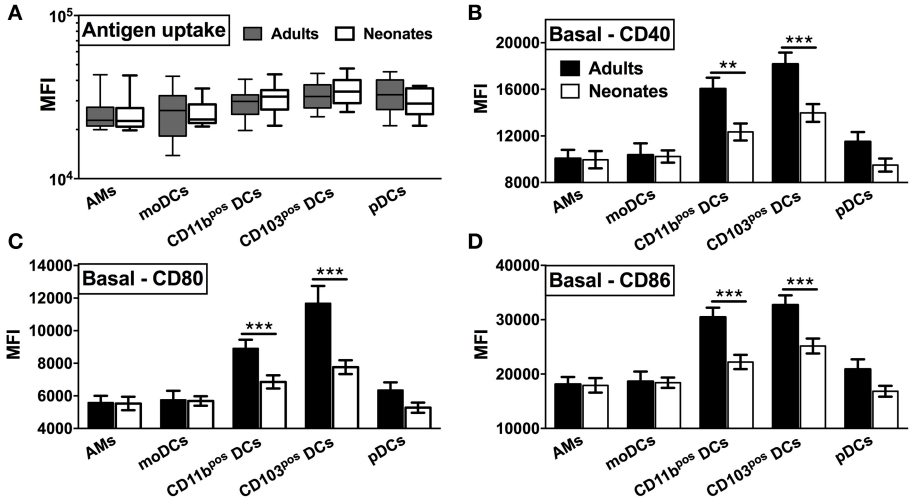

FIGURE 3 | Neonatal murine lung CD103$^+$ DCs and CD11b$^+$ DC subsets demonstrate distinct basal co-stimulatory molecule expression. **(A)** Similar antigen uptake capacity of neonatal and adult APCs was noted across all the DC subsets. **(B–D)** Neonatal CD103$^+$ DCs and CD11b$^+$ lung DC subsets demonstrate a lower expression of co-stimulatory molecules CD40, CD80, and CD86 as compared to adult mice. Results are expressed as mean ± SEM of $n = 12$ per age group. $^{**}p < 0.01$, $^{***}p < 0.001$ determined by repeated measures two-way ANOVA with Sidak *post-hoc test*.

Fold change	
< 1	·
1 - 1.5	●
1.5 - 3	●
3 - 4.5	●
> 4.5	■

Target	In vitro Stimulation	F4/80^{pos} Cells						CD11b^{pos} Cells						CD103^{pos} Cells						pDC					
		CD40		CD80		CD86		CD40		CD80		CD86		CD40		CD80		CD86		CD40		CD80		CD86	
		A	N	A	N	A	N	A	N	A	N	A	N	A	N	A	N	A	N	A	N	A	N	A	N
TLR2/1	PAM3CSK4	●	·	●	●	·	●	·	●	·	·	·	·	●	●	●	●	·	●	·	●	●	●	●	●
TLR2/6	PAM2CSK4	●	●	●	●	·	●	·	●	·	●	·	●	·	●	●	●	●	●	·	●	●	●	●	●
TLR3	Poly (I:C)	●	·	●	·	●	·	·	●	·	●	·	●	●	·	●	●	●	●	·	●	●	·	●	·
TLR4	MPLA	●	●	●	●	●	●	●	●	●	●	●	●	●	·	●	●	●	●	·	●	●	·	●	·
TLR5	Flagellin	●	●	●	●	●	●	●	●	●	●	●	■	●	●	●	●	●	●	·	●	●	·	●	·
TLR8/7	CL075	●	●	●	·	●	·	·	●	●	●	·	·	●	■	●	●	●	●	●	●	●	·	●	·
TLR9	CpG ODN	·	·	●	●	●	●	●	●	·	●	●	●	●	●	●	●	●	●	●	●	●	●	●	·
NOD1	C12 DAP	·	·	·	·	·	·	●	·	·	●	·	●	●	●	●	·	·	·	·	●	·	●	·	·
NOD2	L18-MDP	·	·	●	·	●	·	·	·	·	●	·	·	·	●	●	●	●	●	·	●	●	·	●	·
Mincle	TDB	·	·	●	·	●	·	●	·	·	●	·	●	●	●	●	●	●	●	·	●	●	·	●	·
RIG-I	ppp-dsRNA	·	·	●	·	·	·	●	●	·	●	●	●	●	●	●	●	●	●	·	●	●	·	●	●
STING	cGAMP	●	●	●	●	·	·	●	●	●	●	●	●	●	■	●	●	●	■	●	●	·	●	●	●

Sum activation		
All ages	Adult	Neonate
25	11	14
27	12	15
28	14	14
44	19	24
53	20	33
44	22	22
47	23	24
24	10	14
24	12	13
26	13	12
44	20	24
44	18	26

FIGURE 4 | Functional differences in the major APC subsets in mice lungs identify flagellin and 2′3′-cGAMP as potential activators of mucosal immunity in early life. Summary of flow cytometry all APCs maturation data collected *ex vivo* stimulation. Dot sizes indicate the fold-change (ranging from <1 to >4.5) for CD40, CD80, and CD86, per F4/80, CD11b, CD103 PDCA-1 APC subsets, as compared with un-stimulated controls per age group. Gray-shaded sections indicate adult data. Combined activation total fold-changes are summarized in the right panel. Upon stimulation with PRR agonists TLR2/1 (PAM3CSK4), TLR2/6 (PAM2CSK4), TLR3 (Poly I:C), NOD1, and NOD2 ligands (C12-iE-DAP and L18-MDP, respectively), APC subsets were moderately activated. Contrary to these ligands, the TLR5 agonist flagellin and STING agonist 2′3′-cGAMP specifically and robustly activated neonatal CD103$^+$ and CD11b$^+$ DC subsets, while the TLR4, TLR8/7, TLR9, and RIG-I (5′ppp-dsRNA) demonstrated comparable activity for all the DC subsets from the neonates and adult mice. $n = 5$ per age group.

the migration of DC subsets to draining lymph nodes and initiate adaptive immunity.

To test this hypothesis, we administrated the DQ-OVA antigen either alone or in combination with flagellin by intranasal route and measured migration of lung DCs to draining lymph nodes (**Figure 5D**). DQ-OVA is a self-quenched conjugate of ovalbumin antigen that exhibits bright green fluorescence signal only upon proteolytic cleavage/degradation by endosomal proteases (32) (**Figure 5D**). Since, as we outlined in **Figure 2A**, DC subsets from neonates and adult showed no significant differences in the antigen uptake, we could rely on DQ-OVA mediated labeling for these studies. Also, to rule out any difference which might be because of accessibility of DQ-OVA to lung interstitial resident DCs

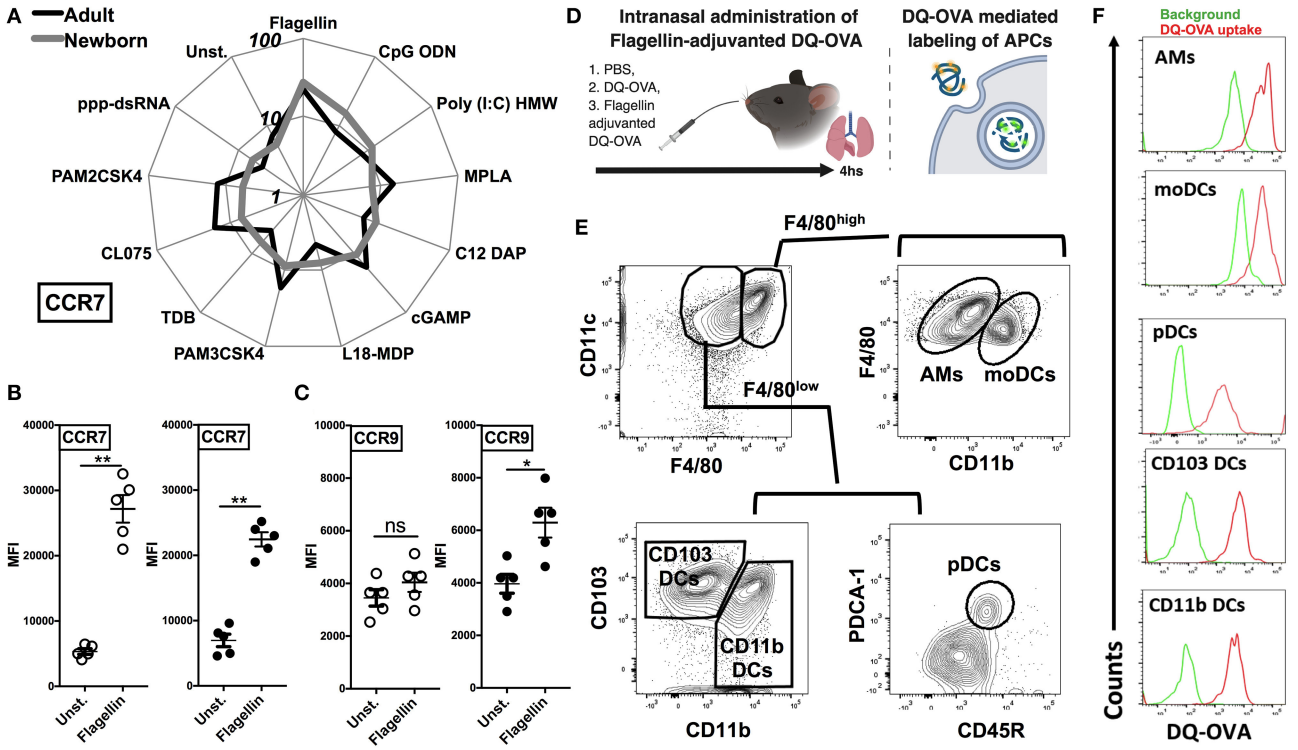

FIGURE 5 | Flagellin upregulates the expression of CCR7 on neonatal CD11c enriched cells and drives the lymph node homing of migDC subsets. **(A)** Characterization of lung CD11c$^+$ cells isolated from the neonatal and adult mice, identifies TLR5 agonist flagellin as the most robust inducer of the expression of lymph node homing receptor CCR7 [MFI ranked clockwise high (flagellin) to low (unstimulated)]. **(B,C)** Flagellin induced CCR7 expression is inversely related to the expression of CCR9 on neonatal lung CD11c$^+$ DCs. **(D)** Overview of Intranasal administration of Flagellin-adjuvanted DQ-OVA and DQ-OVA mediated labeling of APCs. DQ-OVA is a self-quenched conjugate of ovalbumin antigen that exhibits bright green fluorescence signal only upon proteolytic cleavage/degradation by endosomal proteases. **(E)** Representative gating strategy for identification of APC subsets in adult mice lungs. **(F)** DQ-OVA uptake by adult lung APC subsets 4 h after intranasal administration. $n = 5$ per age group. For analyses of individual treatments (e.g., unstimulated vs. flagellin), the unpaired Mann-Whitney test was applied at each concentration, and statistical significance denoted as $^*p < 0.05$, $^{**}p < 0.01$.

(moDCs and CD11b DCs), we looked at DQ-OVA uptake by lung APC subsets 4 h after intranasal administration. Our data clearly demonstrated that all the major APC subsets were labeled (**Figures 5E,F**).

Next, to examine trafficking of leukocytes, we euthanized animals 24 h after intranasal administration of DQ-OVA and isolated the draining lymph nodes (**Figure 6A**). In the lymph node single cell suspension, we gated lung migratory DCs as CD11c$^+$, MHC-II^{high}, and DQ-OVA^{green+} cells (**Figure 6B**) (33). Neonates compared to adults demonstrated lower basal percentages of both the cDC subsets, while mice receiving flagellin-adjuvanted DQ-OVA demonstrated higher trafficking of immunogenic migDCs (**Figure 6C**). Notably, flagellin also increased the percentage of adult CD11b$^+$ cells in mLNs (**Figure 6C**). Moreover, flagellin upregulated the expression of co-stimulatory molecules on neonatal CD103$^+$ DCs, while no significant differences were observed on the other subset studied (**Figures 6D,E**). These observations clearly show that TLR5 agonist adjuvantation mediated stimulation potentially activates the lung CD103$^+$ and CD11b$^+$ migDC subsets in neonates.

Flagellin Regulates Phagosome Maturation and Antigen Degradation by Neonatal Lung CD103$^+$ DCs

By using DQ-OVA, we not only quantified cell trafficking but also characterized antigen uptake, degradation, and cytosolic distribution. DQ-OVA gives green fluorescence following proteolytic degradation in endosomes, and the co-emergence of a red signal reflects the accumulation of cleaved OVA peptides enabling assessment of cytoplasmic differences in organelle distribution after endocytosis. First, we stimulated lung CD11c$^+$ cells *in vitro* with flagellin and measured the phagosome accumulation of DQ-OVA peptides (**Figure 7A**). While there was no overall difference in DQ-OVA uptake and degradation by DCs from neonates and adults (**Figure S2**), we noted the reduction (or a failure to exhibit an increase) in DQ-OVA^{red} signal in neonates CD103$^+$ DCs in a time dependent manner, which was corrected by flagellin stimulation (**Figure 7A**, $P < 0.001$). In line with our *in vitro* studies, we explored this process *in vivo* using our LN migration model. Once again, the flagellin adjuvanted group demonstrated increased OVA^{red} signal, but only in neonatal, and not adult (not shown), CD103^{pos} DCs (**Figure 7B**, $P < 0.001$).

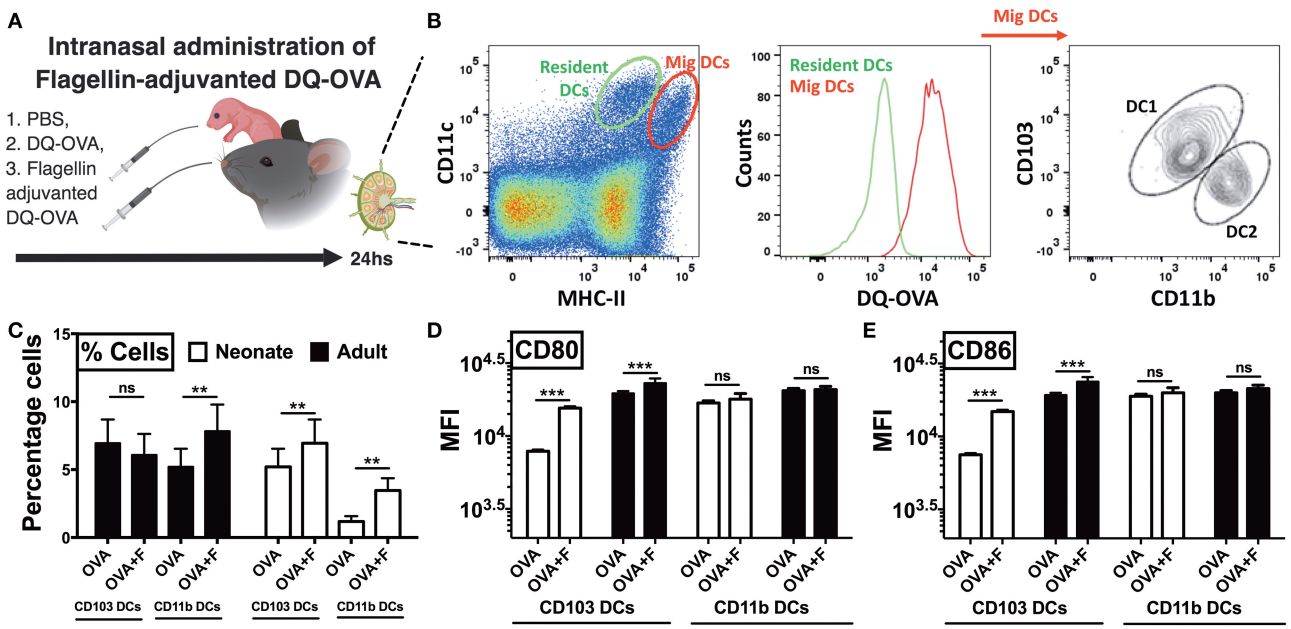

FIGURE 6 | Neonatal mice demonstrate polarized migration of CD103$^+$ and CD11b$^+$ DC subsets to the mediastinal lymph nodes (mLNs) after intranasal administration of flagellin. **(A)** Overview of Intranasal administration of flagellin-adjuvanted DQ-OVA and isolation of draining lymph nodes at 24 h. **(B)** Gating strategy for identification of migratory DC1s and DC2s in draining lymph nodes. **(C)** Flagellin significantly increases the percentage of OVA-specific CD11b$^+$ cells in mLNs of adult mice, but not CD103$^+$ DCs. Flagellin significantly increases the percentage of both OVA-specific CD103$^+$ and CD11b$^+$ DC subsets in neonates. **(D,E)** Flagellin upregulates expression of CD80 and CD86 on neonatal CD103$^+$ migDCs DCs isolated from mLNs. Results are expressed as mean ± SEM of $n = 5$ per age group. $^{**}p < 0.01$, $^{***}p < 0.001$, ns, not significant, determined by repeated measures two-way ANOVA with Sidak *post-hoc* test.

Notably, we did not observe any significance downregulation or impaired phagosome maturation in either adult CD103$^+$ or CD11b$^+$ DCs as compared to their neonatal counterparts subsets (not shown). As slow phagosome maturation is a key step for antigen cross-presentation, these observations suggest that flagellin adjuvant in neonates, but not necessarily adult mice, might enhance a mucosal resident cytotoxic T cell response. These findings were further strengthened by the observations that the CD103$^+$ DC subset from neonatal mice show poor MHC-I presentation of OVA peptides (i.e., SIINFEKL), which was potentially upregulated in the flagellin adjuvanted group in the draining lymph nodes (**Figure 7C**). Together, these studies show that TLR5 signaling plays an important role in the maturation, migration and antigen cross presentation of CD103$^+$ DC subsets which possibly resonate with recent findings which highlight the adjuvanticity of TLR5 ligands via the mucosal route (34–36).

DISCUSSION

Respiratory infection is a major cause of infant mortality, whose susceptibility appears to be due in part to immunological differences in the mucosal compartment (2). Neonatal mucosal barriers are bombarded by environmental, nutritional, microbial, and pathogenic exposures after birth (37). Study of mucosal immune ontogeny may allow us to better understand the establishment of host-microbe homeostasis and responses to pathogens and vaccines. Indeed, the majority of global immunization schedules are focused on the pediatric age group. However, newborns display distinct immune responses, leaving them vulnerable to infections and impairing responses to some vaccines via the slow initiation, deceased magnitude of immunogenicity, reduced persistence of functional Abs, and cell-mediated responses (23). In addition, infectious pathogenesis in neonates might significantly differ from that of older children and adults (23). Vaccine development pipelines typically do not rationally tailor formulations (adjuvants, delivery systems, etc.) for use in early life, but studies such as ours suggest that it is important to take into account early life immune ontogeny to optimize vaccine efficacy (21, 38, 39). For example, early life vaccination against intracellular pathogens has proven difficult (40). Neonates and infants therefore may require different therapeutic vaccine approaches as compared to the established regimen applied to adults.

Innate immune response in early life, especially at the mucosal site is important not only to provide the protection against infections but also to activate adaptive immunity and generate a memory cell pool. Neonates typically demonstrate polarized activation of innate immunity with strong Th2 but limited Th1 responses to most stimuli, low interaction of migratory DCs with lymphocytes in the lymph nodes, and often-inefficient adaptive responses (32). In the present study, we numerically, phenotypically and functionally characterized the APCs isolated

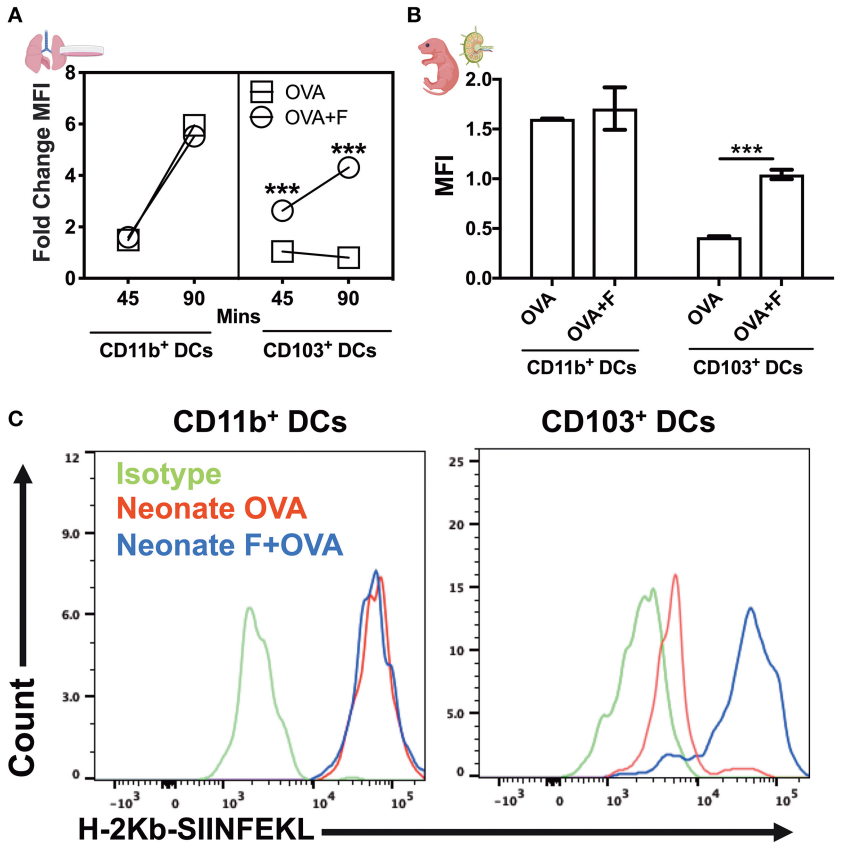

FIGURE 7 | Flagellin enhances antigen cross presentation by neonatal lung CD103$^+$ DCs. **(A)** DQ-OVA gives green fluorescence following uptake, and the co-emergence of a red signal reflects the accumulation of cleaved OVA peptides enabling assessment of cytoplasmic differences in organelle distribution after endocytosis. Stimulation of neonatal lung CD11c$^+$ cells *in vitro* with flagellin measured the phagosome accumulation of DQ-OVA peptides in a time-dependent manner. **(B)** Antigen processing capacities are significantly increased by flagellin in isolated neonatal LN migDC subsets, as determined by the MFI ratio of OVA^{green} to OVA^{red} signal. **(C)** Anti-mouse MHC Class I antibody bound to SIINFEKL specifically reacts with ovalbumin-derived peptide SIINFEKL bound to H-2Kb of MHC class I, but not with unbound H-2Kb or H-2Kb bound with an irrelevant peptide. Draining lymph node CD103$^+$ DC subset from the neonates show poor MHC-I presentation of OVA peptides (SIINFEKL), which was reversed in the flagellin adjuvanted group. $n = 5$ per age group. ***$p < 0.001$, ns, not significant, determined by repeated measures two-way ANOVA with Sidak *post-hoc* test.

from neonatal and adult mouse lungs and monitored their response to different PRR stimuli. In the CD11c enriched cells, we identified mature APCs as MHC-II^{high}, and four major APC precursors were gated based on the expression of Ly6C$^{+/-}$ and CD11b$^{+/-}$ in the MHC-II^{low} population. Compared to adult mice, neonatal mice demonstrated lower frequencies of CD103$^+$ and CD11b$^+$ migDC subsets, while the percentages of Ly6C$^+$ precursor cells were abundant. Low percentages and qualitative differences in migDC subsets correlate with severity of RSV infection in the lungs of neonatal mice (32). However, the Ly6C$^+$CD11b$^+$ monocytic precursor population has not been fully explored for the transcriptional and functional characteristics to identify the molecular pathways, which can be targeted to generate mature APC and cDC populations. Interestingly, precursor cells are more proliferative and replenish DCs and maintain innate responses to microbes, while MHC-II^{pos} mature DCs are migratory and initiate adaptive immunity (41). After viral infections, precursor population depletion and loss of migratory receptor in MHCII$^+$ cells is a mechanism of immune evasion (41, 42), a process that is incompletely characterized in early life. In this study, we focused mainly on mature cell phenotype and how can we overcome a hyporesponsive immune response in early life. Future studies should assess the impact of the high abundance of precursor cells, on infection or intranasal vaccination. Remarkably, we noted that neonatal mice demonstrated a lower percentage of type-I interferon secreting pDCs, while there were no differences noted in the antigen uptake capacities of all the APC subsets isolated from neonates and adults. These observations are consistent with prior reports that neonatal lung contains exceptionally low percentage of pDCs which were more abundant in the spleen, constituting ∼40% of the mature APCs (43). Quantitative differences in lung migDC subsets in the lungs were also accompanied by phenotypic deficiencies of their maturation as they displayed the lower expression of maturation markers CD40, CD80, and CD86. Notably, adult and neonatal CD11c^{pos} cells demonstrated comparable cytokine production after stimulation with TLR5, RIG-I, and STING agonists, while there was no

difference in the basal level of cytokine production. Based on these observations, we speculate that the low abundance or immature phenotype of migDCs and pDCs in the lung may contribute to the greater susceptibility to respiratory infection in early life (44).

To characterize the function of these APC subsets and identify potential innate pathways to overcome neonatal hyporesponsiveness, we stimulated CD11c-enriched cells with different PRR agonists and investigated the expression of maturation markers. Using *in vitro* bone marrow-derived DCs from neonates and adult, we previously identified a STING agonist (2′3′-cGAMP) as an effective adjuvant in early life (mice that were ∼7 days old), that expanded GC B cells and subsequent antigen specific antibody titers, and IgG2c class switching as early as 42 days of life (25). However, the mucosal CD11c$^+$ DCs from neonates and adults demonstrated distinct patterns of activation to the same stimuli, with flagellin the most active of the tested agonists *in vitro*. While responses to PRR agonists PAM3CSK4, PAM2CSK4, and PolyI:C were lower in both ages, we noted that the MPLA, CL075, CpG, and STING induced robust activation of lung DCs from mice lungs. Adjuvant-driven activation of migDC is relevant as these cells not only produce cytokines and induce leukocyte chemotaxis, but also migrate to draining lymph nodes and initiate adaptive immunity.

Among the stimuli studied, TLR5 agonist flagellin activated neonatal migDCs more robustly and upregulated the expression of lymph node homing receptor CCR7 on neonatal migDCs. These findings corroborate many studies which highlight flagellin as a potent mucosal adjuvant and highlight its role in the cytokine induction, leukocyte chemotaxis, cellular interactions, and the generation of protective innate immunity in the mucosal compartment (45, 46). To track migDC mobilization to lymph nodes, we administered DQ-OVA intranasally to neonates and adult mice. DQ-OVA not only acts as an antigen, but is also a very useful tool to study the antigen processing and presentation *in vivo*. While unstimulated DCs from neonates showed poor mobilization from the lung to lymph nodes in response to DQ-OVA antigen, flagellin co-administration strongly potentiated the migration of both the subsets and also upregulated the expression of CD80 and CD86 on CD103$^+$ DC in the lymph nodes. These observations further strengthen our findings and highlight flagellin as a potent mucosal adjuvant in our early life intranasal vaccination model.

Another intriguing finding of our study is the differences in the lysosomal processing of antigens at an early age. DQ-OVA proteolytic cleavage emits the green fluorescence in the endosome, while the accumulation of OVA peptides in the perivascular compartment generates a strong red signal. While there were no differences in antigen uptake across both subsets, neonatal CD103$^+$ DCs showed very rapid cleavage and clearance of DQ-OVA and significantly lower signal in the red channel, which signifies poor antigen cross presentation *in vivo*. We also examined the antigen processing capacities of isolated lung migDC subsets, and observed a striking difference in the DQ-OVA processing which signify the endosomal defects in the cross-presenting machinery of CD103$^+$ DCs. However, flagellin stimulation revived phagosomal maturation and overcame the slow perivascular accumulation of antigens. We also studied OVA peptide presentation on MHC using anti-SIINFEKL antibodies specific for SIINFEKL bound to H-2Kb of MHC class I *in vivo*, and demonstrated that flagellin co-administration significantly increased antigen presentation on MHC-I. These findings suggest that TLR5 signaling in CD103$^+$ DCs plays an important role in the priming of antigen cross-presentation. However, there is also evidence that flagellin-OVA fusion proteins may promote antigen cross-presentation independently of TLR5 or MyD88 signaling, by facilitating antigen processing, presumably dependent upon the maturation stage of DCs (47).

While dealing with the continual process of immune education during postnatal development, early life lung-resident immune cells are faced with the distinct challenge of reacting to pathogenic and non-pathogenic exposures in a manner that protects the organ's critical gas exchange machinery. This "neonatal window of opportunity" is such that early life priming can set the stage for life long host-microbial interaction and immune homeostasis (48–51). Additionally, composition of the early life microbiome may ultimately affect vaccine efficacy (52). For example, several theories are emerging regarding immune ontogeny and exposure during infancy in relation to immune perturbations such as pathogen exposure and vaccination. These include (a) the "hygiene hypothesis" (53), (b) the "appropriate exposure hypothesis" (54), (c) the "founder hypothesis" (55), and (d) "trained immunity" and "local innate immune memory" in the lung (56, 57). Interestingly, human cDC1 and cDC2 subset distribution is a function of tissue site and basal cDC2's preferentially exhibit maturation and migration phenotypes in mucosal-draining lymph nodes of adults and elders (58). However, this high cDC2:cDC1 ratio is (a) largely confined to intestinal sites in early life, and (b) cDC2 maturation dominance only emerges in the lung in later infancy (∼3 months of life) and is maintained throughout life thereafter. Our studies provide further support for an ontologically driven cDC2:cDC1 ratio in the lung, and refine it to specially highlight a cDC1 dominance in the neonatal period that is supplanted by cDC2 subsets in infancy.

Overall, our study features several strengths, including (a) the immunophenotypic characterization of murine five neonatal lung APC subsets, by age; (b) a systematic screening of PRR agonists for activity toward neonatal lung DCs; and (c) while flagellin has been proposed as a promising adjuvant by IM route in NHP infant animals (59), or via the mucosal route in adult mice (60), our study is the first to combine identification of flagellin as an adjuvant active toward neonatal leukocytes *in vitro* and neonatal animals via a mucosal route *in vivo,* (d) distinct from prior investigations of how live infection of neonatal mice with *Staphylococcus aureus* or RSV effect migDCs responses, our study highlights the potential benefit of understating the unique efficacy of well-defined PRR stimuli/adjuvants (i.e., flagellin) enhance lung APC. Together, this information is critically important for evaluating the potential utility of rationally designed vaccine formulations in enabling early life intranasal immunization. Along with its multiple strengths, our study also has limitations, including (a) the neonatal lung APC model represents a mix of cells isolated by mechanical and enzyme

treatment *in vitro* such that they may not fully reflect *in vivo* biology, (b) as a euthanizing agent we employed CO_2 which can induce pulmonary hemorrhage in mice and activate lung APCs (61), and although we did not notice any substantial difference in neonatal and adult lung $CD11c^{pos}$ for the production of IL-1β, we cannot rule out that changes in pH or oxygen tension in the lung may have impacted APC responses, (c) the potential effects of flagellin on migDC1 to lymph organs are intriguing but at this stage inferential, (d) although our studies demonstrated cDC1 maturation with flagellin adjuvanted intranasal ova vaccination, future functional studies (e.g., pathogen challenge) are required to assess the efficacy of this adjuvantation system, and (e) due to species specificity, results in mice may not accurately reflect those in humans.

To our knowledge, ours is the first study to functionally characterize mucosal APC subsets by age combined with evaluation of their responses to different PRR agonists, which can be used as mucosal adjuvants and/or potentiators of innate immunity to enhance resistance to respiratory infections in early life. We also highlight that the neonatal phase of murine development features qualitatively distinct $CD103^{+}$ DCs that are relatively deficient in phagosomal maturation and cross-presenting machinery, which could be functionally enhanced via TLR5 stimulation. As there is an unmet medical need for robust mucosal adjuvants to protect vulnerable populations such as the very young, future studies should further address additional mechanistic differences in the endosomal compartment as well as the effect of flagellin adjuvantation on antigen immunogenicity *in vivo*, including potential protection from live microbial challenge.

DATA AVAILABILITY STATEMENT

The datasets generated for this study are available on request to the corresponding author.

ETHICS STATEMENT

The animal study was reviewed and approved by Animal Care and Use Committee of Boston Children's Hospital and Harvard Medical School (protocol numbers 15-11-3011 and 16-02-3130).

AUTHOR CONTRIBUTIONS

PS, DD, and OL designed the study. PS conducted the experiments. PS and DD analyzed the data and wrote the manuscript. OL provided overall mentorship and assisted in writing the manuscript.

FUNDING

This study within the *Precision Vaccines Program* was supported in part by U.S. National Institutes of Health (NIH)/National Institutes of Allergy and Infectious Diseases (NIAID) awards including Molecular Mechanisms of Combination Adjuvants (1U01AI124284-01), Adjuvant Discovery (HHSN272201400052C and 75N93019C00044), and Development (HHSN272201800047C) Program Contracts and internal awards from the Boston Children's Hospital Department of Pediatrics and Chief Scientific Office. DD's laboratory was supported by NIH grant 1R21AI137932-01A1 and Adjuvant Discovery Program 75N93019C00044.

ACKNOWLEDGMENTS

We authors thank the members of the BCH *Precision Vaccine Program* for their helpful discussions. The authors are grateful for the mentorship and support of Drs. Michael Wessels, Francesco Borriello, Dennis Kim, and Gary R. Fleisher and *Precision Vaccines Program* Coordinator Diana Vo for administrative and programmatic support. This manuscript has been released as a Pre-Print at BioRxiv (62).

SUPPLEMENTARY MATERIAL

The Supplementary Material for this article can be found online at: https://www.frontiersin.org/articles/10.3389/fimmu.2020.00171/full#supplementary-material

Figure S1 | Lung APCs from neonatal mice demonstrate comparable cytokine production to adult mice following stimulation with flagellin and 2′3′-cGAMP. **(A)** Summary of cytokine production after stimulation with different PRR agonists. **(B–E)** TLR5 agonist flagellin and the STING agonist 2′3′-cGAMP induced comparable cytokine production from both neonatal and adult APCs. $n = 3$ per age group, $^{*}p < 0.05$, $^{**}p < 0.01$, $^{***}p < 0.001$, ns, not significant, determined by repeated measures two-way ANOVA with Sidak *post-hoc* test.

Figure S2 | migDC subsets from neonatal and adult mice demonstrate similar antigen uptake and endosomal processing. **(A,B)** CD11c enriched cells from neonatal and adult mouse lungs were stimulated with flagellin and were monitored for kinetics of DQ-OVA degradation. Cells were fixed and fluorescence measured in the green channel via flow cytometry. Mean of fluorescence intensities were compared for mice of different treatment groups.

Table S1 | Antibodies used for flow cytometry study of APC subsets.

REFERENCES

1. Liu L, Oza S, Hogan D, Perin J, Rudan I, Lawn JE, et al. Global, regional, and national causes of child mortality in 2000-13, with projections to inform post-2015 priorities: an updated systematic analysis. *Lancet.* (2015) 385:430–40. doi: 10.1016/S0140-6736(14)61698-6
2. Lycke N. Recent progress in mucosal vaccine development: potential and limitations. *Nat Rev Immunol.* (2012) 12:592–605. doi: 10.1038/nri3251
3. Speers DJ, Moss DM, Minney-Smith C, Levy A, Smith DW. Influenza and respiratory syncytial virus are the major respiratory viruses detected from prospective testing of pediatric and adult coronial autopsies. *Influenza Other Respir Viruses.* (2013) 7:1113–21. doi: 10.1111/irv.12139
4. Shakya AK, Chowdhury MYE, Tao W, Gill HS. Mucosal vaccine delivery: current state and a pediatric perspective. *J Control Release.* (2016) 240:394–413. doi: 10.1016/j.jconrel.2016.02.014
5. Holmgren J, Svennerholm AM. Vaccines against mucosal infections. *Curr Opin Immunol.* (2012) 24:343–53. doi: 10.1016/j.coi.2012.03.014

6. Neutra MR, Kozlowski PA. Mucosal vaccines: the promise and the challenge. *Nat Rev Immunol.* (2006) 6:148–58. doi: 10.1038/nri1777
7. Hu W, Pasare C. Location, location, location: tissue-specific regulation of immune responses. *J Leukoc Biol.* (2013) 94:409–21. doi: 10.1189/jlb.0413207
8. Guilliams M, Ginhoux F, Jakubzick C, Naik SH, Onai N, Schraml BU, et al. Dendritic cells, monocytes and macrophages: a unified nomenclature based on ontogeny. *Nat Rev Immunol.* (2014) 14:571–8. doi: 10.1038/nri3712
9. Kollmann TR, Kampmann B, Mazmanian SK, Marchant A, Levy O. Protecting the newborn and young infant from infectious diseases: lessons from immune ontogeny. *Immunity.* (2017) 46:350–63. doi: 10.1016/j.immuni.2017.03.009
10. Ogra PL, Faden H, Welliver RC. Vaccination strategies for mucosal immune responses. *Clin Microbiol Rev.* (2001) 14:430–45. doi: 10.1128/CMR.14.2.430-445.2001
11. Thwala LN, Preat V, Csaba NS. Emerging delivery platforms for mucosal administration of biopharmaceuticals: a critical update on nasal, pulmonary and oral routes. *Expert Opin Drug Deliv.* (2017) 14:23–36. doi: 10.1080/17425247.2016.1206074
12. Garg R, Theaker M, Martinez EC, van Drunen Littel-van den Hurk S. A single intranasal immunization with a subunit vaccine formulation induces higher mucosal IgA production than live respiratory syncytial virus. *Virology.* (2016) 499:288–97. doi: 10.1016/j.virol.2016.09.023
13. Yang Z, Zhao Q, Gao YA, Zhang W. Combined oral and intravenous immunization stimulates strong IgA responses in both systemic and mucosal compartments. *PLoS ONE.* (2016) 11:e0168037. doi: 10.1371/journal.pone.0168037
14. Rosato PC, Beura LK, Masopust D. Tissue resident memory T cells and viral immunity. *Curr Opin Virol.* (2017) 22:44–50. doi: 10.1016/j.coviro.2016.11.011
15. Riese P, Sakthivel P, Trittel S, Guzman CA. Intranasal formulations: promising strategy to deliver vaccines. *Expert Opin Drug Deliv.* (2014) 11:1619–34. doi: 10.1517/17425247.2014.931936
16. Belyakov IM, Ahlers JD. What role does the route of immunization play in the generation of protective immunity against mucosal pathogens? *J Immunol.* (2009) 183:6883–92. doi: 10.4049/jimmunol.0901466
17. Kim SH, Jang YS. The development of mucosal vaccines for both mucosal and systemic immune induction and the roles played by adjuvants. *Clin Exp Vaccine Res.* (2017) 6:15–21. doi: 10.7774/cevr.2017.6.1.15
18. Beigelman A, Bacharier LB. Early-life respiratory infections and asthma development: role in disease pathogenesis and potential targets for disease prevention. *Curr Opin Allergy Clin Immunol.* (2016) 16:172–8. doi: 10.1097/ACI.0000000000000244
19. Nanishi E, Dowling DJ, Levy O. Toward precision adjuvants: optimizing science and safety. *Curr Opin Pediatr.* (2020) 32:125–38. doi: 10.1097/MOP.0000000000000868
20. Ciabattini A, Pettini E, Fiorino F, Pastore G, Andersen P, Pozzi G, et al. Modulation of primary immune response by different vaccine adjuvants. *Front Immunol.* (2016) 7:427. doi: 10.3389/fimmu.2016.00427
21. Dowling DJ, Levy O. Pediatric vaccine adjuvants: components of the modern vaccinologist's toolbox. *Pediatr Infect Dis J.* (2015) 34:1395–8. doi: 10.1097/INF.0000000000000893
22. Reed SG, Orr MT, Fox CB. Key roles of adjuvants in modern vaccines. *Nat Med.* (2013) 19:1597–608. doi: 10.1038/nm.3409
23. Dowling DJ, Levy O. Ontogeny of early life immunity. *Trends Immunol.* (2014) 35:299–310. doi: 10.1016/j.it.2014.04.007
24. Pabst R. Mucosal vaccination by the intranasal route. Nose-associated lymphoid tissue (NALT)-Structure, function and species differences. *Vaccine.* (2015) 33:4406–13. doi: 10.1016/j.vaccine.2015.07.022
25. Borriello F, Pietrasanta C, Lai JCY, Walsh LM, Sharma P, O'Driscoll DN, et al. Identification and characterization of stimulator of interferon genes as a robust adjuvant target for early life immunization. *Front Immunol.* (2017) 8:1772. doi: 10.3389/fimmu.2017.01772
26. Dowling D, Hamilton CM, O'Neill SM. A comparative analysis of cytokine responses, cell surface marker expression and MAPKs in DCs matured with LPS compared with a panel of TLR ligands. *Cytokine.* (2008) 41:254–62. doi: 10.1016/j.cyto.2007.11.020
27. Chang SY, Song JH, Guleng B, Cotoner CA, Arihiro S, Zhao Y, et al. Circulatory antigen processing by mucosal dendritic cells controls CD8(+) T cell activation. *Immunity.* (2013) 38:153–65. doi: 10.1016/j.immuni.2012.09.018
28. Blom RAM, Amacker M, van Dijk RM, Moser C, Stumbles PA, Blank F, et al. Pulmonary delivery of virosome-bound antigen enhances antigen-specific $CD4^+$ T cell proliferation compared to liposome-bound or soluble antigen. *Front Immunol.* (2017) 8:359. doi: 10.3389/fimmu.2017.00359
29. Clatworthy MR, Aronin CE, Mathews RJ, Morgan NY, Smith KG, Germain RN. Immune complexes stimulate CCR7-dependent dendritic cell migration to lymph nodes. *Nat Med.* (2014) 20:1458–63. doi: 10.1038/nm.3709
30. Cosway EJ, Ohigashi I, Schauble K, Parnell SM, Jenkinson WE, Luther S, et al. Formation of the intrathymic dendritic cell pool requires CCL21-mediated recruitment of CCR7(+) progenitors to the thymus. *J Immunol.* (2018) 201:516–23. doi: 10.4049/jimmunol.1800348
31. Drakes ML, Stiff PJ, Blanchard TG. Inverse relationship between dendritic cell CCR9 expression and maturation state. *Immunology.* (2009) 127:466–76. doi: 10.1111/j.1365-2567.2009.03043.x
32. Ruckwardt TJ, Malloy AM, Morabito KM, Graham BS. Quantitative and qualitative deficits in neonatal lung-migratory dendritic cells impact the generation of the CD8+ T cell response. *PLoS Pathog.* (2014) 10:e1003934. doi: 10.1371/journal.ppat.1003934
33. Lee HK, Zamora M, Linehan MM, Iijima N, Gonzalez D, Haberman A, et al. Differential roles of migratory and resident DCs in T cell priming after mucosal or skin HSV-1 infection. *J Exp Med.* (2009) 206:359–70. doi: 10.1084/jem.20080601
34. Liu F, Su B, Fu Q, Shang M, Gao C, Tan F, et al. Identification, characterization and expression analysis of TLR5 in the mucosal tissues of turbot (Scophthalmus maximus L.) following bacterial challenge. *Fish Shellfish Immunol.* (2017) 68:272–9. doi: 10.1016/j.fsi.2017.07.021
35. Van Maele L, Carnoy C, Cayet D, Songhet P, Dumoutier L, Ferrero I, et al. TLR5 signaling stimulates the innate production of IL-17 and IL-22 by CD3(neg)CD127+ immune cells in spleen and mucosa. *J Immunol.* (2010) 185:1177–85. doi: 10.4049/jimmunol.1000115
36. Van Maele L, Fougeron D, Janot L, Didierlaurent A, Cayet D, Tabareau J, et al. Airway structural cells regulate TLR5-mediated mucosal adjuvant activity. *Mucosal Immunol.* (2014) 7:489–500. doi: 10.1038/mi.2013.66
37. Torow N, Marsland BJ, Hornef MW, Gollwitzer ES. Neonatal mucosal immunology. *Mucosal Immunol.* (2017) 10:5–17. doi: 10.1038/mi.2016.81
38. Dowling DJ. Recent advances in the discovery and delivery of TLR7/8 agonists as vaccine adjuvants. *Immuno Horizons.* (2018) 2:185–97. doi: 10.4049/immunohorizons.1700063
39. Borriello F, van Haren SD, Levy O. First international precision vaccines conference: multidisciplinary approaches to next-generation vaccines. mSphere. (2018) 3:e00214–18. doi: 10.1128/mSphere.00214-18
40. Rappuoli R, Mandl CW, Black S, De Gregorio E. Vaccines for the twenty-first century society. *Nat Rev Immunol.* (2011) 11:865–72. doi: 10.1038/nri3085
41. Wang H, Peters N, Laza-Stanca V, Nawroly N, Johnston SL, Schwarze J. Local CD11c+ MHC class II- precursors generate lung dendritic cells during respiratory viral infection, but are depleted in the process. *J Immunol.* (2006) 177:2536–42. doi: 10.4049/jimmunol.177.4.2536
42. Ruckwardt TJ, Morabito KM, Bar-Haim E, Nair D, Graham BS. Neonatal mice possess two phenotypically and functionally distinct lung-migratory CD103(+) dendritic cell populations following respiratory infection. *Mucosal Immunol.* (2018) 11:186–98. doi: 10.1038/mi.2017.28
43. Sun CM, Fiette L, Tanguy M, Leclerc C, Lo-Man R. Ontogeny and innate properties of neonatal dendritic cells. *Blood.* (2003) 102:585–91. doi: 10.1182/blood-2002-09-2966
44. Sharma A, Sharma P, Vishwakarma AL, Srivastava M. Functional impairment of murine dendritic cell subsets following infection with infective larval stage 3 of *Brugia malayi*. *Infect Immun.* (2017) 85:e00818-16. doi: 10.1128/IAI.00818-16
45. Fulde M, Sommer F, Chassaing B, van Vorst K, Dupont A, Hensel M, et al. Neonatal selection by Toll-like receptor 5 influences long-term gut microbiota composition. *Nature.* (2018) 560:489–93. doi: 10.1038/s41586-018-0395-5
46. McCarron M, Reen DJ. Activated human neonatal CD8+ T cells are subject to immunomodulation by direct TLR2 or TLR5 stimulation. *J Immunol.* (2009) 182:55–62. doi: 10.4049/jimmunol.182.1.55

47. Bates JT, Graff AH, Phipps JP, Grayson JM, Mizel SB. Enhanced antigen processing of flagellin fusion proteins promotes the antigen-specific CD8+ T cell response independently of TLR5 and MyD88. *J Immunol.* (2011) 186:6255–62. doi: 10.4049/jimmunol.1001855
48. Renz H, Adkins BD, Bartfeld S, Blumberg RS, Farber DL, Garssen J, et al. The neonatal window of opportunity-early priming for life. *J Allergy Clin Immunol.* (2018) 141:1212–4. doi: 10.1016/j.jaci.2017.11.019
49. Torow N, Hornef MW. The neonatal window of opportunity: setting the stage for life-long host-microbial interaction and immune homeostasis. *J Immunol.* (2017) 198:557–63. doi: 10.4049/jimmunol.1601253
50. Gensollen T, Iyer SS, Kasper DL, Blumberg RS. How colonization by microbiota in early life shapes the immune system. *Science.* (2016) 352:539–44. doi: 10.1126/science.aad9378
51. Gensollen T, Blumberg RS. Correlation between early-life regulation of the immune system by microbiota and allergy development. *J Allergy Clin Immunol.* (2017) 139:1084–91. doi: 10.1016/j.jaci.2017.02.011
52. Valdez Y, Brown EM, Finlay BB. Influence of the microbiota on vaccine effectiveness. *Trends Immunol.* (2014) 35:526–37. doi: 10.1016/j.it.2014.07.003
53. Haspeslagh E, Heyndrickx I, Hammad H, Lambrecht BN. The hygiene hypothesis: immunological mechanisms of airway tolerance. *Curr Opin Immunol.* (2018) 54:102–8. doi: 10.1016/j.coi.2018.06.007
54. Dowling DJ. Early life immune ontogeny - understanding how we build and sustain immunity to infection. *Perspect Public Health.* (2016) 136:205–7. doi: 10.1177/1757913916641586
55. Litvak Y, Baumler AJ. The founder hypothesis: a basis for microbiota resistance, diversity in taxa carriage, and colonization resistance against pathogens. *PLoS Pathog.* (2019) 15:e1007563. doi: 10.1371/journal.ppat.1007563
56. Netea MG, Joosten LAB. Trained immunity and local innate immune memory in the lung. *Cell.* (2018) 175:1463–5. doi: 10.1016/j.cell.2018.11.007
57. Schulze K, Ebensen T, Babiuk LA, Gerdts V, Guzman CA. Intranasal vaccination with an adjuvanted polyphosphazenes nanoparticle-basedvaccine formulation stimulates protective immune responses in mice. *Nanomedicine.* (2017) 13:2169–78. doi: 10.1016/j.nano.2017.05.012
58. Granot T, Senda T, Carpenter DJ, Matsuoka N, Weiner J, Gordon CL, et al. Dendritic cells display subset and tissue-specific maturation dynamics over human life. *Immunity.* (2017) 46:504–15. doi: 10.1016/j.immuni.2017.02.019
59. Kim JR, Holbrook BC, Hayward SL, Blevins LK, Jorgensen MJ, Kock ND, et al. Inclusion of flagellin during vaccination against influenza enhances recall responses in nonhuman primate neonates. *J Virol.* (2015) 89:7291–303. doi: 10.1128/JVI.00549-15
60. Munoz N, Van Maele L, Marques JM, Rial A, Sirard JC, Chabalgoity JA. Mucosal administration of flagellin protects mice from *Streptococcus pneumoniae* lung infection. *Infect Immun.* (2010) 78:4226–33. doi: 10.1128/IAI.00224-10
61. Fisher S, Burgess WL, Hines KD, Mason GL, Owiny JR. Interstrain differences in CO2-induced pulmonary hemorrhage in mice. *J Am Assoc Lab Anim Sci.* (2016) 55:811–5.
62. Sharma P, Levy O, Dowling DJ. The TLR5 agonist flagellin modifies phenotypical and enhances functional activation of lung mucosal antigen presenting cells in neonatal mice. *bioRxiv.* (2019) 564054. doi: 10.1101/564054

Conflict of Interest: The authors declare that the research was conducted in the absence of any commercial or financial relationships that could be construed as a potential conflict of interest.

frontiers in Immunology

ORIGINAL RESEARCH
published: 05 March 2020
doi: 10.3389/fimmu.2020.00357

Intestinal Dysbiosis and the Developing Lung: The Role of Toll-Like Receptor 4 in the Gut-Lung Axis

*Stephen Wedgwood[1], Kimberly Gerard[1], Katrina Halloran[1], Ashley Hanhauser[1], Sveva Monacelli[1], Cris Warford[1], Phung N. Thai[2], Nipavan Chiamvimonvat[2,3], Satyan Lakshminrusimha[1], Robin H. Steinhorn[4] and Mark A. Underwood[1]**

[1] Department of Pediatrics, UC Davis School of Medicine, Sacramento, CA, United States, [2] Division of Cardiovascular Medicine, Department of Internal Medicine, UC Davis Health System, Sacramento, CA, United States, [3] Department of Veterans Affairs, Northern California Health Care System, Mather, CA, United States, [4] Department of Hospital Medicine, Children's National Health System, Washington, DC, United States

OPEN ACCESS

Edited by:
Duc Ninh Nguyen,
University of Copenhagen, Denmark

Reviewed by:
Chung-Ming Chen,
Taipei Medical University, Taiwan
Claudia Nold,
Hudson Institute of Medical Research, Australia
David Hackam,
Johns Hopkins Medicine, United States

***Correspondence:**
Mark A. Underwood
munderwood@ucdavis.edu

Specialty section:
This article was submitted to Nutritional Immunology, a section of the journal Frontiers in Immunology

Received: 16 November 2019
Accepted: 14 February 2020
Published: 05 March 2020

Citation:
Wedgwood S, Gerard K, Halloran K, Hanhauser A, Monacelli S, Warford C, Thai PN, Chiamvimonvat N, Lakshminrusimha S, Steinhorn RH and Underwood MA (2020) Intestinal Dysbiosis and the Developing Lung: The Role of Toll-Like Receptor 4 in the Gut-Lung Axis. Front. Immunol. 11:357. doi: 10.3389/fimmu.2020.00357

Background: In extremely premature infants, postnatal growth restriction (PNGR) is common and increases the risk of developing bronchopulmonary dysplasia (BPD) and pulmonary hypertension (PH). Mechanisms by which poor nutrition impacts lung development are unknown, but alterations in the gut microbiota appear to play a role. In a rodent model, PNGR plus hyperoxia causes BPD and PH and increases intestinal Enterobacteriaceae, Gram-negative organisms that stimulate Toll-like receptor 4 (TLR4). We hypothesized that intestinal dysbiosis activates intestinal TLR4 triggering systemic inflammation which impacts lung development.

Methods: Rat pups were assigned to litters of 17 (PNGR) or 10 (normal growth) at birth and exposed to room air or 75% oxygen for 14 days. Half of the pups were treated with the TLR4 inhibitor TAK-242 from birth or beginning at day 3. After 14 days, pulmonary arterial pressure was evaluated by echocardiography and hearts were examined for right ventricular hypertrophy (RVH). Lungs and serum samples were analyzed by western blotting and immunohistochemistry.

Results: Postnatal growth restriction + hyperoxia increased pulmonary arterial pressure and RVH with trends toward increased plasma IL1β and decreased IκBα, the inhibitor of NFκB, in lung tissue. Treatment with the TLR4 inhibitor attenuated PH and inflammation.

Conclusion: Postnatal growth restriction induces an increase in intestinal Enterobacteriaceae leading to PH. Activation of the TLR4 pathway is a promising mechanism by which intestinal dysbiosis impacts the developing lung.

Keywords: intestinal dysbiosis, TLR4, pulmonary hypertension, bronchopulmonary dysplasia, premature infant, Enterobacteriaceae

INTRODUCTION

Pulmonary hypertension (PH) is an increase in pulmonary vascular resistance resulting in a decrease in pulmonary blood flow and right ventricular hypertrophy (RVH). The incidence of PH among extremely premature infants (birth weight less than 1000 g) is as high as 18% and increases to 25–40% among premature infants with bronchopulmonary dysplasia (BPD), a chronic lung

disease (1, 2). In this population, PH is associated with very high morbidity and 50% mortality (3). PH is often not diagnosed until the patient develops severe right ventricular dysfunction. Current screening methods are unreliable, and no early biomarkers of PH exist.

A large cohort study found that 79% of premature infants with gestational age <27 weeks displayed poor growth after birth (post-natal growth restriction, PNGR) (4). PNGR is associated with a sustained elevation in C-reactive protein (5) and increases the risk of PH, BPD and other diseases of prematurity including necrotizing enterocolitis (NEC), an inflammatory disease of the intestines (6–8). In a recent prospective study of PH, among extremely preterm infants with BPD (mean gestational age at birth 26 weeks) evaluated at 36 to 38 weeks corrected gestational age, 13/44 (30%) patients with PH had a history of NEC, while only 8/115 (7%) patients without PH had a history of NEC [adjusted odds ratio 5.5 (95% confidence intervals 1.9, 15.4)] (9), suggesting an association between inflammation in the gut and pulmonary vascular disease. A meta-analysis confirmed a strong association between NEC and PH particularly among infants with BPD (RR 3.4 with 95% confidence intervals 1.1 and 10.2) (10).

Similar to preterm infants, rats are born in the saccular stage of lung development. Neonatal rats exposed to hyperoxia (75–95% O_2) for 14 days develop PH, RVH, pulmonary vascular remodeling, and alveolar simplification characteristic of preterm infants with BPD (11). We have shown in a novel rodent model that PNGR, achieved by increasing litter size from 10 to 17 pups, triggers PH and amplifies the adverse effects of hyperoxia at 2 weeks of age (12, 13). This age is roughly equivalent to a human infant at 6–12 months (14), a common time of death for premature infants with PH.

Associations between nutrition, the intestinal microbiota and immune responses in distant sites such as the lung, brain and liver have prompted study of the gut-lung, gut-brain, and gut-liver axes. We recently reported that PNGR, but not hyperoxia, alters the intestinal microbiota in rats at 14 days (15). Partially correcting the dysbiosis with a probiotic strain of *Lactobacillus reuteri* attenuates PNGR-induced PH (15). We also reported an increase in pro-inflammatory Gram-negative Enterobacteriaceae in the distal small bowel of rat pups exposed to both PNGR and hyperoxia (15). Recognition of lipopolysaccharide (LPS) in the cell wall of Enterobacteriaceae by the host Toll-like receptor (TLR)4 is important in the pathogenesis of NEC, and both inhibition of TLR4 and manipulation of the intestinal microbiota with probiotic organisms prevents this disease (16, 17). TLR4 signaling is also important in lung injury and inflammation (18). In a rodent model of NEC, lung injury is prominent and can be attenuated by deletion of TLR4 from the pulmonary epithelium (19). Furthermore, activation of TLR4 in the NEC model induced expression of chemokine ligand 25 (CC25) resulting in recruitment of Th17 cells to the lungs (20). From these studies we hypothesized that TLR4 –induced inflammation in the intestines is an important mechanism by which PNGR-associated dysbiosis triggers PH in rat pups. The goal of this study was to investigate the role of TLR4 in the developing gut-lung axis.

MATERIALS AND METHODS

Animals

The animal protocol was approved by the Institutional Animal Care and Use Committee at UC Davis. Timed-pregnant Sprague Dawley dams at E14-E16 were ordered from Charles River Laboratories (Wilmington, MA, United States). Rats were housed in plastic cages with a 12 h dark:light cycle and allowed to feed *ad libitum* with a standard diet (2018 Teklad from Harlan). After birth, pups were pooled and randomly assigned to litters of 10 pups (normal litter size, N) or 17 pups (restricted litter size, R). Additionally, pups were randomly assigned to cages maintained in room air (A) or exposed to 75% oxygen (O) in a plexiglass chamber (Biospherix, Lacona, NY, United States) continuously, and dams were rotated with the appropriate control or PNGR dam every 24 h. As we have shown previously, the pups tolerate hyperoxia for 14 days without mortality (12). Some pups in each group were injected subcutaneously with the TLR4 inhibitor TAK-242 (Cayman Chemicals, Ann Arbor, MI, United States) (Resatorvid, 3 mg/kg/day from birth) or with vehicle alone (5% ethanol). The dose was chosen based on a previous study in a mouse sepsis model (21). At postnatal day 14, the pups were analyzed by echocardiography, weighed and euthanized for tissue harvest. Pups were euthanized by exposure to CO_2 followed by cardiac puncture and exsanguination, and plasma was collected by centrifugation in heparin-treated tubes (Thermo Fisher Scientific) and stored at −80°C. Hearts and lungs, were snap-frozen in liquid nitrogen and stored at −80°C. The intestinal microbiota was not evaluated for this series of experiments, but has previously been reported for this model (15).

Echocardiography

At day 14, echocardiography was performed on pups under light anesthesia with isoflurane using a VisualSonics VIVO 2100 *in vivo* ultrasound imaging system (VisualSonics, Toronto, ON, Canada) to determine the ratio of the pulmonary acceleration time (PAT) to the total ejection time (ET) a marker of PH as previously described (12).

Measurement of Right Ventricular Hypertrophy (RVH)

Fulton's index [the weight of the right ventricle (RV) divided by the weight of the left ventricle (LV) + septum] was determined to assess RVH. Additionally, RV and LV + septum weights were normalized to body weight (22).

Plasma IL-1b was quantified using the Rat IL-1 beta Platinum ELISA kit (Thermo Fisher Scientific, Waltham, MA, United States) according to the manufacturer's instructions.

Western blots were performed on lung tissue as previously described (12). Briefly, lung tissue was suspended in RIPA buffer containing protease and phosphatase inhibitors and sonicated on ice. Protein content was determined by the Bradford method and Western blotting performed using 1:500 dilution of mouse anti-IκB-α antibody (sc-1643, Santa Cruz Biotechnology, Dallas, TX, United States) at 4°C overnight followed by a 60 min incubation with an anti-mouse secondary antibody conjugated to

horseradish peroxidase (Santa Cruz). Blots were then probed for β-actin (ab6276, 1:4000, Abcam, Cambridge, MA, United States) for 60 min at room temperature. Chemiluminescence generated by Super Signal West Femto substrate (Thermo Fisher Scientific) was detected and quantified using a Kodak Image Station and software. Signals were normalized to β-actin and expressed as fold change relative to OR animals.

Statistical Analysis

Data are presented as means ± SEM. "N" represents the number of animals in each group. Groups were compared with one-way ANOVA (Stata 12.1, College Station, TX, United States). If the *F* test was significant, a Scheffe *post hoc* test was performed. The independent variables were considered significant at $p < 0.05$.

RESULTS

Our previous study identified an increase in Enterobacteriaceae in the distal small bowel of rat pups exposed to PNGR and hyperoxia (15). To determine if activation of TLR4 by Enterobacteriaceae is involved in the development of PH in these rats, we first determined the efficacy of the TLR4 antagonist TAK-242 to attenuate PH. Increased pulmonary artery pressure results in RVH. As we have shown previously (12), PNGR and hyperoxia alone increase Fulton's index (the ratio of RV weight to LV + septum weight) with a further increase in Fulton's index when both are combined (**Figure 1A**). Daily treatment with TAK-242 attenuated RVH in pups exposed to PNGR with and without hyperoxia, but not in pups exposed to hyperoxia alone (**Figure 1A**).

The ratio of the PAT to total ejection time (PAT/ET) detected by echocardiography decreases with increased pulmonary artery pressures. As we have shown previously (12), PAT/ET ratios were significantly decreased in pups exposed to PNGR or hyperoxia alone, and were decreased further in pups exposed to both (**Figure 1B**). Daily treatment with TAK-242 attenuated the decrease in PAT/ET ratios in pups exposed to hyperoxia with PNGR, but not in pups exposed to PNGR or hyperoxia alone (**Figure 1B**).

We opted to focus the remaining experiments on the PNGR and hyperoxia group for four reasons: (1) we have previously demonstrated that intestinal dysbiosis is most severe in the PNGR and hyperoxia group with the largest increases in Enterobacteriaceae, (2) this group consistently has the most severe phenotype in our model, (3) this group had a significant attenuation of both RVH and PAT/ET ratio, with TLR4 inhibition and (4) this group most closely reflects extremely premature infants at the highest risk for PH (those with BPD and poor postnatal growth). We next looked at circulating levels of the cytokine IL-1β, a downstream component of TLR4-induced inflammatory responses. A strong trend toward higher plasma levels was seen in pups exposed to PNGR and hyperoxia relative to controls, while daily treatment with TAK-242 trended toward decreased circulating IL-1β (**Figure 2**).

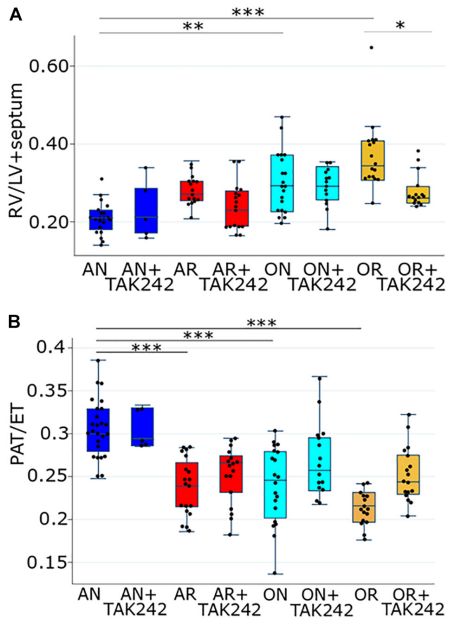

FIGURE 1 | (A) Fulton's index (right ventricular weight divided by the combined weight of the left ventricle and the intraventricular septum) in the four groups of the PNGR model with and without treatment with the TLR4 inhibitor TAK-242. One way ANOVA $p < 0.001$, AN vs. AR $p = 0.2$, AN vs. ON $p = 0.01$, AN vs. OR $p < 0.001$, OR vs. OR + TAK242 $p = 0.04$ (Scheffe). Comparing just the AN vs. AR (not considering the other groups), using a *t*-test, $p < 0.001$. Number of animals AN = 21, AN + TAK242 = 5, AR = 16, AR + TAK242 = 17, ON = 20, ON + TAK242 = 14, OR = 17, OR + TAK242 = 15. **(B)** Ratio of PAT to total ejection time (PAT/ET) in the four groups of the PNGR model with and without treatment with the TLR4 inhibitor TAK-242. One way ANOVA $p < 0.001$, AN vs. AR $p < 0.001$, AN vs. ON $p < 0.001$, AN vs. OR $p < 0.001$, OR vs. OR + TAK242 $p = 0.18$ (Scheffe). Comparing just the OR vs. OR + TAK242 (not considering the other groups), using a *t*-test, $p < 0.001$. Number of animals AN = 25, AN + TAK242 = 5, AR = 19, ARTAK242 = 17, ON = 20, ON + TAK242 = 15, OR = 16, OR + TAK242 = 17. Asterisks in both A and B are from the Scheffe post hoc test: * $p < 0.05$, ** $p < 0.01$, *** $p < 0.001$. AN = room air, normal litter size; AR = room air, growth-restricted litter size; ON = hyperoxia, normal litter size; OR = hyperoxia, growth-restricted litter size.

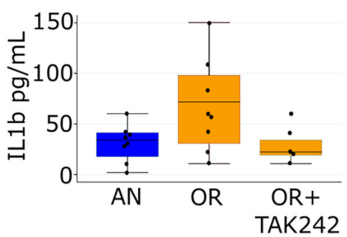

FIGURE 2 | Plasma IL-1β measured by ELISA at day 14 in pups from the air, normal litter size group and the hyperoxia, PNGR group with and without treatment with the TLR4 inhibitor TAK-242. One way ANOVA $p = 0.046$, AN vs. OR $p = 0.08$ and OR vs. OR + TAK242 $p = 0.12$ (Scheffe). Number of animals: AN = 8, OR = 8, OR + TAK242 = 5.

We quantified levels of IκBα protein in lung as a marker of lung inflammation. IκBα is an inhibitory protein of the key pro-inflammatory transcription factor NFκB, and decreases in

IκBα indicate an increase in NFκB-mediated inflammation. IκBα protein trended to a decrease in lungs from rats exposed to PNGR and hyperoxia relative to controls, while daily treatment with TAK-242 significantly increased IκBα levels (**Figure 3**).

In our proposed pathway, intestinal dysbiosis precedes and initiates TLR4 signaling. This raises the possibility that delayed treatment, either to alter the intestinal microbiota or to inhibit TLR4 targeting may be effective in attenuating PH, an advantage in the management of a disease that is not apparent in the premature infant in the first days and weeks of life. To test this hypothesis, we performed additional experiments in which the pups were divided into the four groups on day 1 as usual, but the intervention was not begun until day of life 3. Delaying treatment with TAK-242 until postnatal day 3 still led to significantly increased PAT/ET on day 14 in pups exposed to PNGR and hyperoxia (**Figure 4**) indicating attenuated PH.

DISCUSSION

Postnatal growth restriction is common with very premature birth and increases the risk of BPD and PH. Retrospective cohort studies have demonstrated associations between decreased caloric intake in the first weeks of life and BPD in very preterm infants (6, 7, 23), and limited studies of aggressive nutrition in the first weeks of life have shown benefit in decreasing BPD in this same population (24). NEC is also a risk factor for PH in very preterm infants both with and without BPD (9), supporting the hypothesis that inflammation in the gut impacts the developing lung vasculature.

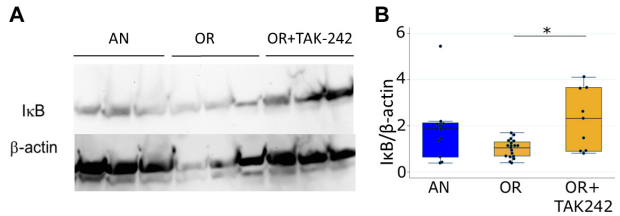

FIGURE 3 | Lung IκBα measured by western blotting at 14 days in pups from the air, normal litter size group and the hyperoxia, PNGR group with and without treatment with the TLR4 inhibitor TAK-242. **(A)** Representative blot **(B)**. Each band was normalized to β-actin and to OR (each point represents a fold change compared to the mean OR value) One way ANOVA $p < 0.01$, AN vs. OR $p = 0.11$ and OR vs. OR + TAK-242 $p < 0.02$ (*Scheffe). Number of animals: AN = 11, OR = 19, OR + TAK242 = 9.

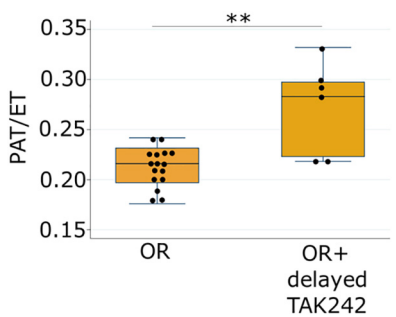

FIGURE 4 | Ratio of pulmonary acceleration time to total ejection time (PAT/ET) in pups exposed to hyperoxia and PNGR model with and without delayed treatment (day 3) with the TLR4 inhibitor TAK-242. **$p < 0.01$. Number of animals: OR = 16, OR + delayed TAK242 = 6.

Many rodent models of PH involve exposing neonatal pups to hyperoxia, although our model including a component of PNGR more closely approximates clinical conditions in extremely premature infants. As such it is a powerful tool to investigate the underlying mechanisms whereby the most vulnerable extremely low birth weight premature infants (those with poor growth receiving supplemental oxygen) are at greatest risk of developing cardiovascular diseases. From these data and our previously published study (15) we hypothesized that PNGR combined with hyperoxia triggers intestinal dysbiosis including elevated Enterobacteriaceae. Blooms of Enterobacteriaceae have been identified just prior to the onset of necrotizing enterocolitis in premature infants (25) and are a signature of dysbiosis in many disease processes (26). We further hypothesized that the resultant activation of TLR4 by Enterobacteriaceae in the intestines triggers an inflammatory response including elevated circulating IL-1β. This transduces the inflammatory signal to the lungs activating NFκB, leading to PH and RVH (**Figure 5**). The present study identifying a role for TLR4 signaling in PH induced by PNGR and hyperoxia supports this hypothesis. We previously demonstrated that the probiotic *L. reuteri* DSM 17938 reverses dysbiosis and attenuates PH and RVH (15), and inhibiting TLR4 signaling likewise attenuates PH and RVH as we show here.

Furthermore, our data suggest that delayed targeting of TLR4 signaling is still effective in attenuating PH. We do not yet know the windows of benefit for either probiotic administration or TLR4 inhibition for successful attenuation of PH in our model, but a potential treatment strategy for preterm infants may involve early probiotic treatment with subsequent targeting of TLR4 signaling in high risk infants.

Studies investigating the gut-lung axis have prompted the hypothesis that intestinal dysbiosis is an important driver of systemic inflammation (27). These associations are particularly important in preterm neonates with immature gut and lung immune responses. Studies of human milk are particularly relevant in this population. Human milk feeding decreases the risk of NEC (28). Meta-analyses suggest a benefit in feeding mother's own milk (29) and pasteurized donor human milk (30) in the prevention of BPD. In organoids derived from the terminal ileum of mouse pups, human milk exosomes have been shown to attenuate LPS induced activation of TLR4 (31). Human milk oligosaccharides interact with TLR4 on the surface of dendritic cells inducing immune tolerance through increased generation of regulatory T cells and attenuation of LPS-induced expression of IL6 and TNFα (32). It is also possible that TLR4 is important in maintenance of stem cells in the developing gut and lung. In the developing intestinal tract, intestinal stem cells express TLR4 which regulates proliferation and apoptosis (33). In a lung injury model, deletion of TLR4 impairs the renewal capacity of lung stem cells (34). Conversely, in a model of neonatal PH triggered by intra-amniotic injection of PBS, human mesenchymal stem

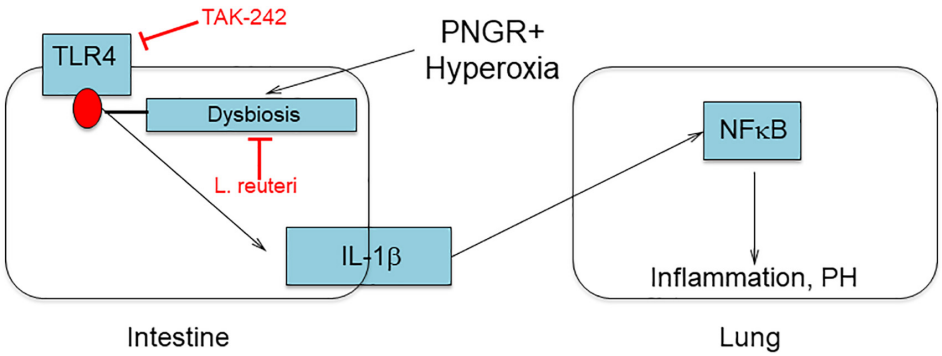

FIGURE 5 | Hypothesized role of dysbiosis and TLR4 signaling in the developing gut-lung axis.

cells decrease expression of TLR4, NFκB, and TNFα in the heart and attenuate PH (35).

Toll-like receptors are important in recognition of pathogen-associated molecular patterns and triggering of innate immune responses in both the gut and the lung, as demonstrated in the studies of TLR4 in NEC-associated lung injury noted in the introduction. TLR4 activates IL-1β transcription via NFκB (36). The role of TLR4 in regulating pulmonary vasculogenesis has also been explored. Adult TLR4-deficient mice do not develop PH when exposed to hypoxia (37). Stimulation of TLR4 on platelets leads to platelet activation and aggregation exacerbating PH (and as a result selective knockout of TLR4 on platelets is protective) (38). The increase in Enterobacteriaceae in our PNGR model suggests a potential role for TLR4 in the intestine and/or the lung in the resultant PH. Probiotic microbes impact host immune responses including downregulation of TLR4 (39), chemokines and cytokines (40–46), suppression of T-helper 2 responses (47) decrease in intestinal permeability (48–51), alteration of intestinal motility (52, 53), and production of short chain fatty acids (54, 55).

Lung inflammation is involved in the development of PH in humans and animal models (56). We believe the current study is the first to demonstrate a potential role for an inflammatory response initiating in the intestines in PNGR/hyperoxia-induced PH. Our studies do not rule out the possibility of a TLR4 response induced in the lung following simultaneous exposure to PNGR and hyperoxia; direct measurement of TLR4 in both the gut and lung would be valuable to address this possibility. Activation of lung TLR4 using aerosolized LPS results in elevated IL-1β in bronchiolar lavage fluid in mice (57), while treatment with the anti-inflammatory molecule dioscin suppresses various pro-inflammatory molecules including TLR4, IL-1β and NFκB in the lungs of rats injected with LPS (58). Our current study indicated that subcutaneous TAK-242 is effective at attenuating PH in our model. Further studies comparing the efficacy of TAK-242 delivered intranasally or via gavage may identify where TLR4 is activated in rats exposed to PNGR and hyperoxia. Measurement of IL1β in both intestinal and lung tissue in this model would be of value in future studies.

In the current study we demonstrate that IκBα levels were decreased in the lungs of rats exposed to PNGR and hyperoxia, while TAK-242 prevented this decrease. Increased NFκB activity is evident in explanted lungs of patients with idiopathic PH (59), and an NFκB decoy delivery into lungs prevents monocrotaline-induced NFκB activity and PH in rats (59) suggesting that elevated lung NFκB activity plays a central role in the pathogenesis of PH. We have previously shown a decrease in IκB in the lungs and pulmonary arteries in a lamb model of persistent PH of the newborn suggesting a potential role for NFκB-target genes in pulmonary vascular remodeling (60). Direct measurement of NFκB in lung tissue in this model would be of value.

In summary, we show that TLR4 inhibition attenuated PH, RVH, and decreased lung IκBα activity in rat pups exposed to PNGR and hyperoxia with a trend toward decreasing elevated circulating IL-1β. Further elucidation of the underlying mechanisms may identify crucial spatial (intestinal and pulmonary) and temporal targets to improve clinical outcomes of low birth weight preterm infants at risk of developing PH.

DATA AVAILABILITY STATEMENT

The datasets generated for this study are available on request to the corresponding author.

ETHICS STATEMENT

The animal study was reviewed and approved by the UC Davis Institutional Animal Care and Use Committee.

AUTHOR CONTRIBUTIONS

SW contributed to study design and data analysis and wrote initial draft. KG, KH, SM, and AH performed the analyses. CW and PT performed the animal experiments. RS, SL, NC, and MU contributed to study design and data analysis. All authors approved the final manuscript.

FUNDING

This work was supported by the National Institutes of Health: R21 HD096241-01 to MU, the Children's Miracle Network to SW, National Institutes of Health R01 HL HL085727, R01 HL085844, R01 HL137228, S10 OD010389 shared equipment grant, VA Merit Review Grant I01 BX000576 and I01 CX001490 to NC, and Postdoctoral Fellowships from NIH T32 Training Grant in Basic & Translational Cardiovascular Science (T32 HL86350) and NIH F32 HL149288 to PT.

REFERENCES

1. Berkelhamer SK, Mestan KK, Steinhorn RH. Pulmonary hypertension in bronchopulmonary dysplasia. *Semin Perinatol.* (2013) 37:124–31. doi: 10.1053/j.semperi.2013.01.009
2. Check J, Gotteiner N, Liu X, Su E, Porta N, Steinhorn R, et al. Fetal growth restriction and pulmonary hypertension in premature infants with bronchopulmonary dysplasia. *J Perinatol.* (2013) 33:553–7. doi: 10.1038/jp.2012.164
3. Khemani E, McElhinney DB, Rhein L, Andrade O, Lacro RV, Thomas KC, et al. Pulmonary artery hypertension in formerly premature infants with bronchopulmonary dysplasia: clinical features and outcomes in the surfactant era. *Pediatrics.* (2007) 120:1260–9.
4. Natarajan G, Johnson YR, Brozanski B, Farrow KN, Zaniletti I, Padula MA, et al. Postnatal weight gain in preterm infants with severe bronchopulmonary dysplasia. *Am J Perinatol.* (2014) 31:223–30. doi: 10.1055/s-0033-1345264
5. Cuestas E, Aguilera B, Cerutti M, Rizzotti A. Sustained neonatal inflammation is associated with poor growth in infants born very preterm during the first year of life. *J Pediatr.* (2019) 205:91–7. doi: 10.1016/j.jpeds.2018.09.032
6. Uberos J, Lardon-Fernandez M, Machado-Casas I, Molina-Oya M, Narbona-Lopez E. Nutrition in extremely low birth weight infants: impact on bronchopulmonary dysplasia. *Minerva Pediatr.* (2016) 68:419–26.
7. Malikiwi AI, Lee YM, Davies-Tuck M, Wong FY. Postnatal nutritional deficit is an independent predictor of bronchopulmonary dysplasia among extremely premature infants born at or less than 28 weeks gestation. *Early Hum Dev.* (2019) 131:29–35. doi: 10.1016/j.earlhumdev.2019.02.005
8. Klevebro S, Lundgren P, Hammar U, Smith LE, Bottai M, Domellof M, et al. Cohort study of growth patterns by gestational age in preterm infants developing morbidity. *BMJ Open.* (2016) 6:e012872. doi: 10.1136/bmjopen-2016-012872
9. Weismann CG, Asnes JD, Bazzy-Asaad A, Tolomeo C, Ehrenkranz RA, Bizzarro MJ. Pulmonary hypertension in preterm infants: results of a prospective screening program. *J Perinatol.* (2017) 37:572–7. doi: 10.1038/jp.2016.255
10. Arjaans S, Zwart EAH, Ploegstra MJ, Bos AF, Kooi EMW, Hillege HL, et al. Identification of gaps in the current knowledge on pulmonary hypertension in extremely preterm infants: a systematic review and meta-analysis. *Paediatr Perinat Epidemiol.* (2018) 32:258–67. doi: 10.1111/ppe.12444
11. Koppel R, Han RN, Cox D, Tanswell AK, Rabinovitch M. Alpha 1-antitrypsin protects neonatal rats from pulmonary vascular and parenchymal effects of oxygen toxicity. *Pediatr Res.* (1994) 36:763–70.
12. Wedgwood S, Warford C, Agvateesiri SC, Thai P, Berkelhamer SK, Perez M, et al. Postnatal growth restriction augments oxygen-induced pulmonary hypertension in a neonatal rat model of bronchopulmonary dysplasia. *Pediatr Res.* (2016) 80:894–902. doi: 10.1038/pr.2016.164
13. La Frano MR, Fahrmann JF, Grapov D, Fiehn O, Pedersen TL, Newman JW, et al. Metabolic perturbations of postnatal growth restriction and hyperoxia-induced pulmonary hypertension in a bronchopulmonary dysplasia model. *Metabolomics.* (2017) 13:32.
14. Sengupta P. The laboratory rat: relating its age with human's. *Int J Prev Med.* (2013) 4:624–30.
15. Wedgwood S, Warford C, Agvatisiri SR, Thai PN, Chiamvimonvat N, Kalanetra KM, et al. The developing gut-lung axis: postnatal growth restriction, intestinal dysbiosis, and pulmonary hypertension in a rodent model. *Pediatr Res.* (2019) doi: 10.1038/s41390-019-0578-2 [Epub ahead of print].
16. Vongbhavit K, Underwood MA. Prevention of necrotizing enterocolitis through manipulation of the intestinal microbiota of the premature infant. *Clin Ther.* (2016) 38:716–32.
17. Hackam DJ, Sodhi CP. Toll-like receptor-mediated intestinal inflammatory imbalance in the pathogenesis of necrotizing enterocolitis. *Cell Mol Gastroenterol Hepatol.* (2018) 6:229–38.e1. doi: 10.1016/j.jcmgh.2018.04.001
18. Hu R, Xu H, Jiang H, Zhang Y, Sun Y. The role of TLR4 in the pathogenesis of indirect acute lung injury. *Front Biosci.* (2013) 18:1244–55. doi: 10.2741/4176
19. Jia H, Sodhi CP, Yamaguchi Y, Lu P, Martin LY, Good M, et al. Pulmonary epithelial TLR4 activation leads to lung injury in neonatal necrotizing enterocolitis. *J Immunol.* (2016) 197:859–71. doi: 10.4049/jimmunol.1600618
20. Jia H, Sodhi CP, Yamaguchi Y, Lu P, Ladd MR, Werts A, et al. Toll like receptor 4 mediated lymphocyte imbalance induces nec-induced lung injury. *Shock (Augusta Ga).* (2019) 52:215–23. doi: 10.1097/SHK.0000000000001255
21. Takashima K, Matsunaga N, Yoshimatsu M, Hazeki K, Kaisho T, Uekata M, et al. Analysis of binding site for the novel small-molecule TLR4 signal transduction inhibitor TAK-242 and its therapeutic effect on mouse sepsis model. *Br J Pharmacol.* (2009) 157:1250–62. doi: 10.1111/j.1476-5381.2009.00297.x
22. Ladha F, Bonnet S, Eaton F, Hashimoto K, Korbutt G, Thebaud B. Sildenafil improves alveolar growth and pulmonary hypertension in hyperoxia-induced lung injury. *Am J Respir Crit Care Med.* (2005) 172:750–6.
23. Wemhoner A, Ortner D, Tschirch E, Strasak A, Rudiger M. Nutrition of preterm infants in relation to bronchopulmonary dysplasia. *BMC Pulm Med.* (2011) 11:7. doi: 10.1186/1471-2466-11-7
24. Panagiotounakou P, Sokou R, Gounari E, Konstantinidi A, Antonogeorgos G, Grivea IN, et al. Very preterm neonates receiving "aggressive" nutrition and early nCPAP had similar long-term respiratory outcomes as term neonates. *Pediatr Res.* (2019) 86:742–8. doi: 10.1038/s41390-019-0514-5
25. Mai V, Young CM, Ukhanova M, Wang X, Sun Y, Casella G, et al. Fecal microbiota in premature infants prior to necrotizing enterocolitis. *PLoS One.* (2011) 6:e20647. doi: 10.1371/journal.pone.0020647
26. Litvak Y, Byndloss MX, Tsolis RM, Baumler AJ. Dysbiotic proteobacteria expansion: a microbial signature of epithelial dysfunction. *Curr Opin Microbiol.* (2017) 39:1–6. doi: 10.1016/j.mib.2017.07.003
27. Budden KF, Gellatly SL, Wood DL, Cooper MA, Morrison M, Hugenholtz P, et al. Emerging pathogenic links between microbiota and the gut-lung axis. *Nat Rev.* (2017) 15:55–63. doi: 10.1038/nrmicro.2016.142
28. Miller J, Tonkin E, Damarell RA, McPhee AJ, Suganuma M, Suganuma H, et al. A systematic review and meta-analysis of human milk feeding and morbidity in very low birth weight infants. *Nutrients.* (2018) 10:707. doi: 10.3390/nu10060707
29. Villamor-Martinez E, Pierro M, Cavallaro G, Mosca F, Villamor E. Mother's own milk and bronchopulmonary dysplasia: a systematic review and meta-analysis. *Front Pediatr.* (2019) 7:224. doi: 10.3389/fped.2019.00224
30. Villamor-Martinez E, Pierro M, Cavallaro G, Mosca F, Kramer BW, Villamor E. Donor human milk protects against bronchopulmonary dysplasia: a systematic review and meta-analysis. *Nutrients* (2018) 10:238. doi: 10.3390/nu10020238
31. Gao R, Zhang R, Qian T, Peng X, He W, Zheng S, et al. A comparison of exosomes derived from different periods breast milk on protecting against intestinal organoid injury. *Pediatr Surg Int.* (2019) 35:1363–8. doi: 10.1007/s00383-019-04562-6
32. Xiao L, van De Worp WR, Stassen R, van Maastrigt C, Kettelarij N, Stahl B, et al. Human milk oligosaccharides promote immune tolerance via direct interactions with human dendritic cells. *Eur J Immunol.* (2019) 49:1001–14. doi: 10.1002/eji.201847971
33. Neal MD, Sodhi CP, Jia H, Dyer M, Egan CE, Yazji I, et al. Toll-like receptor 4 is expressed on intestinal stem cells and regulates their proliferation and apoptosis via the p53 up-regulated modulator of apoptosis. *J Biol Chem.* (2012) 287:37296–308. doi: 10.1074/jbc.M112.375881
34. Liang J, Zhang Y, Xie T, Liu N, Chen H, Geng Y, et al. Hyaluronan and TLR4 promote surfactant-protein-C-positive alveolar progenitor cell renewal

and prevent severe pulmonary fibrosis in mice. *Nat Med.* (2016) 22:1285–93. doi: 10.1038/nm.4192
35. Chou HC, Lin W, Chen CM. Human mesenchymal stem cells attenuate pulmonary hypertension induced by prenatal lipopolysaccharide treatment in rats. *Clin Exp Pharmacol Physiol.* (2016) 43:906–14. doi: 10.1111/1440-1681.12604
36. Lu YC, Yeh WC, Ohashi PS. LPS/TLR4 signal transduction pathway. *Cytokine.* (2008) 42:145–51.
37. Young KC, Hussein SM, Dadiz R, deMello D, Devia C, Hehre D, et al. Toll-like receptor 4-deficient mice are resistant to chronic hypoxia-induced pulmonary hypertension. *Exp Lung Res.* (2010) 36:111–9. doi: 10.3109/01902140903171610
38. Bauer EM, Chanthaphavong RS, Sodhi CP, Hackam DJ, Billiar TR, Bauer PM. Genetic deletion of toll-like receptor 4 on platelets attenuates experimental pulmonary hypertension. *Circ Res.* (2014) 114:1596–600. doi: 10.1161/CIRCRESAHA.114.303662
39. Yao P, Tan F, Gao H, Wang L, Yang T, Cheng Y. Effects of probiotics on tolllike receptor expression in ulcerative colitis rats induced by 2,4,6trinitrobenzene sulfonic acid. *Mol Med Rep.* (2017) 15:1973–80. doi: 10.3892/mmr.2017.6226
40. Izumi H, Minegishi M, Sato Y, Shimizu T, Sekine K, Takase M. *Bifidobacterium breve* alters immune function and ameliorates DSS-induced inflammation in weanling rats. *Pediatr Res.* (2015) 78:407–16. doi: 10.1038/pr.2015.115
41. Philippe D, Favre L, Foata F, Adolfsson O, Perruisseau-Carrier G, Vidal K, et al. *Bifidobacterium lactis* attenuates onset of inflammation in a murine model of colitis. *World J Gastroenterol.* (2011) 17:459–69. doi: 10.3748/wjg.v17.i4.459
42. Lin YP, Thibodeaux CH, Pena JA, Ferry GD, Versalovic J. Probiotic *Lactobacillus reuteri* suppress proinflammatory cytokines via c-Jun. *Inflamm Bowel Dis.* (2008) 14:1068–83. doi: 10.1002/ibd.20448
43. Liu Y, Fatheree NY, Mangalat N, Rhoads JM. *Lactobacillus reuteri* strains reduce incidence and severity of experimental necrotizing enterocolitis via modulation of TLR4 and NF-kappaB signaling in the intestine. *Am J Physiol Gastrointest liver Physiol.* (2012) 302:G608–17. doi: 10.1152/ajpgi.00266.2011
44. Mirpuri J, Sotnikov I, Myers L, Denning TL, Yarovinsky F, Parkos CA, et al. *Lactobacillus rhamnosus* (LGG) regulates IL-10 signaling in the developing murine colon through upregulation of the IL-10R2 receptor subunit. *PLoS One.* (2012) 7:e51955. doi: 10.1371/journal.pone.0051955
45. Borthakur A, Bhattacharyya S, Kumar A, Anbazhagan AN, Tobacman JK, Dudeja PK. *Lactobacillus acidophilus* alleviates platelet-activating factor-induced inflammatory responses in human intestinal epithelial cells. *PLoS One.* (2013) 8:e75664. doi: 10.1371/journal.pone.0075664
46. Liu Y, Fatheree NY, Mangalat N, Rhoads JM. Human-derived probiotic *Lactobacillus reuteri* strains differentially reduce intestinal inflammation. *Am J Physiol Gastrointest Physiol.* (2010) 299:G1087–96. doi: 10.1152/ajpgi.00124.2010
47. Inoue Y, Iwabuchi N, Xiao JZ, Yaeshima T, Iwatsuki K. Suppressive effects of *Bifidobacterium breve* strain M-16V on T-helper type 2 immune responses in a murine model. *Biol Pharm Bull.* (2009) 32:760–3.
48. Putaala H, Salusjarvi T, Nordstrom M, Saarinen M, Ouwehand AC, Bech Hansen E, et al. Effect of four probiotic strains and *Escherichia coli* O157:H7 on tight junction integrity and cyclo-oxygenase expression. *Res Microbiol.* (2008) 159:692–8. doi: 10.1016/j.resmic.2008.08.002
49. Patel RM, Myers LS, Kurundkar AR, Maheshwari A, Nusrat A, Lin PW. Probiotic bacteria induce maturation of intestinal claudin 3 expression and barrier function. *Am J Pathol.* (2012) 180:626–35. doi: 10.1016/j.ajpath.2011.10.025
50. Lin PW, Nasr TR, Berardinelli AJ, Kumar A, Neish AS. The probiotic *Lactobacillus* GG may augment intestinal host defense by regulating apoptosis and promoting cytoprotective responses in the developing murine gut. *Pediatr Res.* (2008) 64:511–6. doi: 10.1203/PDR.0b013e3181827c0f
51. Yan F, Polk DB. Characterization of a probiotic-derived soluble protein which reveals a mechanism of preventive and treatment effects of probiotics on intestinal inflammatory diseases. *Gut Microbes.* (2012) 3:25–8. doi: 10.4161/gmic.19245
52. Kunze WA, Mao YK, Wang B, Huizinga JD, Ma X, Forsythe P, et al. *Lactobacillus reuteri* enhances excitability of colonic AH neurons by inhibiting calcium-dependent potassium channel opening. *J Cell Mol Med.* (2009) 13:2261–70. doi: 10.1111/j.1582-4934.2009.00686.x
53. Wu RY, Pasyk M, Wang B, Forsythe P, Bienenstock J, Mao YK, et al. Spatiotemporal maps reveal regional differences in the effects on gut motility for *Lactobacillus reuteri* and *rhamnosus* strains. *Neurogastroenterol Motil.* (2013) 25:e205–14. doi: 10.1111/nmo.12072
54. Arboleya S, Salazar N, Solis G, Fernandez N, Hernandez-Barranco AM, Cuesta I, et al. Assessment of intestinal microbiota modulation ability of *Bifidobacterium* strains in vitro fecal batch cultures from preterm neonates. *Anaerobe.* (2013) 19:9–16. doi: 10.1016/j.anaerobe.2012.11.001
55. Kumar A, Alrefai WA, Borthakur A, Dudeja PK. *Lactobacillus acidophilus* counteracts enteropathogenic *E. coli*-induced inhibition of butyrate uptake in intestinal epithelial cells. *Am J Physiol Gastrointest Liver Physiol.* (2015) 309:G602–7. doi: 10.1152/ajpgi.00186.2015
56. Kumar R, Graham B. How does inflammation contribute to pulmonary hypertension? *Eur Respir J.* (2018) 51:1702403. doi: 10.1183/13993003.02403-2017
57. Eltom S, Belvisi MG, Yew-Booth L, Dekkak B, Maher SA, Dubuis ED, et al. TLR4 activation induces IL-1beta release via an IPAF dependent but caspase 1/11/8 independent pathway in the lung. *Respir Res.* (2014) 15:87. doi: 10.1186/s12931-014-0087-0
58. Zeng H, Yang L, Zhang X, Chen Y, Cai J. Dioscin prevents LPS-induced acute lung injury through inhibiting the TLR4/MyD88 signaling pathway via upregulation of HSP70. *Mol Med Rep.* (2018) 17:6752–8. doi: 10.3892/mmr.2018.8667
59. Kimura S, Egashira K, Chen L, Nakano K, Iwata E, Miyagawa M, et al. Nanoparticle-mediated delivery of nuclear factor kappaB decoy into lungs ameliorates monocrotaline-induced pulmonary arterial hypertension. *Hypertension.* (2009) 53:877–83. doi: 10.1161/HYPERTENSIONAHA.108.121418
60. Wedgwood S, Lakshminrusimha S, Czech L, Schumacker PT, Steinhorn RH. Increased p22phox/Nox4 expression triggers remodeling through hydrogen peroxide signaling in persistent pulmonary hypertension of the newborn. *Antioxid Redox Signal.* (2013) 18:1765–76.

Conflict of Interest: The authors declare that the research was conducted in the absence of any commercial or financial relationships that could be construed as a potential conflict of interest.

frontiers in Immunology

ORIGINAL RESEARCH
published: 17 March 2020
doi: 10.3389/fimmu.2020.00189

Chronic Intra-Uterine *Ureaplasma parvum* Infection Induces Injury of the Enteric Nervous System in Ovine Fetuses

*Cathelijne Heymans[1], Ilse H. de Lange[1,2], Matthias C. Hütten[2,3,4,5], Kaatje Lenaerts[1], Nadine J. E. de Ruijter[2], Lilian C. G. A. Kessels[2], Glenn Rademakers[6], Veerle Melotte[6], Werend Boesmans[6,7], Masatoshi Saito[8,9], Haruo Usuda[8,9], Sarah J. Stock[10], Owen B. Spiller[11], Michael L. Beeton[12], Matthew S. Payne[8], Boris W. Kramer[2,3], John P. Newnham[8], Alan H. Jobe[8,13], Matthew W. Kemp[8,9,14], Wim G. van Gemert[1,15,16] and Tim G. A. M. Wolfs[2,17]**

[1] Department of Surgery, NUTRIM School of Nutrition and Translational Research in Metabolism, Maastricht University, Maastricht, Netherlands, [2] Department of Pediatrics, School for Oncology and Developmental Biology (GROW), Maastricht University, Maastricht, Netherlands, [3] Neonatology, Department of Pediatrics, Maastricht University Medical Center, Maastricht, Netherlands, [4] Neonatology, Department of Pediatrics, University Hospital Aachen, Aachen, Germany, [5] Neonatology, Department of Pediatrics, University Children's Hospital Würzburg, Würzburg, Germany, [6] Department of Pathology, School for Oncology and Developmental Biology (GROW), Maastricht University Medical Center, Maastricht, Netherlands, [7] Biomedical Research Institute (BIOMED), Hasselt University, Hasselt, Belgium, [8] Division of Obstetrics and Gynecology, University of Western Australia, Perth, WA, Australia, [9] Center for Perinatal and Neonatal Medicine, Tohoku University Hospital, Sendai, Japan, [10] Usher Institute, University of Edinburgh, Edinburgh, United Kingdom, [11] Division of Infection and Immunity, School of Medicine, Cardiff University, Cardiff, United Kingdom, [12] Cardiff School of Sport and Health Sciences, Cardiff Metropolitan University, Cardiff, United Kingdom, [13] Division of Neonatology/Pulmonary Biology, The Perinatal Institute, Cincinnati Children's Hospital Medical Center, University of Cincinnati, Cincinnati, OH, United States, [14] School of Veterinary and Life Sciences, Murdoch University, Perth, WA, Australia, [15] Pediatric Surgery, Department of Surgery, Maastricht University Medical Center, Maastricht, Netherlands, [16] Department of Surgery, University Hospital Aachen, Aachen, Germany, [17] Department of Biomedical Engineering (BMT), School for Cardiovascular Diseases (CARIM), Maastricht University, Maastricht, Netherlands*

OPEN ACCESS

Edited by:
Per T. Sangild, University of Copenhagen, Denmark

Reviewed by:
David Hackam, Johns Hopkins Medicine, United States
Jacqueline Cheuk-Yan Lai, University of Gothenburg, Sweden

***Correspondence:**
Tim G. A. M. Wolfs
tim.wolfs@maastrichtuniversity.nl

Specialty section:
This article was submitted to Microbial Immunology, a section of the journal Frontiers in Immunology

Received: *13 November 2019*
Accepted: *24 January 2020*
Published: *17 March 2020*

Citation:
Heymans C, de Lange IH, Hütten MC, Lenaerts K, de Ruijter NJE, Kessels LCGA, Rademakers G, Melotte V, Boesmans W, Saito M, Usuda H, Stock SJ, Spiller OB, Beeton ML, Payne MS, Kramer BW, Newnham JP, Jobe AH, Kemp MW, van Gemert WG and Wolfs TGAM (2020) Chronic Intra-Uterine Ureaplasma parvum Infection Induces Injury of the Enteric Nervous System in Ovine Fetuses. Front. Immunol. 11:189. doi: 10.3389/fimmu.2020.00189

Background: Chorioamnionitis, inflammation of the fetal membranes during pregnancy, is often caused by intra-amniotic (IA) infection with single or multiple microbes. Chorioamnionitis can be either acute or chronic and is associated with adverse postnatal outcomes of the intestine, including necrotizing enterocolitis (NEC). Neonates with NEC have structural and functional damage to the intestinal mucosa and the enteric nervous system (ENS), with loss of enteric neurons and glial cells. Yet, the impact of acute, chronic, or repetitive antenatal inflammatory stimuli on the development of the intestinal mucosa and ENS has not been studied. The aim of this study was therefore to investigate the effect of acute, chronic, and repetitive microbial exposure on the intestinal mucosa, submucosa and ENS in premature lambs.

Materials and Methods: A sheep model of pregnancy was used in which the ileal mucosa, submucosa, and ENS were assessed following IA exposure to lipopolysaccharide (LPS) for 2 or 7 days (acute), *Ureaplasma parvum* (UP) for 42 days (chronic), or repetitive microbial exposure (42 days UP with 2 or 7 days LPS).

Results: IA LPS exposure for 7 days or IA UP exposure for 42 days caused intestinal injury and inflammation in the mucosal and submucosal layers of the gut. Repetitive microbial exposure did not further aggravate injury of the terminal ileum. Chronic IA UP exposure caused significant structural ENS alterations characterized by loss of PGP9.5

and S100β immunoreactivity, whereas these changes were not found after re-exposure of chronic UP-exposed fetuses to LPS for 2 or 7 days.

Conclusion: The *in utero* loss of PGP9.5 and S100β immunoreactivity following chronic UP exposure corresponds with intestinal changes in neonates with NEC and may therefore form a novel mechanistic explanation for the association of chorioamnionitis and NEC.

Keywords: *Ureaplasma parvum*, intra-amniotic infection, chorioamnionitis, enteric nervous system, sheep, preterm birth, necrotizing enterocolitis

INTRODUCTION

Preterm birth is a common and major worldwide health issue, contributing to significant neonatal morbidity and mortality (1). Around 1 in every 10 births are preterm, accounting for ∼15 million premature newborns each year (2). Due to complications, over one million premature newborns will die shortly after birth (3, 4). Chorioamnionitis, defined as inflammatory cell infiltration of fetal membranes, is frequently associated with preterm birth and typically occurs due to an ascending bacterial infection (5–7) that can be acute or chronic (8). Intrauterine exposure of preterm infants to chorioamnionitis is associated with an increased risk of adverse neonatal outcomes (9, 10), including necrotizing enterocolitis (NEC) (9, 11, 12). Adverse gastrointestinal outcomes have been associated with both systemic fetal inflammatory response syndrome (FIRS) and direct exposure of the gut to the swallowed infected amniotic fluid (11, 13, 14). Chorioamnionitis can occur with intact membranes, which is common for genital mycoplasmas, such as *Ureaplasma* species (spp.), present in the lower genital tract of women (6, 15). *Ureaplasma* spp. can cause chronic chorioamnionitis that does not evoke a maternal response, but is still associated with adverse fetal outcomes (16). In an experimental large animal model, we previously showed that a *Ureaplasma parvum* (UP) serovar 3 infection up to 14 days prior to delivery causes fetal gut inflammation with damaged villus epithelium, gut barrier loss, and severe villus atrophy (17).

The injury caused by intrauterine *Ureaplasma* spp. exposure might derive from the direct inflammatory reaction, as well as from potential interactions with other inflammatory stimuli. Chorioamnionitis is often polymicrobial, as over 65% of positive amniotic fluid cultures lead to the identification of two or more pathogens (7). In this context, we previously showed that cerebral and lung immune activation following intra-amniotic (IA) lipopolysaccharide (LPS) exposure was prevented when these animals were chronically pre-exposed to UP serovar 3 (18, 19). This illustrates that interactions between different microbes can occur, leading to organ-specific sensitization or preconditioning.

The enteric nervous system (ENS) consists of enteric neurons and glial cells, autonomously regulates gastrointestinal activity (i.e., secretion, absorption, and motility), and contributes to gut integrity (20). The formation of the ENS requires coordinated migration, proliferation, and differentiation of neural crest progenitors, directed neurite growth, and establishment of a network of interconnected neurons and glia (21, 22). Although these processes mostly occur *in utero*, an important part of ENS development takes place postnatally (23, 24). Neonates with NEC have structural and functional damage of the submucosal and myenteric plexus, including loss of enteric neurons and glial cells (25–27). The involvement of chorioamnionitis in the induction of adverse intestinal outcomes including NEC, combined with the presence of ENS abnormalities in NEC, prompted us to study the impact of an antenatal infection on the ENS.

The aim of this study was therefore to investigate the effect of acute IA exposure to LPS and chronic exposure to UP on the intestinal mucosa and ENS in fetal lambs using a well-established sheep model of chorioamnionitis. In addition, we investigated the potential interactions of repetitive IA microbial stimuli by acute exposure to LPS in ovine fetuses that were chronically pre-exposed to UP.

MATERIALS AND METHODS

Animal Model and Experimental Procedures

All experiments were approved by the animal ethics committee of the University of Western Australia (Perth, Australia).

The animal model and experimental procedures were previously described (18). Briefly, 39 date-mated merino ewes were randomly assigned to six different groups of between five and eight animals to receive IA injections under ultrasound guidance. Verification of the IA injections was done by amniotic fluid electrolyte analysis. The date-mated pregnant ewes received an IA injection of an *in vitro* cultured strain HPA5 of UP serovar 3 (2×10^5 color-changing units, CCU) (28) 42 days prior to delivery (at 82 days of gestation, which corresponds to the second trimester in humans) or *Escherichia coli*-derived LPS (O55:B5; Merck, Darmstadt, Germany), 10 mg in 2 ml of saline, 2 or 7 days prior to delivery (at respectively, 122 and 117 days of gestation).

Abbreviations: AU, Arbitrary unit; BSA, Bovine serum albumin; CD3, Cluster of differentiation 3; CCU, Color-changing units; *CHAT*, Choline acetyltransferase; ENS, Enteric nervous system; FCS, Fetal calf serum; FIRS, Fetal inflammatory response syndrome; *GAPDH*, Glyceraldehyde 3-phosphate dehydrogenase; GFAP, Glial fibrillary acidic protein; IA, Intra-amniotic; IBD, Inflammatory bowel disease; IL, Interleukin; *IRAK3*, Interleukin-1 receptor-associated kinase 3; LPS, Lipopolysaccharide; MPO, Myeloperoxidase; NEC, Necrotizing enterocolitis; NGS, Normal goat serum; *nNOS*, Neuronal nitric oxide synthase; PBS, Phosphorylated buffer saline; PGP9.5, Protein gene product 9.5; *PPIA*, Peptidylprolyl isomerase A; *RPS15*, Ribosomal protein S15; Spp, Species; *TLR*, Toll-like receptor; *TNF-α*, Tumor necrosis factor alpha; UP, *Ureaplasma parvum*.

Previously, we have shown that the half-life time of LPS in the amniotic fluid is relatively long (1.7 days) and that the LPS amount is higher than the essential threshold of 1 mg for at least 5 days (29, 30). Chronic sustained UP infection was confirmed by positive culture of amniocentesis samples at intermediate time points and sterile amniotic fluid samples collected at cesarean delivery, as previously described (31). Two or seven days LPS exposure (prior to cesarean delivery) represents an acute inflammatory challenge. To evaluate the combined effect between these inflammatory modalities, a subgroup of chronically UP-infected ewes received IA LPS at 35 and 40 days post-UP infection (i.e., 7 or 2 days LPS exposure prior to delivery following 42 days of UP infection). A group receiving IA injections of sterile saline (2 or 7 days prior to delivery, respectively six and two animals which were pooled) served as controls (**Figure 1**). Fetuses were surgically delivered at 124 ± 2 days of gestational age (term gestation in sheep = 150 days), equivalent of ∼30 weeks of human gestation. After delivery, fetuses were euthanized with intravenous pentobarbitone (100 mg/kg). For this experiment, fetuses of both sexes were used.

Sampling

During necropsy, blood and terminal ileum samples were collected. Ileum samples were fixed in 10% formalin and embedded in paraffin, or snap frozen in liquid nitrogen. Where insufficient paraffin-embedded material was available for study, additional material was generated by paraffin embedding snap-frozen tissue samples: frozen tissue blocks were defrosted, fixed in 4% formaldehyde at room temperature overnight, and transferred to 70% ethanol prior to embedding in paraffin with the use of a vacuum infiltration processor.

Antibodies

The following antibodies were used for immunohistochemistry: polyclonal rabbit anti-myeloperoxidase (MPO; A0398, Dakocytomation, Glostrup, Denmark) for the identification of neutrophils, polyclonal rabbit anti-cluster of differentiation 3 (CD3; A0452, Dakocytomation) for the detection of T cells, polyclonal rabbit anti-bovine protein gene product 9.5 (PGP9.5; Z5116, Dakocytomation) for the detection of enteric neurons, polyclonal rabbit anti-doublecortin (Ab18723, Abcam, Cambridge, UK) for the detection of immature neurons, polyclonal rabbit anti-glial fibrillary acidic protein (GFAP; Zo334, Dakocytomation) to detect enteric glial cell reactivity/activation (32), and polyclonal rabbit anti-S100β (PA5-16257, Invitrogen, Carlsbad, CA, USA) as a marker for enteric glial cells.

The following secondary antibodies were used: peroxidase-conjugated polyclonal goat anti-rabbit (111-035-045, Jackson, West Grove, PA, USA) (MPO), peroxidase-conjugated polyclonal swine anti-rabbit (P0399, DakoCytomation) (doublecortin) and BrightVision+ Poly-HRP-Anti Mouse/Rabbit IgG biotin-free (ImmunoLogic, Duiven, Netherlands) (PGP9.5), and biotin-conjugated polyclonal swine anti-rabbit (E0353, DakoCytomation) (CD3, GFAP, S100β).

Immunohistochemistry

Formalin-fixed terminal ileum was embedded in paraffin and 4 μm sections were cut. After deparaffinization and rehydration, endogenous peroxidase activity was blocked with 0.3% H_2O_2 diluted in phosphorylated buffer saline (PBS, pH 7.4). Antigen retrieval was performed with citrate buffer for CD3, PGP9.5, doublecortin, and S100β stainings. Non-specific binding was blocked for 30 min at room temperature with 10% normal goat serum (NGS) in PBS (MPO), 5% NGS in PBS (doublecortin), or 5% bovine serum albumin (BSA) in PBS (CD3, GFAP, and S100β). For PGP9.5, non-specific binding was blocked for 10 min at room temperature with 20% fetal calf serum (FCS). Thereafter, sections were incubated with the primary antibody of interest and subsequently incubated with the respective secondary antibody. MPO, PGP9.5, and doublecortin were detected by using a peroxidase-conjugated secondary antibody and antibodies against CD3, GFAP, and S100β were detected with

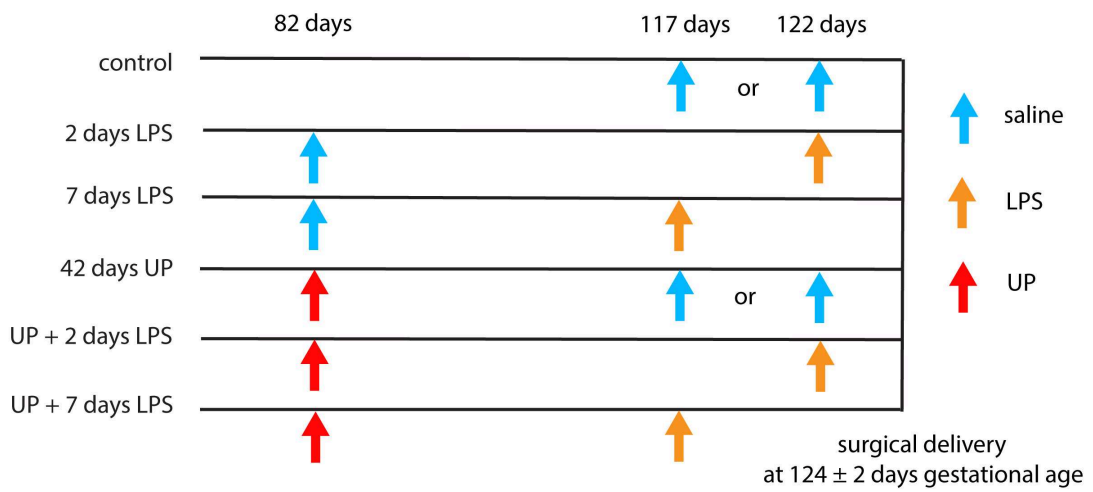

FIGURE 1 | Different intervention study groups. All injections were delivered by ultrasound-guided amniocentesis. Timing is shown in gestational days.

TABLE 1 | Primer sequences.

Primer	Forward	Reverse
RPS15	5′-CGAGATGGTGGGCAGCAT-3′	5′-GCTTGATTTCCACCTGGTTGA-3′
GAPDH	5′-GGAAGCTCACTGGCATGGC-3′	5′-CCTGCTTCACCACCTTCTTG-3′
PPIA	5′-TTATAAAGGTTCCTGCTTTCACAGAA-3′	5′-ATGGACTTGCCACCAGTACCA-3′
IL-1β	5′-AGAATGAGCTGTTATTTGAGGTTGATG-3′	5′-GTGAGAAATCTGCAGCTGGATGT-3′
IL-6	5′-ACATCGTCGACAAAATCTCTGCAA-3′	5′-GCCAGTGTCTCCTTGCTGTTT-3′
IL-10	5′-CATGGGCCTGACATCAAGGA-3′	5′-CGGAGGGTCTTCAGCTTCTC-3′
TNF-α	5′-GCCGGAATACCTGGACTATGC-3′	5′-CAGGGCGATGATCCCAAAGTAG-3′
IRAK3	5′-AGTGTGTAGGTAACACAGCCC-3′	5′-TGCTGGTCATGCTTATGGCA-3′
nNOS	5′-CGGCTTTGGGGGTTATCAGT-3′	5′-TTGCCCCATTTCCACTCCTC-3′
CHAT	5′-CCGCTGGTATGACAAGTCCC-3′	5′-GCTGGTCTTCACCATGTGCT-3′

avidin–biotin complex (Vectastain Elite ABC kit, Bio-connect, Huissen, Netherlands). Substrate staining was performed for MPO with 3-amino-9-ethylcarbazole (AEC; Merck, Darmstadt, Germany). Immunoreactivity for CD3 and GFAP was detected by using nickel-DAB. Immunoreactivity for PGP9.5, doublecortin, and S100β was detected by using DAB. Hematoxylin (MPO, PGP9.5, doublecortin, and S100β) or nuclear fast red (CD3 and GFAP) was used as a counterstain for nuclei.

Qualitative Analysis of Damage of the Terminal Ileum

H&E slides were analyzed by two independent investigators blinded to the experimental setup to assess damage of the terminal ileum. A scoring system from 0 to 4 was used to describe the severity of histological injury. Scoring was as follows: 0, no damage; 1, disrupted epithelial lining, but no loss of enterocytes; 2, disrupted epithelial lining, mild enterocyte loss from the villus tips; 3, disrupted epithelial lining, moderate enterocyte loss from villus tips, some debris in the lumen; and 4, abundant enterocyte loss from villus tips, abundant debris in the lumen, and severe shedding of villus tips.

Quantification of Immunohistochemical Stainings

The stained tissue sections were scanned with the Ventana iScan HT slide scanner (Ventana Medical Systems, Oro Valley, AZ, USA). Of these images, viewed with Panoramic Viewer (version 1.15.4, 3DHISTECH, Budapest, Hungary), random images of regions of interest were taken (×200).

Two investigators blinded to the study groups counted the MPO- and CD3-positive cells in three to five non-overlapping high-power fields in the mucosa and submucosa. The average MPO- and CD3-positive cells per area are reported for each animal. The percentage of area in the submucosal and myenteric ganglia positively stained for PGP9.5, doublecortin, GFAP, and S100β was determined in five non-overlapping high-power fields using Leica QWin Pro software (version 3.4.0, Leica Microsystems, Mannheim, Germany) by an investigator blinded to the study groups. Relative area staining was calculated by dividing the positively stained areas of the ganglia of the submucosal or myenteric plexus by the total area of the muscle layer. The data are expressed as fold increase over the control value.

RNA Extraction and Quantitative Real-Time PCR

RNA was extracted from snap-frozen terminal ileum tissue using TRI reagent (Invitrogen)/chloroform extraction. Isolated RNA was DNase treated to remove possible contamination with genomic DNA by using the RQ1 RNase-Free DNase kit (Promega, Madison, WI, USA) and afterwards reverse transcribed into cDNA using oligo(dT)12–18 primers (Invitrogen) and Moloney murine leukemia virus (M-MLV) reverse transcriptase (Invitrogen). Quantitative real-time PCR (qPCR) reactions were performed with a LightCycler 480 Instrument (Roche Applied Science, Basel, Switzerland) using the SensiMix™ SYBR® No-ROX kit (Bioline, London, UK) for 45 cycles. The mRNA levels of *IL-1β*, *IL-6*, *IL-10*, tumor necrosis factor alpha (*TNF-α*), and interleukin-1 receptor-associated kinase 3 (*IRAK3*) were determined to assess inflammation of the terminal ileum. The mRNA levels of neuronal nitric oxide synthase (*nNOS*) and choline acetyltransferase (*CHAT*) were determined to assess the motility signaling functions of the ENS using LinRegPCR software (version 2016.0, Heart Failure Research Center, Academic Medical Center, Amsterdam, Netherlands). The geometric mean of the mRNA levels of three reference genes [ribosomal protein S15 (*RPS15*), glyceraldehyde 3-phosphate dehydrogenase (*GAPDH*), and peptidylprolyl isomerase A (*PPIA*)] were calculated and used as a normalization factor. The data are expressed as fold increase over the control value. The primer sequences are shown in **Table 1**.

Data Analysis

Data are presented as median with interquartile range. Statistical analyses were performed using GraphPad Prism (version 6.01, GraphPad Software Inc., La Jolla, CA, USA). A non-parametric Kruskal–Wallis test followed by Dunn's *post hoc* test was used to analyze statistically significant group differences. Differences were considered statistically significant at $p < 0.05$. Given the relatively small animal numbers per group, we also reported actual p values between $p \geq 0.05$ and $p < 0.10$ and interpreted these as potentially biologically relevant. This assumption will

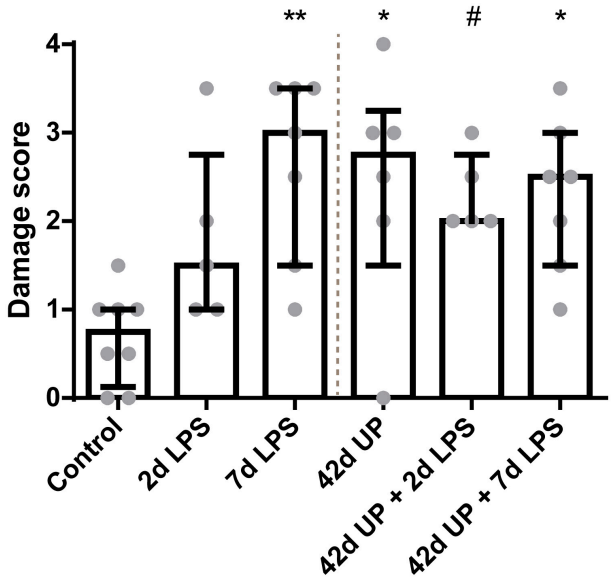

FIGURE 2 | Increased mucosal injury in all groups, except for the animals exposed to 2 days LPS. $^{\#}p = 0.06$, $^{*}p < 0.05$, $^{**}p < 0.005$ compared to the control.

decrease the chance of a type II error, but increases the chance of a type I error.

RESULTS

Intestinal Damage and Inflammation in the Terminal Ileum Due to Chorioamnionitis

There was a higher intestinal damage score for all experimental groups compared to the control ($p < 0.005$ for the 7 days LPS group, $p < 0.05$ for the 42 days UP group and 42 days UP + 7 days LPS group, and $p = 0.06$ for the 42 days UP + 2 days LPS group all compared to the control; **Figure 2**), except for the animals exposed to 2 days of LPS. Pre-exposure with UP did not augment mucosal injury in the LPS-treated groups.

A statistically significant increase in MPO-positive cells was seen in the mucosa 7 days after LPS exposure compared to the control ($p < 0.05$; **Figure 3**). Chronic UP infection also caused an elevation of mucosal MPO-positive cells compared to the control ($p = 0.08$; **Figure 3**). Furthermore, combining these two inflammatory insults resulted in an increased mucosal MPO-positive cell count compared to the control ($p < 0.005$; **Figure 3**), and this experimental group tended to be increased when compared to the UP + 2 days LPS-exposed group ($p = 0.07$; **Figure 3**). LPS exposure 2 days prior to delivery was insufficient to induce mucosal MPO-positive cell infiltration. Pre-exposure to UP in combination with LPS administration did not alter the number of mucosal MPO-positive cells compared to LPS alone, both after 2 and 7 days.

While chronic UP infection and acute LPS exposure 2 days pre-delivery did not have any effect on mucosal CD3-positive T cell presence, those animals receiving LPS 7 days pre-delivery (both uninfected and chronic UP-infected groups) as well as chronic UP-infected animals receiving LPS 2 days pre-delivery all showed apparent elevated levels of CD3-positive T cell infiltration (**Figure 4**). However, the only comparison to achieve $p < 0.05$ significance was that of uninfected and chronic UP-infected animals receiving LPS 2 days pre-delivery (**Figure 4**).

For investigation of submucosal inflammation, there was an increase of MPO-positive cells in the 7 days LPS group and submucosal MPO-positive cells tended to be increased in the chronic UP infection group compared to the control ($p < 0.05$ and $p = 0.06$; **Figure 5**). Additional acute LPS insult (2 or 7 days pre-delivery) in chronic UP-infected animals resulted in increased variability and loss of significance in the MPO cell infiltration compared to 2 or 7 days of LPS alone.

The greatest increase of submucosal CD3-positive cells was observed in 2 day LPS-exposed chronic UP-infected animals, which was significantly increased compared to the control or acute 2 day LPS stimulation alone (both $p < 0.05$; **Figure 6**) and appeared more potent than in chronic UP-infected animals receiving LPS at 7 days pre-delivery ($p = 0.08$; **Figure 6**).

Examination of underlying cytokine levels revealed increased *IL-1β* mRNA levels only in the uninfected or chronic UP-infected animals when LPS was administered 2 days pre-delivery ($p < 0.05$ compared to the 7 days LPS group, $p < 0.01$ compared to the 42 days UP group, $p < 0.05$ compared to the 42 days UP + 7 days LPS group, and $p < 0.05$ compared to the control, respectively; **Figure 7A**), whereas *IL-1β* mRNA levels had dropped to baseline again if LPS was administered 7 days pre-delivery (**Figure 7A**). *IL-6* and *IL-10* mRNA levels were not altered (data not shown), and the only group showing apparent *TNF-α* mRNA level elevation was that of the chronic UP-infected animals additionally receiving LPS 2 days pre-delivery ($p = 0.07$; **Figure 7B**).

IRAK3 mRNA levels were increased significantly only in animals exposed to 2 days of LPS alone compared to the control ($p < 0.05$; **Figure 7C**).

ENS Alterations in the Terminal Ileum Due to Chronic IA UP Exposure

The PGP9.5-positive surface area in the submucosal plexus tended to be decreased in animals chronically infected for 42 days with UP compared to the control ($p = 0.08$; **Figure 8**). Similarly, chronic UP-infected animals had a diminished PGP9.5-positive surface area in the myenteric plexus ($p < 0.05$; **Figure 8**). Doublecortin-positive surface areas were not altered in either the submucosal or the myenteric plexus (data not shown).

In the submucosal plexus, the GFAP-positive surface area tended to be increased in groups receiving LPS either 2 or 7 days pre-delivery compared to the control ($p = 0.07$ and $p = 0.09$; **Figure 9**), while in the myenteric plexus, the GFAP-positive surface area was only increased in the group receiving LPS 7 days pre-delivery compared to the control ($p < 0.05$; **Figure 9**). For both of these regions, concomitant chronic infection by UP appeared to mute these effects.

S100β-positive surface areas were unaltered in the submucosal plexus for all conditions (data not shown), while in the myenteric plexus, the S100β-positive surface area was significantly

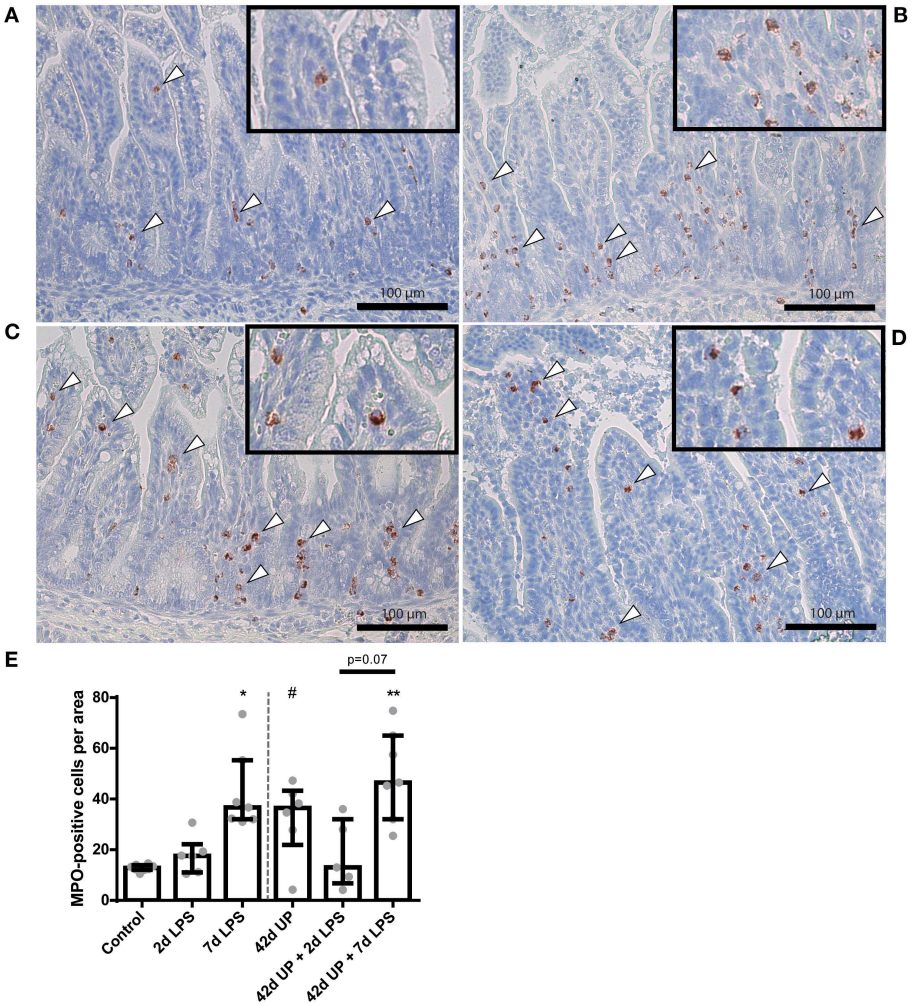

FIGURE 3 | Representative images of mucosal neutrophil influx reflected by myeloperoxidase (MPO)-positive cell (indicated by white triangles) counts of the control **(A)**, 7 days lipopolysaccharide (LPS) **(B)**, *Ureaplasma parvum* (UP) **(C)**, and UP prior to 7 days LPS groups **(D)**. **(E)** Increased MPO count in animals exposed to 7 days LPS, UP, and UP prior to 7 days LPS. $^{\#}p = 0.08$, $^{*}p < 0.01$, $^{**}p < 0.005$ compared to the control.

decreased in the chronic UP-infected group compared to the control ($p < 0.05$; **Figure 10**), but this effect appeared to be counteracted by acute stimulation by LPS at either 2 or 7 days pre-delivery. No differences in *nNOS* and *CHAT* expression were observed between the groups (data not shown).

DISCUSSION

In this study, we investigated the effect of acute, chronic, and combined microbial exposure as an antenatal infectious trigger (chorioamnionitis) on the mucosa, submucosa, and ENS of the terminal ileum of premature lambs.

Both acute LPS and chronic UP exposure caused mucosal inflammation and injury to the terminal ileum. Although the inflammatory signature differed between these groups, mucosal injury was not aggravated in the combined exposure groups. Prenatal IA exposure to 7 days of LPS and to chronic 42 days infection by UP both provoked an influx of neutrophils (MPO-positive cells) in the intestine. In contrast, T cell (CD3-positive cells) numbers remained unaltered in the chronic UP and 2 days LPS groups compared to the control group, but were increased in the UP + 2 days LPS-exposed animals, indicating a potential synergistic effect of both inflammatory stimuli in inducing an adaptive mucosal immune response. We observed a similar effect in the submucosa: while either LPS exposure or UP infection induced innate immune changes in the ileum, T cell alterations only occurred in the presence of combined UP and LPS exposure. Based on the current findings, we can only speculate on the mechanism behind this synergistic effect. In previous *in vitro* studies, signaling via Toll-like receptors (*TLR*) 1, 2, and 6 by *Ureaplasma* spp. increased LPS-mediated inflammation (33, 34). Additionally, *TNF-α* mRNA levels tended to be increased in the UP-infected animals receiving LPS 2 days pre-delivery, while *TNF-α* levels were not increased upon single exposure to either UP or LPS alone. In contrast, no synergistic effect of UP and

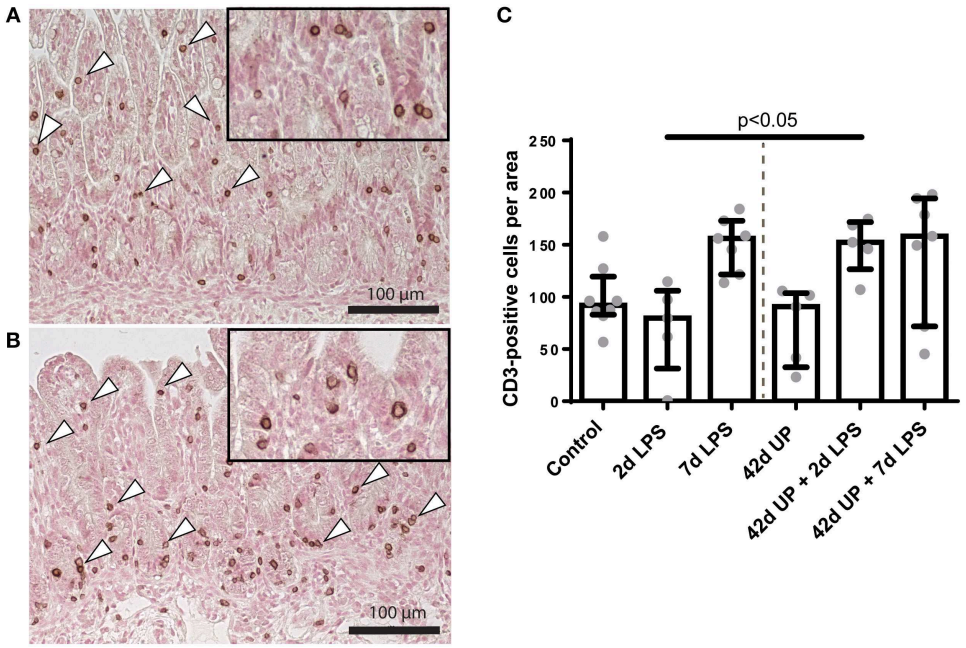

FIGURE 4 | Representative images of mucosal T cell influx reflected by CD3-positive cell (indicated by white triangles) counts of the control **(A)** and *Ureaplasma parvum* (UP) prior to 2 days lipopolysaccharide (LPS) **(B)**. **(C)** Increased CD3 count in animals exposed to UP prior to 2 days LPS compared to the 2 days LPS group.

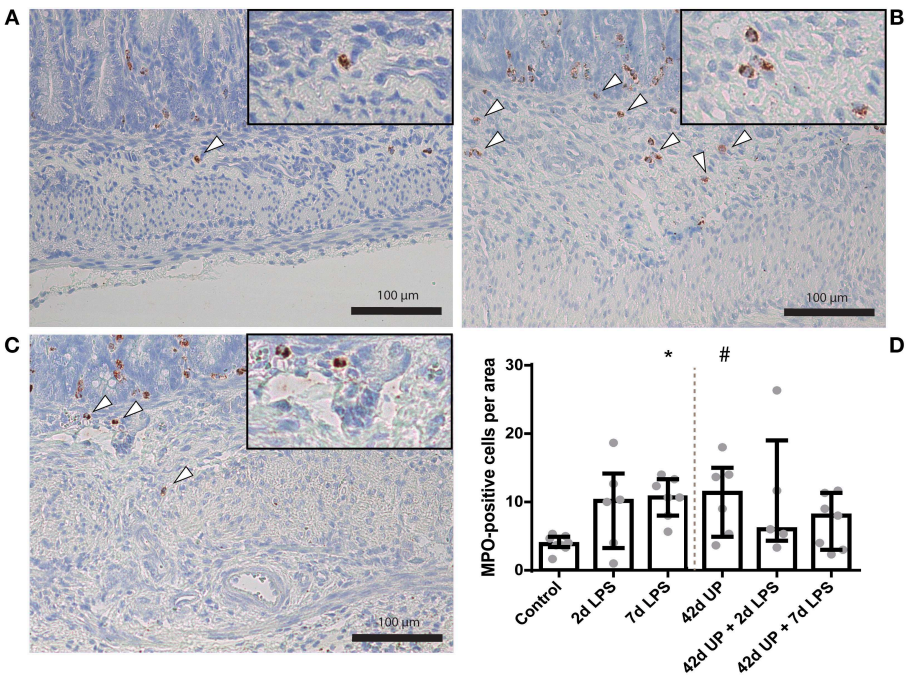

FIGURE 5 | Representative images of submucosal neutrophil influx reflected by myeloperoxidase (MPO)-positive cell (indicated by white triangles) counts of the control **(A)**, 7 days lipopolysaccharide (LPS) **(B)** and *Ureaplasma parvum* (UP) **(C)**. **(D)** Increased MPO count in animals exposed to 7 days LPS and UP. $^{\#}p = 0.06$, $^{*}p < 0.05$ compared to the control.

LPS exposure on intestinal *IL-1β* mRNA levels was found in the current study. This is supported by our *IRAK3* mRNA findings, a negative regulator of *TLR* signaling (35), which remained unaltered in combined exposure of UP-infected animals to LPS. Based on these joined findings, it is tempting to speculate that UP + LPS induced the upregulation of cell adhesion molecules

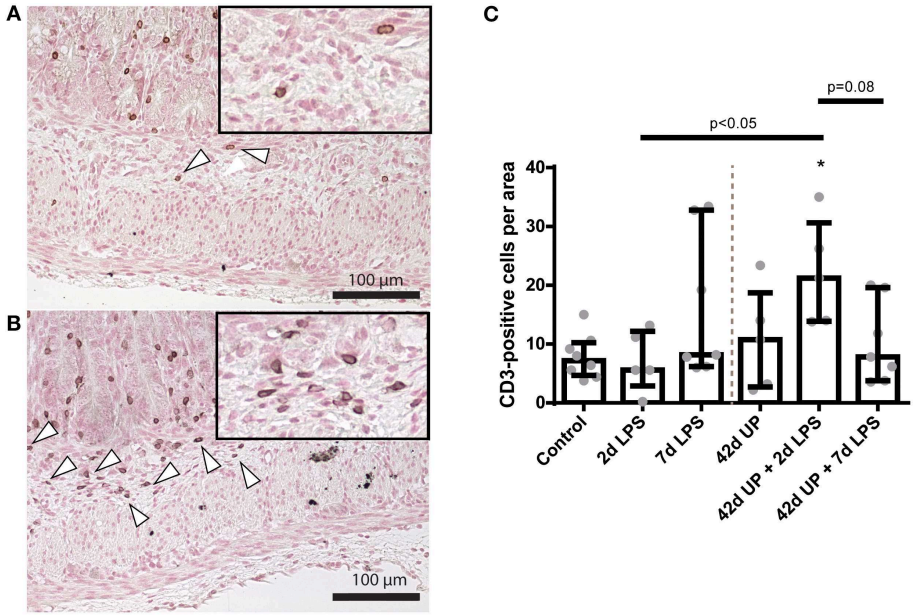

FIGURE 6 | Representative images of submucosal T cell influx reflected by CD3-positive cell (indicated by white triangles) counts of the control **(A)** and *Ureaplasma parvum* (UP) prior to 2 days lipopolysaccharide (LPS) groups **(B)**. **(C)** Increased CD3 count in animals exposed to UP prior to 2 days LPS. $^{*}p < 0.05$ compared to the control.

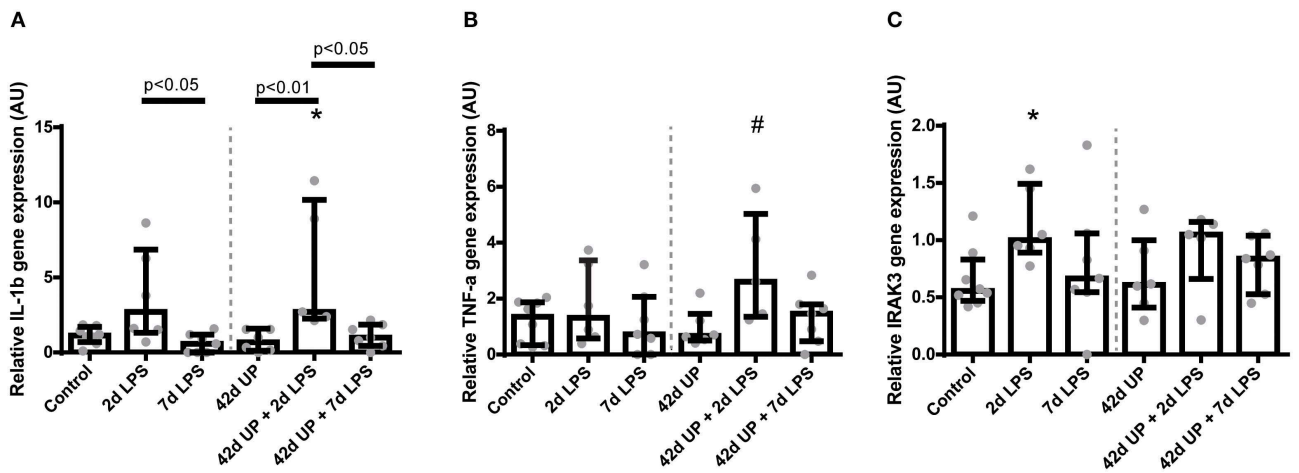

FIGURE 7 | Relative mRNA levels of *IL-1β* **(A)**, *TNF-α* **(B)**, and *IRAK3* **(C)** in arbitrary unit (AU). **(A)** Increased *IL-1β* mRNA level in animals exposed to 2 days lipopolysaccharide (LPS) and *Ureaplasma parvum* (UP) prior to 2 days LPS. $^{*}p < 0.05$ compared to the control. **(B)** Increased *TNF-α* mRNA level in animals exposed to UP prior to 2 days LPS. $^{\#}p = 0.07$ compared to the control. **(C)** Increased *IRAK3* mRNA level in animals exposed to 2 days LPS. $^{*}p < 0.05$ compared to the control.

and, consequently, temporarily increased diapedesis, which could at least in part be responsible for the observed increase in CD3-positive cells. The latter suggestion is supported by previous *in vitro* findings showing enhanced endothelial protein expression of the cell adhesion molecule *CXCR7* following co-incubation with LPS and UP, which was not observed in independently UP- or LPS-exposed cells (36).

Interestingly, other ovine studies have reported a suppressive immune effect in the premature lung and brain after chronic UP exposure prior to acute LPS exposure (18, 19). Taken together, these data show that cells might be sensitized, preconditioned, or remain unaffected following chronic UP infection, indicating organ-dependent responses. The mechanisms responsible for organ-specific effects of a second-hit chorioamnionitis remain to be elucidated.

The ENS closely interacts with intestinal immune cells (37). As such, ENS alterations can both result from intestinal inflammation and modulate it (38, 39). In this study, the most evident signs of ENS alterations were seen after chronic UP infection, which caused a reduced PGP9.5-positive surface area

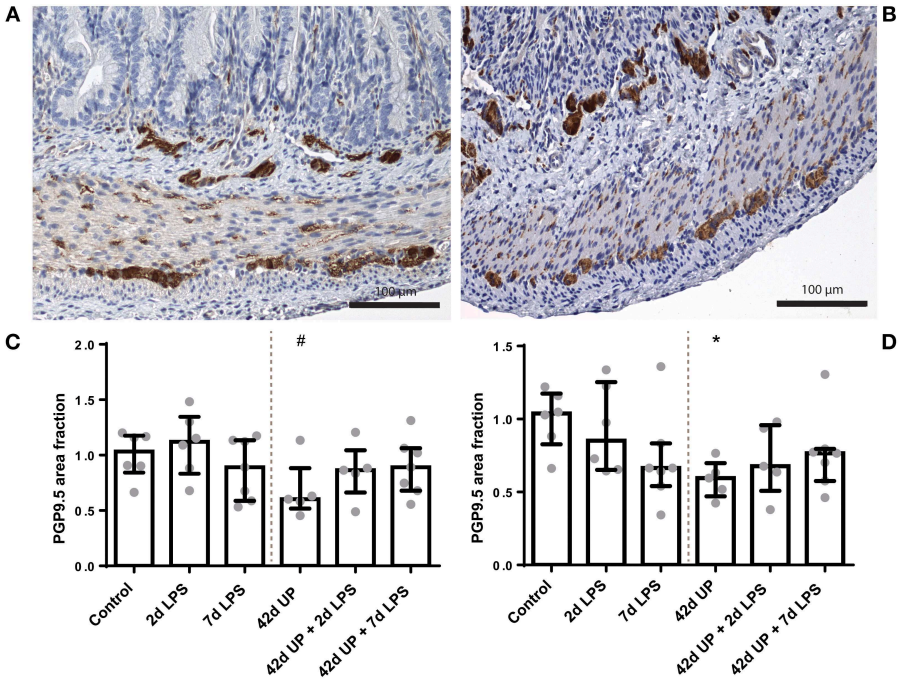

FIGURE 8 | Representative images of PGP9.5 immunoreactivity in the submucosal and myenteric plexus of the control **(A)** and *Ureaplasma parvum* (UP) **(B)** groups. Area fraction of PGP9.5 in the submucosal plexus **(C)** and myenteric plexus **(D)** as fold increase over the control value. **(C)** PGP9.5-positive surface area tended to be decreased in the submucosal plexus of animals exposed to UP. $^{\#}p = 0.08$ compared to the control. **(D)** Decreased PGP9.5-positive surface area in the myenteric plexus of animals exposed to UP. $^{*}p < 0.05$ compared to the control.

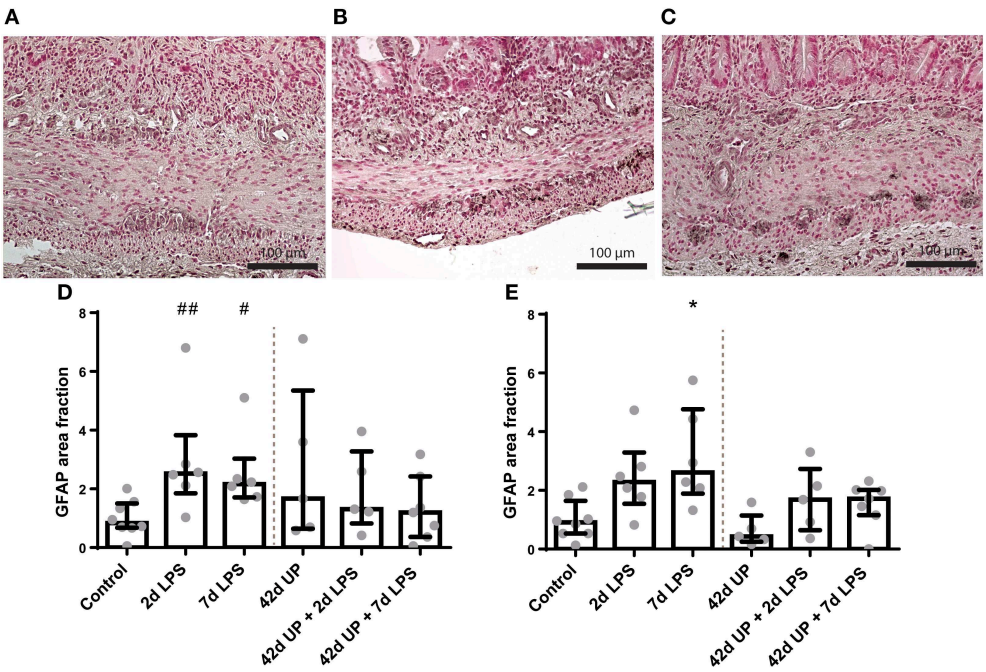

FIGURE 9 | Representative images of glial fibrillary acidic protein (GFAP) immunoreactivity in the submucosal and myenteric plexus of the control **(A)**, 2 days lipopolysaccharide (LPS) **(B)**, and 7 days LPS **(C)** group. Area fraction of GFAP in the submucosal plexus **(D)** and myenteric plexus **(E)** as fold increase over the control value. **(D)** The GFAP-positive surface area tended to be increased in the submucosal plexus of animals exposed to 2- and 7 days LPS. $^{\#\#}p = 0.07$, $^{\#}p = 0.09$ compared to the control. **(E)** Increased GFAP-positive surface area in the myenteric plexus of animals exposed to 7 days LPS. $^{*}p < 0.05$ compared to the control.

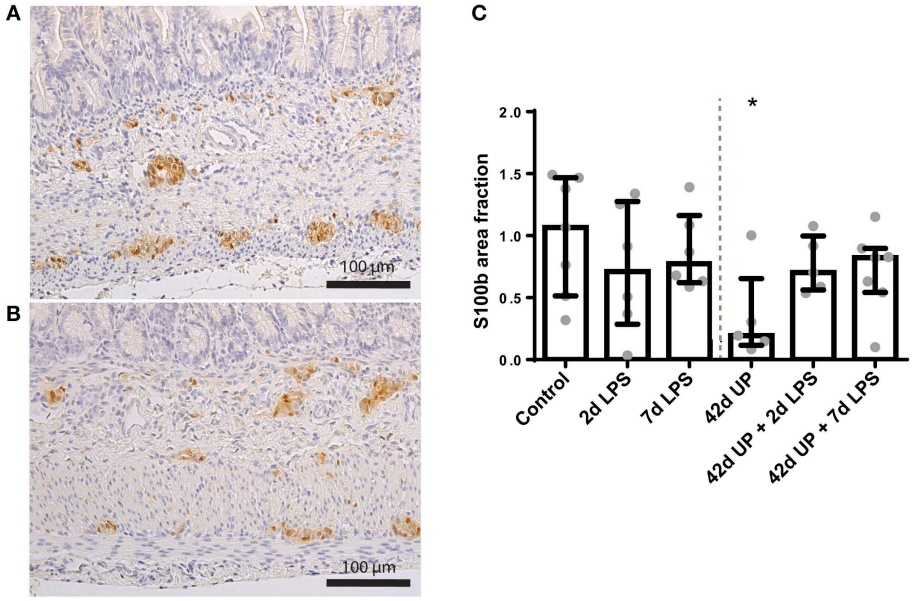

FIGURE 10 | Representative images of S100β immunoreactivity in the submucosal and myenteric plexus of the control **(A)** and *Ureaplasma parvum* (UP) group **(B)**. Area fraction of S100β in the myenteric plexus **(C)** as fold increase over the control value. **(C)** The S100β-positive surface area was decreased in the myenteric plexus of animals exposed to UP. *$p < 0.05$ compared to the control.

in both plexuses, likely representing a loss of enteric neurons. Alternatively, this might represent a loss of PGP9.5 positivity by enteric neurons. The doublecortin-positive (immature neurons) surface area in chronically UP-infected animals was unchanged, indicating that a decrease of mature neurons is responsible for the observed neuronal cell loss. As the period between 10 and 18 weeks of gestation is considered to be of paramount importance for both morphological and functional maturation of the ENS (40, 41), one might assume that the timing of our inflammatory challenge during this vulnerable second trimester is the key determinant for the observed effects rather than the nature of the microbial trigger. The loss of enteric neurons in the myenteric plexus following chronic UP infection coincides with a reduced S100β-positive surface area, suggesting a reduced number of enteric glial cells. However, a reduction of S100β immunoreactivity within glial cells could be involved in the observed effect as well. Enteric glial cells are known to contribute to neuronal maintenance, survival, and function (42). Interestingly, the S100β-positive surface area was less reduced in the groups exposed to an additional LPS challenge in combination with chronic UP infection, and the median of the PGP9.5-positive surface area was higher in these groups. In support, previous studies have shown that enteric glial cells are capable of generating enteric neurons in response to injury (43, 44), indicating that glial cells could be the driving cells behind the loss or gain of neurons in our model. As a hallmark of their high level of cellular plasticity (45), enteric glia can respond to inflammatory cues and ENS damage by alternating their morphology and the expression of key proteins such as GFAP, in a process similar to reactive astrogliosis (46, 47). In this study, GFAP immunoreactivity was increased in both plexuses in the LPS-exposed animals, indicating that a glial response is induced by intestinal inflammation (48). An enteric glial cell response was not detected in chronic UP-infected animals despite signs of intestinal inflammation, suggesting normalization of the GFAP levels within this period. Interestingly, pre-conditioning through chronic UP infection prevented GFAP upregulation in response to the overlapping second challenge with LPS in the glial cells in both plexuses, as no altered GFAP immunoreactivity was seen following subsequent IA LPS exposure. Whether this is solely protective or can contribute to the ENS damage seen in chronic UP exposure is unclear, as activation of enteric glia in the context of intestinal inflammation has been described to be both destructive (49) and potentially neuroregenerative (50). We may conclude from the aforementioned findings that enteric glial cells are already able to react to inflammatory cues prenatally. Importantly, our results suggest that these cells play an important role in neuronal survival and neurogenesis in the intrauterine setting.

At present, the postnatal consequences of the detected loss of mature neurons and glial cells following UP exposure in the second trimester remain unknown. A similar decrease in enteric neurons has been described in models of experimental colitis, which show that neuronal loss persists after recovery of inflammation (51) and is accompanied by a decreased colonic motility (52). Based on these combined findings, it is likely that the observed changes *in utero* will result in ENS dysfunction postnatally.

Interestingly, several studies describe intestinal changes in patients with acute NEC that are similar to those found after chronic UP infection, namely, loss of both enteric neurons (25–27, 53) and glial cells (25–27). Moreover, it has been suggested that ablation of enteric glial cells may be an upstream target of NEC pathology (54). A potential causal role of the

ENS in NEC pathophysiology is further supported by a rat study in which increased NEC survival and intestinal motility was associated with improvement of ENS changes, including an increase in enteric neurons (27). Collectively, our findings form a novel mechanistic explanation for the reported association of chorioamnionitis and NEC.

A limitation of this study is that it only enables us to study the effects of UP and LPS exposure at one time point, preventing us from dissecting the role of the different inflammatory triggers (LPS and UP) of inflammation duration (acute and chronic). In addition, the group sizes are small, which is an inherent shortcoming of the translational ovine model used.

In summary, an acute inflammatory stimulus with LPS or a chronic inflammatory stimulus with UP causes intestinal injury and inflammation in the mucosal and submucosal layers of the gut. Combined overlapping microbial exposure does not aggravate injury of the terminal ileum. Most importantly, chronic UP infection causes structural ENS alterations characterized by PGP9.5 and S100β immunoreactivity loss. Whether the observed ENS alterations result in functional abnormalities after birth remains to be elucidated. However, the observed changes *in utero* correspond with findings in neonates with NEC, which underlines the concept that NEC pathophysiology may already have its origin *in utero*.

DATA AVAILABILITY STATEMENT

The datasets generated for this study are available on request to the corresponding author.

ETHICS STATEMENT

The animal study was reviewed and approved by The Animal Ethics Committee of the University of Western Australia (Perth, Australia).

AUTHOR CONTRIBUTIONS

CH, IL, MH, WG, and TW conceived the original idea. MS, HU, SS, OS, MB, MP, JN, AJ, and MK designed the *in vivo* model and performed the animal experiments. CH carried out the laboratory analyses with the support from NR, LK, and GR. CH, IL, MH, KL, VM, WB, BK, WG, and TW contributed to the interpretation of the results. CH and IL wrote the manuscript with the input from all authors. WG and TW supervised the project. All authors contributed to manuscript revision, read, and approved the submitted version.

FUNDING

This work was supported by the National Institutes of Health (Bethesda, MD, USA) grant (HD 57869) and the Kinderonderzoekfonds Limburg (TW).

ACKNOWLEDGMENTS

The authors would like to thank Ellen Oostenbach for her excellent technical assistance.

REFERENCES

1. Murphy SL, Mathews TJ, Martin JA, Minkovitz CS, Strobino DM. Annual Summary of Vital Statistics: 2013–2014. *Pediatrics*. (2017) 139:e20163239. doi: 10.1542/peds.2016-3239
2. Howson CP, Kinney MV, McDougall L, Lawn JE, Born Too Soon Preterm Birth Action Group. Born too soon: preterm birth matters. *Reprod Health*. (2013) 10(Suppl. 1):S1. doi: 10.1186/1742-4755-10-S1-S1
3. Blencowe H, Cousens S. Addressing the challenge of neonatal mortality. *Trop Med Int Health*. (2013) 18:303–12. doi: 10.1111/tmi.12048
4. Blencowe H, Cousens S, Oestergaard MZ, Chou D, Moller AB, Narwal R, et al. National, regional, and worldwide estimates of preterm birth rates in the year 2010 with time trends since 1990 for selected countries: a systematic analysis and implications. *Lancet*. (2012) 379:2162–72. doi: 10.1016/S0140-6736(12)60820-4
5. Galinsky R, Polglase GR, Hooper SB, Black MJ, Moss TJ. The consequences of chorioamnionitis: preterm birth and effects on development. *J Pregnancy*. (2013) 2013:412831. doi: 10.1155/2013/412831
6. Goldenberg RL, Hauth JC, Andrews WW. Intrauterine infection and preterm delivery. *N Engl J Med*. (2000) 342:1500–7. doi: 10.1056/NEJM200005183422007
7. Tita AT, Andrews WW. Diagnosis and management of clinical chorioamnionitis. *Clin Perinatol*. (2010) 37:339–54. doi: 10.1016/j.clp.2010.02.003
8. Peng CC, Chang JH, Lin HY, Cheng PJ, Su BH. Intrauterine inflammation, infection, or both (Triple I): A new concept for chorioamnionitis. *Pediatr Neonatol*. (2018) 59:231–7. doi: 10.1016/j.pedneo.2017.09.001
9. Silwedel C, Speer CP, Glaser K. Ureaplasma-associated prenatal, perinatal, and neonatal morbidities. *Expert Rev Clin Immunol*. (2017) 13:1073–87. doi: 10.1080/1744666X.2017.1381559
10. Viscardi RM. Ureaplasma species: role in diseases of prematurity. *Clin Perinatol*. (2010) 37:393–409. doi: 10.1016/j.clp.2009.12.003
11. Been JV, Lievense S, Zimmermann LJ, Kramer BW, Wolfs TG. Chorioamnionitis as a risk factor for necrotizing enterocolitis: a systematic review and meta-analysis. *J Pediatr*. (2013) 162:236–42.e2. doi: 10.1016/j.jpeds.2012.07.012
12. Okogbule-Wonodi AC, Gross GW, Sun CC, Agthe AG, Xiao L, Waites KB, et al. Necrotizing enterocolitis is associated with ureaplasma colonization in preterm infants. *Pediatr Res*. (2011) 69(5 Pt 1):442–7. doi: 10.1203/PDR.0b013e3182111827
13. Wolfs TG, Jellema RK, Turrisi G, Becucci E, Buonocore G, Kramer BW. Inflammation-induced immune suppression of the fetus: a potential link between chorioamnionitis and postnatal early onset sepsis. *J Matern Fetal Neonatal Med*. (2012) 25(Suppl. 1):8–11. doi: 10.3109/14767058.2012.664447
14. Wolfs TG, Kramer BW, Thuijls G, Kemp MW, Saito M, Willems MG, et al. Chorioamnionitis-induced fetal gut injury is mediated by direct gut exposure of inflammatory mediators or by lung inflammation. *Am J Physiol Gastrointest Liver Physiol*. (2014) 306:G382–93. doi: 10.1152/ajpgi.00260.2013
15. Kataoka S, Yamada T, Chou K, Nishida R, Morikawa M, Minami M, et al. Association between preterm birth and vaginal colonization

by mycoplasmas in early pregnancy. *J Clin Microbiol*. (2006) 44:51–5. doi: 10.1128/JCM.44.1.51-55.2006
16. Sweeney EL, Dando SJ, Kallapur SG, Knox CL. The human ureaplasma species as causative agents of chorioamnionitis. *Clin Microbiol Rev*. (2017) 30:349–79. doi: 10.1128/CMR.00091-16
17. Wolfs TG, Kallapur SG, Knox CL, Thuijls G, Nitsos I, Polglase GR, et al. Antenatal ureaplasma infection impairs development of the fetal ovine gut in an IL-1-dependent manner. *Mucosal Immunol*. (2013) 6:547–56. doi: 10.1038/mi.2012.97
18. Gussenhoven R, Ophelders DRMG, Kemp MW, Payne MS, Spiller OB, Beeton ML, et al. The paradoxical effects of chronic intra-amniotic *Ureaplasma parvum* exposure on ovine fetal brain development. *Dev Neurosci*. (2017) 39:472–86. doi: 10.1159/000479021
19. Kallapur SG, Kramer BW, Knox CL, Berry CA, Collins JJ, Kemp MW, et al. Chronic fetal exposure to *Ureaplasma parvum* suppresses innate immune responses in sheep. *J Immunol*. (2011) 187:2688–95. doi: 10.4049/jimmunol.1100779
20. Furness JB. *The Enteric Nervous System*. Oxford: Blackwell Publishing (2006). doi: 10.1002/9780470988756
21. Lake JI, Heuckeroth RO. Enteric nervous system development: migration, differentiation, and disease. *Am J Physiol Gastrointest Liver Physiol*. (2013) 305:G1–24. doi: 10.1152/ajpgi.00452.2012
22. Rao M, Gershon MD. Enteric nervous system development: what could possibly go wrong? *Nat Rev Neurosci*. (2018) 19:552–65. doi: 10.1038/s41583-018-0041-0
23. Burns AJ, Roberts RR, Bornstein JC, Young HM. Development of the enteric nervous system and its role in intestinal motility during fetal and early postnatal stages. *Semin Pediatr Surg*. (2009) 18:196–205. doi: 10.1053/j.sempedsurg.2009.07.001
24. Hao MM, Foong JP, Bornstein JC, Li ZL, Vanden Berghe P, Boesmans W. Enteric nervous system assembly: functional integration within the developing gut. *Dev Biol*. (2016) 417:168–81. doi: 10.1016/j.ydbio.2016.05.030
25. Sigge W, Wedel T, Kuhnel W, Krammer HJ. Morphologic alterations of the enteric nervous system and deficiency of non-adrenergic non-cholinergic inhibitory innervation in neonatal necrotizing enterocolitis. *Eur J Pediatr Surg*. (1998) 8:87–94. doi: 10.1055/s-2008-1071128
26. Wedel T, Krammer HJ, Kuhnel W, Sigge W. Alterations of the enteric nervous system in neonatal necrotizing enterocolitis revealed by whole-mount immunohistochemistry. *Pediatr Pathol Lab Med*. (1998) 18:57–70. doi: 10.1080/107710498174227
27. Zhou Y, Yang J, Watkins DJ, Boomer LA, Matthews MA, Su Y, et al. Enteric nervous system abnormalities are present in human necrotizing enterocolitis: potential neurotransplantation therapy. *Stem Cell Res Ther*. (2013) 4:157. doi: 10.1186/scrt387
28. Moss TJ, Knox CL, Kallapur SG, Nitsos I, Theodoropoulos C, Newnham JP, et al. Experimental amniotic fluid infection in sheep: effects of *Ureaplasma parvum* serovars 3 and 6 on preterm or term fetal sheep. *Am J Obstet Gynecol*. (2008) 198:122.e1–8. doi: 10.1016/j.ajog.2007.06.065
29. Kramer BW, Moss TJ, Willet KE, Newnham JP, Sly PD, Kallapur SG, et al. Dose and time response after intraamniotic endotoxin in preterm lambs. *Am J Respir Crit Care Med*. (2001) 164:982–8. doi: 10.1164/ajrccm.164.6.2103061
30. Newnham JP, Kallapur SG, Kramer BW, Moss TJ, Nitsos I, Ikegami M, et al. Betamethasone effects on chorioamnionitis induced by intra-amniotic endotoxin in sheep. *Am J Obstet Gynecol*. (2003) 189:1458–66. doi: 10.1067/S0002-9378(03)00758-0
31. Miura Y, Payne MS, Keelan JA, Noe A, Carter S, Watts R, et al. Maternal intravenous treatment with either azithromycin or solithromycin clears *Ureaplasma parvum* from the amniotic fluid in an ovine model of intrauterine infection. *Antimicrob Agents Chemother*. (2014) 58:5413–20. doi: 10.1128/AAC.03187-14
32. Rao M, Nelms BD, Dong L, Salinas-Rios V, Rutlin M, Gershon MD, et al. Enteric glia express proteolipid protein 1 and are a transcriptionally unique population of glia in the mammalian nervous system. *Glia*. (2015) 63:2040–57. doi: 10.1002/glia.22876
33. Manimtim WM, Hasday JD, Hester L, Fairchild KD, Lovchik JC, Viscardi RM. *Ureaplasma urealyticum* modulates endotoxin-induced cytokine release by human monocytes derived from preterm and term newborns and adults. *Infect Immun*. (2001) 69:3906–15. doi: 10.1128/IAI.69.6.3906-3915.2001
34. Shimizu T, Kida Y, Kuwano K. *Ureaplasma parvum* lipoproteins, including MB antigen, activate NF-{kappa}B through TLR1, TLR2 and TLR6. *Microbiology*. (2008) 154(Pt 5):1318–25. doi: 10.1099/mic.0.2007/016212-0
35. Kobayashi K, Hernandez LD, Galan JE, Janeway CA Jr, Medzhitov R, Flavell RA. IRAK-M is a negative regulator of Toll-like receptor signaling. *Cell*. (2002) 110:191–202. doi: 10.1016/S0092-8674(02)00827-9
36. Silwedel C, Speer CP, Haarmann A, Fehrholz M, Claus H, Buttmann M, et al. Novel insights into neuroinflammation: bacterial lipopolysaccharide, tumor necrosis factor α, and Ureaplasma species differentially modulate atypical chemokine receptor 3 responses in human brain microvascular endothelial cells. *J Neuroinflammation*. (2018) 15:156. doi: 10.1186/s12974-018-1170-0
37. Yoo BB, Mazmanian SK. The enteric network: interactions between the immune and nervous systems of the gut. *Immunity*. (2017) 46:910–26. doi: 10.1016/j.immuni.2017.05.011
38. Brierley SM, Linden DR. Neuroplasticity and dysfunction after gastrointestinal inflammation. *Nat Rev Gastroenterol Hepatol*. (2014) 11:611–27. doi: 10.1038/nrgastro.2014.103
39. Margolis KG, Gershon MD. Enteric neuronal regulation of intestinal inflammation. *Trends Neurosci*. (2016) 39:614–24. doi: 10.1016/j.tins.2016.06.007
40. Fekete E, Resch BA, Benedeczky I. Histochemical and ultrastructural features of the developing enteric nervous system of the human foetal small intestine. *Histol Histopathol*. (1995) 10:127–34.
41. Fekete E, Bagyánszki M, Resch BA. Prenatal development of the myenteric plexus in the human fetal small intestine. *Acta Biol Szeged*. (2000) 44:3–19.
42. De Giorgio R, Giancola F, Boschetti E, Abdo H, Lardeux B, Neunlist M. Enteric glia and neuroprotection: basic and clinical aspects. *Am J Physiol Gastrointest Liver Physiol*. (2012) 303:G887–93. doi: 10.1152/ajpgi.00096.2012
43. Joseph NM, He S, Quintana E, Kim YG, Nunez G, Morrison SJ. Enteric glia are multipotent in culture but primarily form glia in the adult rodent gut. *J Clin Invest*. (2011) 121:3398–411. doi: 10.1172/JCI58186
44. Laranjeira C, Sandgren K, Kessaris N, Richardson W, Potocnik A, Vanden Berghe P, et al. Glial cells in the mouse enteric nervous system can undergo neurogenesis in response to injury. *J Clin Invest*. (2011) 121:3412–24. doi: 10.1172/JCI58200
45. Boesmans W, Lasrado R, Vanden Berghe P, Pachnis V. Heterogeneity and phenotypic plasticity of glial cells in the mammalian enteric nervous system. *Glia*. (2015) 63:229–41. doi: 10.1002/glia.22746
46. Chow AK, Gulbransen BD. Potential roles of enteric glia in bridging neuroimmune communication in the gut. *Am J Physiol Gastrointest Liver Physiol*. (2017) 312:G145–52. doi: 10.1152/ajpgi.00384.2016
47. Rosenbaum C, Schick MA, Wollborn J, Heider A, Scholz CJ, Cecil A, et al. Activation of myenteric glia during acute inflammation *in vitro* and *in vivo*. *PLoS ONE*. (2016) 11:e0151335. doi: 10.1371/journal.pone.0151335
48. Cirillo C, Sarnelli G, Turco F, Mango A, Grosso M, Aprea G, et al. Proinflammatory stimuli activates human-derived enteroglial cells and induces autocrine nitric oxide production. *Neurogastroenterol Motil*. (2011) 23:e372–82. doi: 10.1111/j.1365-2982.2011.01748.x
49. Brown IA, McClain JL, Watson RE, Patel BA, Gulbransen BD. Enteric glia mediate neuron death in colitis through purinergic pathways that require connexin-43 and nitric oxide. *Cell Mol Gastroenterol Hepatol*. (2016) 2:77–91. doi: 10.1016/j.jcmgh.2015.08.007
50. Belkind-Gerson J, Graham HK, Reynolds J, Hotta R, Nagy N, Cheng L, et al. Colitis promotes neuronal differentiation of Sox2+ and PLP1+ enteric cells. *Sci Rep*. (2017) 7:2525. doi: 10.1038/s41598-017-02890-y

51. Linden DR, Couvrette JM, Ciolino A, McQuoid C, Blaszyk H, Sharkey KA, et al. Indiscriminate loss of myenteric neurones in the TNBS-inflamed guinea-pig distal colon. *Neurogastroenterol Motil*. (2005) 17:751–60. doi: 10.1111/j.1365-2982.2005.00703.x
52. Boyer L, Ghoreishi M, Templeman V, Vallance BA, Buchan AM, Jevon G, et al. Myenteric plexus injury and apoptosis in experimental colitis. *Auton Neurosci*. (2005) 117:41–53. doi: 10.1016/j.autneu.2004.10.006
53. Fagbemi AO, Torrente F, Puleston J, Lakhoo K, James S, Murch SH. Enteric neural disruption in necrotizing enterocolitis occurs in association with myenteric glial cell CCL20 expression. *J Pediatr Gastroenterol Nutr*. (2013) 57:788–93. doi: 10.1097/MPG.0b013e3182a86fd4
54. Bush TG. Enteric glial cells. An upstream target for induction of necrotizing enterocolitis and Crohn's disease? *Bioessays*. (2002) 24:130–40. doi: 10.1002/bies.10039

Conflict of Interest: The authors declare that the research was conducted in the absence of any commercial or financial relationships that could be construed as a potential conflict of interest.

The handling editor declared a past co-authorship with several of the authors TW, BK.

frontiers in Immunology

CORRECTION
published: 15 April 2020
doi: 10.3389/fimmu.2020.00672

Corrigendum: Chronic Intra-Uterine *Ureaplasma parvum* Infection Induces Injury of the Enteric Nervous System in Ovine Fetuses

*Cathelijne Heymans[1], Ilse H. de Lange[1,2], Matthias C. Hütten[2,3,4,5], Kaatje Lenaerts[1], Nadine J. E. de Ruijter[2], Lilian C. G. A. Kessels[2], Glenn Rademakers[6], Veerle Melotte[6], Werend Boesmans[6,7], Masatoshi Saito[8,9], Haruo Usuda[8,9], Sarah J. Stock[10], Owen B. Spiller[11], Michael L. Beeton[12], Matthew S. Payne[8], Boris W. Kramer[2,3], John P. Newnham[8], Alan H. Jobe[8,13], Matthew W. Kemp[8,9,14], Wim G. van Gemert[1,15,16] and Tim G. A. M. Wolfs[2,17]**

[1] Department of Surgery, NUTRIM School of Nutrition and Translational Research in Metabolism, Maastricht University, Maastricht, Netherlands, [2] Department of Pediatrics, School for Oncology and Developmental Biology (GROW), Maastricht University, Maastricht, Netherlands, [3] Neonatology, Department of Pediatrics, Maastricht University Medical Center, Maastricht, Netherlands, [4] Neonatology, Department of Pediatrics, University Hospital Aachen, Aachen, Germany, [5] Neonatology, Department of Pediatrics, University Children's Hospital Würzburg, Würzburg, Germany, [6] Department of Pathology, School for Oncology and Developmental Biology (GROW), Maastricht University Medical Center, Maastricht, Netherlands, [7] Biomedical Research Institute (BIOMED), Hasselt University, Hasselt, Belgium, [8] Division of Obstetrics and Gynecology, University of Western Australia, Perth, WA, Australia, [9] Center for Perinatal and Neonatal Medicine, Tohoku University Hospital, Sendai, Japan, [10] Usher Institute, University of Edinburgh, Edinburgh, United Kingdom, [11] Division of Infection and Immunity, School of Medicine, Cardiff University, Cardiff, United Kingdom, [12] Cardiff School of Sport and Health Sciences, Cardiff Metropolitan University, Cardiff, United Kingdom, [13] Division of Neonatology/Pulmonary Biology, The Perinatal Institute, Cincinnati Children's Hospital Medical Center, University of Cincinnati, Cincinnati, OH, United States, [14] School of Veterinary and Life Sciences, Murdoch University, Perth, WA, Australia, [15] Pediatric Surgery, Department of Surgery, Maastricht University Medical Center, Maastricht, Netherlands, [16] Department of Surgery, University Hospital Aachen, Aachen, Germany, [17] Department of Biomedical Engineering (BMT), School for Cardiovascular Diseases (CARIM), Maastricht University, Maastricht, Netherlands

OPEN ACCESS

Approved by:
Frontiers Editorial Office,
Frontiers Media SA, Switzerland

***Correspondence:**
Tim G. A. M. Wolfs
tim.wolfs@maastrichtuniversity.nl

Specialty section:
This article was submitted to Microbial Immunology, a section of the journal Frontiers in Immunology

Received: 24 March 2020
Accepted: 25 March 2020
Published: 15 April 2020

Citation:
Heymans C, de Lange IH, Hütten MC, Lenaerts K, de Ruijter NJE, Kessels LCGA, Rademakers G, Melotte V, Boesmans W, Saito M, Usuda H, Stock SJ, Spiller OB, Beeton ML, Payne MS, Kramer BW, Newnham JP, Jobe AH, Kemp MW, van Gemert WG and Wolfs TGAM (2020) Corrigendum: Chronic Intra-Uterine Ureaplasma parvum Infection Induces Injury of the Enteric Nervous System in Ovine Fetuses. Front. Immunol. 11:672. doi: 10.3389/fimmu.2020.00672

Keywords: *Ureaplasma parvum*, intra-amniotic infection, chorioamnionitis, enteric nervous system, sheep, preterm birth, necrotizing enterocolitis

A Corrigendum on

Chronic Intra-Uterine *Ureaplasma parvum* Infection Induces Injury of the Enteric Nervous System in Ovine Fetuses

by Heymans, C., de Lange, I. H., Hütten, M. C., Lenaerts, K., de Ruijter, N. J. E., Kessels, L. C. G. A., et al. (2020). Front. Immunol. 11:189. doi: 10.3389/fimmu.2020.00189

Michael L. Beeton was not included as an author in the published article. The corrected Author Contributions Statement appears below.

AUTHOR CONTRIBUTIONS

CH, IL, MH, WG, and TW conceived the original idea. MS, HU, SS, OS, MB, MP, JN, AJ, and MK designed the *in vivo* model and performed the animal experiments. CH carried out the laboratory analyses with the support from NR, LK, and GR. CH, IL, MH, KL, VM, WB, BK, WG, and TW

contributed to the interpretation of the results. CH and IL wrote the manuscript with the input from all authors. WG and TW supervised the project. All authors contributed to manuscript revision, read, and approved the submitted version.

The authors apologize for this error and state that this does not change the scientific conclusions of the article in any way. The original article has been updated.

frontiers in Immunology

ORIGINAL RESEARCH
published: 19 March 2020
doi: 10.3389/fimmu.2020.00420

Postnatal Gut Immunity and Microbiota Development Is Minimally Affected by Prenatal Inflammation in Preterm Pigs

Xiaoyu Pan[1†], *Du Zhang*[2†], *Duc Ninh Nguyen*[1], *Wei Wei*[1], *Xinxin Yu*[2], *Fei Gao*[1,2*] and *Per T. Sangild*[1,3,4*]

[1] Comparative Pediatrics and Nutrition, Department of Veterinary and Animal Sciences, Faculty of Health and Medical Sciences, University of Copenhagen, Copenhagen, Denmark, [2] Lingnan Guangdong Laboratory of Modern Agriculture, Genome Analysis Laboratory of the Ministry of Agriculture, Agricultural Genomics Institute at Shenzhen, Chinese Academy of Agricultural Sciences, Shenzhen, China, [3] Department of Neonatology, Rigshospitalet, Copenhagen, Denmark, [4] Department of Pediatrics, Odense University Hospital, Odense, Denmark

OPEN ACCESS

Edited by:
Javier Dominguez,
Instituto Nacional de Investigación y Tecnología Agraria y Alimentaria (INIA), Spain

Reviewed by:
Gloria Isabel Solano-Aguilar,
Agricultural Research Service (USDA), United States
Juan J. Garrido,
Universidad de Córdoba, Spain

***Correspondence:**
Fei Gao
feg@sund.ku.dk
Per T. Sangild
pts@sund.ku.dk

[†]These authors share first authorship

Specialty section:
This article was submitted to Comparative Immunology, a section of the journal Frontiers in Immunology

Received: 17 October 2019
Accepted: 24 February 2020
Published: 19 March 2020

Citation:
Pan X, Zhang D, Nguyen DN, Wei W, Yu X, Gao F and Sangild PT (2020) Postnatal Gut Immunity and Microbiota Development Is Minimally Affected by Prenatal Inflammation in Preterm Pigs. Front. Immunol. 11:420. doi: 10.3389/fimmu.2020.00420

Chorioamnionitis (CA), resulting from intra-amniotic inflammation, is a frequent cause of preterm birth and exposes the immature intestine to bacterial toxins and/or inflammatory mediators before birth via fetal swallowing. This may affect intestinal immune development, interacting with the effects of enteral feeding and gut microbiota colonization just after birth. Using preterm pigs as model for preterm infants, we hypothesized that prenatal exposure to gram-negative endotoxin influences postnatal bacterial colonization and gut immune development. Pig fetuses were given intra-amniotic lipopolysaccharide (LPS) 3 days before preterm delivery by cesarean section and were compared with littermate controls (CON) at birth and after 5 days of formula feeding and spontaneous bacterial colonization. Amniotic fluid was collected for analysis of leukocyte counts and cytokines, and the distal small intestine was analyzed for endotoxin level, morphology, and immune cell counts. Intestinal gene expression and microbiota were analyzed by transcriptomics and metagenomics, respectively. At birth, LPS-exposed pigs showed higher intestinal endotoxin, neutrophil/macrophage density, and shorter villi. About 1.0% of intestinal genes were affected at birth, and *DMBT1*, a regulator of mucosal immune defense, was identified as the hub gene in the co-expression network. Genes related to innate immune response (*TLR2*, *LBP*, *CD14*, *C3*, *SFTPD*), neutrophil chemotaxis (*C5AR1*, *CSF3R*, *CCL5*), and antigen processing (MHC II genes and *CD4*) were also affected, and expression levels correlated with intestinal neutrophil/macrophage density and amniotic fluid cytokine levels. On day 5, LPS and CON pigs showed similar sensitivity to necrotizing enterocolitis, endotoxin levels, morphology, immune cell counts, gene expressions, and microbiota composition (except for difference in some low-abundant species). Our results show that CA markedly affects intestinal genes at preterm birth, including genes related to immune cell infiltration. However, a few days later, following the physiological adaptations to

preterm birth, CA had limited effects on intestinal structure, function, gene expression, bacterial colonization, and necrotizing enterocolitis sensitivity. We conclude that short-term, prenatal intra-amniotic inflammation is unlikely to exert marked effects on intestinal immune development in preterm neonates beyond the immediate neonatal period.

Keywords: chorioamnionitis, small intestine, gene expression, immunity, gut microbiota

INTRODUCTION

When the newborn intestine is exposed to milk and large amount of microbes just after birth, it must be able to mount an effective immune response and tolerance against pathogens and food antigens. In the adult intestine, this homeostasis is maintained by a structured and rapidly renewing epithelium that is reinforced by various aspects of the innate and adaptive immunity (1). For neonates, and especially preterm neonates, the situation is different. Before birth, the intestine is bathed in sterile amniotic fluid through fetal swallowing, contributing up to 20% of fetal energy and protein supply (2). Upon delivery, the neonatal intestine encounters a new microbe-rich environment with oral intake of milk. Meanwhile, both innate and adaptive immune systems still undergo differentiation and adaptation (3). Immaturity-related disruption of the equilibrium may lead to disease susceptibility. Thus, necrotizing enterocolitis (NEC) occurs in many preterm infants during the first weeks of life, and NEC is associated with microbiota dysbiosis and inappropriate immune response (4) with short- and long-term consequences (5, 6). It is important to better understand how the newborn preterm gut develops its immune competence, interacting with the gut microbiota and prenatal insults, to better prevent harmful inflammatory reactions in the postnatal period.

Chorioamnionitis (CA), caused by intra-amniotic inflammation, is a common cause of preterm birth (7). The CA-related inflammatory *in utero* environment may pose an additional challenge for the fetal immature intestine via swallowing of amniotic fluid (8). Using fetal lambs and sheep and rodents, it has been shown that intra-amniotic inflammation affects the neonatal intestine with regard to immune cell infiltration, tight junction proteins, and villus structure (9–13). These studies mainly investigated intestinal outcomes around birth, without demonstrating if such effects were persistent, or even worsened, when transitioning into postnatal life when the normal developmental changes occur associated with hemodynamic stability, enteral nutrition, and gut bacterial colonization within the first 1–2 weeks. It is unknown if these fundamental postnatal adaptations overshadow any effect of intestinal exposure to bacteria, bacterial toxins, and inflammation *in utero*. Prenatal gut inflammation may also influence the postnatal colonization with bacteria and thereby influence intestinal immune development.

Over the past decades, the preterm pig has been extensively used as a valuable biomedical model for preterm infants because of its similarity in size, anatomy, and birth-related clinical complications, such as impaired lung, immunity, gut, and brain functions (14). When kept in a neonatal intensive care unit under high-sanitary conditions, thermoregulation, and nutrition and oxygen support, preterm pigs develop to levels of the their term counterparts within 3–4 weeks, although some functions lack behind for much longer (15). The pig model is generally used to investigate preterm birth independent of the factors leading to preterm birth (e.g., maternal inflammation), but we have recently investigated the specific role of CA, induced by intra-amniotic lipopolysaccharide (LPS) exposure, on organ development in preterm neonates (16). Further building on this model, we hypothesized in this study that exposure of the fetus and the fetal gut (via swallowing of amniotic fluid) to some days of LPS before preterm delivery would influence intestinal gene expressions, not only at birth, but also beyond the neonatal period, after reaching physiological stability and adapting to gut bacterial colonization. By intestinal transcriptome and metagenome profiling, our data showed that CA-like symptoms induced by fetal LPS exposure increased the expression of a number of intestinal genes associated with immune cell infiltration at birth but that these fetal CA symptoms were marginal a few days later, following the start of enteral feeding and spontaneous gut bacterial colonization.

MATERIALS AND METHODS

Animal Procedure and Tissue Analysis

All animal procedures were approved by the Danish National Committee on Animal Experimentation. Details of animal procedures were described previously (16). Briefly, fetuses from 3 sows were assigned to LPS treatment group (LPS, $n = 37$) or control group (CON, $n = 32$), respectively. In the LPS group, each fetus received 1 mg LPS (*Escherichia coli* 055:B5; Sigma-Aldrich, St. Louis, MO, USA) into the amniotic fluid, and fetuses in the CON group received saline or no injection. Preterm piglets were born at day 106 of gestation (3 days after injection) by cesarean section. During the cesarean section, amniotic fluid was collected for analysis of total leukocyte counts (by manual counting under a microscope) and cytokines (by enzyme-linked immunosorbent assay). For each group, piglets were randomly assigned to be euthanized within 1–3 h of birth or to receive parenteral nutrition plus supplemental enteral nutrition with infant formula for 5 days. The formula composition included 75 g/L Liquigen MCT (Nutricia, Allerød, Denmark), 80 g/L Pepdite (Nutricia), and 70 g Lacprodan DI-9224 (Arla Foods Ingredients, Viby, Denmark). The piglets received a gradually increasing amount of infant formula (3–15 mL/kg per 3 h) for 5 days, a

feeding protocol leading to ∼50% of pigs with macroscopically visible NEC lesions in the colon region (16).

From the above fetuses, animals that died *in utero* or within the first 48 h because of respiratory distress were excluded in the study. A subsample of 40 individuals were randomly chosen from the remaining animals for the phenotypic, transcriptomic, and metagenomic analyses in this study and balanced among litters and sexes. Four groups of pigs were sampled either within 1–3 h of delivery (day 1) or on postnatal day 5 and subjected to LPS or control treatment before birth (CON-D1, LPS-D1, CON-D5, LPS-D5, each $n = 10$). The distal small intestines were collected and analyzed for endotoxin levels, morphology (i.e., villus height and crypt depth), brush border enzyme activities, and goblet cell and immune cell counts (including CD3-, Foxp3-, and MPO-positive cells) by immunohistochemistry as previously described (16). Comparisons were made to examine the prenatal LPS effects on the distal intestine at birth (samples collected on day 1 within 1–3 h after delivery) and on day 5, respectively (i.e., LPS-D1 vs. CON-D1 and LPS-D5 vs. CON-D5). Because the phenotypic difference between D1 and D5 pigs involves many more factors than postnatal age alone (e.g., feeding responses, metabolic adaptation, bacterial colonization), no attempts were made to investigate specific age × treatment interactions.

RNA-Seq Analysis

Total RNA from the distal small intestines was isolated with RNeasy Micro Kit (Qiagen), and 1.5 μg RNA per sample was used for RNA-seq library construction. Sequencing libraries were constructed using NEBNext Ultra RNA library Prep Kit for Illumina (NEB, Ipswich, MA, USA) following the manufacturer's recommendations. RNA libraries were sequenced on the Illumina HiSeq 4000 platform with paired-end 150-bp reads production. Quality and adapter trimming of raw reads was performed using TrimGalore (Babraham Bioinformatics, Cambridge, UK). The remaining clean reads were aligned to the porcine genome (Sscrofa11.1) using Tophat (17). The annotated gene information of porcine genome was downloaded from Ensembl. The script *htseq-count* (18) was used to generate gene count matrix, followed by gene-level differential expression analyses using *DESeq2* (19).

Metagenome Analysis

Total genomic DNA from distal intestinal contents was extracted using CTAB/SDS method. Sequencing libraries were generated using TruSeq DNA PCR-Free Sample Preparation Kit (Illumina, USA) following manufacturer's recommendations. The library was sequenced on an Illumina HiSeq Xten platform, and 150-bp paired-end reads were generated. Clean reads after removing host sequence were employed to contigs assembly using MEGAHIT (v1.0.6) (20). Open Reading Frames (ORFs) were identified by MetaGeneMark (v3.38) (21), and the ORFs were clustered for removing redundancy by CD-HIT (v4.7) (22). Taxonomic information of ORFs was annotated by DIAMOND (23) based on pig microbial database (24). Functional information of ORFs was annotated by KAAS (KEGG Automatic Annotation Server) (25) against KEGG database and by DIAMOND against COG (Clusters of Orthologous Groups) and CAZy (carbohydrate-active enzymes) database.

Immunohistochemistry Analysis

Paraformaldehyde- or acetone-fixed distal small intestine sections were examined by immunohistochemistry for DMBT1 (anti-DMBT1, HPA040778; Sigma), SFTPD [mouse anti–pig surfactant protein D (SP-D), MCA2725; Bio-Rad, Hercules, CA, USA] and MHCII (mouse anti–pig SLA CLASS II DQ, MCA1335GA; Bio-Rad). Staining was developed with UltraVision LP Detection System (ThermoFisher Scientific, Waltham, MA, USA). The sections were counterstained with Mayer hematoxylin. Images were acquired using the Leica LAS EZ software (version 3.4.0), Wetzlar, Germany, and the proportion of positive staining was analyzed by the IHC toolbox in ImageJ, National Institutes of Health, USA.

Statistical Analysis

Using R software package (version 3.5.1), Vienna, Austria, amniotic fluid and tissue measures were analyzed by using linear model (lm function), adjusted for litter. The linearity of data, normality of residuals, and homoscedasticity were checked, and data were transformed using Box-Cox transformation when required. $P < 0.05$ was considered statistically significant; $P < 0.10$ was considered a tendency to an effect. For RNA-seq analysis, significant differentially expressed genes (DEGs) with fold change >2 and Benjamini-Hochberg (BH)–adjusted $P < 0.05$ were identified by DESeq2 and adjusted for litter. Correlation between gene expression was performed using Spearman rank correlation based on normalized counts produced from DESeq2, and the correlation with absolute Spearman $\rho > 0.6$ as well as BH-adjusted $P < 0.05$ was considered statistically significant. Gene Ontology and KEGG pathway enrichment analysis were performed using DAVID (26), and BH-adjusted $P < 0.05$ was considered statistically significant. Validation of DEGs was performed by immunohistochemistry analysis, where Wilcoxon rank-sum test was used for the difference test, and $P < 0.05$ was considered statistically significant. For metagenome, diversity analysis was performed based on normalized taxonomy abundance. The difference test of alpha diversity was performed using Wilcoxon rank-sum test, and $P < 0.05$ was considered statistically significant. Analysis of similarities was used to check the difference in beta diversity (based on Bray–Curtis dissimilarity matrix), and $P < 0.05$ was considered statistically significant. Differentially abundant features at different levels were analyzed by Metastats (27), and $P < 0.05$ was considered statistically significant. Differential abundant genes, KEGG pathway, and COGs and CAZymes were identified by the Wilcoxon rank-sum test with BH-adjusted $P < 0.05$.

RESULTS

Prenatal LPS Exposure Induces Intra-Amniotic Inflammation and Intestinal Immune Cell Infiltration at Birth

Intra-amniotic LPS injection induced extensive intra-amniotic inflammation, with increased leukocytes and cytokines [interleukin 1b (IL-1b), IL-6, IL-8, IL-10, and tumor necrosis factor α (TNF-α)] in the amniotic fluid (all $P < 0.05$, **Table S1**).

Focusing on the distal small intestines of these neonates (**Table S2**), we found that shortly after birth (day 1) the LPS-exposed preterm pigs had elevated gut endotoxin level ($P < 0.01$) and tended to have reduced villus height ($P < 0.1$), whereas crypt depth was not affected. There were limited effects of LPS on digestive functions, as measured by lactase, maltase, and sucrase activities. To investigate immune cell infiltration in response to LPS exposure, the distal small intestines were stained for CD3, Foxp3, and myeloperoxidase (MPO, marker of neutrophil/macrophage infiltration). The results showed that the LPS-exposed preterm pigs had increased MPO-positive cell density in the distal small intestines on day 1 ($P < 0.05$). Goblet cells were quantified by Alcian blue and periodic acid–Schiff staining and showed no difference between the LPS and CON groups on day 1. After 5 days, pigs with and without prenatal LPS exposure had similar incidence of intestinal NEC lesions, and all the above measures in the distal small intestine were no longer different between the LPS and CON groups (**Table S2**).

Prenatal LPS Exposure Up-Regulates Intestinal Gene Expression at Birth

The distal small intestinal tissues were used for RNA-seq, and approximately 48 M reads were sequenced for each pig. Of 25,880 pig genes annotated in the Ensembl database (Sscrofa11.1), 20,874 genes were detected in at least one pig and were used for further analysis. Based on the individual expression level of these genes, principal component analysis showed that intestinal gene expression shortly after birth (i.e., day 1) was distinct from that in the postnatal period (i.e., day 5). In addition, there were genes showing moderate variation between the LPS and CON groups on day 1, but not on day 5 (**Figure 1A**).

To detect the changes in gene expression between the LPS and CON groups on days 1 and 5, respectively, we employed a threshold with fold-change >2 and adjusted $P < 0.05$ to identify significant DEGs using DESeq2. The results showed that 176 of 20,874 genes (equivalent to 0.8% of genes analyzed) were identified as DEGs between the two groups on day 1, whereas no significant DEGs were found on day 5 (**Figure 1B** and **Table S3**). The DEGs on day 1 included 166 up-regulated and 10 down-regulated genes, respectively. Based on the current gene annotation in the pig genome, 129 genes with gene symbols were ascertainable according to the Ensembl database. Except for *ADGRG2*, *NEK5*, *ssc-mir-421*, and 7 other genes without gene symbols, all other DEGs showed up-regulation in the LPS vs. CON group on day 1. The top 10 most significant genes were *DMBT1*, *LBP*, *CSF3R*, *SMPDL3B*, *FOLR1*, *SFTPD*, *C3*, *C2*, *RF01973*, and *OLFM4* (**Figure 1C**). *C3*, *DMBT1*, *OLFM4*, and *SMPDL3B* were also among the top 10 DEGs with highest average expression across all pigs on day 1 (**Figure 1D**).

Prenatal LPS Exposure Has Limited Effects on Gut Microbiome Postnatally

To investigate whether intra-amniotic LPS exposure affected the neonatal gut colonization, 5-day-old formula-fed preterm pigs had their distal small intestinal content collected for metagenome analysis. Based on Shannon index and Bray–Curtis dissimilarity, the alpha and beta diversities of gut microbiome were not affected by intra-amniotic LPS exposure, regardless of taxonomic levels (**Figures 2A,B**; all $P > 0.05$). Similar to that in preterm human infants in the first few days after birth (28, 29), these 5-day-old preterm pigs were dominated by phylum Proteobacteria and Firmicutes (mean abundance was 44.2 and 26.6%, respectively). The top abundant genus included *Enterococcus*, *Escherichia*, and *Clostridium* (mean, 17.2, 11.0, and 3.5%, respectively), and the top abundant species were *E. coli*, *Enterococcus hirae*, and *Enterococcus faecium* (mean, 10.6, 5.0, and 2.6%, respectively; **Figure 2C**). The abundance of these features showed no statistical difference between the two groups. However, eight differentially abundant species were identified between the LPS and CON groups ($P < 0.05$) according to Metastats and were detected in at least three pigs (**Figure 2D**). The mean abundance of these eight species was relatively low, and *Streptococcus equi* and *Lactobacillus amylovorus* were among the most abundant (∼0.05%). Their maximum individual abundance was ∼0.58%. These two species were down- and up-regulated in the LPS group, respectively. Moreover, 897 of 21,384 analyzed genes showed differential abundance between the two groups (adjusted $P < 0.05$), and most of them (891/897) were down-regulated in the LPS group. Approximately 11% of the down-regulated genes were annotated to *Streptococcus*, and their top COG annotations were "Replication, recombination, and repair," "Carbohydrate transport and metabolism," and "Defense mechanisms." However, the abundance of these functions was not significantly different between the two groups.

Prenatal LPS Exposure Induced Intestinal Immune Response Associated With DMBT1

Finally, to better understand the relationship of the DEGs identified on day 1, we first conducted a putative co-expression gene network using pairwise correlation to determine possible gene pairs in the expression data. Based on the 129 DEGs with ascertainable gene symbols, 4,205 of 8,256 gene pairs were selected using a threshold of absolute Spearman $\rho > 0.6$ and adjusted $P < 0.05$, and were used to build the co-expression network. Next, to identify the highly connected gene (hub gene) in this network, network analysis was performed using Cytoscape. *DMBT1* (deleted in malignant brain tumors 1) was identified as the hub gene as it had the highest "betweenness centrality," which describes the shortest-path connectors through a network (**Figure 3A**). In addition, experimentally determined protein–protein interaction between these gene pairs was examined using STRING database. We found that DMBT1 interacts with SFTPD (SP-D) and that SFTPD interacts with TLR2 (Toll-like receptor 2), all of which were up-regulated in the newborn pigs exposed to intra-amniotic LPS.

To investigate the biological processes and pathways associated with the DEGs, we performed functional enrichment analyses using the web tool "DAVID" and found that the DEGs identified on day 1 were related to "innate immune response," "neutrophil chemotaxis," "complement and coagulation

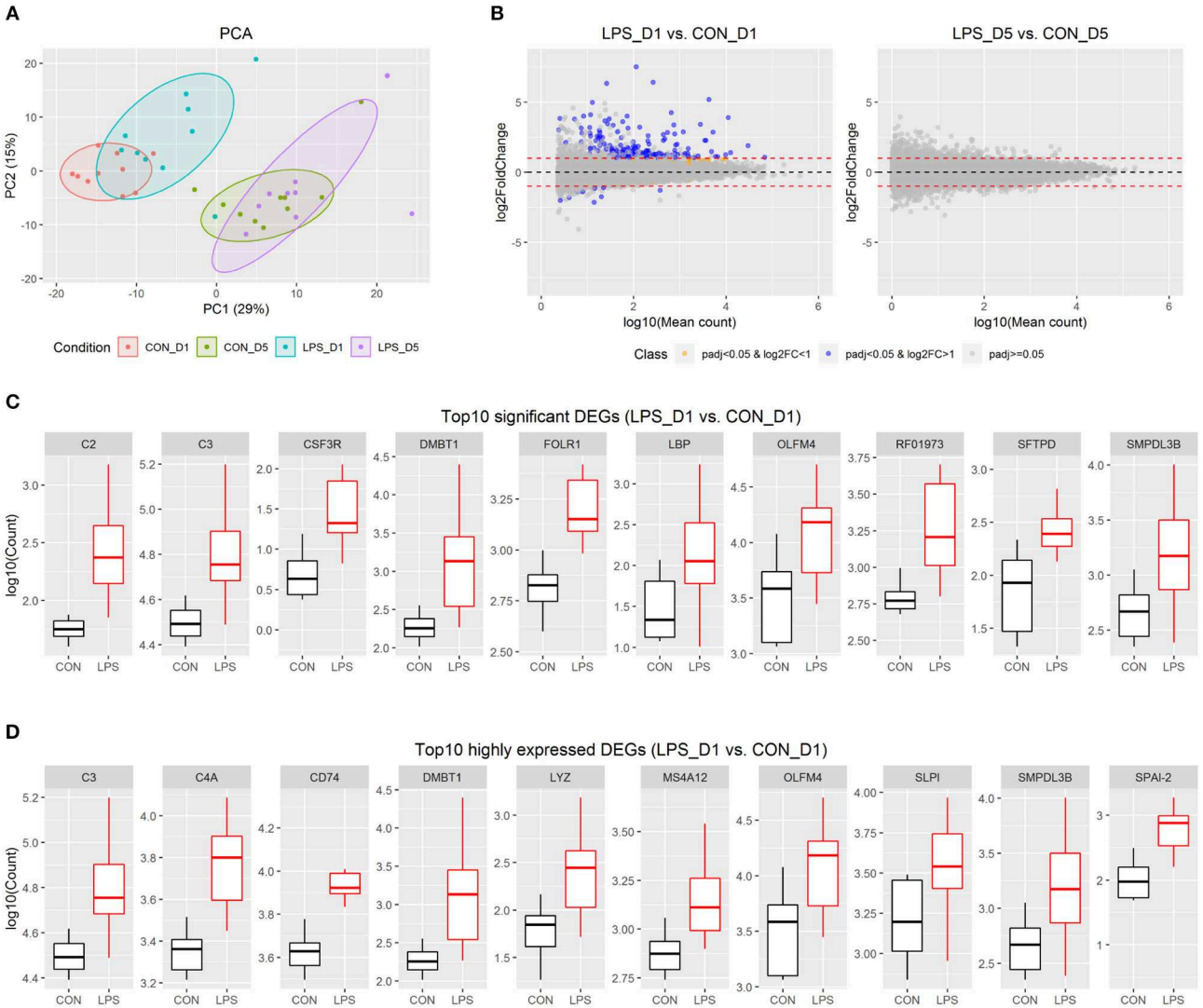

FIGURE 1 | Intestinal transcriptome profile in response to intra-amniotic LPS exposure. **(A)** Scores of the first two principle components from principal component analysis are plotted, with ellipses for the 80% confidence interval for each group. **(B)** MA plot showing fold change (LPS vs. CON) and mean of normalized counts for all the analyzed genes. **(C)** Boxplot of top 10 significant DEGs between LPS-D1 and CON-D1 groups. **(D)** Boxplot of top 10 highly expressed DEGs between LPS-D1 and CON-D1 groups.

cascades," "cell adhesion molecules (CAMs)," and "antigen processing and presentation" (**Table S4**). Thus, both innate and adaptive immune responses were involved in the neonatal intestine exposed to intra-amniotic LPS. Differentially expressed genes involved in the innate immunity were related to pattern recognition (*TLR2*, *CD14*, *LBP*, *DMBT1*, *SFTPD*), complement system (*C1QA*, *C1QB*, *C1QC*, *C1RL*, *C2*, *C3*, *C4A*, *C5*) and neutrophil chemotaxis (*C5AR1*, *CSF3R*, *CCL5*, *CCL17*, *CCL19*). For the adaptive immunity, five DEGs were enriched in the KEGG pathway "antigen processing and presentation," encoding for major histocompatibility complex (MHC) classes I and II, as well as CD4. Consistent with that the recruitment of $CD4^+$ T cells in the mice neonatal small intestine is based on β7 integrin–dependent pathways (30), *ITGB7* (integrin beta-7) was also found to be one of the DEGs and was up-regulated in the LPS group. However, the mRNA expression of co-stimulatory molecules for T-cell activation (i.e., CD80, CD86, CD28, and ICOS), as well as T-cell transcription factors (i.e., T-bet for T_H1, GATA3 for T_H2, RORγt for T_H17, and Foxp3 for Tregs cells), showed no significant difference between the LPS and CON groups.

In addition, pairwise correlation test between each DEG and the measures in the amniotic fluid or small intestine was performed. Consistent with that the DEGs identified on day 1 were enriched in innate immune response and neutrophil chemotaxis as mentioned previously, the correlation test showed that most of the DEGs correlated with the MPO-positive cell density in the small intestine (mean absolute Spearman $\rho = 0.54$; **Figure 3B**). The DEGs were also correlated with cytokine levels, especially TNF-α, in the amniotic fluid

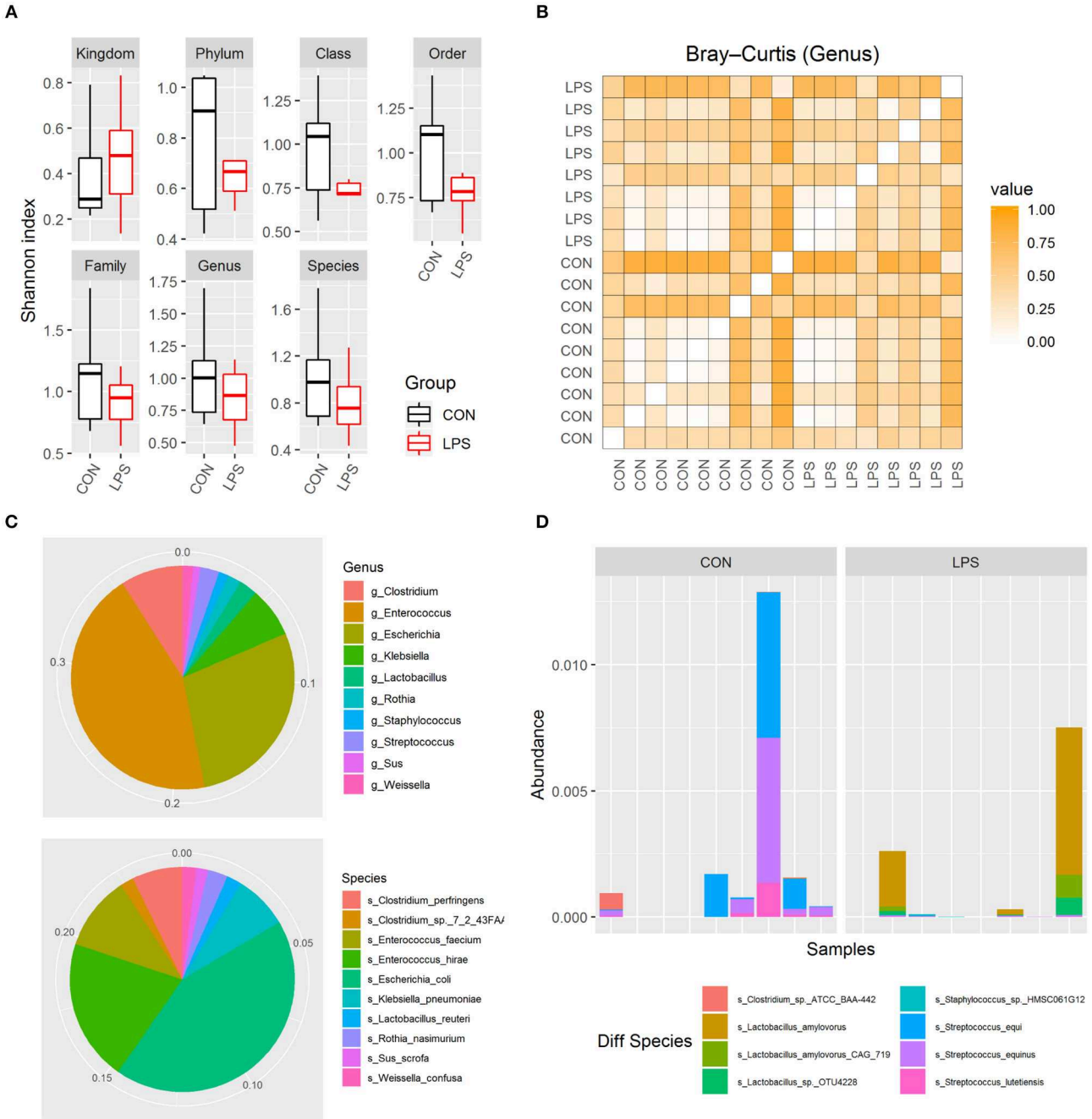

FIGURE 2 | Gut microbiome in LPS and CON groups on postnatal day 5. **(A)** Boxplot of Shannon index in two groups. **(B)** Heatmap derived from dissimilarity matrix of Bray–Curtis distances from all 5-day-old pigs. **(C)** Pie chart of top 10 abundant genus/species in all 5-day-old pigs. **(D)** Bar plot showing eight differential abundant species between the LPS and CON groups.

(mean absolute Spearman $\rho = 0.62$; **Figure 3B**). After multiple testing, 44 and 76 DEGs were significantly and positively correlated with the MPO-positive cell density in the small intestine and TNF-α level in amniotic fluid (adjusted $P < 0.05$, mean $\rho = 0.69$ and 0.71, respectively). Genes significantly correlated with both intestinal MPO-positive cell density and amniotic TNF-α (**Figure 3C**) included *DMBT1*, the hub gene in the putative co-expression network, and those involved in complement system (*C1QA*, *C3*, *C5*) and neutrophil chemotaxis (*C5AR1*, *CSF3R*, *CCL5*), suggesting an underlying mechanism whereby intra-amniotic inflammation affects intestinal immune response via fetal swallowing.

To examine whether the identified DEGs were altered also at the protein level, immunohistochemistry analysis was performed

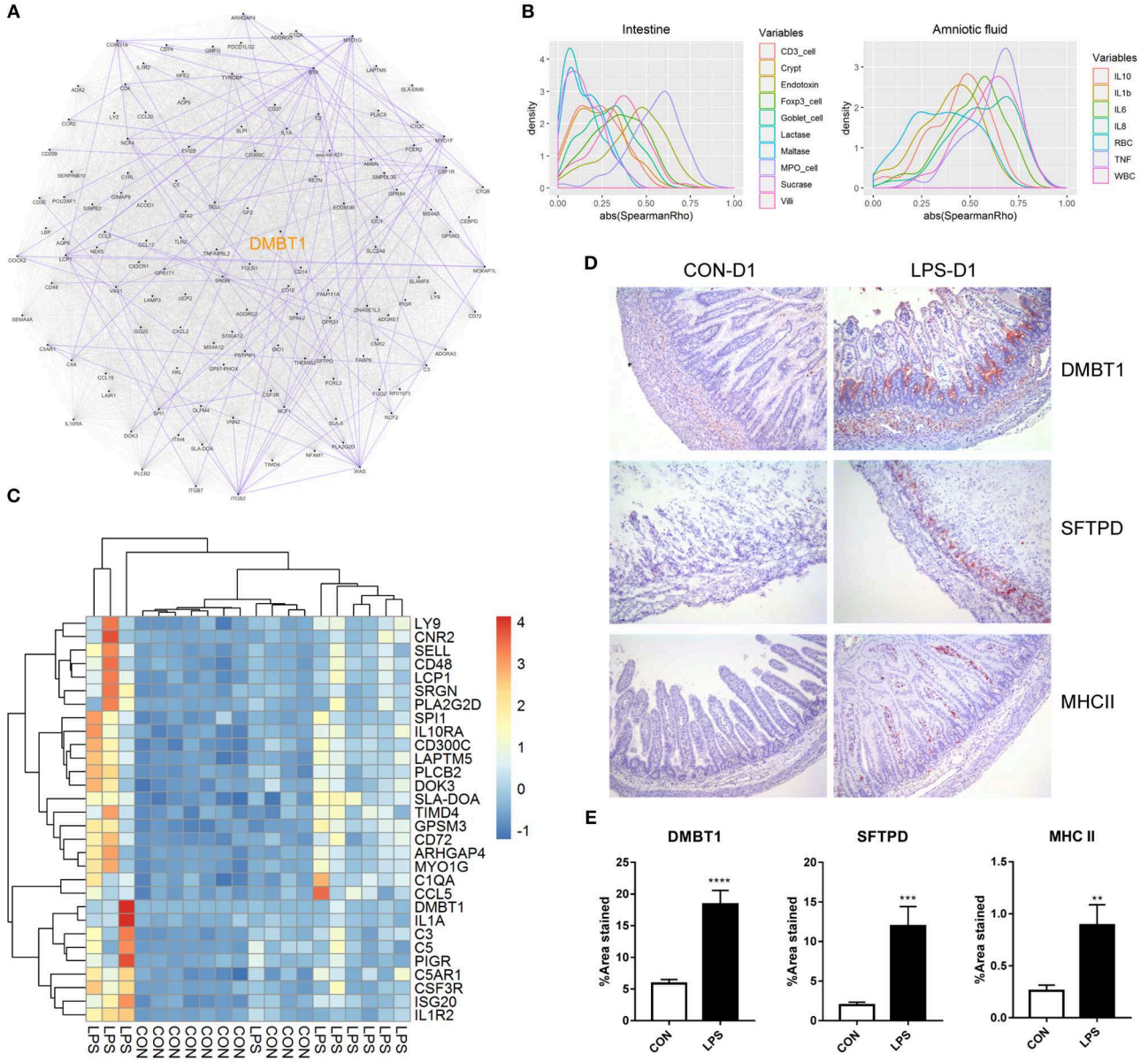

FIGURE 3 | Relationship and functionality of DEGs between LPS and CON groups at birth. **(A)** Putative co-expression network, where each node represents a gene, and each edge represents a significant correlation between gene pairs. Experimentally determined protein–protein interaction between gene pairs is highlighted in purple. Hub gene DMBT1 is highlighted in yellow. **(B)** Density plot of absolute Spearman ρ between DEGs and intestinal/amniotic measures. **(C)** Heatmap showing the relative expression of DEGs that were correlated with intestinal MPO-positive cell density and amniotic TNF-α level. **(D)** Representative images of distal small intestines stained with antibodies to DMBT1, SFTPD, and MHCII. **(E)** Significant difference of the area stained by DMBT1/SFTPD/MHCII between LPS and CON groups was revealed according to Mann–Whitney *U* test. Values are presented as the mean ± SEM, $^{*}P < 0.05$, $^{**}P < 0.01$, $^{***}P < 0.001$, $^{****}P < 0.0001$.

for selected proteins in the newborn pigs (D1 samples). This included DMBT1, the hub gene in the co-expression network, and SFTPD that might interact with DMBT1, both of which are related to innate immunity. In addition, MHCII, related to adaptive immunity, was examined. The results showed that DMBT1 and SFTPD were mainly expressed in the crypts of the distal small intestine and up-regulated in the LPS vs. CON group (mean positive area = 18.4 vs. 5.9% for DMBT1, and 12.0 vs. 2.0% for SFTPD, both $P < 0.05$). MHCII, on the other hand, was distributed within the villi of distal small intestine and also showed higher expression in the LPS vs. CON groups (mean positive area = 0.9 vs. 0.3%, $P < 0.05$; **Figures 3D,E**).

DISCUSSION

Perinatal development of the small intestine, including its immune system, occurs as the combined result of an intrinsic (genetic, endocrinological) program and environmental factors

including oral nutrition/fluid (e.g., amniotic fluid before birth, milk after birth) and exposure to microbiota (e.g., infected amniotic fluid before birth, bacterial colonization after birth). The maturational pattern is partly species- and birth-dependent, and we have previously shown that in pigs the small intestine has a remarkable capacity to mature over the first weeks following the initial deficits in response to preterm birth. We now show that prenatal exposure to inflammation *in utero* induces altered expression of both innate and adaptive immunity-associated genes in the neonatal small intestine, together with marked immune cell infiltration at birth. However, after introduction of enteral feeding and ongoing bacterial colonization, intestinal gene expression, and functions (NEC susceptibility, morphology, digestive enzymes, global gene expression) were similar on day 5 in control and LPS-exposed preterm pigs. In addition, prenatal inflammation had a minor effect on the gut colonization at this time after birth (e.g., the low-abundant *S. equi* and *L. amylovorus* species were reduced and increased, respectively, in LPS-exposed pigs on day 5). Collectively, our results confirm that the birth- and age-related development of intestinal microbiota and gene expressions are remarkably resilient to exposure of a few days of intra-amniotic inflammation before preterm birth. In a translational perspective, intestinal functions of preterm infants born after acute CA may therefore not be markedly compromised in the postnatal period, relative to infants born prematurely without prenatal inflammation. Future studies should address if this conclusion is true also for other periods, doses and types of prenatal inflammatory insults (e.g., using common CA-related pathogens such as *Ureaplasma*), as well as longer postnatal age and interacting factors (e.g., feeding modes, antibiotics, infections).

In the present study, we identified a number of genes that might be co-expressed and up-regulated in the neonatal small intestine exposed to fetal inflammation. The hub gene of this putative co-expression network was *DMBT1*, which is a pattern recognition receptor localized to epithelial cells and binds to a broad range of pathogens (31, 32). Our results show that the intestinal *DMBT1* was up-regulated by prenatal LPS exposure, both at mRNA and protein levels. *DMBT1* in the intestinal epithelial cells (IECs) plays an important role in first-line defense by preventing bacterial invasion into the IECs and inhibiting cytokine secretion (33). Loss of *DMBT1* in mice leads to enhanced dextran sulfate sodium–induced colitis (34). Thus, up-regulation of *DMBT1* in the neonatal intestine in response to CA might play a role in intestinal mucosal protection. In addition to immune cell infiltration, villus structure was moderately compromised around birth following prenatal LPS exposure. Like all the other measures in the small intestine, such effects induced by prenatal LPS exposure disappeared after 5 days. This could be related to *DMBT1*, which negatively affects epithelial cell growth (35) and is associated with a change from proliferation to differentiation in the epithelium and thereby epithelial regeneration following mucosal damage (36).

DMBT1 also binds to mucosal defense proteins, such as SP-D (37). Surfactant protein D exerts antimicrobial effects by bacterial agglutination, enhancing their clearance by phagocytic cells (38). Similar to DMBT1, lack of SP-D in mice also showed increased susceptibility to dextran sulfate sodium–induced colitis (39). Moreover, both DMBT1 and SP-D have been shown to stimulate alveolar macrophage migration (40, 41), suggesting a role of DMBT1 and SP-D in mediating the cross-talk between epithelial cells and the underlying immune cells. Such cross-talk may also exist in the gastrointestinal tract, and MPO-positive cells were increased in density in parallel with the up-regulation of DMBT1 and SP-D, following intra-amniotic endotoxin exposure. Functional enrichment analysis using all the DEGs also revealed pathways related to CAMs and chemokine signaling pathway, which might be relevant to the macrophage migration.

Apart from innate immunity, adaptive immunity may be also involved in the neonatal small intestine in response to CA. We found that genes in the "antigen processing and presentation" pathway were up-regulated, including those that encode for MHC class II and CD4. The MHC molecules are normally expressed on antigen-presenting cells (APCs) such as macrophages, but they are also found in the upper villus under normal physiologic conditions and in the crypts in case of disease (42). By immunohistochemistry analysis, we found that intra-amniotic endotoxin up-regulated MHCII expression that was mainly distributed inside the villi, which suggests CA effects on classic APCs. Our transcriptome data showed that *CD4* was also up-regulated in the LPS-exposed neonatal intestine. However, given the absence of up-regulation of co-stimulatory molecules and T-cell transcription factors in our transcriptome data, it remains unclear if CA activates CD4 T cell in the neonatal intestine. In the lung, T-cell activation could be inhibited by SP-D (43). It remains to be investigated whether this mechanism also exists in the gastrointestinal tract. Nevertheless, in both human and mice intestines, $CD4^+$ T cells are generally naive in the neonatal period (30, 44), and their response to prenatal endotoxin exposure requires further investigation.

There are limitations related to our experimental conditions used to reflect human CA. Thus, our inflammatory insults were induced by a few days of intra-amniotic LPS rather than by giving one or more CA-associated pathogens at various times and doses. Hence, our experimental conditions may not accurately reflect all human CA conditions. It has been shown that the organisms commonly identified in CA include *Ureaplasma urealyticum*, group B *Streptococcus*, and *E. coli*, but it remains unclear whether these are causative agents or only bystanders to the inflammatory effects (45). Thus, in this study, we decided to use intra-amniotic LPS to induce a highly controlled, relatively short-term inflammation of the fetal membranes and evaluated its effects on the neonatal gut independent of source of pathogens. Our result showed increased intestinal MPO, *CD4*, and *TLRs* in response to such prenatal inflammation, which are similar to those that resulted from *Ureaplasma* infection in sheep model (10), suggesting common underlying mechanisms. On the other hand, such intra-amniotic LPS model limits our analysis and interpretation of gut microbiome. During healthy pregnancy, the fetal environment is sterile, and neonatal gut colonization starts in the hours postpartum, whereas for CA neonates, the gut microbial colonization may have started already before birth through ingestion of infected amniotic fluid (46). Thus, CA

neonates may harbor a different initial gut microbiome than healthy infants. We studied here the responses to prenatal inflammation, independently of such pathogen exposure and hence assessed only the postnatal environmentally derived colonization. We show that this colonization is not notably affected by prenatal inflammation. It remains to be investigated how and for how long the gut microbiota may be affected in human preterm infants exposed to pathogens before birth via swallowing amniotic fluid. Another limitation is that in our control group not all the fetuses received saline injection to avoid unnecessary prolonged surgery. However, the pigs with and without saline injection were combined into a joint control group as there was no difference in any amniotic fluid or intestinal phenotypes (parameters listed in **Tables S1**, **S2**) between them. We cannot completely exclude a small effect of the intra-amniotic saline injection, although such minimal manipulation of the uterus and fetus is unlikely to affect the overall pronounced effects of LPS on gut gene expression on D1.

In summary, we characterized the intestinal gene expression and microbiome in a preterm pig model of CA. We found that intra-amniotic LPS exposure affected the expression of intestinal genes in preterm pigs at birth, especially genes related to immune cell infiltration. Following enteral feeding and bacterial colonization, intra-amniotic LPS had limited effects on intestinal structure and function. A short period of intra-amniotic inflammation prior to preterm birth is unlikely to cause longer-lasting pro-inflammatory responses in the gut of preterm infants. This does not exclude, however, that CA with a longer duration of inflammation before birth, and with more aggressive types and doses of pathogens, could have long-term detrimental effects on the developing intestine in preterm infants.

DATA AVAILABILITY STATEMENT

The datasets generated for this study can be found in the Gene Expression Omnibus, accession number GSE139366, and EBI Metagenomics, accession number PRJEB34982.

ETHICS STATEMENT

The animal study was reviewed and approved by Danish National Committee of Animal Experimentation.

AUTHOR CONTRIBUTIONS

XP and DZ analyzed and interpreted the transcriptome and metagenome data. XP was the major contributor in writing the manuscript. WW and XY performed the transcriptome library construction. PS, FG, and DN took part in the main study design and critically reviewed the manuscript. All authors read and approved the final manuscript.

FUNDING

This work was supported by the Center of Arla Foods for Health STIMMUNE project (PS and DN), the Innovation Foundation Denmark NEOCOL project (PS), and the Agricultural Science and Technology Innovation Program (ASTIP) of China (FG). The funders were not involved in the study design, collection, analysis, interpretation of data, the writing of this article or the decision to submit it for publication.

ACKNOWLEDGMENTS

We thank Thomas Thymann, Jane Poulsen, Elin Skytte, Kristina Møller, Katrine V. Kristiansen, Manja Hanegård and Elisabeth Wairimu Petersen (University of Copenhagen), Karin Tarp (Technical University of Denmark), and Nico Kloosterboer (Maastricht University) for their support to animal procedures and laboratory analyses.

SUPPLEMENTARY MATERIAL

The Supplementary Material for this article can be found online at: https://www.frontiersin.org/articles/10.3389/fimmu.2020.00420/full#supplementary-material

REFERENCES

1. McGhee JR, Fujihashi K. Inside the mucosal immune system. *PLoS Biol.* (2012) 10:e1001397. doi: 10.1371/journal.pbio.1001397
2. Trahair JF, Sangild PT. Fetal organ growth in response to oesophageal infusion of amniotic fluid, colostrum, milk or gastrin-releasing peptide: a study in fetal sheep. *Reprod Fertil Dev.* (2000) 12:87–95. doi: 10.1071/RD00024
3. Torow N, Marsland BJ, Hornef MW, Gollwitzer ES. Neonatal mucosal immunology. *Mucosal Immunol.* (2017) 10:5–17. doi: 10.1038/mi.2016.81
4. Neu J, Pammi M. Pathogenesis of NEC: impact of an altered intestinal microbiome. *Semin Perinatol.* (2017) 41:29–35. doi: 10.1053/j.semperi.2016.09.015
5. Shulhan J, Dicken B, Hartling L, Larsen BM. Current knowledge of necrotizing enterocolitis in preterm infants and the impact of different types of enteral nutrition products. *Adv Nutr.* (2017) 8:80–91. doi: 10.3945/an.116.013193
6. Hansen ML, Jensen IV, Gregersen R, Juhl SM, Greisen G. Behavioural and neurodevelopmental impairment at school age following necrotising enterocolitis in the newborn period. *PLoS ONE.* (2019) 14:e0215220. doi: 10.1371/journal.pone.0215220
7. Galinsky R, Polglase GR, Hooper SB, Black MJ, Moss TJ. The consequences of chorioamnionitis: preterm birth and effects on development. *J Pregnancy.* (2013) 2013:412831. doi: 10.1155/2013/412831
8. Wolfs TG, Kramer BW, Thuijls G, Kemp MW, Saito M, Willems MG, et al. Chorioamnionitis-induced fetal gut injury is mediated by direct gut exposure of inflammatory mediators or by lung inflammation. *Am J Physiol Gastrointest Liver Physiol.* (2014) 306:G382–93. doi: 10.1152/ajpgi.00260.2013
9. Wolfs TG, Buurman WA, Zoer B, Moonen RM, Derikx JP, Thuijls G, et al. Endotoxin induced chorioamnionitis prevents intestinal development during gestation in fetal sheep. *PLoS ONE.* (2009) 4:e5837. doi: 10.1371/journal.pone.0005837
10. Wolfs TG, Kallapur SG, Knox CL, Thuijls G, Nitsos I, Polglase GR, et al. Antenatal ureaplasma infection impairs development of the fetal ovine gut in an IL-1-dependent manner. *Mucosal Immunol.* (2013) 6:547–56. doi: 10.1038/mi.2012.97

11. Nikiforou M, Jacobs EM, Kemp MW, Hornef MW, Payne MS, Saito M, et al. Intra-amniotic *Candida albicans* infection induces mucosal injury and inflammation in the ovine fetal intestine. *Sci Rep.* (2016) 6:29806. doi: 10.1038/srep29806
12. Nadeau-Vallee M, Chin PY, Belarbi L, Brien ME, Pundir S, Berryer MH, et al. Antenatal suppression of IL-1 protects against inflammation-induced fetal injury and improves neonatal and developmental outcomes in mice. *J Immunol.* (2017) 198:2047–62. doi: 10.4049/jimmunol.1601600
13. Fricke EM, Elgin TG, Gong H, Reese J, Gibson-Corley KN, Weiss RM, et al. Lipopolysaccharide-induced maternal inflammation induces direct placental injury without alteration in placental blood flow and induces a secondary fetal intestinal injury that persists into adulthood. *Am J Reprod Immunol.* (2018) 79:e12816. doi: 10.1111/aji.12816
14. Sangild PT, Thymann T, Schmidt M, Stoll B, Burrin DG, Buddington RK. Invited review: the preterm pig as a model in pediatric gastroenterology. *J Anim Sci.* (2013) 91:4713–29. doi: 10.2527/jas.2013-6359
15. Andersen AD, Sangild PT, Munch SL, van der Beek EM, Renes IB, Ginneken C, et al. Delayed growth, motor function and learning in preterm pigs during early postnatal life. *Am J Physiol Regul Integr Comp Physiol.* (2016) 310:R481–92. doi: 10.1152/ajpregu.00349.2015
16. Nguyen DN, Thymann T, Goericke-Pesch SK, Ren S, Wei W, Skovgaard K, et al. Prenatal intra-amniotic endotoxin induces fetal gut and lung immune responses and postnatal systemic inflammation in preterm pigs. *Am J Pathol.* (2018) 188:2629–43. doi: 10.1016/j.ajpath.2018.07.020
17. Trapnell C, Pachter L, Salzberg SL. TopHat: discovering splice junctions with RNA-Seq. *Bioinformatics.* (2009) 25:1105–11. doi: 10.1093/bioinformatics/btp120
18. Anders S, Pyl PT, Huber W. HTSeq–a python framework to work with high-throughput sequencing data. *Bioinformatics.* (2015) 31:166–9. doi: 10.1093/bioinformatics/btu638
19. Love MI, Huber W, Anders S. Moderated estimation of fold change and dispersion for RNA-seq data with DESeq2. *Genome Biol.* (2014) 15:550. doi: 10.1186/s13059-014-0550-8
20. Li D, Liu CM, Luo R, Sadakane K, Lam TW. MEGAHIT: an ultra-fast single-node solution for large and complex metagenomics assembly via succinct de Bruijn graph. *Bioinformatics.* (2015) 31:1674–6. doi: 10.1093/bioinformatics/btv033
21. Zhu W, Lomsadze A, Borodovsky M. Ab initio gene identification in metagenomic sequences. *Nucleic Acids Res.* (2010) 38:e132. doi: 10.1093/nar/gkq275
22. Li W, Godzik A. Cd-hit: a fast program for clustering and comparing large sets of protein or nucleotide sequences. *Bioinformatics.* (2006) 22:1658–9. doi: 10.1093/bioinformatics/btl158
23. Buchfink B, Xie C, Huson DH. Fast and sensitive protein alignment using DIAMOND. *Nat Methods.* (2015) 12:59–60. doi: 10.1038/nmeth.3176
24. Xiao L, Estelle J, Kiilerich P, Ramayo-Caldas Y, Xia Z, Feng Q, et al. A reference gene catalogue of the pig gut microbiome. *Nat Microbiol.* (2016) 1:16161. doi: 10.1038/nmicrobiol.2016.161
25. Moriya Y, Itoh M, Okuda S, Yoshizawa AC, Kanehisa M. KAAS: an automatic genome annotation and pathway reconstruction server. *Nucleic Acids Res.* (2007) 35:W182–5. doi: 10.1093/nar/gkm321
26. Huang da W, Sherman BT, Lempicki RA. Systematic and integrative analysis of large gene lists using DAVID bioinformatics resources. *Nat Protoc.* (2009) 4:44–57. doi: 10.1038/nprot.2008.211
27. White JR, Nagarajan N, Pop M. Statistical methods for detecting differentially abundant features in clinical metagenomic samples. *PLoS Comput Biol.* (2009) 5:e1000352. doi: 10.1371/journal.pcbi.1000352
28. Mai V, Young CM, Ukhanova M, Wang X, Sun Y, Casella G, et al. Fecal microbiota in premature infants prior to necrotizing enterocolitis. *PLoS ONE.* (2011) 6:e20647. doi: 10.1371/journal.pone.0020647
29. Morrow AL, Lagomarcino AJ, Schibler KR, Taft DH, Yu Z, Wang B, et al. Early microbial and metabolomic signatures predict later onset of necrotizing enterocolitis in preterm infants. *Microbiome.* (2013) 1:13. doi: 10.1186/2049-2618-1-13
30. Torow N, Yu K, Hassani K, Freitag J, Schulz O, Basic M, et al. Active suppression of intestinal CD4(+)TCRalphabeta(+) T-lymphocyte maturation during the postnatal period. *Nat Commun.* (2015) 6:7725. doi: 10.1038/ncomms8725
31. Mollenhauer J, Herbertz S, Holmskov U, Tolnay M, Krebs I, Merlo A, et al. DMBT1 encodes a protein involved in the immune defense and in epithelial differentiation and is highly unstable in cancer. *Cancer Res.* (2000) 60:1704–10.
32. Ligtenberg AJ, Karlsson NG, Veerman EC. Deleted in malignant brain tumors-1 protein (DMBT1): a pattern recognition receptor with multiple binding sites. *Int J Mol Sci.* (2010) 11:5212–33. doi: 10.3390/ijms11 12521
33. Rosenstiel P, Sina C, End C, Renner M, Lyer S, Till A, et al. Regulation of DMBT1 via NOD2 and TLR4 in intestinal epithelial cells modulates bacterial recognition and invasion. *J Immunol.* (2007) 178:8203–11. doi: 10.4049/jimmunol.178.12.8203
34. Renner M, Bergmann G, Krebs I, End C, Lyer S, Hilberg F, et al. DMBT1 confers mucosal protection *in vivo* and a deletion variant is associated with Crohn's disease. *Gastroenterology.* (2007) 133:1499–509. doi: 10.1053/j.gastro.2007.08.007
35. Lu X, Xu Y, Zhao Y, Tao Q, Wu J. Silenced DMBT1 promotes nasal mucosa epithelial cell growth. *Ann Hum Genet.* (2018) 82:102–8. doi: 10.1111/ahg.12230
36. Kang W, Reid KB. DMBT1, a regulator of mucosal homeostasis through the linking of mucosal defense and regeneration?. *FEBS Lett.* (2003) 540:21–5. doi: 10.1016/S0014-5793(03)00217-5
37. Madsen J, Mollenhauer J, Holmskov U. Review: Gp-340/DMBT1 in mucosal innate immunity. *Innate Immun.* (2010) 16:160–7. doi: 10.1177/1753425910368447
38. Nayak A, Dodagatta-Marri E, Tsolaki AG, Kishore U. An insight into the diverse roles of surfactant proteins, SP-A and SP-D in innate and adaptive immunity. *Front Immunol.* (2012) 3:131. doi: 10.3389/fimmu.2012.00131
39. Sarashina-Kida H, Negishi H, Nishio J, Suda W, Nakajima Y, Yasui-Kato M, et al. Gallbladder-derived surfactant protein D regulates gut commensal bacteria for maintaining intestinal homeostasis. *Proc Natl Acad Sci USA.* (2017) 114:10178–83. doi: 10.1073/pnas.1712837114
40. Tino MJ, Wright JR. Glycoprotein-340 binds surfactant protein-A (SP-A) and stimulates alveolar macrophage migration in an SP-A-independent manner. *Am J Respir Cell Mol Biol.* (1999) 20:759–68. doi: 10.1165/ajrcmb.20.4.3439
41. Tino MJ, Wright JR. Surfactant proteins A and D specifically stimulate directed actin-based responses in alveolar macrophages. *Am J Physiol.* (1999) 276:L164–74. doi: 10.1152/ajplung.1999.276.1.L164
42. Wosen JE, Mukhopadhyay D, Macaubas C, Mellins ED. Epithelial MHC class II expression and its role in antigen presentation in the gastrointestinal and respiratory tracts. *Front Immunol.* (2018) 9:2144. doi: 10.3389/fimmu.2018.02144
43. Borron PJ, Crouch EC, Lewis JF, Wright JR, Possmayer F, Fraher LJ. Recombinant rat surfactant-associated protein D inhibits human T lymphocyte proliferation and IL-2 production. *J Immunol.* (1998) 161:45 99–603.
44. Thome JJ, Bickham KL, Ohmura Y, Kubota M, Matsuoka N, Gordon C, et al. Early-life compartmentalization of human T cell differentiation and regulatory function in mucosal and lymphoid tissues. *Nat Med.* (2016) 22:72–7. doi: 10.1038/nm.4008
45. Ericson JE, Laughon MM. Chorioamnionitis: implications for the neonate. *Clin Perinatol.* (2015) 42:155–65, ix. doi: 10.1016/j.clp.2014.10.011
46. Perez-Munoz ME, Arrieta MC, Ramer-Tait AE, Walter J. A critical assessment of the "sterile womb" and "in utero colonization" hypotheses: implications for research on the pioneer infant microbiome. *Microbiome.* (2017) 5:48. doi: 10.1186/s40168-017-0268-4

Conflict of Interest: The authors declare that the research was conducted in the absence of any commercial or financial relationships that could be construed as a potential conflict of interest

frontiers in Immunology

REVIEW
published: 03 April 2020
doi: 10.3389/fimmu.2020.00587

The Paneth Cell: The Curator and Defender of the Immature Small Intestine

Shiloh R. Lueschow[1†] *and Steven J. McElroy*[1,2*†]

[1] Department of Microbiology and Immunology, University of Iowa, Iowa City, IA, United States, [2] Stead Family Department of Pediatrics, University of Iowa, Iowa City, IA, United States

Paneth cells were first described in the late 19th century by Gustav Schwalbe and Josef Paneth as columnar epithelial cells possessing prominent eosinophilic granules in their cytoplasm. Decades later there is continued interest in Paneth cells as they play an integral role in maintaining intestinal homeostasis and modulating the physiology of the small intestine and its associated microbial flora. Paneth cells are highly specialized secretory epithelial cells located in the small intestinal crypts of Lieberkühn. The dense granules produced by Paneth cells contain an abundance of antimicrobial peptides and immunomodulating proteins that function to regulate the composition of the intestinal flora. This in turn plays a significant role in secondary regulation of the host microvasculature, the normal injury and repair mechanisms of the intestinal epithelial layer, and the levels of intestinal inflammation. These critical functions may have even more importance in the immature intestine of premature infants. While Paneth cells begin to develop in the middle of human gestation, they do not become immune competent or reach their adult density until closer to term gestation. This leaves preterm infants deficient in normal Paneth cell biology during the greatest window of susceptibility to develop intestinal pathology such as necrotizing enterocolitis (NEC). As 10% of infants worldwide are currently born prematurely, there is a significant population of infants contending with an inadequate cohort of Paneth cells. Infants who have developed NEC have decreased Paneth cell numbers compared to age-matched controls, and ablation of murine Paneth cells results in a NEC-like phenotype suggesting again that Paneth cell function is critical to homeostasis to the immature intestine. This review will provide an up to date and comprehensive look at Paneth cell ontogeny, the impact Paneth cells have on the host-microbial axis in the immature intestine, and the repercussions of Paneth cell dysfunction or loss on injury and repair mechanisms in the immature gut.

Keywords: paneth cell, necrotizing enterocolitis, immature intestine, defensins, cathelicidin (LL37), cell death

OPEN ACCESS

Edited by:
Tobias Strunk,
King Edward Memorial Hospital, Australia

Reviewed by:
Claudio Nicoletti,
University of Florence, Italy
Luisa Cervantes-Barragan,
Emory University, United States

***Correspondence:**
Steven J. McElroy
steven-mcelroy@uiowa.edu

†ORCID:
Shiloh R. Lueschow
orcid.org/0000-0001-6185-7612
Steven J. McElroy
orcid.org/0000-0002-4321-723X

Specialty section:
This article was submitted to Mucosal Immunity, a section of the journal Frontiers in Immunology

Received: *17 December 2019*
Accepted: *13 March 2020*
Published: *03 April 2020*

Citation:
Lueschow SR and McElroy SJ (2020) The Paneth Cell: The Curator and Defender of the Immature Small Intestine. Front. Immunol. 11:587. doi: 10.3389/fimmu.2020.00587

INTRODUCTION

In the small intestine, intestinal epithelial cells form an important physical and biochemical barrier that prevents the microbial communities contained within the lumen from accessing the rest of the body and causing infection (1). One particular type of intestinal epithelial cell, the Paneth cell, was first discovered by Gustav Schwalbe in the late 19th century based on the eosinophilic

granules evident in their cytoplasm. A few years later, Paneth cells were described in depth by their namesake, Joseph Paneth (2, 3). They are now well-recognized as pyramidal shaped, columnar, secretory cells situated at the base of the crypts of Lieberkühn, which are small depressions in the mucosal surface along the small intestine (4). While Paneth cells have occasionally also been found patchily dispersed in the stomach and colon, this is generally associated with mucosal inflammation as opposed to homeostasis (4).

Although Paneth cells were first discovered and described in humans, they are not specific to humans. Paneth cells can be found in many other vertebrates including primates, rodents, horses, sheep, certain fish, and chickens (5, 6). While Paneth cells have been found in this wide variety of other organisms aside from humans, the ontogeny and function are not well-understood for most of them aside from the well-studied and characterized rodents as well as humans. Today, Paneth cells still capture the attention of researchers as they serve an essential role in modulating the microbiome, playing a key part of the innate immune response, and aiding in the proliferation and differentiation of the intestinal epithelium. While Paneth cells have been shown to play important roles in the healthy gut of adults, the development and role of Paneth cells in the immature gut of the preterm infant remains an understudied, but crucial avenue of research that could aid in the understanding of the development of intestinal diseases such as necrotizing enterocolitis (NEC). This review sets out to unveil some of the mystery surrounding Paneth cells in the context of the preterm infant gut and how it relates to NEC.

THE ANATOMY OF THE PANETH CELL

The human gastrointestinal surface is the largest surface area of the body that is in contact with the external environment (7, 8). This massive surface area is required to allow sufficient nutrient absorption to support growth and health of the host. The small intestine, where Paneth cells reside, has an estimated surface area of 950 cm^2 at birth, which grows and expands to over 30 m^2 by adulthood (7, 8). To achieve such a massive surface area, the intestinal surface is clad by fingerlike projections that stick out into the intestinal lumen creating an expansive folding system. This systems' entire surface is covered by a single layer of columnar intestinal epithelial cells (IECs). The intestinal epithelium is the most rapidly-renewing tissue in the adult mammal (9) and undergoes continuous turnover that is generated from Intestinal Stem cells (ISC). The ISC reside at or near the base of the pocket-like intestinal crypts (10, 11) and continuously generate daughter cells that differentiate near the top of the crypts before migrating toward their final destinations. The differentiated cell types are generally grouped by their function as belonging to either the absorptive (enterocytes), or secretory (mucus-secreting goblet, antimicrobial-secreting Paneth, hormone-secreting enteroendocrine cells, and chemosensing/immunomodulatory cytokine-secreting tuft cells) lineage, with clear markers (e.g., *hes1* expression of absorptive and *sox9* for secretory) defining commitment to one or the other arm (12). The typical pattern for these cells is to migrate upwards toward the villus tip in a conveyor-belt-type fashion until they are sloughed off the upper villus into the lumen. However, a unique aspect of Paneth cell biology compared to the other intestinal epithelial cell types is that instead of flowing upward out of the crypt, Paneth cells move downwards further into the crypt as they mature. In addition, while most epithelial cells are rapidly turned over in a few days, Paneth cells can persist for just under 1 month (13). Paneth cell presence is an intestinal priority and their density is rapidly repopulated following their depletion (14). Following their descent into the crypts, Paneth cells are interspersed between the ISCs and can be distinguished by their columnar to pyramidal shape and by the presence of eosinophilic granules within their cytoplasm (**Figure 1**).

PANETH CELL ONTOGENY AND DIFFERENTIATION

Paneth cells first appear in the small intestine of humans at 13.5 weeks gestational age (15, 16). Paneth cell density in the developing fetal intestine is relatively low, but gradually increases throughout gestation, with significant increases in the third trimester after 29 weeks completed gestation (17, 18). Paneth cell levels do not reach quantities similar to adult levels until term gestation or later (17). Because Paneth cells are located primarily in the distal small intestine, studies using human tissues have been challenging. Thus, much of our understanding of *in vivo* Paneth cell biology has been generated using animal models, predominantly in mice. It is therefore important to note that not all mammals develop Paneth cells prenatally, but instead develop them mid-way through intestinal development after villus development, but before intestinal maturity according to a normal developmental pattern. For example, the commonly used C57Bl/6 mouse strain does not develop Paneth cells until 7–10 days after birth (18, 19).

Paneth cells, like all other intestinal epithelial cell types, are derived from ISCs. In the last decade, it has become clear that ISCs are quite complex. Current models suggest multiple, potentially interconvertible populations of stem cells exist. The first is the crypt-base columnar (CBC) cells (20), slender cells wedged at the very base of the crypt between the Paneth cells. CBC cells carry the specific marker *LGR5* and are actively proliferating (21, 22). The second ISC population express *Bmi1, mTert,* and *Lrig1* markers, and have been hypothesized to be quiescent stem cells until injury occurs, at which time they actively proliferate and produce daughter progeny (23). Interconversion between the two compartments and overlap between the populations has been demonstrated (24). Under normal conditions, the $LGR5^+$ ISCs proliferate to generate daughter cells that move out of the crypt. These cells become differentiated as they migrate, and both their differentiation and the maintenance of the stem cells in their proper place is driven through gradients and juxtracrine signaling of Bmp, Wnt, Notch, and growth factor pathways (25, 26). Furthermore, while the exact sources of ligands for these pathways are not fully

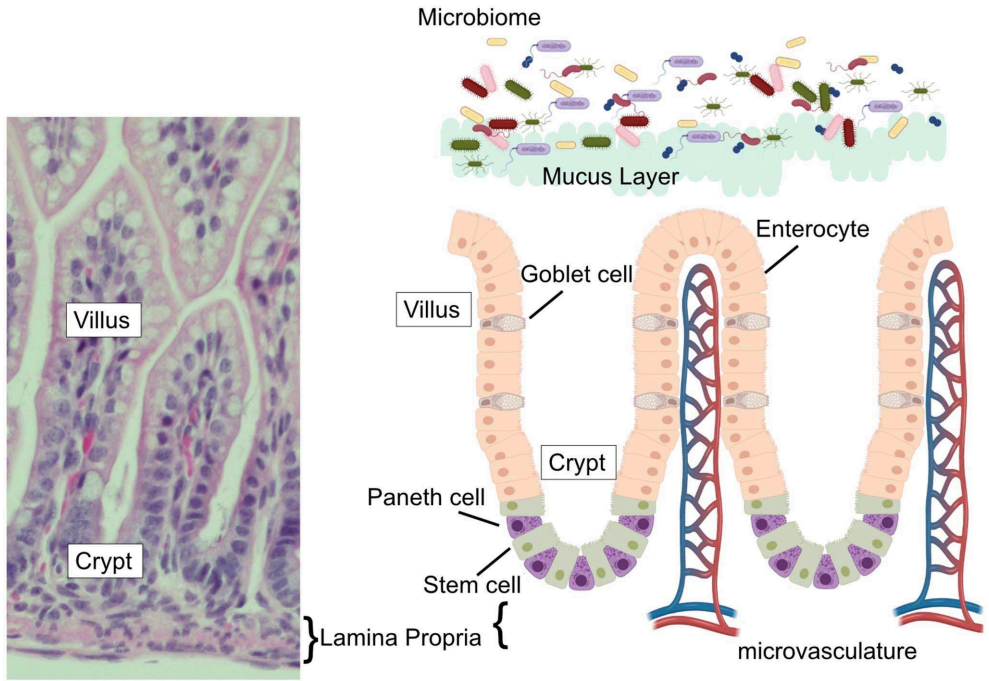

FIGURE 1 | The intestinal epithelium. (Left) H&E stained ileum from P14 C57Bl6 mouse with vilus, crypt, and lamina propria labeled. (Right) Schematic of the intestinal epithelium, associated microbial flora, epithelial cell types (goblet cells, Paneth cells, enterocytes, and stem cells) intestinal microvasculature, and mucus layer. Corresponding labels for vilus, crypt, and lamina propria labeled are placed on the schematic to compare to the H&E stained section.

understood, it is important to note that Paneth cells produce EGF, Notch, and Wnt, which in turn promote stem cell proliferation and maintenance (27). In fact, Paneth cells can support LGR5^{+} cell growth and survival *in vitro*, and have been proposed as a key nurse cell for the actively dividing stem population (27).

Several biochemical pathways have been implicated in the development of Paneth cells (**Figure 2**). Naïve daughter cells are driven to either an absorptive enterocyte phenotype by Notch signaling, or to a secretory phenotype through Wnt signal pathways. The Wnt/β-catenin pathway is an important stimulator of Paneth cell differentiation (28, 29). However, the Wnt signal pathway and its relationship to Paneth cell development is complex and still not completely elucidated. Genetic knockout of LGR-5, a downstream target of Wnt signaling has been shown to produce precocious Paneth cell differentiation in fetal intestine (29, 30). This contradictory data may be due to alterations in negative feedback mediators in the Wnt pathway. Following differentiation into a secretory lineage, activation of the transcription factors Atoh1 (also known as Math1) induces differentiation into a combined goblet/Paneth cell precursor cell lineage (31–35), while genetic ablation of Atoh1 in transgenic mice has been shown to result in loss of Paneth cell lineages (35, 36). Atoh1 has also been shown to be affected by ErbB3, a Receptor Tyrosine Kinase also known as neuregulin (37). Genetic loss of ErbB3 in mice results in unchecked activity of the transcription factor Atoh1 and induces precocious appearance of Paneth cells (37). In addition, activation of ErbB3 can delay normal Paneth cell development. C57Bl/6 mice normally develop Paneth cells by day 10 of life (19). It is however important to note that modifications to Atoh1 signal pathways also affect goblet cell differentiation (36), so understanding of signal pathways that distinguish goblet cell from Paneth cell differentiation downstream of Atoh1 is still incomplete.

PANETH CELL ROLE IN THE SMALL INTESTINE

After their migration to the crypt base and subsequent maturation, Paneth cells can be easily distinguished by their prominent acidophilic granules. The granules hold many of the proteins and peptides that Paneth cells secrete to both modulate the microbiome and mediate the inflammatory response. These include: α-defensins (cryptdins in mice), lysozyme, secretory phospholipase A2 (sPLa2), TNF, RegIII, angiogenin-4, MMP-7, CD15, CD95 ligand, xanthine oxidase, IgA, CRIP, metallothionine, adipokines, serum amyloid A, α-1-antitrypsin IL-17A, IL-1β and lipokines (3, 38, 39). These granular components are assembled and packaged by an extensive endoplasmic reticulum (ER) and Golgi apparatus network into dense core granules. (13, 39–43) It is important to note that it is possible that some components of the granules may be produced elsewhere before being collected and added to the granules. IgA is one such component which may be produced by plasma cells in the lamina propria before

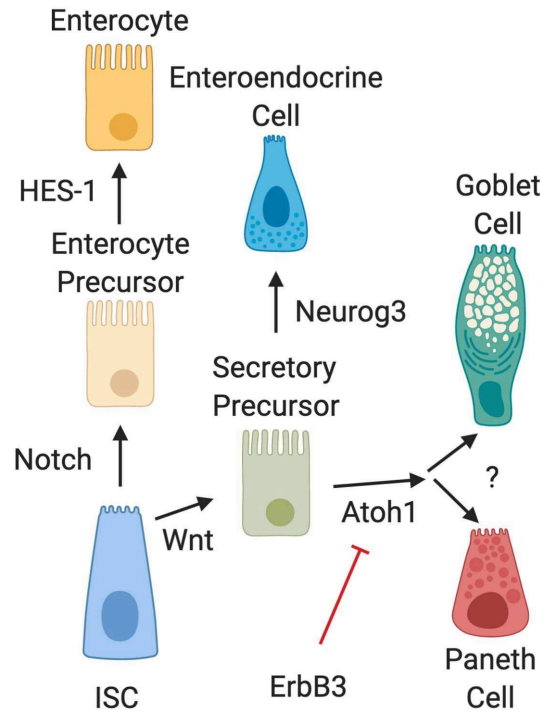

FIGURE 2 | Intestinal epithelial cell differentiation pathways. The intestinal stem cell (ISC) differentiates into absorptive (enterocyte) or secretory precursors through Wnt/Notch signaling. While enterocytes further differentiate through HES-1 signaling, secretory lineages can differentiate into different cell types depending on conditions. Wnt signal pathways drive ISC differentiation into secretory precursor cells. Secretory precursors then develop either into enteroendocrine cells through Neurog3 signaling, or into goblet and Paneth cells following activation of Atoh1. Differentiation signal pathways to separate development of goblet cells and Paneth cells are still unknown. It is also important to note that recent data has shown that activation of ErbB3 acts as a suppressor of Atoh1, while genetic deletion of ErbB3 induces precocious development of Paneth cells.

accumulating and associating in Paneth cell granules (44). Since Paneth cells are not currently able to be cultured without other epithelial and stem cells, most of the data we have on granular contents is from immunohistochemistry techniques. The granules are then released at the apical surface of the cell into the lumen of the intestine where they serve a variety of biological functions, primarily as microbiocidal agents against bacteria, fungi, spirochetes, protozoa, and enveloped viruses (45). Paneth cell granules are secreted both constitutively and in response to pathogenic exposure, with common stimuli including cholinergic stimulation and exposure to bacterial antigens (45–47). This secretion of Paneth cell granular components is under tight regulatory control, as these mediators are vital for maintenance of intestinal homeostasis (38, 48, 49).

Paneth cell health remains a critical priority to the homeostasis of the small intestine. We and others have shown that following dithizone-induced loss, the small intestine replenishes Paneth cell populations within 72 h (14, 50, 51). Since the mammalian intestinal tract represents the largest surface area that communicates with the external environment (7, 52), protection of the host from injury or bacterial invasion from the intestinal flora (53) requires a complex system of defense mechanisms. In the small intestine, a key component of host defense is epithelial derived antimicrobial peptides (AMPs). AMPs are small peptides generally >5 kDa in length, cationic at a neutral pH, and have broad spectrum microbicidal activities at low concentrations (45). These peptides are the main product contained in Paneth cell granules.

In humans, there are two major classes of AMPs: cathelicidins and defensins. Cathelicidins are antimicrobial peptides with broad antibacterial (54), anti-fungal (55), and anti-viral activity (56), and are characterized by a highly conserved N-terminal domain. Only after cleavage of the AMP does the protein exert its myriad activities (57). Humans express only one cathelicidin, LL-37 (originally hCAP-18) (58) and it is expressed in various cells of the body including those of the intestinal epithelium (59–62). However, in the small intestine, cathelicidin expression is restricted to the neonatal period (63, 64) before markedly decreasing and disappearing. The timing of this decrease is important as it coincides with the appearance of Paneth cells (19, 65) and the onset of expression of Paneth cell AMPs such as α-Defensins (18). This "switch" from one AMP to another occurs at roughly the mid-point of development of the small intestine (66). It is important to note that mid-development of the small intestine is also around the time when NEC often occurs in infants born extremely prematurely (67) (**Figure 3**).

The second class of AMP found in the small intestine are defensins. Defensins are abundant in human cells and tissues that are involved in host defense and have two main subtypes: α-defensins, which are found in granule containing cells such as neutrophils and Paneth cells (also known as cryptdins in mice), and β-defensins which are produced by epithelial cells (68–71). Human Paneth cells produce two main α-defensins known as HD-5 and HD-6 (72). In mice, loss of matrilysin (the proteolytic enzyme needed to activate cryptdins) have altered microbiomes and are more susceptible to *Salmonella* infections (73–75). In addition, mice that have been genetically modified to express HD-5 have enhanced resistance to bacterial invasion (74).

AMPs work by inserting themselves into the bacterial membrane and forming pores, which result in the leakage of bacterial cytoplasmic content (76–78). They can also degenerate bacterial cytoplasmic structures and form extracellular net-like structures, which result in bacterial trapping (79). In animal models, AMPs have been shown to preferentially target non-commensal bacteria while sparing commensal normal flora (47, 80). In addition to killing pathogens, AMPs can also influence the immune system through white blood cell chemotaxis (81), activation of dendritic cells (82), and downregulation of immunomodulators such as cortisol (68, 71).

PANETH CELLS AND MECHANISMS OF CELLULAR DEATH

Cells of the body undergo death for a multitude of reasons and through various mechanisms. The mechanisms of cell

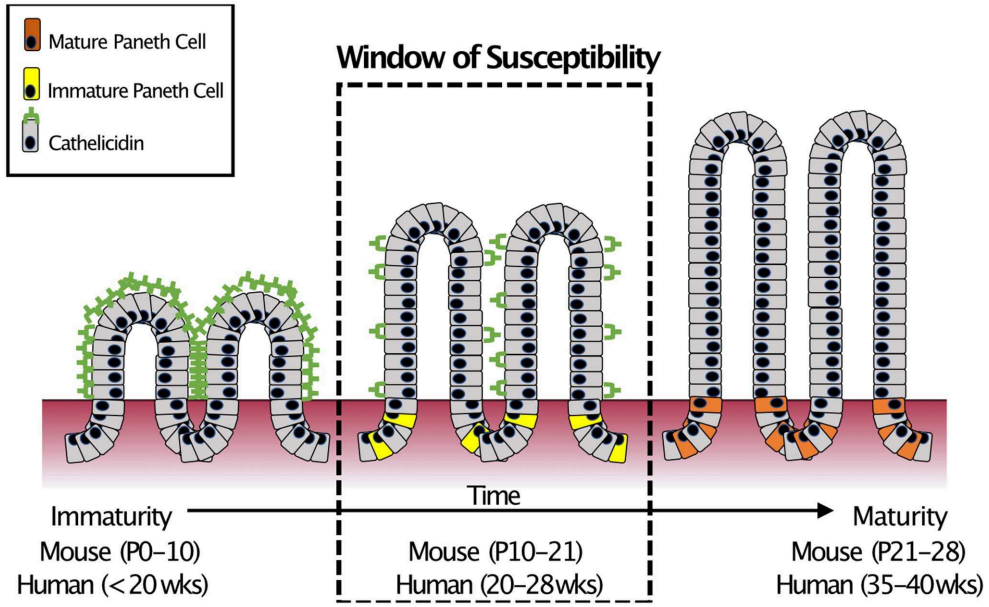

FIGURE 3 | Small intestinal AMP switch during intestinal development. During development, the immature intestine is protected by the AMP CRAMP (LL-37 in humans). However, CRAMP expression decreases around mid-development, at roughly the time that Paneth cells begin to develop. This "switch" occurs during mid-intestinal development which is around post-natal (P) day 10–21 in C57Bl6 mice and in the second trimester (between 20 and 28 weeks of gestation) in humans. In infants born prematurely, this switch is temporally similar to when extremely preterm infants are most susceptible to develop NEC (18).

death include apoptosis, necrosis, necroptosis, pyroptosis, and autophagy. While NEC is defined by necrosis of the intestinal tissue, many of these different cellular death pathways have been implicated in the pathogenesis of NEC. Importantly, several of these pathways are also mechanistically tied to Paneth cell biology.

Apoptosis is a normal part of intestinal health that results in disassembly of the cell and, in general, tends to avoid causing inflammation (83). During apoptosis, cells tend to retract pseudopods, condense chromatin (pyknosis), undergo nuclear fragmentation and then experience blebbing of the plasma membrane (84). This contrasts with cellular necrosis where cells experience organelle swelling, extensive vacuole formation, condensation of nuclei, and release of inflammatory cytokines in a passive or accidental manner (83, 84). One type of apoptosis seen in the intestinal epithelial layer is when the epithelial cells move upward from the crypt toward the tip of the villus. Once they reach the tip, cells are sloughed into the intestinal lumen in a process called anoikis, which is a form of apoptosis (84). There is evidence to show that apoptosis is also involved in the cell death experienced by cells in the stem cell region within the small intestinal crypts although the regulation of the process is not well-understood (84). Apoptosis has been shown by multiple investigators to be important in development of NEC (85–89). Additionally, apoptosis is directly relevant to Paneth cell biology and NEC as our lab has shown that NEC-like injury can be induced in mice by delivering diphtheria toxin to *PC-DTR* mice where a human diphtheria toxin receptor has been attached to the cryptdin-2 promoter of Paneth cells (14, 65). When these mice are exposed to diphtheria toxin, all Paneth cells expressing the construct are lysed through apoptotic pathways (90).

Another form of cell death directly related to Paneth cells is autophagy, which is a self-degradative process thought to help remove cells with misfolded or aggregated proteins or other intracellular damage (91). Autophagy is characterized by creation of an intracellular vacuole known as the autophagosome (83). The autophagosome is formed around damaged intracellular organelles or other selected targets. The autophagosome is then fused with a lysosome allowing for degradation of the components within the autophagosome followed by chromatin condensation (83). The morphologic changes that occur tend to be relatively well-regulated similar to the degree of regulation of apoptosis. Also similar to apoptosis, because the degradation of the dying cell takes place within another cell, this process tends to prevent inflammation (83). Autophagy is also an important process for Paneth cells. Because Paneth cells tend to live longer than most other cells of the gut and have many aggregated proteins that could be recycled by other neighboring cells, as damage and stressors to the cells occur, autophagy becomes activated (92). When mutations occur in the autophagy pathway such as in Atg16l1, Paneth cells can become dysfunctional and ultimately trigger intestinal inflammation, which can have implications for gut health such is suggested to be the case with Crohn's disease (92) and NEC (93). Our laboratory has also shown that autophagy may play a role in development of

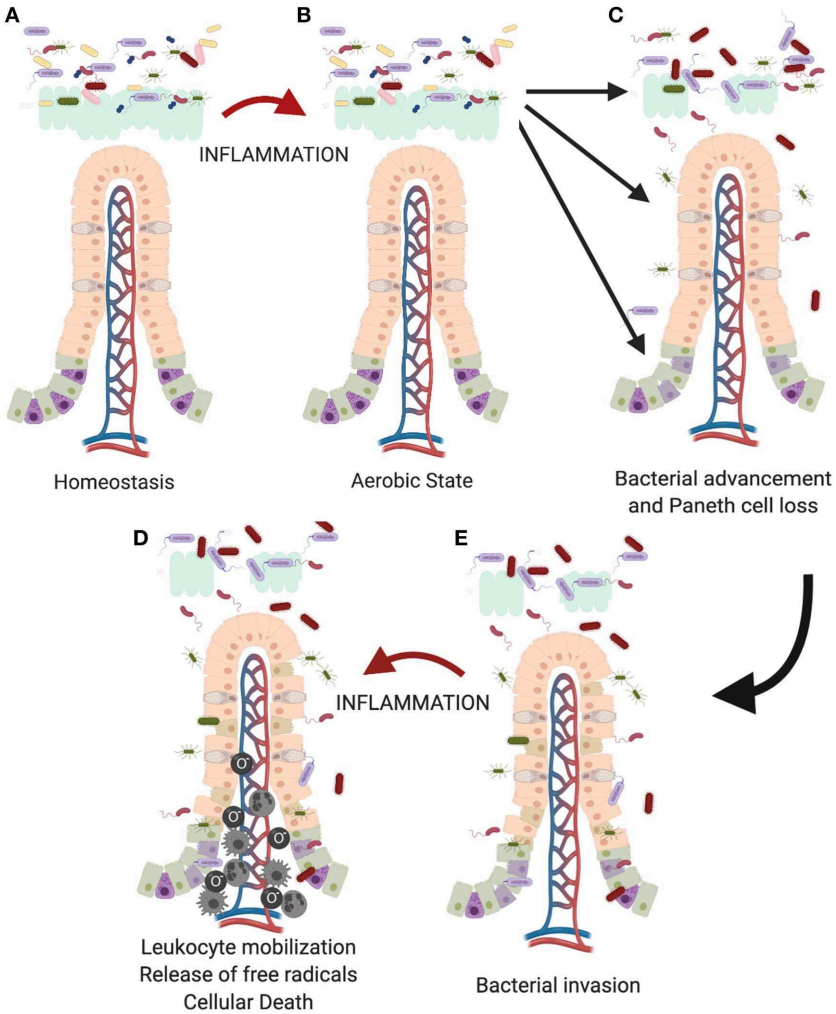

FIGURE 4 | Proposed role of the Paneth cell in development of NEC. As the immature intestine **(A)** is exposed to inflammation **(B)**, oxygen radicals are produced creating a selective advantage for Proteobacteria sp. over obligate anaerobes such as the Firmicutes. This creates a feedback loop for sustaining and increasing the pro-inflammatory state in the immature intestine. Previous work from our lab has shown that intestinal inflammation can reduce intestinal mucus production and cause loss of Paneth cells (112, 129). **(C)** Loss of these important chemical and physical aspects of innate immunity allows bacteria to move from the mucus layer of the intestinal lumen and gain closer proximity to the epithelial surface, **(D)** followed eventually by attachment and invasion of the epithelium. **(E)** Once bacteria invade the intestinal tissue, further inflammation occurs including recruitment of leukocytes including neutrophils, macrophages, and monocytes (133–135) which lead to eventual death of the tissues.

NEC. Lueschow et al. (14) showed that dithizone-induced Paneth cell loss in an experimental murine NEC model resulted in upregulation of autophagy pathways in Paneth cells (14).

Lastly, a more newly described type of cellular death is necroptosis which acts as an intermediate between necrosis and apoptosis. Cells undergoing necroptotic death show features more morphologically similar to necrosis and the immune system creates a highly inflammatory response, but in contrast to necrosis, necroptosis is a well-regulated process, similar to apoptosis (84, 94). Along with this relationship, necroptosis, and apoptosis have a great deal of overlap in their regulation. Apoptosis is promoted by TNFα binding and conversion of the TNFR complex I to the TNFR complex II/alternative TNFR complex (84). Also, the TNFR complex II can regulate as well as induce necroptosis when RIP1 and RIP3 are recruited and deubiquitinated (84). RIP1 and RIP3 are generally under the control of caspase-8, but when an inactivation of the caspase-8 gene occurs, induction of necroptotic cell death ensues although the mechanism by which this occurs is not completely understood (84). Necroptosis is an increasingly important mechanism of cellular death in the intestinal epithelium. Studies have shown that necroptosis of intestinal epithelial cells can result in intestinal inflammation and ultimately produce pathophysiology similar to inflammatory bowel disease (IBD). This was done by creating conditional knockout mice with deletion of FADD or caspase-8, the regulator of necroptosis, in intestinal epithelial cells (54, 95, 96). Interestingly, in addition to induction of necroptosis, this knockout also resulted in

spontaneous inflammation and an absence of Paneth cells (84, 95, 96). On further examination, the authors discovered that Paneth cells were uniquely sensitive to necroptosis. This is now thought to be due to the high expression of RIP3, a key modulator of necroptosis, in Paneth cells of humans and mice (84, 95, 96). Necroptosis has also been recently shown to play a role in development of NEC (94). In preterm infants who develop NEC, there is a higher degree of expression in genes related to necroptosis such as *RIPK1, RIPK2*, and *MLKL* compared to preterm infants who do not develop NEC (94). Moreover, increased expression of these three necroptosis related genes was correlated with a greater degree of NEC severity (94). This trend was also observed in murine experimental NEC conditions (94). Overall, these studies highlight the importance of necroptosis as well as Paneth cells in NEC.

PANETH CELLS AND NECROTIZING ENTEROCOLITIS (NEC)

For preterm infants, one of the leading causes of morbidity and mortality, and the most devastating intestinal complication, is development of NEC (97). The incidence of NEC varies widely among developed countries, ranging from 5 to 22% in infants with birth weight <1,000 g (98), and in the US is around 7% (97). Risk factors associated with development of NEC in the preterm infant include degree of prematurity, low birth weight, formula feeding, intestinal ischemia, prolonged antibiotic use, and anemia (99–102). However, the exact etiologic mechanisms and pathophysiology of NEC is still incomplete. In addition, the NEC phenotype may actually be the result of a final common pathway starting from multiple inciting events that results in an imbalance between mucosal injury and epithelial defense and repair, with activation of an unchecked pro-inflammatory cascade (103). As a disease process, NEC is unique in the Neonatal Intensive Care Unit (NICU) population. While the incidence of NEC is directly correlated to the degree of prematurity (the more premature, the more likely to develop NEC), the onset of NEC doesn't happen at birth, but rather weeks after and this delay is longer in the more premature infants. The result is that the incidence of NEC begins to increase at 28 weeks corrected gestational age, peaks at 32 weeks corrected gestational age, and steadily decreases at older corrected gestational ages (67). Theories have been suggested to explain this delay including feeding practices, development of microbial dysbiosis, or the accumulation of mesenteric hypoxic events (99–102). However, there is currently no universally accepted mechanistic explanation. We propose that another plausible reason may be a disruption in the function or quantity of Paneth cells (17, 67, 104).

As discussed above, Paneth cells play a key role in the homeostasis of the small intestinal epithelial lining, and loss or disruption of these cells has been shown to have significant adverse consequences including a reduction in clearance of bacterial pathogens (105, 106), disruption of normal stem cell function (3, 107), and the development of inflammatory bowel disease (108, 109). Paneth cells do not appear in the intestine until approximately halfway through intestinal development and maturation (22–24 weeks of human gestation and P7-10 or mouse age—normal intestinal development in the mouse occurs following birth while in the human it occurs *in utero*) (19, 65, 110). It is also important to note that these early Paneth cells do not possess all the constituents contained in mature granules (65), and it takes weeks in mice and months in humans before the Paneth cell cohort reaches its optimal density and before it becomes fully functional (17). Because of this developmental pattern, premature infants are thus born before they can develop a full complement of functional Paneth cells. As Paneth cells help regulate the intestinal bacterial flora, and NEC requires bacteria to induce intestinal injury, disruption of normal Paneth cell function, especially in the immature intestine could very well be involved in development of the NEC phenotype. Supporting this theory, decreased numbers of lysozyme positive Paneth cells were documented in infants with surgical NEC compared to similar aged surgical controls in two separate studies (111, 112). These data would suggest that Paneth cells are either lost or degranulated during or prior to development of NEC. However, not all studies have shown decreases in Paneth cell function or biology. A study looking at mRNA levels of Human defensin 5 and 6 found that they were increased in infants who developed NEC compared to controls (113). This discrepancy may be explained by timing of surgical resection following the initial Paneth cell disruption. In mouse models, when Paneth cells are disrupted using the heavy metal chelator dithizone, there is an initial decrease in defensin expression followed by a significant increase starting 72 h after treatment (14). In addition, a recent article that examined presence of HD-6 showed a significant decrease following development of NEC (114). Thus, timing of the surgical collection may play a critical role in determining Paneth cell-specific gene expression following NEC.

Studying Paneth cell mechanistic biology in the immature intestine is challenging in humans due to the difficulty of obtaining tissue specimens for preterm infants (115, 116). To help understand the potential role of Paneth cell biology in NEC, several laboratories have instead utilized animal models (100). Interestingly, when Paneth cells are disrupted in neonatal rats followed by enteral exposure to *E. coli*, there is not only an increase in bacterial translocation, but also a development of NEC-like injury to the small intestinal tract (105). In adapting this model to mice, our laboratory and others have shown that selective ablation of Paneth cells followed by enteric gavage of *Klebsiella pneumoniae* in 14-days old mice results in grossly necrotic intestines (89, 117–119), an increase in serum inflammatory markers (119), and alterations in the microbiome (14) that are consistent with human NEC. The use of 2-weeks old mice in this model is potentially advantageous as well as they possess a gene expression profile of epithelial cell genes that matches the expression profile seen in preterm human infants during the window when they are most susceptible to develop NEC (18, 67). Interestingly, disruption of Paneth cell biology via administration of the heavy metal chelator dithizone prior to normal Paneth cell development (5 days old mice) does not result in a NEC-like phenotype (117). One critique of this methodology is that dithizone is not specific to Paneth cells but

instead is a general chelator of heavy metals. To help resolve this issue, we developed the *PC-DTR* mouse (14, 119, 120). The *PC-DTR* mouse has a human diphtheria toxin receptor (DTR) inserted into mouse Paneth cells targeting the cryptdin-2 promotor (65). Treatment with diphtheria toxin induces apoptosis of any cells possessing DTR while sparing all other cells. In this model, treatment with diphtheria toxin followed by *Klebsiella pneumoniae* exposure also produces intestinal injury that is equivalent to human NEC (14, 119). These data provide further evidence that it is a disruption of, and not an absence of Paneth cells that contributes to development of NEC-like injury in the immature small intestine.

While these studies show a strong association for Paneth cell disfunction or loss with human NEC as well as a mechanistic relationship in mice, questions about how Paneth cell dysfunction may result in NEC remain (104, 121). It is well-established that prior to the development of NEC there is a dysbiotic change to the microbiome that is marked by a bloom of Proteobacteria, more specifically Enterobacteriaceae species (122–124). This phenomenon has also been replicated in our Paneth cell disruption model of NEC (14). In the normal homeostatic state, the microbiome acts to suppress inflammation through several mechanisms including induction of anti-inflammatory mediators such as IL-10, suppression of pro-inflammatory mediators such as IL-17, and by breaking down and fermenting complex, non-digestible complex polysaccharides into short-chain fatty acids, which possess anti-inflammatory properties (125–127). However, a result of inflammation is increased production of nitric oxide (NO) and superoxide radicals (O_2^-), which can then react to form nitrates (NO_3^-). These nitrates can be fermented by facultative anaerobic bacteria such as *Enterobacteriaceae* sp. that belong to the Proteobacteria phyla by utilizing anaerobic respiration with host-derived nitrates as alternative electron acceptors. Since obligate anaerobes cannot use nitrates as a growth substrate, Proteobacteria are able to use this selective pressure to out-compete the obligate anaerobic Firmicutes and Bacteroidetes that rely on fermentation for growth (128). As the proportion of commensal bacteria such as Firmicutes and Bacteroidetes decrease, the production of anti-inflammatory mediators also decreases which further facilitates increased inflammation and dysbiosis. Our laboratory has previously shown that in the immature murine small intestine, exposure to inflammation can significantly decrease the density and function of Paneth cells (129–131).

Thus, we think that as the premature infant is exposed to foreign antigens such as formula feedings (132), there is an increase in production of inflammatory cytokines (**Figure 4**). This creates a more aerobic state leading to a competitive advantage for Proteobacteria, such as Enterobacteriaceae species. As the microbiome becomes more dysbiotic, it suppresses anti-inflammatory mechanisms creating a cycle of increasing intestinal inflammation (136). This increasing inflammation can then impact Paneth cell biology leading to a loss in Paneth cells (14, 129, 137). In an already dysbiotic environment, this combination is exactly the milieu that is modeled in our animal model and predisposes to development of injury. This is further compounded because the Paneth cells present in the immature intestine are not fully mature or functional at a baseline (18). This limited Paneth cell cohort also means that there is a limited capacity for protection via AMPs (40). As Paneth cells are lost, AMP levels will further fall, likely reaching a critical threshold under which bacterial invasion of the epithelial tissue can begin to occur (105). Lastly, it is important to remember that Paneth cell loss may also impact the stem cell niche. A healthy stem cell cohort is critical to induce epithelial restitution following injury as Paneth cells support the stem cell niche through the production of EGF, Notch, and Wnt (27, 88, 104, 138).

In summary, the Paneth cell plays a critical role in many facets of intestinal homeostasis, from regulating the microbiota that closely associate with the epithelium, to maintaining the health of the stem cell niche, to helping to regulate levels of inflammation. Disruption of these secretory cells can have an important effect on the ability of the intestinal epithelium to not only protect itself from foreign invaders, but to promote growth and development of the intestine. These functions are especially critical in the immature intestine of premature infants who have a developing intestinal tract associated with a dysbiotic microbiome. Thus, it is reasonable that Paneth cell disruption has been linked mechanistically to development of NEC-like injury. As mortality rates for NEC remain static, a greater understanding of Paneth cell biology may provide a critical novel pathway to understand the development of NEC.

AUTHOR CONTRIBUTIONS

SM and SL contributed equally to the drafting and editing of the work.

FUNDING

Funding was provided by the Stead Family Department of Pediatrics and the Carver College of Medicine at the University of Iowa.

REFERENCES

1. Peterson LW, Artis D. Intestinal epithelial cells: regulators of barrier function and immune homeostasis. *Nat Rev Immunol*. (2014) 14:141–53. doi: 10.1038/nri3608
2. Paneth J. Ueber die secernirenden Zellen des Dünndarm-Epithels. *Arc Mikrosk Anat*. (1887) 31:113–91. doi: 10.1007/BF02955706
3. Clevers HC, Bevins CL. Paneth cells: maestros of the small intestinal crypts. *Annu Rev Physiol*. (2013) 75:289–311. doi: 10.1146/annurev-physiol-030212-183744
4. Bevins CL, Salzman NH. Paneth cells, antimicrobial peptides and maintenance of intestinal homeostasis. *Nat Rev Microbiol*. (2011) 9:356–68. doi: 10.1038/nrmicro2546

5. Paulsen SM, Engstad RE, Robertsen B. Enhanced lysozyme production in Atlantic salmon. (Salmo salar L.) macrophages treated with yeast beta-glucan and bacterial lipopolysaccharide. *Fish Shellfish Immunol.* (2001) 11:23–37. doi: 10.1006/fsim.2000.0291
6. Poindexter BJ, Klein GL, Milner SM, Bick RJ. Upregulation of defensins in burn sheep small intestine. *Eplasty*. (2009) 10:e6.
7. Helander HF, Fandriks L. Surface area of the digestive tract - revisited. *Scand J Gastroenterol*. (2014) 49:681–9. doi: 10.3109/00365521.2014.898326
8. Martin RJ, Fanaroff AA, Walsh MC. *Fanaroff and Martin's Neonatal-Perinatal Medicine: Diseases of the Fetus and Infant*. Philadelphia, PA: Elsevier/Saunders (2015).
9. Cheng H, Leblond CP. Origin, differentiation and renewal of the four main epithelial cell types in the mouse small intestine. *I Columnar cell Am J Anat*. (1974) 141:461–79. doi: 10.1002/aja.1001410403
10. Crosnier C, Stamataki D, Lewis J. Organizing cell renewal in the intestine: stem cells, signals and combinatorial control. *Nat Rev Genet*. (2006) 7:349–59. doi: 10.1038/nrg1840
11. Van Der Flier LG, Clevers H. Stem cells, self-renewal, and differentiation in the intestinal epithelium. *Annu Rev Physiol*. (2009) 71:241–60. doi: 10.1146/annurev.physiol.010908.163145
12. Gerbe F, Van Es JH, Makrini L, Brulin B, Mellitzer G, Robine S, et al. Distinct ATOH1 and Neurog3 requirements define tuft cells as a new secretory cell type in the intestinal epithelium. *J Cell Biol*. (2011) 192:767–80. doi: 10.1083/jcb.201010127
13. Porter EM, Bevins CL, Ghosh D, Ganz T. The multifaceted Paneth cell. *Cell Mol Life Sci*. (2002) 59:156–70. doi: 10.1007/s00018-002-8412-z
14. Lueschow SR, Stumphy J, Gong H, Kern SL, Elgin TG, Underwood MA, et al. Loss of murine Paneth cell function alters the immature intestinal microbiome and mimics changes seen in neonatal necrotizing enterocolitis. *PLoS ONE*. (2018) 13:e0204967. doi: 10.1371/journal.pone.0204967
15. Rumbo M, Schiffrin EJ. Ontogeny of intestinal epithelium immune functions: developmental and environmental regulation. *Cell Mol Life Sci*. (2005) 62:1288–96. doi: 10.1007/s00018-005-5033-3
16. Kandasamy J, Huda S, Ambalavanan N, Jilling T. Inflammatory signals that regulate intestinal epithelial renewal, differentiation, migration and cell death: implications for necrotizing enterocolitis. *Pathophysiology*. (2014) 21:67–80. doi: 10.1016/j.pathophys.2014.01.001
17. Heida FH, Beyduz G, Bulthuis ML, Kooi EM, Bos AF, Timmer A, et al. *Paneth cells in the* developing gut: when do they arise and when are they immune competent? *Pediatr Res*. (2016) 80:306–10. doi: 10.1038/pr.2016.67
18. Stanford AH, Gong H, Noonan M, Lewis AN, Gong Q, Lanik WE, et al. A direct comparison of mouse and human intestinal development using epithelial gene expression patterns. *Pediatr Res*. (2019). doi: 10.1038/s41390-019-0472-y. [Epub ahead of print].
19. Bry L, Falk P, Huttner K, Ouellette A, Midtvedt T, Gordon JI. Paneth cell differentiation in the developing intestine of normal and transgenic mice. *Proc Natl Acad Sci USA*. (1994) 91:10335–9. doi: 10.1073/pnas.91.22.10335
20. Cheng H, Leblond CP. Origin, differentiation and renewal of the four main epithelial cell types in the mouse small intestine. V Unitarian Theory of the origin of the four epithelial cell types. *Am J Anat*. (1974) 141:537–61. doi: 10.1002/aja.1001410407
21. Barker N, Van Es JH, Kuipers J, Kujala P, Van Den Born M, Cozijnsen M, et al. Identification of stem cells in small intestine and colon by marker gene Lgr5. *Nature*. (2007) 449:1003–7. doi: 10.1038/nature06196
22. Barker N, Huch M, Kujala P, Van De Wetering M, Snippert HJ, Van Es JH, et al. Lgr5(+ve) stem cells drive self-renewal in the stomach and build long-lived gastric units *in vitro*. *Cell Stem Cell*. (2010) 6:25–36. doi: 10.1016/j.stem.2009.11.013
23. Yan KS, Chia LA, Li X, Ootani A, Su J, Lee JY, et al. The intestinal stem cell markers Bmi1 and Lgr5 identify two functionally distinct populations. *Proc Natl Acad Sci USA*. (2012) 109:466–71. doi: 10.1073/pnas.1118857109
24. Munoz J, Stange DE, Schepers AG, Van De Wetering M, Koo BK, Itzkovitz S, et al. The Lgr5 intestinal stem cell signature: robust expression of proposed quiescent '+4' cell markers. *EMBO J*. (2012) 31:3079–91. doi: 10.1038/emboj.2012.166
25. Kosinski C, Li VS, Chan AS, Zhang J, Ho C, Tsui WY, et al. Gene expression patterns of human colon tops and basal crypts and BMP antagonists as intestinal stem cell niche factors. *Proc Natl Acad Sci USA*. (2007) 104:15418–23. doi: 10.1073/pnas.0707210104
26. Miyazono K, Kamiya Y, Morikawa M. Bone morphogenetic protein receptors and signal transduction. *J Biochem*. (2010) 147:35–51. doi: 10.1093/jb/mvp148
27. Sato T, Van Es JH, Snippert HJ, Stange DE, Vries RG, Van Den Born M, et al. Paneth cells constitute the niche for Lgr5 stem cells in intestinal crypts. *Nature*. (2011) 469:415–8. doi: 10.1038/nature09637
28. Van Es JH, Jay P, Gregorieff A, Van Gijn ME, Jonkheer S, Hatzis P, et al. Wnt signalling induces maturation of Paneth cells in intestinal crypts. *Nat Cell Biol*. (2005) 7:381–6. doi: 10.1038/ncb1240
29. Andreu P, Peignon G, Slomianny C, Taketo MM, Colnot S, Robine S, et al. A genetic study of the role of the Wnt/beta-catenin signalling in Paneth cell differentiation. *Dev Biol*. (2008) 324:288–96. doi: 10.1016/j.ydbio.2008.09.027
30. Garcia MI, Ghiani M, Lefort A, Libert F, Strollo S, Vassart G. LGR5 deficiency deregulates Wnt signaling and leads to precocious Paneth cell differentiation in the fetal intestine. *Dev Biol*. (2009) 331:58–67. doi: 10.1016/j.ydbio.2009.04.020
31. Ben-Arie N, Bellen HJ, Armstrong DL, Mccall AE, Gordadze PR, Guo Q, et al. Math1 is essential for genesis of cerebellar granule neurons. *Nature*. (1997) 390:169–72. doi: 10.1038/36579
32. Bermingham NA, Hassan BA, Price SD, Vollrath MA, Ben-Arie N, Eatock RA, et al. Math1: an essential gene for the generation of inner ear hair cells. *Science*. (1999) 284:1837–41. doi: 10.1126/science.284.5421.1837
33. Jensen P, Smeyne R, Goldowitz D. Analysis of cerebellar development in math1 null embryos and chimeras. *J Neurosci*. (2004) 24:2202–11. doi: 10.1523/JNEUROSCI.3427-03.2004
34. Shroyer NF, Helmrath MA, Wang VY, Antalffy B, Henning SJ, Zoghbi HY. Intestine-specific ablation of mouse atonal homolog 1 (Math1) reveals a role in cellular homeostasis. *Gastroenterology*. (2007) 132:2478–88. doi: 10.1053/j.gastro.2007.03.047
35. Nakanishi Y, Reina-Campos M, Nakanishi N, Llado V, Elmen L, Peterson S, et al. Control of paneth cell fate, intestinal inflammation, and tumorigenesis by PKCLAMBDA/iota. *Cell Rep*. (2016) 16:3297–310. doi: 10.1016/j.celrep.2016.08.054
36. Durand A, Donahue B, Peignon G, Letourneur F, Cagnard N, Slomianny C, et al. Functional intestinal stem cells after Paneth cell ablation induced by the loss of transcription factor Math1. (Atoh1). *Proc Natl Acad Sci USA*. (2012) 109:8965–70. doi: 10.1073/pnas.1201652109
37. Almohazey D, Lo YH, Vossler CV, Simmons AJ, Hsieh JJ, Bucar EB, et al. The ErbB3 receptor tyrosine kinase negatively regulates Paneth cells by PI3K-dependent suppression of Atoh1. *Cell Death Differ*. (2017) 24:855–65. doi: 10.1038/cdd.2017.27
38. Ouellette AJ. Paneth cells and innate mucosal immunity. *Curr Opin Gastroenterol*. (2010) 26:547–53. doi: 10.1097/MOG.0b013e32833dccde
39. Johnson LR. *Physiology of the Gastrointestinal Tract*. Amsterdam: Elsevier/AP (2012).
40. Satoh Y. Effect of live and heat-killed bacteria on the secretory activity of Paneth cells in germ-free mice. *Cell Tissue Res*. (1988) 251:87–93. doi: 10.1007/BF00215451
41. Porter EM, Liu L, Oren A, Anton PA, Ganz T. Localization of human intestinal defensin 5 in Paneth cell granules. *Infect Immun*. (1997) 65:2389–95. doi: 10.1128/IAI.65.6.2389-2395.1997
42. Takahashi N, Vanlaere I, De Rycke R, Cauwels A, Joosten LA, Lubberts E, et al. IL-17 produced by Paneth cells drives TNF-induced shock. *J Exp Med*. (2008) 205:1755–61. doi: 10.1084/jem.20080588
43. Park SW, Kim M, Brown KM, D'agati VD, Lee HT. Paneth cell-derived interleukin-17A causes multiorgan dysfunction after hepatic ischemia and reperfusion injury. *Hepatology*. (2011) 53:1662–75. doi: 10.1002/hep.24253
44. Satoh Y, Ishikawa K, Tanaka H, Ono K. Immunohistochemical observations of immunoglobulin A in the Paneth cells of germ-free and formerly-germ-free rats. *Histochemistry*. (1986) 85:197–201. doi: 10.1007/BF00494804
45. Ouellette AJ. Paneth cell alpha-defensins: peptide mediators of innate immunity in the small intestine. *Springer Semin Immunopathol*. (2005) 27:133–46. doi: 10.1007/s00281-005-0202-x

46. Ayabe T, Satchell DP, Wilson CL, Parks WC, Selsted ME, Ouellette AJ. Secretion of microbicidal alpha-defensins by intestinal Paneth cells in response to bacteria. *Nat Immunol*. (2000) 1:113–8. doi: 10.1038/77783
47. Nakamura K, Sakuragi N, Takakuwa A, Ayabe T. Paneth cell alpha-defensins and enteric microbiota in health and disease. *Biosci Microbiota Food Health*. (2016) 35:57–67. doi: 10.12938/bmfh.2015-019
48. Mizrahi A, Barlow O, Berdon W, Blanc WA, Silverman WA. Necrotizing Enterocolitis in Premature Infants. *J Pediatr*. (1965) 66:697–705. doi: 10.1016/S0022-3476(65)80003-8
49. Salzman NH, Underwood MA, Bevins CL. Paneth cells, defensins, and the commensal microbiota: a hypothesis on intimate interplay at the intestinal mucosa. *Semin Immunol*. (2007) 19:70–83. doi: 10.1016/j.smim.2007.04.002
50. Sawada M, Takahashi K, Sawada S, Midorikawa O. Selective killing of Paneth cells by intravenous administration of dithizone in rats. *Int J Exp Pathol*. (1991) 72:407–21.
51. Sawada M, Nishikawa M, Adachi T, Midorikawa O, Hiai H. A Paneth cell specific zinc-binding protein in the rat. Purification and immunohistochemical localization. *Lab Invest*. (1993) 68:338–44.
52. Hooper LV, Midtvedt T, Gordon JI. How host-microbial interactions shape the nutrient environment of the mammalian intestine. *Annu Rev Nutr*. (2002) 22:283–307. doi: 10.1146/annurev.nutr.22.011602.092259
53. Gilbert JA, Blaser MJ, Caporaso JG, Jansson JK, Lynch SV, Knight R. Current understanding of the human microbiome. *Nat Med*. (2018) 24:392–400. doi: 10.1038/nm.4517
54. Chromek M, Arvidsson I, Karpman D. The antimicrobial peptide cathelicidin protects mice from *Escherichia coli* O157:H7-mediated disease. *PLoS ONE*. (2012) 7:e46476. doi: 10.1371/journal.pone.0046476
55. Wong JH, Ng TB, Legowska A, Rolka K, Hui M, Cho CH. Antifungal action of human cathelicidin fragment. (LL13-37) on Candida albicans. *Peptides*. (2011) 32:1996–2002. doi: 10.1016/j.peptides.2011.08.018
56. Barlow PG, Svoboda P, Mackellar A, Nash AA, York IA, Pohl J, et al. Antiviral activity and increased host defense against influenza infection elicited by the human cathelicidin LL-37. *PLoS ONE*. (2011) 6:e25333. doi: 10.1371/journal.pone.0025333
57. Durr UH, Sudheendra US, Ramamoorthy A. LL-37, the only human member of the cathelicidin family of antimicrobial peptides. *Biochim Biophys Acta*. (2006) 1758:1408–25. doi: 10.1016/j.bbamem.2006.03.030
58. Larrick JW, Hirata M, Balint RF, Lee J, Zhong J, Wright SC. Human CAP18: a novel antimicrobial lipopolysaccharide-binding protein. *Infect Immun*. (1995) 63:1291–7. doi: 10.1128/IAI.63.4.1291-1297.1995
59. Frohm M, Agerberth B, Ahangari G, Stahle-Backdahl M, Liden S, Wigzell H, et al. The expression of the gene coding for the antibacterial peptide LL-37 is induced in human keratinocytes during inflammatory disorders. *J Biol Chem*. (1997) 272:15258–63. doi: 10.1074/jbc.272.24.15258
60. Bals R, Wang X, Zasloff M, Wilson JM. The peptide antibiotic LL-37/hCAP-18 is expressed in epithelia of the human lung where it has broad antimicrobial activity at the airway surface. *Proc Natl Acad Sci USA*. (1998) 95:9541–6. doi: 10.1073/pnas.95.16.9541
61. Frohm Nilsson M, Sandstedt B, Sorensen O, Weber G, Borregaard N, Stahle-Backdahl M. The human cationic antimicrobial protein (hCAP18), a peptide antibiotic, is widely expressed in human squamous epithelia and colocalizes with interleukin-6. *Infect Immun*. (1999) 67:2561–6. doi: 10.1128/IAI.67.5.2561-2566.1999
62. Hase K, Eckmann L, Leopard JD, Varki N, Kagnoff MF. Cell differentiation is a key determinant of cathelicidin LL-37/human cationic antimicrobial protein 18 expression by human colon epithelium. *Infect Immun*. (2002) 70:953–63. doi: 10.1128/IAI.70.2.953-963.2002
63. Kai-Larsen Y, Bergsson G, Gudmundsson GH, Printz G, Jornvall H, Marchini G, et al. Antimicrobial components of the neonatal gut affected upon colonization. *Pediatr Res*. (2007) 61:530–6. doi: 10.1203/pdr.0b013e318045be83
64. Menard S, Forster V, Lotz M, Gutle D, Duerr CU, Gallo RL, et al. Developmental switch of intestinal antimicrobial peptide expression. *J Exp Med*. (2008) 205:183–93. doi: 10.1084/jem.20071022
65. Garabedian EM, Roberts LJ, Mcnevin MS, Gordon JI. Examining the role of Paneth cells in the small intestine by lineage ablation in transgenic mice. *J Biol Chem*. (1997) 272:23729–40. doi: 10.1074/jbc.272.38.23729
66. Mcelroy SJ, Weitkamp JH. Innate Immunity in the Small Intestine of the Preterm Infant. *NeoReviews*. (2011) 12:e517–26. doi: 10.1542/neo.12-9-e517
67. Yee WH, Soraisham AS, Shah VS, Aziz K, Yoon W, Lee SK. Incidence and timing of presentation of necrotizing enterocolitis in preterm infants. *Pediatrics*. (2012) 129:e298–304. doi: 10.1542/peds.2011-2022
68. Ganz T. Defensins: antimicrobial peptides of innate immunity. *Nat Rev Immunol*. (2003) 3:710–20. doi: 10.1038/nri1180
69. Wehkamp J, Schauber J, Stange EF. Defensins and cathelicidins in gastrointestinal infections. *Curr Opin Gastroenterol*. (2007) 23:32–8. doi: 10.1097/MOG.0b013e32801182c2
70. Kolls JK, Mccray PB Jr, Chan YR. Cytokine-mediated regulation of antimicrobial proteins. *Nat Rev Immunol*. (2008) 8:829–35. doi: 10.1038/nri2433
71. Ganz T. The role of antimicrobial peptides in innate immunity. *Integr Comp Biol*. (2003) 43:300–4. doi: 10.1093/icb/43.2.300
72. De Smet K, Contreras R. Human antimicrobial peptides: defensins, cathelicidins and histatins. *Biotechnol Lett*. (2005) 27:1337–47. doi: 10.1007/s10529-005-0936-5
73. Wilson CL, Ouellette AJ, Satchell DP, Ayabe T, Lopez-Boado YS, Stratman JL, et al. Regulation of intestinal alpha-defensin activation by the metalloproteinase matrilysin in innate host defense. *Science*. (1999) 286:113–7. doi: 10.1126/science.286.5437.113
74. Salzman NH, Ghosh D, Huttner KM, Paterson Y, Bevins CL. Protection against enteric salmonellosis in transgenic mice expressing a human intestinal defensin. *Nature*. (2003) 422:522–6. doi: 10.1038/nature01520
75. Salzman NH, Hung K, Haribhai D, Chu H, Karlsson-Sjoberg J, Amir E, et al. Enteric defensins are essential regulators of intestinal microbial ecology. *Nat Immunol*. (2010) 11:76–83. doi: 10.1038/ni.1825
76. Ulm H, Wilmes M, Shai Y, Sahl HG. Antimicrobial host defensins - specific antibiotic activities and innate defense modulation. *Front Immunol*. (2012) 3:249. doi: 10.3389/fimmu.2012.00249
77. Hemshekhar M, Anaparti V, Mookherjee N. Functions of Cationic Host Defense Peptides in Immunity. *Pharmaceuticals*. (2016) 9:40. doi: 10.3390/ph9030040
78. Ho J, Zhang L, Liu X, Wong SH, Wang MHT, Lau BWM, et al. Pathological role and diagnostic value of endogenous host defense peptides in adult and neonatal sepsis: a systematic review. *Shock*. (2017) 47:673–9. doi: 10.1097/SHK.0000000000000815
79. Schroeder BO, Ehmann D, Precht JC, Castillo PA, Kuchler R, Berger J, et al. Paneth cell alpha-defensin 6 (HD-6) is an antimicrobial peptide. *Mucosal Immunol*. (2015) 8:661–71. doi: 10.1038/mi.2014.100
80. Masuda K, Sakai N, Nakamura K, Yoshioka S, Ayabe T. Bactericidal activity of mouse alpha-defensin cryptdin-4 predominantly affects noncommensal bacteria. *J Innate Immun*. (2011) 3:315–26. doi: 10.1159/000322037
81. Yang D, Chertov O, Bykovskaia SN, Chen Q, Buffo MJ, Shogan J, et al. Beta-defensins: linking innate and adaptive immunity through dendritic and T cell CCR6. *Science*. (1999) 286:525–8. doi: 10.1126/science.286.5439.525
82. Yang D, Chen Q, Chertov O, Oppenheim JJ. Human neutrophil defensins selectively chemoattract naive T and immature dendritic cells. *J Leukoc Biol*. (2000) 68:9–14. doi: 10.1189/jlb.68.1.9
83. Fink SL, Cookson BT. Apoptosis, pyroptosis, and necrosis: mechanistic description of dead and dying eukaryotic cells. *Infect Immun*. (2005) 73:1907–16. doi: 10.1128/IAI.73.4.1907-1916.2005
84. Gunther C, Neumann H, Neurath MF, Becker C. Apoptosis, necrosis and necroptosis: cell death regulation in the intestinal epithelium. *Gut*. (2013) 62:1062–71. doi: 10.1136/gutjnl-2011-301364
85. Jilling T, Lu J, Jackson M, Caplan MS. Intestinal epithelial apoptosis initiates gross bowel necrosis in an experimental rat model of neonatal necrotizing enterocolitis. *Pediatr Res*. (2004) 55:622–9. doi: 10.1203/01.PDR.0000113463.70435.74
86. Clark JA, Lane RH, Maclennan NK, Holubec H, Dvorakova K, Halpern MD, et al. Epidermal growth factor reduces intestinal apoptosis in an experimental model of necrotizing enterocolitis. *Am J Physiol Gastrointest Liver Physiol*. (2005) 288:G755–62. doi: 10.1152/ajpgi.00172.2004
87. Feng JX, Besner GE. Heparin-binding epidermal growth factor-like growth factor promotes enterocyte migration and proliferation in neonatal

rats with necrotizing enterocolitis. *J Pediatr Surg*. (2007) 42:214–20. doi: 10.1016/j.jpedsurg.2006.09.055
88. Neal MD, Sodhi CP, Jia H, Dyer M, Egan C, Yazji I, et al. Toll like receptor 4 is expressed on intestinal stem cells and regulates their proliferation and apoptosis via the p53-upregulated modulator of apoptosis. *J Biol Chem*. (2012) 287:37296–308. doi: 10.1074/jbc.M112.375881
89. Mcelroy SJ, Castle SL, Bernard JK, Almohazey D, Hunter CJ, Bell BA, et al. The ErbB4 ligand neuregulin-4 protects against experimental necrotizing enterocolitis. *Am J Pathol*. (2014) 184:2768–78. doi: 10.1016/j.ajpath.2014.06.015
90. Alouf JE, Popoff MR. The comprehensive sourcebook of bacterial protein toxins. Amsterdam; Boston: Elsevier (2006).
91. Glick D, Barth S, Macleod KF. Autophagy: cellular and molecular mechanisms. *J Pathol*. (2010) 221:3–12. doi: 10.1002/path.2697
92. Van Es JH, Clevers H. Paneth cells. *Curr Biol*. (2014) 24:R547–8. doi: 10.1016/j.cub.2014.04.049
93. Sampath V, Bhandari V, Berger J, Merchant D, Zhang L, Ladd M, et al. A functional ATG16L1 (T300A) variant is associated with necrotizing enterocolitis in premature infants. *Pediatr Res*. (2017) 81:582–8. doi: 10.1038/pr.2016.260
94. Werts AD, Fulton WB, Ladd MR, Saad-Eldin A, Chen YX, Kovler ML, et al. A novel role for necroptosis in the pathogenesis of necrotizing enterocolitis. *Cell Mol Gastroenterol Hepatol*. (2019) 9:403–23. doi: 10.1016/j.jcmgh.2019.11.002
95. Gunther C, Martini E, Wittkopf N, Amann K, Weigmann B, Neumann H, et al. Caspase-8 regulates TNF-alpha-induced epithelial necroptosis and terminal ileitis. *Nature*. (2011) 477:335–9. doi: 10.1038/nature10400
96. Welz PS, Wullaert A, Vlantis K, Kondylis V, Fernandez-Majada V, Ermolaeva M, et al. FADD prevents RIP3-mediated epithelial cell necrosis and chronic intestinal inflammation. *Nature*. (2011) 477:330–4. doi: 10.1038/nature10273
97. Patel RM, Kandefer S, Walsh MC, Bell EF, Carlo WA, Laptook AR, et al. Causes and timing of death in extremely premature infants from 2000 through 2011. *N Engl J Med*. (2015) 372:331–40. doi: 10.1056/NEJMoa1403489
98. Battersby C, Santhalingam T, Costeloe K, Modi N. Incidence of neonatal necrotising enterocolitis in high-income countries: a systematic review. *Arch Dis Child Fetal Neonatal Ed*. (2018) 103:F182–9. doi: 10.1136/archdischild-2017-313880
99. Lin PW, Nasr TR, Stoll BJ. Necrotizing enterocolitis: recent scientific advances in pathophysiology and prevention. *Semin Perinatol*. (2008) 32:70–82. doi: 10.1053/j.semperi.2008.01.004
100. Ares GJ, Mcelroy SJ, Hunter CJ. The science and necessity of using animal models in the study of necrotizing enterocolitis. *Semin Pediatr Surg*. (2018) 27:29–33. doi: 10.1053/j.sempedsurg.2017.11.006
101. Hackam D, Caplan M. Necrotizing enterocolitis: pathophysiology from a historical context. *Semin Pediatr Surg*. (2018) 27:11–8. doi: 10.1053/j.sempedsurg.2017.11.003
102. Hackam DJ, Sodhi CP, Good M. New insights into necrotizing enterocolitis: from laboratory observation to personalized prevention and treatment. *J Pediatr Surg*. (2019) 54:398–404. doi: 10.1016/j.jpedsurg.2018.06.012
103. Caplan MS, Underwood MA, Modi N, Patel R, Gordon PV, Sylvester KG, et al. Necrotizing enterocolitis: using regulatory science and drug development to improve outcomes. *J Pediatr*. (2019) 212:208–15 e201. doi: 10.1016/j.jpeds.2019.05.032
104. Mcelroy SJ, Underwood MA, Sherman MP. Paneth cells and necrotizing enterocolitis: a novel hypothesis for disease pathogenesis. *Neonatology*. (2013) 103:10–20. doi: 10.1159/000342340
105. Sherman MP, Bennett SH, Hwang FF, Sherman J, Bevins CL. Paneth cells and antibacterial host defense in neonatal small intestine. *Infect Immun*. (2005) 73:6143–6. doi: 10.1128/IAI.73.9.6143-6146.2005
106. Vaishnava S, Behrendt CL, Ismail AS, Eckmann L, Hooper LV. Paneth cells directly sense gut commensals and maintain homeostasis at the intestinal host-microbial interface. *Proc Natl Acad Sci USA*. (2008) 105:20858–63. doi: 10.1073/pnas.0808723105
107. Clevers H. Stem cells: a unifying theory for the crypt. *Nature*. (2013) 495:53–4. doi: 10.1038/nature11958
108. Bel S, Pendse M, Wang Y, Li Y, Ruhn KA, Hassell B, et al. Paneth cells secrete lysozyme via secretory autophagy during bacterial infection of the intestine. *Science*. (2017) 357:1047–52. doi: 10.1126/science.aal4677
109. Delorme-Axford E, Klionsky DJ. Secretory autophagy holds the key to lysozyme secretion during bacterial infection of the intestine. *Autophagy*. (2018) 14:1–3. doi: 10.1080/15548627.2017.1401425
110. Moxey PC, Trier JS. Specialized cell types in the human fetal small intestine. *Anat Rec*. (1978) 191:269–85. doi: 10.1002/ar.1091910302
111. Coutinho HB, Da Mota HC, Coutinho VB, Robalinho TI, Furtado AF, Walker E, et al. Absence of lysozyme (muramidase) in the intestinal Paneth cells of newborn infants with necrotising enterocolitis. *J Clin Pathol*. (1998) 51:512–4. doi: 10.1136/jcp.51.7.512
112. Mcelroy SJ, Prince LS, Weitkamp JH, Reese J, Slaughter JC, Polk DB. Tumor necrosis factor receptor 1-dependent depletion of mucus in immature small intestine: a potential role in neonatal necrotizing enterocolitis. *Am J Physiol Gastrointest Liver Physiol*. (2011) 301:G656–66. doi: 10.1152/ajpgi.00550.2010
113. Salzman NH, Polin RA, Harris MC, Ruchelli E, Hebra A, Zirin-Butler S, et al. Enteric defensin expression in necrotizing enterocolitis. *Pediatr Res*. (1998) 44:20–6. doi: 10.1203/00006450-199807000-00003
114. Markasz L, Wanders A, Szekely L, Lilja HE. Diminished DEFA6 expression in paneth cells is associated with necrotizing enterocolitis. *Gastroenterol Res Pract*. (2018) 2018:7345426. doi: 10.1155/2018/7345426
115. Ralls MW, Gadepalli SK, Sylvester KG, Good M. Development of the necrotizing enterocolitis society registry and biorepository. *Semin Pediatr Surg*. (2018) 27:25–8. doi: 10.1053/j.sempedsurg.2017.11.005
116. Chaaban H, Markel TA, Canvasser J, Good M. Biobanking for necrotizing enterocolitis: Needs and standards. *J Pediatr Surg*. (2019). doi: 10.1016/j.jpedsurg.2019.05.002. [Epub ahead of print].
117. Zhang C, Sherman MP, Prince LS, Bader D, Weitkamp JH, Slaughter JC, et al. Paneth cell ablation in the presence of Klebsiella pneumoniae induces necrotizing enterocolitis (NEC)-like injury in the small intestine of immature mice. *Dis Model Mech*. (2012) 5:522–32. doi: 10.1242/dmm.009001
118. Eckert J, Scott B, Lawrence SM, Ihnat M, Chaaban H. FLLL32, a curcumin analog, ameliorates intestinal injury in necrotizing enterocolitis. *J Inflamm Res*. (2017) 10:75–81. doi: 10.2147/JIR.S131051
119. White JR, Gong H, Pope B, Schlievert P, Mcelroy SJ. Paneth-cell-disruption-induced necrotizing enterocolitis in mice requires live bacteria and occurs independently of TLR4 signaling. *Dis Model Mech*. (2017) 10:727–36. doi: 10.1242/dmm.028589
120. Berger JN, Gong H, Good M, Mcelroy SJ. Dithizone-induced Paneth cell disruption significantly decreases intestinal perfusion in the murine small intestine. *J Pediatr Surg*. (2019) 54:2402–7. doi: 10.1016/j.jpedsurg.2019.02.021
121. Underwood MA. Paneth cells and necrotizing enterocolitis. *Gut Microbes*. (2012) 3:562–5. doi: 10.4161/gmic.21738
122. Gritz EC, Bhandari V. The human neonatal gut microbiome: a brief review. *Front Pediatr*. (2015) 3:17. doi: 10.3389/fped.2015.00060
123. Lu CY, Ni YH. Gut microbiota and the development of pediatric diseases. *J Gastroenterol*. (2015) 50:720–6. doi: 10.1007/s00535-015-1082-z
124. Niemarkt HJ, De Meij TG, Van De Velde ME, Van Der Schee MP, Van Goudoever JB, Kramer BW, et al. Necrotizing enterocolitis: a clinical review on diagnostic biomarkers and the role of the intestinal microbiota. *Inflamm Bowel Dis*. (2015) 21:436–44. doi: 10.1097/MIB.0000000000000184
125. Mazmanian SK, Round JL, Kasper DL. A microbial symbiosis factor prevents intestinal inflammatory disease. *Nature*. (2008) 453:620–5. doi: 10.1038/nature07008
126. Spees AM, Lopez CA, Kingsbury DD, Winter SE, Baumler AJ. Colonization resistance: battle of the bugs or Menage a Trois with the host? *PLoS Pathog*. (2013) 9:e1003730. doi: 10.1371/journal.ppat.1003730
127. Shin NR, Whon TW, Bae JW. Proteobacteria: microbial signature of dysbiosis in gut microbiota. *Trends Biotechnol*. (2015) 33:496–503. doi: 10.1016/j.tibtech.2015.06.011
128. Winter SE, Winter MG, Xavier MN, Thiennimitr P, Poon V, Keestra AM, et al. Host-derived nitrate boosts growth of *E. coli* in the inflamed gut. *Science*. (2013) 339:708–11. doi: 10.1126/science.1232467

129. Brown KS, Gong H, Frey MR, Pope B, Golden M, Martin K, et al. Tumor necrosis factor induces developmental stage-dependent structural changes in the immature small intestine. *Mediators Inflamm*. (2014) 2014:852378. doi: 10.1155/2014/852378
130. Fricke EM, Elgin TG, Gong H, Reese J, Gibson-Corley KN, Weiss RM, et al. Lipopolysaccharide-induced maternal inflammation induces direct placental injury without alteration in placental blood flow and induces a secondary fetal intestinal injury that persists into adulthood. *Am J Reprod Immunol*. (2018) 79:e12816. doi: 10.1111/aji.12816
131. Elgin TG, Fricke EM, Gong H, Reese J, Mills DA, Kalantera KM, et al. Fetal exposure to maternal inflammation interrupts murine intestinal development and increases susceptibility to neonatal intestinal injury. *Dis Model Mech*. (2019) 12:dmm040808. doi: 10.1242/dmm.040808
132. Liu Y, Zhu L, Fatheree NY, Liu X, Pacheco SE, Tatevian N, et al. Changes in intestinal Toll-like receptors and cytokines precede histological injury in a rat model of necrotizing enterocolitis. *Am J Physiol Gastrointest Liver Physiol*. (2009) 297:G442–50. doi: 10.1152/ajpgi.00182.2009
133. Anand RJ, Gribar SC, Li J, Kohler JW, Branca MF, Dubowski T, et al. Hypoxia causes an increase in phagocytosis by macrophages in a HIF-1alpha-dependent manner. *J Leukoc Biol*. (2007) 82:1257–65. doi: 10.1189/jlb.0307195
134. Egan CE, Sodhi CP, Good M, Lin J, Jia H, Yamaguchi Y, et al. Toll-like receptor 4-mediated lymphocyte influx induces neonatal necrotizing enterocolitis. *J Clin Invest*. (2016) 126:495–508. doi: 10.1172/JCI83356
135. Mohankumar K, Namachivayam K, Song T, Jake Cha B, Slate A, Hendrickson JE, et al. A murine neonatal model of necrotizing enterocolitis caused by anemia and red blood cell transfusions. *Nat Commun*. (2019) 10:3494. doi: 10.1038/s41467-019-11199-5
136. Elgin TG, Kern SL, Mcelroy SJ. Development of the neonatal intestinal microbiome and its association with necrotizing enterocolitis. *Clin Ther*. (2016) 38:706–15. doi: 10.1016/j.clinthera.2016.01.005
137. Fung CM, White JR, Brown AS, Gong H, Weitkamp JH, Frey MR, et al. Intrauterine growth restriction alters mouse intestinal architecture during development. *PLoS ONE*. (2016) 11:e0146542. doi: 10.1371/journal.pone.0146542
138. Li B, Lee C, Cadete M, Zhu H, Koike Y, Hock A, et al. Impaired Wnt/beta-catenin pathway leads to dysfunction of intestinal regeneration during necrotizing enterocolitis. *Cell Death Dis*. (2019) 10:743. doi: 10.1038/s41419-019-1987-1

Conflict of Interest: The authors declare that the research was conducted in the absence of any commercial or financial relationships that could be construed as a potential conflict of interest.

frontiers in Immunology

ORIGINAL RESEARCH
published: 15 April 2020
doi: 10.3389/fimmu.2020.00565

Rapid Gut Adaptation to Preterm Birth Involves Feeding-Related DNA Methylation Reprogramming of Intestinal Genes in Pigs

Xiaoyu Pan[1], *Thomas Thymann*[1], *Fei Gao*[1,2]* *and Per T. Sangild*[1,3,4]*

[1] *Comparative Pediatrics and Nutrition, Department of Veterinary and Animal Sciences, Faculty of Health and Medical Sciences, University of Copenhagen, Copenhagen, Denmark,* [2] *Genome Analysis Laboratory of the Ministry of Agriculture, Agricultural Genomics Institute at Shenzhen, Chinese Academy of Agricultural Sciences, Shenzhen, China,* [3] *Department of Neonatology, Rigshospitalet, Copenhagen, Denmark,* [4] *Department of Pediatrics, Odense University Hospital, Odense, Denmark*

Following preterm birth, the immature gut function and immunology must rapidly adapt to cope with bacterial colonization and enteral milk feeding. We hypothesized that intestinal epigenetic changes are involved in the gut response to preterm birth and the first feeding. Using piglets as models for infants, preterm, and term pigs were fed total parenteral nutrition (TPN) or partial enteral feeding for 5 days, followed by exclusive enteral feeding with bovine milk until day 26 (weaning age). Intestinal structure, function, microbiome, DNA methylome, and gene expressions were compared between preterm and term pigs on days 0, 5, and 26 (n = 8 in each group). At birth, the intestine of preterm pigs showed villus atrophy and global hypermethylation, affecting genes related to the Wnt signaling pathway. Hypermethylation-associated lowered expression of lipopolysaccharide-binding protein and genes related to the Toll-like receptor 4 pathway were evident during the first 5 days of life, but most early methylation differences disappeared by day 26. Regardless, sucrase and maltase activities (adult-type brush border enzymes) remained reduced, and the gut microbiota altered (fewer *Akkermansia*, more Lachnoclostridia and Lactobacilli) until day 26 in preterm pigs. During the 0- to 5-day period, many new preterm–term methylation differences appeared, but mainly when no enteral feed was provided (TPN feeding). These methylation differences affected intestinal genes related to cell metabolism, including increased GCK (glucokinase) expression via promoter hypomethylation. In conclusion, the immature intestine has a remarkable capacity to adapt its gene methylation and expression after preterm birth, and only few preterm-related defects persisted until weaning. Early enteral feeding may be important to stimulate the methylation reprogramming of intestinal genes, allowing rapid intestinal adaptation to preterm birth.

Keywords: preterm birth, small intestine, DNA methylation, nutrition, immunity, metabolism

OPEN ACCESS

Edited by:
Lijuan Yuan,
Virginia Tech, United States

Reviewed by:
Marie C. Lewis,
University of Reading, United Kingdom
Xiaofei Sun,
University of California, San Francisco, United States

***Correspondence:**
Fei Gao
flys828@gmail.com
Per T. Sangild
pts@sund.ku.dk

Specialty section:
This article was submitted to Nutritional Immunology, a section of the journal Frontiers in Immunology

Received: *20 December 2019*
Accepted: *12 March 2020*
Published: *15 April 2020*

Citation:
Pan X, Thymann T, Gao F and Sangild PT (2020) Rapid Gut Adaptation to Preterm Birth Involves Feeding-Related DNA Methylation Reprogramming of Intestinal Genes in Pigs. Front. Immunol. 11:565. doi: 10.3389/fimmu.2020.00565

INTRODUCTION

Preterm birth accounts for ∼10% of all live births and remains a major global health problem (1). For survival after preterm birth, the structure and function of the immature gut must rapidly adapt to the new nutritional and microbial environment. This adaptation may fail, or take some time to develop, as indicated by a high sensitivity to feeding intolerance, gut inflammation, and necrotizing

enterocolitis (NEC) in preterm infants during the first weeks after birth (2, 3). Later, children born preterm may show elevated risks of neurologic and metabolic disorders (4–7), whereas persistent gut complications are less often reported. Both short- and long-term gut complications may result from a combination of three critical factors, shortened gestational age at birth, premature transition to enteral feeding, and inappropriate bacterial colonization. Thus, the optimal dietary strategy (e.g., timing, volume, and type of diet) and most appropriate bacterial colonization of the immature gut remain unknown. A better understanding of how the immature gut interacts with environmental factors, such as nutrition and microbes, is required to define how early feeding strategies can best secure optimal adaptation of the preterm infant to postnatal life.

Adequate nutrient supply is critical for growth and organ development in preterm infants, but mother's milk is often insufficient or delayed in supply during the first weeks after preterm birth. Partial or total parenteral nutrition (TPN) is often used to support nutritional intake during the first 1–2 weeks, and this helps to combat the high sensitivity to feeding intolerance and NEC (8). On the other hand, lack of milk-derived immunomodulatory and trophic factors during TPN may compromise intestinal maturation (9, 10) and lead to more systemic infections and metabolic disorders (11). Preterm pigs, an animal model of preterm birth with a full range of prematurity signs (e.g., high sensitivity to NEC, sepsis, respiratory distress, neurological impairment, metabolic disorders) (12), respond to fast increases in enteral feeding (e.g., >120 mL/kg per day within few days) with marked intestine-trophic responses, but also with a high NEC sensitivity, especially when the diet is infant formula vs. more protective milk diets, such as sow's or cow's colostrum (12–14). The NEC risk is much less when enteral feeding is advanced slowly, in parallel with parenteral nutrition (15), similar to the situation for most preterm infants. There are differences in transfer of passive immunity between pigs and infants (e.g., immunoglobulin transferred postnatally via the gut in piglets vs. transplacental transport before birth in infants), but these differences do not appear to explain differences in NEC sensitivity (16). Even small volumes of formula may be detrimental in both preterm infants and pigs, and gradual feeding with natural milk or colostrum products may benefit intestinal maturation (15, 17, 18). Early enteral feeding (ENT) with small volumes is therefore recommended for preterm infants (10) despite that its diet dependency and the benefits vs. risks remain debated. It is therefore important to investigate the intestinal molecular functions affected by early TPN and early supplemental ENT feeding to understand the biological pathways and mechanisms of gut adaptation in preterm neonates. In an ongoing clinical trial in very preterm infants (ClinicalTrials.gov identifier NCT03085277), ENT with small volumes of bovine colostrum is being investigated.

As one of the important epigenetic mechanisms of tissue adaptation, DNA methylation plays a key role in sensing environmental exposures, thereby regulating transcription and cellular function during development (19). Because of the shortened gestation, intestines of preterm neonates may be subject to an accelerated adaptation after birth to adjust cellular functions, together with distinct DNA methylation profiles that reflect developmental immaturity at birth and postnatal exposure to enteral milk and microbes. We previously showed that formula feeding and bacterial colonization have marked short-term effects on intestinal DNA methylation in preterm pigs (18, 20), but it is not known if such changes are stable more long-term and ENT-dependent. Preterm–term comparisons of the intestinal methylome with advancing postnatal age help to elucidate if the phenotypic and molecular differences observed at birth may have long-term consequences for gut development in preterm neonates.

We hypothesized that the intestine of preterm neonates has a distinct epigenetic signature at birth and that DNA methylation changes in the postnatal period depending on the presence of ENT stimulation, to help adapt the immature intestine to postnatal life. Cesarean-delivered preterm or term pigs were euthanized for tissue collection shortly after birth or fed TPN or gradually increasing amounts of enteral nutrition (ENT) using bovine colostrum for 5 days, followed by transition to the same milk diet until day 26 (weaning age). The two feeding regimen, both of which minimize NEC risk (15), allowed us to examine how the immature intestine responded to the presence of enteral nutrition without confounded by NEC. Intestinal phenotypes (including morphology, digestive and absorptive function, microbiota composition), genome-wide DNA methylation, and targeted gene expression were compared between preterm and matched term pigs.

MATERIALS AND METHODS

Animal Experimental Procedure

All animal procedures were approved by the Danish National Committee on Animal Experimentation. One hundred sixty-eight piglets from eight sows (Danish Landrace × Large White × Duroc) were delivered by cesarean section at full term (day 118 or 100% gestation, n = 56 pigs from three sows) or preterm (day 106, 90% of gestation, $n = 112$ pigs from five sows) (21, 22). Based on immaturities in the intestine and other organs (e.g., lungs, liver, kidney, immunity), preterm 90% gestation pigs can be considered a relevant model for corresponding aspects in human infants delivered at ∼70% gestation (12). Immediately after cesarean section, all pigs were transferred to our piglet neonatal intensive care unit and reared in individual incubators. Within 3 h of delivery, all pigs were fitted with orogastric and umbilical arterial catheters. Preterm and term pigs were randomly assigned to be euthanized immediately after birth ($n = 8$, sodium pentobarbital, 200 mg/kg, intraarterial) or to receive total parental nutrition (TPN) or parenteral nutrition plus supplemental enteral nutrition (ENT) for 5 days. Total parenteral nutrition–treated pigs were given parenteral nutrition with gradually increasing volume (from 96 mL/kg per day on day 1– 114 mL/kg per day on day 5). Enteral feeding–treated pigs were given bovine colostrum with gradually increasing volume (from 16 mL/kg per day on day 1–64 mL/kg per day on day 5), accompanied by a reduction in parental nutrition, such that the two dietary regimens both provided similar fluid volumes and

were isoenergetic. In this setting, parental nutrition was infused continuously, while bovine colostrum was given every 3 h using the orogastric catheter. Importantly, the volume progression (16–64 mL/kg per day) was relatively slow, representing a careful approach to advance enteral nutrition.

On day 5, TPN and ENT pigs were randomly assigned to be euthanized for tissue collection or transitioned to full enteral nutrition with cow's milk, a gut-protective diet for preterm pigs (23), until euthanasia on day 26. For the latter ones, parental nutrition was discontinued on day 5, and pigs started to receive full enteral nutrition via a trough until the end of the study (8–10 feedings per day). During the period when pigs learned drinking milk from the trough (2–3 days), any remaining milk left in the trough was given to the pigs via the orogastric catheter. Therefore, during transition from TPN or partial ENT to full ENT, all pigs received the preplanned milk amount. All animals were reared individually throughout the study. Incubators with controlled ventilation and heating (from 0 to 5 days), larger home boxes (from 5 to 12 days), and even larger home cages (from 12 to 26 days) were used. All details of animal procedures were described previously (21, 22).

Consequently, intestinal tissues were collected on days 0, 5, and 26, from a total of 10 groups of pigs. Eight pigs from each group were randomly selected for this study (**Figure 1A**, total $n = 80$). Shortly before euthanasia, intestinal permeability was measured by the lactulose-mannitol technique, glucose

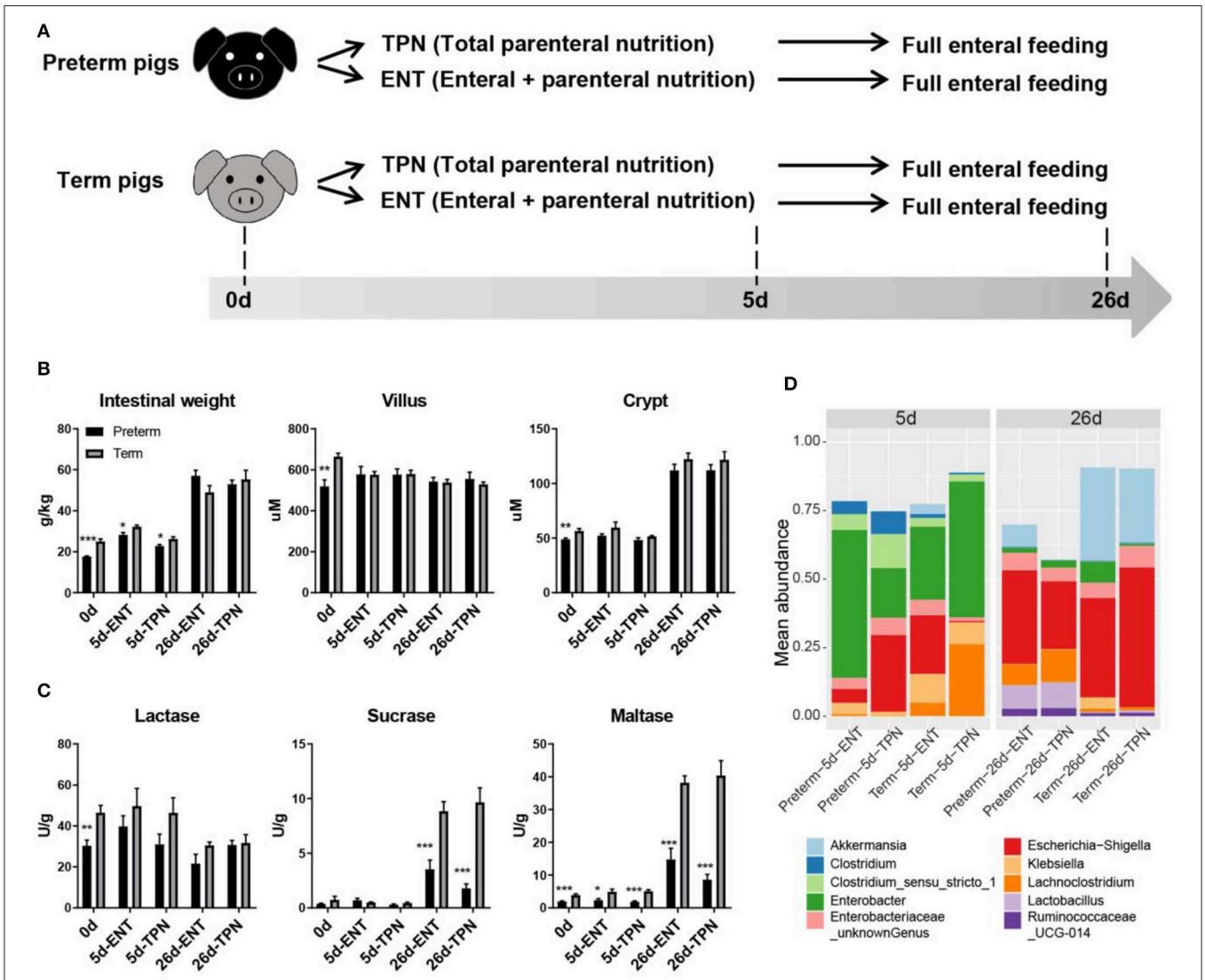

FIGURE 1 | Study design and intestinal phenotypes of preterm and term pigs. **(A)** Study design showing feeding regimens and sampling time points of preterm and term pigs ($n = 8$ from two to three litters in each group). **(B)** Intestinal morphology (i.e., weight, villus height, crypt depth), **(C)** digestive function (i.e., brush border enzymes activities), and **(D)** colon bacterial abundance between preterm and term pigs were compared. The top 10 abundant genera were plotted. Differential colon bacterial abundance was detected in *Akkermansia, Lachnoclostridia*, and *Lactobacilli* on day 26. Values in barplots **(B,C)** are presented as mean ± SEM. $^{*}P < 0.05$, $^{**}P < 0.01$, $^{***}P < 0.001$.

absorptive capacity by performing a galactose absorption test, plasma levels of glucose-dependent insulinotropic polypeptide (GIP) by radioimmunoassay, and diarrhea was evaluated by a diarrhea score, as described previously (22). Immediately after euthanasia, two 1-cm pieces of the middle of small intestine (jejunum, 50% along the length) were collected, snap frozen in liquid nitrogen, and kept at −80°C for subsequent analysis of enzyme activities, DNA methylome, and gene expression. Considering our aim to characterize the overall intestinal methylation differences, involving all interacting cell populations, we decided to analyze full-thickness intestine. Two additional full-thickness 1-cm sections of the middle intestine were fixed in 4% paraformaldehyde for later histological analysis. Luminal content from colon was collected for later microbiota analysis.

Intestinal Morphology and Enzyme Activity Analyses

To evaluate the mucosal morphology, two paraformaldehyde-fixed jejunum samples were embedded in paraffin, sectioned, mounted on slides, and stained with hematoxylin and eosin before measuring villus height and crypt depth as described previously (23). For each pig, villus height and crypt depth were measured from 10 representative well-oriented villus-crypt axes by ImageJ software, National Institutes of Health, USA. The mean of 10 villus heights and crypt depths were used as representative value for one pig. To estimate the proportion of epithelial cells in the middle small intestine, immunohistochemistry (IHC) using the epithelial cell marker (cytokeratin) was performed, and the proportion of the positive staining for cytokeratin in cross-sectional areas was calculated by the IHC toolbox in ImageJ. Finally, activities of brush border enzymes (lactase, maltase, and sucrase) were analyzed in homogenates of the middle intestinal tissues by spectrophotometry and were expressed as units per gram of wet tissue, as described previously (20, 22).

Reduced Representation Bisulfite Sequencing

Genomic DNA from the middle intestinal tissues was extracted using DNeasy Blood & Tissue Kit (Qiagen, Hilden, Germany) and was subjected to reduced representation bisulfite sequencing (RRBS), as previously described (24). Raw sequencing data were processed by the Illumina base-calling pipeline. Low-quality reads that contained more than 30% N's or >10% of the sequence with low-quality value (quality value <20) per read were omitted from the data analysis. Bisulfite sequence mapping program was used for sequence alignment to the Ensembl pig reference genome (Sscrofa10.2). Methylation level of individual cytosine was calculated as the ratio of sequenced depth of methylated cytosine to the total sequenced depth of the individual cytosine. One of 80 samples failed in RRBS and was excluded in DNA methylation analysis.

Gene Expression Analysis

Gene expression was analyzed as previously described (25). Briefly, total RNA was isolated from middle intestinal tissues ($n = 8$ in each group), using the RNeasy Mini Kit (Qiagen), and cDNA was synthesized using 2 μg total RNA by High-Capacity cDNA Reverse Transcription Kit (ThermoFisher, Waltham, MA, USA) according to the manufacturer's instructions. Primers for real-time quantitative polymerase chain reaction (RT-qPCR) were designed using Primer-BLAST. Real-time qPCR analysis was performed using QuantiTect SYBR Green PCR Kit (Qiagen) on LightCycler 480 (Roche, Basel, Switzerland), and results were analyzed according to double delta Ct method. Relative quantification of target genes was normalized to the housekeeping gene *HPRT1* and was presented as mean values ± SEM.

Microbiota Analysis

Total DNA was extracted, and the v3–v4 hypervariable regions of the 16S rRNA sequence were amplified through PCR. The resultant amplicons were sequenced using the Illumina MiSeq system (Illumina, San Diego, CA, USA), producing paired-end reads. The raw data set containing pair-ended reads was merged, trimmed, filtered from chimeric reads, and subjected to operational taxonomic units (OTUs) clustering using the UPARSE pipeline. Representative sequences were aligned to the SILVA reference alignment (version: SILVA123). The OTU annotation results were employed to determine the microbiota composition in the colon region of each pig.

Statistical Analysis

Comparisons of phenotypic variables (villus height, crypt depth, brush border enzyme activities, gene expressions) were made using Student *t*-test, and a two-tailed $p < 0.05$ was considered as statistically significant. Comparison of epithelial proportion was made using Mann–Whitney *U*-test, and a two-tailed $p < 0.05$ was considered as statistically significant. Differentially methylated regions (DMRs) were identified as previously described (20). Briefly, the methylation levels between the two groups were tested using the Mann–Whitney *U*-test, and false discovery rate (FDR) of DMRs was controlled at level 0.05 with the Benjamini–Hochberg procedure. For microbiome analysis, Shannon diversity differences were tested using Mann–Whitney *U*-test, and a two-tailed $p < 0.05$ was considered statistically significant. Comparisons of relative abundance were made using Mann–Whitney *U*-test, and all *p*-values were adjusted for multiple comparisons with FDR correction.

RESULTS

Intestinal Morphology, Digestive Function, and Gut Microbiota Differ Between Preterm and Term Pigs

Preterm pigs had lower relative intestinal weight than term pigs at birth (17.7 ± 0.3 vs. 25.0 ± 1.3 g/kg, $p < 0.05$) and day 5 (28.3 ± 1.1 vs. 32.2 ± 0.8 g/kg for ENT, 22.8 ± 0.8 vs. 26.2 ± 1.1 g/kg for TPN, both $p < 0.05$), but not at weaning (57.1 ± 2.7 vs. 49.0 ± 3.4 g/kg for ENT, 53.0 ± 2.0 vs. 55.3 ± 4.5 g/kg for TPN, both $p > 0.05$; **Figure 1B**). Villus height in the middle intestine was similar among 0-, 5-, and 26-day-old pigs (586.2 ± 27.8 μm for 0 days, 577.5 ± 13.2 μm for 5 days, 541.4 ± 10.2 μm for 26 days, $p > 0.05$). Crypt depth was similar between 0- and

5-day-old pigs (52.4 ± 1.6 vs. 52.7 ± 1.5 μm, $p > 0.05$), but there was a sharp increase from days 5 to 26 (52.7 ± 1.5 vs. 117.0 ± 3.0 μm, $p < 0.0001$; **Figure 1B**). Only at birth did preterm pigs show shorter villi (519.0 ± 32.3 vs. 664.6 ± 16.3 μm, $p < 0.01$) and crypts (48.9 ± 1.1 vs. 56.5 ± 2.1 μm, $p < 0.01$) than term pigs. The proportion of epithelial cells (59% on average), as estimated by IHC staining of cross sections of the intestine, was similar between the preterm and term pigs ($p > 0.05$), and regardless of age. For activity of brush border enzymes in the middle intestine, lactase was high relative to sucrase and maltase at birth (37.9 ± 3.0 vs. 0.6 ± 0.2 and 2.9 ± 0.3 U/g, both $p < 0.0001$). Preterm pigs had lower lactase activity than term pigs at birth (30.4 ± 2.7 vs. 46.5 ± 3.5 U/g, $p < 0.01$; **Figure 1C**). Sucrase and maltase activities increased markedly from days 5 to 26 (0.5 ± 0.1 vs. 6.0 ± 0.8 U/g and 3.6 ± 0.4 vs. 25.5 ± 2.9 U/g, respectively, both $p < 0.0001$), but remained to be lower in preterm than term pigs (2.7 ± 0.5 vs. 9.3 ± 0.8 U/g and 11.7 ± 2.0 vs. 39.3 ± 2.4 U/g, respectively, both $p < 0.001$; **Figure 1C**). Despite their immature state at birth, preterm pigs had similar gut permeability, glucose absorptive capacity, and diarrhea scores as term pigs during the postnatal period (data not shown). No preterm or term pigs showed any signs of NEC. Analyses of the colon microbiota by 16s rRNA gene sequencing showed no difference in alpha diversity or relative abundances of genera between preterm and term pigs on day 5, due to large individual variation. However, on day 26, the preterm pigs had lower abundance of *Akkermansia* (4.0 vs. 30.7%) and higher abundance of *Lachnoclostridium* (9.6 vs. 1.1%) and *Lactobacillus* (9.1 vs. 0.7%, all adjusted $p < 0.05$), compared with term pigs (**Figure 1D**). Except that early ENT feeding significantly increased the relative intestinal weight in both groups on day 5 (28.30 ± 1.09 vs. 22.77 ± 0.76 for preterms and 32.23 ± 0.80 vs. 26.23 ± 1.09 for terms, both $p < 0.001$), none of the other measured phenotypic characteristics of the gut were consistently affected by ENT vs. TPN feeding.

The Intestinal DNA Methylome Is Hypermethylated at Birth in Preterm Pigs

A total of 39.7 mio reads per sample were generated from RRBS (mean across samples). Among the reads passing QC (∼33.8 mio/sample), 67.7% could be mapped to the Ensembl pig reference genome (Sscrofa10.2, **Table S1**). DNA methylation mainly occurred on CpG cytosines (mean methylation level, $m = 60.4\%$), rather than CHG ($m = 0.7\%$) or CHH cytosines ($m = 0.6\%$). Thus, only CpG cytosines were analyzed thereafter. To avoid the potentially confounding influence of X chromosome inactivation on DNA methylation patterns between male and female pigs, only autosomal data were used. A total of 1,772,546 CpG cytosines detected in 10 groups of pigs were used for analysis.

Based on the individual cytosines, principal component analysis (PCA) showed that intestinal DNA methylomes were distinct for each age group. Moreover, the preterm and term groups remained separated postnatally (**Figure 2A**). Next, we started with a comprehensive genome-wide characterization of the intestinal CpG methylation in preterm and term pigs at birth (before any feeding). Similar to other mammalian DNA methylation landscape (26), the overall DNA methylation level of the gene body, that is, the genomic region from transcription start site (TSS) of a gene to its transcription end site (TES), was higher than that of adjacent intergenic regions (72.5 vs. 41.8%, $p < 0.0001$), and there was a marked hypomethylation (7.4%) around the TSS (**Figure 2B**, **Table S2**). The preterm intestines showed global hypermethylation compared to the term group (64.3 vs. 63.6%, paired Mann–Whitney *U*-test $p < 0.0001$; **Figure 2B**). A total of 103 genomic regions were identified as significantly DMRs between preterm and term pigs (**Figure 2C**, **Table S3**). There were more hypermethylated DMRs ($n = 82$) than hypomethylated DMRs ($n = 21$). These DMRs included 941 CpG cytosines, equivalent to 0.05% of all the cytosines analyzed. In preterm pigs, 76% of these cytosines showed relative hypermethylation, and 37% was highly methylated (methylation level >75%).

Among the total 103 DMRs, 59 overlapped with genic regions, particularly in introns. Fifty-five genes contained at least one DMR in either their putative promoters or the gene bodies. Genes that contained DMR in their putative promoter included BHLHA9, SLC5A10, COX17, lipopolysaccharide-binding protein (LBP), STK11, CPTP, RD3L, FGFR3, C4orf46, NAP1L5, and ZPBP. Gene ontology enrichment analysis on all the 55 genes resulted in multiple biological processes, including steroid hormone receptor activity and canonical Wnt signaling pathway (**Table S4**). STK11 (also called LKB1) was involved in canonical Wnt signaling pathway that is important for epithelium development (27) and possessed a DMR in the putative promoter where methylation level was higher in preterm vs. term newborns (74 vs. 50%). Consistent with that promoter methylation may suppress gene expression, the mRNA expression of STK11 was down-regulated in the preterm newborns (0.7-fold, $p < 0.001$; **Figure 2D**). Similar to that the villus height and crypt depth differed between preterm and term pigs only at birth, differential methylation and gene expression of STK11 were detected at birth, but not on day 5 or 26.

Persistent Abnormal Methylation and Expression of Intestinal Genes Related to Innate Immunity

To investigate whether the observed differences of intestinal methylation between preterm and term newborns persist into the postnatal period, DMRs in 5- and 26-day-old pigs, fed either TPN or ENT during the first 5 days, were identified and compared with the 103 DMRs detected at birth. Only 6 and 28 of the 103 newborn DMRs persisted until day 5 in ENT- or TPN-feeding groups, respectively. On day 26, just before weaning, all the DMRs detected at birth were no longer different between preterm and term pigs (**Figure 2E**). The 34 DMRs that lasted until day 5 in preterm pigs were associated with 13 genes, of which four genes (LBP, LHPP, NR3C1, WHSC1) were identified both in the ENT and TPN groups. The remaining nine intestinal genes with preterm–term gene methylation differences that lasted until day 5 were found only among TPN-fed pigs.

Among the above four common genes containing persistent DMRs until day 5, only LBP (lipopolysaccharide binding protein) contained a DMR within its putative promoter region, showing

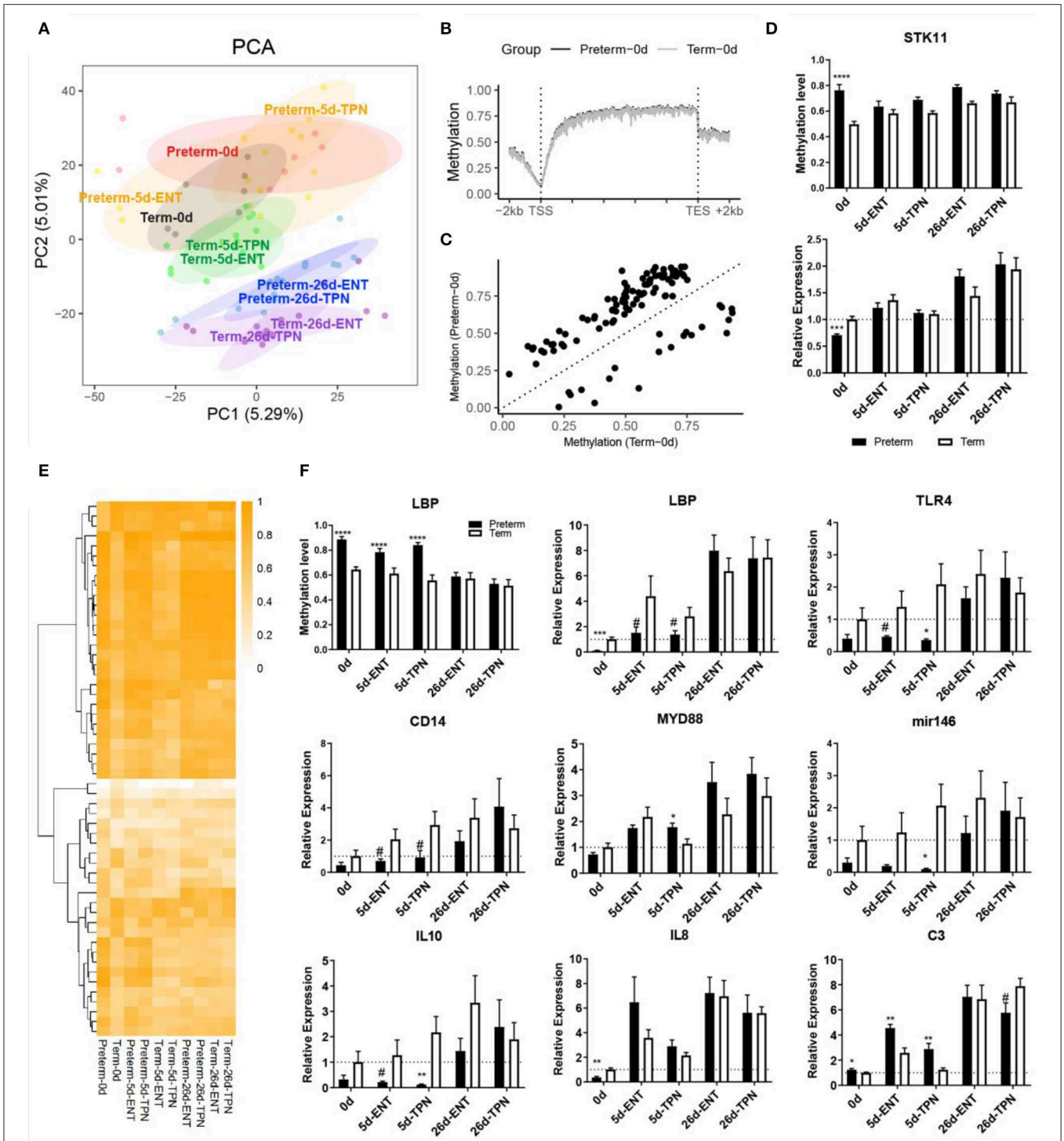

FIGURE 2 | DNA methylation and gene expression difference at birth and their postnatal changes. **(A)** Scores of first two principle components from PCA are plotted, with ellipses for the 80% confidence interval for each group. Pigs with the same age after either preterm or term delivery are labeled with the same colors. **(B)** Birth DNA methylation levels along the gene bodies and 2-kb upstream of the TSS and 2-kb downstream of the TES of all Ensembl genes. **(C)** Scatterplot showing mean methylation level of DMRs in preterm and term pigs at birth. **(D)** Barplot showing promoter methylation level and mRNA expression of STK11. **(E)** Heatmap depicting methylation level of birth DMRs in postnatal period. Hierarchical clustering was performed using complete linkage method with euclidean distance. **(F)** Barplot showing promoter methylation level and mRNA expression of LBP, and mRNA expression of immunity-related genes. Values in barplots are presented as mean ± SEM. $^{\#}P < 0.1$, $^{*}P < 0.05$, $^{**}P < 0.01$, $^{***}P < 0.001$, $^{****}P < 0.0001$.

hypermethylation in preterm pigs (89 vs. 64% at birth and 84 vs. 57% by day 5; **Figure 2F**). The mRNA expression of LBP was negatively correlated with its promoter methylation level (Spearman $\rho = -0.54$, $p < 0.0001$) and was less expressed in preterm vs. term pigs at birth (0.1-fold, $p < 0.001$) and day 5 (0.3-fold for ENT, 0.5-fold for TPN, both $p < 0.1$; **Figure 2F**). Lipopolysaccharide-binding protein is important for initiating Toll-like receptor 4 (TLR4) signaling, which is essential for neonatal intestinal immune tolerance (28) and was proposed to impact the risk of NEC in preterm infants (29). Thus, expression of genes involved in TLR4 signaling was also examined. Similar to LBP, both TLR4 and the accessory protein CD14 tended to be less expressed in 5-day-old preterm vs. term pigs (both 0.3-fold, $p < 0.1$). MYD88, which mediates signal transduction for TLR4, was comparable between preterm and term pigs or even up-regulated in TPN-fed 5-day-old preterm pigs (1.6-fold, $p < 0.05$; **Figure 2F**). Moreover, microRNA-146a and interleukin 10 (IL-10), representative for intestinal anti-inflammation, were less expressed in 5-day-old preterm pig, especially those fed TPN (0.05- and 0.06-fold, respectively, both $p < 0.05$), whereas proinflammatory cytokine IL-8 was less expressed in preterm pigs at birth (0.4 fold, $p < 0.01$) and increased to a similar level to that in term pigs on day 5 (**Figure 2F**). C3 that is involved in complement cascade, another component of the innate immune response, showed persistent overexpression in preterm vs. term pigs from birth (1.2-fold) to day 5 (1.8-fold for ENT, 2.3-fold for TPN, all $p < 0.05$; **Figure 2F**).

Another DMR was located within a CpG island in the gene body region of NR3C1 encoding for the glucocorticoid receptor (GR), which may interfere with TLR4 signaling. This DMR showed hypermethylation in preterm vs. term pigs (89 vs. 69% at birth and 90 vs. 70% on day 5), but the DNA methylation level was not correlated with gene expression (Spearman $\rho = 0.15$, $p > 0.05$). Except that C3 was up-regulated by ENT vs. TPN during the first week regardless of gestation (1.6-fold for preterm, 2.1-fold for term, both $p < 0.05$), no differences in DNA methylation or mRNA expression in the above genes were detected between the ENT- and TPN-treated pigs.

Reprogramming of the Intestinal DNA Methylome in Preterm Neonates Is Feeding-Dependent

Although most of the DNA methylation differences observed at birth disappeared by day 5 and especially day 26, PCA showed persistent separation between the preterm and term groups in postnatal period (**Figure 2A**). A detailed look into the four postnatal groups of DMRs, that is, 5d-ENT, 5d-TPN, 26d-ENT, and 26d-TPN pigs, revealed a number of new postnatal DMRs that did not overlap with the DMRs detected at birth. On day 5, there were more new DMRs in the TPN group ($n = 800$) than in the ENT group ($n = 60$; **Figure 3A**, **Tables S5, S6**). The 800 new DMRs in the TPN group consisted of 6,767 CpG cytosines, equivalent to 0.38% of all the cytosines analyzed. Approximately 89% of the involved cytosines showed hypermethylation in the preterm group. These 800 TPN-specific DMRs overlapped with putative promoters of 54 genes and gene bodies of 255 genes.

Pathway enrichment analysis based on all the genes containing the TPN-specific DMRs revealed nine KEGG pathways being significantly enriched (**Figure 3B**, **Table S7**), including multiple metabolic pathways (e.g., galactose metabolism, amino sugar, and nucleotide sugar metabolism). Among the 20 genes involved in the above nine KEGG pathways, one gene (GCK, encoding glucokinase) was involved in multiple pathways and had a DMR located within its putative promoter region, where methylation level was correlated with gene expression (Spearman $\rho = -0.54$, $p < 0.01$). Glucokinase showed promoter hypomethylation (51 vs. 75%) and increased gene expression in 5-day-old TPN-fed preterm vs. term pigs (1.7-fold, $p < 0.05$; **Figure 3C**). This GCK expression also correlated negatively with the plasma level of GIP, a sensor for luminal glucose (30) ($p < 0.0001$, $r = -0.52$; **Figure 3D**). To explore additional effects of the gene methylation–regulated intestinal GCK, a protein–protein interaction analysis with the remaining 19 genes involved in the enriched pathways was performed. Result showed that GCK was directly or indirectly related to seven genes (GMPPA, GMDS, GALE, GALK1, PPARA, PPARD, and FABP1).

Next, to examine whether the new postnatal preterm–term methylation difference persisted until weaning, we searched for overlapped DMRs in 5- and 26-day groups. The result revealed only two genes (ZIP4 and DTX4), which showed no methylation difference at birth. However, hypermethylation of these two genes occurred after 5 days of TPN (but not ENT) feeding (55 vs. 31% for ZIP4, 59 vs. 34% for DTX4), and hypermethylation persisted until 26 days (56 vs. 39% for ZIP4, 61 vs. 39% for DTX4), although all pigs received full ENT from 5 to 26 days (**Figure 3E**). Subsequent analysis of mRNA expression of these two genes showed hypermethylation-associated down-regulation in TPN-fed preterm pigs on day 5 (0.1-fold for ZIP4, 0.2-fold for DTX4, both $p < 0.05$), but not day 26 (**Figure 3E**).

On day 26, the number of new DMRs in the TPN group ($n = 31$) was similar to that in the ENT group ($n = 39$), and these were associated with a similar number of genes (14 and 15 for TPN and ENT, respectively, **Tables S8, S9**). In both ENT and TPN groups, DMRs associated with CAMK2G, BRD3, and BAHCC1 were detected. Methylation level of DMRs in these three genes was higher (79 vs. 53% for CAMK2G, 81 vs. 53% for BRD3, and 69 vs. 40% for BAHCC1) in preterm vs. term pigs on day 26. As sucrase activity differed between preterm and term pigs only on day 26, correlation between sucrase activity and the methylation of these three genes was analyzed using all pigs. Significant negative correlation was found (all Spearman $\rho < -0.6$, $p < 0.0001$). In summary, the above results described a feeding-dependent DNA methylation reprogramming pattern in the neonatal intestine following preterm birth.

DISCUSSION

Perinatal intestinal maturation is determined by intrinsic genetic mechanisms (a predetermined "biological clock"), as well as external stimuli, including the birth process, nutrition, and microbes. When born preterm, the intestine needs to rapidly adapt to tolerate the transition from parenteral to enteral

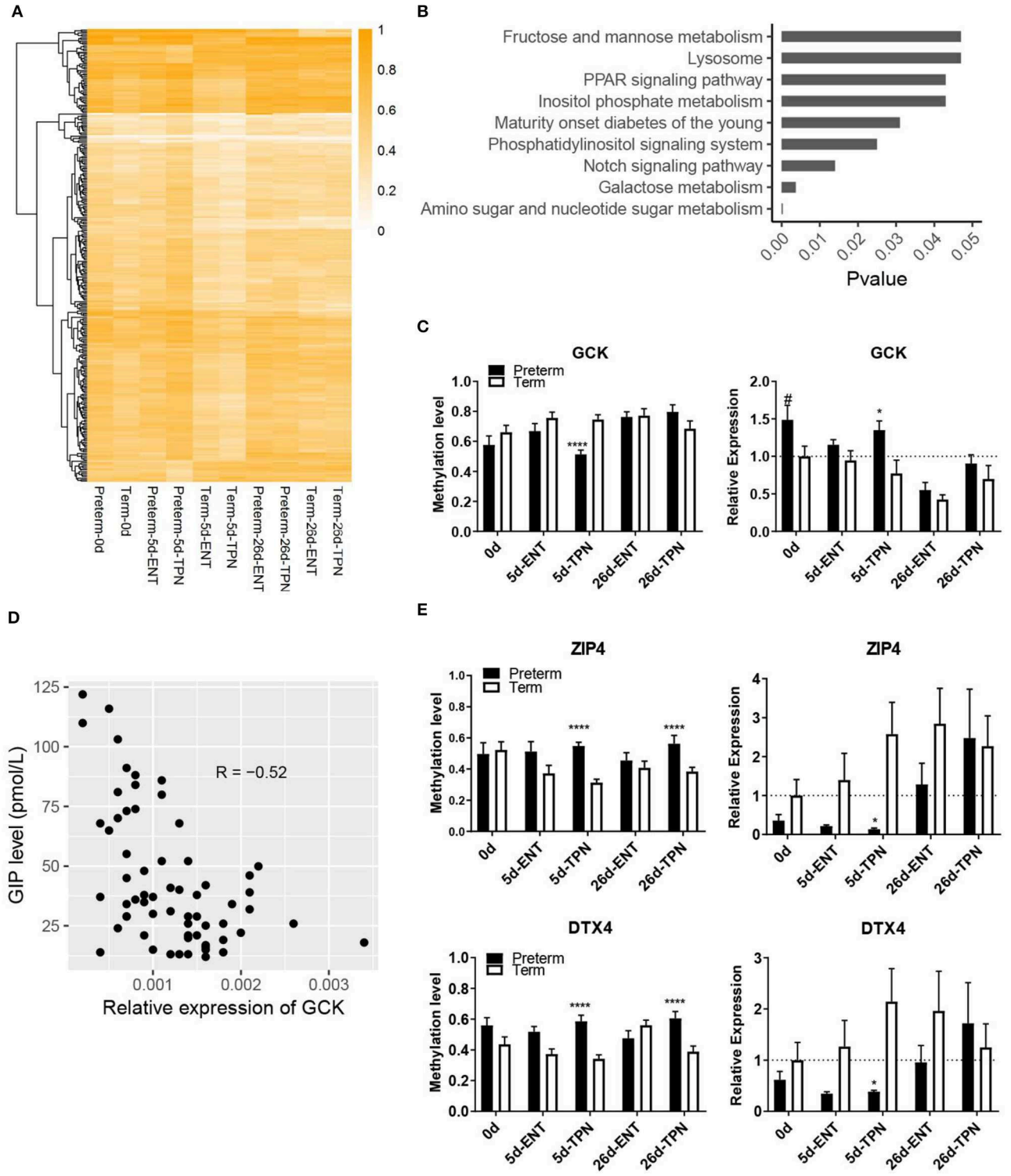

FIGURE 3 | Methylation differences between preterm and term intestines after birth. **(A)** Heatmap depicting methylation level of DMRs that present in postnatal period. Hierarchical clustering was performed using complete linkage method with euclidean distance. **(B)** KEGG pathways enriched from genes with TPN-specific DMRs. **(C)** Barplots showing methylation level of the DMR and mRNA expression of GCK. Values in barplots are presented as mean ± SEM. $^{\#}P < 0.1$, $^{*}P < 0.05$, $^{**}P < 0.01$, $^{***}P < 0.001$. **(D)** Scatterplot illustrating the correlation between mRNA expression of GCK in the small intestine and plasma GIP level. **(E)** Barplots showing methylation level of the DMR and mRNA expression of ZIP4 and DTX4. Values in barplots are presented as mean ± SEM. $^{*}P < 0.05$, $^{**}P < 0.01$, $^{***}P < 0.001$, $^{****}P < 0.0001$.

nutrition while avoiding NEC. Total parenteral nutrition or parenteral nutrition together with small volume of natural milk or colostrum is NEC-protective in preterm infants (31) and preterm pigs (15). It is critical to understand the molecular mechanisms that make the preterm intestine adapt, or fail to adapt, and characterize the subclinical differences between these two feeding regimen. Considering that DNA methylation can be affected by nutrition and plays a key role in regulating gene expression, our study provides new knowledge on feeding-dependent intestinal adaptation in preterm neonates. We show that reduced gestational age at birth (independent of other birth-related factors) is associated with a marked hypermethylation of intestinal genes that largely disappears by weaning. The two NEC-protective feeding regimens used in this study for the first 5 days (TPN, ENT) modulated the immune response in similar ways, but differed in their effects on specific genes related to intestinal metabolism. Preterm birth and the early diet differences may not have major long-lasting effects on intestinal functions, as indicated by the limited number of persistent gene methylation changes. However, it cannot be excluded that a more NEC-provocative early feeding regimen, using fast advancement of infant formula, would have more lasting effects on gene expressions and its regulation by gene methylation differences.

The global intestinal hypermethylation at preterm birth included a key gene, STK11/LKB1, which is a tumor suppressor gene in the Wnt/β-catenin pathway to regulate intestinal epithelial cells apoptosis and control cell proliferation (32). Here we showed that at preterm birth the immature intestine had shorter villus height and crypt depth, together with less expression of STK11 via promoter hypermethylation. The down-regulation of STK11 in the immature intestine may facilitate intestinal epithelial cell growth after preterm birth, and consistently, difference in the villus height and crypt depth disappeared within the first week of life. Thus, our results suggest that DNA methylation plays an important role in helping the immature intestine to adapt to postnatal life, both when fed enterally and parenterally during the first day after birth.

Intestinal hypermethylation in preterm neonates included another key gene related to innate immunity, LBP, and hypermethylation of its promoter-reduced LBP mRNA expression within the first week in preterm vs. term newborns. Lipopolysaccharide-binding protein presents LPS to host cells through TLR4 (33), and we previously showed that the expression of LBP is positively correlated with bacterial adherence to the intestinal epithelium in preterm pigs (18). Reduced neonatal LBP expression following preterm birth may indicate for an immature gut immunity in preterm pigs, also reflected by reduced expression of genes in the TLR4 signaling pathway. In mice pups, the newborn intestine develops tolerance to LPS stimulation by expressing TLR4-dependent microRNA-146a, which represses the TLR4 signaling molecule IRAK1 and prevents nuclear factor κB (NF-κB) translocation (28). Correspondingly, we found that TLR4 and its accessory protein CD14 as well as microRNA-146a, but not MYD88, were down-regulated in the preterm intestine by day 5, probably leading to impaired LPS tolerance in an MYD88-independent manner. Consistently, the anti-inflammatory cytokine IL-10, which could be induced by microRNA-146a (34), was also less expressed in the preterm intestine by day 5. The proinflammatory cytokine IL-8 (a NF-κB target gene) was less expressed in the preterm intestine at birth but increased to a level comparable to that in term pigs already by day 5. In addition, C3, which is central for activation of the complement system, was persistently higher expressed in the preterm vs. term intestine during the first week. These results suggest that preterm birth is a risk factor for the immature intestine via an immature TLR4 signaling pathway, regardless of the initial feeding regimen (TPN or ENT) and at least partly regulated by epigenetic changes. It is important to note that both feeding regimens in the current study were NEC-protective (TPN or ENT with bovine colostrum). Only when fed infant formula, LBP expression increases more markedly in response to bacterial contact and results in much lower microRNA-146a, as well as much higher C3 levels, as shown previously (18). This helps to explain the well-known difference in NEC risk among TPN-, colostrum-, and formula-fed preterm newborn pigs and infants.

Unlike in the case of LBP, hypermethylation of NR3C1, encoding GR, was observed in the gene body with no difference in mRNA expression between newborn preterm and term pigs. Hypermethylation of NR3C1 in the preterm intestine may be associated with lack of cortisol stimulation before preterm birth, because methylation of this gene is sensitive to cortisol and stress responses (35). In both pigs and humans, circulating glucocorticoid levels increase markedly prior to term (36) to regulate final maturation of many organ functions, including the intestine (37, 38). A better understanding of the potential regulatory role of methylation in NR3C1 gene body is required.

While most newborn intestinal methylation defects in preterm pigs disappeared rapidly postnatally, novel preterm–term differences were identified, especially in relation to metabolic pathways in 5-day-old pigs fed TPN. These TPN-specific methylation changes covered 0.38% genome-wide cytosines, which were much more than that detected at birth (0.05%). Pathway enrichment analysis identified one gene, GCK (glucokinase), whose promotor hypomethylation likely upregulated the corresponding GCK transcription in TPN-treated preterm pigs. This may reflect a specific adaptation of the preterm TPN-fed intestine to facilitate glucose metabolism (relative to fat and amino acid metabolism). The inverse correlation with circulating GIP levels, an important sensor to luminal glucose (30), supports this hypothesis. In addition, protein–protein interaction analysis indicated that GCK might interact with PPARA (peroxisome proliferator-activated receptor α) and FABP1 (fatty acid binding protein 1), both of which are major regulators of fatty acid metabolism (39–41) and showed aberrant DNA methylation in TPN-fed preterm pigs. Thus, gene methylation of GCK may help to adapt intestinal nutrient metabolism in preterm neonates during the important transition from parenteral to enteral nutrition. Despite the marked feeding-dependent DNA methylation reprogramming in the first week of life, the intestinal DNA methylation in preterm neonates converges toward the pattern observed in term counterparts, with advancing postnatal age and transition to full ENT.

The present study used whole intestinal tissue samples, not isolated cell types (e.g., enterocytes) for DNA methylation analysis. This approach likely better represents the *in vivo* state of the intestine with many different cell types interacting during development and in response to feeding and diseases. On the other hand, this approach limited our ability to identify cell type–specific methylation changes associated with preterm birth and early feeding regimens. As DNA methylation is known to vary across cell types (42), changes in the intestinal cell composition may also contribute to DNA methylation changes in the intestinal tissue. However, as we did not observe any difference in the proportion of epithelial cells between preterm and term pigs along development, the reported DNA methylation differences are unlikely to be due to major changes in relative cell compositions.

In conclusion, the preterm intestine has a remarkable capacity to adapt to postnatal life, and this may involve highly dynamic gene methylation changes. At preterm birth, the intestinal epigenetic patterns may reflect incomplete fetal programming associated with immature morphology, digestive capacity and elevated risk of inflammation. The immature intestine has a high reprogramming capacity, involving both immunological and metabolic plasticity. The first week after preterm birth is an important window of opportunity, and early and gradual introduction of protective milk diets (e.g., mother's own milk or colostrum) may be important to facilitate optimal adaptation.

DATA AVAILABILITY STATEMENT

The data sets generated for this study can be found in the NCBI Gene Expression Omnibus (GEO) with accession GSE108284.

ETHICS STATEMENT

The animal study was reviewed and approved by the Danish National Committee on Animal Experimentation.

AUTHOR CONTRIBUTIONS

XP and FG analyzed and interpreted the data. XP, FG, and PS were major contributors in writing the manuscript. TT took part in the main study design. All authors read and approved the final manuscript.

FUNDING

This work was supported by the Innovation Foundation Denmark NEOMUNE project (PS), the Agricultural Science and Technology Innovation Program (ASTIP) of China (FG), and the China Scholarship Council (XP).

ACKNOWLEDGMENTS

We thank Anders Daniel Andersen, Jane Povlsen, and Karina Ryom for their support to animal procedures, and Elin Skytte, Kristina Møller, Duc Ninh Nguyen, Jens Juul Holst, and Bolette Hartmann for support to laboratory analyses.

SUPPLEMENTARY MATERIAL

The Supplementary Material for this article can be found online at: https://www.frontiersin.org/articles/10.3389/fimmu.2020.00565/full#supplementary-material

REFERENCES

1. Beck S, Wojdyla D, Say L, Betran AP, Merialdi M, Requejo JH, et al. The worldwide incidence of preterm birth: a systematic review of maternal mortality and morbidity. *Bull World Health Organ.* (2010) 88:31–8. doi: 10.2471/BLT.08.062554
2. Ward RM, Beachy JC. Neonatal complications following preterm birth. *BJOG.* (2003) 110(Suppl 20):8–16. doi: 10.1046/j.1471-0528.2003.00012.x
3. Siggers RH, Siggers J, Thymann T, Boye M, Sangild PT. Nutritional modulation of the gut microbiota and immune system in preterm neonates susceptible to necrotizing enterocolitis. *J Nutr Biochem.* (2011) 22:511–21. doi: 10.1016/j.jnutbio.2010.08.002
4. Marlow N, Wolke D, Bracewell MA, Samara M, Group EPS. Neurologic and developmental disability at six years of age after extremely preterm birth. *N Engl J Med.* (2005) 352:9–19. doi: 10.1056/NEJMoa041367
5. Moster D, Lie RT, Markestad T. Long-term medical and social consequences of preterm birth. *N Engl J Med.* (2008) 359:262–73. doi: 10.1056/NEJMoa0706475
6. Wang G, Divall S, Radovick S, Paige D, Ning Y, Chen Z, et al. Preterm birth and random plasma insulin levels at birth and in early childhood. *JAMA.* (2014) 311:587–96. doi: 10.1001/jama.2014.1
7. Kajantie E, Strang-Karlsson S, Hovi P, Wehkalampi K, Lahti J, Kaseva N, et al. Insulin sensitivity and secretory response in adults born preterm: the Helsinki Study of Very Low Birth Weight Adults. *J Clin Endocrinol Metab.* (2015) 100:244–50. doi: 10.1210/jc.2014-3184
8. Heird WC, Gomez MR. Total parenteral nutrition in necrotizing enterocolitis. *Clin Perinatol.* (1994) 21:389–409. doi: 10.1016/S0095-5108(18)30352-X
9. Kudsk KA. Current aspects of mucosal immunology and its influence by nutrition. *Am J Surg.* (2002) 183:390–8. doi: 10.1016/S0002-9610(02)00821-8
10. Neu J. Gastrointestinal development and meeting the nutritional needs of premature infants. *Am J Clin Nutr.* (2007) 85:629S–34S. doi: 10.1093/ajcn/85.2.629S
11. Stoll B, Horst DA, Cui L, Chang X, Ellis KJ, Hadsell DL, et al. Chronic parenteral nutrition induces hepatic inflammation, steatosis, and insulin resistance in neonatal pigs. *J Nutr.* (2010) 140:2193–200. doi: 10.3945/jn.110.125799
12. Sangild PT, Thymann T, Schmidt M, Stoll B, Burrin DG, Buddington RK. Invited review: the preterm pig as a model in pediatric gastroenterology. *J Anim Sci.* (2013) 91:4713–29. doi: 10.2527/jas.2013-6359
13. Sangild PT, Siggers RH, Schmidt M, Elnif J, Bjornvad CR, Thymann T, et al. Diet- and colonization-dependent intestinal dysfunction predisposes to necrotizing enterocolitis in preterm pigs. *Gastroenterology.* (2006) 130:1776–92. doi: 10.1053/j.gastro.2006.02.026
14. Bjornvad CR, Thymann T, Deutz NE, Burrin DG, Jensen SK, Jensen BB, et al. Enteral feeding induces diet-dependent mucosal dysfunction, bacterial proliferation, and necrotizing enterocolitis in preterm pigs on parenteral nutrition. *Am J Physiol Gastrointest Liver Physiol.* (2008) 295:G1092–103. doi: 10.1152/ajpgi.00414.2007
15. Shen RL, Thymann T, Ostergaard MV, Stoy AC, Krych L, Nielsen DS, et al. Early gradual feeding with bovine colostrum improves gut function and NEC resistance relative to infant formula in preterm pigs. *Am J Physiol Gastrointest Liver Physiol.* (2015) 309:G310–23. doi: 10.1152/ajpgi.00163.2015
16. Sangild PT. Gut responses to enteral nutrition in preterm infants and animals. *Exp Biol Med.* (2006) 231:1695–711. doi: 10.1177/153537020623101106

17. Willems R, Krych L, Rybicki V, Jiang P, Sangild PT, Shen RL, et al. Introducing enteral feeding induces intestinal subclinical inflammation and respective chromatin changes in preterm pigs. *Epigenomics*. (2015) 7:553–65. doi: 10.2217/epi.15.13
18. Pan X, Gong D, Gao F, Sangild PT. Diet-dependent changes in the intestinal DNA methylome after introduction of enteral feeding in preterm pigs. *Epigenomics*. (2018) 10:395–408. doi: 10.2217/epi-2017-0122
19. Reik W. Stability and flexibility of epigenetic gene regulation in mammalian development. *Nature*. (2007) 447:425–32. doi: 10.1038/nature05918
20. Pan X, Gong D, Nguyen DN, Zhang X, Hu Q, Lu H, et al. Early microbial colonization affects DNA methylation of genes related to intestinal immunity and metabolism in preterm pigs. *DNA Res*. (2018) 25:287:96. doi: 10.1093/dnares/dsy001
21. Andersen AD, Sangild PT, Munch SL, van der Beek EM, Renes IB, Ginneken C, et al. Delayed growth, motor function and learning in preterm pigs during early postnatal life. *Am J Physiol Regul Integr Comp Physiol*. (2016) 310:R481–92. doi: 10.1152/ajpregu.00349.2015
22. Hansen CF, Thymann T, Andersen AD, Holst JJ, Hartmann B, Hilsted L, et al. Rapid gut growth but persistent delay in digestive function in the postnatal period of preterm pigs. *Am J Physiol Gastrointest Liver Physiol*. (2016) 310:G550–60. doi: 10.1152/ajpgi.00221.2015
23. Li Y, Jensen ML, Chatterton DE, Jensen BB, Thymann T, Kvistgaard AS, et al. Raw bovine milk improves gut responses to feeding relative to infant formula in preterm piglets. *Am J Physiol Gastrointest Liver Physiol*. (2014) 306:G81–90. doi: 10.1152/ajpgi.00255.2013
24. Meng M, Li X, Ge H, Chen F, Han M, Zhang Y, et al. Noninvasive prenatal testing for autosomal recessive conditions by maternal plasma sequencing in a case of congenital deafness. *Genet Med*. (2014) 16:972–6. doi: 10.1038/gim.2014.51
25. Li Y, Nguyen DN, de Waard M, Christensen L, Zhou P, Jiang P, et al. Pasteurization procedures for donor human milk affect body growth, intestinal structure, and resistance against bacterial infections in preterm pigs. *J Nutr*. (2017) 147:1121–30. doi: 10.3945/jn.116.244822
26. Guo H, Zhu P, Yan L, Li R, Hu B, Lian Y, et al. The DNA methylation landscape of human early embryos. *Nature*. (2014) 511:606–10. doi: 10.1038/nature13544
27. van der Flier LG, Clevers H. Stem cells, self-renewal, and differentiation in the intestinal epithelium. *Annu Rev Physiol*. (2009) 71:241–60. doi: 10.1146/annurev.physiol.010908.163145
28. Chassin C, Kocur M, Pott J, Duerr CU, Gutle D, Lotz M, et al. miR-146a mediates protective innate immune tolerance in the neonate intestine. *Cell Host Microbe*. (2010) 8:358–68. doi: 10.1016/j.chom.2010.09.005
29. Nino DF, Sodhi CP, Hackam DJ. Necrotizing enterocolitis: new insights into pathogenesis and mechanisms. *Nat Rev Gastroenterol Hepatol*. (2016) 13:590–600. doi: 10.1038/nrgastro.2016.119
30. Andersen DK, Elahi D, Brown JC, Tobin JD, Andres R. Oral glucose augmentation of insulin secretion. Interactions of gastric inhibitory polypeptide with ambient glucose and insulin levels. *J Clin Invest*. (1978) 62:152–61. doi: 10.1172/JCI109100
31. Corpeleijn WE, Kouwenhoven SM, Paap MC, van Vliet I, Scheerder I, Muizer Y, et al. Intake of own mother's milk during the first days of life is associated with decreased morbidity and mortality in very low birth weight infants during the first 60 days of life. *Neonatology*. (2012) 102:276–81. doi: 10.1159/000341335
32. Yoo LI, Chung DC, Yuan J. LKB1–a master tumour suppressor of the small intestine and beyond. *Nat Rev Cancer*. (2002) 2:529–35. doi: 10.1038/nrc843
33. Lee CC, Avalos AM, Ploegh HL. Accessory molecules for Toll-like receptors and their function. *Nat Rev Immunol*. (2012) 12:168–79. doi: 10.1038/nri3151
34. Luo X, Han M, Liu J, Wang Y, Luo X, Zheng J, et al. Epithelial cell-derived micro RNA-146a generates interleukin-10-producing monocytes to inhibit nasal allergy. *Sci Rep*. (2015) 5:15937. doi: 10.1038/srep15937
35. Turner JD, Alt SR, Cao L, Vernocchi S, Trifonova S, Battello N, et al. Transcriptional control of the glucocorticoid receptor: CpG islands, epigenetics and more. *Biochem Pharmacol*. (2010) 80:1860–8. doi: 10.1016/j.bcp.2010.06.037
36. Fowden AL, Valenzuela OA, Vaughan OR, Jellyman JK, Forhead AJ. Glucocorticoid programming of intrauterine development. *Domest Anim Endocrinol*. (2016) 56(Suppl):S121–32. doi: 10.1016/j.domaniend.2016.02.014
37. Arsenault P, Menard D. Influence of hydrocortisone on human fetal small intestine in organ culture. *J Pediatr Gastroenterol Nutr*. (1985) 4:893–901. doi: 10.1097/00005176-198512000-00008
38. Sangild PT, Sjostrom H, Noren O, Fowden AL, Silver M. The prenatal development and glucocorticoid control of brush-border hydrolases in the pig small intestine. *Pediatr Res*. (1995) 37:207–12. doi: 10.1203/00006450-199502000-00014
39. Bunger M, van den Bosch HM, van der Meijde J, Kersten S, Hooiveld GJ, Muller M. Genome-wide analysis of PPARalpha activation in murine small intestine. *Physiol Genomics*. (2007) 30:192–204. doi: 10.1152/physiolgenomics.00198.2006
40. Piomelli D. A fatty gut feeling. *Trends Endocrinol Metab*. (2013) 24:332–41. doi: 10.1016/j.tem.2013.03.001
41. Gajda AM, Storch J. Enterocyte fatty acid-binding proteins (FABPs): different functions of liver and intestinal FABPs in the intestine. *Prostaglandins Leukot Essent Fatty Acids*. (2015) 93:9–16. doi: 10.1016/j.plefa.2014.10.001
42. Roadmap Epigenomics C, Kundaje A, Meuleman W, Ernst J, Bilenky M, Yen A, et al. Integrative analysis of 111 reference human epigenomes. *Nature*. (2015) 518:317–30. doi: 10.1038/nature14248

Conflict of Interest: The authors declare that the research was conducted in the absence of any commercial or financial relationships that could be construed as a potential conflict of interest.

frontiers in Immunology

ORIGINAL RESEARCH
published: 21 April 2020
doi: 10.3389/fimmu.2020.00516

Staphylococcus epidermidis Sensitizes Perinatal Hypoxic-Ischemic Brain Injury in Male but Not Female Mice

Giacomo Gravina[1], *Pernilla Svedin*[1], *Maryam Ardalan*[1], *Ofer Levy*[2,3,4], *C. Joakim Ek*[1], *Carina Mallard*[1*†] and *Jacqueline C. Y. Lai*[1†]

[1] Institute of Neuroscience and Physiology, Sahlgrenska Academy, University of Gothenburg, Gothenburg, Sweden, [2] Precision Vaccines Program, Boston Children's Hospital, Boston, MA, United States, [3] Department of Pediatrics, Harvard Medical School, Boston, MA, United States, [4] Broad Institute of MIT and Harvard, Cambridge, MA, United States

Background: *Staphylococcus epidermidis* is the most common nosocomial infection and the predominant pathogen in late-onset sepsis in preterm infants. Infection and inflammation are linked to neurological and developmental sequelae and bacterial infections increase the vulnerability of the brain to hypoxia-ischemia (HI). We thus tested the hypothesis that *S. epidermidis* exacerbates HI neuropathology in neonatal mice.

Methods: Male and female C57Bl/6 mice were injected intraperitoneally with sterile saline or 3.5×10^7 colony-forming units of *S. epidermidis* on postnatal day (PND) 4 and then subjected to HI on PND5 (24 h after injection) or PND9 (5 d after injection) by left carotid artery ligation and exposure to 10% O_2. White and gray matter injury was assessed on PND14-16. In an additional group of animals, the plasma, brain, and liver were collected on PND5 or PND9 after infection to evaluate cytokine and chemokine profiles, C5a levels and C5 signaling.

Results: HI induced 24 h after injection of *S. epidermidis* resulted in greater gray and white matter injury compared to saline injected controls in males, but not in females. Specifically, males demonstrated increased gray matter injury in the cortex and striatum, and white matter loss in the subcortical region, hippocampal fimbria and striatum. In contrast, there was no potentiation of brain injury when HI occurred 5 d after infection in either sex. In the plasma, *S. epidermidis*-injected mice demonstrated increased levels of pro- and anti-inflammatory cytokines and chemokines and a reduction of C5a at 24 h, but not 5 d after infection. Brain CCL2 levels were increased in both sexes 24 h after infection, but increased only in males at 5 d post infection.

Conclusion: Ongoing *S. epidermidis* infection combined with neonatal HI increases the vulnerability of the developing brain in male but not in female mice. These sex-dependent effects were to a large extent independent of expression of systemic cytokines or brain CCL2 expression. Overall, we provide new insights into how systemic *S. epidermidis* infection affects the developing brain and show that the time interval between infection and HI is a critical sensitizing factor in males.

Keywords: *Staphylococcus epidermidis*, bacterial infection, sepsis, hypoxia-ischemia, neonatal mice, brain injury, complement activation

OPEN ACCESS

Edited by:
Per T. Sangild,
University of Copenhagen, Denmark

Reviewed by:
Anders Brunse,
University of Copenhagen, Denmark
Tim Wolfs,
Maastricht University, Netherlands

***Correspondence:**
Carina Mallard
carina.mallard@neuro.gu.se

† These authors have contributed equally to this work

Specialty section:
This article was submitted to Microbial Immunology, a section of the journal Frontiers in Immunology

Received: *15 November 2019*
Accepted: *06 March 2020*
Published: *21 April 2020*

Citation:
Gravina G, Svedin P, Ardalan M, Levy O, Ek CJ, Mallard C and Lai JCY (2020) Staphylococcus epidermidis Sensitizes Perinatal Hypoxic-Ischemic Brain Injury in Male but Not Female Mice. Front. Immunol. 11:516. doi: 10.3389/fimmu.2020.00516

INTRODUCTION

Extreme prematurity is associated with increased mortality and morbidity (1). Despite improved survival rates of preterm infants over the years, preterm birth remains a major health problem, especially for infants experiencing sepsis (2). Due to invasive procedures and extensive use of medical devices, certain infections pose a special risk to preterm infants (3, 4). The coagulase-negative staphylococci *Staphylococcus epidermidis* forms biofilms on medical devices and is one of the most common nosocomial infections in preterm infants and has emerged as the predominant pathogen in late-onset sepsis (5, 6).

Clinical and experimental evidence link perinatal infection and inflammation to subsequent neurological and developmental sequelae (7). Sepsis can induce neuroinflammation resulting in activation of neurotoxic processes (8). There is increased risk of neurodevelopmental impairment in infants that experience sepsis and a meta-analysis demonstrated that coagulase-negative staphylococci sepsis in very low birth weight infants is associated with a higher incidence of cerebral palsy (9). Furthermore, infection in preterm infants is associated with a greater incidence of subsequent cardiorespiratory events, such as apnoea and hypoxemia (10), and it is recognized that neonatal encephalopathy is likely multifactorial where both maternal and neonatal infections can exacerbate hypoxic-ischemic (HI) brain injury (11).

We and others have demonstrated that synthetic compounds, such as Pam_3CSK_4, a Toll-like receptor (TLR) 2 agonist that mimics aspects of inflammation driven by Gram-positive bacteria, increases the vulnerability of the brain to subsequent HI in neonatal mice (12, 13). Recently we extended these findings to show that live *S. epidermidis* bacterial infection induced 14 h prior to HI also sensitizes the brain to increased injury (14). However, the time interval between infection and subsequent HI is known to be important in experimental studies (15). Thus, to test the hypothesis that *S. epidermidis* infection increases the vulnerability to HI mainly during an ongoing infection, we used our model of self-clearing systemic *S. epidermidis* infection in neonatal mice to investigate the effects of infection on HI injury over time.

The complement system is an important component of innate host defense, enhancing killing of pathogens, and clearance of microbes. The complement system is impaired in preterm infants and has been associated with preterm birth and susceptibility to neonatal sepsis (16). The complement component 5 (C5) protein cleaves into two protein fragments upon activation: C5a and C5b. C5a signaling through C5a receptors plays an important role in the development of sepsis (17). C5 has also been implicated in cerebral injury (18, 19) and C5a is elevated in CSF of preterm infants (20). We therefore also investigated the involvement of C5 signaling following *S. epidermidis* infection. We demonstrate that the time interval between *S. epidermidis* infection and HI is critical in sensitizing the brain to HI injury and that the effects are sex-dependent as they were evident only in male mice.

MATERIALS AND METHODS

Animals

C57Bl/6J wild-type mice were purchased from Janvier Labs (Le Genest-Saint-Isle, France) and Charles River Laboratories (Sulzfeld, Germany) and were bred in the animal facility at the University of Gothenburg (Experimental Biomedicine, University of Gothenburg). Mice were housed with a normal 12-h light/dark cycle (lights on at 06:00) and *ad libidum* access to standard laboratory chow diet (B&K, Solna, Sweden) and drinking water in a temperature controlled environment (20–22°C). All animal experiments were approved by the Gothenburg Animal Ethical Committee (No 663/2017). Mice of both sexes were used. Sex was established by visual inspection. In each experimental group, mice were obtained from at least three different litters.

Study Design

We have previously shown that *S epidermidis* infection can increase the vulnerability of the developing brain to HI (14). To evaluate the potentiation of brain injury after *S. epidermidis* infection over time, mice were subjected to a combination of *S. epidermidis* infection and HI. For exposure to neonatal infection, mice were intraperitoneally injected with sterile saline or 3.5×10^7 colony-forming units (CFU) of *S. epidermidis* at postnatal day (PND) 4 as previously described (14). HI was induced at 24 h (PND5) or 5 d (PND9) after *S. epidermidis* injection. The timing of HI was based on our previous study which showed that infection was ongoing at 24 h but largely cleared at 5 d (14). Animals were sacrificed on PND14-PND16 for neuropathological examination (**Figure 1A**).

To understand molecular mechanisms underlying brain sensitization at the time of HI, another group of animals was injected intraperitoneally at PND4 with 3.5×10^7 CFU of *S. epidermidis* or saline (without HI). Twenty-four hours or 5 d after *S. epidermidis*/saline injection, blood, liver, and brain samples were collected for biochemical analysis (**Figure 1B**).

Hypoxia-Ischemia Procedure

PND5 and PND9 pups were exposed to neonatal HI as previously described (21, 22). Pups were anesthetized with isoflurane (IsoFlo vet 100%; Abbott Laboratories Ltd, Illinois, USA), 5% for induction and 1.5% for maintenance, in 1:1 oxygen-nitrogen gas mixture. The left common carotid artery was ligated with a 7.0 silk suture (Ethicon; Vömel, Germany) and the incision was closed and infiltrated with a local anesthetic (Xylocain 20 mg/ml, lidocaine hydrochloride; Astra Zeneca, Södertälje, Sweden). After surgery, mice were returned to their dams for 1 h, before being placed in a chamber with circulating humidified air (36 °C). In the chamber, PND5 mice were exposed to 10 min of air, followed by 60 min of hypoxia (10% O_2 in 90% N_2) followed by another 10 min of air. PND9 mice were treated in the same manner except the hypoxia time was 50 min. This procedure results in a similar degree of brain injury in PND5 and PND9 mice as previously shown (21, 23) and **Supplementary Figure 1**. Following the hypoxic exposure, pups were returned to their dams until sacrifice.

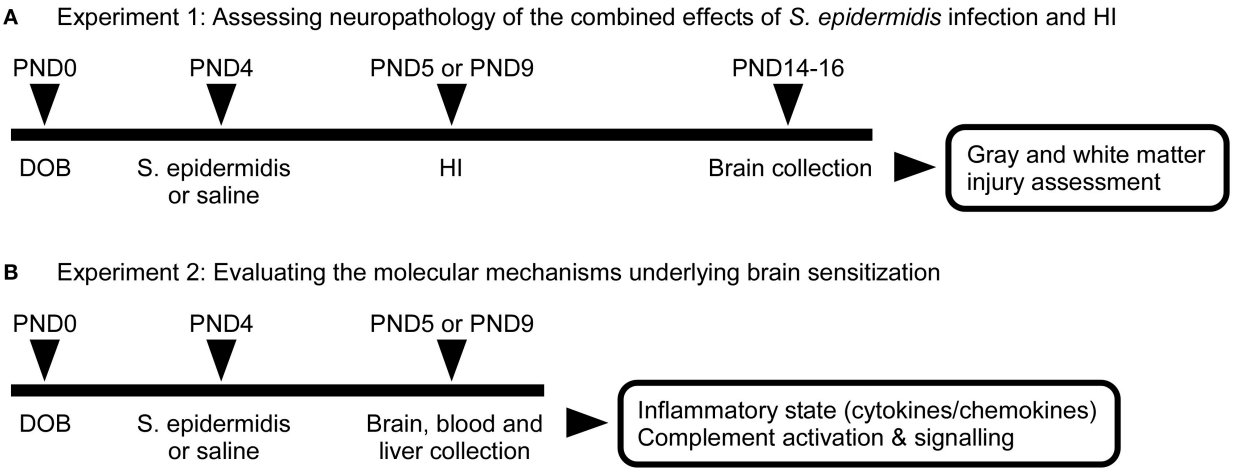

FIGURE 1 | Schematic overview of experimental study design**. (A)** C57Bl/6J mice were injected intraperitoneally at PND4 with 3.5×10^7 CFU of *S. epidermidis* or saline followed by hypoxia-ischemia (HI) procedure at 24 h (PND5) or 5 days (PND9) after injection. Brains were collected on PND14 or 16 for evaluation of neuropathology. **(B)** A second group of animals was sacrificed prior to HI for the evaluation of inflammatory response and complement activation and signaling in blood, liver, and brain.

Tissue Preparation and Immunohistochemistry

PND14 (i.e., 9 d after HI at PND5) or PND16 (i.e., 7 d after HI at PND9) mice were deeply anesthetized via intraperitoneal administration of pentobarbital (Pentacour) and intracardially perfused with 0.9% saline followed by 6% buffered formaldehyde (Histofix; Histolab). The brains were collected and kept in the same fixative solution at 4°C until dehydration and paraffin embedding. For the immunohistochemistry analysis, brains were sectioned at 7-μm coronal thickness on a microtome and based on a systematic sampling principle every 50th section was used for immunohistochemical staining. Brain sections were heated at 65°C for 30 min, followed by deparaffinization in xylene and graded alcohol. Antigen retrieval was performed by boiling the tissue sections in 0.01 M citric acid buffer (pH 6.0). Brain sections were then washed in PBS, blocked for endogenous peroxidase activity with 3% H_2O_2 in PBS, followed by blocking for non-specific binding with 4% goat serum in PBS. Sections were incubated at 4°C overnight with primary antibody against microtubule-associated protein-2 (MAP-2; clone HM-2, 1:1,000; Sigma-Aldrich catalog # M4403) or myelin basic protein (MBP; clone SMI-94, 1:1,000; BioLegend catalog # 836504), followed by 1 h of incubation with horse-anti-mouse biotinylated secondary antibody (1:250; Vector Laboratories catalog # BA-2001) and VECTASTAIN Elite ABC HRP Kit (Vector Laboratories) according to manufacturer's instructions. Sections were visualized with a solution of 0.5 mg/ml 3,3-diaminobenzidine enhanced with 15 mg/ml ammonium nickel sulfate, 2 mg/ml β-D-glucose, 0.4 mg/ml ammonium chloride, and 0.01 mg/ml β-glucose oxidase (all from Sigma-Aldrich). In the last step, stained sections were dehydrated through a graded series of alcohol (70, 95, 99%), cleared in xylene and cover-slipped.

Brain Injury Analysis

Gray matter injury was quantified on sections stained for MAP-2, which labels neurons and dendrites, and white matter was quantified on sections stained for MBP, which labels myelin. Images were captured on a light microscope (Olympus BX60) using a 4X objective lens. The region of interest (ROI) with MAP-2 or MBP positive immunoreactivity in the hemispheres ipsilateral and contralateral to the ligated artery were outlined and measured with ImageJ software (v1.52a, NIH, USA). Gray matter analysis was performed in brain regions ranging from the anterior striatum to the middle of the hippocampal structure (5 levels including the cortex, 3 levels including the dorsal hippocampus and thalamus, and 3 levels including the striatum). The sum of the MAP-2 positive areas in the cortex, hippocampus, thalamus, and striatum was considered as a measurement of the whole cerebral hemisphere.

Myelinated areas were determined as integrated density of MBP-positive staining (i.e., the product of area and mean gray value in the ROI). MBP staining was measured at 2 levels in the subcortical white matter, at 2 levels of the hippocampal fimbria, and at 3 levels in the striatum. The percentage of MAP-2 and MBP-positive tissue loss were calculated at each level as follows: [(contralateral side – ipsilateral side)/contralateral side × 100%]. The mean of the percentage tissue loss for all levels was compared between animals.

Sample Collection for Biochemical Analysis

At 24 h (PND5) or 5 d (PND9) post infection or injection of saline (n = 10/treatment group/sex), mice were deeply anesthetized via intraperitoneal administration of pentobarbital (Pentacour). Approximately 20 μl of blood was collected via

cardiac puncture and mixed with 5 μl of 50 mM EDTA. Mice were then transcardially perfused with 0.9% saline and brain and liver were collected and flash frozen in dry ice.

For protein analysis, brain and liver were homogenized in 1,000 μl of RNase-free PBS containing 0.5% protease inhibitor cocktail (Sigma catalog # P8340), 5 mM EDTA and 1% Triton X-100 by sonication (40% amplitude, 10 pulses, 1.2 s each). Lysates were then centrifuged (10,000 x g, 10 min, 4°C) and cleared supernatants were stored at −80°C. Protein concentrations were measured using the Pierce BCA Protein Assay Kit (Thermo Fisher Scientific) according to the manufacturer's instructions.

Cytokine and Chemokine Assay

Bio-Plex Pro Mouse Cytokine Standard 23-Plex kit (Bio-Rad, catalog # M600009RDPD), analyzed on a Bio-Plex 200 System (Bio-Rad), was used to perform cytokine profiling of plasma from PND5 and PND9 mice according to the manufacturer's instructions. Plasma samples were diluted 1/5 in Bio-plex sample diluent prior to assaying.

Measurement of Brain CCL2

Protein concentration of CCL2 from brain lysates was analyzed by enzyme-linked immunosorbent assay (ELISA) kit and standard (CCL2/JE/MCP-1 DuoSet ELISA kit, R&D Systems, catalog # DY479-05) as per manufacturer's instructions.

Measurement of Plasma, Brain, and Liver C5a

C5a concentrations were measured using the mouse C5a DuoSet ELISA kit (R&D Systems, catalog # DY2150) as per manufacturer's instructions. Plasma from both PND5 and PND9 mice were diluted 1/200, whereas brain lysates were diluted 1/50 in reagent diluent. Liver lysates from PND5 and PND9 samples were diluted 1/50 and 1/200 respectively.

Measurement of C5, C5aR1, and C5aR2 mRNA Expression in Brain and Liver

Total RNA was prepared from the brain and liver lysates in RNase-free PBS using RNeasy Mini Kit (Qiagen), following the manufacturer's instructions and measured using NanoDrop 2000 (Thermo Fisher Scientific). RNA was reversed transcribed into cDNA using QuantiTect Reverse Transcription Kit (Qiagen). All cDNA samples were diluted with nuclease-free water to a final volume of 50 μl. Quantitative real-time RT-qPCR was performed with a Touch real-time cycler (Bio-Rad, Hercules, CA, USA). Each 20 μl reaction contained 10 μl Fast SYBR master mix (Qiagen), 2 μl of 10x Primer set (Qiagen) for C5 - QT00102032; C5a receptor 1 (C5aR1) - QT00288232 and C5a receptor 2 (C5aR2) - QT02532803, 6 μl of H_2O and 2 μl of cDNA. The PCR temperature profile was 95 °C for 2 min followed by 40 cycles of amplification (95 °C for 10 s and 60 °C for 30 s).

The values for each gene were normalized to the concentration of cDNA in each RT sample measured using the QUANT-IT™ OLIGREEN ssDNA assay kit (Invitrogen), according to the manufacturer's instructions. The amount of target gene expression was calculated as follows: ([$cDNA_{targetgene}$/average of $cDNA_{total}$ in all samples]/total $cDNA_{target\ gene}$).

Statistical Analysis

Statistical analyses were performed using GraphPad Prism v.8. Descriptive data are presented as box plots with median and the whiskers at 10–90th percentile. Normal distribution of the data was examined by generating Q-Q plot and in cases of non-normal distribution, log transformation of data was performed. The interaction between the independent variables (bacterial infection and sex) and the main effect of sex or bacterial infection on brain injury were tested using two-way analysis of variance (Two-way ANOVA). *Post-hoc* analysis between the groups was performed using the Sidak's multiple comparison test. *P*-values < 0.05 were considered statistically significant.

RESULTS

Staphylococcus epidermidis Sensitizes Hypoxic-Ischemic Brain Injury in Males but Not in Females

To assess the window of increased vulnerability to HI after *S. epidermidis* bacteraemia, we induced HI either at 24 h post infection, when bacteraemia was high, or at 5 d after infection, when bacteria was significantly reduced in the blood (14). We assessed changes in the white and gray matter at PND14—PND16, corresponding to an age when myelination is established and detectable by immunohistochemical staining in mice (24). As infection and inflammation can affect perinatal brain injury in a sex-dependent manner, reviewed in Ardalan et al. (25), neuropathological outcome was determined in male and female pups separately.

S. epidermidis bacteraemia initiated 24 h before HI potentiated brain injury in male but not in female mice (**Figure 2**). Two-way ANOVA of regional gray matter analysis revealed a significant interaction between sex and bacterial infection in the cortex [$F_{(1,48)} = 4.28$, $p = 0.04$]. Significant main effects of bacterial infection were seen in the striatum and total hemispheres [$F_{(1,48)} = 8.08$, $p = 0.006$; $F_{(1,48)} = 4.68$, $p = 0.03$], while significant main effects of sex were observed in the cortex, thalamus, striatum, and total hemispheres respectively [$F_{(1,48)} = 12.13$, $p = 0.001$; $F_{(1,48)} = 8.03$, $p = 0.006$; $F_{(1,48)} = 6.47$, $p = 0.01$; $F_{(1,48)} = 7.81$, $p = 0.006$]. Tissue loss in the entire cerebral hemisphere was greater in *S. epidermidis* infected male mice compared to saline treated males ($p = 0.01$), but not in female mice. Specifically, regional gray matter analysis revealed that *S. epidermidis* infected male mice had increased tissue loss in the cerebral cortex ($p = 0.02$) and in the striatum ($p = 0.01$) compared to saline treated male mice. Significantly increased injury in infected male mice compared to female mice was found when analyzing the entire hemisphere ($p = 0.004$), cortex ($p = 0.0008$), thalamus ($p = 0.005$) and striatum ($p = 0.01$). *S. epidermidis* did not increase gray matter tissue

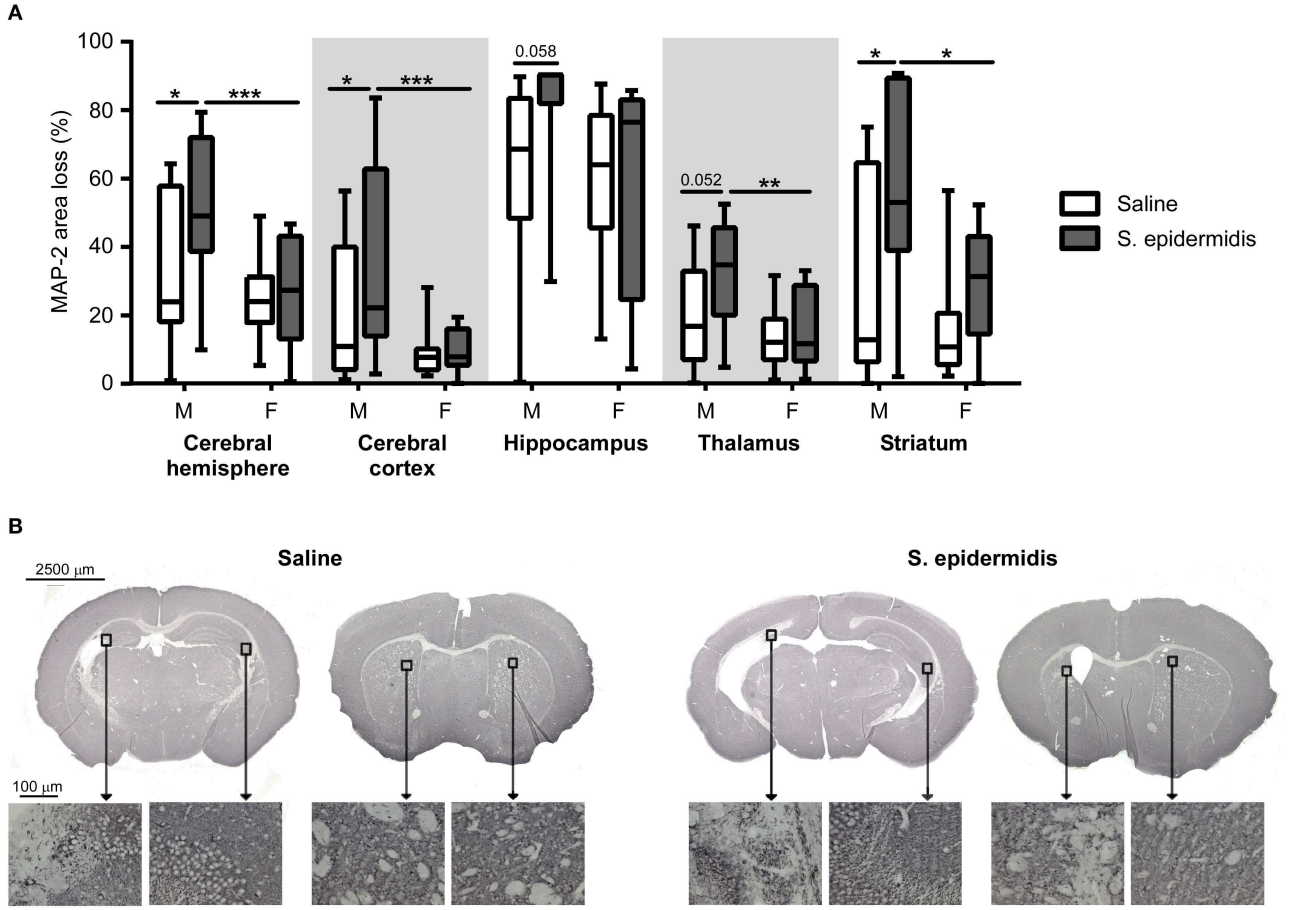

FIGURE 2 | *S. epidermidis* 24 h prior to hypoxia-ischemia potentiates gray matter injury in neonatal male mice. PND4 mice were injected with saline or *S. epidermidis* and subjected to hypoxia-ischemia 24 h later. **(A)** Gray matter brain injury was assessed by microtubule-associated protein 2 (MAP-2) immunohistochemistry at PND14 in the entire cerebral hemisphere, cerebral cortex, hippocampus, thalamus, and striatum ($n = 12$ saline males; $n = 11$ *S. epidermidis* males; $n = 17$ saline females, and $n = 13$ *S. epidermidis* females). **(B)** Representative images (4 × objective lens) of PND14 male mice brain sections stained with MAP-2 at the hippocampal and striatal levels following saline or *S. epidermidis* injection at PND4 in combination with hypoxia-ischemia 24 h later. Images of CA3 region of the hippocampus and striatum captured on a light microscope with a 20× objective lens. Data are presented as median and 10–90th percentile. Statistical comparison between the *S. epidermidis* and saline groups for each brain region was performed using Two-way ANOVA with Sidak's multiple comparison *post-hoc* test; $^{*}p < 0.05$, $^{**}p < 0.01$, and $^{***}p < 0.001$.

loss in female mice compared to saline-injected controls in any region examined.

S. epidermidis bacteraemia initiated 24 h before HI potentiated white matter injury in male but not female mice (**Figure 3**). There was a significant interaction between sex and bacterial infection and main effect of sex on white matter injury in the subcortical region [$F_{(1,47)} = 4.82$, $p = 0.01$; $F_{(1,47)} = 7.92$, $p = 0.007$] and hippocampal fimbria [$F_{(1,47)} = 4.82$, $p = 0.03$; $F_{(1,47)} = 7.58$, $p = 0.008$]. Additionally, an effect of bacterial infection on white matter loss was detected in the fimbria [$F_{(1,47)} = 8.36$, $p = 0.005$] and striatum [$F_{(1,47)} = 8.48$, $p = 0.005$]. *Post-hoc* analysis demonstrated an increased white matter tissue loss in *S. epidermidis* infected male mice compared with saline controls in the subcortical white matter ($p = 0.01$), hippocampal fimbria ($p = 0.003$), and striatum ($p = 0.004$). Consistent with MAP-2 results, a significant increase in tissue loss was found in the subcortical white matter ($p = 0.001$), hippocampal fimbria ($p = 0.003$), and striatum ($p = 0.02$) in *S. epidermidis* infected male mice compared to *S. epidermidis* infected female mice. *S. epidermidis* did not increase white matter tissue loss in female mice compared to saline-injected controls in any region examined.

When the time interval between *S. epidermidis* infection and HI was extended to 5 days, there was no significant interaction between sex and bacterial infection, and no significant effects of sex and bacterial infection on the degree of gray or white matter tissue loss (**Figure 4**). No significant differences in baseline HI injury were seen between male and female mice at either age after saline and HI treatment (**Figures 2–4**). Similarly, there was no difference in overall hemispheric injury between animals subjected to saline and HI at PND5 and PND9 (**Supplementary Figure 1**).

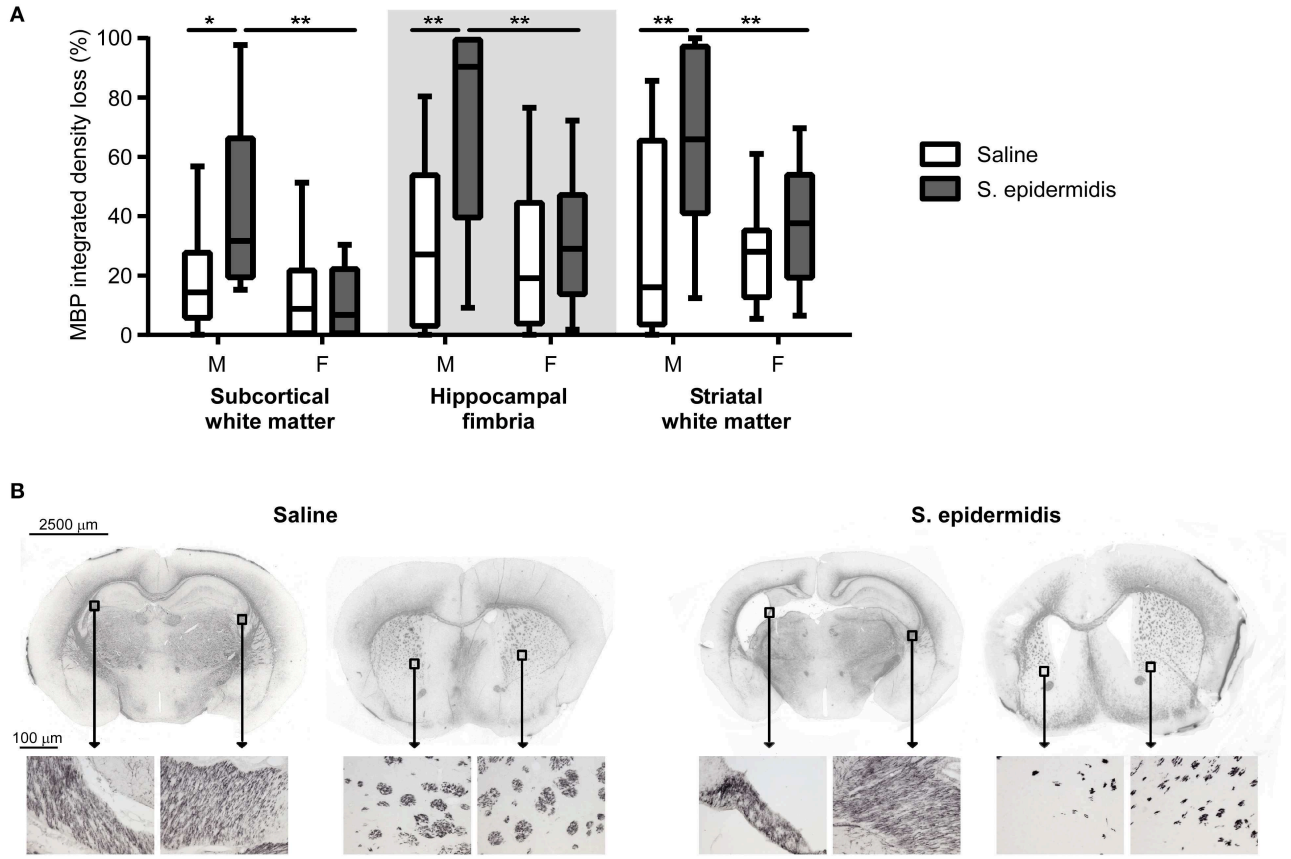

FIGURE 3 | *S. epidermidis* 24 h prior to hypoxia-ischemia potentiates white matter injury in neonatal male mice. PND4 mice were injected with saline or *S. epidermidis* and subjected to hypoxia-ischemia 24 h later. **(A)** White matter brain injury was assessed by myelin basic protein (MBP) immunohistochemistry at PND14 in the subcortical region, hippocampal fimbria, and striatum of male (M) and female (F) mice ($n = 12$ saline males; $n = 11$ *S. epidermidis* males; $n = 16$ saline females, and $n = 13$ *S. epidermidis* females). **(B)** Representative images (4 × objective lens) of PND14 male mice brain sections stained with MBP at the hippocampal and striatal levels following saline or *S. epidermidis* injection at PND4 in combination with hypoxia-ischemia 24 h later. Images of the hippocampal fimbria and striatum captured on a light microscope with a 20× objective lens. Data are presented as median and 10–90th percentile. Statistical comparison between the *S. epidermidis* and saline groups for each brain region was performed using Two-way ANOVA with Sidak's multiple comparison *post-hoc* test; $^{*}p < 0.05$ and $^{**}p < 0.01$.

S. epidermidis Induced Cytokine and Chemokine Production in Blood

To evaluate inflammatory processes associated with increased vulnerability to HI injury, we examined animals 24 h and 5 d after *S. epidermidis* or saline injection, prior to HI. We first measured inflammatory cytokine concentrations in the plasma using a 23-plex cytometry bead array. Two-way ANOVA of plasma cytokine concentrations revealed no significant interaction between sex and bacterial infection at 24 h or 5 d after infection (**Tables 1**, **2**), but there was a significant main effect of bacterial infection on the plasma cytokine and chemokines levels at 24 h, including IL-1b [$F_{(1,36)} = 48.45$, $p < 0.0001$], IL-2 [$F_{(1,36)} = 16.53$, $p = 0.0002$], IL-5 [$F_{(1,36)} = 21.71$, $p < 0.0001$], IL-6 [$F_{(1,36)} = 19.32$, $p < 0.0001$], IL-10 [$F_{(1,36)} = 31.16$, $p < 0.0001$], IL-12(p40) [$F_{(1,36)} = 33.7$, $p < 0.0001$], IL-13 [$F_{(1,36)} = 44.09$, $p < 0.0001$], IL-17 [$F_{(1,36)} = 6.99$, $p = 0.012$], G-CSF [$F_{(1,36)} = 41.28$, $p < 0.0001$], GM-CSF [$F_{(1,36)} = 16.36$, $p = 0.0003$], KC [$F_{(1,36)} = 34.86$, $p < 0.0001$], CCL2 (MCP-1) [$F_{(1,36)} = 45.44$, $p < 0.0001$], CCL3 (MIP1a) [$F_{(1,36)} = 34.57$, $p < 0.0001$], CCL4 (MIP1b) [$F_{(1,36)} = 30.77$, $p < 0.0001$], and CCL5 (RANTES) [$F_{(1,36)} = 10.51$, $p = 0.002$] (**Figure 5A**). The levels of IL-2, IL-17 and CCL5 at 24 h after infection were regulated in a sex-dependent manner. Specifically, we observed an upregulation of IL-2 ($p = 0.02$) in males and CCL5 ($p = 0.01$) in females, while IL-17 was downregulated in males ($p = 0.02$) (**Figure 5A**, **Table 1**). At 5 days after infection, IL-6 and G-CSF were increased in males, whereas IL-5 and G-CSF were reduced in *S. epidermidis* infected females compared to control animals (**Figure 5B**, **Table 2**).

To assess whether *S. epidermidis* induces an inflammatory response in the immature brain, concentrations of CCL2 in brain homogenates 24 h and 5 d after infection were evaluated by ELISA (**Figure 6**). CCL2 levels in the brain ranged from 6.2 to 255 μg/ml at 24 h (**Figure 6A**), but from 1.5 to 17.1 μg/ml at 5 d (**Figure 6B**) after infection. Analysis of brain CCL2 concentrations revealed no significant interaction between sex and bacterial infection at 24 h or 5 days after infection, but there was a significant effect of bacterial infection on brain CCL2 levels

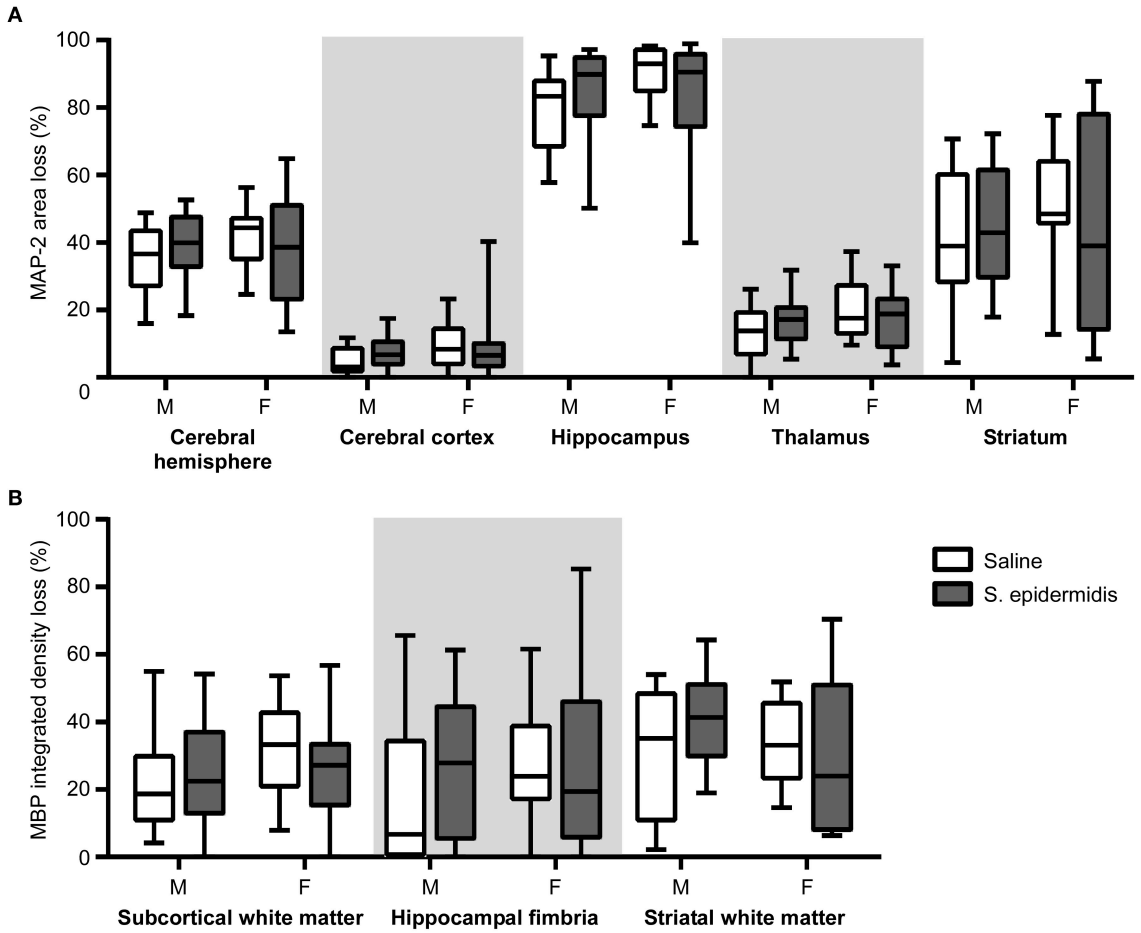

FIGURE 4 | *S. epidermidis* 5 days prior to hypoxia-ischemia does not potentiate neonatal brain injury**.** PND4 mice were injected with saline or *S. epidermidis* and subjected to hypoxia-ischemia 5 days later. **(A)** Gray matter brain injury was assessed by MAP-2 immunohistochemistry at PND16 in the entire cerebral hemisphere, cerebral cortex, hippocampus, thalamus, and striatum of male (M) and female (F) mice. **(B)** White matter brain injury was assessed by MBP immunohistochemistry at PND16 in the subcortical region, hippocampal fimbria, and striatum. $n = 12$ saline males; $n = 15$ *S. epidermidis* males; $n = 16$ saline females, and $n = 14$ *S. epidermidis* females. Data are presented as median and 10–90th percentile. Statistical comparison was performed between the *S. epidermidis* and saline groups for each brain region using Two-way ANOVA with Sidak's multiple comparison *post-hoc* test.

at 24 h [$F_{(1,17)} = 36.84$, $p < 0.0001$] and 5 d [$F_{(1,19)} = 7.20$, $p = 0.01$]. Compared to their respective saline cohorts, brain CCL2 concentrations in infected mice at 24 h were significantly higher in both males and females (18.2-fold in males, $p = 0.007$; 16.4-fold in females, $p = 0.001$) (**Figure 6A**). At 5 days post infection, there was still an increase in CCL2 in infected males (2.1-fold, $p = 0.006$), although less augmented than at 24 h (**Figure 6B**).

S. epidermidis Bacteraemia Affects Complement Component C5a Release in the Plasma

To study the effect of *S. epidermidis* infection on complement protein activation, we measured C5a levels in the plasma, brain, and liver by ELISA. Two-way ANOVA revealed no significant interaction between sex and bacterial infection at 24 h and 5 d after infection; but there was a significant main effect of bacterial infection on C5a levels in the plasma at both time points [$F_{(1,36)} = 16.53$, $p = 0.0002$; $F_{(1,36)} = 21.71$, $p < 0.0001$, respectively, **Figures 7A,B**]. Specifically, plasma C5a levels were significantly decreased 24 h after *S. epidermidis* injection in males compared to saline treated controls ($p = 0.001$). This difference was not observed in females ($p = 0.09$, **Figure 7A**). In contrast, there was an increase in the plasma level of C5a in both sexes 5 d after *S. epidermidis* injection ($p = 0.002$ in males and $p = 0.007$ in females, **Figure 7B**). No difference in C5a levels were found in the brain (**Figures 7C,D**) or in the liver (**Figures 7E,F**) in either sex or time point.

S. epidermidis Alters C5 Signaling in the Liver

To evaluate C5 signaling after *S. epidermidis* infection, we measured the mRNA expression of C5, C5aR1, and C5aR2 in the brain and liver. Analysis of C5, C5aR1, and C5aR2 expression

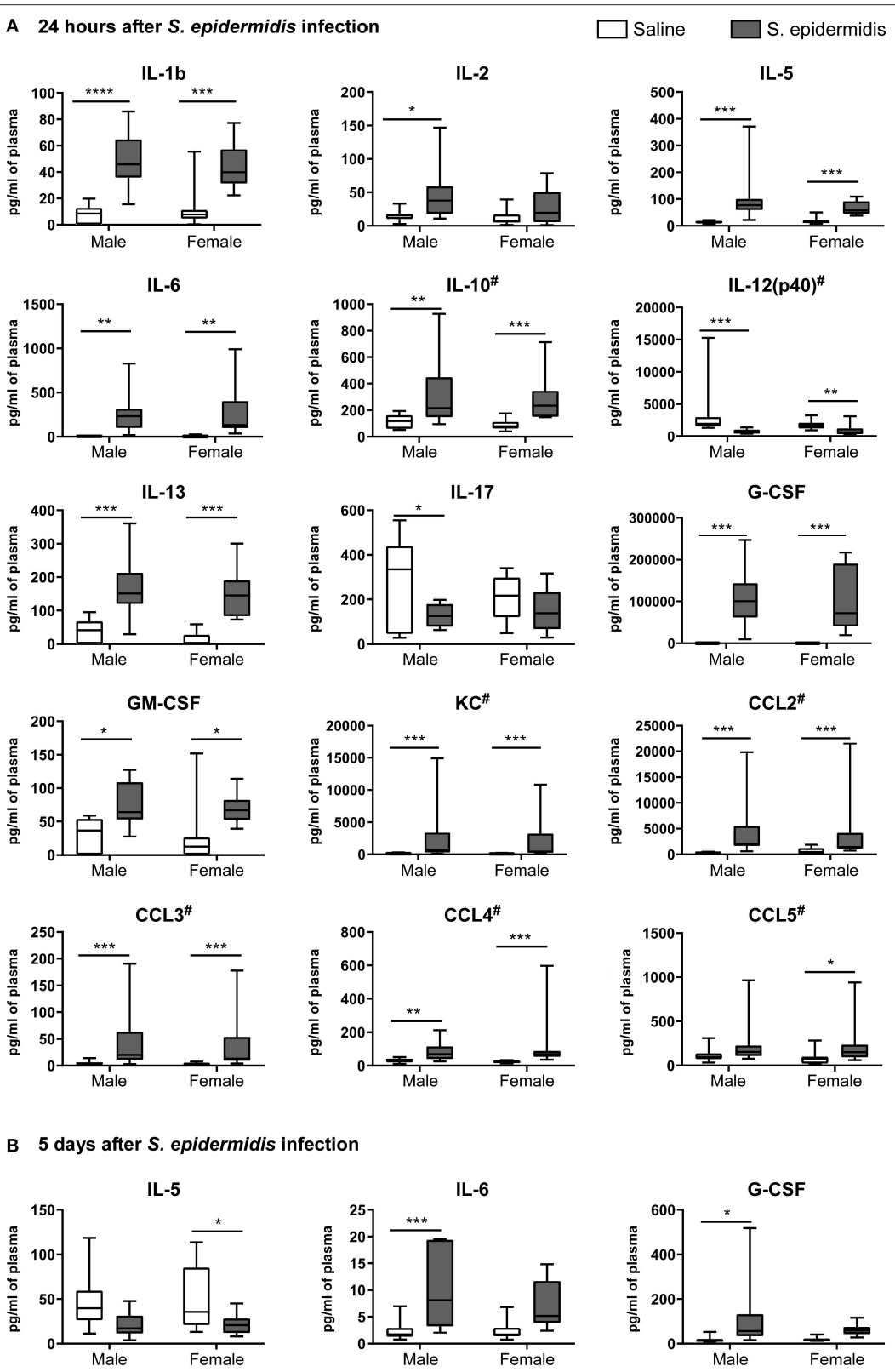

FIGURE 5 | *S. epidermidis* infection induces plasma pro-inflammatory cytokines and chemokines**.** PND4 mice were injected with saline or *S. epidermidis* and the plasma analyzed for cytokines and chemokines at **(A)** 24 h or **(B)** 5 days ($n = 10$ mice/sex/group). Data are presented as median and 10–90th percentile. Statistical comparison between the *S. epidermidis* and saline groups was performed using Two-way ANOVA with Sidak's multiple comparison *post-hoc* test; $^{*}p < 0.05$, $^{**}p < 0.01$, and $^{***}p < 0.001$. # indicates data presented before log transformation.

TABLE 1 | Cytokines and chemokines 24 h after *S. epidermidis* infection.

Treatment	Saline		*S. epidermidis*		*p*-value[a,b,c]
Sex	**Male**	**Female**	**Male**	**Female**	
Cytokines					
IL-1a	138.6 ± 221.5	73.2 ± 179.8	112.4 ± 43.3	102.6 ± 64.8	n.s.
IL-1b	7.6 ± 7.4	12.1 ± 17.2	48.4 ± 21.0	44.7 ± 17.7	***; ###
IL-2	15.2 ± 8.6	12.1 ± 12.2	47 ± 42.4	28.5 ± 27.2	*
IL-3	15.3 ± 11.3	12.5 ± 8.3	16.6 ± 5.8	17.4 ± 6.5	n.s.
IL-4	11.3 ± 21.2	0.4 ± 0.5	5.1 ± 10.6	5.2 ± 10.3	n.s.
IL-5	13.8 ± 5.1	18.2 ± 13.3	104.4 ± 106.7	66.7 ± 25.2	***; ###
IL-6	3.5 ± 2.2	4.7 ± 8.3	267.2 ± 239.7	285.9 ± 310.1	**; ##
IL-9	26.8 ± 17.4	19.4 ± 14.9	19.5 ± 12.0	19.7 ± 11.5	n.s.
IL-10	113.6 ± 54.5	89.3 ± 41.9	328 ± 280.7	283.9 ± 187.0	**; ###
IL-12 (p40)	3511 ± 4642	1769 ± 713.8	701.0 ± 354.4	895.9 ± 906.7	***; ##
IL-12 (p70)	344.3 ± 230.0	181.7 ± 140.7	194.0 ± 158.7	199.7 ± 140.6	n.s.
IL-13	41.1 ± 36.0	14.4 ± 22.2	169.1 ± 95.4	153.4 ± 72.5	***; ###
IL-17	280.3 ± 202.3	206.2 ± 104.6	127.9 ± 49.3	148.2 ± 95.0	*
Eotaxin	1082 ± 297.5	882.1 ± 300.5	1069 ± 454.3	1000 ± 423.7	n.s.
G-CSF	55.9 ± 69.9	38.6 ± 45.3	108582 ± 70384	104658 ± 77792	***; ###
GM-CSF	28.8 ± 25.6	26.9 ± 50.1	74.3 ± 33.6	70.4 ± 23.5	*; #
IFN-g	40.9 ± 27.4	25.2 ± 15.9	29.8 ± 14.4	29.7 ± 16.1	n.s.
KC	121.7 ± 75.4	96.4 ± 61.2	2735 ± 4909	2237 ± 3567	***; ###
CCL2	318.1 ± 143.2	671.9 ± 606.1	4581 ± 6254	4284 ± 6872	***; ###
CCL3	4.8 ± 4.1	3.0 ± 2.0	45.2 ± 61.6	41.1 ± 56.6	***; ###
CCL4	31.8 ± 13.4	23.1 ± 7.5	85.1 ± 62.5	124.6 ± 186.3	**; ###
CCL5	117.9 ± 81.6	86.5 ± 82.8	248.1 ± 285.7	236.1 ± 281.7	#
TNF-a	126.9 ± 88.3	99.2 ± 54.8	141.4 ± 57.4	136.0 ± 44.7	#

Postnatal day 4 mice were intraperitoneally injected with saline or 3.5 × 10^7 CFU of S. epidermidis. Plasma samples were obtained 24 h later for cytometric bead array analysis.
*[a]Saline vs. S. epidermidis-injected male mice *p < 0.05, **p < 0.01, and ***p < 0.001.*
[b]Saline vs. S. epidermidis-injected female mice #p < 0.05, ##p < 0.01, and ###p < 0.001.
[c]No statistical differences were observed between male and female mice injected with saline, or between male and female mice injected with S. epidermidis.

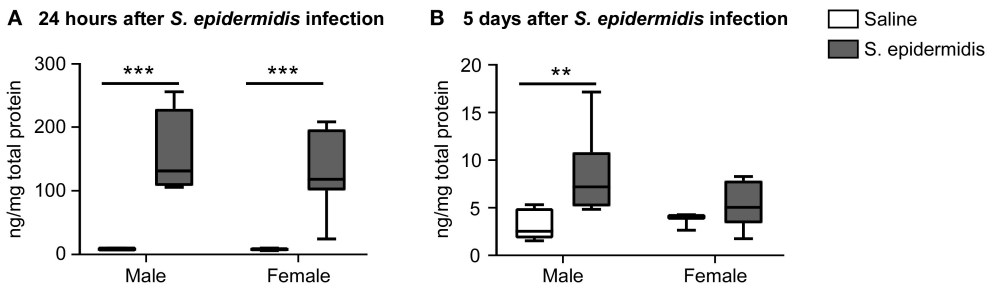

FIGURE 6 | CCL2 levels are increased in the brain following *S. epidermidis* infection**.** PND4 mice were injected with saline or *S. epidermidis* and analyzed at **(A)** 24 h ($n = 5$ saline males; $n = 4$ *S. epidermidis* males; $n = 4$ saline females, and $n = 8$ *S. epidermidis* females) or **(B)** 5 days ($n = 7$ saline males; $n = 6$ *S. epidermidis* females; $n = 3$ saline females, and $n = 7$ *S. epidermidis* females) after infection. CCL2 brain concentrations are presented as median and 10–90th percentile. Statistical comparison between the *S. epidermidis* and saline groups was done using Two-way ANOVA followed by Sidak's multiple comparison *post-hoc* test; $^{**}p < 0.01$ and $^{***}p < 0.001$.

in the brain and liver at 24 h and 5 d post infection revealed no significant interaction between sex and bacterial infection, but there was a significant effect of bacterial infection on the expression of C5aR1 and C5aR2 in the liver 5 d post infection [$F_{(1,36)} = 49.11$, $p < 0.0001$; $F_{(1,36)} = 5.25$, $p = 0.02$, respectively] and an effect of sex on the expression of C5aR1 in liver 5 d post infection [$F_{(1,36)} = 5.55$, $p = 0.02$] (**Figure 8**). At 5 d after the infection, C5aR2 was only significantly upregulated in the liver of infected males compared to the saline group ($p = 0.02$), while C5aR1 expression in the liver was consistently upregulated in both sexes ($p < 0.0001$ in males and $p = 0.002$ in females; **Figure 8B**). The expression of C5aR2 was upregulated in the

TABLE 2 | Cytokines and chemokines 5 days after *S. epidermidis* infection.

Treatment	Saline		*S. epidermidis*		*p*-value[a,b,c]
Sex	**Male**	**Female**	**Male**	**Female**	
Cytokines					
IL-1a	48.2 ± 55.5	47.3 ± 51.1	10.5 ± 5.6	21.8 ± 19.8	n.s.
IL-1b	7.3 ± 8.2	3.3 ± 5.7	8.7 ± 8.5	7.5 ± 11.3	n.s.
IL-2	10.0 ± 5.4	12 ± 9.3	8.6 ± 4.9	13.2 ± 11.1	n.s.
IL-3	11.1 ± 4.9	11.7 ± 9.8	10.6 ± 6.5	12.5 ± 8.4	n.s.
IL-4	0.2 ± 0.0	2.4 ± 6.9	0.4 ± 0.7	1.5 ± 4.1	n.s.
IL-5	46.6 ± 32.4	51 ± 37.3	20.8 ± 13.7	21.7 ± 11.8	#
IL-6	2.4 ± 1.9	2.4 ± 1.9	10.3 ± 7.3	6.9 ± 4.3	***
IL-9	16.1 ± 11.8	17.0 ± 15.9	13.6 ± 9.4	14.7 ± 13.0	n.s.
IL-10	102.0 ± 87.4	74.9 ± 36.5	111.6 ± 45.7	110.3 ± 49.1	n.s.
IL-12 (p40)	1294 ± 304.6	1316 ± 390.8	1221 ± 536.1	1036 ± 463.8	n.s.
IL-12 (p70)	212.5 ± 156.6	213.3 ± 229.6	131.9 ± 115.1	186.4 ± 198.4	n.s.
IL-13	3.164 ± 6.2	7.6 ± 22.8	4.5 ± 12.9	9.9 ± 30.2	n.s.
IL-17	290.9 ± 83.5	276.6 ± 202.0	187.5 ± 142.5	259.8 ± 147.2	n.s.
Eotaxin	806.0 ± 254.4	877.3 ± 278.3	574.4 ± 190.3	617 ± 180.3	n.s.
G-CSF	18.0 ± 13.6	18.3 ± 9.0	115.6 ± 161.8	62.3 ± 27.7	*
GM-CSF	7.7 ± 13.0	14.3 ± 20.9	15.1 ± 20.2	12.6 ± 19.0	n.s.
IFN-g	28.3 ± 16.4	25.3 ± 25.5	18.8 ± 15.9	23.7 ± 19.1	n.s.
KC	71.2 ± 31.4	86.9 ± 46.2	98.9 ± 36.1	90.2 ± 30.4	n.s.
CCL2	874.2 ± 989.7	271.2 ± 396.5	529.1 ± 750.0	783 ± 1017	n.s.
CCL3	2.6 ± 1.3	2.7 ± 2.0	3.5 ± 1.6	3.8 ± 1.6	n.s.
CCL4	21.8 ± 8.6	22.6 ± 11.9	27.3 ± 9.9	28.9 ± 11.5	n.s.
CCL5	61.2 ± 22.7	61.2 ± 29.7	109.3 ± 63.5	121.8 ± 113.1	n.s.
TNF-a	94.8 ± 48.1	99.6 ± 81.2	79.6 ± 50.8	96.5 ± 63.5	n.s.

Postnatal day 4 mice were intraperitoneally injected with saline or 3.5 × 10^7 CFU of S. epidermidis. Plasma samples were obtained 5 days later for cytometric bead array analysis.
[a]*Saline vs. S. epidermidis-injected male mice *p < 0.05, and ***p < 0.001.*
[b]*Saline vs. S. epidermidis-injected female mice #p < 0.05.*
[c]*No statistical differences were observed between male and female mice injected with saline, or between male and female mice injected with S. epidermidis.*

brain of infected female ($p = 0.04$) but not in male mice 24 h after *S. epidermidis* infection (**Figure 8A**).

DISCUSSION

To study the effects of perinatal infection on cerebral vulnerability, we examined the impact of *S. epidermidis*, the most common nosocomial infection in preterm infants, on HI injury in neonatal mice. Here, we show for the first time that the vulnerability to HI brain injury subsequent to *S. epidermidis* infection is both time and sex-dependent, with an increased sensitivity in males.

We have previously reported that *S. epidermidis* infection 14 h prior to HI in neonatal (PND4) mice sensitizes the brain to cerebral injury (14) and that intravenous injection of *S. epidermidis* at PND0 impairs brain development (26). *S. epidermidis* is known to activate TLR2 (27), but *S. epidermidis* induction of neonatal brain injury is both TLR2 dependent and independent (26). Furthermore, innate immune responses to *S. epidermidis* in preterm infants is known to be age-dependent (28). We and others have demonstrated that administration of specific TLR2 agonists prior to HI increases vulnerability to brain injury (12, 13). Previous studies have also demonstrated that vulnerability to HI following LPS-induced inflammation is dependent on the time interval between LPS and HI (15). This suggests that timing of the infection is important. Supporting this, we find in the present study that the time interval between *S. epidermidis* infection and HI induction determines the neuropathological outcome, at least in male mice.

Brain development is a sexually dimorphic process, including neurotransmission and/or genetic and metabolic responses (29, 30). Furthermore, perinatal complications are dependent on sex. For example, a higher incidence of preterm birth is observed in males (31) and HI affects male more often than female infants (32). Increased male prevalence has also been observed in several neurodevelopmental disorders such as autism (33) and attention deficit hyperactivity disorder (34, 35). Significant evidence points to sexual dimorphism of the inflammatory response being an underlying factor for the sexual bias in neuro-psychiatric disorders (25). An elegant experiment by Villa et al. recently demonstrated that female and male microglia are different and that female microglia transplanted into the brain of male mice maintain their sex-specific features and provide neuroprotection in males following adult stroke (36). Supporting

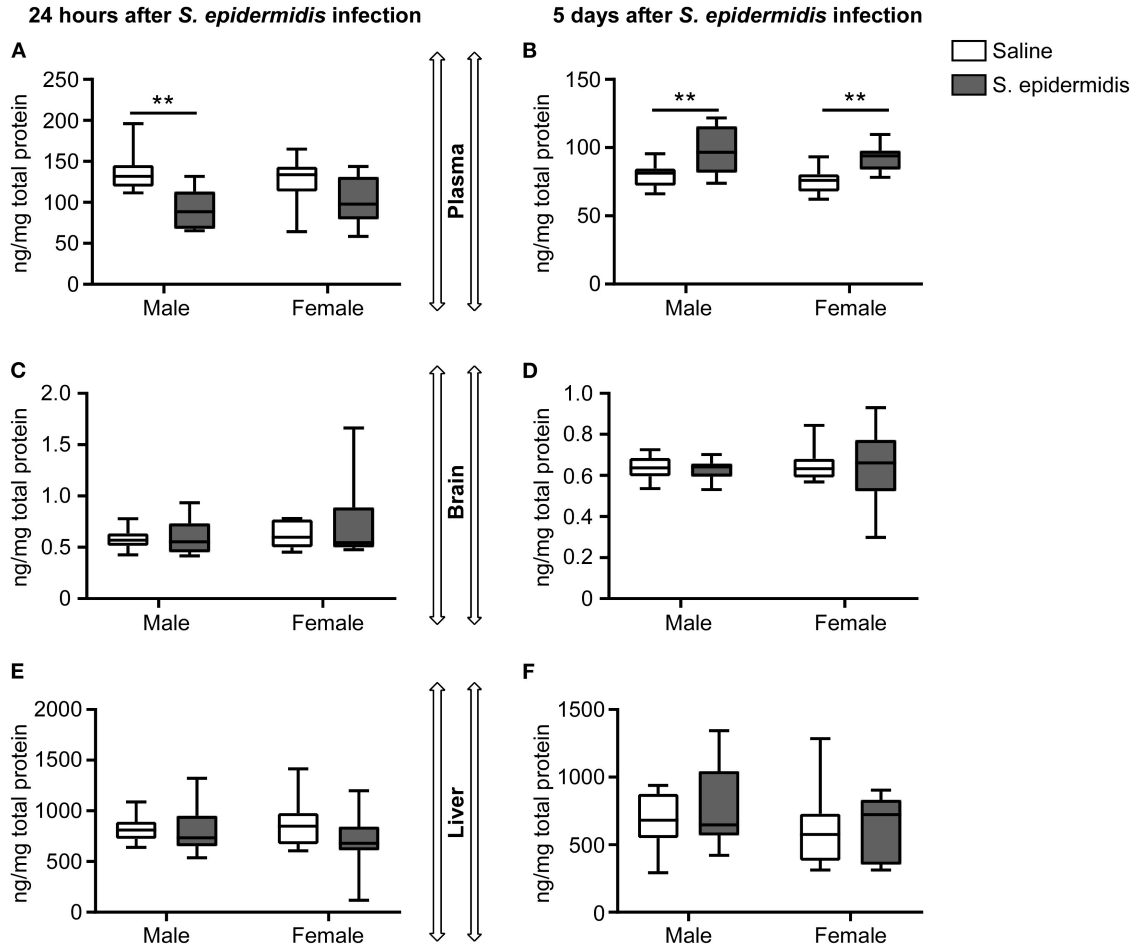

FIGURE 7 | Plasma concentrations of C5a is reduced 24 h following *S. epidermidis* infection. PND4 mice were injected with saline or *S. epidermidis* and analyzed for C5a levels in the plasma, brain, and liver at **(A,C,E)** 24 h or **(B,D,F)** 5 days post infection ($n = 10$ mice/sex/group). Data are presented as median and 10–90th percentile. Statistical comparison between the *S. epidermidis* and saline groups was done using Two-way ANOVA followed by *post-hoc* Sidak's multiple comparison test; $^{**}p < 0.01$.

previous evidence demonstrating increased male vulnerability to inflammation and brain injury, our present study shows that *S. epidermidis* selectively sensitizes males to HI brain injury.

In the present study, increased brain vulnerability in males was only observed when HI was induced at 24 h, but not 5 days post infection. To investigate the role of inflammation at these two time points, when sensitization was and was not identified, we performed cytokine and chemokine assays in the blood and brain of male and female mice. Although we observed a significant upregulation of several pro- and anti-inflammatory cytokines in the blood 24 h post *S. epidermidis* infection, only IL-2, CCL5, and IL-17 were regulated in a sex-dependent manner. At 5 d after infection, most cytokines had tapered back to baseline levels and only IL-6 and G-CSF remained upregulated in males. Consistent with our findings, PND10 rats of both sexes challenged with either a mix of bacterial or viral components showed an upregulation of blood (serum) cytokines and chemokines at PND12, returning to constitutive levels 5 d later (37).

There is increasing evidence supporting sex dimorphism in the cytokine response to certain bacterial infections, such as an overproduction of IL-2 in males (38). However, to our knowledge, there are no studies investigating sex-dependent differences of IL-2, CCL5, or IL-17 in neonatal sepsis. Clinical studies are conflicting and demonstrate either decreased (39) or increased CCL5 levels in the blood during neonatal sepsis (40). IL-17 is important for immune surveillance and reduced levels of IL-17A in human preterm neonates is associated with increased risk of bacteraemia (41). On the other hand, pathologically elevated IL-17 can be harmful in the neonate as it is also associated with inflammatory diseases such as asthma (42).

IL-6 and G-CSF have predictive value in neonatal sepsis (43, 44) and IL-6 remains high in newborns with poor outcome following hypoxic-ischemic encephalopathy (45). In this study,

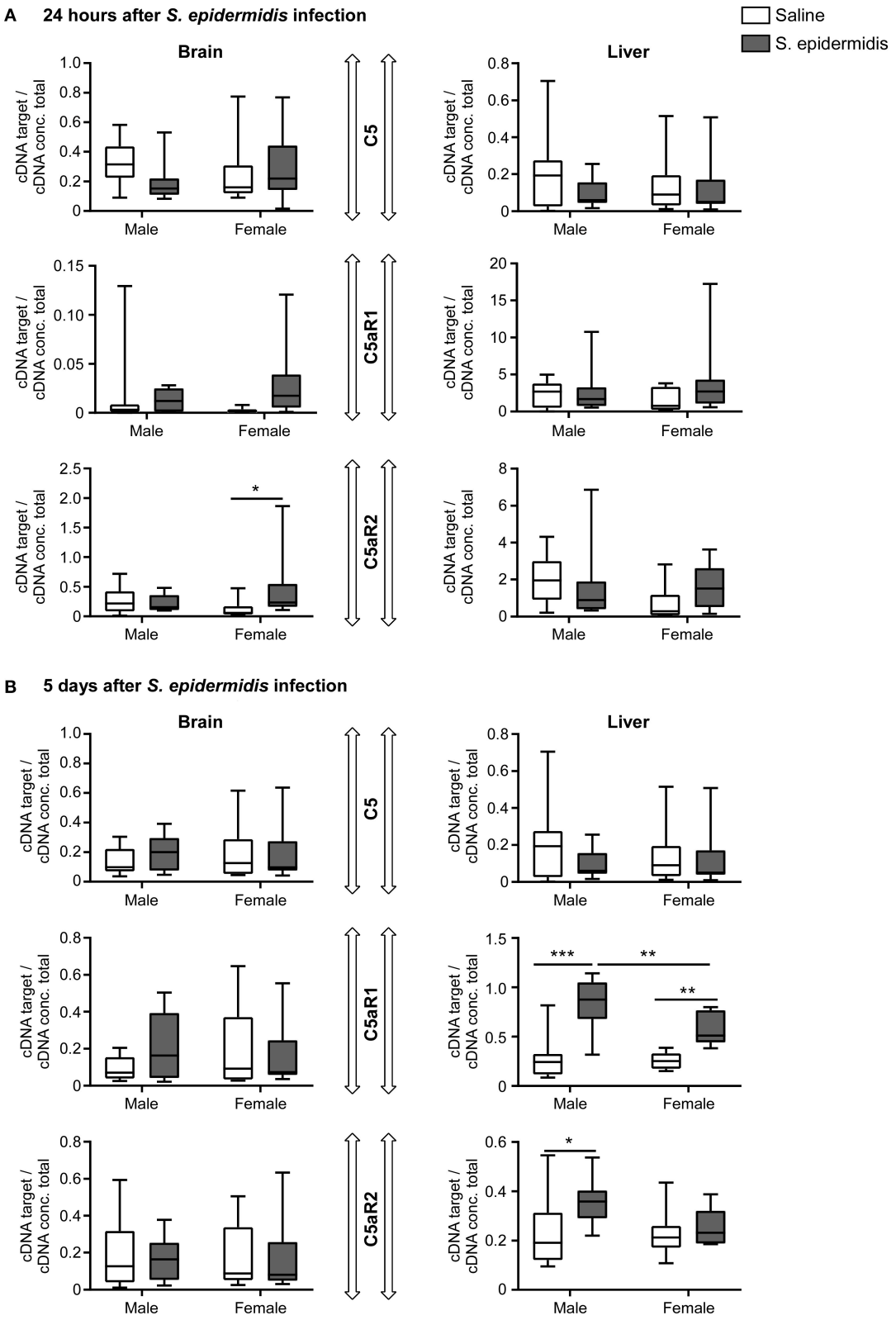

FIGURE 8 | Complement component C5 and receptor expression following *S. epidermidis* infection. PND4 mice were injected with saline or *S. epidermidis* and mRNA involved in C5 signaling (C5, C5aR1, C5aR2) was analyzed by PCR at **(A)** 24 h or **(B)** 5 days in the brain and liver ($n = 10$ mice/sex/group). Data are presented as median and 10–90th percentile. Statistical comparison between the *S. epidermidis* and saline groups was done using Two-way ANOVA followed by Sidak's multiple comparison *post-hoc* test; $^{*}p < 0.05$, $^{**}p < 0.01$, and $^{***}p < 0.001$.

plasma IL-6 and G-CSF were upregulated in both sexes at 24 h, but stayed elevated at 5 days only in males. Similarly, in the brain, CCL2 was upregulated in both males and females at 24 h but only in males at 5 d after the infection. Thus, these cytokines and chemokines may be important factors that are more pronounced in males. Interestingly, in line with our previous findings, there was no clear translation of CCL2 concentration in the blood to expression in the brain (46).

Complement proteins and their proteolytic fragments are important for phagocytosis by neutrophils and monocytes (47) and deficiency of proteins in the complement cascade is associated with increased susceptibility to perinatal infection, mortality and low birthweight (48). We found a biphasic C5a response in the plasma of male mice following *S. epidermidis* infection, with reduced C5a levels 24 h later and an increase in C5a levels 5 d after infection. A similar trend was seen in females at 24 h and we cannot exclude that females may have had an initial significant decrease in C5a levels at other time points from those we evaluated in the present study. The biphasic pattern of C5a is similar to patients admitted to hospitals with different types of trauma leading to systemic inflammatory response syndrome where the downstream complement membrane attack complex (MAC) is decreased at day 1 and increased on days 2–7 (49). The initial decrease in C5a levels could be due to temporary complement depletion in the presence of the bacteria or inflammation. In addition, the production of extracellular proteases from *S. epidermidis* can inactivate human plasma serine and cysteine proteinase inhibitors and thereby degrade C5 (50, 51), which may also explain the early decrease in plasma C5a we observed. Consistent with this hypothesis, we found a reversal, or even an increase in plasma C5a levels 5 days after infection, a time when the bacterial load is significantly reduced in the blood (14).

The decrease in C5a levels may lead to worsened disease outcome as C5-deficient mice demonstrate impaired bacterial clearance (52) and a study of adult patients with sepsis-induced brain dysfunction revealed a correlation between decreased C5a levels with increased mortality (53). Neonatal rats demonstrate elevated expression of C5a and C5 receptors in the blood and brain following HI, which is reduced with therapeutic hypothermia, suggesting that C5a has an injurious effect in cerebral tissue (18, 19). In contrast, even though C5 receptor expression was increased in the liver, we did not find any major changes in the mRNA expression of C5 or C5 receptors in the brain of infected mice prior to HI. Future studies examining C5 signaling following the combination of *S. epidermidis* infection and HI may reveal stronger evidence for a role of C5 complement in brain injury. Furthermore, as C5 receptors are mainly expressed in microglia, future studies that examine cellular expression of C5 receptors upon *S. epidermidis* infection may provide additional supporting data.

In conclusion, our results demonstrate that neonatal hypoxia-ischemia added to an ongoing *S. epidermidis* infection in combination with enhanced inflammation increases the vulnerability of the developing brain in a time- and sex-specific manner. Increased expression of a number of cytokines and chemokines and decreased C5a protein in the blood were associated with increased vulnerability in males. These findings are consistent with a higher incidence of perinatal brain injury in newborn males (32). Overall, we provide fresh insight into how systemic *S. epidermidis* infection affects the developing brain.

DATA AVAILABILITY STATEMENT

All datasets generated for this study are included in the article/**Supplementary Material**.

ETHICS STATEMENT

The animal study was reviewed and approved by Gothenburg Animal Ethical Committee (No. 663/2017).

AUTHOR CONTRIBUTIONS

This study was conceived and designed and the manuscript drafted by GG, JL, and CM. Experiments were performed by GG, PS, JL, and MA. Data analysis was performed by GG, JL, MA, and CE. All authors critically reviewed and edited the work.

FUNDING

This study was supported by VINNOVA VINNMER Marie-Curie Incoming (2015-01505—JL), Wilhelm & Martina Lundgrens Foundation (2016-1323, 2017-1966, 2018-2465—JL) (2019-2902—MA), Lilla Barnets Fund (20170806—JL), Anna-Brita & Bo Castegrens Memorial Foundation (LA2017-0269—JL), Stiftelsen Mary von Sydows, född Wijk, donationsfond (2019-2419—GG), Swedish Research Council (VR-2017-01409—CM), Åhlen Foundation (CM), Public Health Service at the Sahlgrenska University Hospital (ALFGBG-722491—CM), and Swedish Brain Foundation (FO2017-0063, FO2019-0270—CM).

SUPPLEMENTARY MATERIAL

The Supplementary Material for this article can be found online at: https://www.frontiersin.org/articles/10.3389/fimmu.2020.00516/full#supplementary-material

REFERENCES

1. Serenius F, Kallen K, Blennow M, Ewald U, Fellman V, Holmstrom G, et al. Neurodevelopmental outcome in extremely preterm infants at 2.5 years after active perinatal care in Sweden. *JAMA*. (2013) 309:1810–20. doi: 10.1001/jama.2013.3786
2. Strunk T, Inder T, Wang X, Burgner D, Mallard C, Levy O. Infection-induced inflammation and cerebral injury in preterm infants. *Lancet Infect Dis*. (2014) 14:751–62. doi: 10.1016/S1473-3099(14)70710-8
3. Ramasethu J. Prevention and treatment of neonatal nosocomial infections. *Matern Health Neonatol Perinatol*. (2017) 3:5. doi: 10.1186/s40748-017-0043-3

4. Rupp ME. Clinical characteristics of infections in humans due to *Staphylococcus epidermidis*. *Methods Mol Biol*. (2014) 1106:1–16. doi: 10.1007/978-1-62703-736-5_1
5. Dong Y, Speer CP. Late-onset neonatal sepsis: recent developments. *Arch Dis Child Fetal Neonatal Ed*. (2015) 100:F257–63. doi: 10.1136/archdischild-2014-306213
6. Otto M. *Staphylococcus epidermidis* pathogenesis. *Methods Mol Biol*. (2014) 1106:17–31. doi: 10.1007/978-1-62703-736-5_2
7. Hagberg H, Mallard C, Ferriero DM, Vannucci SJ, Levison SW, Vexler ZS, et al. The role of inflammation in perinatal brain injury. *Nat Rev Neurol*. (2015) 11:192–208. doi: 10.1038/nrneurol.2015.13
8. Meneses G, Cardenas G, Espinosa A, Rassy D, Perez-Osorio IN, Barcena B, et al. Sepsis: developing new alternatives to reduce neuroinflammation and attenuate brain injury. *Ann N Y Acad Sci*. (2019) 1437:43–56. doi: 10.1111/nyas.13985
9. Alshaikh B, Yusuf K, Sauve R. Neurodevelopmental outcomes of very low birth weight infants with neonatal sepsis: systematic review and meta-analysis. *J Perinatol*. (2013) 33:558–64. doi: 10.1038/jp.2012.167
10. Hofstetter AO, Legnevall L, Herlenius E, Katz-Salamon M. Cardiorespiratory development in extremely preterm infants: vulnerability to infection and persistence of events beyond term-equivalent age. *Acta Paediatr*. (2008) 97:285–92. doi: 10.1111/j.1651-2227.2007.00618.x
11. Aslam S, Strickland T, Molloy EJ. Neonatal encephalopathy: need for recognition of multiple etiologies for optimal management. *Front Pediatr*. (2019) 7:142. doi: 10.3389/fped.2019.00142
12. Mottahedin A, Svedin P, Nair S, Mohn CJ, Wang X, Hagberg H, et al. Systemic activation of toll-like receptor 2 suppresses mitochondrial respiration and exacerbates hypoxic-ischemic injury in the developing brain. *J Cereb Blood Flow Metab*. (2017) 37:1192–8. doi: 10.1177/0271678X17691292
13. Falck M, Osredkar D, Maes E, Flatebo T, Wood TR, Walloe L, et al. Hypothermia is neuroprotective after severe hypoxic-ischaemic brain injury in neonatal rats pre-exposed to PAM3CSK4. *Dev Neurosci*. (2018) 40:189–97. doi: 10.1159/000487798
14. Lai JCY, Svedin P, Ek CJ, Mottahedin A, Wang X, Levy O, et al. Vancomycin is protective in a neonatal mouse model of *Staphylococcus epidermidis*-potentiated hypoxic-ischemic brain injury. *Antimicrob Agents Chemother*. (2020) 64: e02003-19. doi: 10.1128/AAC.02003-19
15. Eklind S, Mallard C, Arvidsson P, Hagberg H. Lipopolysaccharide induces both a primary and a secondary phase of sensitization in the developing rat brain. *Pediatr Res*. (2005) 58:112–6. doi: 10.1203/01.PDR.0000163513.03619.8D
16. Galindo-Sevilla N, Reyes-Arroyo F, Mancilla-Ramirez J. The role of complement in preterm birth and prematurity. *J Perinat Med*. (2019) 47:793–803. doi: 10.1515/jpm-2019-0175
17. Yan C, Gao H. New insights for C5a and C5a receptors in sepsis. *Front Immunol*. (2012) 3:368. doi: 10.3389/fimmu.2012.00368
18. Pavlovski D, Thundyil J, Monk PN, Wetsel RA, Taylor SM, Woodruff TM. Generation of complement component C5a by ischemic neurons promotes neuronal apoptosis. *FASEB J*. (2012) 26:3680–90. doi: 10.1096/fj.11-202382
19. Shah TA, Nejad JE, Pallera HK, Lattanzio FA, Farhat R, Kumar PS, et al. Therapeutic hypothermia modulates complement factor C3a and C5a levels in a rat model of hypoxic ischemic encephalopathy. *Pediatr Res*. (2017) 81:654–62. doi: 10.1038/pr.2016.271
20. Pataky R, Howie FA, Girardi G, Boardman JP. Complement C5a is present in CSF of human newborns and is elevated in association with preterm birth. *J Matern Fetal Neonatal Med*. (2017) 30:2413–6. doi: 10.1080/14767058.2016.1251896
21. Albertsson AM, Bi D, Duan L, Zhang X, Leavenworth JW, Qiao L, et al. The immune response after hypoxia-ischemia in a mouse model of preterm brain injury. *J Neuroinflammation*. (2014) 11:153. doi: 10.1186/s12974-014-0153-z
22. Svedin P, Hagberg H, Savman K, Zhu C, Mallard C. Matrix metalloproteinase-9 gene knock-out protects the immature brain after cerebral hypoxia-ischemia. *J Neurosci*. (2007) 27:1511–8. doi: 10.1523/JNEUROSCI.4391-06.2007
23. Zhu C, Wang X, Xu F, Bahr BA, Shibata M, Uchiyama Y, et al. The influence of age on apoptotic and other mechanisms of cell death after cerebral hypoxia-ischemia. *Cell Death Differ*. (2005) 12:162–76. doi: 10.1038/sj.cdd.4401545
24. Vincze A, Mazlo M, Seress L, Komoly S, Abraham H. A correlative light and electron microscopic study of postnatal myelination in the murine corpus callosum. *Int J Dev Neurosci*. (2008) 26:575–84. doi: 10.1016/j.ijdevneu.2008.05.003
25. Ardalan M, Chumak T, Vexler Z, Mallard C. Sex-dependent effects of perinatal inflammation on the brain: implication for neuro-psychiatric disorders. *Int J Mol Sci*. (2019) 20:E2270. doi: 10.3390/ijms20092270
26. Bi D, Qiao L, Bergelson I, Ek CJ, Duan L, Zhang X, et al. *Staphylococcus epidermidis* bacteremia induces brain injury in neonatal mice via toll-like receptor 2-dependent and -independent pathways. *J Infect Dis*. (2015) 212:1480–90. doi: 10.1093/infdis/jiv231
27. Strunk T, Power Coombs MR, Currie AJ, Richmond P, Golenbock DT, Stoler-Barak L, et al. TLR2 mediates recognition of live *Staphylococcus epidermidis* and clearance of bacteremia. *PLoS ONE*. (2010) 5:e10111. doi: 10.1371/journal.pone.0010111
28. Strunk T, Prosser A, Levy O, Philbin V, Simmer K, Doherty D, et al. Responsiveness of human monocytes to the commensal bacterium *Staphylococcus epidermidis* develops late in gestation. *Pediatr Res*. (2012) 72:10–8. doi: 10.1038/pr.2012.48
29. Lim S, Han CE, Uhlhaas PJ, Kaiser M. Preferential detachment during human brain development: age- and sex-specific structural connectivity in diffusion tensor imaging (DTI) data. *Cereb Cortex*. (2015) 25:1477–89. doi: 10.1093/cercor/bht333
30. Cahill L. Why sex matters for neuroscience. *Nat Rev Neurosci*. (2006) 7:477–84. doi: 10.1038/nrn1909
31. Challis J, Newnham J, Petraglia F, Yeganegi M, Bocking A. Fetal sex and preterm birth. *Placenta*. (2013) 34:95–9. doi: 10.1016/j.placenta.2012.11.007
32. Charriaut-Marlangue C, Besson VC, Baud O. Sexually dimorphic outcomes after neonatal stroke and hypoxia-ischemia. *Int J Mol Sci*. (2017) 19:E61. doi: 10.3390/ijms19010061
33. Xu G, Strathearn L, Liu B, Bao W. Prevalence of autism spectrum disorder among US children and adolescents, 2014-2016. *JAMA*. (2018) 319:81–2. doi: 10.1001/jama.2017.17812
34. Polanczyk G, de Lima MS, Horta BL, Biederman J, Rohde LA. The worldwide prevalence of ADHD: a systematic review and metaregression analysis. *Am J Psychiatry*. (2007) 164:942–8. doi: 10.1176/ajp.2007.164.6.942
35. Rucklidge JJ. Gender differences in attention-deficit/hyperactivity disorder. *Psychiatr Clin North Am*. (2010) 33:357–73. doi: 10.1016/j.psc.2010.01.006
36. Villa A, Gelosa P, Castiglioni L, Cimino M, Rizzi N, Pepe G, et al. Sex-Specific features of microglia from adult mice. *Cell Rep*. (2018) 23:3501–11. doi: 10.1016/j.celrep.2018.05.048
37. Bruce M, Streifel KM, Boosalis CA, Heuer L, Gonzalez EA, Li S, et al. Acute peripheral immune activation alters cytokine expression and glial activation in the early postnatal rat brain. *J Neuroinflammation*. (2019) 16:200. doi: 10.1186/s12974-019-1569-2
38. Vazquez-Martinez ER, Garcia-Gomez E, Camacho-Arroyo I, Gonzalez-Pedrajo B. Sexual dimorphism in bacterial infections. *Biol Sex Differ*. (2018) 9:27. doi: 10.1186/s13293-018-0187-5
39. Sugitharini V, Prema A, Berla Thangam E. Inflammatory mediators of systemic inflammation in neonatal sepsis. *Inflamm Res*. (2013) 62:1025–34. doi: 10.1007/s00011-013-0661-9
40. Stojewska M, Wasek-Buko M, Jakub B, Wisniewska-Ulfig D, Goleniowska-Krol A, Szymanska A, et al. Evaluation of serum chemokine RANTES concentration as a biomarker in the diagnosis of early-onset severe infections in neonates. *Postepy Hig Med Dosw*. (2016) 70:272–9. doi: 10.5604/17322693.1198990
41. Schelonka RL, Maheshwari A, Carlo WA, Taylor S, Hansen NI, Schendel DE, et al. T cell cytokines and the risk of blood stream infection in extremely low birth weight infants. *Cytokine*. (2011) 53:249–55. doi: 10.1016/j.cyto.2010.11.003
42. Lawrence SM, Ruoss JL, Wynn JL. IL-17 in neonatal health and disease. *Am J Reprod Immunol*. (2018) 79:e12800. doi: 10.1111/aji.12800
43. Ye Q, Du LZ, Shao WX, Shang SQ. Utility of cytokines to predict neonatal sepsis. *Pediatr Res*. (2017) 81:616–21. doi: 10.1038/pr.2016.267
44. Leal YA, Alvarez-Nemegyei J, Lavadores-May AI, Giron-Carrillo JL, Cedillo-Rivera R, Velazquez JR. Cytokine profile as diagnostic and prognostic factor in neonatal sepsis. *J Matern Fetal Neonatal Med*. (2019) 32:2830–6. doi: 10.1080/14767058.2018.1449828

45. Orrock JE, Panchapakesan K, Vezina G, Chang T, Harris K, Wang Y, et al. Association of brain injury and neonatal cytokine response during therapeutic hypothermia in newborns with hypoxic-ischemic encephalopathy. *Pediatr Res*. (2016) 79:742–7. doi: 10.1038/pr.2015.280
46. Mottahedin A, Smith PL, Hagberg H, Ek CJ, Mallard C. TLR2-mediated leukocyte trafficking to the developing brain. *J Leukoc Biol*. (2017) 101:297–305. doi: 10.1189/jlb.3A1215-568R
47. Basha S, Surendran N, Pichichero M. Immune responses in neonates. *Expert Rev Clin Immunol*. (2014) 10:1171–84. doi: 10.1586/1744666X.2014.942288
48. Cedzynski M, Swierzko AS, Kilpatrick DC. Factors of the lectin pathway of complement activation and their clinical associations in neonates. *J Biomed Biotechnol*. (2012) 2012:363246. doi: 10.1155/2012/363246
49. Li Y, Zhao Q, Liu B, Dixon A, Cancio L, Dubick M, et al. Early complementopathy predicts the outcomes of patients with trauma. *Trauma Surg Acute Care Open*. (2019) 4:e000217. doi: 10.1136/tsaco-2018-000217
50. Dubin G, Chmiel D, Mak P, Rakwalska M, Rzychon M, Dubin A. Molecular cloning and biochemical characterisation of proteases from *Staphylococcus epidermidis*. *Biol Chem*. (2001) 382:1575–82. doi: 10.1515/BC.2001.192
51. Moon JL, Banbula A, Oleksy A, Mayo JA, Travis J. Isolation and characterization of a highly specific serine endopeptidase from an oral strain of *Staphylococcus epidermidis*. *Biol Chem*. (2001) 382:1095–9. doi: 10.1515/BC.2001.138
52. Flierl MA, Rittirsch D, Nadeau BA, Day DE, Zetoune FS, Sarma JV, et al. Functions of the complement components C3 and C5 during sepsis. *FASEB J*. (2008) 22:3483–90. doi: 10.1096/fj.08-110595
53. Orhun G, Tuzun E, Ozcan PE, Ulusoy C, Yildirim E, Kucukerden M, et al. Association between inflammatory markers and cognitive outcome in patients with acute brain dysfunction due to sepsis. *Noro Psikiyatr Ars*. (2019) 56:63–70. doi: 10.29399/npa.23212

Conflict of Interest: The authors declare that the research was conducted in the absence of any commercial or financial relationships that could be construed as a potential conflict of interest.

frontiers in Immunology

REVIEW
published: 30 April 2020
doi: 10.3389/fimmu.2020.00688

S100-Alarmins Are Essential Pilots of Postnatal Innate Immune Adaptation

Dorothee Viemann [1,2,3]*

[1] Department of Pediatric Pneumology, Allergy and Neonatology, Hannover Medical School, Hanover, Germany, [2] Cluster of Excellence RESIST (EXC 2155), Hannover Medical School, Hanover, Germany, [3] PRIMAL Consortium, Hanover, Germany

The restricted capacity of newborn infants to mount inflammatory responses toward microbial challenges has traditionally been linked to the high risk of septic diseases during the neonatal period. In recent years, substantial evidence has been provided that this characteristic of the neonatal immune system is actually a meaningful physiologic state that is based on specific transiently active cellular and molecular mechanisms and required for a favorable course of postnatal immune adaptation. The identification of physiologically high amounts of S100-alarmins in neonates has been one of the crucial pieces in the puzzle that contributed to the change of concept. In this context, innate immune immaturity could be redefined and assigned to the epigenetic silence of adult-like cell-autonomous regulation at the beginning of life. S100-alarmins represent an alternative age-specific mechanism of immune regulation that protects neonates from hyperinflammatory immune responses. Here, we summarize how infants are provided with S100-alarmins and why these allow an uneventful clash between the innate immune system and the extrauterine world. The mode of action of S100-alarmins is highlighted including their tuning functions at multiple levels for establishing a state of homeostasis with the environment in the newborn individual.

Keywords: neonate, S100A8/A9, systemic immunity, innate immunity, trained immunity, immune adaptation, inflammatory diseases

Edited by:
Andrew Currie,
Murdoch University, Australia

Reviewed by:
Markus Sperandio,
Ludwig Maximilian University of Munich, Germany
Daniel Scott-Algara,
Institut Pasteur, France

***Correspondence:**
Dorothee Viemann
Viemann.Dorothee@mh-hannover.de

Specialty section:
This article was submitted to Inflammation, a section of the journal Frontiers in Immunology

Received: *17 December 2019*
Accepted: *26 March 2020*
Published: *30 April 2020*

Citation:
Viemann D (2020) S100-Alarmins Are Essential Pilots of Postnatal Innate Immune Adaptation. Front. Immunol. 11:688. doi: 10.3389/fimmu.2020.00688

INTRODUCTION

After transition from the largely sterile intrauterine environment, the immune system encounters a flood of antigenic stimuli in the new extrauterine world. This represents an enormous challenge for the newborn infant and initiates a process of immune adaptation. Ideally, early-life immune adaptation is a training by new antigens that goes along with the acquisition of protecting immune memory. Especially during the neonatal window of life, responses to new antigens have lifelong imprinting effects by transcriptional and epigenetic reprogramming of systemic and mucosal immunity (1–8). Therefore, early-life immune adaptation critically determines the long-term development of health and disease. Successful immune adaptation achieves an energy-efficient state of homeostasis which balances tolerizing and defending activities of the immune system toward the environment. If immune adaptation fails, the activity of the immune system remains unbalanced which sooner or later leads to the development of chronic inflammatory diseases and an increased susceptibility to infections (2, 3, 5, 9–14). With respect to systemic immunity, important direct reprogramming immune challenges are commensal microbes colonizing the host's barrier sites including thereof translocating metabolites, infections, vaccines, and metabolized food components (2, 3, 5, 7). Therefore, in terms of promotion of successful immune adaptation,

a myriad of excellent work has been done and still goes into identifying the ideal pattern of developing microbiota compositions, dissecting "bad" and "good" early-life infections, testing optimized kinds, and combinations of vaccines and defining the most favorable diet including probiotics for infants and young children. On the other side, the mechanisms and molecular options, the newborn infant has to impact on the process of immune adaptation, are still barely elucidated. The interindividual differences in coping with the flood of new antigens after birth and the postnatal development of immunity indicate that host factors must play an important role for the outcome of immune adaptation. Host factors might exert direct imprinting effects and/or determine how the neonate meets its new environment by regulating the neonatal immune response. In this respect, the alarmins S100A8 and S100A9 have been identified as important host factors warranting uneventful and favorable postnatal immune adaptation. In this review, we highlight the current knowledge about the sources of S100A8/A9 supply to the newborn infant and the mode of action of S100A8/A9 in controlling postnatal innate immune adaptation.

PROTEIN BIOCHEMISTRY AND SIGNALING OF S100A8/A9

S100A8 (also named calgranulin A; myeloid-related protein 8, MRP8) and S100A9 (calgranulin B; MRP14) are two members of the S100 protein family specifically linked to innate immune functions. They are calcium-binding proteins characterized by two calcium binding EF-hand motifs, which are connected by a central hinge region. Physiologically, S100A8 and S100A9 exist only as heterodimer S100A8/A9 (termed calprotectin) that can form heterotetramers in the presence of calcium or zinc, but not or at most very little as S100A8/A8 or S100A9/A9 homodimers (15, 16). The reason for it is the instability of the homodimers. Two independent laboratories have shown that myeloid cells of the *S100a9*-knockout mouse express *S100a8* mRNA but no S100a8 protein, suggesting that the posttranscriptional *in vivo* stability of S100a8 protein is dependent on S100A9 expression (17, 18). Interestingly, the deletion of the mouse *S100a8* gene results in an embryonically lethal phenotype without detectability of S100A9 homodimers, pointing to an important role of S100A8 during embryogenesis (19). Once released to the extracellular space, S100A8/A9 impacts on immune cells through binding to different cell surface receptors.

In inflammatory disease states, S100A8/A9 has been shown to bind to endothelial cells (ECs) and chondrocytes by a mechanism involving heparan sulfate proteoglycans and carboxylated N-glycans (20–22). The multiligand receptor for advanced glycation end products (RAGE) was also proposed to act as an S100A8/A9 receptor (23, 24). However, in healthy conditions, the physiological relevance is debatable as RAGE is widespread (on vascular ECs, neutrophils, monocytes/macrophages, lymphocytes, dendritic cells, cardiomyocytes, and neurons) but relatively low expressed (25). Moreover, the binding of S100A8/A9 to RAGE is rather weak and was shown to rely on S100A9 and the presence of Ca^{2+} or Zn^{2+} ions (26). Therefore, it is still controversial and questionable that RAGE mediates S100A8/A9 signal transduction.

The main signaling pathway of S100A8/A9 has been delineated by Vogl et al. who demonstrated that S100A8/A9 is a ligand of the Toll-like receptor 4 (TLR4) (27–30). A direct binding of S100A8 and S100A9 to the TLR4–myeloid differentiation factor 2 (MD2) complex was confirmed by surface plasmon resonance studies (29) and comprehensive binding assays (30). The discovery of S100A8/A9 as endogenous TLR4 ligand has been groundbreaking as before TLR4 was only known as a pattern recognition receptor (PRR) for the exogenous TLR4 ligand lipopolysaccharide (LPS), the integral part of the outer membrane of gram-negative bacteria. Fueled by this work, the concept of endogenous damage-associated molecular pattern molecules (DAMPs, also termed alarmins) evolved in analogy to the exogenous microbe-associated respective pathogen-associated pattern molecules (MAMPs respective PAMPs) as activators of PRRs. The canonical downstream signaling induced by TLR4 ligation through S100A8/A9 and LPS has a huge overlap (27–29). Similar to LPS (31, 32), the binding of S100A8/A9 induces the translocation of the adaptor molecule MyD88 from the cytosol to the TLR4 receptor complex which subsequently activates interleukin-1 receptor–associated kinase-1 (IRAK-1) and the transcription factor nuclear factor (NF)-κB p65/p50, thereby increasing the expression of a classical pro-inflammatory gene program including, e.g., tumor necrosis factor (*TNF*), interleukin (*IL*)*6*, *IL1B*, C-X-C motif chemokine ligand 2 (*CXCL2*), and C-C motif chemokine ligand 2 (*CCL2*) (8, 27–30). However, in contrast to LPS, at least in neonatal monocytes, it was shown that S100A8/A9 does not activate the TLR4 adaptor molecule TIR domain-containing adaptor protein-inducing interferon-β (TRIF)-TRIF-related adaptor molecule (TRAM) (8). The reason for it has not been completely elucidated yet, but S100A8/A9 seems to bind different domains of the TLR4/MD2 receptor complex than LPS (29, 30). TRIF-dependent TLR4 signaling shifts the transcription factors IFN regulatory factor (IRF)3 and IRF7 into the nucleus and activates a regulatory gene program including, e.g., *CCL5*, *CXCL9*, *CXCL10*, *CD80*, and IFN-response genes that in turn regulates the LPS response in a cell-autonomous manner and also links the innate to the adaptive immune system (33–36).

When released secondarily during a primary acute inflammatory process like sepsis and infection or autoimmune and autoinflammatory reactions, S100A8/A9 amplifies the primary pro-inflammatory response by activating the MyD88-dependent TLR4 signaling pathway (29, 37–42) (**Figure 1**). In adults, the sepsis amplifying effect was proposed to be pathogenetically relevant. In a small study in 17 septic shock patients, S100A8/A9 levels decreased in surviving patients during recovery while non-survivors were characterized by high S100A8/A9 serum levels (43). This could be validated in another cohort of 49 septic shock patients with high plasma levels of S100A8/A9 being associated with a higher risk of death (42). However, under sterile stress conditions with no underlying primary inflammatory stimulus, S100A8/A9 does not induce an inflammatory disease state but contrary a state of inflammatory hyporesponsiveness to subsequent inflammatory

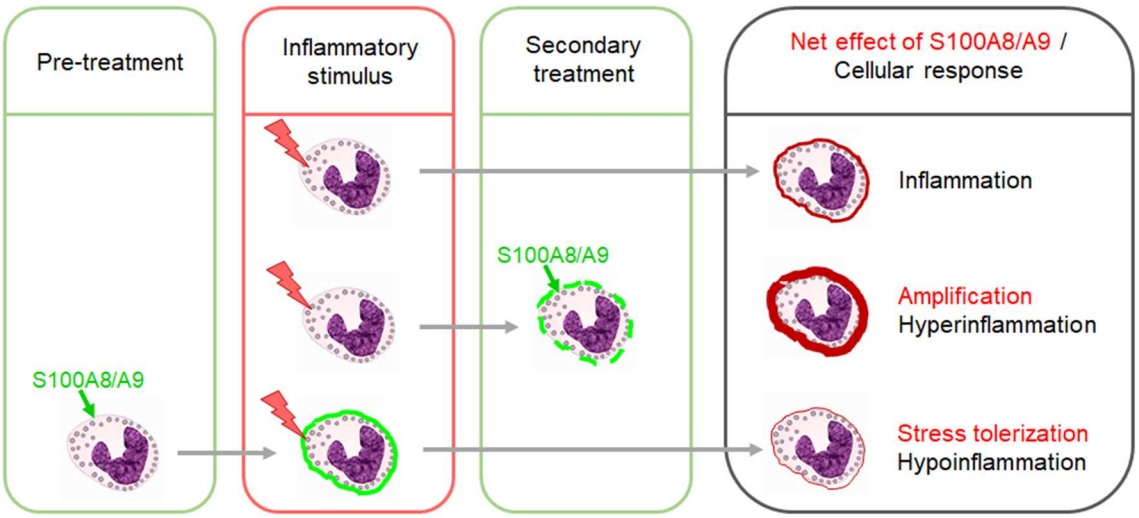

FIGURE 1 | Dual impact of S100A8/A9 on the outcome of inflammatory responses. The secondary release of S100A8/A9 during an inflammatory response upon a preceding stimulus has amplifying effects. Excessive S100A8/A9 release in such settings increases the risk of hyperinflammation. In contrast, pretreatment of immune cells with S100A8/A9 induces a state of hyporesponsiveness of innate signaling pathways which dampens the response to subsequent inflammatory stimuli.

stimuli, particularly microbial challenges (**Figure 1**) (8, 27, 44). However, S100A8/A9 was shown to tolerize not only for a subsequent TLR4 signaling but also TLR2 signaling (27). This work led to the introduction of the concept of "stress tolerance" by endogenous DAMPs and completed the proof of principle that DAMPs similar as PAMPs are able to act in a dual manner, i.e., pro-inflammatory when released secondary and regulatory under sterile conditions. No matter whether pro-inflammatory or regulatory, the S100a8 homodimer proved in several studies as much more potent than the S100a9 homodimer or the heterodimer S100A8/A9 (8, 27, 45). The question of the reason for it could be solved recently. S100A8 and S100A9 bind to the TLR4 complex *via* specific peptide sequences (29, 30). It was shown that calcium-induced $(S100A8/A9)_2$ tetramer formation hides the TLR4-binding site and blocks the ability of the heterodimer to further bind to TLR4 which prevents undesirable systemic effects (30). This work provided the explanation for how S100A8/A9 effects are locally restricted in sterile settings.

An important molecular mechanism of stress tolerance induction is the S100A8/A9-TLR4-MyD88-mediated preactivation of NF-κB. After activation, cytosolic NF-κB shifts into the nucleus and is then subjected to rapid proteasomal degradation (8, 46, 47). Thus, after S100A8/A9-conditioning, cytosolic NF-κB is no longer available for the canonical signaling cascades of subsequently activated innate signaling pathways which except for TLR3 all depend essentially on NF-κB (31). Yet, recently, it could be revealed that S100A8/A9 priming induces still more in-depth reprogramming of immune cells than only "NF-κB consumption." In human as well as murine monocytes/macrophages, two major pathways responsible for the S100A8/A9-primed hyporesponsiveness could be identified (44). Firstly, S100A8/A9 induced a lasting inactivation of the phosphatidylinositol 3-kinase (PI3K)/AKT/GSK-3β pathway which resulted in an accumulation of NF-κB inhibitors. Secondly, IL-10-dependent STAT3 activation and nuclear BCL-3 accumulation were identified as master regulators of S100A8/A9-induced tolerance, with the latter resulting in an inhibition of NF-κB transactivation.

SYSTEMIC SUPPLY OF THE NEWBORN INFANT WITH S100A8/A9

In health, significant expression of S100A8 and S100A9 has been found only in cells of myeloid origin, i.e., granulocytes, monocytes, and macrophages (48, 49). S100A8 and S100A9 constitute up to 40% of cytosolic proteins in granulocytes and 5% in monocytes (50). Inducible expression in microvascular ECs has been described (51, 52) in experimental lung cancer but not under physiologic conditions (51). In psoriasis and other inflammatory skin diseases, S100A8 and S100A9 are highly overexpressed in keratinocytes, while levels are low in normal epidermis (53, 54). Moreover, S100A8/A9 has been identified as a differentiation marker of mammary epithelial cells suppressing malignant transition (55).

In healthy neonates, the concentration of S100A8/A9 in the serum is massively increased in the first days of life up to mean levels of >3,000 ng/ml that in adults are only detectable in inflammatory diseases (27). The high serum levels of S100A8/A9 after birth rapidly decrease but reach normal adult levels (≤330 ng/ml) not before the second week of life. Hitherto, two sources have been identified that contribute to the high serum levels of S100A8/A9 in newborn infants. Firstly, neonatal blood monocytes and macrophages overexpress and strongly release S100A8/A9, while expression in the corresponding cell types in healthy adult individuals is low (8, 27, 45). Neonatal granulocytes

probably also express S100A8 and S100A9 at high levels, but this still needs to be demonstrated. Secondly, human breast milk contains the highest amounts of S100A8/A9 hitherto found under physiologic conditions (56). In healthy term newborns, the levels in breast milk are in average at least six times higher than the already elevated S100A8/A9 serum levels. The kinetics of S100A8/A9 breast milk levels resemble much that in the neonate's serum, i.e., levels are highest in the colostrum and then gradually decrease over time, reaching normal adult serum levels 1 month after birth. In exclusively breast milk-fed human infants, fecal levels of S100A8/A9 were shown to be significantly higher than in formula-fed ones (57). In mice, enterally supplied S100A8/A9 was demonstrated to be systemically bioavailable in the blood circulation (56). In humans, the dependence of the height of S100A8/A9 levels in the serum on the supply by breast milk awaits quantification. Maternal myeloid cells certainly represent a major production site of the high amounts of S100A8/A9 in human breast milk (58) as levels are three times higher if breast milk samples are analyzed without prior depletion of cells (unpublished data of the authors). To what extent mammary epithelial cells (55) increase the production of S100A8/A9 in the lactating human breast and release it into the milk is currently unknown.

A remarkable aspect related to the physiologically high levels of S100A8/A9 in newborn infants is its unsuitability as an inflammatory biomarker, underlining once more the importance and different role of S100A8/A9 in the neonatal period as compared to later childhood and adulthood. In children and adults, the serum level of S100A8/A9 is clinically used as an excellent biomarker in inflammatory processes like sepsis (42, 43), rheumatoid arthritis, juvenile idiopathic arthritis, and autoinflammatory diseases (40, 59–62). In contrast, in neonates, attempts to establish S100A8/A9 as a clinical biomarker of neonatal sepsis remained without tangible success. Two groups proposed serum S100A8/A9 as a promising sepsis marker in very low birth weight infants (63) respective of infants of all gestational ages (64). Both groups surprisingly claimed that S100A8/A9 values were not influenced by postnatal age and the area under receiver operating characteristic (ROC) curve of 0.6 at a cutoff level of 2,200 ng/ml (64) unveiled S100A8/A9 as a rather poor discriminator.

The release of S100A8/A9 from myeloid cells is a specific and energy-dependent process (65). Any sort of stress and cell damage triggers the release of S100A8/A9 like infections, malignancies, burns, and trauma (22, 27, 29, 37–39, 41, 51, 54, 59–62, 66, 67). The interaction of activated endothelium with phagocytes was also described as an important stimulus for S100A8/A9 secretion (66). A study in marathon runners was the first one revealing that heavy exercise represents a physiologic stress trigger leading to increased S100A8/A9 serum levels during the early post-exercise period that returned to normal levels 1 day after the run (68). Labor and birth are certainly one of the most exhausting conditions in life, imposing heavy stress on the mother as well as the newborn infant. Thus, birth-related stress is probably the main trigger of perinatal S100A8/A9 release, and the gradual resolution of stress after birth well explains the postnatal decrease of S100A8/A9 in breast milk (56) and the infant's blood circulation (27). Therewith in line is a previous report that glucocorticoids can induce the expression of S100-alarmins (69). S100A8-producing macrophages were significantly elevated in rheumatoid arthritis patients treated with high-dose steroids. Further trigger for the release of S100A8/A9 in the perinatal context are thinkable but would need validation, e.g., the hormonal changes upon birth giving like the strong increase of estrogens and oxytocin or the withdrawal of progesterone (70).

The major determinant of birth-induced stress is the extent of labor and uterine contractions which is absent in elective cesarean section (CS) (71). This explains why S100A8/A9 levels in breast milk were significantly higher after vaginal delivery (VD) compared to delivery by CS (56). Moreover, the gestational age has an influence on the height of S100A8/A9 levels. S100A8/A9 levels in breast milk of mothers who gave birth to term babies were significantly higher than of mothers with premature born infants (56). The same holds true for S100A8/A9 levels in cord blood of preterm infants compared to term ones (8). Various other parameters like birth weight, gender, Apgar score, hormonal status of the neonate and the mother, maternal body mass index, and perinatal medications might also influence the early-life S100A8/A9 levels and are currently analyzed in the frame of a prospective multicenter clinical study (BMBF 01GL1746B, DRKS00013197) (72).

Summarized, clearly identified states of early-life S100A8/A9 deficiency are premature birth, elective CS, and formula feeding. The manifold reported associations of all these conditions with an unfavorable short-term as well as long-term immune adaptation including an increased susceptibility to infections (5, 9, 10, 14) and a higher risk for developing chronic inflammatory diseases (2, 3, 11, 12, 14) are a strong indicator for S100-alarmins being a possible common molecular denominator setting the stage for successful postnatal immune adaptation.

ROLE OF S100A8/A9 FOR THE POSTNATAL ADAPTATION OF SYSTEMIC IMMUNITY

The neonatal immune system has traditionally been regarded as "deficient" and the high susceptibility to infections has been understood as a "general weakness." This concept referred to numerous experimental studies that found impaired inflammatory responses of neonatal immune cells to different microbial challenges (5, 13, 14, 73). The expansion of certain suppressive cell types, e.g., regulatory T cells (Tregs) and granulocytic myeloid suppressor cells (MDSCs) observed in neonates was interpreted as part of this concept (74, 75). However, the hallmark of neonatal sepsis is an extremely rapid course with a hyperinflammatory immune response (76), and the inconsistency of experimental and clinical findings remained unsolved for a long time. The disclosure of diverse molecular and cellular effects of physiologically high amounts of S100-alarmins on the neonatal immune system (**Figure 2**) significantly contributed to the change of concept that the previously misunderstood characteristics of neonatal immunity actually

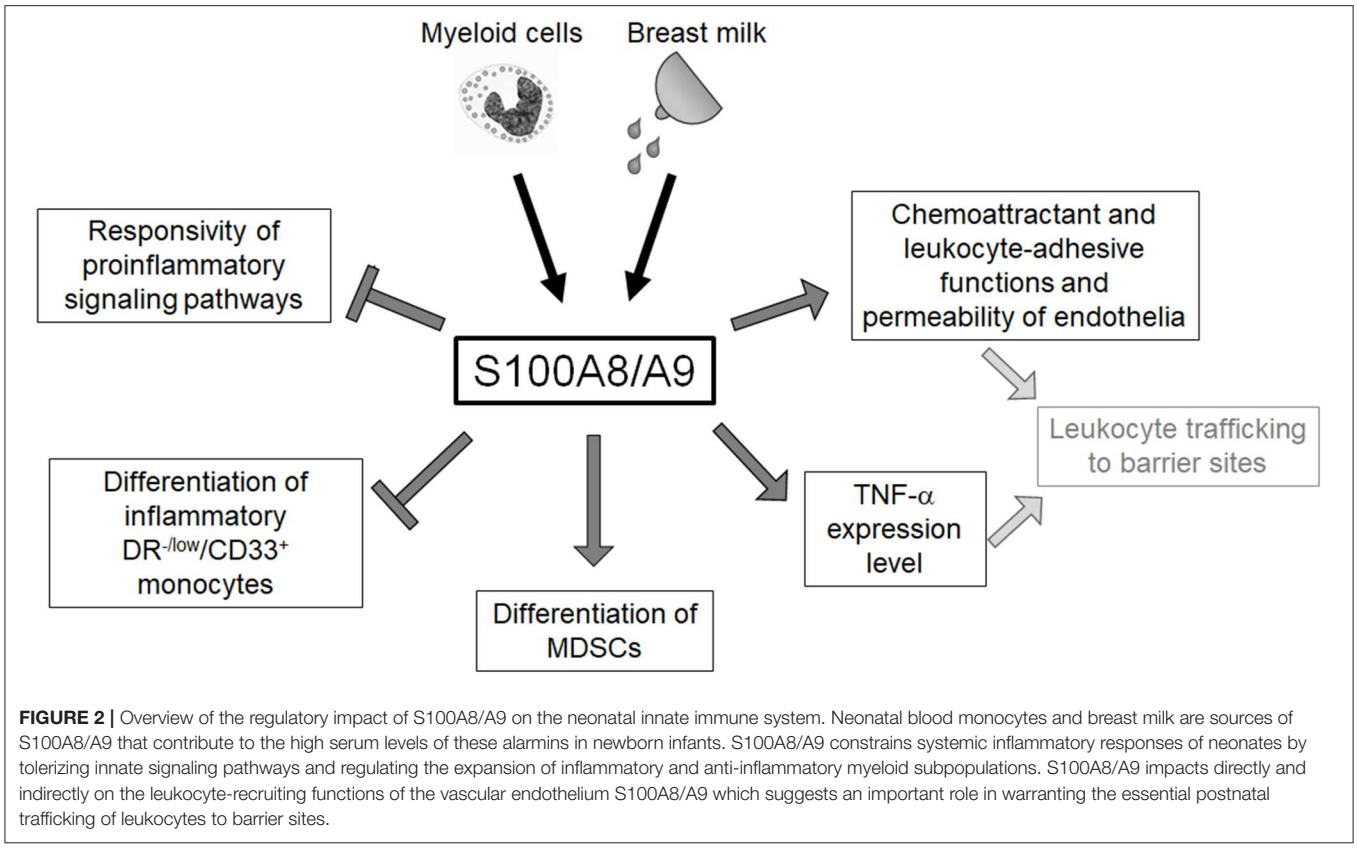

FIGURE 2 | Overview of the regulatory impact of S100A8/A9 on the neonatal innate immune system. Neonatal blood monocytes and breast milk are sources of S100A8/A9 that contribute to the high serum levels of these alarmins in newborn infants. S100A8/A9 constrains systemic inflammatory responses of neonates by tolerizing innate signaling pathways and regulating the expansion of inflammatory and anti-inflammatory myeloid subpopulations. S100A8/A9 impacts directly and indirectly on the leukocyte-recruiting functions of the vascular endothelium S100A8/A9 which suggests an important role in warranting the essential postnatal trafficking of leukocytes to barrier sites.

represent an essential programming that warrants postnatal immune adaptation.

First of all, it was recognized that the high release and supply of S100A8/A9 directly at the beginning of life corresponds to a conditioning of the neonatal immune system with S100-alarmins and that such pretreatment with S100-alarmins results in stress tolerization of immune cells toward subsequent microbial stimuli (27). The importance and biological relevance of this specific mechanism in newborn infants was further elucidated by Ulas et al. (8) who could link the impaired response of neonatal monocytes to LPS to an activated initial state of MyD88-dependent gene expression at baseline. They further identified S100A8/A9 as an inducer of this specific activation state of neonatal monocytes that was transcriptionally as well as epigenetically fixed as long as serum levels of S100A8/A9 were high. Withdrawal or blocking of S100A8/A9 terminated the activation of the MyD88-dependent gene program and came along with an increased inflammatory response toward microbial stimuli *in vitro* and *in vivo* in experimental sepsis models (8, 27, 45). Furthermore, S100A8/A9 also caused a metabolic programming in cord blood macrophages that was characterized by an impaired glycolysis pathway and suppressed mammalian target of rapamycin (mTOR) activation linked to the inflammatory hyporesponsiveness (77). Importantly, S100A8/A9 regulated the inflammatory responsivity without impairing the antimicrobial functions of neonatal phagocytes (8), a decisive requirement to achieve the critical balance between unimpaired defense and uneventful tolerance development. Consequently, the pretreatment of *S100a9*-knockout mice with the S100A8/A9 heterodimer or the more potent S100A8 homodimer directly after birth rescued murine neonates from fatal courses of later sepsis (8, 45). In human neonates, S100A8/A9 serum levels were negatively associated with the risk of sepsis and significantly higher in term compared to preterm infants. Additionally, in preterm infants, levels higher than 2,000 ng/ml in cord blood were associated with a 25-fold lower risk of late-onset sepsis compared with levels <330 ng/ml (8). This finding closed the gap regarding the seeming discrepancy between the *in vitro* inflammatory hyporesponsiveness of S100-conditioned neonatal immune cells and the clinical characteristic of hyperdynamic neonatal sepsis with overshooting inflammatory responses in S100-deficient states (**Figure 3**).

This relationship became even more important when evidence was provided that TRIF-dependent regulatory gene programs including IFN-response genes are low expressed and epigenetically silent in neonatal monocytes (8). Their expression tonus was not affected by S100A8/A9 and only gradually increased over a prolonged period of time during the first year of life, which suggests environment-dependent initiation. In parallel, another group demonstrated that preterm infants specifically differ from term infants by an even lower baseline expression of regulatory IFN-response genes (78). The profound immaturity of cell-autonomous regulation together with the impaired age-specific alternative kind of

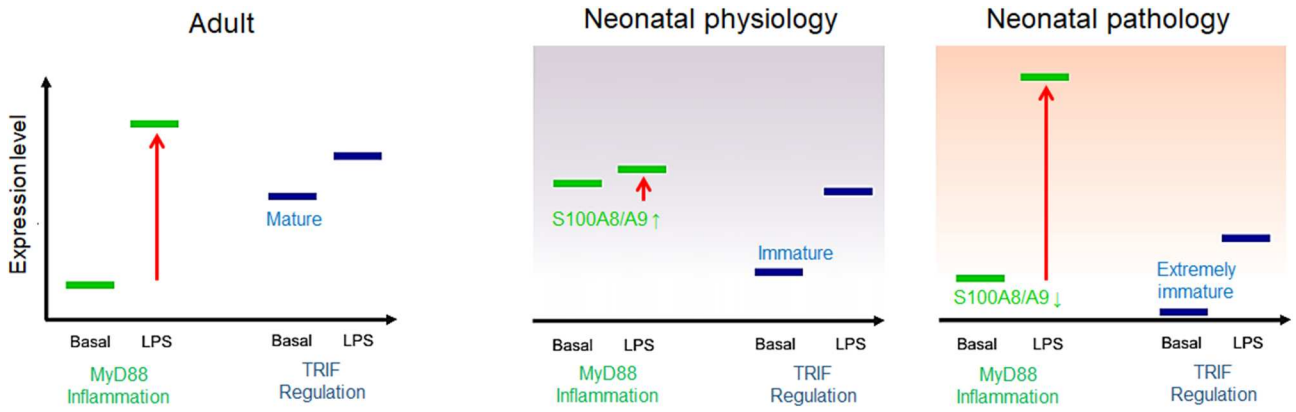

FIGURE 3 | Model of adult and neonatal regulation of lipopolysaccharide (LPS)-responsive gene expression. In healthy adults, MyD88-dependent pro-inflammatory genes are not expressed at baseline but strongly induced by LPS; the basal expression tonus of regulatory TIR domain-containing adaptor protein-inducing interferon (IFN)-β (TRIF)-dependent genes in adults is high and moderately increased by LPS stimulation. In healthy neonates, MyD88-dependent gene expression is physiologically pre-activated by S100A8/A9 and thereby tolerized toward subsequent LPS activation. TRIF-dependent genes are barely expressed at baseline but initiated by a first LPS challenge after birth. In S100A8/A9-deficient neonates, insufficient tolerization of the MyD88-dependent pro-inflammatory response and/or an immature expression tonus or altered postnatal initiation of TRIF-dependent regulatory gene programs results in unregulated hyperinflammatory LPS responses, increasing the risk of severe sepsis.

regulation by S100A8/A9 provided an explanation for the massively increased sepsis risk of individual preterm infants (**Figure 3**). Moreover, identifying this period as a critical phase in which the regulation of inflammatory responsiveness shifts from S100A8/A9-programming to an adult-like endogenous regulation allowed understanding why the incidence of late-onset sepsis is highest in the first 2 weeks of life (79).

Next to the outlined molecular effects of S100 programming, S100A8/A9 has influence on the differentiation of several cell types of the innate immune system. In humans and mice, high levels of S100A8/A9 prevented the expansion a specific subpopulation of inflammatory blood monocytes in neonates ($DR^{-/low}/CD33^{+}$ monocytes in humans and $CD11b^{+}/Gr\text{-}1^{int}/Ly6G^{-}/Ly6C^{hi}$ cells in mice) which promoted systemic hyperinflammatory responses (45). Treating *S100a9*-knockout neonates directly after birth with S100A8/A9 prevented excessive expansion of this inflammatory monocyte population and death from septic shock. Among the rapidly growing list of mechanisms controlling overshooting inflammation in newborn infants are granulocytic MDSCs. Similar as S100A8/A9 levels, MDSCs are expanded in breast milk and the blood circulation of newborn infants and drop down to low adult-like levels 1 month after birth (75, 80, 81). Initially considered as a sign of immune immaturity, their suppressive activity on the inflammatory phenotype of neonatal T cells and monocytes has meanwhile been included into the concept of alternative immune regulation during the neonatal period (81–83). S100A8 and S100A9 are two of the most important positive regulators of the number and function of MDSCs by acting on hematopoietic progenitor cells (84–88). It was recently shown that S100A8/A9 triggers the suppressive activity and also the antibacterial activity of neonatal MDSCs, thereby controlling inflammation (82). Another important process in the neonatal period is the exchange of fetal tissue-resident leukocytes by hematopoietic blood-derived leukocytes, which is an integral part of immune adaptation and results in the reorganization of the leukocyte profiles at barrier sites (89–92). In this context, the impact of S100A8/A9 on the vascular endothelium as well as on monocytes/macrophages might be of biological relevance. S100A8/A9 induces a specific endothelial response characterized by the induction of chemokines and adhesion molecules and a loss of cell–cell contacts that increases the vascular permeability and promotes leukocyte recruitment (67). Furthermore, TNF-α has been demonstrated to be a pivotal mediator maintaining the postnatal trafficking of leukocyte to barrier sites in the neonatal period (93). By increasing the expression of TNF-α in neonatal monocytes/macrophages (8) together with its impact on the chemoattractant and leukocyte-adhesive function and the permeability of endothelia S100A8/A9 might be crucially involved in orchestrating the extravasation and redistribution of leukocytes in the neonatal period.

Finally, it should be noted that glucocorticoids induce the expression and release of S100-alarmins (69). Antenatal corticosteroids for women at risk of imminent preterm birth are the major perinatal intervention to reduce the incidence of respiratory distress syndrome and neonatal mortality associated with preterm birth (94). The effects of steroid-induced S100-alarmins on neonatal immunity are probably part of the beneficial impact of antenatal corticosteroids in promoting fetal maturation and improving postnatal adaptation.

CONCLUDING REMARKS

A large body of evidence suggests that S100A8/A9 programs the inflammatory responsivity of systemic innate immunity of newborn infants at multiple molecular and cellular levels. Current data suggest that the tuning of the initial programming of immunity by S100-alarmins is an important determinant of

how newborn infants react toward the new antigenic challenges in the extrauterine world. Deficient priming by S100-alarmins increases the risk of life-threatening systemic inflammatory response syndromes, which hampers uneventful immune adaptation and regulated reprogramming of immunity by the environment. Better understanding of how the host contributes to the postnatal development of immunity is an opportunity to exploit endogenous mechanisms like S100-alarmins for intervention strategies, which ensure favorable immune adaptation and could benefit health not only in infancy but also in adulthood.

AUTHOR CONTRIBUTIONS

DV conceptualized and composed the manuscript.

FUNDING

The Volkswagen Foundation (Az 90 005), the Appenrodt Foundation and the Deutsche Forschungsgemeinschaft (DFG) (VI 538/6-1), and the DFG under Germany's Excellence Strategy–EXC 2155 RESIST–Project ID 39087428 supported research in this area.

REFERENCES

1. Garand M, Cai B, Kollmann TR. Environment impacts innate immune ontogeny. *Innate Immun*. (2017) 23:3–10. doi: 10.1177/1753425916671018
2. Gensollen T, Blumberg RS. Correlation between early-life regulation of the immune system by microbiota and allergy development. *J Allergy Clin Immunol*. (2017) 139:1084–91. doi: 10.1016/j.jaci.2017.02.011
3. Gluckman PD, Hanson MA, Cooper C, Thornburg KL. Effect of *in utero* and early-life conditions on adult health and disease. *N Engl J Med*. (2008) 359:61–73. doi: 10.1056/NEJMra0708473
4. Hornef MW, Torow N. 'Layered immunity' and the 'neonatal window of opportunity' - timed succession of non-redundant phases to establish mucosal host-microbial homeostasis after birth. *Immunology*. (2020) 159:15–25. doi: 10.1111/imm.13149
5. Kollmann TR, Kampmann B, Mazmanian SK, Marchant A, Levy O. Protecting the newborn and young infant from infectious diseases: lessons from immune ontogeny. *Immunity*. (2017) 46:350–63. doi: 10.1016/j.immuni.2017.03.009
6. Netea MG, Joosten LA, Latz E, Mills KH, Natoli G, Stunnenberg HG, et al. Trained immunity: a program of innate immune memory in health and disease. *Science*. (2016) 352:aaf1098. doi: 10.1126/science.aaf1098
7. Renz H, Adkins BD, Bartfeld S, Blumberg RS, Farber DL, Garssen J, et al. The neonatal window of opportunity-early priming for life. *J Allergy Clin Immunol*. (2018) 141:1212–4. doi: 10.1016/j.jaci.2017.11.019
8. Ulas T, Pirr S, Fehlhaber B, Bickes MS, Loof TG, Vogl T, et al. S100-alarmin-induced innate immune programming protects newborn infants from sepsis. *Nat Immunol*. (2017) 18:622–32. doi: 10.1038/ni.3745
9. Burgner DP, Doherty D, Humphreys J, Currie A, Simmer K, Charles A, et al. Maternal chorioamnionitis and postneonatal respiratory tract infection in ex-preterm infants. *J Pediatr*. (2017) 184:62–7.e2. doi: 10.1016/j.jpeds.2017.01.037
10. Doyle LW, Ford G, Davis N. Health and hospitalistions after discharge in extremely low birth weight infants. *Semin Neonatol*. (2003) 8:137–45. doi: 10.1016/S1084-2756(02)00221-X
11. Harju M, Keski-Nisula L, Georgiadis L, Raisanen S, Gissler M, Heinonen S. The burden of childhood asthma and late preterm and early term births. *J Pediatr*. (2014) 164:295–9.e1. doi: 10.1016/j.jpeds.2013.09.057
12. Holsti A, Adamsson M, Hagglof B, Farooqi A, Serenius F. Chronic conditions and health care needs of adolescents born at 23 to 25 weeks' gestation. *Pediatrics*. (2017) 139:e20162215–25. doi: 10.1542/peds.2016-2215
13. Kan B, Razzaghian HR, Lavoie PM. An immunological perspective on neonatal sepsis. *Trends Mol Med*. (2016) 22:290–302. doi: 10.1016/j.molmed.2016.02.001
14. Zhang X, Zhivaki D, Lo-Man R. Unique aspects of the perinatal immune system. *Nat Rev Immunol*. (2017) 17:495–507. doi: 10.1038/nri.2017.54
15. Vogl T, Gharibyan AL, Morozova-Roche LA. Pro-inflammatory S100A8 and S100A9 proteins: self-assembly into multifunctional native and amyloid complexes. *Int J Mol Sci*. (2012) 13:2893–917. doi: 10.3390/ijms13032893
16. Vogl T, Leukert N, Barczyk K, Strupat K, Roth J. Biophysical characterization of S100A8 and S100A9 in the absence and presence of bivalent cations. *Biochim Biophys Acta*. (2006) 1763:1298–306. doi: 10.1016/j.bbamcr.2006.08.028
17. Manitz M-P, Horst B, Seeliger S, Strey A, Skryabin BV, Gunzer M, et al. Loss of S100A9 (MRP14) results in reduced interleukin-8-induced CD11b surface expression, a polarized microfilament system, and diminished responsiveness to chemoattractants *in vitro*. *Mol Cell Biol*. (2003) 23:1034–43. doi: 10.1128/MCB.23.3.1034-1043.2003
18. Hobbs JA, May R, Tanousis K, McNeill E, Mathies M, Gebhardt C, et al. Myeloid cell function in MRP-14 (S100A9) null mice. *Mol Cell Biol*. (2003) 23:2564–76. doi: 10.1128/MCB.23.7.2564-2576.2003
19. Passey RJ, Williams E, Lichanska AM, Wells C, Hu S, Geczy CL, et al. A null mutation in the inflammation-associated S100 protein S100A8 causes early resorption of the mouse embryo. *J Immunol*. (1999) 163:2209–16.
20. Robinson MJ, Tessier P, Poulsom R, Hogg N. The S100 family heterodimer, MRP-8/14, binds with high affinity to heparin and heparan sulfate glycosaminoglycans on endothelial cells. *J Biol Chem*. (2002) 277:3658–65. doi: 10.1074/jbc.M102950200
21. Srikrishna G, Panneerselvam K, Westphal V, Abraham V, Varki A, Freeze HH. Two proteins modulating transendothelial migration of leukocytes recognize novel carboxylated glycans on endothelial cells. *J Immunol*. (2001) 166:4678–88. doi: 10.4049/jimmunol.166.7.4678
22. van Lent PL, Grevers LC, Blom AB, Arntz OJ, van de Loo FA, van der Kraan P, et al. Stimulation of chondrocyte-mediated cartilage destruction by S100A8 in experimental murine arthritis. *Arthritis Rheum*. (2008) 58:3776–87. doi: 10.1002/art.24074
23. Turovskaya O, Foell D, Sinha P, Vogl T, Newlin R, Nayak J, et al. RAGE, carboxylated glycans and S100A8/A9 play essential roles in colitis-associated carcinogenesis. *Carcinogenesis*. (2008) 29:2035–43. doi: 10.1093/carcin/bgn188
24. Gebhardt C, Riehl A, Durchdewald M, Nemeth J, Furstenberger G, Muller-Decker K, et al. RAGE signaling sustains inflammation and promotes tumor development. *J Exp Med*. (2008) 205:275–85. doi: 10.1084/jem.20070679
25. Sims GP, Rowe DC, Rietdijk ST, Herbst R, Coyle AJ. HMGB1 and RAGE in inflammation and cancer. *Annu Rev Immunol*. (2010) 28:367–88. doi: 10.1146/annurev.immunol.021908.132603
26. Bjork P, Bjork A, Vogl T, Stenstrom M, Liberg D, Olsson A, et al. Identification of human S100A9 as a novel target for treatment of autoimmune disease via binding to quinoline-3-carboxamides. *PLoS Biol*. (2009) 7:e97. doi: 10.1371/journal.pbio.1000097
27. Austermann J, Friesenhagen J, Fassl SK, Petersen B, Ortkras T, Burgmann J, et al. Alarmins MRP8 and MRP14 induce stress tolerance in phagocytes under sterile inflammatory conditions. *Cell Rep*. (2014) 9:2112–23. doi: 10.1016/j.celrep.2014.11.020
28. Fassl SK, Austermann J, Papantonopoulou O, Riemenschneider M, Xue J, Bertheloot D, et al. Transcriptome assessment reveals a dominant role for TLR4 in the activation of human monocytes by the alarmin MRP8. *J Immunol*. (2015) 194:575–83. doi: 10.4049/jimmunol.1401085
29. Vogl T, Tenbrock K, Ludwig S, Leukert N, Ehrhardt C, van Zoelen, et al. Mrp8 and Mrp14 are endogenous activators of toll-like receptor 4, promoting lethal, endotoxin-induced shock. *Nat Med*. (2007) 13:1042–9. doi: 10.1038/nm1638
30. Vogl T, Stratis A, Wixler V, Voller T, Thurainayagam S, Jorch SK, et al. Autoinhibitory regulation of S100A8/S100A9 alarmin activity locally restricts sterile inflammation. *J Clin Invest*. (2018) 128:1852–66. doi: 10.1172/JCI89867

31. Takeuchi O, Akira S. Pattern recognition receptors and inflammation. *Cell*. (2010) 140:805–20. doi: 10.1016/j.cell.2010.01.022
32. Escoubet-Lozach L, Benner C, Kaikkonen MU, Lozach J, Heinz S, Spann NJ, et al. Mechanisms establishing TLR4-responsive activation states of inflammatory response genes. *PLoS Genet*. (2011) 7:e1002401. doi: 10.1371/journal.pgen.1002401
33. Fitzgerald KA, Rowe DC, Barnes BJ, Caffrey DR, Visintin A, Latz E, et al. LPS-TLR4 signaling to IRF-3/7 and NF-kappaB involves the toll adapters TRAM and TRIF. *J Exp Med*. (2003) 198:1043–55. doi: 10.1084/jem.20031023
34. Biswas SK, Lopez-Collazo E. Endotoxin tolerance: new mechanisms, molecules and clinical significance. *Trends Immunol*. (2009) 30:475–87. doi: 10.1016/j.it.2009.07.009
35. Yamamoto M, Sato S, Hemmi H, Hoshino K, Kaisho T, Sanjo H, et al. Role of adaptor TRIF in the MyD88-independent toll-like receptor signaling pathway. *Science*. (2003) 301:640–3. doi: 10.1126/science.1087262
36. Yamamoto M, Sato S, Hemmi H, Uematsu S, Hoshino K, Kaisho T, et al. TRAM is specifically involved in the toll-like receptor 4-mediated MyD88-independent signaling pathway. *Nat Immunol*. (2003) 4:1144–50. doi: 10.1038/ni986
37. van Zoelen MA, Vogl T, Foell D, van Veen SQ, van Till JW, Florquin S, et al. Expression and role of myeloid-related protein-14 in clinical and experimental sepsis. *Am J Respir Crit Care Med*. (2009) 180:1098–106. doi: 10.1164/rccm.200810-1552OC
38. Frosch M, Ahlmann M, Vogl T, Wittkowski H, Wulffraat N, Foell D, et al. The myeloid-related proteins 8 and 14 complex, a novel ligand of toll-like receptor 4, and interleukin-1beta form a positive feedback mechanism in systemic-onset juvenile idiopathic arthritis. *Arthritis Rheum*. (2009) 60:883–91. doi: 10.1002/art.24349
39. Frosch M, Vogl T, Seeliger S, Wulffraat N, Kuis W, Viemann D, et al. Expression of myeloid-related proteins 8 and 14 in systemic-onset juvenile rheumatoid arthritis. *Arthritis Rheum*. (2003) 48:2622–6. doi: 10.1002/art.11177
40. Chan JK, Roth J, Oppenheim JJ, Tracey KJ, Vogl T, Feldmann M, et al. Alarmins: awaiting a clinical response. *J Clin Invest*. (2012) 122:2711–9. doi: 10.1172/JCI62423
41. Wang S, Song R, Wang Z, Jing Z, Wang S, Ma J. S100A8/A9 in inflammation. *Front Immunol*. (2018) 9:1298. doi: 10.3389/fimmu.2018.01298
42. Dubois C, Marce D, Faivre V, Lukaszewicz A-C, Junot C, Fenaille F, et al. High plasma level of S100A8/S100A9 and S100A12 at admission indicates a higher risk of death in septic shock patients. *Sci Rep*. (2019) 9:15660. doi: 10.1038/s41598-019-52184-8
43. Payen D, Lukaszewicz A-C, Belikova I, Faivre V, Gelin C, Russwurm S, et al. Gene profiling in human blood leucocytes during recovery from septic shock. *Intensive Care Med*. (2008) 34:1371–6. doi: 10.1007/s00134-008-1048-1
44. Freise N, Burghard A, Ortkras T, Daber N, Imam Chasan A, Jauch S-L, et al. Signaling mechanisms inducing hyporesponsiveness of phagocytes during systemic inflammation. *Blood*. (2019) 134:134–46. doi: 10.1182/blood.2019000320
45. Heinemann AS, Pirr S, Fehlhaber B, Mellinger L, Burgmann J, Busse M, et al. In neonates S100A8/S100A9 alarmins prevent the expansion of a specific inflammatory monocyte population promoting septic shock. *FASEB J*. (2017) 31:1153–64. doi: 10.1096/fj.201601083R
46. Tanaka T, Grusby MJ, Kaisho T. PDLIM2-mediated termination of transcription factor NF-kappaB activation by intranuclear sequestration and degradation of the p65 subunit. *Nat Immunol*. (2007) 8:584–91. doi: 10.1038/ni1464
47. Geng H, Wittwer T, Dittrich-Breiholz O, Kracht M, Schmitz ML. Phosphorylation of NF-kappaB p65 at Ser468 controls its COMMD1-dependent ubiquitination and target gene-specific proteasomal elimination. *EMBO Rep*. (2009) 10:381–6. doi: 10.1038/embor.2009.10
48. Lagasse E, Clerc RG. Cloning and expression of two human genes encoding calcium-binding proteins that are regulated during myeloid differentiation. *Mol Cell Biol*. (1988) 8:2402–10. doi: 10.1128/MCB.8.6.2402
49. Marenholz I, Heizmann CW, Fritz G. S100 proteins in mouse and man: from evolution to function and pathology (including an update of the nomenclature). *Biochem Biophys Res Commun*. (2004) 322:1111–22. doi: 10.1016/j.bbrc.2004.07.096
50. Edgeworth J, Gorman M, Bennett R, Freemont P, Hogg N. Identification of p8,14 as a highly abundant heterodimeric calcium binding protein complex of myeloid cells. *J Biol Chem*. (1991) 266:7706–13.
51. Hiratsuka S, Watanabe A, Aburatani H, Maru Y. Tumour-mediated upregulation of chemoattractants and recruitment of myeloid cells predetermines lung metastasis. *Nat Cell Biol*. (2006) 8:1369–75. doi: 10.1038/ncb1507
52. Yen T, Harrison CA, Devery JM, Leong S, Iismaa SE, Yoshimura T, et al. Induction of the S100 chemotactic protein, CP-10, in murine microvascular endothelial cells by proinflammatory stimuli. *Blood*. (1997) 90:4812–21. doi: 10.1182/blood.V90.12.4812.4812_4812_4821
53. Gabrielsen TO, Dale I, Brandtzaeg P, Hoel PS, Fagerhol MK, Larsen TE, et al. Epidermal and dermal distribution of a myelomonocytic antigen (L1) shared by epithelial cells in various inflammatory skin diseases. *J Am Acad Dermatol*. (1986) 15(2 Pt 1):173–9. doi: 10.1016/S0190-9622(86)70152-7
54. Kunz M, Roth J, Sorg C, Kolde G. Epidermal expression of the calcium binding surface antigen 27E10 in inflammatory skin diseases. *Arch Dermatol Res*. (1992) 284:386–90. doi: 10.1007/BF00372067
55. Cormier K, Harquail J, Ouellette RJ, Tessier PA, Guerrette R, Robichaud GA. Intracellular expression of inflammatory proteins S100A8 and S100A9 leads to epithelial-mesenchymal transition and attenuated aggressivity of breast cancer cells. *Anticancer Agents Med Chem*. (2014) 14:35–45. doi: 10.2174/18715206113136660333
56. Pirr S, Richter M, Fehlhaber B, Pagel J, Hartel C, Roth J, et al. High amounts of S100-alarmins confer antimicrobial activity on human breast milk targeting pathogens relevant in neonatal sepsis. *Front Immunol*. (2017) 8:1822. doi: 10.3389/fimmu.2017.01822
57. Savino F, Castagno E, Calabrese R, Viola S, Oggero R, Miniero R. High faecal calprotectin levels in healthy, exclusively breast-fed infants. *Neonatology*. (2010) 97:299–304. doi: 10.1159/000255161
58. Witkowska-Zimny M, Kaminska-El-Hassan E. Cells of human breast milk. *Cell Mol Biol Lett*. (2017) 22:11. doi: 10.1186/s11658-017-0042-4
59. Foell D, Wittkowski H, Vogl T, Roth J. S100 proteins expressed in phagocytes: a novel group of damage-associated molecular pattern molecules. *J Leukoc Biol*. (2007) 81:28–37. doi: 10.1189/jlb.0306170
60. Foell D, Roth J. Proinflammatory S100 proteins in arthritis and autoimmune disease. *Arthritis Rheum*. (2004) 50:3762–71. doi: 10.1002/art.20631
61. Frosch M, Roth J. New insights in systemic juvenile idiopathic arthritis–from pathophysiology to treatment. *Rheumatology*. (2008) 47:121–5. doi: 10.1093/rheumatology/kem271
62. Holzinger D, Frosch M, Kastrup A, Prince FH, Otten MH, Van Suijlekom-Smit, et al. The toll-like receptor 4 agonist MRP8/14 protein complex is a sensitive indicator for disease activity and predicts relapses in systemic-onset juvenile idiopathic arthritis. *Ann Rheum Dis*. (2012) 71:974–80. doi: 10.1136/annrheumdis-2011-200598
63. Terrin G, Passariello A, Manguso F, Salvia G, Rapacciuolo L, Messina F, et al. Serum calprotectin: an antimicrobial peptide as a new marker for the diagnosis of sepsis in very low birth weight newborns. *Clin Dev Immunol*. (2011) 2011:291085. doi: 10.1155/2011/291085
64. Decembrino L, De Amici M, Pozzi M, De Silvestri A, Stronati M. Serum calprotectin: a potential biomarker for neonatal sepsis. *J Immunol Res*. (2015) 2015:147973. doi: 10.1155/2015/147973
65. Rammes A, Roth J, Goebeler M, Klempt M, Hartmann M, Sorg C. Myeloid-related protein (MRP) 8 and MRP14, calcium-binding proteins of the S100 family, are secreted by activated monocytes via a novel, tubulin-dependent pathway. *J Biol Chem*. (1997) 272:9496–502. doi: 10.1074/jbc.272.14.9496
66. Frosch M, Strey A, Vogl T, Wulffraat NM, Kuis W, Sunderkotter C, et al. Myeloid-related proteins 8 and 14 are specifically secreted during interaction of phagocytes and activated endothelium and are useful markers for monitoring disease activity in pauciarticular-onset juvenile rheumatoid arthritis. *Arthritis Rheum*. (2000) 43:628–37. doi: 10.1002/1529-0131(200003)43:3<628::AID-ANR20>3.0.CO;2-X
67. Viemann D, Strey A, Janning A, Jurk K, Klimmek K, Vogl T, et al. Myeloid-related proteins 8 and 14 induce a specific inflammatory response in human microvascular endothelial cells. *Blood*. (2005) 105:2955–62. doi: 10.1182/blood-2004-07-2520

68. Mooren FC, Lechtermann A, Fobker M, Brandt B, Sorg C, Volker K, et al. The response of the novel pro-inflammatory molecules S100A8/A9 to exercise. *Int J Sports Med*. (2006) 27:751–8. doi: 10.1055/s-2005-872909
69. Harrison CA, Raftery MJ, Walsh J, Alewood P, Iismaa SE, Thliveris S, et al. Oxidation regulates the inflammatory properties of the murine S100 protein S100A8. *J Biol Chem*. (1999) 274:8561–9. doi: 10.1074/jbc.274.13.8561
70. Kota SK, Gayatri K, Jammula S, Kota SK, Krishna SV, Meher LK, et al. Endocrinology of parturition. *Indian J Endocrinol Metab*. (2013) 17:50–9. doi: 10.4103/2230-8210.107841
71. Kiriakopoulos N, Grigoriadis S, Maziotis E, Philippou A, Rapani A, Giannelou P, et al. Investigating stress response during vaginal delivery and elective cesarean section through assessment of levels of cortisol, interleukin 6 (IL-6), growth hormone (GH) and insulin-like growth factor 1 (IGF-1). *J Clin Med*. (2019) 8:1112–27. doi: 10.3390/jcm8081112
72. Marissen J, Haiss A, Meyer C, van Rossum T, Bunte LM, Frommhold D, et al. Efficacy of *bifidobacterium longum*, B. infantis and *Lactobacillus* acidophilus probiotics to prevent gut dysbiosis in preterm infants of 28+0-32+6 weeks of gestation: a randomised, placebo-controlled, double-blind, multicentre trial: the PRIMAL Clinical Study protocol. *BMJ Open*. (2019) 9:e032617. doi: 10.1136/bmjopen-2019-032617
73. Levy O. Innate immunity of the newborn: basic mechanisms and clinical correlates. *Nat Rev Immunol*. (2007) 7:379–90. doi: 10.1038/nri2075
74. Pagel J, Hartz A, Figge J, Gille C, Eschweiler S, Petersen K, et al. Regulatory T cell frequencies are increased in preterm infants with clinical early-onset sepsis. *Clin Exp Immunol*. (2016) 185:219–27. doi: 10.1111/cei.12810
75. Rieber N, Gille C, Kostlin N, Schafer I, Spring B, Ost M, et al. Neutrophilic myeloid-derived suppressor cells in cord blood modulate innate and adaptive immune responses. *Clin Exp Immunol*. (2013) 174:45–52. doi: 10.1111/cei.12143
76. Zhao J, Kim KD, Yang X, Auh S, Fu Y-X, Tang H. Hyper innate responses in neonates lead to increased morbidity and mortality after infection. *Proc Natl Acad Sci USA*. (2008) 105:7528–33. doi: 10.1073/pnas.0800152105
77. Dreschers S, Ohl K, Lehrke M, Mollmann J, Denecke B, Costa I, et al. Impaired cellular energy metabolism in cord blood macrophages contributes to abortive response toward inflammatory threats. *Nat Commun*. (2019) 10:1685. doi: 10.1038/s41467-019-09359-8
78. Singh VV, Chauhan SK, Rai R, Kumar A, Singh SM, Rai G. Decreased pattern recognition receptor signaling, interferon-signature, and bactericidal/permeability-increasing protein gene expression in cord blood of term low birth weight human newborns. *PLoS ONE*. (2013) 8:e62845. doi: 10.1371/journal.pone.0062845
79. Brook B, Harbeson D, Ben-Othman R, Viemann D, Kollmann TR. Newborn susceptibility to infection vs. disease depends on complex *in vivo* interactions of host and pathogen. *Semin Immunopathol*. (2017) 39:615–25. doi: 10.1007/s00281-017-0651-z
80. Schwarz J, Scheckenbach V, Kugel H, Spring B, Pagel J, Hartel C, et al. Granulocytic myeloid-derived suppressor cells (GR-MDSC) accumulate in cord blood of preterm infants and remain elevated during the neonatal period. *Clin Exp Immunol*. (2018) 191:328–37. doi: 10.1111/cei.13059
81. Kostlin N, Schoetensack C, Schwarz J, Spring B, Marme A, Goelz R, et al. Granulocytic myeloid-derived suppressor cells (GR-MDSC) in breast milk (BM) GR-MDSC accumulate in human BM and modulate T-Cell and monocyte function. *Front Immunol*. (2018) 9:1098. doi: 10.3389/fimmu.2018.01098
82. He Y-M, Li X, Perego M, Nefedova Y, Kossenkov AV, Jensen EA, et al. Transitory presence of myeloid-derived suppressor cells in neonates is critical for control of inflammation. *Nat Med*. (2018) 24:224–31. doi: 10.1038/nm.4467
83. Kostlin N, Vogelmann M, Spring B, Schwarz J, Feucht J, Hartel C, et al. Granulocytic myeloid-derived suppressor cells from human cord blood modulate T-helper cell response towards an anti-inflammatory phenotype. *Immunology*. (2017) 152:89–101. doi: 10.1111/imm.12751
84. Chen X, Eksioglu EA, Zhou J, Zhang L, Djeu J, Fortenbery N, et al. Induction of myelodysplasia by myeloid-derived suppressor cells. *J Clin Invest*. (2013) 123:4595–611. doi: 10.1172/JCI67580
85. Cheng P, Corzo CA, Luetteke N, Yu B, Nagaraj S, Bui MM, et al. Inhibition of dendritic cell differentiation and accumulation of myeloid-derived suppressor cells in cancer is regulated by S100A9 protein. *J Exp Med*. (2008) 205:2235–49. doi: 10.1084/jem.20080132
86. Gabrilovich DI, Nagaraj S. Myeloid-derived suppressor cells as regulators of the immune system. *Nat Rev Immunol*. (2009) 9:162–74. doi: 10.1038/nri2506
87. Petersen B, Wolf M, Austermann J, van Lent P, Foell D, Ahlmann M, et al. The alarmin Mrp8/14 as regulator of the adaptive immune response during allergic contact dermatitis. *EMBO J*. (2013) 32:100–11. doi: 10.1038/emboj.2012.309
88. Sinha P, Okoro C, Foell D, Freeze HH, Ostrand-Rosenberg S, Srikrishna G. Proinflammatory S100 proteins regulate the accumulation of myeloid-derived suppressor cells. *J Immunol*. (2008) 181:4666–75. doi: 10.4049/jimmunol.181.7.4666
89. Ginhoux F, Schultze JL, Murray PJ, Ochando J, Biswas SK. New insights into the multidimensional concept of macrophage ontogeny, activation and function. *Nat Immunol*. (2016) 17:34–40. doi: 10.1038/ni.3324
90. Guilliams M, De Kleer I, Henri S, Post S, Vanhoutte L, De Prijck S, et al. Alveolar macrophages develop from fetal monocytes that differentiate into long-lived cells in the first week of life via GM-CSF. *J Exp Med*. (2013) 210:1977–92. doi: 10.1084/jem.20131199
91. Perdiguero EG, Geissmann F. The development and maintenance of resident macrophages. *Nat Immunol*. (2016) 17:2–8. doi: 10.1038/ni.3341
92. van de Laar L, Saelens W, De Prijck S, Martens L, Scott CL, van Isterdael G, et al. Yolk sac macrophages, fetal liver, and adult monocytes can colonize an empty niche and develop into functional tissue-resident macrophages. *Immunity*. (2016) 44:755–68. doi: 10.1016/j.immuni.2016.02.017
93. Bickes MS, Pirr S, Heinemann AS, Fehlhaber B, Halle S, Vollger L, et al. Constitutive TNF-α signaling in neonates is essential for the development of tissue-resident leukocyte profiles at barrier sites. *FASEB J*. (2019) 33:10633–47. doi: 10.1096/fj.201900796R
94. World Health Organization. *WHO Recommendations on Interventions to Improve Preterm Birth Outcomes*. Geneva: WHO (2015).

Conflict of Interest: The author declares that the research was conducted in the absence of any commercial or financial relationships that could be construed as a potential conflict of interest.

frontiers in Immunology

REVIEW
published: 12 May 2020
doi: 10.3389/fimmu.2020.00793

Cytomegaloviruses and Macrophages—Friends and Foes From Early on?

Sebastian Baasch[1,2], *Zsolt Ruzsics*[3] *and Philipp Henneke*[1,2]*

[1] Institute for Immunodeficiency, Center for Chronic Immunodeficiency (CCI), Medical Center - University of Freiburg, Faculty of Medicine, University of Freiburg, Freiburg, Germany , [2] Center for Pediatrics and Adolescent Medicine, University of Freiburg, Freiburg, Germany, [3] Institute of Virology, Medical Center - University of Freiburg, Faculty of Medicine, University of Freiburg, Freiburg, Germany

Starting at birth, newborn infants are exposed to numerous microorganisms. Adaptation of the innate immune system to them is a delicate process, with potentially advantageous and harmful implications for health development. Cytomegaloviruses (CMVs) are highly adapted to their specific mammalian hosts, with which they share millions of years of co-evolution. Throughout the history of mankind, human CMV has infected most infants in the first months of life without overt implications for health. Thus, CMV infections are intertwined with normal immune development. Nonetheless, CMV has retained substantial pathogenicity following infection *in utero* or in situations of immunosuppression, leading to pathology in virtually any organ and particularly the central nervous system (CNS). CMVs enter the host through mucosal interfaces of the gastrointestinal and respiratory tract, where macrophages (MACs) are the most abundant immune cell type. Tissue MACs and their potential progenitors, monocytes, are established target cells of CMVs. Recently, several discoveries have revolutionized our understanding on the pre- and postnatal development and site-specific adaptation of tissue MACs. In this review, we explore experimental evidences and concepts on how CMV infections may impact on MAC development and activation as part of host-virus co-adaptation.

Keywords: macrophage, monocyte, CMV (cytomegalovirus), innate immunity, pathogen-host coevolution, mucosal immune barrier, virus-host adaptation, macrophage heterogeneity

OPEN ACCESS

Edited by:
Tobias Strunk, King Edward Memorial Hospital, Australia

Reviewed by:
Cecilia Söderberg-Naucler, Karolinska Institutet (KI), Sweden
Luka Cicin-Sain, Helmholtz Association of German Research Centers (HZ), Germany

***Correspondence:**
Philipp Henneke
philipp.henneke@uniklinik-freiburg.de

Specialty section:
This article was submitted to Mucosal Immunity, a section of the journal Frontiers in Immunology

Received: *18 December 2019*
Accepted: *07 April 2020*
Published: *12 May 2020*

Citation:
Baasch S, Ruzsics Z and Henneke P (2020) Cytomegaloviruses and Macrophages—Friends and Foes From Early on? Front. Immunol. 11:793. doi: 10.3389/fimmu.2020.00793

INTRODUCTION

The human body harbors diverse communities of microorganisms, in particular bacteria and fungi colonizing the outer and inner surfaces of the body (microbiome), as well as latently infecting viruses (virome) (1). This ecosystem is subject to influences, e.g. nutrient supply, interspecies competition and diffusible immunological effector molecules. At the same time, microbiome and virome shape host immunity via direct interaction with immune and non-immune cells, and indirectly, e.g. via secreted metabolites (2). In contrast to extracellular bacteria and fungi, which are largely controlled on the population level, viruses can be expected to rely on reciprocal adaptations with the individually infected host cell. The genus of cytomegaloviruses (CMVs), which belong to the subfamily of betaherpesvirinae, have co-evolved with their mammalian hosts for millions of years (3). In humans, infection with human CMV (HCMV) usually occurs in the first months of life, although infection has been pushed toward later life in highly industrialized societies (4–6).

Therefore, HCMV is part of a "physiological" virome in immunocompetent individuals. Infants are infected via smear infections or via HCMV-containing milk as seropositive mothers reactivate HCMV locally (7) and transmit the virus to their children in more than 30% of cases (8).

CMVs have co-evolved with their specific hosts. Therefore, cross species infection models to study virus-host interactions are not available *in vivo*. Murine CMV (MCMV) and HCMV share only 45% of their genes (9), but have many similarities in cell tropism and immune modulatory properties. Hence, MCMV infection of mice is regarded as a useful experimental model to understand HCMV pathology (10). In the subsequent text we will use the abbreviation "CMV" in the case of general statements and if features are shared by the CMVs, which were studied.

Intraperitoneal and subcutaneous (foot pad) infections have provided valuable information on MCMV biology in the complex *in vivo* situation. However, since breast milk and saliva are regarded as important HCMV and MCMV sources, intragastric and intranasal infections have more recently been exploited (11). HCMV may infect cells of the mouth/upper gastro-intestinal tract, or it may reach the intestine. Moreover, HCMV may infect the respiratory tract via aspiration of virus containing milk. MACs and their potential progenitors, circulating monocytes, are well-known target cells for CMV (12–16). In the barrier tissues of intestinal and respiratory tracts, MACs represent the most abundant immune cells. However, tissue resident MACs are highly heterogeneous and undergo age specific changes during the individual host development, with respect to their origin and the tissue they inhere (17). For example, lamina propria MACs (LpMAC) in the intestine and microglia in the CNS represent two extremes with and without replenishment by monocytes, respectively. Models on how the phenotypic and functional MAC diversity impacts on CMV infections and vice versa are still in infancy.

In this review we focus on the ability of MACs to recognize CMV early after infection, and the known cellular consequences of infected MACs with regard of cytokine production and polarization. We summarize mechanisms of how CMV exploits monocyte influx and discuss potential consequences in putative target tissues. We propose that early CMV infections train the monocyte-macrophage-axis and are therefore beneficial in the immunocompetent host. Finally, we highlight the central role of monocytes and MACs in CMV infection serving as latent reservoirs and reactivation sites.

CMV RECOGNITION BY MACROPHAGES AND MONOCYTES

The high frequency of tissue MACs in CMV entry sites, e.g. the lamina propria (intestinal tract) or alveolar spaces, allows for a potent response to epithelial barrier disruption and invasion of microorganisms, such as bacteria, or viruses. In order to cover a huge variety of pathogens with distinct extracellular or intracellular lifestyles, MACs and monocytes are equipped with pattern recognition receptors on plasma and endosomal membranes and in the cytosol. Together, these receptors recognize conserved microbial molecules or alterations in host structures, such as nucleic acids occurring at atypical sites. The engagement of pattern recognition receptors leads to the formation of cytokines, which are suited to initiate an appropriate immune response. During viral infections, type I interferons (IFN I) play an important role in creating a hostile cellular environment for viral replication and spread (18). Accordingly, mice deficient in the IFN I receptor ($IFNAR^{-/-}$) succumb to CMV infection (19). Furthermore, inflammasome-dependent secretion of interleukin 18 (IL-18) augments NK-cell function in MCMV infections (20).

CMV and Toll-Like Receptors

Upon ligand binding Toll-like receptors (TLRs) transduce signals via the cytosolic adapter molecule myeloid differentiation primary response 88 (MyD88). In this respect, TLR3 is an exception, since it uses TIR-domain-containing adapter inducing interferon-β (TRIF) and TRIF-related adaptor molecule (TRAM) as sole adapters (21). To induce IFN I transcription, dimerization of transcription factors interferon regulatory factor (IRF) 3 (through TLR3-TRIF) and/or IRF7 (through TLR9-MyD88) is essential. Accordingly, peritoneal MAC from IRF3 and IRF7 double knockout mice do not produce IFN-β when infected with MCMV (22). The role of upstream MyD88 in IFN I production in MCMV infection was confirmed in several studies (23–25). A loss-of-function frameshift mutation in TRIF increases susceptibility and diminishes circulating IFN I in MCMV infection (26). Moreover, bone marrow cells from mice with a combined deficiency in MyD88 and TRIF, showed an impaired IFN I formation in MCMV infection *in vitro*. However, residual IFN I formation in these cells suggests the existence of a TLR-independent pathway (27).

The strictly intracellular lifestyle of CMV requires expression of host cell receptors that provide docking sites for viral ligands and facilitate cellular entry. Complexes of the CMV glycopoteins B and H (gB, gH) mediate host cell entry (28). Although, the entry-mediating host receptors for these protein complexes are still controversial (29), TLR2, which is expressed on the cell membrane, is known to interact with gB/ gH (30). TLR2 binding drives HCMV-induced nuclear factor kappa-light-chain-enhancer of activated B cells (NFκB)-dependent production of inflammatory cytokines in MACs (31) (**Figure 1**) and mediates the control of CMV in immunocompromised humans and mice (32, 33). Interestingly, TLR2-dependent IFN I production has been found to be specific for inflammatory monocytes (27) (**Figure 1**), while dendritic cells did not mount an IFN I response through TLR2 (27).

In addition, endosomal TLRs, e.g. TLR 3, 7 and 9, are involved in MCMV recognition, since a missense mutation in their adapter UNC-93B leads to substantially decreased formation of interferon gamma (IFN-γ), IL-12, tumor necrosis factor (TNF) and IFN I in the plasma of mice after intraperitoneal MCMV infection (34).

Although the cell specific contribution of individual TLRs remains unclear, interaction of MCMV with TLR2 on monocytes and MACs may contribute to the rapid mounting

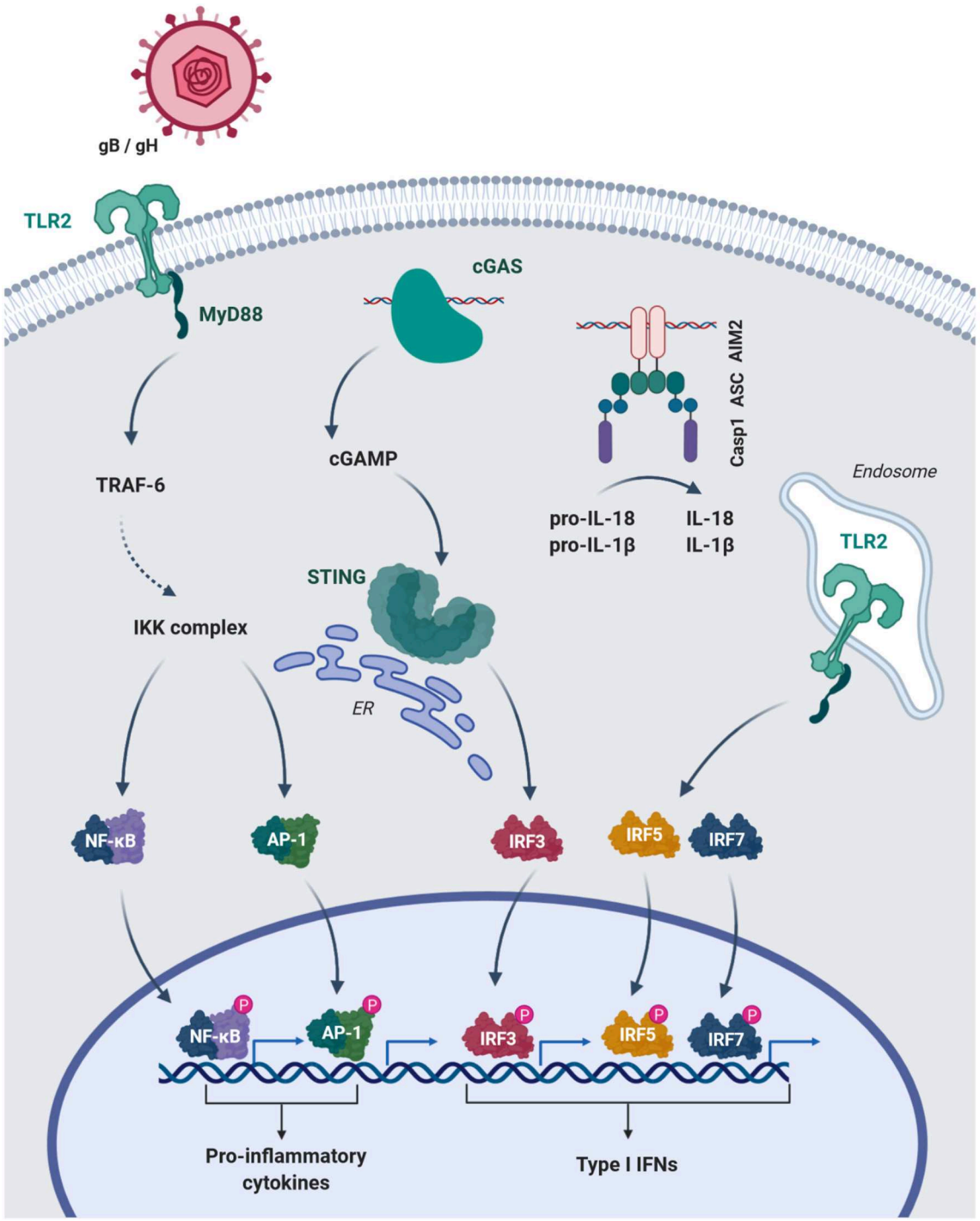

FIGURE 1 | HCMV glycoproteins B and H (gB/gH) engange TLR2 of MAC on the surface and activate NFκB and AP-1 mediated transcription of pro-inflammatory cytokines. The cytosolic sensors cGAS and AIM2 recognize CMV-DNA. cGAS produces the signaling mediator cGAMP, which leads to STING activation and IRF3-dependent type I IFN transcription. Engagement of DNA by the HIN domain of AIM2 leads to interaction with the adaptor ASC (PYD-PYD) and subsequent recruitment of pro-caspase 1 via their CARD domains. Activated caspase 1 (Casp1) can cleave the pro-forms of IL-18 and IL-1β converting them into their mature bioactive forms. Additionally, inflammatory monocytes can uptake DNA viruses into endosomal compartments and induce type I IFN via IRF5 and 7. TRAF-6, TNF receptor associated factor-6; IKK-complex, IκB kinase-complex; AP-1, Activator protein-1; ER, endoplasmatic reticulum; ASC, Apoptosis-asspciated speck-like protein containing a CARD; PYD, pyrin domain.

TABLE 1 | Genes of MCMV and their HCMV homologs in this review.

Gene	m129 (Mck2)	M36 (vICA)	m139, m140, m141	M35	M45 (vIRA)
MAC specific	Partly	Yes	Yes	Partly	No
Function	Viral CC chemokine homolog to attract monocytes; essential for *in vitro* infection of MAC in MCMV	Inhibition of caspase 8 activation (apoptosis); inhibition of innate immune response of MAC; essential for *in vitro* replication in MAC	Capsid formation in MAC	Interference with NFκB-dependent IFN I transcription; essential for *in vitro* replication in MAC	Inhibition of necroptosis (inhibition of RIP3 activation); activation of NFκB (early); inhibition of NFκB essential modulator (NEMO) (late)
HCMV ortholog/ homolog	Yes (UL128)	Yes (UL36)	No	Yes (UL35)	Yes (UL45); not a functional homolog
Literature	(63–65)	(66–68)	(69, 70)	(46)	(57, 71, 72)

of inflammatory and antiviral mediators in case of viremia. In contrast, TLR9 in dendritic cells seems to be crucial for IFN I in later stages of infection (24, 34–37).

CMV and Cytosolic Sensors

The observation that MACs, which accumulate DNA in phagosomes due to a DNAse II-deficiency, induce interferon-mediated anemia, which was reversed by deletion of *IFNAR* (38), suggested a TLR9-independent DNA sensor in the cytosol. Moreover, MACs deficient in MyD88, TRIF and mitochondrial antiviral signaling (MAVS) protein maintained a IFN I response in MCMV infection (39). The identification of the stimulator of interferon genes (STING) (40, 41) and cyclic guanosin monophosphate-adenosine monophosphate synthase (cGAS) (42), the upstream sensor for cytosolic DNA, provided mechanisms for the recognition of self and microbial DNA, e.g. from herpesviruses (43, 44). Tegtmeyer et al. recently demonstrated the importance of cGAS-STING-signaling in MCMV infection (45). STING-mediated IFN I was induced as early as 4 h post infection (hpi) (45). Kupffer cells, the liver resident MACs, were a main source of STING-dependent IFN I and restrained viral dissemination to the lymphnodes (45). These results support data generated *in vitro* in immortalized bone marrow-derived MACs, which responded to MCMV infection with IFN-β in a cGAS-STING-dependent fashion (46). Accordingly, HCMV induces IFN I in human monocyte-derived MACs via cGAS and STING (47) (**Figure 1**).

The DNA-dependent activator of IFN-regulatory factors (DAI) has been identified as another cytosolic sensor of nucleic acids (48). DAI interacts with TANK binding kinase 1 (TBK1) and IRF3, suggesting IRF3-mediated transcription of IFN I (48). Moreover, DAI can activate NFκB via RHIM/RIP1 and 3 recruitment (49, 50). However, the importance of DAI-mediated activation of NFκB and IRF3 in the IFN I response to cytosolic DNA seems marginal (51). Moreover, DAI has been recently challenged as a specific DNA sensor, since it was shown to interact with genomic RNA of influenza A virus (52) and with newly synthesized MCMV RNA (53), ultimately leading to necroptosis of fibroblasts (52, 53). This is in line with previous studies, where infection with MCMV, lacking the viral inhibitor of RIP activation (vIRA/m45) (54–56), induced DAI-RIPK3-dependent necroptosis in MACs (57). These findings support a role of DAI-dependent cell death induction in infected cells, rather than in direct innate immune activation.

The interaction of CMV with intracellular sensors appears to induce cellular activation beyond IFN I. A prominent example is the engagement of the absent in melanoma 2 (AIM2) by MCMV DNA in MACs, which leads to the maturation of IL-1β and IL-18 via caspase 1 cleavage (22) (**Figure 1**). Inflammasome activation and IL-18 secretion is essential for NK cell activation, as the formation of IFN-γ by these cells is reduced in $ASC^{-/-}$ and $AIM2^{-/-}$ mice (22).

Overall, MACs recognize CMV particles and form IFN I to restrict viral spread within hours after infections (45, 58). *In vitro* data generated in MACs further suggest that they induce NK-cell recruitment and IFN-γ production via inflammasome activation during the early response (**Figure 1**). On the other hand, MCMV and HCMV have evolved numerous strategies to evade the IFN I response (59–62). As an example, the MCMV protein M35 antagonizes IFN I induction downstream of STING and TLRs and thus ensures MCMV replication in MACs (46) (**Table 1**).

CYTOMEGALOVIRUS AFFECTS DYNAMICS OF MONOCYTE RECRUITMENT TO INFECTED TISSUES

As outlined above, MACs can be a major source of IFN I in CMV infections. IFN I induce CCL2 and, to a lesser extent, CCL7 and 12 in the liver and the bone-marrow in MCMV infections (73, 74). A gradient of CCL2, which binds to its receptor CCR2, facilitates the egress of inflammatory monocytes from the bone marrow into the blood stream and the entry into infected tissues (75–79). Notably, all CMV species encode for viral chemokines located directly downstream to their major immediate early locus, corresponding to the UL128-UL131A region in HCMV. In MCMV, the viral chemokine is encoded by the m131 and m129 ORFs, which are fused by splicing. The resulting transcript encodes for a single protein called MCK-2 (80), which cooperates with CCL2 to attract monocytes (63) (**Table 1**). In HCMV, the chemokine homolog is encoded by the UL128 gene. The chemokine function of this gene product has not been well-studied yet. This may change in the near future by exploiting primate CMV models (81).

At the site of infection, Ly6C^{hi} inflammatory monocytes can differentiate into monocyte-derived dendritic cells or MACs, which express the inducible nitric oxide synthase iNOS (82, 83). Nitric oxide formed by inflammatory monocytes inhibits CD8^{+} T-cells and thus modulates adaptive immunity in MCMV infection (84). Additionally, recruitment of inflammatory monocytes increases the number of NK-cells via CCL3 in the liver (85). NK-cells contain the T-cell response by killing of infected antigen presenting cells (86). This process contributes to MCMV persistence (86).

In a foot pad infection model with MCMV, a second subset of monocytes, Ly6C^{lo} CX_3CR1^{hi} patrolling monocytes, are rapidly recruited (64). Intravital microscopy revealed that patrolling monocytes crawl along the inner lining of blood vessels (87) to remove particles inside the vessel lumen (88). Accordingly, patrolling monocytes may acquire MCMV from Tie2^{+} endothelial cells (89) and outmatch inflammatory monocytes as primary targets of MCMV. They harbor viral DNA and serve as vehicles to disseminate MCMV to the spleen and salivary gland (64). However, the roles of the chemokine receptor CX_3CR1, which is highly expressed on patrolling monocytes, and MCK-2, which supports the recruitment of patrolling monocytes, are controversial in the context of viral spread (64, 90). In contrast to an earlier study (64), Farrell et al. did not find significant differences in MCMV salivary gland titers between CX_3CR1-deficient and control mice after foot pad infection (90). Furthermore, MCK-2-deficient MCMV spreads in similar magnitude as wt-MCMV to the salivary gland 5 days after lung infection. A significant role of MCK-2 in MCMV dissemination was found only late, i.e. 10 days post infection (90). These findings highlight the value of kinetic experiments especially in elaborate *in vivo* experiments.

Collectively, MCMV infection leads to the recruitment of inflammatory and patrolling monocytes. While this appears to assist viral spread during initial infection, the monocyte influx changes the tissue-specific cell composition and might thus ultimately affect adaptive immunity and tissue integrity.

MONOCYTE CONTRIBUTION TO TISSUE MACROPHAGES IN STEADY STATE AND INFECTIONS

It has been appreciated for a long time that circulating monocytes can be the direct progenitors of tissue MACs (91). However, in the last decade, substantial heterogeneity of MACs in different organs with respect to origin, renewal and immunophenotype has been uncovered (92–94). Resident MACs are seeded already in the embryo, either directly from the yolk-sac or via fetal liver-derived monocytes (17, 95). Postnatally, with increasing age and adaptation to the outer world, monocytes replenish MACs of the heart (96), the skin (97) and the intestine (98) even in steady state. This situation changes during inflammation or infection, when monocytes are recruited in great numbers also to other tissues (17, 99).

The depletion of MACs, e.g. via lytic infection of CMV, opens niches in the resident tissue MAC pool, which may be filled by invading monocytes (100). In mice, Ly6C^{hi} monocytes give rise to MACs in the skin (97). Patrolling monocytes, on the other hand, fail to populate the intestine after depletion of CD11c^{+} MACs (101). Accordingly, inflammatory and not patrolling monocytes are considered to be the source of tissue MACs under described conditions. However, it seems highly context and tissue dependent, whether monocyte-derived MACs fully adapt and turn into long lived resident MACs or act as "transitory" cells (102). Monocytes cease to engraft into some tissues once inflammation has resolved (103–105). While they poorly perform tissue specific functions to prevent pulmonary alveolar proteinosis in the lung (106), they successfully replace and functionally restore resident cells in other organs, e.g. Kupffer cells in the liver (107). Therefore, origin and time of tissue invasion can impact on MAC function. Interestingly, monocyte-derived MACs may also show context and tissue-specific functional properties during inflammation (108, 109). As examples, monocytes ensure tissue regeneration after skeletal muscle injury (109), yet they show high inflammatory activity during DSS-induced colitis (108). This suggests that fine tuning of MAC function is largely influenced by local cues of the target tissue (110).

In summary, CMV infections and subsequent monocyte recruitment most likely have tissue specific consequences for the resident MAC population and therefore function, which can be either beneficial or deleterious. Thus, all organs, which are targeted in CMV infection deserve individual investigation.

MACROPHAGES—A SPECIAL TARGET FOR CMV?

MACs are defined by morphology, phenotype and function, i.e. phagocytosis and cytokine secretion (111). Tissue MACs are terminally differentiated, however they retain plasticity to react on changing environmental cues, like those induced in infections (112). Next to their prominent role as a first line of defense, MACs in barrier tissues also bear central functions to maintain an anti-inflammatory state in homeostasis. Attempts to grasp the response capacity of MACs to different stimuli have led to a conceptionally useful, but oversimplifying view of pro-inflammatory (M1) and anti-inflammatory, or regulatory (M2) MAC polarization states (113).

Interestingly, polarization of MACs toward either a pro-inflammatory or regulatory state before exposure to HCMV and MCMV alters their susceptibility to infection *in vitro* (114, 115). With respect to putative MCMV virulence factors, MCK-2 deficiency limits CMV infectivity of MACs *in vitro* (65) and *in vivo* (116). MCK-2 appears to be incorporated in infectious particles via binding to virion glycoproteins gH and gL. Since gH/gL is curtail for cell entry, MCK-2 binding to gH/gL has a potential to modulate viral tropism (65) (**Table 1**). In contrast to the relatively clear *in vitro* phenotype, MCK-2 deficiency does not show a strong tropism phenotype *in vivo* (117). In HCMV, the MCK-2 homolog UL128 participates in the formation of the alternative gH/gL envelop glycoprotein complex, which also appears to influence viral host cell tropism (118).

HCMV can induce inflammatory transcriptional programs in MACs as soon as 4 hpi, with upregulation of genes of the ontology

"Anti-viral response" (119). Within 24 hpi inflammatory cytokines are secreted (114) involving NFκB, phosphoinositide 3-kinase (PI3K) (120) and IRF signal transduction. The interplay of NFκB and PI3K seems necessary for early transcription of inflammatory cytokines, e.g. TNFα, but also anti-inflammatory cytokines, e.g. IL-10 (120). Accordingly, MCMV induces IL-10 production in peritoneal MACs leading to downregulation of MHCII (121). HCMV and rhesus CMV encode for a viral IL-10 homolog, which reduces migration of dendritic cells to the lymph node, as well as T-cell activation (122, 123). On the other hand, IL-10 producing $CD4^+$ T-cells are induced via IFN I signaling in MACs during MCMV infection (124). IL-10 dampens inflammatory cytokines, such as IFN-γ and IL-6, attenuates tissue damage after MCMV infection (125, 126) and promotes persistence of infection in the salivary gland (127). Finally, TGFβ is secreted by infected human fibroblasts and in rat splenocytes after infection with the respective CMV species (128, 129). Thus, there is strong evidence that CMV induces immunoregulatory cytokines in MACs in addition to viral IL-10, e.g. in HCMV.

CMV inhibits apoptosis and necroptosis in MACs via its proteins pM36 (66) and pM45 (57), respectively (**Table 1**). The M36 gene is conserved among all CMVs and encodes for a cytosolic protein, binds to and blocks the activation of caspase-8 (66). Mutants lacking the M36 gene fail to inhibit apoptosis, show poor viral growth in MAC cell cultures, and loose *in vivo* fitness (67, 130, 131). vIRA/m45 and the cell death regulator vICA/M36 (66, 132) are essential for CMV replication in MACs. After intraperitoneal infection $F4/80^+$ MACs seeded MCMV into the blood and brown adipose tissue, while $CD11c^+$ myeloid cells, which can be expected to comprise dendritic cells, MACs and monocytes, were necessary for dissemination to the salivary gland after lung infection (133, 134). These findings indicate a migratory character of otherwise resident MACs. Interestingly, MCMV mutants lacking M36 (ΔM36) cannot disseminate after peripheral infection (67), and they grow normally in most of the cell types *in vitro* except for MACs. The growth impairment of MCMV mutants lacking M36 in mice with a defect adaptive immunity was rescued by the depletion of MACs. Accordingly, activated MACs were sufficient to impair ΔM36 growth in normally permissive MEFs *in vitro*. This could be reverted by caspase inhibition. TNFα from activated MAC synergized with IFN-γ in MEFs to inhibit ΔM36 growth. Hence, the altered ΔM36 growth in MAC and probably the altered virulence of this mutant does not reflect a defect in tropism, but rather a defect in the suppression of innate immune mediators secreted by infected and/or bystander MACs (67). The vICA in HCMV is encoded by the UL36 gene. The protein pUL36 also binds to pro-caspase-8, inhibits apoptosis and allows for viral replication in THP-1 cells (135). *In vivo* studies on the function of UL36 are limited due to the strict host specificity of CMVs. However, the cloning of UL36 into ΔM36 MCMV completely rescues the viral function both *in vitro* and *in vivo* (68). This indicates functional conservation of vICA in MCMV and HCMV.

Similar to M36, the complex of the products of MCMV genes m139, m140, and m141 is dispensable for the viral growth in fibroblasts, but it is essential for lytic MAC infection (66, 69) (**Table 1**). The products of these genes aid efficient capsid formation, which is apparent only in MACs (70). The underlying mechanism is not clear. It was proposed that the complex of pm139/pm140/pm141 influences cell type specific regulation of transport processes, which are important for assembly of infectious particles (69).

Together, cytokines formed by CMV-infected MACs, such as IFN I, TNFα and IFN-γ, help to contain viral infection (45, 58, 136), while viral and host IL-10 ensure replication and persistence of CMV. Simultaneously, IL-10 maintains a tolerogenic environment, which prevents tissue damage and may benefit the host during CMV infection. Regulatory or "unprimed" MACs can be considered to be more susceptible to CMV infections. This and the notion that neonatal innate immune cells produce lower amounts of IFN I (137), may explain, why newborn infants shed HCMV in higher concentrations than adults in primary HCMV infection (138). Furthermore, CMVs encode viral gene products (**Table 1**) to specifically target MACs and modulate their functions. This is decisive for viral dissemination and confers a central role to MACs in CMV infections.

CMV INFECTION OF THE RESPIRATORY TRACT, THE INTESTINE AND THE CNS

In the lung, a potential CMV entry site, two major MAC types can be discriminated: Alveolar MACs (aMACs), which reside in the alveolar space to safeguard the lung from inhaled particles or pathogens (139), and interstitial MACs (iMACs) (**Table 2**). Fetal liver-monocytes colonize the lung to differentiate and mature into aMACs in the first week of life (140). Under steady state conditions, the aMAC population does not receive a monocyte influx (140, 157). IMACs are a heterogeneous population of at least two sub-populations (145–147). One subset bears significant self-renewal properties, whereas the other is constantly replenished by patrolling monocytes (146), which is unique for tissue resident MACs. Under steady state conditions, iMACs constantly produce IL-10, which alters DC function and maintains regulatory T-cells (104, 108, 146, 148–150, 158–160). At the same time, aMAC secrete TGFβ to induce differentiation of naïve T-cells into $FoxP3^+$ regulatory T-cells (141, 161, 162). Thus, both aMACs and iMACs contribute to an anti-inflammatory tolerogenic environment in homeostasis (141, 142, 148, 149, 161, 162). AMACs are primarily targeted after intranasal infection with MCMV and their depletion leads to higher viral burden (163). After infection $Ly6C^{hi}$ monocytes infiltrate the lung in high numbers and are infected too (163). However, data to further define the consequences of monocyte recruitment, i.e. the fate of infected and uninfected monocytes, in intranasal MCMV infections are missing. Interestingly, inflammatory monocytes are able to enter the tissue and traffic to the draining lymph nodes (164), a sequence also described after intranasal MCMV infection (133).

In MCMV latency, the infection may be reactivated in immunosuppressive conditions also in the lung (165). Thus, monocytes (64, 166) could carry CMV to the lung, where

TABLE 2 | MAC heterogeneity in CMV target tissues (steady state).

MAC	Alveolar MACs	Interstitial MACs	Lamina propria MACs	Microglia	CNS-associated MACs
Localization	Lung: Inside alveoli	Lung interstitium: 1. Alveolar interstitium/ nerves 2. Bronchial interstitium/ blood vessels	Intestine: Lamina propria	Brain parenchyma	CNS-interfaces: 1. Meninges, 2. Perivascular space, 3. Choroid plexus
Immunophenotypic markers	F4/80^{+} CD64^{+} CX3CR1^{-} MerTK^{+} CD11b^{lo} CD11c^{+} SiglecF^{+}	1. F4/80^{+} CD64^{+} CX3CR1^{++} CD206^{-} Lyve-1^{lo} CD11c^{+} MCHII^{hi} 2. F4/80^{+} CD64^{+} CX3CR1^{+} CD206^{+} Lyve-1^{hi} CD11c^{lo} MHCII^{lo}	F4/80^{+} CD64^{+} CX3CR1^{+} MHCII^{+}	F4/80^{+} CD64^{+} CX3CR1^{+} MerTK^{+} CD206^{-} CD45^{lo} Iba1^{+}	F4/80^{+} CD64^{+} CX3CR1^{+} MerTK^{+} CD206^{+} Lyve-1^{+} (1., 2.) CD45$^{lo/hi}$ CD36^{+} (2.) Iba1^{+}
Ontogeny	Embryonic (fetal liver)	Definitive hematopoiesis	Definitive hematopoiesis and embryonic (yolk sac)	Embryonic (yolk sac)	Embryonic (yolk sac, fetal liver) and definitive hematopoiesis
Monocyte replenishment	No	Yes; inflammatory and patrolling monocytes	Yes; microbiota dependent	No	Partial turnover (choroid plexus)
Function	Phagocytosis of surfactant, apoptotic cells and inhaled particles; TGFβ production; maintenance of tolerance against allergens	IL-10 formation; prevention of type 2 response to inhaled allergens; antigen presentation, regulation of T-cell response	Phagocytosis; maintenance of regulatory T cells; epithelial cell renewal;	Phagocytosis; supply of neurotrophic factors; synaptic pruning; guidance of developing vasculature	Filtering of cerebrospinal fluid; immune surveillance; regulation of blood-brain barrier permeability
Literature	(105, 139–144)	(145–149)	(98, 104, 108, 150, 151)	(152, 153)	(154–156)

they can reactivate the virus upon differentiation into iMACs. Accordingly, CMV may exploit the physiological recruitment of patrolling monocytes (167–169), which serve as vehicles in MCMV infections (64).

Intestinal LpMACs represent the largest MAC subset in the mouse (170) (**Table 2**). They form a dense network close to the basal site of epithelial cells. Moreover, LpMACs directly reach into the intestinal lumen with their protrusions (171). The majority of LpMACs are constantly replenished by circulating inflammatory monocytes (Ly6C^{hi}) after week 3 of life, i.e. starting with weaning (98). Accordingly, CCR2-deficient mice, which are impaired in monocyte egress from the bone-marrow, are deficient in LpMACs (98, 108). This process is dependent on the microbiota (98).

Once monocytes enter the lamina propria they differentiate and mature into LpMACs, which are characterized by a site specific response program to TLR-stimuli (172). Moreover, maturation of intestinal tolerogenic LpMACs and subsequent tolerance of the gut, similar to the lung, depends on IL-10 and TGFβ signaling (104, 108, 150, 158, 173). Inflammation interferes with this maturation process and leads to the formation of inflammatory effector cells (174), which control neutrophil activation and limit commensal-mediated tissue damage (175). In neonatal mice, an enteral challenge with MCMV-containing milk leads to viral dissemination (176). Yet, adult mice seem largely resistant to this infection mode (11). In HCMV associated intestinal inflammation, CD14^{+} monocytes, the putative human analog of mouse Ly6C^{hi} monocytes (177), upregulate the TGFβ antagonist Smad7, which leads to the acquisition of inflammatory properties of intestinal MACs (178). It is tempting to speculate that early postnatal infections with CMV promote the monocyte influx into the intestine and thus protect against the invasion of commensals and opportunistic pathogens (179).

CMV-infections in fetuses cause severe symptoms and can lead to permanent damage of the CNS with immediate consequences and late sequelae, such as hearing loss. Microglia, the resident MACs of the brain parenchyma, are yolk sac-derived and maintain their population size exclusively via self-renewal (180) (**Table 2**). Monocyte-derived MACs only populate the brain after blood-brain-barrier disruption (181). In contrast to microglia, CNS-associated MACs include resident tissue MACs of barriers and interfaces of the CNS parenchyma and the periphery, such as perivascular space, meninges and the choroid plexus (154) (**Table 2**). They are also predominantly embryonically seeded and mainly self-renew (155, 182). Congenital transmission of CMV is best modeled by early postnatal intraperitoneal infection of mice (PND0-2), because a cell-free or cell-associated viremia is preceding focal encephalitis (183, 184) similar to the situation in humans (185). Thus, regions around blood vessels are infected first, including the choroid plexus of the periventricular region (186) and the meninges (187). In these regions MACs identified via F4/80^{+}

(186) and Iba1$^+$ (ionized calcium-binding adaptor molecule 1) (187) are infected or activated, respectively. In human brain aggregate culture systems, microglia or monocyte-derived MACs also appear to be initially infected (188). From the periventricular region, the meningoencephalitis caused by MCMV spreads to the hippocampus and cortex (186). In mice, MCMV-encephalitis leads to monocyte recruitment, diapedesis and subsequent differentiation into monocyte-derived MACs (189), which were also found to be infected. Thereby, monocyte-derived MACs might represent a potential way of viral dissemination from CNS interfaces into the brain parenchyma (186, 190). Accordingly, infection of MACs in the CNS may lead to heavy reorganization of otherwise tightly regulated immune cell populations, which may contribute to different pathologies (191–193).

Since resident MACs ensure the structural and functional integrity of their respective tissue (194), an exchange with monocyte-derived MACs after postnatal CMV infection bears opportunities, but also risks. On the one hand, tissue resident MACs are terminally differentiated and less plastic compared to monocytes (106). Postnatal infection could induce an early turnover of MACs in tissues like the intestine (98) and more distal, the skin (97). Thereby monocyte-derived MAC may foster maturation of the immune system and change the Th2-biased immune state (138) to a more inflammatory state, which may promote resistance to future infections. On the other hand, in organs, where MACs are largely maintained through self-renewal, invasion of monocytes could lead to exaggerated inflammation and subsequently tissue damage.

DO CMV INFECTIONS PROTECT AGAINST CONSECUTIVE CHALLENGES OR ALLERGY?—IMMUNOMODULATION OF THE INNATE IMMUNE SYSTEM

Individual immune memory is conventionally attributed to the adaptive immune system. However, it has been known for decades that innate immune cells can be primed by infection for long-lasting alterations in the response to subsequent challenges. These changes in activation programs were variably coined immune priming, immune tolerance, and most recently trained immunity (195–197). As an example for the latter, Rag1$^{-/-}$ mice without T- and B-cells, but not CCR2$^{-/-}$ mice, which are deficient in circulating monocytes, survived a lethal dose of *Candida albicans*, when they had been subjected to a low dose fungal infection one week before (198). Human monocyte and MAC training have been found to involve altered cytokine formation and epigenetic changes (198, 199).

In case of herpesvirus infection models, latent murid herpesvirus 4 (MuHV4) infection leads to the replacement of aMACs with regulatory monocyte-derived MACs, which generate tolerance to house dust mite extracts (200). Furthermore, peritoneal MACs of latently (>28 days) MCMV or mouse gamma-herpesvirus 68 infected mice showed an activated phenotype with increased MHC II expression and a higher killing capacity when re-infected with *Listeria monocytogenes ex vivo*. Latently infected mice were protected against infections with a lethal dose of *L. monocytogenes*. This mode of host resistance was dependent on IFN-γ, but differed from classical IFN-γ-induced protection with respect to both, duration and quality (201).

The fetal and neonatal immune systems have been suggested to be polarized toward protection against extracellular pathogens, which may render them especially vulnerable to viral infections, e.g. by HCMV (138). In contrast, postnatal HCMV infections often pass without overt symptoms and lead to a latent infection with sporadic viral reactivation. It constitutes an attractive model that reactivation occurs, when cues (e.g. interferons) from initial postnatal CMV infection wear off allowing for viral replication (202, 203). In other words, immune priming and recruitment of regulatory myeloid cells may quite rapidly fade. Subsequently, CMV reactivation and containment may induce a further wave of protection/tolerance by innate immune cells without provoking overt disease in immunocompetent individuals. Therefore, infection with CMV may keep the immune system in an alert state, which allows for a rapid response against potentially harmful agents. At the same time, recruitment of regulatory monocytes may maintain tissue integrity and tolerance at mucocutaneous surfaces.

MYELOPOIESIS, LATENCY, AND REACTIVATION IN CMV INFECTIONS

The development along the monocyte-macrophage-axis may be involved in lifelong persistence of CMV (**Figure 2**). Human CD34$^+$ hematopoietic stem and progenitor cells (HSPC) and CD14$^+$ monocytes can be latently infected without ongoing replication and virus release (166, 205–209). The proportion of mononuclear cells carrying HCMV genome in latently infected individuals is rather low (1:10^4-10^5) (210). Yet, CD14$^+$ CD74^{lo} MHCII^{lo} monocytes contain more virus genomes as compared to CD14$^+$ CD74$^+$ and MHCII$^+$ cells (211) (**Figure 2**). Furthermore, new techniques have allowed for the enrichment and characterization of latency-associated transcripts (212). Expression of US28 and UL138 in HCMV is important to establish latency in HSPC (213–215). Notably, *in vitro* infected HSPC and peripheral blood mononuclear cells (PBMC) from clinical samples showed similar HCMV transcriptome profiles (212), pointing to a potent antiviral program already in immature cells.

The HCMV protein pUL7 binds to the Fms-like tyrosine kinase 3 receptor (Flt3R) and further steers HSPC toward myeloid monocyte commitment (216). Moreover, pUL111A, a viral IL-10 analog, impairs HSPC differentiation into dendritic cells (217) (**Figure 2**). This is in line with recent single cell sequencing data, where HCMV-infected HSPC predominantly differentiated into monocytes (211). Thus, during the course of infection, viral IL-10 ensures a supply of monocytes, which may aid in HCMV dissemination.

In the absence of acute inflammation, inflammatory monocytes recirculate to the bone marrow (101), where they differentiate into patrolling monocytes (218, 219). Interestingly, inflammatory monocytes are short lived (half-life: 20h in mice; ∼1d in humans), yet they control the lifespan of patrolling

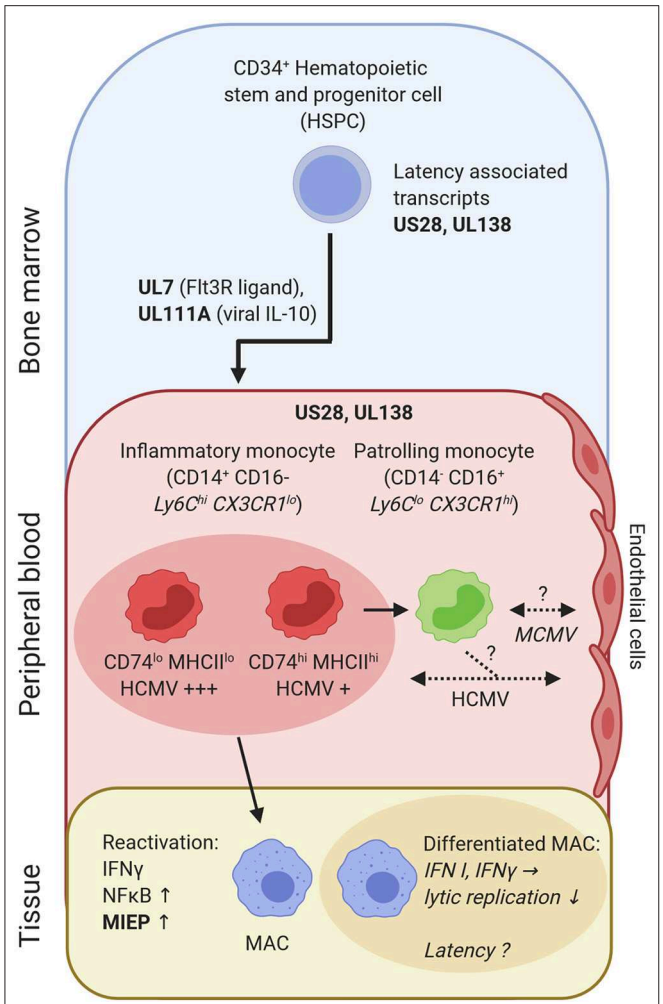

FIGURE 2 | HCMV-derived transcripts (*US28* and *UL138*) are needed to establish latency in CD34$^+$ HSPC and CD14$^+$ monocytes. HCMV gene products (pUL7, pUL111A) promote preferential differentiation of HSPC into monocytes. CD14$^+$ inflammatory monocytes can be subdivided into CD74^{hi} and CD74^{lo} cells, which differ in latent HCMV content and reactivation. Inflammatory monocytes can differentiate into patrolling monocytes. Patrolling monocytes may transfer CMV to uninfected endothelial cells or acquire infection from previously infected endothelial cells [as shown for human CD14$^+$ monocytes *in vitro* (204)]. Upon tissue entry and differentiation into monocyte-derived MACs reactivation and lytic replication occurs, once MIEP is activated. IFN-γ and NFκB are central in this process. In contrast, IFN I and IFN-γ protect against active/lytic replication of MCMV in differentiated MACs, which may explain viral latent states observed in MACs. Bold letters, CMV transcripts/genes; italic, mouse data; non-italic, human data; consistent arrow, differentiation; dashed arrow, CMV transmission.

monocytes (half-life: ∼2.2d in mice; ∼7.5d in humans) via M-CSF consumption in mice (219, 220). Thus, it seems conceivable that inflammatory monocytes can be infected, harbor CMV and continue to differentiate into patrolling monocytes. This may lead to complex changes in the composition of circulating monocytes. Moreover, infected monocytes could pass CMV on to endothelial cells (204), another cell type discussed for life-long latency in mice (221) and persistent infection in humans (222) (**Figure 2**). In a mouse model of latency, IFN-β prevents immediate early (IE) gene expression, which confers protection of lytic MCMV replication in endothelial cells. Reactivation of lytic infection occurred, once the effect of IFN-β wore off (203).

Upon activation and differentiation of monocytes into MACs, viral replication can restart (223, 224). *Ex vivo* infection and culturing of primary human CD34$^+$ cells until differentiation into MACs, resembling the sequence of myelopoiesis and MAC determination, was associated with HCMV reactivation (225). Transcriptional activation of the major immediate early promoter (MIEP) and subsequent expression of IE1, IE2 (HCMV) or ie1, ie3 (MCMV) genes is a key switch to lytic infection. The enhancer of the MIE locus contains binding sites for NFκB (226). Hence, inflammation and cytokine production, e.g. TNF, may lead to reactivation, which is controlled in immunocompetent individuals. However, in case of an impaired inflammation control, reactivation causes complications as seen in the gut, lung or skin (227–230). Interestingly, in HCMV seropositive individuals IFN-γ producing T-cells appear to be more frequent as in seronegative individuals (231). IFN-γ represents a crucial factor for viral reactivation during the differentiation of human monocyte-derived MACs (224) (**Figure 2**). However, the presence of IFN-γ also leads to MAC activation and confers protection against lytic MCMV infection in already differentiated MACs (202) (**Figure 2**).

Early studies suggested that MACs are also a cellular reservoir for viral latency. After administering MCMV into the abdominal cavity, peritoneal MACs were found to bear MCMV DNA 3–9 months after infection. Furthermore, co-culturing with mouse embryonic fibroblasts resulted in reactivation of lytic viral replication, arguing for latently infected MACs (232). Another study used PCR *in situ* hybridization (PISH) to label viral DNA in tissue sections 6 months after peritoneal infection with MCMV. LAMP-2$^+$ (CD107b$^+$/Mac-3$^+$) bona fide lung MACs were found to carry MCMV genome. However, the association of MCMV PISH- and LAMP-2-positivity were based on colocalisation in interalveolar tissue and not determined on the single cell level, which hampers the interpretation of these data (233).

In summary, CMV latency in myeloid cells may provide solutions for several puzzles in CMV disease progression and control, yet further data are required to robustly establish this scenario. In particular the discrimination between human inflammatory/classical and patrolling/non-classical monocytes could serve well to translate murine *in vivo* models into the human system.

CONCLUSIONS

In CMV infection, barrier tissue MACs are both targets and effector cells. The early formation of antiviral IFNs, which control several thousand of genes (234), is essential for regulating the immune response. The expression of numerous IFN inhibitory proteins by both HCMV and MCMV (235) is in full support of a model, where the armament of host and virus ultimately serves

both sides. Subsequent signaling events, including the formation of IL-10, impact on restricting CMV-induced immunopathology and antiviral immunity, thus allowing for reestablishment of tissue immune homeostasis, as well as viral latency for years. When CMV infection occurs very early in life, as it has in most of human history, antiviral immunity and individual development of myeloid cells are intertwined. This is particular true for organs with high turnover of MACs, since monocytes as MAC progenitors integrate cues from CMV into the site specific differentiation program. Accordingly, in the case of an immunocompetent host, CMV and tissue MACs are primarily not foes. On the contrary, given the ancient CMV adaptation to mammalian hosts, it is a relationship with reciprocal benefits, e.g. the tuning of basal activation for a better response against more harmful microbial invaders, the renewal of tissue resident cells and modulation of autoimmunity (as it has been shown for gamma herpesviruses). At the same time, CMV has developed strategies to manipulate host immunity for lifelong persistence and inter-individual spread. Therefore, adverse consequences of CMV in the elderly, e.g. T-cell inflation (236) may be due to a CMV-human co-evolution tailored for a shorter host lifespan. Currently, direct evidence for such "mutual friendship" is just emerging. Yet, a scenario, where the benefits and harms of CMV infection are tissue and context specific, is highly attractive.

AUTHOR CONTRIBUTIONS

SB, ZR, and PH wrote and edited the manuscript.

FUNDING

Funding was provided by the Else-Kröner-Fresenius Foundation, the German Ministry of Education and Research (grant Nos: 01EO0803, 01GL1746A and 01EK1602A to PH) and the German Research Council (grant Nos: HE3127/9-1, HE3127/12-1, and SFB/TRR167 to PH and 406922110 to ZR). The article processing charge was funded by the University of Freiburg in the funding programme Open Access Publishing.

REFERENCES

1. Wylie KM, Weinstock GM, Storch GA. Emerging view of the human virome. *Transl Res.* (2012) 160:283–90. doi: 10.1016/j.trsl.2012.03.006
2. Hooper LV, Littman DR, Macpherson AJ. Interactions between the microbiota and the immune system. *Science.* (2012) 336:1268–73. doi: 10.1126/science.1223490
3. McGeoch DJ, Rixon FJ, Davison AJ. Topics in herpesvirus genomics and evolution. *Virus Res.* (2006) 117:90–104. doi: 10.1016/j.virusres.2006.01.002
4. Bello C, Whittle H. Cytomegalovirus infection in Gambian mothers and their babies. *J Clin Pathol.* (1991) 44:366–9. doi: 10.1136/jcp.44.5.366
5. Lanzieri TM, Dollard SC, Bialek SR, Grosse SD. Systematic review of the birth prevalence of congenital cytomegalovirus infection in developing countries. *Int J Infect Dis.* (2014) 22:44–8. doi: 10.1016/j.ijid.2013.12.010
6. Voigt S, Schaffrath Rosario A, Mankertz A. Cytomegalovirus Seroprevalence among children and adolescents in Germany: data from the German health interview and examination survey for children and adolescents (KiGGS), 2003-2006. *Open forum Infect Dis.* (2016) 3:ofv193. doi: 10.1093/ofid/ofv193
7. Stagno S, Cloud GA. Working parents: the impact of day care and breast-feeding on cytomegalovirus infections in offspring. *Proc Natl Acad Sci USA.* (1994) 91:2384–9. doi: 10.1073/pnas.91.7.2384
8. Hamprecht K, Maschmann J, Vochem M, Dietz K, Speer CP, Jahn G. Epidemiology of transmission of cytomegalovirus from mother to preterm infant by breastfeeding. *Lancet.* (2001) 357:513–8. doi: 10.1016/S0140-6736(00)04043-5
9. Rawlinson WD, Farrell HE, Barrell BG. Analysis of the complete DNA sequence of murine cytomegalovirus. *J Virol.* (1996) 70:8833–49. doi: 10.1128/JVI.70.12.8833-8849.1996
10. Reddehase MJ. Antigens and immunoevasins: opponents in cytomegalovirus immune surveillance. *Nat Rev Immunol.* (2002) 2:831–44. doi: 10.1038/nri932
11. Oduro JD, Redeker A, Lemmermann NA, Ebermann L, Marandu TF, Dekhtiarenko I, et al. Murine cytomegalovirus (CMV) infection via the intranasal route offers a robust model of immunity upon mucosal CMV infection. *J Gen Virol.* (2016) 97:185–95. doi: 10.1099/jgv.0.000339
12. Smith PD, Saini SS, Raffeld M, Manischewitz JF, Wahl SM. Cytomegalovirus induction of tumor necrosis factor-alpha by human monocytes and mucosal macrophages. *J Clin Invest.* (1992) 90:1642–8. doi: 10.1172/JCI116035
13. Sinzger C, Plachter B, Grefte A, The TH, Jahn G. Tissue macrophages are infected by human cytomegalovirus *in vivo*. *J Infect Dis.* (1996) 173:240–5. doi: 10.1093/infdis/173.1.240
14. Mims CA, Gould J. The role of macrophages in mice infected with murine cytomegalovirus. *J Gen Virol.* (1978) 41:143–53. doi: 10.1099/0022-1317-41-1-143
15. Brautigam AR, Dutko FJ, Olding LB, Oldstone MB. Pathogenesis of murine cytomegalovirus infection: the macrophage as a permissive cell for cytomegalovirus infection, replication and latency. *J Gen Virol.* (1979) 44:349–59. doi: 10.1099/0022-1317-44-2-349
16. Ibanez CE, Schrier R, Ghazal P, Wiley C, Nelson JA. Human cytomegalovirus productively infects primary differentiated macrophages. *J Virol.* (1991) 65:6581–8. doi: 10.1128/JVI.65.12.6581-6588.1991
17. Ginhoux F, Guilliams M. Tissue-resident macrophage ontogeny and homeostasis. *Immunity.* (2016) 44:439–49. doi: 10.1016/j.immuni.2016.02.024
18. McNab F, Mayer-Barber K, Sher A, Wack A, O'Garra A. Type I interferons in infectious disease. *Nat Rev Immunol.* (2015) 15:87–103. doi: 10.1038/nri3787
19. Presti RM, Pollock JL, Dal Canto AJ, O'Guin AK, Virgin IV HW. Interferon γ regulates acute and latent murine cytomegalovirus infection and chronic disease of the great vessels. *J Exp Med.* (1998) 188:577–88. doi: 10.1084/jem.188.3.577
20. Madera S, Sun JC. Cutting edge: stage-specific requirement of IL-18 for antiviral NK cell expansion. *J Immunol.* (2015) 194:1408–12. doi: 10.4049/jimmunol.1402001
21. Kawai T, Akira S. The role of pattern-recognition receptors in innate immunity: update on toll-like receptors. *Nat Immunol.* (2010) 11:373–84. doi: 10.1038/ni.1863
22. Rathinam VA, Jiang Z, Waggoner SN, Sharma S, Cole LE, Waggoner L, et al. The AIM2 inflammasome is essential for host defense against cytosolic bacteria and DNA viruses. *Nat Immunol.* (2010) 11:395–402. doi: 10.1038/ni.1864
23. Delale T, Paquin A, Asselin-Paturel C, Dalod M, Brizard G, Bates EE, et al. MyD88-dependent and -independent murine cytomegalovirus sensing for IFN-alpha release and initiation of immune responses *in vivo*. *J Immunol.* (2005) 175:6723–32. doi: 10.4049/jimmunol.175.10.6723
24. Krug A, French AR, Barchet W, Fischer JA, Dzionek A, Pingel JT, et al. TLR9-dependent recognition of MCMV by IPC and DC generates coordinated cytokine responses that activate antiviral NK cell function. *Immunity.* (2004) 21:107–19. doi: 10.1016/j.immuni.2004.06.007
25. Hokeness-Antonelli KL, Crane MJ, Dragoi AM, Chu WM, Salazar-Mather TP. IFN-alphabeta-mediated inflammatory responses and antiviral defense in liver is TLR9-independent but MyD88-dependent during murine cytomegalovirus infection. *J Immunol.* (2007) 179:6176–83. doi: 10.4049/jimmunol.179.9.6176

26. Hoebe K, Du X, Georgel P, Janssen E, Tabeta K, Kim SO, et al. Identification of Lps2 as a key transducer of MyD88-independent TIR signalling. *Nature.* (2003) 424:743–8. doi: 10.1038/nature01889
27. Barbalat R, Lau L, Locksley RM, Barton GM. Toll-like receptor 2 on inflammatory monocytes induces type I interferon in response to viral but not bacterial ligands. *Nat Immunol.* (2009) 10:1200–7. doi: 10.1038/ni.1792
28. Nguyen CC, Kamil JP. Pathogen at the gates: human cytomegalovirus entry and cell tropism. *Viruses.* (2018) 10:704. doi: 10.3390/v10120704
29. Ryckman BJ, Chase MC, Johnson DC. HCMV gH/gL/UL128-131 interferes with virus entry into epithelial cells: evidence for cell type-specific receptors. *Proc Natl Acad Sci USA.* (2008) 105:14118–23. doi: 10.1073/pnas.0804365105
30. Boehme KW, Guerrero M, Compton T. Human cytomegalovirus envelope glycoproteins B and H are necessary for TLR2 activation in permissive cells. *J Immunol.* (2006) 177:7094–102. doi: 10.4049/jimmunol.177.10.7094
31. Compton T, Kurt-Jones EA, Boehme KW, Belko J, Latz E, Golenbock DT, et al. Human cytomegalovirus activates inflammatory cytokine responses via CD14 and Toll-like receptor 2. *J Virol.* (2003) 77:4588–96. doi: 10.1128/JVI.77.8.4588-4596.2003
32. Kijpittayarit S, Eid AJ, Brown RA, Paya CV, Razonable RR. Relationship between Toll-like receptor 2 polymorphism and cytomegalovirus disease after liver transplantation. *Clin Infect Dis.* (2007) 44:1315–20. doi: 10.1086/514339
33. Szomolanyi-Tsuda E, Liang X, Welsh RM, Kurt-Jones EA, Finberg RW. Role for TLR2 in NK cell-mediated control of murine cytomegalovirus *in vivo*. *J Virol.* (2006) 80:4286–91. doi: 10.1128/JVI.80.9.4286-4291.2006
34. Tabeta K, Hoebe K, Janssen EM, Du X, Georgel P, Crozat K, et al. The Unc93b1 mutation 3d disrupts exogenous antigen presentation and signaling via Toll-like receptors 3, 7 and 9. *Nat Immunol.* (2006) 7:156–64. doi: 10.1038/ni1297
35. Andoniou CE, van Dommelen SL, Voigt V, Andrews DM, Brizard G, Asselin-Paturel C, et al. Interaction between conventional dendritic cells and natural killer cells is integral to the activation of effective antiviral immunity. *Nat Immunol.* (2005) 6:1011–9. doi: 10.1038/ni1244
36. Tabeta K, Georgel P, Janssen E, Du X, Hoebe K, Crozat K, et al. Toll-like receptors 9 and 3 as essential components of innate immune defense against mouse cytomegalovirus infection. *Proc Natl Acad Sci USA.* (2004) 101:3516–21. doi: 10.1073/pnas.0400525101
37. Puttur F, Francozo M, Solmaz G, Bueno C, Lindenberg M, Gohmert M, et al. Conventional dendritic cells confer protection against mouse cytomegalovirus infection via TLR9 and MyD88 signaling. *Cell Rep.* (2016) 17:1113–27. doi: 10.1016/j.celrep.2016.09.055
38. Yoshida H, Okabe Y, Kawane K, Fukuyama H, Nagata S. Lethal anemia caused by interferon-beta produced in mouse embryos carrying undigested DNA. *Nat Immunol.* (2005) 6:49–56. doi: 10.1038/ni1146
39. Doring M, Lessin I, Frenz T, Spanier J, Kessler A, Tegtmeyer P, et al. M27 expressed by cytomegalovirus counteracts effective type I interferon induction of myeloid cells but not of plasmacytoid dendritic cells. *J Virol.* (2014) 88:13638–50. doi: 10.1128/JVI.00216-14
40. Ishikawa H, Barber GN. STING is an endoplasmic reticulum adaptor that facilitates innate immune signalling. *Nature.* (2008) 455:674–8. doi: 10.1038/nature07317
41. Sun L, Wu J, Du F, Chen X, Chen ZJ. Cyclic GMP-AMP synthase is a cytosolic DNA sensor that activates the type I interferon pathway. *Science.* (2013) 339:786–91. doi: 10.1126/science.1232458
42. Ablasser A, Goldeck M, Cavlar T, Deimling T, Witte G, Rohl I, et al. cGAS produces a 2'-5'-linked cyclic dinucleotide second messenger that activates STING. *Nature.* (2013) 498:380–4. doi: 10.1038/nature12306
43. Ishikawa H, Ma Z, Barber GN. STING regulates intracellular DNA-mediated, type I interferon-dependent innate immunity. *Nature.* (2009) 461:788–92. doi: 10.1038/nature08476
44. Schoggins JW, MacDuff DA, Imanaka N, Gainey MD, Shrestha B, Eitson JL, et al. Pan-viral specificity of IFN-induced genes reveals new roles for cGAS in innate immunity. *Nature.* (2014) 505:691–5. doi: 10.1038/nature12862
45. Tegtmeyer PK, Spanier J. STING induces early IFN-beta in the liver and constrains myeloid cell-mediated dissemination of murine cytomegalovirus. *Nat Commun.* (2019) 10:2830. doi: 10.1038/s41467-019-10863-0
46. Chan B, Goncalves Magalhaes V. The murine cytomegalovirus M35 protein antagonizes type I IFN induction downstream of pattern recognition receptors by targeting NF-kappaB mediated transcription. *PLoS pathogens.* (2017) 13:e1006382. doi: 10.1371/journal.ppat.1006382
47. Paijo J, Doring M, Spanier J, Grabski E, Nooruzzaman M, Schmidt T, et al. cGAS senses human cytomegalovirus and induces type I interferon responses in human monocyte-derived cells. *PLoS Pathog.* (2016) 12:e1005546. doi: 10.1371/journal.ppat.1005546
48. Takaoka A, Wang Z, Choi MK, Yanai H, Negishi H, Ban T, et al. DAI (DLM-1/ZBP1) is a cytosolic DNA sensor and an activator of innate immune response. *Nature.* (2007) 448:501–5. doi: 10.1038/nature06013
49. Rebsamen M, Heinz LX, Meylan E, Michallet MC, Schroder K, Hofmann K, et al. DAI/ZBP1 recruits RIP1 and RIP3 through RIP homotypic interaction motifs to activate NF-kappaB. *EMBO Rep.* (2009) 10:916–22. doi: 10.1038/embor.2009.109
50. Kaiser WJ, Upton JW, Mocarski ES. Receptor-interacting protein homotypic interaction motif-dependent control of NF-kappa B activation via the DNA-dependent activator of IFN regulatory factors. *J Immunol.* (2008) 181:6427–34. doi: 10.4049/jimmunol.181.9.6427
51. Ishii KJ, Kawagoe T, Koyama S, Matsui K, Kumar H, Kawai T, et al. TANK-binding kinase-1 delineates innate and adaptive immune responses to DNA vaccines. *Nature.* (2008) 451:725–9. doi: 10.1038/nature06537
52. Thapa RJ, Ingram JP, Ragan KB, Nogusa S, Boyd DF, Benitez AA, et al. DAI senses influenza a virus genomic RNA and activates RIPK3-dependent cell death. *Cell Host Microbe.* (2016) 20:674–81. doi: 10.1016/j.chom.2016.09.014
53. Maelfait J, Liverpool L. Sensing of viral and endogenous RNA by ZBP1/DAI induces necroptosis. *EMBO J.* (2017) 36:2529–43. doi: 10.15252/embj.201796476
54. Brune W, Menard C, Heesemann J, Koszinowski UH. A ribonucleotide reductase homolog of cytomegalovirus and endothelial cell tropism. *Science.* (2001) 291:303–5. doi: 10.1126/science.291.5502.303
55. Upton JW, Kaiser WJ, Mocarski ES. Virus inhibition of RIP3-dependent necrosis. *Cell Host Microbe.* (2010) 7:302–13. doi: 10.1016/j.chom.2010.03.006
56. Koehler HS, Feng Y, Mandal P, Mocarski ES. Recognizing limits of Z-nucleic acid binding protein (ZBP1/DAI/DLM1) function. *FEBS J.* (2020). doi: 10.1111/febs.15242. [Epub ahead of print].
57. Daley-Bauer LP, Roback L, Crosby LN, McCormick AL, Feng Y, Kaiser WJ, et al. Mouse cytomegalovirus M36 and M45 death suppressors cooperate to prevent inflammation resulting from antiviral programmed cell death pathways. *Proc Natl Acad Sci USA.* (2017) 114:E2786–95. doi: 10.1073/pnas.1616829114
58. Farrell HE, Bruce K, Lawler C, Cardin RD, Davis-Poynter NJ. Type 1 interferons and NK cells limit murine cytomegalovirus escape from the lymph node subcapsular sinus. *PLoS Pathog.* (2016) 12:e1006069. doi: 10.1371/journal.ppat.1006069
59. Zimmermann A, Trilling M, Wagner M, Wilborn M, Bubic I, Jonjic S, et al. A cytomegaloviral protein reveals a dual role for STAT2 in IFN-γ signaling and antiviral responses. *J Exp Med.* (2005) 201:1543–53. doi: 10.1084/jem.20041401
60. Browne EP, Shenk T. Human cytomegalovirus UL83-coded pp65 virion protein inhibits antiviral gene expression in infected cells. *Proc Natl Acad Sci USA.* (2003) 100:11439–44. doi: 10.1073/pnas.1534570100
61. Taylor RT, Bresnahan WA. Human cytomegalovirus immediate-early 2 gene expression blocks virus-induced beta interferon production. *J Virol.* (2005) 79:3873–7. doi: 10.1128/JVI.79.6.3873-3877.2005
62. Stempel M, Chan B, Juranic Lisnic V, Krmpotic A, Hartung J, Paludan SR, et al. The herpesviral antagonist m152 reveals differential activation of STING-dependent IRF and NF-kappaB signaling and STING's dual role during MCMV infection. *EMBO J.* (2019) 38:e100983. doi: 10.15252/embj.2018100983
63. Saederup N, Lin YC, Dairaghi DJ, Schall TJ, Mocarski ES. Cytomegalovirus-encoded beta chemokine promotes monocyte-associated viremia in the host. *Proc Natl Acad Sci USA.* (1999) 96:10881–6. doi: 10.1073/pnas.96.19.10881
64. Daley-Bauer LP, Roback LJ, Wynn GM, Mocarski ES. Cytomegalovirus hijacks CX3CR1(hi) patrolling monocytes as immune-privileged

vehicles for dissemination in mice. *Cell Host Microbe.* (2014) 15:351–62. doi: 10.1016/j.chom.2014.02.002
65. Wagner FM, Brizic I, Prager A, Trsan T, Arapovic M, Lemmermann NA, et al. The viral chemokine MCK-2 of murine cytomegalovirus promotes infection as part of a gH/gL/MCK-2 complex. *PLoS Pathog.* (2013) 9:e1003493. doi: 10.1371/journal.ppat.1003493
66. Menard C, Wagner M, Ruzsics Z, Holak K, Brune W, Campbell AE, et al. Role of murine cytomegalovirus US22 gene family members in replication in macrophages. *J Virol.* (2003) 77:5557–70. doi: 10.1128/JVI.77.10.5557-5570.2003
67. Ebermann L, Ruzsics Z, Guzman CA, van Rooijen N, Casalegno-Garduno R, Koszinowski U, et al. Block of death-receptor apoptosis protects mouse cytomegalovirus from macrophages and is a determinant of virulence in immunodeficient hosts. *PLoS Pathog.* (2012) 8:e1003062. doi: 10.1371/journal.ppat.1003062
68. Chaudhry MZ, Kasmapour B, Plaza-Sirvent C, Bajagic M, Casalegno Garduño R, Borkner L, et al. UL36 rescues apoptosis inhibition and *in vivo* replication of a Chimeric MCMV Lacking the M36 Gene. *Front Cell Infect Microbiol.* (2017) 7:312. doi: 10.3389/fcimb.2017.00312
69. Hanson LK, Slater JS, Karabekian Z, Ciocco-Schmitt G, Campbell AE. Products of US22 genes M140 and M141 confer efficient replication of murine cytomegalovirus in macrophages and spleen. *J Virol.* (2001) 75:6292–302. doi: 10.1128/JVI.75.14.6292-6302.2001
70. Hanson LK, Slater JS, Cavanaugh VJ, Newcomb WW, Bolin LL, Nelson CN, et al. Murine cytomegalovirus capsid assembly is dependent on US22 family gene M140 in infected macrophages. *J Virol.* (2009) 83:7449–56. doi: 10.1128/JVI.00325-09
71. Krause E, de Graaf M, Fliss PM, Dölken L, Brune W. Murine cytomegalovirus virion-associated protein M45 mediates rapid NF-κB activation after infection. *J Virol.* (2014) 88:9963–75. doi: 10.1128/JVI.00684-14
72. Fliss PM, Jowers TP, Brinkmann MM, Holstermann B, Mack C, Dickinson P, et al. Viral mediated redirection of NEMO/IKKγ to autophagosomes curtails the inflammatory cascade. *PLoS Pathog.* (2012) 8:e1002517. doi: 10.1371/journal.ppat.1002517
73. Hokeness KL, Kuziel WA, Biron CA, Salazar-Mather TP. Monocyte chemoattractant protein-1 and CCR2 interactions are required for IFN-alpha/beta-induced inflammatory responses and antiviral defense in liver. *J Immunol.* (2005) 174:1549–56. doi: 10.4049/jimmunol.174.3.1549
74. Crane MJ, Hokeness-Antonelli KL, Salazar-Mather TP. Regulation of inflammatory monocyte/macrophage recruitment from the bone marrow during murine cytomegalovirus infection: role for type I interferons in localized induction of CCR2 ligands. *J Immunol.* (2009) 183:2810–7. doi: 10.4049/jimmunol.0900205
75. Huffnagle GB, Strieter RM, Standiford TJ, McDonald RA, Burdick MD, Kunkel SL, et al. The role of monocyte chemotactic protein-1 (MCP-1) in the recruitment of monocytes and CD4+ T cells during a pulmonary Cryptococcus neoformans infection. *J Immunol.* (1995) 155:4790–7.
76. Lu B, Rutledge BJ, Gu L, Fiorillo J, Lukacs NW, Kunkel SL, et al. Abnormalities in monocyte recruitment and cytokine expression in monocyte chemoattractant protein 1-deficient mice. *J Exp Med.* (1998) 187:601–8. doi: 10.1084/jem.187.4.601
77. Boring L, Gosling J, Chensue SW, Kunkel SL, Farese RV, Jr., Broxmeyer HE, et al. Impaired monocyte migration and reduced type 1 (Th1) cytokine responses in C-C chemokine receptor 2 knockout mice. *J Clin Invest.* (1997) 100:2552–61. doi: 10.1172/JCI119798
78. Kuziel WA, Morgan SJ, Dawson TC, Griffin S, Smithies O, Ley K, et al. Severe reduction in leukocyte adhesion and monocyte extravasation in mice deficient in CC chemokine receptor 2. *Proc Natl Acad Sci USA.* (1997) 94:12053–8. doi: 10.1073/pnas.94.22.12053
79. Serbina NV, Pamer EG. Monocyte emigration from bone marrow during bacterial infection requires signals mediated by chemokine receptor CCR2. *Nat Immunol.* (2006) 7:311–7. doi: 10.1038/ni1309
80. MacDonald MR, Burney MW, Resnick SB, Virgin HW. Spliced mRNA encoding the murine cytomegalovirus chemokine homolog predicts a β chemokine of novel structure. *J Virol.* (1999) 73:3682–91. doi: 10.1128/JVI.73.5.3682-3691.1999
81. Assaf BT, Mansfield KG, Strelow L, Westmoreland SV, Barry PA, Kaur A. Limited dissemination and shedding of the UL128 complex-intact, UL/b'-defective rhesus cytomegalovirus strain 180.92. *J Virol.* (2014) 88:9310–20. doi: 10.1128/JVI.00162-14
82. Menezes S, Melandri D, Anselmi G, Perchet T, Loschko J, Dubrot J, et al. The heterogeneity of Ly6Chi monocytes controls their differentiation into iNOS+ macrophages or monocyte-derived dendritic cells. *Immunity.* (2016) 45:1205–18. doi: 10.1016/j.immuni.2016.12.001
83. Auffray C, Sieweke MH, Geissmann F. Blood monocytes: development, heterogeneity, and relationship with dendritic cells. *Ann Rev Immunol.* (2009) 27:669–92. doi: 10.1146/annurev.immunol.021908.132557
84. Daley-Bauer LP, Wynn GM, Mocarski ES. Cytomegalovirus impairs antiviral CD8+ T cell immunity by recruiting inflammatory monocytes. *Immunity.* (2012) 37:122–33. doi: 10.1016/j.immuni.2012.04.014
85. Salazar-Mather TP, Orange JS, Biron CA. Early murine cytomegalovirus (MCMV) infection induces liver natural killer (NK) cell inflammation and protection through macrophage inflammatory protein 1alpha (MIP-1alpha)-dependent pathways. *J Exp Med.* (1998) 187:1–14. doi: 10.1084/jem.187.1.1
86. Andrews DM, Estcourt MJ, Andoniou CE, Wikstrom ME, Khong A, Voigt V, et al. Innate immunity defines the capacity of antiviral T cells to limit persistent infection. *J Exp Med.* (2010) 207:1333–43. doi: 10.1084/jem.20091193
87. Auffray C, Fogg D, Garfa M, Elain G, Join-Lambert O, Kayal S, et al. Monitoring of blood vessels and tissues by a population of monocytes with patrolling behavior. *Science.* (2007) 317:666–70. doi: 10.1126/science.1142883
88. Carlin LM, Stamatiades EG, Auffray C, Hanna RN, Glover L, Vizcay-Barrena G, et al. Nr4a1-dependent Ly6C(low) monocytes monitor endothelial cells and orchestrate their disposal. *Cell.* (2013) 153:362–75. doi: 10.1016/j.cell.2013.03.010
89. Sacher T, Podlech J, Mohr CA, Jordan S, Ruzsics Z, Reddehase MJ, et al. The major virus-producing cell type during murine cytomegalovirus infection, the hepatocyte, is not the source of virus dissemination in the host. *Cell Host Microbe.* (2008) 3:263–72. doi: 10.1016/j.chom.2008.02.014
90. Farrell HE, Bruce K, Redwood AJ, Stevenson PG. Murine cytomegalovirus disseminates independently of CX3CR1, CCL2 or its m131/m129 chemokine homologue. *J Gen Virol.* (2019) 100:1695–700. doi: 10.1099/jgv.0.001333
91. van Furth R, Cohn ZA. The origin and kinetics of mononuclear phagocytes. *J Exp Med.* (1968) 128:415–35. doi: 10.1084/jem.128.3.415
92. Sieweke MH, Allen JE. Beyond stem cells: self-renewal of differentiated macrophages. *Science.* (2013) 342:1242974. doi: 10.1126/science.1242974
93. Ginhoux F, Schultze JL, Murray PJ, Ochando J, Biswas SK. New insights into the multidimensional concept of macrophage ontogeny, activation and function. *Nat Immunol.* (2016) 17:34–40. doi: 10.1038/ni.3324
94. Ginhoux F, Jung S. Monocytes and macrophages: developmental pathways and tissue homeostasis. *Nat Rev Immunol.* (2014) 14:392–404. doi: 10.1038/nri3671
95. Gomez Perdiguero E, Klapproth K, Schulz C, Busch K, Azzoni E, Crozet L, et al. Tissue-resident macrophages originate from yolk-sac-derived erythro-myeloid progenitors. *Nature.* (2015) 518:547–51. doi: 10.1038/nature13989
96. Molawi K, Wolf Y, Kandalla PK, Favret J, Hagemeyer N, Frenzel K, et al. Progressive replacement of embryo-derived cardiac macrophages with age. *J Exp Med.* (2014) 211:2151–8. doi: 10.1084/jem.20140639
97. Kolter J, Feuerstein R, Zeis P, Hagemeyer N, Paterson N, d'Errico P, et al. A subset of skin macrophages contributes to the surveillance and regeneration of local nerves. *Immunity.* (2019) 50:1482–97.e7. doi: 10.1016/j.immuni.2019.05.009
98. Bain CC, Bravo-Blas A, Scott CL, Gomez Perdiguero E. Constant replenishment from circulating monocytes maintains the macrophage pool in the intestine of adult mice. *Nat Immunol.* (2014) 15:929–37. doi: 10.1038/ni.2967
99. Shi C, Pamer EG. Monocyte recruitment during infection and inflammation. *Nat Rev Immunol.* (2011) 11:762–4. doi: 10.1038/nri3070
100. Guilliams M, Scott CL. Does niche competition determine the origin of tissue-resident macrophages? *Nat Rev Immunol.* (2017) 17:451-60. doi: 10.1038/nri.2017.42

101. Varol C, Landsman L, Fogg DK, Greenshtein L, Gildor B, Margalit R, et al. Monocytes give rise to mucosal, but not splenic, conventional dendritic cells. *J Exp Med.* (2007) 204:171–80. doi: 10.1084/jem.20061011
102. Perdiguero EG, Geissmann F. The development and maintenance of resident macrophages. *Nat Immunol.* (2016) 17:2–8. doi: 10.1038/ni.3341
103. Ajami B, Bennett JL, Krieger C, McNagny KM, Rossi FM. Infiltrating monocytes trigger EAE progression, but do not contribute to the resident microglia pool. *Nat Neurosci.* (2011) 14:1142–9. doi: 10.1038/nn.2887
104. Zigmond E, Bernshtein B, Friedlander G, Walker CR, Yona S, Kim KW, et al. Macrophage-restricted interleukin-10 receptor deficiency, but not IL-10 deficiency, causes severe spontaneous colitis. *Immunity.* (2014) 40:720–33. doi: 10.1016/j.immuni.2014.03.012
105. Hashimoto D, Chow A, Noizat C, Teo P, Beasley MB, Leboeuf M, et al. Tissue-resident macrophages self-maintain locally throughout adult life with minimal contribution from circulating monocytes. *Immunity.* (2013) 38:792–804. doi: 10.1016/j.immuni.2013.04.004
106. van de Laar L, Saelens W, De Prijck S, Martens L, Scott CL, Van Isterdael G, et al. Yolk sac macrophages, fetal liver, and adult monocytes can colonize an empty niche and develop into functional tissue-resident macrophages. *Immunity.* (2016) 44:755–68. doi: 10.1016/j.immuni.2016.02.017
107. Scott CL, Zheng F, De Baetselier P, Martens L, Saeys Y, De Prijck S, et al. Bone marrow-derived monocytes give rise to self-renewing and fully differentiated Kupffer cells. *Nat Commun.* (2016) 7:10321. doi: 10.1038/ncomms10321
108. Bain CC, Scott CL, Uronen-Hansson H, Gudjonsson S, Jansson O, Grip O, et al. Resident and pro-inflammatory macrophages in the colon represent alternative context-dependent fates of the same Ly6Chi monocyte precursors. *Mucosal Immunol.* (2013) 6:498–510. doi: 10.1038/mi.2012.89
109. Arnold L, Henry A, Poron F, Baba-Amer Y, van Rooijen N, Plonquet A, et al. Inflammatory monocytes recruited after skeletal muscle injury switch into antiinflammatory macrophages to support myogenesis. *J Exp Med.* (2007) 204:1057–69. doi: 10.1084/jem.20070075
110. Okabe Y, Medzhitov R. Tissue biology perspective on macrophages. *Nat Immunol.* (2016) 17:9–17. doi: 10.1038/ni.3320
111. Gunther P, Schultze JL. Mind the map: technology shapes the myeloid cell space. *Front Immunol.* (2019) 10:2287. doi: 10.3389/fimmu.2019.02287
112. Lawrence T, Natoli G. Transcriptional regulation of macrophage polarization: enabling diversity with identity. *Nat Rev Immunol.* (2011) 11:750–61. doi: 10.1038/nri3088
113. Murray PJ, Allen JE, Biswas SK, Fisher EA, Gilroy DW, Goerdt S, et al. Macrophage activation and polarization: nomenclature and experimental guidelines. *Immunity.* (2014) 41:14–20. doi: 10.1016/j.immuni.2014.06.008
114. Bayer C, Varani S, Wang L, Walther P, Zhou S, Straschewski S, et al. Human cytomegalovirus infection of M1 and M2 macrophages triggers inflammation and autologous T-cell proliferation. *J Virol.* (2013) 87:67–79. doi: 10.1128/JVI.01585-12
115. Presti RM, Popkin DL, Connick M, Paetzold S, Virgin IV HW. Novel cell type–specific antiviral mechanism of interferon γ action in macrophages. *J Exp Med.* (2001) 193:483–96. doi: 10.1084/jem.193.4.483
116. Noda S, Aguirre SA, Bitmansour A, Brown JM, Sparer TE, Huang J, et al. Cytomegalovirus MCK-2 controls mobilization and recruitment of myeloid progenitor cells to facilitate dissemination. *Blood.* (2006) 107:30–8. doi: 10.1182/blood-2005-05-1833
117. Lemmermann NA, Krmpotic A, Podlech J, Brizic I, Prager A, Adler H, et al. Non-redundant and redundant roles of cytomegalovirus gH/gL complexes in host organ entry and intra-tissue spread. *PLoS Pathog.* (2015) 11:e1004640. doi: 10.1371/journal.ppat.1004640
118. Ryckman BJ, Rainish BL, Chase MC, Borton JA, Nelson JA, Jarvis MA, et al. Characterization of the human cytomegalovirus gH/gL/UL128-131 complex that mediates entry into epithelial and endothelial cells. *J Virol.* (2008) 82:60–70. doi: 10.1128/JVI.01910-07
119. Chan G, Bivins-Smith ER, Smith MS, Smith PM, Yurochko AD. Transcriptome analysis reveals human cytomegalovirus reprograms monocyte differentiation towards a M1 macrophage. *J Immunol.* (2008) 181:698–711. doi: 10.4049/jimmunol.181.1.698
120. Chan G, Bivins-Smith ER, Smith MS, Yurochko AD. NF-κB and phosphatidylinositol 3-kinase activity mediates the HCMV-induced Atypical M1/M2 polarization of monocytes. *Virus Res.* (2009) 144:329–33. doi: 10.1016/j.virusres.2009.04.026
121. Redpath S, Angulo A, Gascoigne NR, Ghazal P. Murine cytomegalovirus infection down-regulates MHC class II expression on macrophages by induction of IL-10. *J Immunol.* (1999) 162:6701–7.
122. Avdic S, Cao JZ, McSharry BP, Clancy LE, Brown R, Steain M, et al. Human cytomegalovirus interleukin-10 polarizes monocytes toward a deactivated M2c phenotype to repress host immune responses. *J Virol.* (2013) 87:10273–82. doi: 10.1128/JVI.00912-13
123. Chang WW, Barry PA. Attenuation of innate immunity by cytomegalovirus IL-10 establishes a long-term deficit of adaptive antiviral immunity. *Proc Natl Acad Sci USA.* (2010) 107:22647–52. doi: 10.1073/pnas.1013794108
124. Clement M, Marsden M, Stacey MA, Abdul-Karim J, Brias SG, Bento DC, et al. Cytomegalovirus-specific IL-10-producing CD4+ T cells are governed by type-I IFN-induced IL-27 and promote virus persistence. *PLoS Pathog.* (2016) 12:e1006050. doi: 10.1371/journal.ppat.1006050
125. Oakley OR, Garvy BA, Humphreys S, Qureshi MH, Pomeroy C. Increased weight loss with reduced viral replication in interleukin-10 knock-out mice infected with murine cytomegalovirus. *Clin Exp Immunol.* (2008) 151:155–64. doi: 10.1111/j.1365-2249.2007.03533.x
126. Tang-Feldman YJ, Lochhead GR, Lochhead SR, Yu C, Pomeroy C. Interleukin-10 repletion suppresses pro-inflammatory cytokines and decreases liver pathology without altering viral replication in murine cytomegalovirus (MCMV)-infected IL-10 knockout mice. *Inflammation Res.* (2011) 60:233–43. doi: 10.1007/s00011-010-0259-4
127. Humphreys IR, De Trez C, Kinkade A, Benedict CA, Croft M, Ware CF. Cytomegalovirus exploits IL-10–mediated immune regulation in the salivary glands. *J Exp Med.* (2007) 204:1217–25. doi: 10.1084/jem.20062424
128. Michelson S, Alcami J, Kim S, Danielpour D, Bachelerie F, Picard L, et al. Human cytomegalovirus infection induces transcription and secretion of transforming growth factor beta 1. *J Virol.* (1994) 68:5730–7. doi: 10.1128/JVI.68.9.5730-5737.1994
129. Haagmans B, Teerds K, van den Eijnden-van Raaij A, Horzinek M, Schijns V. Transforming growth factor beta production during rat cytomegalovirus infection. *J Gen Virol.* (1997) 78:205–13. doi: 10.1099/0022-1317-78-1-205
130. Cičin-Šain L, Podlech J, Messerle M, Reddehase MJ, Koszinowski UH. Frequent coinfection of cells explains functional *in vivo* complementation between cytomegalovirus variants in the multiply infected host. *J Virol.* (2005) 79:9492–502. doi: 10.1128/JVI.79.15.9492-9502.2005
131. Cicin-Sain L, Ruzsics Z, Podlech J, Bubic I, Menard C, Jonjic S, et al. Dominant-negative FADD rescues the *in vivo* fitness of a cytomegalovirus lacking an antiapoptotic viral gene. *J Virol.* (2008) 82:2056–64. doi: 10.1128/JVI.01803-07
132. Skaletskaya A, Bartle LM, Chittenden T, McCormick AL, Mocarski ES, Goldmacher VS. A cytomegalovirus-encoded inhibitor of apoptosis that suppresses caspase-8 activation. *Proc Natl Acad Sci USA.* (2001) 98:7829–34. doi: 10.1073/pnas.141108798
133. Farrell HE, Bruce K, Lawler C, Stevenson PG. Murine cytomegalovirus spread depends on the infected myeloid cell type. *J Virol.* (2019) 93:e00540-19. doi: 10.1128/JVI.00540-19
134. Farrell HE, Bruce K, Lawler C, Oliveira M, Cardin R, Davis-Poynter N, et al. Murine cytomegalovirus spreads by dendritic cell recirculation. *mBio.* (2017) 8:e01264-17. doi: 10.1128/mBio.01264-17
135. McCormick AL, Roback L, Livingston-Rosanoff D, Clair CS. The human cytomegalovirus UL36 gene controls caspase-dependent and-independent cell death programs activated by infection of monocytes differentiating to macrophages. *J Virol.* (2010) 84:5108–23. doi: 10.1128/JVI.01345-09
136. Farrell HE, Davis-Poynter N, Bruce K, Lawler C, Dolken L, Mach M, et al. Lymph node macrophages restrict murine cytomegalovirus dissemination. *J Virol.* (2015) 89:7147–58. doi: 10.1128/JVI.00480-15
137. Kollmann TR, Crabtree J, Rein-Weston A, Blimkie D, Thommai F, Wang XY, et al. Neonatal innate TLR-mediated responses are distinct from those of adults. *J Immunol.* (2009) 183:7150–60. doi: 10.4049/jimmunol.0901481
138. Prendergast AJ, Klenerman P, Goulder PJ. The impact of differential antiviral immunity in children and adults. *Nat Rev Immunol.* (2012) 12:636-48. doi: 10.1038/nri3277

139. Westphalen K, Gusarova GA, Islam MN, Subramanian M, Cohen TS, Prince AS, et al. Sessile alveolar macrophages communicate with alveolar epithelium to modulate immunity. *Nature*. (2014) 506:503–6. doi: 10.1038/nature12902
140. Guilliams M, De Kleer I, Henri S, Post S, Vanhoutte L, De Prijck S, et al. Alveolar macrophages develop from fetal monocytes that differentiate into long-lived cells in the first week of life via GM-CSF. *J Exp Med*. (2013) 210:1977–92. doi: 10.1084/jem.20131199
141. Soroosh P, Doherty TA, Duan W, Mehta AK, Choi H, Adams YF, et al. Lung-resident tissue macrophages generate Foxp3+ regulatory T cells and promote airway tolerance. *J Exp Med*. (2013) 210:775–88. doi: 10.1084/jem.20121849
142. Holt PG, Oliver J, Bilyk N, McMenamin C, McMenamin PG, Kraal G, et al. Downregulation of the antigen presenting cell function(s) of pulmonary dendritic cells *in vivo* by resident alveolar macrophages. *J Exp Med*. (1993) 177:397–407. doi: 10.1084/jem.177.2.397
143. Watanabe Y, Hashimoto Y, Shiratsuchi A, Takizawa T, Nakanishi Y. Augmentation of fatality of influenza in mice by inhibition of phagocytosis. *Biochem Biophys Res Commun*. (2005) 337:881–6. doi: 10.1016/j.bbrc.2005.09.133
144. Misharin AV, Morales-Nebreda L, Mutlu GM, Budinger GR, Perlman H. Flow cytometric analysis of macrophages and dendritic cell subsets in the mouse lung. *Am J Respir Cell Mol Biol*. (2013) 49:503–10. doi: 10.1165/rcmb.2013-0086MA
145. Gibbings SL, Thomas SM, Atif SM, McCubbrey AL, Desch AN, Danhorn T, et al. Three unique interstitial macrophages in the murine lung at steady state. *Am J Respir Cell Mol Biol*. (2017) 57:66–76. doi: 10.1165/rcmb.2016-0361OC
146. Schyns J, Bai Q. Non-classical tissue monocytes and two functionally distinct populations of interstitial macrophages populate the mouse lung. *Nat Commun*. (2019) 10:3964. doi: 10.1038/s41467-019-11843-0
147. Chakarov S, Lim HY. Two distinct interstitial macrophage populations coexist across tissues in specific subtissular niches. *Science*. (2019) 363:eaau0964. doi: 10.1126/science.aau0964
148. Bedoret D, Wallemacq H, Marichal T, Desmet C, Quesada Calvo F, Henry E, et al. Lung interstitial macrophages alter dendritic cell functions to prevent airway allergy in mice. *J Clin Investig*. (2009) 119:3723–38. doi: 10.1172/JCI39717
149. Kawano H, Kayama H, Nakama T, Hashimoto T, Umemoto E, Takeda K. IL-10-producing lung interstitial macrophages prevent neutrophilic asthma. *Int Immunol*. (2016) 28:489–501. doi: 10.1093/intimm/dxw012
150. Shouval DS, Biswas A, Goettel JA, McCann K, Conaway E, Redhu NS, et al. Interleukin-10 receptor signaling in innate immune cells regulates mucosal immune tolerance and anti-inflammatory macrophage function. *Immunity*. (2014) 40:706–19. doi: 10.1016/j.immuni.2014.03.011
151. Kayama H, Ueda Y, Sawa Y, Jeon SG, Ma JS, Okumura R, et al. Intestinal CX3C chemokine receptor 1high (CX3CR1high) myeloid cells prevent T-cell-dependent colitis. *Proc Natl Acad Sci USA*. (2012) 109:5010–5. doi: 10.1073/pnas.1114931109
152. Kolter J, Kierdorf K, Henneke P. Origin and differentiation of nerve-associated macrophages. *J Immunol*. (2020) 204:271–9. doi: 10.4049/jimmunol.1901077
153. Prinz M, Erny D, Hagemeyer N. Ontogeny and homeostasis of CNS myeloid cells. *Nat Immunol*. (2017) 18:385-92. doi: 10.1038/ni.3703
154. Kierdorf K, Masuda T. Macrophages at CNS interfaces: ontogeny and function in health and disease. *Nat Rev Neurosci*. (2019) 20:547–62. doi: 10.1038/s41583-019-0201-x
155. Goldmann T, Wieghofer P, Jordão MJC, Prutek F, Hagemeyer N, Frenzel K, et al. Origin, fate and dynamics of macrophages at central nervous system interfaces. *Nat Immunol*. (2016) 17:797–805. doi: 10.1038/ni.3423
156. Mrdjen D, Pavlovic A, Hartmann FJ, Schreiner B, Utz SG, Leung BP, et al. High-dimensional single-cell mapping of Central nervous system immune cells reveals distinct myeloid subsets in health, aging, and disease. *Immunity*. (2018) 48:380–95.e6. doi: 10.1016/j.immuni.2018.01.011
157. Schneider C, Nobs SP, Heer AK, Kurrer M, Klinke G, van Rooijen N, et al. Alveolar macrophages are essential for protection from respiratory failure and associated morbidity following influenza virus infection. *PLoS Pathog*. (2014) 10:e1004053. doi: 10.1371/journal.ppat.1004053
158. Schridde A, Bain CC, Mayer JU, Montgomery J, Pollet E, Denecke B, et al. Tissue-specific differentiation of colonic macrophages requires TGFbeta receptor-mediated signaling. *Mucosal Immunol*. (2017) 10:1387–99. doi: 10.1038/mi.2016.142
159. Hadis U, Wahl B, Schulz O, Hardtke-Wolenski M, Schippers A, Wagner N, et al. Intestinal tolerance requires gut homing and expansion of FoxP3+ regulatory T cells in the lamina propria. *Immunity*. (2011) 34:237–46. doi: 10.1016/j.immuni.2011.01.016
160. Murai M, Turovskaya O, Kim G, Madan R, Karp CL, Cheroutre H, et al. Interleukin 10 acts on regulatory T cells to maintain expression of the transcription factor Foxp3 and suppressive function in mice with colitis. *Nat Immunol*. (2009) 10:1178–84. doi: 10.1038/ni.1791
161. Munger JS, Huang X, Kawakatsu H, Griffiths MJ, Dalton SL, Wu J, et al. The integrin alpha v beta 6 binds and activates latent TGF beta 1: a mechanism for regulating pulmonary inflammation and fibrosis. *Cell*. (1999) 96:319–28. doi: 10.1016/S0092-8674(00)80545-0
162. Lloyd CM, Hawrylowicz CM. Regulatory T cells in asthma. *Immunity*. (2009) 31:438–49. doi: 10.1016/j.immuni.2009.08.007
163. Farrell HE, Lawler C, Oliveira MT, Davis-Poynter N, Stevenson PG. Alveolar macrophages are a prominent but nonessential target for murine cytomegalovirus infecting the lungs. *J Virol*. (2015) 90:2756–66. doi: 10.1128/JVI.02856-15
164. Jakubzick C, Gautier EL, Gibbings SL, Sojka DK, Schlitzer A, Johnson TE, et al. Minimal differentiation of classical monocytes as they survey steady-state tissues and transport antigen to lymph nodes. *Immunity*. (2013) 39:599–610. doi: 10.1016/j.immuni.2013.08.007
165. Polić B, Hengel H, Krmpotić A, Trgovcich J, Pavić I, Lučin P, et al. Hierarchical and redundant lymphocyte subset control precludes cytomegalovirus replication during latent infection. *J Exp Med*. (1998) 188:1047–54. doi: 10.1084/jem.188.6.1047
166. Taylor-Wiedeman J, Sissons JG, Borysiewicz LK, Sinclair JH. Monocytes are a major site of persistence of human cytomegalovirus in peripheral blood mononuclear cells. *J Gen Virol*. (1991) 72:2059–64. doi: 10.1099/0022-1317-72-9-2059
167. Smith MS, Bentz GL, Alexander JS, Yurochko AD. Human cytomegalovirus induces monocyte differentiation and migration as a strategy for dissemination and persistence. *J Virology*. (2004) 78:4444–53. doi: 10.1128/JVI.78.9.4444-4453.2004
168. Chan G, Nogalski MT, Yurochko AD. Human cytomegalovirus stimulates monocyte-to-macrophage differentiation via the temporal regulation of caspase 3. *J Virol*. (2012) 86:10714–23. doi: 10.1128/JVI.07129-11
169. Noriega VM, Haye KK, Kraus TA, Kowalsky SR, Ge Y, Moran TM, et al. Human cytomegalovirus modulates monocyte-mediated innate immune responses during short-term experimental latency *in vitro*. *J Virol*. (2014) 88:9391–405. doi: 10.1128/JVI.00934-14
170. Lee SH, Starkey PM, Gordon S. Quantitative analysis of total macrophage content in adult mouse tissues. Immunochemical studies with monoclonal antibody F4/80. *J Exp Med*. (1985) 161:475–89. doi: 10.1084/jem.161.3.475
171. Cerovic V, Bain CC, Mowat AM, Milling SW. Intestinal macrophages and dendritic cells: what's the difference? *Trends Immunol*. (2014) 35:270–7. doi: 10.1016/j.it.2014.04.003
172. Hirotani T, Lee PY, Kuwata H, Yamamoto M, Matsumoto M, Kawase I, et al. The nuclear IkappaB protein IkappaBNS selectively inhibits lipopolysaccharide-induced IL-6 production in macrophages of the colonic lamina propria. *J Immunol*. (2005) 174:3650–7. doi: 10.4049/jimmunol.174.6.3650
173. Maheshwari A, Kelly DR, Nicola T, Ambalavanan N, Jain SK, Murphy-Ullrich J, et al. TGF-beta2 suppresses macrophage cytokine production and mucosal inflammatory responses in the developing intestine. *Gastroenterology*. (2011) 140:242–53. doi: 10.1053/j.gastro.2010.09.043
174. Zigmond E, Varol C, Farache J, Elmaliah E, Satpathy AT, Friedlander G, et al. Ly6C hi monocytes in the inflamed colon give rise to proinflammatory effector cells and migratory antigen-presenting cells. *Immunity*. (2012) 37:1076–90. doi: 10.1016/j.immuni.2012.08.026

175. Grainger JR, Wohlfert EA, Fuss IJ, Bouladoux N, Askenase MH, Legrand F, et al. Inflammatory monocytes regulate pathologic responses to commensals during acute gastrointestinal infection. *Nat Med.* (2013) 19:713–21. doi: 10.1038/nm.3189
176. Wu CA, Paveglio SA, Lingenheld EG, Zhu L, Lefrancois L, Puddington L. Transmission of murine cytomegalovirus in breast milk: a model of natural infection in neonates. *J Virol.* (2011) 85:5115–24. doi: 10.1128/JVI.01934-10
177. Geissmann F, Jung S, Littman DR. Blood monocytes consist of two principal subsets with distinct migratory properties. *Immunity.* (2003) 19:71–82. doi: 10.1016/S1074-7613(03)00174-2
178. Dennis EA, Smythies LE, Grabski R, Li M, Ballestas ME, Shimamura M, et al. Cytomegalovirus promotes intestinal macrophage-mediated mucosal inflammation through induction of Smad7. *Mucosal Immunol.* (2018) 11:1694–704. doi: 10.1038/s41385-018-0041-4
179. Kolter J, Henneke P. Codevelopment of microbiota and innate immunity and the risk for group B streptococcal disease. *Front Immunol.* (2017) 8:1497. doi: 10.3389/fimmu.2017.01497
180. Ginhoux F, Greter M, Leboeuf M, Nandi S, See P, Gokhan S, et al. Fate mapping analysis reveals that adult microglia derive from primitive macrophages. *Science.* (2010) 330:841–5. doi: 10.1126/science.1194637
181. Mildner A, Schmidt H, Nitsche M, Merkler D, Hanisch U-K, Mack M, et al. Microglia in the adult brain arise from Ly-6C hi CCR2+ monocytes only under defined host conditions. *Nat Neurosci.* (2007) 10:1544. doi: 10.1038/nn2015
182. Van Hove H, Martens L, Scheyltjens I, de Vlaminck K, Antunes ARP, de Prijck S, et al. A single-cell atlas of mouse brain macrophages reveals unique transcriptional identities shaped by ontogeny and tissue environment. *Nat Neurosci.* (2019) 22:1021–35. doi: 10.1038/s41593-019-0393-4
183. Cekinovic D, Golemac M, Pugel EP, Tomac J, Cicin-Sain L, Slavuljica I, et al. Passive immunization reduces murine cytomegalovirus-induced brain pathology in newborn mice. *J Virol.* (2008) 82:12172–80. doi: 10.1128/JVI.01214-08
184. Koontz T, Bralic M, Tomac J, Pernjak-Pugel E, Bantug G, Jonjic S, et al. Altered development of the brain after focal herpesvirus infection of the central nervous system. *J Exp Med.* (2008) 205:423–35. doi: 10.1084/jem.20071489
185. Renard T, Daumas-Duport B, Auffray-Calvier E, Bourcier R, Desal H. Cytomegalovirus encephalitis: undescribed diffusion-weighted imaging characteristics. Original aspects of cases extracted from a retrospective study, and from literature review. *J Neuroradiol.* (2016) 43:371–7. doi: 10.1016/j.neurad.2016.03.004
186. Kosugi I, Kawasaki H, Arai Y, Tsutsui Y. Innate immune responses to cytomegalovirus infection in the developing mouse brain and their evasion by virus-infected neurons. *Am J Pathol.* (2002) 161:919–28. doi: 10.1016/S0002-9440(10)64252-6
187. Kosmac K, Bantug GR, Pugel EP, Cekinovic D, Jonjic S, Britt WJ. Glucocorticoid treatment of MCMV infected newborn mice attenuates CNS inflammation and limits deficits in cerebellar development. *PLoS Pathog.* (2013) 9:e1003200. doi: 10.1371/journal.ppat.1003200
188. Pulliam L. Cytomegalovirus preferentially infects a monocyte derived macrophage/microglial cell in human brain cultures: neuropathology differs between strains. *J Neuropathol Exp Neurol.* (1991) 50:432–40. doi: 10.1097/00005072-199107000-00004
189. Seleme MC, Kosmac K, Jonjic S, Britt WJ. TNFalpha induced recruitment of inflammatory mononuclear cells leads to inflammation and altered brain development in MCMV infected newborn mice. *J Virol.* (2017) 91:JVI.01983-16. doi: 10.1128/JVI.01983-16
190. Bentz GL, Jarquin-Pardo M, Chan G, Smith MS, Sinzger C, Yurochko AD. Human cytomegalovirus (HCMV) infection of endothelial cells promotes naive monocyte extravasation and transfer of productive virus to enhance hematogenous dissemination of HCMV. *J Virol.* (2006) 80:11539–55. doi: 10.1128/JVI.01016-06
191. Djukic M, Mildner A, Schmidt H, Czesnik D, Brück W, Priller J, et al. Circulating monocytes engraft in the brain, differentiate into microglia and contribute to the pathology following meningitis in mice. *Brain.* (2006) 129:2394–403. doi: 10.1093/brain/awl206
192. Gres V, Kolter J, Erny D, Henneke P. The role of CNS macrophages in streptococcal meningoencephalitis. *J Leukoc Biol.* (2019) 106:209–18. doi: 10.1002/JLB.4MR1118-419R
193. Jordao MJC, Sankowski R. Single-cell profiling identifies myeloid cell subsets with distinct fates during neuroinflammation. *Science.* (2019) 363:eaat7554. doi: 10.1126/science.aat7554
194. Wynn TA, Chawla A, Pollard JW. Macrophage biology in development, homeostasis and disease. *Nature.* (2013) 496:445–55. doi: 10.1038/nature12034
195. Foster SL, Hargreaves DC, Medzhitov R. Gene-specific control of inflammation by TLR-induced chromatin modifications. *Nature.* (2007) 447:972–8. doi: 10.1038/nature05836
196. Netea MG, Quintin J, van der Meer JW. Trained immunity: a memory for innate host defense. *Cell Host Microbe.* (2011) 9:355–61. doi: 10.1016/j.chom.2011.04.006
197. Netea MG, Domínguez-Andres J, Barreiro LB, Chavakis T, Divangahi M, Fuchs E, et al. Defining trained immunity and its role in health and disease. *Nat Rev Immunol.* (2020). doi: 10.1038/s41577-020-0285-6. [Epub ahead of print].
198. Quintin J, Saeed S, Martens JHA, Giamarellos-Bourboulis EJ, Ifrim DC, Logie C, et al. Candida albicans infection affords protection against reinfection via functional reprogramming of monocytes. *Cell Host Microbe.* (2012) 12:223–32. doi: 10.1016/j.chom.2012.06.006
199. Saeed S, Quintin J, Kerstens HH, Rao NA, Aghajanirefah A, Matarese F, et al. Epigenetic programming of monocyte-to-macrophage differentiation and trained innate immunity. *Science.* (2014) 345:1251086. doi: 10.1126/science.1251086
200. Machiels B, Dourcy M, Xiao X, Javaux J, Mesnil C, Sabatel C, et al. A gammaherpesvirus provides protection against allergic asthma by inducing the replacement of resident alveolar macrophages with regulatory monocytes. *Nat Immunol.* (2017) 18:1310–20. doi: 10.1038/ni.3857
201. Barton ES, White DW, Cathelyn JS, Brett-McClellan KA, Engle M, Diamond MS, et al. Herpesvirus latency confers symbiotic protection from bacterial infection. *Nature.* (2007) 447:326–9. doi: 10.1038/nature05762
202. Kropp KA, Robertson KA, Sing G, Rodriguez-Martin S, Blanc M, Lacaze P, et al. Reversible inhibition of murine cytomegalovirus replication by gamma interferon (IFN-γ) in primary macrophages involves a primed type I IFN-signaling subnetwork for full establishment of an immediate-early antiviral state. *J Virol.* (2011) 85:10286–99. doi: 10.1128/JVI.00373-11
203. Dag F, Dolken L, Holzki J, Drabig A, Weingartner A, Schwerk J, et al. Reversible silencing of cytomegalovirus genomes by type I interferon governs virus latency. *PLoS Pathog.* (2014) 10:e1003962. doi: 10.1371/journal.ppat.1003962
204. Waldman WJ, Knight DA, Huang EH, Sedmak DD. Bidirectional transmission of infectious cytomegalovirus between monocytes and vascular endothelial cells: an *in vitro* model. *J Infect Dis.* (1995) 171:263–72. doi: 10.1093/infdis/171.2.263
205. Mendelson M, Monard S, Sissons P, Sinclair J. Detection of endogenous human cytomegalovirus in CD34+ bone marrow progenitors. *J Gen Virol.* (1996) 77:3099–102. doi: 10.1099/0022-1317-77-12-3099
206. von Laer D, Meyer-Koenig U, Serr A, Finke J, Kanz L, Fauser AA, et al. Detection of cytomegalovirus DNA in CD34+ cells from blood and bone marrow. *Blood.* (1995). 86:4086-90. doi: 10.1182/blood.V86.11.4086
207. Taylor-Wiedeman J, Sissons P, Sinclair J. Induction of endogenous human cytomegalovirus gene expression after differentiation of monocytes from healthy carriers. *J Virol.* (1994) 68:1597–604. doi: 10.1128/JVI.68.3.1597-1604.1994
208. Sindre H, Tjoonnfjord G, Rollag H, Ranneberg-Nilsen T, Veiby OP, Beck S, et al. Human cytomegalovirus suppression of and latency in early hematopoietic progenitor cells. *Blood.* (1996) 88:4526–33. doi: 10.1182/blood.V88.12.4526.bloodjournal88124526
209. Kondo K, Kaneshima H, Mocarski ES. Human cytomegalovirus latent infection of granulocyte-macrophage progenitors. *Proc Natl Acad Sci USA.* (1994) 91:11879–83. doi: 10.1073/pnas.91.25.11879
210. Slobedman B, Mocarski ES. Quantitative analysis of latent human cytomegalovirus. *J Virol.* (1999) 73:4806–12. doi: 10.1128/JVI.73.6.4806-4812.1999

211. Shnayder M, Nachshon A, Rozman B, Bernshtein B, Lavi M, Fein N, et al. Single cell analysis reveals human cytomegalovirus drives latently infected cells towards an anergic-like monocyte state. *eLife*. (2020) 9:e52168. doi: 10.7554/eLife.52168.sa2
212. Cheng S, Caviness K, Buehler J, Smithey M, Nikolich-Žugich J, Goodrum F. Transcriptome-wide characterization of human cytomegalovirus in natural infection and experimental latency. *Proc Natl Acad Sci USA*. (2017) 114:E10586–95. doi: 10.1073/pnas.1710522114
213. Humby MS, O'Connor CM. Human cytomegalovirus US28 is important for latent infection of hematopoietic progenitor cells. *J Virol*. (2016) 90:2959–70. doi: 10.1128/JVI.02507-15
214. Petrucelli A, Rak M, Grainger L, Goodrum F. Characterization of a novel Golgi apparatus-localized latency determinant encoded by human cytomegalovirus. *J Virol*. (2009) 83:5615–29. doi: 10.1128/JVI.01989-08
215. Weekes MP, Tan SY, Poole E, Talbot S, Antrobus R, Smith DL, et al. Latency-associated degradation of the MRP1 drug transporter during latent human cytomegalovirus infection. *Science*. (2013) 340:199–202. doi: 10.1126/science.1235047
216. Crawford LB, Kim JH, Collins-McMillen D, Lee B-J, Landais I, Held C, et al. Human cytomegalovirus encodes a novel FLT3 receptor ligand necessary for hematopoietic cell differentiation and viral reactivation. *mBio*. (2018) 9:e00682–18. doi: 10.1128/mBio.00682-18
217. Avdic S, Cao JZ, Cheung AK, Abendroth A, Slobedman B. Viral interleukin-10 expressed by human cytomegalovirus during the latent phase of infection modulates latently infected myeloid cell differentiation. *J Virol*. (2011) 85:7465–71. doi: 10.1128/JVI.00088-11
218. Mildner A, Schonheit J, Giladi A, David E, Lara-Astiaso D, Lorenzo-Vivas E, et al. Genomic characterization of murine monocytes reveals C/EBPbeta transcription factor dependence of Ly6C- cells. *Immunity*. (2017) 46:849–62.e7. doi: 10.1016/j.immuni.2017.04.018
219. Patel AA, Zhang Y. The fate and lifespan of human monocyte subsets in steady state and systemic inflammation. *J Exp Med*. (2017) 214:1913–23. doi: 10.1084/jem.20170355
220. Yona S, Kim KW, Wolf Y, Mildner A, Varol D, Breker M, et al. Fate mapping reveals origins and dynamics of monocytes and tissue macrophages under homeostasis. *Immunity*. (2013) 38:79–91. doi: 10.1016/j.immuni.2013.05.008
221. Seckert CK, Renzaho A, Tervo HM, Krause C, Deegen P, Kuhnapfel B, et al. Liver sinusoidal endothelial cells are a site of murine cytomegalovirus latency and reactivation. *J Virol*. (2009) 83:8869–84. doi: 10.1128/JVI.00870-09
222. Fish KN, Soderberg-Naucler C, Mills LK, Stenglein S, Nelson JA. Human cytomegalovirus persistently infects aortic endothelial cells. *J Virol*. (1998) 72:5661–8. doi: 10.1128/JVI.72.7.5661-5668.1998
223. Soderberg-Naucler C, Streblow DN, Fish KN, Allan-Yorke J, Smith PP, Nelson JA. Reactivation of latent human cytomegalovirus in CD14(+) monocytes is differentiation dependent. *J Virol*. (2001) 75:7543–54. doi: 10.1128/JVI.75.16.7543-7554.2001
224. Soderberg-Naucler C, Fish KN, Nelson JA. Reactivation of latent human cytomegalovirus by allogeneic stimulation of blood cells from healthy donors. *Cell*. (1997) 91:119–26. doi: 10.1016/S0092-8674(01)80014-3
225. Zhuravskaya T, Maciejewski JP, Netski DM, Bruening E, Mackintosh FR, St Jeor S. Spread of human cytomegalovirus (HCMV) after infection of human hematopoietic progenitor cells: model of HCMV latency. *Blood*. (1997) 90:2482–91. doi: 10.1182/blood.V90.6.2482
226. Dorsch-Hasler K, Keil GM, Weber F, Jasin M, Schaffner W, Koszinowski UH. A long and complex enhancer activates transcription of the gene coding for the highly abundant immediate early mRNA in murine cytomegalovirus. *Proc Natl Acad Sci USA*. (1985) 82:8325–9. doi: 10.1073/pnas.82.24.8325
227. Riddell SR. Pathogenesis of cytomegalovirus pneumonia in immunocompromised hosts. *Semin Respir Infect*. (1995) 10:199–208.
228. Goodgame RW. Gastrointestinal cytomegalovirus disease. *Ann Int Med*. (1993) 119:924–35. doi: 10.7326/0003-4819-119-9-199311010-00010
229. Lee JY. Cytomegalovirus infection involving the skin in immunocompromised hosts: a clinicopathologic study. *Am J Clin Pathol*. (1989) 92:96–100. doi: 10.1093/ajcp/92.1.96
230. Smyth RL, Scott JP, Borysiewicz LK, Sharples LD, Stewart S, Wreghitt TG, et al. Cytomegalovirus infection in heart-lung transplant recipients: risk factors, clinical associations, and response to treatment. *J Infect Dis*. (1991) 164:1045–50. doi: 10.1093/infdis/164.6.1045
231. Dunn HS, Haney DJ, Ghanekar SA, Stepick-Biek P, Lewis DB, Maecker HT. Dynamics of CD4 and CD8 T cell responses to cytomegalovirus in healthy human donors. *J Infect Dis*. (2002) 186:15–22. doi: 10.1086/341079
232. Pollock JL, Presti RM, Paetzold S, Virgin HWt. Latent murine cytomegalovirus infection in macrophages. *Virology*. (1997) 227:168–79. doi: 10.1006/viro.1996.8303
233. Koffron AJ, Hummel M, Patterson BK, Yan S, Kaufman DB, Fryer JP, et al. Cellular localization of latent murine cytomegalovirus. *J Virol*. (1998) 72:95–103. doi: 10.1128/JVI.72.1.95-103.1998
234. Rusinova I, Forster S, Yu S, Kannan A, Masse M, Cumming H, et al. Interferome v2. 0: an updated database of annotated interferon-regulated genes. *Nucleic Acids Res*. (2012) 41:D1040–6. doi: 10.1093/nar/gks1215
235. Hengel H, Koszinowski UH, Conzelmann K-K. Viruses know it all: new insights into IFN networks. *Trends Immunol*. (2005) 26:396–401. doi: 10.1016/j.it.2005.05.004
236. Klenerman P, Oxenius A. T cell responses to cytomegalovirus. *Nat Rev Immunol*. (2016) 16:367–77. doi: 10.1038/nri.2016.38

Conflict of Interest: The authors declare that the research was conducted in the absence of any commercial or financial relationships that could be construed as a potential conflict of interest.

frontiers in Immunology

REVIEW
published: 15 May 2020
doi: 10.3389/fimmu.2020.00899

Dysregulated Mucosal Immunity and Associated Pathogeneses in Preterm Neonates

*Maame Efua S. Sampah and David J. Hackam**

Division of Pediatric Surgery, Department of Surgery, Johns Hopkins University School of Medicine, Baltimore, MD, United States

Many functions of the immune system are impaired in neonates, allowing vulnerability to serious bacterial, viral and fungal infections which would otherwise not be pathogenic to mature individuals. This vulnerability is exacerbated in compromised newborns such as premature neonates and those who have undergone surgery or who require care in an intensive care unit. Higher susceptibility of preterm neonates to infections is associated with delayed immune system maturation, with deficiencies present in both the innate and adaptive immune components. Here, we review recent insights into early life immunity, and highlight features associated with compromised newborns, given the challenges of studying neonatal immunity in compromised neonates due to the transient nature of this period of life, and logistical and ethical obstacles posed by undertaking studies newborns and infants. Finally, we highlight how the unique immunological characteristics of the premature host play key roles in the pathogenesis of diseases that are unique to this population, including necrotizing enterocolitis and the associated sequalae of lung and brain injury.

Keywords: necrotizing enterocolitis, toll like receptors, sepsis, intestinal epithelial barrier, lymphocytes, regulatory lymphocytes, neonatal immunity

OPEN ACCESS

Edited by:
Duc Ninh Nguyen, University of Copenhagen, Denmark

Reviewed by:
Stine Brandt Bering, University of Copenhagen, Denmark
Simon Eaton, University College London, United Kingdom
Douglas G. Burrin, Baylor College of Medicine, United States

****Correspondence:***
David J. Hackam
dhackam1@jhmi.edu

Specialty section:
This article was submitted to Mucosal Immunity, a section of the journal Frontiers in Immunology

Received: *05 February 2020*
Accepted: *17 April 2020*
Published: *15 May 2020*

Citation:
Sampah MES and Hackam DJ (2020) Dysregulated Mucosal Immunity and Associated Pathogeneses in Preterm Neonates. Front. Immunol. 11:899. doi: 10.3389/fimmu.2020.00899

INTRODUCTION

Early maturation of the immune system is a complex process that involves molecular, cellular and epigenetic programs. While *in utero*, the fetal immune system has traditionally been thought to exist in a sterile environment with no antigenic exposure (1) with a need for modulation to allow coexistence with the mother's immune system. However, a growing body of evidence suggests that the intrauterine environment may not be entirely sterile, as previously thought, and that the formation of a neonatal microbiome may originate *in utero* (2–4). Bacterial DNA has been found in the human placenta as well as amniotic fluid (5, 6), suggesting a unique placental microbiome that might impact the immunity of the fetus. While this area is still under active study, there is no question that the neonate becomes quickly exposed to a storm of pathogens immediately following birth. Importantly, the infant is inoculated with varying species of commensal microbiota as he or she passes through the birth canal. These initially include facultative aerobes such as *Escherichia* and *Enterococcus*, and subsequently obligate anaerobes, including Firmicutes such as *Clostridia*, Bacteroidetes, and especially *Bifidobacteria*

(7). Evolution and variations in this commensal population play a critical role in shaping immunity and allergy, food digestion as well as brain and other bodily functions. Thus, the immune system must be appropriately primed to fight potential infections, while also modulating itself to allow for beneficial microbial colonization and to avoid potentially harmful inflammation and autoimmunity.

Initially, the innate immune system is mainly responsible for surveillance in the neonate, involving cellular players which include phagocytes, natural killer (NK) cells, antigen-presenting cells (APCs), humoral mediators of inflammation, and complement. This surveillance occurs while the components of the acquired immune system mature and gain antigenic experience. The importance of breastfeeding is evident, as breastfed infants are able to receive antibodies and antimicrobial components in breast milk that help prevent certain acute infections (8, 9).

While the relevance of environmental factors such as pathogens, commensals, and the maternal-fetal interface to development of the early immune system is clear, it is important to note that regulation of the immune response to microbial and environmental cues takes place at the genetic level. A large number of transcription factors control critical aspects of immunity such as hematopoietic cell differentiation, determination of myeloid and lymphoid cell fates, immune cell activation, expression of antimicrobial proteins and cytokines, expression of cell surface receptors, and the establishment of memory, to name a few. These transcriptional networks are well-characterized and involve factors such as GATA3, Tbet, Bcl6, NFκB, STATs, IRFs, and AP-1. Overall, a multifactorial mechanism prevails where both genes and environmental factors interact in shaping the immune system. Furthermore, it is now well-understood that post-transcriptional mechanisms regulating transcription factor activity, nuclear architecture, and epigenetic mechanisms are crucial in the development and differentiation of immune system and related pathologies. These mechanisms include DNA and histone protein methylation, acetylation and other modifications, nucleosome remodeling, as well as the formation of higher-order chromatin structures (10). The consequences of these transcriptional, post-transcriptional and epigenetic programs can be short-term or have lifelong implications.

Given the above, this review aims to examine immune system dysfunction in compromised newborns and the related increased risk of complications such as necrotizing enterocolitis. Data from studies investigating components of both the innate and adaptive immune systems will be presented, as well as the effect of the immature immune system on the risk of infections such as necrotizing enterocolitis.

INNATE IMMUNITY

Innate protective mechanisms against pathogens are provided by the skin, respiratory and gastrointestinal epithelia, and other mucous membranes. These mechanisms are complemented by humoral factors, such as cytokines and complement components present in tissue fluids, blood, and secretions such as tears and saliva. These factors are present at birth and do not require gene rearrangements. The functions of innate immunity need to be both rapid (to prevent spread of the infection) and broad (enabling protection against multiple diverse pathogens at the same time). Soluble (e.g., complement and acute phase proteins) as well as cellular components contribute to this first level of defense. Important but often underappreciated determinants of immunity fall under this broad category, including immunosuppressive erythroid precursors, granulocyte/neutrophil function, and pattern recognition receptor (PRR)-based responses (see **Figure 1**).

Physical Epithelial Barriers, Associated Signaling, and the Microbiome

Neonatal skin is easily disrupted and lacks the advantage of a protective lipid layer and acidic pH until ∼1 month of postnatal age. This phenomenon is exacerbated in preterm infants, in whom it takes longer for these features to develop (11). The vernix caseosa, a naturally occurring biofilm that covers fetal skin, functions as a barrier against water loss, regulating temperature, and preventing microbial access. Development of the vernix caseosa begins in the third trimester, hence, it is often not fully developed in premature infants. It has also been shown that neonatal skin keratinocytes, and particularly the vernix, constitutively produce a broader array of antimicrobial peptides (AMPs) compared to older infants and adults (12) which provides an extra level of protection. AMPs generally include α-defensins and β-defensins and the cathelicidin LL-37, which have direct antimicrobial activity against gram-positive and gram-negative bacteria and some fungi, as well as the influenza virus, respiratory syncytial virus (RSV); and protozoa. These defensins and cathelicidins destroy pathogens by insertion into the membranes of a broad range of gram-positive and gram-negative bacteria, fungi, protozoa, spirochetes, and enveloped viruses (1). Once inside the microbial cell membrane, they form pores allowing the passage of anions through the membrane, thus depolarizing and killing the organism (13). The immaturity of premature skin is exacerbated by the iatrogenic insults inflicted as a part of lifesaving intensive care.

The neonatal skin epithelium is also rapidly colonized by a normal flora of commensal bacteria following birth that help to prevent colonization by pathogens (14, 15). Coagulase-negative staphylococci such as *Staphylococcus epidermidis*, micrococci, and other species constitute the majority of this flora, and have been shown play a protective role in the skin by secreting lipopeptides that bind to toll-like receptor 2 (TLR2) on neonatal keratinocytes and stimulating them to produce the AMPs hBD-2 and hBD-3. These features are not functional in preterm infants (16).

Like the skin epithelium, the epithelial surface of the neonatal stomach also lacks an acidic pH, which is thought to facilitate the establishment of commensal flora (14) mainly belonging to the phyla *Firmicutes* and *Proteobacteria* (17). AMP-producing Paneth cells are decreased in number in the small intestine of preterm and, to a lesser degree, term neonates, which may increase the risk of enterocolitis and invasion by pathogens. Some animal models have demonstrated more robust production of antimicrobial peptides by intestinal epithelial cells which

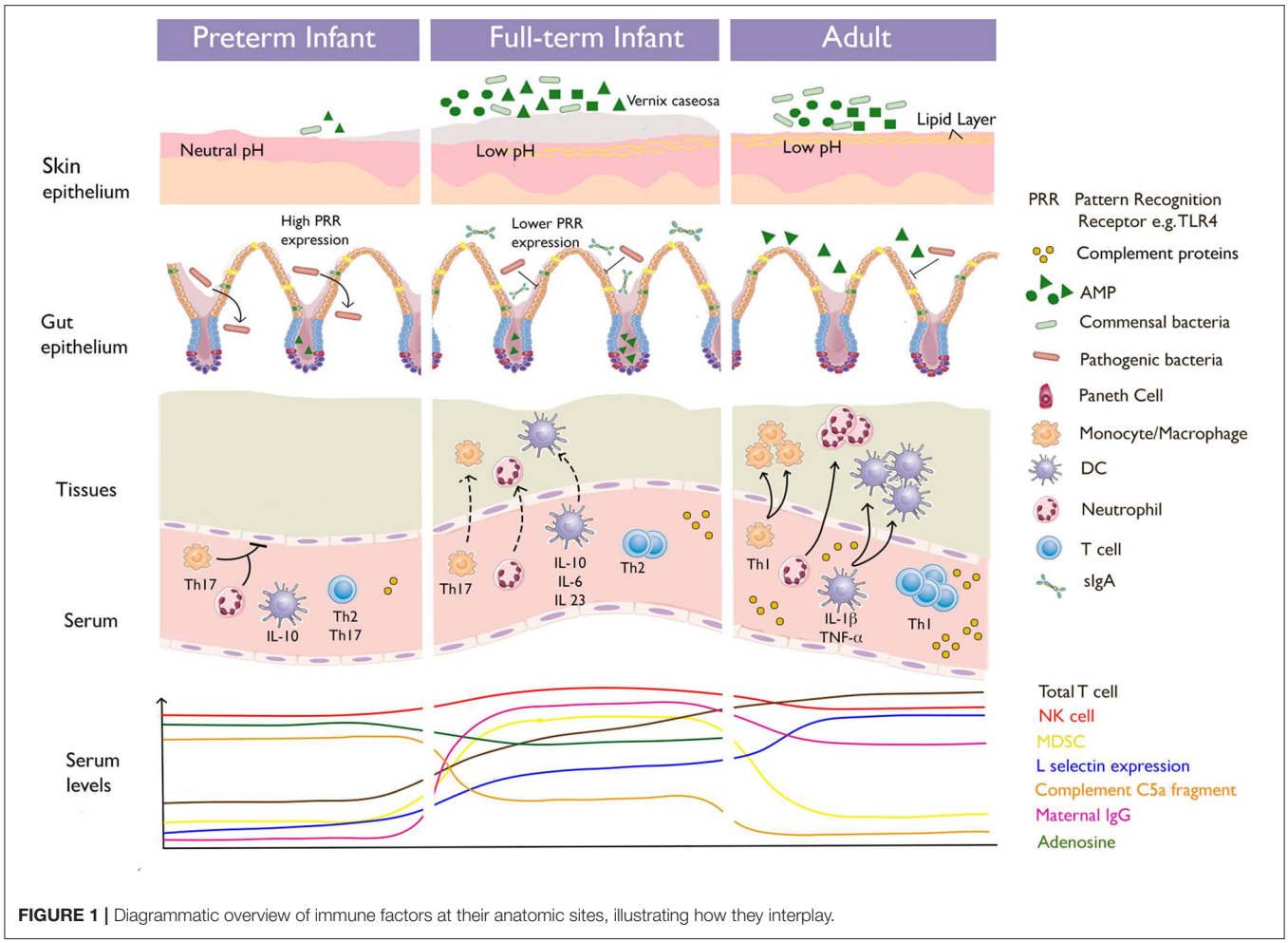

FIGURE 1 | Diagrammatic overview of immune factors at their anatomic sites, illustrating how they interplay.

may counteract this phenomenon, but this has been yet to be confirmed in humans *in vivo* (18).

In a full-term infant, enterocytes within the gut epithelium sample and identify antigens introduced into the intestinal lumen, signaling to intraepithelial lymphocytes via PRR (19–21) such as toll-like receptors (TLRs) and nucleotide-binding oligomerization domains (NODs). These receptors recognize antigens on pathogenic bacteria and elicit an immune response against infection.

It has been shown that higher levels of innate immune receptor expression in premature neonates compared to full-term controls lead to increased inflammation within the gut epithelium, leading to loss of epithelial integrity, and subsequent introduction of pathogens into circulation (22–24). This is often in the setting of an increased number of activating mutations in the signaling pathways associated with these receptors. For instance, TLR4 hyperactivation in premature mice and humans has been shown to lead to increased enterocyte apoptosis, reduced enterocyte proliferation and migration, and the eventual breakdown of the intestinal epithelium (25–28) that is a hallmark of necrotizing enterocolitis (NEC). Further, we have shown that TLR4 activation can reduce expression of endothelial nitric oxide synthase (eNOS) in the intestinal endothelium, causing decreased blood flow and ischemia that exacerbates the clinical course of NEC (29).

The gut epithelium, similar to the skin, houses cells that also produce defensins and cathelicidins. Intestinal epithelial cells (IECs) secrete β-defensins (hBD1, 2, and 3) (30–32) while Paneth cells secrete lysozyme, phospholipase A2, the AMPs, defensins (α and β), and cathelicidins (33, 34) in response to microbial or cholinergic stimuli. This creates a relative sterile and protected intestinal crypt environment. Microscopic and molecular analysis of tissue from non-viable fetuses and adults has demonstrated that Paneth cells are normally present by 12 weeks gestation, antimicrobial defensins at 13 weeks and lysozyme at 20 weeks (35–37). However, premature infants have been shown to have few Paneth cells with decreased antimicrobial producing function (36, 38).

Another parallel between skin and gut epithelium is the presence of commensal bacterial flora. The immune system is able to distinguish these microbes from harmful pathogens in part by limiting the location of innate immune receptors. For instance, in the full term gut, intestinal epithelial cells normally express few or no TLRs on their luminal surface

(22), where they are in contact with commensals. Pathogenic microbes that invade through the epithelial cell layer are however recognized by endosomal TLRs, cytosolic innate immune recognition receptors, and TLRs located on the basolateral surface of epithelial cells, triggering an inflammatory response. On the other hand, commensal bacteria are able to inhibit signaling and inflammatory mediator production downstream of these receptors or induce anti-inflammatory cytokine production, thereby actively suppressing gut inflammation. However, the underdeveloped preterm intestinal epithelium is highly permeable and more easily colonized by pathogenic bacteria because of reduced gastrointestinal motility as well as limited enteric nervous system function (39), all of which set the stage for destructive dysbiosis, chronic inflammation, and microbial translocation through the weakened intestinal barrier, leading to potentially lethal diseases of prematurity. Additionally, the premature intestinal epithelium expresses high levels of TLR4, which causes an overreaction by the host immune system to gut bacteria that leads to excessive inflammation (25, 40). The elevated TLR4 expression in the premature gut is explained by the non-immune role that we discovered for TLR4 in the regulation of gut development, through its activation of Notch and Wnt pathways (41–43). Thus, in the relatively sterile environment of the fetus, TLR4 serves a predominantly developmental role, while the premature infant, in which TLR4 expression remains persistently elevated, mounts an exaggerated inflammatory response to bacteria upon colonization of the intestine by microbes (44). This elevated inflammatory state leads to mucosal barrier breakdown, bacterial translocation and the development of NEC in the premature host (45). Based upon these findings, we have embarked upon a strategy of TLR4 inhibition for the prevention and treatment of NEC, and have discovered a novel class of TLR4 inhibitors to serve as potential therapies (46, 47). We also note that breast milk, which is a powerful material capable of reducing NEC, is rich in molecules that inhibit TLR4 signaling, explaining in part their mechanisms of action in achieving NEC protection (48).

The respiratory epithelium is also known to express TLRs and the AMPs, SP-A, and SP-D, which mature in the last trimester of fetal development (49). Preterm infants therefore may lack these defenses, which is exacerbated by reduced numbers of resident alveolar macrophages compared to term infants. NEC-induced lung injury is particularly severe as compared to the lung injury that develops in premature infants who do not develop NEC. We have shown that TLR4 expression on the lung epithelium is required for the recruitment of proinflammatory neutrophils into the lung through the upregulation of CCL25 (50, 51), and that strategies to either inhibit TLR4 via the administration of aerosolized inhibitors, or through genetic deletion, can serve as novel lung protective strategies in the setting of NEC (50).

Extracellular Components

In response to infection and inflammation, multiple mediators in the plasma are activated to fight pathogens. These mediators include the complement and kinin systems, mannose-binding lectin (MBL), fibronectin, coagulation factors, arachidonic acid metabolites, amines, and lysosomal enzymes. Many of these mechanisms are known to be impaired in the neonate, and more-so in compromised newborns.

Complement

The complement system, composed of three pathways for pathogen recognition, subsequent permeabilization, opsonization, and lysis of harmful microbes, also plays a significant role in priming the adaptive immune system. These include the classic, alternative, and the lectin pathways. Complement expression may vary in newborns secondary to common genetic variants as well as rare deficiencies. Fetal complement synthesis is detected as early as 6 weeks gestation, with gradual age-dependent maturation (52). Levels increase after birth and reach adult levels between 6 and 18 months of age (53). Serum complement activity is known to be decreased in term newborns compared with adults and further diminished in preterm infants. Levels of complement proteins in pre-terms, specifically C3 and C9 have been measured to be as low as 10% of adult levels, remaining low until up to 1 year of age (54). These components are known to be responsible for recognition of polysaccharide antigens and formation of the membrane attack complex in bacterial lysis, respectively. On the other hand, the complement activation product, C5a, a strong chemoattractant peptide and a mediator of mesenteric ischemia/reperfusion injury is found to be highly expressed in cases of NEC and is under study for its utility as a clinical marker for diagnosis of infants with NEC in combination with radiographical findings (55).

The Lectin Pathway

The lectin pathway of complement recognizes conserved carbohydrate moieties on pathogens, leading to opsonization and phagocytosis in an antibody independent manner, and making it an important pathway in neonates, who are relatively antibody deficient. This pathway is mainly activated by mannose-binding lectin (MBL) which serves as an opsonin for the ingestion of gram-negative and gram-positive bacteria by neutrophils and monocytes. Baseline polymorphisms are known to exist at the MBL locus, leading to reduced circulating MBL levels in approximately one-third of the population. However, levels of serum MBL have been measured to be about 70% that of adults in term infants and 5% that of adults in premature infants (56). Low MBL levels have been associated with pneumonia and sepsis in premature infants. Mannose-binding lectin (MBL) recognizes microorganisms and activates the complement system via MBL-associated serine protease-2 (MASP-2), which in a small case control study was found to be in higher concentrations in cord blood levels in premature infants predisposed to NEC and associated with a 3-fold increased risk to develop NEC (57). Given that extremely low MASP-2 concentrations was found in most premature neonates overall in the study, authors concluded that MASP-2 deficiency may represent a protective mechanism against excessive proinflammatory stimuli during the neonatal period.

Acute Phase Proteins

Acute phase proteins (APPs) are released by the liver, leukocytes, epithelial cells, and mucosal sites (58) in response to infection and trauma to resolve inflammation. Some of these APPs exhibit antimicrobial activities similar to antimicrobial peptides (AMP). APPs bind to pathogens and permeabilize their membranes. They are also capable of binding and neutralizing microbial toxins (59). Maturation of soluble APP is age-dependent, and preterm newborns have been found to be deficient (60), as is the case with levels of fibronectin, a glycoprotein that promotes neutrophil adherence to endothelium as part of their migration from blood to the tissues. This deficit likely results in reduced neutrophil function and increased susceptibility to bacterial infections, which is discussed further in the following section.

Cellular Components

The workhorses of the innate immune system are comprised of the cellular components that include granulocytes (particularly neutrophils), monocytes, macrophages, dendritic cells (DCs), and natural killer (NK) cells. The cells generally phagocytose microbes, present antigens, and are responsible for killing pathogenic organisms.

Monocytes and Macrophages

These innate immune system antigen-presenting cells that secrete inflammatory mediators, perform their function by phagocytosis of microbes and subsequent antigen presentation to T and B cells, linking the innate and adaptive arms of the immune system. Following release from the bone marrow, monocytes circulate in the bloodstream and then differentiate into macrophages as they enter tissues. They subsequently become resident throughout the body, becoming specialized as distinct populations in the alveoli, interstitial connective tissue, bone, brain, and liver (58). There, they play the important roles of phagocytosis, killing microbes, producing cytokines and AMPs, clearing dead host cells, and antigen presentation. Neonates have comparable numbers of monocytes to adults (61). However, preterm monocytes have been found to be defective in their ability to be recruited to sites of inflammation via chemotaxis (62).

In vitro analysis of cells derived from preterm neonates have also demonstrated impairment in phagocytosis, as well as low expression of costimulatory molecules such as MHCII, CD40, and CD80 required for antigen presentation, a finding which has been associated with increased incidence of sepsis (63, 64). Other receptors such as TLR-4, CD14, and MD-2 which, together as a complex on the extracellular surface of macrophages, are involved in inflammatory signaling via LPS, an antigen derived from the wall of gram-negative bacteria. Neonatal cells appear to have normal levels of each of these molecules. However, the consequences of TLR activation in preterm infants and neonates are different compared to adults. Downstream cytokine response from interaction of LPS with these molecules in adults is consistent with a proinflammatory Th1 profile leading to expression of interferon gamma (IFNγ), IL-12 and tumor necrosis factor alpha (TNFα), which predominantly target intracellular pathogens. This response is different in neonates and especially preterm infants, where a Th17 dominant profile is observed, with IL-6 and IL2-3, which defend against extracellular bacterial and fungal pathogens, being produced. The anti-inflammatory and immunoregulatory cytokine IL-10 is also seen to play a dominant role. It is thought that this polarization prevents excessive production of the proinflammatory cytokines such as TNFα and IFNγ, which are associated with spontaneous abortion and intrauterine growth retardation (65, 66). However, this pattern of polarization nonetheless sensitizes preterm infants and newborns to infection by a broad range of intracellular micro-organisms which would normally require Th1 mediated clearance, such as *Listeria monocytogenes* and herpes simplex virus (HSV) (66). Interestingly, studies looking specifically at the neonatal response to the latter pathogen have demonstrated that an overly vigorous immune response via proinflammatory cytokines IL-6 and IL-8 may also occur, which is associated with an exacerbated clinical course (67, 68). In this regard, we have found that TLR4 signaling on the premature newborn epithelium leads to the differentiation of immature lymphocytes into Th17 cells, leading to the release of IL-17, and subsequent injury to the intestinal mucosa (28). Accordingly, strategies which inhibit IL-17 signaling were found to significantly attenuate NEC in pre-clinical models (28).

Levels of early response cytokines produced by innate cells such as macrophages are modulated by the neonatal metabolic state. The preterm infant metabolic state is characterized by stress induced by low oxygen tension that leads to increased expression of proinflammatory cytokines such as IL-6 and IL-8 via a HIF independent pathway (67). However, the response to low oxygen levels also involves a rise in adenosine levels. Adenosine is produced by cells in response to stress via breakdown of adenosine triphosphate (ATP) and is hence found to be elevated during hypoxia. This molecule has been well-studied and been found to play an immunomodulatory role through inhibition of TLR-mediated proinflammatory cytokines including TNFα, IL-12, and MIP1α (69). Specifically, in pre-term and term neonates, adenosine has been shown to downregulate proinflammatory/Th1 cytokine responses, instead mediating an alternative acute-phase response pathway via MBL, soluble CD14, C-reactive protein, LPS-binding protein, and the anti-inflammatory IL-10. Hence, in preterm neonates, adenosine attenuates pathologic inflammation by downregulating the inflammatory Th1 pathway. Recent studies have shown that administration of a probiotic *Lactobacillus reuteri* increases serum levels of adenosine and Tregs and results in lower susceptibility to NEC in stressed newborn mice by inhibiting the TLR4-mediated NFκB pathway (70–72).

Dendritic Cells

Like monocytes and macrophages, dendritic cells link the innate and adaptive immune responses (73–75) by serving as the main APCs for naïve T cells. DCs are classified into the plasmacytoid DC (pDC) and conventional DCs (cDC) groups. pDCs represent a small subset of DCs that circulate mainly in blood and lymphoid, producing massive amounts of type I IFN (IFNα/β) upon recognizing foreign antigens (74). They then acquire the ability to present these antigens to T cells (76). cDCs refer to all DCs other than pDCs. They mainly circulate in

tissues, constantly acquiring antigens and have superior antigen processing and presentation functions. They produce IL-12 p70, which is strongly pro-inflammatory. DC-like cells are detected in the human fetal thymus, liver and lymph nodes as early as 12 weeks of gestation (77). In cord blood, the pDC: cDC ratio is 3:1 compared to a 1:3 pDC-cDC ratio in adults (78). Much like monocytes, DC populations in preterm infants and neonates are found to express lower MHC-II, CD80, and CD86 compared to adult cells, reflective of their defective ability to fully activate antigen specific T and B cell responses. As a consequence, neonates and especially preterm infants have impaired immune responses to most vaccines (74, 79, 80).

In parallel with the monocyte and macrophage populations described above, TLR expression in preterm, full-term and adult DCs have been found to be generally equivalent. However, in response to stimulation, preterm infant DCs induce production of the anti-inflammatory cytokine, IL-10 compared to term infant DCs that produce elevated levels of IL-10, IL-6, and Th17 inducing IL-23 (81). This cytokine production in term neonates declines over the first year of life while levels of pro-inflammatory cytokines such as IL-1β and TNFα increase. Further, neonatal pDCs exhibit severe defects in IFNα/β production upon TLR activation.

Neonatal lungs have been found to contain fewer cDCs, and a markedly lower number of pDCs in comparison with adult lungs (82). In laboratory studies, neonatal pDCs responded poorly to respiratory syncytial virus (RSV), a common pathogen encountered by neonates. pDCs from premature neonates have been found to mount a weaker response than those from full-term neonates to both RSV and to TLR9 agonists (83). The lower numbers of pDCs in preterm neonates likely translate into compromised antiviral function.

A specific population of cDCs that express CD103 are known to drive the induction of the chemokine receptor CCR9 and alpha4 beta7 integrin, both known as gut-homing receptors. CD103(+) DCs also contribute to control inflammatory responses and intestinal homeostasis by fostering the conversion of naive T cells into induced Foxp3(+) regulatory T cells. These cells have been found to be missing in neonatal gut tissue, resulting in susceptibility to *Cryptosporidium parvum* infections (84) and increased prevalence of food allergies (85).

Neutrophils

Neutrophils belong to a group of white blood cells known as granulocytes that have cytoplasmic granules containing cationic AMPs. They are present in the fetal liver parenchyma as early as week 5 of gestation (86). In response to stimulus, neutrophils must travel from the bloodstream to the site of inflammation, enter the tissue via diapedesis, phagocytose the pathogen, and kill it in its phagolysosome. Preterm neutrophils have been found to have deficiencies in each of these functions (87). First, selectin mediated rolling occurs at the vascular endothelium, which is required for neutrophil entry from the bloodstream into tissues. Compared with adults, neonatal neutrophils express <50% L-selectin on their cell surface compared to adult neutrophils. Preterm endothelium has decreased P-selectin expression compared to term infants (88). β2 integrin expression is required for arrest of rolling and adhesion to the endothelium but these are decreased on preterm neutrophils and are unable to be upregulated in response to stimulus (89). Diapedesis through the endothelial lining requires that the neutrophil actin cytoskeleton undertake significant structural reorganization, which neonatal neutrophils are unable to achieve (90). Levels of opsonins such as immunoglobulin G (IgG), complement, and their receptors required for antigen recognition and phagocytosis are reduced in preterm neutrophils (91, 92). This phenomenon of diminished opsonization in preterm neutrophils has been demonstrated in *in vitro* studies that show impaired adult neutrophilic phagocytosis following incubation in preterm serum (93).

Pathogenic killing in the neutrophil phagolysosome occurs primarily via an NADPH oxidase-dependent respiratory burst. Term neonates have been shown to have a largely intact respiratory burst, however preterm neonates, especially those that are critically ill (94), display decreased respiratory burst and killing on exposure to group B *Streptococcus*, *Staphylococcus,* and *Pseudomonas* (95). Other bactericidal molecules normally found in neutrophilic granules, such as lactoferrin, myeloperoxidase and BPI are also decreased in quantity in neonatal neutrophils (∼30–50% of adult levels) (11), and more so in preterm infants, a phenomenon that has been correlated with increased risk of NEC (96, 97). This is also thought to confer susceptibility specifically to *Pseudomonas aeruginosa*, *Staphylococcus aureus*, and some strains of group B streptococci based on *in vitro* assays (98, 99). Neutrophils are able to form neutrophil extracellular traps (NET) by extruding DNA, chromatin and antibacterial proteins in order to sequester bacteria. NET formation has been found to be diminished by inhibitors present in cord blood of preterm and term neonates (100). Recent studies have examined whether NETs play a role in NEC pathogenesis. For instance, in one study, protein arginine deiminase (PAD) inhibited mice, which are incapable of producing NETs, were found to be protected from NEC compared to controls in a NEC model (101). Similarly, human NEC intestinal samples appeared to have increased neutrophil activation and NET formation.

Finally, neonates are unable to ramp up robust neutrophil production in response to infection, mainly due to a diminished bone marrow pool. This deficit is exacerbated in premature infants (102), in whom neutropenia is a clinical indicator of poor prognosis in cases of bacterial sepsis (103). Unfortunately, clinical trials for granulocyte colony-stimulating factor (G-CSF) or granulocyte-macrophage colony-stimulating factor (GM-CSF) as either prophylaxis or therapy for neonatal sepsis resulted in increased cell counts with no concurrent reduction in mortality (104).

Myeloid-Derived Suppressor Cells

Related to neutrophils and monocytes are a population known as myeloid-derived suppressor cells (MDSCs), which have been found to play a major regulatory role in inflammation and immune function in many pathological conditions (105–108). They are distinct from the former immune cell populations in their morphological, phenotypic, and functional heterogeneity. They produce high levels of ROS, NO, arginase (ARG1), an

immunosuppressive enzyme as well as prostaglandin E2 (PGE2). They have also been found to highly express a number of anti-inflammatory cytokines, including IL-10, all of which mediate their potent inhibition of immune responses from T cells, B cells, and NK cells (109–111).

A recent *in vivo* study examining PBMC from preterm and term neonates determined that the levels of MDSCs in the blood of preterm infants was substantially lower than that observed in full-term infants (112). More so, low numbers of MDSCs in preterm infants was associated with the development of NEC. MDSC levels were also correlated with serum lactoferrin levels. Finally, *in vitro* treatment of newborn neutrophils and monocytes with lactoferrin converted these cells to MDSCs. These lactoferrin-induced MDSCs improved survival following treatment of newborn mice. Taken together, these findings suggest an important clinical and therapeutic role for MDSCs in disorders such as NEC.

Natural Killer Cells

NK cells play a significant role in defense to virus-infected and malignant cells by expressing receptors that mediate killing of these harmful cells. The percentage of NK cells in cord blood from preterm and term neonates is often slightly lower than in the blood of children and adults; however, the absolute number is slightly higher, due to overall higher lymphocyte count in infancy (113). Fetal and neonatal NK cells are mainly deficient in IFNγ and TNFα production and exhibit reduced cytotoxic function compared to adult cells.

Like cytolytic $CD8^+$ T cells, NK cells mediate cytotoxicity, though they differ in accomplishing this via an MHC independent mechanism (114). CD56 is an NK cell-specific marker whose presence on the cell surface reflects cytolytic function. About half of neonatal NK cells do not express CD56, corresponding to a 50% capacity of full-term and premature infant cord blood NK cells to mediate cytolysis (measured at 15–60% in various studies) compared to adult NK cells (115–117).

NK cells kill infected target cells that are coated with IgG antibodies in a process known as antibody-dependent cellular cytotoxicity (ADCC) (117). Neonatal NK cell ADCC activity has been measured at ∼50% that of adult NK cells. This phenotype is rescued upon addition of cytokines such as IL2, IL12, IL15, and IFNγ *in vitro* (118). Similarly, when exposed to HSV, IFNγ production is identical in neonatal and adult NK cells (119). These studies suggest the neonatal NK cell ADCC activity *in vivo* may be comparable to adult levels in the setting of an appropriate stimulus.

In general, there is scarcity of data examining the role of NK cells in NEC, however, one small prospective study found that preterm infants with NEC showed a reduction in their NK cell proportion compared to controls (120).

ADAPTIVE IMMUNITY

The adaptive immune system consists of a cell-mediated response involving T helper cells ($CD4^+$) and cytotoxic T cells (CTL, $CD8^+$), humoral responses involving immunoglobulins and immunoregulatory actors including T regulatory cells (Tregs).

T Cells

$CD4^+$ T cells, known as "helper cells," function by activating other lymphocytes to kill infected cells. After being presented with antigens by MHC class II molecules expressed by APCs, they produce cytokines that regulate the immune response. Depending on the kind of stimulus and resulting cytokine environment, they may differentiate into Th1, Th2, Th17, or Treg cells. Th1 cells mediate cellular immunity, Th2 cells are involved in humoral immunity, while Th17 cells produce the proinflammatory cytokine IL-17. Tregs are immune suppressor cells. $CD8^+$ or cytotoxic T cells kill infected cells and cancer cells directly via antigen recognition using class I MHC molecules.

There are several features of preterm T cells which limit their function. First, preterm neonates have been found to have marked lymphopenia (up to 50% reduction) with a significant decrease in the percentage of total, $CD4^+$, and $CD8^+$ lymphocytes compared with full term infants (121). The reduction is most notable among the $CD8^+$ population, resulting in an increased CD4/CD8 ratio.

DC and macrophages induce the production of IL-12 after encountering antigens. IL-12 in turn stimulates NK cells and induces naive $CD4^+$ T cells to become Th1-type effector cells which produce IFNγ, initiating the expression of proinflammatory cytokines, such as IL-1β, TNFα, and further upregulation of IL-12 production (122, 123). Preterm naive $CD4^+$ T cells have reduced activation and impaired early Th1 differentiation including IFNγ production (124). Upon encountering stimuli, these T cells express a Th2 and Th17 polarization, weak Th1 polarization, and low innate antiviral type 1 interferon responses (65, 125). They are therefore referred to as Th2 skewed (126). IFNγ production by stimulated naive cord blood $CD4^+$ T cells has been measured as 5 to 10-fold less relative to adult $CD4^+$ T cells, resulting in susceptibility to viral infections such as human cytomegalovirus (HCMV) and HIV (127). The transcription factors T-bet, GATA3, and RORγt, regulate differentiation into Th1, Th2, and Th17 phenotypes, respectively. Accordingly, recent studies have shown that the proportion of T-bet expressing $CD4^+$ T cells is reduced within the preterm T cell population (121).

Given the relatively preserved Th2 response, preterm T cells are still able to provide help to newborn B cells for antibody synthesis. CD8 function is also relatively intact in the preterm infant, with IFNγ production by stimulated naive cord blood $CD8^+$ T cells comparable to adults' (127). It is unclear if the marked reduction in $CD8^+$ T cell frequency, contributes to the increased risk of infections in these extremely premature neonates.

Tregs, which suppress fetal anti-maternal immunity and persist at least until early adulthood are abundant in the peripheral blood and tissues of the human fetus and preterm infant. *In vitro* studies looking at cord blood have shown no quantitative differences within the Treg compartment between full term and preterm neonates. However, Tregs are also involved in T cell migration to tissues such as skin and gut in a process that

depends on the expression of the homing receptors CCR9/α4β7 and CCR4, respectively. CCR9 signaling is also known to regulate the immune response by inhibiting Treg development (128). The preterm Treg cell compartment has been shown to have lower frequency of α4β7-expressing but higher proportions of CCR4- and CCR9-expressing cells compared with full-term infants. This reflects an altered homing capacity of T cells to their target tissues in preterm infants compared to full-term. The premature newborn intestinal mucosa is characterized by an abundance of proinflammatory IL-17-producing Th17 cells which comes at the expense of anti-inflammatory $Foxp3^+$ Treg cells, and the relative skew toward a pro-inflammatory state contributes to the excessive inflammatory response that leads to development of neonatal necrotizing enterocolitis (28).

B Cells and Immunoglobulins

The B cell receptor is made up of antibodies specific for antigen detection. Upon binding of the antigen to the receptor, the former is endocytosed, processed, and presented on the B cell surface by MHC-II proteins which bind to a helper T cell. This triggers T cell activation, cytokine release to induce B cell proliferation and differentiation into antibody-producing plasma cells or memory cells. Antibodies that encounter antigens neutralize the associated pathogens and/or attract macrophages or killer cells to attack them.

Passive transfer of antibodies to the fetus and newborn occurs via transfer of maternal IgG from the placenta or secretory IgA (IgA) from breast milk. *In utero*, fetal serum immunoglobulin concentrations are significantly low until 18–20 weeks of gestation. Concentration of fetal immunoglobulins rises with the transfer of maternal immunoglobulin G (IgG) across the placenta during the third trimester of pregnancy. Preterm infants at <22 weeks gestation have 10% the level of maternal antibodies, increasing to 50% by 28–32 weeks, and elevating to 20–30% above maternal levels by term (129). This lower level of IgG compared to term neonates is likely due to less time for transfer, lower production levels and impaired placental transport. Antibodies from these infants therefore demonstrate low opsonic activity for all types of organisms (130). IgG concentrations may drop further after birth in these preterm infants due to the normal physiologic hypogammaglobulinemia that occurs in all infants. However, breast milk from mothers of preterm infants have been found to have higher levels of sIgA compared to term mothers' milk (131–133). Clinical trials evaluating the effect of oral immunoglobulin administration in preterm infants (134) have found no effect of oral immunoglobulin administration on risk of immune mediated conditions such as NEC. This is of interest, given that a recent study using a mouse NEC model showed that secretory IgA from maternal milk was protective for NEC (135). This data was correlated with levels of secretory IgA levels from preterm infant fecal samples.

In spite of limitations in the quality and quantity of immunoglobulins, even premature infants as young as 24 weeks gestation respond vigorously to protein vaccines (136, 137) such as tetanus and diphtheria toxoids, hepatitis B surface antigen, and OPV (138, 139). In contrast, responses to polysaccharide, T cell-independent antigens, such as the capsular polysaccharides of *Haemophilus influenzae* type b or Group B streptococci, are severely blunted in both preterm and term neonates until ∼18–24 months (140). Pneumococcal and *H. influenzae* conjugate vaccines were designed as a solution to this phenomenon of poor response to polysaccharide antigens. In complexing polysaccharide antigens to immunogenic proteins, a T cell mediated mechanism is required (141).

IMMATURE IMMUNITY AND DISEASE

As discussed above, the lack of maturation of intestinal innate and adaptive immune defense mechanisms in premature infants explains their susceptibility to diseases of infectious and inflammatory etiology such as NEC (see **Table 1**). As demonstrated, the components of adaptive immunity regulate the innate immune system which can cause disease when allowed to respond unchecked. Preterm infants, who are born with underdeveloped adaptive immunity also have reduced transfer of maternal antibodies, especially formula fed infants (142) placing them at greater risk for inflammatory diseases such as NEC. The role of dysfunctional TLR4 signaling and other immature immune activation, compromised barrier function as well as deficits in humoral and cellular immunity have been discussed elsewhere in this article.

Because infants with immature host innate and adaptive immune systems also have abnormal patterns of colonizing gut bacteria, there is disruption of bacterial homeostasis referred to as dysbiosis, which causes gut bacteria over-reactivity that may lead to further inflammation. The resulting high proinflammatory and pro-oxidant stress inevitably leads to irreversible damage to vital organs, including brain and intestine that often results in neurodevelopment impairment (143). Systemic inflammation during the first weeks of life is predictive of neonatal cerebral white matter injury (144), microcephaly (145), and cognitive impairment at 2 years of age (146). We have recently shown that NEC-induced brain injury, which is more severe than the brain injury that occurs in age-matched premature infants who do not develop NEC, and is characterized by significant white matter injury leading to cognitive impairment, develops as a result of cytokine release from the injured intestinal epithelium, which causes microglial activation, and the release of ROS (147). Accordingly, strategies which target the microglia and dampen the ROS response were shown in pre-clinical models to protect against the development of histologic NEC-induced brain injury, and importantly to prevent the development of cognitive impairment even in the setting of severe NEC (147).

The link between the gut and lung microbiome's development is an area of active study. Gut and lung microbiota participate in a complex interaction that shapes the host immune system, evidenced by the bidirectional association of gut dysbiosis with lung disease. For instance, infants with early life asthma have

TABLE 1 | Summary of differences in development between preterm infant, term infant and adult immune components.

	Preterm infant	Full term infant	Adult
Skin epithelium	Thin epidermis	More developed	Normal
	No lipid layer	Lipid layer present	Normal
	Neutral pH	Acidic pH	Acidic pH
	Vernix caseosa develops late	Vernix caseosa present	Not present
	–	Broad array of AMPs	Less AMP diversity
	Keratinocytes underdeveloped	Commensal bacteria interact with keratinocytes to make AMPs	–
Gut epithelium	Higher levels of PRR expressed on epithelial cells	Fewer PRR	Normal levels
	Few Paneth cells; decreased AMPs	Paneth cells make lysozyme and AMPs	Paneth cells make lysozyme and AMPs
	Epithelium more permeable to pathogenic bacteria	Epithelium more resistant to pathogenic bacteria	Normal
Complement	Low levels	Increased levels	High levels
	High level C5a fragment	Lower levels	Low levels
MBL	Low 5%	10%	100%
APPs	Low soluble APP	Increased	High
Monocytes	Comparable levels	Comparable levels	Comparable levels
	Cannot be recruited to tissue	Recruited to tissues, but fewer tissue macrophages than adult	Normal
	Poor phagocytic ability	Normal phagocytic ability	Normal
	Low receptor levels	Normal receptor levels	Normal levels
	Trigger Th17 response	Trigger Th17 response	Th1 response
Metabolic state	Low O_2 tension	Low O_2 tension	Normal O_2 tension
	Proinflammatory cytokines	Proinflammatory cytokines	No cytokine stress response
	High adenosine levels → Immunomodulation	Lower adenosine levels	–
Dendritic cells	–	High plasmacytoid DC (pDC:cDC ratio 3:1) in serum	High conventional DC (pDC:cDC ratio 1:3) in serum
	Low receptor levels	Low receptor levels	Normal
	Impaired vaccine response	Impaired vaccine response	Normal response
	Very low levels in tissues	Low levels in tissues	Higher levels in tissues
	Induce anti-inflammatory IL-10	Induce IL-10, IL-6, and IL-23	Induce IL1β and TNFα
	Poor antiviral response	Improved antiviral response	Intact antiviral response
	Poor induction of Foxp3(+) Treg	Poor induction of Foxp3(+) Treg	Normal induction of Foxp3(+) Treg
	Increased allergy prevalence	Increased allergy prevalence	
Neutrophils	Very low levels of L-selectin	Low levels of L-selectin <50%	Normal
	Low β2 integrin	Low β2 integrin	Normal
	Unable to diapedese	Poor diapedesis	Normal
	Diminished opsonization	Improved opsonization	Normal
	Impaired respiratory burst	Intact respiratory burst	Normal
	Very low levels of bactericidal molecules in neutrophilic granules	Low levels of bactericidal molecules in neutrophilic granules	Normal
	Poor NET formation	Poor NET formation	Normal
	No reserve in the setting of infection	No reserve in the setting of infection	Normal
MDSC	Low	High	Low
NK cells	Normal to slightly higher number	Normal to slightly higher number	Normal
	Deficient in IFNγ and TNFα production	Deficient in IFNγ and TNFα production	Normal
	About 50% do not express CD56; reduced cytotoxic function	About 50% do not express CD56; reduced cytotoxic function	Normal
	Unknown	50% ADCC compared to adults	Normal
T cells	50% lymphopenia compared to full term	Higher counts	Normal
	Low CD8 count, but CD8 cytolytic activity intact	Normal counts; Intact CD8 activity	Normal

(Continued)

TABLE 1 | Continued

	Preterm infant	Full term infant	Adult
	Impaired Th1 differentiation, favor Th2 and Th17	Impaired Th1 differentiation, favor Th2	Th1 differentiation intact
	Normal Treg levels	Normal Treg levels	Normal Treg levels
	Impaired homing of T cells to target tissues	–	Normal homing capacity
Serum Maternal IgG	10–50% of maternal levels	20–30% above maternal levels	–
	Low opsonic activity	Low opsonic activity	Normal
sIgA	Low in Serum	Higher in serum	–
	High in Mother's breastmilk	Lower in mothers breastmilk	–

been found to have increased levels of *Clostridia* and reduced *Bifidobacteria* in the gut (148).

SUMMARY

The response of the compromised neonate to potential infection reflects a pattern of unique features of the premature host, that stem in part from a variety of under-developed innate and adaptive immune responses. Such responses leave the premature neonate vulnerable to significant infection, while also playing an important role in the pathogenesis of diseases that are unique to this population, including necrotizing enterocolitis, as well as the sequelae of lung and brain injury. A greater understanding of the genetic, cellular, hormonal and metabolic regulation of the immune pathways of the newborn is likely to yield novel insights into how this population responds to infection and develops disease, and will hopefully unlock new avenues for prophylaxis and therapy of newborn septic disorders.

AUTHOR CONTRIBUTIONS

All authors conceived, wrote, and edited the manuscript.

REFERENCES

1. Lim ES, Wang D, Holtz LR. The bacterial microbiome and virome milestones of infant development. *Trends Microbiol.* (2016) 24:801–10. doi: 10.1016/j.tim.2016.06.001
2. Mshvildadze M, Neu J, Shuster J, Theriaque D, Li N, Mai V. Intestinal microbial ecology in premature infants assessed with non-culture-based techniques. *J Pediatr.* (2010) 156:20–5. doi: 10.1016/j.jpeds.2009.06.063
3. Ardissone AN, De La Cruz DM, Davis-Richardson AG, Rechcigl KT, Li N, Drew JC, et al. Meconium microbiome analysis identifies bacteria correlated with premature birth. *PLoS ONE.* (2014) 9:e90784. doi: 10.1371/journal.pone.0090784
4. Willyard C. Could baby's first bacteria take root before birth? *Nature.* (2018) 553:264–6. doi: 10.1038/d41586-018-00664-8
5. Gerber S, Vial Y, Hohlfeld P, Witkin SS. Detection of *Ureaplasma urealyticum* in second-trimester amniotic fluid by polymerase chain reaction correlates with subsequent preterm labor and delivery. *J Infect Dis.* (2003) 187:518–21. doi: 10.1086/368205
6. Nguyen DP, Gerber S, Hohlfeld P, Sandrine G, Witkin SS. *Mycoplasma hominis* in mid-trimester amniotic fluid: relation to pregnancy outcome. *J Perinat Med.* (2004) 32:323–6. doi: 10.1515/JPM.2004.060
7. Clarke RTJ. The gut and its micro-organisms. In: Clarke RTJ, Bauchop T, editors. *Microbial Ecology of the Gut*. New York, NY: Academic Press (1977). p. 35–71.
8. Jakaitis BM, Denning PW. Human breast milk and the gastrointestinal innate immune system. *Clin Perinatol.* (2014) 41:423–35. doi: 10.1016/j.clp.2014.02.011
9. Collins A, Weitkamp JH, Wynn JL. Why are preterm newborns at increased risk of infection? *Arch Dis Child Fetal Neonatal Ed.* (2018) 103:F391–4. doi: 10.1136/archdischild-2017-313595
10. Saccani S, Natoli G. Dynamic changes in histone H3 Lys 9 methylation occurring at tightly regulated inducible inflammatory genes. *Genes Dev.* (2002) 16:2219–24. doi: 10.1101/gad.232502
11. Levy O. Innate immunity of the newborn: basic mechanisms and clinical correlates. *Nat Rev Immunol.* (2007) 7:379–90. doi: 10.1038/nri2075
12. Oranges T, Dini V, Romanelli M. Skin physiology of the neonate and infant: clinical implications. *Adv Wound Care.* (2015) 4:587–95. doi: 10.1089/wound.2015.0642
13. Fabisiak A, Murawska N, Fichna J. LL-37: cathelicidin-related antimicrobial peptide with pleiotropic activity. *Pharmacol Rep.* (2016) 68:802–8. doi: 10.1016/j.pharep.2016.03.015
14. Capone KA, Dowd SE, Stamatas GN, Nikolovski J. Diversity of the human skin microbiome early in life. *J Invest Dermatol.* (2011) 131:2026–32. doi: 10.1038/jid.2011.168
15. Li D, Lei H, Li Z, Li H, Wang Y, Lai Y. A novel lipopeptide from skin commensal activates TLR2/CD36-p38 MAPK signaling to increase antibacterial defense against bacterial infection. *PLoS ONE.* (2013) 8:e58288. doi: 10.1371/journal.pone.0058288
16. Dominguez-Bello MG, Costello EK, Contreras M, Magris M, Hidalgo G, Fierer N, et al. Delivery mode shapes the acquisition and structure of the initial microbiota across multiple body habitats in newborns. *Proc Natl Acad Sci USA.* (2010) 107:11971–5. doi: 10.1073/pnas.1002601107
17. Moles L, Gómez M, Jiménez E, Bustos G, de Andrés J, Melgar A, et al. Bacterial diversity of the gastric content of preterm infants during their first month of life at the hospital. *Front Nutr.* (2017) 4:12. doi: 10.3389/fnut.2017.00012
18. Shen L, Turner JR. Role of epithelial cells in initiation and propagation of intestinal inflammation. Eliminating the static: tight junction dynamics exposed. *Am J Physiol Gastrointest Liver Physiol.* (2006) 290:577. doi: 10.1152/ajpgi.00439.2005
19. Miron N, Cristea V. Enterocytes: active cells in tolerance to food and microbial antigens in the gut. *Clin Exp Immunol.* (2012) 167:405–12. doi: 10.1111/j.1365-2249.2011.04523.x
20. Hackam DJ, Good M, Sodhi CP. Mechanisms of gut barrier failure in the pathogenesis of necrotizing enterocolitis: toll-like receptors throw the switch. *Semin Pediatr Surg.* (2013) 22:76–82. doi: 10.1053/j.sempedsurg.2013.01.003

21. Vitale S, Picascia S, Gianfrani C. The cross-talk between enterocytes and intraepithelial lymphocytes. *Mol Cell Pediatr.* (2016) 3:20. doi: 10.1186/s40348-016-0048-4
22. Fusunyan RD, Nanthakumar NN, Baldeon ME, Walker WA. Evidence for an innate immune response in the immature human intestine: toll-like receptors on fetal enterocytes. *Pediatr Res.* (2001) 49:589–93. doi: 10.1203/00006450-200104000-00023
23. Nanthakumar N, Meng D, Goldstein AM, Zhu W, Lu L, Uauy R, et al. The mechanism of excessive intestinal inflammation in necrotizing enterocolitis: an immature innate immune response. *PLoS ONE.* (2011) 6:e17776. doi: 10.1371/journal.pone.0017776
24. Neal MD, Sodhi CP, Dyer M, Craig BT, Good M, Jia H, et al. A critical role for TLR4 induction of autophagy in the regulation of enterocyte migration and the pathogenesis of necrotizing enterocolitis. *J Immunol.* (2013) 190:3541–51. doi: 10.4049/jimmunol.1202264
25. Gribar SC, Sodhi CP, Richardson WM, Anand RJ, Gittes GK, Branca MF, et al. Reciprocal expression and signaling of TLR4 and TLR9 in the pathogenesis and treatment of necrotizing enterocolitis. *J Immunol.* (2009) 182:636–46. doi: 10.4049/jimmunol.182.1.636
26. Good M, Siggers RH, Sodhi CP, Afrazi A, Alkhudari F, Egan CE, et al. Amniotic fluid inhibits Toll-like receptor 4 signaling in the fetal and neonatal intestinal epithelium. *Proc Natl Acad Sci USA.* (2012) 109:11330–5. doi: 10.1073/pnas.1200856109
27. Afrazi A, Branca MF, Sodhi CP, Good M, Yamaguchi Y, Egan CE, et al. Toll-like receptor 4-mediated endoplasmic reticulum stress in intestinal crypts induces necrotizing enterocolitis. *J Biol Chem.* (2014) 289:9584–99. doi: 10.1074/jbc.M113.526517
28. Egan CE, Sodhi CP, Good M, Lin J, Jia H, Yamaguchi Y, et al. Toll-like receptor 4-mediated lymphocyte influx induces neonatal necrotizing enterocolitis. *J Clin Invest.* (2016) 126:495–508. doi: 10.1172/JCI83356
29. Good M, Sodhi CP, Yamaguchi Y, Jia H, Lu P, Fulton WB, et al. The human milk oligosaccharide 2′-fucosyllactose attenuates the severity of experimental necrotising enterocolitis by enhancing mesenteric perfusion in the neonatal intestine. *Br J Nutr.* (2016) 116:1175–87. doi: 10.1017/S0007114516002944
30. Harder J, Bartels J, Christophers E, Schroder JM. A peptide antibiotic from human skin. *Nature.* (1997) 387:861. doi: 10.1038/43088
31. Harder J, Bartels J, Christophers E, Schröder JM. Isolation and characterization of human β-defensin-3, a novel human inducible peptide antibiotic. *J Biol Chem.* (2001) 276:5707–13.doi: 10.1074/jbc.M008557200
32. Valore EV, Park CH, Quayle AJ, Wiles KR, McCray PB, Ganz T. Human β-defensin-1: an antimicrobial peptide of urogenital tissues. *J Clin Invest.* (1998) 101:1633–42. doi: 10.1172/JCI1861
33. Ganz T. Defensins: antimicrobial peptides of innate immunity. *Nat Rev Immunol.* (2003) 3:710–20. doi: 10.1038/nri1180
34. Otte JM, Kiehne K, Herzig KH. Antimicrobial peptides in innate immunity of the human intestine. *J Gastroenterol.* (2003) 38:717–26. doi: 10.1007/s00535-003-1136-5
35. Moxey PC, Trier JS. Specialized cell types in the human fetal small intestine. *Anat Rec.* (1978) 191:269–85. doi: 10.1002/ar.1091910302
36. Mallow EB, Harris A, Salzman N, Russell JP, DeBerardinis RJ, Ruchelli E, et al. Human enteric defensins: gene structure and developmental expression. *J Biol Chem.* (1996) 271:4038–45. doi: 10.1074/jbc.271.8.4038
37. Rumbo M, Schiffrin EJ. Ontogeny of intestinal epithelium immune functions: developmental and environmental regulation. *Cell Mol Life Sci.* (2005) 62:1288–96. doi: 10.1007/s00018-005-5033-3
38. Heida FH, Beyduz G, Bulthuis MLC, Kooi EMW, Bos AF, Timmer A, et al. Paneth cells in the developing gut: when do they arise and when are they immune competent? *Pediatr Res.* (2016) 80:306–10. doi: 10.1038/pr.2016.67
39. Van Belkum M, Mendoza Alvarez L, Neu J. Preterm neonatal immunology at the intestinal interface. *Cell Mol Life Sci.* (2019) 77:1209–27. doi: 10.1007/s00018-019-03316-w
40. Gribar SC, Richardson WM, Sodhi CP, Hackam DJ. No longer an innocent bystander: epithelial toll-like receptor signaling in the development of mucosal inflammation. *Mol Med.* (2008) 14:645–59. doi: 10.2119/2008-00035.Gribar
41. Sodhi CP, Shi XH, Richardson WM, Grant ZS, Shapiro RA, Prindle TJ, et al. Toll-like receptor-4 inhibits enterocyte proliferation via impaired beta-catenin signaling in necrotizing enterocolitis. *Gastroenterology.* (2010) 138:185–96. doi: 10.1053/j.gastro.2009.09.045
42. Sodhi CP, Neal MD, Siggers R, Sho S, Ma C, Branca MF, et al. Intestinal epithelial Toll-like receptor 4 regulates goblet cell development and is required for necrotizing enterocolitis in mice. *Gastroenterology.* (2012) 143:708–18.e5. doi: 10.1053/j.gastro.2012.05.053
43. Hackam DJ, Sodhi CP. Toll-like receptor-mediated intestinal inflammatory imbalance in the pathogenesis of necrotizing enterocolitis. *Cell Mol Gastroenterol Hepatol.* (2018) 6:229–38.e1. doi: 10.1016/j.jcmgh.2018.04.001
44. Nino DF, Sodhi CP, Hackam DJ. Necrotizing enterocolitis: new insights into pathogenesis and mechanisms. *Nat Rev Gastroenterol Hepatol.* (2016) 13:590–600. doi: 10.1038/nrgastro.2016.119
45. Hackam DJ, Sodhi CP, Good M. New insights into necrotizing enterocolitis: from laboratory observation to personalized prevention and treatment. *J Pediatr Surg.* (2019) 54:398–404. doi: 10.1016/j.jpedsurg.2018.06.012
46. Neal MD, Jia H, Eyer B, Good M, Guerriero CJ, Sodhi CP, et al. Discovery and validation of a new class of small molecule toll-like receptor 4 (TLR4) inhibitors. *PLoS ONE.* (2013) 8:e65779. doi: 10.1371/journal.pone.0065779
47. Wipf P, Eyer BR, Yamaguchi Y, Zhang F, Neal MD, Sodhi CP, et al. Synthesis of anti-inflammatory alpha-and beta-linked acetamidopyranosides as inhibitors of toll-like receptor 4 (TLR4). *Tetrahedron Lett.* (2015) 56:3097–100. doi: 10.1016/j.tetlet.2014.11.048
48. Good M, Sodhi CP, Egan CE, Afrazi A, Jia H, Yamaguchi Y, et al. Breast milk protects against the development of necrotizing enterocolitis through inhibition of Toll-like receptor 4 in the intestinal epithelium via activation of the epidermal growth factor receptor. *Mucosal Immunol.* (2015) 8:1166–79. doi: 10.1038/mi.2015.30
49. Starner TD, Agerberth B, Gudmundsson GH, McCray PB. Expression and activity of β-defensins and LL-37 in the developing human lung. *J Immunol.* (2005) 174:1608–15. doi: 10.4049/jimmunol.174.3.1608
50. Jia H, Sodhi CP, Yamaguchi Y, Lu P, Martin LY, Good M, et al. Pulmonary epithelial TLR4 activation leads to lung injury in neonatal necrotizing enterocolitis. *J Immunol.* (2016) 197:859–71. doi: 10.4049/jimmunol.1600618
51. Jia H, Sodhi CP, Yamaguchi Y, Lu P, Ladd MR, Werts A, et al. Toll like receptor 4 mediated lymphocyte imbalance induces nec-induced lung injury. *Shock.* (2018) 52:215–23.doi: 10.1097/shk.0000000000001255
52. Kohler PF. Maturation of the human complement system. I. Onset time and sites of fetal C1q, C4, C3, and C5 synthesis. *J Clin Invest.* (1973) 52:671–77. doi: 10.1172/JCI107228
53. Davis CA, Vallota EH, Forristal J. Serum complement levels in infancy: age related changes. *Pediatr Res.* (1979) 13:1043–6. doi: 10.1203/00006450-197909000-00019
54. Johnston RB, Altenburger KM, Atkinson AW, Curry RH. Complement in the newborn infant. *Pediatrics.* (1979) 64:781–6.
55. Tayman C, Tonbul A, Kahveci H, Uysal S, Koseoglu B, Tatli MM, et al. C5a, a complement activation product, is a useful marker in predicting the severity of necrotizing enterocolitis. *Tohoku J Exp Med.* (2011) 224:143–50. doi: 10.1620/tjem.224.143
56. Dzwonek AB, Neth OW, ThiIbaut R, Gulczynska E, Chilton M, Hellwig T, et al. The role of mannose-binding lectin in susceptibility to infection in preterm neonates. *Pediatr Res.* (2008) 63:680–5. doi: 10.1203/PDR.0b013e31816fdbff
57. Schlapbach LJ, Aebi C, Fisch U, Ammann RA, Otth M, Bigler S, et al. Higher cord blood levels of mannose-binding lectin-associated serine protease-2 in infants with necrotising enterocolitis. *Pediatr Res.* (2008) 64:562–6. doi: 10.1203/PDR.0b013e3181841335
58. Levy O. A pediatric perspective on antimicrobial proteins and peptides: expression, function, and clinical relevance. In: Gallo RL, editor. *Antimicrobial Peptides in Human Health and Disease.* Norfolk: Horizon Bioscience (2005). p. 305–329.
59. Galli SJ, Borregaard N, Wynn TA. Phenotypic and functional plasticity of cells of innate immunity: macrophages, mast cells and neutrophils. *Nat Immunol.* (2011) 12:1035–44. doi: 10.1038/ni.2109
60. Strunk T, Doherty D, Richmond P, Simmer K, Charles A, Levy O, et al. Reduced levels of antimicrobial proteins and peptides in human cord blood plasma. *Arch Dis Child Fetal Neonatal Ed.* (2009) 94:F230–1. doi: 10.1136/adc.2008.143438

61. Ueno Y, Koizumi S, Yamagami M, Miura M, Taniguchi N. Characterization of hemopoietic stem cells [CFU(C)] in cord blood. *Exp Hematol.* (1981) 9:716–22.
62. Maródi L, Goda K, Palicz A, Szabó G. Cytokine receptor signalling in neonatal macrophage: defective STAT-1 phosphorylation in response to stimulation with ifn-γ. *Clin Exp Immunol.* (2001) 126:456–60. doi: 10.1046/j.1365-2249.2001.01693.x
63. Azizia M, Lloyd J, Allen M, Klein N, Peebles D. Immune status in very preterm neonates. *Pediatrics.* (2012) 129:e967–74. doi: 10.1542/peds.2011-1579
64. Ygberg S, Nilsson A. The developing immune system - from foetus to toddler. *Acta Paediatr Int J Paediatr.* (2012) 101:120–7. doi: 10.1111/j.1651-2227.2011.02494.x
65. Lewis DB, Wilson CB. Developmental immunology and role of host defenses in fetal and neonatal susceptibility to infection. In: Remington JS, Klein JO, Wilson CB, Baker CJ, editors. *Infectious Diseases of the Fetus and Newborn Infant.* Philadelphia, PA: W.B. Saunders (2006). p. 87–210. doi: 10.1016/B0-72-160537-0/50006-2
66. Dowling DJ, Levy O. Ontogeny of early life immunity. *Trends Immunol.* (2014) 35:299–310. doi: 10.1016/j.it.2014.04.007
67. Schultz C, Rott C, Temming P, Schlenke P, Möller JC, Bucsky P. Enhanced interleukin-6 and interleukin-8 synthesis in term and preterm infants. *Pediatr Res.* (2002) 51:317–22. doi: 10.1203/00006450-200203000-00009
68. Kurt-Jones EA, Belko J, Yu C, Newburger PE, Wang J, Chan M, et al. The role of toll-like receptors in herpes simplex infection in neonates. *J Infect Dis.* (2005) 191:746–8. doi: 10.1086/427339
69. Haskó G, Cronstein BN. Adenosine: an endogenous regulator of innate immunity. *Trends Immunol.* (2004) 25:33–9. doi: 10.1016/j.it.2003.11.003
70. Liu Y, Fatheree NY, Mangalat N, Rhoads JM. Lactobacillus reuteri strains reduce incidence and severity of experimental necrotizing enterocolitis via modulation of TLR4 and NF-κB signaling in the intestine. *Am J Physiol Gastrointest Liver Physiol.* (2012) 302:G608–G617. doi: 10.1152/ajpgi.00266.2011
71. Liu Y, Tran DQ, Fatheree NY, Rhoads JM. Lactobacillus reuteri DSM 17938 differentially modulates effector memory T cells and Foxp3+ regulatory T cells in a mouse model of necrotizing enterocolitis. *Am J Physiol Gastrointest Liver Physiol.* (2014) 307:G177–86. doi: 10.1152/ajpgi.00038.2014
72. Liu Y, Tian X, He B, Hoang TK, Taylor CM, Blanchard E, et al. Lactobacillus reuteri DSM 17938 feeding of healthy newborn mice regulates immune responses while modulating gut microbiota and boosting beneficial metabolites. *Am J Physiol Gastrointest Liver Physiol.* (2019) 317:G824–38. doi: 10.1152/ajpgi.00107.2019
73. Adkins B, Leclerc C, Marshall-Clarke S. Neonatal adaptive immunity comes of age. *Nat Rev Immunol.* (2004) 4:553–64. doi: 10.1038/nri1394
74. Willems F, Vollstedt S, Suter M. Phenotype and function of neonatal DC. *Eur J Immunol.* (2009) 39:26–35. doi: 10.1002/eji.200838391
75. Zaghouani H, Hoeman CM, Adkins B. Neonatal immunity: faulty T-helpers and the shortcomings of dendritic cells. *Trends Immunol.* (2009) 30:585–91. doi: 10.1016/j.it.2009.09.002
76. Cao W, Liu YJ. Innate immune functions of plasmacytoid dendritic cells. *Curr Opin Immunol.* (2007) 19:24–30. doi: 10.1016/j.coi.2006.11.004
77. Wu L, Liu YJ. Development of Dendritic-Cell Lineages. *Immunity.* (2007) 26:741–50. doi: 10.1016/j.immuni.2007.06.006
78. Borràs FE, Matthews NC, Lowdell MW, Navarrete CV. Identification of both myeloid CD11c+and lymphoid CD11c-dendritic cell subsets in cord blood. *Br J Haematol.* (2001) 113:925–31. doi: 10.1046/j.1365-2141.2001.02840.x
79. De Wit D, Tonon S, Olislagers V, Goriely S, Boutriaux M, Goldman M, et al. Impaired responses to toll-like receptor 4 and toll-like receptor 3 ligands in human cord blood. *J Autoimmun.* (2003) 21:277–81. doi: 10.1016/j.jaut.2003.08.003
80. Langrish CL, Buddle JC, Thrasher AJ, Goldblatt D. Neonatal dendritic cells are intrinsically biased against Th-1 immune responses. *Clin Exp Immunol.* (2002) 128:118–23. doi: 10.1046/j.1365-2249.2002.01817.x
81. Angelone DF, Wessels MR, Coughlin M, Suter EE, Valentini P, Kalish LA, et al. Innate immunity of the human newborn is polarized toward a high ratio of IL-6/TNF-α production *in vitro* and *in vivo*. *Pediatr Res.* (2006) 60:205–9. doi: 10.1203/01.pdr.0000228319.10481.ea
82. Ruckwardt TJ, Malloy AMW, Morabito KM, Graham BS. Quantitative and qualitative deficits in neonatal lung-migratory dendritic cells impact the generation of the $CD8^+$ T cell response. *PLoS Pathog.* (2014) 10:e1003934. doi: 10.1371/journal.ppat.1003934
83. Marr N, Wang T-I, Kam SHY, Hu YS, Sharma AA, Lam A, et al. Attenuation of respiratory syncytial virus–induced and RIG-I–dependent type I IFN responses in human neonates and very young children. *J Immunol.* (2014) 192:948–57. doi: 10.4049/jimmunol.1302007
84. Lantier L, Lacroix-Lamandé S, Potiron L, Metton C, Drouet F, Guesdon W, et al. Intestinal CD103+ dendritic cells are key players in the innate immune control of *Cryptosporidium parvum* infection in neonatal mice. *PLoS Pathog.* (2013) 9:e1003801. doi: 10.1371/journal.ppat.1003801
85. Stern A, Wold AE, Östman S. Neonatal mucosal immune stimulation by microbial superantigen improves the tolerogenic capacity of CD103+ dendritic cells. *PLoS ONE.* (2013) 8:e75594. doi: 10.1371/journal.pone.0075594
86. De Kleer I, Willems F, Lambrecht B, Goriely S. Ontogeny of myeloid cells. *Front Immunol.* (2014) 5:423. doi: 10.3389/fimmu.2014.00423
87. Raymond SL, Mathias BJ, Murphy TJ, Rincon JC, López MC, Ungaro R, et al. Neutrophil chemotaxis and transcriptomics in term and preterm neonates. *Transl Res.* (2017) 190:4–15. doi: 10.1016/j.trsl.2017.08.003
88. Anderson DC, Abbassi O, Kishimoto TK, Koenig JM, McIntire LV, Smith CW. Diminished lectin-, epidermal growth factor-, complement binding domain-cell adhesion molecule-1 on neonatal neutrophils underlies their impaired CD18-independent adhesion to endothelial cells *in vitro*. *J Immunol.* (1991) 146:3372–9.
89. Lorant DE, Li W, Tabatabaei N, Garver MK, Albertine KH. P-selectin expression by endothelial cells is decreased in neonatal rats and human premature infants. *Blood.* (1999) 94:600–9. doi: 10.1182/blood.V94.2.600
90. McEvoy LT, Zakem-Cloud H, Tosi MF. Total cell content of CR3 (CD11b/CD18) and LFA-1 (CD11a/CD18) in neonatal neutrophils: relationship to gestational age. *Blood.* (1996) 87:3929–33. doi: 10.1182/blood.V87.9.3929.bloodjournal8793929
91. Abughali N, Berger M, Tosi MF. Deficient total cell content of CR3 (CD11b) in neonatal neutrophils. *Blood.* (1994) 83:1086–92. doi: 10.1182/blood.V83.4.1086.1086
92. Linden JR, De Paepe ME, Laforce-Nesbitt SS, Bliss JM. Galectin-3 plays an important role in protection against disseminated candidiasis. *Med Mycol.* (2013) 51:641–51. doi: 10.3109/13693786.2013.770607
93. Linderkamp O, Ruef P, Brenner B, Gulbins E, Lang F. Passive deformability of mature, immature, and active neutrophils in healthy and septicemic neonates. *Pediatr Res.* (1998) 44:946–50. doi: 10.1203/00006450-199812000-00021
94. Strunk T, Temming P, Gembruch U, Reiss I, Bucsky P, Schultz C. Differential maturation of the innate immune response in human fetuses. *Pediatr Res.* (2004) 56:219–26. doi: 10.1203/01.PDR.0000132664.66975.79
95. Källman J, Schollin J, Schalèn C, Erlandsson A, Kihlström E. Impaired phagocytosis and opsonisation towards group B streptococci in preterm neonates. *Arch Dis Child Fetal Neonatal Ed.* (1998) 78:F46–50. doi: 10.1136/fn.78.1.F46
96. Anderson DC, Freeman KLB, Heerdt B, Hughes BJ, Jack RM, Smith CW. Abnormal stimulated adherence of neonatal granulocytes: impaired induction of surface MAC-1 by chemotactic factors or secretagogues. *Blood.* (1987) 70:740–50. doi: 10.1182/blood.V70.3.740.bloodjournal703740
97. Pammi M, Abrams SA. Oral lactoferrin for the prevention of sepsis and necrotizing enterocolitis in preterm infants. *Cochrane Database Syst. Rev.* (2015) 2:CD007137. doi: 10.1002/14651858.CD007137.pub4
98. Levy O, Martin S, Eichenwald E, Ganz T, Valore E, Carroll SF, et al. Impaired innate immunity in the newborn: newborn neutrophils are deficient in bactericidal/permeability-increasing protein. *Pediatrics.* (1999) 104:1327–33. doi: 10.1542/peds.104.6.1327
99. Stroobant J, Harris MC, Cody CS, Polin RA, Douglas SD. Diminished bactericidal capacity for group b streptococcus in neutrophils from "stressed" and healthy neonates. *Pediatr Res.* (1984) 18:634–7. doi: 10.1203/00006450-198407000-00013
100. Yost CC, Schwertz H, Cody MJ, Wallace JA, Campbell RA, Vieira-De-Abreu A, et al. Neonatal NET-inhibitory factor and related peptides inhibit

neutrophil extracellular trap formation. *J Clin Invest.* (2016) 126:3783–98. doi: 10.1172/JCI83873
101. Vincent D, Klinke M, Eschenburg G, Trochimiuk M, Appl B, Tiemann B, et al. NEC is likely a NETs dependent process and markers of NETosis are predictive of NEC in mice and humans. *Sci Rep.* (2018) 8:12612. doi: 10.1038/s41598-018-31087-0
102. Carr R, Huizinga TWJ. Low soluble FcRIII receptor demonstrates reduced neutrophil reserves in preterm neonates. *Arch Dis Child Fetal Neonatal Ed.* (2000) 83:F160. doi: 10.1136/fn.83.2.F160
103. Carr R. Neutrophil production and function in newborn infants. *Br J Haematol.* (2000) 110:18–28. doi: 10.1046/j.1365-2141.2000.01992.x
104. Miura E, Procianoy RS, Bittar C, Miura CS, Miura MS, Mello C, et al. A randomized, double-masked, placebo-controlled trial of recombinant granulocyte colony-stimulating factor administration to preterm infants with the clinical diagnosis of early-onset sepsis. *Pediatrics.* (2001) 107:30–5. doi: 10.1542/peds.107.1.30
105. Youn J-I, Collazo M, Shalova IN, Biswas SK, Gabrilovich DI. Characterization of the nature of granulocytic myeloid-derived suppressor cells in tumor-bearing mice. *J Leukoc Biol.* (2012) 91:167–81. doi: 10.1189/jlb.0311177
106. Zhang YL, Luan B, Wang XF, Qiao JY, Song L, Lei RR, et al. Peripheral blood MDSCs, IL-10 and IL-12 in children with asthma and their importance in asthma development. *PLoS ONE.* (2013) 8:e63775. doi: 10.1371/journal.pone.0063775
107. He YM, Li X, Perego M, Nefedova Y, Kossenkov AV, Jensen EA, et al. Transitory presence of myeloid-derived suppressor cells in neonates is critical for control of inflammation. *Nat Med.* (2018) 24:224–31. doi: 10.1038/nm.4467
108. Schwarz J, Scheckenbach V, Kugel H, Spring B, Pagel J, Härtel C, et al. Granulocytic myeloid-derived suppressor cells (GR-MDSC) accumulate in cord blood of preterm infants and remain elevated during the neonatal period. *Clin Exp Immunol.* (2018) 191:328–37. doi: 10.1111/cei.13059
109. Huang B, Pan PY, Li Q, Sato AI, Levy DE, Bromberg J, et al. Gr-1+CD115+ immature myeloid suppressor cells mediate the development of tumor-induced T regulatory cells and T-cell anergy in tumor-bearing host. *Cancer Res.* (2006) 66:1123–31. doi: 10.1158/0008-5472.CAN-05-1299
110. Hanson EM, Clements VK, Sinha P, Ilkovitch D, Ostrand-Rosenberg S. Myeloid-derived suppressor cells down-regulate l-selectin expression on CD4 + and CD8 + T cells. *J Immunol.* (2009) 183:937–44. doi: 10.4049/jimmunol.0804253
111. Li H, Han Y, Guo Q, Zhang M, Cao X. Cancer-expanded myeloid-derived suppressor cells induce anergy of NK cells through membrane-bound TGF-β1. *J Immunol.* (2009) 182:240–9. doi: 10.4049/jimmunol.182.1.240
112. Liu Y, Perego M, Xiao Q, He Y, Fu S, He J, et al. Lactoferrin-induced myeloid-derived suppressor cell therapy attenuates pathologic inflammatory conditions in newborn mice. *J Clin Invest.* (2019) 129:4261–75.doi: 10.1172/JCI128164
113. Shearer WT, Rosenblatt HM, Gelman RS, Oyomopito R, Plaeger S, Stiehm ER, et al. Lymphocyte subsets in healthy children from birth through 18 years of age: the pediatric AIDS Clinical Trials Group P1009 study. *J Allergy Clin Immunol.* (2003) 112:973–80. doi: 10.1016/j.jaci.2003.07.003
114. Phillips JH, Hori T, Nagler A, Bhat N, Spits H, Lanier LL. Ontogeny of Humanliller (NK) cells: fetal NK lasmic CD3ε, δ Proteins. *J Exp Med.* (1992) 175:1055–66. doi: 10.1084/jem.175.4.1055
115. Baley JE, Schacter BZ. Mechanisms of diminished natural killer cell activity in pregnant women and neonates. *J Immunol.* (1985) 134:3042–8.
116. Nair MPN, Schwartz SA, Menon M. Association of decreased natural and antibody-dependent cellular cytotoxicity and production of natural killer cytotoxic factor and interferon in neonates. *Cell Immunol.* (1985) 94:159–71. doi: 10.1016/0008-8749(85)90093-0
117. Merrill JD, Sigaroudinia M, Kohl S. Characterization of natural killer and antibody-dependent cellular cytotoxicity of preterm infants against human immunodeficiency virus-infected cells. *Pediatr Res.* (1996) 40:498–503. doi: 10.1203/00006450-199609000-00021
118. Kohl S. Human neonatal natural killer cell cytotoxicity function. *Pediatr Infect Dis J.* (1999) 18:635–7. doi: 10.1097/00006454-199907000-00015
119. Hayward AR, Herberger M, Saunders D. Herpes simplex virus-stimulated γ-interferon production by newborn mononuclear cells. *Pediatr Res.* (1986) 20:398–401. doi: 10.1203/00006450-198605000-00004
120. Bochennek K, Fryns E, Wittekindt B, Buxmann H, Quaiser A, Fischer D, et al. Immune cell subsets at birth may help to predict risk of late-onset sepsis and necrotizing enterocolitis in preterm infants. *Early Hum Dev.* (2016) 93:9–16. doi: 10.1016/j.earlhumdev.2015.10.018
121. Qazi KR, Jensen GB, van der Heiden M, Björkander S, Holmlund U, Haileselassie Y, et al. Extremely preterm infants have significant alterations in their conventional T cell compartment during the first weeks of life. *J Immunol.* (2020) 204:68–77. doi: 10.4049/jimmunol.1900941
122. Shuai K, Schindler C, Prezioso V, Darnell J. Activation of transcription by IFN-gamma: tyrosine phosphorylation of a 91-kD DNA binding protein. *Science.* (1992) 258:1808–12. doi: 10.1126/science.1281555
123. Shuai K, Stark GR, Kerr IM, Darnell JE. A single phosphotyrosine residue of Stat91 required for gene activation by interferon-γ. *Science.* (1993) 261:1744–6. doi: 10.1126/science.7690989
124. Chen L, Cohen AC, Lewis DB. Impaired allogeneic activation and T-helper 1 differentiation of human cord blood naive CD4 T cells. *Biol Blood Marrow Transplant.* (2006) 12:160–71. doi: 10.1016/j.bbmt.2005.10.027
125. Palin AC, Ramachandran V, Acharya S, Lewis DB. Human neonatal naive CD4 + T cells have enhanced activation-dependent signaling regulated by the MicroRNA miR-181a. *J Immunol.* (2013) 190:2682–91. doi: 10.4049/jimmunol.1202534
126. Wilson CB, Westall J, Johnston L, Lewis DB, Dower SK, Alpert AR. Decreased production of interferon-gamma by human neonatal cells. Intrinsic and regulatory deficiencies. *J Clin Invest.* (1986) 77:860–7. doi: 10.1172/JCI112383
127. Cimini E, Castilletti C, Sacchi A, Casetti R, Bordoni V, Romanelli A, et al. Human Zika infection induces a reduction of IFN-γ producing CD4 T-cells and a parallel expansion of effector Vδ2 T-cells. *Sci Rep.* (2017) 7:6313. doi: 10.1038/s41598-017-06536-x
128. Evans-Marin HL, Cao AT, Yao S, Chen F, He C, Liu H, et al. Unexpected regulatory role of CCR9 in regulatory T cell development. *PLoS ONE.* (2015) 10:e0134100. doi: 10.1371/journal.pone.0134100
129. Palmeira P, Quinello C, Silveira-Lessa AL, Zago CA, Carneiro-Sampaio M. IgG placental transfer in healthy and pathological pregnancies. *Clin Dev Immunol.* (2012) 2012:985646. doi: 10.1155/2012/985646
130. Buckley RH. The immunologic system and disorders. In: Kliegman RM, Behrman RE, Jenson Nelson's HB, editors. *Textbook of Pediatrics.* Philadelphia, PA: WB Saunders (2004). p. 681.
131. Gross SJ, Buckley RH, Wakil SS, McAllister DC, David RJ, Faix RG. Elevated IgA concentration in milk produced by mothers delivered of preterm infants. *J Pediatr.* (1981) 99:389–93. doi: 10.1016/S0022-3476(81)80323-X
132. Schlesinger L, Muñoz C, Arevalo M, Arredondo S, Mendez G. Functional capacity of colostral leukocytes from women delivering prematurely. *J Pediatr Gastroenterol Nutr.* (1989) 8:89–94. doi: 10.1097/00005176-198901000-00017
133. Mehta R, Petrova A. Biologically active breast milk proteins in association with very preterm delivery and stage of lactation. *J Perinatol.* (2011) 31:58–62. doi: 10.1038/jp.2010.68
134. Foster JP, Cole MJ, Seth R. Oral immunoglobulin for preventing necrotizing enterocolitis in preterm and low birth weight neonates. *Cochrane Database Syst Rev.* (2016) 2016:CD001816. doi: 10.1002/14651858.CD001816.pub3
135. Gopalakrishna KP, Macadangdang BR, Rogers MB, Tometich JT, Firek BA, Baker R, et al. Maternal IgA protects against the development of necrotizing enterocolitis in preterm infants. *Nat Med.* (2019) 25:1110–5. doi: 10.1038/s41591-019-0480-9
136. Smolen P, Bland R, Heiligenstein E, Lawless MR, Dillard R, Abramson J. Antibody response to oral polio vaccine in premature infants. *J Pediatr.* (1983) 103:917–9. doi: 10.1016/S0022-3476(83)80714-8
137. Koblin BA, Townsend TR, Muñtoz A, Onorato I, Wilson M, Polk BF. Response of preterm infants to diphtheria–tetanus-pertussis vaccine. *Pediatr Infect Dis J.* (1988) 7:704–11. doi: 10.1097/00006454-198810000-00008
138. Bernbaum JC, Daft A, Anolik R, Samuelson J, Barkin R, Douglas S, et al. Response of preterm infants to diphtheria-tetanus-pertussis immunizations. *J Pediatr.* (1985) 107:184–8. doi: 10.1016/S0022-3476(85)80122-0

139. Adenyi-Jones SCA, Faden H, Ferdon MB, Kwong MS, Ogra PL. Systemic and local immune responses to enhanced-potency inactivated poliovirus vaccine in premature and term infants. *J Pediatr.* (1992) 120:686–9. doi: 10.1016/S0022-3476(05)80228-8
140. Landers CD, Chelvarajan RL, Bondada S. The role of B cells and accessory cells in the neonatal response to TI-2 antigens. *Immunol Res.* (2005) 31:25–36. doi: 10.1385/IR:31:1:25
141. van den Biggelaar AHJ, Pomat WS. Immunization of newborns with bacterial conjugate vaccines. *Vaccine.* (2013) 31:2525–30. doi: 10.1016/j.vaccine.2012.06.019
142. Cheng MM, Huang CF, Yang LY, Lin YG, Peng HJ, Chang CY, et al. Development of serum IgA and IgM levels in breast-fed and formula-fed infants during the first week of life. *Early Hum Dev.* (2012) 88:743–5. doi: 10.1016/j.earlhumdev.2012.03.005
143. Walker JC, Smolders MAJC, Gemen EFA, Antonius TAJ, Leuvenink J, De Vries E. Development of lymphocyte subpopulations in preterm infants. *Scand J Immunol.* (2011) 73:53–8. doi: 10.1111/j.1365-3083.2010.02473.x
144. Procianoy RS, Silveira RC. Association between high cytokine levels with white matter injury in preterm infants with sepsis. *Pediatr Crit Care Med.* (2012) 13:183–7. doi: 10.1097/PCC.0b013e3182231074
145. Leviton A, Kuban KCK, Allred EN, Fichorova RN, O'Shea TM, Paneth N. Early postnatal blood concentrations of inflammation-related proteins and microcephaly two years later in infants born before the 28th post-menstrual week. *Early Hum Dev.* (2011) 87:325–30. doi: 10.1016/j.earlhumdev.2011.01.043
146. O'Shea TM, Allred EN, Kuban KCK, Dammann O, Paneth N, Fichorova R, et al. Elevated concentrations of inflammation-related proteins in postnatal blood predict severe developmental delay at 2 years of age in extremely preterm infants. *J Pediatr.* (2012) 160:395–401.e4. doi: 10.1016/j.jpeds.2011.08.069
147. Niño DF, Zhou Q, Yamaguchi Y, Martin LY, Wang S, Fulton WB, et al. Cognitive impairments induced by necrotizing enterocolitis can be prevented by inhibiting microglial activation in mouse brain. *Sci Transl Med.* (2018) 10:eaan0237. doi: 10.1126/scitranslmed.aan0237
148. Kalliomäki M, Kirjavainen P, Eerola E, Kero P, Salminen S, Isolauri E. Distinct patterns of neonatal gut microflora in infants in whom atopy was and was not developing. *J Allergy Clin Immunol.* (2001) 107:129–34. doi: 10.1067/mai.2001.111237

Conflict of Interest: The authors declare that the research was conducted in the absence of any commercial or financial relationships that could be construed as a potential conflict of interest.

frontiers in Immunology

MINI REVIEW
published: 19 May 2020
doi: 10.3389/fimmu.2020.00855

Maternal Immunoglobulins in Infants—Are They More Than Just a Form of Passive Immunity?

Kateryna Pierzynowska[1,2,3]*, *Jarosław Woliński*[1], *Björn Weström*[2] and *Stefan G. Pierzynowski*[2,3,4]

[1] Department of Animal Physiology, The Kielanowski Institute of Animal Physiology and Nutrition, Polish Academy of Sciences, Jabłonna, Poland, [2] Department of Biology, Lund University, Lund, Sweden, [3] SGP + GROUP, Trelleborg, Sweden, [4] Department of Medical Biology, Institute of Rural Health, Lublin, Poland

In the present review, we highlight the possible "extra-immunological" effects of maternal immunoglobulins (Ig) transferred to the blood circulation of offspring, either via the placenta before birth or via the colostrum/milk across the gut after birth in different mammalian species. Using the newborn pig as a model, since they are naturally born agammaglobulinemic, intravenously (i.v.) infused purified serum Ig rapidly improved the vitality, suckling behavior, and ensured the survival of both preterm and term piglets. In further studies, we found that proper brain development requires i.v. Ig supplementation. Studies have reported on the positive effects of i.v. Ig treatment in children with epilepsy. Moreover, feeding newborn pigs an elementary diet supplemented with Ig improved the gut structure, and recently a positive impact of enteral or parenteral Ig supplementation on the absorption of polyunsaturated fatty acids (PUFAs) was observed in the newborn pig. Summarized, our own results and those found in the literature, indicate the existence of important extra-immune effects of maternal Ig, in addition to the classical protective effects of transferred maternal passive immunity, including effects on the development of the brain, gut, and possibly other organ systems in the neonate. These additional properties of circulating Ig could have an impact on care guidelines for human neonates, especially those born prematurely with low plasma Ig levels.

Keywords: immunoglobulins, extra-immunological effects, neonatal, brain development, gut development

OPEN ACCESS

Edited by:
Andrew Currie,
Murdoch University, Australia

Reviewed by:
Xi Ma,
China Agricultural University, China
Marjolein Meijerink,
Netherlands Organisation for Applied Scientific Research (TNO), Netherlands

***Correspondence:**
Kateryna Pierzynowska
Katerina.Goncharova@biol.lu.se

Specialty section:
This article was submitted to Nutritional Immunology, a section of the journal Frontiers in Immunology

Received: *15 December 2019*
Accepted: *14 April 2020*
Published: *19 May 2020*

Citation:
Pierzynowska K, Woliński J, Weström B and Pierzynowski SG (2020) Maternal Immunoglobulins in Infants—Are They More Than Just a Form of Passive Immunity? Front. Immunol. 11:855. doi: 10.3389/fimmu.2020.00855

INTRODUCTION

Human infants receive the majority of maternal immunoglobulins (Ig), predominantly immunoglobulin G (IgG), via the placenta. Maternal antibody transfer to the fetus starts as early as during the 13th week of gestation. The level of IgG in the fetal circulation is relatively low (5–10% of maternal levels) between weeks 17 and 22, reaching 50% of maternal levels by week 32 and usually exceeding the maternal plasma IgG level at birth (1).

In ungulate species, in contrast to humans, Ig are exclusively transferred from the mother to the newborn after birth through the ingestion of the "first milk" or colostrum, which is rich in IgG. The Ig are transferred across the "open" gut to the general circulation during the first few days of life. Thus, since piglets are born agammaglobulinemic, they serve as an excellent model for studying the biological effects of maternal Ig transfer in the newborn. In addition, since the pig is multiparous and may give birth to 10–20 piglets at a time, it is possible to form several treatment groups from one litter, making comparative studies easier.

Newborn, unsuckled piglets are in a biological sense transiently immunodeficient, and Ig are not always optimally transmitted from mother to offspring, e.g., because of premature delivery in humans or problems with suckling in ungulates. This raises the question as to whether a transient immunodeficiency could result in symptoms similar to those observed in classical primary immunodeficiency (PID) later in life. Patients with classical PID, as a result of various gene defects, develop various immune disorders later in life (2) with variable clinical manifestations, e.g., autoimmune disorders and malignancies or allergic disorders (3).

MATERNAL Ig INFLUENCE ON THE STRUCTURAL AND FUNCTIONAL DEVELOPMENT OF THE BRAIN

Maternal Ig, transferred to the offspring's blood stream, either before birth (in the case of human infants) or after birth (in the case of ungulates), are omnipresent and may function as regulators for those organs and systems undergoing drastic developmental changes after birth, e.g., the gut, brain, immune system, etc. However, any extra-immune regulatory effects of Ig are difficult to recognize at "first glance," and are probably often overlooked because of "the most obvious role of Ig in protecting the offspring from infections during the first few weeks of life." Hence, the aim of our review is to highlight and summarize the knowledge obtained from previous studies by our lab, as well as previous literature concerning the possible extra-immunological effects of maternal Ig transfer during the early post-natal period and their (Ig) role in further development of the offspring.

In the case of livestock praxis with regard to goat breeding, it is well-known that careful surveillance of the pasture should be carried out during delivery time in order to locate newborn kids. If the kids do not receive colostrum containing high levels of IgG timeously, they become apathetic and die within a few hours after birth, with no obvious symptoms of infection (4). Similarly, pig breeders usually keep some colostrum in reserve in order to vitalize piglets, which are not able to suckle from their mothers. Nowadays, sows, which have a maximum of 14 teats, usually give birth to over 20 piglets. Thus, in order for all the piglets to survive (5), breeders need to feed the surplus piglets Ig-rich colostrum collected from other sows or from cows. If piglets do not get a sufficient amount of colostrum for absorption over the gut during the first few hours of life, they become apathetic, often have watery diarrhea, and finally die—generally not as a result of infection.

To study this inexplicable effect of colostrum, we performed some simple experiments to determine whether provision of purified Ig, the major protein in colostrum whey, using different approaches, would be beneficial for term and preterm newborn piglets (6). A preparation of porcine serum Ig was infused i.v. in an amount sufficient to ensure the attainment of blood levels of IgG similar to those found in piglets fed with sow colostrum. Infusion of the Ig preparation in both preterm and term newborn (un-suckled) piglets ensured their active suckling behavior, growth, and survival, as well as blood IgG and protein levels similar to those observed in piglets fed colostrum. In contrast, piglets completely deprived of Ig exhibited no willingness to suckle and exhibited very low blood levels of IgG and lower protein levels compared to colostrum-fed or Ig-infused animals. Moreover, piglets infused with sow serum, containing less IgG than the Ig preparation, displayed significantly lower blood IgG levels, compared to those infused with the Ig preparation or those fed colostrum, and did not develop proper suckling behavior. In conclusion, the experiments suggest that early systemic infusion of Ig is key to stimulating behavioral survival instincts and ensuring the well-being of newborn piglets, either preterm or full term. In addition, the experiments indicated that the agammaglobulinemic newborn pig can be used as an animal model for the human infant.

Neurological disorders are among the main clinical problems affecting preterm children and often cause communication problems and learning disabilities later on in life (7, 8). Several factors are important for brain development, but the role of maternal Ig transfer has not yet been investigated with regard to this aspect. The first results indicating positive effects of Ig administration on protein synthesis in the brain were obtained by Burrin et al. (9). Colostrum was found to be the best stimulator of protein synthesis in vital organs of newborn piglets, e.g., the brain and heart, compared to an isoenergetic diet of milk formula or mature milk. The authors attributed the stimulation of specific protein synthesis in the brain and heart to the colostrum that was fed to the piglets, and not to the intake of certain macronutrients. These findings suggested to us that it was the high content of Ig in the colostrum that had the stimulatory effect on brain growth, development and metabolism. Moreover, Harada et al. (10) have shown that following colostrum feeding, the IgG can penetrate into the cerebrospinal fluid (CSF) of neonatal piglets.

Thus, the main objective in a study performed in our lab (11), was to evaluate the effects of colostrum (Ig) on brain development in neonatal pigs during the first 3 days after birth. Positive correlations were found between growth and hippocampal development and the levels of total protein and IgG in blood plasma of sow-reared piglets. Piglets that were exclusively fed an elemental diet exhibited reduced counts of microglial cells and neurons in the CA1 area of the hippocampus 72 h after birth. However, supplementation of an elemental diet with Ig or rearing the piglets with sow colostrum improved the cellular structure and supported the trophic status of the hippocampus. The data obtained indicated that the development of the hippocampus requires Ig in order to stimulate protein synthesis and brain development during the early post-natal period. In order to focus on the specific role of IgG, further investigations are required, since the Ig preparation used in our studies contained a mixture of Ig classes. However, though colostrum contains several Ig classes, predominantly IgG is absorbed over the gut before gut closure (12).

In a follow-up study by our lab, newborn piglets were fed an infant formula or colostrum supplemented, orally or i.v., with either species-specific, porcine, or foreign, human, Ig and compared to newborn un-suckled piglets or sow-reared piglets (13). After 2 days, behavioral tests were performed on the piglets. Both neuronal plasticity parameters, i.e., neuronal maturation

and synapse-associated proteins, and behavioral test parameters seemed to only be improved by the presence of the species-specific porcine Ig in the circulation and in the cerebrospinal fluid (CSF). In fact, Kowal et al. (14) have discussed the possible role of Ig on the development of the blood–brain barrier in humans. Why during the early stages of development are Ig permitted to enter the CSF, since the presence of Ig in the CSF of adults is considered a pathological sign? An indication might be that the presence of Fc gamma receptors have been described in the developing rat brain (15, 16) and the same type of Fc receptor is known to be of importance in the development of the cerebellum (17). Despite the expression profile and functionality of Fc receptors in neurons being not well-investigated and controversial, there is accumulating evidence that all four types of Fc receptors are expressed in neurons (17–22). Moreover, stimulation of mouse superior cervical ganglions with IgG *in vitro* leads to an increase in intracellular calcium (18). Thus, maternal Ig appear to play some sort of regulatory role, e.g., enabling the transfer of maternal experience to the developing brain.

MATERNAL Ig AND THE DEVELOPMENT OF EPILEPSY

A positive influence of i.v. Ig treatment on epilepsy in children, with a decrease in frequency and severity of seizures, was observed as early as 1977 by Pechadre et al. (23). At the time, this finding supported the allergic theory of epilepsy and was recognized as a form of immunological treatment. However, both animal and human studies suggest non-immunological effects of i.v. Ig treatment. Patients with both idiopathic and symptomatic forms of epilepsy demonstrated an immediate response to Ig infusion. I.v. Ig infusion has also been shown to have anticonvulsant effects in the kindled cat model (24) and in a model of direct cortical stimulation, where i.v. treatment with Ig significantly decreased seizure threshold (25). All these observations suggest a direct neuro-modulatory effect of i.v. Ig treatment (25).

It has been reported that an increase in gestational age is negatively correlated with the risk of epilepsy (26). Taking into consideration that i.v. Ig treatment has been used in different forms of the intractable childhood epilepsy with promising results (up to 70% of patients obtaining a seizure-free status) (27, 28), and the fact that plasma levels of IgG are positively correlated with gestational age increase (1), one should consider Ig as possible neuromodulators, which regulate excitability of neuronal membranes and protect the immature brain of newborn infants against over excitation. Furthermore, Ig have been shown to be taken up by neurons (20), causing direct neuroprotective effects via the modulation of NF-kB and MAPK activities, through the reduced expression and activation of neuronal toll-like receptors, as well as by decreasing caspase-3 cleavage leading to decreased apoptosis of neurons (29–32).

We postulate possible positive clinical effects of i.v. infusion of human Ig in terms of stimulating neuronal plasticity and development of cognitive function in preterm infants born with low immunoglobulin levels in their blood. This is supported by the review by Chavoshzadeh et al. (33) who postulate that early recognition and treatment of primary immunodeficiencies (PID) is important to prevent or reduce future irreversible neurological sequelae. Diverse neurological deficits accompanying certain PID may be mild. However, they may greatly influence the course of the disease with major impacts on the quality of life of these patients.

MATERNAL Ig SUPPORT STRUCTURAL AND FUNCTIONAL DEVELOPMENT OF THE GUT

Nowadays, a lot of research is performed on the influence of the gut microbiota on infant development and metabolism, a lot of which involves maternal Ig derived from mother's milk or retro-transported via the FcRn receptor from the serum to the gut (34). Gut microbiota develops via interactions with nutrients (35), both endogenous and exogenous agents, such as melatonin (36) or fructans (37), and even viral infections (38), with involvement of maternal and infant Ig. Recently (39), it has been shown that maternal IgA decreases the risk of development of necrotizing enterocolitis through its (IgA) influence on the host–microbiota relationship in preterm neonates. However, all these investigations focus on the classical functions of the immune system and its impact on overall gut function.

To better address this issue, we investigated whether Ig administration affects the structure of the gastrointestinal tract in newborn piglets (40). Enteral feeding with an elementary diet supplemented with purified Ig resulted in a significant increase in the thickness of the stomach, duodenal and jejunal mucosa, and muscularis layers compared to that observed in the group fed an elementary diet without Ig. The parameters measured in the Ig-fed group reached values similar to those observed in sow-reared piglets. Finally, colostrum and Ig may have a protective effect via blockage of the pro-inflammatory reaction of the enteral nervous system (40). Our results show that a diet supplemented with Ig stimulates growth of the gut and affects intestinal structure by altering it toward that observed in colostrum-fed piglets, which indicates a direct beneficial effect of Ig on gut development in neonatal pigs.

In a recent study, we investigated the impact of Ig on intestinal function and the absorption of polyunsaturated fatty acids (PUFAs) in the newborn pig (41). The high plasma levels of PUFAs found in newborn, un-suckled piglets decrease by between 40 and 50% in piglets fed an infant formula for 48 h. However, piglets fed the infant formula supplemented with Ig, either orally or through feeding with swine or bovine colostrum, or by swine serum infusion, or by i.v. infusion of swine or human Ig preparations, demonstrated improved growth and enhanced plasma PUFA levels, similar to those observed at birth. These results indicate the importance of the presence of Ig in the blood for the appropriate absorption of dietary PUFAs and overall gut function and, thus, the absorption of other nutrients in newborn piglets. This may have an impact on the dietary guidelines for human neonates, especially those born prematurely with low

plasma Ig levels, since PUFAs are important factors for brain development in early life.

IMPLICATIONS

The extra-immunological effects of circulating maternal Ig, presumably more specifically IgG, in the newborn are summarized in this review highlighting the importance of maternal Ig transfer in stimulating organ growth and maturation after birth. The classical immune-protecting features of maternal Ig can be replaced by, e.g., antibiotics and sterile conditions, while the extra-immunological stimulatory effects probably cannot be replaced. Thus, the properties and role of maternal Ig transmitted to the offspring in late pregnancy or directly after birth need to be further explored and recognized as vital components of early development with possible long-lasting effects on health and performance later in life.

AUTHOR CONTRIBUTIONS

KP, JW, BW, and SP were responsible for preparing the manuscript. KP, SP, and BW designed the review and critically reviewed the manuscript. All authors contributed to manuscript revision, have read, and approved the submitted version.

ACKNOWLEDGMENTS

The authors would like to express their thanks to Dr. Janine Donaldson for her constructive feedback and valuable input with regard to the writing of the manuscript.

REFERENCES

1. Palmeira P, Quinello C, Silveira-Lessa AL, Zago CA, Carneiro-Sampaio M. IgG placental transfer in healthy and pathological pregnancies. *Clin Dev Immunol.* (2012) 2012:985646. doi: 10.1155/2012/985646
2. Picard C, Gaspar HB, Al-Herz W, Bousfiha A, Casanova J-L, Chatila T, et al. International Union of Immunological Societies: 2017 Primary Immunodeficiency Diseases Committee report on inborn errors of immunity. *J Clin Immunol.* (2018) 38:96–128. doi: 10.1007/s10875-017-0464-9
3. Samarghitean C, Ortutay C, Vihinen M. Systematic classification of primary immunodeficiencies based on clinical, pathological, and laboratory parameters. *J Immunol.* (2009) 183:7569–75. doi: 10.4049/jimmunol.0901837
4. Hermandez-Castellano LE, Morales-dela Nuez A, Sanchez-Macias D, Moreno-Indias I, Torres A, Capote, et al. The effect of colostrum source (goat vs. sheep) and timing of the first colostrum feeding. (2 h vs. 14 h after birth) on body weight and immune status of artificially reared newborn lambs. *J Dairy Sci.* (2015) 98:204–10. doi: 10.3168/jds.2014-8350
5. Aumaitre A, Seve B. Nutritional importance of colostrum in the piglet. *Ann Rech Vet.* (1978) 9:181–92.
6. Socha-Banasiak A, Pierzynowski SG, Wolinski J, Grujic D, Boryczka M, Grzesiak P, et al. The pig as a model for premature infants - the importance of immunoglobulin supplementation for growth and development. *Biol Regul Homeost Agents*. (2017) 31:87–92.
7. Synnes A, Hicks M.Neurodevelopmental outcomes of preterm children at school age and beyond. *Clin Perinatol.* (2018) 45:393–408. doi: 10.1016/j.clp.2018.05.002
8. Ådén U, Sävman K, Norman M. [Children born too soon and outcomes]. *Lakartidningen*. (2019) 116:FR6D.
9. Burrin DG, Davis TA, Ebner S, Schonknecht PA, Firotto ML, Reed PJ. Colostrum in neonatal pig enhances the nutritional stimulation of vital organ protein synthesis. *J Nutr.* (1977) 127:1284–98. doi: 10.1093/jn/127.7.1284
10. Harada E, Araki Y, Furumura E, Takeuchi T, Sitizyo K, Yajima T, et al. Characteristic transfer of colostrum-derived biologically active substances into cerebrospinal fluid via blood in natural suckling neonatal pigs. *J Vet Med A Physiol Pathol Clin Med.* (2002) 49:358–64. doi: 10.1046/j.1439-0442.2002.00457.x
11. Pierzynowski SG, Ushakova G, Kovalenko T, Osadchenko I, Goncharova K, Gustavsson P, et al. Impact of colostrum and plasma immunoglobulin intake on hippocampus structure during early postnatal development in pig. *Int J Dev Neurosci.* (2014) 35:64–71. doi: 10.1016/j.ijdevneu.2014.03.003
12. Hurley WL, Theil PK. Perspectives on immunoglobulins in colostrum and milk. *Nutrients.* (2011) 3:442–74. doi: 10.3390/nu3040442
13. Goncharova K, Lozinska L, Arevalo Sureda E, Wolinski J, Weström B, Pierzynowski S. Importance of neonatal immunoglobulin transfer for hippocampal development and behaviour in the newborn pig. *PLoS ONE.* (2017) 12:e0180002. doi: 10.1371/journal.pone.0180002
14. Kowal C, Athanassiou A, Chen H, Diamond B. Maternal antibodies and developing blood–brain barrier. *Immunol Res.* (2015) 63:18–25. doi: 10.1007/s12026-015-8714-5
15. Stamou M, Grodzki ACh, van Oostrum M, Wollscheid B, Lein PJ. Fc gamma receptors are expressed in the developing rat brain and activate downstream signaling molecules upon cross-linking with immune complex. *J Inflam.* (2018) 15:7. doi: 10.1186/s12974-017-1050-z
16. Stamou M, Lein PJ. Commentary: Fc gamma receptors are expressed in the developing rat brain and activate downstream signaling molecules upon cross-linking with immune complex. *Neurol Neuromed.* (2019) 4:26–29. doi: 10.29245/2572.942X/2019/1.1243
17. Nakamura K, Hirai H, Torashima T, Miyazaki T, Tsurui H, Xiu Y, et al. CD3 and immunoglobulin G Fc receptor regulate cerebellar functions. *Mol Cell Biol.* (2007) 27:5128–34. doi: 10.1128/MCB.01072-06
18. van der Kleij H, Charles N, Karimi K, Mao YK, Foster J, Janssen L, et al. Evidence for neuronal expression of functional Fc (epsilon and gamma) receptors. *J Allergy Clin Immunol.* (2010) 125:757–60. doi: 10.1016/j.jaci.2009.10.054
19. Qu L, Zhang P, LaMotte RH, Ma C. Neuronal Fc-gamma receptor I mediated excitatory effects of IgG immune complex on rat dorsal root ganglion neurons. *Brain Behav Immun.* (2011) 25:1399–407. doi: 10.1016/j.bbi.2011.04.008
20. Congdon EE, Gu J, Sait HBR, Sigurdsson EM. Antibody uptake into neurons occurs primarily via clathrin-dependent Fcγ receptor endocytosis and is a prerequisite for acute tau protein clearance. *J Biol Chem.* (2013) 288:35452–65. doi: 10.1074/jbc.M113.491001
21. Fernandez-Vizarra P, Lopez-Franco O, Mallavia B, Higuera-Matas A, Lopez-Parra V, Ortiz-Muñoz G, et al. Immunoglobulin G Fc receptor deficiency prevents Alzheimer-like pathology and cognitive impairment in mice. *Brain.* (2012) 135(Pt 9):2826–37. doi: 10.1093/brain/aws195
22. Kam T-I, Song S, Gwon Y, Park H, Yan J-J, Im I, et al. FcγRIIb mediates amyloid-B neurotoxicity and memory impairment in Alzheimer's disease. *J Clin Invest.* (2013) 123:2791–802. doi: 10.1172/JCI66827
23. Pechadre JC, Sauvezie B, Osier C, Gibert J. Traitement des encephalopathies epileptiques de l'enfant par les gammaglobulines. *Rev Elettroencephalogr Neurophysiol.* (1977) 7:443–7. doi: 10.1016/S0370-4475(77)80049-X
24. Hirayama H, Kurimoto T, Wada S, Machida N, Shikuma H, Shoji S, et al. Antiepileptic effects of globulin-N, an intact human immunoglobulin and its tissue-distribution in kindled cats. *Int J Clin Pharm.* (1986) 24:109–22.
25. Villani F, Avanzini G. The use of immunoglobulins in the treatment of human epilepsy. *Neurol Sci.* (2002) 23(Suppl. 1):S33–7. doi: 10.1007/s100720200013
26. Hirvonen M, Ojala R, Korhonen P, Haataja P, Eriksson K, Gissler M, et al. The incidence and risk factors of epilepsy in children born preterm: a nationwide register study. *Epilepsy Res.* (2017) 138:32–8. doi: 10.1016/j.eplepsyres.2017.10.005
27. van Engelen BG, Reiner WO, Weemaes CM, Strengers PF, Bernsen PJ, Notermans SL. High-dose intravenous immunoglobulin treatment in

cryptogenic West and Lennox- Gastaut syndromes; an add-on study. *Eur J Pediatr.* (1994) 153:762–9. doi: 10.1007/BF01954498
28. Duse M, Notarangelo LD, Tiberti S, Menegati E, Plebani A Ugazio AG. Intravenous immune globulin in the treatment of intractable childhood epilepsy. *Clin Exp Immunol.* (1996) 104(Suppl. 1):71–6. doi: 10.1111/cei.1996.104.s1.71
29. Arumugam TV, Tang SC, Lathia JD, Cheng A, Mughal MR, Chigurupati S, et al. Intravenous immunoglobulin (IVIG) protects the brain against experimental stroke by preventing complement-mediated neuronal cell death. *Proc Natl Acad Sci USA.* (2007) 104:14104–9. doi: 10.1073/pnas.0700506104
30. Widiapradja A, Vegh V, Lok KZ, Manzanero S, Thundyil J, Gelderblom M, et al. Intravenous immunoglobulin protects neurons against amyloid betapeptide toxicity and ischemic stroke by attenuating multiple cell death pathways. *J Neurochem.* (2012) 122:321–32. doi: 10.1111/j.1471-4159.2012.07754.x
31. Lok KZ, Basta M, Manzanero S, Arumugam TV. Intravenous immunoglobulin (IVIg) dampens neuronal toll-like receptor-mediated responses in ischemia. *J Neuroinflammation.* (2015) 12:73. doi: 10.1186/s12974-015-0294-8
32. Thom V, Arumugam TV, Magnus T, Gelderblom M. Therapeutic potential of intravenous immunoglobulin in acute brain injury. *Front Immunol.* (2017) 8:875. doi: 10.3389/fimmu.2017.00875
33. Chavoshzadeh Z, Hashemitari A, Darougar S. Neurological manifestations of primary immunodeficiencies. *Iran J Child Neurol.* (2018) 12:7–23.
34. Harris NL, Spoerri I, Schopfer JF, Nembrini C, Merky P, Massacand J, et al. Mechanisms of neonatal mucosal antibody protection. *J Immunol.* (2006) 177:6256–62. doi: 10.4049/jimmunol.177.9.6256
35. Ma N, Guo P, Zhang J, He T, Kim SW, Zhang G, Ma X Nutrients mediate intestinal bacteria–mucosal immune crosstalk. *Front Immunol.* (2018) 9:5. doi: 10.3389/fimmu.2018.00005
36. Ma N, Zhang J, Reiter RJ, Ma X. Melatonin mediates mucosal immune cells, microbial metabolism, and rhythm crosstalk: a therapeutic target to reduce intestinal inflammation. *Med Res Rev.* (2020) 40:606–32. doi: 10.1002/med.21628
37. Valcheva R, Koleva P, Martínez I, Walter J, Gänzle MG, Dieleman LA. Inulin-type fructans improve active ulcerative colitis associated with microbiota changes and increased short-chain fatty acids levels. *Gut Microbes.* (2019) 10:334–57. doi: 10.1080/19490976.2018.1526583
38. Machiavelli A, Duarte RTD, Pires MMS, Zárate-Bladés CR, Pinto AR. The impact of *in utero* HIV exposure on gut microbiota, inflammation, and microbial translocation. *Gut Microbes.* (2019) 10:599–614. doi: 10.1080/19490976.2018.1560768
39. Gopalakrishna KP, Macadangdang BR, Rogers MB, Tometich JT, Firek BA, Baker R, et al. Maternal IgA protects against the development of necrotizing enterocolitis in preterm infants. *Nat Med.* (2019) 25:1110–5. doi: 10.1038/s41591-019-0480-9
40. Wolinski J, Słupecka M, Weström B, Prykhodko O, Ochniewicz P, Arciszewski M, et al. Effect of feeding colostrum versus exogenous immunoglobulin G on gastrointestinal structure and enteric nervous system in newborn pig. *J Anim Sci.* (2012) 90(Suppl. 4):327–30. doi: 10.2527/jas.53926
41. Pierzynowska K, Wolinski J, Weström B, Jazwiec R, Shmigel H, Pierzynowski SG. Polyunsaturated fatty acid (PUFA) absorption is related to IgG blood levels of neonatal pig during the first 48 hours postpartum. *J Immunol Res.* (2020) 2020:3813250. doi: 10.1155/2020/3813250

Conflict of Interest: SP is the owner of SGP+ Group, Sweden; KP is employed by the SGP+ Group, Sweden.

The remaining authors declare that the research was conducted in the absence of any commercial or financial relationships that could be construed as a potential conflict of interest.

frontiers in Immunology

ORIGINAL RESEARCH
published: 27 May 2020
doi: 10.3389/fimmu.2020.01019

Diet Modulates the High Sensitivity to Systemic Infection in Newborn Preterm Pigs

Ole Bæk[1†], Anders Brunse[1†], Duc Ninh Nguyen[1], Arshnee Moodley[2], Thomas Thymann[1] and Per Torp Sangild[1,3,4]*

[1] Comparative Pediatrics and Nutrition, Department of Veterinary and Animal Sciences, Faculty of Health and Medical Sciences, University of Copenhagen, Copenhagen, Denmark, [2] Veterinary Clinical Microbiology, Department of Veterinary and Animal Sciences, Faculty of Health and Medical Sciences, University of Copenhagen, Copenhagen, Denmark, [3] Department of Neonatology, Rigshospitalet, Copenhagen, Denmark, [4] Department of Pediatrics, Odense University Hospital, Odense, Denmark

OPEN ACCESS

Edited by:
Philip John Griebel,
University of Saskatchewan, Canada

Reviewed by:
Gregers Jungersen,
Statens Serum Institute, Denmark
Martin Faldyna,
Veterinary Research Institute (VRI), Czechia

***Correspondence:**
Per Torp Sangild
pts@sund.ku.dk

[†]These authors have contributed equally to this work and share first authorship

Specialty section:
This article was submitted to Comparative Immunology, a section of the journal Frontiers in Immunology

Received: 01 October 2019
Accepted: 28 April 2020
Published: 27 May 2020

Citation:
Bæk O, Brunse A, Nguyen DN, Moodley A, Thymann T and Sangild PT (2020) Diet Modulates the High Sensitivity to Systemic Infection in Newborn Preterm Pigs. Front. Immunol. 11:1019. doi: 10.3389/fimmu.2020.01019

Background: Preterm infants are born with an immature immune system, limited passive immunity, and are at risk of developing bacteremia and sepsis in the postnatal period. We hypothesized that enteral feeding, with or without added immunoglobulins, improves the clinical response to systemic infection by coagulase negative staphylococci.

Methods: Using preterm cesarean delivered pigs as models for preterm infants, we infused live *Staphylococcus epidermidis* (SE, 5×10^9 colony forming units per kg) systemically 0–3 days after birth across five different experiments. SE infection responses were assessed following different gestational age at birth (preterm vs. term), enteral milk diets (bovine colostrum, infant formula with or without added porcine plasma) and with/without systemic immunoglobulins. Pigs infected with SE were assessed 12–48 h for clinical variables, blood bacteriology, chemistry, hematology, and gut dysfunction (intestinal permeability, necrotizing enterocolitis lesions).

Results: Adverse clinical responses and increased mortality were observed in preterm vs. term pigs, when infected with SE just after birth. Feeding bovine colostrum just after birth improved blood SE clearance and clinical status (improved physical activity and intestinal structure, fewer bone marrow bacteria), relative to pigs fed infant formula. A few days later, clinical responses to SE bacteremia (hematology, neutrophil phagocytic capacity, T cell subsets) were less severe, and less affected by different milk diets, with or without added immunoglobulins.

Conclusion: Prematurity increases the sensitivity of newborn pigs to SE bacteremia, potentially causing sepsis. Sensitivity to systemic SE infection decreases rapidly in the days after preterm birth. Both age and diet (parenteral nutrition, colostrum, milk, formula) may influence gut inflammation, bacterial translocation and systemic immune development in the days after birth in preterm newborns.

Keywords: sepsis, bacteremia, preterm, infant, diet, immunity, passive, feeding

INTRODUCTION

Preterm infants have an increased risk of infection in the neonatal period. The risk of late onset sepsis (LOS) is 20–40%, with increasing risks at lower gestational ages (1, 2). Use of infant formula, or prolonged use of parenteral nutrition, and associated use of catheters, increases the risk of LOS (3). Use of milk based diets shorten the time to full enteral feeding, and thereby removal of central venous catheters as well as reduces the incidence of necrotizing enterocolitis (NEC) (4, 5). Severe inflammation of the gut is associated with sepsis in preterm neonates, but it is unknown if this effect is due mainly to increased bacterial translocation, or if local gut inflammatory conditions adversely affect systemic immunity. The type of nutrition after birth (parenteral, or enteral feeding with formula, milk or colostrum) rapidly affects gut maturation in immunocompromised preterm infants and pigs (6). Whether the first enteral feeding also influences systemic immunity in such infants is less clear, although clinical outcomes may be improved after early feeding with milk or colostrum of either human or animal origin (7–9).

Across the world, some of the most common pathogens causing LOS in preterm neonates are coagulase negative staphylococci (CoNS) (2, 10–12). The defense against systemic CoNS infection is dependent on opsonization of the bacteria by immunoglobulins and complement factors (13–15). Immunoglobulin G (IgG) is actively transported across the placenta, starting in the second trimester, and accelerates toward term (16). Preterm infants are therefore born with lower levels of maternally derived IgG (16, 17). As a result, opsonization and clearance of CoNS is more dependent on complement activation in these infants (14, 18). However, levels of complement factors are also lower in preterm infants, as their capacity to synthetize them is diminished (19). Overall, levels of IgG in preterm infants have been correlated to the risk of neonatal sepsis, but providing these infants prophylactic immunoglobulins does not prevent sepsis (20, 21). A Cochrane review found that infusion of immunoglobulins led to a slight reduction in nosocomial infections, but did not affect the incidence of neonatal sepsis or overall mortality (22). Likewise, providing specific anti-staphylococcal IgG, did not prevent infection with CoNS (23). Finally, administration of intravenous IgG during neonatal sepsis had no effects on clinical outcomes (24).

Oral administration of IgG to preterm infants has been speculated to prevent NEC as immunoglobulins may survive passage through the gastrointestinal tract (25). In two randomized controlled trials, orally administered human IgG and IgA reduced NEC incidence in preterm infants (26, 27), but a later Cochrane review concluded that there was no overall effect of oral IgG on NEC incidence in preterm infants (28). In other studies, enteral feeding with either porcine or bovine colostrum to preterm pigs prevented NEC, and improved gut maturation and parameters of systemic immunity (29–33). Feeding of porcine plasma (PP) has also been shown to improve survival, growth and diarrhea resistance in growing pigs (34), probably mediated by diminished pro-inflammatory and increased anti-inflammatory responses in both gut and lung derived immune cells (35–37). Dietary PP supplementation was not associated with adverse events in healthy or malnourished infants (38, 39) and oral immunoglobulins improved gut symptoms, recovery and virus clearance in children with rotavirus diarrhea (40). Collectively, the above studies suggest that feeding immunoglobulin rich milk diets improves the response to bacteremia in immature animals and humans. Regardless, the mechanisms remain unclear and until now scientific results have not led to general recommendations to feed immunoglobulin enriched diets to bacteremia sensitive infants. Thus, it remains unknown how postnatal age, diet (e.g., mother's own milk, formula, donor milk), type of immunoglobulin (IgG, IgA and their species specificity) affect systemic immune responses.

Bovine colostrum (BC), the first milk after birth in cows, is rich in immunoglobulins and other immunomodulatory factors (41), inhibits growth of *Staphylococcus epidermidis* (SE) *in vitro* (42) and prevents septic shock and neuroinflammation in newborn preterm pigs (within 2 d of birth), relative to pigs not fed enterally (43). To further validate preterm pigs as models for preterm infants sensitive to blood stream infections, we investigated responses to SE infection across five different experiments with varying postnatal ages and exposures to immunoglobulin-containing diets. First, we compared the effect of SE infusion on newborn preterm and term pigs lacking maternal immunoglobulins and enteral feeding. Then we tested effects of feeding BC or infant formula (IF) to preterm pigs infected shortly after birth or 2 days later, with or without immunization with maternal plasma. Finally, we tested the effects of feeding preterm pigs IF, supplemented with porcine plasma, for 3 days, followed by SE inoculation.

MATERIALS AND METHODS

Animal Experimental Procedures

In five separate experiments, 145 piglets from 10 pregnant sows [(Landrace x Large White) x Duroc crossbreeds] were delivered by cesarean section at the 106th day (preterm birth, ∼90% gestation) or 116th (term birth, ∼100% gestation) day of gestation. Animals were housed in individual, heated (37°C) and ventilated incubators with 1–2 l/min oxygen supply. Shortly after delivery, animals were fitted with orogastric catheters (6 Fr, Portex, Kent, UK) for enteral feeding and vascular catheters (4 Fr, Portex) into the dorsal aorta via the transected umbilical cord for arterial access. Both control and infected animals were euthanized according to predefined humane endpoints. All animal procedures were approved by the Danish National Committee on Animal Experimentation.

Across all experiments, animals were stratified by birth weight and randomly allocated to treatment groups. In *Experiment 1*, preterm ($n = 23$) and term ($n = 21$) pigs were inoculated with either SE (SE-PRE, $n = 15$; SE-TERM, $n = 14$) or control saline (CON-PRE, $n = 8$; CON-TERM, $n = 7$) within 2 h after birth. Animals received no enteral nutrition and were followed for 48 h. In *Experiment 2*, preterm pigs ($n = 15$) were inoculated with SE 2 h after birth and were fed either BC (SE-BC, $n = 8$) or IF (SE-IF, $n = 7$) and followed for 12 h. In *Experiment 3*, preterm pigs were fed either BC or IF for further 2 days, and inoculated

TABLE 1 | Overview of experiments.

Experiment	Gestational age at birth	Saline controlled	Supplemental maternal immunity*	Age at SE infusion	Follow-up time	Diet comparison	Enteral volumes
1	Term or preterm	+	-	2 h	48 h	-	-
2	Preterm	-	-	2 h	12 h	BC vs. IF	40–56 ml/kg/d
3	Preterm	+	+	48 h	48 h	BC vs. IF	40–56 ml/kg/d
4	Preterm	-	-	48 h	24 h	BC vs. IF	40–56 ml/kg/d
5	Preterm	-	+	72 h	24 h	PP vs. IF	24–120 ml/kg/d

**Animals immunized with systemic infusion of maternal plasma. BC, bovine colostrum; IF, infant formula; PP, porcine plasma; SE, Staphylococcus epidermidis.*

TABLE 2 | Diet compositions, energy, and macronutrient contents.

Diet	Product	Amount (g/L)	Energy (kJ/L)	Protein (g/L)	Carbohydrate (g/L)	Fat (g/L)
BC			4,416	121	20	54
	Bovine colostrum powder*	203				
IF			3,990	73	42	56
	Lacprodan DI-9224†	70				
	Pepdite‡	80				
	SHS Liquigen MCT‡	75				
PP			3,940	81	35	53
	Lacprodan DI-9224†	70				
	Pepdite‡	66.5				
	AP 820 porcine plasma#	13.5				
	SHS Liquigen MCT‡	75				

**Biofiber-Damino (Gesten, Denmark), †Arla Foods Ingredients (Aarhus, Denmark), ‡Nutricia (Allerød, Denmark), #APC Europe (Barcelona, Spain). BC, bovine colostrum; IF, infant formula; PP, porcine plasma.*

with SE (SE-BC, $n = 13$; SE-IF, $n = 13$) or control saline (CON-BC, $n = 9$; CON-IF, $n = 12$) and followed for 48 h. Further, these animals were infused with maternal plasma to confer a low level of maternally-derived IgG similar to preterm infants. In *Experiment 4*, in an attempt to increase the sensitivity to SE, preterm pigs were fed BC (SE-BC, $n = 10$) or IF (SE-IF, $n = 10$) for 2 days, but not infused with maternal plasma before receiving a systemic SE challenge. In *Experiment 5*, preterm pigs, supplemented with maternal plasma, were fed with a PP enriched IF (SE-PP, $n = 11$) or a control IF (SE-IF, $n = 8$) and received a systemic SE challenge after 3 days. An overview of conditions in the five experiments is shown in **Table 1**.

Feeding Regimens and Bacterial Administration

In *Experiment 1,* animals received no enteral feed and were kept on 6 ml/kg/h of total parenteral nutrition. In *Experiments 2, 3,* and *4*, animals were fed 40 ml/kg/d on day 1, increasing to 56 ml/kg/d on day 5 of either BC or IF, with 4–6 ml/kg/h of supplementary parenteral nutrition. In *Experiment 5*, animals were fed 24 ml/kg/d of IF with or without added PP on day 1, increasing to 96–120 ml/kg/d on day 5 with 3 ml/kg/d of supplementary parenteral nutrition.

The BC powder was produced from first and second milking of Danish Holstein dairy cattle and gently processed to preserve bioactivity (Biofiber Damino, Gesten, Denmark). The IF diet consisted of a nutritionally complete IF powder (Pepdite, Nutricia, Allerød, Denmark) with added whey and medium chain triglycerides. In the PP enriched IF diet, a fraction (8%) of the IF powder was replaced with a gently processed porcine plasma powder (AP 920 P APC Europe, Spain). The parenteral formulation used in all experiments (Kabiven, Fresenius Kabi, Bad Homburg, Germany) was supplemented with vitamins and minerals (Soluvit, Vitalipid and Peditrace, all Fresenius Kabi), and modified to meet macronutrient requirements of newborn pigs (30). Detailed diet compositions and macronutrient contents are presented in **Table 2**.

In *Experiments 3* and *5*, animals were supplemented with a vascular infusion of 16 ml/kg body weight maternal plasma within the first 24 h after birth. This was done to confer some level of immunoglobulins, mimicking the situation in preterm infants.

Preparation of the SE inoculum was performed, as previously described (43). Briefly, wildtype SE strain 1,457 (a kind gift from Dr. Xiaoyang Wang, University of Gothenburg, Sweden) was incubated for 17 h in tryptic soy broth, enumerated with spectrophotometry and a working solution containing 1.67×10^9 colony forming units (CFU)/ml in sterile saline was prepared. Animals received 5.0×10^9 CFU/kg body weight SE as a continuous arterial infusion over 3 min. A similar volume of sterile saline was administered to control animals in *Experiments 1* and *3*.

Clinical Assessment and Euthanasia

Animals were monitored and clinically assessed (gastrointestinal symptoms, circulation, respiration, consciousness) at least every 3 h prior to, and continuously after SE administration. Animals were euthanized if they showed clinical signs of circulatory and/or respiratory collapse (Pale skin, cold extremities, cyanosis, lethargy, irregular/shallow breathing and/or bradycardia). Rectal temperature was measured before and at 6- or 12-h intervals after SE administration. Motor activity was captured by continuous infrared video surveillance of each incubator connected to a motion detection software (PigLWin, Ellegaard Systems, Faaborg, Denmark).

Sample Collection

Arterial blood was collected at regular intervals after SE administration for hematology and blood gas analysis. After a follow up period of 12–48 h, animals were sedated with 0.1 ml/kg Zoletil mixture, mixed blood was drawn by cardiac puncture and euthanasia performed with a lethal cardiac injection of barbiturate. In *Experiments 3* and *5*, animals were fed a 5/5% w/v lactulose and mannitol watery solution 3 h before scheduled euthanasia for intestinal permeability measurement. After euthanasia, the abdominal cavity was opened, and urine collected by bladder puncture. Urinary levels of lactulose and mannitol were measured as previously described (30). In *Experiments 3, 4* and *5*, the stomach and intestines were examined, and gastrointestinal pathology graded according to an established NEC scoring system (30). Specifically, in *Experiment 3*, the left hind leg was released at the hip joint, and femur dissected and sterilized in ethanol. Using a sterile scalpel, bone marrow was dissected at the distal epiphysis and a biopsy was obtained for bacterial enumeration.

Blood Analyses

Enumeration of SE was determined in blood samples taken 3, 6, and 12 h after SE inoculation in *Experiment 2* and at euthanasia in *Experiments 3* and *4*, as previously described elsewhere (43). Briefly, whole blood was cooled after collection, stepwise diluted in sterile saline (undilute, 1:10 and 1:100), plated out on agar plates and incubated for 24 h at 37°C.Colonies were counted and identification of bacteria was performed by Matrix Assisted Laser Desorption/Ionization-Time of Flight Mass Spectrometry. In a similar manner, bacterial enumeration, and identification in bone marrow homogenate were performed in *Experiment 3*.

In *Experiments 3, 4,* and *5*, levels of bovine and porcine IgG in euthanasia blood plasma samples were measured by enzyme-linked immunosorbent assay (ELISA) using species specific antibodies (AAI23AB and AAI41, Bio-Rad, Kidlington, UK). Blood hematology was performed using the Advia 2120i Clinical Chemistry System (Siemens Healthcare GmbH, Erlangen, Germany). In plasma samples from euthanasia from *Experiments 1, 3, 4,* and *5*, we determined levels of soluble terminal complement complex by ELISA (sC5b-9, OptEIA, BD Biosciences, Eysins, Switzerland). Additionally, in *Experiments 3* and *4*, plasma levels of tumor necrosis factor alpha (TNF-α) and interleukin 6 (IL-6) were determined by ELISA (porcine DuoSet DY686 and DY690B, R&D systems, Abingdon, UK).

Arterial blood gas was measured in *Experiments 1, 2,* and *4*, using a GEM Premier 3000 (Instrumentation Laboratory, MA, USA). Hemostatic function in citrate stabilized whole blood was tested in *Experiment 5* by thromboelastography (TEG) using a TEG 5000 Hemostasis Analyzer System (Haemonetics, Braintree, MA, USA).

T cell phenotyping in whole blood at 12, 24, and 48 h (euthanasia) after SE inoculation was done in *Experiment 3* by flow cytometry. Briefly, whole blood samples were subjected to red blood cell lysis, fixation and permeabilization before Fc-receptor blocking using porcine serum. Next, cells were stained for 30 min with CD3-PerCP Cy5.5 (clone BB23-8E6-8C8, BD biosciences, Eysins, Switzerland), CD4a-FITC (clone MIL17, Bio-Rad), CD8α-PE (clone MIL12, Bio-Rad) and Foxp3-APC (clone FJK-16s, ThermoFisher Scientific, Waltham, MA, USA) or respective isotype controls PerCP Cy5.5 mouse IgG2a (clone G155-178, Becton Dickinson), FITC mouse IgG2b (clone MCA691, Bio-Rad), PE mouse IgG2a (clone OX-34, Bio-Rad) or APC mouse IgG2a (clone eBR2a, ThermoFisher Scientific). Samples were acquired on a BD Accuri C6 Plus (BD Biosciences, Eysins, Switzerland) and analyzed using BD Accuri software. The fractions of total T cells ($CD3^+$), CD4 positive T cells ($CD3^+CD4^+CD8^-$), CD8 positive T cells ($CD3^+CD4^-CD8^+$), double positive T cells ($CD3^+CD4^+CD8^+$) and regulatory T cells ($CD3^+CD4^+FOXP3^+$) were determined. Due to the limitation on antibodies used, the CD8 positive T cell population would include cytotoxic T cells as well as γδ T cells and CD8 positive NK cells. Both these cell types are estimated to account for 1% of CD8 positive T cells in pigs (44, 45).

Neutrophil phagocytic function was investigated in *Experiments 3* and *5*, using a commercial kit (pHRodo, ThermoFisher, Roskilde, Denmark), as described elsewhere (46). Briefly, whole blood was incubated at 37°C for 30 min with phrodo conjugated *E. coli.* Afterwards the samples were run on the above mentioned flow cytometer and the neutrophil population was identified. The phagocytic rate was defined as the fraction of neutrophils with internalized bacteria and phagocytic capacity as the median fluorescent intensity of neutrophils.

Statistics

All statistics were performed in STATA v. 14.2 (StataCorp, Texas, USA). Continuous data were analyzed by a linear mixed effects model with litter as a fixed factor. Due to the factorial design of *Experiments 1* and *3,* we used a linear multilevel model to determine interactions between gestational age (*Experiment 1*) or diet (*Experiment 3*) and SE inoculation. For significant results a *post hoc* group comparison by Tukey's test, these results are reported in the text of the results section. If data were not normally distributed, logarithmic transformation was performed. Data that did not conform to normal distribution after transformation was analyzed by Kruskal Wallis' test. Categorical data was analyzed by Chi^2 test. Overall, $p < 0.05$ were considered significant and those under 0.1 as tendency to effect. Unless stated otherwise, data shown in text are presented as means with corresponding standard errors and *p*-values.

RESULTS

Experiment 1

In this experiment, to investigate the influence of gestational age on the response to SE inoculation, we tested the effects of SE or saline infusion (SE or CON) shortly after term or preterm birth (TERM or PRE). Resulting in four groups: SE-TERM, SE-PRE, CON-TERM, and CON-PRE.

One animal in the CON-TERM group died due to bleeding from the catheter shortly after SE inoculation and was excluded from the analysis. In the SE-PRE group, 53% (8/14) of animals were euthanized ahead of schedule, compared to only 12.5% (1/8) of CON-PRE pigs (**Figure 1A**). For the term animals, 14% (2/14) of SE-TERM were euthanized early (both within 24 h of SE inoculation) compared with none (0/6) of CON-TERM pigs. Considering the high clinical affection from the SE infusion, remaining preterm pigs were euthanized after 24 h.

Motor activity was higher in term animals after 6 h but decreased by SE in both term and preterm animals at 12 and 18 h (**Figure 1B**). Term animals showed increased body temperature after 2 h and SE led to increased body temperature at 6 and 24 h in both term and preterm animals (**Figure 1C**). *Post hoc* testing showed higher body temperatures in SE-TERM vs. SE-PRE pigs for all time points after 2 h (*post hoc* test, all $p < 0.05$). Blood pH decreased after SE inoculation with corresponding increases in lactate levels at 12 h (**Figures 1D,E**), which was more pronounced in SE-PRE vs. SE-TERM pigs (*post hoc* test, $p < 0.001$). Total leucocyte and neutrophil numbers increased less in SE-PRE vs. SE-TERM pigs (**Table 3**). In addition, SE inoculation reduced the platelet and leucocyte counts after 12 h, the latter explained mainly by reductions in neutrophil and lymphocyte numbers. This reduction persisted after 24 h for lymphocytes and platelets while neutrophil counts then increased, but only in SE-TERM animals (e.g., significant gestational age × SE interaction, **Table 3**). Levels of sC5b-9 in plasma at euthanasia tended to be lower for SE-TERM vs. CON-TERM animals (15 ± 3 vs. 26 ± 8 ng/mL, $p = 0.06$), while for surviving preterm animals, there

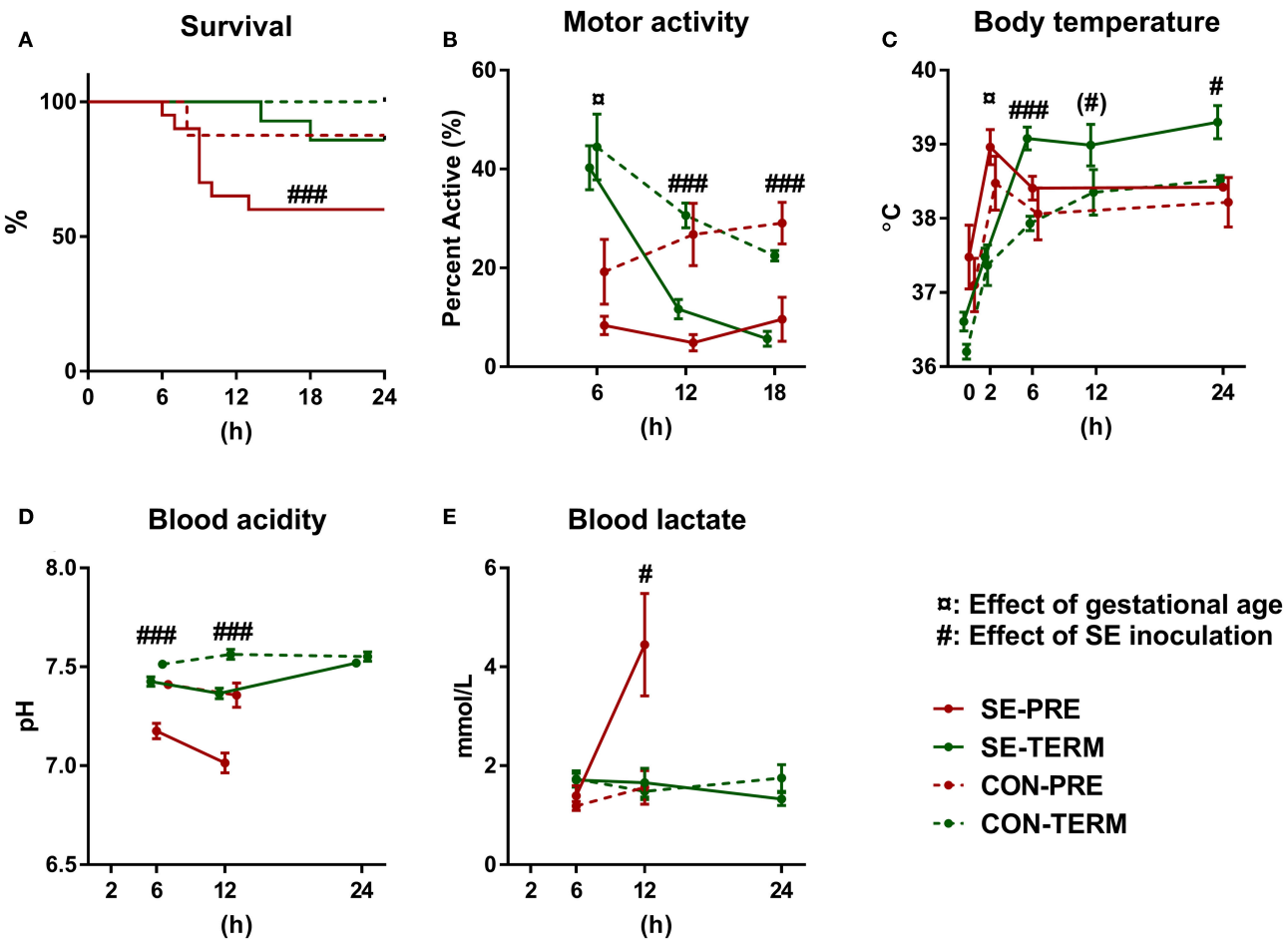

FIGURE 1 | Preterm birth increases susceptibility to Staphylococcus epidermidis bacteremia. Results of *Experiment 1* comparing term (TERM) and preterm (PRE) pigs infused with *Staphylococcus epidermidis* (SE) or saline (CON) immediately after birth, without any enteral feeding. **(A)** Survival rates 24 h post inoculation. **(B)** Motor activity, shown as the fraction of time when pigs were physically moving at 2–18 h post inoculation. **(C)** Body temperature 2–24 h post inoculation. **(D)** Blood pH 6–24 h post inoculation. **(E)** Blood lactate levels 6–24 h post inoculation. **(A)** Presented as Kaplan Meyer curves. **(B–E)** Presented as means with corresponding standard errors. (#): Effect of SE ($p \leq 0.1 \geq 0.05$), #: Effect of SE ($p < 0.05$), ###: Effect of SE ($p < 0.001$), ¤: Effect of gestational age ($p < 0.05$).

TABLE 3 | Hematological parameters in *Experiment 1*.

	Time after SE (hours)	SE-PRE	CON-PRE	SE-TERM	CON-TERM	p interaction	p SE effect	p gestation
Total leucocytes (10^9 cells/L)	12	1.0 (0.2)	3.1 (0.5)	2.3 (0.9)	4.2 (0.2)	NS	<0.001	<0.05
	24	2.0 (0.5)	3.3 (0.5)	5.4 (1.0)	4.3 (0.5)	NS	NS	NS
	48	-	-	7.5 (0.6)	4.5 (0.4)	-	<0.001	-
Neutrophils (10^9 cells/L)	12	0.3 (0.1)	1.1 (0.2)	1.4 (0.5)	2.6 (0.1)	NS	<0.001	<0.001
	24	0.5 (0.1)	1.4 (0.2)	3.0 (0.6)	2.6 (0.2)	<0.01	NS	<0.001
	48	-	-	3.6 (0.3)	2.6 (0.5)	-	NS	-
Lymphocytes (10^9 cells/L)	12	0.7 (0.1)	1.9 (0.3)	0.3 (0.1)	1.5 (0.1)	<0.01	<0.001	NS
	24	1.5 (0.5)	1.8 (0.3)	0.7 (0.2)	1.6 (0.3)	NS	<0.01	NS
	48	-	-	2.3 (0.2)	1.8 (0.2)	-	<0.05	-
Monocytes (10^9 cells/L)	12	0.0 (0.0)	0.1 (0.0)	0.0 (0.0)	0.1 (0.0)	NS	<0.05	NS
	24	0.0 (0.0)	0.1 (0.0)	0.0 (0.0)	0.1 (0.0)	NS	NS	NS
	48	-	-	0.2 (0.0)	0.0 (0.0)	-	<0.001	-
Platelets (10^9cells/L)	12	247 (8)	331 (8)	206 (11)	359 (15)	<0.05	<0.001	NS
	24	181 (15)	322 (20)	202 (10)	314 (21)	NS	<0.001	NS
	48	-	-	123 (8)	211 (26)	-	<0.001	-

Hematological parameters for preterm (PRE) or term (TERM) animals, infused with Staphylococcus epidermidis (SE) or saline (CON). Data presented as means with corresponding standard error, p < 0.1 are presented p < 0.05 are considered significant. NS, Not significant.

was no difference between groups (35 ± 7 vs. 27 ± 8 ng/mL for SE-PRE and CON-PRE, respectively, $p > 0.1$). However, levels tending to be increased in animals euthanized prematurely compared with those that survived (42 ± 4 vs. 31 ± 5 ng/mL, $p = 0.06$).

Experiment 2

In this experiment we investigated if clearance of SE from the bloodstream was affected by enteral feeding of BC vs. IF. Preterm pigs infused with SE shortly after birth and fed either BC (SE-BC) or IF (SE-IF) and followed for 12 h.

No animals were euthanized before the end of the 12 h follow up period. Due to the short intervals between blood samplings and intensive handling of the pigs, data on movement activity and body temperature were not collected. The SE-BC group showed consistently lower levels of SE in blood, though only significantly after 3 and 12 h (**Figure 2A**). Blood lactate tended to be lower in SE-BC after 3 h (**Figure 2B**) and standard bicarbonate after 6 h (**Figure 2C**) whereas blood pH did not differ between groups (**Figure 2D**). Likewise, there was no difference in total leucocyte, neutrophil or lymphocyte counts 12 h after infusion of SE (**Figure 2E**).

Experiment 3

In this experiment, investigating if 2 days of BC feeding improves systemic responses to SE, preterm pigs received maternal plasma and were fed either BC or IF until postnatal day 2 where they were infused with either SE or saline (CON). Resulting in four groups: SE-BC, SE-IF, CON-BC and CON-IF.

There was no difference in the proportion of animals euthanized prematurely, with 12% (4/24) in the SE groups and 5% (1/22) in CON ($p > 0.1$) and these few animals all showed signs of severe NEC upon necropsy. SE inoculation led to increased body temperature in both SE-BC and SE-IF groups, lasting for at least 48 h (**Figure 3A**). There was no effect of SE on motor activity, but IF-fed pigs showed reduced activity compared with BC-fed pigs (**Figure 3B**).

No effect of SE inoculation or interaction with diet was observed for the neutrophil phagocytic rate or capacity (**Figures 3C,D**). For cellular immune parameters, there were no interactions between SE and diet but SE inoculation alone led to several effects, the most important being lower total leucocytes and monocyte counts at 12 and 24 h, corresponding with lower lymphocyte and platelet counts at 12, 24, and 48 h in the SE inoculated groups (**Table 4**). Diet in itself had little impact on the hematological parameters (**Table 4**) T cells were also affected by SE infection, with a lower total T cell fraction at 12 h and lower CD4 positive T cell fraction at 24 h (**Figures 3E,F**). There were no differences observed for CD8 positive or regulatory T cells (**Figures 3G,H**). Also, there were no differences in fractions of double positive T cells between the groups at any time point (data not shown).

No interactions between SE and diet were seen for non-immunological hematological parameters, although SE alone led to increased hemoglobin and hematocrit values in the SE groups at 12, 24, and 48 h (**Table 4**). SE inoculation also led to increased relative spleen weight (3.2 ± 0.1 vs. 2.3 ± 0.1 g/kg, $p < 0.001$) but no other organ weights were affected by SE inoculation.

There were similar levels of SE CFUs in bone marrow of SE-BC and SE-IF pigs ($1.1 \times 10^9 \pm 7.0 \times 10^8$ vs. $4.7 \times 10^8 \pm 2.1 \times 10^8$ CFU/mL, $p < 0.1$). *Staphylococcus aureus* and *Enterococcus spp.* were also detected in the bone marrow and these were less prevalent in BC vs. IF animals (3 vs. 26%, $p < 0.05$). Levels of porcine IgG were similar in all four groups (overall mean 406 ± 18 mg/L), however the levels of bovine IgG were significantly higher in the groups fed BC (**Figure 3I**), making overall IgG levels higher in BC fed animals compared to IF (572 ± 40 vs. 406 ± 28 mg/L, $p < 0.001$). There was no influence of SE infection

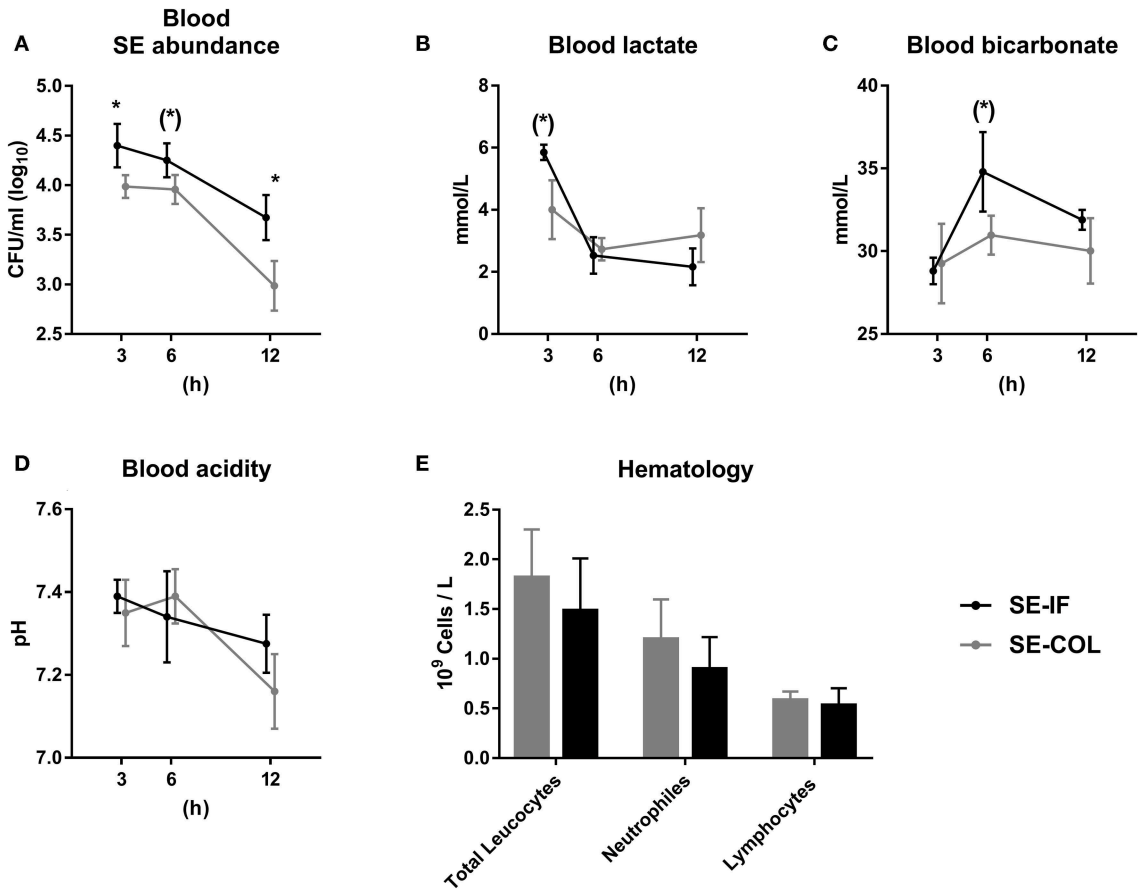

FIGURE 2 | Feeding of bovine colostrum improves clearance of *Staphylococcus epidermidis* in newborn preterm pigs. Results of *Experiment 2* comparing preterm pigs infused with *Staphylococcus epidermidis* (SE) immediately after birth and fed either bovine colostrum or infant formula. **(A)** Abundance of SE in blood 3–12 h post inoculation, shown as colony-forming units per milliliter of whole blood. **(B)** Blood lactate levels 3-12 h post inoculation. **(C)** Blood bicarbonate levels 3–12 h post inoculation. **(D)** Blood pH 3–12 h post inoculation. **(E)** Total leucocyte, neutrophil and lymphocyte counts, taken 12 h post inoculation. **(A–E)** Presented as means with corresponding standard errors. (*): Effect of diet ($p \leq 0.1 \geq 0.05$), *Effect of diet ($p < 0.05$).

on porcine or bovine IgG levels. For gut related parameters, milk diet influenced the lactulose/mannitol ratio, in that ratios were lower in BC vs. IF animals (2.6 ± 0.5 vs. 18.2 ± 3.3%, $p < 0.001$). Incidence of NEC was also lower in BC fed animals over IF (29 vs. 72 %, $p < 0.01$). No direct effects of SE were observed for the gut related parameters.

Regardless of diet, the levels of sC5b-9 were lower in SE inoculated than in CON animals (15 ± 4 vs. 22 ± 4 ng/mL, $p < 0.05$), whereas levels of TNF-α (102 ± 30 vs. 62 ± 11 pg/mL, $p > 0.1$) or IL-6 (430 ± 136 vs. 329 ± 69 pg/mL, $p > 0.1$) did not differ. There was no influence of diet on levels of sC5b-9, TNF-α or IL-6 (data not shown).

Experiment 4

To further investigate the effects of BC feeding we increased the overall susceptibility to infection by withholding maternal plasma in all animals. As in *Experiment 3*, preterm pigs were fed either BC or IF for 2 days where after all animals were inoculated with SE, resulting in two groups: SE-BC and SE-IF.

There were no differences in body temperature between pigs fed BC or IF (**Figure 4A**), but motor activity was highest in the SE-BC pigs (**Figure 4B**). The SE-BC group showed higher blood acidity 6 h after SE inoculation (**Figure 4C**) together with higher oxygen pressure (**Figure 4D**) and bicarbonate at 24 h (**Figure 4E**). Milk diets did not markedly influence hematology except the reduced monocyte and elevated red blood cell counts at 6–12 h in SE-BC vs. SE-IF pigs (**Supplementary Table 1**).

In this experiment, we also collected plasma 6 and 12 h after inoculation. Levels of TNF-α were increased at 6 h after the SE challenge and dropped throughout the study, with no difference between SE-BC and SE-IF (**Figure 4F**). Likewise, sC5b-9 levels were elevated 6 h after inoculation with no difference between BC and IF fed animals, and hardly detectable after 24 h (**Figure 4G**). In addition, plasma levels of IL-6 at euthanasia did not differ between SE-BC and SE-IF (336 ± 67 vs. 351 ± 42 pg/mL, $p > 0.1$). At 24 h, the majority of administered SE was cleared from the blood stream with no difference in clearance capacity between groups (**Figure 4H**). Levels of porcine IgG also did not differ between SE-BC and SE-IF (6 ± 2 vs. 4 ± 1 mg/L, $p > 0.1$), but

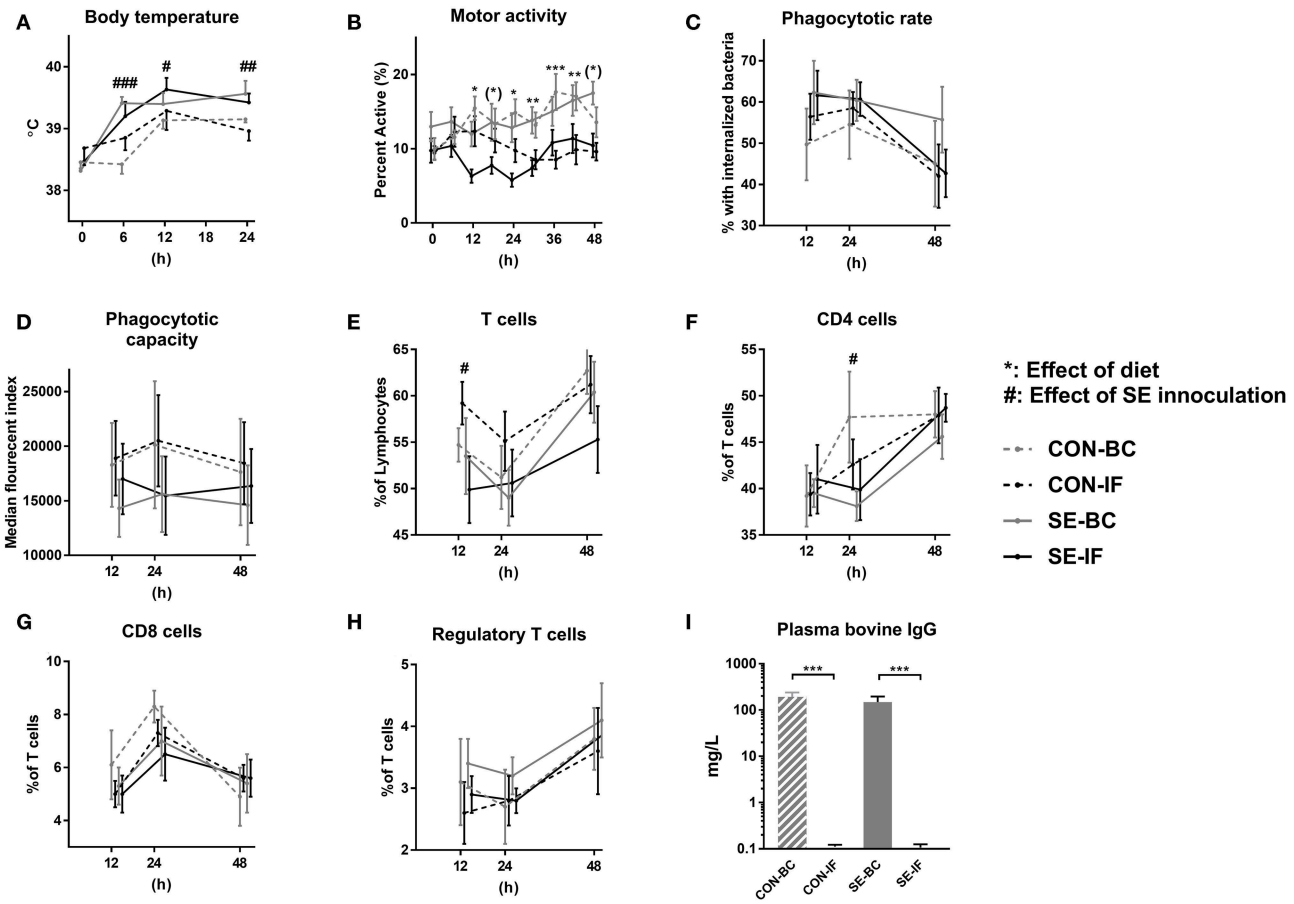

FIGURE 3 | Two days of bovine colostrum feeding has no impact on response to *Staphylococcus epidermidis* bacteremia. Results of *Experiment 3* comparing preterm pigs infused with *Staphylococcus epidermidis* (SE) or saline (CON) at day 3, after being infused with maternal plasma and fed bovine colostrum (BC) or infant formula (IF) from after birth. **(A)** Body temperature 0–48 h post inoculation. **(B)** Motor activity, shown as the fraction of time with physical activity at 0–48 h post inoculation. **(C)** Neutrophil phagocytic rate 12–48 h post inoculation, defined as fraction of neutrophils with internalized bacteria. **(D)** Neutrophil phagocytic capacity 12–48 h post inoculation, defined as median fluorescent index of neutrophils with internalized bacteria. **(E)** T cells 12–48 h post inoculation, defined as fraction of CD3 positive lymphocytes. **(F)** CD4 cells 12–48 h post inoculation, defined as the CD4 positive, CD8 and FOXP3 negative fraction of T cells. **(G)** CD8 cells 12–48 h post inoculation, defined as the CD8 positive, CD4 and FOXP3 negative fraction of T cells. **(H)** Regulatory T cells 12–48 h post inoculation, defined as the FOXP3 and CD4 positive, CD8 negative fraction of T cells. CD4 positive as fraction **(I)** Plasma levels of bovine immunoglobulin G (IgG) at euthanasia. **(A–I)** Presented as means with corresponding standard errors. #: Effect of SE ($p < 0.05$), ##: Effect of SE ($p < 0.01$), ###: Effect of SE ($p < 0.001$), (*): Effect of diet ($p \leq 0.1 \geq 0.05$), *: Effect of diet ($p < 0.05$), **: Effect of diet ($p < 0.01$), ***: Effect of diet ($p < 0.001$).

as expected, levels were much lower than in *Experiment 3*. Bovine IgG levels were significantly higher in SE-BC (**Figure 4I**), making overall IgG levels higher (209 ± 42 vs. 5 ± 1 mg/L, $p < 0.001$). For gut related parameters, mean NEC incidence was lower in SE-BC than SE-IF pigs, although not significantly (33 vs. 71%, $p > 0.1$). In addition, SE-BC pigs showed higher relative weight of the proximal small intestine (10.2 ± 0.5 vs. 7.3 ± 0.7, $p < 0.001$), relative to SE-IF.

Experiment 5

To investigate if oral feeding of porcine immunoglobulins affected the systemic response to SE, preterm pigs were fed IF with or without added porcine plasma proteins (PP) for 3 days, at which time all animals were inoculated with SE, resulting in two groups: SE-IF and SE-PP.

One animal was euthanized ahead of time from the SE-PP group with signs of NEC at necropsy. Like in the previous studies, body temperature rose after SE inoculation, but the changes were not affected by PP supplementation (**Figure 5A**) and neither was motor activity (**Figure 5B**). Like in *Experiment 4*, most of the administered SE were cleared from the blood stream 24 h after infection, but again, with no effect of PP supplementation (**Figure 5E**).

At baseline, monocyte counts were higher in SE-PP than SE-IF pigs (data not shown). After SE inoculation, total leucocyte counts and lymphocyte counts (**Figures 5C,D**) were higher in SE-PP vs. SE-IF pigs at 12 h. No other differences in hematological or hemostatic parameters were observed (**Supplementary Table 2**). Levels of sC5b-9 (18.5 ± 8.2 vs. 5.8 ± 2.0 ng/mL, $p > 0.1$) and porcine immunoglobulins (**Figure 5F**) did not differ between

TABLE 4 | Hematological parameters in *Experiment 3*.

	Time after SE (hours)	SE-IF	SE-BC	CON-IF	CON-BC	p interaction	p SE	P diet
Total leucocytes (10^9 cells/L)	12	1.5 (0.4)	2.0 (0.7)	2.2 (1.0)	2.9 (0.7)	NS	<0.01	<0.05
	24	1.6 (0.4)	2.1 (1.0)	2.3 (1.0)	2.8 (1.0)	NS	0.06	NS
	48	2.7 (0.9)	2.3 (0.5)	2.4 (0.8)	2.7 (0.7)	NS	NS	NS
Neutrophils (10^9 cells/L)	12	0.8 (0.3)	1.3 (0.6)	0.8 (0.5)	1.2 (0.7)	NS	NS	NS
	24	0.8 (0.3)	1.2 (0.9)	0.8 (0.4)	1.3 (0.9)	NS	NS	NS
	48	1.1 (0.6)	1.3 (0.4)	0.9 (0.4)	1.4 (0.7)	NS	NS	NS
Lymphocytes (10^9 cells/L)	12	0.5 (0.1)	0.6 (0.2)	1.3 (0.9)	1.6 (0.8)	NS	<0.001	NS
	24	0.7 (0.2)	0.8 (0.4)	1.3 (0.9)	1.3 (0.8)	NS	<0.01	NS
	48	1.0 (0.3)	0.8 (0.3)	1.1 (0.5)	1.1 (0.2)	NS	<0.05	NS
Monocytes (10^9 cells/L)	12	0.05 (0.06)	0.05 (0.05)	0.05 (0.03)	0.09 (0.07)	NS	<0.05	NS
	24	0.04 (0.02)	0.04 (0.02)	0.07 (0.03)	0.08 (0.06)	NS	<0.05	NS
	48	0.21 (0.26)	0.05 (0.02)	0.11 (0.07)	0.19 (0.10)	NS	NS	NS
Platelets (10^9cells/L)	12	141 (24)	170 (33)	370 (278)	409 (188)	NS	<0.001	NS
	24	154 (43)	209 (61)	413 (230)	455 (186)	NS	<0.001	NS
	48	225 (49)	257 (61)	341 (81)	496 (153)	NS	<0.001	<0.05
Red blood cells (10^{12}cells/L)	12	3.6 (0.5)	3.6 (0.4)	3.6 (0.6)	3.4 (0.7)	NS	NS	NS
	24	3.3 (0.4)	3.4 (0.4)	3.5 (0.6)	3.3 (0.8)	NS	NS	NS
	48	3.1 (0.2)	3.0 (0.2)	3.1 (0.6)	2.7 (0.6)	NS	NS	NS
Hemoglobin (g/L)	12	4.8 (0.7)	4.7 (0.5)	4.4 (0.9)	3.9 (0.8)	NS	<0.01	NS
	24	4.4 (0.5)	4.4 (0.5)	4.3 (0.8)	3.7 (0.8)	NS	<0.05	NS
	48	4.0 (0.3)	4.1 (0.2)	4.0 (0.8)	3.4 (0.5)	NS	<0.05	NS
Hematocrit (%)	12	26.7 (3.9)	25.9 (2.4)	24.9 (4.6)	22.7 (3.7)	NS	<0.05	NS
	24	24.8 (2.9)	24.6 (2.1)	24.3 (4.2)	21.5 (4.3)	NS	<0.05	NS
	48	22.0 (1.7)	22.5 (0.9)	22.4 (4.2)	19.0 (3.7)	NS	<0.05	NS

Hematological parameters for preterm animals, immunized with maternal plasma, infused with Staphylococcus epidermidis (SE) or saline (CON) and fed either bovine colostrum (BC) or infant formula (IF). Data presented as means with corresponding standard error, $p < 0.1$ are presented $p < 0.05$ are considered significant. NS, Not significant.

the SE-PP and SE-IF groups. Supplementation with PP had no significant effect on NEC incidence (60 vs. 33%, $p > 0.1$), lactulose/mannitol ratio (9 ± 2 vs. 5 ± 1%, $p > 0.1$) or weight of internal organs (data not shown, all $p > 0.1$).

DISCUSSION

Bacterial infection remains a major contributor to neonatal mortality in preterm infants and understanding the response of preterm infants to bacteremia is key for early diagnosis and treatment. Postnatal immune system maturation in preterm infants is not well-understood and may be influenced by environmental factors, such as diet and microbial colonization in the gut, lungs and skin epithelia. Regardless, it remains unclear how postnatal factors influence systemic immunity development and responses to bacteremia. Using a recently established model of neonatal bloodstream infection, we first demonstrate that preterm pigs were markedly more affected than term pigs by systemic SE exposure shortly after birth, leading to clear signs of sepsis and high mortality. The clinical responses were much less pronounced when similar SE doses were infused after initiation of enteral feeding, either shortly after birth or after 2 days. However, the responses were not markedly affected by the type of milk diet, although BC fed animals showed lower levels of circulating SE when inoculated shortly after birth. After day 3, luminal supplementation with porcine plasma proteins into IF also failed to improve responses. Furthermore, we have done preliminary studies in preterm pigs that showed limited effects of BC feeding for 4 days, relative to un-fed animals on total parenteral nutrition (unpublished observations). Thus, enteral feeding, even with a highly immunomodulatory milk diet like bovine colostrum, is unlikely to influence systemic immunity development and bacteremia responses in preterm neonates beyond its effectiveness in the immediate neonatal period (first 1–2 days after birth), as shown also in our previous study (43). A general effect of enteral feeding on the immune response is possible, as enterally fed animals had lower blood acidity, lactate and mortality both when comparing *Experiments 1* and *2*, and in the previous preterm pig study (43). However, we have not yet fully investigated the effect of early enteral feeding shortly after birth, and further studies are necessary. Whether a similar age or diet dependency of clinical responses to systemic bacterial infection is valid for preterm infants remains to be investigated following different gestational ages, diet regimens and bacterial exposures.

Regarding gestational age, both preterm and term pigs showed clinical and immunological responses to SE exposure shortly after birth (i.e., increasing body temperature, reduced physical activity and blood pH), but these conditions only became fatal in

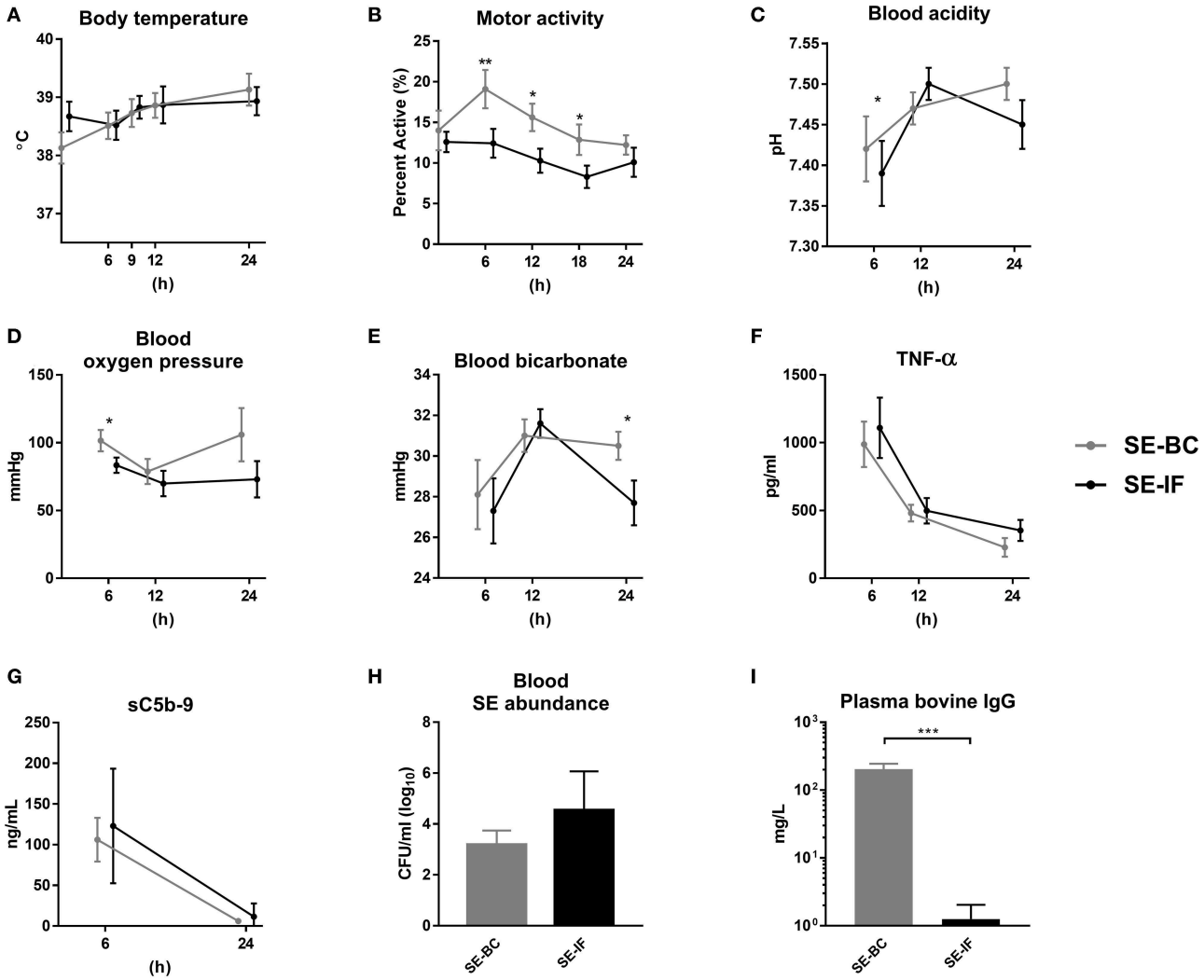

FIGURE 4 | Two days of bovine colostrum feeding has no impact on response to *Staphylococcus epidermidis* bacteremia, even when maternal antibodies are withheld. Results of *Experiment 4* where preterm pigs were infused with *Staphylococcus epidermidis* (SE) on day 3, without any previous immunization (plasma infusion) and fed bovine colostrum (SE-BC) or infant formula (SE-IF). **(A)** Body temperature 0–24 h post inoculation. **(B)** Motor activity, shown as the fraction of time with physical activity at 0–24 h post inoculation. **(C)** Blood pH 6–24 h post inoculation. **(D)** Blood oxygen pressure 6–24 h post inoculation. **(C)** Blood bicarbonate levels 6–24 h post inoculation. **(F)** Plasma levels of tumor necrosis factor alpha (TNF-α) 6–24 h post inoculation. **(G)** Plasma levels of soluble terminal complement complexes (sC5b-9) 6–12 h post inoculation. **(H)** Abundance of SE in blood at euthanasia, shown as colony-forming units per milliliter of whole blood. **(I)** Plasma levels of bovine immunoglobulin G (IgG) at euthanasia. **(A–F)** Presented as means with corresponding standard errors. *: Effect of diet ($p < 0.05$), **: Effect of diet ($p < 0.01$), ***: Effect of diet ($p < 0.001$).

preterm pigs, requiring early euthanasia of half of these animals. Conversely, term pigs maintained a higher body temperature and their neutrophil counts even exceeded baseline levels at 24 h after SE infection. Thus, preterm pigs seemed to have a lower capacity in their bone marrow to replace neutrophils after SE infection challenge. Neutropenia is often observed in preterm infants (47, 48).

In the later preterm pig experiments, preterm animals showed limited diet-dependent differences in systemic responses to SE, beyond the lowered SE levels in newborn preterm pigs (<24 h old) fed BC vs. IF. The other para-clinical outcomes such as leucocyte subsets and blood acidity/lactate did however not differ. In pigs that were fed BC or IF for 2 days before SE inoculation, no clear differences in SE responses could be demonstrated. Also, withholding maternal plasma did not reveal any further effects of feeding BC over IF on the immune response during SE bacteremia.

Consistent with protective effects of feeding BC vs. IF on gut parameters (reduced intestinal permeability and NEC incidence) in this study, BC feeding is associated with a long series of structural, functional and immunological changes locally in the gut of preterm pigs (29–32, 49). In this study, the BC fed animals were less likely to have enteric bacteria (i.e., *Enterococcus* spp. and *Staphylococcus aureus)* in their bone marrow (*Experiment 3)*,

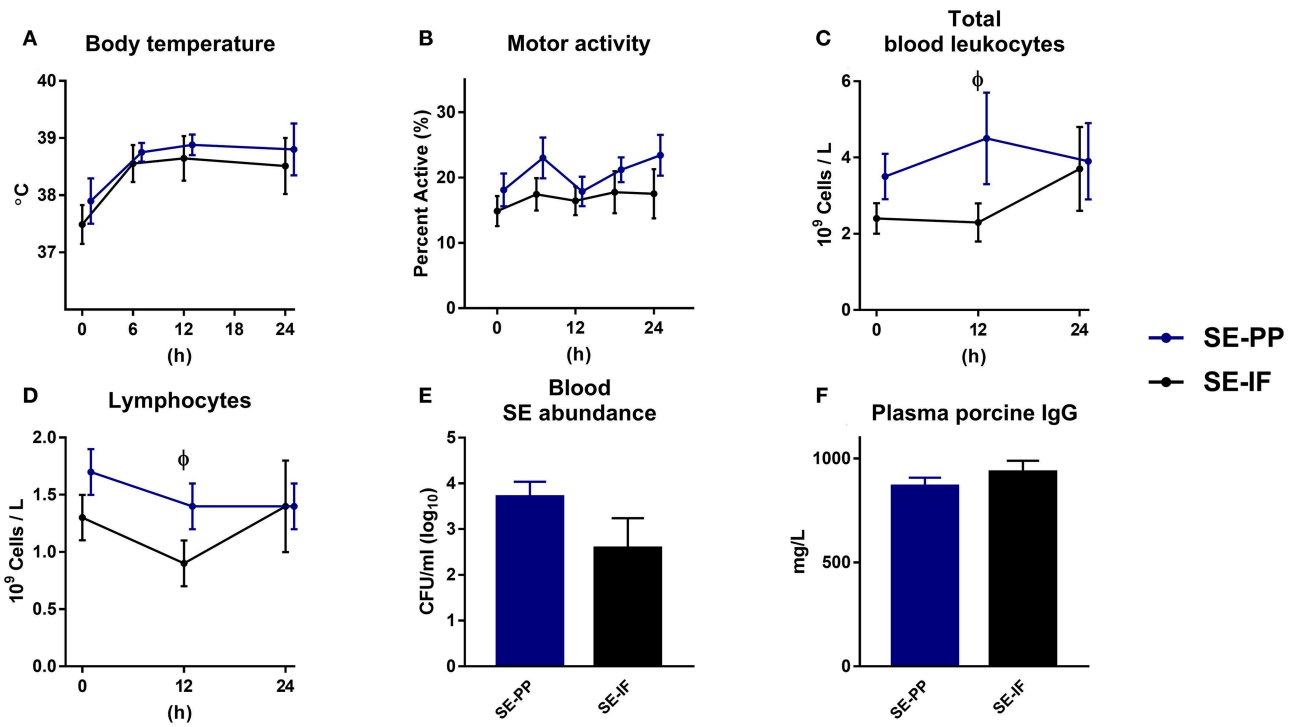

FIGURE 5 | Feeding of infant formula, enriched with porcine plasma, has no effect on responses to *Staphylococcus epidermidis* bacteremia. Results of *Experiment 5* where preterm pigs were infused with *Staphylococcus epidermidis* (SE) on day 4, after infusion of maternal plasma at birth, and then fed infant formula supplemented with porcine plasma powder (SE-PP) or whey protein (SE-IF). **(A)** Body temperature 0–24 h post inoculation. **(B)** Motor activity, shown as the fraction of time with physical movements at 0–24 h post inoculation. **(C)** Total blood leucocyte counts 0–24 h post inoculation. **(D)** Lymphocyte counts in blood, 0–24 h post inoculation **(E)** Abundance of SE in blood at euthanasia, shown colony-forming units per milliliter of whole blood. **(F)** Plasma levels of porcine immunoglobulin G (IgG) at euthanasia. **(A–F)** Presented as means with corresponding standard errors. ϕ: Effect of PP ($p < 0.05$).

suggesting a protective effect of BC against bacterial translocation across the intestine. Also, we consistently found higher levels of motor activity in BC fed animals, suggesting an overall better clinical status. We have previously shown that BC feeding of preterm pigs prevented bacterial translocation within the first 1–2 weeks of life, but not later (29, 50, 51), further suggesting that a critical window exists early after preterm birth where intestinal permeability, and therefore the risk of gut derived systemic infections, can be reduced by protective milk diets. Whether such bioactive milk diets could affect systemic immunity development directly, independent of any maturational and protective effects on the immature gut, remains unclear and may take longer than just a few days after preterm birth to manifest. In preterm infants, risk of sepsis is associated with length of parenteral nutrition (and thereby presence of central catheters), but alleviated by human milk feeding (3). Possibly, direct systemic immune effects of enteral milk diets, beyond the first days after preterm birth, depend on associated changes in the gut microbiota. An observational study in preterm infants has shown that gut dysbiosis, with accumulation of fermentation products, precedes neonatal sepsis (52). However, diet-induced changes to the gut microbiota may occur mainly after the first week of life, as shown in previous studies on preterm pigs (30, 31, 53). This may explain why no marked differences between BC and IF fed animals were apparent for the systemic response to SE.

A clear effect of SE inoculation on several immunological parameters was observed already 12 h after inoculation, including a marked reduction in monocytes, lymphocytes and platelets. Following the SE inoculations, bacteria would permeate the tissues, likely prompting monocytes to leave the vasculature, explaining the reduced number of circulating monocytes. Lymphocytes would mostly stay in the blood stream and we therefore suspect that SE bacteremia induced apoptosis of peripheral lymphocytes, as indicated from adult sepsis. Here, a substantial sepsis-induced loss of helper T cells and B lymphocytes has been observed, compared with trauma patients and non-septic controls (54, 55). Likewise, thrombocytopenia is a common finding in preterm infants with neonatal sepsis (56, 57). Loss of lymphocytes and platelets were observed across experiments in the SE treated groups. Hematocrit and hemoglobin values were generally higher in SE infected animals, likely indicating a greater loss of fluid from the vasculature. Loss of intravascular fluid is a well-known phenomenon in both adult and neonatal sepsis caused by increased capillary permeability (58). Furthermore, we found that circulating levels of sC5b-9 were lower in SE animals indicating that complement factors had been depleted. The sC5b-9 protein complex is the end product

of the complement cascade and only has a half-life of 1–2 h (59), so any product generated by the initial SE inoculation would be gone by 48 h. Complement activation by SE sepsis shortly after birth was seen in *Experiment 1*, as levels were increased in non-surviving animals and in *Experiment 4* with higher levels shortly after SE inoculation. Although enterally fed animals, inoculated after 2 days, were less clinically affected by SE, they remained to have some immunological responses reflecting neonatal sepsis, but with limited effects of milk diet (colostrum, formula), regardless of provision of maternal plasma (*Experiment 3)* or not (*Experiment 4)*. Thus, this experimentally induced bacteremia in preterm pigs mimicked many of the signs and symptoms seen in neonatal sepsis patients.

SE is considered a relatively low-virulent pathogen that would not normally cause serious systemic responses in healthy individuals, but SE is often isolated from preterm infants suspected of sepsis (2). Preterm pigs provide a good model for studying infections in preterm infants, as the overall values for hematological and immunological parameters are similar (46). In addition, the developing pig fetus does not receive IgG via the placenta, which mimics the situation in preterm infants, born with low levels of IgG. This allows for experimentally changing the degree of immunodeficiency, through infusion of immunoglobulins and other plasma proteins. Neonatal pigs have the ability to effectively transfer immunoglobulins and other macromolecules across the intestine within the first 12–24 h (60, 61). This ability is severely reduced in fetal pigs (62) and preterm newborn pigs (63, 64) but an ability remains, as observed by the higher overall plasma IgG levels seen in animals fed BC or IF-PP. We do not know to what degree these absorbed bovine immunoglobulins were directed against SE. Since SE is a common pathogen in cattle (65) it is probable that the BC powder contains SE specific IgG's that would improve opsonisation and clearance of bacteria. However, improved clearance of SE was only observed in BC fed animals just after birth (*Experiment 2*), not those fed for two full days (*Experiment 4*), indicating that absorbed immunoglobulins played a minor role. Absorption of smaller macromolecules across the intestine has been demonstrated to be increased in very preterm infants (66–68), as a sign of enhanced gut permeability, as no specific immunoglobulin uptake mechanism exists. The overall immunoglobulin levels that we achieved in preterm pigs by maternal plasma supplementation were far lower than what is reported in term human neonates, where cord blood IgG levels range from 4 to 10 g/L (16, 69). The IgG levels of preterm infants are dependent on gestational age at birth, but were reported to be only ∼3 g/L by 22 weeks gestation (16, 70).

In conclusion, preterm newborn pigs are more sensitive to SE bacteremia than term pigs. Enteral feeding immediately after birth dampened the clinical responses to SE, and feeding with a highly bioactive milk diet, like bovine colostrum, improved clearance of SE from the bloodstream, relative to infant formula, with subtle improvements in blood gas parameters. A further 2 days of enteral feeding after preterm birth attenuated the SE response but the marked effect of BC vs. IF feeding disappeared. Early feeding with immunomodulatory milk diets may provide protection against neonatal systemic infection in preterm infants mainly via improving intestinal maturation and reducing the need for parenteral nutrition and fluid via indwelling central catheters. Nevertheless, early feeding with a protective milk diet, like colostrum, may improve the ability of preterm infants to resist systemic infections in the first days after birth.

DATA AVAILABILITY STATEMENT

The datasets generated for this study are available on request to the corresponding author.

ETHICS STATEMENT

The animal study was reviewed and approved by The Danish National Committee on Animal Experimentation.

AUTHOR CONTRIBUTIONS

OB, AB, DN, and PS planned the research. OB and AB conducted experiments, did data analysis and interpretation of results, and wrote the manuscript. TT supervised animal procedure. DN and AM did laboratory procedures. PS had primary responsibility for the final content. All authors read and approved the final paper.

FUNDING

The studies were part of the NEOCOL (Innovation Fund Denmark) and STIMMUNE (Arla Foods for Health) projects.

ACKNOWLEDGMENTS

We would like to thank Elin Skytte, Jane C. Povlsen, and Kristina Møller for their help performing these experiments.

SUPPLEMENTARY MATERIAL

The Supplementary Material for this article can be found online at: https://www.frontiersin.org/articles/10.3389/fimmu.2020.01019/full#supplementary-material

REFERENCES

1. Tröger B, Göpel W, Faust K, Müller T, Jorch G, Felderhoff-Müser U, et al. Risk for late-onset blood-culture proven sepsis in very-low-birth weight infants born small for gestational age: a large multicenter study from the German neonatal network. *Pediatr Infect Dis J.* (2014) 33:238–43. doi: 10.1097/INF.0000000000000031
2. Stoll BJ, Hansen N, Fanaroff AA, Wright LL, Carlo WA, Ehrenkranz RA, et al. Late-onset sepsis in very low birth weight neonates: the experience of the NICHD Neonatal Research Network. *Pediatrics.* (2002) 110:285–91. doi: 10.1542/peds.110.2.285

3. el Manouni el Hassani S, Berkhout DJC, Niemarkt HJ, Mann S, de Boode WP, Cossey V, et al. Risk factors for late-onset sepsis in preterm infants: a multicenter case-control study. *Neonatology*. (2019) 116:42–51. doi: 10.1159/000497781
4. Sisk PM, Lovelady CA, Gruber KJ, Dillard RG, O'Shea TM. Human milk consumption and full enteral feeding among infants who weigh. *Pediatrics*. (2008) 121:e1528–33. doi: 10.1542/peds.2007-2110
5. Sangild PT. Gut responses to enteral nutrition in preterm infants and animals. *Exp Biol Med*. (2006) 231:1695–711. doi: 10.1177/153537020623101106
6. Cleminson JS, Zalewski SP, Embleton ND. Nutrition in the preterm infant: what's new? *Curr Opin Clin Nutr Metab Care*. (2016) 19:220–5.
7. Corpeleijn WE, Kouwenhoven SMP, Paap MC, van Vliet I, Scheerder I, Muizer Y, et al. Intake of own mother's milk during the first days of life is associated with decreased morbidity and mortality in very low birth weight infants during the first 60 days of life. *Neonatology*. (2012) 102:276–81. doi: 10.1159/000341335
8. Nasuf AWA, Ojha S, Dorling J. Oropharyngeal colostrum in preventing mortality and morbidity in preterm infants. *Cochrane Database Syst Rev*. (2018) 9:CD011921. doi: 10.1002/14651858.CD011921.pub2
9. Juhl SM, Ye X, Zhou P, Li Y, Iyore EO, Zhang L, et al. Bovine colostrum for preterm infants in the first days of life. *J Pediatr Gastroenterol Nutr*. (2018) 66:471–78. doi: 10.1097/MPG.0000000000001774
10. Jiang Y, Kuang L, Wang H, Li L, Zhou W, Li M. The clinical characteristics of neonatal sepsis infection in southwest china. *Intern Med.* (2016) 55:597–603. doi: 10.2169/internalmedicine.55.3930
11. Shivanna V, Sunkappa S, Venkatesha D. The rising trend of coagulase-negative staphylococci in neonatal septicemia. *Indian J Pathol Microbiol*. (2016) 59:510. doi: 10.4103/0377-4929.191806
12. Dong Y, Speer CP, Glaser K. Beyond sepsis: *Staphylococcus epidermidis* is an underestimated but significant contributor to neonatal morbidity. *Virulence*. (2018) 9:621–33. doi: 10.1080/21505594.2017.1419117
13. Krediet TG, Beurskens FJ, van Dijk H, Gerards LJ, Fleer A. Antibody responses and opsonic activity in sera of preterm neonates with coagulase-negative staphylococcal septicemia and the effect of the administration of fresh frozen plasma. *Pediatr Res.* (1998) 43:645–51. doi: 10.1203/00006450-199805000-00013
14. Fleer A, Gerards LJ, Aerts P, Westerdaal NAC, Senders RC, van Dijk H, et al. Opsonic defense to *Staphylococcus epidermidis* in the premature neonate. *J Infect Dis*. (1985) 152:930–7. doi: 10.1093/infdis/152.5.930
15. Peterson PK, Wilkinson BJ, Kim Y, Schmeling D, Douglas SD, Quie PG, et al. The key role of peptidoglycan in the opsonization of Staphylococcus aureus. *J Clin Invest*. (1978) 61:597–609. doi: 10.1172/JCI108971
16. Malek A, Sager R, Kuhn P, Nicolaides KH, Schneider H. Evolution of maternofetal transport of immunoglobulins during human pregnancy. *Am J Reprod Immunol*. (1996) 36:248–55. doi: 10.1111/j.1600-0897.1996.tb00172.x
17. van den Berg JP, Westerbeek EAM, van der Klis FRM, Berbers GAM, van Elburg RM. Transplacental transport of IgG antibodies to preterm infants: a review of the literature. *Early Hum Dev*. (2011) 87:67–72. doi: 10.1016/j.earlhumdev.2010.11.003
18. Cates KL, Goetz C, Rosenberg N, Pantschenko A, Rowe JC, Ballow M. Longitudinal development of specific and functional antibody in very low birth weight premature infants. *Pediatr Res.* (1988) 23:14–22. doi: 10.1203/00006450-198801000-00005
19. Strunk T, Currie A, Richmond P, Simmer K, Burgner D. Innate immunity in human newborn infants: prematurity means more than immaturity. *J Matern Neonatal Med*. (2011) 24:25–31. doi: 10.3109/14767058.2010.482605
20. Sandberg K, Fasth A, Berger A, Eibl M, Isacson K, Lischka A, et al. Preterm infants with low immunoglobulin G levels have increased risk of neonatal sepsis but do not benefit from prophylactic immunoglobulin G. *J Pediatr*. (2000) 137:623–8. doi: 10.1067/mpd.2000.109791
21. Fanaroff AA, Korones SB, Wright LL, Wright EC, Poland RL, Bauer CB, et al. A controlled trial of intravenous immune globulin to reduce nosocomial infections in very-low-birth-weight infants. *N Engl J Med.* (1994) 330:1107–13. doi: 10.1056/NEJM199404213301602
22. Ohlsson A, Lacy JB. Intravenous immunoglobulin for preventing infection in preterm and/or low birth weight infants. *Cochrane Database Syst Rev*. (2013). 2:CD000361. doi: 10.1002/14651858.CD000361.pub3
23. Shah PS, Kaufman DA. Antistaphylococcal immunoglobulins to prevent staphylococcal infection in very low birth weight infants. *Cochrane Database Syst Rev*. (2009). 15:CD006449. doi: 10.1002/14651858.CD006449.pub2
24. INIS Collaborative Group, Brocklehurst P, Farrell B, King A, Juszczak E, Darlow B, et al. Treatment of neonatal sepsis with intravenous immune globulin. *N Engl J Med.* (2011) 365:1201–11. doi: 10.1056/NEJMoa1100441
25. Blum PM, Phelps DL, Ank BJ, Krantman HJ, Stiehm ER. Survival of oral human immune serum globulin in the gastrointestinal tract of low birth weight infants. *Pediatr Res.* (1981) 15:1256–60. doi: 10.1203/00006450-198109000-00006
26. Eibl MM, Wolf HM, Fürnkranz H, Rosenkranz A. Prevention of necrotizing enterocolitis in low-birth-weight infants by IGA-IGG feeding. *N Engl J Med.* (1988) 319:1–7. doi: 10.1056/NEJM198807073190101
27. Rubaltelli FF, Benini F, Sala M. Prevention of necrotizing enterocolitis in neonates at risk by oral administration of monomeric IgG. *Dev Pharmacol Ther.* (1991) 17:138–43. doi: 10.1159/000457513
28. Foster JP, Seth R, Cole MJ. Oral immunoglobulin for preventing necrotizing enterocolitis in preterm and low birth weight neonates. *Cochrane Database Syst. Rev.* (2016) CD001816. doi: 10.1002/14651858.CD001816.pub3
29. Sun J, Li Y, Pan X, Nguyen DN, Brunse A, Bojesen AM, et al. Human milk fortification with bovine colostrum is superior to formula-based fortifiers to prevent gut dysfunction, necrotizing enterocolitis, and systemic infection in preterm pigs. *J Parenter Enter Nutr*. (2018) 43:252–62. doi: 10.1002/jpen.1422
30. Shen RL. Thymann T, Østergaard MV., Støy ACF, Krych Ł, Nielsen DS, et al. Early gradual feeding with bovine colostrum improves gut function and NEC resistance relative to infant formula in preterm pigs. *Am J Physiol Gastrointest Liver Physiol.* (2015) 309:G310–23. doi: 10.1152/ajpgi.00163.2015
31. Rasmussen SO, Martin L, Østergaard MV, Rudloff S, Li Y, Roggenbuck M, et al. Bovine colostrum improves neonatal growth, digestive function and gut immunity relative to donor human milk and infant formula in preterm pigs. *Am J Physiol Gastrointest Liver Physiol*. (2016) 311:G480–91. doi: 10.1152/ajpgi.00139.2016
32. Bjornvad CR, Thymann T, Deutz NE, Burrin DG, Jensen SK, Jensen BB, et al. Enteral feeding induces diet-dependent mucosal dysfunction, bacterial proliferation, and necrotizing enterocolitis in preterm pigs on parenteral nutrition. *Am J Physiol Gastrointest Liver Physiol*. (2008) 295:G1092–103. doi: 10.1152/ajpgi.00414.2007
33. Bjornvad CR, Schmidt M, Petersen YM, Jensen SK, Offenberg H, Elnif J, et al. Preterm birth makes the immature intestine sensitive to feeding-induced intestinal atrophy. *Am J Physiol Integr Comp Physiol*. (2005) 289:R1212–22. doi: 10.1152/ajpregu.00776.2004
34. Pérez-Bosque A, Polo J, Torrallardona D. Spray dried plasma as an alternative to antibiotics in piglet feeds, mode of action and biosafety. *Porc Heal Manag*. (2016) 2:1–10. doi: 10.1186/s40813-016-0034-1
35. Pe A, Polo J, Russell L, Campbell J, Weaver E, Crenshaw J, et al. Dietary plasma protein supplements prevent the release of mucosal proinflammatory mediators in intestinal inflammation in rats 1, 2. *J Nutr*. (2010) 140:25–30. doi: 10.3945/jn.109.112466
36. Maijo M, Miro L, Polo J, Campbell J, Russell L, Crenshaw J, et al. Dietary plasma proteins modulate the adaptive immune response in mice with acute lung inflammation. *J Nutr*. (2012) 142:264–70. doi: 10.3945/jn.111.149070
37. Pérez-Bosque A, Miró L, Maijó M, Polo J, Campbell JM, Russell L, et al. Oral serum-derived bovine immunoglobulin/protein isolate has immunomodulatory effects on the colon of mice that spontaneously develop colitis. *PLoS ONE*. (2016) 11:e154823. doi: 10.1371/journal.pone.0154823
38. Bégin F, Santizo M-C, Peerson JM, Torún B, Brown KH. Effects of bovine serum concentrate, with or without supplemental micronutrients, on the growth, morbidity, and micronutrient status of young children in a low-income, peri-urban guatemalan community. *Eur J Clin Nutr*. (2008) 62:39–50. doi: 10.1038/sj.ejcn.1602682
39. Lembcke JL, Peerson JM, Brown KH. Acceptability, safety, and digestibility of spray-dried bovine serum added to diets of recovering malnourished children. *J Pediatr Gastroenterol Nutr*. (1997) 25:381–4. doi: 10.1097/00005176-199710000-00003
40. Sarker SA, Casswall TH, Mahalanabis D, Alam NH, Albert MJ, Brüssow H, et al. Successful treatment of rotavirus diarrhea in children with immunoglobulin from immunized bovine colostrum. *Pediatr Infect Dis J*. (1998) 17:1149–54. doi: 10.1097/00006454-199812000-00010

41. Pakkanen R, Aalto J. Growth factors and antimicrobial factors of bovine colostrum. *Int Dairy J*. (1997) 7:285–97. doi: 10.1016/S0958-6946(97)00022-8
42. Nguyen DN, Currie AJ, Ren S, Bering SB, Sangild PT. Heat treatment and irradiation reduce anti-bacterial and immune-modulatory properties of bovine colostrum. *J Funct Foods*. (2019) 57:182–9. doi: 10.1016/j.jff.2019.04.012
43. Brunse A, Worsøe P, Pors SE, Skovgaard K, Sangild PT. Oral supplementation with bovine colostrum prevents septic shock and brain barrier disruption during bloodstream infection in preterm newborn pigs. *Shock*. (2018) 51:337–47. doi: 10.1097/SHK.0000000000001131
44. Wen K, Li G, Zhang W, Azevedo MSP, Saif LJ, Liu F, et al. Development of γδ T cell subset responses in gnotobiotic pigs infected with human rotaviruses and colonized with probiotic lactobacilli. *Vet Immunol Immunopathol*. (2011) 141:267–75. doi: 10.1016/j.vetimm.2011.03.016
45. Schäfer A, Hühr J, Schwaiger T, Dorhoi A, Mettenleiter TC, Blome S, et al. Porcine invariant natural killer T cells: functional profiling and dynamics in steady state and viral infections. *Front Immunol*. (2019) 10:1380. doi: 10.3389/fimmu.2019.01380
46. Nguyen DN, Jiang P, Frøkiær H, Heegaard PMH, Thymann T, Sangild PT. Delayed development of systemic immunity in preterm pigs as a model for preterm infants. *Sci Rep*. (2016) 6:36816. doi: 10.1038/srep36816
47. Carr R. Neutrophil production and function in newborn infants. *Br J Haematol*. (2000) 110:18–28. doi: 10.1046/j.1365-2141.2000.01992.x
48. Gessler P, Lüders R, König S, Haas N, Lasch P, Kachel W. Neonatal neutropenia in low birthweight premature infants. *Am J Perinatol*. (1995) 12:34–8. doi: 10.1055/s-2007-994396
49. Li Y, Jensen ML, Chatterton DEW, Jensen BB, Thymann T, Kvistgaard AS, et al. Raw bovine milk improves gut responses to feeding relative to infant formula in preterm piglets. *Am J Physiol Gastrointest Liver Physiol*. (2014) 306:G81–90. doi: 10.1152/ajpgi.00255.2013
50. Li Y, Nguyen DN, de Waard M, Christensen L, Zhou P, Jiang P, et al. Pasteurization procedures for donor human milk affect body growth, intestinal structure, and resistance against bacterial infections in preterm pigs. *J Nutr*. (2017) 147:1121–30. doi: 10.3945/jn.116.244822
51. Sun J, Li Y, Nguyen DN, Mortensen MS, van den Akker CHP, Skeath T, et al. Nutrient fortification of human donor milk affects intestinal function and protein metabolism in preterm pigs. *J Nutr*. (2018) 148:336–47. doi: 10.1093/jn/nxx033
52. Graspeuntner S, Waschina S, Künzel S, Twisselmann N, Rausch TK, Cloppenborg-Schmidt K, et al. Gut dysbiosis with bacilli dominance and accumulation of fermentation products precedes late-onset sepsis in preterm infants. *Clin Infect Dis*. (2019) 69:268–77. doi: 10.1093/cid/ciy882
53. Cilieborg MS, Boye M, Sangild PT. Bacterial colonization and gut development in preterm neonates. *Early Hum Dev*. (2012) 88:S41–9. doi: 10.1016/j.earlhumdev.2011.12.027
54. Hotchkiss RS, Tinsley KW, Swanson PE, Schmieg RE, Hui JJ, Chang KC, et al. Sepsis-induced apoptosis causes progressive profound depletion of B and CD4+ T lymphocytes in humans. *J Immunol*. (2001) 166:6952–63. doi: 10.4049/jimmunol.166.11.6952
55. Hotchkiss RS, Swanson PE, Freeman BD, Tinsley KW, Cobb JP, Matuschak GM, et al. Apoptotic cell death in patients with sepsis, shock, and multiple organ dysfunction. *Crit Care Med*. (1999) 27:1230–51. doi: 10.1097/00003246-199907000-00002
56. Guida JD, Kunig AM, Leef KH, McKenzie SE, Paul DA. Platelet count and sepsis in very low birth weight neonates: is there an organism-specific response? *Pediatrics*. (2003) 111:1411–5. doi: 10.1542/peds.111.6.1411
57. Bhat MA, Bhat JI, Kawoosa MS, Ahmad SM, Ali SW. Organism-specific platelet response and factors affecting survival in thrombocytopenic very low birth weight babies with sepsis. *J Perinatol*. (2009) 29:702–8. doi: 10.1038/jp.2009.72
58. Lee WL, Slutsky AS. Sepsis and endothelial permeability. *N Engl J Med*. (2010) 363:689–91. doi: 10.1056/NEJMcibr1007320
59. Hugo F, Berstecher C, Krämer S, Fassbender W, Bhakdi S. *In vivo* clearance studies of the terminal fluid-phase complement complex in rabbits. *Clin Exp Immunol*. (1989) 77:112–6.
60. Porter P. Transfer of immunoglobulins IgG, IgA and IgM to lacteal secretions in the parturient sow and their absorption by the neonatal piglet. *Biochim Biophys Acta Protein Struct*. (1969) 181:381–92. doi: 10.1016/0005-279590271-2
61. Jensen AR, Elnif J, Burrin DG, Sangild PT. Development of intestinal immunoglobulin absorption and enzyme activities in neonatal pigs is diet dependent. *J Nutr*. (2001) 131:3259–65. doi: 10.1093/jn/131.12.3259
62. Sangild PT, Trahair JF, Loftager MK, Fowden AL. Intestinal macromolecule absorption in the fetal pig after infusion of colostrum *in utero*. *Pediatr Res*. (1999) 45:595–602. doi: 10.1203/00006450-199904010-00021
63. Sangild PT, Schmidt M, Elnif J, Björnvad CR, Weström BR, Buddington RK. Prenatal development of gastrointestinal function in the pig and the effects of fetal esophageal obstruction. *Pediatr Res*. (2002) 52:416–24. doi: 10.1203/00006450-200209000-00019
64. Sangild PT, Petersen YM, Schmidt M, Elnif J, Petersen TK, Buddington RK, et al. Preterm birth affects the intestinal response to parenteral and enteral nutrition in newborn pigs. *J Nutr*. (2002) 132:2673–81. doi: 10.1093/jn/132.9.2673
65. Jenkins SN, Okello E, Rossitto PV, Lehenbauer TW, Champagne J, Penedo MCT, et al. Molecular epidemiology of coagulase-negative staphylococcus species isolated at different lactation stages from dairy cattle in the United States. *Peer J*. (2019) 7:e6749. doi: 10.7717/peerj.6749
66. Axelsson I, Jakobsson I, Lindberg T, Polberger S, Benediktson B, Räihä N. Macromolecular absorption in preterm and term infants. *Acta Paediatr*. (1989) 78:532–7. doi: 10.1111/j.1651-2227.1989.tb17932.x
67. Roberton DM, Paganelli R, Dinwiddie R, Levinsky RJ. Milk antigen absorption in the preterm and term neonate. *Arch Dis Child*. (1982) 57:369–72. doi: 10.1136/adc.57.5.369
68. Weaver LT, Laker MF, Nelson R. Intestinal permeability in the newborn. *Arch Dis Child*. (1984) 59:236–41. doi: 10.1136/adc.59.3.236
69. Oxelius V-A. IgG subclass levels in infancy and childhood. *Acta Paediatr*. (1979) 68:23–7. doi: 10.1111/j.1651-2227.1979.tb04424.x
70. Ballow M, Cates KL, Rowe JC, Goetz C, Desbonnet C. Development of the immune system in very low birth weight (less than 1500 g) premature infants: concentrations of plasma immunoglobulins and patterns of infections. *Pediatr Res*. (1986) 20:899–904. doi: 10.1203/00006450-198609000-00019

Conflict of Interest: The University of Copenhagen holds a patent on the use of bovine colostrum for pediatric patients. PS is listed as a sole inventor but has declined any share of potential revenue arising from commercial exploitation of such a patent.

The remaining authors declare that the research was conducted in the absence of any commercial or financial relationships that could be construed as a potential conflict of interest.

frontiers in Immunology

MINI REVIEW
published: 02 June 2020
doi: 10.3389/fimmu.2020.01035

T Cells in Preterm Infants and the Influence of Milk Diet

Thomas Sproat[1,2]*, *Rebecca Pamela Payne*[2], *Nicholas D. Embleton*[1,3], *Janet Berrington*[1,2] *and Sophie Hambleton*[2]

[1] Neonatal Intensive Care Unit, Royal Victoria Infirmary, Newcastle upon Tyne, United Kingdom, [2] Immunity and Inflammation Theme, Translational and Clinical Research Institute, Newcastle University, Newcastle upon Tyne, United Kingdom, [3] Population Health Science Institute, Newcastle University, Newcastle upon Tyne, United Kingdom

Preterm infants born before 32 weeks gestational age (GA) have high rates of late onset sepsis (LOS) and necrotizing enterocolitis (NEC) despite recent improvements in infection control and nutrition. Breast milk has a clear protective effect against both these outcomes likely due to multiple mechanisms which are not fully understood but may involve effects on both the infant's immune system and the developing gut microbiota. Congregating at the interface between the mucosal barrier and the microbiota, innate and adaptive T lymphocytes (T cells) participate in this interaction but few studies have explored their development after preterm delivery. We conducted a literature review of T cell development that focuses on fetal development, postnatal maturation and the influence of milk diet. The majority of circulating T cells in the preterm infant display a naïve phenotype but are still able to initiate functional responses similar to those seen in term infants. T cells from preterm infants display a skew toward a T-helper 2(T_h2) phenotype and have an increased population of regulatory cells (T_{reg}s). There are significant gaps in knowledge in this area, particularly in regards to innate-like T cells, but work is emerging: transcriptomics and mass cytometry are currently being used to map out T cell development, whilst microbiomic approaches may help improve understanding of events at mucosal surfaces. A rapid rise in organoid models will allow robust exploration of host-microbe interactions and may support the development of interventions that modulate T-cell responses for improved infant health.

Keywords: T-lymphocytes, infant, premature, mucosal immunity, necrotizing enterocolitis, extremely premature

OPEN ACCESS

Edited by:
Per T. Sangild, University of Copenhagen, Denmark

Reviewed by:
Alberto Finamore, Council for Agricultural and Economics Research (CREA), Italy
Claudia Nold, Hudson Institute of Medical Research, Australia

***Correspondence:**
Thomas Sproat
tsproat@nhs.net

Specialty section:
This article was submitted to Nutritional Immunology, a section of the journal Frontiers in Immunology

Received: *15 December 2019*
Accepted: *29 April 2020*
Published: *02 June 2020*

Citation:
Sproat T, Payne RP, Embleton ND, Berrington J and Hambleton S (2020) T Cells in Preterm Infants and the Influence of Milk Diet. Front. Immunol. 11:1035. doi: 10.3389/fimmu.2020.01035

INTRODUCTION

Infants born prematurely, especially before 32 weeks gestational age (GA) are susceptible to diseases associated with invasive bacterial infections, specifically late onset sepsis (LOS) and necrotizing enterocolitis (NEC). These occur in around 30 and 6% of very preterm infants, respectively, according to recent data (1), most occur in the first 4 weeks of life, and both diseases are associated with changes in the gut microbiota (2, 3). Feeding preterm infants with their mother's breast milk has been shown to reduce the risk of NEC and LOS (4, 5). T lymphocytes (T cells) are an important component of the immune response to infection, however, this role is balanced against their emerging role in tissue regeneration and repair. The newborn, who is exposed to diverse microbes including many potential pathogens soon after birth, requires an appropriate T cell response to navigate the potentially conflicting requirements of growth, repair and infection control.

This review focuses on fetal T cell development, postnatal T cell maturation, and the potential for dietary modulation of gut mucosal T cells in the preterm environment. T cells of particular interest

TABLE 1 | Summary of differences between peripheral blood T cell populations in preterm infants compared to term infants.

T cell type	Description of role	Relative abundance (preterm compared to term infants, population as % of T cells)	Relative function (preterm compared to term infants)	Relevance of difference	References
CD4+ T (T_h)	Regulate immune response Help B cells produce immunoglobulin	↑↑	↑IL-5 ↓IFN-γ	Limited T_h1 response limits response to intracellular infections	(6, 7)
T_{reg}	Suppress immune response	↑↑	↑IL-10	Suppress immune response, leading to tolerogenic state (limiting inflammation)	(6, 8–10)
CD8+ T	Cytotoxic T cells	↔	Not known ↑IFN-γ* ↑TNF-α* ↓IL-2*	Potentially increased ability to respond to viral infections	(11, 12)
γδ T	Innate-like, predominantly mucosa-based range of cytotoxic functions	↓↓	↑IFN-γ ↑IL-10	Potentially compensates for decreased T_h1 response.	(13–15)
iNKT	Innate-like, some roles similar to natural killer cells	Not known/↑*	Not known	Unclear if beneficial or detrimental	(16)
MAIT	Innate-like, cytotoxic and inflammatory functions	↓	Not known	Unclear if beneficial or detrimental	(17, 18)

**Umbilical cord blood. ↑Increased; ↑↑Greatly increased; ↓Decreased; ↓↓Greatly decreased; ↔Similar.*

in the preterm infant comprise those with innate-like properties such as γδ T, invariant natural killer T (iNKT) and mucosa-associated invariant T (MAIT) cells, which have the capacity to deliver effector functions without prior clonal expansion. Among conventional TCRαβ-expressing T cells, regulatory T cells (T_{reg}s) are known for their ability to mediate tolerance but also have emerging roles in tissue regeneration of potential relevance to NEC (**Table 1**).

A challenge of studying T cells in preterm infants is that it is difficult to obtain suitable samples purely for research purposes. Umbilical cord blood is often used to represent the immune system of preterm infants, however a recent systems level analysis suggests it is more representative of the fetal state than the *ex-utero* infant (6). Therefore, where possible, we focus on studies using postnatal blood, but supplement these data with studies on umbilical cord blood, fetuses, and animal studies as necessary.

FETAL T-CELL DEVELOPMENT

Bone marrow-derived T progenitor cells enter the thymus at around 8 weeks gestation (19). These early thymocytes do not display the full range of T cell receptors (TCR) until 16 weeks GA (20). Fetal T cells can be detected in peripheral blood from 8 weeks GA, with the capacity to proliferate and produce cytokines (21). T cell migration to secondary lymphoid tissue has been confirmed with identification of T cells in the mesenteric lymph nodes (MLN) from 12 weeks GA (20) and the spleen and intestinal mucosa from 14 weeks GA (20–23).

Abbreviations: GA, gestational age; iNK T, invariant natural killer T cells; MAIT, mucosal associated invariant T cells; MHC, major histocompatibility complex; MLN, mesenteric lymph nodes; PNA, postnatal age; TCR, T cell receptor; T_h, T-helper; T_{reg}s, regulatory T cells.

Unsurprisingly, the majority of T cells derived from cord blood in newborns are naïve (24). The proportion of naive T cells has been shown to remain high (median 85%) at 6–8 weeks age [postnatal age (PNA)] in preterm infants, however this is significantly less than term infants at this PNA (25). This may reflect increased antigen exposure or reduced thymic output in preterm infants.

The size, composition, and function of the immune cell compartment varies from one tissue to another (26, 27). Interestingly, fetal CD4 T (T_h) cells in the intestinal lamina propria but not spleen or liver display a predominantly memory phenotype (22, 23). This suggests priming as a result of prior "antigen" exposure, the nature of which is not known (22). Fetal MLN-derived T cells have capacity to respond to stimulation by proliferating and secreting a broad range of cytokines. Both proliferation and cytokine production by fetal MLN-derived T cells are augmented upon the removal of T_{reg}s (20) suggesting T_{reg}s play an important role in limiting fetal tissue inflammation.

SKEWING OF THE T-helper (T_h) RESPONSE

Naïve T_h cells can differentiate toward alternative cell fates depending on the context in which they receive antigenic stimulation (8). Preterm infants have been suggested to have a skewed T_h2 response based on their increased production of a classical T_h2 cytokine, IL-5, and decreased production of a T_h1 cytokine, IFN-γ, upon stimulation of peripheral blood compared to term cord blood (7). Postnatally, the ability of preterm T_h cells to secrete IFN-γ remains low with single cell RNA-seq analysis of term and preterm infants at 12 weeks of age demonstrating up-regulation of genes that suppress IFN-γ, together with longitudinal sampling of preterm infants displaying

low expression (6, 13). An effective T_h1 response is key to preventing intracellular infections, including bacteria, and this may explain why preterm infants have increased susceptibility.

In contrast to the T_h2 skewing observed in peripheral blood, fetal intestinal T_h cells instead have a tendency to secrete TNF-α and IL-2 (T_h1 cytokine), when compared to term infant intestinal samples. TNF-α was shown in a human fetal organoid model to be important in intestinal epithelial growth by its effects on intestinal stem cells, albeit high levels of TNF-α suppress epithelial growth. Infants with NEC have an increased production of TNF-α from intestinal T_h cells, although the temporal relationship to disease is unknown (23).

The tissue T_h response is affected by human milk oligosaccharides (HMO's), which comprise 1–2% of human milk and are the third largest non-water component by weight (after lactose and lipids). HMO's are not digestible by the infant but are believed to modulate the gut microbiota. HMO's appear to promote the growth of *Bifidobacteria* and suppress potentially pathogenic organisms (28, 29). When adding HMO's to fetal *in vitro* organ cultures, gene transcripts associated with T_h differentiation were found only with HMO's from early, not mature human milk, believed to reflect variation in the concentration of the HMO's. These transcriptional changes were deduced to promote a T_h1 response whilst suppressing a T_h2, T_h17, and IL-8 expression (30). It is possible that these alterations play a role in the reduction of NEC and LOS seen in preterm infants fed breast milk.

SUPPRESSION OF THE IMMUNE RESPONSE

T_{reg}s are a population of T_h cells defined by their suppressive function toward effector T cell responses. T_{reg} abundance is inversely correlated with GA and higher in infants compared to adults (9, 31). T_{reg}s have been identified in the thymus as early as 13 weeks GA and in the periphery (spleen) from 14 weeks GA (21). The proportion of T_{reg}s in the fetal MLN is significantly increased compared to adults and T_{reg}s are functional even at a fetal stage (20, 23).

Interleukin- (IL-) 10 is amongst the factors that mediate the suppressive function as well as induce expansion of T_{reg}s (8–10). IL-10 is produced following bacterial invasion or in stimulated tissues. IL-10 has been shown to contribute to bacterial clearance, yet minimize host damage from infection (10). Interestingly, germline mutations causing loss of function in the IL-10 receptor, as well as deficiency of the critical T_{reg} transcription factor *FOXP3*, cause early-onset enterocolitis (32). The ability of lamina propria T_{reg}s to produce IL-10 is greatly reduced in preterm infants with NEC compared to term infants (23). An impaired T_{reg} IL-10 response to bacterial invasion may have a role in development of NEC, or it may be that the microbial dysbiosis seen before the development of NEC leads to an impaired IL-10 response (2).

Similar to humans, mice harbor an increased density of T_{reg}s in the intestine compared with other organs. In mice, the introduction of gut bacteria induces an increase in the population of colonic but not small intestinal T_{reg}s, apparently driven by *Clostridium*. These T_{reg}s are thought to be peripherally induced (rather than thymus-derived) as judged by their lack of expression of the transcription factor, Helios (33). *Bacteroides fragilis* has also been shown to induce T_{reg}s in mice through its production of polysaccharide A (PSA) in the presence of the toll-like receptor, TLR-2 (34, 35). In mice, induction of T_{reg}s upon treatment by PSA in the presence of *Bacteroides fragilis* is protective against not only intestinal inflammation but also encephalitis, suggesting there could be a systemic effect of this interaction (34–36). No preterm human work on this aspect currently exists.

UNIMPAIRED CD8 EFFECTOR POTENTIAL?

CD8 T cells have been demonstrated in the fetal intestine as early as 16 weeks GA (20, 37). Whilst they display mainly a naive phenotype in the first 12 weeks of postnatal life, little is known about their postnatal effector potential (11). Fetal (term and preterm cord blood) and adult CD8 T cells develop a similar memory phenotype and ability to produce perforin and cytokines in response to a common neonatal virus, cytomegalovirus (CMV) (38). Furthermore, using cord blood derived CD8 T cells from varying gestations (23–41 weeks GA), an increased ability to secrete IFN-γ, TNF-α, and IL-2 has been demonstrated at earlier gestations (12).

These limited data suggest prematurity does not prevent CD8 effector T cell function in newborns. Indeed, it is possible that they display an excessive response to viral infection, which may be harmful, particularly as many infants are postnatally exposed to CMV.

INNATE-LIKE T CELLS

Innate-like T cells can display effector function without prior antigen priming. This would suggest they could be important in early life (17, 39). Innate-like T cells include γδ T, iNKT, and MAIT cells.

Gamma-Delta (γδ) T Cells

Unlike αβ T cells, a large number of γδ T cells reside in non-lymphoid tissues including the gut, spleen and lungs. They have a small range of antigen receptors but are able to respond to a large repertoire of antigens including peptide not bound to classical major histocompatibility complex (MHC) molecules (39). They comprise 4–10%, 1–3%, and <1% of T cells in the peripheral blood of adults, term and preterm cord blood of infants, respectively (14).

γδ T cells develop a memory phenotype in the first month of life (15) and preterm γδ T cells have an increased ability to secrete IFN-γ and IL-10 upon stimulation with PMA and ionomycin compared to both term γδ T cells and preterm αβ T cells (15). The ability to secrete IFN-γ increases over time, which is in contrast to preterm T_h cells (13). However, when challenged with influenza virus, cord blood γδ T cells show a

decreased ability to proliferate and produce IFN-γ compared to term infants and adults (14). The differences in these results could be due to experimental design, however these data suggest at least the potential for preterm γδ T cells to contribute to the cellular immune response. Little is known about preterm mucosal γδ T cells or their responses to alternative ligands.

Invariant Natural Killer T (iNKT) Cells

Natural killer T (NKT) cells define a population of T cells that bear TCR's restricted by a non-classical MHC molecule, CD1d, and express cell surface markers associated with NK cells. Invariant/ type 1 NKT (or iNKT) cells express the invariant TCR (Vα24-Jα18). iNKT cells vary in abundance depending on tissue, comprising 0.01–0.1% of lymphocytes in peripheral blood but 10% of lymphocytes in the omentum (40). There is an increased abundance of iNKT cells in preterm cord blood compared to term cord blood (16).

iNKT's are able to secrete cytokines that mediate T_h1, T_h2, or T_h17 responses, and recognize specific glycolipid antigens presented by CD1d (41). The ability of preterm iNKT cells to produce these T_h cytokines is not known but has been demonstrated in the case of term cord blood iNKT's. The secretion of IL-10 is particularly increased compared to adults suggesting a potential regulatory role of iNKT's in term infants (41).

iNKT cells have been associated with colitis in mouse models. Germ-free mice have an increased proportion of iNKT cells in their colon and increased susceptibility to colitis, however colonization of the intestine with bacteria early in life leads to a reduction in iNKT density and provides protection from colitis (42). iNKT cells able to produce IL-13 have been implicated in the pathogenesis of colitis (43). Furthermore, iNKT-deficient mice differ in gut microbial composition compared to wild-type mice, as well as showing increased intestinal leucocyte infiltration (44). Whether iNKT cells are involved in the pathogenesis of NEC in preterm infants is not known.

Mucosa-Associated Invariant T (MAIT) Cells

MAIT cells are a population of T cells predominantly found in the lung and intestinal mucosa, that display a semi-invariant TCR (Vα 7.2 – Jα3.3/20/12). MAIT cells have been demonstrated in the fetal thymus from 18 weeks GA. MAIT cells represent <1% of peripheral blood T cells in newborns compared to up to 10% in adults, suggesting a postnatal expansion (17). MAIT cells are of particular interest as they recognize MR-1, an MHC-1 like molecule that presents microbial derived metabolites of the essential vitamin, riboflavin (17). Riboflavin is synthesized by gut commensal bacteria, and has a variable concentration in human milk dependent on maternal intake (45, 46). Thus, the postnatal expansion of MAIT cells is likely driven both by bacteria and by diet.

In contrast to thymic MAIT cells, those in fetal intestine, spleen, and MLN express a marker of activation (PLZF), suggesting peripheral maturation. They develop this mature phenotype in the first 2 months of life (17, 47) and display inflammatory and cytotoxic abilities. Indeed, fetal intestinal, liver and lung but not thymic or spleen MAIT cells can produce IFN-γ following stimulation (18). Functional changes in MAIT cells have been associated with inflammation in adults with inflammatory bowel disease (48). However, no study has examined their relationship with NEC.

DIETARY INTERACTIONS WITH MUCOSAL T CELLS

When considering modulation of the preterm T cell populations, we have described how key dietary exposures such as HMOs and bacteria appear important. Breast milk contains a vast array of components that may directly or indirectly affect gut mucosal T cell populations, as demonstrated in both human and animal models of early life (**Figure 1**). The gut microbiota is likely to be a key mediator of such dietary effects, implying the possibility of therapeutic modulation either by dietary modifications or the use of prebiotics or probiotics.

Colostrum

Compared to more mature human milk, colostrum has a higher concentration of bioactive components including HMOs, lactoferrin, immune cells, and immunoglobulin. In a porcine model, pregnant sows were given NEC-inducing intra-amniotic lipopolysaccharide injections *in-utero* and offspring pups were then fed varying diets before euthanasia. Pups fed colostrum had decreased levels of distal ileal IL-8 and IL-1β, combined with increased abundance of blood T_h cells (as % of lymphocytes). The authors concluded that a colostrum diet led to maturation of the intestinal mucosa as well as the systemic immune system (50).

Translocation of Milk Derived Immune Cells

Human milk contains stem cells and leucocytes (51, 58). Studies using mice show that maternal immune cells can translocate from the intestine into the circulation or distal organs (53, 54, 59). Stem cells derived from milk have been shown to translocate into the brains of mice, and once there to traffic and differentiate (53, 54). In these mouse models, T cells are the predominant cell type that transfers across the intestinal epithelium despite their relative paucity in milk (58, 59). CD8 T cells, in particular, translocate into the intestinal Peyer's patches, possibly based on their expression of a gut homing receptor (CCR9). Once there, they show an increased ability to produce cytokines upon stimulation compared with peripheral blood CD8 T cells (59). It is unclear whether diet-derived T cells migrate beyond the MLN in mice as studies conflict (52, 59) but it is plausible that milk-derived maternal CD8 T cells translocate into the mucosa in humans and compensate for "deficiencies" of preterm T cells.

Lactoferrin

Lactoferrin is the major whey glycoprotein of human milk and subject to intense research for over 50 years due to its ability to inhibit bacteria by multiple mechanisms (55, 60). Lactoferrin has also been shown to bind to immune cells and influence their function (61). Most lymphocytes can express a lactoferrin receptor including stimulated αβ and γδ T cells

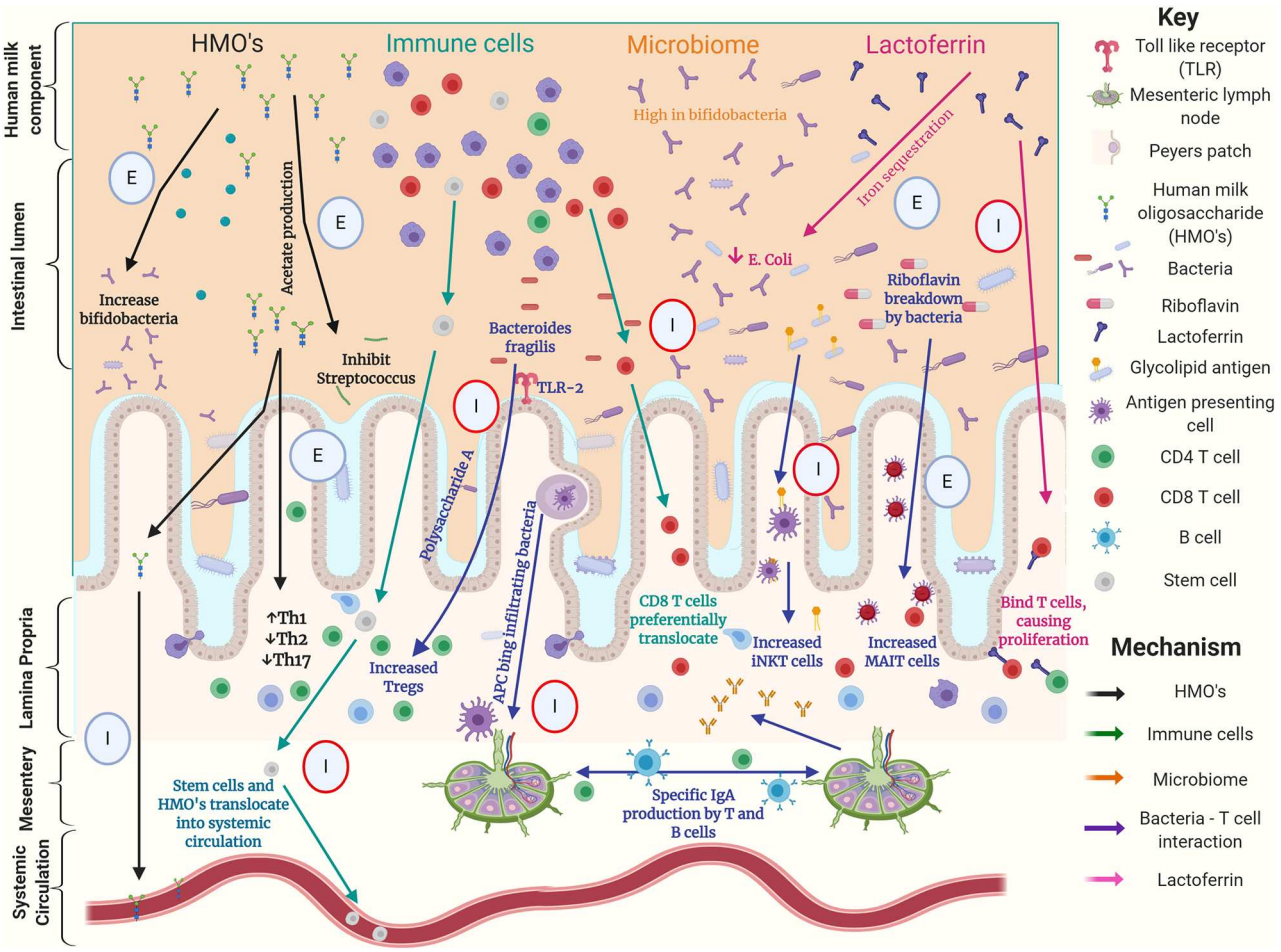

FIGURE 1 | Graphical summary of possible interactions between components of human milk, the gut microbiome and T cells in the preterm intestine. This summarizes work using human, animal and laboratory-based experiments. Circles highlight experiment type with; E denoting an *ex-vivo* experiment, I denoting an *in-vivo* experiment, red circles denoting animal experiments (16, 28–30, 32, 34, 35, 42, 44, 49–57).

(56). Furthermore, T cells in the lamina propria of pigs bind lactoferrin (57). In a mouse model, T cells in the lamina propria proliferated upon administration of enteral bovine lactoferrin in the presence or absence of colon cancer. These T cells secreted IFN-γ and IL-18, suggesting that they were immunologically active (62).

CONCLUSION

Preterm infants have a T cell population that was designed for fetal life and therefore differs systematically from term infants (**Table 1**). In particular, they have a diminished T_h1 response leaving them susceptible to infection by intracellular pathogens. T_{reg}s protect the preterm infant from an excessive innate response which may reduce the risk of NEC but may also increase the risk of LOS. This variation in function of T_{reg}s is modulated by IL-10.

There are multiple mechanisms by which the diet, gut microbiome, and T cell populations have been demonstrated to interact in human, mouse, and laboratory experiments demonstrated in **Figure 1**. However, there is a paucity of data comparing the effects of alternative feeding strategies on the preterm infant's immune system, including T cells, and there remains substantial uncertainty about when and how donor human milk and human milk derived fortifiers should be used. Clinical studies aimed at identifying changes in the immune system associated with these dietary interventions will improve understanding and enable more informed nutritional management.

The functions of innate-like cells such as iNKT and MAIT cells in preterm infants have yet to be unraveled but a number of compelling studies on animals imply an important role in preventing intestinal inflammation. Alterations in gut mucosal T cells may occur in preterm infants as a result of dietary or microbiome manipulations. A

better understanding of the interplay of diet, microbiome and host immunity will underpin efforts to develop interventions that modulate T-cell responses for improved infant health.

AUTHOR CONTRIBUTIONS

TS wrote the initial manuscript. All authors contributed to manuscript revision, read, and approved the submitted version.

REFERENCES

1. Griffiths J, Jenkins P, Vargova M, Bowler U, Juszczak E, King, et al. Enteral lactoferrin supplementation for very preterm infants: a randomised placebo-controlled trial. *The Lancet.* (2019) 393:423–33. doi: 10.1016/S0140-6736(18)32221-9
2. Stewart CJ, Embleton ND, Marrs ECL, Smith DP, Smith DP, Nelson A, et al. Temporal bacterial and metabolic development of the preterm gut reveals specific signatures in health and disease. *Microbiome.* (2016) 4:67. doi: 10.1186/s40168-016-0216-8
3. Stewart CJ, Embleton ND, Marrs ECL, Smith DP, Fofanova T, Nelson, et al. Longitudinal development of the gut microbiome and metabolome in preterm neonates with late onset sepsis and healthy controls. *Microbiome.* (2017) 5:1. doi: 10.1186/s40168-017-0295-1
4. Patel AL, Johnson TJ, Engstrom JL, Fogg LF, Jegier BJ, Bigger R, et al. Impact of early human milk on sepsis and health-care costs in very low birth weight infants. *J Perinatol.* (2013) 33:514–19. doi: 10.1038/jp.2013.2
5. Corpeleijn WE, Kouwenhoven MP, Paap M, Vliet I, Scheerder I, Muizer Y, et al. Intake of own mother's milk during the first days of life is associated with decreased morbidity and mortality in very low birth weight infants during the first 60 days of life. *Neonatology.* (2012) 102:276–81. doi: 10.1159/000341335
6. Olin A, Henckel E, Chen Y, Lakshmikanth T, Pou C, Mikes, et al. Stereotypic immune system development in newborn children. *Cell.* (2018) 174:1277–92.e14. doi: 10.1016/j.cell.2018.06.045
7. Dirix V, Vermeulen F, Mascart F. Maturation of CD4+ regulatory T lymphocytes and of cytokine secretions in infants born prematurely. *J Clin Immunol.* (2013) 33:1126–33. doi: 10.1007/s10875-013-9911-4
8. Raphael I, Nalawade S, Eagar TN, Forsthuber TG. T cell subsets and their signature cytokines in autoimmune and inflammatory diseases. *Cytokine.* (2015) 74:5–17. doi: 10.1016/j.cyto.2014.09.011
9. Zahran AM, Saad K, Abdel-Raheem YF, Elsayh KI, El-Houfey AA, Aboul-Khair MD, et al. Characterization of regulatory T cells in preterm and term infants. *Archivum Immunologiae et Therapiae Experimentalis.* (2019) 67:49–54. doi: 10.1007/s00005-018-0530-x
10. Penaloza HF, Noguera LP, Riedel CA, Bueno SM. Expanding the current knowledge about the role of interleukin-10 to major concerning bacteria. *Front Microbiol.* (2018) 9:2047. doi: 10.3389/fmicb.2018.02047
11. Walker JC, Smolders MAJC, Gemen EFA, Antonius TAJ, Leuvenink J, De Vries E. Development of lymphocyte subpopulations in preterm infants. *Scand J Immunol.* (2010) 73:53–8. doi: 10.1111/j.1365-3083.2010.02473.x
12. Scheible KM, Erno J, Yang H, Holden-Wiltse J, Straw A, Huyck H, et al. Developmentally determined reduction in CD31 during gestation is associated with CD8+ T cell effector differentiation in preterm infants. *Clin Immunol.* (2015) 161:65–74. doi: 10.1016/j.clim.2015.07.003
13. *Kamdar* S, Hutchinson R, *Laing* A, Stacey F, Ansbro K, Millar MR, et al. Perinatal inflammation influences but does not arrest rapid immune development in preterm babies. *Nat Commun*. (2012) 11:1284. doi: 10.1038/s41467-020-14923-8
14. Li J, Li H, Mao H, Yu M, Feng T, Yang F, et al. Vgamma9Vdelta2-T lymphocytes have impaired antiviral function in small-for-gestational-age and preterm neonates. *Cell Mol Immunol.* (2013) 10:253–60. doi: 10.1038/cmi.2012.78
15. Gibbons DL, Haque SF, Silberzahn T, Hamilton K, Langford C, Ellis P, et al. Neonates harbour highly active gammadelta T cells with selective impairments in preterm infants. *Eur J Immunol.* (2009) 39:1794–806. doi: 10.1002/eji.200939222
16. Ladd M, Sharma A, Huang Q, Wang AY, Xu L, Genowiti I, et al. Natural killer T cells constitutively expressing the interleukin-2 receptor α chain early in life are primed to respond to lower antigenic stimulation. *Immunology.* (2010) 131:289–99. doi: 10.1111/j.1365-2567.2010.03304.x
17. Ben Youssef G, Tourret M, Salou M, Ghazarian L, Houdouin V, Mondot S, et al. Ontogeny of human mucosal-associated invariant T cells and related T cell subsets. *J Exp Med.* (2018) 215:459–79. doi: 10.1084/jem.20171739
18. Leeansyah E, Loh L, Nixon DF, Sandberg JK. Acquisition of innate-like microbial reactivity in mucosal tissues during human fetal MAIT-cell development. *Nat Commun.* (2014) 5:3143. doi: 10.1038/ncomms4143
19. Haynes BF, Heinly CS. Early human T cell development: analysis of the human thymus at the time of initial entry of hematopoietic stem cells into the fetal thymic microenvironment. *J Exp Med.* (1995) 181:1445–58. doi: 10.1084/jem.181.4.1445
20. Michaelsson J, Mold JE, McCune JM, Nixon DF. Regulation of T cell responses in the developing human fetus. *J Immunol.* (2006) 176:5741–8. doi: 10.4049/jimmunol.176.10.5741
21. Darrasse-Jeze G, Marodon G, Salomon BL, Catala B, Klatzmann, D. Ontogeny of CD4+CD25+ regulatory/suppressor T cells in human fetuses. *Blood.* (2005) 105:4715–21. doi: 10.1182/blood-2004-10-4051
22. Li N, van Unen V, Abdelaal T, Guo N, Kasatskaya SA, Ladell K et al. Memory CD4(+) T cells are generated in the human fetal intestine. *Nat Immunol.* (2019) 20:301–12. doi: 10.1038/s41590-018-0294-9
23. Schreurs R, Baumdick ME, Sagebiel AF, Kaufmann M, Mokry M, Klarenbeek PL, et al. Human fetal TNF-alpha-cytokine-producing CD4(+) effector memory T cells promote intestinal development and mediate inflammation early in life. *Immunity.* (2019) 50:462–76.e8. doi: 10.1016/j.immuni.2018.12.010
24. Quinello C, Silveira-Lessa AL, Ceccon, MEJR, Cianciarullo MA, Carneiro-Sampaio M, Palmeira P. Phenotypic differences in leucocyte populations among healthy preterm and full-term newborns. *Scand J Immunol.* (2014) 80:57–70. doi: 10.1111/sji.12183
25. Berrington JE, Barge D, Fenton AC, Cant AJ, Spickett GP. Lymphocyte subsets in term and significantly preterm UK infants in the first year of life analysed by single platform flow cytometry. *Clin Exp Immunol.* (2005) 140:289–92. doi: 10.1111/j.1365-2249.2005.02767.x
26. Wong MT, Ong DE, Lim FS, Teng KW, McGovern N, Narayanan S, et al. A high-dimensional atlas of human T cell diversity reveals tissue-specific trafficking and cytokine signatures. *Immunity.* (2016) 45:442–56. doi: 10.1016/j.immuni.2016.07.007
27. Thome JJ, Bickham KL, Ohmura Y, Kubota M, Matsuoka N, Gordon, et al. Early-life compartmentalization of human T cell differentiation and regulatory function in mucosal and lymphoid tissues. *Nat Med.* (2016) 22:72–7. doi: 10.1038/nm.4008
28. Gonia S, Tuepker M, Heisel T, Autran C, Bode L, Gale A, et al. Human milk oligosaccharides inhibit *Candida albicans* invasion of human premature intestinal epithelial cells. *J Nutr.* (2015) 145:1992–8. doi: 10.3945/jn.115.214940
29. Bode L. Human milk oligosaccharides: every baby needs a sugar mama. *Glycobiology.* (2012) 22:1147–62. doi: 10.1093/glycob/cws074
30. He Y, Liu S, Leone S, Newburg DS. Human colostrum oligosaccharides modulate major immunologic pathways of immature human intestine. *Mucosal Immunol.* (2014) 7:1326–39. doi: 10.1038/mi.2014.20
31. Pagel J, Hartz A, Figge J, Gille C, Eschweiler S, Petersen K, et al. Regulatory T cell frequencies are increased in preterm infants with clinical early-onset sepsis. *Clin Exp Immunol.* (2016) 185:219–27. doi: 10.1111/cei.12810
32. Glocker EO, Kotlarz D, Boztug K, Gertz EM, Schaffer AA, Noyan F, et al. Inflammatory bowel disease and mutations affecting the interleukin-10 receptor. *N Engl J Med.* (2009) 361:2033–45. doi: 10.1056/NEJMoa0907206
33. Atarashi K, Tanoue T, Shima T, Imaoka A, Kuwahara T, Momose Y, et al. Induction of colonic regulatory T cells by indigenous clostridium species

- murine model of Treg and Th population being changed by microbiota. *Science.* (2011) 331:337–41. doi: 10.1126/science.1198469
34. Round JL, Lee SM, Li J, Tran G, Jabri B, Chatila TA, et al. The Toll-like receptor 2 pathway establishes colonization by a commensal of the human microbiota. *Science.* (2011) 332:974. doi: 10.1126/science.1206095
35. Ramakrishna C, Kujawski M, Chu H, Li L, Mazmanian SK, Cantin M, et al. Bacteroides fragilis polysaccharide A induces IL-10 secreting B and T cells that prevent viral encephalitis. *Nat Commun.* (2019) 10:2153. doi: 10.1038/s41467-019-09884-6
36. Sittipo P, Lobionda S, Choi K, Sari IN, Kwon HY, Lee K, et al. Toll-like receptor 2-mediated suppression of colorectal cancer pathogenesis by polysaccharide A from *Bacteroides fragilis*. *Front Microbiol.* (2018) 9:1588. doi: 10.3389/fmicb.2018.01588
37. Zhang X, Mozelski B, Lemoine S, Deriaud E, Lim A, Zhivaki D, et al. CD4 T cells with effector memory phenotype and function develop in the sterile environment of the fetus. *Sci Transl Med.* (2014) 6:238ra72. doi: 10.1126/scitranslmed.3008748
38. Marchant A, Appay V, van der Sande M, Dulphy N, Liesnard C, Kidd M, et al. Mature CD8+ T lymphocyte response to viral infection during fetal life. *J Clin Investig.* (2003) 111:1747–55. doi: 10.1172/JCI200317470
39. Vantourout, P, Hayday A. Six-of-the-best: unique contributions of gammadelta T cells to immunology. *Nat Rev Immunol.* (2013) 13:88–100. doi: 10.1038/nri3384
40. Berzins SP, Smyth MJ, Baxter AG. Presumed guilty: natural killer T cell defects and human disease. *Nat Rev Immunol.* (2011) 11:131–42. doi: 10.1038/nri2904
41. Moreira-Teixeira L, Resende M, Coffre M, Devergne O, Herbeuval JP, Hermine O, et al. Proinflammatory environment dictates the IL-17-producing capacity of human invariant NKT cells. *J Immunol.* (2011) 186:5758–65. doi: 10.4049/jimmunol.1003043
42. Olszak T, An D, Zeissig S, Vera MP, Richter J, Franke A, et al. Microbial exposure during early life has persistent effects on natural killer T cell function. *Science.* (2012) 336:489–93. doi: 10.1126/science.1219328
43. Heller F, Fuss IJ, Niewenhuis EE, Blumberg RS, Strober W. Oxazolone colitis, a Th2 colitis model resembling ulcerative colitis, is mediated by IL-13-producing NK-T cells. *Immunity*. (2002). 17:629–38. doi: 10.1016/S1074-7613(02)00453-3
44. Shen S, Prame Kumar K, Stanley D, Moore RJ, Van TTH, Wen SW, et al. Invariant natural killer T cells shape the gut microbiota and regulate neutrophil recruitment and function during intestinal inflammation. *Front Immunol.* (2018) 9:999. doi: 10.3389/fimmu.2018.00999
45. Hampel D, Shabab-Ferdows S, Islam MM, Peerson JM, Allen LH. Vitamin concentrations in human milk vary with time within feed. Circadian rhythm, single-dose supplementation. *J Nutr.* (2017) 147:603–11. doi: 10.3945/jn.116.242941
46. Tastan C, Karhan E, Zhou W, Fleming E, Voigt AY, Yao X, et al. Tuning of human MAIT cell activation by commensal bacteria species and MR1-dependent T-cell presentation. *Mucosal Immunol.* (2018) 11:1591–605. doi: 10.1038/s41385-018-0072-x
47. Walker LJ, Tharmalingam H, Klenerman P. The rise and fall of MAIT cells with age. *Scand J Immunol.* (2014) 80:462–3. doi: 10.1111/sji.12237
48. Chiba A, Murayama G, Miyake S. Mucosal-associated invariant T cells in autoimmune diseases. *Front Immunol.* (2018) 9:1333. doi: 10.3389/fimmu.2018.01333
49. Le Bourhis L, Guerri L, Dusseaux M, Martin E, Soudais C, Lantz, et al. Mucosal-associated invariant T cells: unconventional development and function. *Trends Immunol.* (2011) 32:212–8. doi: 10.1016/j.it.2011.02.005
50. Ren S, Hui Y, Goericke-Pesch S, Pankratova S, Kot W, Pan X, et al. Gut and immune effects of bioactive milk factors in preterm pigs exposed to prenatal inflammation. *Am J Physiol Gastrointest Liver Physiol.* (2019) 317:G67–77. doi: 10.1152/ajpgi.00042.2019
51. Hassiotou F, Beltran A, Chetwynd E, Stuebe AM, Twigger, A-J., et al. Breastmilk is a novel source of stem cells with multilineage differentiation potential. *Stem Cells.* (2012) 30:2164–74. doi: 10.1002/stem.1188
52. Ma LJ, Walter B, Deguzman A, Muller HK, Walker AM. Trans-epithelial immune cell transfer during suckling modulates delayed-type hypersensitivity in recipients as a function of gender. *PLoS ONE.* (2008) 3:e3562. doi: 10.1371/journal.pone.0003562
53. Hassiotou F, Mobley A, Geddes D, Hartmann P, Walkie T. Breastmilk imparts the mother's stem cells to the infant. *FASEB J.* (2015) 29:876.
54. Aydin MS, Yigit EN, Vatandaslar E, Erdogan E, Ozturk G. Transfer, and integration of breast milk stem cells to the brain of suckling pups. *Sci Rep.* (2018). 8:14289. doi: 10.1038/s41598-018-32715-5
55. Oram JD, Reiter B. Inhibition of bacteria by lactoferrin and other iron-chelating agents. *Biochim Biophys Acta.* (1968) 170:351–65. doi: 10.1016/0304-4165(68)90015-9
56. Mincheva-Nilsson L, Hammarstrom S, Hammarstrom M. Activated human yd T lymphocytes express functional lactoferrin receptors. *Scand J Immunol.* (1997) 46:609–18. doi: 10.1046/j.1365-3083.1997.d01-165.x
57. Nielsen SM, Hansen GH, Danielsen EM. Lactoferrin targets T cells in the small intestine. *J Gastroenterol.* (2010) 45:1121–8. doi: 10.1007/s00535-010-0271-z
58. Trend S, de Jong E, Lloyd ML, Kok CH, Richmond P, Doherty DA, et al. Leukocyte populations in human preterm and term breast milk identified by multicolour flow cytometry. *PLoS ONE.* (2015) 10:e0135580. doi: 10.1371/journal.pone.0135580
59. Cabinian A, Sinsimer D, Tang M, Zumba O, Mehta H, Toma A, et al. Transfer of maternal immune cells by breastfeeding: maternal cytotoxic T lymphocytes present in breast milk localize in the Peyer's patches of the nursed infant. *PLoS ONE.* (2016) 11:e0156762. doi: 10.1371/journal.pone.0156762
60. Ward P, Conneely OM. Lactoferrin: role in iron homeostasis and host defense against microbial infection. *BioMetals.* (2004) 17:203–8. doi: 10.1023/B:BIOM.0000027693.60932.26
61. Legrand D. Overview of lactoferrin as a natural immune modulator. *J Pediatr.* (2016) 173(Suppl.):S10–5. doi: 10.1016/j.jpeds.2016.02.071
62. Wang, W.-P., Iigo M, Sato J, Sekine K, Adachi I, et al. Activation of intestinal mucosal immunity in tumour-bearing mice by lactoferrin. *Jap J Cancer Res.* (2000) 91:1022–7. doi: 10.1111/j.1349-7006.2000.tb00880.x

Conflict of Interest: NE declares research funding from Danone Early Life Nutrition and Prolacta Biosciences, as well as speaker honoraria from Baxter and Nestle Nutrition Institute.

The remaining authors declare that the research was conducted in the absence of any commercial or financial relationships that could be construed as a potential conflict of interest.

The handling editor declared a past co-authorship with the JB and NE.

frontiers in Immunology

SYSTEMATIC REVIEW
published: 05 June 2020
doi: 10.3389/fimmu.2020.00972

Association of Histological and Clinical Chorioamnionitis With Neonatal Sepsis Among Preterm Infants: A Systematic Review, Meta-Analysis, and Meta-Regression

*Eduardo Villamor-Martinez, George A. Lubach, Owais Mohammed Rahim, Pieter Degraeuwe, Luc J. Zimmermann, Boris W. Kramer and Eduardo Villamor**

Department of Pediatrics, Maastricht University Medical Center (MUMC+), School for Oncology and Developmental Biology (GROW), Maastricht, Netherlands

OPEN ACCESS

Edited by:
Duc Ninh Nguyen, University of Copenhagen, Denmark

Reviewed by:
David Burgner, Royal Children's Hospital, Australia
Ivana Musilova, Charles University, Czechia

***Correspondence:**
Eduardo Villamor
e.villamor@mumc.nl

Specialty section:
This article was submitted to Microbial Immunology, a section of the journal Frontiers in Immunology

Received: *15 November 2019*
Accepted: *24 April 2020*
Published: *05 June 2020*

Citation:
Villamor-Martinez E, Lubach GA, Rahim OM, Degraeuwe P, Zimmermann LJ, Kramer BW and Villamor E (2020) Association of Histological and Clinical Chorioamnionitis With Neonatal Sepsis Among Preterm Infants: A Systematic Review, Meta-Analysis, and Meta-Regression. Front. Immunol. 11:972. doi: 10.3389/fimmu.2020.00972

Chorioamnionitis (CA) is considered a key risk factor for very preterm birth and for developing early onset sepsis (EOS) in preterm infants, but recent data suggest that CA might be protective against late onset sepsis (LOS). We performed a systematic review and meta-analysis of studies exploring the association between CA and sepsis. A comprehensive literature search was performed in PubMed/MEDLINE and EMBASE, from their inception to December 1, 2018. A random-effects model was used to calculate odds ratios (OR) and 95% confidence intervals (CI). Sources of heterogeneity were analyzed by subgroup and meta-regression analyses. The following categories of sepsis were analyzed: EOS, LOS, unspecified onset sepsis (UOS), culture-proven, and clinical sepsis. CA was subdivided into clinical and histological chorioamnionitis. Funisitis was also analyzed. We found 3,768 potentially relevant studies, of which 107 met the inclusion criteria (387,321 infants; 44,414 cases of CA). Meta-analysis showed an association between any CA and any EOS (OR 4.29, CI 3.63–5.06), any LOS (OR 1.29, CI 1.11–1.54), and any UOS (OR 1.59, CI 1.11–1.54). Subgroup analysis showed that CA was associated with culture-proven EOS (OR 4.69, CI 3.91–5.56), clinical EOS (OR 3.58, CI 1.90–6.76), and culture-proven LOS (OR 1.31, CI 1.12–1.53), but not with clinical LOS (OR 1.52, CI 0.78–2.96). The presence of funisitis did not increase the risk of either EOS or LOS when compared with CA without funisitis. CA-exposed infants had lower gestational age (−1.11 weeks, CI −1.37 to −0.84) than the infants not exposed to CA. Meta-regression analysis showed that the lower gestational age of the CA group correlated with the association between CA and LOS but not with the association between CA and EOS. In conclusion, our data suggest that the positive association between chorioamnionitis and LOS may be modulated by the effect of chorioamnionitis on gestational age.

Keywords: chorioamnionitis, neonatal sepsis, immunomodulation, very preterm birth, extremely preterm birth, meta-analysis, meta-regression, systematic review

INTRODUCTION

Very preterm birth is defined by a gestational age (GA) below 32 weeks, and extremely preterm birth is defined by a GA below 28 weeks (1). The etiological background of very/extremely preterm birth can be divided into two main categories: intrauterine infection/inflammation and placental vascular dysfunction (2–4). The first category is associated with chorioamnionitis (CA), preterm labor, premature rupture of membranes (PROM), placental abruption, and cervical insufficiency, whereas the second category is associated with gestational hypertensive disorders and condition known as fetal indication/fetal growth restriction (2–4). Belonging to the first group, CA is the maternal response to an intrauterine infection/inflammation and implies the presence of inflammatory cells in the extraplacental membranes (chorion and amnion) (5, 6). Acute CA generally represents the presence of intraamniotic infection or "amniotic fluid infection syndrome" but can also occur in the in the absence of proven infection (6). This may partly be due to lack of detection of some bacterial species by the culturing methods routinely employed (7, 8).

CA is not only considered to be a leading cause of very/extremely preterm birth but also a main factor in the development of subsequent neonatal complications (9–11). Numerous individual studies and meta-analyses have addressed the association between CA and complications of very/extremely preterm birth such as bronchopulmonary dysplasia (12, 13), necrotizing enterocolitis (14), retinopathy of prematurity (15, 16), patent ductus arteriosus (17, 18), intraventricular hemorrhage (19), cerebellar hemorrhage (20), neonatal brain injury (21), or cerebral palsy (22).

Very/extremely preterm infants are at high risk for neonatal sepsis (23–27). Early onset sepsis (EOS) is defined as a blood or cerebrospinal fluid culture obtained within 72 h after birth. EOS is typically caused by microorganisms transmitted vertically from the mother to the infant before birth or during delivery (23, 24). Frequently, preterm EOS begins in the uterus and the microbial-induced maternal inflammation initiates labor and elicits an inflammatory response in the fetus (23–25). Therefore, CA and/or intraamniotic infection are strongly associated with EOS in preterm infants (23–25).

Late-onset sepsis (LOS) occurs after 72 h of life and may be caused by microorganisms acquired at delivery or during the course of hospital care (23, 25). Very/extremely preterm infants are at an increased risk of LOS because of the relative immaturity of their immune system as well as the frequently required prolonged hospitalization, with ongoing risk of infection, and exposure to invasive procedures and devices (23, 25, 26, 28). Coagulase-negative staphylococci (CoNS) are the most frequent pathogens causing nosocomial sepsis among preterm infants. Interestingly, Strunk et al. reported in a cohort of infants with a GA below 30 weeks that histological CA was associated with reduced risk of developing LOS, both with CoNS and other bacteria (25). They speculate that "chorioamnionitis may result in maturation of the fetal and neonatal immune system and therefore indirectly modulates the risk of LOS with nosocomial organisms" (25).

Surprisingly, to the best of our knowledge, the association between CA and neonatal sepsis has not yet been the subject of a systematic review. We therefore aimed to carry out a systematic review and meta-analysis of observational studies reporting on the association between CA and EOS and/or LOS in preterm infants. We paid particular attention to how the criteria used to define CA and sepsis affected the potential association between the two conditions. We also analyzed the role of potential confounders or intermediate factors, such as GA, birth weight (BW), presence of fetal inflammatory response (i.e., funisitis), or exposure to antenatal corticosteroids, on the association between CA and neonatal sepsis.

METHODS

We used a similar methodology to earlier meta-analyses on the association of CA and short-term outcomes of prematurity (13, 16, 17, 19). A protocol (available at https://www.crd.york.ac.uk/prospero/display_record.php?RecordID=117190) was developed and published a priori in which the objectives, inclusion criteria, method for evaluating study quality, included outcomes and covariates, and statistical methodology were specified (29) We report the study according to the guidelines for the Preferred Reporting Items for Systematic Reviews and Meta-Analysis (PRISMA) (30).

Sources and Search Strategy

A comprehensive literature search was performed in the PubMed/MEDLINE and EMBASE databases from their inception to December 1, 2018. The search strategy involved the following keywords in various combinations: "chorioamnionitis," "intrauterine infection," "intrauterine inflammation," "antenatal infection," antenatal inflammation," "funisitis," "preterm infant," "prematurity," "cohort," "sepsis," "(neonatal) early-onset sepsis," and "(neonatal) late-onset sepsis." The full search strategy can be found in the **Supplementary Data 1**.

Study Selection

Studies were included if they examined preterm (GA < 37 weeks) infants and reported primary data that could be used to measure the association between exposure to CA and the development of neonatal sepsis. Studies using BW instead of GA as the inclusion criteria were included only when inclusion BW was below 1,500 g. Therefore, we selected studies assessing the outcomes of infants exposed to CA when sepsis was one of the reported outcomes, and studies assessing the risk factors for sepsis when CA was one of the reported risk factors. We also included studies reporting on intra-amniotic infection resulting from microbial invasion of the amniotic cavity (MIAC) because MIAC is also within the spectrum of CA (31). MIAC was defined as a positive amniotic fluid culture for microorganisms. The results of the total search were screened independently by two reviewers (G. A. L. and O. M. R.) in several rounds: first by title only, second by title and abstract and thirdly by consulting the full text. The reviewers resolved discrepancies in inclusion through discussion and by consulting a third reviewer (P. D.).

Data Extraction

Utilizing a predetermined worksheet, data was extracted from the included studies by three researchers (G. A. L., O. M. R., and E. V.-M). Two additional researchers (P. D. and E. V.) checked the extracted data for accuracy and completeness. Discrepancies were resolved by checking the primary data report and by discussion. We extracted the following data from each study: citation information, the language of the publication, the location where research was conducted, the time period of the study, study objectives, study design, inclusion/exclusion criteria, patient characteristics, definitions of CA (clinical, histological, or microbiological), definitions of sepsis (culture-proven or clinical), and results (including raw numbers, summary statistics, and adjusted analyses on CA and sepsis where available). Onset of sepsis was classified in three groups: EOS, LOS, and unspecified onset sepsis (UOS).

Quality Assessment

The Newcastle-Ottawa Scale (NOS) for cohort or case-control studies was used to assess the methodological quality of the included studies (32). The NOS evaluates three aspects of a given study: selection, comparability, and exposure/outcome. These are scored individually and tallied up to a possible total of 9 points. The NOS was independently used by two researchers (G. A. L. and E. V.-M) to evaluate the quality of each study. Discrepancies were resolved by reaching consensus through discussion.

Statistical Analysis

Studies were combined and analyzed using COMPREHENSIVE META-ANALYSIS V 3.0 software (CMA, RRID:SCR_012779, Biostat Inc., Englewood, NJ, USA). The odds ratio (OR) and the 95% confidence interval (CI) for dichotomous variables were calculated from the extracted data of the studies. For continuous variables, the mean difference (MD) was calculated together with the 95% CI. When studies reported continuous variables as the median and the range/interquartile range, we estimated the mean and standard deviation using the method of Wan et al. (33). Due to anticipated heterogeneity, summary statistics were calculated with a random-effects model. This accounts for the variability between studies as well as within studies. For subgroup analyses the mixed-effects model was used (34). With this approach, a random-effects model is used within each subgroup, while a fixed-effect model is used to combine subgroups to generate the overall effect. The study-to-study variance (tau-squared) was calculated across all studies. Statistical heterogeneity was tested using Cochran's Q statistic and the I^2 statistic (34). Publication bias was assessed with Egger's regression test (35) and visual inspection of funnel plots. K represents the number of studies used in each analysis.

Univariate random-effects meta-regression was used to explore whether the differences in covariates between studies might influence the outcome effect size (34). We carried out meta-regression analysis only if there were more than 10 studies that reported on a covariate. The following possible sources of variability were defined beforehand: CA type (clinical or histological), sepsis type (culture-proven or clinical), differences in GA and BW between infants with and without CA, use of antenatal corticosteroids, mode of delivery, rate of GA, rate of PROM, and rate of preeclampsia.

RESULTS

Description of Studies

We screened 3,768 studies after removing duplicates, of which 107 studies met the inclusion criteria (4, 25, 36–141). The PRISMA flow diagram of the search is shown in **Figure 1**. The included studies evaluated 387,321 infants, including 44,414 infants with CA. An overview of the characteristics of the included studies can be found in **Supplementary Table 1**. There were 75 studies that evaluated the outcomes of CA, and sepsis was one of these outcomes, and 26 studies that looked at potential risk factors for sepsis, including CA. Seven studies were designed to primarily examine the association between CA and sepsis. From the included studies, 58 used a histological definition of CA and 28 studies used a clinical definition of CA. Nine studies distinguished between both definitions of CA in their reporting (36, 45, 65, 80, 93, 97, 104, 106, 108). Five studies reported on MIAC (77, 83, 84, 105, 113). In six studies, the CA definition was not further specified and categorized as "unspecified" for further analysis (37, 42, 75, 103, 129). Nine studies (37, 46, 77, 98, 115, 118, 129, 139, 141) used the 7-day limit to differentiate between EOS and LOS.

Quality Assessment

A summary of the NOS quality assessment can be found in **Supplementary Table 2**. Four studies received a quality score of 5 points, 24 studies a score of 6 points, 57 studies a score of 7 points, 9 studies a score of 8 points and 13 studies received a score 9 points. Studies lost points for quality for not adjusting the risk of sepsis for confounders ($k = 90$), for not defining sepsis clearly ($k = 6$), for not defining CA clearly ($k = 21$), and for adjusting the risk of sepsis only for one confounder ($k = 6$).

Meta-Analysis Based on Unadjusted Data

Early Onset Sepsis

As shown in **Figure 2A**, meta-analysis found a positive association between CA (any type) and EOS (any type) ($k = 70$, OR 4.29, 95% CI 3.63–5.06). When subdividing by CA definition, meta-analysis showed that histological CA ($k = 43$, OR 3.46, 95% CI 2.74–4.4.38, **Figure 3**), clinical CA ($k = 20$, OR 4.76, 95% CI 3.68–6.15, **Figure 4**), histological/clinical CA ($k = 1$, OR 6.17, 95% CI 1.18–32.23, **Figure 4**), MIAC ($k = 3$, OR 5.38, 95% CI 1.76–16.44, **Figure 4**), and unspecified CA ($k = 3$, OR 14.14, 95% CI 6.46–30.95, **Figure 4**) were associated with EOS (any type). The exclusion of the studies reporting on MIAC, combined clinical/histological CA, and unspecified CA did not substantially affect the OR of the association between CA and EOS (**Table 1**).

When subdividing by EOS definition, meta-analysis showed that CA (any type) was associated with culture-proven EOS ($k = 56$, OR 4.69, 95% CI 3.93–5.60, **Figure 2B**) and clinical EOS ($k = 15$, OR 3.58, 95% CI 1.90–6.76, **Figure 2C**). As shown in **Figure 2B**, subgroup analysis based on CA type showed that histological CA ($k = 26$, **Supplementary Figure 1**), clinical CA ($k = 24$ **Supplementary Figure 2**), MIAC (k

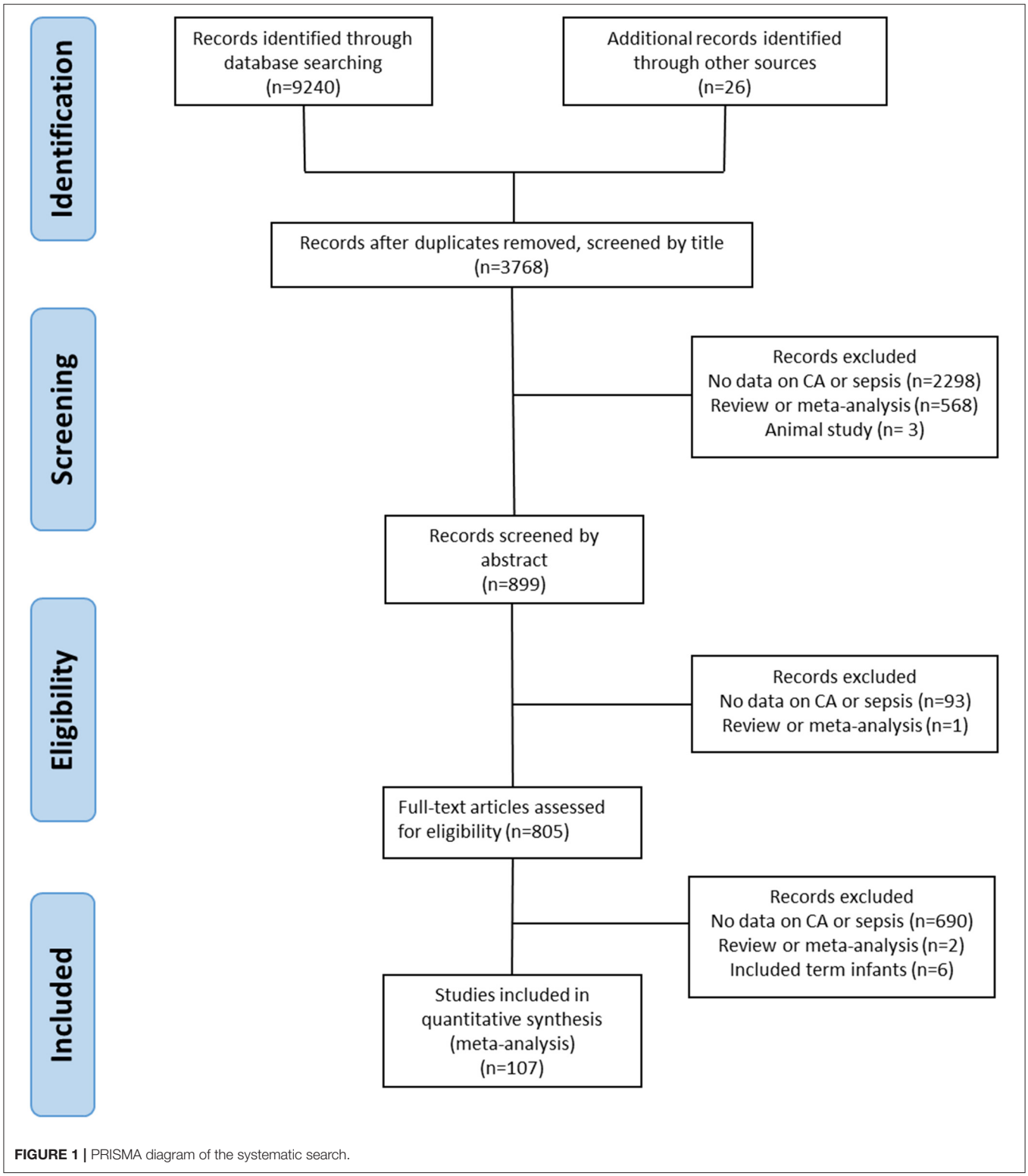

FIGURE 1 | PRISMA diagram of the systematic search.

= 3, **Supplementary Figure 2**), and unspecified CA (k = 3, **Supplementary Figure 2**) were associated with culture-proven EOS. In contrast, as shown in **Figure 2C** and **Supplementary Figure 3**, clinical EOS was associated with clinical CA ($k = 4$), but not with histological CA ($k = 9$), or MIAC ($k = 2$). Meta-regression could not find differences between the effect size of the association CA-culture-proven EOS and the effect size of the association CA-clinical EOS (p

A Any early onset sepsis

Chorioamnionitis definition	k	Odds ratio	Lower limit	Upper limit	p-Value
Histological	43	3.46	2.74	4.38	< 0.001
Clinical	20	4.76	3.68	6.15	< 0.001
MIAC	3	5.40	1.76	16.57	0.003
Unspecified	3	14.14	6.46	30.95	< 0.001
Histol./Clin.	1	6.17	1.18	32.41	0.031
OVERALL	**70**	**4.29**	**3.63**	**5.06**	**< 0.001**

Heterogeneity: I^2 = 66%; p < 0.001

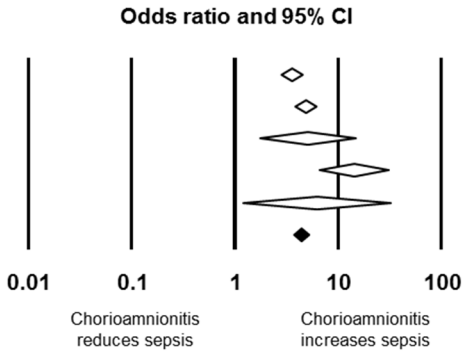

B Culture proven early onset sepsis

Chorioamnionitis definition	k	Odds ratio	Lower limit	Upper limit	p-Value
Histological	26	3.57	2.69	4.74	< 0.001
Clinical	24	5.14	4.03	6.55	< 0.001
MIAC	3	4.41	1.43	13.57	0.010
Unspecified	3	14.30	6.66	30.72	< 0.001
OVERALL	**56**	**4.69**	**3.93**	**5.60**	**< 0.001**

Heterogeneity: I^2 = 68%; p < 0.001

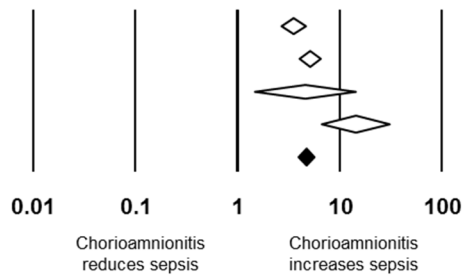

C Clinical early onset sepsis

Chorioamnionitis definition	k	Odds ratio	Lower limit	Upper limit	p-Value
Histological	9	2.28	0.96	5.43	0.061
Clinical	4	5.97	2.05	17.38	0.001
MIAC	2	6.17	0.91	41.67	0.062
OVERALL	**15**	**3.58**	**1.90**	**6.76**	**< 0.001**

Heterogeneity: I^2 = 83%; p < 0.001

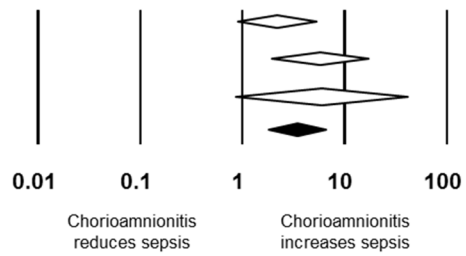

D

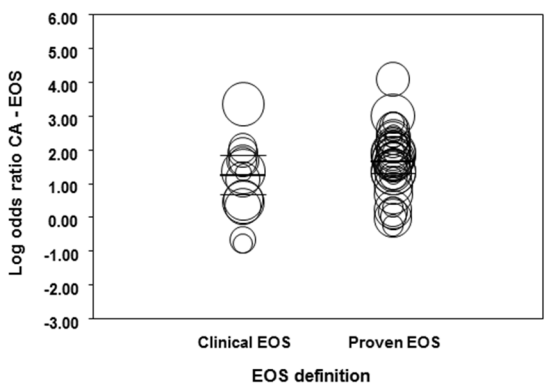

FIGURE 2 | Random effects meta-analyses of chorioamnionitis and early onset sepsis (EOS), subdivided by definition of chorioamnionitis. **(A)** Any EOS; **(B)** culture-proven EOS; **(C)** clinical EOS; **(D)** meta-regression comparing culture-proven and clinical EOS. MIAC, microbial invasion of the amniotic cavity.

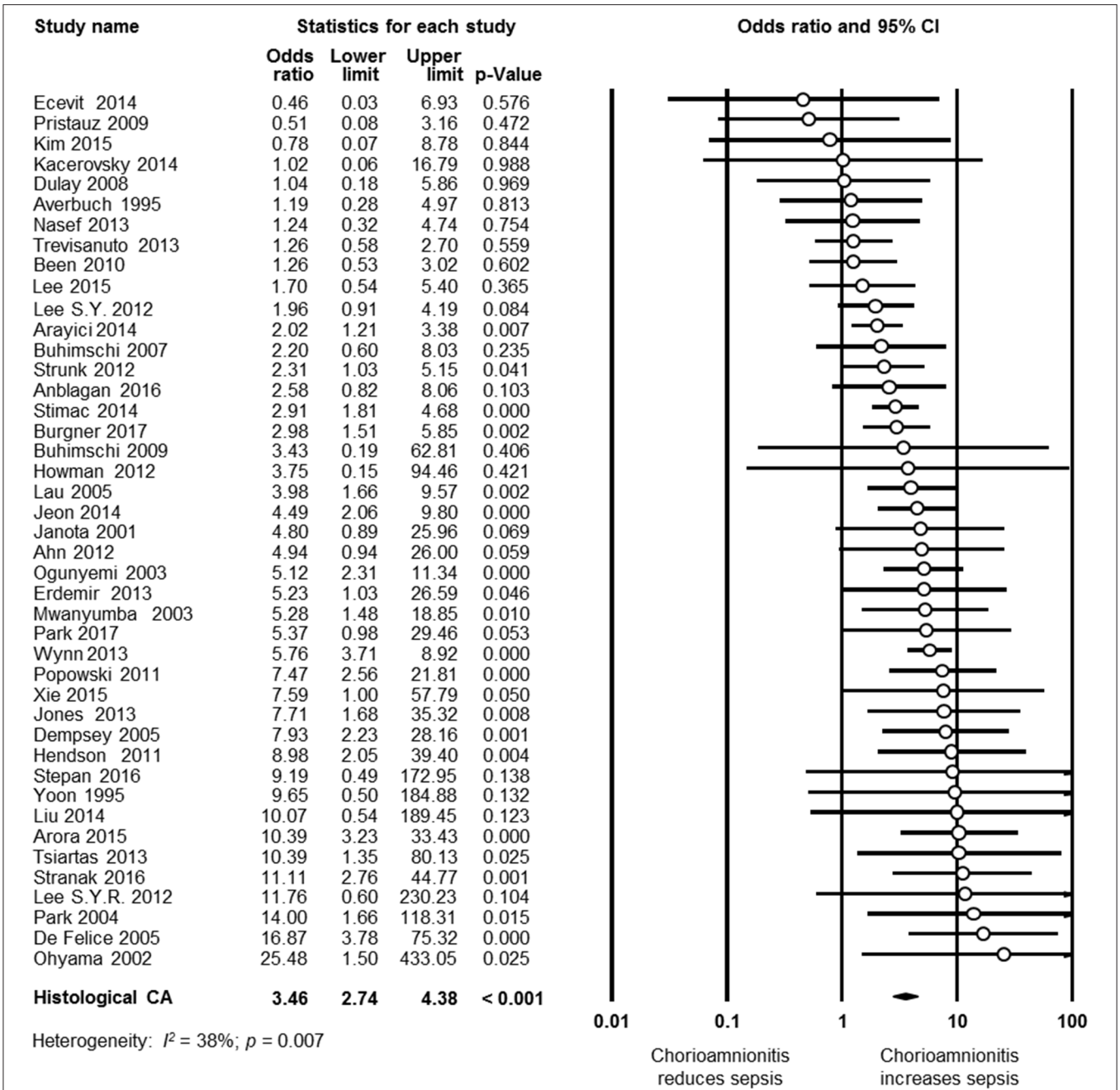

FIGURE 3 | Random effects meta-analysis of histological chorioamnionitis (CA) and all early onset sepsis (culture proven or clinical).

= 0.150, **Figure 2D**). There was no evidence of publication bias for studies reporting on EOS (**Supplementary Figure 4**), assessed with Egger's regression test and visual inspection of the funnel plots.

Late Onset Sepsis

As shown in **Figures 5A**, **6**, meta-analysis found a positive association between CA (any type) and LOS (any type) (k = 29, OR 1.29, 95% CI 1.11–1.54). When subdividing by CA definition, meta-analysis showed that histological CA (k = 21, OR 1.38, 95% CI 1.13–1.68, **Figure 6**), and MIAC (k = 1, OR 9.90, 95% CI 1.90–51.54, **Figure 6**) were associated with LOS (any type). In contrast, subgroup analysis could not find an association between LOS (any type) and clinical CA (k = 6, OR 1.21, 95% CI 0.95–1.55, **Figure 6**), or unspecified CA (k = 1 OR 0.61, 95% CI 0.28–1.33, **Figure 6**). The exclusion of the studies reporting on MIAC, combined clinical/histological CA, and unspecified CA did not substantially

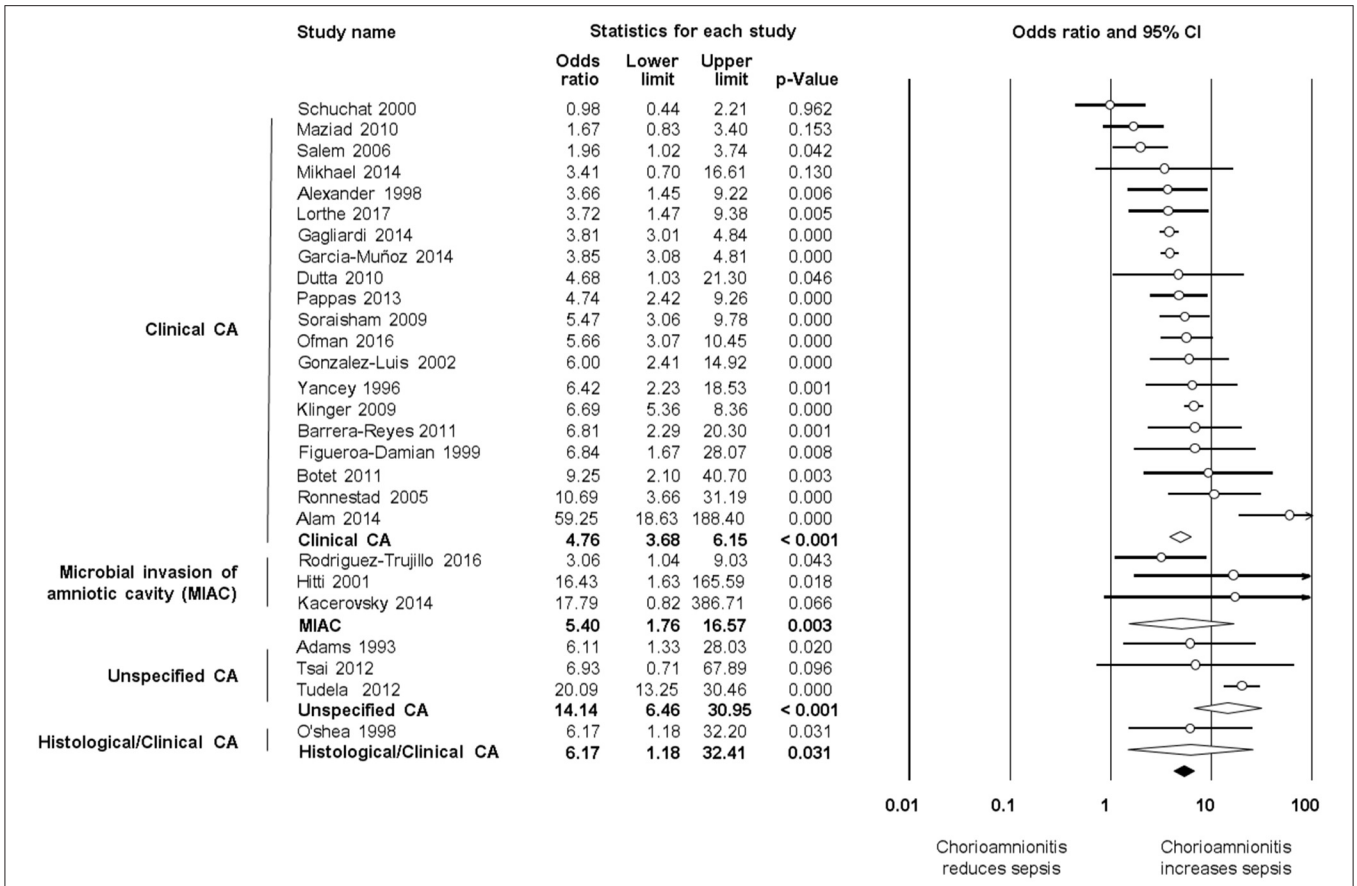

FIGURE 4 | Random effects meta-analyses of clinical, microbiological, unspecified, and histological/clinical chorioamnionitis (CA) and all early onset sepsis (culture proven or clinical).

TABLE 1 | Meta-analysis on the association between any chorioamnionitis[a] and sepsis, divided by onset, and definition of sepsis.

Sepsis onset	Sepsis definition	Number of studies (k)			OR	95% CI	*P*
		Total	Histological	Clinical			
Early	Any sepsis	64	42	22	4.10	3.45–4.86	<0.001
	Culture proven	50	26	24	4.40	3.66–5.29	<0.001
	Clinical	13	9	4	3.34	1.71–6.53	<0.001
Late	Any sepsis	27	21	6	1.31	1.12–1.53	0.001
	Culture proven	16	12	4	1.33	1.13–1.57	0.001
	Clinical	5	5	0	1.52	0.78–2.96	0.216
Unspecified	Any sepsis	29	22	7	1.61	1.30 - 1.99	<0.001
	Culture proven	20	15	5	1.48	1.16 - 2.27	<0.001
	Clinical	6	5	1	2.13	1.30 - 3.48	0.003

[a] *Studies reporting on microbial invasion of the amniotic cavity (MIAC), combined clinical/histological chorioamnionitis, or on unspecified chorioamnionitis were excluded from the analysis.*

affect the OR of the association between CA and LOS (**Table 1**).

When subdividing by LOS definition, meta-analysis showed that CA (any type) was associated with culture-proven LOS ($k = 18$, OR 1.31, 95% CI 1.12–1.53, **Figure 5B** and **Supplementary Figure 5**), but not with clinical LOS ($k = 5$, OR 1.52, 95% CI 0.78–2.96, **Figure 5C** and **Supplementary Figure 6**). The analysis on the association between clinical LOS and CA was exclusively based on data on histological CA. As shown in **Figure 5B** and **Supplementary Figure 5**, subgroup analysis based on CA type showed that histological CA ($k = 12$), clinical CA ($k = 4$), and MIAC ($k = 1$) were associated with culture-proven LOS. Meta-regression could not find differences between the effect size of the association CA-culture-proven LOS and the effect size of the association CA-clinical LOS ($p = 0.920$, **Figure 5D**). There

A Any late onset sepsis

Chorioamnionitis definition	k	Odds ratio	Lower limit	Upper limit	p-Value
Histological	21	1.38	1.13	1.68	0.001
Clinical	6	1.21	0.95	1.55	0.127
MIAC	1	9.90	1.90	51.54	0.006
Unspecified	1	0.61	0.28	1.33	0.218
OVERALL	**29**	**1.29**	**1.11**	**1.54**	**0.001**

Heterogeneity: I^2 = 69%; p < 0.001

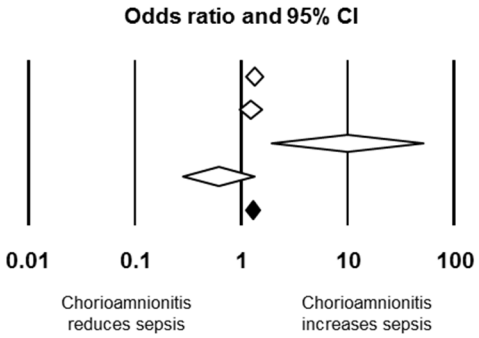

B Culture proven late onset sepsis

Chorioamnionitis definition	k	Odds ratio	Lower limit	Upper limit	p-Value
Histological	12	1.34	1.07	1.68	0.011
Clinical	4	1.32	1.05	1.67	0.017
MIAC	1	9.90	1.96	49.98	0.005
Unspecified	1	0.61	0.30	1.24	0.176
OVERALL	**18**	**1.31**	**1.12**	**1.53**	**0.001**

Heterogeneity: I^2 = 64%; p < 0.001

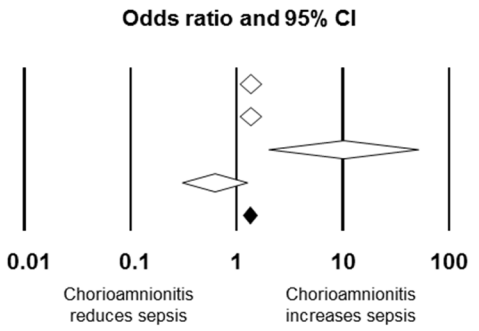

C Clinical late onset sepsis

Chorioamnionitis definition	k	Odds ratio	Lower limit	Upper limit	p-Value
Histological	5	1.52	0.78	2.96	0.216

Heterogeneity: I^2 = 53%; p = 0.073

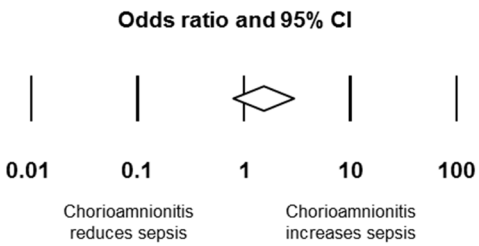

D

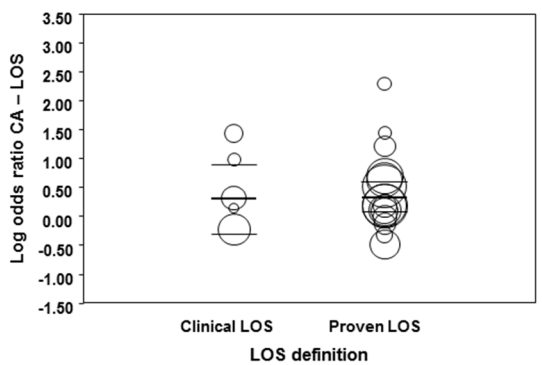

FIGURE 5 | Random effects meta-analyses of chorioamnionitis and late onset sepsis (LOS), subdivided by definition of chorioamnionitis. **(A)** Any LOS; **(B)** culture-proven LOS; **(C)** clinical LOS; **(D)** meta-regression comparing culture-proven and clinical LOS. MIAC, microbial invasion of the amniotic cavity.

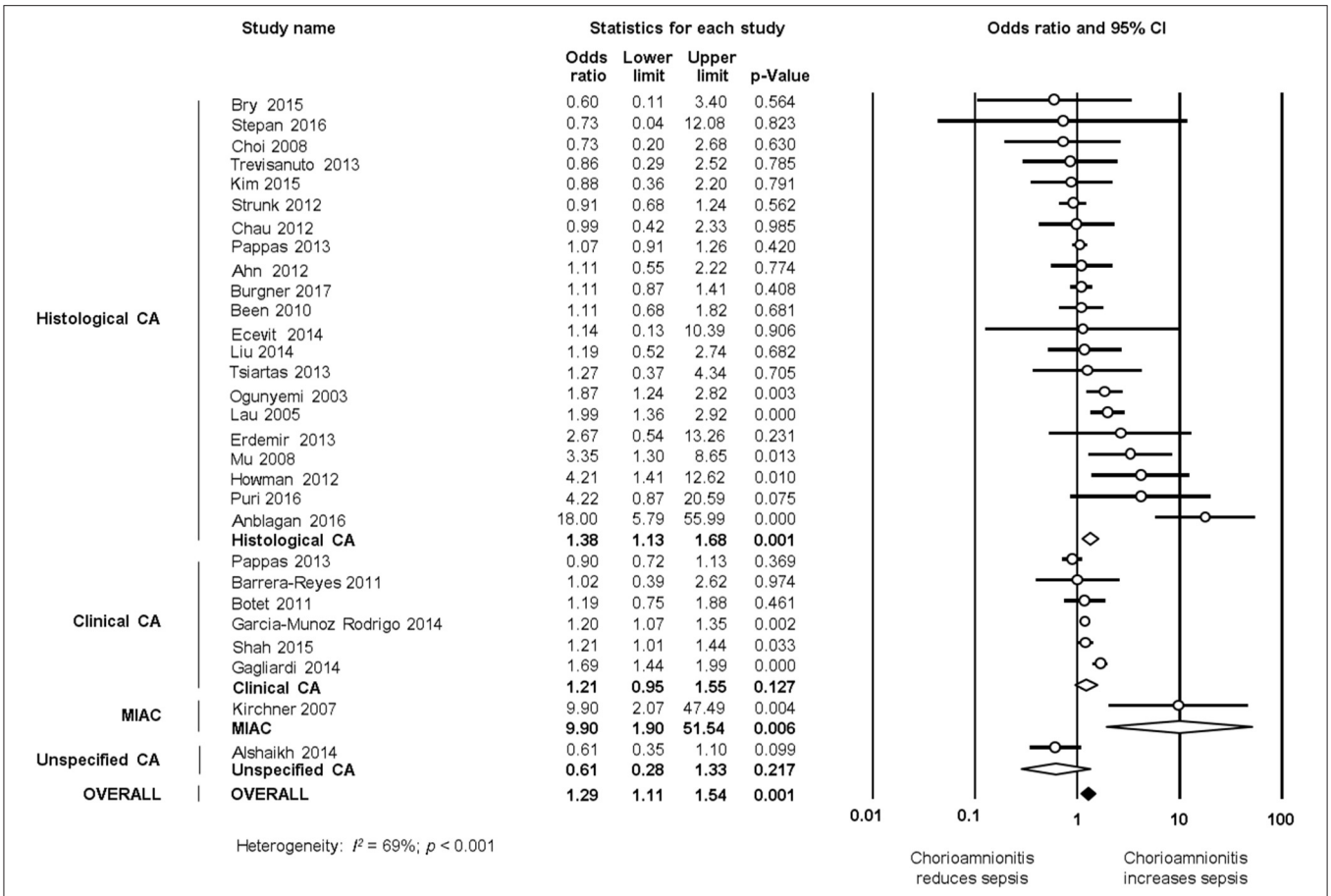

FIGURE 6 | Random effects meta-analyses of histological, clinical, microbiological, and unspecified chorioamnionitis (CA) and all late onset sepsis.

was no evidence of publication bias for studies reporting on LOS (**Supplementary Figure 4**), assessed with Egger's regression test and visual inspection of funnel plots.

Unspecified Onset Sepsis

As shown in **Figure 7A** and **Supplementary Figure 7**, meta-analysis found a significant positive association between CA (any type) and UOS (any type) (k = 31, OR 1.59, 95% CI 1.11–1.54). When subdividing by CA definition, meta-analysis showed that histological CA (k = 22, OR 1.61, 95% CI 1.30–1.99), and clinical CA (k = 7, OR 1.63, 95% CI 1.16–2.29) were significantly associated with UOS (any type, **Supplementary Figure 7**).

When subdividing by UOS definition, meta-analysis showed that CA (any type) was associated with culture-proven UOS (k = 22, OR 1.48, 95% CI 1.23–1.76, **Figure 7B** and **Supplementary Figure 8**) and clinical UOS (k = 6, OR 2.13, 95% CI 1.30–3.48, **Figure 7C** and **Supplementary Figure 9**). As shown in **Figure 7B** and **Supplementary Figure 8**, subgroup analysis based on CA type showed that histological CA (k = 15), and clinical CA (k = 5) were associated with culture-proven UOS. In contrast, only histological CA was associated with clinical UOS (k = 5, **Figure 7C** and **Supplementary Figure 9**). Meta-regression could not find differences between the effect size of the association CA-culture proven UOS and the effect size of the association CA-clinical UOS (**Figure 7D**). There was no evidence of publication bias for studies reporting on UOS (**Supplementary Figure 4**), assessed with Egger's regression test and visual inspection of funnel plots.

Funisitis

Additional meta-analyses were performed to determine if funisitis, as a fetal-inflammatory response, was associated with the development of neonatal sepsis. As shown in **Figure 8,** 10 studies reported on EOS and infants with histological CA with or without funisitis; eight studies on LOS and infants with histological CA with or without funisitis; and five studies on UOS and infants with histological CA with or without funisitis. Meta-analysis showed that funisitis did not increase the risk of sepsis (EOS, LOS, or UOS), when compared with CA without funisitis (**Figure 8**).

Meta-Analysis of Covariates and Meta-Regression

We performed additional meta-analyses to explore the possible differences in baseline characteristics between the groups exposed and non-exposed to CA. Exposure to CA was

A **Any unspecified onset sepsis**

Chorioamnionitis definition	k	Odds ratio	Lower limit	Upper limit	p-Value
Histological	22	1.61	1.30	1.99	< 0.001
Clinical	7	1.63	1.16	2.29	0.005
Both	1	0.63	0.13	2.98	0.564
Unspecified	1	1.69	0.76	3.74	0.195
OVERALL	**31**	**1.59**	**1.11**	**1.54**	**< 0.001**

Heterogeneity: I^2 = 62%; p < 0.001

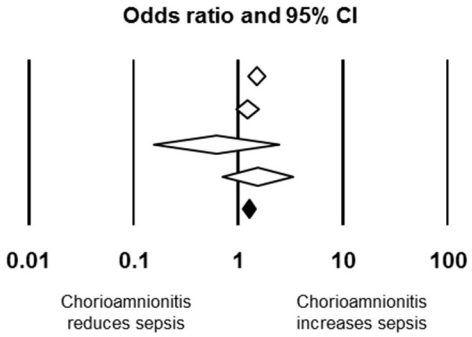

B **Culture proven unspecified onset sepsis**

Chorioamnionitis definition	k	Odds ratio	Lower limit	Upper limit	p-Value
Histological	15	1.42	1.14	1.78	0.002
Clinical	5	1.62	1.16	2.27	0.005
Both	1	0.63	0.14	2.86	0.552
Unspecified	1	1.69	0.83	3.42	0.145
OVERALL	**22**	**1.48**	**1.23**	**1.76**	**< 0.001**

Heterogeneity: I^2 = 59%; p < 0.001

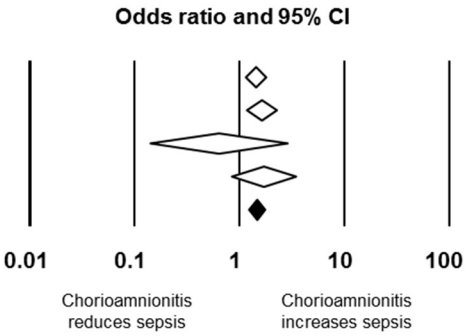

C **Clinical unspecified onset sepsis**

Chorioamnionitis definition	k	Odds ratio	Lower limit	Upper limit	p-Value
Histological	5	2.04	1.23	3.37	0.006
Clinical	1	5.38	0.53	55.04	0.156
OVERALL	**6**	**2.13**	**1.30**	**3.48**	**0.003**

Heterogeneity: I^2 = 51%; p = 0.069

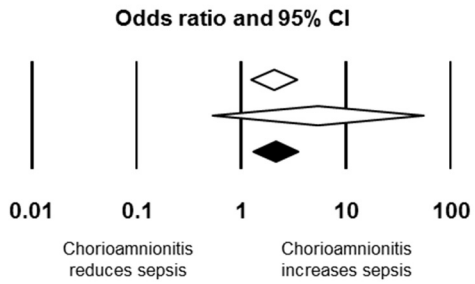

D

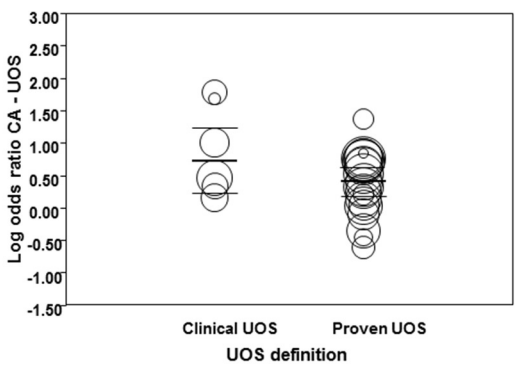

FIGURE 7 | Random effects meta-analyses of unspecified onset sepsis (UOS), subdivided by definition of chorioamnionitis. **(A)** Any UOS; **(B)** culture-proven UOS; **(C)** clinical UOS; **(D)** meta-regression comparing culture-proven and clinical UOS.

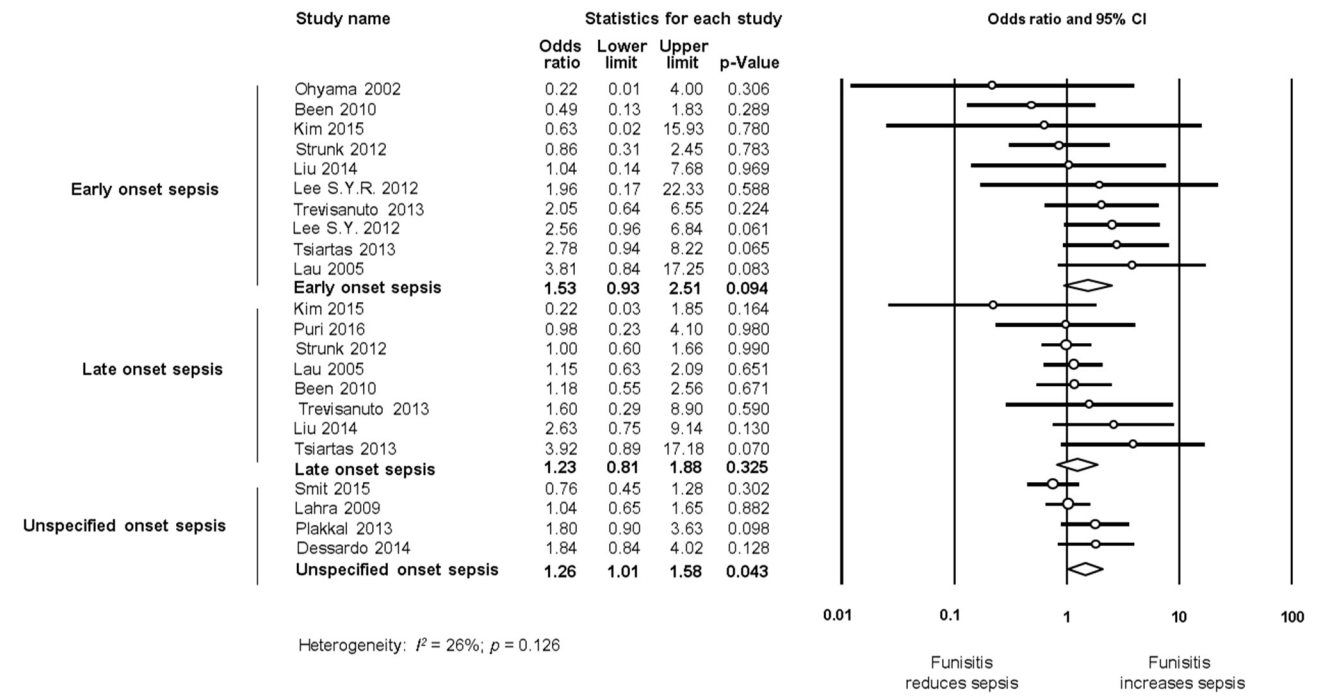

FIGURE 8 | Random effects meta-analyses of funisitis (compared with chorioamnionitis without funisitis) and sepsis (culture proven or clinical), subdivided by onset of sepsis.

significantly associated with lower GA and BW, as shown in **Table 2**. Additionally, when compared with CA-unexposed, CA-exposed infants had significantly higher rates of exposure to antenatal corticosteroids and PROM, and significantly increased rates of mortality, but significantly lower rates of preeclampsia, cesarean section, or small for GA (**Table 3**).

Meta-regression was performed to determine the potential modulatory effect of GA and BW on the association between sepsis and CA. As shown in **Figure 9A**, the effect size of the association between CA and EOS was not affected by the differences in GA between the CA-exposed and CA-unexposed group ($R^2 = 0.0$; $p = 0.490$). In contrast, meta-regression showed that mean differences in GA modified the effect size of the association between CA and LOS ($R^2 = 0.54$, $p = 0.001$, **Figure 9B**). Meta-regression for mean differences in BW could not show a correlation with the effect size of the association CA-EOS (**Supplementary Figure 10A**) or with the effect size of the association CA-LOS (**Supplementary Figure 10B**). Meta-regressions of the associations CA-EOS and CA-LOS with other covariates (antenatal corticosteroids, cesarean section, small for GA, PROM) did not show correlations with these covariates (**Supplementary Table 2**).

Meta-Analysis Subdivided by Gestational Age

To further assess the effect of GA on the association CA-sepsis, we pooled the studies where the mean difference in GA was, according to the classical threshold of p-value ($p \geq 0.05$) (142), "non-significant" and compared it with meta-analysis of studies where the mean difference in GA was "statistically significant" ($p < 0.05$). Meta-analysis found that CA was a risk factor for EOS both in studies where infants had a similar GA across groups ($k = 15$, OR 3.76, 95% CI 2.66–5.32, **Supplementary Figure 11**), and in studies where infants had significantly lower GA in the CA group ($k = 22$, OR 3.95, 95% CI 3.11–5.02, **Supplementary Figure 11**). In contrast, the association between CA and LOS was only observed in the subgroup meta-analysis of studies where CA-exposed infants had lower GA ($k = 16$, OR 1.33, 95% CI 1.11–1.60, **Supplementary Figure 12**), but not in the subgroup of studies where infants had similar GA across groups ($k = 7$, OR 1.06, 95% CI 0.72–1.57, **Supplementary Figure 12**).

Meta-Analysis Based on Adjusted Data

We pooled studies that provided adjusted data on the association between CA and sepsis. Meta-analysis of adjusted data found an association between CA and EOS ($k = 15$, OR 2.51, 95% CI 1.51–4.14, **Supplementary Figure 13**), but not between CA and LOS ($k = 7$, OR 1.04, 95% CI 0.79–1.38, **Supplementary Figure 14**). Meta-analysis of unadjusted data of the same group of studies found that CA was associated with both EOS (OR 5.10, 95% CI 3.07–8.46, **Supplementary Figure 13**) and LOS (OR 1.42, 95% CI 1.08–1.87, **Supplementary Figure 14**).

TABLE 2 | Meta-analysis of chorioamnionitis and continuous variables.

Meta-analysis	CA Type	*K*	Mean difference	95% CI	*Z*	*p*	Heterogeneity		
							Q	*p*	I^2(%)
Gestational age (weeks)	Clinical	13	−0.84	−1.32 to −0.36	−20.8	0.000	1358.6	0.000	99.1
	Histological	47	−1.11	−1.37 to −0.84	−20.8	0.000	888.5	0.000	94.8
	Microbiological	5	−2.23	−3.10 to −1.36	−14.8	0.000	160.4	0.000	97.5
	Any Type	67	−1.11	−1.34 to −0.89	−70.8	0.000	2961.5	0.000	97.8
Birth weight (g)	Clinical	12	−19.12	−83.9 to 45.6	−1.3	0.563	490.5	0.000	97.8
	Histological	47	−49.96	−73.6 to −26.1	−64.9	0.000	255.9	0.000	82.0
	Microbiological	4	−226.8	−434.5 to −19.14	−4.93	0.032	12.1	0.007	75.2
	Any Type	65	−48.30	−70.25 to −26.35	−62.6	0.000	1078.8	0.000	94.0
Maternal age (years)	Clinical	6	0.62	−0.50 to 1.76	−10.9	0.280	59.4	0.000	91.6
	Histological	25	−0.11	−0.48 to 0.27	−2.2	0.580	40.3	0.027	40.5
	Any Type	33	−0.01	−0.34 to 0.33	−10.4	0.976	116.1	0.000	72.4

CA, chorioamnionitis; k, number of studies included. Mean difference represent the mean of the CA-exposed group minus the mean of the CA-unexposed group.

TABLE 3 | Meta-analysis of chorioamnionitis and dichotomous variables.

Meta-analysis	CA Type	*k*	OR	95% CI	*Z*	*P*	Heterogeneity		
							Q	*p*	I^2(%)
Diabetes	Any Type	8	0.20	0.01 to 4.38	−1.5	0.310	3.4	0.844	0.0
Antenatal corticosteroids[a]	Clinical	6	1.54	1.38 to 1.71	7.2	0.000	181.3	0.000	97.8
	Histological	28	1.36	1.25 to 1.48	7.9	0.000	103.8	0.000	75.9
	Any Type	37	1.42	1.33 to 1.52	10.3	0.000	262.9	0.000	86.3
Pre-eclampsia	Histological	14	0.16	0.10 to 0.27	−17.4	0.000	47.7	0.000	72.7
	Any Type	16	0.09	0.09 to 0.21	−18.2	0.000	61.5	0.000	75.6
Preterm rupture of membranes	Clinical	7	3.80	2.27 to 6.38	37.2	0.000	111.3	1.000	94.6
	Histological	28	2.74	2.18 to 3.44	22.4	0.000	102.3	0.000	73.6
	Any Type	36	2.84	2.32 to 3.47	43.4	0.000	220.4	0.000	0.45
Cesarean section	Clinical	11	0.55	0.20 to 1.57	22.5	0.267	2721.7	0.000	99.6
	Histological	26	0.40	0.30 to 0.52	−18.9	0.000	140.1	0.000	82.1
	Any Type	39	0.43	0.34 to 0.55	10.7	0.000	3613.7	0.000	98.9
Small for gestational age	Clinical	3	0.33	0.16 to 0.66	−5.3	0.002	4.8	0.089	58.7
	Histological	16	0.36	0.23 to 0.55	−13.7	0.000	70.6	0.000	78.7
	Any Type	19	0.35	0.14 to 0.81	−5.3	0.000	76.1	0.000	76.2
Mortality	Clinical	9	1.64	1.34 to 2.01	1442.1	0.000	23.5	0.003	65.9
	Histological	32	1.54	1.28 to 1.85	6.1	0.000	51.0	0.013	39.3
	Any Type	44	1.59	1.39 to 1.82	13.3	0.000	84.1	0.000	48.9

CA, chorioamnionitis; k, number of studies included; OR, odds ratio. An OR higher than 1 indicates that CA is a risk factor for the outcome, an OR below indicates that CA is a protective factor for the outcome. [a]Complete or partial course.

DISCUSSION

This is the first meta-analysis investigating the association between CA and sepsis in preterm infants. The meta-analysis based on unadjusted data showed a strong association between CA and EOS and a weaker, but still positive, association between CA and LOS. Exposure to funisitis was not associated with a higher risk of sepsis when compared with exposure to CA in the absence of funisitis. As in previous meta-analysis on the association between CA and short term outcomes of prematurity (12, 13, 16, 17, 19), we observed differences in basal characteristics between the CA-exposed and the CA-unexposed group. CA was associated with a lower GA and BW, higher rates of exposure to antenatal corticosteroids, and the preterm rupture of membranes, as well as lower rates of cesarean section and small for gestational age. Meta-regression analysis showed that the lower GA of the CA group correlated with the association between CA and LOS but not with the association between CA and EOS. Therefore, the pathogenic effect of CA on LOS appears to be modulated by the effect of chorioamnionitis on GA.

We chose to combine studies by using ORs rather than risk ratios (RRs) because it allowed us to compare the unadjusted ORs

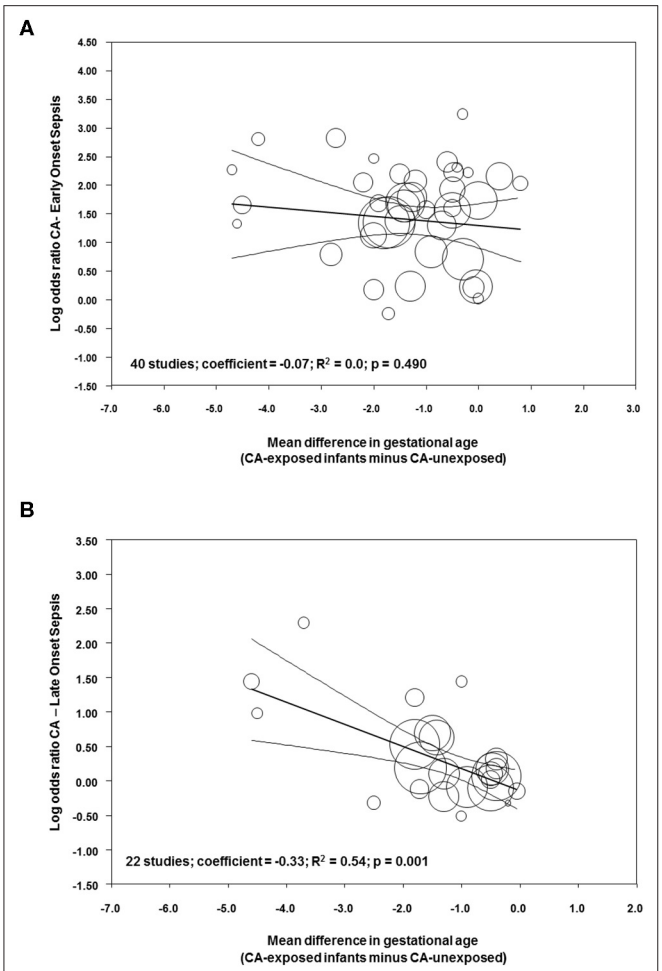

FIGURE 9 | Meta-regression plot of association between chorioamnionitis and **(A)** early onset sepsis, and **(B)** late onset sepsis controlling for difference in gestational age between exposed and non-exposed groups.

with the adjusted ORs reported in some studies. However, while the RR has a relatively simple interpretation, OR interpretation is less intuitive, as the concept of "odds" is less easy to grasp (143, 144). Interpretation of ORs in the same way as RRs can lead to overestimation of effect sizes when the risk in either group is high (above 20%) and the OR is large (144). In order to check if there were important discrepancies between ORs and RRs in our study, we calculated the RRs for some analyses. In the case of the association between CA and EOS, the RR was 3.45, whereas the OR was 4.29 (∼24% higher). In the case of the association between CA and LOS, the RR was 1.21 whereas the OR was 1.29 (∼6.6% higher). Therefore, in CA-exposed infants, the risk of EOS was 3.5-fold higher and the risk of LOS was 1.2-fold higher than the respective risk in infants non-exposed to CA. These increases in risk were slightly overestimated by the OR.

Since very/extremely preterm birth is always a pathological condition, any study aimed to analyze the association between its etiology and its outcome will face the limitation of the absence of a healthy control group (145). As mentioned in the introduction, very/extremely preterm birth etiology can be divided into two main categories: intrauterine infection/inflammation and placental vascular dysfunction (2–4). The distribution of these two etiological entities across the different gestational ages is not uniform: the lower the GA, the greater the possibility that an infectious/inflammatory process is the trigger for preterm birth (2, 146). Our meta-analysis showed that infants exposed to CA were born ∼1.1 weeks earlier than "control" infants. Meta-regression showed that this difference in GA did not affect the association between CA and EOS but modulated the association between CA and LOS. The difference in GA was associated with 54% (R^2) of the variance in the association between CA and LOS across studies and each week that infants with CA were born earlier than control infants resulted in an increase in LOS log OR of 0.33 (the equivalent of going from an OR of 1.00 to an OR of 2.14). This modulatory role of GA may be related to the maturation of the immunological system (26, 147), but also to the fact that CA-exposed preterm infants would require longer hospitalization and more days of invasive therapies, rendering them more susceptible to LOS.

Besides the meta-regression analysis, other data of the present study underline the modulatory role of GA on the association between CA and LOS. When we performed a subgroup analysis of studies without a significant difference ($p > 0.05$) in GA between the CA-exposed group and the CA-unexposed group, the association between CA and EOS was still strong (odds ratio 3.76), but the association between CA and LOS could not be demonstrated. When we pooled the few studies that corrected for GA, as well as for other potential confounders, the association between CA and EOS was tempered but still positive, and the association between CA and LOS could not be further demonstrated. This effect of the use of adjusted data has been previously described in meta-analyses on the association between CA and bronchopulmonary dysplasia (12, 13), cerebral palsy (22), retinopathy of prematurity (16), patent ductus arteriosus (17), and intraventricular hemorrhage (19). Moreover, the decreased risk of LOS in CA-exposed infants previously reported by Strunk et al. was only observed after correction for GA (25). Adjustment for GA is commonly used in observational studies examining predictors of outcomes in preterm infants (3, 148, 149). However, GA may represent both a risk factor *per se* and a mediator in the causal pathway linking cause of preterm birth (i.e., CA) to outcome (i.e., LOS). As pointed out by Ananth and Schisterman, GA is often mislabeled as a confounder when it may be an intermediate (149). Adjustment for GA in the presence of unmeasured factors that may affect both GA and neonatal outcome, may result in bias (3, 148–151). This bias may even change the direction of estimates, unless all mediator–outcome confounders are taken into account in the analysis, a condition that is unlikely to be achieved (3, 148–152). Therefore, observational studies and meta-analyses of observational studies that analyze the association between conditions like CA or pre-eclampsia and outcome of preterm birth provide valuable information for descriptive or prognostic purposes. However, inferring causal effects is not possible (145, 149).

There is a reasonable biological plausibility for the immunomodulatory role of intrauterine infection/inflammation

on the etiopathogenesis of neonatal sepsis. Nevertheless, our comprehension of the mechanisms that link intrauterine infection/inflammation and preterm birth is still incomplete. The maternal lower genital tract is generally considered to be the primary source of bacteria, but other potential sources, such as the oral cavity, need to be considered (7, 8). The microorganisms more frequently cultivated from amniotic fluid in pregnancies complicated by preterm birth are *Ureaplasma urealyticum*, *Mycoplasma hominis*, *Fusobacterium nucleatum*, *Gardnerella vaginalis*, and *Bacteroides* spp. (7, 8). These microorganisms are able to stimulate the intrauterine inflammatory process but have relatively low virulence and rarely induce EOS, which is mainly related to such bacteria as group B streptococcus or *Escherichia coli* (153). In addition, an important proportion of the organisms associated with intra-amniotic infection are uncultivated or difficult-to-cultivate bacteria (7, 8). Nevertheless, as suggested by Strunk et al., even culture-negative, asymptomatic CA that does not result in EOS might lead to a persistent alteration of the neonatal immune system (11). Accordingly, evidence from animal and human studies supports that CA could diminish innate immune responses and thereby increase the susceptibility of preterm infants to LOS (154–157).

Not all the situations of intrauterine infection/inflammation will lead to an inflammatory process reaching the fetus (158). Funisitis is considered the histologic counterpart of the fetal inflammatory response syndrome (9, 158). Our meta-analysis could not demonstrate a stronger association between funisitis and the risk of developing neonatal sepsis (EOS, LOS, or UOS), when compared with CA in the absence of funisitis (**Figure 8**). This is an argument against the role of the immunomodulation induced by the fetal inflammatory response in the etiopathogenesis of neonatal sepsis. Similarly, we observed in previous meta-analyses that funisitis was not an additional risk factor for developing intraventricular hemorrhage (19), patent ductus arteriosus (17), respiratory distress syndrome (13), or bronchopulmonary dysplasia (13) in preterm infants. In contrast, funisitis significantly increased the risk of retinopathy of prematurity (16). However, all these meta-analyses, as well as the present one, are limited by the small number of studies providing data on funisitis.

Besides the immunomodulatory role of prenatal infection/inflammation, some differences between CA-exposed infants and CA-unexposed infants may also play a role in the association between CA and neonatal sepsis. Our meta-analysis showed a higher rate of exposure to antenatal corticosteroids among CA-exposed infants, but meta-regression could not demonstrate that this affected the association between CA and sepsis. In addition, alterations in infant's microbiome due to mode of delivery, or antibiotic exposure in early life may be related to the increased risk of LOS in CA-exposed infants (159). Concerns that an intrauterine infection is the trigger for prematurity lead to the initiation of empirical antibiotics in the majority of very and extremely preterm infants (160). If the newborn has a true infection, these antibiotics will save his life, but overuse may lead to the development of antibiotic resistance. Moreover, growing evidence shows that prolonged initial empirical antibiotic treatment may be associated with adverse outcomes, such as LOS, necrotizing enterocolitis, bronchopulmonary dysplasia, or death (160, 161).

Our study has several limitations. The studies showed great heterogeneity in their definition of CA, particularly pertaining to criteria used in defining clinical CA. Recent recommendations propose to restrict the term CA to pathologic diagnosis (162). With regard to histological CA, the definition and staging criteria of Redline et al. (163) were the most frequently used but only 11 studies (25, 41, 43, 50, 55, 61, 81, 90, 111, 120, 141) used this classification and only two studies (81, 141) stratified the outcomes according to the grade of histological CA. In addition, few studies had the association between CA and sepsis as their main study objective, while at the same time this may have acted in favor of avoiding publication bias. Furthermore, the generalized definition of EOS, LOS, clinical, and culture-proven sepsis did not allow for analysis of individual pathogen associations. Such an approach was simply not feasible given the overall lack of such specific data across all analyzed studies. Currently, no consensus exists on the definition of neonatal bacterial sepsis unlike pediatric sepsis (164, 165). Pediatric sepsis is defined as a "systemic inflammatory response syndrome in the presence of a suspected or proven infection," conditions that do not necessarily apply to neonatal sepsis (166). Neonatal sepsis in most cases may present itself with a negative blood culture, and with non-specific clinical symptoms (167). Providing a clear disease definition of neonatal sepsis remains therefore in part challenging due to current limitations of ancillary diagnostics (165, 168).

CONCLUSIONS

Infant's immaturity plays a key role in the morbidity associated with very/extremely preterm birth but the pathological processes causing preterm birth may also influence the outcome. Our data suggest that when infection/inflammation is the trigger of preterm birth, infants are more susceptible to develop sepsis not only immediately after birth, but also during the first weeks of life. The association between CA and EOS seems to be GA-independent, whereas the lower GA of CA-exposed infants modulated the effect size of the association between CA and LOS. CA may initiate the immunomodulatory sequence leading to LOS but also may alter the rate of exposure to other stimuli such as antenatal and post-natal corticosteroids, antenatal and post-natal antibiotics, invasive therapies, lung damage, patent ductus arteriosus, or necrotizing enterocolitis, which render very/extremely preterm infants more vulnerable to sepsis. A meta-analysis of individual patient data would help determine the role of some of these factors in the different outcomes of preterm children exposed to chorioamnionitis.

DATA AVAILABILITY STATEMENT

The raw data supporting the conclusions of this article will be made available by the authors, without undue reservation, to any qualified researcher.

AUTHOR'S NOTE

This study was presented at the 3rd Congress of Joint European Neonatal Societies (jENS 2019). Abstract available at https://www.nature.com/articles/s41390-019-0521-6.

AUTHOR CONTRIBUTIONS

EV-M contributed to the search and inclusion of studies, carried out data collection, carried out statistical analyses, assessed methodological quality, contributed to interpretation of results, helped draft the initial manuscript, and reviewed and revised the manuscript. GL contributed to the search and inclusion of studies, contributed to data collection, assessed methodological quality, contributed to interpretation of results, and drafted the initial manuscript. OR selected studies for inclusion, carried out data collection, and carried out statistical analyses. PD carried out and supervised data collection, contributed to interpretation of results, and reviewed and revised the manuscript. LZ contributed to interpretation of results and reviewed and revised the manuscript. BK contributed to interpretation of results, contributed to drafting the manuscript, and reviewed and revised the manuscript. EV conceptualized and designed the study, carried out the search and selected studies for inclusion, supervised data collection, contributed to statistical analyses and interpretation of results, helped draft the initial manuscript, and reviewed and revised the manuscript. All authors approved the final manuscript as submitted.

SUPPLEMENTARY MATERIAL

The Supplementary Material for this article can be found online at: https://www.frontiersin.org/articles/10.3389/fimmu.2020.00972/full#supplementary-material

REFERENCES

1. Moutquin JM. Classification and heterogeneity of preterm birth. *BJOG.* (2003) 110(Suppl. 20):30–3. doi: 10.1046/j.1471-0528.2003.00021.x
2. McElrath TF, Hecht JL, Dammann O, Boggess K, Onderdonk A, Markenson G, et al. Pregnancy disorders that lead to delivery before the 28th week of gestation: an epidemiologic approach to classification. *Am J Epidemiol.* (2008) 168:980–9. doi: 10.1093/aje/kwn202
3. Gagliardi L, Rusconi F, Da Fre M, Mello G, Carnielli V, Di Lallo D, et al. Pregnancy disorders leading to very preterm birth influence neonatal outcomes: results of the population-based ACTION cohort study. *Pediatr Res.* (2013) 73:794–801. doi: 10.1038/pr.2013.52
4. Gagliardi L, Rusconi F, Bellu R, Zanini R, Italian Neonatal N. Association of maternal hypertension and chorioamnionitis with preterm outcomes. *Pediatrics.* (2014) 134:e154–61. doi: 10.1542/peds.2013-3898
5. Park CW, Moon KC, Park JS, Jun JK, Romero R, Yoon BH. The involvement of human amnion in histologic chorioamnionitis is an indicator that a fetal and an intra-amniotic inflammatory response is more likely and severe: clinical implications. *Placenta.* (2009) 30:56–61. doi: 10.1016/j.placenta.2008.09.017
6. Kim CJ, Romero R, Chaemsaithong P, Chaiyasit N, Yoon BH, Kim YM. Acute chorioamnionitis and funisitis: definition, pathologic features, and clinical significance. *Am J Obstet Gynecol.* (2015) 213(4 Suppl.):S29–52. doi: 10.1016/j.ajog.2015.08.040
7. Han YW, Shen T, Chung P, Buhimschi IA, Buhimschi CS. Uncultivated bacteria as etiologic agents of intra-amniotic inflammation leading to preterm birth. *J Clin Microbiol.* (2009) 47:38–47. doi: 10.1128/JCM.01206-08
8. DiGiulio DB. Diversity of microbes in amniotic fluid. *Semin Fetal Neonatal Med.* (2012) 17:2–11. doi: 10.1016/j.siny.2011.10.001
9. Gantert M, Been JV, Gavilanes AW, Garnier Y, Zimmermann LJ, Kramer BW. Chorioamnionitis: a multiorgan disease of the fetus? *J Perinatol.* (2010) 30(Suppl):S21–30. doi: 10.1038/jp.2010.96
10. Thomas W, Speer CP. Chorioamnionitis: important risk factor or innocent bystander for neonatal outcome? *Neonatology.* (2011) 99:177–87. doi: 10.1159/000320170
11. Strunk T, Inder T, Wang X, Burgner D, Mallard C, Levy O. Infection-induced inflammation and cerebral injury in preterm infants. *Lancet Infect Dis.* (2014) 14:751–62. doi: 10.1016/S1473-3099(14)70710-8
12. Hartling L, Liang Y, Lacaze-Masmonteil T. Chorioamnionitis as a risk factor for bronchopulmonary dysplasia: a systematic review and meta-analysis. *Arch Dis Child Fetal Neonatal Ed.* (2012) 97:F8–17. doi: 10.1136/adc.2010.210187
13. Villamor-Martinez E, Alvarez-Fuente M, Ghazi AMT, Degraeuwe P, Zimmermann LJI, Kramer BW, et al. Association of chorioamnionitis with bronchopulmonary dysplasia among preterm infants: a systematic review, meta-analysis, and metaregression. *JAMA Netw Open.* (2019) 2:e1914611. doi: 10.1001/jamanetworkopen.2019.14611
14. Been JV, Lievense S, Zimmermann LJ, Kramer BW, Wolfs TG. Chorioamnionitis as a risk factor for necrotizing enterocolitis: a systematic review and meta-analysis. *J Pediatr.* (2013) 162:236–42.e2. doi: 10.1016/j.jpeds.2012.07.012
15. Mitra S, Aune D, Speer CP, Saugstad OD. Chorioamnionitis as a risk factor for retinopathy of prematurity: a systematic review and meta-analysis. *Neonatology.* (2014) 105:189–99. doi: 10.1159/000357556
16. Villamor-Martinez E, Cavallaro G, Raffaeli G, Mohammed Rahim OMM, Gulden S, Ghazi AMT, et al. Chorioamnionitis as a risk factor for retinopathy of prematurity: an updated systematic review and meta-analysis. *PLoS ONE.* (2018) 13:e0205838. doi: 10.1371/journal.pone.0205838
17. Behbodi E, Villamor-Martinez E, Degraeuwe PL, Villamor E. Chorioamnionitis appears not to be a risk factor for patent ductus arteriosus in preterm infants: a systematic review and meta-analysis. *Sci Rep.* (2016) 6:37967. doi: 10.1038/srep37967
18. Park HW, Choi YS, Kim KS, Kim SN. Chorioamnionitis and patent ductus arteriosus: a systematic review and meta-analysis. *PLoS ONE.* (2015) 10:e0138114. doi: 10.1371/journal.pone.0138114
19. Villamor-Martinez E, Fumagalli M, Mohammed Rahim O, Passera S, Cavallaro G, Degraeuwe P, et al. Chorioamnionitis is a risk factor for intraventricular hemorrhage in preterm infants: a systematic review and meta-analysis. *Front Physiol.* (2018) 9:1253. doi: 10.3389/fphys.2018.01253
20. Villamor-Martinez E, Fumagalli M, Alomar YI, Passera S, Cavallaro G, Mosca F, et al. Cerebellar hemorrhage in preterm infants: a meta-analysis on risk factors and neurodevelopmental outcome. *Front Physiol.* (2019) 10:800. doi: 10.3389/fphys.2019.00800
21. De Felice C, Toti P, Laurini RN, Stumpo M, Picciolini E, Todros T, et al. Early neonatal brain injury in histologic chorioamnionitis. *J Pediatr.* (2001) 138:101–4. doi: 10.1067/mpd.2001.109605
22. Wu YW, Colford JM Jr. Chorioamnionitis as a risk factor for cerebral palsy: a meta-analysis. *JAMA.* (2000) 284:1417–24. doi: 10.1001/jama.284.11.1417
23. Hornik CP, Fort P, Clark RH, Watt K, Benjamin DK Jr, Smith PB, et al. Early and late onset sepsis in very-low-birth-weight infants from a large group of neonatal intensive care units. *Early Hum Dev.* (2012) 88(Suppl. 2):S69–74. doi: 10.1016/S0378-3782(12)70019-1
24. Puopolo KM, Benitz WE, Zaoutis TE, Committee On F, Newborn, Committee On Infectious D. Management of neonates born at </=34 6/7 weeks' gestation with suspected or proven early-onset bacterial sepsis. *Pediatrics.* (2018) 142:e20182894. doi: 10.1542/peds.2018-2896
25. Strunk T, Doherty D, Jacques A, Simmer K, Richmond P, Kohan R, et al. Histologic chorioamnionitis is associated with reduced risk

of late-onset sepsis in preterm infants. *Pediatrics.* (2012) 129:e134–41. doi: 10.1542/peds.2010-3493
26. Schuller SS, Kramer BW, Villamor E, Spittler A, Berger A, Levy O. Immunomodulation to prevent or treat neonatal sepsis: past, present, and future. *Front Pediatr.* (2018) 6:199. doi: 10.3389/fped.2018.00199
27. Ng S, Strunk T, Jiang P, Muk T, Sangild PT, Currie A. Precision medicine for neonatal sepsis. *Front Mol Biosci.* (2018) 5:70. doi: 10.3389/fmolb.2018.00070
28. Hocevar SN, Edwards JR, Horan TC, Morrell GC, Iwamoto M, Lessa FC. Device-associated infections among neonatal intensive care unit patients: incidence and associated pathogens reported to the national healthcare safety network, 2006–2008. *Infect Control Hosp Epidemiol.* (2012) 33:1200–6. doi: 10.1086/668425
29. Villamor-Martinez E, Lubach G, Mohammed Rahim OM, Degraeuwe P, Kramer BW, Villamor E. *Chorioamnionitis as a Risk Factor for Neonatal Sepsis: A Systematic Review and Meta-Analysis CRD42018117190 2018.* (2019). Available online at: https://www.crd.york.ac.uk/prospero/display_record.php?RecordID=117190 (accessed November 15, 2019).
30. Moher D, Liberati A, Tetzlaff J, Altman DG, Group P. Preferred reporting items for systematic reviews and meta-analyses: the PRISMA statement. *PLoS Med.* (2009) 6:e1000097. doi: 10.1371/journal.pmed.1000097
31. Kachikis A, Eckert LO, Walker C, Bardají A, Varricchio F, Lipkind HS, et al. Chorioamnionitis: case definition & guidelines for data collection, analysis, and presentation of immunization safety data. *Vaccine.* (2019) 37:7610–22. doi: 10.1016/j.vaccine.2019.05.030
32. Wells GA, Shea B, O'Connell D, Peterson J, Welch V, Losos M. *The Newcastle-Ottawa Scale (NOS) for Assessing the Quality of Nonrandomized Studies in Meta-Analyses.* Available online at: http://www.ohri.ca/programs/clinical_epidemiology/oxford.htm (accessed February 02, 2019).
33. Wan X, Wang W, Liu J, Tong T. Estimating the sample mean and standard deviation from the sample size, median, range and/or interquartile range. *BMC Med Res Methodol.* (2014) 14:135. doi: 10.1186/1471-2288-14-135
34. Borenstein M (editor). *Introduction to Meta-Analysis*. Chichester, WS: John Wiley & Sons Ltd (2009). doi: 10.1002/9780470743386
35. Egger M, Smith GD, Schneider M, Minder C. Bias in meta-analysis detected by a simple, graphical test. *BMJ.* (1997) 315:629–34. doi: 10.1136/bmj.315.7109.629
36. Abu-Maziad A, Schaa K, Bell EF, Dagle JM, Cooper M, Marazita ML, et al. Role of polymorphic variants as genetic modulators of infection in neonatal sepsis. *Pediatr Res.* (2010) 68:323–9. doi: 10.1203/PDR.0b013e3181e6a068
37. Adams WG, Kinney JS, Schuchat A, Collier CL, Papasian CJ, Kilbride HW, et al. Outbreak of early onset group B streptococcal sepsis. *Pediatr Infect Dis J.* (1993) 12:565–70. doi: 10.1097/00006454-199307000-00003
38. Ahn HM, Park EA, Cho SJ, Kim YJ, Park HS. The association of histological chorioamnionitis and antenatal steroids on neonatal outcome in preterm infants born at less than thirty-four weeks' gestation. *Neonatology.* (2012) 102:259–64. doi: 10.1159/000339577
39. Alam MM, Saleem AF, Shaikh AS, Munir O, Qadir M. Neonatal sepsis following prolonged rupture of membranes in a tertiary care hospital in Karachi, Pakistan. *J Infect Dev Ctries.* (2014) 8:67–73. doi: 10.3855/jidc.3136
40. Alexander JM, Gilstrap LC, Cox SM, McIntire DM, Leveno KJ. Clinical chorioamnionitis and the prognosis for very low birth weight infants. *Obstet Gynecol.* (1998) 91(5 Pt 1):725–9. doi: 10.1097/00006250-199805000-00016
41. Alfiero Bordigato M, Piva D, Di Gangi IM, Giordano G, Chiandetti L, Filippone M. Asymmetric dimethylarginine in ELBW newborns exposed to chorioamnionitis. *Early Hum Dev.* (2011) 87:143–5. doi: 10.1016/j.earlhumdev.2010.11.004
42. Alshaikh B, Yee W, Lodha A, Henderson E, Yusuf K, Sauve R. Coagulase-negative staphylococcus sepsis in preterm infants and long-term neurodevelopmental outcome. *J Perinatol.* (2014) 34:125–9. doi: 10.1038/jp.2013.155
43. Anblagan D, Pataky R, Evans MJ, Telford EJ, Serag A, Sparrow S, et al. Association between preterm brain injury and exposure to chorioamnionitis during fetal life. *Sci Rep.* (2016) 6:37932. doi: 10.1038/srep37932
44. Arayici S, Kadioglu Simsek G, Oncel MY, Eras Z, Canpolat FE, Oguz SS, et al. The effect of histological chorioamnionitis on the short-term outcome of preterm infants </=32 weeks: a single-center study. *J Matern Fetal Neonatal Med.* (2014) 27:1129–33. doi: 10.3109/14767058.2013.850668
45. Arora P, Bagga R, Kalra J, Kumar P, Radhika S, Gautam V. Mean gestation at delivery and histological chorioamnionitis correlates with early-onset neonatal sepsis following expectant management in pPROM. *J Obstet Gynaecol.* (2015) 35:235–40. doi: 10.3109/01443615.2014.958143
46. Averbuch B, Mazor M, Shoham-Vardi I, Chaim W, Vardi H, Horowitz S, et al. Intra-uterine infection in women with preterm premature rupture of membranes: maternal and neonatal characteristics. *Eur J Obstet Gynecol Reprod Biol.* (1995) 62:25–9. doi: 10.1016/0301-2115(95)02176-8
47. Aziz N, Cheng YW, Caughey AB. Neonatal outcomes in the setting of preterm premature rupture of membranes complicated by chorioamnionitis. *J Matern Fetal Neonatal Med.* (2009) 22:780–4. doi: 10.3109/14767050902922581
48. Ballard AR, Mallett LH, Pruszynski JE, Cantey JB. Chorioamnionitis and subsequent bronchopulmonary dysplasia in very-low-birth weight infants: a 25-year cohort. *J Perinatol.* (2016) 36:1045–8. doi: 10.1038/jp.2016.138
49. Barrera-Reyes RH, Ruiz-Macias H, Segura-Cervantes E. Neurodevelopment at one year of age [corrected] in preterm newborns with history of maternal chorioamnionitis. *Ginecol Obstet Mex.* (2011) 79:31–7.
50. Been JV, Rours IG, Kornelisse RF, Lima Passos V, Kramer BW, Schneider TA, et al. Histologic chorioamnionitis, fetal involvement, and antenatal steroids: effects on neonatal outcome in preterm infants. *Am J Obstet Gynecol.* (2009) 201:587.e1–8. doi: 10.1016/j.ajog.2009.06.025
51. Botet F, Figueras J, Carbonell-Estrany X, Arca G, The Castrillo Study G. Effect of maternal clinical chorioamnionitis on neonatal morbidity in very-low birthweight infants: a case-control study. *J Perinat Med.* (2010) 38:269–73. doi: 10.1515/jpm.2010.029
52. Bry KJ, Jacobsson B, Nilsson S, Bry K. Gastric fluid cytokines are associated with chorioamnionitis and white blood cell counts in preterm infants. *Acta Paediatr.* (2015) 104:575–80. doi: 10.1111/apa.12947
53. Buhimschi CS, Buhimschi IA, Abdel-Razeq S, Rosenberg VA, Thung SF, Zhao G, et al. Proteomic biomarkers of intra-amniotic inflammation: relationship with funisitis and early-onset sepsis in the premature neonate. *Pediatr Res.* (2007) 61:318–24. doi: 10.1203/01.pdr.0000252439.48564.37
54. Buhimschi CS, Dulay AT, Abdel-Razeq S, Zhao G, Lee S, Hodgson EJ, et al. Fetal inflammatory response in women with proteomic biomarkers characteristic of intra-amniotic inflammation and preterm birth. *BJOG.* (2009) 116:257–67. doi: 10.1111/j.1471-0528.2008.01925.x
55. Burgner DP, Doherty D, Humphreys J, Currie A, Simmer K, Charles A, et al. Maternal chorioamnionitis and postneonatal respiratory tract infection in ex-preterm infants. *J Pediatr.* (2017) 184:62–7.e2. doi: 10.1016/j.jpeds.2017.01.037
56. Chau V, Brant R, Poskitt KJ, Tam EW, Synnes A, Miller SP. Postnatal infection is associated with widespread abnormalities of brain development in premature newborns. *Pediatr Res.* (2012) 71:274–9. doi: 10.1038/pr.2011.40
57. Choi CW, Kim BI, Joung KE, Lee JA, Lee YK, Kim EK, et al. Decreased expression of transforming growth factor-beta1 in bronchoalveolar lavage cells of preterm infants with maternal chorioamnionitis. *J Korean Med Sci.* (2008) 23:609–15. doi: 10.3346/jkms.2008.23.4.609
58. Churgay CA, Smith MA, Blok B. Maternal fever during labor–what does it mean? *J Am Board Fam Pract.* (1994) 7:14–24.
59. De Felice C, Toti P, Parrini S, Del Vecchio A, Bagnoli F, Latini G, et al. Histologic chorioamnionitis and severity of illness in very low birth weight newborns. *Pediatr Crit Care Med.* (2005) 6:298–302. doi: 10.1097/01.PCC.0000160658.35437.65
60. Dempsey E, Chen MF, Kokottis T, Vallerand D, Usher R. Outcome of neonates less than 30 weeks gestation with histologic chorioamnionitis. *Am J Perinatol.* (2005) 22:155–9. doi: 10.1055/s-2005-865020
61. Dessardo NS, Dessardo S, Mustac E, Banac S, Petrovic O, Peter B. Chronic lung disease of prematurity and early childhood wheezing: is foetal inflammatory response syndrome to blame? *Early Hum Dev.* (2014) 90:493–9. doi: 10.1016/j.earlhumdev.2014.07.002
62. Dexter SC, Malee MP, Pinar H, Hogan JW, Carpenter MW, Vohr BR. Influence of chorioamnionitis on developmental outcome in very low birth weight infants. *Obstet Gynecol.* (1999) 94:267–73. doi: 10.1097/00006250-199908000-00022

63. Dexter SC, Pinar H, Malee MP, Hogan J, Carpenter MW, Vohr BR. Outcome of very low birth weight infants with histopathologic chorioamnionitis. *Obstet Gynecol.* (2000) 96:172–7. doi: 10.1097/00006250-200008000-00004
64. Dollner H, Vatten L, Halgunset J, Rahimipoor S, Austgulen R. Histologic chorioamnionitis and umbilical serum levels of pro-inflammatory cytokines and cytokine inhibitors. *BJOG.* (2002) 109:534–9. doi: 10.1111/j.1471-0528.2002.01028.x
65. Dulay AT, Buhimschi IA, Zhao G, Luo G, Abdel-Razeq S, Cackovic M, et al. Nucleated red blood cells are a direct response to mediators of inflammation in newborns with early-onset neonatal sepsis. *Am J Obstet Gynecol.* (2008) 198:426.e1–9. doi: 10.1016/j.ajog.2008.01.040
66. Dutta S, Reddy R, Sheikh S, Kalra J, Ray P, Narang A. Intrapartum antibiotics and risk factors for early onset sepsis. *Arch Dis Child Fetal Neonatal Ed.* (2010) 95:F99–103. doi: 10.1136/adc.2009.163220
67. Ecevit A, Anuk-Ince D, Yapakci E, Kupana-Ayva S, Kurt A, Yanik FF, et al. Association of respiratory distress syndrome and perinatal hypoxia with histologic chorioamnionitis in preterm infants. *Turk J Pediatr.* (2014) 56:56–61.
68. Elimian A, Verma U, Beneck D, Cipriano R, Visintainer P, Tejani N. Histologic chorioamnionitis, antenatal steroids, and perinatal outcomes. *Obstet Gynecol.* (2000) 96:333–6. doi: 10.1097/00006250-200009000-00003
69. Erdemir G, Kultursay N, Calkavur S, Zekioglu O, Koroglu OA, Cakmak B, et al. Histological chorioamnionitis: effects on premature delivery and neonatal prognosis. *Pediatr Neonatol.* (2013) 54:267–74. doi: 10.1016/j.pedneo.2013.03.012
70. Figueroa-Damian R, Arredondo-Garcia JL, Mancilla-Ramirez J. Amniotic fluid interleukin-6 and the risk of early-onset sepsis among preterm infants. *Arch Med Res.* (1999) 30:198–202. doi: 10.1016/S0188-0128(99)00015-9
71. Garcia-Munoz Rodrigo F, Galan Henriquez G, Figueras Aloy J, Garcia-Alix Perez A. Outcomes of very-low-birth-weight infants exposed to maternal clinical chorioamnionitis: a multicentre study. *Neonatology.* (2014) 106:229–34. doi: 10.1159/000363127
72. Gonzalez-Luis G, Jordan Garcia I, Rodriguez-Miguelez J, Botet Mussons F, Figueras Aloy J. [Neonatal morbidity and mortality in very low birth weight infants according to exposure to chorioamnionitis]. *An Esp Pediatr.* (2002) 56:551–5. doi: 10.1016/S1695-4033(02)77863-6
73. Group E. Incidence of and risk factors for neonatal morbidity after active perinatal care: extremely preterm infants study in Sweden (EXPRESS). *Acta Paediatr.* (2010) 99:978–92. doi: 10.1111/j.1651-2227.2010.01846.x
74. Guzick DS, Winn K. The association of chorioamnionitis with preterm delivery. *Obstet Gynecol.* (1985) 65:11–6.
75. Gyamfi-Bannerman C, Son M. Preterm premature rupture of membranes and the rate of neonatal sepsis after two courses of antenatal corticosteroids. *Obstet Gynecol.* (2014) 124:999–1003. doi: 10.1097/AOG.0000000000000460
76. Hendson L, Russell L, Robertson CM, Liang Y, Chen Y, Abdalla A, et al. Neonatal and neurodevelopmental outcomes of very low birth weight infants with histologic chorioamnionitis. *J Pediatr.* (2011) 158:397–402. doi: 10.1016/j.jpeds.2010.09.010
77. Hitti J, Tarczy-Hornoch P, Murphy J, Hillier SL, Aura J, Eschenbach DA. Amniotic fluid infection, cytokines, and adverse outcome among infants at 34 weeks' gestation or less. *Obstet Gynecol.* (2001) 98:1080–8. doi: 10.1016/S0029-7844(01)01567-8
78. Howman RA, Charles AK, Jacques A, Doherty DA, Simmer K, Strunk T, et al. Inflammatory and haematological markers in the maternal, umbilical cord and infant circulation in histological chorioamnionitis. *PLoS ONE.* (2012) 7:e51836. doi: 10.1371/journal.pone.0051836
79. Janota J, Stranak Z, Belohlavkova S, Mudra K, Simak J. Post-natal increase of procalcitonin in premature newborns is enhanced by chorioamnionitis and neonatal sepsis. *Eur J Clin Invest.* (2001) 31:978–83. doi: 10.1046/j.1365-2362.2001.00912.x
80. Jeon JH, Namgung R, Park MS, Park KI, Lee C. Positive maternal C-reactive protein predicts neonatal sepsis. *Yonsei Med J.* (2014) 55:113–7. doi: 10.3349/ymj.2014.55.1.113
81. Jones MH, Corso AL, Tepper RS, Edelweiss MI, Friedrich L, Pitrez PM, et al. Chorioamnionitis and subsequent lung function in preterm infants. *PLoS ONE.* (2013) 8:e81193. doi: 10.1371/journal.pone.0081193
82. Kacerovsky M, Musilova I, Andrys C, Hornychova H, Pliskova L, Kostal M, et al. Prelabor rupture of membranes between 34 and 37 weeks: the intraamniotic inflammatory response and neonatal outcomes. *Am J Obstet Gynecol.* (2014) 210:325.e1–e10. doi: 10.1016/j.ajog.2013.10.882
83. Kim SY, Choi CW, Jung E, Lee J, Lee JA, Kim H, et al. Neonatal morbidities associated with histologic chorioamnionitis defined based on the site and extent of inflammation in very low birth weight infants. *J Korean Med Sci.* (2015) 30:1476–82. doi: 10.3346/jkms.2015.30.10.1476
84. Kirchner L, Helmer H, Heinze G, Wald M, Brunbauer M, Weninger M, et al. Amnionitis with ureaplasma urealyticum or other microbes leads to increased morbidity and prolonged hospitalization in very low birth weight infants. *Eur J Obstet Gynecol Reprod Biol.* (2007) 134:44–50. doi: 10.1016/j.ejogrb.2006.09.013
85. Klinger G, Levy I, Sirota L, Boyko V, Reichman B, Lerner-Geva L, et al. Epidemiology and risk factors for early onset sepsis among very-low-birthweight infants. *Am J Obstet Gynecol.* (2009) 201:38.e1–6. doi: 10.1016/j.ajog.2009.03.006
86. Lahra MM, Beeby PJ, Jeffery HE. Intrauterine inflammation, neonatal sepsis, and chronic lung disease: a 13-year hospital cohort study. *Pediatrics.* (2009) 123:1314–9. doi: 10.1542/peds.2008-0656
87. Lau J, Magee F, Qiu Z, Hoube J, Von Dadelszen P, Lee SK. Chorioamnionitis with a fetal inflammatory response is associated with higher neonatal mortality, morbidity, and resource use than chorioamnionitis displaying a maternal inflammatory response only. *Am J Obstet Gynecol.* (2005) 193(3 Pt 1):708–13. doi: 10.1016/j.ajog.2005.01.017
88. Lee SY, Leung CW. Histological chorioamnionitis - implication for bacterial colonization, laboratory markers of infection, and early onset sepsis in very-low-birth-weight neonates. *J Matern Fetal Neonatal Med.* (2012) 25:364–8. doi: 10.3109/14767058.2011.579208
89. Lee SY, Park KH, Jeong EH, Oh KJ, Ryu A, Park KU. Relationship between maternal serum C-reactive protein, funisitis and early-onset neonatal sepsis. *J Korean Med Sci.* (2012) 27:674–80. doi: 10.3346/jkms.2012.27.6.674
90. Liu Z, Tang Z, Li J, Yang Y. Effects of placental inflammation on neonatal outcome in preterm infants. *Pediatr Neonatol.* (2014) 55:35–40. doi: 10.1016/j.pedneo.2013.05.007
91. Lorthe E, Ancel PY, Torchin H, Kaminski M, Langer B, Subtil D, et al. Impact of latency duration on the prognosis of preterm infants after preterm premature rupture of membranes at 24 to 32 weeks' gestation: a national population-based cohort study. *J Pediatr.* (2017) 182:47–52.e2. doi: 10.1016/j.jpeds.2016.11.074
92. Mehta R, Nanjundaswamy S, Shen-Schwarz S, Petrova A. Neonatal morbidity and placental pathology. *Indian J Pediatr.* (2006) 73:25–8. doi: 10.1007/BF02758255
93. Mikhael M, Brown LS, Rosenfeld CR. Serial neutrophil values facilitate predicting the absence of neonatal early-onset sepsis. *J Pediatr.* (2014) 164:522–8.e1–3. doi: 10.1016/j.jpeds.2013.10.080
94. Miyazaki K, Furuhashi M, Ishikawa K, Tamakoshi K, Hayashi K, Kai A, et al. Impact of chorioamnionitis on short- and long-term outcomes in very low birth weight preterm infants: the neonatal research network Japan. *J Matern Fetal Neonatal Med.* (2016) 29:331–7. doi: 10.3109/14767058.2014.1000852
95. Mu SC, Lin CH, Chen YL, Ma HJ, Lee JS, Lin MI, et al. Impact on neonatal outcome and anthropometric growth in very low birth weight infants with histological chorioamnionitis. *J Formos Med Assoc.* (2008) 107:304–10. doi: 10.1016/S0929-6646(08)60091-1
96. Mwanyumba F, Inion I, Gaillard P, Mandaliya K, Praet M, Temmerman M. Placental inflammation and perinatal outcome. *Eur J Obstet Gynecol Reprod Biol.* (2003) 108:164–70. doi: 10.1016/S0301-2115(02)00438-4
97. Nasef N, Shabaan AE, Schurr P, Iaboni D, Choudhury J, Church P, et al. Effect of clinical and histological chorioamnionitis on the outcome of preterm infants. *Am J Perinatol.* (2013) 30:59–68. doi: 10.1055/s-0032-1321501
98. O'Shea TM, Klinepeter KL, Meis PJ, Dillard RG. Intrauterine infection and the risk of cerebral palsy in very low-birthweight infants. *Paediatr Perinat Epidemiol.* (1998) 12:72–83. doi: 10.1111/j.1365-3016.1998.00081.x
99. Ofman G, Vasco N, Cantey JB. Risk of early-onset sepsis following preterm, prolonged rupture of membranes with or without chorioamnionitis. *Am J Perinatol.* (2016) 33:339–42. doi: 10.1055/s-0035-1556758
100. Ogunyemi D, Murillo M, Jackson U, Hunter N, Alperson B. The relationship between placental histopathology findings and perinatal outcome in preterm infants. *J Matern Fetal Neonatal Med.* (2003) 13:102–9. doi: 10.1080/jmf.13.2.102.109

101. Oh S-H, Kim J-J, Do H-J, Lee BS, Kim K-S, Kim EA-R. Preliminary study on neurodevelopmental outcome and placental pathology among extremely low birth weight infants. *Korean J Perinatol.* (2015) 26:67–77. doi: 10.14734/kjp.2015.26.1.67
102. Ohyama M, Itani Y, Yamanaka M, Goto A, Kato K, Ijiri R, et al. Re-evaluation of chorioamnionitis and funisitis with a special reference to subacute chorioamnionitis. *Hum Pathol.* (2002) 33:183–90. doi: 10.1053/hupa.2002.31291
103. Ozkan H, Cetinkaya M, Koksal N, Celebi S, Hacimustafaoglu M. Culture-proven neonatal sepsis in preterm infants in a neonatal intensive care unit over a 7 year period: coagulase-negative *Staphylococcus* as the predominant pathogen. *Pediatr Int.* (2014) 56:60–6. doi: 10.1111/ped.12218
104. Pappas A, Kendrick DE, Shankaran S, Stoll BJ, Bell EF, Laptook AR, et al. Chorioamnionitis and early childhood outcomes among extremely low-gestational-age neonates. *JAMA Pediatr.* (2014) 168:137–47. doi: 10.1001/jamapediatrics.2013.4248
105. Park JW, Park KH, Jung EY. Clinical significance of histologic chorioamnionitis with a negative amniotic fluid culture in patients with preterm labor and premature membrane rupture. *PLoS ONE.* (2017) 12:e0173312. doi: 10.1371/journal.pone.0173312
106. Park KH, Yoon BH, Shim SS, Jun JK, Syn HC. Amniotic fluid tumor necrosis factor-alpha is a marker for the prediction of early-onset neonatal sepsis in preterm labor. *Gynecol Obstet Invest.* (2004) 58:84–90. doi: 10.1159/000078492
107. Plakkal N, Soraisham AS, Trevenen C, Freiheit EA, Sauve R. Histological chorioamnionitis and bronchopulmonary dysplasia: a retrospective cohort study. *J Perinatol.* (2013) 33:441–5. doi: 10.1038/jp.2012.154
108. Popowski T, Goffinet F, Maillard F, Schmitz T, Leroy S, Kayem G. Maternal markers for detecting early-onset neonatal infection and chorioamnionitis in cases of premature rupture of membranes at or after 34 weeks of gestation: a two-center prospective study. *BMC Pregnancy ChildB.* (2011) 11:26. doi: 10.1186/1471-2393-11-26
109. Prendergast M, May C, Broughton S, Pollina E, Milner AD, Rafferty GF, et al. Chorioamnionitis, lung function and bronchopulmonary dysplasia in prematurely born infants. *Arch Dis Child Fetal Neonatal Ed.* (2011) 96:F270–4. doi: 10.1136/adc.2010.189480
110. Pristauz G, Bader AA, Schwantzer G, Kutschera J, Lang U. Assessment of risk factors for survival of neonates born after second-trimester PPROM. *Early Hum Dev.* (2009) 85:177–80. doi: 10.1016/j.earlhumdev.2008.09.012
111. Puri K, Taft DH, Ambalavanan N, Schibler KR, Morrow AL, Kallapur SG. Association of chorioamnionitis with aberrant neonatal gut colonization and adverse clinical outcomes. *PLoS ONE.* (2016) 11:e0162734. doi: 10.1371/journal.pone.0162734
112. Rocha G, Proenca E, Quintas C, Rodrigues T, Guimaraes H. Chorioamnionitis and neonatal morbidity. *Acta Med Port.* (2006) 19:207–12. doi: 10.1016/j.ajog.2004.11.035
113. Rodriguez-Trujillo A, Cobo T, Vives I, Bosch J, Kacerovsky M, Posadas DE, et al. Gestational age is more important for short-term neonatal outcome than microbial invasion of the amniotic cavity or intra-amniotic inflammation in preterm prelabor rupture of membranes. *Acta Obstet Gynecol Scand.* (2016) 95:926–33. doi: 10.1111/aogs.12905
114. Ronnestad A, Abrahamsen TG, Medbo S, Reigstad H, Lossius K, Kaaresen PI, et al. Septicemia in the first week of life in a norwegian national cohort of extremely premature infants. *Pediatrics.* (2005) 115:e262–8. doi: 10.1542/peds.2004-1834
115. Salem SY, Sheiner E, Zmora E, Vardi H, Shoham-Vardi I, Mazor M. Risk factors for early neonatal sepsis. *Arch Gynecol Obstet.* (2006) 274:198–202. doi: 10.1007/s00404-006-0135-1
116. Sato M, Nishimaki S, Yokota S, Seki K, Horiguchi H, An H, et al. Severity of chorioamnionitis and neonatal outcome. *J Obstet Gynaecol Res.* (2011) 37:1313–9. doi: 10.1111/j.1447-0756.2010.01519.x
117. Schlapbach LJ, Ersch J, Adams M, Bernet V, Bucher HU, Latal B. Impact of chorioamnionitis and preeclampsia on neurodevelopmental outcome in preterm infants below 32 weeks gestational age. *Acta Paediatr.* (2010) 99:1504–9. doi: 10.1111/j.1651-2227.2010.01861.x
118. Schuchat A, Zywicki SS, Dinsmoor MJ, Mercer B, Romaguera J, O'Sullivan MJ, et al. Risk factors and opportunities for prevention of early-onset neonatal sepsis: a multicenter case-control study. *Pediatrics.* (2000) 105(1 Pt 1):21–6. doi: 10.1542/peds.105.1.21
119. Shah J, Jefferies AL, Yoon EW, Lee SK, Shah PS, Canadian Neonatal N. Risk factors and outcomes of late-onset bacterial sepsis in preterm neonates born at < 32 weeks' gestation. *Am J Perinatol.* (2015) 32:675–82. doi: 10.1055/s-0034-1393936
120. Smit AL, Been JV, Zimmermann LJ, Kornelisse RF, Andriessen P, Vanterpool SF, et al. Automated auditory brainstem response in preterm newborns with histological chorioamnionitis. *J Matern Fetal Neonatal Med.* (2015) 28:1864–9. doi: 10.3109/14767058.2014.971747
121. Smulian JC, Shen-Schwarz S, Vintzileos AM, Lake MF, Ananth CV. Clinical chorioamnionitis and histologic placental inflammation. *Obstet Gynecol.* (1999) 94:1000–5. doi: 10.1097/00006250-199912000-00018
122. Soraisham AS, Singhal N, McMillan DD, Sauve RS, Lee SK, Canadian Neonatal N. A multicenter study on the clinical outcome of chorioamnionitis in preterm infants. *Am J Obstet Gynecol.* (2009) 200:372.e1–6. doi: 10.1016/j.ajog.2008.11.034
123. Soraisham AS, Trevenen C, Wood S, Singhal N, Sauve R. Histological chorioamnionitis and neurodevelopmental outcome in preterm infants. *J Perinatol.* (2013) 33:70–5. doi: 10.1038/jp.2012.49
124. Stepan M, Cobo T, Maly J, Navratilova M, Musilova I, Hornychova H, et al. Neonatal outcomes in subgroups of women with preterm prelabor rupture of membranes before 34 weeks. *J Matern Fetal Neonatal Med.* (2016) 29:2373–7. doi: 10.3109/14767058.2015.1086329
125. Stimac M, Juretic E, Vukelic V, Matasic NP, Kos M, Babic D. Effect of chorioamnionitis on mortality, early onset neonatal sepsis and bronchopulmonary dysplasia in preterm neonates with birth weight of < 1,500 grams. *Coll Antropol.* (2014) 38:167–71.
126. Stranak Z, Feyereisl J, Korcek P, Feyereislova S, Krofta L. Procalcitonin is more likely to be released by the fetus rather than placental tissue during chorioamnionitis. *Biomed Pap Med Fac Univ Palacky Olomouc Czech Repub.* (2016) 160:499–502. doi: 10.5507/bp.2016.041
127. Sung JH, Choi SJ, Oh SY, Roh CR, Kim JH. Revisiting the diagnostic criteria of clinical chorioamnionitis in preterm birth. *BJOG.* (2017) 124:775–83. doi: 10.1111/1471-0528.14176
128. Trevisanuto D, Peruzzetto C, Cavallin F, Vedovato S, Cosmi E, Visentin S, et al. Fetal placental inflammation is associated with poor neonatal growth of preterm infants: a case-control study. *J Matern Fetal Neonatal Med.* (2013) 26:1484–90. doi: 10.3109/14767058.2013.789849
129. Tsai CH, Chen YY, Wang KG, Chen CY, Chen CP. Characteristics of early-onset neonatal sepsis caused by *Escherichia coli*. *Taiwan J Obstet Gynecol.* (2012) 51:26–30. doi: 10.1016/j.tjog.2012.01.006
130. Tsiartas P, Kacerovsky M, Musilova I, Hornychova H, Cobo T, Savman K, et al. The association between histological chorioamnionitis, funisitis and neonatal outcome in women with preterm prelabor rupture of membranes. *J Matern Fetal Neonatal Med.* (2013) 26:1332–6. doi: 10.3109/14767058.2013.784741
131. Tudela CM, Stewart RD, Roberts SW, Wendel GD Jr, Stafford IA, McIntire DD, et al. Intrapartum evidence of early-onset group B streptococcus. *Obstet Gynecol.* (2012) 119:626–9. doi: 10.1097/AOG.0b013e31824532f6
132. Van Marter LJ, Dammann O, Allred EN, Leviton A, Pagano M, Moore M, et al. Chorioamnionitis, mechanical ventilation, and post-natal sepsis as modulators of chronic lung disease in preterm infants. *J Pediatr.* (2002) 140:171–6. doi: 10.1067/mpd.2002.121381
133. van Vliet EO, de Kieviet JF, van der Voorn JP, Been JV, Oosterlaan J, van Elburg RM. Placental pathology and long-term neurodevelopment of very preterm infants. *Am J Obstet Gynecol.* (2012) 206:489.e1–7. doi: 10.1016/j.ajog.2012.03.024
134. Vander Haar E, Gyamfi-Bannerman C. Chorioamnionitis and neurocognitive development at age 2 years. *Obstet Gynecol.* (2016) 127:437–41. doi: 10.1097/AOG.0000000000001295
135. Vinnars MT, Papadogiannakis N, Nasiell J, Holmstrom G, Westgren M. Placental pathology in relation to stillbirth and neonatal outcome in an extremely preterm population: a prospective cohort study. *Acta Obstet Gynecol Scand.* (2015) 94:584–90. doi: 10.1111/aogs.12610
136. Watterberg KL, Gerdes JS, Gifford KL, Lin HM. Prophylaxis against early adrenal insufficiency to prevent chronic lung disease in premature infants. *Pediatrics.* (1999) 104:1258–63. doi: 10.1542/peds.104.6.1258

137. Wynn JL, Hansen NI, Das A, Cotten CM, Goldberg RN, Sanchez PJ, et al. Early sepsis does not increase the risk of late sepsis in very low birth weight neonates. *J Pediatr.* (2013) 162:942–8.e1–3. doi: 10.1016/j.jpeds.2012.11.027
138. Xie A, Zhang W, Chen M, Wang Y, Wang Y, Zhou Q, et al. Related factors and adverse neonatal outcomes in women with preterm premature rupture of membranes complicated by histologic chorioamnionitis. *Med Sci Monit.* (2015) 21:390–5. doi: 10.12659/MSM.891203
139. Yancey MK, Duff P, Kubilis P, Clark P, Frentzen BH. Risk factors for neonatal sepsis. *Obstet Gynecol.* (1996) 87:188–94. doi: 10.1016/0029-7844(95)00402-5
140. Yoon BH, Romero R, Kim CJ, Jun JK, Gomez R, Choi JH, et al. Amniotic fluid interleukin-6: a sensitive test for antenatal diagnosis of acute inflammatory lesions of preterm placenta and prediction of perinatal morbidity. *Am J Obstet Gynecol.* (1995) 172:960–70. doi: 10.1016/0002-9378(95)90028-4
141. Lee Y, Kim H-J, Choi S-J, Oh S-Y, Kim J-S, Roh C-R, et al. Is there a stepwise increase in neonatal morbidities according to histological stage (or grade) of acute chorioamnionitis and funisitis?: effect of gestational age at delivery. *J Perinatal Med*. (2015) 43:259–67. doi: 10.1515/jpm-2014-0035
142. McShane BB, Gal D, Gelman A, Robert C, Tackett JL. Abandon statistical significance. *Am Stat.* (2019) 73(Supp1):235–45. doi: 10.1080/00031305.2018.1527253
143. Ciolino JD, Martin RH, Zhao W, Jauch EC, Hill MD, Palesch YY. Covariate imbalance and adjustment for logistic regression analysis of clinical trial data. *J Biopharm Stat*. (2013) 23:1383–402. doi: 10.1080/10543406.2013.834912
144. Davies HTO, Crombie IK, Tavakoli M. When can odds ratios mislead? *BMJ.* (1998) 316:989–91. doi: 10.1136/bmj.316.7136.989
145. Snowden JM, Basso O. Causal inference in studies of preterm babies: a simulation study. *BJOG.* (2018) 125:686–92. doi: 10.1111/1471-0528.14942
146. Durrmeyer X, Kayem G, Sinico M, Dassieu G, Danan C, Decobert F. Perinatal risk factors for bronchopulmonary dysplasia in extremely low gestational age infants: a pregnancy disorder-based approach. *J Pediatr.* (2012) 160:578–83.e2. doi: 10.1016/j.jpeds.2011.09.025
147. van Well GTJ, Daalderop LA, Wolfs T, Kramer BW. Human perinatal immunity in physiological conditions and during infection. *Mol Cell Pediatr.* (2017) 4:4. doi: 10.1186/s40348-017-0070-1
148. Wilcox AJ, Weinberg CR, Basso O. On the pitfalls of adjusting for gestational age at birth. *Am J Epidemiol.* (2011) 174:1062–8. doi: 10.1093/aje/kwr230
149. Ananth CV, Schisterman EF. Confounding, causality, and confusion: the role of intermediate variables in interpreting observational studies in obstetrics. *Am J Obstet Gynecol.* (2017) 217:167–75. doi: 10.1016/j.ajog.2017.04.016
150. Basso O, Wilcox A. Mortality risk among preterm babies: immaturity vs. underlying pathology. *Epidemiology (Cambridge, Mass).* (2010) 21:521–7. doi: 10.1097/EDE.0b013e3181debe5e
151. Hernández-Díaz S, Schisterman EF, Hernán MA. The birth weight "paradox" uncovered? *Am J Epidemiol.* (2006) 164:1115–20. doi: 10.1093/aje/kwj275
152. Braun D, Bromberger P, Ho NJ, Getahun D. Low rate of perinatal sepsis in term infants of mothers with chorioamnionitis. *Am J Perinatol.* (2016) 33:143–50. doi: 10.1055/s-0035-1560045
153. Puopolo KM, Mukhopadhyay S, Hansen NI, Cotten CM, Stoll BJ, Sanchez PJ, et al. Identification of extremely premature infants at low risk for early-onset sepsis. *Pediatrics.* (2017) 140:e20170925. doi: 10.1542/peds.2017-0925
154. Azizia M, Lloyd J, Allen M, Klein N, Peebles D. Immune status in very preterm neonates. *Pediatrics.* (2012) 129:e967–74. doi: 10.1542/peds.2011-1579
155. Wolfs TG, Jellema RK, Turrisi G, Becucci E, Buonocore G, Kramer BW. Inflammation-induced immune suppression of the fetus: a potential link between chorioamnionitis and post-natal early onset sepsis. *J Matern Fetal Neonatal Med.* (2012) 25(Suppl. 1):8–11. doi: 10.3109/14767058.2012.664447
156. Kallapur SG, Kramer BW, Knox CL, Berry CA, Collins JJ, Kemp MW, et al. Chronic fetal exposure to ureaplasma parvum suppresses innate immune responses in sheep. *J Immunol.* (2011) 187:2688–95. doi: 10.4049/jimmunol.1100779
157. Kramer BW, Kallapur SG, Moss TJ, Nitsos I, Newnham JP, Jobe AH. Intra-amniotic LPS modulation of TLR signaling in lung and blood monocytes of fetal sheep. *Innate Immun.* (2009) 15:101–7. doi: 10.1177/1753425908100455
158. Revello R, Alcaide MJ, Dudzik D, Abehsera D, Bartha JL. Differential amniotic fluid cytokine profile in women with chorioamnionitis with and without funisitis. *J. Matern. Fetal Neonatal Med.* (2015) 29:2161–5. doi: 10.3109/14767058.2015.1077512
159. Groer MW, Luciano AA, Dishaw LJ, Ashmeade TL, Miller E, Gilbert JA. Development of the preterm infant gut microbiome: a research priority. *Microbiome.* (2014) 2:38. doi: 10.1186/2049-2618-2-38
160. Ting JY, Roberts A, Sherlock R, Ojah C, Cieslak Z, Dunn M, et al. Duration of initial empirical antibiotic therapy and outcomes in very low birth weight infants. *Pediatrics.* (2019) 143:e20182286. doi: 10.1542/peds.2018-2286
161. Flannery DD, Dysart K, Cook A, Greenspan J, Aghai ZH, Jensen EA. Association between early antibiotic exposure and bronchopulmonary dysplasia or death. *J Perinatol.* (2018) 38:1227–34. doi: 10.1038/s41372-018-0146-3
162. Higgins RD, Saade G, Polin RA, Grobman WA, Buhimschi IA, Watterberg K, et al. Evaluation and management of women and newborns with a maternal diagnosis of chorioamnionitis: summary of a workshop. *Obst Gynecol.* (2016) 127:426–36. doi: 10.1097/AOG.0000000000001246
163. Redline RW, Heller D, Keating S, Kingdom J. Placental diagnostic criteria and clinical correlation-a workshop report. *Placenta.* (2005) 26:S114–S7. doi: 10.1016/j.placenta.2005.02.009
164. Wynn JL. Defining neonatal sepsis. *Curr Opin Pediatr.* (2016) 28:135–40. doi: 10.1097/MOP.0000000000000315
165. Hofer N, Zacharias E, Muller W, Resch B. Performance of the definitions of the systemic inflammatory response syndrome and sepsis in neonates. *J Perinat Med.* (2012) 40:587–90. doi: 10.1515/jpm-2011-0308
166. Wynn JL, Wong HR, Shanley TP, Bizzarro MJ, Saiman L, Polin RA. Time for a neonatal-specific consensus definition for sepsis. *Pediatr Crit Care Med.* (2014) 15:523–8. doi: 10.1097/PCC.0000000000000157
167. Wynn JL, Guthrie SO, Wong HR, Lahni P, Ungaro R, Lopez MC, et al. Post-natal age is a critical determinant of the neonatal host response to sepsis. *Mol Med.* (2015) 21:496–504. doi: 10.2119/molmed.2015.00064
168. Wortham JM, Hansen NI, Schrag SJ, Hale E, Van Meurs K, Sanchez PJ, et al. Chorioamnionitis and culture-confirmed, early-onset neonatal infections. *Pediatrics.* (2016) 137:e20152323. doi: 10.1542/peds.2015-2323

Conflict of Interest: The authors declare that the research was conducted in the absence of any commercial or financial relationships that could be construed as a potential conflict of interest.

The handling Editor declared a past co-authorship with one of the authors BK.

frontiers in Immunology

REVIEW
published: 09 June 2020
doi: 10.3389/fimmu.2020.01153

The Immature Gut Barrier and Its Importance in Establishing Immunity in Newborn Mammals

Björn Weström[1]*, *Ester Arévalo Sureda*[2], *Kateryna Pierzynowska*[1,3], *Stefan G. Pierzynowski*[1,4] and *Francisco-José Pérez-Cano*[5,6]

[1] Department of Biology, Lund University, Lund, Sweden, [2] Precision Livestock and Nutrition Unit, TERRA Teaching and Research Centre, Gembloux Agro-Biotech, University of Liège, Gembloux, Belgium, [3] Department of Animal Physiology, Kielanowski Institute of Animal Physiology and Nutrition, Jablonna, Poland, [4] Department of Medical Biology, Institute of Rural Health, Lublin, Poland, [5] Physiology Section, Department of Biochemistry and Physiology, Faculty of Pharmacy and Food Science, University of Barcelona, Barcelona, Spain, [6] Research Institute of Nutrition and Food Safety of the University of Barcelona (INSA-UB), Santa Coloma de Gramenet, Spain

The gut is an efficient barrier which protects against the passage of pathogenic microorganisms and potential harmful macromolecules into the body, in addition to its primary function of nutrient digestion and absorption. Contrary to the restricted macromolecular passage in adulthood, enhanced transfer takes place across the intestines during early life, due to the high endocytic capacity of the immature intestinal epithelial cells during the fetal and/or neonatal periods. The timing and extent of this enhanced endocytic capacity is dependent on animal species, with a prominent non-selective intestinal macromolecular transfer in newborn ungulates, e.g., pigs, during the first few days of life, and a selective transfer of mainly immunoglobulin G (IgG), mediated by the FcRn receptor, in suckling rodents, e.g., rats and mice. In primates, maternal IgG is transferred during fetal life via the placenta, and intestinal macromolecular transfer is largely restricted in human neonates. The period of intestinal macromolecular transmission provides passive immune protection through the transfer of IgG antibodies from an immune competent mother; and may even have extra-immune beneficial effects on organ maturation in the offspring. Moreover, intestinal transfer during the fetal/neonatal periods results in increased exposure to microbial and food antigens which are then presented to the underlying immune system, which is both naïve and immature. This likely stimulates the maturation of the immune system and shifts the response toward tolerance induction instead of activation or inflammation, as usually seen in adulthood. Ingestion of mother's milk and the dietary transition to complex food at weaning, as well as the transient changes in the gut microbiota during the neonatal period, are also involved in the resulting immune response. Any disturbances in timing and/or balance of these parallel processes, i.e., intestinal epithelial maturation, luminal microbial colonization and mucosal immune maturation due to, e.g., preterm birth, infection, antibiotic use or nutrient changes during the neonatal period, might affect the establishment of the immune system in the infant.

OPEN ACCESS

Edited by:
Per T. Sangild,
University of Copenhagen, Denmark

Reviewed by:
Viviana Parreño,
National Agricultural Technology Institute, Argentina
Isabelle Le Huërou-Luron,
INRA Centre Bretagne-Normandie, France

***Correspondence:**
Björn Weström
bjorn.westrom@biol.lu.se

Specialty section:
This article was submitted to Nutritional Immunology, a section of the journal Frontiers in Immunology

Received: *31 January 2020*
Accepted: *11 May 2020*
Published: *09 June 2020*

Citation:
Weström B, Arévalo Sureda E, Pierzynowska K, Pierzynowski SG and Pérez-Cano F-J (2020) The Immature Gut Barrier and Its Importance in Establishing Immunity in Newborn Mammals. Front. Immunol. 11:1153. doi: 10.3389/fimmu.2020.01153

This review will focus on how differing developmental processes in the intestinal epithelium affect the macromolecular passage in different species and the possible impact of such passage on the establishment of immunity during the critical perinatal period in young mammals.

Keywords: intestine, permeability, fetal, transcytosis, FcRn, tolerance, immunity

INTRODUCTION

The gut, in addition to its primary function of nutrient digestion and absorption, constitutes an effective barrier to protect against the invasion of pathogenic microorganisms and passage of potential harmful macromolecules into the body. However, as opposed to the restricted macromolecular passage in the adult, enhanced transfer of macromolecules across the immature intestinal epithelium takes place during the fetal and neonatal periods (1). The high intestinal permeability during these periods is due to the high endocytic capacity of the immature (fetal-type) enterocytes (2–4). These fetal-type enterocytes internalize luminal content containing macromolecules, by fluid-phase or receptor-mediated endocytosis, either for intracellular digestion in digestive vacuoles or for their vesicular transfer through the cell and release on the basolateral side (transcytosis). The intestinal transfer can either be non-selective, with uptake and passage of an array of luminal macromolecules, or the transfer can be more selective due to epithelial expression of the neonatal Fc (fragment crystallizable) receptor (FcRn) that binds and mediates the transepithelial transfer of immunoglobulin G (IgG) (5–11).

This property of the intestinal epithelium is largely lost with the progress of development and maturation, during the fetal and neonatal periods, until macromolecular transepithelial transfer ceases at the time of the so-called "gut closure." In the mature intestine, after gut closure, some macromolecular transfer still takes place, but the extent of transfer is limited and it is restricted in terms of intestinal area, with transfer occurring mainly in the follicle-associated epithelium, especially over the membranous cells (M-cells), overlaying the immune-cell rich regions in the small intestine known as the Peyer's patches (12). Recent research also suggests passage of antigenic molecules through intestinal goblet cells (13). In addition, a paracellular leakage of larger molecules after an inflammatory-induced opening of the epithelial tight junctions may also occur (14).

This review will focus on the developmental processes taking place in the intestinal epithelium, highlighting the high macromolecular passage during the critical perinatal period and the impact of such passage on the development of immunity in the young, with possible effects later in life. In addition, the review will describe the differences in timing and amount of such macromolecular transfer between species, in particular those used as animal models for humans, and the impact this could have when comparing different species.

ENHANCED INTESTINAL MACROMOLECULAR TRANSFER IN FETAL/NEONATAL LIFE

The extent and time period of macromolecular transfer over the immature intestine, before gut closure, is dependent on animal species (1). In eutherian (placental) species, this appears to be linked to the type of placentation and number of tissue layers separating the fetal and maternal blood circulations, hence affecting the extent of the macromolecular transfer between mother and offspring. In non-mammalian vertebrates, such as fish and birds, maternal macromolecular transfer takes place from the yolk, over the yolk sac endoderm, and finally to the offspring's blood circulation (1, 15, 16). In mammalian species, such as rodents, the yolk sac is everted and participates in some macromolecular transfer from the uterus, however, the immature neonatal gut takes over this role and constitutes the main route of macromolecular transmission in rats and mice (1, 4). In other mammalian species, such as ungulates and primates, the yolk sac either atrophies during gestation or is absent (17). In ungulates macromolecular transfer occurs from the first milk, known as colostrum, via the immature gut for a short period after birth, while in primates the main macromolecular transfer is occurs via the placenta and intestinal macromolecular transfer is largely restricted to fetal life (**Table 1**).

Lagomorph and Rodent Species

In the lagomorph rabbit and in precocious rodent species, i.e., the guinea pig, macromolecular transfer takes place from uterine secretion via the everted yolk sac during the fetal period (15, 29). Even though the yolk sac endoderm may endocytose macromolecules indiscriminately, this transfer is selective since the yolk sac endoderm expresses FcRn that binds and mediates the transfer of IgG to the fetal circulation (18, 19). Thus, guinea pigs are born relatively mature, equipped with their mother's IgG repertoire, and intestinal macromolecular transfer is negligible postnatally (20, 22).

In altricial rodents such as rats and mice, similar to guinea pigs, some macromolecular transfer takes place *in utero* during the late fetal period, via the endocytic cells of the everted yolk sac endoderm. However, this is quantitatively less important compared to the postnatal intestinal transfer (9, 23), which is selective and occurs during the entire suckling period until weaning (24, 25).

The macromolecular uptake and transepithelial transfer takes place with regional differences along the small intestine. In the proximal part (jejunum), highly endocytic fetal-type enterocytes

TABLE 1 | Overview and comparison of macromolecular transmission between mother and offspring in different species.

Taxon/species	Pre- or Postnatal	Gestation length	Maternal source	Route of transfer to offspring	Transfer mechanism	Gut closure age	Weaning age	Age at immune maturity	Literature
Aves (chicken)			Yolk	Yolk sac endoderm	Receptor-mediated endocytosis, FcRY/IgY	–	–	>2–3 weeks	(1, 16)
Lagomorphs (rabbit)	Prenatal	3–4 weeks	Uterine secretion	Everted yolk sac	Receptor-mediated endocytosis, FcRn/IgG	–	5–6 weeks	After Infancy (>6 weeks)	(18–21)
Rodents (rat, mouse)	Prenatal	3 weeks	Blood	Everted yolk sac	Receptor-mediated endocytosis, FcRn/IgG	–		After Infancy (>6 weeks)	(9, 20, 22–28)
	Postnatal		Milk	Proximal small intestine	Receptor-mediated endocytosis, FcRn/IgG	3 weeks	2–3 weeks		
Rodents (guinea pig)	Prenatal	8–10 weeks	Uterine secretion	Everted yolk sac	Receptor-mediated endocytosis, FcRn/IgG	–	4–6 weeks	Post weaning (>6 weeks)	(15, 20, 29–31)
Ungulates (pig, sheep)	Prenatal	16 weeks						Post weaning (>7 weeks)	(32–36)
	Postnatal		Colostrum	Proximal small intestine	Macropinocytosis, (FcRn)	1–2 days	4–12 weeks		
Carnivores (cat, dog)	Prenatal	9 weeks (dog)	Blood	Placenta				After infancy (>6 months)	(37–39)
	Postnatal		Milk	Small intestine	Macropinocytosis	1–2 days	4 weeks		
Primates (human)	Prenatal	9 months	Amniotic fluid	Small intestine	Macropinocytosis, FcRn	≈22 weeks	4–6 months	After infancy (>10 years)	(4, 5, 7, 8, 40–46)
			Blood	Placenta	Receptor-mediated endocytosis, FcRn/IgG	–			

Summary data including, pre- and/or postnatal transfer period, gestation length, maternal source, transfer route and mechanism of transfer, i.e., selective transfer of antibodies (IgG or IgY) by receptor-mediated (FcRn or FcRY) endocytosis or by macro-pinocytosis (free-fluid endocytosis). The age at gut closure, i.e., cessation of transepithelial macromolecular passage, age at weaning from mothers milk to a complex diet and approximative age of reaching immune maturity is also indicated.

express FcRn receptors that bind and mediate the transepithelial transfer of IgG, as well as minor quantities of other milk proteins (24, 25, 47–49). The intestinal expression of the FcRn receptor is consistent with the high percentage of IgG (∼80% of total Ig) present in rodent milk in comparison with that of human breast milk (∼10%) (50). In fact, intestinal FcRn expression in premature rat pups is higher than that observed in term rats, suggesting a compensatory mechanism to counteract the low IgG passage during the fetal period (51).

In contrast, in the distal small intestine (ileum), the fetal-type epithelium internalizes luminal material via the apical endocytic complex and forms large digestive vacuoles that make up most of the cytoplasmic content (26, 52), allowing little macromolecules to pass the epithelium intact. The endocytosis machinery in mouse ileal enterocytes was recently identified and described as consisting of the multi-ligand scavenger (protein) receptors, Cubulin and Amnionless, together with the adaptor protein, Dab2, as mediators of the endocytosis mechanism (53, 54). In fact, these highly endocytic intestinal cells equipped with this multi-ligand endocytic machinery were also found in the zebrafish, indicating a conserved presence and function in vertebrates. Thus, instead of mediating transepithelial transfer of macromolecules; the cells of the rodent distal small intestine play a nutritional role with intracellular digestion, especially of protein, sustaining the rapid post-natal growth.

At about 2 weeks of age, when pups open their eyes and start to become interested in nibbling solid food in addition to suckling milk, adult-type epithelial enterocytes with drastically reduced endocytic capacity and decreased FcRn expression appear in the crypts and move up the villi, in both the proximal and distal parts of the small intestine. By 3 weeks of age, at weaning (27), this maturation process has finished and gut-closure is completed, so all fetal-type enterocytes have been replaced by the adult-type epithelium (49, 55–58).

Precocious intestinal maturation may be induced by premature weaning (59) or by luminal stimulation of suckling rats by, e.g., exposure to the lectin, phytohaemagglutinin (PHA), binding to the mucosa (60); experimental feeding of the polyamine, spermine (61, 62); administration of exogenous corticosteroids (63, 64) and by provocation with proteases (65). All these treatments stimulate crypt-cell proliferation, and thus, increase intestinal epithelial cell turnover and renewal to adult-type enterocytes with heavily decreased endocytic activity and macromolecular transfer capacity along the villi.

Ungulate (Hoofed) Species

In ungulate species, the epitheliochorial placenta consists of four epithelial/endothelial layers between the maternal and the fetal circulations, which constitutes an impermeable and effective barrier to macromolecules. Therefore, ungulates, i.e., piglets, lambs, calves and foals; are agammaglobulinemic at birth and during the first 1–2 days of life they display an extensive macromolecular transmission, including that of colostral antibodies over the intestines, making suckling essential for survival (32). The macromolecular transfer takes place by free-fluid endocytosis (macro-pinocytosis) in the proximal part of the small intestine and it is essentially a non-selective process. The enterocytes in the distal small intestine are also highly endocytic but the vesicles coalesce and form giant cell vacuoles designated for intra-cellular digestion and little, if any, of the macromolecules will survive intact and reach the basolateral side (4, 33). The period of intestinal transmission in newborn ungulates (piglets) matches the maternal (sow) production of colostrum, which is not only rich in nutrients, but also has a high content of IgG and other bioactive proteins. The FcRn receptor has been identified in the intestinal epithelium in piglets and lambs (34, 66) but it does not seem to be essential for the transfer of IgG, since a variety of macromolecules, including non-proteins like polyvinyl pyrrolidone (Mw 60.000) (67) and FITC-dextrans (Mw 3.000–70.000) (35, 68), can be absorbed. During this period, transfer of intact IgG and other colostrum whey proteins is facilitated by the high colostral protein content, that *per se* stimulates endocytosis (35), as well as the presence of a specific colostrum protease inhibitor (SCTI), which in turn decreases luminal protein degradation (69, 70).

At 1–2 days of life, if feeding has been initiated, gut closure takes place and the epithelium in the proximal small intestine loses its macromolecular transfer capacity (1, 68). The exact mechanism is not yet known, but the luminal proteolytic activity increases as the colostrum inhibitor level rapidly decreases, and the intestinal epithelial cells either lose their highly endocytic capacity or this capacity is limited and ceases after being fully utilized. In contrast, the endocytic capacity of the epithelium in the distal small intestine remains until up to 3 weeks of life and endocytosis of luminal material for intracellular vacuolar digestion continues (4, 33) until the epithelium of the entire small intestine is exchanged to adult-type epithelium and the endocytic capacity ceases. Thus, in ungulate species, macromolecular closure occurs early after birth in the proximal intestine without substantial cell replacement and unrelated to the weaning process.

Carnivore Species

In cats and dogs some maternal IgG is transmitted over the placental structures to the fetus, but the main macromolecular transfer occurs postnatally from colostrum, in a similar manner to that of ungulate species (37, 38). Characteristically, the intestinal epithelium is heavily vacuolated, indicating extensive endocytosis and closure of transepithelial macromolecular transfer occurs 1–2 days after birth. After this, macromolecular uptake and intracellular vacuolar digestion continues for some weeks until these epithelial cells are replaced and intestinal maturation is completed.

Primate Species

In contrast to the previously discussed mammalian phyla, primates, i.e., humans, show profound transfer of immunoglobulins already during the fetal period, across the hemochorial (chorioallantoic) placenta. Due to the "simple" human placenta being formed by one epithelial layer between fetal and maternal circulations, it allows for maternal-fetal macromolecular transfer. This transfer is selective and takes place by receptor-mediated transcytosis, binding of IgG to FcRn, across the syncytiotrophoblast cells (71). The transmission of IgG

is low during the early fetal period (1st and 2nd trimesters) but increases significantly during the late fetal period (3rd trimester). Hence, premature infants are born with lower IgG levels in the blood than full term infants.

In addition to the major placental IgG transfer, some macromolecular passage can also take place *in utero* over the intestine, since vacuolated enterocytes have been observed in the mid-distal intestine from about 13–14 weeks of fetal life (72) and a capacity for endocytosis has been described (40). Moreover, FcRn receptors have been identified in the apical membrane of intestinal epithelial cells and are able to bind IgG molecules present in the amniotic fluid after swallowing, mediating their endocytic transfer to the fetus (5, 8, 41). This capacity is lost at mid-gestation since the fetal-type enterocytes are exchanged for enterocytes lacking endocytic properties and gut closure appears to occur already *in utero* in humans (4, 40). At birth, full term neonates are equipped with an essentially adult-type intestinal epithelium, with low expression of the FcRn receptor and thus the endocytic capacity is largely lost. Hence, macromolecular transfer in the newborn is low, albeit somewhat higher than in the adult (42). The oral sugar (lactulose/mannitol) test has indicated increased intestinal permeability for a short period of about 1 week after birth, which can be prolonged by prematurity or formula-feeding (43, 73–76). Since the intestinal epithelium still expresses some FcRn receptors, it has been suggested that luminal IgG/antigen complexes might be transported over the intestinal barrier into the lamina propria, to interact with antigen presenting cells and other immune cells (44, 77).

In general, different strategies for macromolecular transfer from mother to offspring have evolved, from taking place via the yolk sac endoderm and/or fetal intestine to occurring after birth via the immature intestine, and lastly mainly via the placenta in primates (4). Nonetheless, all mammalian species undergo a period of high endocytic activity of the immature intestinal epithelium and/or yolk sac epithelium, which are all cells of endodermal origin, allowing for an enhanced transcellular transfer of maternal macromolecules to her progeny. Mostly, it is a selective transfer of IgG, shuttled and regulated by epithelial expression of FcRn, to secure the transfer of protective maternal immunity. However, dietary and microbial macromolecules can also be transmitted, either as part of a complex with IgG, selected due to the maternal antibody specificity, or in free antigenic form by non-selective endocytosis. In all cases this period of decreased epithelial barrier function with increased transfer of maternal antibodies and environmental antigens will have an impact on the activation and maturation of the submucosal immune system.

THE IMMATURE IMMUNE SYSTEM IN FETAL/NEONATAL LIFE

The formation of the immune system in humans starts in the embryo, develops during fetal life and only reaches maturity some years after birth (78). However, the precise organization and functionality of the early life, immature immune system is still poorly understood, both at systemic and local levels.

A Species Comparison

The formation and development of the immune system in rodents is delayed compared to humans, due to their short gestation period (3 vs. 42 weeks, respectively) and consequently, their relative immaturity after birth. Thus, it is established that the lymphoid architecture forms prenatally in humans while it occurs mainly during the postnatal period in rodents, and for that reason newborn rodents resemble and can be used as a model for prematurity in humans. However, overall, in both cases, they develop with similar schemes (79).

In rodents, and particularly in rats, development of inductor lymphoid aggregates, as Peyer's patches, and effector immune cells found scattered in the epithelial layer (i.e., Intraepithelial lymphocytes, IEL) or in the lamina propria (i.e., Lamina propria lymphocytes, LPL), have been well characterized (28). Almost all major IEL and LPL subsets identified in adults are already present in suckling rats, but in different proportions. After birth, both IELs and LPLs expand in numbers based on the generation of precursors and their migration from the thymus to peripheral tissues, especially increasing during the second week of life which coincides with the contact with new antigens due to the start of solid food ingestion or weaning, which has been proven crucial (80, 81). Intestinal IgA production is very low during early life and the number of IgA-secreting B-cells at the end of the suckling period is far lower than that in adult rats (81). Many of these immune features are even less developed when rats are born prematurely (51, 82).

It has been proposed that T-cells are mediators of intestinal epithelial cell differentiation and they contribute to the maintenance of the epithelial barrier function (83). It is also known that T-cells, in the neonatal intestine of mice, are inhibited by T-regs and IgA-mediated antigen translocation (84). Innate lymphocytes (ILCs) in the GI tract have been suggested to constitute the counterpart of T-lymphocytes in innate immunity (85), with a role as integrative factors being both receivers and regulators of multisystem signaling in the gut (86). Noteworthy, in the neonatal intestine, a specific type of ILCs (type 3) has been described as the first immune cell colonizer (87), and they have been proposed to function as inhibitors of the immune response in early life (88).

In ungulate pigs, the complex maternal-fetal placental separation prevents the transfer of maternal immune components, such as Ig or cytokines, to the fetus, thus making intestinal passage during suckling essential for development of the immune system. The structure of innate immunity in pigs is similar to that of other mammals, with natural killer cells (NK) being the key cell-type in early life, even though their functionality is only achieved after birth when immunoregulatory bioactive molecules appear during breastfeeding (36). Although there is significant lymphopoietic activity in the fetal liver, bone marrow and thymus, the adaptive immunity at birth is comprised mostly of immature, low effector/memory T cells and mainly un-primed B–cells. Accordingly, the mucosal adaptive immune system in the neonatal piglet is also immature (36).

In human fetuses, B- and T-cells are found in the intestine as early as between 12 and 14 weeks gestation and their abundance and maturation increases until birth (89). It has been recently demonstrated that both the innate and adaptive immune systems are present as early as 16 weeks of gestation. Furthermore, fetal leukocytes display a distinctive differential clustering compared to neonatal intestinal tissues and have established T-cell and B-cell receptor diversity. In addition, most effector memory cells have a tissue resident memory (TRM) phenotype and secrete TNF-α and IFN-γ (90). Despite this, the low levels of immune cells observed in the intestine during early life, among them TRM cells and NK cells, with a lower proliferative or cytotoxic response of T cells, and dysregulated cytokine or lower IgA production, indicates a general immaturity of the immune system, leading to increased susceptibility to infections (91).

In early life, the immaturity of the immune system is paralleled with the immaturity of the intestinal barrier function, resulting in a higher passage of antigens across the intestine. Thus, within this particular time period it is essential that a balance is reached between avoiding infection while at the same time activating the immune system and inducing antigen tolerance.

Immunomodulatory Breast Milk Components

In all mammalian neonates, breast milk is the principal nutrient source, but also the main driving factor in the maturation, activation and expansion of immune cells, particularly at mucosal sites. Even though 87% of breast milk content is water, the remaining 13% contains nutrients, as well as important bioactive compounds that have beneficial, non-nutritional functions (92). These compounds include, in addition to IgG in some species as discussed above, secretory IgA, antimicrobial factors like lactoferrin and lysozyme, cytokines, growth hormones and digestive enzymes, among others (43, 93–95). These milk-borne bioactive compounds are involved in the acquisition and appropriate establishment of the newborn's intestinal microbiota and immune system development (96). Secretory IgA (sIgA) in particular, contributes to shaping the microbiota during the suckling period and the breast milk oligosaccharides modulate the infant's microbiota by promoting the selective growth of health beneficial bacteria, like bifidobacteria, in the intestine.

Maternal immune cells are also present in breast milk and have been shown to be able to survive and pass the intestinal epithelial barrier and translocate into the newborn's tissues (97–101). Transfer of maternal immune cells may also occur during gestation, when maternal and fetal cells are exchanged across the placenta (102). However, this fetal cell transfer is quantitatively less marked than that which occurs following the ingestion of colostrum, due to its high content of immune cells. Furthermore, translocation of immunocompetent cells from mother to offspring has been shown to provide offspring with effective immunity and has been shown to have modulatory effects on the immune response in the young, thus influencing the development of their own immune system (103).

Breast milk contains an array of cytokines and growth factors involved in the newborn's immune system development, i.e., IL-6 stimulates differentiation of IgA-producing cells; IL-10 promotes tolerance to dietary and microbiota derived antigens, downregulates inflammation and promotes healing of damaged intestinal cells (104). In addition, the presence of pro-inflammatory cytokines, such as IL-8 and TNF-α, has also been reported in human milk. The growth factors in breast milk, TGF-β1 and TGF-β2, promote functional development of the gastrointestinal mucosa and are immunoregulators, whereas the epidermal growth factor (EGF) participates in tissue repair and growth and may contribute to the tightening of intercellular junctions (102). The cytokine profile of breast milk changes during the lactation period with differences in relative cytokine content in colostrum, transition milk and mature milk and, in addition, breast milk composition is also adapted to the delivery period, being different in term, preterm and very preterm neonates (104). Some of these bioactive factors, such as the EGF, have a low intestinal absorption ratio and they function mainly in the development of the gut and mucosal immune system, while others such as IL-2, are mostly absorbed and by entering the systemic circulation they can influence the maturing immune system (105).

Recently, the microbiomes of breast milk from humans (106), rats (50) and pigs (107) have been described. Milk microbiota have been suggested to function in the establishment of the infant's gut microbiota through the initial inoculum of the GI tract with microorganisms, and thus has been named "mother nature's prototypical probiotic food." It is estimated that infants consuming about 800 mL of breast milk per day obtain $\sim 10^5$-10^7 bacteria from the milk (108, 109). Thus, the maternal microbiome and maternal diet influences not only the composition of the breast milk, but also the composition of the infant's microbiome (110, 111).

Effects of Microbial Colonization

The colonization and expansion of beneficial bacteria in mucosal tissues during early life is not only important in the reduction of enteric infections, through competition with pathogens for the ecological niche and the production of antimicrobial agents or improvements in intestinal barrier function (108), but also through the stimulation and education of the host's immune system (109).

Among the many factors involved in the maturation of the intestinal immune system during early life, the colonization and establishment of a dynamic and appropriate microbiota is crucial. Exposure to microbes during early childhood is associated with protection from immune-mediated diseases later in life by permanently impacting the function of natural killer T (NKT) cells (112). NKT cells are a subset of cells which connect the innate and acquired immunity essential in early life (113) and are related to the development of allergic diseases in human subjects and mice (114). Additionally, similar levels of receptors that recognizes microbes and microbial components, such as the toll-like receptors (TLRs), have been found in human neonates and adults, although their activation causes immune reactions that are not as strong during early life (115). In fact, dysbiosis in infants seems to correlate with altered immune shaping and a chronic pro-inflammatory state later in adulthood (116).

In newborns, microbial antigens from the intestinal environment cannot be counteracted by a typical antibacterial and antiviral T helper type 1 (Th1) cell response, they induce a T helper type 2 (Th2) response instead, activating T cells and neutrophils via interleukin 8 (IL-8) (117). In contrast, an infant's dysbiotic microbiota would promote the Th1 response involving the production of pro-inflammatory cytokines, such as IL-12 and interferon (IFN)-γ (110). Regulation of the immune response seems to involve myeloid-derived suppressor cells that are already present in early life, which have demonstrated a strong ability to suppress T cells in mice and humans (118). These specific actions of the intestinal immune system limits continuous inflammatory damage and allows for intestinal colonization by the microbiota.

Overall, the time window for appropriate host-microbe cross-talk and therefore immune imprinting by microbiota, mainly takes place from birth to weaning, a period that involves a large expansion and diversification of the intestinal microbiota (119) and which coincides with the time window of increased antigen passage across the intestine.

The microbial and immunomodulatory components, at both the maternal and infant levels, are dependent on several factors which are considered as positive or beneficial when they promote the growth of bacterial genera, such as lactobacilli and bifidobacteria. Factors which positively shape the neonatal microbiome include vaginal delivery, maternal health status, long duration of lactation and the absence of antibiotic treatment during both pre- and post-natal periods. In contrast, factors that cause alterations in the infant's microbiota are C-section delivery, maternal disease status, especially infections that require antibiotics use; or absence of lactation that results in formula feeding (106, 110, 120, 121). These negative factors, such as antibiotics, not only reduce the previously mentioned bifidobacteria and lactobacilli beneficial bacterial groups, but also seem to affect other bacterial groups such as Proteobacteria, Firmicutes or the Clostridium cluster XIVa (121).

The microbial colonization of the intestine after birth will generate a diversity of new antigens that will play an important role in stimulating epithelial function and establishing the offspring's immune system (122). Weaning, with the loss of milk-born sIgA and other anti-microbial factors and the transition from mothers' milk to a complex diet will have a major impact on the dynamic microbiota development and thus in the resulting immune response during the neonatal period.

IMPACT OF INTESTINAL MACROMOLECULAR TRANSFER IN THE FETAL/NEONATAL PERIOD

At birth, when the offspring leaves the safety of the mother's womb, the intestinal barrier function is of utmost importance due to its dual function in preventing the passage of potentially harmful molecules and selectively allowing bioactive molecules and antigens to pass through. The barrier function is accomplished by several components including the luminal content, formed by endogenous secretions; the microbiota and the mucus layer; the intestinal epithelium itself, and the underlying immune system. The intestinal epithelium, a single layer of polarized cells, forms a key portion of the selective barrier, due to the endocytic capacity of the immature intestinal epithelium to select and shuttle those molecules which are allowed to pass through and reach the sub-mucosa and general circulation. Among the important macromolecules that require selective passage are the maternal antibodies, especially IgG, as well as the bioactive components in the amniotic fluid and breast milk and the microbial and dietary antigens (**Figure 1**).

Passive Immune Protection by Maternal Antibodies (IgG)

The transfer of antibodies from immune competent mothers, either during fetal life or after birth, independent of route, provides newborns with effective immune protection, especially taking into account that they will most likely be exposed to the same environmental pathogens. These passively acquired maternal antibodies enter the blood circulation and provide the same protective function as actively produced antibodies. The benefit of acquiring the mother's cumulative antibody repertoire has been shown in both human and animal studies (1, 123, 124). For example, newborn husbandry ungulates, e.g., lambs or piglets, that for some reason are not able to or are not allowed to suckle and are thus deprived of naturally receiving the IgG in colostrum, will rapidly weaken and will usually develop post-natal diarrhea and succumb (125). In human neonates, since IgG is already transferred across the placenta, difficulties with regards to breast-feeding has less dramatic consequences. Even children that are genetically incapable of producing IgG (X-linked agammaglobulinemia) are protected against most infections for a few months by maternal antibodies. However, antibodies, like all proteins, are metabolized over time and IgG declines to non-protective levels, rendering these children extremely sensitive to infections (126). Previous studies in both rodents and humans have shown that maternally acquired IgG can also be transported back into the intestinal lumen, from the circulation, via the FcRn receptor (44). This can exert local protective effects, which are especially important in humans, in instances where milk contains low levels of IgG or when infants are fed with formula (127).

In addition to immune protection, passively acquired maternal antibodies reduce the metabolic costs of generating an active immune response in the offspring. Thus, passive immunity minimizes growth-suppressive effects that may be caused by activation of the immune system in species with rapid growth after birth (128). However, there is also a drawback with regards to the transfer of maternal antibodies, since it can inhibit active immunization and cause problems concerning the efficacy of vaccination of young infants, as described in both in human and veterinary medicine (129).

Recent results also indicate the existence of extra-immunological effects of maternal antibody transfer in addition to the classical protective immune effects, including direct effects on growth and functional development of the brain, the gut and possibly other organ systems in the neonate (130–132). The

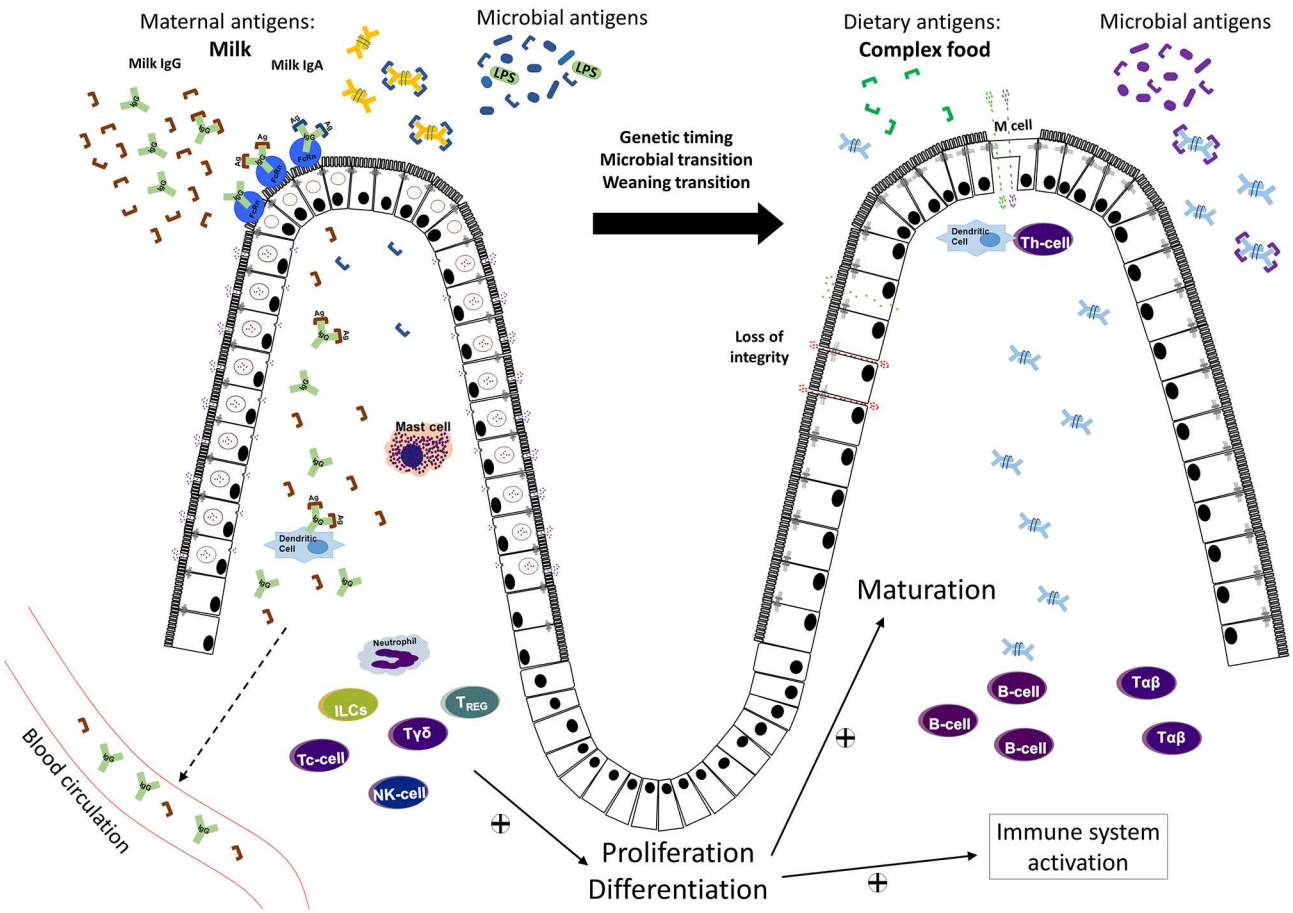

FIGURE 1 | Schematic illustration of the maturational changes taking place in the small intestine, with the replacement of endocytic fetal-type epithelial cells by mature adult-type cells lacking these features during fetal/neonatal development of young mammals. Maternal macromolecules/antigens in amniotic fluid or milk (colostrum), as well as microbial antigens, may pass over the fetal and neonatal epithelial barrier and activate the underlying immature immune system. The transfer of maternal IgG is facilitated by receptor-mediated endocytosis by epithelial FcRn receptors. With maturation, at gut closure, epithelial cell endocytosis ceases and the transepithelial macromolecular passage is largely restricted. In addition to low physiological antigen passage over the adult-type epithelium, a loss of barrier integrity due to e.g., inflammation, can increase the passage of dietary or microbial antigens and impact the immune system.

additional properties of circulating maternal Ig could have an impact on human neonates, especially those born prematurely with low plasma IgG levels.

Effects of Transfer of Antigenic Macromolecules

In addition to the passive immunization by maternal transfer of antibodies (IgG), milk cells and bioactive molecules; enhanced macromolecular passage over the intestines during the fetal and neonatal periods also results, although with some variation in quantity and timing between various species, in increased microbial and dietary antigen exposure and presentation to the underlying immature immune system. The outcome of antigenic exposure and the resulting immune response during this critical time window will be dependent on the maturity of the immune system and can either result in effector cell activation or tolerance induction.

Gut Luminal Effects on Antigen Transfer

During the fetal and neonatal periods, intestinal luminal digestion is generally low due to the immature stomach and pancreatic function and the presence of milk-borne protease inhibitors (27, 55, 133). The reduced luminal enzymatic activity during these periods functions to keep molecules intact until they reach the intestinal epithelium, thus preserving antigenicity and possibly increasing the extent of their subsequent transepithelial passage (134). Antenatally, components in the amniotic fluid like proteinase inhibitors, and, postnatally, bioactive components in colostrum and milk, will influence the luminal environment and hence the formation and stability of antigenic molecules. In addition, milk oligosaccharides can bind to viral and bacterial antigens

blocking their interaction with host cell-surface glycans, and thus prevent infection or dysbiosis, as well as their translocation into sub-mucosal sites (135). Hence, increased amounts of accessible antigenic molecules in the lumen will add to the enhanced intestinal macromolecular transfer, boosting the exposure of the immune system to these macromolecules during the perinatal period.

Forms and Routes of Antigen Transfer

The antigen format, free vs. immune-complex bound, is a factor of importance for the immunological outcome. Thus, transepithelial passage of antigens, bound in complex to maternal IgG and transported via FcRn, has been observed in both rodents and humans, and the subsequent interaction of these immune-complexes with lamina propria antigen presenting cells might be facilitated by their binding to Fc-receptors on these cells (11, 44, 77, 136–138). In fact, microbial antigens, of maternal intestinal origin, in complex with maternal antibodies (antigen-IgG complexes) are transferred via the placenta in primates or via colostrum/milk and intestinal transfer in other species, and hence induce immune activation in the offspring (139–141). Thus, the FcRn receptor appears to be important for the protection of antigens in complex with IgG from degradation and for guiding the antigen through the epithelial cells during transport and sub-epithelial exposure.

Free dietary antigens may also pass materno-fetal barriers, since proteins experimentally fed to pregnant rats have been detected in antigenic form in both amniotic fluid and fetal blood (142). This may affect the immune response in neonates and shift it causing immune activation and inflammation as usually seen in the adult (143, 144) instead of induction of tolerance.

Experiments in neonatal rats have shown that anti-nutritional factors, such as lectins, block intestinal absorption (145), and oral provocation with the lectin PHA severely decreases endocytosis immediately after exposure (146, 147), due to the binding to the epithelial surface (146, 148, 149). Hence, PHA is thought to have blocked epithelial "receptors" needed for endocytosis. In contrast, provocation feeding with a protease caused an instant decrease in receptor-mediated endocytosis, a gradual decrease in the non-specific endocytic pathway and a temporary increase in paracellular leakiness (147).

Changes in paracellular permeability are caused by the disassembling of intestinal tight junctions, regulated by proteins such as claudins, zonulin, and occludin, causing a loosened pore diameter which in turn allows "larger" molecules to pass through (150–154). Tight junction proteins, specifically zonulin, have been associated with activation of the protease-activated receptors (PAR-2) in the intestinal epithelium, which has been linked to the development of cancer and autoimmune diseases (152, 155). Activation of the PAR-2 receptor in the small intestine has also been described as a trigger for pro-inflammatory responses such as immune cell recruitment, mucus secretion, and signaling to enterocytes, immune cells and the enteric nervous system (156–159).

In general, it would seem that the pathway of antigen transfer across the intestinal epithelial barrier could affect the immune system response. Transcellular passage of antigen complexes act as an educational pathway for the newborn's developing immune system, whereas paracellular passage would cause a primary immune response against those free antigens. Hence, during this critical period of early life, there is a continuous balance between tolerance induction and effector immune responses (13).

Effects of Antigen Transfer on the Immune System

The communication between the luminal content, including microorganisms and dietary macromolecules, and the immune system has been studied mostly with regards to their interaction via the intestinal epithelial cells and their receptors, while less emphasis has been placed on the direct interaction of antigenic molecules after passage across the intestinal epithelium. Moreover, the route for transepithelial passage of antigens, either by the transcellular endocytic pathway (160) or by paracellular "leakage" between the epithelial cells, might also be of importance for the resulting immune response (13). After epithelial passage of luminal antigens and interaction with the local immune system this might either result in tolerance induction or priming of a protective immune response, but could also result in immune activation and inflammation.

Early studies on tissue transplantation suggest that the fetal/neonatal immune system is immature and predisposed to induction of tolerance (161). Transfer of macromolecules or intact antigens across the intestinal epithelium induces differentiation of regulatory T-cells (Tregs) and tolerance, and further protection from allergic diseases. Recently, Ohsaki et al., showed that maternal cutaneous sensitization to an antigen could prevent against antigen-specific IgE production, intestinal mast cell expansion and food allergy in the offspring (162). The observed effects were mediated by neonatal FcRn–mediated transfer of maternal IgG or antigen-IgG immune complexes via breast milk. FcRn-dependent antigen presentation to CD11c+ dendritic cells was also required to induce oral tolerance in the offspring (163).

Dietary macromolecules that induce Treg cells at weaning appear to be required to suppress the immune response to dietary antigens that are important in controlling inflammatory or allergic responses (144). Moreover, maternal IgG against maternal gut microbiota, that are transferred after birth in mice and possible via the placenta in humans, limits the activation of both mucosal T-cells and B-cells against the gut microbiota in her young offspring (164).

Natural weaning has been classified as "physiological inflammation," with the recruitment of immune cells to the gut, mediated by chemokines and cytokines released by the enterocytes (165). T-cell recruitment to the neonatal mucosa has proven crucial for gut maturation and immune system activation, as well as for the establishment of oral tolerance in early life (80, 166–171). The prominent changes in microbiota induced by weaning seem to be required for immune maturation and the induction of Treg cells, while disturbances in the weaning reaction lead to pathological conditions, with increased susceptibility to allergy and inflammation later in life (172).

As discussed above the route of transepithelial passage of antigens is important in determining the immune response/outcome, where transcellular passage with enterocyte processing and FcRn biding may be preferable compared to

paracellular passage (leakage), which instead might result in inflammation and/or sensitization. The high endocytic activity of fetal-type enterocytes and increased macromolecular intestinal permeability might contribute to the increased susceptibility of preterm and term neonates to enteric infection and allergies. The immaturity of the intestine, together with the high epithelial endocytic activity, is possibly involved in the high risk of developing necrotizing enterocolitis (NEC) in preterm infants (173, 174).

PERSPECTIVES AND CONCLUSIONS

Selecting an appropriate animal species to serve as an ideal model to study the gut and immune system of human infants is not an easy task. The neonatal suckling rat (28, 82) and the newborn pig (175, 176) have often been used for this purpose. The rat is an altricial species, born very immature and with a permeable intestine during the entire suckling period, which is quite different from human infants. The suckling rat should probably rather be used as a model for premature infants. The newborn piglet on the other hand, is born agammaglobulinemic with a highly permeable intestine during the first day of life, which is essential in the acquisition of passive immunity. However, this also differs from that which occurs in newborn human infants. Instead, newborn guinea pigs (21) or rabbit pups, which are precocious species, born with their mothers' immunity and a relative mature gut, exhibiting low intestinal permeability, might be more suitable models for newborn humans. However, the latter species are often considered as less favorable from an experimental, practical and economic perspective, since among other things, the rat and the pig are multiparous species that normally give birth to between 10 and 20 or more offspring. Nevertheless, it is of utmost importance to keep in mind the particularities of each species, and to adapt each model species to the human model, such as the relevance of using piglets before or after ingestion of colostrum, as well as the gestational time in the case of using premature animal models.

This review contributes to a better understanding of how macromolecules of dietary and microbial origin in the intestinal lumen are delivered to the underlying immune system and how this transfer changes during development in perinatal life. Any disturbances in the timing and/or balance of these parallel processes, i.e., intestinal maturation, gut immune maturation and luminal microbial colonization, e.g., due to preterm birth, perinatal infection, antibiotic use or nutrient changes during the neonatal period, might affect the establishment of the immune system in the infant. Understanding the development of intestinal macromolecular permeability, in different animal models, will increase our understanding of intestinal barrier function and provide strategies for the prevention of infection and inappropriate antigen transport affecting the immune response. This might also contribute to a better understanding of the etiology of inflammatory diseases of the gastrointestinal tract and in potential preventive and therapeutic strategies.

AUTHOR CONTRIBUTIONS

BW planned the manuscript. BW, EA, and F-JP-C researched and wrote the manuscript and made the figures and tables. BW, EA, KP, SP, and F-JP-C edited the manuscript.

ACKNOWLEDGMENTS

The authors thank Dr. Janine Donaldson for her constructive feedback and language editing of the manuscript.

REFERENCES

1. Brambell FWR. *The Transmission of Passive Immunity from Mother to Young*. Amsterdam: North-Holland Publishing Company (1970).
2. Clark SL Jr. The ingestion of proteins and colloidal materials by columnar absorptive cells of the small intestine in suckling rats and mice. *J Biophys Biochem Cytol*. (1959) 5:41–50. doi: 10.1083/jcb.5.1.41
3. Wilson JM, Casanova JE. Chapter 5: development of endocytosis in the intestinal epithelium. In: Sanderson IR, Walker WA, editors. *Development of the Gastrointestinal Tract*. Hamilton, ON: B.C. Decker Inc. (2000).
4. Baintner K. Chapter 2: vacuolation in the young. In: Zabielski R, Gregory PC, Weström B, editors. *Biology of the Intestine in Growing Animals*. Amsterdam: Elsevier Science B.V. (2002).
5. Israel EJ, Simister N, Freiberg E, Caplan A, Walker WA. Immunoglobulin G binding sites on the human foetal intestine: a possible mechanism for the passive transfer of immunity from mother to infant. *Immunology*. (1993) 79:77–81.
6. Story CM, Mikulska JE, Simister NE. A major histocompatibility complex class I-like Fc receptor cloned from human placenta: possible role in transfer of immunoglobulin G from mother to fetus. *J Exp Med*. (1994) 180:2377–81. doi: 10.1084/jem.180.6.2377
7. Israel EJ, Taylor S, Wu Z, Mizoguchi E, Blumberg RS, Bhan A, et al. Expression of the neonatal Fc receptor, FcRn, on human intestinal epithelial cells. *Immunology*. (1997) 92:69–74. doi: 10.1046/j.1365-2567.1997.00326.x
8. Shah U, Dickinson BL, Blumberg RS, Simister NE, Lencer WI, Walker WA. Distribution of the IgG Fc receptor, FcRn, in the human fetal intestine. *Pediatr Res*. (2003) 53:295–301. doi: 10.1203/00006450-200302000-00015
9. Simister NE. Placental transport of immunoglobulin G. *Vaccine*. (2003) 21:3365–9. doi: 10.1016/S0264-410X(03)00334-7
10. Latvala S, Jacobsen B, Otteneder MB, Herrmann A, Kronenberg S. Distribution of FcRn across species and tissues. *J Histochem Cytochem*. (2017) 65:321–33. doi: 10.1369/00221554177 05095
11. Pyzik M, Sand KMK, Hubbard JJ, Andersen JT, Sandlie I, Blumberg RS. The neonatal Fc receptor. (FcRn): a misnomer? *Front Immunol*. (2019) 10:1540. doi: 10.3389/fimmu.2019.01540
12. Neutra MR, Mantis NJ, Kraehenbuhl JP. Collaboration of epithelial cells with organized mucosal lymphoid tissues. *Nat Immunol*. (2001) 2:1004–9. doi: 10.1038/ni1101-1004
13. Kulkarni DH, Gustafsson JK, Knoop KA, Mcdonald KG, Bidani SS, Davis JE, et al. Goblet cell associated antigen passages support the induction and maintenance of oral tolerance. *Mucosal Immunol*. (2020) 13:271–82. doi: 10.1038/s41385-019-0240-7
14. Edelblum KL, Turner JR. The tight junction in inflammatory disease: communication breakdown. *Curr Opin Pharmacol*. (2009) 9:715–20. doi: 10.1016/j.coph.2009.06.022
15. Baintner K. *Intestinal Absorption of Macromolecules and Immune Transmission from Mother to Young*. Boca Raton, FL: CRC Press (1986).
16. Ulmer-Franco AM. Transfer of Chicken immunoglobulin Y (IgY) from the hen to the chick. *Avian Biol Res*. (2019) 5:81–7. doi: 10.3184/175815512X13350053184471
17. Carter AM, Enders AC. The evolution of epitheliochorial placentation. *Annu Rev Anim Biosci*. (2013) 1:443–67. doi: 10.1146/annurev-animal-031412-103653

18. Meads TJ, Wild AE. Evidence that Fc gamma receptors in rabbit yolk sac endoderm do not depend upon an acid pH to effect IgG binding and transcytosis *in vitro*. *Placenta*. (1994) 15:525–39. doi: 10.1016/S0143-4004(05)80421-7
19. Szikora B, Hiripi L, Bender B, Kacskovics I, Ilias A. Characterization of the interactions of rabbit neonatal Fc receptor (FcRn) with rabbit and human IgG isotypes. *PLoS ONE*. (2017) 12:e0185662. doi: 10.1371/journal.pone.0185662
20. Williams RM, Beck F. A histochemical study of gut maturation. *J Anat*. (1969) 105:487–501.
21. Mage RG, Sehgal D, Schiaffella E, Anderson AO. Gene-conversion in rabbit B-cell ontogeny and during immune responses in splenic germinal centers. *Vet Immunol Immunopathol*. (1999) 72:7–15. doi: 10.1016/S0165-2427(99)00110-5
22. Halliday R. Prenatal and postnatal transmission of passive immunity to young rats. *Proc R Soc Lond B Biol Sci*. (1955) 144:427–30. doi: 10.1098/rspb.1955.0068
23. Kristoffersen EK. Placental Fc receptors and the transfer of maternal IgG. *Transfus Med Rev*. (2000) 14:234–43. doi: 10.1053/tm.2000.7393
24. Jones EA, Waldmann TA. The mechanism of intestinal uptake and transcellular transport of IgG in the neonatal rat. *J Clin Invest*. (1972) 51:2916–27. doi: 10.1172/JCI107116
25. Rodewald R, Kraehenbuhl JP. Receptor-mediated transport of IgG. *J Cell Biol*. (1984) 99:159s–64s. doi: 10.1083/jcb.99.1.159s
26. Baba R, Fujita M, Tein CE, Miyoshi M. Endocytosis by absorptive cells in the middle segment of the suckling rat small intestine. *Anat Sci Int*. (2002) 77:117–23. doi: 10.1046/j.0022-7722.2002.00017.x
27. Walthall K, Cappon GD, Hurtt ME, and Zoetis T. (2005). Postnatal development of the gastrointestinal system: a species comparison. *Birth Defects Res B Dev Reprod Toxicol*. 74:132–56. doi: 10.1002/bdrb.20040
28. Perez-Cano FJ, Franch A, Castellote C, Castell M. The suckling rat as a model for immunonutrition studies in early life. *Clin Dev Immunol*. (2012) 2012:537310. doi: 10.1155/2012/537310
29. King BF. An electron microscopic study of absorption of peroxidase-conjugated immunoglobulin G by guinea pig visceral yolk sac *in vitro*. *Am J Anat*. (1977) 148:447–55. doi: 10.1002/aja.1001480403
30. Rehling A, Trillmich. Weaning in the guinea pig (*Cavia aperea* f. porcellus): who decides and by what measure? *Behav Ecol Sociobiol*. (2007) 62:149–57. doi: 10.1007/s00265-007-0449-4
31. Molski M. Theoretical modeling of pre and postnatal growth. *J Theor Biol*. (2018) 458:58–67. doi: 10.1016/j.jtbi.2018.09.002
32. Sangild PT, Trahair JF, Loftager MK, Fowden AL. Intestinal macromolecule absorption in the fetal pig after infusion of colostrum in utero. *Pediatr Res*. (1999) 45:595–602. doi: 10.1203/00006450-199904010-00021
33. Ekstrom GM, Westrom BR, Telemo E, Karlsson BW. The uptake of fluorescein-conjugated dextran 70,000 by the small intestinal epithelium of the young rat and pig in relation to macromolecular transmission into the blood. *J Dev Physiol*. (1988) 10:227–33.
34. Stirling CM, Charleston B, Takamatsu H, Claypool S, Lencer W, Blumberg RS, et al. Characterization of the porcine neonatal Fc receptor–potential use for trans-epithelial protein delivery. *Immunology*. (2005) 114:542–53. doi: 10.1111/j.1365-2567.2004.02121.x
35. Westrom BR, Ohlsson BG, Svendsen J, Tagesson C, Karlsson BW. Intestinal transmission of macromolecules (BSA and FITC-dextran) in the neonatal pig: enhancing effect of colostrum, proteins and proteinase inhibitors. *Biol Neonate*. (1985) 47:359–66. doi: 10.1159/000242140
36. Sinkora M, Butler JE. The ontogeny of the porcine immune system. *Dev Comp Immunol*. (2009) 33:273–83. doi: 10.1016/j.dci.2008.07.011
37. Claus MA, Levy JK, Macdonald K, Tucker SJ, Crawford PC. Immunoglobulin concentrations in feline colostrum and milk, and the requirement of colostrum for passive transfer of immunity to neonatal kittens. *J Feline Med Surg*. (2006) 8:184–91. doi: 10.1016/j.jfms.2006.01.001
38. Chastant-Maillard S, Freyburger L, Marcheteau E, Thoumire S, Ravier JF, Reynaud K. Timing of the intestinal barrier closure in puppies. *Reprod Domest Anim*. (2012) 47 (Suppl. 6):190–3. doi: 10.1111/rda.12008
39. Pereira M, Valério-Bolas A, Saraiva-Marques C, Alexandre-Pires G, Pereira da Fonseca I, Santos-Gomes G. Development of dog immune system: from in uterus to elderly. *Vet Sci*. (2019) 6:83. doi: 10.3390/vetsci6040083
40. Trier JS, Colony Moxey P. Morphogenesis of the small intestine during fetal development. In: *Ciba Foundation Symposium 70 - Development of Mammalian Absorptive Processes*, Amsterdam. (2008) p. 3–29.
41. Wagner CL, Taylor SN, Johnson D. Host factors in amniotic fluid and breast milk that contribute to gut maturation. *Clin Rev Allergy Immunol*. (2008) 34:191–204. doi: 10.1007/s12016-007-8032-3
42. Axelsson I, Jakobsson I, Lindberg T, Polberger S, Benediktsson B, Raiha N. Macromolecular absorption in preterm and term infants. *Acta Paediatr Scand*. (1989) 78:532–7. doi: 10.1111/j.1651-2227.1989.tb17932.x
43. Catassi C, Bonucci A, Coppa GV, Carlucci A, Giorgi PL. Intestinal permeability changes during the first month: effect of natural versus artificial feeding. *J Pediatr Gastroenterol Nutr*. (1995) 21:383–6. doi: 10.1097/00005176-199511000-00003
44. Yoshida M, Claypool SM, Wagner JS, Mizoguchi E, Mizoguchi A, Roopenian DC, et al. Human neonatal Fc receptor mediates transport of IgG into luminal secretions for delivery of antigens to mucosal dendritic cells. *Immunity*. (2004) 20:769–83. doi: 10.1016/j.immuni.2004.05.007
45. Martin R, Nauta A, Ben Amor K, Knippels L, Knol J, Garssen J. Early life: gut microbiota and immune development in infancy. *Benef Microbes*. (2010) 1:367–82. doi: 10.3920/BM2010.0027
46. Renz H, Brandtzaeg P, Hornef M. The impact of perinatal immune development on mucosal homeostasis and chronic inflammation. *Nat Rev Immunol*. (2012) 12:9–23. doi: 10.1038/nri3112
47. Abrahamson DR, Rodewald R. Evidence for the sorting of endocytic vesicle contents during the receptor-mediated transport of IgG across the newborn rat intestine. *J Cell Biol*. (1981) 91:270–80. doi: 10.1083/jcb.91.1.270
48. Jakoi ER, Cambier J, Saslow S. Transepithelial transport of maternal antibody: purification of IgG receptor from newborn rat intestine. *J Immunol*. (1985) 135:3360–4.
49. Martin MG, Wu SV, Walsh JH. Ontogenetic development and distribution of antibody transport and Fc receptor mRNA expression in rat intestine. *Dig Dis Sci*. (1997) 42:1062–9. doi: 10.1023/A:1018853506830
50. Azagra-Boronat I, Tres A, Massot-Cladera M, Franch A, Castell M, Guardiola F, et al. Associations of breast milk microbiota, immune factors, and fatty acids in the rat mother-offspring pair. *Nutrients*. (2020) 12:319. doi: 10.3390/nu12020319
51. Grases-Pinto B, Torres-Castro P, Marin-Morote L, Abril-Gil M, Castell M, Rodriguez-Lagunas MJ, et al. Leptin and EGF supplementation enhance the immune system maturation in preterm suckling rats. *Nutrients*. (2019) 11:2380. doi: 10.3390/nu11102380
52. Kumagai N, Baba R, Sakuma Y, Arita K, Shinohara M, Kourogi M, et al. Origin of the apical transcytic membrane system in jejunal absorptive cells of neonates. *Med Mol Morphol*. (2011) 44:71–8. doi: 10.1007/s00795-010-0506-3
53. Vazquez-Carretero MD, Palomo M, Garcia-Miranda P, Sanchez-Aguayo I, Peral MJ, Calonge ML, et al. Dab2, megalin, cubilin and amnionless receptor complex might mediate intestinal endocytosis in the suckling rat. *J Cell Biochem*. (2014) 115:510–22. doi: 10.1002/jcb.24685
54. Park J, Levic DS, Sumigray KD, Bagwell J, Eroglu O, Block CL, et al. Lysosome-rich enterocytes mediate protein absorption in the vertebrate gut. *Dev Cell*. (2019) 51:7–20.e26. doi: 10.1016/j.devcel.2019.08.001
55. Telemo E, Westrom BR, Ekstrom G, Karlsson BW. Intestinal macromolecular transmission in the young rat: influence of protease inhibitors during development. *Biol Neonate*. (1987) 52:141–8. doi: 10.1159/000242703
56. Skrzypek T, Valverde Piedra JL, Skrzypek H, Kazimierczak W, Biernat M, Zabielski R. Gradual disappearance of vacuolated enterocytes in the small intestine of neonatal piglets. *J Physiol Pharmacol*. (2007) 58 (Suppl. 3):87–95.
57. Parker GA, Picut CA, Swanson C, Toot JD. Histologic features of postnatal development of immune system organs in the sprague-dawley rat. *Toxicol Pathol*. (2015) 43:794–815. doi: 10.1177/0192623315578720
58. Arevalo Sureda E, Westrom B, Pierzynowski SG, Prykhodko O. Maturation of the intestinal epithelial barrier in neonatal rats coincides with decreased FcRn expression, replacement of vacuolated enterocytes and changed blimp-1 expression. *PLoS ONE*. (2016) 11:e0164775. doi: 10.1371/journal.pone.0164775
59. Koldovsky O. Search for role of milk-borne biologically active peptides for the suckling. *J Nutr*. (1989) 119:1543–51. doi: 10.1093/jn/119.11.1543
60. Linderoth A, Biernat M, Prykhodko O, Kornilovska I, Pusztai A, Pierzynowski SG, et al. Induced growth and maturation of the gastrointestinal tract after Phaseolus vulgaris lectin exposure in

suckling rats. *J Pediatr Gastroenterol Nutr*. (2005) 41:195–203. doi: 10.1097/01.mpg.0000172262.05297.98
61. Harada E, Hashimoto Y, Syuto B. Orally administered spermine induces precocious intestinal maturation of macromolecular transport and disaccharidase development in suckling rats. *Comp Biochem Physiol A Physiol*. (1994) 109:667–73. doi: 10.1016/0300-9629(94)90208-9
62. Peulen O, Pirlet C, Klimek M, Goffinet G, Dandrifosse G. Comparison between the natural postnatal maturation and the spermine-induced maturation of the rat intestine. *Arch Physiol Biochem*. (1998) 106:46–55. doi: 10.1076/apab.106.1.46.4392
63. Daniels VG, Hardy RN, Malinowska KW, Nathanielsz PW. The influence of exogenous steroids on macromolecule uptake by the small intestine of the new-born rat. *J Physiol*. (1973) 229:681–95. doi: 10.1113/jphysiol.1973.sp010160
64. Nanthakumar NN, Henning SJ. Distinguishing normal and glucocorticoid-induced maturation of intestine using bromodeoxyuridine. *Am J Physiol*. (1995) 268:G139–45. doi: 10.1152/ajpgi.1995.268.1.G139
65. Prykhodko O, Pierzynowski SG, Nikpey E, Arevalo Sureda E, Fedkiv O, Westrom BR. Pancreatic and pancreatic-like microbial proteases accelerate gut maturation in neonatal rats. *PLoS One*. (2015) 10:e0116947. doi: 10.1371/journal.pone.0116947
66. Mayer B, Zolnai A, Frenyo LV, Jancsik V, Szentirmay Z, Hammarstrom L, et al. Redistribution of the sheep neonatal Fc receptor in the mammary gland around the time of parturition in ewes and its localization in the small intestine of neonatal lambs. *Immunology*. (2002) 107:288–96. doi: 10.1046/j.1365-2567.2002.01514.x
67. Clarke RM, Hardy RN. Histological changes in the small intestine of the young pig and their relation to macromolecular uptake. *J Anat*. (1971) 108:63–77.
68. Westrom BR, Svendsen J, Ohlsson BG, Tagesson C, Karlsson BW. Intestinal transmission of macromolecules (BSA and FITC-labelled dextrans) in the neonatal pig. Influence of age of piglet and molecular weight of markers. *Biol Neonate*. (1984) 46:20–6. doi: 10.1159/000242028
69. Laskowski M, Kassell B, Hagerty G. A crystalline trypsine inhibitor from swine colostrum. *Biochim Biophys Acta*. (1957) 24:300–5. doi: 10.1016/0006-3002(57)90198-1
70. Carlsson LC, Westrom BR, Karlsson BW. Intestinal absorption of proteins by the neonatal piglet fed on sow's colostrum with either natural or experimentally eliminated trypsin-inhibiting activity. *Biol Neonate*. (1980) 38:309–20. doi: 10.1159/000241381
71. Chen K, Magri G, Grasset EK, Cerutti A. Rethinking mucosal antibody responses: IgM, IgG and IgD join IgA. *Nat Rev Immunol*. (2020). doi: 10.1038/s41577-019-0261-1
72. Grand RJ, Watkins JB, Torti FM. Development of the human gastrointestinal tract. A review. *Gastroenterology*. (1976) 70:790–810. doi: 10.1016/S0016-5085(76)80277-6
73. Van Elburg RM, Uil JJ, Kokke FTM, Mulder AM, Van De Broek WGM, Mulder CJJ, et al. Repeatability of the sugar-absorption test, using lactulose and mannitol, for measuring intestinal permeability for sugars. *J Pediatr Gastroenterol Nutr*. (1995) 20:184–8. doi: 10.1097/00005176-199502000-00008
74. Van Elburg RM, Fetter WP, Bunkers CM, Heymans HS. Intestinal permeability in relation to birth weight and gestational and postnatal age. *Arch Dis Child Fetal Neonatal Ed*. (2003) 88:F52–5. doi: 10.1136/fn.88.1.F52
75. Taylor SN, Basile LA, Ebeling M, Wagner CL. Intestinal permeability in preterm infants by feeding type: mother's milk versus formula. *Breastfeed Med*. (2009) 4:11–5. doi: 10.1089/bfm.2008.0114
76. Saleem B, Okogbule-Wonodi AC, Fasano A, Magder LS, Ravel J, Kapoor S, et al. Intestinal barrier maturation in very low birthweight infants: relationship to feeding and antibiotic exposure. *J Pediatr*. (2017) 183:31–6.e31. doi: 10.1016/j.jpeds.2017.01.013
77. Yoshida M, Kobayashi K, Kuo TT, Bry L, Glickman JN, Claypool SM, et al. Neonatal Fc receptor for IgG regulates mucosal immune responses to luminal bacteria. *J Clin Invest*. (2006) 116:2142–51. doi: 10.1172/JCI27821
78. Chirico G. Development of the immune system in neonates. *J Arab Neonatal Forum*. (2005) 2:5–11.
79. Hoorweg K, Cupedo T. Development of human lymph nodes and Peyer's patches. *Semin Immunol*. (2008) 20:164–70. doi: 10.1016/j.smim.2008.02.003
80. Perez-Cano FJ, Castellote C, Gonzalez-Castro AM, Pelegri C, Castell M, Franch A. Developmental changes in intraepithelial T lymphocytes and NK cells in the small intestine of neonatal rats. *Pediatr Res*. (2005) 58:885–91. doi: 10.1203/01.pdr.0000182187.88505.49
81. Perez-Cano FJ, Castellote C, Marin-Gallen S, Franch A, Castell M. Neonatal immunoglobulin secretion and lymphocyte phenotype in rat small intestine lamina propria. *Pediatr Res*. (2005) 58:164–9. doi: 10.1203/01.PDR.0000156367.60769.36
82. Grases-Pinto B, Torres-Castro P, Abril-Gil M, Castell M, Rodriguez-Lagunas MJ, Perez-Cano FJ, et al. A preterm rat model for immunonutritional studies. *Nutrients*. (2019) 11:999. doi: 10.3390/nu11050999
83. Dahan S, Rabinowitz KM, Martin AP, Berin MC, Unkeless JC, Mayer L. Notch-1 signaling regulates intestinal epithelial barrier function, through interaction with CD4+ T cells, in mice and humans. *Gastroenterology*. (2011) 140:550–9. doi: 10.1053/j.gastro.2010.10.057
84. Torow N, Yu K, Hassani K, Freitag J, Schulz O, Basic M, et al. Active suppression of intestinal CD4(+)TCRalphabeta(+) T-lymphocyte maturation during the postnatal period. *Nat Commun*. (2015) 6:7725. doi: 10.1038/ncomms8725
85. Eberl G, Marmon S, Sunshine MJ, Rennert PD, Choi Y, Littman DR. An essential function for the nuclear receptor RORgamma(t) in the generation of fetal lymphoid tissue inducer cells. *Nat Immunol*. (2004) 5:64–73. doi: 10.1038/ni1022
86. Ibiza S, Garcia-Cassani B, Ribeiro H, Carvalho T, Almeida L, Marques R, et al. Glial-cell-derived neuroregulators control type 3 innate lymphoid cells and gut defence. *Nature*. (2016) 535:440–3. doi: 10.1038/nature18644
87. Eberl G, Colonna M, Di Santo JP, Mckenzie AN. Innate lymphoid cells. Innate lymphoid cells: a new paradigm in immunology. *Science*. (2015) 348:aaa6566. doi: 10.1126/science.aaa6566
88. Hepworth MR, Monticelli LA, Fung TC, Ziegler CG, Grunberg S, Sinha R, et al. Innate lymphoid cells regulate CD4+ T-cell responses to intestinal commensal bacteria. *Nature*. (2013) 498:113–7. doi: 10.1038/nature12240
89. Spencer J, Macdonald TT, Finn T, Isaacson PG. The development of gut associated lymphoid tissue in the terminal ileum of fetal human intestine. *Clin Exp Immunol*. (1986) 64:536–43.
90. Stras SF, Werner L, Toothaker JM, Olaloye OO, Oldham AL, Mccourt CC, et al. Maturation of the human intestinal immune system occurs early in fetal development. *Dev Cell*. (2019) 51:357–73.e355. doi: 10.1016/j.devcel.2019.09.008
91. Gasparoni A, Ciardelli L, Avanzini A, Castellazzi AM, Carini R, Rondini G, et al. Age-related changes in intracellular TH1/TH2 cytokine production, immunoproliferative T lymphocyte response and natural killer cell activity in newborns, children and adults. *Biol Neonate*. (2003) 84:297–303. doi: 10.1159/000073638
92. Martin CR, Ling PR, Blackburn GL. Review of infant feeding: key features of breast milk and infant formula. *Nutrients*. (2016) 8:279. doi: 10.3390/nu8050279
93. Westrom BR, Ekman R, Svendsen L, Svendsen J, Karlsson BW. Levels of immunoreactive insulin, neurotensin, and bombesin in porcine colostrum and milk. *J Pediatr Gastroenterol Nutr*. (1987) 6:460–5. doi: 10.1097/00005176-198705000-00025
94. Donovan SM, Mcneil LK, Jimenez-Flores R, Odle J. Insulin-like growth factors and insulin-like growth factor binding proteins in porcine serum and milk throughout lactation. *Pediatr Res*. (1994) 36:159–68. doi: 10.1203/00006450-199408000-00005
95. Admyre C, Johansson SM, Qazi KR, Filen JJ, Lahesmaa R, Norman M, et al. Exosomes with immune modulatory features are present in human breast milk. *J Immunol*. (2007) 179:1969–78. doi: 10.4049/jimmunol.179.3.1969
96. Gila-Diaz A, Arribas SM, Algara A, Martin-Cabrejas MA, Lopez De Pablo AL, Saenz De Pipaon M, et al. A review of bioactive factors in human breastmilk: a focus on prematurity. *Nutrients*. (2019) 11:1307. doi: 10.3390/nu11061307
97. Hale ML, Hanna EE, Hansen CT. Nude mice from homozygous nude parents show smaller PFC responses to sheep erythrocytes than nude mice from heterozygous mothers. *Nature*. (1976) 260:44–5. doi: 10.1038/260044a0
98. Goldman AS, Garza C, Nichols BL, Goldblum RM. Immunologic factors in human milk during the first year of lactation. *J Pediatr*. (1982) 100:563–7. doi: 10.1016/S0022-3476(82)80753-1
99. Sheldrake RF, Husband AJ. Intestinal uptake of intact maternal lymphocytes by neonatal rats and lambs. *Res Vet Sci*. (1985) 39:10–5. doi: 10.1016/S0034-5288(18)31762-4

100. Tuboly S, Bernath S, Glavits R, Medveczky I. Intestinal absorption of colostral lymphoid cells in newborn piglets. *Vet Immunol Immunopathol*. (1988) 20:75–85. doi: 10.1016/0165-2427(88)90027-X
101. Cabinian A, Sinsimer D, Tang M, Zumba O, Mehta H, Toma A, et al. Transfer of maternal immune cells by breastfeeding: maternal cytotoxic T lymphocytes present in breast milk localize in the Peyer's Patches of the nursed infant. *PLoS ONE*. (2016) 11:e0156762. doi: 10.1371/journal.pone.0156762
102. Moles JP, Tuaillon E, Kankasa C, Bedin AS, Nagot N, Marchant A, et al. Breastmilk cell trafficking induces microchimerism-mediated immune system maturation in the infant. *Pediatr Allergy Immunol*. (2018) 29:133–43. doi: 10.1111/pai.12841
103. Laouar A. Maternal leukocytes and infant immune programming during breastfeeding. *Trends Immunol*. (2020) 41:225–39. doi: 10.1016/j.it.2020.01.005
104. Castellote C, Casillas R, Ramirez-Santana C, Perez-Cano FJ, Castell M, Moretones MG, et al. Premature delivery influences the immunological composition of colostrum and transitional and mature human milk. *J Nutr*. (2011) 141:1181–7. doi: 10.3945/jn.110.133652
105. Nolan LS, Parks OB, Good M. A review of the immunomodulating components of maternal breast milk and protection against necrotizing enterocolitis. *Nutrients*. (2019) 12:14. doi: 10.3390/nu12010014
106. Gomez-Gallego C, Garcia-Mantrana I, Salminen S, Collado MC. The human milk microbiome and factors influencing its composition and activity. *Semin Fetal Neonatal Med*. (2016) 21:400–5. doi: 10.1016/j.siny.2016.05.003
107. Chen W, Mi J, Lv N, Gao J, Cheng J, Wu R, et al. Lactation stage-dependency of the sow milk microbiota. *Front Microbiol*. (2018) 9:945. doi: 10.3389/fmicb.2018.00945
108. Fernandez L, Langa S, Martin V, Maldonado A, Jimenez E, Martin R, et al. The human milk microbiota: origin and potential roles in health and disease. *Pharmacol Res*. (2013) 69:1–10. doi: 10.1016/j.phrs.2012.09.001
109. Gensollen T, Iyer SS, Kasper DL, Blumberg RS. How colonization by microbiota in early life shapes the immune system. *Science*. (2016) 352:539–44. doi: 10.1126/science.aad9378
110. Tamburini S, Shen N, Wu HC, Clemente JC. The microbiome in early life: implications for health outcomes. *Nat Med*. (2016) 22:713–22. doi: 10.1038/nm.4142
111. Garcia-Mantrana I, Selma-Royo M, Gonzalez S, Parra-Llorca A, Martinez-Costa C, Collado MC. Distinct maternal microbiota clusters are associated with diet during pregnancy: impact on neonatal microbiota and infant growth during the first 18 months of life. *Gut Microbes*. (2020) 13:1–17. doi: 10.1080/19490976.2020.1730294
112. Olszak T, An D, Zeissig S, Vera MP, Richter J, Franke A, et al. Microbial exposure during early life has persistent effects on natural killer T cell function. *Science*. (2012) 336:489–93. doi: 10.1126/science.1219328
113. Marin-Gallen S, Perez-Cano FJ, Castell M, Castellote C, Franch A. Intestinal intraepithelial NK and NKT cell ontogeny in Lewis rats. *Dev Comp Immunol*. (2008) 32:1405–8. doi: 10.1016/j.dci.2008.06.011
114. Gensollen T, Blumberg RS. Correlation between early-life regulation of the immune system by microbiota and allergy development. *J Allergy Clin Immunol*. (2017) 139:1084–91. doi: 10.1016/j.jaci.2017.02.011
115. Fleer A, Krediet TG. Innate immunity: toll-like receptors and some more. A brief history, basic organization and relevance for the human newborn. *Neonatology*. (2007) 92:145–57. doi: 10.1159/000102054
116. Nyangahu DD, Jaspan HB. Influence of maternal microbiota during pregnancy on infant immunity. *Clin Exp Immunol*. (2019) 198:47–56. doi: 10.1111/cei.13331
117. Gibbons D, Fleming P, Virasami A, Michel ML, Sebire NJ, Costeloe K, et al. Interleukin-8 (CXCL8) production is a signatory T cell effector function of human newborn infants. *Nat Med*. (2014) 20:1206–10. doi: 10.1038/nm.3670
118. He YM, Li X, Perego M, Nefedova Y, Kossenkov AV, Jensen EA, et al. Transitory presence of myeloid-derived suppressor cells in neonates is critical for control of inflammation. *Nat Med*. (2018) 24:224–31. doi: 10.1038/nm.4467
119. Al Nabhani Z, Eberl G. Imprinting of the immune system by the microbiota early in life. *Mucosal Immunol*. (2020) 13:183–9. doi: 10.1038/s41385-020-0257-y
120. Ximenez C, Torres J. Development of microbiota in infants and its role in maturation of gut mucosa and immune system. *Arch Med Res*. (2017) 48:666–80. doi: 10.1016/j.arcmed.2017.11.007
121. Nogacka AM, Salazar N, Arboleya S, Suarez M, Fernandez N, Solis G, et al. Early microbiota, antibiotics and health. *Cell Mol Life Sci*. (2018) 75:83–91. doi: 10.1007/s00018-017-2670-2
122. Dzidic M, Boix-Amoros A, Selma-Royo M, Mira A, Collado MC. Gut microbiota and mucosal immunity in the neonate. *Med Sci*. (2018) 6:56. doi: 10.3390/medsci6030056
123. Hanson LA, Korotkova M, Lundin S, Haversen L, Silfverdal SA, Mattsby-Baltzer I, et al. The transfer of immunity from mother to child. *Ann N Y Acad Sci*. (2003) 987:199–206. doi: 10.1111/j.1749-6632.2003.tb06049.x
124. Hasselquist D, Nilsson JA. Maternal transfer of antibodies in vertebrates: trans-generational effects on offspring immunity. *Philos Trans R Soc Lond B Biol Sci*. (2009) 364:51–60. doi: 10.1098/rstb.2008.0137
125. Devillers N, Le Dividich J, Prunier A. Influence of colostrum intake on piglet survival and immunity. *Animal*. (2011) 5:1605–12. doi: 10.1017/S175173111100067X
126. Smith CIE, Berglof A. X-linked agammaglobulinemia. In: Adam MP, Ardinger HH, Pagon RA, Wallace SE, Bean LJH, Stephens K, et al., editors. *GeneReviews[(R)]*. Seattle, WA: GeneReviews, University of Washington, Seattle, USA (1993).
127. Harris NL, Spoerri I, Schopfer JF, Nembrini C, Merky P, Massacand J, et al. Mechanisms of neonatal mucosal antibody protection. *J Immunol*. (2006) 177:6256–62. doi: 10.4049/jimmunol.177.9.6256
128. Grindstaff JL. Maternal antibodies reduce costs of an immune response during development. *J Exp Biol*. (2008) 211:654–60. doi: 10.1242/jeb.012344
129. Niewiesk S. Maternal antibodies: clinical significance, mechanism of interference with immune responses, and possible vaccination strategies. *Front Immunol*. (2014) 5:446. doi: 10.3389/fimmu.2014.00446
130. Wolinski J, Slupecka M, Westrom B, Prykhodko O, Ochniewicz P, Arciszewski M, et al. Effect of feeding colostrum versus exogenous immunoglobulin G on gastrointestinal structure and enteric nervous system in newborn pigs. *J Anim Sci*. (2012) 90 (Suppl. 4):327–30. doi: 10.2527/jas.53926
131. Pierzynowski S, Ushakova G, Kovalenko T, Osadchenko I, Goncharova K, Gustavsson P, et al. Impact of colostrum and plasma immunoglobulin intake on hippocampus structure during early postnatal development in pigs. *Int J Dev Neurosci*. (2014) 35:64–71. doi: 10.1016/j.ijdevneu.2014.03.003
132. Goncharova K, Lozinska L, Arevalo Sureda E, Wolinski J, Westrom B, Pierzynowski S. Importance of neonatal immunoglobulin transfer for hippocampal development and behaviour in the newborn pig. *PLoS ONE*. (2017) 12:e0180002. doi: 10.1371/journal.pone.0180002
133. Henning SJ. Ontogeny of enzymes in the small intestine. *Annu Rev Physiol*. (1985) 47:231–45. doi: 10.1146/annurev.ph.47.030185.001311
134. Rakhimov KR, Karimov OR, Kurbanov AS, Kuchkarova LS. Rearrangement of spectrum of digestive proteases in postnatal ontogenesis of rats. *J Evol Biochem Physiol*. (2002) 38:184–8. doi: 10.1023/A:1016558421099
135. Azagra-Boronat I, Massot-Cladera M, Knipping K, Van't Land B, Stahl B, Garssen J, et al. Supplementation with 2'-FL and scGOS/lcFOS ameliorates rotavirus-induced diarrhea in suckling rats. *Front Cell Infect Microbiol*. (2018) 8:372. doi: 10.3389/fcimb.2018.00372
136. Roopenian DC, Christianson GJ, Sproule TJ, Brown AC, Akilesh S, Jung N, et al. The MHC class I-like IgG receptor controls perinatal IgG transport, IgG homeostasis, and fate of IgG-Fc-coupled drugs. *J Immunol*. (2003) 170:3528–33. doi: 10.4049/jimmunol.170.7.3528
137. Qiao SW, Kobayashi K, Johansen FE, Sollid LM, Andersen JT, Milford E, et al. Dependence of antibody-mediated presentation of antigen on FcRn. *Proc Natl Acad Sci USA*. (2008) 105:9337–42. doi: 10.1073/pnas.0801717105
138. Menard S, Cerf-Bensussan N, Heyman M. Multiple facets of intestinal permeability and epithelial handling of dietary antigens. *Mucosal Immunol*. (2010) 3:247–59. doi: 10.1038/mi.2010.5
139. Baker K, Qiao SW, Kuo TT, Aveson VG, Platzer B, Andersen JT, et al. Neonatal Fc receptor for IgG. (FcRn) regulates cross-presentation of IgG immune complexes by CD8-CD11b+ dendritic cells. *Proc Natl Acad Sci USA*. (2011) 108:9927–32. doi: 10.1073/pnas.1019037108
140. Ganal-Vonarburg SC, Fuhrer T, Gomez De Aguero M. Maternal microbiota and antibodies as advocates of neonatal health. *Gut Microbes*. (2017) 8:479–85. doi: 10.1080/19490976.2017.1299847
141. Blumberg LJ, Humphries JE, Jones SD, Pearce LB, Holgate R, Hearn A, et al. Blocking FcRn in humans reduces circulating IgG levels and inhibits IgG immune complex-mediated immune responses. *Sci Adv*. (2019) 5:eaax9586. doi: 10.1126/sciadv.aax9586

142. Dahl GM, Telemo E, Westrom BR, Jakobsson I, Lindberg T, Karlsson BW. The passage of orally fed proteins from mother to foetus in the rat. *Comp Biochem Physiol A Comp Physiol*. (1984) 77:199–201. doi: 10.1016/0300-9629(84)90046-X
143. Pasternak JA, Ng SH, Buchanan RM, Mertins S, Mutwiri GK, Gerdts V, et al. Oral antigen exposure in newborn piglets circumvents induction of oral tolerance in response to intraperitoneal vaccination in later life. *BMC Vet Res*. (2015) 11:50. doi: 10.1186/s12917-015-0350-8
144. Kim KS, Hong SW, Han D, Yi J, Jung J, Yang BG, et al. Dietary antigens limit mucosal immunity by inducing regulatory T cells in the small intestine. *Science*. (2016) 351:858–63. doi: 10.1126/science.aac5560
145. Vasconcelos IM, Oliveira JT. Antinutritional properties of plant lectins. *Toxicon*. (2004) 44:385–403. doi: 10.1016/j.toxicon.2004.05.005
146. Linderoth A, Prykhod'ko O, Ahren B, Fak F, Pierzynowski SG, Westrom BR. Binding and the effect of the red kidney bean lectin, phytohaemagglutinin, in the gastrointestinal tract of suckling rats. *Br J Nutr*. (2006) 95:105–15. doi: 10.1079/BJN20051612
147. Arevalo Sureda E, Prykhodko O, Westrom B. Early effects on the intestinal barrier and pancreatic function after enteral stimulation with protease or kidney bean lectin in neonatal rats. *Br J Nutr*. (2018) 119:992–1002. doi: 10.1017/S0007114518000168
148. Pusztai A, Ewen SW, Grant G, Peumans WJ, Van Damme EJ, Rubio L, et al. Relationship between survival and binding of plant lectins during small intestinal passage and their effectiveness as growth factors. *Digestion*. (1990) 46 (Suppl. 2):308–16. doi: 10.1159/000200402
149. Otte JM, Chen C, Brunke G, Kiehne K, Schmitz F, Folsch UR, et al. Mechanisms of lectin. (phytohemagglutinin)-induced growth in small intestinal epithelial cells. *Digestion*. (2001) 64:169–78. doi: 10.1159/000048858
150. Jacob C, Yang PC, Darmoul D, Amadesi S, Saito T, Cottrell GS, et al. Mast cell tryptase controls paracellular permeability of the intestine. Role of protease-activated receptor 2 and beta-arrestins. *J Biol Chem*. (2005) 280:31936–48. doi: 10.1074/jbc.M506338200
151. Groschwitz KR, Wu D, Osterfeld H, Ahrens R, Hogan SP. Chymase-mediated intestinal epithelial permeability is regulated by a protease-activating receptor/matrix metalloproteinase-2-dependent mechanism. *Am J Physiol Gastrointest Liver Physiol*. (2013) 304:G479–89. doi: 10.1152/ajpgi.00186.2012
152. Vanuytsel T, Vermeire S, Cleynen I. The role of Haptoglobin and its related protein, Zonulin, in inflammatory bowel disease. *Tissue Barriers*. (2013) 1:e27321. doi: 10.4161/tisb.27321
153. Bischoff SC, Barbara G, Buurman W, Ockhuizen T, Schulzke JD, Serino M, et al. Intestinal permeability–a new target for disease prevention and therapy. *BMC Gastroenterol*. (2014) 14:189. doi: 10.1186/s12876-014-0189-7
154. Ronaghan NJ, Shang J, Iablokov V, Zaheer R, Colarusso P, Dion S, et al. The serine protease-mediated increase in intestinal epithelial barrier function is dependent on occludin and requires an intact tight junction. *Am J Physiol Gastrointest Liver Physiol*. (2016) 311:G466–79. doi: 10.1152/ajpgi.00441.2015
155. Fasano A. Zonulin and its regulation of intestinal barrier function: the biological door to inflammation, autoimmunity, and cancer. *Physiol Rev*. (2011) 91:151–75. doi: 10.1152/physrev.00003.2008
156. Kong W, Mcconalogue K, Khitin LM, Hollenberg MD, Payan DG, Bohm SK, et al. Luminal trypsin may regulate enterocytes through proteinase-activated receptor 2. *Proc Natl Acad Sci USA*. (1997) 94:8884–9. doi: 10.1073/pnas.94.16.8884
157. Vergnolle N. Proteinase-activated receptor-2-activating peptides induce leukocyte rolling, adhesion, and extravasation *in vivo*. *J Immunol*. (1999) 163:5064–9.
158. Kawabata A, Kinoshita M, Nishikawa H, Kuroda R, Nishida M, Araki H, et al. The protease-activated receptor-2 agonist induces gastric mucus secretion and mucosal cytoprotection. *J Clin Invest*. (2001) 107:1443–50. doi: 10.1172/JCI10806
159. Vergnolle N. Protease inhibition as new therapeutic strategy for GI diseases. *Gut*. (2016) 65:1215–24. doi: 10.1136/gutjnl-2015-309147
160. Kliwinski C, Cooper PR, Perkinson R, Mabus JR, Tam SH, Wilkinson TM, et al. Contribution of FcRn binding to intestinal uptake of IgG in suckling rat pups and human FcRn-transgenic mice. *Am J Physiol Gastrointest Liver Physiol*. (2013) 304:G262–70. doi: 10.1152/ajpgi.00340.2012
161. Billingham RE, Brent L, Medawar PB. Actively acquired tolerance of foreign cells. *Nature*. (1953) 172:603–6. doi: 10.1038/172603a0
162. Ohsaki A, Venturelli N, Buccigrosso TM, Osganian SK, Lee J, Blumberg RS, et al. Maternal IgG immune complexes induce food allergen-specific tolerance in offspring. *J Exp Med*. (2018) 215:91–113. doi: 10.1084/jem.20171163
163. Mosconi E, Rekima A, Seitz-Polski B, Kanda A, Fleury S, Tissandie E, et al. Breast milk immune complexes are potent inducers of oral tolerance in neonates and prevent asthma development. *Mucosal Immunol*. (2010) 3:461–74. doi: 10.1038/mi.2010.23
164. Koch MA, Reiner GL, Lugo KA, Kreuk LS, Stanbery AG, Ansaldo E, et al. Maternal IgG and IgA antibodies dampen mucosal T helper cell responses in early life. *Cell*. (2016) 165:827–41. doi: 10.1016/j.cell.2016.04.055
165. Fiocchi C. What is "physiological" intestinal inflammation and how does it differ from "pathological" inflammation? *Inflamm Bowel Dis*. (2008) 14 (Suppl. 2):S77–78. doi: 10.1002/ibd.20618
166. Mengheri E, Ciapponi L, Vignolini F, Nobili F. Cytokine gene expression in intestine of rat during the postnatal developmental period: increased IL-1 expression at weaning. *Life Sci*. (1996) 59:1227–36. doi: 10.1016/0024-3205(96)00446-8
167. Thompson FM, Mayrhofer G, Cummins AG. Dependence of epithelial growth of the small intestine on T-cell activation during weaning in the rat. *Gastroenterology*. (1996) 111:37–44. doi: 10.1053/gast.1996.v111.pm8698223
168. Schaeffer C, Diab-Assef M, Plateroti M, Laurent-Huck F, Reimund JM, Kedinger M, et al. Cytokine gene expression during postnatal small intestinal development: regulation by glucocorticoids. *Gut*. (2000) 47:192–8. doi: 10.1136/gut.47.2.192
169. Pie S, Lalles JP, Blazy F, Laffitte J, Seve B, Oswald IP. Weaning is associated with an upregulation of expression of inflammatory cytokines in the intestine of piglets. *J Nutr*. (2004) 134:641–7. doi: 10.1093/jn/134.3.641
170. D'cruz LM, Klein L. Development and function of agonist-induced CD25+Foxp3+ regulatory T cells in the absence of interleukin 2 signaling. *Nat Immunol*. (2005) 6:1152–9. doi: 10.1038/ni1264
171. Fontenot JD, Rasmussen JP, Gavin MA, Rudensky AY. A function for interleukin 2 in Foxp3-expressing regulatory T cells. *Nat Immunol*. (2005) 6:1142–51. doi: 10.1038/ni1263
172. Al Nabhani Z, Dulauroy S, Marques R, Cousu C, Al Bounny S, Dejardin F, et al. A weaning reaction to microbiota is required for resistance to immunopathologies in the adult. *Immunity*. (2019) 50:1276–88.e1275. doi: 10.1016/j.immuni.2019.02.014
173. Schnabl KL, Van Aerde JE, Thomson AB, Clandinin MT. Necrotizing enterocolitis: a multifactorial disease with no cure. *World J Gastroenterol*. (2008) 14:2142–61. doi: 10.3748/wjg.14.2142
174. Halpern MD, Denning PW. The role of intestinal epithelial barrier function in the development of NEC. *Tissue Barriers*. (2015) 3:e1000707. doi: 10.1080/21688370.2014.1000707
175. Sangild PT, Thymann T, Schmidt M, Stoll B, Burrin DG, Buddington RK. Invited review: the preterm pig as a model in pediatric gastroenterology. *J Anim Sci*. (2013) 91:4713–29. doi: 10.2527/jas.2013-6359
176. Mudd AT, Dilger RN. Early-life nutrition and neurodevelopment: use of the piglet as a translational model. *Adv Nutr*. (2017) 8:92–104. doi: 10.3945/an.116.013243

Conflict of Interest: The authors declare that the research was conducted in the absence of any commercial or financial relationships that could be construed as a potential conflict of interest.

frontiers in Immunology

ORIGINAL RESEARCH
published: 10 June 2020
doi: 10.3389/fimmu.2020.00903

Effects of Low-Dose Antibiotics on Gut Immunity and Antibiotic Resistomes in Weaned Piglets

Qi Hu[1†], Cong Liu[1†], Du Zhang[1], Ru Wang[2], Linlin Qin[2], Qin Xu[2], Lianqiang Che[2] and Fei Gao[1,3*]*

[1] Lingnan Guangdong Laboratory of Modern Agriculture, Genome Analysis Laboratory of the Ministry of Agriculture, Agricultural Genomics Institute at Shenzhen, Chinese Academy of Agricultural Sciences, Shenzhen, China, [2] Animal Nutrition Institute, Sichuan Agricultural University, Ya'an, China, [3] Comparative Pediatrics and Nutrition, Department of Veterinary and Animal Sciences, Faculty of Health and Medical Sciences, University of Copenhagen, Frederiksberg, Denmark

Widespread antibiotic use increases the risk of livestock acting as potential reservoirs of antimicrobial resistance genes (ARGs) that may be transferred to human and animal pathogens. Particularly, maternal-infant transmission of antibiotics via breastmilk represents a great concern regarding infant health. In this study, we investigated the effects of 4-week low-dose antibiotic (LDA) treatment on the host immunity and antibiotic resistomes in weaned piglets. Transcriptomic analyses of ileum tissues revealed that the affected genes were largely enriched in innate immunity-related pathways. Significantly reduced protein expression of inflammatory factors, i.e., *IFN-γ, IL-6* were observed. In addition, analyses of antibiotic resistomes identified a total of 1,021 ARGs related to 39 classes of antibiotics. The samples exhibited highly individual-specific diversity and no significant difference in the structure and diversity of ARGs and mobile gene elements (MGE) after LDA exposure for both colon and ileum samples. Despite of that, there were significant changes in the abundance of two transferrable ARGs [Erm(T) and tcr3] related to the antibiotics administered, implying an increased risk of transferrable antibiotic resistance. There was a significant change in the abundance of one pathogenic species after LDA exposure in the colon samples and one in the ileum samples, but there were no significant differences in the matched ARGs. Collectively, our findings reveal considerable changes in intestinal immunity-related genes, but minimal effects on gut antibiotic resistomes (ARGs and MGEs) in weaned piglets after 4 weeks LDA exposure. Our study provides a foundation for evaluating the longer-term cumulative effects of LDA use, especially the effects of maternal–infant LDA transmission, on antibiotic resistance and risks to infant health.

Keywords: low-dose antibiotics, antimicrobial resistance genes, mobile genetic elements, immunity, intestine, weaned piglet

OPEN ACCESS

Edited by:
Andrew Currie, Murdoch University, Australia

Reviewed by:
Zhihong Sun, Inner Mongolia Agricultural University, China
Gislane Lelis Vilela de Oliveira, São Paulo State University, Brazil

***Correspondence:**
Lianqiang Che
clianqiang@hotmail.com
Fei Gao
flys828@gmail.com

[†]These authors have contributed equally to this work

Specialty section:
This article was submitted to Microbial Immunology, a section of the journal Frontiers in Immunology

Received: *15 January 2020*
Accepted: *20 April 2020*
Published: *10 June 2020*

Citation:
Hu Q, Liu C, Zhang D, Wang R, Qin L, Xu Q, Che L and Gao F (2020) Effects of Low-Dose Antibiotics on Gut Immunity and Antibiotic Resistomes in Weaned Piglets. Front. Immunol. 11:903. doi: 10.3389/fimmu.2020.00903

INTRODUCTION

In-feed antibiotics have been widely used in livestock production to prevent and treat infectious diseases and to control the gut microbiota (1, 2). Non-therapeutic low-dose antibiotics (LDA) are commonly used as feed additives for piglets during the difficult weaning transition period to increase growth, promote gut health, and improve feed efficiency (3). However, antimicrobial

resistance is a worldwide public health concern and multidrug antibiotic resistance is partly related to excessive use of antibiotics for livestock. Food-producing animals may act as potential reservoirs of antimicrobial resistance genes (ARGs) that are transferred to and survive in their gut microbiota and then are transferred to human or animal pathogens that enter the gut via the food chain or the environment (4). Previous studies reported antibiotic residue in dairy products (5) and breastmilk (6), regardless of whether the mothers received antibiotics during pregnancy or lactation. Transmission of LDA residue to infants' guts may represent a risk factor for poor infant health. It is important to understand the potential negative side effects of LDA, especially as this preventive antibiotic-related approach is currently being banned in many countries around the world.

The complex and dense microbial environment of the gut is an important natural reservoir of ARGs, and it is also important for the development of the host immune system, thereby influencing infection by intestinal pathogens and the development of allergic and inflammatory bowel diseases (7–11). Metagenomics analyses have indicated the presence of ARGs in the microbiota of human and animal fecal samples and the correlation between the fecal antibiotic resistome and the microbiome (12–14). Further, due to the interactions between microbiota and the host immune system, the antibiotic-mediated alterations to the microbiota composition can result in different immunological consequences. For example, with the antibiotics intake, antibiotics also reduced production of interferon (*IFN*)-γ and interleukin (*IL*)-*17* cytokines by CD4+ T lymphocytes in the small intestine by perturbing microbial communities, which would affect the development and differentiation of immune system (9, 15). However, there are few studies on the microbiome-immunity-resistome interactions based on samples from biologically important sites along the gastrointestinal tract, such as the small intestine and colon. The resistome-microbiome-immunity interactions may differ between different gastrointestinal sites due to their widely differing conditions (e.g., luminal pH, metabolites, endogenous antimicrobial peptides and other secretions, gut motility, and food passage).

In a previous study (16), we established a LDA-treated piglet model and demonstrated that 4 weeks of LDA exposure induced clear growth promotion and significantly reduced total bacterial load in the ileum content, but not the colon content. In the present study, we further performed serum immonological analyses and ileum transcriptome analyses to study whether the same LDA regimen influences the systemic or gut immunity. The expression levels of immune-related proteins of ileum tissues were also validated. In addition, we applied deep metagenomic sequencing on samples of ileum and colon contents to investigate the antibiotic resistomes, including ARGs and mobile gene elements (MGEs).

MATERIALS AND METHODS

Animal Treatments and Ileum and Colon Sample Collection

The study was approved by the Sichuan Agriculture University animal welfare committee and carried out in accordance with the National Research Council's Guide for the Care and Use of Laboratory Animals. Twenty-four 21-day-old female weaned piglets were supplied by Sichuan Agricultural University, with a mean body weight of 6.50 ± 0.20 kg. They were randomly divided into two groups, which were fed a basic diet ($n = 13$) or a diet supplemented with LDA ($n = 11$). The LDA regimen involved a premix of the chlortetracycline (10% purity) and the virginiamycin (50% purity) at 750 and 50 mg/kg of feed, respectively. The feed consumed by the piglets was recorded daily and the growth of each piglet was measured weekly. After 4 weeks of LDA exposure, the piglets were euthanized, ileum tissues, and contents of the ileum and colon of each piglet were obtained and flash frozen in liquid nitrogen.

Blood Sample Collection and Immunological Analysis

Eight milliliter of blood samples were placed in heparinized tubes, followed by centrifugation at 3,000 × g and 4°C for 15 min and then removal and immediate storage of the plasma at −80°C for later analysis. The parameters of routine blood test were analyzed using an automatic blood analyzer (Advia 120, Bayer HealthCare, Tarrytown, NY, USA). Moreover, plasma concentrations of complement 3 (C3), C-Reactive Protein (C-RP), immunoglobulin G (IgG), and immunoglobulin M (IgM) were measured by an automatic biochemical analyzer (Model 7020, Hitachi, Tokyo, Japan) through corresponding commercial kits (Sichuan Maker Biotechnology Inc., Chengdu, China). There was <5% variation between intra-assay and inter-assay coefficients for each assay. Each plasma sample was analyzed in duplicate.

Transcriptomics Analyses of Ileum Tissues

Total RNA was extracted from the frozen ileum tissue samples (∼100 mg each) using Trizol Reagent (Invitrogen, Carlsbad, CA, USA) according to the manufacturer's instructions. The integrity and quality of the RNA were determined by agarose gel electrophoresis (1%) and an assessment of the absorbance (A260/A280). RNA purity was checked using the NanoPhotometer® spectrophotometer (IMPLEN, CA, USA). RNA concentration was measured using Qubit® RNA Assay Kit in Qubit® 2.0 Flurometer (Life Technologies, CA, USA). RNA integrity was assessed using the RNA Nano 6000 Assay Kit of the Agilent Bioanalyzer 2100 system (Agilent Technologies, CA, USA). Sequencing libraries were generated using NEBNext® UltraTM Directional RNA Library Prep Kit for Illumina® (NEB, USA) following the manufacturer's recommendations. Briefly, mRNA was purified from total RNA using poly-T oligo-attached magnetic beads. Fragmentation was carried out using divalent cations under elevated temperature in NEBNext First Strand Synthesis Reaction Buffer (5X). First-strand cDNA was synthesized using random hexamer primer and M-MuLV Reverse Transcriptase (RNaseH-). Second strand cDNA synthesis was subsequently performed using DNA Polymerase I and RNase H. In the reaction buffer, dNTPs with dTTP were replaced by dUTP. Remaining overhangs were converted into blunt ends via exonuclease/polymerase activities. After the adenylation of 3′ ends of DNA fragments, NEBNext Adaptor with a hairpin loop structure was ligated to prepare for hybridization. In order to select cDNA fragments with the right length, the library

fragments were purified with AMPure XP system (Beckman Coulter, Beverly, USA). Then 3 μl USER Enzyme (NEB, USA) was used with size-selected, adaptor-ligated cDNA at 37°C for 15 min followed by 5 min at 95°C before PCR. Then PCR was performed with Phusion High-Fidelity DNA polymerase, Universal PCR primers and Index (X) Primer. At last, products were purified (AMPure XP system) and library quality was assessed on the Agilent Bioanalyzer 2100 system. From these libraries, 150-bp paired-end and strand-specific sequence reads were produced with Illumina HiSeq 4000. Hisat2 (v 2.1.0) was employed for performing read mapping to Sus scrofa genome reference (v11.1) (17). Gene expression profiling was based on the number of reads. FPKM (fragments per kb of exon model per million mapped reads) values were used to estimate the expressed values and transcript levels. DEGs were obtained with an *P*-value cutoff <= 0.05 and an absolute fold-change of >= 1.5. KEGG (Kyoto Encyclopedia of Genes and Genome) is the main public database related to the pathway, and it contained 20 pathways related to the immune system. The DEGs related to the immune pathways were identified. KEGG functional enrichment analysis was performed on the clusterProfile R package.

Enzyme-Linked Immunosorbent Assay (ELISA)

The concentrations of 10 cytokines, including Claudin (*CLDN*)*-1*, interferon (*IFN*)*-γ*, interleukin (*IL*)*-22*, *IL-6*, myeloid differentiation factor *(MYD)88*, nuclear factor (*NF*)*-κB*, transforming growth factor *(TGF)-β*, toll-like receptor (*TLR*)*4*, *TLR9*, and TNF receptor associated factor (*TRAF*)*6,* related to innate immune responses were quantified by ELISA (Jianglai Industrial Company, Shanghai, China) according to the manufacturer's instructions.

DNA Extraction and Shotgun Metagenomic Sequencing

DNA was extracted from the ileum and colon content using a cetyltrimethylammonium bromide (CTAB)/sodium dodecyl sulfate (SDS) method. DNA concentrations were measured using a Qubit® 3.0 Fluorometer (Life Technologies, ThermoFisher Scientific, USA) and DNA purity was assessed on 1% agarose gels. Extracted DNA was stored at −20°C for later use. Samples with a bright main band at 400–450 bp were chosen for further analysis. Next, the DNA was diluted to 1 ng/μl using sterile water. Thereafter, sequencing libraries were generated using a TruSeq® DNA PCR-Free Sample Preparation Kit (Illumina, Inc., San Diego, CA, USA) following the manufacturer's recommendations, and index codes were added. Briefly, 250 ng of DNA was end repaired, purified with AmpureXP beads (Agencourt; Beckman Coulter), adenylated, and adapters ligated. The libraries were cleaned up and size-selected to remove adapter monomers and dimers. The library quality was assessed using a Qubit® 2.0 Fluorometer (Life Technologies, ThermoFisher Scientific, USA) and a 2100 Bioanalyzer system (Agilent Technologies, Inc., Santa Clara, CA, USA). Lastly, the library was sequenced on a HiSeq X ten platform (Illumina), generating 150-bp paired-end reads.

Metagenome Assembly and Non-redundant Gene Set Prediction and Annotation

According to the unique barcode and primer sequences, paired-end reads were accurately assigned to the relevant samples. High-quality clean reads were generated by removing the adaptor sequences and low-quality sequences (default low quality threshold: 5, default low quality rate: 0.5, and default N rate threshold: 0.05), and PCR duplications were removed. Host DNA was removed according to the Human Sequence Removal protocol of the National Center for Biotechnology Information (NCBI) using a pig reference genome (Sscrofa11.1). The clean reads were assembled into contigs using megahit (v1.0.6) (18). Open reading frames (ORFs) were predicted by prodigal (v2.6.3) and the clean reads were aligned to ORFs to calculate the mapped read count. Thereafter, the ORFs were clustered to remove redundancy for building a set of representative genes through CD-HIT software (v4.7). To avoid bias related to variation in the ORF size, both ORF sequence length and sequencing depth were included in the data normalization process prior to statistical comparisons. The normalized abundance matrix (G) was calculated for all samples:

$$G = (g_{kh})_{m\times n} = \begin{bmatrix} g_{11} & \cdots & g_{1m} \\ \vdots & \ddots & \vdots \\ g_{n1} & \cdots & g_{nm} \end{bmatrix},\ g_{kh} = \frac{\sum_{i=1}^{p} \frac{D_{ki}}{L_{ki}}}{\sum_{h=1}^{n}\sum_{i=1}^{p} \frac{D_{ki}}{L_{ki}}}$$

where m is the number of samples, *n* is the number of representative genes, g_{kh} is the normalized abundance of representative gene h for sample k, p is the total number of ORFs clustered for representative gene h and sample k, D_{ki} is the mapped reads count of ORF i for sample k, and L_{ki} is the length of ORF i for sample k.

ORFs were annotated with taxonomic information using Diamond based on the NCBI-nr database (cutoff *E*-value $\leq 10^{-6}$). The annotated results were revised by MEGAN6 using the lowest common ancestor algorithm. Further, we specially identified the ORFs related to pathogenic bacteria based on the common pathogenic bacteria list of our laboratory (**Supplementary Table S1**) according to the above ORFs taxonomic information. Subsequent diversity analyses were all performed based on normalized taxonomy abundance. ORFs were annotated with functional information using the Kyoto Encyclopedia of Genes and Genomes (KEGG) Automatic Annotation Server (KAAS) (19) based on the KEGG database with default parameters.

ARG and MGE Analysis

ARGs were characterized by mapping ORFs to the Comprehensive Antibiotic Resistance Database (CARD) (V3.0.0) using the Resistance Gene Identifier (RGI) application. The CARD is a rigorously curated collection of characterized, peer-reviewed antibiotic resistance determinants (20). We identified the 16S rRNA genes in the ORF gene set by aligning the ORFs to the SILVA database (v132). The ARG count data were normalized based on the 16S rRNA gene copy number

in order to express the ARG abundance as "ARG copy per 16S rRNA gene copy", as suggested by Li et al. using the following formula:

$$A = (a_{uv})_{x\times y} = \begin{bmatrix} a_{11} & \cdots & a_{1x} \\ \vdots & \ddots & \vdots \\ a_{y1} & \cdots & a_{yx} \end{bmatrix},\ a_{uv} = \frac{\sum_{j=1}^{q} G_{uj}}{\sum G_{16S}}$$

where x is the number of samples, y is the number of ARGs, a_{uv} is the normalized abundance of ARG v for sample u, q is the total number of representative genes annotated to ARG v of sample u, G_{uj} is the normalized abundance of representative gene j for sample u, and $\sum_{j=1}^{q} G_{uj}$ means the abundance sum of all representative genes annotated to ARG v of sample u. $\sum G_{16s}$ is the total normalized abundance of the 16S rRNA gene for sample u.

Transferrable ARGs (T-ARGs) are typically of greater clinical concern than non-transferable ARGs. To specifically assess the T-ARGs, a separate ARG database, ResFinder (v3.2), which focuses on acquired ARGs, was used. Briefly, ORFs were submitted to the ResFinder webpage (https://cge.cbs.dtu.dk/services/ResFinder/) and the identity threshold was set to ≥90% with ≥60% minimum length match. T-ARG count data were normalized based on the 16S rRNA gene copy number (as for the ARG count data).

Diamond was used to map the ORFs to the MGE database. The MGE database contains genes with 278 different gene name annotations (annotated as IS*, ISCR*, intI1, int2, istA*, istB*, qacEdelta, tniA*, tniB*, tnpA*, and Tn916 transposon in the NCBI nucleotide database) and more than 2,000 unique sequences, excluding the sequences from the PlasmidFinder database (12). Subsets of ORFs that were mapped to MGEs were used to produce the MGE profiles. MGE count data were also normalized based on the 16S rRNA gene copy number (as for the ARG count data).

In order to identify the ARGs and MGEs in pathogenic bacteria, the ORFs related to pathogenic bacteria were chose and were calculated according to the above methods.

Statistical Analysis

Alpha diversity analysis, which indicates the complexity of species diversity for each sample, was conducted using R package VEGAN (V2.5-3). The alpha diversity of different groups was compared using Wilcoxon rank-sum tests. Beta diversity was calculated based on the Bray–Curtis distance and weighted UniFrac distance using the R package VEGAN (V2.5-3) (21). Differences in beta diversity were identified using analysis of similarity (ANOSIM), with the effect size being indicated by an *R*-value [between −1 and +1, with 0 indicating that the null hypothesis cannot be rejected (22)], and permutational multivariate analysis of variance (PERMANOVA) leveraged by stress, with the effect size being indicated by R^2 (between 0 and 1). Differences in community structure based on beta diversity were visualized using principal coordinate analysis (PCoA) with the R package ape and the non-metric multi-dimensional scaling (NMDS) method using the R package VEGAN. Significantly different phylum and genus were identified between LAD and CON groups for colon and ileum using STAMP (v2.1.3) (23), respectively. The correlation analysis between pathogeny microbes and cytokines was performed using R package corrplot. Statistical significance was defined as $P < 0.05$ for all analyses.

RESULTS

Effects of LDA on Systemic and Intestinal Immunity

To investigate the effects of LDA on immunity in weaned piglets, we first assessed the serum immunological parameters. No significant differences in the levels of IgG, IgM, complement C3, and C- Reactive Protein (C-RP) were observed in the serum samples between the LDA and CON groups (**Supplementary Figure S1**). Considering that LDA exposure induced significantly reduced total bacterial load in the ileum content, we then focused on the transcriptomics analyses of the ileum tissues by RNA-seq technology. A total of 22.98 ± 1.96 million clean reads for each sample were generated from ileum tissues of 19 piglets, of which 89.67 ± 1.72% could be aligned to the pig reference genome (**Supplementary Table S2**). Based on these data, pair-wise comparisons between the LDA group and CON groups revealed 52 immune-related differentially expressed genes (DEGs) out of totally 1,247 DEGs (FC > 1.5, $p < 0.05$) (**Supplementary Table S3**). KEGG enrichment analysis indicated that these immune-related DEGs were enriched in 17 pathways, majority of which were innate-immunity pathways (**Figure 1A**; **Supplementary Table S4**). Thereby, we further analyzed the protein expression of 10 innate immunity-related genes, including four cytokines, by ELISA in ileum tissues of piglets (**Figure 1B**; **Supplementary Figure S2**). The results showed that the LDA group had significantly decreased levels of *IFN-γ*, *IL-6*, and *TLR4* (all $P < 0.05$), suggesting that LDA exposure for 4 weeks may induce an early anti-inflammatory response. In addition, the *CLDN-1* protein expression was significantly elevated ($P < 0.05$), indicated that the intestinal barrier might be improved upon LDA exposure for 4 weeks.

Community Structure of ARG-Containing Bacteria

Deep metagenomic sequencing was then performed on 23 samples of ileum content (10 LDA samples and 13 CON samples) and 24 samples of colon content (11 LDA samples and 13 CON samples) of the weaned piglets (**Supplementary Table S5**). From these samples, 456 Gb of high-quality reads, with an average of 9.7 Gb per sample, were generated. The clean data from each sample allowed successful assembly, with a mean N50 (minimum contig length needed to cover 50% of the genome) of 2.09 kb. Thereafter, a total of 5,306,978 ORFs were obtained. We obtained a similar bacterial community structure as in our previous study (which was based on 16S rRNA sequencing), which indicated apparent differences (based on the Shannon index) between the colon and ileum samples, while no clear structural divergence was found between the LDA and CON groups (**Supplementary Figure S3**). A total of 939,519 core ORFs were obtained, comprising 48,668 in the colon subgroup of

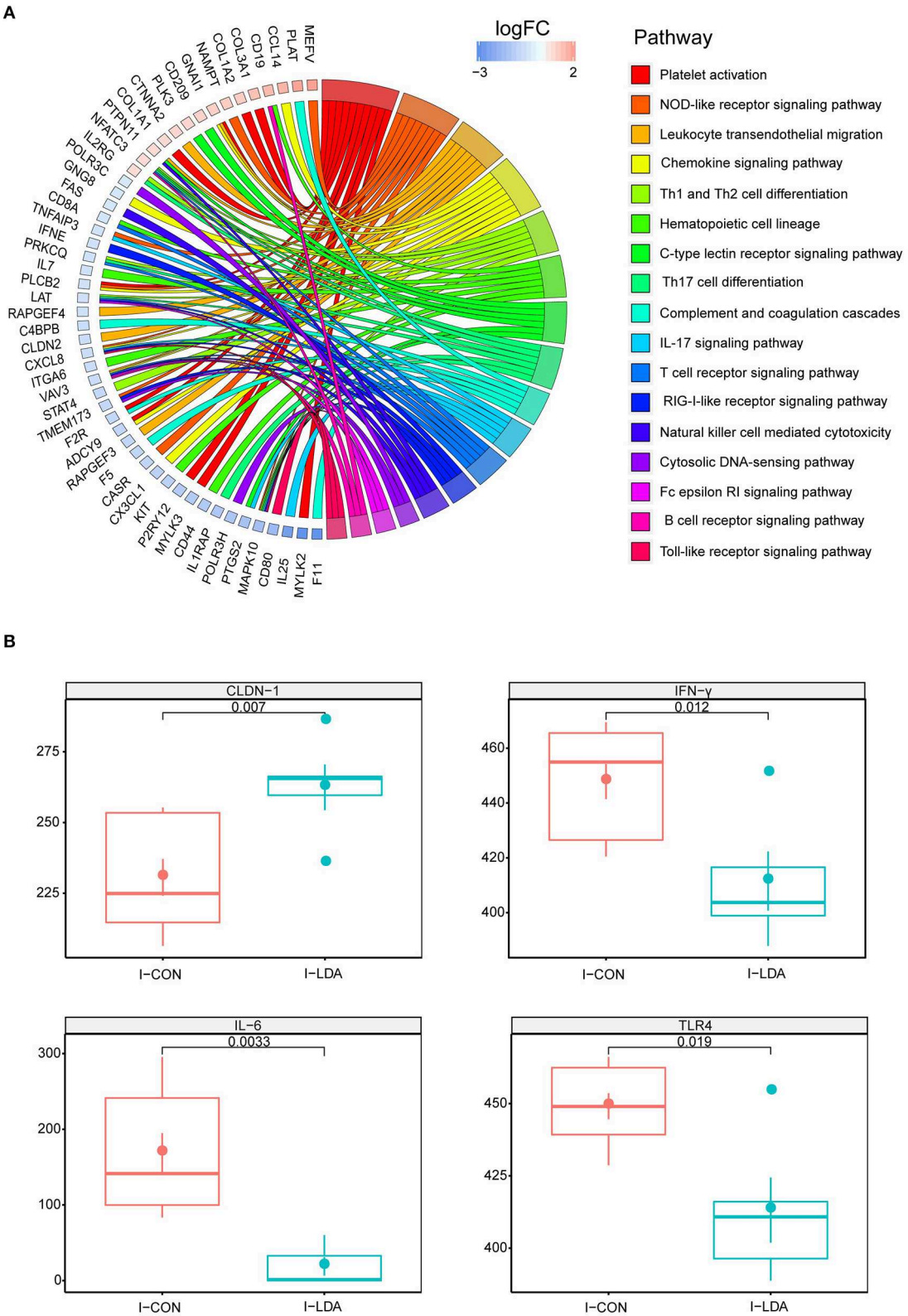

FIGURE 1 | Intestinal immunity analysis between I-LDA, and I-CON groups. **(A)** GOChord plot displays the relationship between a list of pathway and corresponding genes. The DEGs located in plot left were ordered according to their logFC. The GO terms located in plot right were cluster as server category. **(B)** Between-group comparisons of four immune-related proteins using two-sided independent Wilcoxon tests. I-CON, ileum subgroup of CON group; I-LDA, ileum subgroup of LDA group.

the LDA group (C-LDA), 63,749 in the colon subgroup of the CON group (C-CON), 1,707 in the ileum subgroup of the LDA group (I-LDA), and 10,569 in the ileum subgroup of the CON group (I-CON).

Based on this gene set, we further identified 4941 ORFs that comprised the gut resistomes, involving ARGs and MGEs. The bacteria that contained these ORFs were then identified. There were no clear differences in alpha diversity between the C-LDA and C-CON groups or the I-LDA and I-CON groups (**Figure 2A**). Beta diversity analysis indicated for clear divergence between colon and ileum samples (ANOSIM $R = 0.413$, $P = 0.001$), but not between the LDA and CON groups of colon or ileum.

Escherichia coli was the most abundant resistome-containing species in the ileum samples, while *Bacteroides fragilis* was the most abundant resistome-containing species in the colon samples. *Alistipes* sp. CAG_435 and *Ruminococcaceae bacterium* were significantly decreased and *Bacteroides fragilis* and *Prevotella* sp. P3-122 were significantly increased in the C-LDA group compared to the C-CON group (all $P < 0.05$). *Romboutsia timonensis* was significantly decreased ($P = 1.58e^{-3}$) in the I-LDA group compared to the I-CON group (**Figures 2B,C**). Furthermore, KEGG pathway annotations were assigned to the four groups (**Figures 2D,E**).

Changes in Antibiotic Resistance After LDA Exposure

In total, 1,021 ARGs were detected across all samples, which belonged to 182 gene families (**Supplementary Tables S6**, **S7**; **Supplementary Figures S4A,B**). Only 265 (26%) ARGs were common among the four groups. Between the I-CON and I-LDA groups, 393 ARGs were common and between the C-LDA and C-CON groups, 492 ARGs were common (**Figure 3A**). There were no significant differences in the total amount, structure, or diversity of ARGs between the I-LDA and I-CON groups or the C-LDA and C-CON groups. Furthermore, the highly individual-specific composition of ARGs was revealed by a rarefaction analysis of the pan and core resistome genes (**Figure 3B**).

Over 50.66% of the ARGs in the samples were predicted to confer multidrug resistance (involving up to six antibiotic resistance mechanisms). Overall, the ARGs were predicted to confer resistance to 39 classes of antibiotics, with a range of 0–0.14 ARG copies per 16S rRNA gene copy among the samples. The top five most abundant antibiotic resistance classes were tetracycline, macrolide, aminoglycoside, lincosamide, and streptogramin in the C-LDA and C-CON groups, and tetracycline, penam, fluoroquinolone, aminoglycoside, and cephalosporin in the I-LDA and I-CON groups (**Figure 4A**). NMDS analyses indicated that the antibiotic resistance classes were significantly different between the C-LDA and I-LDA groups and the C-CON and I-CON groups (ANOSIM $R = 0.354$, $P = 0.001$) (**Figure 4B**). The differences of ARG levels between colon and ileum samples (i.e., between the C-LDA and I-LDA groups and the C-CON and I-CON groups) were larger than between the LDA and CON groups (i.e., between the I-LDA and I-CON groups and the C-LDA and C-CON groups) (**Supplementary Figure S4C**).

Pair-wise comparisons revealed only one and two significantly different antibiotic classes (based on the abundance of ARGs) between the C-LDA and C-CON groups and the I-LDA and I-CON groups, respectively, and there were no significantly different antibiotic mechanisms. Rifamycin resistance was the only significantly different antibiotic resistance class ($P < 0.05$) between the C-LDA and C-CON groups; it involved 30 ARGs, which had non-significant differences between the C-LDA and C-CON groups. Oxazolidinone and sulfone resistance were the only significantly different antibiotic resistance classes (all $P < 0.05$) between the I-LDA and I-CON groups (**Supplementary Table S8**). Eight and three ARGs were predicted to confer the oxazolidinone and sulfone resistances, respectively, and three of the oxazolidinone resistance genes were significantly different (all $P < 0.05$) between the I-LDA and I-CON groups (**Supplementary Figure S5**). We also revealed a number of differential ARG gene families and ARGs (**Supplementary Tables S9**, **S10**).

Dissemination of Antibiotic Resistance After LDA Exposure

We examined two elements that greatly contribute to the dissemination of antibiotic resistance: T-ARGs and MGEs. The representative ORFs were aligned to a ResFinder database containing only acquired ARGs and a customized MGE database. As a result, 148 T-ARGs were detected, conferring resistance to 12 classes of antibiotics, mainly including aminoglycoside, beta-lactam, tetracycline, macrolide, and phenicol. Among them, there was one significantly different T-ARG between the C-LDA and C-CON groups and four significantly different T-ARGs between the I-LDA and I-CON groups. Erm(T) was significantly increased ($P < 0.05$) in the C-LDA group compared to the C-CON group, whereas, cfr(B), aac (3)-IId, cfxA6, and tcr3 had significant differences ($P < 0.05$) between the I-LDA and I-CON groups (**Figure 5A**). Notably, the T-ARGs Erm(T) and tcr3 confer macrolide and tetracycline resistance, respectively, which reflected the LDA drugs used in this study (i.e., the virginiamycin contains macrolide and the chlortetracycline belongs to tetracycline). This confirms that LDA use significantly enriches the T-ARGs related to the specific antibiotic classes administered.

MGEs can transfer ARGs between members of the gut microbial community (24). In total, 129 MGEs (level 2) were detected across all four groups, while 38 (29%) MGEs were common to the four groups. Between the I-LDA and I-CON groups, 83 MGEs were common, and between the C-LDA and C-CON groups, 47 MGEs were common (**Supplementary Figure S6**). Among these MGEs, tnpA was the most abundant MGE in all four groups, followed by IS91, tnpA-IS683, and ISCrsp1 in C-LDA and C-CON groups; IS91, tnpA-IS683, and tnpA10 in I-CON group; IS91, tnpA10, and rep18 in I-LDA group (**Figure 5B**). NMDS analyses indicated that the MGEs (level 2) were not significantly different between the C-LDA and C-CON groups (ANOSIM $R = 0.0592$,

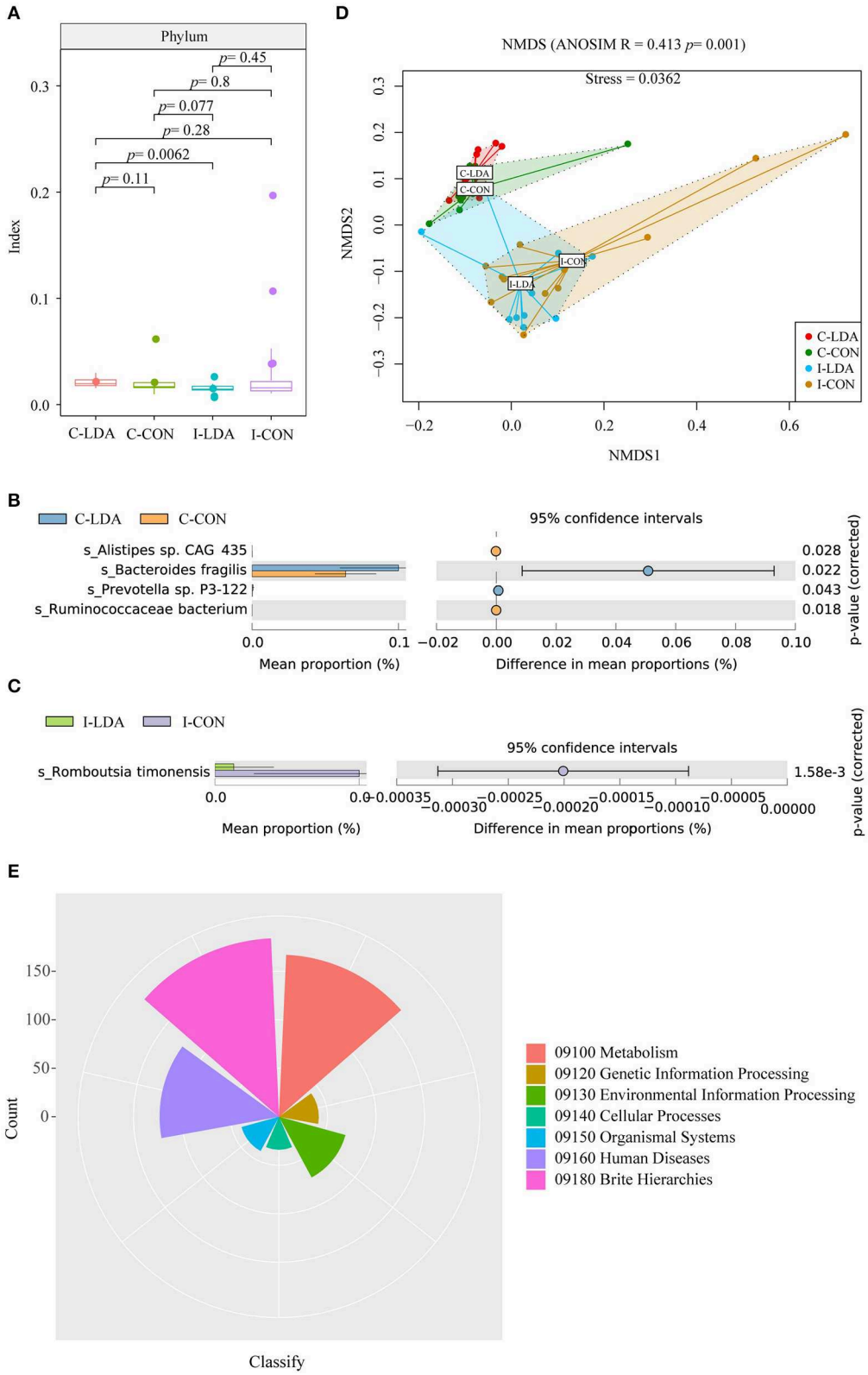

FIGURE 2 | Analysis of the community structure of the resistome-containing bacteria among the C-LDA, C-CON, I-LDA, and I-CON groups. **(A)** Alpha diversity analysis of the resistome-containing bacteria in all four groups using the Shannon index. Species with significantly different ($P < 0.05$) mean abundances (using

(Continued)

FIGURE 2 | two-sided Welch's *t*-tests) between the **(B)** C-LDA and C-CON groups and **(C)** I-LDA and I-CON groups, based on SILVA database annotation. **(D)** Beta diversity analysis of the functions of four groups using NMDS analysis based on Bray–Curtis distance among all samples. Analysis of similarity (ANOSIM) was conducted, with the effect size being indicated by an R-value (between −1 and +1, with 0 indicating that the null hypothesis cannot be rejected). **(E)** KEGG pathway annotation in all four groups. C-CON, colon subgroup of control (CON) group; C-LDA, colon subgroup of low-dose antibiotic (LDA) group; I-CON, ileum subgroup of CON group; I-LDA, ileum subgroup of LDA group.

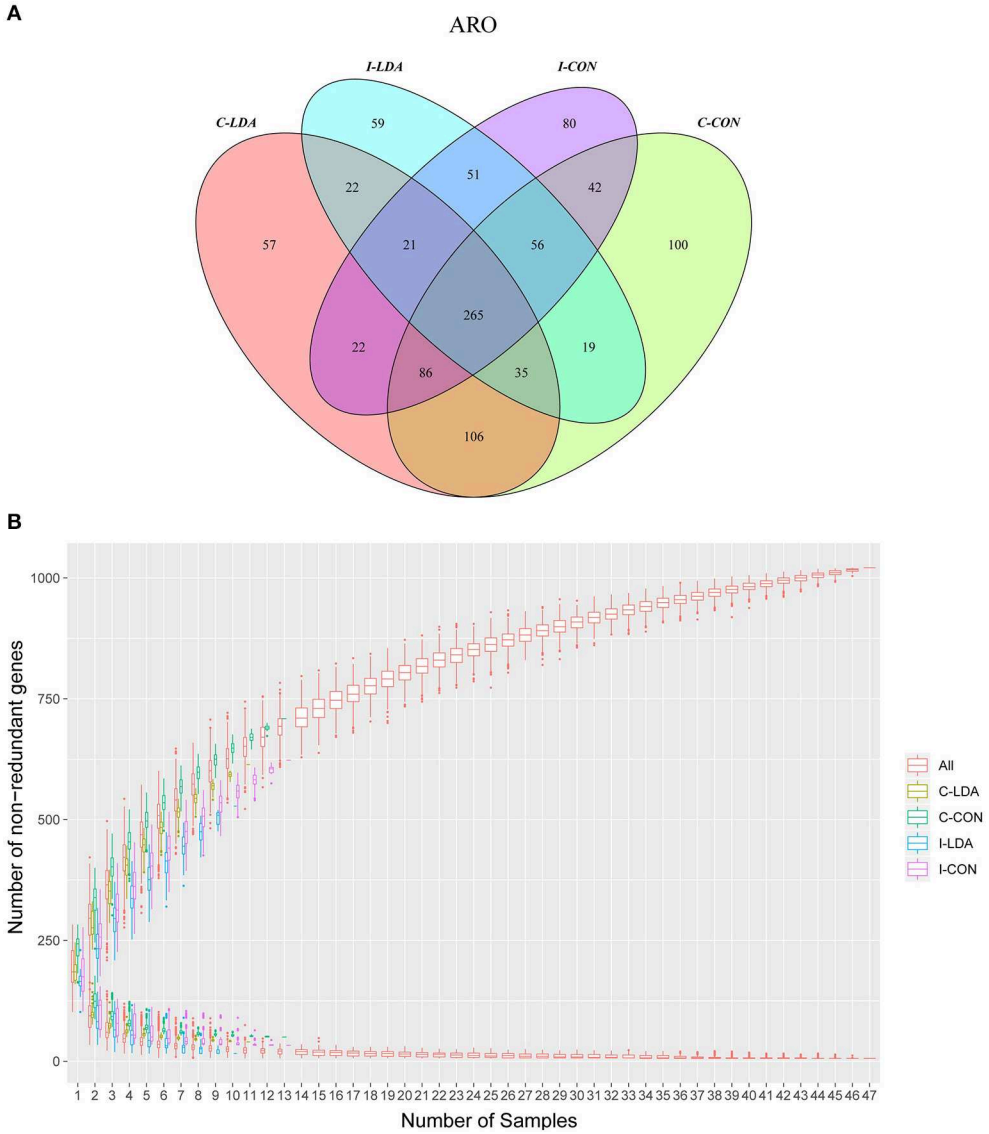

FIGURE 3 | Antimicrobial resistance gene (ARG) catalog analysis between the C-LDA, C-CON, I-LDA, and I-CON groups. **(A)** Venn diagram showing distribution of the ARGs in the four groups. **(B)** Rarefaction analysis of pan and core resistome genes including all samples in each group. C-CON, colon subgroup of control (CON) group; C-LDA, colon subgroup of low-dose antibiotic (LDA) group; I-CON, ileum subgroup of CON group; I-LDA, ileum subgroup of LDA group.

$P = 0.106$) or the I-LDA and I-CON groups (ANOSIM $R = -0.0214$, $P = 0.508$) (**Supplementary Figure S7**). In contrast, MGE differences between colon and ileum samples within group (i.e., between the C-LDA and I-LDA groups and the C-CON and I-CON groups) were larger than between the LDA and CON groups (i.e., between the I-LDA and I-CON groups and the C-LDA and C-CON groups) (**Figure 5C**). Pair-wise comparisons revealed that the abundance of nine MGEs (level 2) were significantly decreased (all $P < 0.05$) in the C-LDA group compared to the C-CON group, comprising int3, rep18, Tn*916–orf14*, Tn*916–orf15*, Tn*916–orf16*, Tn*916–orf17*, Tn*916–orf18*, Tn*916–orf20*, and Tn*916–orf7* (**Supplementary Table S11**). Additionally, five significantly different MGEs (level 2) were identified (all $P < 0.05$) in the

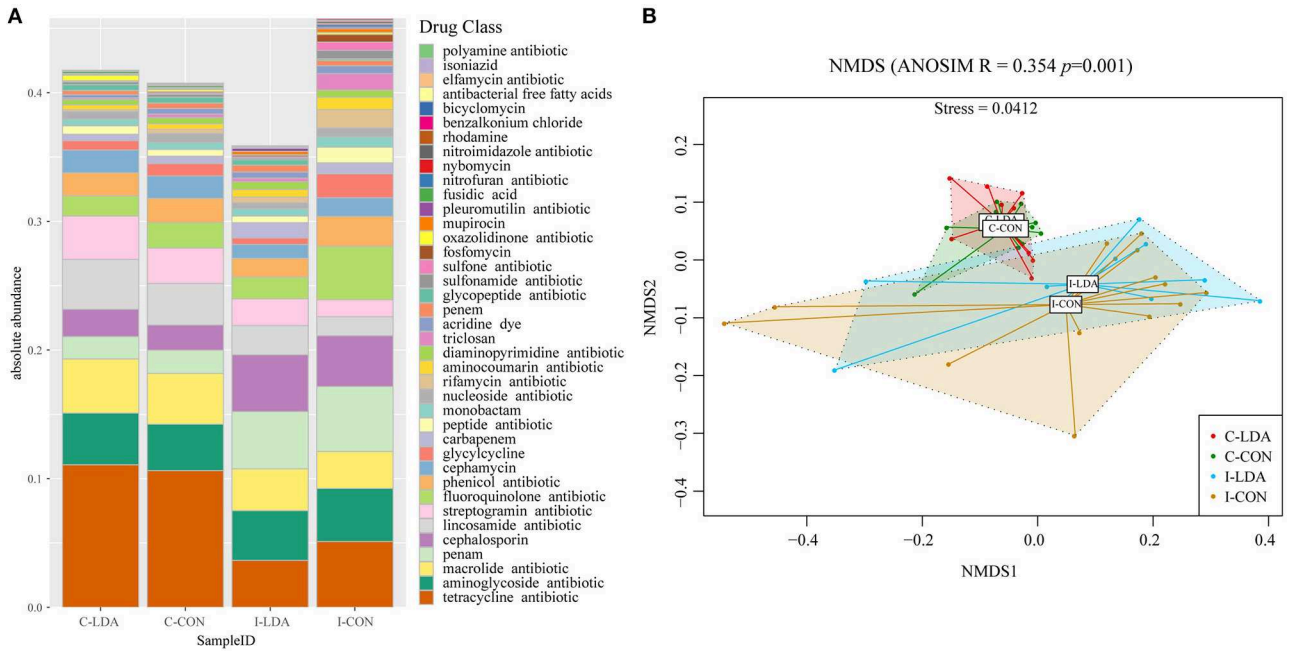

FIGURE 4 | Composition and structure of antimicrobial resistance genes (ARGs) between the C-LDA, C-CON, I-LDA, and I-CON groups. **(A)** Absolute abundance of antibiotic resistance classes in the four groups. **(B)** Beta diversity analysis of antibiotic resistance classes in the four groups using NMDS analysis based on Bray–Curtis distance. Analysis of similarity (ANOSIM) was conducted, with the effect size being indicated by an *R*-value (between −1 and +1, with 0 indicating that the null hypothesis cannot be rejected). C-CON, colon subgroup of control (CON) group; C-LDA, colon subgroup of low-dose antibiotic (LDA) group; I-CON, ileum subgroup of CON group; I-LDA, ileum subgroup of LDA group.

ileum analysis, comprising three MGEs that were significantly decreased (int3, Tn*916–orf7,* and rep14) and two MGEs that were significantly increased (tnpA1B1–IS1068, and tnpA3B3–ISLL6) in the I-LDA group compared to the I-CON group (**Supplementary Table S12**).

Antibiotic Resistomes–Pathogenic Bacteria–Innate Immunity Interactions

To examine the antibiotic resistance status of specific pathogenic bacteria, we matched the identified ARGs to common enteral pathogens and identified four pathogens in the samples (**Supplementary Figure S8**), comprising *Campylobacter coli, Streptococcus suis*, *Clostridium perfringens,* and *Klebsiella pneumoniae*. Thereafter, we found that *Campylobacter coli*, which is a commensal in the gastrointestinal tract but can sometimes cause enteritis in pigs and humans, was significantly increased in the I-LDA group ($P = 0.014$) compared to the I-CON group. Additionally, *Streptococcus suis*, which is a zoonotic pathogen that is an emerging threat to human health (25), was significantly decreased in the C-LDA group ($P = 0.0099$) compared to the C-CON group.

Campylobacter coli, which was the significantly different pathogenic bacterial species between the I-LDA and I-CON groups, was only matched to one ARG [APH(2")-If]. There were no significant differences in antibiotic resistance (based on the abundance of ARG) in *Campylobacter coli* between the I-LDA and I-CON groups. The ARG in *Campylobacter coli* was predicted to confer aminoglycoside resistance. There were no differences in MGEs in *Campylobacter coli* between the I-LDA and I-CON groups.

Streptococcus suis, which was the significantly different pathogenic bacterial species between the C-LDA and C-CON groups, was matched to two ARGs, comprising SAT-4, and Erm(T). There was no significant difference in these ARGs between the C-LDA and C-CON groups. The ARGs in *Streptococcus suis* were predicted to confer macrolide, lincosamide, nucleoside, and streptogramin resistance and one ARG [Erm(T)] had transfer potential. However, pairwise comparisons revealed no significant differences in antibiotic resistance (based on the abundance of ARGs) in *Streptococcus suis* between the C-LDA and C-CON groups. Five MGEs were detected in *Streptococcus suis*, comprising tnpA, repUS17, rep18, rep22, and Tn*916-orf7*. Among them, there was one significantly different MGE, Tn*916-orf7*, in *Streptococcus suis* between the C-LDA and C-CON groups.

We further performed the correlations between identified four pathogens in the samples and the 10 immune-related proteins (**Figure 6**). As a result, *Campylobacter coli* has strongly positive correlation with *IL-6*, *NF-κB*, *TGF-β* and *TLR9*, and negative correlation only with *IL-22*. Whereas, both *Clostridium perfringens* and *Klebsiella pneumoniae* were positively correlated with almost half of cytokines. In contrast, *Streptococcus suis* was only negatively correlated with *MyD88, IL-6,* and *TLR9*.

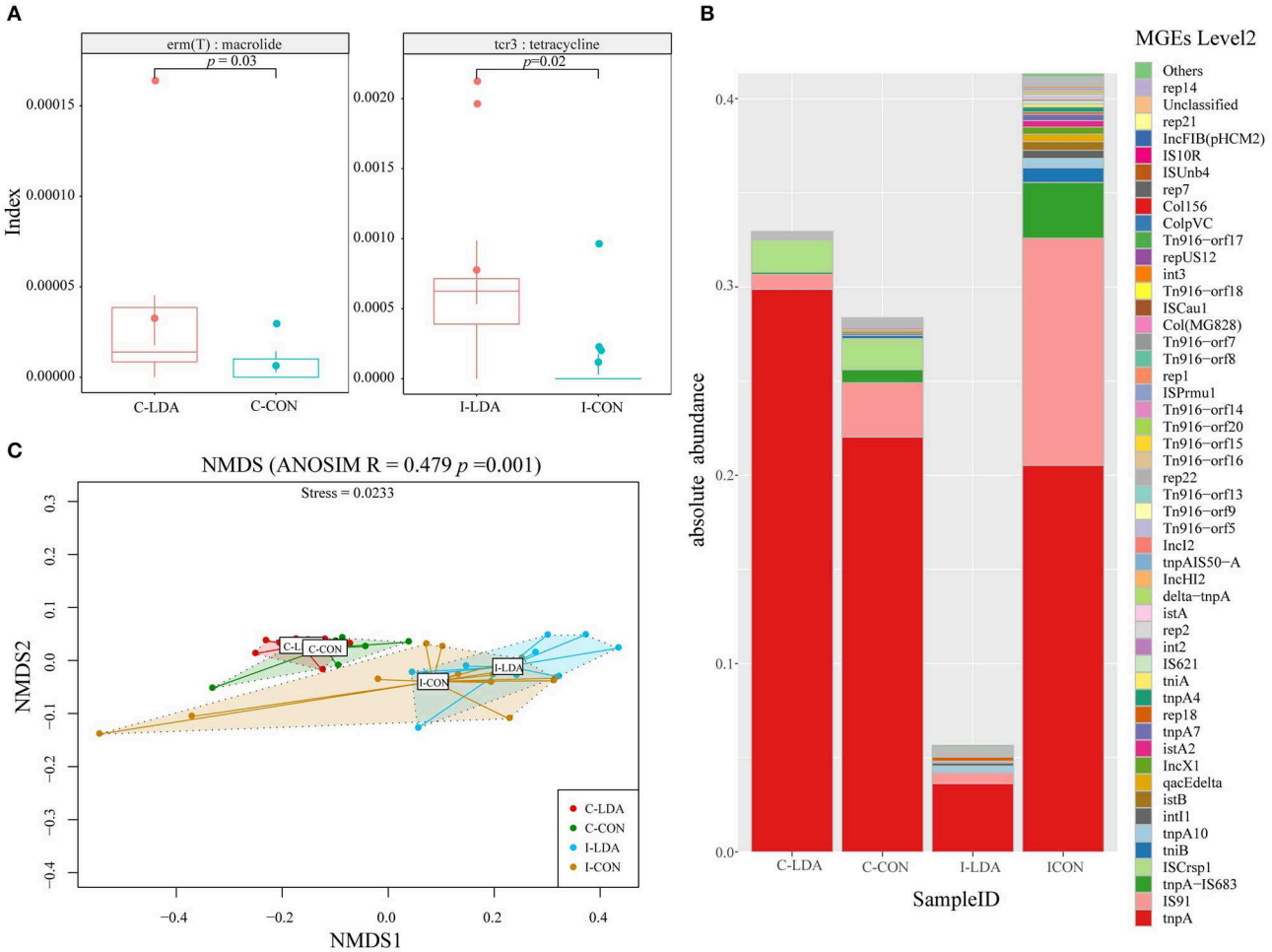

FIGURE 5 | Comparison of antibiotic resistance elements between the C-LDA, C-CON, I-LDA, and I-CON groups. **(A)** Between-group comparisons of two T-ARGs using two-sided independent Wilcoxon tests. **(B)** Absolute abundance of mobile gene elements (MGEs; level 2) in the four groups. **(C)** Beta diversity analysis of MGEs in the four groups using NMDS analysis based on Bray–Curtis distance. Analysis of similarity (ANOSIM) was conducted, with the effect size being indicated by an *R*-value (between −1 and +1, with 0 indicating that the null hypothesis cannot be rejected). C-CON, colon subgroup of control (CON) group; C-LDA, colon subgroup of low-dose antibiotic (LDA) group; I-CON, ileum subgroup of CON group; I-LDA, ileum subgroup of LDA group.

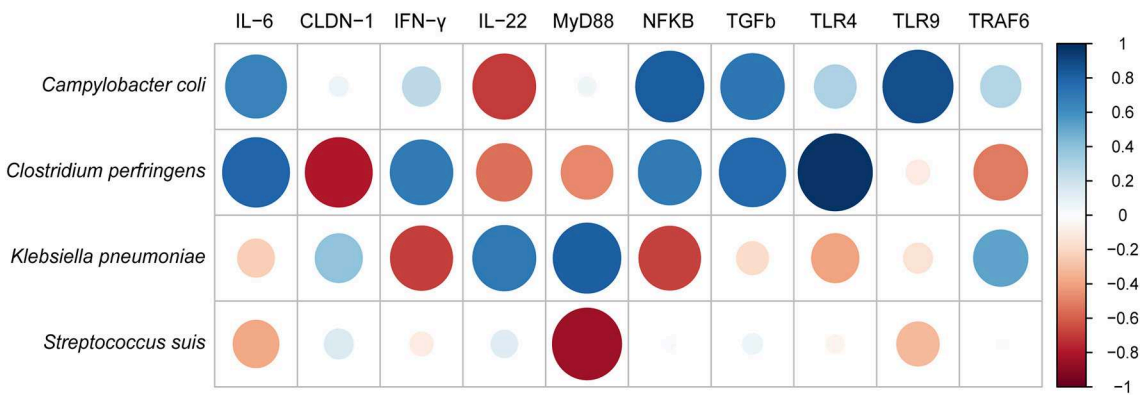

FIGURE 6 | The correlation analysis between pathogenic bacteria and innate immune cytokines measured by ELISA using corrplot package of R.

DISCUSSION

High-dose antibiotics are used for the clinical management of diseases in humans and animals, and LDAs are used as feed additives to promote the growth of livestock. The use of high-dose antibiotics enriches ARGs, which may lead to an uncoupling of the mutualistic relationships that have evolved over long periods between the gut microbiota and the host (26, 27). LDA accumulation is believed to disrupt the microbiota composition and consequently promote host growth (28–30). Furthermore, LDA residue in breastmilk can be transferred to the infant gut (6), and therefore LDA may also affect the gut microbiota of infants. Using a pig model of LDA exposure for 4 weeks, our study aimed to evaluate the effects of LDA on intestinal immunity and antibiotic resistance, including ARGs and MGEs, based on colon and ileum samples, over a relatively short period. In general, we revealed the intestinal innate immunity was considerably affected upon LDA exposure, as well as the highly individual-specific diversity regarding the resistomes and, probably because of this, the structure and diversity of the resistomes were not significantly different between the I-LDA and I-CON groups or C-LDA and C-CON groups.

Despite the highly individual-specific diversity, we identified significantly different antibiotic classes (based on the abundance of ARGs and MGEs) between the LDA and CON groups. Notably, although the ARG divergence was large, the classes and mechanisms of antibiotic resistance were highly consistent between the ileum and the colon. This suggested that the microbiota and ARGs, but not the overall resistomes, were different between different intestinal segments. Furthermore, T-ARGs that were predicted to confer macrolide and tetracycline resistance, including Erm(T) and tcr3, respectively, were revealed to be significantly increased after LDA exposure in the colon and ileum samples. Therefore, even over a relatively short period of 4 weeks, levels of antibiotic resistance to administered antibiotics can be changed. Two previous studies reported negligible impacts of LDA on antibiotic resistance based on testing fecal microbiota over both long and short periods (31, 32). There were between-study differences in the antibiotics, source of microbiota, and time period, and our results suggest that a more comprehensive evaluation should be conducted before concluding that the impacts of LDA are negligible.

We not only identified antibiotic resistance in the LDA group, but also in the CON group not exposed to antibiotics, and both groups exhibited highly individual-specific diversity. The infant's gut microbiota is shaped by many factors (33–35), but the most studied aspect is the correlation of the gut microbiota between infants and mothers (36, 37). It has been reported that infants derive their first microbiota from their mother and so it is very likely that infants share gut resistomes (including MGEs) with their mother's gut and breastmilk microbiota during pregnancy, birth, and lactation (38, 39), which may be acquired from the mother. Additionally, the resistomes of the infants might be influenced by the antibiotics in the breastmilk, which may also underlie the highly individual-specific diversity of the gut resistomes in infants.

The composition of the microbiota affects immune responses, susceptibility to infection by intestinal pathogens, and the development of inflammatory bowel diseases (40), while antibiotics alter the intestinal microbiota and thereby influence the intestinal immune defenses, which can involve reductions or increases in the expression of intestinal innate immunity-related genes (41, 42). In this study, there were two bacterial pathogens with significantly different abundances between the I-LDA and I-CON groups and C-LDA and C-CON groups (based on matching the ARGs to common enteral bacterial pathogens), which composed limited ARGs in the pathogens with non-significant differences in abundances. Further, the intestinal immunity was considerably changed between the LDA and CON groups. This revealed that with short-term LDA exposure, the changes in intestinal immunity were considerable, probably because of the changes in pathogenic bacterial species and the early anti-inflammation response [significantly decreased *TLR4* and *two* pro-inflammatory cytokines (*IFN-γ* and *IL-6*)] and improved intestine barrier (significantly increased *CLDN-1*). Moreover, the correlations between bacterial pathogens and immune-related proteins indicated differential abundance of specific gut bacteria was associated with cytokine responses, it has been reported that this effect was exerted directly on the intrinsic cytokine production capacity (43).

Overall, our findings revealed considerable changes in intestinal immunity, but minimal changes in the gut antibiotic resistomes (ARGs and MGEs), in weaned piglets after LDA exposure for 4 weeks. Our study focused on the short-term impact of LDA on the colon and ileum resistomes and intestinal immunity in the first 4 weeks after weaning. As the duration of LDA exposure in this study was only 4 weeks, the antibiotic resistome profiles reported here may not be representative of the longer-term effects. It would be interesting to continue to assess piglets for a longer period after weaning to investigate how the minor changes impact the future health and productivity of growing piglets.

DATA AVAILABILITY STATEMENT

The datasets generated in this study are available in the NCBI Sequence Read Archive (SRA) repository. The metagenome data is linked to accession numbers SRR11489746-SRR11489792. The strand-specific RNA-seq data is linked to accession numbers SRR7779786-SRR7779804.

ETHICS STATEMENT

The animal study was reviewed and approved by the Sichuan Agricultural University animal welfare committee.

AUTHOR CONTRIBUTIONS

FG and LC conceived of and designed the study. RW, LQ, and QX collected samples and performed the animal experiments. RW performed the qPCR experiment. QH and DZ processed and analyzed the data. FG, QH, and CL interpreted the data and wrote the manuscript. All authors read and approved the final manuscript.

FUNDING

This work was funded by the Central Public-interest Scientific Institution Basal Research Fund (Y2017JC26), the Agricultural Science and Technology Innovation Program (ASTIP), the Agricultural Science and Technology Innovation Program Cooperation and Innovation Mission (CAAS-XTCX2016), and the National Key Research and Development Program of China (2016YFD0501204).

ACKNOWLEDGMENTS

We thank Prof. Per Sangild (Copenhagen University) for editing the manuscript and providing helpful advice on the study.

SUPPLEMENTARY MATERIAL

The Supplementary Material for this article can be found online at: https://www.frontiersin.org/articles/10.3389/fimmu.2020.00903/full#supplementary-material

REFERENCES

1. Cho I, Yamanishi S, Cox L, Methe BA, Zavadil J, Li K, et al. Antibiotics in early life alter the murine colonic microbiome and adiposity. *Nature.* (2012) 488:621–6. doi: 10.1038/nature11400
2. Modi SR, Collins JJ, Relman DA. Antibiotics and the gut microbiota. *J Clin Invest.* (2014) 124:4212–8. doi: 10.1172/JCI72333
3. Chattopadhyay MK. Use of antibiotics as feed additives: a burning question. *Front Microbiol.* (2014) 5:334. doi: 10.3389/fmicb.2014.00334
4. Thanner S, Drissner D, Walsh F. Antimicrobial resistance in agriculture. *Mbio.* (2016) 7:e02227–15. doi: 10.1128/mBio.02227-15
5. Gajda A, Nowacka-Kozak E, Gbylik-Sikorska M, Posyniak A. Tetracycline antibiotics transfer from contaminated milk to dairy products and the effect of the skimming step and pasteurisation process on residue concentrations. *Food Addit Contam Part A Chem Anal Control Expo Risk Assess.* (2018) 35:66–76. doi: 10.1080/19440049.2017.1397773
6. Dinleyici M, Yildirim GK, Aydemir O, Kaya TB, Bildirici Y, Carman KB. Human milk antibiotic residue levels and their relationship with delivery mode, maternal antibiotic use and maternal dietary habits. *Eur Rev Med Pharmacol Sci.* (2018) 22:6560–6. doi: 10.26355/eurrev_201810_16072
7. Abreu MT, Fukata M, Arditi M. TLR signaling in the gut in health and disease. *J Immunol.* (2005) 174:4453–60. doi: 10.4049/jimmunol.174.8.4453
8. Brandl K, Plitas G, Mihu CN, Ubeda C, Jia T, Fleisher M, et al. Vancomycin-resistant enterococci exploit antibiotic-induced innate immune deficits. *Nature.* (2008) 455:804–7. doi: 10.1038/nature07250
9. Hill DA, Artis D. Intestinal bacteria and the regulation of immune cell homeostasis. *Annu Rev Immunol.* (2010) 28:623–67. doi: 10.1146/annurev-immunol-030409-101330
10. Qin JJ, Li RQ, Raes J, Arumugam M, Burgdorf KS, Manichanh C, et al. A human gut microbial gene catalogue established by metagenomic sequencing. *Nature.* (2010) 464:59–U70. doi: 10.1038/nature08821
11. Hill DA, Siracusa MC, Abt MC, Kim BS, Kobuley D, Kubo M, et al. Commensal bacteria-derived signals regulate basophil hematopoiesis and allergic inflammation. *Nat Med.* (2012) 18:538–46. doi: 10.1038/nm.2657
12. Parnanen K, Karkman A, Hultman J, Lyra C, Bengtsson-Palme J, Larsson DGJ, et al. Maternal gut and breast milk microbiota affect infant gut antibiotic resistome and mobile genetic elements. *Nat Commun.* (2018) 9:3891. doi: 10.1038/s41467-018-06393-w
13. Joyce A, Mccarthy CGP, Murphy S, Walsh F. Antibiotic resistomes of healthy pig faecal metagenomes. *Microbial Genomics.* (2019) 5:e000272. doi: 10.1099/mgen.0.000272
14. Liu JX, Taft DH, Maldonado-Gomez MX, Johnson D, Treiber ML, Lemayq DG, et al. The fecal resistome of dairy cattle is associated with diet during nursing. *Nat Commun.* (2019) 10:4406. doi: 10.1038/s41467-019-12111-x
15. Hill DA, Hoffmann C, Abt MC, Du Y, Kobuley D, Kirn TJ, et al. Metagenomic analyses reveal antibiotic-induced temporal and spatial changes in intestinal microbiota with associated alterations in immune cell homeostasis. *Mucosal Immunol.* (2010) 3:148–58. doi: 10.1038/mi.2009.132
16. Che LQ, Hu Q, Wang R, Zhang D, Liu C, Zhang YH, et al. Inter-correlated gut microbiota and SCFAs changes upon antibiotics exposure links with rapid body-mass gain in weaned piglet model. *J Nutrit Biochem.* (2019) 74:108246. doi: 10.1016/j.jnutbio.2019.108246
17. Kim D, Langmead B, Salzberg SL. HISAT: a fast spliced aligner with low memory requirements. *Nat Methods.* (2015) 12:357–60. doi: 10.1038/nmeth.3317
18. Li DH, Luo RB, Liu CM, Leung CM, Ting HF, Sadakane K, et al. MEGAHIT v1.0: a fast and scalable metagenome assembler driven by advanced methodologies and community practices. *Methods.* (2016) 102:3–11. doi: 10.1016/j.ymeth.2016.02.020
19. Moriya Y, Itoh M, Okuda S, Yoshizawa AC, Kanehisa M. KAAS: an automatic genome annotation and pathway reconstruction server. *Nucleic Acids Res.* (2007) 35:W182–5. doi: 10.1093/nar/gkm321
20. Mcarthur AG, Waglechner N, Nizam F, Yan A, Azad MA, Baylay AJ, et al. The comprehensive antibiotic resistance database. *Antimicrob Agents Chemother.* (2013) 57:3348–57. doi: 10.1128/AAC.00419-13
21. Oksanen J, Blanchet FG, Kindt R, Legendre P, Minchin PR, O'hara R, et al. Package 'vegan'. *Community Ecology Package, Version 2.* (2015). Available online at: http://CRAN.R-project.org/package=vegan
22. Clarke KR. Non-parametric multivariate analyses of changes in community structure. *Austral J Ecol.* (1993) 18:117–43. doi: 10.1111/j.1442-9993.1993.tb00438.x
23. Parks DH, Tyson GW, Hugenholtz P, Beiko RG. STAMP: statistical analysis of taxonomic and functional profiles. *Bioinformatics.* (2014) 30:3123–4. doi: 10.1093/bioinformatics/btu494
24. Frost LS, Leplae R, Summers AO, Toussaint A. Mobile genetic elements: the agents of open source evolution. *Nat Rev Microbiol.* (2005) 3:722–32. doi: 10.1038/nrmicro1235
25. Rajahram GS, Hameed AA, Menon J, William T, Tambyah PA, Yeo TW. Case report: two human Streptococcus suis infections in Borneo, Sabah, Malaysia. *BMC Infect Dis.* (2017) 17:188. doi: 10.1186/s12879-017-2294-z
26. Dethlefsen L, Mcfall-Ngai M, Relman DA. An ecological and evolutionary perspective on human-microbe mutualism and disease. *Nature.* (2007) 449:811–8. doi: 10.1038/nature06245
27. Costello EK, Stagaman K, Dethlefsen L, Bohannan BJ, Relman DA. The application of ecological theory toward an understanding of the human microbiome. *Science.* (2012) 336:1255–62. doi: 10.1126/science.1224203
28. Ray K. Gut microbiota: adding weight to the microbiota's role in obesity–exposure to antibiotics early in life can lead to increased adiposity. *Nat Rev Gastroenterol Hepatol.* (2012) 9:615. doi: 10.1038/nrgastro.2012.175
29. Cox LM, Blaser MJ. Antibiotics in early life and obesity. *Nat Rev Endocrinol.* (2015) 11:182–90. doi: 10.1038/nrendo.2014.210
30. Yoshimoto A, Uebanso T, Nakahashi M, Shimohata T, Mawatari K, Takahashi A. Effect of prenatal administration of low dose antibiotics on gut microbiota and body fat composition of newborn mice. *J Clin Biochem Nutr.* (2018) 62:155–60. doi: 10.3164/jcbn.17-53
31. Choo JM, Abell GCJ, Thomson R, Morgan L, Waterer G, Gordon DL, et al. Impact of long-term erythromycin therapy on the oropharyngeal microbiome and resistance gene reservoir in non-cystic fibrosis bronchiectasis. *mSphere.* (2018) 3:e00103–18. doi: 10.1128/mSphere.00103-18
32. Zeineldin MM, Megahed A, Blair B, Burton B, Aldridge B, Lowe J. Negligible impact of perinatal tulathromycin metaphylaxis on the developmental dynamics of fecal microbiota and their accompanying antimicrobial resistome in piglets. *Front Microbiol.* (2019) 10:726. doi: 10.3389/fmicb.2019.00726

33. Forsgren M, Isolauri E, Salminen S, Rautava S. Late preterm birth has direct and indirect effects on infant gut microbiota development during the first six months of life. *Acta Paediatr.* (2017) 106:1103–9. doi: 10.1111/apa.13837
34. Akkerman R, Faas MM, De Vos P. Non-digestible carbohydrates in infant formula as substitution for human milk oligosaccharide functions: effects on microbiota and gut maturation. *Crit Rev Food Sci Nutr.* (2019) 59:1486–97. doi: 10.1080/10408398.2017.1414030
35. Wang Y, Liu YQ, Bai JB, Chen XL. The effect of maternal postpartum practices on infant gut microbiota: a chinese cohort study. *Microorganisms.* (2019) 7:511. doi: 10.3390/microorganisms7110511
36. Vaishampayan PA, Kuehl JV, Froula JL, Morgan JL, Ochman H, Francino MP. Comparative metagenomics and population dynamics of the gut microbiota in mother and infant. *Genome Biol Evol.* (2010) 2:53–66. doi: 10.1093/gbe/evp057
37. De Vries LE, Valles Y, Agerso Y, Vaishampayan PA, Garcia-Montaner A, Kuehl JV, et al. The gut as reservoir of antibiotic resistance: microbial ant. *PLoS ONE.* (2011) 6:e21644. doi: 10.1371/journal.pone.0021644
38. Kozak K, Charbonneau D, Sanozky-Dawes R, Klaenhammer T. Characterization of bacterial isolates from the microbiota of mothers' breast milk and their infants. *Gut Microbes.* (2015) 6:341–51. doi: 10.1080/19490976.2015.1103425
39. Yassour M, Vatanen T, Siljander H, Hamalainen AM, Harkonen T, Ryhanen S. J, et al. Natural history of the infant gut microbiome and impact of antibiotic treatment on bacterial strain diversity and stability. *Sci Transl Med.* (2016) 8:343ra81. doi: 10.1126/scitranslmed.aad0917
40. Abraham C, Cho J. InterIeukin-23/Th17 pathways and inflammatory bowel disease. *Inflamm Bowel Dis.* (2009) 15:1090–100. doi: 10.1002/ibd.20894
41. Schumann A, Nutten S, Donnicola D, Comelli EM, Mansourian R, Cherbut C, et al. Neonatal antibiotic treatment alters gastrointestinal tract developmental gene expression and intestinal barrier transcriptome. *Physiol Genomics.* (2005) 23:235–45. doi: 10.1152/physiolgenomics.00057.2005
42. Wlodarska M, Willing B, Keeney KM, Menendez A, Bergstrom KS, Gill N, et al. Antibiotic treatment alters the colonic mucus layer and predisposes the host to exacerbated citrobacter rodentium-induced colitis. *Infect Immun.* (2011) 79:1536–45. doi: 10.1128/IAI.01104-10
43. Schirmer M, Smeekens SP, Vlamakis H, Jaeger M, Oosting M, Franzosa EA, et al. Linking the human gut microbiome to inflammatory cytokine production capacity. *Cell.* (2016) 167:1897. doi: 10.1016/j.cell.2016.11.046

Conflict of Interest: The authors declare that the research was conducted in the absence of any commercial or financial relationships that could be construed as a potential conflict of interest.

frontiers in Immunology

ORIGINAL RESEARCH
published: 16 June 2020
doi: 10.3389/fimmu.2020.01194

Expression of S100A Alarmins in Cord Blood Monocytes Is Highly Associated With Chorioamnionitis and Fetal Inflammation in Preterm Infants

Veronika Golubinskaya[1], Henri Puttonen[2], Ing-Marie Fyhr[2], Halfdan Rydbeck[1], Ann Hellström[3], Bo Jacobsson[4,5,6], Holger Nilsson[1], Carina Mallard[1†] and Karin Sävman[7,8†]*

[1] Department of Physiology, Institute of Neuroscience and Physiology, University of Gothenburg, Sahlgrenska Academy, Gothenburg, Sweden, [2] Department of Pathology, Sahlgrenska University Hospital, Gothenburg, Sweden, [3] Department of Clinical Neuroscience, Institute of Neuroscience and Physiology, University of Gothenburg, Sahlgrenska Academy, Gothenburg, Sweden, [4] Department of Obstetrics and Gynecology, Institute of Clinical Science, University of Gothenburg, Sahlgrenska Academy, Gothenburg, Sweden, [5] Department of Obstetrics and Gynecology, Sahlgrenska University Hospital, Gothenburg, Sweden, [6] Department of Genetics and Bioinformatics, Domain of Health Data and Digitalization, Institute of Public Health, Oslo, Norway, [7] Department of Pediatrics, Institute of Clinical Sciences, University of Gothenburg, Sahlgrenska Academy, Gothenburg, Sweden, [8] Department of Neonatology, The Queen Silvia Children's Hospital, Sahlgrenska University Hospital, Gothenburg, Sweden

OPEN ACCESS

Edited by:
Per T. Sangild,
University of Copenhagen, Denmark

Reviewed by:
Pietro Presicce,
UCLA Department of Pediatrics, United States
Xiaoyu Pan,
University of Copenhagen, Denmark

***Correspondence:**
Karin Sävman
karin.savman@pediat.gu.se

† These authors have contributed equally to this work

Specialty section:
This article was submitted to Inflammation, a section of the journal Frontiers in Immunology

Received: *06 December 2019*
Accepted: *13 May 2020*
Published: *16 June 2020*

Citation:
Golubinskaya V, Puttonen H, Fyhr I-M, Rydbeck H, Hellström A, Jacobsson B, Nilsson H, Mallard C and Sävman K (2020) Expression of S100A Alarmins in Cord Blood Monocytes Is Highly Associated With Chorioamnionitis and Fetal Inflammation in Preterm Infants. Front. Immunol. 11:1194. doi: 10.3389/fimmu.2020.01194

Background: Preterm infants exposed to chorioamnionitis and with a fetal inflammatory response are at risk for neonatal morbidity and adverse outcome. Alarmins S100A8, S100A9, and S100A12 are expressed by myeloid cells and have been associated with inflammatory activation and monocyte modulation.

Aim: To study S100A alarmin expression in cord blood monocytes from term healthy and preterm infants and relate results to clinical findings, inflammatory biomarkers and alarmin protein levels, as well as pathways identified by differentially regulated monocyte genes.

Methods: Cord blood CD14+ monocytes were isolated from healthy term ($n = 10$) and preterm infants (<30 weeks gestational age, $n = 33$) by MACS technology. Monocyte RNA was sequenced and gene expression was analyzed by Principal Component Analysis and hierarchical clustering. Pathways were identified by Ingenuity Pathway Analysis. Inflammatory proteins were measured by Multiplex ELISA, and plasma S100A proteins by mass spectrometry. Histological chorioamnionitis (HCA) and fetal inflammatory response syndrome (FIRS) were diagnosed by placenta histological examination.

Results: S100A8, S100A9, and S100A12 gene expression was significantly increased and with a wider range in preterm vs. term infants. High S100A8 and S100A9 gene expression ($n = 17$) within the preterm group was strongly associated with spontaneous onset of delivery, HCA, FIRS and elevated inflammatory proteins in cord blood, while low expression ($n = 16$) was associated with impaired fetal growth and physician-initiated

delivery. S100A8 and S100A9 protein levels were significantly lower in preterm vs. term infants, but within the preterm group high S100A gene expression, spontaneous onset of labor, HCA and FIRS were associated with elevated protein levels. One thousand nine hundred genes were differentially expressed in preterm infants with high vs. low S100A alarmin expression. Analysis of 124 genes differentially expressed in S100A high as well as FIRS and HCA groups identified 18 common pathways and S100A alarmins represented major hubs in network analyses.

Conclusion: High expression of S100A alarmins in cord blood monocytes identifies a distinct clinical risk group of preterm infants exposed to chorioamnionitis and with a fetal inflammatory response. Gene and pathway analyses suggest that high S100A alarmin expression also affects monocyte function. The connection with monocyte phenotype and inflammation-stimulated S100A expression in other cell types (e.g., neutrophils) warrants further investigation.

Keywords: alarmins, S100A8, S100A9, preterm birth, chorioamnionitis, fetal inflammation, monocytes, cord blood

INTRODUCTION

Preterm infants are at increased risk for severe neonatal morbidities as well as long term cognitive and motor impairment (1). The risk is inversely related to gestational age at birth (1), but there are also additional risk factors that may affect neonatal morbidities and long term outcome. One distinct clinical risk group are infants born to mothers with intrauterine infection and/or inflammation, commonly referred to as chorioamnionitis.

Chorioamnionitis is a major cause of preterm labor (PTL), preterm prelabor rupture of membranes (PPROM) and subsequent preterm delivery (2–4) and present in >50% of extremely preterm deliveries (5). Chorioamnionitis is commonly asymptomatic in the mother and spontaneous onset of labor or rupture of membranes are often the only clinical symptoms (5, 6). Reliable diagnosis is commonly obtained only after birth following histological examination of the placenta. Histological chorioamnionitis (HCA) is defined as a maternal inflammatory response in the placenta and may be associated with a fetal inflammatory response syndrome (FIRS) characterized by inflammation in fetal blood vessels and/or umbilical cord (funisitis) (5, 7). Preterm infants exposed to HCA and FIRS have an increased risk of early onset sepsis (8, 9) and may have elevated inflammatory parameters in cord blood as an additional sign of fetal inflammation (10, 11), but most infants have no clinical symptoms and there are no biochemical markers for FIRS in clinical use.

In spite of a lack of early symptoms, exposure to chorioamnionitis, and FIRS in particular, has been linked to an increased risk for severe neonatal morbidities (12–14), preterm brain injury (11, 15), and long term adverse outcomes (16, 17), suggesting that inflammatory mechanisms may contribute to injury. In addition to a possible risk of inflammation-induced injury, chorioamnionitis may also affect the immune response and the risk of severe infections in the preterm infant (18). It is thus of vital importance to characterize the fetal immune response associated with exposure to intrauterine infection/inflammation and to identify underlying mechanisms that may lead to inflammation-induced injury or affect the defense against infections. Recent studies suggest that monocyte phenotype is affected by the intrauterine environment and that alterations in monocyte function may change susceptibility to additional infectious or inflammatory insults (19, 20).

Alarmins are endogenous proteins/peptides that are released from cells in response to stress, immune activation, or cellular injury (21). Alarmins act as damage-associated molecular patterns (DAMPs) on pattern recognition receptors to initiate an immune-response (21). Proteins from the S100 family; S100A, S100A9, and S100A12 (also called calgranulin a, b, and c), are highly expressed in myeloid cells including neutrophils and monocytes (22). They make up a considerable part of cytoplasmic proteins in these cells (23), where they are important for phagocytosis and facilitate cell adhesion and migration (21). Neutrophil cells represent a larger circulating population than monocytes and also contain a larger percentage of S100A proteins and may therefore be a major source of proteins released under inflammatory conditions (23). When released following cellular injury or as a response to inflammatory stimuli, the S100A8 and S100A9 alarmins preferably form a heterodimer complex (calprotectin) and act as a DAMP by activating the RAGE and TLR4 receptors resulting in cytokine release and chemotaxis (21, 24). In the clinical setting, the S100A8/A9 dimer is released in response to local inflammatory processes into stool or plasma (25). In adults, it serves a preferable biomarker for certain inflammatory conditions such as inflammatory bowel disease and rheumatoid arthritis (25, 26).

S100A8/A9 has also been studied in the neonatal setting, mainly by studies of protein levels in association with various conditions. Protein levels of S100A8/A9 are increased in healthy term infants compared with adults and equal those found in adult patients during inflammation (19, 27), while preterm infants not exposed to chorioamnionitis have lower levels than term infants, but still significantly higher than in adults (19). S100A8/A9 proteins are also elevated in neonatal sepsis in preterm infants

(28), while no elevation was seen in association with clinical intraamniotic infection (29). Recent studies also suggest that increased S100A8/A9 protein levels are responsible for specific characteristics of neonatal monocytes (19). In healthy term infants without signs of inflammation, S100A8/A9 modulates TLR responses resulting in a decreased risk for potentially tissue damaging hyperinflammation with preserved bacterial clearance. Low S100A8/A9 protein levels in cord blood are also associated with an increased risk of late onset sepsis in preterm infants (19). In addition, elevated levels of S100A9 and S100A12 proteins in amniotic fluid are associated with elevated inflammatory markers in cord blood and an increased risk for early onset sepsis (EOS) (30). To our knowledge, monocyte gene expression of S100A alarmins has not been studied in clinical inflammatory conditions or in the neonatal setting.

In this study, we investigate S100A8, S100A9, and S100A12 gene expression in cord blood monocytes from term healthy infants and preterm infants with exposure to chorioamnionitis or with a fetal inflammatory response. To characterize clinically relevant monocyte phenotypes, we relate our findings to clinical features, to inflammatory biomarkers and S100A proteins in cord blood and to potentially important pathways and networks identified by differentially regulated monocyte genes.

METHODS

Study Population

The study was conducted at Sahlgrenska University Hospital, and at the Sahlgrenska Academy, University of Gothenburg, Sweden. The study was approved by the Regional Ethic's Committee (EPN Gbg 933-16, T350-18) at the Sahlgrenska University Hospital, Gothenburg, Sweden and children were enrolled following written informed parental consent. The preterm group consisted of 33 infants born at <30 weeks gestational age and the term group of 10 term infants born after normal vaginal delivery and without perinatal complications.

Data regarding maternal morbidity and pregnancy complications as well as data on deliveries and neonatal morbidities was obtained from medical charts. Pre-eclampsia was diagnosed in mothers with elevated blood pressure and significant proteinuria, and suspected clinical chorioamnionitis in mothers with fever >38.0°C and/or elevated CRP that received antibiotics on suspicion of intrauterine infection. Spontaneous onset of delivery was recorded when delivery was started by either spontaneous contractions (PTL) or rupture of membranes (PPROM) and physician-initiated delivery when infants were delivered by cesarean section without PTL or PPROM. Inflammatory markers were analyzed according to clinical routine within 1 h of birth and were considered elevated with CRP > 10 mg/L and/or Interleukin (IL)-6 >1,000 ng/L. Sepsis was diagnosed when clinical symptoms of infection were accompanied by positive blood cultures, except for *Staphylococcus epidermidis* where, in addition, a CRP > 20 mg/L was required for diagnosis. Additional severe neonatal morbidities were recorded, including intraventricular hemorrhage (IVH) grade 3–4, necrotizing enterocolitis (NEC) with clinical and radiological signs, patent ductus arteriosus (PDA) requiring medical or surgical treatment, and chronic lung disease (CLD) with oxygen need at 36 weeks gestational age.

Placenta Histology

The diagnoses of HCA and FIRS were based on joint analyses by two trained perinatal pathologists. Tissue samples were obtained from umbilical cord (proximal and distal samples), roll of chorioamniotic membranes, umbilical cord insertion, and full-thickness samples of placenta. Histological examination of the placenta was performed following College of American Pathologists guidelines and findings were classified according to the ELGAN protocol as previously described (7). HCA was defined as a maternal inflammatory response with neutrophil infiltration of subchorionic space, chorionic plate, and amnion (Stages 1–3) while FIRS was defined as inflammation of the umbilical cord (funisitis) and/or neutrophilic infiltration of fetal stem vessels. Placentas from twins were examined and classified individually.

Cord Blood Sampling and Storage

Cord blood was collected by gentle needle aspiration and transferred to EDTA tubes. After sampling, blood was stored vertically in closed tubes at +4°C without agitation until processing. Samples were stored for a median of 5.7 h (range 1.6–21.5 h). Storage time did not significantly affect gene expressions of S100A8, A9, or A12 (Spearman rank test, $p > 0.05$, correlation coefficients < 0.3).

Blood Plasma Preparation and CD14+ Monocyte Isolation

Blood was mixed by repeated inversion of the tube and then spun at room temperature for 2 min at 2,000×g. Plasma was separated to a new tube, spun for 5 min at 2,000×g and the supernatant was aliquoted and saved frozen at −80°C until analysis.

Removed plasma was replaced by a corresponding volume of EasySep™ cell separation buffer (STEMCELL Technologies Inc., cat.#20144), and the cell pellet was carefully resuspended. For preparing the peripheral blood mononuclear cell (PBMC) fraction, the samples were diluted 1:2 in EasySep™ cell separation buffer and spun with brakes off in Lymphoprep™ density gradient medium (STEMCELL Technologies Inc., cat.#07801) at 1,200×g for 20 min at room temperature.

All further steps of the monocyte isolation protocol were conducted at +4°C. CD14+ monocytes were purified from PBMC fraction with the help of magnetic cell separation (MACS) technology according to the manufacturer protocol (CD14 MicroBeads, human, cat.#130-050-201; autoMACS running buffer, cat.#130-091-221; MiniMACS Separation columns, type MS, cat.#130-042-201; Miltenyi Biotec). The last washing step was made with D-PBS without calcium and magnesium (STEMCELL Technologies Inc., cat.#37350). The CD14+ monocyte cell pellets were then stored at −80°C for later RNA extraction.

Prior to the last washing step the purified monocytes were counted and number of dead cells was determined based on positive TrypanBlue staining. Cell samples were also placed on

+-charged glasses, quickly dried, fixed with ice-cold acetone-methanol and stored frozen at −20°C for further analysis of the monocyte fraction purity. Cells on the slides were stained with anti-CD14+ antibodies (1:200, HPA001887, Atlas Antibodies AB), and the number of positive cells, as well as the morphology of the cells and the cell nuclei were evaluated. Purity of the CD14+ monocyte fraction was >96% and cell viability on average 93%.

RNA Sequencing

Monocyte cell pellets were homogenized in QIAzol Lysis Reagent (Qiagen, cat.# 79306) and then total RNA was purified by miRNeasy Micro Kit (Qiagen, cat.# 217084) according to the manufacturer's protocol. RNA quantity and purity were analyzed by NanoDrop (Thermo Fisher Scientific), and RNA integrity was determined by Experion™ automated electrophoresis system (BioRad). Samples that proceeded to RNA sequencing had a mean (SD) RQI of 9.2 (1.0). RNA sequencing experiments and basic data analysis were conducted at QIAGEN Genomic Services, as described below.

Library Preparation and Next Generation Sequencing

The library preparation was done using Illumina TruSeq Stranded Total RNA Library Prep Kit with rRNA depletion (Illumina Inc.). A total of 100 ng RNA was used. Sequencing was performed on a NextSeq500 instrument, with an average number of reads 60 million paired-end reads/per sample and number of sequencing cycles (read length) 2 × 75 nt. Sequencing was performed according the manufacturer's instructions (Illumina Inc.). The NGS data analysis pipeline was based on the Tuxedo software package. Briefly, abundant sequences were filtered after aligning the raw data with Bowtie2. Tophat was used to perform alignment to the reference genome (GRCh37, annotation from ENSEMBL_75). Cufflinks was used to assemble transcripts, Cuffmerge to merge transcripts and Cuffquant to quantify expression levels. Counts were converted to fpkm (fragments per kilobase million) values and the data set was filtered.

After preparing library, all samples passed the internal quality check (Qiagen, Genomic Services). Following sequencing, intensity correction and base calling (into BCL files), and FASTQ files were generated using the appropriate bcl2fastq software (Illumina Inc.). Average read *Q*-score was above 30 (high quality data). On average 33.0 million reads were obtained for each sample and the average genome mapping rate was 90.5%. All samples in the study had similar call rates (similar numbers of genes identified) and were considered to be comparable. In the analysis the fpkm values are normalized with median of the geometric mean (31).

Further analyses included only the transcripts where, in all groups, 10% or more of individual reads were at least 2 fpkm. Unmapped transcripts, clone-based genes, ribosome-related RNA transcripts, small nuclear and nucleolar RNA-related transcripts, Y-RNA and non-unique transcripts were also eliminated. Zero fpkm values for the individual reads were replaced by 1 fpkm, and then all fpkm values were transformed to log2 fpkm values for further analysis.

To validate RNA sequencing results, qPCR analysis was conducted at QIAGEN Genomic Services on 4 samples each from high and low S100A preterm groups as identified by RNAseq. Samples were analyzed using a PCR array panel (Human aging panel, Cat.# PAHS-178Z, product # 33023) which included S100A8 and S100A9, as well as 5 additional genes from the top 500 differentially expressed (DE) genes between S100 high and S100 low groups (ANXA3, FCER1G, FCGR1A, LMNB1, WRN). Five housekeeping genes (ACTB, B2M, GAPDH, HPRT1, RPLP0) were also included. The average of Ct values for the housekeeping genes were calculated, and for further analysis delta Ct for each gene was used (dCt = average Ct for 5 housekeeping genes – Ct for the gene of interest). In the sequencing data analysis log2(fpkm) values were used.

Measurements of Inflammatory Proteins in Plasma

A comprehensive screening of plasma cytokines, chemokines, and growth factors was performed by Bio-Plex ELISA (Bio-Rad Laboratories, Inc., Bio-Plex Pro™ Human Cytokine Screening Panel, 48-Plex #12007283, Bio-Plex Pro™ Human Inflammation Panel 1, 37-Plex #171AL001M) according to the manufacturer's instructions. Samples were diluted according to the manufacturer protocol (1:4 in sample diluent). Low "out-of-range" values were replaced by 1/8 of the detection limit value for the protein measured. No high "out-of-range" values were registered. For the proteins that were included in both of the Bio-Plex panels, reads from only one assay were included, based on best fit of the measurements to the standard curve.

Quantitative Analysis of Plasma S100A8 and S100A9 Proteins by Mass Spectrometry

Each plasma sample (0.6 μl) was reduced in 100 mM DTT with 2% SDS and 50 mM TEAB, and processed by the FASP method (32) including alkylation with 10 mM MMTS, and digestion using trypsin (MS Grade, Thermo Fisher Scientific). Peptides were labeled with TMT 11-plex (Thermo Fisher Scientific), pooled per TMT set, and subjected to basic reverse-phase fractionation. The 40 collected fractions were pooled into 20, and analyzed on an Easy nanoLC 1200 liquid chromatography system, coupled to an Orbitrap Fusion Lumos Tribrid instrument (Thermo Fisher Scientific). Peptides were trapped on an Acclaim Pepmap 100 C18 trap column (100 μm × 2 cm, particle size 5 μm, Thermo Fischer Scientific) and separated on an in-house packed analytical column (75 μm × 300 mm, particle size 3 μm, Reprosil-Pur C18, Dr. Maisch) using a gradient from 5 to 100% acetonitrile in 0.2% Formic Acid. The nLC MS analysis was performed in a data-dependent multinotch mode using an m/z of 400–1,400 and a dynamic exclusion of 45 s.

Identification and relative quantification was performed using Proteome Discoverer v. 2.2 (Thermo Fisher Scientific). Mascot v. 2.5.1 (Matrix Science, London, UK) was used to match to the H. sapiens database (SwissProt, September 2019) with MS peptide tolerance of 5 ppm and fragment ion tolerance of 0.6 Da. Miscleavages were set on 0, methionine oxidation was set

as variable modification; cysteine methylthiolation; and TMT-modification were set as fixed. Percolator was used for PSM validation with an FDR threshold of 1%. Normalization of all TMT reporter intensities for each sample on the total peptide amount was performed. Only unique identified peptides were used for relative quantification, and ratios were calculated by dividing the samples with the reference sample.

Gene Co-expression Network Analysis

Only samples from preterm infants were analyzed. For network analysis the expression values of genes left after filtering (10,533 genes) were processed with the R package WGCNA (33) following a pipeline adapted from tutorial I, available from the website (https://horvath.genetics.ucla.edu/html/CoexpressionNetwork/Rpackages/WGCNA/). The WGCNA function for network and module construction, blockwiseModules, uses the soft threshold (power), the minimum module size and mergeCutHeight parameters when calculating the network and the modules, which in turn will affect the GO analysis. We used the settings in the tutorial, except for using minimum module size of 100. For each module, representative eigengenes were defined as the first principal component of gene expression in a given module. The correlation between eigengenes (Pearson correlation) and S100A high or low expression, as well as clinical conditions (FIRS, HCA, PTL/PPROM, elevated CRP/IL-6) was determined. The Gene Ontology Enrichment analysis was performed with the WGCNA function GO enrichment Analysis. Networks were exported for filtering and visualization in the software VisAnt. For selecting hub genes, we used code adapted from Tutorial III, section 7. Connectivity for each gene was calculated with the WGCNA function intramodular Connectivity. This function sums all adjacency entries to other genes, both within the module for intramodular connectivity and to all analyzed genes for total connectivity.

Hub-genes were selected as the top 5% genes with the highest within-module connectivity in order to capture genes with the highest connectivity according to the connectivity distribution (34). The adapted code is available at https://github.com/halryd/~high_S100A_hub_genes.

Data Analysis

For creating lists of differentially expressed genes and inflammatory proteins for principal component analysis (PCA), for hierarchical clustering, and for visual representation in the form of heat maps, the commercial software Qlucore Omics Explorer v3.4 (Qlucore AB, Sweden) was used. Pathway analysis was performed by commercial software Ingenuity Pathway Analysis (IPA) (Qiagen Bioinformatics). Network co-expression analysis is described in detail above.

Clinical data, single genes and proteins were compared using unpaired *t*-tests or Fisher's exact test, following either normality tests or log transformation (GraphPad Prism Software). A $p < 0.05$ was considered statistically significant.

Statistical comparisons of groups of parameters (genes and inflammatory proteins) between study groups were made using Qlucore software (multiple *t*-tests with Benajmini-Hochberg multiple correction procedure). A $q < 0.05$ was considered statistically significant.

Correlations were calculated as either Spearman's rank correlation coefficient, or Pearson's correlation coefficient as appropriate, and correction for confounding factors was performed by linear regression.

RESULTS

Gene Expression in Cord Blood Monocytes and Plasma Inflammatory Protein Profiles Differ Between Preterm and Term Infants

In a first set of experiments we investigated cord blood monocyte gene expression in preterm ($n = 33$) and term ($n = 10$) infants. Background data on infants included is shown in **Table 1**. In summary, 1,924 genes were differentially expressed between the preterm group and the healthy term group. PCA analyses of all genes (**Figure 1A**) and heat maps based on hierarchical clustering of top 500 differentially expressed (DE) genes (**Figure 1B**, $q < 0.008$) show a homogenous pattern of expression within the term group. The preterm group is distinctly different from the term group, and demonstrates a significantly larger variability with clear differences in gene expression between individual preterm infants.

To investigate whether differences in inflammatory activation could help to explain differences in gene expression between preterm and term infants we performed gene pathway analyses. An overview of the 20 most affected pathways based on DE genes are listed in **Table 2**. In summary, more than half of the identified pathways were clearly related to inflammation and immune regulation, including several pathways associated with monocyte maturation and, in particular, monocyte recruitment and extravasation.

In addition, inflammatory plasma proteins were analyzed by Bio-Plex Elisa, and concentrations differed between preterm and term groups for 36 out of 77 measured proteins (**Figure 1D**, $q < 0.049$). Similar to gene expression, term infants exhibited a homogenous protein profile while the preterm group included infants with varying protein patterns thus suggesting differences in inflammatory phenotypes within the preterm group as demonstrated by PCA analysis (**Figure 1C**) and heat map (**Figure 1D**). Detailed data on inflammatory protein analyses is found in **Supplementary Tables 1, 2**.

TABLE 1 | Background data on preterm and term infants.

	Preterm infants ($n = 33$)	Term infants ($n = 10$)
Gestational age (days), mean (SD)	185 (14)	284 (7)
Gestational age (weeks + days), median (range)	26 + 3 (23 + 0 – 29 + 5)	40 + 5 (38 + 2 – 41 + 4)
Birth weight (g), mean (SD)	920 (307)	3,620 (520)
Boys (%)	23/33 (69.7)	7/10 (70)

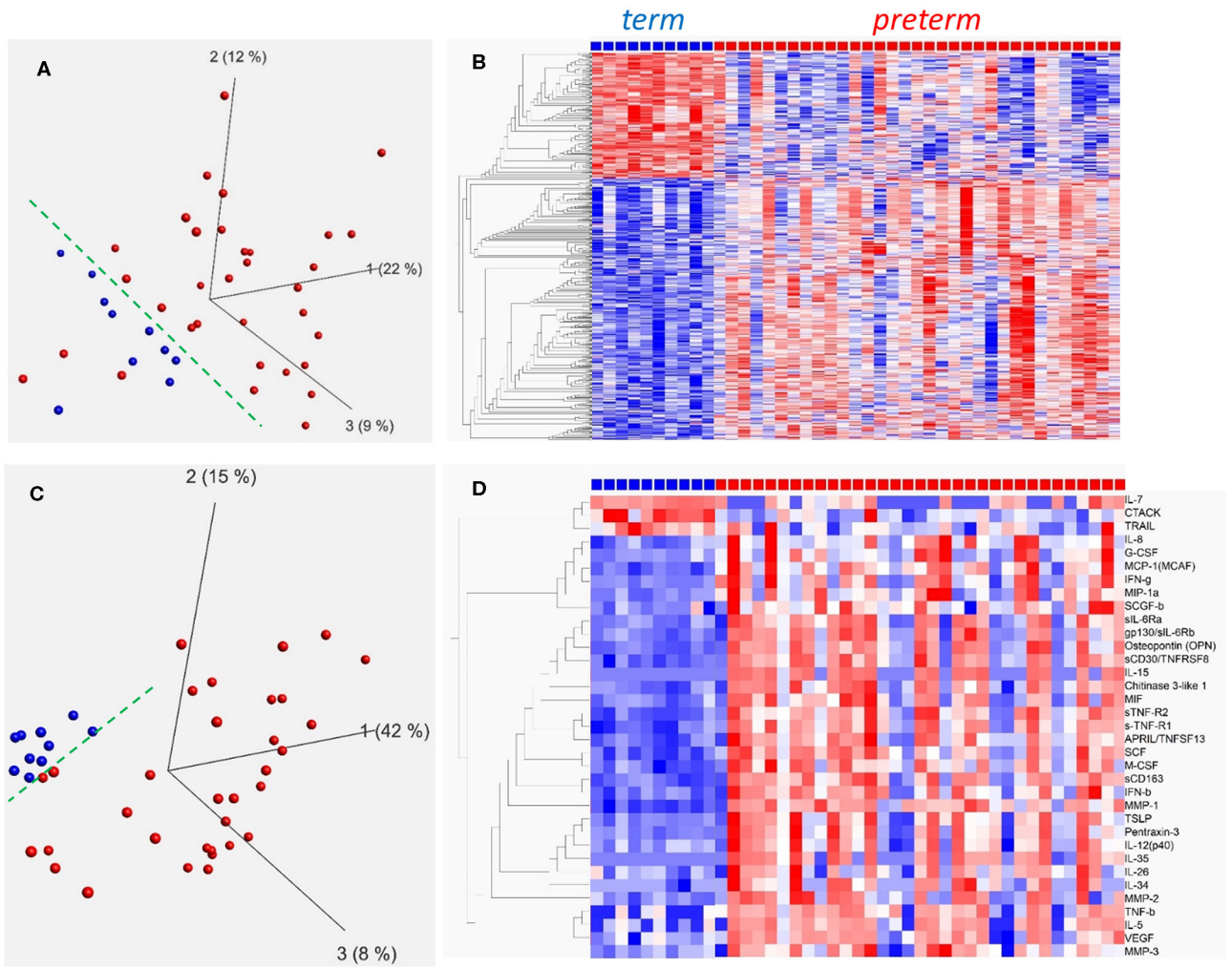

FIGURE 1 | Gene expression in CD14+ cord blood monocytes **(A,B)** and plasma inflammatory protein profiles **(C,D)** in term and preterm infants presented by PCA analysis **(A,C)** and hierarchical clustering **(B,D)**. Principal component analysis (PCA) plots for monocyte gene expression **(A)** and plasma inflammatory proteins **(C)** indicate that term infants (blue, $n = 10$) are better grouped than preterm infants (red, $n = 33$). Heat maps with hierarchical clustering present top 500 differentially expressed genes ($q < 0.008$, Qlucore software; multiple t-tests with Benajmini-Hochberg multiple correction procedure) in monocytes **(B)** and all significantly different ($q \leq 0.049$) inflammatory proteins in plasma **(D)**. Heatmaps and hierarchical clustering are based on fpkm (fragments per kilobase million) values where each value is normalized to mean = 0 and variance = 1. Red color denotes up-regulation and blue down-regulation within a range of −2 to +2.

Preterm Infants Have a Different Pattern of S100A Alarmin Expression in Cord Blood Monocytes Compared With Term Infants

Since S100A alarmins are associated with inflammatory activation and modulate monocyte function in the neonatal period (19), gene expression for alarmins S100A8, S100A9, and S100A12 in cord blood monocytes was analyzed separately and compared between preterm and term infants. Expression was significantly higher and had a wider range in preterm infants for all three genes (**Figure 2A**).

To further investigate the association of alarmin expression and inflammatory phenotypes in the preterm group, we divided the infants into two groups using the median log2 fpkm expression for the different genes (**Figure 2A**, red line). In our experiments, gene expressions of the different S100A alarmins were strongly correlated with each other with correlation coefficients > 0.95 (**Figure 2B**). As S100A8 and S100A9 proteins commonly form biologically active heterodimers and gene expression of S100A8 and S100A9 identified exactly the same infants with high ($n = 17$, at or above median) and low ($n = 16$, under median) gene expression, these groups were used for further analyses and referred to as "S100A high" and "S100A low," respectively. All term infants had alarmin gene expression defined as low by this division.

qPCR analysis was performed for S100A8, S100A9 and 5 of the top 500 DE genes between S100A high and S100A low groups to confirm RNA sequencing results. In summary, gene expression by qPCR was strongly correlated with RNA sequencing data

TABLE 2 | Top 20 canonical IPA pathways differentially regulated in cord blood monocytes from preterm and term infants.

Ingenuity canonical pathways	Signaling pathway categories (IPA)	–log (*p*-value)	Relation to inflammation and/or monocyte function (select references)
Regulation of Actin-based Motility by Rho	Neurotransmitters and Other Nervous System Signaling	5.72	Rho is a family of GTPases, important in innate and adaptive immunity (35)
Thrombin Signaling	Cardiovascular Signaling	5.54	Involved in monocyte regulation of systemic coagulation in (36)
RhoGDI Signaling	Intracellular and Second Messenger Signaling	4.98	Involved in Rho-regulation; important for innate and adaptive immunity (35, 37)
Integrin Signaling	Cell Cycle Regulation; Cellular Growth, Proliferation and Development; Intracellular and Second Messenger Signaling	4.75	Critical in monocyte trafficking and vessel wall adhesion (38)
Actin Cytoskeleton Signaling	Cell Cycle Regulation; Cellular Growth, Proliferation and Development; Intracellular and Second Messenger Signaling	4.63	Regulates locomotion, phagocytosis, and cell shape in leukocytes including monocytes (39)
Relaxin Signaling	Growth Factor Signaling; Organismal Growth and Development	4.5	An insulin-like peptide with properties important for recruitment of peripheral blood mononuclear cells to sites of inflammation (40)
Cellular Effects of Sildenafil (Viagra)	Cardiovascular Signaling; Disease-Specific Pathways	4.34	N/A
Ephrin B Signaling	Neurotransmitters and Other Nervous System Signaling; Organismal Growth and Development	4.15	Ephrin proteins are involved in inflammation in vascular endothelium (41) including in monocytes (42)
Signaling by Rho Family GTPases	Intracellular and Second Messenger Signaling	4.11	Rho is a family of GTPases, important in innate and adaptive immunity (35)
Molecular Mechanisms of Cancer	Cancer; Disease-Specific Pathways	4.1	N/A
Cardiac β-adrenergic Signaling	Cardiovascular Signaling	4.07	N/A
Protein Kinase A Signaling	Intracellular and Second Messenger Signaling	4	N/A
Synaptogenesis Signaling Pathway	Neurotransmitters and Other Nervous System Signaling; Organismal Growth and Development	3.91	N/A
Leukocyte Extravasation Signaling	Cellular Immune Response	3.9	Monocytes immune surveillance and trafficking across vasculature (42)
Germ Cell-Sertoli Cell Junction Signaling	Cellular Growth, Proliferation and Development	3.89	N/A
IL-8 Signaling	Cellular Immune Response; Cytokine Signaling	3.88	Commonly found in early-onset neonatal sepsis (43)
Breast Cancer Regulation by Stathmin1	Cancer; Disease-Specific Pathways	3.86	N/A
Epithelial Adherens Junction Signaling	Cellular Growth, Proliferation and Development	3.73	N/A
Androgen Signaling	Nuclear Receptor Signaling	3.52	N/A
CXCR4 Signaling	Cellular Immune Response; Cytokine Signaling	3.4	Involved in maturation and replenishment of monocytes (44)

Analysis is based on 500 genes differentially expressed between term and preterm groups and analyzed by Ingenuity Pathway Analysis (IPA) (Qiagen Bioinformatics).

(**Table 3**) and differences between groups remained significant for all genes examined (**Supplementary Table 3**).

High Expression of S100A Alarmins in Cord Blood Monocytes From Preterm Infants Is Associated With Clinical Features Associated With Chorioamnionitis and Fetal Inflammation

Clinical background data on preterm infants divided by high or low alarmin S100A gene expression is presented in **Table 4**. High expression of S100A alarmins in cord blood monocytes was associated with several conditions indicative of chorioamnionitis and fetal inflammation. Infants with high expression of S100A alarmins were born at significantly lower gestational ages and all mothers had spontaneous onset of delivery with either PTL or PPROM and with a significantly higher proportion of HCA and FIRS. Elevated CRP and/or IL-6 in clinical routine samples from cord blood were found in the high S100A group only, while the only significant difference regarding neonatal morbidities was a higher percentage in need of treatment for patent ductus arteriosus in the high S100A group. Low S100A expression was

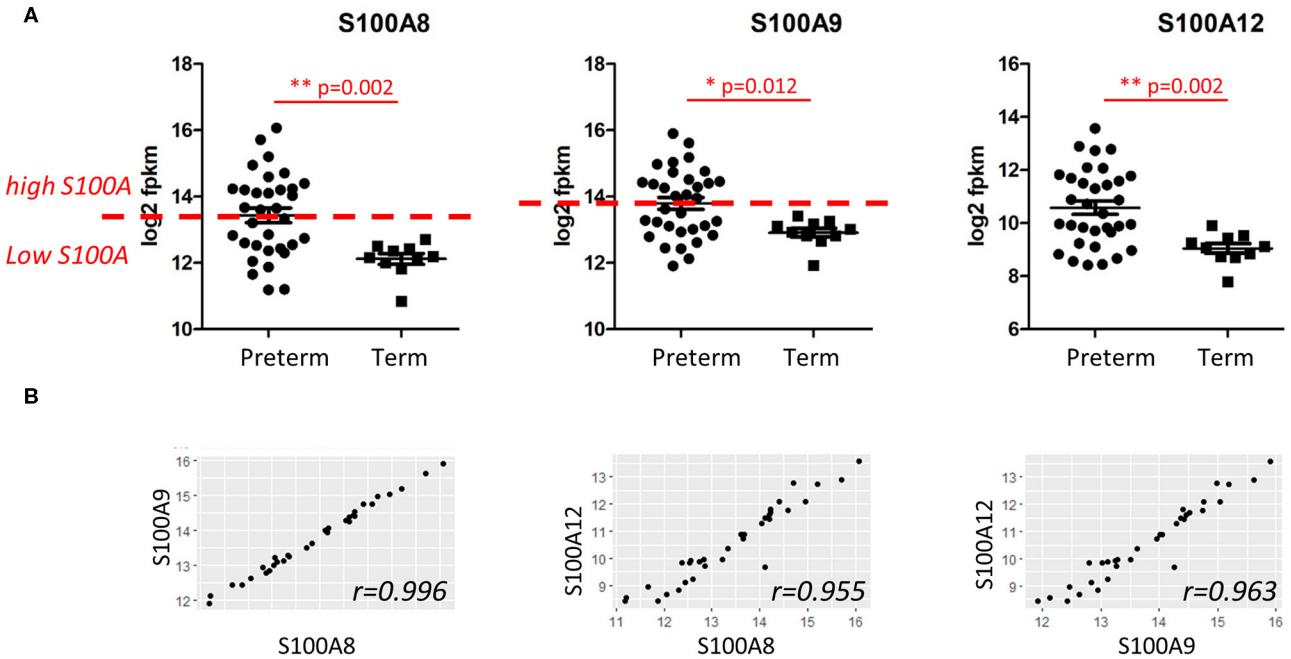

FIGURE 2 | Expression of S100A alarmin genes in CD14+ cord blood monocytes from preterm and term infants. **(A)** Expression of S100A8, S100A9, and S100A12 alarmins was significantly higher and with a wider range in preterm ($n = 33$) compared to term infants ($n = 10$). Data presented as mean ± SEM and compared with unpaired *t*-test for log2-transformed fpkm (fragments per kilobase million) values, *p*-values in figure. Red line indicate division of preterm infants into a S100A high group (S100A8 and S100A9 at or above median, $n = 17$) and a S100A low group (S100A8 and S100A9 below median, $n = 16$). **(B)** Gene expressions of the different S100A alarmins were strongly correlated with each other, Pearson's correlation coefficients > 0.95.

TABLE 3 | Correlation between gene expression analyzed by RNA sequencing or qPCR for S100A8, S100A9 and 5 genes differentially expressed between preterm infants with high or low S100A expression in cord blood monocytes.

Gene	*R*	Slope	*p*-value
S100A8	0.97	1.23	0.0001
S100A9	0.95	1.20	0.0003
ANXA3	1.00	1.09	<0.0001
FCER1G	0.92	1.71	0.0013
FCGR1A	0.94	1.43	0.0005
LMNB1	0.99	1.24	<0.0001
WRN	0.77	0.54	0.0259

N = 8, r, Pearson's correlation coefficient; slope, linear regression coefficient; P, P-values for r.

associated with a different clinical risk profile, with a significantly higher number of small for gestational age (SGA) infants, with lower mean weight for gestational age and a higher proportion of physician-initiated deliveries. Placenta data was missing in six preterm infants, four in the S1000A low group and two in the S100A high group. Only two out of 11 infants with FIRS were found in the low S100A group. Interestingly, one was a twin with a sibling in the S100A high group. Both twins filled criteria for FIRS and exposure to HCA, but differed in degree of neutrophil infiltration.

To further investigate the association between S100A gene expression and risk groups, we identified a set of clinical conditions associated with chorioamnionitis and fetal inflammation, namely PTL/PPROM (spontaneous onset of delivery), HCA, FIRS and elevated CRP/IL-6. We then compared total gene expression between high ($n = 17$) and low ($n = 16$) S100A groups with respect to these clinical conditions. **Figure 3** presents a heat map based on the 500 top DE genes ($q < 0.002$) with added clinical characteristics of the individual infants, showing a clustering of inflammatory features within the S100A high expression group.

In additional analyses of the association between S100A8 and S100A9 monocyte gene expression and clinical characteristics, we found that gene expression of both genes was significantly elevated in association with PTL/PPROM, HCA, FIRS, and elevated IL-6/CRP (**Figure 4**). A similar pattern with significant differences for all clinical groups was seen for S100A12 (data not shown).

Infants in the high S100A group were born at significantly lower gestational age than those in the low S100A group (**Table 4**). To exclude that gestational age in itself could explain differences in S100A expression, a linear regression was performed to adjust for gestational age as a confounding factor. In summary, regression analyses showed that gestational age alone could not explain differences in S100A gene expression between groups (**Supplementary Figure 1**).

TABLE 4 | Clinical data on preterm infants divided by high or low gene expression of S100A alarmins in cord blood monocytes.

	High expression of S100A ($n = 17$)	Low expression of S100A ($n = 16$)	p-value
Gestational age (days), mean (SD)	177 (11)	193 (11)	<0.001
Gestational age (weeks + days), median (range)	25 + 6 (23 + 0 – 27 + 5)	27 + 6 (24 + 6 – 29 + 5)	
Birth weight (g), mean (SD)	825 (220)	1,020 (360)	ns
Boys	14/17 (82.4%)	9/16 (56.2%)	ns
Standard deviation score (SDS) for weight, mean (SD)	−0.047 (0.73)	−1.49 (1.63)	0.02
Small for Gestational Age (SGA)< −2 SD for weight	0/17 (0%)	4/16 (25%)	<0.05
Twin infants	4/17 (23.5%)	6/16 (37.5%)	ns
Preeclampsia	0/17 (0%)	2/16 (12.5%)	ns
Suspected clinical chorioamnionitis	6/17 (35.3%)	5/16 (41.2%)	ns
Antenatal steroids	17/17 (100%)	16/16 (100%)	ns
Preterm Labor (PTL)	7/17 (41.2%)	4/16 (25%)	ns
Preterm Prelabor Rupture of Membranes (PPROM)	10/17 (58.8%)	5/16 (31.2%)	ns
Spontaneous onset of delivery (PTL/PPROM)	17/17 (100%)	9/16 (56.2%)	0.03
Physician-initiated delivery	0/17 (0%)	7/16 (43.8%)	0.03
Delivered by cesarean section	8/17 (47.1%)	12/16 (75%)	ns
Histological chorioamnionitis (HCA)	12/15 (80%)	2/12 (16.7%)	0.002
Fetal Inflammatory Response Syndrome (FIRS)	9/15 (60%)	2/12 (16.7%)	<0.05
Infant elevated CRP and/or IL-6 at birth	5/17 (29.4%)	0/16 (0%)	<0.05
Early onset sepsis (<3 d of age)	1/17 (5.8%)	0/16 (0%)	ns
Late onset sepsis (>3 d of age)	0/14 (0%)	2/14 (14.3%)	ns
Death	1/17 (5.8%)	2/16 (12.5%)	ns
Intraventricular hemorrhage (IVH) grade 3–4	2/17 (11.8%)	3/16 (18.8%)	ns
Necrotizing Enterocolitis (NEC)	2/17 (11.8%)	1/16 (6.2%)	ns
Patent ductus arteriosus (PDA)	11/17 (76.5%)	3/14 (21.4%)	0.03
Chronic Lung Disease (CLD)	8/15 (53.3%)	5/14 (35.7%)	ns

Following normality tests, groups were compared using unpaired t-test or Fisher's Exact Test. Placenta data was not available in all infants and PDA and CLD could only be diagnosed in infants that survived until examination.

High Expression of S100A Alarmins in Cord Blood Monocytes Is Associated With Elevated Inflammatory Proteins in Cord Blood Plasma

To determine if high expression of S100A alarmins was associated also with biochemical markers for inflammation, inflammatory proteins in cord blood plasma were analyzed in relation to alarmin expression. Thirteen out of 77 inflammatory proteins were increased in the high alarmin group as demonstrated in **Figure 5**, $q < 0.049$. The heat map also demonstrates a clear relation between an inflammatory protein pattern and clinical conditions associated with chorioamnionitis and fetal inflammation. In spite of this correlation, the differences between clinical groups regarding elevated inflammatory proteins were less pronounced than for groups with different S100A expression. Eleven out of 77 proteins were elevated in infants with FIRS ($n = 11$) vs. no FIRS ($n = 16$); 10/77 proteins in infants exposed to HCA ($n = 14$) vs. no HCA ($n = 13$); 7/77 in infants with elevated CRP/IL-6 ($n = 5$) vs. infants without elevated markers ($n = 28$) and no significantly elevated proteins were found in cord blood from infants born after spontaneous onset of delivery (PTL/PPROM, $n = 26$) compared with physician-initiated delivery ($n = 7$). Detailed data is found in **Supplementary Table 1**.

Alarmin Proteins Are Elevated in Cord Blood Plasma From Preterm Infants With High Expression of S100A8 and S100A9 Genes in Monocytes and in Association With Spontaneous Onset of Labor, HCA and FIRS

To evaluate alarmin protein levels in preterm vs. term infants and in relation to clinical characteristics in the preterm group, proteins S100A8 and S100A9 were analyzed in cord blood plasma from term infants ($n = 10$) and in all preterm infants where monocyte gene expression was analyzed and with either high ($n = 17$) or low ($n = 16$) S100A8 and S100A9 gene expression. Protein levels were significantly higher in the term vs. the preterm group. Within the preterm group, spontaneous onset of labor (PTL/PPROM), HCA and FIRS were associated with

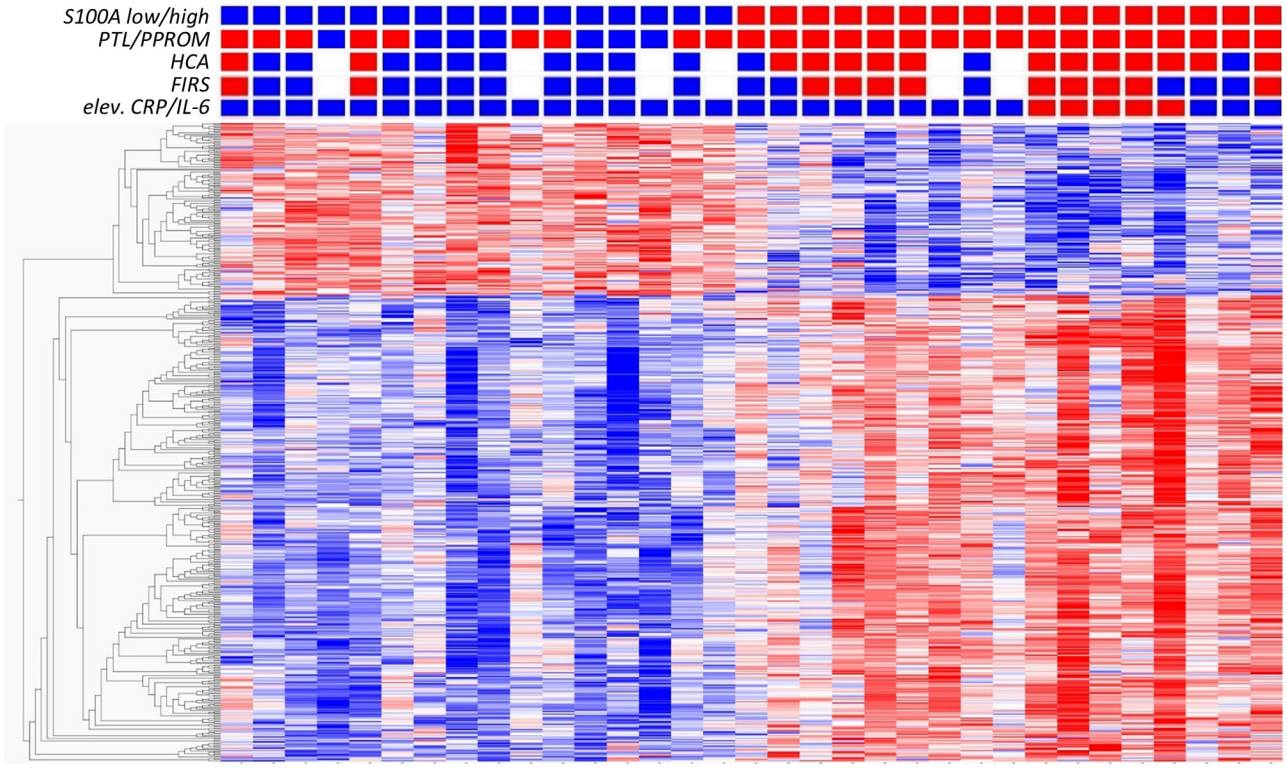

FIGURE 3 | Analysis of gene expression in CD14+ cord blood monocytes in preterm infants based on expression levels of S100A alarmins and in relation to clinical features associated with chorioamnionitis and fetal inflammation. Heat map with hierarchical clustering of top 500 DE genes between high S100A (red squares, $n = 17$) and low S100A (blue squares, $n = 16$) groups ($q < 0.0021$, Qlucore software, multiple *t*-tests with Benajmini-Hochberg multiple correction procedure). Red squares also indicate presence of preterm labor (PTL)/preterm prelabor rupture of membranes (PPROM); exposure to histological chorioamnionitis (HCA), histological fetal inflammatory response syndrome (FIRS) and elevated CRP/IL-6 in cord blood plasma while blue squares indicate the absence of these conditions. White squares indicate missing data. Heatmaps and hierarchical clustering are based on fpkm (fragments per kilobase million) values where each value is normalized to mean = 0 and variance = 1. Red color denotes up-regulation and blue down-regulation within a range of −2 to +2.

elevated S100A8 and S100A9 plasma protein levels. High S100A monocyte gene expression was associated with elevated plasma levels of protein S100A8, while the elevation of protein S100A9 was borderline significant ($p = 0.056$) (**Figure 6**).

Multiple Differentially Expressed Genes and Several Pathways Are Common to Preterm Infants With High Expression of S100A Alarmins and Clinical Features Associated With Chorioamnionitis and Fetal Inflammation

To obtain insight into possible mechanisms affecting preterm monocyte phenotype and function, we further analyzed differentially expressed genes and affected pathways in infants with high vs. low S100A gene expression under various clinical conditions. Out of 1936 DE genes ($q < 0.049$), top 500 DE genes were identified between the two S100A expression groups. Similarly, top 500 DE genes (based on *p*-values) were identified for clinical conditions indicative of inflammatory exposure, namely HCA vs. no HCA; FIRS vs. no FIRS, PTL/PPROM vs. physician-initiated delivery, and laboratory signs of early inflammation (elevated CRP/IL-6) vs. no such signs. When statistical significance was identical for the least regulated DE genes, a cut-off of exactly 500 could not be applied and numbers of DE genes therefore differ slightly between groups. Genes and pathways common to high S100A expression and the clinical conditions are demonstrated in **Figure 7**. In summary, 16–46% of ∼500 top DE genes were common to high S100A groups and groups with different clinical features, with the largest overlap with PTL/PPROM and HCA (**Figure 7A**). A similar pattern was seen for top 50 regulated pathway with 12–52% of pathways common to high S100A groups and groups with different clinical features and the largest overlap was again seen with PTL/PPROM and HCA (**Figure 7B**). The weakest association in both cases was seen for high S100A group and elevated CRP/IL-6 at birth.

To narrow down the number of interesting genes and associated pathways, we excluded elevated CRP/IL-6 (low number of infants, poor overlap with S100A high group) and PTL/PPROM (large overlap with S100A high group but a significant number of infants also in the S100A low group). We conducted further analyses with the S100A high group in relation to HCA and FIRS, two clinical factors that are associated

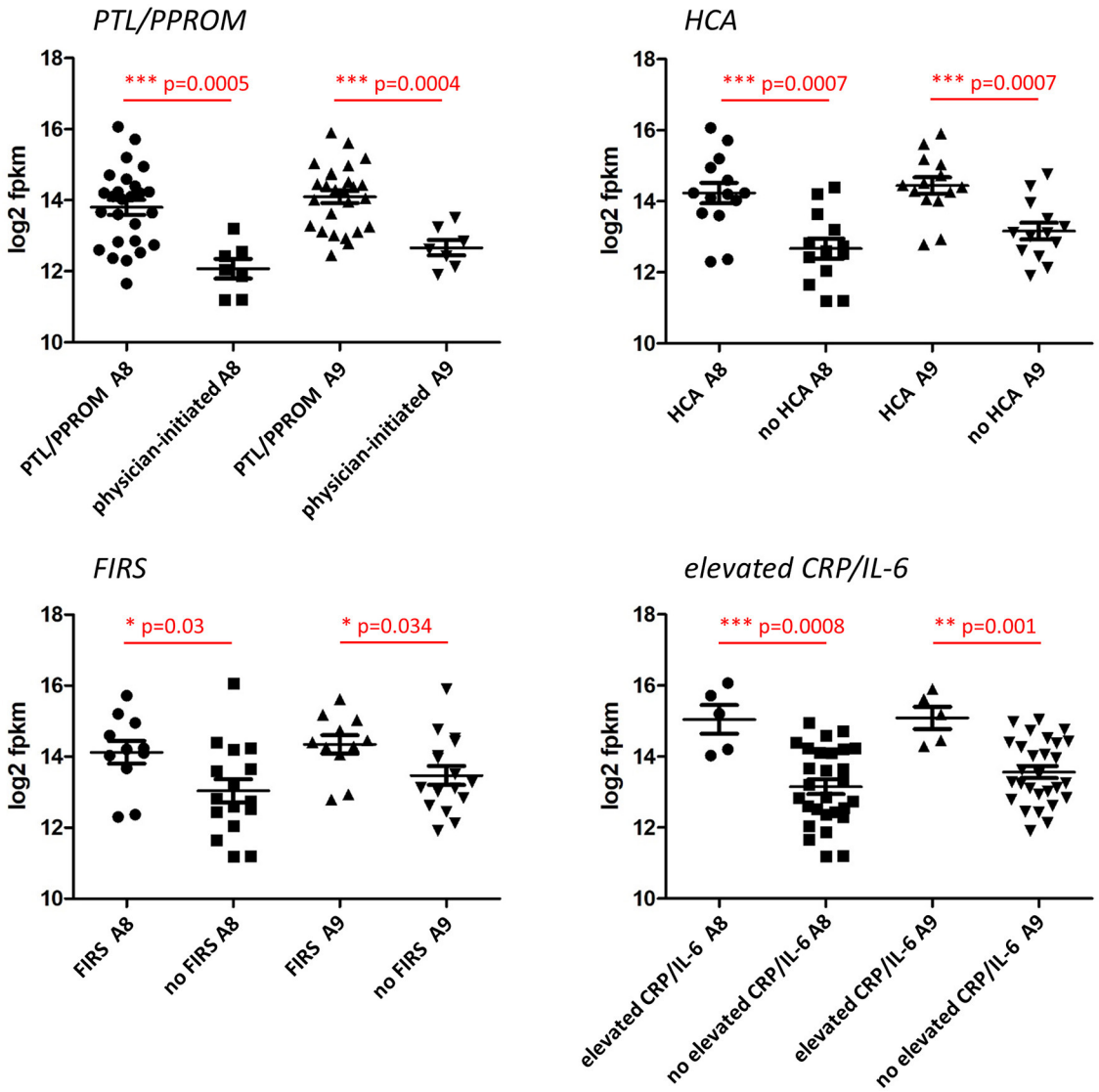

FIGURE 4 | Expression of S100A alarmin genes in CD14+ cord blood monocytes in relation to clinical features associated with chorioamnionitis and fetal inflammation within the preterm group. Monocyte gene expression levels of S100A8 and S100A9 were significantly elevated in association with preterm labor (PTL)/preterm prelabor rupture of membranes (PPROM), exposure to histological chorioamnionitis (HCA), histological fetal inflammatory response syndrome (FIRS) as well as elevated CRP/IL-6 in cord blood plasma (individual samples demonstrated in figure). Data presented as mean ± SEM and compared with unpaired *t*-test for log2-transformed fpkm (fragments per kilobase million) values, *p*-values in figure.

with inflammatory activation in the fetus as well as neonatal morbidity and outcome. Our analyses revealed that 124 DE genes and 18 affected pathways were common to all three groups (**Figures 7C,D**). Genes are listed in **Table 5** and pathways with select references in **Table 6**. Further details for the 124 DE genes including fold change and fpkm levels are provided in **Supplementary Table 4**. In summary, affected pathways were largely inflammatory and associated with cytokine/chemokine signaling, chemotaxis and leukocyte trafficking as well as phagocytosis. Some of these 18 pathways were common to those affected by preterm vs. term birth, including pathways associated RhoA GTPases.

Network Analysis Show That S100A8 and S100A9 Are Hub Genes in a Network Based on Genes Common to High S100A, FIRS and HCA and With Strong Correlation to Clinical Inflammatory Conditions

For co-expression network analyses, we obtained 13 modules with sizes between 205 and 2,290 genes. The heatmap plot showing the correlation and significance of the eigengenes in relation to S100A expression and relevant clinical conditions is shown in **Figure 8A**. Of the modules identified, the red module was negatively correlated, and the green and

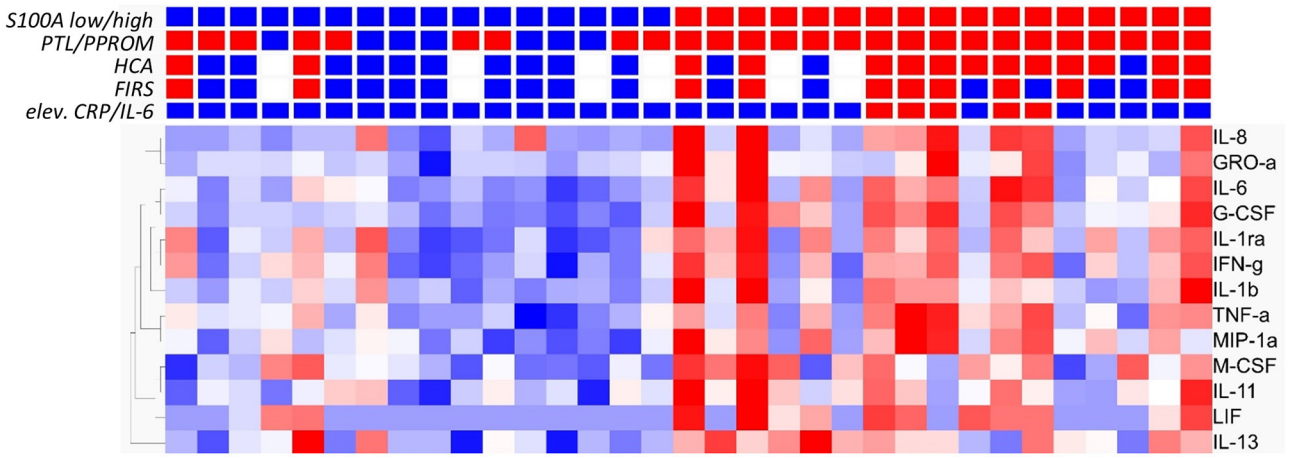

FIGURE 5 | Analysis of inflammatory proteins in cord blood plasma from preterm infants based on expression levels of S100A alarmins and in relation to clinical features associated with chorioamnionitis and fetal inflammation. Heat map with hierarchical clustering demonstrates significant elevation of 13/77 inflammatory proteins analyzed by Multiplex ELISA in S100A high (red squares, $n = 17$) and S100A low (blue squares, $n = 16$) groups ($q \leq 0{,}049$, multiple t-tests with Benajmini-Hochberg multiple correction procedure). Red squares also indicate presence of preterm labor (PTL)/preterm prelabor rupture of membranes (PPROM); exposure to histological chorioamnionitis (HCA), histological fetal inflammatory response syndrome (FIRS) and elevated CRP/IL-6 in cord blood plasma while blue squares indicate the absence of these conditions. White squares indicate missing data. Heatmaps and hierarchical clustering are based on fpkm fragments per kilobase million) values where each value is normalized to mean = 0 and variance = 1. Red color denotes up-regulation and blue down-regulation within a range of −2 to +2.

the yellow modules were positively correlated with high S100A expression as well as PTL/PPROM, HCA, FIRS and elevated CRP/IL-6. In addition, 21 of the 124 DE genes we previously identified as common to FIRS, HCA and high S100A expression were identified as hub genes when considering all modules.

As S100A8, S100A9, and S100A12 genes were all found in the yellow module, this module was studied in further detail. The yellow module also showed the highest correlation with S100A expression in monocytes (**Figure 8A**). This module consisted of a total 836 genes and 41 of them were identified as hub genes within the module. The yellow module was to the greatest extent enriched with the 124 DE genes common to high S100A expression, HCA, and FIRS. 73/124 genes (58.9%) were found within the 836 genes of the module and 13/124 genes were among the 41 hub genes. S100A8 and S100A9 were identified as hub genes, while S100A12 was not.

Visualization of the network within the yellow module (**Figure 8B**) shows that S100A8 and S100A9 are major hubs with connectivities of 78 and 77, respectively. The other major hub nodes in this module are ANXA3, CYSTM1, B4GALT5, and GCA with connectivities of 98 96, 88, and 83, respectively. A list of hub genes for the yellow module is presented in **Supplementary Table 5**.

Gene Ontology enrichment for all the genes in the yellow module showed that these genes are highly relevant to inflammatory and leukocyte activation processes (**Supplementary Table 6**). The GO enrichment analysis made only for the hub genes showed similar enrichment with inflammation and immunity-related processes (data not shown).

DISCUSSION

In this study we found that gene expression of S100A alarmins in cord blood monocytes was associated with specific monocyte phenotypes characterized by their associations to inflammatory pathways and strong correlations to clinically relevant conditions. S100A alarmin genes were significantly up-regulated in preterm infants with exposure to chorioamnionitis, a fetal inflammatory response and gene expression changes associated with inflammatory pathways. In contrast, low S100A expression in preterm infants was associated with a clinical risk profile of SGA infants and a high proportion of physician-initiated deliveries.

In our first analyses, we found that gene expression in cord blood monocytes significantly differed between preterm and term infants and that the differences could largely be attributed to genes associated with inflammatory pathways. In addition to up-regulated genes and inflammatory proteins in the preterm vs. the term group, there was also a large variability of gene expression as well as inflammatory protein profiles within the preterm group, suggesting different patterns of inflammatory activation. This is in accordance with previous findings from global transcriptome analyses of cord blood monocytes where differences between term and preterm groups were accentuated in the presence of HCA in the preterm group (20). The number of genes that were differentially expressed between term and preterm infants was, however, 10-fold lower than in our study even when term and HCA-exposed preterm infants were compared (20). This may be explained by differences in analyses methods including the use of frozen and cultured vs. directly isolated monocytes in our study, but also by the fact that our study included a larger

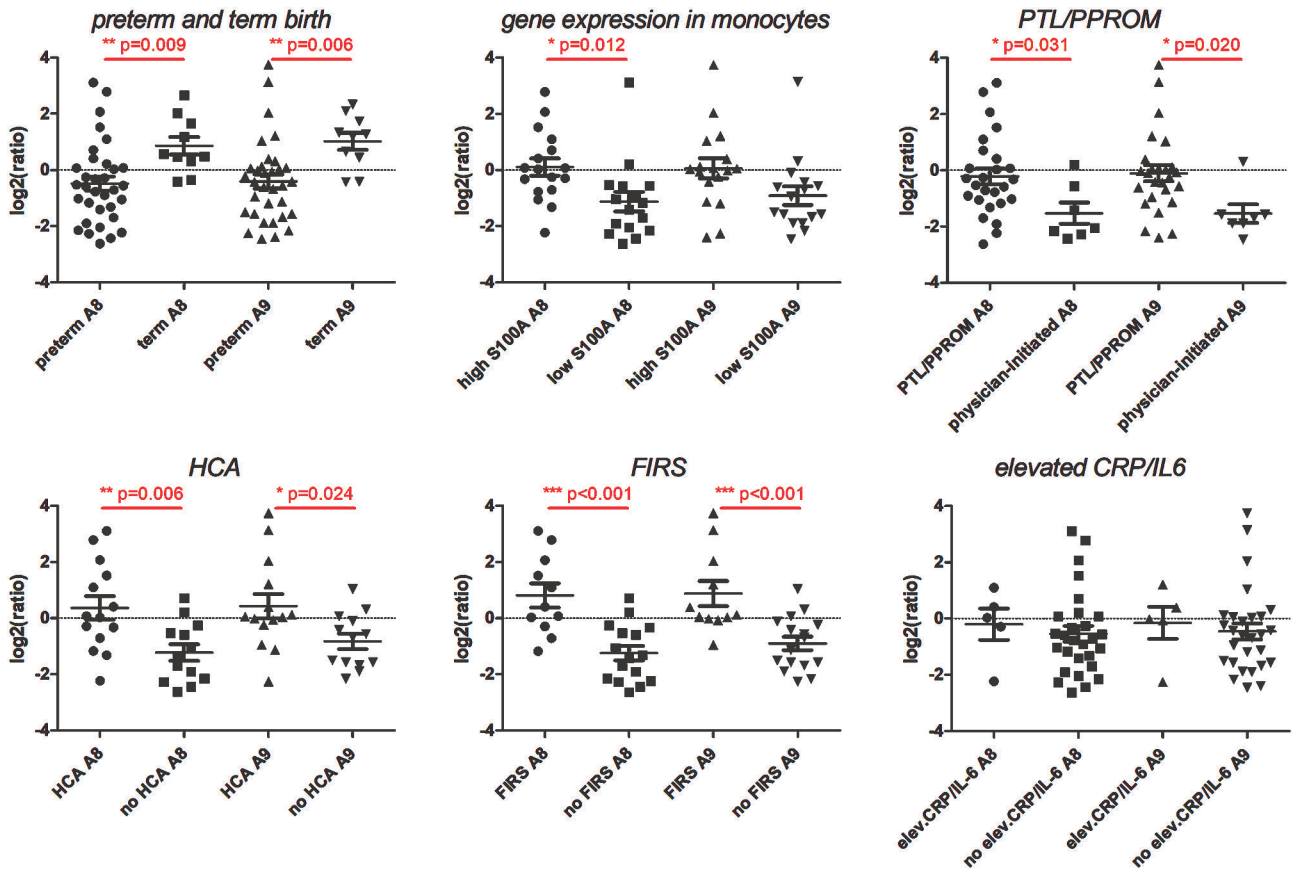

FIGURE 6 | S100A8 and S100A9 proteins in cord blood plasma in preterm and term newborns and in relation to S100A gene expression and clinical features associated with chorioamnionitis and fetal inflammation within the preterm group. Plasma protein levels of S1000A8 and S100A9 were analyzed by mass-spectrometry and relative concentrations were compared between groups. The first panel shows that term infants ($n = 10$) had significantly higher levels than preterm infants ($n = 33$). The remaining panels all refer to differences in plasma protein levels within the preterm group. Elevated plasma protein levels were seen in infants with high ($n = 17$) compared with low ($n = 16$) S100A8 and S100A9 gene expression. Preterm labor (PTL)/preterm prelabor rupture of membranes (PPROM), histological chorioamnionitis (HCA), and histological fetal inflammatory response syndrome (FIRS) were also associated with increased protein levels, while exposure to elevated CRP/IL-6 in cord blood plasma was not (individual samples demonstrated in figure). Data presented as mean ± SEM and compared with unpaired *t*-test for log2-transformed relative concentrations of S100A8 and S100A9 proteins, *p*-values in figure.

number of infants (33 preterm and 10 term vs. 11 preterm and 4 term) born at lower gestational ages (23–30 vs. 29–32 weeks) (20). The variable inflammatory protein profiles within the preterm group are also likely to reflect differences in prenatal exposure to infection or inflammation as previous studies show a significant association between inflammatory markers in cord blood and histological findings of HCA and, in particular, FIRS (10, 11, 51).

To identify monocyte gene expression associated with clinical and biochemical inflammatory signs within the preterm group, we investigated gene expression of alarmins S100A8, S100A9, and S100A12. We found an increased and highly correlated expression of all three genes in the preterm group with a variability suggesting association to different inflammatory patterns. In spite of a relatively small study group and an arbitrary cut-off based on median expression of S100A8 and S100A9 only, we found a strong correlation between S100A gene expression and clinical conditions that are associated with chorioamnionitis and fetal inflammation. As discussed below, there are numerous studies of S100A protein levels but, to our knowledge, this is the first study linking differences in monocyte S100A alarmin expression to a specific clinical inflammatory syndrome.

Identifying preterm infants with an increased risk of inflammation-related injury is of great importance in the clinical setting. Histological signs of HCA, and FIRS in particular, are associated with severe neonatal morbidities (12–14) as well as brain injury (11, 15) and neurodevelopmental sequels (11, 15). In addition, spontaneous onset of delivery has been related to preterm cerebral palsy (52) and elevated inflammatory markers in cord blood has been related not only to early onset sepsis but also to brain injury (11) and poor neurodevelopmental outcome (53). Characterizing the fetal immune response associated with exposure to chorioamnionitis and fetal inflammation is important to identify infants at risk for inflammatory injury and distinguish them from infants with other risk profiles and different mechanisms of injury. Remarkably, S100A8/A9 monocyte gene expression, with an arbitrary cut-off defined as

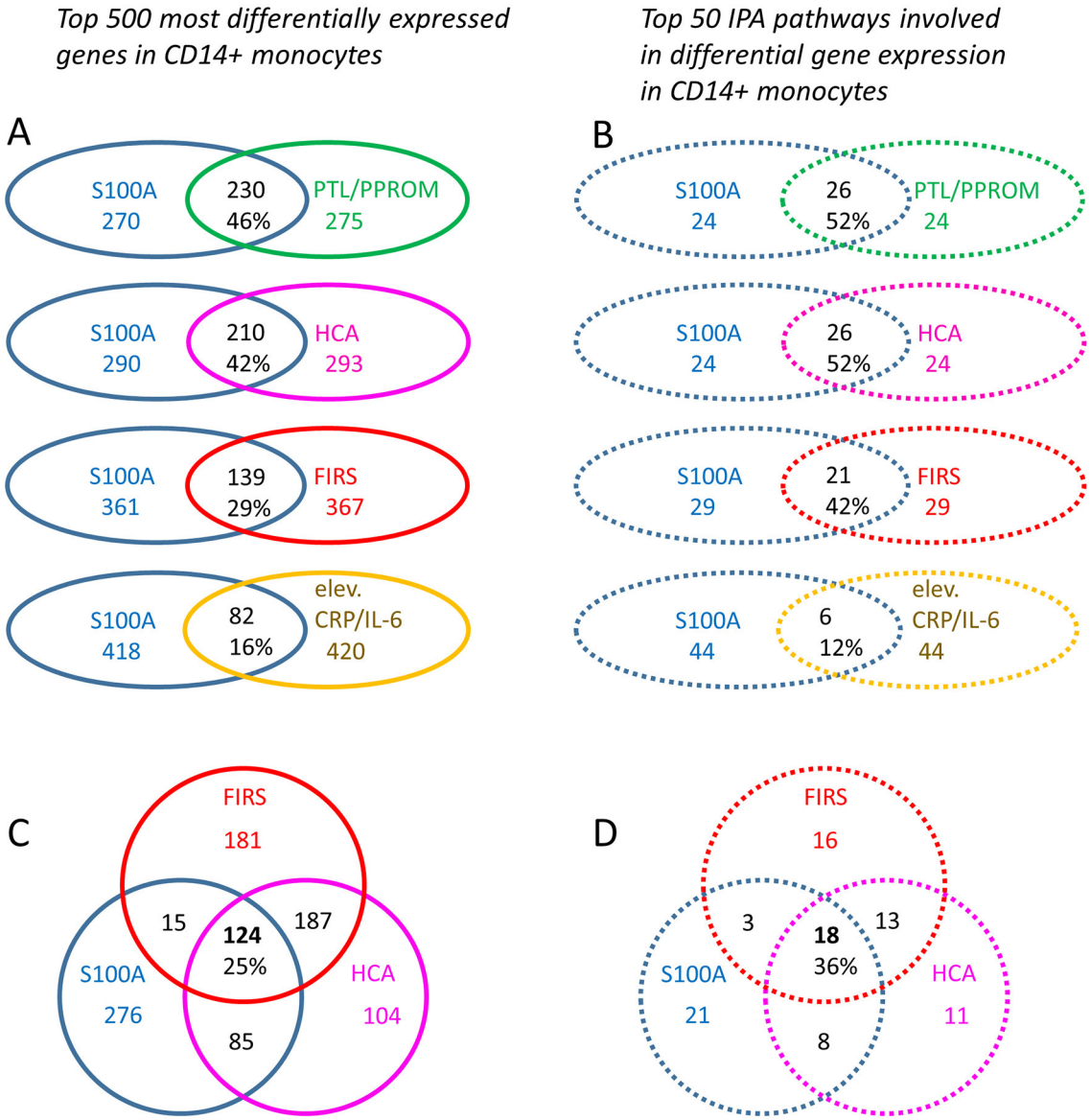

FIGURE 7 | Differentially expressed monocyte genes and affected IPA pathways common to high monocyte S100A alarmin gene expression and clinical features associated with chorioamnionitis and a fetal inflammatory response in preterm infants. Top 500 differentially expressed (DE) genes (based on *p*-values) **(A)** and top 50 affected IPA pathways **(B)** were identified for each clinical grouping parameter. Common genes and pathways for the S100 high group in relation to HCA and FIRS are shown in **(C)** and **(D)**, respectively. When statistical significance was identical for the least regulated DE genes, a cut-off of exactly 500 could not be applied and numbers of DE genes may therefore differ slightly between groups. S100A high vs. low gene expression (500 genes, $p < 0.0001$, blue outline), presence of preterm labor (PTL)/preterm prelabor rupture of membranes (PPROM) (505 genes, $p < 0.003$, green outline); exposure to histological chorioamnionitis (HCA) (503 genes, $p < 0.002$, violet outline); histological fetal inflammatory response syndrome (FIRS) (502 genes, $p < 0.0006$, red outline); and elevated CRP/IL-6 in cord blood (506 genes, $p < 0.013$, yellow outline). The Venn diagrams demonstrate numbers and percentages for overlapping genes and pathways.

above median of the preterm group, correctly identified 87% of HCA and 82% of FIRS exposed infants. In addition, all mothers in the S100A high group had spontaneous onset of delivery (PTL/PPROM) and all infants with clinically relevant elevation of CRP and/or IL-6 had high expression of S100A alarmins. Similarly, infants with the most pronounced pro-inflammatory protein profiles were found in the S100A high group. Equally important, infants with risk factors not related to inflammation (poor fetal growth, physician-initiated delivery due to maternal conditions or fetal compromise) were largely found in the low S100A group. This suggests that transcription of S100A defines a monocyte phenotype closely related to clinically defined risk factors.

In our study, single cases of HCA and FIRS were not correctly classified by S100A gene expression. This may be explained by the choice of cut-off value or by factors related to classification

TABLE 5 | Differentially expressed genes in cord blood monocytes common to high expression of S100A alarmins as well as HCA and FIRS ($n = 124$).

Gene symbol	Official full name	Aliases	Corresponding protein function
ACSS2	Acyl-CoA synthetase short chain family member 2	ACAS2, ACECS, ACS, ACSA, AceCS1, dJ1161H23.1	A cytosolic enzyme that catalyzes the activation of acetate for use in lipid synthesis and energy generation
ACTR3	Actin related protein 3	ARP3	A major constituent of the ARP2/3 complex
ADAM10	ADAM metallopeptidase domain 10	AD10, AD18, CD156c, CDw156, HsT18717, MADM, RAK, kuz	An ADAM family member that cleaves many proteins including TNF-alpha and E-cadherin
ADCK3	Coenzyme Q8A	COQ8A; ARCA2, CABC1, COQ10D4, COQ8, SCAR9	A mitochondrial protein similar to yeast ABC1, which functions in an electron-transferring membrane protein complex in the respiratory chain
AKAP1	A-kinase anchoring protein 1	AKAP21, AKAP149, AKAP84, D-AKAP1, PPP1R43, PRKA1, SAKAP84, TDRD17, AKAP1	A member of the AKAP family, binds to type I and type II regulatory subunits of PKA and anchors them to the mitochondrion
ALOX5	Arachidonate 5-lipoxygenase	5-LO, 5-LOX, 5LPG, LOG5	A member of the lipoxygenase gene family, plays a dual role in the synthesis of leukotrienes from arachidonic acid
ASGR2	Asialoglycoprotein receptor 2	ASGP-R2, ASGPR2, CLEC4H2, HBXBP, HL-2	A subunit of the asialoglycoprotein receptor
ATP6V0D1	ATPase H+ transporting V0 subunit d1	ATP6D, ATP6DV, P39, VATX, VMA6, VPATPD	A component of vacuolar ATPase (V-ATPase)
B4GALT5	Beta-1,4-galactosyltransferase 5	B4Gal-T5, BETA4-GALT-IV, beta4Gal-T5, beta4GalT-V, gt-V	Type II membrane-bound glycoproteins that appear to have exclusive specificity for the donor substrate UDP-galactose
BATF	Basic leucine zipper ATF-like transcription factor	B-ATF1, SFA-2, SFA2, BATF	A nuclear basic leucine zipper protein that belongs to the AP-1/ATF superfamily of transcription factors
BTAF1	B-TFIID TATA-box binding protein associated factor 1	MOT1, TAF(II)170, TAF172, TAFII170	A TAF (TATA box-binding protein-associated factor), which associates with TBP (TATA box-binding protein) to form the B-TFIID complex that is required for transcription initiation of genes by RNA polymerase II
C17orf62	Cytochrome b-245 chaperone 1	CYBC1, Eros	–
C9orf84	Shortage in chiasmata 1	SHOC1; ZIP2; MZIP2; ZIP2H	–
CALM3	Calmodulin 3	CALM, CAM1, CAM2, CAMB, CaM, CaMIII, HEL-S-72, PHKD, PHKD3	A member of a family of proteins that binds calcium and functions as a enzymatic co-factor
CAMK2D	Calcium/calmodulin dependent protein kinase II delta	CAMKD	A member of the serine/threonine protein kinase family and the Ca(2+)/calmodulin-dependent protein kinase subfamily
CARS	Cysteinyl-tRNA synthetase 1	CARS1, CYSRS, MGC:11246	A class 1 aminoacyl-tRNA synthetase, cysteinyl-tRNA synthetase
CD177	CD177 molecule	HNA-2a, HNA2A, NB1, NB1 GP, PRV-1, PRV1	A glycosyl-phosphatidylinositol (GPI)-linked cell surface glycoprotein that plays a role in neutrophil activation
CD63	CD63 molecule	LAMP-3, ME491, MLA1, OMA81H, TSPAN30	A member of the transmembrane 4 superfamily, also known as the tetraspanin family, the encoded protein is a cell surface glycoprotein that is known to complex with integrins
CEACAM1	CEA cell adhesion molecule 1	BGP, BGP1, BGPI	A member of the carcinoembryonic antigen (CEA) gene family, which belongs to the immunoglobulin superfamily, mediates cell adhesion via homophilic as well as heterophilic binding to other proteins of the subgroup
CEACAM3	CEA cell adhesion molecule 3	CD66D, CEA, CGM1, W264, W282	A member of the family of carcinoembryonic antigen-related cell adhesion molecules (CEACAMs)
CFL1	Cofilin 1	CFL, HEL-S-15, cofilin	An intracellular actin-modulating protein that binds and depolymerizes filamentous F-actin and inhibits the polymerization of monomeric G-actin in a pH-dependent manner
CHMP2A	Charged multivesicular body protein 2A	BC-2, BC2, CHMP2, VPS2, VPS2A	Protein belongs to the chromatin-modifying protein/charged multivesicular body protein (CHMP) family
CNNM3	Cyclin and CBS domain divalent metal cation transport mediator 3	ACDP3	–
CPSF2	Cleavage and polyadenylation specific factor 2	CPSF100	–

(Continued)

TABLE 5 | Continued

Gene symbol	Official full name	Aliases	Corresponding protein function
CR1	Complement C3b/C4b receptor 1 (Knops blood group)	C3BR, C4BR, CD35, KN	A member of the receptors of complement activation (RCA) family, a monomeric single-pass type I membrane glycoprotein, mediates cellular binding to particles and immune complexes that have activated complement
CREB5	cAMP responsive element binding protein 5	CRE-BPA, CREB-5, CREBPA	Belongs to the CRE (cAMP response element)-binding protein family containing zinc-finger and bZIP DNA-binding domains, functions as a CRE-dependent trans-activator
CSF2RB	Colony stimulating factor 2 receptor beta common subunit	CD131, CDw131, IL3RB, IL5RB, SMDP5, betaGMR	A common beta chain of the high affinity receptor for IL-3, IL-5, and CSF
CYSTM1	Cysteine rich transmembrane module containing 1	C5orf32, ORF1-FL49	–
DOK3	Docking protein 3	DOKL	–
DYRK2	Dual specificity tyrosine phosphorylation regulated kinase 2		Belongs to a family of protein kinases whose members are presumed to be involved in cellular growth and/or development
EIF2AK4	Eukaryotic translation initiation factor 2 alpha kinase 4	GCN2, PVOD2	A member of a family of kinases that phosphorylate the alpha subunit of eukaryotic translation initiation factor-2 (EIF2), resulting in the downregulaton of protein synthesis
ERI1	Exoribonuclease 1	3′HEXO, HEXO, THEX1	–
EXOC6	Exocyst complex component 6	EXOC6A, SEC15, SEC15L, SEC15L1, SEC15L3, Sec15p	Similar to the yeast gene product, which is essential for vesicular traffic from the Golgi apparatus to the cell surface, one of the components of a multiprotein complex required for exocytosis
EXOC7	Exocyst complex component 7	2-5-3p, BLOM4, EX070, EXO70, EXOC1, Exo70p, YJL085W	A component of the exocyst complex, is required for assembly of the exocyst complex and docking of the complex to the plasma membrane
FAM109A	PH domain containing endocytic trafficking adaptor 1	PHETA1; SES1; IPIP27A	A protein that localizes to the endosome and interacts with inositol polyphosphate 5-phosphatase OCRL-1
FAM151B	Family with sequence similarity 151 member B	UNQ9217	–
FAM20A	FAM20A golgi associated secretory pathway pseudokinase	AI1G, AIGFS, FP2747	A protein that is likely secreted and may function in hematopoiesis
FCER1G	Fc fragment of IgE receptor Ig	FCRG	A high affinity IgE receptor
FCGR1A	Fc fragment of IgG receptor Ia	CD64, CD64A, FCRI, IGFR1	A high-affinity Fc-gamma receptor
FCGR1B	Fc fragment of IgG receptor Ib	CD64b, FCG1, FCGR1, FCGR1A, FcRI, FcgammaRIa, IGFR1, IGFRB	A low affinity FcgammaRIB receptor that may play an important role in humoral immune response
FCGR1C	Fc fragment of IgG receptor Ic, pseudogene	FCGR1CP; CD64c; FCRIC; IGFR1; IGFRC	–
FKBP1A	FKBP prolyl isomerase 1A	FKBP-12, FKBP-1A, FKBP1, FKBP12, PKC12, PKCI2, PPIASE	A member of the immunophilin protein family, which play a role in immunoregulation and basic cellular processes involving protein folding and trafficking
FNDC3B	Fibronectin type III domain containing 3B	FAD104, PRO4979, YVTM2421	–
FXN	Frataxin	CyaY, FA, FARR, FRDA, X25	A mitochondrial protein which belongs to the FRATAXIN family, participates in regulating mitochondrial iron transport and respiration
GBA	Glucosylceramidase beta	GBA1, GCB, GLUC	A lysosomal membrane protein that cleaves the beta-glucosidic linkage of glycosylceramide
GFRA2	GDNF family receptor alpha 2	GDNFRB, NRTNR-ALPHA, NTNRA, RETL2, TRNR2	A member of the GDNF receptor family, a glycosylphosphatidylinositol(GPI)-linked cell surface receptor for GDNF and NTN, mediates activation of the RET tyrosine kinase receptor
GK	Glycerol kinase	GK1D, GK	Protein belongs to the FGGY kinase family, it is a key enzyme in the regulation of glycerol uptake and metabolism
GNG5	G protein subunit gamma 5		A member of a family of G proteins
GPR84	G protein-coupled receptor 84	EX33, GPCR4	–
GTF2A2	General transcription factor IIA subunit 2	HsT18745, T18745, TF2A2, TFIIA, TFIIA-12, TFIIA-gamma, TFIIAS	Factor for transcription initiation on TATA-containing class II genes

(Continued)

TABLE 5 | Continued

Gene symbol	Official full name	Aliases	Corresponding protein function
GUSBP3	GUSB pseudogene 3	GUSBP1, SMA3	–
HCK	HCK proto-oncogene, Src family tyrosine kinase	JTK9, p59Hck, p61Hck	A member of the Src family of tyrosine kinases. This protein is primarily hemopoietic, particularly in cells of the myeloid and B-lymphoid lineages
HDAC1	Histone deacetylase 1	GON-10, HD1, KDAC1, RPD3, RPD3L1	Belongs to the histone deacetylase/acuc/apha family and is a component of the histone deacetylase complex
HSD3B7	Hydroxy-delta-5-steroid dehydrogenase, 3 beta- and steroid delta-isomerase 7	CBAS1, PFIC4, SDR11E3	A member of the short-chain dehydrogenase/reductase superfamily
IFNAR1	Interferon alpha and beta receptor subunit 1	AVP, IFN-alpha-REC, IFNAR, IFNBR, IFRC	A type I membrane protein that forms one of the two chains of a receptor for interferons alpha and beta
IGSF6	Immunoglobulin superfamily member 6	DORA	–
IL4R	Interleukin 4 receptor	CD124, IL-4RAA, IL4R	Encodes the alpha chain of the interleukin-4 receptor, a type I transmembrane protein that can bind interleukin 4 and interleukin 13
ITGB2	Integrin subunit beta 2	CD18, LAD, LCAMB, LFA-1, MAC-1, MF17, MFI7	An integrin beta chain, which combines with multiple different alpha chains to form different integrin heterodimers
JAK3	Janus kinase 3	JAK-3_HUMAN, JAKL, L-JAK, LJAK, JAK3	A member of the Janus kinase (JAK) family of tyrosine kinases involved in cytokine receptor-mediated intracellular signal transduction
KDM1A	Lysine demethylase 1A	AOF2, BHC110, CPRF, KDM1, LSD1	A nuclear protein containing a SWIRM domain, a FAD-binding motif, and an amine oxidase domain. This protein silences genes by functioning as a histone demethylase
KREMEN1	Kringle containing transmembrane protein 1	ECTD13, KREMEN, KRM1	A high-affinity dickkopf homolog 1 (DKK1) transmembrane receptor that functionally cooperates with DKK1 to block wingless (WNT)/beta-catenin signaling
L3MBTL3	L3MBTL histone methyl-lysine binding protein 3	MBT-1, MBT1	A member of the malignant brain tumor (MBT) family of chromatin interacting transcriptional repressors, is associated with the repression of gene expression
LAMTOR2	Late endosomal/lysosomal adaptor, MAPK and MTOR activator 2	ENDAP, HSPC003, MAPBPIP, MAPKSP1AP, ROBLD3, Ragulator2, p14	Protein with suggested role in endosomal biogenesis
LCP1	Lymphocyte cytosolic protein 1	CP64, HEL-S-37, L-PLASTIN, LC64P, LPL, PLS2	A member of a family of actin-binding proteins plastins
LGALS1	Galectin 1	GAL1, GBP	A protein from a family of beta-galactoside-binding proteins implicated in modulating cell-cell and cell-matrix interactions
LIMK2	LIM domain kinase 2		Belongs to a small subfamily of LIM proteins with 2 N-terminal LIM motifs and a C-terminal protein kinase domain, phosphorylates cofilin, inhibiting its actin-depolymerizing activity
LITAF	Lipopolysaccharide induced TNF factor	PIG7, SIMPLE, TP53I7	Lipopolysaccharide-induced TNF-alpha factor, which is a DNA-binding protein and can mediate the TNF-alpha expression by direct binding to the promoter region of the TNF-alpha gene
LMNB1	Lamin B1	ADLD, LMN, LMN2, LMNB	B-type lamin protein, is a component of the nuclear lamina
LUC7L	LUC7 like	LUC7B1, Luc7, SR+89, hLuc7B1	–
MAP3K14-AS1	MAP3K14 antisense RNA 1		
MAP4K1	Mitogen-activated protein kinase kinase kinase kinase 1	HPK1	–
MARVELD1	MARVEL domain containing 1	GB14, MARVD1, MRVLDC1, bA548K23.8	–
METTL7B	Methyltransferase like 7B	ALDI	–
MILR1	Mast cell immunoglobulin like receptor 1	Allergin-1, C17orf60, MCA-32, MCA32	–

(Continued)

TABLE 5 | Continued

Gene symbol	Official full name	Aliases	Corresponding protein function
MRPL28	Mitochondrial ribosomal protein L28	MAAT1, p15	A 39S subunit protein, belongs to mitochondrial ribosomal proteins
MTR	5-methyltetrahydrofolate-homocysteine methyltransferase	HMAG, MS, cblG	5-methyltetrahydrofolate-homocysteine methyltransferase, catalyzes the final step in methionine biosynthesis
MTRR	5-methyltetrahydrofolate-homocysteine methyltransferase reductase	MSR, cblE	A member of the ferredoxin-NADP(+) reductase (FNR) family of electron transferases, functions in the synthesis of methionine by regenerating methionine synthase to a functional state
MYO10	Myosin X		A member of the myosin superfamily, represents an unconventional myosin
MYO7B	Myosin VIIB		Is involved in linking protocadherins to the actin cytoskeleton and is essential for proper microvilli function
NCF4	Neutrophil cytosolic factor 4	CGD3, NCF, P40PHOX, SH3PXD4	A cytosolic regulatory component of the superoxide-producing phagocyte NADPH-oxidase
PART1	Prostate androgen-regulated transcript 1	NCRNA00206	–
PIK3AP1	Phosphoinositide-3-kinase adaptor protein 1	BCAP	–
PIK3IP1	Phosphoinositide-3-kinase interacting protein 1	HGFL, TrIP, hHGFL(S)	–
PIM1	Pim-1 proto-oncogene, serine/threonine kinase	PIM	The protein encoded by this gene belongs to the Ser/Thr protein kinase family, and PIM subfamily. It plays a role in signal transduction in blood cells, contributing to both cell proliferation and survival
PLB1	Phospholipase B1	PLB, PLB/LIP	A membrane-associated phospholipase that displays lysophospholipase and phospholipase A2 activities through removal of sn-1 and sn-2 fatty acids of glycerophospholipids
PLSCR1	Phospholipid scramblase 1	MMTRA1B	–
PLXNC1	Plexin C1	CD232, PLXN-C1, VESPR	A member of the plexin family of transmembrane receptors for semaphorins
POLR1E	RNA polymerase I subunit E	PAF53, PRAF1	–
PPM1M	Protein phosphatase, Mg2+/Mn2+ dependent 1M	PP2C-eta, PP2CE, PP2Ceta	–
PPP1R18	Protein phosphatase 1 regulatory subunit 18	HKMT1098, KIAA1949	Protein phosphatase-1 interacts with regulatory subunits that target the enzyme to different cellular locations and change its activity toward specific substrates
PSMB7	Proteasome 20S subunit beta 7	Z	A member of the proteasome B-type family, it is a 20S core beta subunit in the proteasome
PTPN2	Protein tyrosine phosphatase non-receptor type 2	PTN2, PTPT, TC-PTP, TCELLPTP, TCPTP	A member of the protein tyrosine phosphatase (PTP) family known to be signaling molecules that regulate cell growth, differentiation, mitotic cycle, and oncogenic transformation
RAB31	RAB31, member RAS oncogene family	Rab22B	A small GTP-binding protein of the RAB family, participates in vesicle and granule targeting
RGL4	Ral guanine nucleotide dissociation stimulator like 4	Rgr	A protein similar to guanine nucleotide exchange factor Ral guanine dissociation stimulator
RHBDD2	Rhomboid domain containing 2	NPD007, RHBDL7	A member of the rhomboid family of membrane-bound proteases
RHOG	Ras homolog family member G	ARHG	A member of the Rho family of small GTPases, which cycle between inactive GDP-bound and active GTP-bound states and function as molecular switches in signal transduction cascades
S100A11	S100 calcium binding protein A11	HEL-S-43, MLN70, S100C	A member of the S100 family of proteins containing 2 EF-hand calcium-binding motifs
SBNO2	Strawberry notch homolog 2	KIAA0963, SNO, STNO	–
SERPINA1	Serpin family A member 1	A1A, A1AT, AAT, PI, PI1, PRO2275, alpha1AT, nNIF	A serine protease inhibitor whose targets include elastase, plasmin, thrombin, trypsin, chymotrypsin, and plasminogen activator

(Continued)

TABLE 5 | Continued

Gene symbol	Official full name	Aliases	Corresponding protein function
SIPA1L2	Signal induced proliferation associated 1 like 2	SPAL2, SPAR2	A member of the signal-induced proliferation-associated 1 like family containing a GTPase activating domain, a PDZ domain and a C-terminal coiled-coil domain with a leucine zipper
SLC2A3	Solute carrier family 2 member 3	GLUT3	–
SNX20	Sorting nexin 20	SLIC1	–
SRF	Serum response factor	MCM1	A member of the MADS box superfamily of transcription factors, stimulates both cell proliferation and differentiation
SRP14	Signal recognition particle 14	ALURBP	–
ST3GAL2	ST3 beta-galactoside alpha-2,3-sialyltransferase 2	Gal-NAc6S, SIAT4B, ST3GALII, ST3GalA.2	A type II membrane protein that catalyzes the transfer of sialic acid from CMP-sialic acid to galactose-containing substrates
TCAIM	T cell activation inhibitor, mitochondrial	TOAG1; TOAG-1; C3orf23	–
TESC	Tescalcin	CHP3, TSC	–
TMBIM6	Transmembrane BAX inhibitor motif containing 6	BAXI1, BI-1, TEGT	–
TMEM117	Transmembrane protein 117		–
TMEM120A	Transmembrane protein 120A	NET29, TMPIT	–
TNFRSF1A	TNF receptor superfamily member 1A	CD120a, FPF, TBP1, TNF-R, TNF-R-I, TNF-R55, TNFAR, TNFR1, TNFR55, TNFR60, p55, p55-R, p60	A member of the TNF receptor superfamily of proteins
TPRKBP2	TP53RK binding protein pseudogene 2		–
TYSND1	Trypsin domain containing 1	NET41	A protease that removes the N-terminal peroxisomal targeting signal (PTS2) from proteins produced in the cytosol, thereby facilitating their import into the peroxisome
UBE2L3	Ubiquitin conjugating enzyme E2 L3	E2-F1, L-UBC, UBCH7, UbcM4	A member of the E2 ubiquitin-conjugating enzyme family, participates in ubiquitination of proteins
UFD1L	Ubiquitin recognition factor in ER associated degradation 1	UFD1L	The encoded protein forms a complex with nuclear protein localization-4 and valosin-containing protein, and this complex is necessary for the degradation of ubiquitinated proteins
URB1	URB1 ribosome biogenesis homolog	C21orf108, NPA1	–
WDFY3	WD repeat and FYVE domain containing 3	ALFY, BCHS, MCPH18, ZFYVE25	A phosphatidylinositol 3-phosphate-binding protein that functions as a master conductor for aggregate clearance by autophagy
WDFY3-AS1	WDFY3 antisense RNA 1		ncRNA
WDR59	WD repeat domain 59	CDW12, FP977, p90-120	–
VOPP1	VOPP1 WW domain binding protein	ECOP, GASP, WBP1L2	–
ZBTB41	Zinc finger and BTB domain containing 41	FRBZ1, ZNF924	–
ZNF337	Zinc finger protein 337		A zinc finger domain containing protein
ZNF438	Zinc finger protein 438		–
ZNF529	Zinc finger protein 529		–

Lists of differentially expressed genes were created using Qlucore Omics Explorer v3.4. Description of the genes (Gene Official Full Name, Aliases, info about corresponding protein transcript) are adapted from Gene ncbi database https://www.ncbi.nlm.nih.gov/gene/.

and severity of the intrauterine infection/inflammation. We have not related our findings to severity of placenta inflammation due to a limited number of patients, and without access to amniotic fluid it cannot be determined if there was intra-amniotic infection without placenta findings, or whether the inflammatory process was infectious or sterile (5, 54).

There are a number of factors apart from chorioamnionitis that could potentially affect the inflammatory response in cord monocytes in our preterm infants. Gestational age was significantly lower in the S100A high group, but differences between groups remained after statistical correction for gestational age at birth. Labor and vaginal delivery is in itself associated with an inflammatory response in the fetus (55, 56), and spontaneous onset of delivery was significantly more common in the group with high S100A gene expression. There was, however, a significant number of infants with spontaneous

TABLE 6 | Canonical IPA pathways regulated in cord blood monocytes and common to high expression of S100A alarmins as well as HCA and FIRS ($n = 18$).

Canonical pathways	Signaling pathway categories	Relation to inflammation and/or monocyte function (select references)
fMLP Signaling in Neutrophils	Cellular Immune Response; Cytokine Signaling	
RhoGDI Signaling	Intracellular and Second Messenger Signaling	Involved in Rho-regulation, important for innate and adaptive immunity (35, 37)
STAT3 Pathway	Cellular Growth, Proliferation and Development; Transcriptional Regulation	Transcription activator, responds to cytokines and growth factors (45)
Production of Nitric Oxide and Reactive Oxygen Species in Macrophages	Cellular Immune Response	Plasma oxidative stress markers significantly increased in preterm infants (46)
Signaling by Rho Family GTPases	Intracellular and Second Messenger Signaling	Rho is a family of GTPases, important in innate and adaptive immunity (35)
Ephrin Receptor Signaling	Cell Morphology; Cellular Movement; Connective Tissue Development and Function	Ephrin proteins are involved in inflammation in vascular endothelium (41) including in monocytes (42)
Opioid Signaling Pathway	Neurotransmitters and Other Nervous System Signaling	N/A
CCR3 Signaling in Eosinophils	Cellular Immune Response; Cytokine Signaling	Important in leukocyte trafficking (47)
GNRH Signaling	Neurotransmitters and Other Nervous System Signaling	N/A
Protein Kinase A Signaling	Intracellular and Second Messenger Signaling	N/A
Breast Cancer Regulation by Stathmin1	Cancer; Disease-Specific Pathways	N/A
Rac Signaling	Intracellular and Second Messenger Signaling	Involved in monocyte migration (48)
Regulation of Actin-based Motility by Rho	Neurotransmitters and Other Nervous System Signaling	Rho is a family of GTPases, important in innate and adaptive immunity (35)
Chemokine Signaling	Cytokine Signaling; Organismal Growth and Development	
Fcy Receptor-mediated Phagocytosis in Macrophages and Monocytes	Cellular Immune Response	
Phospholipase C Signaling	Intracellular and Second Messenger Signaling	Chemotaxis in monocytes (49)
Synaptic Long Term Potentiation	Neurotransmitters and Other Nervous System Signaling	N/A
Phagosome Formation	Cellular Immune Response; Pathogen-Influenced Signaling	Important in innate and adaptive host defense against pathogens (50)

Analysis of pathways was performed by Ingenuity Pathway Analysis (IPA) (Qiagen Bioinformatics). IPA signaling pathway categories are used to briefly describe each pathway. HCA, histological chorioamnionitis; FIRS, fetal inflammatory response syndrome with a fetal inflammatory response in placent.

onset of delivery also in the S100A low group, and in addition, cesarian section and the frequency of vaginal delivery did not significantly differ between groups with or without spontaneous onset of labor. In addition, the term group included only infants born after vaginal delivery, and all infants had low expression of S100A alarmins. These findings suggest that labor or way of delivery could not in itself explain increased S100A gene expression. There is also a risk that fetal monocyte response could be related to infection or inflammation in the mother, not related to chorioamnionitis. In our study, we identified mothers with fever and/or elevated CRP that were clinically diagnosed and treated as chorioamnionitis and found that symptoms in the mothers did not differ between groups with high or low S100A gene expression. Comprehensive studies show that most cases of verified HCA are subclinical and that a significant number of "clinical chorioamnionitis" is unrelated to intrauterine infection or inflammation (6). In our study, fetal S100A monocyte expression had a stronger association with definite histological signs than with unspecific clinical symptoms.

Based on our findings of S100A monocyte gene upregulation in association with clinical signs of inflammation, we investigated if S100A8 and S100A9 proteins in cord blood could serve as markers for exposure to chorioamnionitis and fetal inflammation. We found that plasma levels of both proteins were increased in term vs. preterm infants and in association with HCA, FIRS and spontaneous onset of delivery (PTL/PPROM) within the preterm group. Elevated levels of the S100A8/A9 protein dimer has previously been described in healthy term infants compared with preterm infants in the absence of exposure to chorioamnionitis or signs of infection (19). In preterm infants, lower S100A8/A9 protein levels are associated with an *increased* risk for late onset sepsis (19), while another study shows that HCA and FIRS are associated with a *decreased* risk for late onset sepsis in preterm infants (18). Our novel findings of elevated S100A8 and S100A9 proteins in association with HCA and FIRS may provide a link between these findings, but further studies are needed to confirm such a connection. The S100A8/A9 protein dimer is elevated in neonatal sepsis in preterm infants (28), but to our knowledge, only one study has previously studied S100A8/A9 in preterm cord blood in association with chorioamnionitis and no changes were found (29). In that study, diagnosis of chorioamnionitis was based on clinical signs only, and proteins were analyzed in supernatant from whole blood cultures which may explain the differing findings (29).

In our study, high expression of S100A8 and S100A9 genes in cord blood monocytes was accompanied by elevated protein levels within the preterm group, which is contrary to the inverse relation seen in term infants. The inverse relation in term infants suggest that cells other than monocytes, most

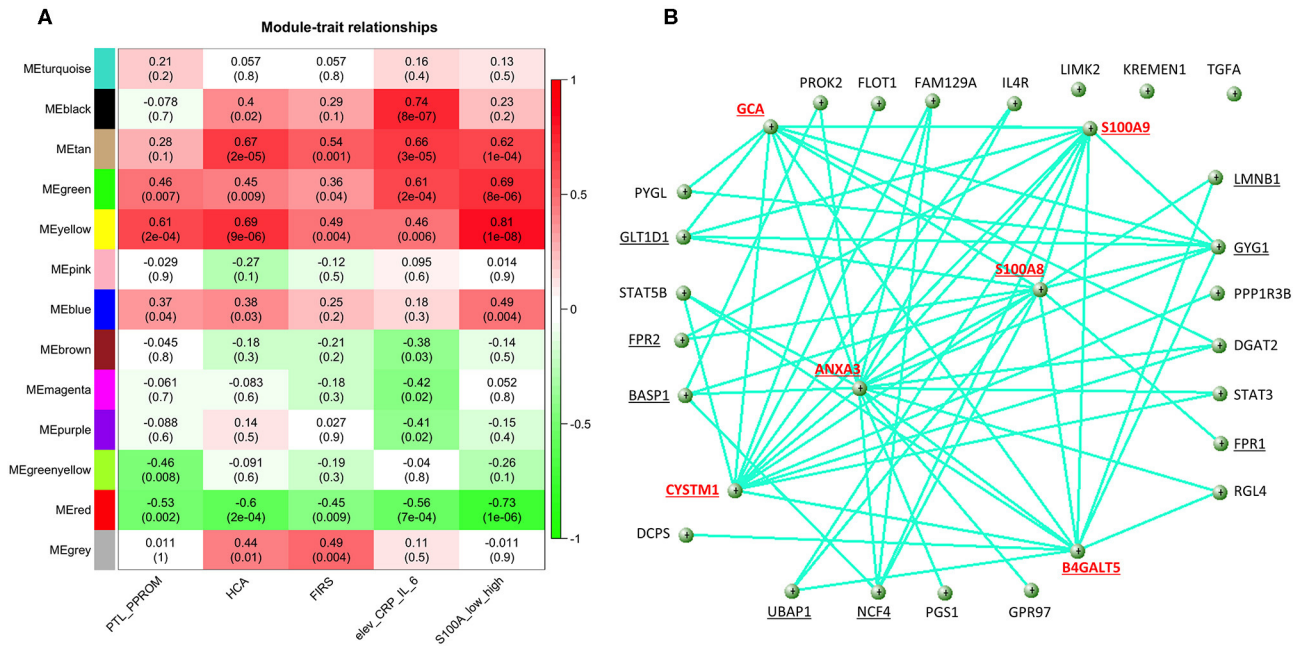

FIGURE 8 | Results of weighted correlation network analysis of gene expression in cord blood monocytes from preterm infants. **(A)** The heatmap shows correlation and (significance) of the eigengenes of the modules in relation to S100A alarmin expression and clinical inflammatory conditions [preterm labor (PTL)/preterm prelabor rupture of membranes (PPROM); exposure to histological chorioamnionitis (HCA), histological fetal inflammatory response syndrome (FIRS), and elevated CRP/IL-6 in cord blood plasma]. Significant positive correlations for all traits were seen for green and yellow modules and negative correlations for the red module. **(B)** Visualization of the network for the top 30 hub genes in the yellow module (weight cutoff set from 0.19 to 1) with the most pronounced hub nodes marked in red and genes connected with S100A8 and S100A9 underlined.

likely neutrophils, are the main source of S100A proteins in this group. S100A8 and S100A9 represents ∼5% of cytosolic proteins in monocytes, but nearly half of cytosolic proteins in neutrophils (23). Neutrophils may also be of importance as a protein source in preterm infants under inflammatory conditions. While neutrophils of maternal origin are found in the placenta during HCA (57), fetal neutrophils invading umbilical cord is the hallmark of FIRS (7). Neutrophils of fetal as well as maternal origin are found in amniotic fluid in association with intraamniotic infection/inflammation and extremely preterm birth (58, 59). Neutrophils also release S100A alarmins under other inflammatory conditions in the preterm infant (60). In addition, elevated proteins S100A8, S100A9, and S100A12 have been identified as biomarkers for intra-amniotic infection and inflammation (61, 62) and, as reviewed by Buhimschi et al. (62), a panel of amniotic fluid proteins including S100A8 and S100A12 predicts clinically relevant HCA and FIRS as well as early onset sepsis and elevated inflammatory proteins in cord blood in preterm infants. Furthermore, increased gene expression of alarmins S100A8, A9, and A12 is found in umbilical cord tissue from preterm infants with FIRS and GO enrichment analysis show associations with neutrophil extravasation as well as monocyte migration (63). These findings suggest that fetal cells, other than circulating monocytes could be the source of proteins S100A8 and S100A9 released into the fetal blood stream also in the preterm infant. The positive correlation between high monocyte S100A gene expression and elevated protein levels in preterm infants under inflammatory conditions suggests, however, that monocytes may contribute to the increase in S100A protein levels, either by direct release of proteins or by inducing protein release from other cell types. As discussed below, S100A8/A9 proteins in cord blood could affect monocyte phenotype, and it is also possible that increased expression of S100A alarmins in cord tissue and increased levels of S100A8/A9 plasma proteins precede and contribute to monocyte phenotype changes rather than being caused by increased monocyte gene expression.

We found that close to 2,000 genes were differentially regulated in monocytes with either high or low expression of S100A8 and S100A9 genes. This was at the same level as number of genes differentially regulated between term and preterm infants. It is likely that this pronounced difference in gene expression pattern is associated with different functional monocyte phenotypes. Preterm monocytes are commonly characterized by a hypo-responsive phenotype with attenuated pro-inflammatory gene response (64). Exposure to HCA accentuates this pattern with reduced expression of key inflammatory genes associated with TLR activation and results in an attenuated response to Staphylococcus epidermis challenge (20). These findings suggest that exposure to chorioamnionitis may alter monocyte phenotype and later susceptibility to infections (20) and explain the decreased risk of late onset sepsis in preterm infants exposed to HCA (18). Recent studies have also suggested a role for S100A8/A9 protein dimer in induction

of a hypo-responsive phenotype (19). Monocytes from healthy term infants demonstrate a hypo-responsive phenotype when compared with adult monocytes, and this phenotype is induced by high levels of S100A8/A9 in term cord blood (19, 27). The altered phenotype is explained by an altered transcription of genes in TRIF and MyD88 associated pathways following TLR4 activation by the S100A alarmins. The resulting imbalance leads to an attenuated cytokine response with decreased risk for hyperinflammation but with adequate pathogen defense and a decreased risk for sepsis (19). Preterm infants had generally lower levels of S100A8/A9 in cord blood than term infants and low levels within the preterm group were associated with an increased risk for sepsis (19). No infants with exposure to chorioamnionitis or with laboratory signs of fetal inflammation were included in this study (19).

In our study, preterm infants had lower levels of proteins S100A8 and S100A9 compared to term infants as found in previous studies (19), but HCA and FIRS resulted in significantly elevated concentrations within the preterm group with levels similar to those seen in term infants. It is thus possible that S100A8/A9 could alter monocyte phenotype in infants exposed to FIRS as in term infants (19) and help explain the transcriptional differences regarding S100A alarmins. However, none of the key down-regulated genes in HCA-exposed monocytes (20) or TLR4-related genes associated with S100A8/A9 immune-programming (19) were among the 124 genes that were differentially expressed in association with high S100A8/A9 gene expression as well as FIRS and HCA in our study. The connection between clinical inflammatory conditions, S100A8/A9 protein activity and monocyte phenotype warrants further investigation.

The monocyte hypo-responsiveness previously described in association with exposure to HCA (18, 20) and implied by increased levels of S100A8/A9 proteins in association with HCA and FIRS in our study is difficult to link to neonatal morbidities associated with HCA and FIRS. However, elevated S100A8/A9 are normalized within a week after birth in term infants (27) and experimental studies show that early endotoxin tolerance induced in fetal sheep is followed by an accentuated inflammatory monocyte response (65). It is thus possible that an early hypo-responsiveness induced by FIRS could be combined with a delayed, and potentially harmful hyper-inflammation. Longitudinal studies of monocyte phenotype and changes in S100A8/A9 protein levels in preterm infants are needed.

The most important reason to investigate monocyte phenotypes in preterm infants is to find associations with early morbidities that will help us identify underlying mechanisms of inflammation-induced injury. In our study, only the proportion of infants with patent ductus arteriosus differed between S100A high and low groups. An association between patent ductus arteriosus and chorioamnionitis is previously described (13). No differences for other morbidities were seen. Possible explanations are small study groups, few infants with severe disease and high risk infants with poor fetal growth within the S100A low group. It is, however, notable that the only case of early onset sepsis was found in the S100A high group and the only two cases of late onset sepsis in the S100A low group.

Pathway analysis based on genes that were differentially expressed in the S100A high group as well as FIRS and HCA groups identified several pathways that warrant further investigation. Cytokine/chemokine signaling and pathways associated with phagocytosis and oxygen free radical formation were, not unexpectedly, affected as these functions are well-described in monocytes in response to infectious and inflammatory challenges. Less well-described in monocytes than in other innate immune cells such as neutrophils and macrophages, are the small GTPases RhoA and RAC. These GTPases regulate the remodeling of actin cytoskeleton that is required for immune cell functions such as migration and phagocytosis (35, 48). Notably, 4/13 inflammation-related pathways were directly associated with RhoA and RAC signaling and at least one other more loosely [STAT3 signaling (66)]. RhoA GTPase signaling pathways have been implicated in preterm births (67), but have, to our knowledge, not been studied in cord blood monocytes or in association with chorioamnionitis.

Network analysis revealed that S100A8 and S100A9 are hub nodes in a network strongly related to clinical inflammatory conditions. Gene ontology enrichment analyses of genes within this network confirmed a strong relation to inflammatory and immune-related mechanisms within the monocytes and confirmed previous finding in analyses of genes and pathways common to high S100A expression, HCA and FIRS. Our findings suggest that S100A alarmins are not only responder genes but may be central in networks associated with specific monocyte phenotypes.

S100A8 and S100A9 were among the genes with the highest number of connectivities. In contrast, S100A12 was found within the same network but was not identified as a hub gene. This suggests that, in spite of very strong co-expression with S100A8 and S100A9, alarmin S100A12 may have other functions in relation to monocyte phenotype and outcome.

Network analysis also revealed connections between S100A8 and S100A9 and other major hub nodes that may be important in mechanisms related to monocyte function. This is exemplified by the hub gene ANXA3, that was also among the 500 DE genes in monocytes with high or low S100A expression. Annexin 3 is found in myeloid cells in specific granules that are translocated upon cell activation (68) and interactions between the annexin family proteins and S100A proteins have previously been described (69). ANXA3 is also upregulated together with S100A9 and S100A12 in peripheral blood in children with severe infections (70). These findings suggest that interactions between annexin 3 and S100A alarmins in relation to monocyte function and immune activation warrant further investigation.

In summary, we show that gene expression of S100A alarmins in cord blood monocytes was significantly up-regulated in preterm compared with term infants. A high expression of S100A alarmins within the preterm group was accompanied by pronounced changes in overall gene expression and was strongly associated with spontaneous onset of delivery, HCA, FIRS and a pro-inflammatory protein profile. This implies a direct link between exposure to chorioamnionitis and an altered monocyte phenotype characterized by high expression of S100A8 and S100A9 genes. These findings were supported

by differential gene expression and network analyses showing a strong association between S100A alarmin expression and inflammation-associated pathways in the preterm infant. We also show that S100A8 and S100A9 proteins were elevated in cord blood plasma from preterm infants with high monocyte S100A alarmin gene expression and inflammatory conditions, to levels resembling those seen in term infants. Our study is, however, limited by a small sample size and the exploratory nature of the study using complex methods aimed at characterizing monocyte phenotypes. Our findings may help to identify clinically relevant markers (not limited to S100A proteins) to identify high-risk infants in the future, but this warrants further extensive studies in larger patient groups. In addition, the connection between elevated protein levels, monocyte phenotype and risk for inflammation-associated morbidities warrants further investigation as changes in monocyte gene expression may also be important for the adaptation of preterm infants to a postnatal life with additional inflammatory and infectious challenges. Furthermore, our study is limited to clinical findings and additional mechanistic studies are needed. A deeper understanding of immune regulation in the compromised preterm infants may help us clarify mechanisms of injury and identify infants for potential therapeutic interventions.

DATA AVAILABILITY STATEMENT

The raw data supporting the conclusions of this article will be made available by the authors, without undue reservation, to any qualified researcher.

ETHICS STATEMENT

The studies involving human participants were reviewed and approved by Regional Ethic's Committee at the Sahlgrenska University Hospital, Gothenburg; application (EPN Gbg 933-16, T350-18). Written informed consent to participate in this study was provided by the participants' legal guardian/next of kin.

AUTHOR CONTRIBUTIONS

This study was conceived and designed by VG, CM, and KS. Clinical sampling and experiments were performed by VG, HP, I-MF, BJ, AH, and KS. Results were analyzed by VG, HN, HR, and KS. VG, HN, CM, and KS drafted the manuscript. All authors critically reviewed and edited the work.

FUNDING

This work was supported by Swedish Research Council (VR-2017-01409—CM), Public Health Service at the Sahlgrenska University Hospital (ALFGBG-722491—CM/KS), Region Västra Götalan, for Collaborative Research (VGFOUREG-932182—KS), The Swedish Brain Foundation (FO2017-0063; FO2019-0270—CM), Torsten Söderberg Foundation (M98/15—CM), Wilhelm and Martina Lundgren Foundation (CM and VG), and Åhlen Foundation (CM), Märta Lundqvist Foundation (VG).

ACKNOWLEDGMENTS

We thank Dr. Pernilla Svedin for technical support of Bio-Plex analysis and Dr. Evelin Berger at the Proteomic Core Facility, Sahlgrenska Academy for excellent data generation on plasma S100A proteins.

SUPPLEMENTARY MATERIAL

The Supplementary Material for this article can be found online at: https://www.frontiersin.org/articles/10.3389/fimmu.2020.01194/full#supplementary-material

REFERENCES

1. Serenius F, Ewald U, Farooqi A, Fellman V, Hafstrom M, Hellgren K, et al. Neurodevelopmental outcomes among extremely preterm infants 6.5 years after active perinatal care in Sweden. *JAMA Pediatr.* (2016) 170:954–63. doi: 10.1001/jamapediatrics.2016.1210
2. Goldenberg RL, Hauth JC, Andrews WW. Intrauterine infection and preterm delivery. *N Eng J Med.* (2000) 342:1500–7. doi: 10.1056/NEJM200005183422007
3. Jacobsson B, Mattsby-Baltzer I, Andersch B, Bokstrom H, Holst RM, Nikolaitchouk N, et al. Microbial invasion and cytokine response in amniotic fluid in a Swedish population of women with preterm prelabor rupture of membranes. *Acta Obstetr Gynecol Scand.* (2003) 82:423–31. doi: 10.1034/j.1600-0412.2003.00157.x
4. Jacobsson B, Mattsby-Baltzer I, Andersch B, Bokstrom H, Holst RM, Wennerholm UB, et al. Microbial invasion and cytokine response in amniotic fluid in a Swedish population of women in preterm labor. *Acta Obstetr Gynecol Scand.* (2003) 82:120–8. doi: 10.1034/j.1600-0412.2003.00047.x
5. Kim CJ, Romero R, Chaemsaithong P, Chaiyasit N, Yoon BH, Kim YM. Acute chorioamnionitis and funisitis: definition, pathologic features, and clinical significance. *Am J Obstet Gynecol.* (2015) 213(4 Suppl.):S29–52. doi: 10.1016/j.ajog.2015.08.040
6. Sung JH, Choi SJ, Oh SY, Roh CR. Should the diagnostic criteria for suspected clinical chorioamnionitis be changed? *J Matern Fetal Neonatal Med.* (2019) 3:1–10. doi: 10.1080/14767058.2019.1618822
7. Hecht JL, Allred EN, Kliman HJ, Zambrano E, Doss BJ, Husain A, et al. Histological characteristics of singleton placentas delivered before the 28th week of gestation. *Pathology.* (2008) 40:372–6. doi: 10.1080/00313020802035865
8. Tsiartas P, Kacerovsky M, Musilova I, Hornychova H, Cobo T, Sävman K, et al. The association between histological chorioamnionitis, funisitis and neonatal outcome in women with preterm prelabor rupture of membranes. *J Mater Fetal Neonatal Med.* (2013) 26:1332–6. doi: 10.3109/14767058.2013.784741
9. Mukhopadhyay S, Puopolo KM. Clinical and microbiologic characteristics of early-onset sepsis among very low birth weight infants: opportunities for antibiotic stewardship. *Pediatr Infect Dis J.* (2017) 36:477–81. doi: 10.1097/INF.0000000000001473
10. Mestan K, Yu Y, Thorsen P, Skogstrand K, Matoba N, Liu X, et al. Cord blood biomarkers of the fetal inflammatory response. *J Mater Fetal Neonatal Med.* (2009) 22:379–87. doi: 10.1080/14767050802609759
11. Lu HY, Zhang Q, Wang QX, Lu JY. Contribution of histologic chorioamnionitis and fetal inflammatory response syndrome to increased risk of brain injury in infants with preterm premature rupture of membranes. *Pediatr Neurol.* (2016) 61:94–8.e1. doi: 10.1016/j.pediatrneurol.2016.05.001

12. Pugni L, Pietrasanta C, Acaia B, Merlo D, Ronchi A, Ossola MW, et al. Chorioamnionitis and neonatal outcome in preterm infants: a clinical overview. *J Mater Fetal Neonatal Med.* (2016) 29:1525–9. doi: 10.3109/14767058.2015.1053862
13. Park HW, Choi YS, Kim KS, Kim SN. Chorioamnionitis and patent ductus arteriosus: a systematic review and meta-analysis. *PLoS ONE.* (2015) 10:e0138114. doi: 10.1371/journal.pone.0138114
14. Been JV, Lievense S, Zimmermann LJ, Kramer BW, Wolfs TG. Chorioamnionitis as a risk factor for necrotizing enterocolitis: a systematic review and meta-analysis. *J Pediatr.* (2013) 162:236–42.e2. doi: 10.1016/j.jpeds.2012.07.012
15. Leviton A, Allred EN, Kuban KC, Hecht JL, Onderdonk AB, O'Shea TM, et al. Microbiologic and histologic characteristics of the extremely preterm infant's placenta predict white matter damage and later cerebral palsy. The ELGAN study. *Pediatr Res.* (2010) 67:95–101. doi: 10.1203/PDR.0b013e3181bf5fab
16. Shatrov JG, Birch SC, Lam LT, Quinlivan JA, McIntyre S, Mendz GL. Chorioamnionitis and cerebral palsy: a meta-analysis. *Obstetr Gynecol.* (2010) 116:387–92. doi: 10.1097/AOG.0b013e3181e90046
17. Pappas A, Kendrick DE, Shankaran S, Stoll BJ, Bell EF, Laptook AR, et al. Chorioamnionitis and early childhood outcomes among extremely low-gestational-age neonates. *JAMA Pediatr.* (2014) 168:137–47. doi: 10.1001/jamapediatrics.2013.4248
18. Strunk T, Doherty D, Jacques A, Simmer K, Richmond P, Kohan R, et al. Histologic chorioamnionitis is associated with reduced risk of late-onset sepsis in preterm infants. *Pediatrics.* (2012) 129:e134–41. doi: 10.1542/peds.2010-3493
19. Ulas T, Pirr S, Fehlhaber B, Bickes MS, Loof TG, Vogl T, et al. S100-alarmin-induced innate immune programming protects newborn infants from sepsis. *Nat Immunol.* (2017) 18:622–32. doi: 10.1038/ni.3745
20. de Jong E, Hancock DG, Wells C, Richmond P, Simmer K, Burgner D, et al. Exposure to chorioamnionitis alters the monocyte transcriptional response to the neonatal pathogen staphylococcus epidermidis. *Immunol Cell Biol.* (2018) 96:792–804. doi: 10.1111/imcb.12037
21. Pruenster M, Vogl T, Roth J, Sperandio M. S100A8/A9: from basic science to clinical application. *Pharmacol Ther.* (2016) 167:120–31. doi: 10.1016/j.pharmthera.2016.07.015
22. Foell D, Wittkowski H, Vogl T, Roth J. S100 proteins expressed in phagocytes: a novel group of damage-associated molecular pattern molecules. *J Leukocyte Biol.* (2007) 81:28–37. doi: 10.1189/jlb.0306170
23. Hessian PA, Edgeworth J, Hogg N. MRP-8 and MRP-14, two abundant Ca(2+)-binding proteins of neutrophils and monocytes. *J Leukocyte Biol.* (1993) 53:197–204. doi: 10.1002/jlb.53.2.197
24. Vogl T, Tenbrock K, Ludwig S, Leukert N, Ehrhardt C, van Zoelen MA, et al. Mrp8 and Mrp14 are endogenous activators of toll-like receptor 4, promoting lethal, endotoxin-induced shock. *Nat Med.* (2007) 13:1042–9. doi: 10.1038/nm1638
25. Foell D, Frosch M, Sorg C, Roth J. Phagocyte-specific calcium-binding S100 proteins as clinical laboratory markers of inflammation. *Clin Chim Acta.* (2004) 344:37–51. doi: 10.1016/j.cccn.2004.02.023
26. Jonsson MK, Sundlisaeter NP, Nordal HH, Hammer HB, Aga AB, Olsen IC, et al. Calprotectin as a marker of inflammation in patients with early rheumatoid arthritis. *Ann Rheum Dis.* (2017) 76:2031–7. doi: 10.1136/annrheumdis-2017-211695
27. Austermann J, Friesenhagen J, Fassl SK, Petersen B, Ortkras T, Burgmann J, et al. Alarmins MRP8 and MRP14 induce stress tolerance in phagocytes under sterile inflammatory conditions. *Cell Rep.* (2014) 9:2112–23. doi: 10.1016/j.celrep.2014.11.020
28. Terrin G, Passariello A, Manguso F, Salvia G, Rapacciuolo L, Messina F, et al. Serum calprotectin: an antimicrobial peptide as a new marker for the diagnosis of sepsis in very low birth weight newborns. *Clin Dev Immunol.* (2011) 2011:291085. doi: 10.1155/2011/291085
29. Faust K, Gopel W, Moser K, Temole G, Bartels M, Wieg C, et al. Differential expression of antimicrobial polypeptides in cord blood samples of preterm and term infants. *Acta Paediatr.* (2014) 103:e143–7. doi: 10.1111/apa.12544
30. Buhimschi CS, Dulay AT, Abdel-Razeq S, Zhao G, Lee S, Hodgson EJ, et al. Fetal inflammatory response in women with proteomic biomarkers characteristic of intra-amniotic inflammation and preterm birth. *BJOG.* (2009) 116:257–67. doi: 10.1111/j.1471-0528.2008.01925.x
31. Anders S, Huber W. Differential expression analysis for sequence count data. *Genome Biol.* (2010) 11:R106. doi: 10.1186/gb-2010-11-10-r106
32. Wisniewski JR, Zougman A, Nagaraj N, Mann M. Universal sample preparation method for proteome analysis. *Nat Methods.* (2009) 6:359–62. doi: 10.1038/nmeth.1322
33. Langfelder P, Horvath S. WGCNA: an R package for weighted correlation network analysis. *BMC Bioinform.* (2008) 9:559. doi: 10.1186/1471-2105-9-559
34. Yang Y, Han L, Yuan Y, Li J, Hei N, Liang H. Gene co-expression network analysis reveals common system-level properties of prognostic genes across cancer types. *Nat Commun.* (2014) 5:3231. doi: 10.1038/ncomms4231
35. Bros M, Haas K, Moll L, Grabbe S. RhoA as a key regulator of innate and adaptive immunity. *Cells.* (2019) 8:733. doi: 10.3390/cells8070733
36. Wang Y, Braun OO, Zhang S, Norstrom E, Thorlacius H. Monocytes regulate systemic coagulation and inflammation in abdominal sepsis. *Am J Physiol Heart Circ Physiol.* (2015) 308:H540–7. doi: 10.1152/ajpheart.00336.2014
37. Kim JG, Islam R, Cho JY, Jeong H, Cap KC, Park Y, et al. Regulation of RhoA GTPase and various transcription factors in the RhoA pathway. *J Cell Physiol.* (2018) 233:6381–92. doi: 10.1002/jcp.26487
38. Ley K, Laudanna C, Cybulsky MI, Nourshargh S. Getting to the site of inflammation: the leukocyte adhesion cascade updated. *Nat Rev Immunol.* (2007) 7:678–89. doi: 10.1038/nri2156
39. Jones GE. Cellular signaling in macrophage migration and chemotaxis. *J Leukocyte Biol.* (2000) 68:593–602. doi: 10.1189/jlb.68.5.593
40. Figueiredo KA, Mui AL, Nelson CC, Cox ME. Relaxin stimulates leukocyte adhesion and migration through a relaxin receptor LGR7-dependent mechanism. *J Biol Chem.* (2006) 281:3030–9. doi: 10.1074/jbc.M506665200
41. Coulthard MG, Morgan M, Woodruff TM, Arumugam TV, Taylor SM, Carpenter TC, et al. Eph/Ephrin signaling in injury and inflammation. *Am J Pathol.* (2012) 181:1493–503. doi: 10.1016/j.ajpath.2012.06.043
42. Gerhardt T, Ley K. Monocyte trafficking across the vessel wall. *Cardiovasc Res.* (2015) 107:321–30. doi: 10.1093/cvr/cvv147
43. Simonsen KA, Anderson-Berry AL, Delair SF, Davies HD. Early-onset neonatal sepsis. *Clin Microbiol Rev.* (2014) 27:21–47. doi: 10.1128/CMR.00031-13
44. Chong SZ, Evrard M, Devi S, Chen J, Lim JY, See P, et al. CXCR4 identifies transitional bone marrow premonocytes that replenish the mature monocyte pool for peripheral responses. *J Exp Med.* (2016) 213:2293–314. doi: 10.1084/jem.20160800
45. Hillmer EJ, Zhang H, Li HS, Watowich SS. STAT3 signaling in immunity. *Cytokine Growth Factor Rev.* (2016) 31:1–15. doi: 10.1016/j.cytogfr.2016.05.001
46. Norishadkam M, Andishmand S, Zavar Reza J, Zare Sakhvidi MJ, Hachesoo VR. Oxidative stress and DNA damage in the cord blood of preterm infants. *Mutat Res.* (2017) 824:20–4. doi: 10.1016/j.mrgentox.2017.10.003
47. Olson TS, Ley K. Chemokines and chemokine receptors in leukocyte trafficking. *Am J Physiol Regul Integr Comp Physiol.* (2002) 283:R7–28. doi: 10.1152/ajpregu.00738.2001
48. Hu Y, Hu X, Boumsell L, Ivashkiv LB. IFN-gamma and STAT1 arrest monocyte migration and modulate RAC/CDC42 pathways. *J Immunol.* (2008) 180:8057–65. doi: 10.4049/jimmunol.180.12.8057
49. Cathcart MK. Signal-activated phospholipase regulation of leukocyte chemotaxis. *J Lipid Res.* (2009) 50:S231–6. doi: 10.1194/jlr.R800096-JLR200
50. Tjelle TE, Lovdal T, Berg T. Phagosome dynamics and function. *Bioessays.* (2000) 22:255–63. doi: 10.1002/(SICI)1521-1878(200003)22:3<255::AID-BIES7>3.0.CO;2-R
51. Andrys C, Drahosova M, Hornychova H, Tambor V, Musilova I, Tosner J, et al. Umbilical cord blood concentrations of IL-6, IL-8, and MMP-8 in pregnancy complicated by preterm premature rupture of the membranes and histological chorioamnionitis. *Neuro Endocrinol Lett.* (2010) 31:857–63.
52. Morken NH, Kallen K, Jacobsson B. Outcomes of preterm children according to type of delivery onset: a nationwide population-based study. *Paediatr Perinatal Epidemiol.* (2007) 21:458–64. doi: 10.1111/j.1365-3016.2007.00823.x
53. Hansen-Pupp I, Hallin AL, Hellstrom-Westas L, Cilio C, Berg AC, Stjernqvist K, et al. Inflammation at birth is associated with subnormal development in very preterm infants. *Pediatr Res.* (2008) 64:183–8. doi: 10.1203/PDR.0b013e318176144d

54. Romero R, Miranda J, Chaemsaithong P, Chaiworapongsa T, Kusanovic JP, Dong Z, et al. Sterile and microbial-associated intra-amniotic inflammation in preterm prelabor rupture of membranes. *J Mater Fetal Neonatal Med.* (2015) 28:1394–409. doi: 10.3109/14767058.2014.958463
55. Nandanan B, Chua MC, Chiang WC, Goh A, Kumar D, Knippels L, et al. Influence of mode of delivery on cytokine expression in cord blood. *Hum Immunol.* (2019) 80:533–6. doi: 10.1016/j.humimm.2019.03.018
56. Sundqvist M, Osla V, Jacobsson B, Rudin A, Savman K, Karlsson A. Cord blood neutrophils display a galectin-3 responsive phenotype accentuated by vaginal delivery. *BMC Pediatr.* (2013) 13:128. doi: 10.1186/1471-2431-13-128
57. McNamara MF, Wallis T, Qureshi F, Jacques SM, Gonik B. Determining the maternal and fetal cellular immunologic contributions in preterm deliveries with clinical or subclinical chorioamnionitis. *Infect Dis Obstetr Gynecol.* (1997) 5:273–9. doi: 10.1155/S1064744997000471
58. Gomez-Lopez N, Romero R, Xu Y, Leng Y, Garcia-Flores V, Miller D, et al. Are amniotic fluid neutrophils in women with intraamniotic infection and/or inflammation of fetal or maternal origin*? Am J Obstet Gynecol.* (2017) 217:693.e1–e16. doi: 10.1016/j.ajog.2017.09.013
59. Gomez-Lopez N, Romero R, Leng Y, Xu Y, Slutsky R, Levenson D, et al. The origin of amniotic fluid monocytes/macrophages in women with intra-amniotic inflammation or infection. *J Perinatal Med.* (2019) 47:822–40. doi: 10.1515/jpm-2019-0262
60. Vento G, Lio A, Tirone C, Aurilia C, Tana M, Piras A, et al. Association of high levels of α-defensins and S100A proteins with Candida mannan detection in bronchoalveolar lavage fluid of preterm neonates. *Pediatr Res.* (2013) 74:19–25. doi: 10.1038/pr.2013.60
61. Ruetschi U, Rosen A, Karlsson G, Zetterberg H, Rymo L, Hagberg H, et al. Proteomic analysis using protein chips to detect biomarkers in cervical and amniotic fluid in women with intra-amniotic inflammation. *J Proteome Res.* (2005) 4:2236–42. doi: 10.1021/pr050139e
62. Buhimschi CS, Bhandari V, Han YW, Dulay AT, Baumbusch MA, Madri JA, et al. Using proteomics in perinatal and neonatal sepsis: hopes and challenges for the future. *Curr Opin Infect Dis.* (2009) 22:235–43. doi: 10.1097/QCO.0b013e32832a5963
63. Costa D, Castelo R. Umbilical cord gene expression reveals the molecular architecture of the fetal inflammatory response in extremely preterm newborns. *Pediatr Res.* (2016) 79:473–81. doi: 10.1038/pr.2015.233
64. de Jong E, Strunk T, Burgner D, Lavoie PM, Currie A. The phenotype and function of preterm infant monocytes: implications for susceptibility to infection. *J Leukocyte Biol.* (2017) 102:645–56. doi: 10.1189/jlb.4RU0317-111R
65. Kramer BW, Joshi SN, Moss TJ, Newnham JP, Sindelar R, Jobe AH, et al. Endotoxin-induced maturation of monocytes in preterm fetal sheep lung. *Am J Physiol Lung Cell Mol Physiol.* (2007) 293:L345–53. doi: 10.1152/ajplung.00003.2007
66. Debidda M, Wang L, Zang H, Poli V, Zheng Y. A role of STAT3 in Rho GTPase-regulated cell migration and proliferation. *J Biol Chem.* (2005) 280:17275–85. doi: 10.1074/jbc.M413187200
67. Nadeau-Vallee M, Quiniou C, Palacios J, Hou X, Erfani A, Madaan A, et al. Novel noncompetitive IL-1 receptor-biased ligand prevents infection- and inflammation-induced preterm birth. *J Immunol.* (2015) 195:3402–15. doi: 10.4049/jimmunol.1500758
68. Le Cabec V, Maridonneau-Parini I. Annexin 3 is associated with cytoplasmic granules in neutrophils and monocytes and translocates to the plasma membrane in activated cells. *Biochem J.* (1994) 303:481–7. doi: 10.1042/bj3030481
69. Gerke V, Moss SE. Annexins: from structure to function. *Physiol Rev.* (2002) 82:331–71. doi: 10.1152/physrev.00030.2001
70. Kulohoma BW, Marriage F, Vasieva O, Mankhambo L, Nguyen K, Molyneux ME, et al. Peripheral blood RNA gene expression in children with pneumococcal meningitis: a prospective case-control study. *BMJ Paediatr Open.* (2017) 1:e000092. doi: 10.1136/bmjpo-2017-000092

Conflict of Interest: The authors declare that the research was conducted in the absence of any commercial or financial relationships that could be construed as a potential conflict of interest.

frontiers in Immunology

ORIGINAL RESEARCH
published: 13 August 2020
doi: 10.3389/fimmu.2020.01808

Impaired Neonatal Immunity and Infection Resistance Following Fetal Growth Restriction in Preterm Pigs

*Ole Bæk†, Shuqiang Ren†, Anders Brunse, Per Torp Sangild and Duc Ninh Nguyen**

Section for Comparative Pediatrics and Nutrition, University of Copenhagen, Copenhagen, Denmark

OPEN ACCESS

Edited by:
Anastasia N. Vlasova, The Ohio State University, United States

Reviewed by:
Pascal M. Lavoie, BC Children's Hospital Research Institute, Canada
Satoshi Kusuda, Tokyo Women's Medical University, Japan

***Correspondence:**
Duc Ninh Nguyen
dnn@sund.ku.dk

†These authors share first authorship

Specialty section:
This article was submitted to Comparative Immunology, a section of the journal Frontiers in Immunology

Received: *27 May 2020*
Accepted: *07 July 2020*
Published: *13 August 2020*

Citation:
Bæk O, Ren S, Brunse A, Sangild PT and Nguyen DN (2020) Impaired Neonatal Immunity and Infection Resistance Following Fetal Growth Restriction in Preterm Pigs. Front. Immunol. 11:1808. doi: 10.3389/fimmu.2020.01808

Background: Infants born preterm or small for gestational age (SGA, due to fetal growth restriction) both show an increased risk of neonatal infection. However, it remains unclear how the co-occurrence of preterm birth and SGA may affect neonatal immunity and infection risk. We hypothesized that fetal growth restricted (FGR) preterm newborns possess impaired immune competence and increased susceptibility to systemic infection and sepsis, relative to corresponding normal birth weight (NBW) newborns.

Methods: Using preterm pigs as a model for preterm infants, gene expression in lipopolysaccharide (LPS) stimulated cord blood was compared between NBW and FGR (lowest 25% birth weight percentile) preterm pigs. Next, clinical responses to a systemic *Staphylococcus epidermidis* (SE) challenge were investigated in newborn FGR and NBW preterm pigs. Finally, occurrence of spontaneous infections were investigated in 9 d-old FGR and NBW preterm pigs, with or without neonatal antibiotics treatment.

Results: At birth, preterm FGR piglets showed diminished *ex vivo* cord blood responses to LPS for genes related to both innate and adaptive immunity, and also more severe septic responses following SE infection (e.g., higher blood lactate, decreased blood pH, neutrophil and platelet counts, relative to NBW pigs). After 9 d, FGR pigs had higher incidence and severity of spontaneous infections (e.g., higher bacterial densities in the bone marrow), increased regulatory T cell numbers, reduced neutrophil phagocytosis capacity, and impaired *ex vivo* blood gene responses to LPS, especially when receiving neonatal antibiotics.

Conclusion: FGR at preterm birth is associated with poor immune competence, impaired infection resistance, and greater sepsis susceptibility in the immediate postnatal period. Our results may explain the increased morbidity and mortality of SGA preterm infants and highlight the need for clinical vigilance for this highly sensitive subgroup of preterm neonates.

Keywords: preterm, infant, small for gestation age, fetal growth restriction, immunity, neonatal sepsis

BACKGROUND

Preterm infants (born before 37 weeks of gestation) are at a higher risk of life threatening infections than their term born counterparts, risk increasing with lower gestational age (1–3). The causes of this are multifaceted, including an immature immune system, comorbidities related to prematurity, and iatrogenic interventions during hospital admission (3, 4). In addition, intrauterine complications that could lead to premature birth, may also affect nutrient supply to the fetus. If fetal growth is severely affected, infants could be born small for gestational age (SGA), defined as a birth weight in the lower 10th percentile of the expected weight for gestational age. Infants born SGA, whether preterm or not, show a higher postnatal mortality than infants of adequate birth weight (5). They also display lower blood neutrophil counts at birth and less responsive leucocytes to *ex vivo* infectious challenges (6, 7). Some studies even suggested that this impaired immune status may persist for years after birth with SGA (8, 9). From animal studies, low birth weight following term birth has been correlated with negative long term effects on growth as well as systemic and gut immune functions (10–13). The possible effects of being both premature and SGA on immune development and infection risks during the first few days of life, remain elusive. Few observational studies indicate an association between SGA and increased mortality and sepsis in preterm infants (3, 14–16) and cord blood from SGA preterm infants may be less responsive to *ex vivo* lipopolysaccharide (LPS) challenge (17). Regardless, the separate effects of prematurity and SGA remain unclear because both overlapping and independent factors may predispose to preterm delivery and growth restriction at birth (e.g., maternal infection/inflammation, poor placental function, reduced blood supply/oxygenation, or genetic factors).

Systemic infection in preterm infants is difficult to diagnose due to the lack of precise biomarkers and poor sensitivity of blood culture assays using small blood volumes (18–20). Therefore, empirical antibiotics are used for a majority of preterm infants in the days after birth despite that only a fraction these infants may indeed be infected (21, 22). Such antibiotic treatments in the neonatal period may affect gut bacterial colonization and immune development early in life, although the evidence from infants are limited. In preterm pigs, neutrophil status is affected by prophylactic oral antibiotics (23). In term pigs, short term neonatal antibiotics altered immune response several weeks after exposure, even though the changes to gut microbiota disappeared after 1 week (24). In term infants, early life antibiotic use is associated with later development of asthma and eczema (25, 26), but such studies are of limited value for the special condition of preterm birth. More information is required on the possible interacting effects of antibiotics treatment and growth restriction on immune development in the early life of preterm neonates.

Preterm pigs are acknowledged as a clinically relevant model for preterm infants as they show many complications similar to preterm infants, including impaired immunity, immature organ systems, and increased susceptibility to sepsis and necrotizing enterocolitis (27, 28). Planned delivery by preterm cesarean section on pregnant sows makes it possible to study factors related to reduced gestational age at birth (e.g., developmental immaturity), independent from the pathological factors that may predispose to and affect outcomes in preterm infants, besides reduced fetal age. Using the preterm pig model, we hypothesized that fetal growth restriction (FGR) would further impair immune competence and increase the risk of systemic infection and sepsis in preterm pigs, relative to preterm pigs with a normal body weight (NBW) for their gestational age. FGR was defined as the lowest 25% birth weight percentile to include both moderately and extremely growth restricted neonates in evaluating immune status, spontaneous infections and responses to infection challenges, with or without antibiotic treatment just after preterm birth. Different from our previous longer term study on systemic immune status in FGR and NBW preterm pigs with optimal feeding to avoid clinical complications (10), we now focused on the *in vitro* and *in vivo* responses to systemic infection in the first week after preterm birth when both preterm pigs and infants are highly sensitive to infections.

METHODS

All animal experiments were approved by the Danish National Committee on Animal Experimentation (2014-15-0201-00418). We performed three experiments to determine the immune competence, sepsis outcomes following infection challenges and spontaneous infection in FGR preterm pigs. All pigs were of the same race (Duroc x Yorkshire x Danish Landrace) and delivered by cesarean section at the same gestational age (106 days, ∼90% gestation), probably reflecting an immune system development of human preterm infants born at 24–28 weeks of gestation, as described previously (27). Within each litter across these experiments, FGR animals were defined as those in the lower 25th percentile for birth weight, while remaining animals were designated as normal birth weight (NBW).

Experiment 1

In order to explore immune competence at birth, cord blood was collected from 81 preterm pigs (21 FGR, 60 NBW) across 4 litters from the umbilical cord at delivery. Fresh blood was then immediately used for *ex vivo* stimulation assay as described later.

Experiment 2

Fifty-seven preterm pigs across 5 litters were delivered, immediately resuscitated in heated and oxygenated incubators (2 L/min) and manual ventilation was performed if deemed necessary. While still affected by anesthesia, each pig was fitted with an umbilical arterial catheter (4F, Portex, UK) for arterial blood sampling and administration of parenteral nutrition. Shortly after birth, 38 animals were infused with live *Staphylococcus epidermidis* (SE) bacteria ($1*10^8 - 5*10^9$ colony forming units/kg) via the umbilical catheter, as previously described (29). The pigs were stratified by the predefined FGR criteria, resulting in two groups SE-FGR ($n = 9$) and SE-NBW ($n = 29$). The remaining pigs received the same volume of control saline, and were not divided by birth weight due to the low number (CON, $n = 19$). Following administration of SE or saline, pigs were closely monitored for the next 24 h for signs of sepsis, pain, and circulatory collapse. If severe symptoms appeared, animals were euthanized ahead of schedule according to predefined, humane endpoints. During

the experiment, animals were kept on total parenteral nutrition (Kabiven, Fresenius-Kabi, Swenden, 6 mL/kg/h). Blood samples were drawn from the umbilical catheter 6, 12, and 24 h after inoculation and used for hematology and arterial blood gas analysis, as described later. After 24 h, all pigs were euthanized by intracardial injection of pentobarbital.

Experiment 3

Preterm pigs ($n = 127$) across 7 litters were delivered by cesarean section, resuscitated and fitted with umbilical catheters as in *Exp 2*. In addition, the pigs were fitted with an orogastric feeding tube (6F, Portex, UK) for administration of enteral nutrition and antibiotics. A proportion of animals ($n = 30$) received oral antibiotics within the first 4 days of life. All pigs were reared until postnatal day 9. The animals were divided by birth weight (NBW or FGR) and antibiotic use (CON or AB), resulting in four groups: NBW-CON ($n = 78$), FGR-CON ($n = 19$), NBW-AB ($n = 22$), and FGR-AB ($n = 8$).

The pigs were weighed daily and clinically assessed twice a day, for signs of illness or pain. If necessary, a pain relief drug was given as an intramuscular injection of meloxicam or butorphanol (Metacam, Denmark or Torbugesic, Finland). According to predefined humane endpoints, animals were euthanized ahead of schedule if they exhibited treatment resistant pain or severe morbidities. The pigs were fed, via the orogastric catheter, increasing amounts of infant formula (16–112 mL/kg/day). Pigs received different bovine milk based diets, that were prepared daily, as described previously (30). The enteral nutrition was supported by decreasing amount of parenteral nutrition (same formulation as in *Exp 2*, from 6 mL/kg/h at birth to 2 mL/kg/h on days 6–9). For NBW-AB and FGR-AB pigs, a combination of amoxicillin with clavulanic acid (50/25 mg/kg, Bioclavid, Sandoz GmbH, Austria) and neomycin (50 mg/kg, Neomay, ScanVet, Denmark) was given through the orogastric tube twice daily for the first 4 days. Blood samples for the evaluation of hematology, neutrophil phagocytosis, T cell profiling, and gene expression analysis were drawn from the umbilical catheter on day 5, 7, and 9, after which all pigs were euthanized by intercardial injection of pentobarbital. After euthanasia the left hind leg was severed, the femur head dissected and immersed in 70% ethanol for 10 min, and a bone marrow biopsy was collected in a sterile manner, for bacterial enumeration.

Immune Cell Characterization

Hematology and immune cell counts on all blood samples from *Exp 2* and *3* were performed on an Advia 2120 hematology system (Siemens Healthcare Diagnostics, USA). In *Exp 2* arterial blood gas analysis was performed using a GEM Premier 3000 (Instrumentation Laboratory, USA).

In *Exp 3*, T cell characterization was performed as previously described (31). Briefly, blood leucocytes were stained with fluorescent antibodies against porcine CD3, CD4, CD8, and FOXP3. Leucocytes were then analyzed using a BD Accuri C6 flow cytometer (BD Biosciences, USA). T cell subsets were defined as follows: T cells ($CD3^+$ lymphocytes), CD4 positive T cells ($CD3^+CD4^+CD8^-$ lymphocytes), CD8 positive T cells ($CD3^+CD4^-CD8^+$ lymphocytes) and regulatory T cells ($CD3^+CD4^+FOXP3^+$ lymphocytes).

Whole Blood Stimulation and Neutrophil Phagocytosis Assays

Ex vivo whole blood stimulation and leucocyte gene expression was performed in *Exp 1* and in a subgroup of *Exp 3* (NBW-CON, $n = 25$; FGR-CON $n = 5$; NBW-AB, $n = 19$; FGR-AB, $n = 7$). Briefly, fresh whole blood was incubated at 37°C for 5 h with or without 1 μg/ml LPS added. After stimulation, whole blood was stabilized with a mixture of lysis/binding solution concentrate and isopropanol (MagMax 96 blood RNA isolation kit, Thermofisher, Roskilde, Denmark), and stored at −80°C until RNA extraction. RNA was extracted and prepared for quantitative polymerase chain reaction (qPCR) as described elsewhere (10). Using a LightCycler 480 system (Roche, Switzerland) and a commercial qPCR kit (QuantiTect SYBR Green PCR Kit, Qiagen, Netherlands), gene expressions were determined for a panel of 23 genes related to innate and adaptive immunity, as well as cellular metabolism. The genes and corresponding primers are shown in **Table 1**, primers were designed using the *Genes* database and Primer-BLAST software (both National Center for Biotechnology Information, USA). *HPRT1* was used as a housekeeping gene. If a gene in a sample could not be detected by qPCR the sample was rerun, if no expression could be obtained the gene was censored from analysis. If *HPRT1* could not be determined, the entire sample was censored from analysis. Differences in expression of specific genes were calculated relative to the expression of the housekeeping gene, done separately in LPS and non-LPS stimulated samples.

In the same subgroup of *Exp 3*, neutrophil phagocytic function was assessed using commercial fluorescently labeled *E. coli* kit (pHrodo, ThermoFisher, Roskilde, Denmark), as described previously (32). In short, whole blood was incubated with the fluorescent bacteria, and thereafter analyzed on the above mentioned flow cytometer. Neutrophils were identified and phagocytic rate was defined as the fraction of neutrophils with internalized bacteria and phagocytic capacity, as the median fluorescent index of neutrophils with internalized bacteria.

Microbiology

In *Exp 3* we assessed spontaneous bacterial accumulation in the bone marrow. Bone marrow homogenate was serially diluted, plated out on blood agar plates and incubated for 24 h at 37°C. Colonies were counted and bacterial density was assessed as colony forming units per milliliter of bone marrow homogenate. Later, bacteria were identified at species level by Matrix Assisted Laser Desorption/Ionization time of flight mass spectroscopy, as previously described (23).

Statistics

Stata 14.2 (StataCorp, Texas, USA) was used for all calculations. For all comparisons, we used a linear mixed effect model, with relevant intervention as the fixed factor and litter as the random factor. If a variable could not conform to normal distribution after logistic transformation it was assessed by a non-parameteric,

TABLE 1 | List of genes and primers used in gene expression analysis.

Protein	Gene	Forward sequence (5′-3′)	Reverse sequence (5′–3′)	Amplicon length
CXC chemokine ligand 9	*CXCL9*	GAAAAGCAGTGTTGCCTTGCT	TGATGCAGGAACAACGTCCAT	98
CXC chemokine ligand 10	*CXCL10*	ATCATCCCGAGCTGTTGAGC	CCAGGACTTGGCACATTCAC	94
GATA binding protein 3	*GATA3*	ACCCCTTATTAAGCCCAAGC	TCCAGAGAGTCGTCGTTGTG	92
Hypoxia inducible factor 1 alpha	*HIF1A*	TGTGTTATCTGTCGCTTTGAGTC	TTTCGCTTTCTCTGAGCATTC	96
Hexokinase 1	*HK1*	TTTCCCTTGTCGGCAATCCA	CCTCCACTCCGCTTGCTTTA	80
Hypoxanthine phosphoribosyltransferase 1	*HPRT1*	TATGGACAGGACTGAACGGC	ACACAGAGGGCTACGATGTG	75
Interferon gamma	*IFNG*	AGCTTTGCGTGACTTTGTGT	ATGCTCCTTTGAATGGCCTG	247
Interleukin 2	*IL2*	AAGCTCTGGAGGGAGTGCTA	CAACAGCAGTTACTGTCTCATCA	159
Interleukin 4	*IL4*	GTACCAGCAACTTCGTCCAC	CCTTCTCCGTCGTGTTCTCT	150
Interleukin 6	*IL6*	TGCCACCTCAGACAAAATGC	AGGTTCAGGTTGTTTTCTGCC	159
Interleukin 10	*IL10*	GTCCGACTCAACGAAGAAGG	GCCAGGAAGATCAGGCAATA	73
Interleukin 12	*IL12*	TCCTGGGAAAGTCCTGTCGT	GGTGAGGTCGCTAGTTTGGA	81
Interleukin 17	*IL17*	GCACACGGGCTGCATCAACG	TGCAACCAACAGTGACCCGCA	149
Myeloperoxidase	*MPO*	CCCGAGTTGCTTTCCTCACT	AAGAAGGGGATGCAGTCACG	127
Pyruvate dehydrogenase α1	*PDHA1*	GTCAGGAAGCTTGTTGCGTG	GGTAAAGCCATGAGCTCGGT	86
Pyruvate kinase	*PKM*	GCCCTGGACACTAAAGGACC	CAGCCACAGGACATTCTCGT	147
Peroxisome proliferator activated receptor alpha	*PPARA*	CCGAGACCGCAGATCTCAAG	GACGAAAGGCGGGTTATTGC	128
RAR-related orphan receptor alpha	*RORrt*	CAGCGCTCCAACATCTTCTC	GACCAGCACCACTTCCATTG	207
S100 Calcium Binding Protein A9	*S100A9*	GCCAAACTTTCTCAAGAAGCA	AGTGTCCAGGTCTTCCAGGAT	70
T-Box transcription factor	*TBET*	CTGAGAGTCGCGCTCAACAA	ACCCGGCCACAGTAAATGAC	121
Transforming growth factor beta 1	*TGFB1*	GCAAGGTCCTGGCTCTGTA	TAGTACACGATGGGCAGTGG	97
Toll-like receptor 2	*TLR2*	CGTGTGCTATGACGCTTTCG	GTACTTGCACCACTCGCTCT	232
Toll-like receptor 4	*TLR4*	TGGTGTCCCAGCACTTCATA	CAACTTCTGCAGGACGATGA	116
Tumor necrosis factor alpha	*TNFA*	ATTCAGGGATGTGTGGCCTG	CCAGATGTCCCAGGTTGCAT	120

Kruskal Wallis' test. In *Exp 1* differences between FGR and NBW animals in gene expression were assessed separately with or without LPS stimulation. Afterwards the effect of LPS stimulations was determined by a similar model using LPS as the fixed factor and the individual pigs as the random factor. In *Exp 2*, within the animals inoculated with SE we first tested the effect of FGR, separately for each post inoculation time point. To elucidate the effect of SE inoculation we compared all SE infused animals (both FGR and NBW) to all saline infused animals (CON). One litter ($n = 24$) was removed from this comparison as it only included SE infused pigs and no saline infused control group. In *Exp 3* we first tested the effects of FGR on bone marrow infection and blood endpoints separately in antibiotic and non-antibiotic treated preterm pigs at each postnatal time point. The gene expression analysis on day 5 and 9 was assessed in the same manner as in *Exp 1*.

RESULTS

Impaired Immune Competence in FGR Pigs at Birth Assessed by Cord Blood LPS Stimulation

In *Exp 1,* the mean birth weight was lower in the FGR group compared to the NBW (723 ± 30 vs. 1,119 ± 19 g, $P < 0.001$). Before LPS stimulation in cord blood, FGR preterm pigs showed diminished expression of *TBET* and *SA100A9* as well slightly higher expression of *IL4* ($P < 0.01$, 0.001, and 0.05, respectively, **Figures 1A–C**). After LPS stimulation, the FGR group showed lower expression of *TNFA, IL6* and *TLR2* ($P < 0.01$, 0.001, and 0.05, respectively, **Figures 1A–C**), with tendencies toward lower expression of *IL4* ($P = 0.07$, **Figure 1B**), relative to NBW pigs. In the FGR group, LPS stimulation increased expression of *TBET, IL6, IL10, TLR2, TLR4*, and *S100A9* (all $P < 0.05$, **Figures 1A–C**), with tendencies toward higher expression of *TNFA* and *CXCL10* ($P = 0.09$ and 0.06, respectively, **Figures 1A,C**) and lower expression of *GATA3* ($P = 0.06$, **Figure 1B**). Within the NBW group, LPS stimulation increased expression of *TNFA, IL6, IL10, TLR2, TLR4, S100A9, CXCL9*, and *CXCL10* (all $P < 0.01$, **Figures 1A–C**) and diminished expression of *TBET, IL2* and *IL4* ($P < 0.05$, 0.05, and 0.01, respectively, **Figures 1A,B**). There was also a tendency toward less expression of *IL12* ($P = 0.07$, **Figure 1A**).

For genes related to cellular metabolism, FGR pigs showed lower expression of *PPARA* and *PKM* before LPS stimulation (all $P < 0.01$, **Figure 1D**), with a tendency toward lower expression of *HIF1A* and *TGFB* ($P = 0.08$ and 0.07, respectively, **Figure 1D**) than NBW pigs. After LPS stimulation, the FGR group still showed lower expression of *PPARA* and *PKM* (all $P < 0.05$, **Figure 1D**) and a tendency toward lower expression of *HIF1A*

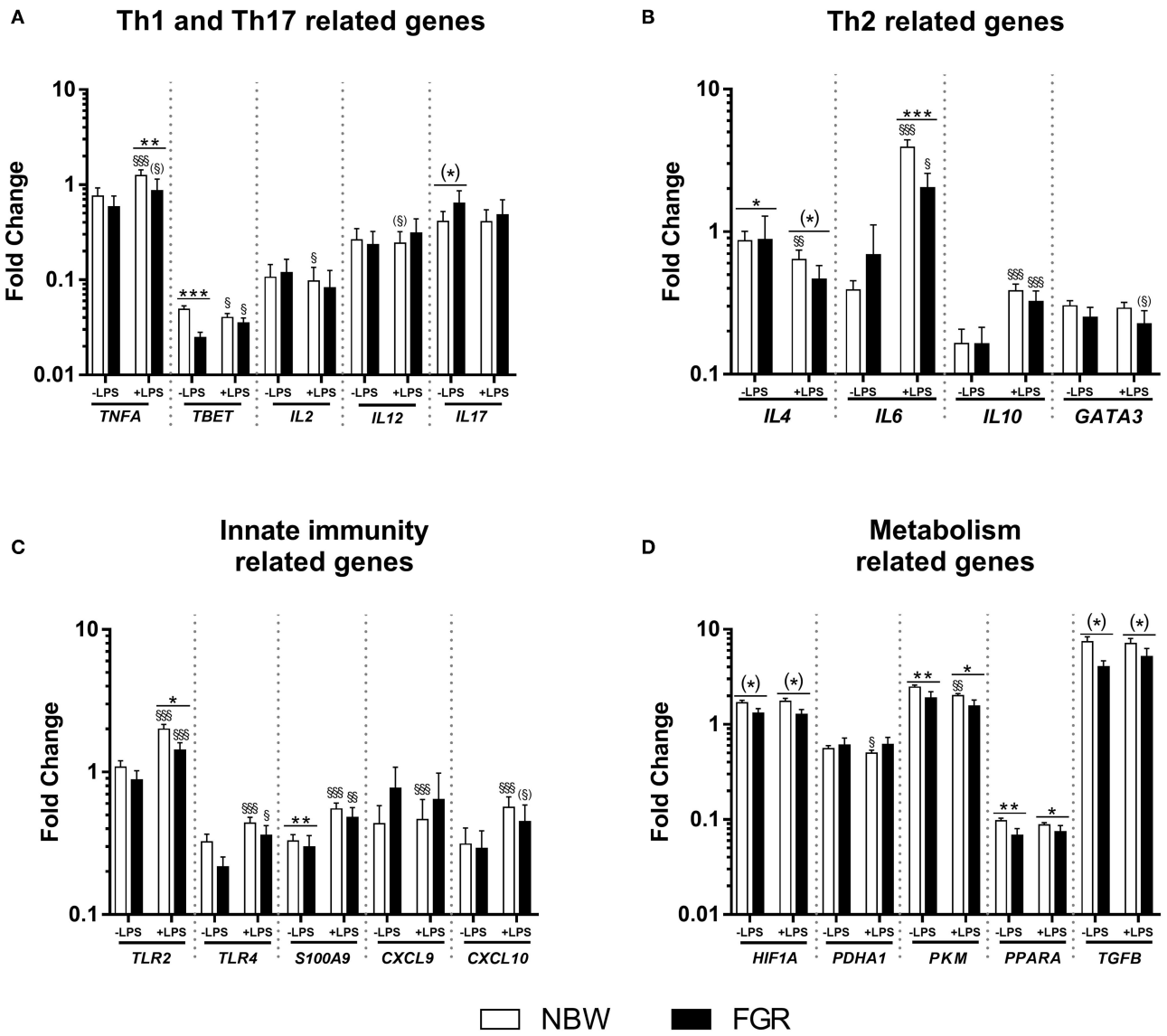

FIGURE 1 | Cord blood leucocyte gene expressions in normal birth weight (NBW, $n = 60$) and fetal growth restricted (FGR, $n = 21$) preterm pigs. Expression of **(A)** Th1 and Th17–, **(B)** Th2–, **(C)** innate immunity-, and **(D)** cellular metabolism-related genes. Data are shown as fold changes in relation to housekeeping gene, all presented on a logarithmic scale, before and after stimulation with lipopolysaccharide (LPS). Data are presented as means with corresponding standard error. *: Difference between NBW and FGR; (*) $P < 0.1$, *$P < 0.05$, **$P < 0.01$, ***$P < 0.001$. §: Effect of LPS stimulation; (§)$P < 0.1$, §$P < 0.05$, §§$P < 0.01$, §§§$P < 0.001$.

and *TGFB* (both $P = 0.07$, **Figure 1D**). Within the NBW group, LPS stimulation lead to lower expression of *PADHA1 and PKM* (all $P < 0.05$, **Figure 1D**). Within the FGR group, LPS stimulation did not affect the expression of any metabolism related gene.

Severe Sepsis Outcomes in Newborn Preterm FGR Pigs Following SE Infection

In *Exp 2*, the mean birth weight was lower in SE-FGR than SE-NBW (701 ± 38 vs. 993 ± 34 g, $P < 0.001$). The overall birth weight did not differ between SE inoculated animals and CON (data not shown). Following SE infusion, SE inoculated pigs showed septic responses with lower blood pH and higher blood carbon dioxide pressure at 6 and 12 h (all $P < 0.01$, **Figures 2A,B**), and higher bicarbonate levels and lower oxygen pressure at 12 h after inoculation ($P < 0.05$ and 0.001, respectively, **Figures 2C,F**). Relative to SE-NBW pigs, SE-FGR preterm pigs had lower blood pH 6 h after inoculation with corresponding higher carbon dioxide pressure (all $P < 0.01$, **Figures 2A,B**). After 12 h, pH was still lower in SE-FGR with higher bicarbonate and lactate levels (**Figures 2A,C,E**). Blood glucose levels were consistently higher in SE-FGR than SE-NBW pigs at both 6 and 12 h ($P < 0.05$, **Figure 2F**).

For the cellular immune parameters, relative to controls, SE infected pigs experienced depletion of blood neutrophils,

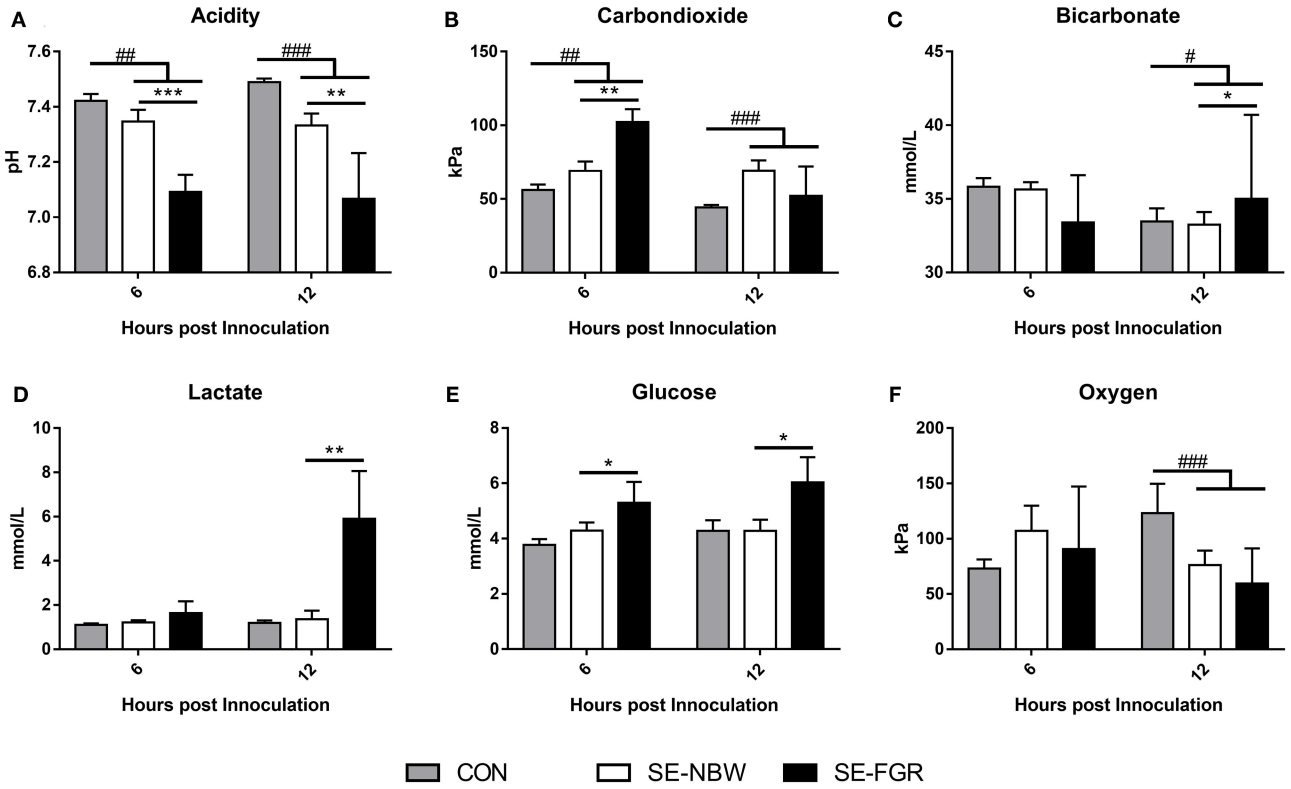

FIGURE 2 | Blood gas parameters in normal birth weight and fetal growth restricted preterm pigs inoculated with live *Staphylococcus epidermidis* (SE-NBW, $n = 29$ and SE-FGR, $n = 9$, respectively), as well as preterm pigs inoculated with control saline (CON, $n = 19$). **(A)** Blood pH. **(B)** Blood carbondioxide pressure. **(C)** Blood levels of bicarbonate. **(D)** Blood levels of lactate. **(E)** Blood glucose levels. **(F)** Blood oxygen pressure Data are presented as means with corresponding standard error, 6 and 12 h after inoculation. $^{\#}$: Difference between all SE inoculated preterm pigs and CON; $^{\#}P < 0.05$, $^{\#\#}P < 0.01$, $^{\#\#\#}P < 0.001$. *: Difference between SE-NBW and SE-FGR; $^{*}P < 0.05$, $^{**}P < 0.01$, $^{***}P < 0.001$.

lymphocytes, and monocytes at 6 and 12 h (all $P < 0.001$, **Figures 3A,B,D**) with lower platelet counts only at 12 h ($P < 0.001$, **Figure 3B**). Relative to SE-NBW pigs, SE-FGR pigs showed blood lower neutrophil and platelet counts after 12 h ($P < 0.05$ and 0.001, respectively, **Figures 3A,B**). Blood lymphocyte and monocyte counts were higher in SE-FGR vs. SE-NBW pigs after 6 and 12 h (all $P < 0.05$, respectively, **Figure 3C**). The full panel of hematological parameters at 6, 12, and 24 h after inoculation was shown in **Supplementary Table 1**.

Impaired Immune Competence and Increased Nosocomial Infection in Neonatal Preterm FGR Pigs

In *Exp 3*, the overall birth weight were significantly lower in FGR than NBW animals (740 ± 30 vs. 1,141 ± 19 g, $P < 0.001$). At euthanasia on day 9, FGR-CON pigs showed a higher incidence of spontaneous aerobic bacterial infection of the bone marrow than their NBW-CON counterparts ($P < 0.05$, **Figure 4A**). The effect was still significant when comparing all FGR preterm pigs to all NBW (95 vs. 67%, Fisher's exact test: $P < 0.01$). The density of aerobic bacteria in the bone marrow was higher in FGR-CON pigs compared to NBW-CON ($P < 0.01$), but not in FGR-AB compared to NBW-AB (**Figure 4B**). When comparing all pigs, FGR preterm pigs had higher densities of aerobic bacteria in the bone marrow compared to NBW (3.9 vs. 2.6 × 10^9 CFU/ml, $P < 0.01$). The incidence of anaerobic bacterial infection in bone marrow did not differ between groups (**Figure 4C**). However, the density of anaerobically cultured bacteria was higher in FGR-CON than NBW-CON ($P < 0.05$, **Figure 4D**). The dominant strains of aerobically cultured bacteria isolated from the bone marrow are shown in **Figure 4E** with the dominance of *Enterococcus* and *Staphyloccocus* spp.

For hematological parameters, FGR-CON pigs showed higher blood neutrophil counts on day 5 than NBW-CON ($P < 0.05$, **Figure 5A**). On day 9, FGR-CON still had higher blood neutrophil counts than NBW-CON, but FGR-AB had lower neutrophil counts than NBW-AB (all $P < 0.05$, **Figure 5A**). Blood neutrophil phagocytosis function was also affected, as FGR-AB treated pigs had a lower phagocytic rate on both day 5 and 9 ($P < 0.01$ and 0.001, respectively), with a correspondingly lower phagocytic capacity only on day 5 ($P < 0.05$, **Figures 5B,C**). When comparing all FGR pigs to all NBW, only the phagocytic rate at day 5 differed, being lower in FGR pigs (85 ± 4 vs. 91

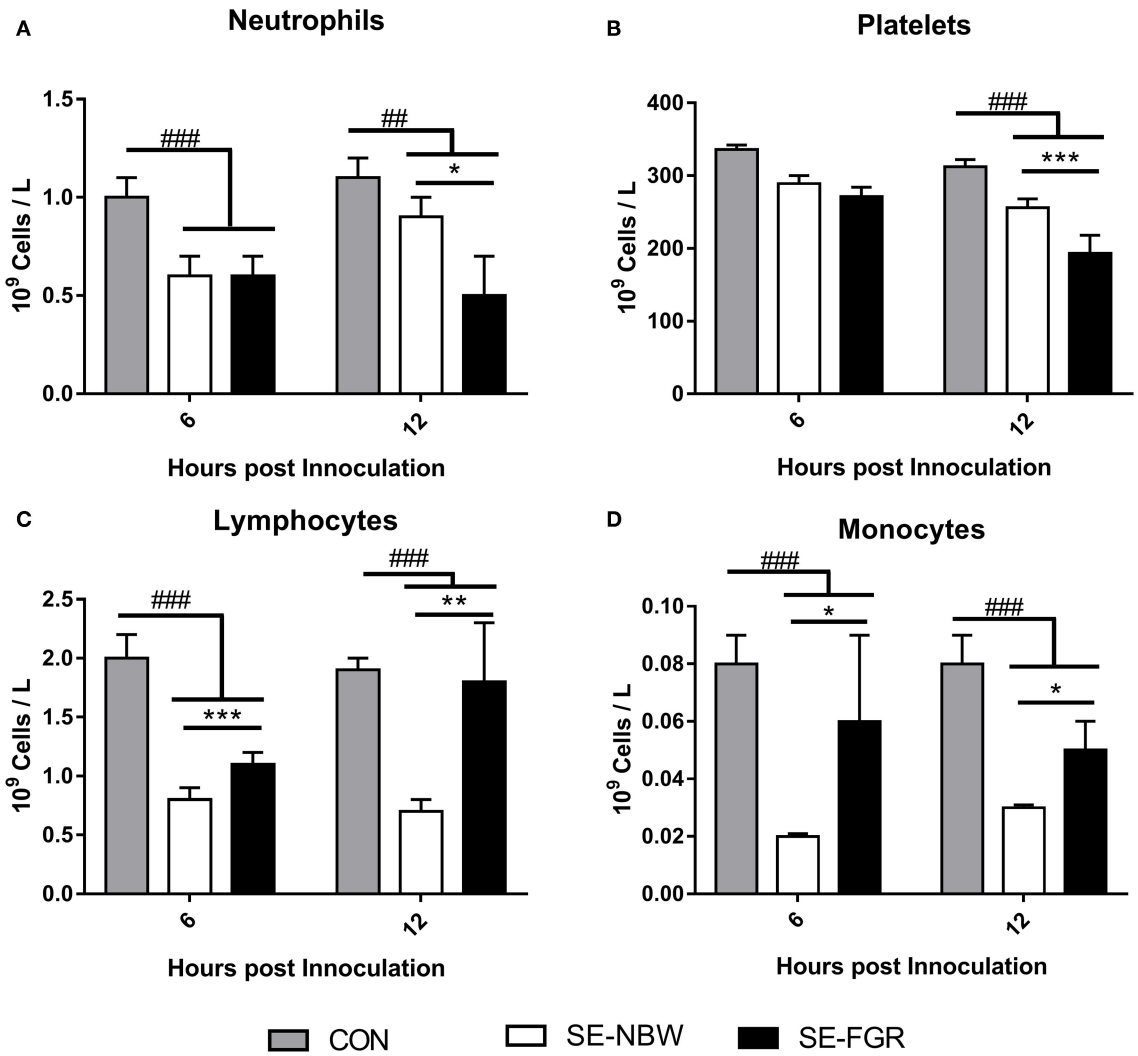

FIGURE 3 | Hematological parameters in normal birth weight and fetal growth restricted preterm pigs inoculated with live *Staphylococcus epidermidis* (SE-NBW, $n = 29$ and SE-FGR, $n = 9$, respectively), as well as preterm pigs inoculated with control saline (CON, $n = 19$). **(A–D)** Blood neutrophil, lymphocyte, platelet, and monocyte counts. Data are presented as means with corresponding standard error, 6 and 12 h after inoculation. #: Difference between all SE inoculated preterm pigs and CON. $^{\#\#}P < 0.01$, $^{\#\#\#}P < 0.001$. *: Difference between SE-NBW and SE-FGR; $^{*}P < 0.05$, $^{**}P < 0.01$, $^{***}P < 0.001$.

± 1%, $P < 0.01$). Blood platelet counts were lower in FGR-CON than NBW-CON on day 5, but higher on day 7 ($P < 0.05$, **Figure 5D**). For FGR-AB, the platelets counts were lower on day 7 and 9 than in NBW-AB (all $P < 0.05$, **Figure 5D**). For blood T cell subsets in non-antibiotics treated animals, the fraction of regulatory T cells was higher on day 7 in the FGR-CON group relative to NBW-CON ($P < 0.05$). In antibiotics treated animals, FGR-AB had increased fractions of both CD4 positive and regulatory T cells on days 5, 7, and 9 compared to NBW-AB ($P < 0.05$, except CD4 positive T cells on day 5 and regulatory T cells on day 9, $P < 0.01$, **Figures 5E,F**). In addition, the ratio of CD4 to CD8 positive T cells was increased in FGR-AB pigs, compared to NBW-AB on day 9 (9.2 ± 1.1 vs. 5.8 ± 0.6, $P < 0.001$). Besides these findings, FGR pigs showed higher levels of total leucocytes, red blood cells, and hematocrit over the course of the experiment, compared to their NBW counterparts (**Supplementary Table 2**).

Gene expression analysis after blood stimulation on day 5 and 9 was performed to support the hematological and T cell findings (**Figures 6A–F**). On day 5, baseline gene expressions did not differ between FGR-CON and NBW-CON or FGR-AB or NBW-AB. After stimulation with LPS, expressions of *TLR2*, *TLR4*, and *CXCL9* were increased only in NBW-CON pigs, but not FGR-CON (all $P < 0.05$, **Figures 6A–C**). For these same genes, LPS effects were similar in FGR-AB and NBW-AB pigs. Only *TBET* was expressed slightly more in FGR-AB pigs after LPS stimulation, than in NBW-AB ($P < 0.01$, **Figure 6E**). By day 9, the baseline expression of *TLR2* was higher in FGR-CON

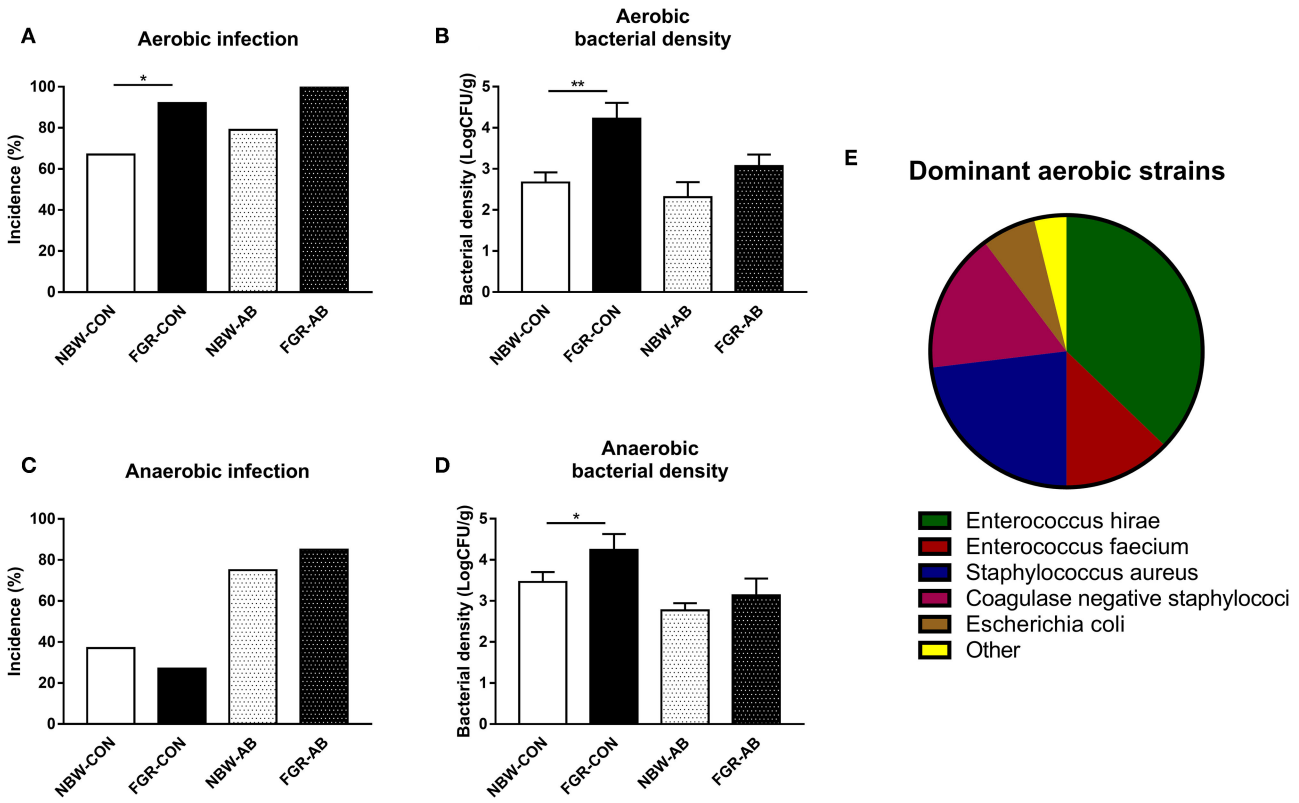

FIGURE 4 | Spontaneous bacterial infection of the bone marrow of normal birth weight or fetal growth restricted preterm pigs, reared for 9 days, receiving either antibiotics (NBW-AB, $n = 22$ and FGR-AB, $n = 8$) or not (NBW-CON, $n = 78$ and FGR-CON, $n = 19$). **(A)** Incidence of aerobically cultured bacterial growth in the bone marrow. **(B)** Density of aerobically cultured bacteria in the bone marrow. **(C)** Incidence of anaerobically cultured bacterial growth in the bone marrow. **(D)** Density of anaerobically cultured bacteria in the bone marrow. **(E)** Distribution of dominant aerobically cultured bacterial strains. **(A,C)** Presented as fraction of animals with bacterial growth. **(B,D)** Presented as means with corresponding standard error. **(E)** Each bacterial group, shown as a fraction of the whole. *: Difference between either NBW-CON and FGR-CON or NBW-AB and FGR-AB; $^*P < 0.05$, $^{**}P < 0.01$.

pigs than NBW-CON ($P < 0.05$, **Figure 6A**) but tended to be lower for *CXCL9* ($P = 0.07$, **Figure 6C**). Furthermore, FGR-CON pigs were not able to mount expressions of *TLR2* and *TLR4* after stimulation with LPS, whereas NBW-CON pigs were more competent ($P < 0.01$ and 0.001, respectively, **Figures 6A,B**). Baseline expression of genes did not differ between FGR-AB and NBW-AB on day 9. However, after stimulation with LPS, FGR-AB pigs showed lower expression of *TLR2*, *CXCL9*, *CXCL10*, and *TBET* than NBW-AB (all $P < 0.05$, **Figures 1A,C–E**) with a tendency toward lower expression of *TLR4* and *IL10* ($P = 0.07$ and 0.06, respectively, **Figures 6B,F**). Likewise, the FGR-AB pigs did not increase expression of *IL10* after LPS stimulation, whereas NBW-AB did ($P < 0.01$, **Figure 6F**). For the remaining tested genes, there were no or minor differences among the groups (**Supplementary Table 3**).

DISCUSSION

Following preterm birth, immune status, and infection resistance during the first days and weeks of life are critical factors for survival and long-term health. We show that preterm pigs born following fetal growth-restriction, show clear evidence of impaired immune competence in the critical neonatal period, with adverse clinical outcome after infection challenge and an increased rate of spontaneous infections. Interestingly, the effects of being born growth restricted were in part exacerbated by antibiotic use in the immediate postnatal period, although more studies are required to confirm this and investigate mechanisms. Collectively, our data help to explain why infants born both premature and SGA have increased morbidity and mortality. Although antibiotics seemed to reduce bacterial densities in bone marrow, the results suggest a need for increased critical care, but also cautious antibiotics use, for this special subpopulation of preterm newborn infants.

Cord blood of FGR and NBW pigs was initially used to examine immune competence at birth by a whole blood stimulation assay with LPS. Before LPS stimulation, FGR preterm pigs showed lower baseline expressions of few genes, However, we did not measure the leucocyte levels in *Exp 1*, but we have previously shown that FGR piglets tend to have lower lymphocyte counts (but not neutrophil and monocyte counts) in cord blood (10). Therefore, it is possible that differences in expressions of some lymphocytes-related genes at baseline may be influenced by the leucocyte levels. Still, after stimulation with LPS, it appeared

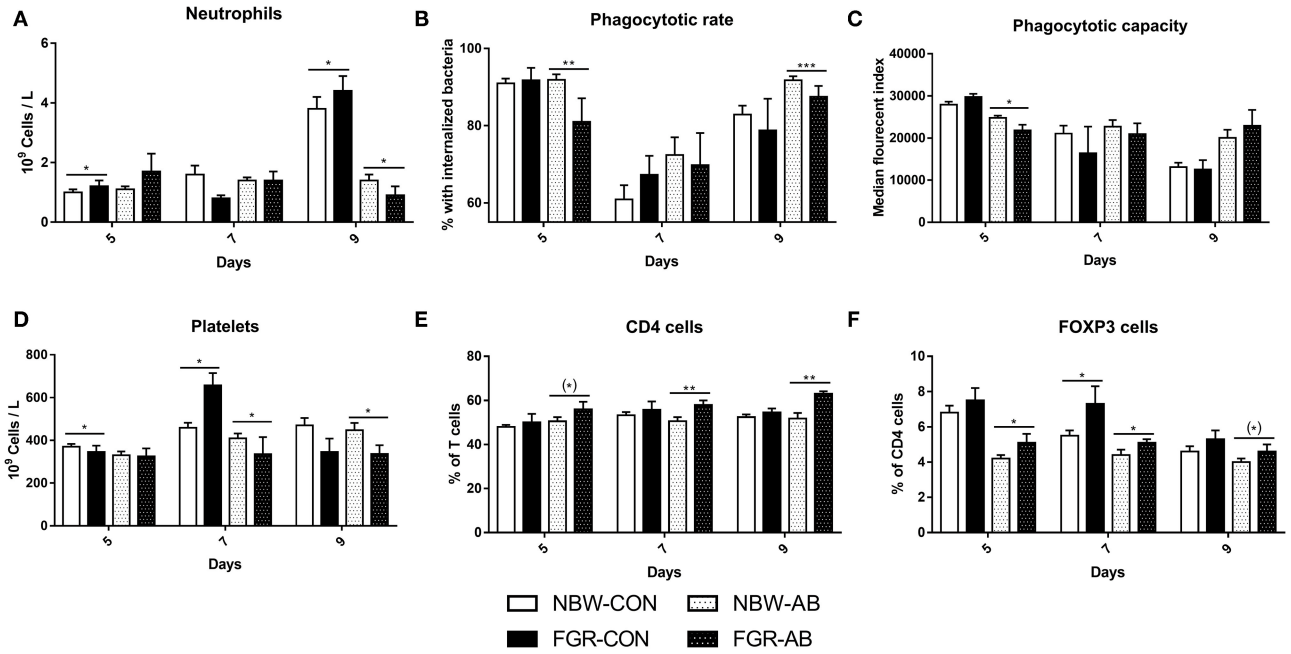

FIGURE 5 | Blood immune cell subsets of normal birth weight or fetal growth restricted preterm pigs, reared for 9 days, receiving either antibiotics (NBW-AB, n = 13–19 and FGR-AB, n = 5–7) or not (NBW-CON, n = 47–54 and FGR-CON, n = 12–14). **(A)** Blood neutrophil counts. **(B)** Neutrophil phagocytic rate. **(C)** Neutrophil phagocytic capacity. **(D)** Blood platelets counts. **(E)** Fraction of CD4 positive T cells, as a percentage of all T cells. **(F)** Fraction of regulatory T cells, as a percentage of CD4 positive T cells. Data are presented as means with corresponding standard error, 5, 7, and 9 days after birth. *: Difference between either NBW-CON and FGR-CON or NBW-AB and FGR-AB; (*)$P < 0.1$, *$P < 0.05$, **$P < 0.01$, ***$P < 0.001$.

that blood leucocytes of FGR animals had a diminished response with regards to several genes related to innate and adaptive immunity as well as cellular metabolism. This indicates an overall impaired capacity to mount sufficient immune response to infectious challenges in newborn preterm pigs with fetal growth restriction. This is similar to the diminished immune function at birth observed in cord blood of SGA preterm infants (17).

To be able to relate the *ex vivo* immune response to the actual infection outcomes in FGR preterm pigs, we performed an *in vivo* infection challenge with systemic administration of SE to induce neonatal sepsis (*Exp 2*), in a similar manner to previous studies (29). SE is normally considered a low virulent pathogen and was previously often considered a contamination if cultured from the blood (33). However, coagulase negative staphylococci, like SE, are among the most common organism isolated from preterm infants with LOS (3, 34). As expected, SE infected pigs appeared to undergo respiratory acidosis 6 h after infusion (low blood pH and oxygen pressure with high carbon dioxide pressure), similar to what have been observed in preterm infants with neonatal sepsis (35). The overall effects of SE challenge, when compared to saline infused pigs (drop in pH and leucocyte subsets after SE inoculation), were also similar to those that we have observed in previous experiments, using the same model (29). This confirms that pigs underwent a relevant immunological challenge. Interestingly, SE infected FGR animals showed more severe clinical and cellular responses, relative to their littermates of adequate birth weight. Their drop in blood pH and bicarbonate was followed by a corresponding rise in lactate, indicating that the FGR preterm pigs were undergoing a more severe septic response to the SE challenge. This was also accompanied by a more severe drop in neutrophils and platelets in SE-FGR pigs. Collectively, it was clear that newborn growth restricted preterm pigs were more affected by the SE inoculation than their preterm normal birth weight counterparts. The combined data in *Exp 1* and *2* suggest that infants born with prematurity and fetal growth restriction have impaired immune competence that may lead to higher susceptibility to neonatal sepsis following systemic infection, in the immediate neonatal period.

We also attempted to characterize the immune development and test the susceptibility to spontaneous infection, over the first few days after preterm birth in FGR pigs. It was evident that FGR preterm pigs, were more prone to infection of aerobically cultured bacteria in their bone marrow, with higher densities of bacteria than pigs of adequate birth weight. The effect was less apparent for antibiotics treated pigs that showed bacterial densities comparable to the NBW-CON pigs. For anaerobically cultured bacteria there were no effects, possibly a result of the high blood flow in the bone marrow, somewhat restricting anaerobic bacterial growth. In fact, very few strictly anaerobic bacteria could be cultured (data not shown). The species of aerobically cultured bacteria found in the bone marrow are all known to inhabit the gut of preterm infants and pigs (34, 36). This indicates that preterm SGA infants may be either more

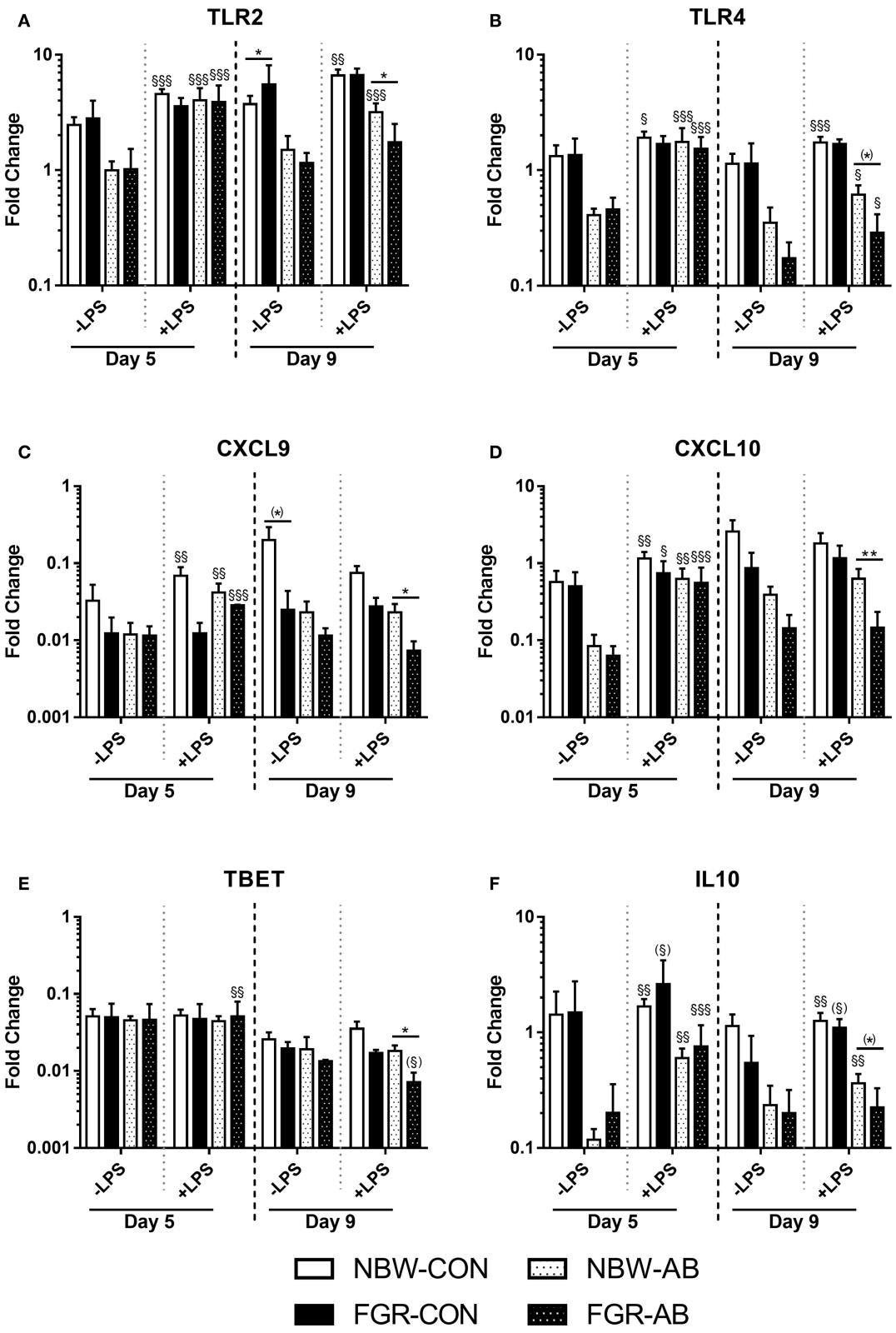

FIGURE 6 | Blood leucocyte gene expressions of normal birth weight or fetal growth restricted preterm pigs, reared for 9 days, receiving either antibiotics (NBW-AB, $n = 8$–17 and FGR-AB, $n = 2$–5) or not (NBW-CON, $n = 14$–22 and FGR-CON, $n = 3$). **(A–F)** Expression of *TLR2, TLR4, CXCL9, CXCL10, TBET*, and *IL10*. Data are presented as means with corresponding standard error, 5 and 9 days after birth. *: Difference between either NBW-CON and FGR-CON or NBW-AB and FGR-AB; (*): $P < 0.1$, $^{*}P < 0.05$, $^{**}P < 0.01$. §: Effect of LPS stimulation; (§):$P < 0.1$, $^{§}P < 0.05$, $^{§§}P < 0.01$, $^{§§§}P < 0.001$.

prone to bacterial translocation across the gut or have a reduced capacity to clear the gut derived systemic bacteria. In this study, we have not investigated gut permeability *per se*, so differentiating between the two factors is difficult. The supporting data showed that over the first week of life, FGR preterm pigs consistently had poorer systemic immune functions and an immune suppressed status, with less capacity to response to an *ex vivo* challenge.

The development of immune cell subsets, including T cell subsets, was affected by neonatal antibiotic treatment, as expected (24). Interestingly though, adverse immune effects of being born FGR were more pronounced in animals treated with antibiotics. The FGR-AB preterm pigs showed lower neutrophil counts with poorer phagocytosis capacity, as well as higher fractions of CD4 positive and regulatory T cells, relative to NBW-AB. The FGR-CON pigs also showed higher counts of regulatory T cells on day 7, indicating the effect of low birth weight was not entirely dependent on antibiotics. These results suggest that FGR preterm pigs, irrespective of antibiotic treatment, had decreased immune function, relative to their NBW counterparts. The whole blood LPS stimulation assays could support this conclusion in that blood leucocytes of FGR-AB pigs expressed less *TBET* than NBW-AB pigs, indicating that the increased number of CD4 positive T cells in FGR-AB pigs were skewed toward a Th2 phenotype. As in *Exp 1*, the baseline leucocyte gene expression levels could be influenced by the differences in neutrophil counts observed. However, several innate immune related genes were also expressed less in FGR-AB and FGR-CON pigs following LPS stimulation than in their NBW counterparts. The increased fraction of regulatory T cells may act to dampen the immune competence or delay immune maturation in FGR preterm pigs. This immune suppressive status may lead to less systemic bacterial clearance and more bacterial accumulation in the bone marrow of FGR preterm pigs. However, these longer term immune effects are more suggestive and require further exploration.

Interestingly, in *Exp 1*, we found that cord blood leucocytes of newborn growth restricted preterm pigs had a lower expression of genes related to cellular energy metabolism (*PPARA, HIF1A*, and *PKM*), both before and after LPS stimulation. The *PPARA* gene encodes the protein peroxisome proliferator–activated receptor α, which is crucial for fatty acid metabolism and ketogenesis (37). The gene is mostly expressed in hepatocytes, where it plays a major role in fasting responses (38). However, higher levels of peroxisome proliferator–activated receptors in monocytes has been linked to anti-inflammatory cytokine production and differentiation to macrophages (39–41) as well as increased activity of cellular fatty acid oxidation and oxidative phosphorylation (42). Pyruvate kinase (encoded by *PKM*) is a glycolytic enzyme crucial for the generation of adenosine triphosphate (ATP), the last step of the glycolysis process, normally occurring under anaerobic conditions (43). However, it is well-established that pro-inflammatory leucocytes rely on glycolysis to exude their function, even when oxygen is abundant, a phenomenon known as the Warburg effect (44, 45). Hypoxia-inducible factor-1a (encoded by *HIF1A*) is also a regulator in glycolysis and has been proposed as a mediator of the Warburg effect (46, 47) via the mTOR immune pathway and therefore can also be considered an immune related factor (48, 49). The drop in expressions of *PKM, HIF1A*, and *PPARA* in *Exp 1* may reflect less ATP production, possibly due to lower energy reservoirs, and therefore could impair energy-consuming immune responses in the FGR preterm pigs. This observation was similar to the poor immune responses and low expressions of monocyte genes related to both glycolysis and oxidative phosphorylation in preterm vs. term infants (50). Further, following SE inoculation in *Exp 2*, the FGR pigs had higher glucose levels, which could indicate a dysregulated metabolism during infections or endogenous glucose generation associated with more excessive inflammatory response. This could possibly be part of the explanation for their poorer outcome, compared to NBW preterm piglets subjected to the same experimental SE inoculation.

Preterm pigs have emerged as good models for preterm infants, with many similarities in size, physiology, and immune system (27, 32). Due to the large litter sizes of pigs there is a sizable variation in birth weight, making it possible to compare low and high birth weight individuals (51). The causes of this birth weight variation may be a combination of placental variation in blood flow and intrinsic fetal genetic determinants. In humans, the causes leading to slow intrauterine growth are more diverse, including other associated pathologies, like maternal infections and preeclampsia playing a role (52). These conditions could separately affect postnatal immune development, regardless of birth weight. Using elective cesarean section of preterm pigs from uncomplicated sow pregnancies, we can study the effects of fetal growth restriction, independent of such inflammatory and pathological maternal conditions, leading to preterm birth with/without SGA in infants. Since there were no prenatal complications prior to delivery of piglets, the observed immunity effects in this study are likely to arise from slow intrauterine growth *per se*, independent of any fetal or maternal inflammatory or pathological conditions.

We conclude that there are clear effects on the neonatal immune system of being born SGA after preterm birth, with greater sensitivity and adverse response to bacterial infection, less responsive leucocytes *in vitro*, and increased fraction of regulatory T cells. Collectively, our results suggest that preterm pigs born moderately growth restricted were immune suppressed or experienced some delay in immune maturation, which may be further exacerbated by neonatal antibiotic use. Such effects may be most pronounced in the immediate neonatal period (e.g., the first 1–2 weeks), as supported by the limited effects of moderate FGR and prematurity on blood immune parameters (10, 53) and gut and brain development beyond the first 2 weeks of life (53, 54). Correspondingly, a dysfunctional immune system and an increased risk of infections in preterm infants with fetal growth restriction suggest special care and medical attention in this population to avoid damaging infections in the critical neonatal period.

DATA AVAILABILITY STATEMENT

The raw data supporting the conclusions of this article will be made available by the authors, without undue reservation.

ETHICS STATEMENT

The animal study was reviewed and approved by Danish National Committee on Animal Experimentation (2014-15-0201-00418).

AUTHOR CONTRIBUTIONS

DN designed the study. DN, AB, and SR carried out the experiments and laboratory analysis. OB performed data analysis and wrote the manuscript. OB, SR, AB, PS, and DN provided critical interpretation and revised the manuscript. OB and DN had primary responsibility for the final content. All authors approved the final paper.

ACKNOWLEDGMENTS

We would like to thank Thomas Thymann, Yanqi Li, Xiaoyu Pan, Elin Skytte, Jane C. Povlsen, and Kristina Møller for their help performing these experiments. This study was supported by NEOCOL project funded by Innovation Foundation Denmark.

SUPPLEMENTARY MATERIAL

The Supplementary Material for this article can be found online at: https://www.frontiersin.org/articles/10.3389/fimmu.2020.01808/full#supplementary-material

REFERENCES

1. Fanaroff AA, Korones SB, Wright LL, Verter J, Poland RL, Bauer CR, et al. Incidence, presenting features, risk factors and significance of late onset septicemia in very low birth weight infants. the national institute of child health and human development neonatal research network. *Pediatr Infect Dis J.* (1998) 17:593–8. doi: 10.1097/00006454-199807000-00004
2. el Manouni el Hassani S, Berkhout DJC, Niemarkt HJ, Mann S, de Boode WP, Cossey V, et al. Risk factors for late-onset sepsis in preterm infants: a multicenter case-control study. *Neonatology.* (2019) 116:42–51. doi: 10.1159/000497781
3. Stoll BJ, Hansen N, Fanaroff AA, Wright LL, Carlo WA, Ehrenkranz RA, et al. Late-onset sepsis in very low birth weight neonates: the experience of the NICHD neonatal research network. *Pediatrics.* (2002) 110:285–91. doi: 10.1542/peds.110.2.285
4. Strunk T, Currie A, Richmond P, Simmer K, Burgner D. Innate immunity in human newborn infants: prematurity means more than immaturity. *J Matern Neonatal Med.* (2011) 24:25–31. doi: 10.3109/14767058.2010.482605
5. Kristensen S, Salihu HM, Keith LG, Kirby RS, Fowler KB, Pass MAB. SGA subtypes and mortality risk among singleton births. *Early Hum Dev.* (2007) 83:99–105. doi: 10.1016/j.earlhumdev.2006.05.008
6. Watts T, Roberts I. Haematological abnormalities in the growth-restricted infant. *Semin Neonatol.* (1999) 4:41–54. doi: 10.1016/S1084-2756(99)80006-2
7. Li J, Li H, Mao H, Yu M, Yang F, Feng T, et al. Impaired NK cell antiviral cytokine response against influenza virus in small-for-gestational-age neonates. *Cell Mol Immunol.* (2013) 10:437–43. doi: 10.1038/cmi.2013.31
8. Ferguson AC. Prolonged impairment of cellular immunity in children with intrauterine growth retardation. *J Pediatr.* (1978) 93:52–56. doi: 10.1016/S0022-3476(78)80599-X
9. McDade TW, Beck MA, Kuzawa CW, Adair LS. Prenatal undernutrition and postnatal growth are associated with adolescent thymic function. *J Nutr.* (2001) 131:1225–31. doi: 10.1093/jn/131.4.1225
10. Bæk O, Sangild PT, Thymann T, Nguyen DN. Growth restriction and systemic immune development in preterm piglets. *Front Immunol.* (2019) 10:2402. doi: 10.3389/fimmu.2019.02402
11. Amdi C, Lynegaard JC, Thymann T, Williams AR. Intrauterine growth restriction in piglets alters blood cell counts and impairs cytokine responses in peripheral mononuclear cells 24 days post-partum. *Sci Rep.* (2020) 10:4683. doi: 10.1038/s41598-020-61623-w
12. Hu L, Peng X, Chen H, Yan C, Liu Y, Xu Q, et al. Effects of intrauterine growth retardation and Bacillus subtilis PB6 supplementation on growth performance, intestinal development and immune function of piglets during the suckling period. *Eur J Nutr.* (2017) 56:1753–65. doi: 10.1007/s00394-016-1223-z
13. Han F, Hu L, Xuan Y, Ding X, Luo Y, Bai S, et al. Effects of high nutrient intake on the growth performance, intestinal morphology and immune function of neonatal intra-uterine growth-retarded pigs. *Br J Nutr.* (2013) 110:1819–27. doi: 10.1017/S0007114513001232
14. Tröger B, Göpel W, Faust K, Müller T, Jorch G, Felderhoff-Müser U, et al. Risk for late-onset blood-culture proven sepsis in very-low-birth weight infants born small for gestational age: a large multicenter study from the German neonatal network. *Pediatr Infect Dis J.* (2014) 33:238–43. doi: 10.1097/INF.0000000000000031
15. Zeitlin J, El Ayoubi M, Jarreau PH, Draper ES, Blondel B, Künzel W, et al. Impact of fetal growth restriction on mortality and morbidity in a very preterm birth cohort. *J Pediatr.* (2010) 157:733–9.e1. doi: 10.1016/j.jpeds.2010.05.002
16. Bernstein IM, Horbar JD, Badger GJ, Ohlsson A, Golan A. Morbidity and mortality among very-low-birth-weight neonates with intrauterine growth restriction. the vermont oxford network. *Am J Obstet Gynecol.* (2000) 182:198–206. doi: 10.1016/S0002-9378(00)70513-8
17. Tröger B, Müller T, Faust K, Bendiks M, Bohlmann MK, Thonnissen S, et al. Intrauterine growth restriction and the innate immune system in preterm infants of $\leq$32 weeks gestation. *Neonatology.* (2013) 103:199–204. doi: 10.1159/000343260
18. Vincent JL, Beumier M. Diagnostic and prognostic markers in sepsis. *Expert Rev Anti Infect Ther.* (2013) 11:265–75. doi: 10.1586/eri.13.9
19. Hedegaard SS, Wisborg K, Hvas AM. Diagnostic utility of biomarkers for neonatal sepsis - a systematic review. *Infect Dis.* (2015) 47:117–24. doi: 10.3109/00365548.2014.971053
20. Ng PC, Ang IL, Chiu RWK, Li K, Lam HS, Wong RPO, et al. Host-response biomarkers for diagnosis of late-onset septicemia and necrotizing enterocolitis in preterm infants. *J Clin Invest.* (2010) 120:2989–3000. doi: 10.1172/JCI40196
21. Clark RH, Bloom BT, Spitzer AR, Gerstmann DR. Empiric use of ampicillin and cefotaxime, compared with ampicillin and gentamicin, for neonates at risk for sepsis is associated with an increased risk of neonatal death. *Pediatrics.* (2006) 117:67–74. doi: 10.1542/peds.2005-0179
22. Stoll BJ, Hansen NI, Higgins RD, Fanaroff AA, Duara S, Goldberg R, et al. Very low birth weight preterm infants with early onset neonatal sepsis: the predominance of gram-negative infections continues in the national institute of child health and human development neonatal research network, 2002-2003. *Pediatr Infect Dis J.* (2005) 24:635–9. doi: 10.1097/01.inf.0000168749.82105.64
23. Nguyen DN, Fuglsang E, Jiang P, Birck MM, Pan X, Kamal SBS, et al. Oral antibiotics increase blood neutrophil maturation and reduce bacteremia and necrotizing enterocolitis in the immediate postnatal period of preterm pigs. *Innate Immun.* (2016) 22:51–62. doi: 10.1177/1753425915615195
24. Fouhse JM, Yang K, More-Bayona J, Gao Y, Goruk S, Plastow G, et al. Neonatal exposure to amoxicillin alters long-term immune response despite transient effects on gut-microbiota in piglets. *Front Immunol.* (2019) 10:2059. doi: 10.3389/fimmu.2019.02059
25. Ni J, Friedman H, Boyd BC, McGurn A, Babinski P, Markossian T, et al. Early antibiotic exposure and development of asthma and allergic rhinitis in childhood. *BMC Pediatr.* (2019) 19:225. doi: 10.1186/s12887-019-1594-4
26. Tsakok T, McKeever TM, Yeo L, Flohr C. Does early life exposure to antibiotics increase the risk of eczema? A systematic review. *Br J Dermatol.* (2013) 169:983–91. doi: 10.1111/bjd.12476

27. Sangild PT, Thymann T, Schmidt M, Stoll BJ, Burrin DG, Buddington RK. The preterm pig as a model in pediatric gastroenterology. *J Anim Sci.* (2013) 91:4713–6359. doi: 10.2527/jas.2013-6359
28. Bæk O, Brunse A, Nguyen DN, Moodley A, Thymann T, Sangild PT. Diet modulates the high sensitivity to systemic infection in newborn preterm pigs. *Front Immunol.* (2020) 11:1019. doi: 10.3389/fimmu.2020.01019
29. Brunse A, Worsøe P, Pors SE, Skovgaard K, Sangild PT. Oral supplementation with bovine colostrum prevents septic shock and brain barrier disruption during bloodstream infection in preterm newborn pigs. *SHOCK.* (2018) 51:337–47. doi: 10.1097/SHK.0000000000001131
30. Li Y, Pan X, Nguyen DN, Ren S, Moodley A, Sangild PT. Bovine colostrum before or after formula feeding improves systemic immune protection and gut function in newborn preterm pigs. *Front Immunol.* (2020) 10:3062. doi: 10.3389/fimmu.2019.03062
31. Ren S, Hui Y, Goericke-Pesch S, Pankratova S, Kot W, Pan X, et al. Gut and immune effects of bioactive milk factors in preterm pigs exposed to prenatal inflammation. *Am J Physiol - Gastrointest Liver Physiol.* (2019) 317:G67–G77. doi: 10.1152/ajpgi.00042.2019
32. Nguyen DN, Jiang P, Frøkiær H, Heegaard PMH, Thymann T, Sangild PT. Delayed development of systemic immunity in preterm pigs as a model for preterm infants. *Sci Rep.* (2016) 6:36816. doi: 10.1038/srep36816
33. Padari H, Oselin K, Tasa T, Metsvaht T, Lõivukene K, Lutsar I. Coagulase negative staphylococcal sepsis in neonates: do we need to adapt vancomycin dose or target? *BMC Pediatr.* (2016) 16:206. doi: 10.1186/s12887-016-0753-0
34. Graspeuntner S, Waschina S, Künzel S, Twisselmann N, Rausch TK, Cloppenborg-Schmidt K, et al. Gut dysbiosis with bacilli dominance and accumulation of fermentation products precedes late-onset sepsis in preterm infants. *Clin Infect Dis.* (2019) 69:268–77. doi: 10.1093/cid/ciy882
35. Shane AL, Sánchez PJ, Stoll BJ. Neonatal sepsis. *Lancet.* (2017) 390:1770–80. doi: 10.1016/S0140-6736(17)31002-4
36. Rasmussen SO, Martin L, Østergaard MV, Rudloff S, Li Y, Roggenbuck M, Bering SB, et al. Bovine colostrum improves neonatal growth, digestive function and gut immunity relative to donor human milk and infant formula in preterm pigs. *Am J Physiol - Gastrointest Liver Physiol.* (2016) 311:G480–91. doi: 10.1152/ajpgi.00139.2016
37. Desvergne B, Ijpenberg A, Devchand PR, Wahli W. The peroxisome proliferator-activated receptors at the cross-road of diet and hormonal signalling. *J Steroid Biochem Mol Biol.* 65:65–74. doi: 10.1016/S0960-0760(97)00182-9
38. Kersten S, Seydoux J, Peters JM, Gonzalez FJ, Desvergne B, Wahli W. Peroxisome proliferator-activated receptor α mediates the adaptive response to fasting. *J Clin Invest.* (1999) 103:1489–98. doi: 10.1172/JCI6223
39. Jiang C, Ting AT, Seed B. PPAR-γ agonists inhibit production of monocyte inflammatory cytokines. *Nature.* (1998) 391:82–86. doi: 10.1038/34184
40. Ricote M, Li AC, Willson TM, Kelly CJ, Glass CK. The peroxisome proliferator-activated receptor-γ is a negative regulator of macrophage activation. *Nature.* (1998) 391:79–82. doi: 10.1038/34178
41. Maess MB, Sendelbach S, Lorkowski S. Selection of reliable reference genes during THP-1 monocyte differentiation into macrophages. *BMC Mol Biol.* (2010) 11:90. doi: 10.1186/1471-2199-11-90
42. Harbeson D, Francis F, Bao W, Amenyogbe NA, Kollmann TR. Energy demands of early life drive a disease tolerant phenotype and dictate outcome in neonatal bacterial sepsis. *Front Immunol.* (2018) 9:1918. doi: 10.3389/fimmu.2018.01918
43. Meisenberg G. *Principles of Medical Biochemistry*. 2nd Edn. Philadelphia, PA: Elsevier (2006).
44. Warburg O, Wind F, Negelein E. The metabolism of tumors in the body. *J Gen Physiol.* (1927) 8:519–30. doi: 10.1085/jgp.8.6.519
45. Palsson-Mcdermott EM, O'Neill LAJ. The warburg effect then and now: from cancer to inflammatory diseases. *BioEssays.* (2013) 35:965–73. doi: 10.1002/bies.201300084
46. Larbi A, Zelba H, Goldeck D, Pawelec G. Induction of HIF-1alpha and the glycolytic pathway alters apoptotic and differentiation profiles of activated human T cells. *J Leukoc Biol.* (2010) 87:265–73. doi: 10.1189/jlb.0509304
47. Darekar S, Georgiou K, Yurchenko M, Yenamandra SP, Chachami G, Simos G, et al. Epstein-Barr virus immortalization of human B-cells leads to stabilization of hypoxia-induced factor 1 alpha, congruent with the warburg effect. *PLoS ONE.* (2012) 7:e42072. doi: 10.1371/journal.pone.0042072
48. Rius J, Guma M, Schachtrup C, Akassoglou K, Zinkernagel AS, Nizet V, et al. NF-κB links innate immunity to the hypoxic response through transcriptional regulation of HIF-1α. *Nature.* (2008) 453:807–11. doi: 10.1038/nature06905
49. Wouters BG, Koritzinsky M. Hypoxia signalling through mTOR and the unfolded protein response in cancer. *Nat Rev Cancer.* (2008) 8:851–64. doi: 10.1038/nrc2501
50. Kan B, Michalski C, Fu H, Au HHT, Lee K, Marchant EA, et al. Cellular metabolism constrains innate immune responses in early human ontogeny. *Nat Commun.* (2018) 9:4822. doi: 10.1038/s41467-018-07215-9
51. Ferenc K, Pietrzak P, Godlewski MM, Piwowarski J, Kilianczyk R, Guilloteau P, et al. Intrauterine growth retarded piglet as a model for humans – studies on the perinatal development of the gut structure and function. *Reprod Biol.* (2014) 14:51–60. doi: 10.1016/j.repbio.2014.01.005
52. Sankaran S, Kyle PM. Aetiology and pathogenesis of IUGR. *Best Pract Res Clin Obstet Gynaecol.* (2009) 23:765–77. doi: 10.1016/j.bpobgyn.2009.05.003
53. Ren S, Hui Y, Obelitz-Ryom K, Brandt AB, Kot W, Nielsen DS, et al. Neonatal gut and immune maturation is determined more by postnatal age than by post-conceptional age in moderately preterm pigs. *Am J Physiol Gastrointest Liver Physiol.* (2018) 315:G855–67. doi: 10.1152/ajpgi.00169.2018
54. Holme Nielsen C, Bladt Brandt A, Thymann T, Obelitz-Ryom K, Jiang P, Vanden Hole C, et al. Rapid postnatal adaptation of neurodevelopment in pigs born late preterm. *Dev Neurosci.* 40:586–600. doi: 10.1159/000499127

Conflict of Interest: The authors declare that the research was conducted in the absence of any commercial or financial relationships that could be construed as a potential conflict of interest.

frontiers in Immunology

ORIGINAL RESEARCH
published: 23 September 2020
doi: 10.3389/fimmu.2020.577878

A Neonatal Murine *Escherichia coli* Sepsis Model Demonstrates That Adjunctive Pentoxifylline Enhances the Ratio of Anti- vs. Pro-inflammatory Cytokines in Blood and Organ Tissues

Esther M. Speer[1], Elizabet Diago-Navarro[2], Lukasz S. Ozog[1], Mahnoor Raheel[1], Ofer Levy[3,4,5†] and Bettina C. Fries[2,6†]*

[1] Department of Pediatrics, Renaissance School of Medicine at Stony Brook University, Stony Brook, NY, United States, [2] Department of Medicine, Renaissance School of Medicine at Stony Brook University, Stony Brook, NY, United States, [3] Precision Vaccine Program, Division of Infectious Diseases, Boston Children's Hospital, Boston, MA, United States, [4] Harvard Medical School, Boston, MA, United States, [5] Broad Institute of MIT and Harvard, Cambridge, MA, United States, [6] U.S. Department of Veterans Affairs, Northport VA Medical Center, Northport, NY, United States

OPEN ACCESS

Edited by:
Duc Ninh Nguyen,
University of Copenhagen, Denmark

Reviewed by:
Basilia Zingarelli,
Cincinnati Children's Hospital Medical Center, United States
Regina Sordi,
Federal University of Santa Catarina, Brazil

***Correspondence:**
Esther M. Speer
esther.speer@stonybrookmedicine.edu

† These authors have contributed equally to this work

Specialty section:
This article was submitted to Inflammation, a section of the journal Frontiers in Immunology

Received: 30 June 2020
Accepted: 18 August 2020
Published: 23 September 2020

Citation:
Speer EM, Diago-Navarro E, Ozog LS, Raheel M, Levy O and Fries BC (2020) A Neonatal Murine Escherichia coli Sepsis Model Demonstrates That Adjunctive Pentoxifylline Enhances the Ratio of Anti- vs. Pro-inflammatory Cytokines in Blood and Organ Tissues. Front. Immunol. 11:577878. doi: 10.3389/fimmu.2020.577878

Introduction: Neonatal sepsis triggers an inflammatory response that contributes to mortality and multiple organ injury. Pentoxifylline (PTX), a phosphodiesterase inhibitor which suppresses pro-inflammatory cytokines, is a candidate adjunctive therapy for newborn sepsis. We hypothesized that administration of PTX in addition to antibiotics decreases live bacteria-induced pro-inflammatory and/or enhances anti-inflammatory cytokine production in septic neonatal mice without augmenting bacterial growth.

Methods: Newborn C57BL/6J mice (<24 h old) were injected intravenously with 10^5 colony forming units (CFUs)/g weight of a bioluminescent derivative of the encapsulated clinical isolate *Escherichia coli* O18:K1. Adequacy of intravenous injections was validated using *in vivo* bioluminescence imaging and Evans blue. Pups were treated with gentamicin (GENT), PTX, (GENT + PTX) or saline at 0, 1.5, or 4 h after sepsis initiation, and euthanized after an additional 4 h. CFUs and cytokines were measured from blood and homogenized organ tissues.

Results: GENT alone inhibited bacterial growth, IL-1β, and IL-6 production in blood and organs. Addition of PTX to GENT profoundly inhibited *E. coli*-induced TNF and enhanced IL-10 in blood of newborn mice at all timepoints, whereas it primarily upregulated IL-10 production in peripheral organs (lung, spleen, brain). PTX, whether alone or adjunctive to GENT, did not increase microbial colony counts in blood and organs.

Conclusion: Addition of PTX to antibiotics in murine neonatal *E. coli* sepsis promoted an anti-inflammatory milieu through inhibition of plasma TNF and enhancement of IL-10 production in plasma and organs without increasing bacterial growth, supporting its utility as a potential adjunctive agent for newborn sepsis.

Keywords: newborn, sepsis, *Escherichia coli*, anti-inflammatory, pentoxifylline, interleukin 10, cytokines

INTRODUCTION

Sepsis remains the leading cause of neonatal morbidity and mortality worldwide, especially among the 11% of all newborns that are born preterm (1–3). In the United States alone bacterial sepsis affects > 30,000 live births annually (4). Despite major advances in neonatal care in developed countries, 40% of septic neonates still die or suffer from major neurodevelopmental disability, and little progress has been made over the past three decades (1, 5). The distinct neonatal inflammatory immune response to severe infections, while key to reducing microbial invasion, has been associated with mortality and multiple organ injury including the brain (6–8). Adjunctive anti-inflammatory agents may mitigate the deleterious effects of the associated neonatal systemic inflammatory response syndrome, thereby improving survival and outcome (9–11). However, corticosteroids are associated with significant side effects and are generally not recommended for neonatal sepsis (12), and other adjunctive immunologic interventions for neonatal sepsis have not demonstrated clinical benefit in randomized controlled trials (10, 11). This unfortunate state of affairs is in part due to inadequate sample sizes and unique physiological, pharmacological, and ethical challenges in conducting clinical studies in this vulnerable population (11, 13). Thus, there continues to be an urgent unmet clinical need for approaches to prevent or treat hyper-inflammation associated with sepsis in the newborn.

Pentoxifylline (PTX) is a low molecular weight phosphodiesterase inhibitor that increases intracellular cyclic adenosine monophosphate (cAMP) and decreases transcription of pro-inflammatory cytokines (14). PTX is a candidate for adjunctive therapy of newborn sepsis and necrotizing enterocolitis (15, 16), which could potentially be licensed for use in neonates. Small sample sizes and risk of selection, detection and attrition biases limit the rigor of human neonatal trials thus far (15). We have demonstrated that when tested in human blood *in vitro*, PTX inhibits production of pro-inflammatory cytokines [e.g., tumor necrosis factor (TNF) and the inflammasome-mediated cytokine interleukin-1β (IL-1β)] in response to pure *Toll*-like receptor (TLR) and inflammasome agonists as well as live neonatal pathogens (17, 18). Importantly, a greater effect was observed in newborn cord blood compared to adult blood, and endogenous expression of anti-inflammatory and pro-resolution cytokines (IL-10, IL-6) (17, 19) was preserved.

Studies of the effect of PTX on preterm and term newborn animals are encouraging but thus far limited. In neonatal mice, PTX decreased death from subcutaneous *Staphylococcus aureus* infections (20). In preterm rabbits infected with aerosolized group B streptococci, PTX enhanced pulmonary clearance of bacteria and decreased inflammatory mediators in bronchoalveolar lavage fluid (21). Furthermore, PTX reduced incidence and severity of necrotizing enterocolitis in newborn rats (22). Activated leukocytes in septic patients may contribute to sustained inflammation and organ failure (23), and inflammatory cytokines and chemokines (e.g., TNF, IL-1β, CXCL-8) have been associated with perinatal brain injury (6, 24, 25). On the other hand, bone marrow stromal cells administered to aged adult mice reduced sepsis-induced mortality and improved multiple organ function via reprogramming of host monocytes and macrophages that led to increased IL-10 production (26). Treatment with either anti-TNF-α or IL-10 significantly improved survival in 1 day old neonatal mice *with E. coli* sepsis (27). Suppressing pro-inflammatory cytokines such as TNF and/or enhancing endogenous IL-10 production might therefore be beneficial in neonatal sepsis. How infection-induced systemic or local inflammatory responses can interrupt normal tissue structure and organ function such as the neonatal brain (24, 28), and how anti-inflammatory therapeutics such as PTX could restore homeostasis remains unknown. Furthermore, the effects of timing of anti-inflammatory treatment in relation to sepsis initiation (23), its interaction with antimicrobial agents (18), the relationship of systemic *vs.* organ-specific inflammation (23) and the systemic and organ-specific effects of anti-inflammatory agents such as PTX, as well as potential sex differences in response to anti-inflammatory approaches (29, 30), remain largely unknown.

Based on our *in vitro* experiments in human neonatal cord blood, wherein PTX inhibited live bacteria-induced inflammatory responses without enhancing bacterial proliferation (18), and previous reports of increased bacterial clearance with PTX (31), we hypothesized that adjunctive PTX in addition to antibiotics decreases live *E. coli*-induced pro-inflammatory and/or enhances anti-inflammatory cytokine production in blood and peripheral organs of septic neonatal mice without enhancing bacterial growth. To investigate our hypothesis and address these questions, we developed and validated a neonatal murine sepsis model, which we adapted from a previously published model of neonatal *Staphylococcus epidermidis* sepsis (32), consisting of intravenous (IV) live bacterial injections of the most frequently encountered neonatal pathogen of early-onset sepsis, namely *Escherichia coli* (33), in mice < 24 h old. We then employed this model to characterize the inhibitory efficacy of adjunctive PTX treatment in addition to antibiotics on the systemic and organ-specific inflammatory response to *E. coli* sepsis, its effects on systemic and organ-specific bacterial growth, the impact of timing of antimicrobial and/or anti-inflammatory treatment in relation to sepsis initiation on systemic and organ-specific innate immune responses, the interaction of PTX and antimicrobial treatment on these immune responses, and its potential gender-specific immunomodulatiory effects. We demonstrate for the first time that addition of PTX to gentamicin (GENT) suppresses systemic pro-inflammatory and enhances production of anti-inflammatory cytokines in blood and organ tissues without increase of bacterial burden, thus supporting the potential utility of PTX as an adjunctive anti-inflammatory agent for newborn sepsis.

MATERIALS AND METHODS

Preparation of Microorganisms

Live *E. coli* K1 strain [# 700973, American Type Culture Collection; Manassas, VA, or a bioluminescent K1 strain A192PP-*lux2,* which was derived from the neonatal septicemia

clinical isolate *E. coli* A192 by two rounds of passage through neonatal rat pups with bacterial recovery from the blood and subsequent introduction of the *lux* operon, as described by Witcomb et al. (34)] was used to induce experimental murine neonatal sepsis. Single colonies of *E. coli,* stored at 4°C on Luria-Bertani (LB) agar plates containing kanamycin (50 μg/ml), were grown overnight in LB media (Becton Dickinson; Franklin Lakes, NJ) under kanamycin pressure [since the bioluminescent derivative *E. coli* strain A192PP-*lux2* was engineered by introduction of the *lux* operon (*luxCDABE*) from the bacterium *Photorhabdus luminescens* on a disarmed mini-Tn5 transposon by conjugation under kanamycin-selection pressure (34)] in a Forma Scientific Orbital Shaker (Thermo Fisher Scientific; Waltham, MA) at 150 RPM at 37°C to stationary phase. An aliquot was then transferred to fresh growth medium at 1:100 dilution and grown (150 RPM, 37°C) to exponential phase for 2 h. After centrifugation and washing of microbial suspensions in sterile saline, bacterial colonies per ml were determined spectrophotometrically at 600 nm and confirmed by plating of serial (1:10) dilutions and manual counting of colony forming units (CFU) as described below. Microbial suspensions were diluted in sterile saline to yield the desired inoculum concentration, i.e., 4×10^6 CFU per ml, thus resulting in 10^5 CFU per g body weight when administering an injection volume of 25 μl per g weight. Gentamicin susceptibility was confirmed by plating these microorganisms onto agar plates containing different antimicrobial concentrations. The minimal inhibitory concentration was determined, which was well below the clinically relevant concentration ranges for this agent.

Animal Model and Experimental Protocol

C57BL/6J female and male breeders were obtained from Jackson Laboratories (Bar Harbor, ME), and were mated in-house at our animal facility. Pups were delivered naturally at term gestation, and remained with their dams except for brief interruptions due to experimental procedures. Animals were fed *ad libitum* with a standard chow diet, and maintained in a year-around climate-controlled environment with a 12-h light-dark cycle. Pups of both sexes were used for all experimental procedures. BSL 2 containment was employed for all experiments involving live bacteria. The research protocol and all animal procedures were approved by the Institutional Animal Care and Use Committee at Stony Brook University, Stony Brook, NY.

Murine Newborn Sepsis Model

Newborn mice pups under 24 h old were injected IV via the external jugular route with live *E. coli* in 25 μl sterile saline per g body weight. Injections were performed with a two-person technique as previously described (32). Mice pups were manually restrained by one investigator, while the other investigator located the external jugular vein and performed the injection. In order to aid visualization and success of IV cannulation, transillumination, and magnifying glasses were used (35), in addition to brief (< 30 s) sedation/anesthesia with isoflurane open drip and Mepilex^{TM} tape (Mölnlycke Health Care; Norcross, GA) as needed. Following the injection, mice pups were monitored for signs of distress, marked with a pen for identification, and returned to their cages once fully recovered from sedation/anesthesia. As previously reported, the intravenous injection procedure itself lasts ∼1 min and is generally well-tolerated by mice pups with 100% procedure-related survival (32). For our treatment experiments, following IV bacterial injections, pups were treated with either 5 μg per g body weight gentamicin (Fresenius Kabi; Lake Zurich, IL), 60 μg per g weight PTX (VWR International, LLC; Buffalo Grove, IL), combined gentamicin and pentoxifylline, or an equal volume of sterile saline control (Hospira Inc.; Lake Forest, IL) (20 μl per g weight), administered intraperitonally (IP) once at different time points in relation to the initial bacterial inoculation. In order to investigate the effects of timing of antimicrobial and/or anti-inflammatory treatment in relation to sepsis initiation, these agents were administered either simultaneously (immediately after bacterial inoculation, 0 h delay), early (1.5 h after bacterial injections) or late (4 h after bacterial injections). All pharmacological agents used in these animal experiments were United States Pharmacopeia (USP) grade. 32 G Hamilton syringes (Hamilton Company; Reno, NV) were employed to enable dosing at 1μl precision for injections of live bacteria as well as antibiotic and anti-inflammatory agents. Following sepsis treatment, mice pups were euthanized after an additional 4 h, i.e., after 4, 5.5, or 8 h following bacterial inoculation (see **Figure 1** for a schematic representation of our treatment protocol), and blood and organ tissues were obtained under sterile conditions for further processing as described below. Bacterial injections were performed in the morning, and mice were monitored for the specified durations until euthanized in the afternoon or evening.

Validation of Sepsis Model With Evans Blue

In order to confirm the successful performance of IV injections, low concentration (0.05%) Evans blue, a dye which is not detectable in the extravascular space shortly after intravenous injections, was mixed to the bacterial inoculum prior to injections (36–38). Successful IV bacterial injections led to homogenous discoloration of neonatal mice (assigned score = 3), partial extravasation led to local discoloration at the injection site with slight general discoloration (score = 2), and failed IV injections appeared as localized blue discoloration without general color changes (score = 1). Photographs of all injected animals were obtained for documentation of color changes (see representative images in **Figure 2**). Only Evans blue injection scores of 3 were used for further analyses for all sepsis-related treatment experiments.

Validation of Sepsis Model With Optical Imaging

In order to confirm the adequacy of IV bacterial injections with an objective quantitative method, in addition to the subjective semiquantitative Evans blue scoring system based on the observed color change, we utilized the bioluminescent *E. coli* K1 strain A192PP-*lux2* (34), and measured photon emission with an IVIS Lumina III *In Vivo* Imaging System (PerkinElmer; Waltham. MA) soon after IV bacterial injections. Our standard settings for optical imaging consisted of 2 min acquisition time, subject height of 0.5 cm (which provided the

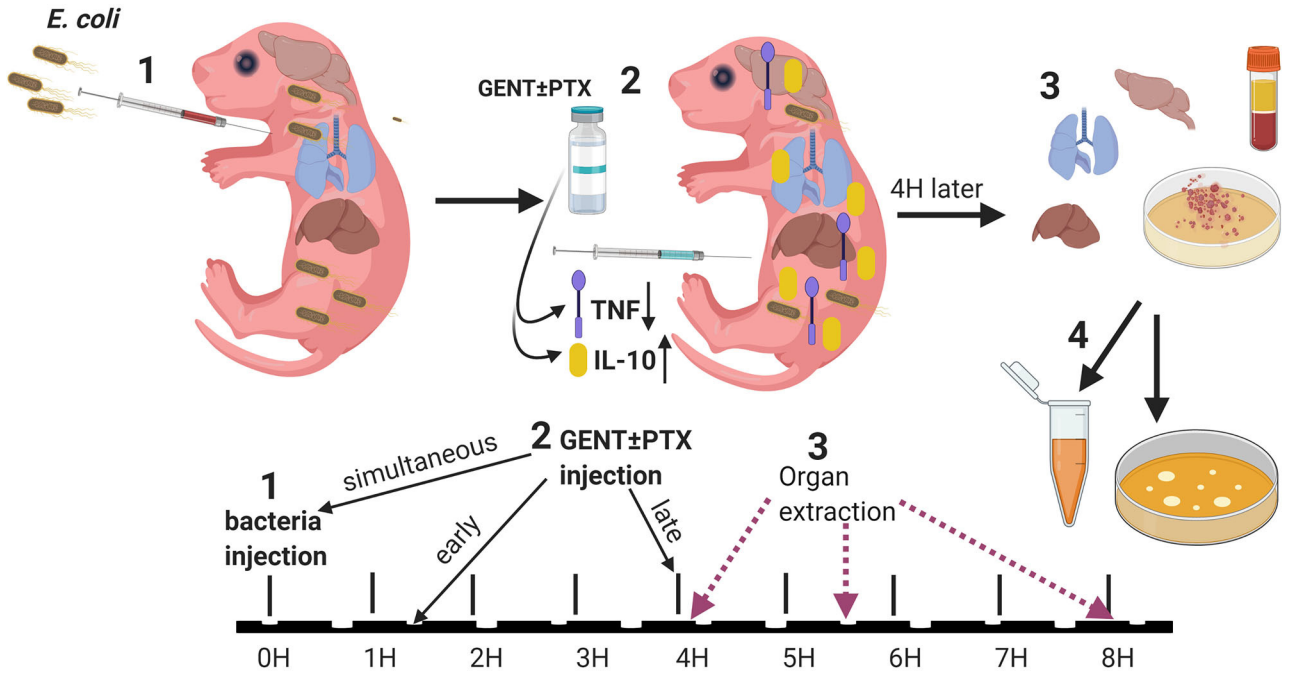

FIGURE 1 | Experimental design. (1) Neonatal mice (< 24 h old) were injected with *E. coli* via the right intra-jugular route at the start of the experiment (0H time point). (2) Subsequently, pups were injected intraperitoneally with GENT, PTX, (GENT + PTX), or saline control immediately following bacteria injection (simultaneously, at the 0H time point), early (1.5H after bacteria injection), or late (4H after bacteria injection). (3) After additional 4H of incubation, i.e., at the 4H, 5.5H, or 8H time point from the start of the experiment, mice were euthanized and blood and organs obtained for (4) bacterial plating and cytokine measurements.

FIGURE 2 | Evans blue IV injection quality score. 0.05% Evans blue dye was added to the bacterial inoculum prior to injection, and images were taken immediately after IV injection. Successful IV bacterial injections led to homogenous discoloration of neonatal mice (score = 3), partial extravasation led to local discoloration at the injection site with slight general discoloration (score = 2), and failed IV injections appeared as localized blue discoloration without general color changes (score = 1), as demonstrated on these representative photographs.

maximal sensitivity), and settings of 2, 4, and 8 for binning. Animals were placed supine with their right side (injection site) up and were kept under anesthesia using isoflurane 2 to 3% on the preheated instrument platform, in order to avoid any artifacts due to movements. Optical images were analyzed by placing regions of interest (ROIs) of standard size and shape over the region of the bacterial injection site of each animal image. Images were obtained for 2, 4, and 8 binning settings and the average radiance of all images was calculated for each animal. Higher concentrations of bacteria around the injection

site, i.e., extravascular leakage of bacteria, led to higher photon emission around the area of the injection site on subsequent optical imaging. Using these instrument settings and based on data derived from initial images of animals with Evans blue injection scores of 3 *vs.* < 3, indicating adequate *vs.* unsuccessful IV bacterial injections, a cutoff point of equal or $< 4 \times 10^4$ p/s/cm^2/sr radiance was employed in order to classify an IV bacterial injection as successful.

Determination of Sex

The sex of neonatal mice was determined through Transnetyx Genotyping^{TM} of tissue for the presence of the y chromosome (Transnetyx; Cordova, TN). Several undetermined samples during the initial run were subsequently repeated. For quality control purposes, 10 tissue samples from C57BL/6J mice of known male and female sex were submitted for genotyping in a blinded fashion.

Preparation of Organ Tissues for Bacteriological Studies

After completion of predetermined incubation periods, mice were euthanized by decapitation, and blood, and organ tissues were harvested under sterile conditions. Small volume blood sampling (∼20–30 μl) employed sterile capillary tubes (Drummond Scientific Company; Broomall, PA), and blood was immediately mixed with sodium citrate and kept on ice. The left lung (to minimize the possibility of bacterial contamination from potential residual extravasated microorganisms at the time of bacterial inoculation into the right external jugular vein), liver, spleen, and brain were dissected and immediately placed into 1.7 ml microcentrifuge tubes pre-filled with 500 μl sterile endotoxin-free saline and kept on ice. Upon completion of organ dissections, an aliquot of blood samples was used for bacterial plating with serial (1:10) dilutions using sterile endotoxin-free saline onto kanamycin-containing LB agar plates (Becton Dickinson). The remaining blood samples were centrifuged at 500 g for 10 min at room temperature, and plasma supernatants were carefully removed without disturbing the cell pellets and stored at −80°C. The weight of organ tissues was determined by subtracting the measured tube weights prior to the addition of organ tissues from their respective weights measured after addition of organ tissues using a Mettler Toledo AT261 Delta Range Analytical Balance (Mettler Toledo; Columbus, OH). Organ tissues were mixed with sterile 2.3 mm zirconia/silica beads (Biospec Products Inc.; Bartlesville, OK) and homogenized with a Mini-Beadbeater-16 (Biopec Products Inc.), as previously described (32). An aliquot of each tissue homogenate was then used for bacterial plating with serial (1:10) dilutions onto kanamycin-containing LB agar plates. The remaining tissue samples were centrifuged at 13,000 g for 10 min at 4 °C, and supernatants were harvested and stored at −80°C for subsequent cytokine measurements. Bacterial plates of blood and tissue homogenates were incubated at 37°C in a humidified incubator for ∼18–24 h, and microbial colonies were then manually counted with an eCount Colony Counter (Heathrow Scientific; Vernon Hills, IL) as previously described (18). All colony count results were expressed as CFU counts per ml blood and CFUs per mg organ tissue, respectively.

Measurement of Cytokine Concentrations in Plasma and Tissue Homogenates

Cytokine concentrations (TNF, IL-1β, IL-6, and IL-10) in blood plasma samples and tissue homogenate supernatants were determined with Bio-Plex Pro magnetic multiplex assays (Bio-Rad; Hercules, CA) and analyzed on the Bio-Plex 200 system with Bio-Plex Manager 5.0 software (Bio-Rad). Results were expressed as cytokine concentrations in pg per ml plasma and pg per mg protein concentration for supernatants of organ tissue homogenates. Duplicate technical replicates were used for all immunological studies. Protein concentrations in supernatant tissue homogenate samples were determined with the Bradford method (Bio-Rad Laboratories; Richmond, CA) and measured on a Spectramax 190 Plate Reader (Molecular Devices LLC; San Jose, CA).

Statistical Analysis

All microbial counts were expressed as CFUs per ml *vs.* CFUs per mg tissue for plasma and organ tissue samples, respectively, and cytokine concentrations were expressed as pg per ml plasma *vs.* pg per mg protein for supernatant tissue homogenates. In order to account for the possibility of litter effects on these findings, cytokine concentrations of samples derived from septic animals treated with antibiotics and/or PTX were also expressed as a percentage compared to cytokine concentrations of plasma and organ tissue samples from untreated septic animals within the same litter, which were defined as 100%. Likewise, in addition to the absolute CFUs per ml or per mg tissue, CFU results from samples of septic animals that were treated with GENT, PTX, or (GENT + PTX) were also expressed as percentage change compared to those results obtained from untreated septic animals within the same litter, defined as 100%. Only samples from animals with a good Evans blue injection score of 3 were analyzed for comparisons of antimicrobial and/or anti-inflammatory treatment effects. Similarily, only samples from animals with Evans blue scores of 3 were analyzed to determine the relationships between bacterial inoculum and subsequent recovery of CFUs from blood and organ tissues as well as cytokine concentrations in these samples.

Means and standard errors were estimated for normally distributed data, and median and interquartile ranges (IQR) for non-normally distributed data, whereby the assumption of normality was assessed graphically using Q-Q-plots and through the application of Kolmogorov-Smirnov tests for normal distribution. Group comparisons between untreated and treated [GENT, PTX, or (GENT + PTX)] septic animals employed one-way ANOVA or Kruskal-Wallis tests for multiple group comparisons that were corrected by false discovery rates, for parametric and non-parametric data, respectively. Unpaired Welch *t*-tests, which do not assume variances homogeneity, and Mann Whitney *U*-tests were used for pair-wise group comparisons, as indicated. *GraphPad* Prism Version 8.4 (GraphPad Software; San Diego, CA) was used for analyses and

for graphing of results. All statistical tests were two-sided and $p < 0.05$ were determined significant.

For animal ethical reasons, we used the lowest estimated number of animals for each experiment expected to achieve reliable results. Due to differences in the expected effect sizes between different groups and experimental conditions, the number of animals used varied accordingly among the different types of experiments (e.g., only few animals were required for our validation experiments that employed injections with 10-fold increasing bacterial inoculum). In order to assure adequate statistical power in light of limited numbers of experimental animals, we therefore computed a *post hoc* analysis of the achieved power to detect treatment-related group differences in bacterial CFUs and cytokine concentrations (TNF, IL-10) in blood and lung tissue between animals receiving GENT, (GENT + PTX) and saline controls (SAL), employing an alpha error of 0.05 and the given sample and effect sizes of our study. This analysis was conducted using G*Power software for Wilcoxon-Mann-Whitney test version 3.1 (https://www.psychologie.hhu.de/arbeitsgruppen/allgemeine-psychologie-und-arbeitspsychologie/gpower.html; Allgemeine Psychologie und Arbeitspsychologie, Heinrich Heine Universität Düsseldorf, Germany) (39).

RESULTS

Validation of Murine Neonatal Sepsis Model With Evans Blue and Optical Imaging

In order to overcome the challenge of confirming successful small volume IV injections of bacteria in neonatal mice, we developed two new injection quality scoring systems based on Evans-blue dye and optical imaging of bioluminescent bacteria.

As shown in the representative image and graph (**Figures 3A,B**), the average radiance measured shortly after IV injections correlated with the estimated Evans blue-based injection score (Spearman correlation $r = -0.51$, 95% confidence interval -0.41 to -0.61, $p < 0.001$). Furthermore, a high Evans blue injection score of 3, representing successful IV bacterial injections, resulted in significantly lower median radiance compared to Evans blue injection scores < 3 (32,567 *vs.* 56,977 p/s/cm^2/sr, $p < 0.001$).

An Evans blue injection score of 3, representing successful IV injection, was associated with significantly higher bacterial CFUs in all peripheral organs tested at 5.5 h after sepsis initiation (**Figure 4B**), and in the lung, liver, and spleen at 4 h after injection of bacteria with a trend toward higher CFU counts in brain tissue for Evans blue injection scores of 3 as compared to injection scores < 3 ($p = 0.08$) (**Figure 4A**). Comparable CFU counts in blood samples observed after good Evans blue injection scores *vs.* scores below 3 at 4 h after sepsis initiation (**Figure 4A**) are likely due to dissemination of bacteria from the blood to peripheral organs. This interpretation is further suggested by the finding of significantly decreased CFU counts in blood after good Evans blue scores compared to low scores at 5.5 h after bacterial injections, whereas CFUs in all peripheral organs were increased in animals with high *vs.* low injection scores at that timepoint (**Figure 4B**). CFU counts in lung and liver tissue achieved after bacterial injections with a high Evans blue score of 3 remained significantly elevated after 8 h of incubation as compared to CFU counts in these organ tissues after bacterial injections with low Evans blue scores ($p < 0.05$) (*data not shown*). Of note, the addition of Evans blue did not alter the viability of the bacteria used in this study nor the bacteria-induced cytokine production in human blood tested *in vitro* (*data not shown*).

Effect of Bacterial Inoculum on CFU Counts and Cytokine Production in Blood and Organ Tissue in Newborn Mice

Among animals with an Evans blue score of 3, i.e., animals with successful IV bacterial injection, *E. coli* CFUs from newborn mice blood and organ tissue cultures were all bacterial inoculum-dependent (10^4, 10^5, and 10^6 CFUs per g weight; **Figure 5A**) CFU counts. Furthermore, these were significantly associated with inoculum-dependent production of IL-1β in blood, lung, and spleen (**Figure 5B**), IL-6 in blood and all organ tissues tested (**Figure 5C**), and IL-10 in blood, lung, and liver with a non-significant trend in spleen tissue (**Figure 5D**). These data confirm the validity and feasibility of our model, i.e., successful injection of increasing bacterial inocula leads to increased recovery of bacterial CFUs accompanied by enhanced inflammatory responses in blood and peripheral organs of experimentally infected newborn mice.

Standardization of Optical Imaging of Bioluminescent *E. coli* Injections in Neonatal Mice

In order to determine the cut-off value for good radiance representing successful IV bacterial injection, neonatal mice were injected subcutaneously into their right neck area with decreasing loads of bioluminescent *E. coli*. The average radiance measured shortly after injections correlated highly with the injected bacterial inoculum (Spearman correlation $r = +0.91$, $p < 0.001$) (see **Supplementary Figure 1A**). Furthermore, the median radiance of mice injected with 3.3×10^3 CFUs/g weight subcutaneously differed significantly from the measured median radiance after injection of 10^5 CFUs/g weight (median: 4.7×10^5 p/s/cm^2/sr, IQR: 2.6×10^5 to 6.7×10^5 p/s/cm^2/sr) as well as 3.3×10^4 CFUs/g weight, which correspond to 100% and 33% of the bacterial load used for IV injections in our sepsis mouse model. The measured median radiance after injection of 10^4 CFU/g weight (median 3.1×10^4 p/s/cm^2/sr, IQR: 2.3×10^4 to 3.5×10^4 p/s/cm^2/sr), which corresponds to 10% of the total injected bacterial inoculum for IV injections in this study, still showed a non-significant trend toward lower values compared to 10^5 CFUs/g weight. We thus determined a radiance of 4×10^4 p/s/cm^2/sr as cut-off value (depicted as interrupted line in **Supplementary Figure 1A**), which corresponds to ∼10% of the bacterial inoculum used, below which an IV injection was determined acceptable for inclusion in our study. Since the measured radiance also depends on the ROI chosen, we employed ROIs of standard size and shape, which were placed over the injection site on the corresponding optical images as shown in the example in **Supplementary Figure 1B**.

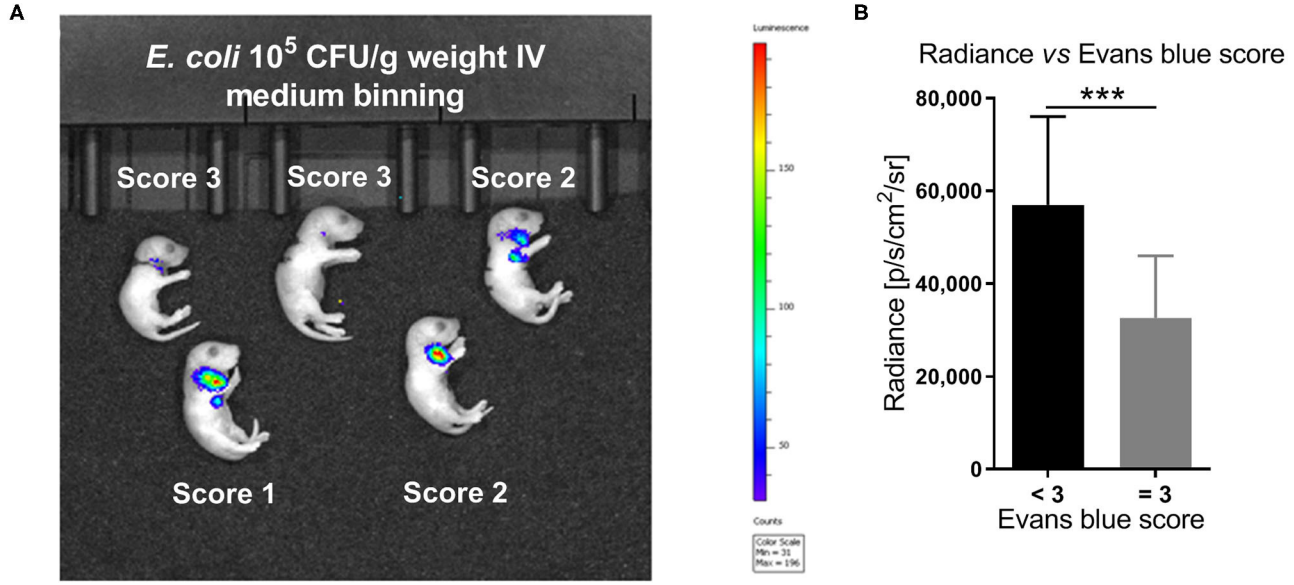

FIGURE 3 | *In vivo* imaging of bioluminescent *E. coli* correlated with Evans blue IV injection score. **(A)** Optical imaging following IV injection of 10^5 CFU per g body weight of the bioluminescent *E. coli* A192PP-*lux2* strain (34). The representative image shows the corresponding Evans blue IV injection score for each animal. **(B)** The average radiance measured shortly after IV injections correlated with the estimated Evans blue IV injection score (Spearman correlation $r = -0.51$, 95% confidence interval: −0.61 to −0.41, $p < 0.001$, $n = 230$). Significant difference between median (IQR) radiance derived from animals with Evans blue scores < 3 *vs.* =3 was as indicated: ***$p < 0.001$, 2-sided Mann-Whitney *U*-test.

On the basis of the above findings, we thus defined successful IV injections in neonatal mice as Evans blue score of 3 or as measured radiance $\leq 4 \times 10^4$ p/s/cm^2/sr, and only animals fulfilling these criteria were included in the analyses of all subsequent sepsis-related treatment experiments. These therapeutic experiments all employed 10^5 CFUs/g weight of bioluminescent *E. coli* delivered in a volume of 25 μl/g weight, i.e., 4×10^6 CFUs/ml, and optical imaging was performed upon completion of IV injections.

Characteristics of Mice in Treatment Experiments of Neonatal Sepsis

A total of 227 pups (39.5% male, 60.5% female) with a mean (± SEM) weight of 1.5 ± 0.02 g were used to investigate treatment effects of GENT and/or PTX in *E. coli* sepsis on their first day of life. Since our study examined the short-term effects of adjunctive anti-inflammatory treatment of neonatal murine sepsis on bacterial colony counts and cytokine production in blood and organs, the overall mortality among experimental animals was low. All simultaneously treated pups survived the observation period. Among early treated neonatal mice, only one out of 27 (3.7%) pups [male, treated with (GENT + PTX)] died, whereas a total of 9 (12%) late treated pups did not survive the intended duration of observation. These consisted of 2 (10%, 2 males) saline-controls, 2 (10.5%, 2 females) GENT-treated, 2 (10.5%, 1 male and 1 female) (GENT + PTX)-treated, and 3 (17.6%, 3 females) PTX alone-treated septic mice. Due to these low overall mortality numbers, further analyses and group comparisons could not be performed. However, this indicated that addition of PTX to GENT did not increase mortality in neonatal murine *E. coli* sepsis compared to GENT alone, a finding that requires further investigation under experimental conditions specifically designed to study the mortality risk of adjunctive PTX use and longer observation periods. Although it remains to be determined if the 17.6% mortality among septic mice treated with PTX alone might be relevant, prudent use of PTX under appropriate antibiotic coverage in cases of potential neonatal sepsis would be warranted.

Microbial Colony Counts in Blood and Organ Tissue of Newborn Mice With Experimental *E. coli* Sepsis

Next we tested if PTX increases the replication of microorganisms, which would prohibit its clinical use. We quantified growth of *E. coli* in blood and peripheral organ tissue of newborn mice intravenously infected with 10^5 CFUs per g body weight, followed by immediate (0 h), early (1.5 h), or late (4 h) treatment with GENT, PTX, (GENT + PTX) or saline control (SAL) administered IP. As shown in **Figure 6**, *E. coli* CFUs recovered from blood and all organ tissues (lung, liver, spleen, and brain) of untreated (SAL) septic neonatal mice significantly increased over time (4, 5.5, and 8 h). CFU counts in blood samples were very high already at 4 h after sepsis initiation (mean of 1.1×10^6 CFU per ml), and further increased to more than 30-fold after 8 h of sepsis duration. CFU counts of untreated neonatal mice after 4 h of sepsis were moderately high in lung and liver (mean of 1.9×10^3 and 1.5×10^3 CFU per mg tissue, respectively), and low in spleen and brain tissue (mean

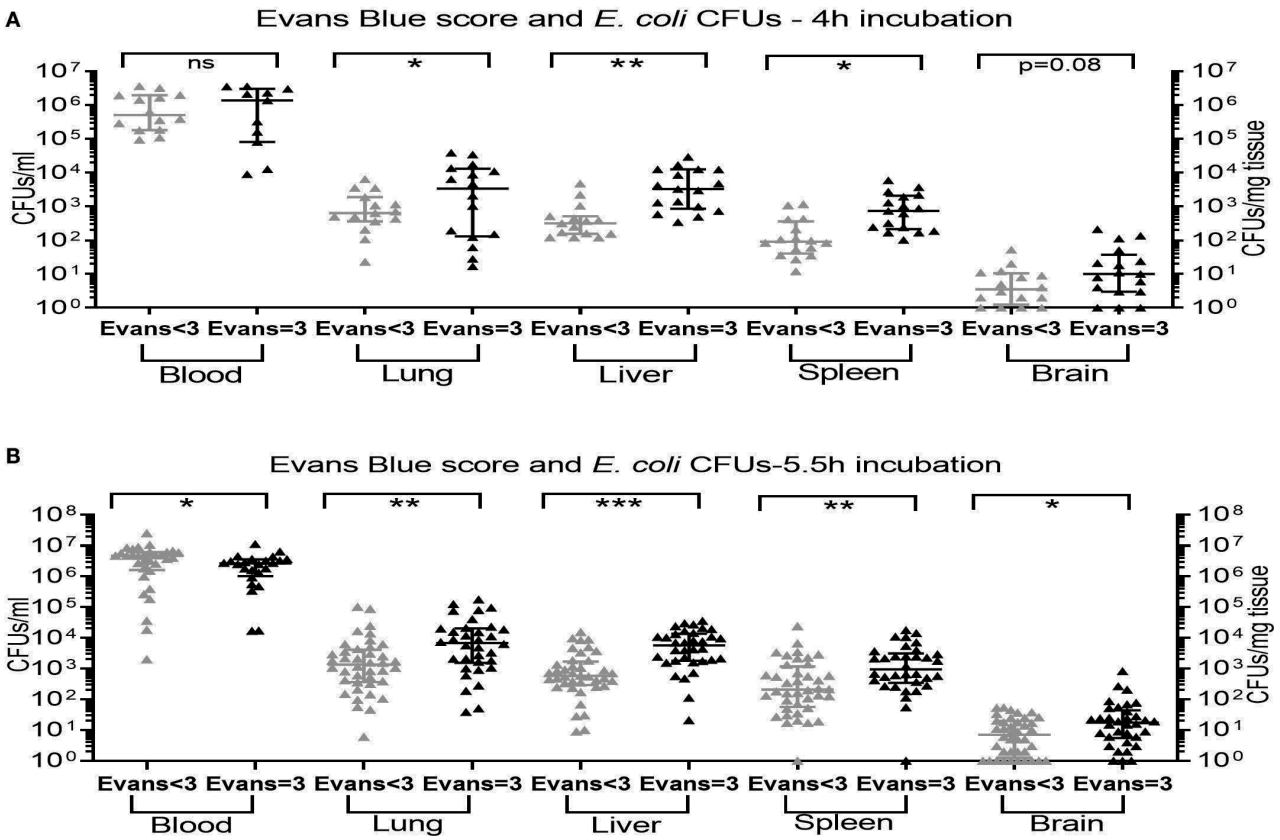

FIGURE 4 | Recovery of *E. coli* CFUs in organ tissue was associated with a high Evans blue score. Neonatal mice < 24 h old were injected IV with *E. coli* 10^5 CFU/g body weight suspended in saline with 0.05% Evans blue dye. Evans blue injection scores were assigned immediately following IV injections. After **(A)** 4 h ($n = 11–17$) and **(B)** 5.5 h ($n = 24–40$) of incubation, mice were euthanized and blood and homogenized organ tissue serially plated for bacterial counting. Significant differences of CFU counts for each organ and blood (plotted as median and IQR) derived from animals with low Evans blue score < 3 *vs.* high Evans blue score = 3 (successful IV injection) were as indicated: $^*p < 0.05$, $^{**}p < 0.01$, $^{***}p < 0.001$, 2-sided *t*-tests with Welch's correction **(A)** and Mann-Whitney *U*-tests **(B)**.

of 297 and 11 CFU per mg tissue, respectively). However, tissue CFU counts increased rapidly with increasing sepsis duration, showing an ∼50-fold increase of mean CFUs in liver tissue, ∼150-fold higher mean CFUs in lung, ∼170-fold higher mean CFUs in spleen, and ∼60-fold increased median CFUs per mg tissue in the brain (**Figure 6**).

As expected, GENT significantly diminished CFU counts in blood and all tested organ tissues, whether administered simultaneously, early, or late in relation to bacterial inoculation (**Figure 7**). Addition of PTX to GENT in neonatal mice infected with *E. coli* did not change their CFU counts derived from blood and peripheral organ tissues (lung, liver, spleen, and brain) at all three time points investigated. Likewise, simultaneous, early, and late PTX treatment alone without antimicrobial agents did not increase CFUs in blood and organ tissues compared to untreated septic neonatal mice after 4, 5.5, and 8 h of sepsis (**Figures 7A–C**), suggesting that PTX does not affect microbial proliferation and/or viability *in vivo*. *Post hoc* analysis for an alpha error of 0.05 revealed a power > 99% to detect differences between (GENT + PTX)-treated *vs.* control animals for CFUs in blood and 87% for CFUs in lung tissue. Based on our sample sizes, a difference in effect sizes between GENT- *vs.* (GENT + PTX)-treated animals of 0.77 for CFUs in blood samples and 0.71 for CFUs in lung tissue would have been detectable with a power of 80% and an alpha error of 0.05.

Pro- and Anti-inflammatory Cytokine Production Show Characteristic Time-Dependent Systemic and Organ-Specific Patterns During Murine Neonatal Sepsis

E. coli induced high concentrations of both pro- and anti-inflammatory cytokines in untreated septic newborn mice (**Figure 8**). Whereas, plasma concentrations for TNF (mean concentration of 6,142 pg/ml), IL-6 (31,000 pg/ml), and IL-10 (2,322 pg/ml) were already very high after 4 h of sepsis duration and subsequently remained elevated, IL-1β plasma concentrations increased only after 5.5 h of sepsis initiation to levels comparable to the other cytokines (mean concentrations of 1,273 pg/ml after 8 h). By contrast, plasma TNF concentrations as an early responding pro-inflammatory cytokine started to trend

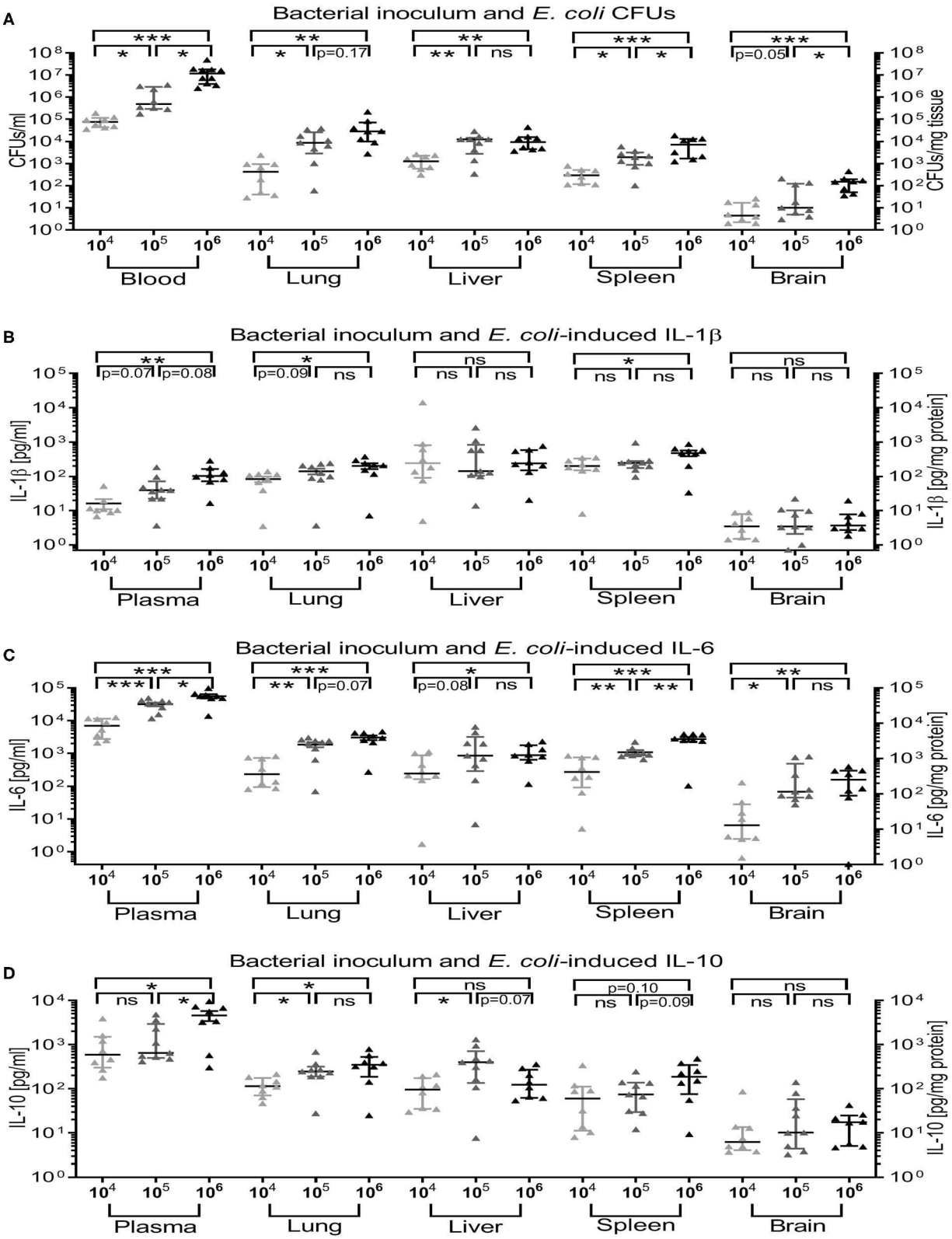

FIGURE 5 | Recovery of *E. coli* CFUs and magnitude of cytokine production in blood and organ tissue was inoculum-dependent. Neonatal mice < 24 h old were injected IV with *E. coli* 10^4, 10^5, or 10^6 CFU/g body weight suspended in saline with 0.05% Evans blue. After 4 h of incubation, mice were euthanized and blood, and homogenized organ tissue serially plated for bacterial counting, and cytokine concentrations measured. Mean (± SEM) or median (IQR) were plotted and one-way

(Continued)

FIGURE 5 | ANOVA employed. Significant differences of **(A)** CFU counts ($n = 5$–7 each), **(B)** IL-1β, **(C)** IL-6, and **(D)** IL-10 cytokine concentrations ($n = 8$–9 each) for each organ and blood or plasma from animals injected with different bacterial loads were as indicated: $^{*}p < 0.05$, $^{**}p < 0.01$, $^{***}p < 0.001$, ns, non-significant; Kruskal-Wallis tests **(A)** or one-way ANOVA **(B–D)** corrected for false discovery rate.

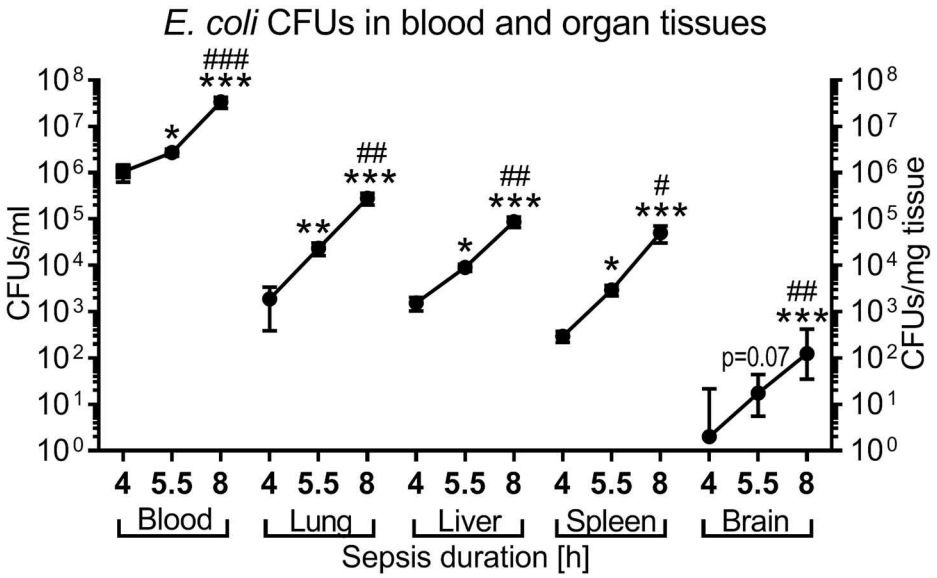

FIGURE 6 | Time-dependent *E. coli* bacterial growth pattern in murine neonatal sepsis. Neonatal mice < 24 h old were injected IV with *E. coli* 10^5 CFU/g body weight. After 4 h ($n = 10$), 5.5 h ($n = 34$), and 8 h ($n = 19$) of incubation, mice were euthanized and blood, and homogenized organ tissue serially plated for bacterial counting. Mean (± SEM) or median (IQR) CFUs were plotted for each time point as indicated. Significant differences of CFU counts for each organ and blood recovered after increasing incubation periods were as follows: $^{*}p < 0.05$, $^{**}p < 0.01$, $^{***}p < 0.001$ for 4 *vs.* 5.5 h and 4 *vs.* 8 h comparisons; $^{\#}p < 0.05$, $^{\#\#}p < 0.01$, $^{\#\#\#}p < 0.001$ for 5.5 *vs.* 8 h comparisons, Kruskal-Wallis tests corrected for false discovery rate.

down after 8 h of sepsis duration (mean 1,607 pg/ml, $p < 0.001$) (**Figure 8A**). Comparable to the time course of TNF in plasma, TNF concentrations in lung and liver tissue were already high at 4 h of sepsis duration and significantly decreased in liver tissue by 8 h after sepsis initiation. TNF in spleen tissue, on the other hand, showed a different time course for production of this pro-inflammatory cytokine, which was characterized by initially relatively low levels of TNF (mean 220 pg/mg protein) that then rapidly increased to 3,901 pg/mg protein by 5.5 h and 9,908 pg/mg protein after 8 h of sepsis duration. Brain tissue reached its peak tissue TNF concentration (mean 950 pg/mg protein) after 5.5 h of sepsis duration.

IL-1β concentrations in lung and spleen tissue mirror the delayed increase of this cytokine in plasma, whereas cerebral tissue levels of this cytokine remain low with a peak mean concentration of 33 pg/mg protein after 5.5 h of sepsis duration (**Figure 8B**). While IL-6 plasma concentrations remained steadily elevated, IL-6 tissue concentrations in peripheral organs (lung. liver, and brain) continued to rise between 4 and 8 h after sepsis initiation (**Figure 8C**). Similarily, whereas IL-10 plasma concentrations remained at a high level throughout the observation period, peripheral tissue concentrations of this anti-inflammatory cytokine increased in all organs studied after 4 h of sepsis duration and began to decline in liver tissue after 8 h of sepsis (mean of 1,335 *vs.* 467 pg/mg protein, $p < 0.01$, after 5.5 and 8 h of sepsis duration, respectively) (**Figure 8D**).

Addition of PTX to Antimicrobial Treatment Inhibits *E. coli*-Induced TNF Production in Blood and Enhances Anti-inflammatory IL-10 in Blood and Peripheral Organs of Septic Newborn Mice

Addition of adjunctive PTX to GENT in septic newborn mice significantly and profoundly inhibited TNF plasma concentrations compared to untreated saline control animals with simultaneous and early treatment, with a non-significant trent for decreased concentrations compared to GENT alone [mean TNF plasma concentrations for SAL, GENT, and (GENT + PTX) of 6,142 *vs.* 285 *vs.* 133 pg/ml with simultaneous, and 8,180 *vs.* 5,868 *vs.* 2,128 pg/ml with early treatment], and still decreased TNF plasma concentrations compared to saline controls after late treatment (**Figure 9A**). By contrast, GENT alone only led to a non-significant decrease of plasma TNF after simultaneous treatment. GENT alone, on the other hand, significantly diminished IL-1β concentrations in plasma of septic mice with simultaneous, early and late treatment, without any additional inhibitory effect of adjunctive PTX (**Figure 9B**). Likewise, IL-6 production in plasma of septic newborn mice

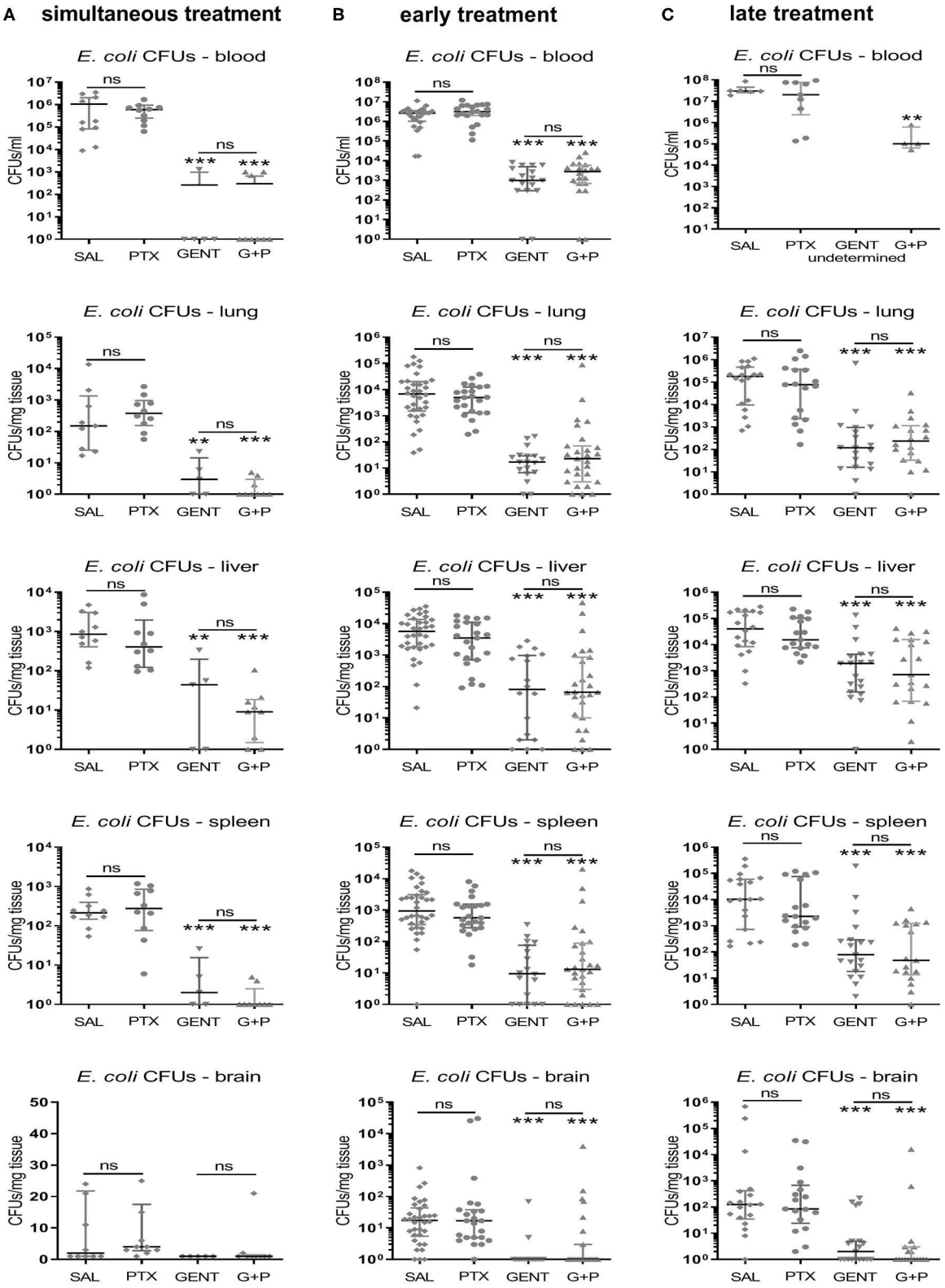

FIGURE 7 | PTX did not increase *E. coli* bacterial growth in neonatal mice. Neonatal mice < 24 h old were injected IV with *E. coli* 10^5 CFU/g body weight, followed by **(A)** simultaneous (0 h, $n = 9$–10), **(B)** early (1.5 h, $n = 17$–34), or **(C)** late (4 h, $n = 17$–19) IP injection of saline control (SAL), GENT, PTX, or GENT + PTX (G + P). After an additional 4 h of incubation, i.e., 4, 5.5, or 8 h from the time of sepsis initiation, mice were euthanized and blood and homogenized organ tissue serially plated for

(Continued)

FIGURE 7 | bacterial counting. Median (IQR) CFU counts for each organ and blood recovered after each treatment condition and time point are shown. Significant differences between SAL *vs.* each treatment condition as well as between GENT *vs.* (G + P) were as indicated: $^{**}p < 0.01$, $^{***}p < 0.001$, ns, non-significant; 2-sided Mann-Whitney *U*-tests. No results available for late treatment with GENT for blood due to insufficient samples.

was significantly diminished with simultaneous, early and late GENT, whereas addition of PTX did not show any further inhibitory effects (**Figure 9C**). Addition of PTX to GENT enhanced the production of the anti-inflammatory IL-10 in septic neonatal mice compared to GENT alone (∼5-fold increase in mean IL-10 plasma concentrations) as well as untreated saline controls (∼3.6-fold increase) after simultaneous treatment, and compared to GENT alone (∼2-fold increase) after late treatment (**Figure 9D**). Similarily, early and late treatment with PTX alone significantly enhanced plasma IL-10 production compared to untreated saline controls, with a non-significant trent toward higher plasma IL-10 concentrations compared to (GENT + PTX)-treated septic neonatal mice after late treatment, indicative of a strongly enhancing effect of PTX on IL-10 production that might partially be counteracted in the presence of GENT. Consistent with the plasma TNF-inhibiting and IL-10-enhancing actions of adjunctive PTX in addition to GENT in our murine neonatal sepsis model, (GENT + PTX) decreased the plasma TNF-to-IL-10 concentration ratio compared to GENT alone as well as untreated saline controls with simultaneous, early and late treatment in relation to sepsis initiation (**Figure 9E**), whereas GENT alone only resulted in a non-significant decline in the plasma TNF-to-IL-10 ratio after simultaneous treatment that immediately followed the injection of bacteria. According to these findings, the addition of PTX to GENT in septic newborn mice thus shifts their plasma cytokine production profile toward an anti-inflammatory milieu that might mitigate the bacteria-induced inflammatory response syndrome associated with *E. coli* sepsis.

While adjunctive PTX to GENT exerted inhibitory actions on *E. coli*-induced plasma TNF production in neonatal mice (achieved power of 95%), addition of PTX to antibiotics did not alter TNF production in peripheral organ tissues such as lung, liver, spleen, and brain of our experimental animals (**Figure 10A**). Similar to its effect on IL-1β and IL-6 in plasma of septic newborn mice, GENT alone decreased production of these two cytokines in lung, liver, and spleen tissue, and inhibited IL-6 but not IL-1β production in brain tissue compared to saline control animals (**Figures 10B,C**). Of note, cerebral IL-1β concentrations were low compared to other organ tissues. Adjunctive PTX in addition to GENT, on the other hand, increased IL-10 tissue concentrations compared to saline control and GENT alone in lung (achieved power of 82%), spleen, and brain tissue (**Figure 10D**). However, compared to GENT alone, (GENT + PTX) did not modify hepatic IL-10 production nor the TNF-to-IL-10 production ratio in liver tissue of septic neonatal mice. Although GENT effectively reduced *E. coli* CFUs in lung tissue (**Figure 7**), GENT alone led to an increased TNF-to-IL-10 production ratio in the lung of septic neonatal mice, i.e., a shift toward a more pro-inflammatory state, compared to untreated septic mice. Addition of PTX to GENT after 1.5 and 4 h of sepsis duration, on the other hand, reduced the TNF-to-IL-10 ratio in lung tissue and effectively prevented this pro-inflammatory response observed with GENT treatment alone at the later stages of sepsis in our model (**Figure 10E**). Likewise, adjunctive PTX to GENT when administered simultaneous with sepsis initiation significantly decreased the TNF-to-IL-10 concentration ratio in the lung compared to saline controls. (GENT + PTX) significantly reduced the ratio of TNF-to-IL-10 concentrations in spleen tissue as compared to untreated septic animals, and in cerebral tissue as compared to GENT alone as well as untreated septic newborn mice (**Figure 10E**). Since TNF concentrations in lung and brain tissue of infected mice were not modified by the addition of PTX to antibiotics, the observed shift toward an anti-inflammatory milieu was primarily achieved through upregulation of IL-10 production in these organs of our *E. coli*-septic newborn mice. Adjunctive PTX in addition to GENT for *E. coli* sepsis appears to exert its anti-inflammatory effects in plasma through inhibition of TNF and enhancement of IL-10 production, whereas it primarily exerts its actions through upregulation of IL-10 production in peripheral organ tissues including the lung and brain.

Relative Treatment-Related Changes of Bacterial CFUs and Cytokine Concentrations Compared to Untreated Septic Neonatal Animals

As shown in **Figure 11A**, *E. coli* CFU counts for GENT- and (GENT + PTX)-treated as compared to untreated septic neonatal mice at 5.5 h after sepsis initiation were comparable between absolute CFUs and relative percentage changes of colony counts, except for increased relative CFU counts in brain tissue among PTX-alone treated compared to untreated mice. Absolute and relative TNF concentrations between GENT- and (GENT + PTX)-treated *vs.* untreated mice were also comparable, except for decreased relative but not absolute TNF concentrations in lung tissue after GENT or (GENT + PTX)-treatment and in plasma after GENT alone (**Figure 11B**). Likewise, absolute and relative IL-10 concentrations between GENT- and (GENT + PTX)-treated *vs.* untreated septic animals remained comparable, except for decreased relative IL-10 in plasma, lung, liver, and brain of GENT-alone treated mice, elevated relative plasma IL-10 in (GENT + PTX)-treated *vs.* GENT alone treated pups, and decreased relative IL-10 in the liver of (GENT + PTX)-treated septic neonatal mice compared to saline controls (**Figure 11C**). These findings demonstrate that absolute cytokine data therefore is more conservative compared to relative treatment-related effects on cytokine production in plasma and organ tissues. Since the TNF-to-IL-10 production ratios were derived from the absolute cytokine values, litter effects are unlikely to be relevant. These data support therefore the conclusion that (GENT +

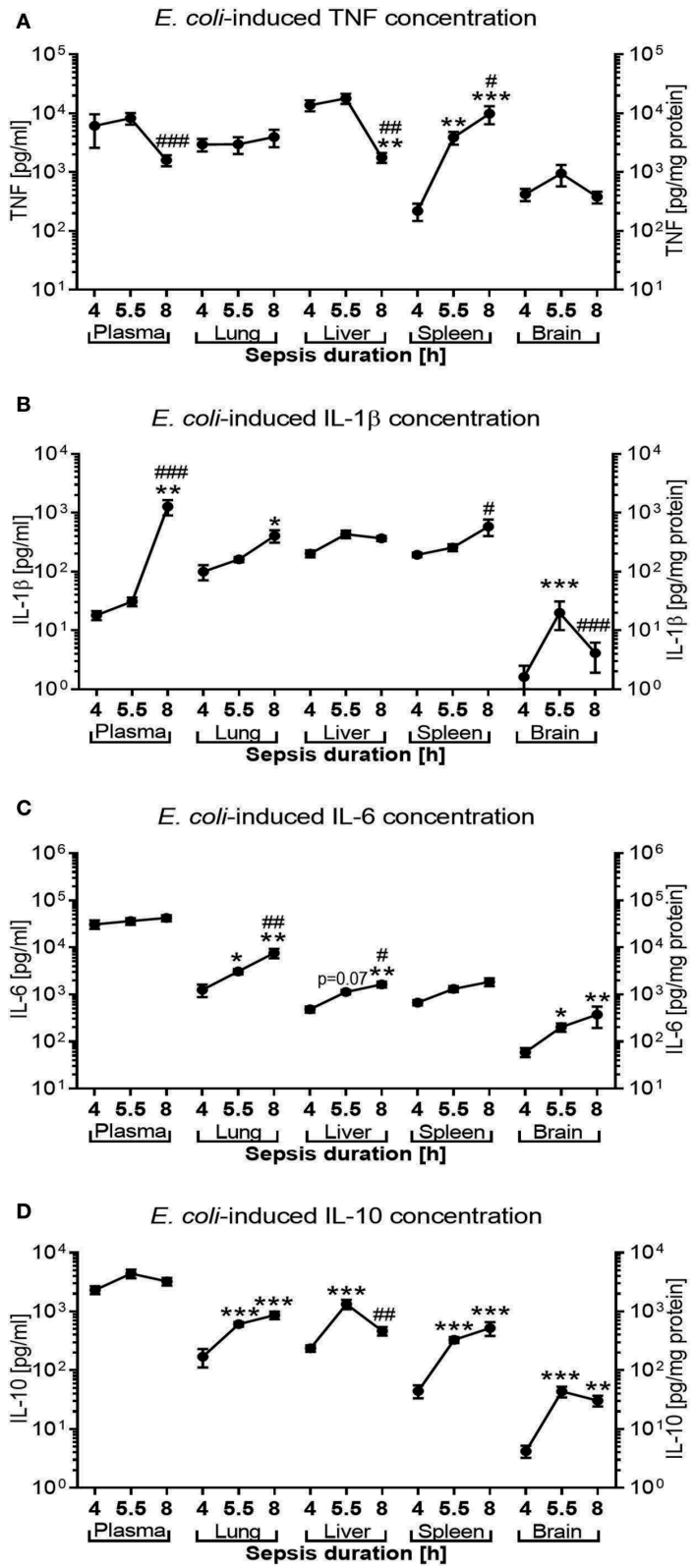

FIGURE 8 | *E. coli*-induced cytokine production in neonatal mice as a function of sepsis duration. Neonatal mice < 24 h old were injected IV with *E. coli* 10^5 CFU/g body weight. After 4 h ($n = 8$), 5.5 h ($n = 34$), and 8 h ($n = 18$) of incubation, mice were euthanized, and pro- and anti-inflammatory cytokines were measured in plasma and homogenized organ tissue. Mean (± SEM) or median (IQR) concentrations for **(A)** TNF, **(B)** IL-1β, **(C)** IL-6, and **(D)** IL-10 were plotted for each time point

(Continued)

FIGURE 8 | as indicated. Significant differences were as follows: $^{*}p < 0.05$, $^{**}p < 0.01$, $^{***}p < 0.001$ for 4 *vs.* 5.5 h and 4 *vs.* 8 h comparisons; $^{\#}p < 0.05$, $^{\#\#}p < 0.01$, $^{\#\#\#}p < 0.001$ for 5.5 *vs.* 8 h comparisons, Kruskal-Wallis tests corrected for false discovery rate.

PTX) treatment of *E. coli*-infected neonatal mice significantly diminished the TNF-to-IL-10 concentration ratios in plasma and all organ tissues except the liver as compared to GENT alone and/or saline controls, thus indicating a shift toward an anti-inflammatory milieu through addition of PTX to antimicrobial therapy in murine neonatal sepsis.

E. coli CFUs and Cytokine Production in Murine Neonatal Sepsis Analyzed by Sex

To determine if sex affects immune responses to immunomodulatory therapies, we analyzed bacterial growth patterns as well as *E. coli*-induced cytokine responses in blood and organs of male and female septic neonatal mice that were untreated or treated with antimicrobials and/or anti-inflammatory agents. Due to low numbers sex-specific analysis had to be limited to the early treatment groups only. *E. coli* CFU counts showed no significant differences between male and female mice among any of the treatment groups (see **Supplementary Table 1**). Likewise, TNF and IL-10 concentrations were similar among male and female untreated and treated [GENT or (GENT + PTX)] septic mice. The pro-inflammatory cytokine IL-1β, however, demonstrated significantly higher (1.6-fold) tissue concentrations in the lung of untreated, 2.5-fold increased concentrations in plasma of GENT-treated, and 2.2-fold higher concentrations in the spleen of GENT-treated female mice, and higher concentrations in the lung (1.7-fold) and spleen (1.7-fold) of (GENT + PTX)-treated male mice after 5.5 h of sepsis (**Table 1**). Additionally, GENT-treated female mice had 4-fold higher IL-6 in lung, whereas (GENT + PTX)-treated male mice presented with higher IL-6 concentrations in lung (∼2.5-fold), spleen (2.3-fold), and brain tissues (6-fold) at 5.5 h after sepsis initiation compared to their female counterparts (**Table 1**). Mice treated with PTX alone revealed no significant differences in cytokine concentrations in any of the organs when analyzed by sex (see **Supplementary Table 2**).

DISCUSSION

The immune system of preterm and term neonates has traditionally been viewed as immature and more susceptible to infections and adverse outcomes resulting from damage caused by invading microorganisms. However, recent findings support the concept of the immune-mediated damage framework (40), specifically that the infection-induced neonatal host response contributes to organ damage including brain injury (6, 24, 28, 41, 42), suggesting that appropriately formulated and timed anti-inflammatory agents such as the phosphodiestarease inhibitor PTX may be of benefit to reduce harmful hyper-inflammation in the newborn. To investigate the actions of PTX or alternative anti-inflammatory agents in newborns, who express distinct innate immunity and suffer the greatest burden of infection (3), we further developed an intravenous live bacterial neonatal mouse sepsis model starting from the first post-natal day of life, followed by anti-microbial and anti-inflammatory treatment (32), and rigorously validated this model by applying two new IV quality scoring systems. Whereas the Evans blue dye-based method to evaluate the quality of IV injections in neonatal rodents is easily applicable to any IV injection including non-microbial injections without the need for any additional equipment, it remains subjective and dependent on user training, and therefore potentially prone to bias. Review of images of experimental animals injected with Evans blue by a trained investigator, or comparison of Evans blue scores with optical imaging results, as performed in this study, can mitigate the risk of bias. Optical imaging to verify the quality of IV bacterial injections in a quantitative and objective manner, on the other hand, besides the need for a suitable bioluminescent microbial strain requires determining a cut-off radiance value for successful IV injections. This cut-off value depends in part on the bioluminescent strain itself, as well as the volume and concentration of the injected bacterial inoculum, the site of injection, the size and position of the animal during optical imaging, as well as the instrument settings and the selected measurement region of interest. Once such a cut-off point has been determined and standard experimental settings are established, optical imaging provides a user-independent and quantitative comparable method to determine the quality of IV injections in neonatal rodents. Depending on the experimental requirements, both quality scoring systems may therefore be employed to verify quality IV injections in rodent pups in future studies.

Applying IV injection quality scoring systems to a murine neonatal sepsis model, our findings support the hypothesis that PTX decreased live *E. coli*-induced systemic inflammatory cytokine production and enhanced the production of the anti-inflammatory IL-10 in blood of newborn mice without increasing bacterial proliferation. This *in vivo* finding is consistent with our previous report on the TNF- suppressive and IL-10-enhancing effects of PTX added to GENT in human cord blood exposed to live *E. coli in vitro* (18). Likewise, these results on reduction of pro-inflammatory cytokine production especially TNF in blood and organs are consistent with other adult and neonatal animal studies. For instance, PTX injection prior to intravenous injection of live *E. coli* in adult rats decreased plasma TNF, IL-1β, and IL-6 concentrations (43). PTX-treated preterm rabbits infected with aerosolized group B streptococci had lower levels of lysozyme and TNF in bronchoalveolar lavage fluid compared to untreated controls (21). Combined PTX and indomethacin treatment of neonatal piglets with group B streptococcal sepsis led to significant reduction of TNF serum levels (44). Other studies have demonstrated that PTX also reduced bacterial endotoxin-induced TNF, interferon γ, and other acute phase reactants in young sheep (45), reversed cerebral ischemia-reperfusion-induced TNF and IL-6 levels in adult rats (46),

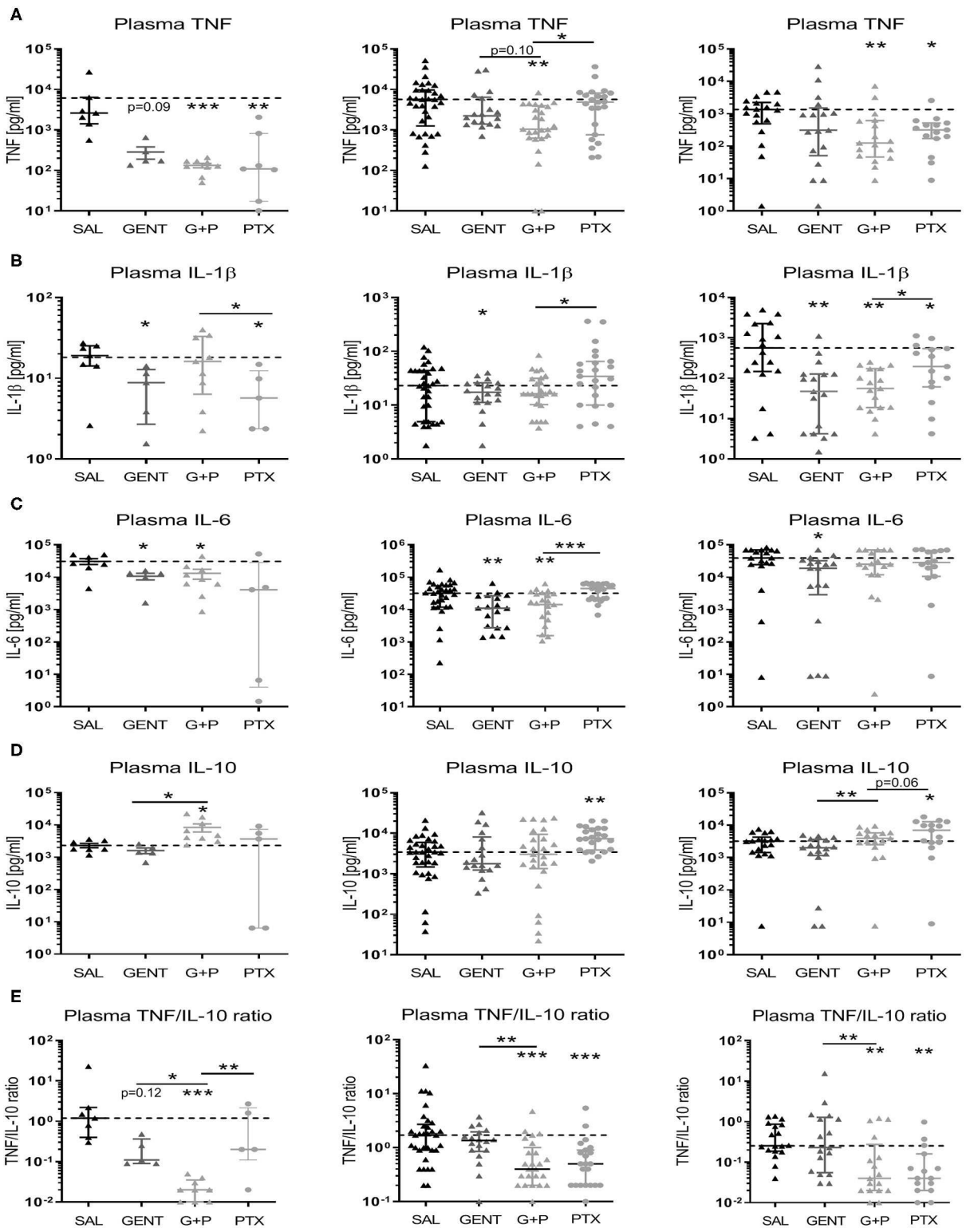

FIGURE 9 | Addition of PTX to GENT profoundly inhibited *E. coli*-induced plasma TNF and enhanced plasma IL-10 in septic newborn mice. Neonatal mice < 24 h old were injected IV with *E. coli* 10^5 CFU/g body weight, followed by simultaneous (0 h, $n = 7–9$), early (1.5 h, $n = 18–33$), or late (4 h, $n = 15–18$) IP injection of SAL, GENT, PTX, or GENT + PTX (G + P). After an additional 4 h of incubation, i.e., 4, 5.5, or 8 h from the time of sepsis initiation, mice were euthanized and plasma

(Continued)

FIGURE 9 | cytokines were measured. Mean (± SEM) or median (IQR) plasma cytokine concentrations for **(A)** TNF, **(B)** IL-1β, **(C)** IL-6, **(D)** IL-10, and **(E)** TNF-to-IL-10 ratios after each treatment condition and time point are shown. Significant differences between SAL *vs.* each treatment condition as well as between GENT *vs.* (G + P) and PTX *vs.* (G + P) were as indicated: $^{*}p < 0.05$, $^{**}p < 0.01$, $^{***}p < 0.001$, one-way ANOVA with Welch's correction or Kruskal-Wallis tests corrected for false discovery rate.

and protected against LPS-induced white matter injury in the developing rat brain (47), suggesting that PTX can inhibit microbial-induced as well as sterile inflammation.

To our knowledge ours is the first study that demonstrated a PTX-induced enhancement of IL-10 production in a neonatal sepsis model *in vivo*, suggesting that this anti-inflammatory mechanism may be relevant in peripheral organ tissues especially during the later phases of sepsis. This novel finding also mirrors our results with newborn cord blood stimulated with purified TLR agonists and live microbes. There PTX inhibited lipopolysaccharide-induced *TNF* mRNA but enhanced *IL10* mRNA expression in newborn cord blood (17), and addition of PTX to antibiotics inhibited *E. coli*-induced pro-inflammatory cytokine production of TNF and IL-1β without decreasing IL-10 (18). Similarly, PTX inhibited TLR agonist-induced pro-inflammatory cytokines in newborn and adult blood (48), consistent with its enhancement of the cAMP-dependent pathway (14). Both anti-TNF-α and recombinant murine IL-10 injected subcutaneously improved survival of *E. coli* sepsis in neonatal mice (27), indicating a role of IL-10 in improved outcome of sepsis in these animals. In contrast to the other organs studied, addition of PTX to GENT did not inhibit hepatic TNF, and did not modify IL-10 production nor the TNF-to-IL-10 ratio in liver tissue of septic neonatal mice compared to GENT alone, an observation that warrants further investigation. PTX might protect against lipopolysaccharide-induced liver injury (49), however this has not been demonstrated for bacterial sepsis-induced hepatic inflammation.

The kinetics of E. coli-induced cytokine concentrations demonstrated striking differences between plasma and peripheral organ tissue responses to murine neonatal sepsis. Whereas TNF appeared to rise early in plasma as well as several peripheral organs (lung and liver), there was a time delay in the pro-inflammatory response of other organs such as the spleen and the brain. Absolute cytokine concentrations in plasma as well as changes in cytokine concentrations are therefore not necessarily predictive of pro-inflammatory cytokines in peripheral organs, which might exhibit a delayed inflammatory response. Thus, characteristic plasma and organ-specific pro- and anti-inflammatory cytokine concentrations and time-course of elevated cytokine levels are encountered during neonatal murine sepsis that need to be accounted for when investigating immunomodulatory treatment strategies that aim to reduce the sepsis-induced inflammatory response syndrome. The fact that adjunctive PTX to GENT inhibited TNF and increased IL-10 concentrations in plasma, but primarily promoted IL-10 production in peripheral organ tissues emphasizes such differences between the systemic and organ responses to immunopharmacological interventions, and might be a consequence of differences in the time-course and stage of sepsis between systemic and peripheral compartments. The effects of treatment on the sepsis-induced inflammatory response in blood and organ tissues were each determined 4 h after PTX and GENT treatment, i.e., at the 4 h time point for simultaneous treatment, at 5.5 h for early, and at 8 h for late treatment (see **Figure 1**), thus providing an equal period of time for treatment effects, and enabling the study of treatment effects during different phases of the inflammatory response to sepsis. *In vitro* studies of microbe-stimulated blood samples as a model of experimental sepsis are useful as a screening tool for the identification of potential candidate adjunctive anti-inflammatory agents (18, 50), but may not be entirely predictive of inflammatory immune responses in peripheral organs, as activated leukocytes in septic patients may contribute to sustained inflammation in peripheral organs und subsequent organ damage (23).

Of particular interest are the responses to sepsis in the murine neonatal brain. The changes in cerebral tissue CFU counts from very low to absent after 4 h of sepsis to moderately high CFU loads at later time-points suggest that the blood-brain barrier initially protected the brain from invading microorganisms, but lost its protective effects with progressing sepsis, thus allowing cerebral microbial invasion. Despite this delay in cerebral microbial invasion by *E. coli* in neonatal septic mice, TNF concentrations were already elevated after 4 h of sepsis and did not significantly change with further progression of sepsis, indicating that systemic pro-inflammatory cytokines such as TNF can enter cerebral tissue in the early stages of sepsis while the blood-brain barrier might still provide protection against invading microorganisms. Cerebral IL-10, on the other hand, remained initially low, thus resulting in the highest TNF-to-IL-10 concentration ratios in the brain compared to the other organ tissues investigated in this study. Addition of PTX to GENT in neonatal sepsis, which resulted in significantly diminished TNF-to-IL-10 ratios in cerebral tissue of *E. coli*-infected mice in our study, might therefore be of particular benefit to protect the vulnerable neonatal brain from sepsis-induced inflammatory injury.

While GENT alone decreased IL-1β and IL-6 concentrations in plasma and all organs tested except for cerebral IL-1β, it exerted only limited decreases in TNF concentrations in the spleen and liver with early treatment, and did not augment IL-10 concentrations nor diminish the ratio of TNF-to-IL-10 in any of the compartments. Adjunctive PTX to GENT, on the other hand, did not demonstrate any additional inhibitory effect on IL-1β and IL-6 in plasma and organ tissues, but actually increased IL-6 concentrations in lung and spleen tissue of *E. coli* septic neonatal mice, which is consistent with its previously reported enhancing effect of this pro-resolution cytokine, bearing in mind that IL-6, for example, reduces tissue neutrophilia (17, 19, 51).

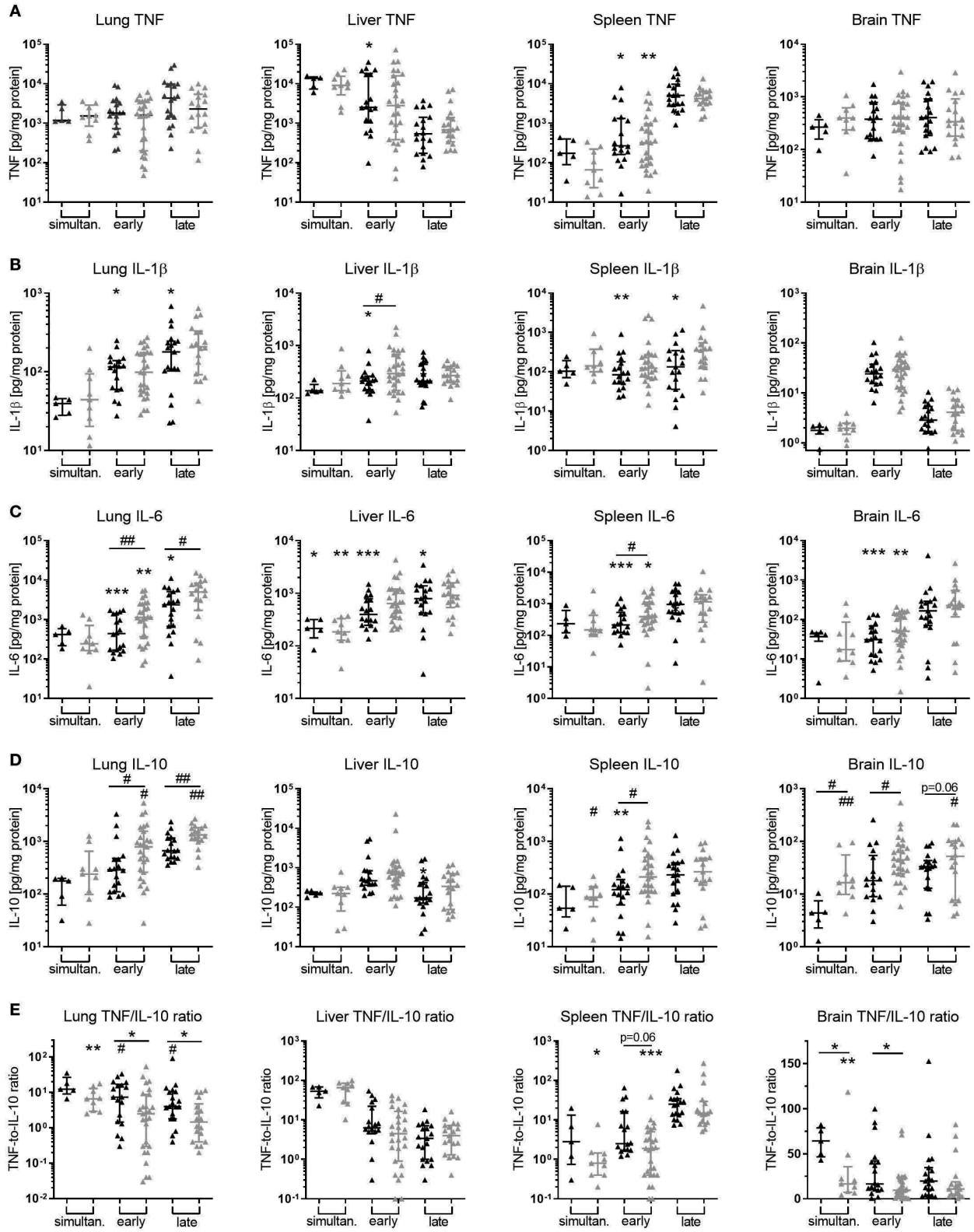

FIGURE 10 | Addition of PTX to GENT enhanced *E. coli*-induced IL-10 production in peripheral organ tissues. Neonatal mice < 24 h old were injected IV with *E. coli* 10^5 CFU/g body weight, followed by simultaneous (0 h, $n = 7–9$), early (1.5 h, $n = 18–34$), or late (4 h, $n = 19–20$) IP injection of SAL, GENT, or (GENT + PTX). After an additional 4 h of incubation, i.e., 4, 5.5, or 8 h from the time of sepsis initiation, mice were euthanized and homogenized organ tissue **(A)** TNF, **(B)** IL-1β, **(C)** IL-6, *(Continued)*

FIGURE 10 | (D) IL-10, and **(E)** TNF-to-IL-10 for lung, liver, spleen, and brain were measured. Mean (± SEM) or median (IQR) cytokine concentrations for GENT (black bars) and (GENT + PTX) (gray bars) for each time point are shown. Significant differences of each treatment condition *vs.* untreated controls and between GENT *vs.* (GENT + PTX) were as indicated: significant increase $^{*}p < 0.05$, $^{**}p < 0.01$, $^{***}p < 0.001$; significant decrease $^{\#}p < 0.05$, $^{\#\#}p < 0.01$, 2-sided *t*-tests with Welch's correction **(A–D)** or Mann-Whitney *U*-tests **(E)** as indicated.

By contrast, adjunctive PTX to GENT significantly inhibited TNF plasma concentrations at all treatment time points tested and spleen TNF with early treatment, and enhanced IL-10 in plasma, lung, spleen, and brain tissues with resulting reduction in TNF-to-IL-10 concentration ratios demonstrating a shift toward an anti-inflammatory milieu. GENT alone even diminished IL-10 in the spleen and elevated the TNF-to-IL-10 ratio in lung tissue, thereby promoting pro-inflammatory responses, which were effectively prevented by the addition of PTX to GENT. Since GENT and PTX both exert different immunomodulatory effects, with GENT primarily decreasing IL-1β and PTX inhibiting TNF and enhancing IL-10, it is conceivable that the combination effect of PTX and an appropriate antimicrobial agent such as GENT provides the greatest suppression of sepsis-induced pro-inflammatory cytokine responses, as demonstrated in our murine neonatal sepsis model. This observation has potential clinical implications, i.e., it is possible that PTX in the context of infections including sepsis may be most helpful when used as an adjunctive agent in combination with appropriate antimicrobial therapy. The observation that concurrent administration of subtherapeutic doses of amphotericin B and a PTX analog led to increased survival times in experimental candidiasis in mice (52) further supports the potential benefit of combined antimicrobial and anti-inflammatory sepsis therapy. On the other hand, TNF may be beneficial for host immunity at low bacterial inoculum and harmful at higher inoculum, and TNF blockade with monoclonal antibodies may be beneficial or harmful depending on the microbial inoculum and strain involved (53–56). The effects of TNF-suppressing anti-inflammatory agents such as PTX in addition to antibiotics in sepsis should therefore be investigated with different bacterial loads and strains prior to its recommendation as adjunctive sepsis therapeutic.

We did not observe any increase of bacterial growth with PTX in our murine neonatal *E. coli* sepsis model, which is consistent with our previous *in vitro* studies (18) as well as published *in vivo* reports, wherein PTX even enhanced clearance of GBS from infected preterm rabbits (21) and improved bacterial clearance in the context of hemorrhage and endotoxemia in rabbits (31). While PTX decreased mortality from experimental *S. aureus* infection in newborn mice at lower doses, high dose PTX actually increased mortality in *S. aureus*-infected newborn mice (20), and led to greater fungal burden and shortened survival in murine *Candida albicans* sepsis (57). Based on limited clinical trials in human septic neonates, PTX may decrease mortality in newborn sepsis when administered in addition to antibiotics (15). Adjunctive PTX, when added to appropriate antibiotics and at recommended doses, therefore does not appear to compromise the antimicrobial host immune response, which was also suggested by our own albeit limited mortality data. PTX added to antibiotics might under certain circumstances even support bacterial clearance, and it might protect the host from inflammatory organ injury through the promotion of an anti-inflammatory milieu. On the other hand, adjunctive PTX might exert microbe-specific changes in the host immune response to sepsis. In a model of *Staphylococcus epidermidis*-induced murine neonatal sepsis that was further potentiated by hypoxic-ischemic brain injury, vancomycin reduced bacterial growth and cytokine production in plasma and alleviated the resulting brain injury, whereas the addition of PTX did not provide any additional beneficial effects (58). Likewise, whereas PTX alone or combined with GENT significantly suppressed *E. coli*-induced TNF and IL-1β expression in newborn cord blood monocytes *in vitro*, this agent only led to a minor decrease in *S. epidermidis*-induced IL-1β without modifying intramonocytic TNF expression, and did not alter the expression of any *S. epidermidis*-induced cytokine-encoding genes (18). According to these animal and limited human studies and our own findings, PTX may be a beneficial and feasible adjuvant therapy for neonatal sepsis due to its ability to reduce systemic and peripheral organ inflammation without compromising antibacterial host immunity.

Sex differences in immune function such as distinct vaccine responses, autoimmune diseases, or cancer, is a well-recognized phenomenon and has been extensively reviewed (30, 59, 60). Sex-specific differences in immune functions appear to play a role in the increased manifestation and severity of many complications among male preterm neonates such as perinatal brain injury, bronchopulmonary dysplasia and sepsis (29). To the best of our knowledge, no sex differences in the anti-inflammatory immune responses of adjunctive PTX to infections have been reported to date. Since our study was not powered for the detection of sex differences in cytokine responses, it is possible that small differences in immune responses to our treatment interventions might have remained undetected. Since we did not apply multiple comparison correction to this exploratory analysis of sex-specific cytokine responses, the statistical differences in IL-1β and IL-6 tissue concentrations observed between male and female neonatal mice for several treatment conditions might have occurred by chance alone. The observation that (GENT + PTX) did not suppress IL-6 and IL-1β as much in male *vs.* female neonatal mice in several organ tissues warrants further investigation in future studies.

Our study is novel and has important strengths. We employed a rigorously validated murine neonatal sepsis model, consisting of high quality intravenous live bacterial injections on the first day of life, thereby mimicking human preterm neonatal sepsis (61). Our study demonstrated substantial differences in the effects of adjunctive PTX on systemic *vs.* peripheral organ inflammation as well as organ-specific responses, such that PTX inhibited plasma TNF and enhanced plasma IL-10 concentrations while primarily increasing IL-10 production in

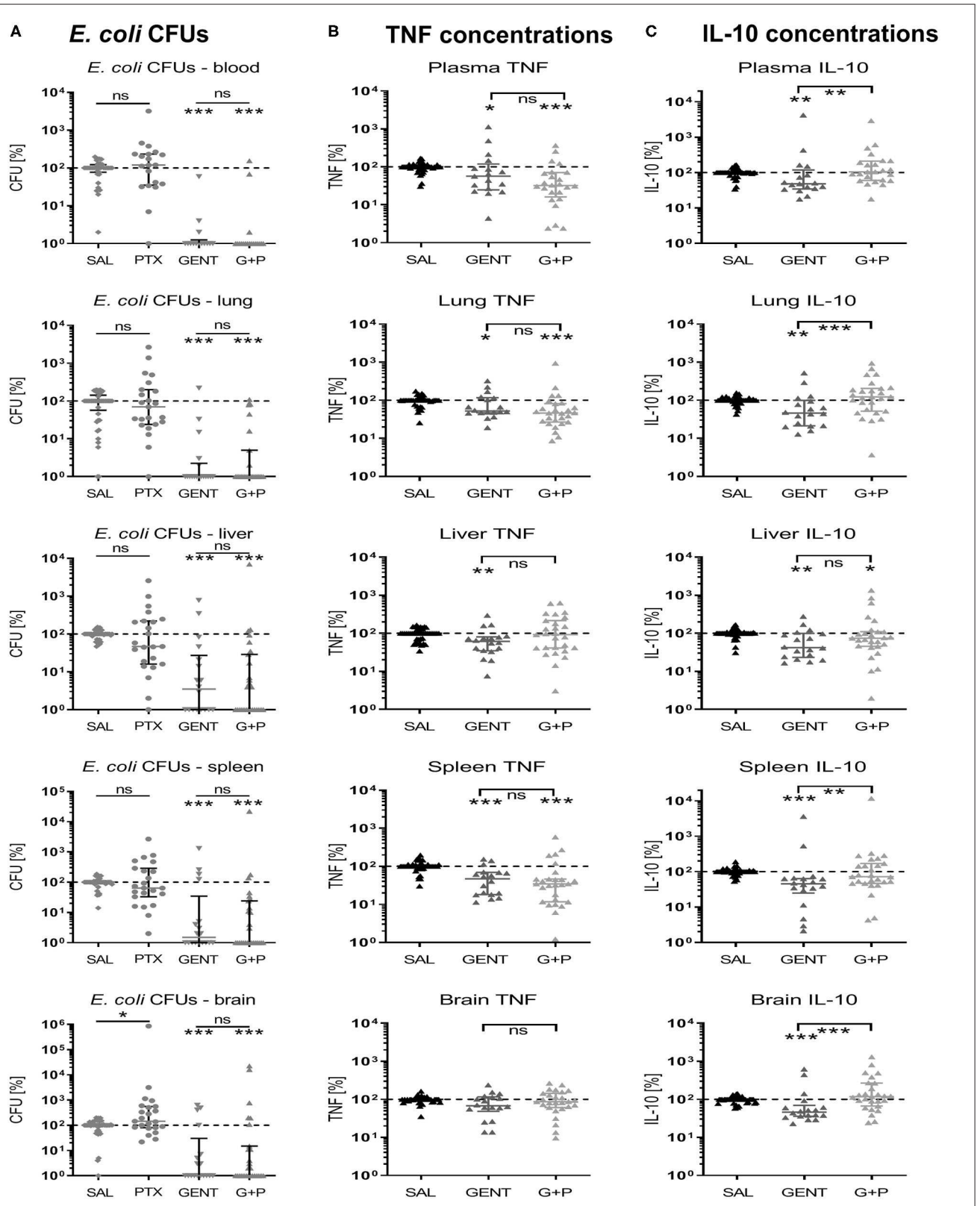

FIGURE 11 | Effect of GENT, PTX, and (GENT + PTX) on *E. coli* CFUs and cytokine production in neonatal mice relative to untreated septic mice. Neonatal mice < 24 h old were injected IV with *E. coli* 10^5 CFU/g body weight, followed by 1.5 h delayed IP injection of SAL, GENT, PTX, or GENT + PTX (G + P). After an additional 4 h of incubation mice were euthanized, blood and homogenized organ tissues serially plated for bacterial counting, and cytokine concentrations measured. **(A)** CFU

(Continued)

FIGURE 11 | counts, **(B)** TNF, and **(C)** IL-10 concentrations for each organ and blood or plasma from animals subjected to different treatment conditions were expressed as a percentage compared to untreated septic mice within the same litter (defined as 100%). Significant differences of relative median (IQR) CFUs and cytokine concentrations of animals treated with antibiotics and/or anti-inflammatory agents *vs.* untreated controls and between GENT- *vs.* (G + P)-treated animals were as follows: $*p < 0.05$, $**p < 0.01$, $***p < 0.001$, ns, non-significant; Mann-Whitney *U* **(A)** and Kruskal-Wallis tests with correction for false discovery rate **(B,C)**, $n = 15–27$.

TABLE 1 | Effects of early GENT and PTX on *E. coli*-induced cytokines in murine neonatal sepsis by sex.

Cytokine	Organ	Sex	SAL control				GENT				GENT + PTX			
			N	Mean	± SEM	Median	*N*	Mean	± SEM	Median	*N*	Mean	± SEM	Median
TNF	Plasma	Fem.	21	7,214	± 1,701	5,845	13	7,289	± 2,828	2,439	13	2,072	± 646	1,046
		Male	12	9,870	± 4,239	4,810	5	1,914	± 347	1,619	12	2,189	± 528	1,451
	Lung	Fem.	22	2,795	± 1,093	777	13	2,668	± 808	1,536	14	2,202	± 495	1,669
		Male	12	1,942	± 959	568	5	2,188	± 655	1,860	13	1,751	± 464	1,497
	Liver	Fem.	22	19,338	± 4,425	11,697	13	10,214	± 3,205	3,420	14	12,658	± 5,265	4,362
		Male	12	17,057	± 5,652	6,003	5	5,198	± 4,041	1,226	13	7,362	± 3,075	2,780
	Spleen	Fem.	22	3,331	± 730	2,099	13	1,426	± 642	316	14	752	± 317	158
		Male	11	5,284	± 2,492	2,281	5	884	± 769	122	13	1,037	± 437	341
	Brain	Fem.	22	973	± 556	335	13	516	± 135	357	14	392	± 86	733
		Male	12	848	± 236	657	5	465	± 139	413	13	734	± 217	308
IL-1β	Plasma	Fem.	21	33	± 6	25	13	**23****	**± 3**	**23****	13	22	± 6	16
		Male	12	27	± 10	15	5	**9****	**± 3**	**11****	12	23	± 4	18
	Lung	Fem.	22	**187***	**± 22**	**168***	13	120	± 18	120	14	**87***	**± 16**	**62***
		Male	12	**114***	**± 18**	**118***	5	85	± 11	84	13	**153***	**± 21**	**172***
	Liver	Fem.	22	479	± 89	336	13	261	± 51	216	14	481	± 153	247
		Male	12	350	± 65	360	5	186	± 40	207	13	486	± 118	354
	Spleen	Fem.	22	285	± 49	190	13	197	± 64	**118****	14	452	± 230	**80***
		Male	11	200	± 32	196	5	42	± 8	**53****	13	397	± 159	**254***
	Brain	Fem.	22	35	± 16	18	13	32	± 8	22	14	30	± 5	27
		Male	12	30	± 8	20	5	26	± 3	26	13	36	± 9	33
IL-6	Plasma	Fem.	21	38,724	± 7,874	35,492	13	19,065	± 4,950	12,267	13	12,044	± 3,581	4,832
		Male	12	31,756	± 8,472	26,226	5	6,452	± 2,505	3,130	12	22,542	± 5,596	17,685
	Lung	Fem.	22	3,178	± 490	2,583	13	**874***	**± 177**	870	14	**966***	**± 202**	**1,026***
		Male	12	2,879	± 746	2,755	5	**220***	**± 51**	173	13	**2,384***	**± 508**	**2,465***
	Liver	Fem.	22	1,225	± 166	882	13	630	± 112	495	14	914	± 291	520
		Male	12	950	± 167	697	5	304	± 55	247	13	951	± 188	822
	Spleen	Fem.	22	1,381	± 245	1,177	13	458	± 120	335	14	**465***	**± 149**	**301***
		Male	11	1,182	± 287	890	5	170	± 38	187	13	**1,085***	**± 251**	**985***
	Brain	Fem.	22	166	± 44	120	13	57	± 12	49	14	**50***	**± 13**	**31***
		Male	12	269	± 86	148	5	15	± 4	13	13	**304***	**± 18**	**111***
IL-10	Plasma	Fem.	21	4,042	727	3,445	13	5,439	1,741	2,270	13	7,477	± 2,563	2,190
		Male	12	5,066	± 1,662	3,344	5	7,475	± 6,273	1,244	12	5,550	± 1,815	4,159
	Lung	Fem.	22	566	± 56	485	13	489	± 151	302	14	1,165	± 405	464
		Male	12	689	± 124	588	5	777	± 633	164	13	1,078	± 264	913
	Liver	Fem.	22	996	± 118	1,045	13	952	± 335	515	14	2,274	± 1,589	797
		Male	12	1,957	± 627	1,326	5	1,312	± 1,013	385	13	1,279	± 633	699
	Spleen	Fem.	22	352	± 53	233	13	204	± 80	138	14	444	± 196	131
		Male	11	286	± 50	261	5	205	± 133	98	13	435	± 96	318
	Brain	Fem.	22	40	± 13	25	13	33	± 9	19	14	92	38	32
		Male	12	51	± 12	45	5	60	± 50	9	13	58	± 10	47

Neonatal mice < 24 h old were injected IV with E. coli 10^5 CFU/g body weight, followed by early (1.5 h) IP injection of SAL, GENT, or (GENT + PTX). After an additional 4 h of incubation, i.e., 5.5 h from the time of sepsis initiation, mice were euthanized, and plasma, and homogenized organ tissue cytokines were measured. Mean (± SEM) and median cytokine concentrations in pg/ml (plasma) or pg/mg protein for each organ and treatment condition and separate for both sexes were calculated. Significant sex differences (in bold) employing 2-sided t-tests and Mann-Whitney U-tests were indicated as follows: $*p < 0.05$, $**p < 0.01$.

organ tissues with little or no effect on tissue TNF levels. The IL-10-promoting effect of PTX might be particularly relevant in the brain, which showed the highest TNF-to-IL-10 concentrations compared to other organ tissues among untreated septic neonatal mice. Our results indicate that the combination of PTX with antibiotics such as GENT might further improve the anti-inflammatory efficacy of these agents. Anti-inflammatory effects of adjunctive PTX to antibiotics were achieved at different time points in relation to sepsis duration, whether anti-inflammatory and antimicrobial treatment was administered simultaneously, early or late after sepsis initiation. And importantly, the shift of bacterial sepsis-induced cytokine responses toward an anti-inflammatory mileu was achieved without an increase of bacterial growth and mortality, suggesting that the adjunctive use of PTX to antibiotics for neonatal sepsis might be safe and beneficial.

On the other hand, our study has several limitations. Our findings were based on murine neonatal *E. coli* sepsis, the most frequently encountered organism of early-onset sepsis in the human neonate. However, the effects of PTX on immune responses in human newborns and those induced by other neonatal pathogens, including the Gram-positive organisms *S. epidermidis* and *S. aureus*, *Candida* or viral infections such as *Herpes simplex*, will need to be investigated prior to recommending this agent as empiric adjunctive therapy for newborn sepsis syndromes. Neonatal immunity changes rapidly over the course of the first several weeks of life, and preterm neonates are especially vulnerable to microbial infections and infection-induced organ damage including brain injury. Therefore, neonatal sepsis models investigating the effects of adjunctive anti-inflammatory treatment regimens should also study the effects on different gestational and post-natal age groups. As demonstrated in our current study as well as our previous *in vitro* experiments on human cord blood (18), combinations of PTX with antibiotics may lead to different treatment interactions including additive or synergistic anti-inflammatory responses. Our observations pave the way for future studies to: (a) investigate additional antimicrobial agents, such as those with intrinsic anti-inflammatory mechanisms of action (e.g., azithromycin) (62); and (b) assess the potential impact of PTX and other anti-inflammatory agents on metabolites and metabolic pathways relevant to the progression and severity of sepsis, such as lactate. Our study examined the short-term effects of adjunctive PTX on microbe-induced inflammatory cytokine responses and bacterial growth in murine neonatal sepsis. However, longitudinal survival and outcome studies of adjunctive PTX treatment are needed, as well as comprehensive studies on the structural and functional outcome of organs that are adversely affected by neonatal sepsis such as the brain.

In summary, our study demonstrated that adjunctive PTX when added to GENT inhibited *E. coli*-induced TNF and enhanced *E. coli*-induced IL-10 production in blood plasma while also increasing anti-inflammatory IL-10 concentrations in peripheral organ tissues including the brain. This PTX-induced shift toward anti-inflammatory immune responses was achieved whether treatment was administered simultaneously, early or late in relation to sepsis initiation, and without increasing the bacterial burden or mortality in septic neonatal mice. To the extent that sepsis-induced organ damage in newborns is driven by TNF and other pro-inflammatory mediators, our observations raise the possibility that PTX might be a safe and effective anti-inflammatory adjunctive agent to treat sepsis.

DATA AVAILABILITY STATEMENT

The raw data supporting the conclusions of this article will be made available by the authors, without undue reservation.

ETHICS STATEMENT

The animal study was reviewed and approved by Institutional Animal Care and Use Committee, Stony Brook University, Stony Brook, NY.

AUTHOR CONTRIBUTIONS

ES initiated the project, performed formal data analysis, and wrote the original manuscript. ES, ED-N, OL, and BF conceptualized the study and developed the hypothesis and design. ES, ED-N, and LO developed the methodology. LO, ES, ED-N, and MR performed and validated the experiments. OL, BF, and ED-N critically reviewed and edited the manuscript. All authors reviewed the final version of the manuscript.

FUNDING

ES was supported by the U.S. National Institutes of Health (NIH) National Institute of Allergy and Infectious Diseases NIAID (R21AI149296), the Department of Pediatrics, Stony Brook Children's Hospital and the Renaissance School of Medicine at Stony Brook University. OL was supported by the U.S. National Institutes of Health (NIH) National Institute of Allergy and Infectious Diseases (NIAID) Infant Immunity grant R01AI100135-01 and its administrative supplements. BF is an attending at the U.S. Department of Veterans Affairs—Northport VA Medical Center, Northport, NY. She was supported by US Veterans Affairs Merit Review Award 5I01 BX003741 and NIAID R01 AI127704. The contents of this article do not represent the views of VA or the United States Government. The funders had no role in study design, data collection and interpretation, or the decision to submit the work for publication.

ACKNOWLEDGMENTS

The authors thank Laurie Levine, Jean Rooney, and Thomas Zimmerman, Division of Laboratory Animal Resources, Stony Brook University, for their assistance with our animal breeding colony, and assistance and advice with animal procedures and protocols. Furthermore, we acknowledge the biostatistical consultation and support provided by the Biostatistical

Consulting Core at the Renaissance School of Medicine at Stony Brook University. The authors also thank Prof. Peter Taylor, University College London School of Pharmacy, London, United Kingdom, for providing us with the bioluminescent *E. coli* strain.

SUPPLEMENTARY MATERIAL

The Supplementary Material for this article can be found online at: https://www.frontiersin.org/articles/10.3389/fimmu.2020.577878/full#supplementary-material

REFERENCES

1. Lawn JE, Cousens S, Zupan J. 4 million neonatal deaths: When? Where? Why? *Lancet*. (2005) 365:891–900. doi: 10.1016/S0140-6736(05)71048-5
2. Goldenberg RL, Hauth JC, Andrews WW. Intrauterine infection and preterm delivery. *N Engl J Med*. (2000) 342:1500–7. doi: 10.1056/NEJM200005183422007
3. Stoll BJ, Hansen NI, Bell EF, Walsh MC, Carlo WA, Shankaran S, et al. Trends in care practices, morbidity, and mortality of extremely preterm neonates, 1993-2012. *JAMA*. (2015) 314:1039–51. doi: 10.1001/jama.2015.10244
4. Lukacs SL, Schoendorf KC, Schuchat A. Trends in sepsis-related neonatal mortality in the United States, 1985-1998. *Pediatr Infect Dis J*. (2004) 23:599–603. doi: 10.1097/01.inf.0000131633.74921.90
5. Wynn JL. Defining neonatal sepsis. *Curr Opin Pediatr*. (2016) 28:135–40. doi: 10.1097/MOP.0000000000000315
6. Kuban KC, O'Shea TM, Allred EN, Paneth N, Hirtz D, Fichorova RN, et al. Systemic inflammation and cerebral palsy risk in extremely preterm infants. *J Child Neurol*. (2014) 29:1692–8. doi: 10.1177/0883073813513335
7. Cornette L. Fetal and neonatal inflammatory response and adverse outcome. *Semin Fetal Neonatal Med*. (2004) 9:459–70. doi: 10.1016/j.siny.2004.08.004
8. Mallard C, Wang X. Infection-induced vulnerability of perinatal brain injury. *Neurol Res Int*. (2012) 2012:102153. doi: 10.1155/2012/102153
9. Wittebole X, Collienne C, Castanares-Zapatero D, Laterre PF. Adjunctive therapies for severe sepsis. *Int J Antimicrob Agents*. (2008) 32(Suppl. 1):S34–8. doi: 10.1016/j.ijantimicag.2008.06.005
10. Schüller SS, Kramer BW, Villamor E, Spittler A, Berger A, Levy O. Immunomodulation to prevent or treat neonatal sepsis: past, present, and future. *Front Pediatr*. (2018) 6:199. doi: 10.3389/fped.2018.00199
11. Tarnow-Mordi W, Isaacs D, Dutta S. Adjunctive immunologic interventions in neonatal sepsis. *Clin Perinatol*. (2010) 37:481–99. doi: 10.1016/j.clp.2009.12.002
12. Du Pont-Thibodeau G, Joyal JS, Lacroix J. Management of neonatal sepsis in term newborns. *F1000Prime Rep*. (2014) 6:67. doi: 10.12703/P6-67
13. Coppini R, Simons SHP, Mugelli A, Allegaert K. Clinical research in neonates and infants: challenges and perspectives. *Pharmacol Res*. (2016) 108:80–7. doi: 10.1016/j.phrs.2016.04.025
14. Serezani CH, Ballinger MN, Aronoff DM, Peters-Golden M. Cyclic AMP: master regulator of innate immune cell function. *Am J Respir Cell Mol Biol*. (2008) 39:127–32. doi: 10.1165/rcmb.2008-0091TR
15. Pammi M, Haque KN. Pentoxifylline for treatment of sepsis and necrotizing enterocolitis in neonates. *Cochrane Database Syst Rev*. (2015) 3:CD004205. doi: 10.1002/14651858.CD004205.pub3
16. Salman S, Hibbert J, Page-Sharp M, Manning L, Simmer K, Doherty DA, et al. Effects of maturation and size on population pharmacokinetics of pentoxifylline and its metabolites in very preterm infants with suspected late-onset sepsis or necrotizing enterocolitis: a pilot study incorporating clinical outcomes. *Br J Clin Pharmacol*. (2019) 85:147–59. doi: 10.1111/bcp.13775
17. Speer EM, Dowling DJ, Ozog LS, Xu J, Yang J, Kennady G, et al. Pentoxifylline inhibits TLR- and inflammasome-mediated *in vitro* inflammatory cytokine production in human blood with greater efficacy and potency in newborns. *Pediatr Res*. (2017) 81:806–16. doi: 10.1038/pr.2017.6
18. Speer EM, Diago-Navarro E, Ozog LS, Dowling DJ, Huo W, Raheel M, et al. Pentoxifylline alone or in combination with gentamicin or vancomycin inhibits live microbe-induced pro-inflammatory cytokine production in human cord blood and cord blood monocytes *in vitro*. *Antimicrob Agents Chemother*. (2018) 62:e01462–18. doi: 10.1128/AAC.01462-18
19. Jones SA. Directing transition from innate to acquired immunity: defining a role for IL-6. *J Immunol*. (2005) 175:3463–8. doi: 10.4049/jimmunol.175.6.3463
20. Maderazo EG, Breaux S, Woronick CL, Krause PJ. Efficacy, toxicity, and pharmacokinetics of pentoxifylline and its analogs in experimental Staphylococcus aureus infections. *Antimicrob Agents Chemother*. (1990) 34:1100–6. doi: 10.1128/AAC.34.6.1100
21. Mah MP, Aeberhard EE, Gilliam MB, Sherman MP. Effects of pentoxifylline on *in vivo* leukocyte function and clearance of group B streptococci from preterm rabbit lungs. *Crit Care Med*. (1993) 21:712–20. doi: 10.1097/00003246-199305000-00015
22. Travadi J, Patole S, Charles A, Dvorak B, Doherty D, Simmer K. Pentoxifylline reduces the incidence and severity of necrotizing enterocolitis in a neonatal rat model. *Pediatr Res*. (2006) 60:185–9. doi: 10.1203/01.pdr.0000228325.24945.ac
23. Cavaillon JM, Eisen D, Annane D. Is boosting the immune system in sepsis appropriate? *Crit Care*. (2014) 18:216. doi: 10.1186/cc13787
24. Strunk T, Inder T, Wang X, Burgner D, Mallard C, Levy O. Infection-induced inflammation and cerebral injury in preterm infants. *Lancet Infect Dis*. (2014) 14:751–62. doi: 10.1016/S1473-3099(14)70710-8
25. Procianoy RS, Silveira RC. Association between high cytokine levels with white matter injury in preterm infants with sepsis. *Pediatr Crit Care Med*. (2012) 13:183–7. doi: 10.1097/PCC.0b013e3182231074
26. Németh K, Leelahavanichkul A, Yuen PST, Mayer B, Parmelee A, Doi K, et al. Bone marrow stromal cells attenuate sepsis via prostaglandin E(2)-dependent reprogramming of host macrophages to increase their interleukin-10 production. *Nat Med*. (2009) 15:42–9. doi: 10.1038/nm.1905
27. Lally KP, Cruz E, Xue H. The role of anti-tumor necrosis factor-α and interleukin-10 in protecting murine neonates from *Escherichia coli* sepsis. *J Pediatr Surg*. (2000) 35:852–5. doi: 10.1053/jpsu.2000.6862
28. Wynn J, Cornell TT, Wong HR, Shanley TP, Wheeler DS. The host response to sepsis and developmental impact. *Pediatrics*. (2010) 125:1031–41. doi: 10.1542/peds.2009-3301
29. O'Driscoll DN, Greene CM, Molloy EJ. Immune function? A missing link in the gender disparity in preterm neonatal outcomes. *Expert Rev Clin Immunol*. (2017) 13:1061–71. doi: 10.1080/1744666X.2017.1386555
30. Brown MA, Su MA. An inconvenient variable: sex hormones and their impact on T cell responses. *J Immunol*. (2019) 202:1927–33. doi: 10.4049/jimmunol.1801403
31. Heller S, Weber K, Heller A, Urbaschek R, Koch T. Pentoxifylline improves bacterial clearance during hemorrhage and endotoxemia. *Crit Care Med*. (1999) 27:756–63. doi: 10.1097/00003246-199904000-00031
32. Kronforst KD, Mancuso CJ, Pettengill M, Ninkovic J, Power Coombs MR, Stevens C, et al. A neonatal model of intravenous *Staphylococcus epidermidis* infection in mice <24 h old enables characterization of early innate immune responses. *PLoS ONE*. (2012) 7:e43897. doi: 10.1371/journal.pone.0043897
33. Cortese F, Scicchitano P, Gesualdo M, Filaninno A, De Giorgi E, Schettini F, et al. Early and late infections in newborns: where do we stand? A review. *Pediatr Neonatol*. (2016) 57:265–73. doi: 10.1016/j.pedneo.2015.09.007
34. Witcomb LA, Collins JW, McCarthy AJ, Frankel G, Taylor PW. Bioluminescent imaging reveals novel patterns of colonization and invasion in systemic *Escherichia coli* K1 experimental infection in the neonatal rat. *Infect Immun*. (2015) 83:4528–40. doi: 10.1128/IAI.00953-15
35. Kienstra KA, Freysdottir D, Gonzales NM, Hirschi KK. Murine neonatal intravascular injections: modeling newborn disease. *J Am Assoc Lab Anim Sci*. (2007) 46:50–4.
36. Radu M, Chernoff J. An *in vivo* assay to test blood vessel permeability. *J Vis Exp*. (2013) 73:e50062. doi: 10.3791/50062
37. Bany BM, Hamilton GS. Assessment of permeability barriers to macromolecules in the rodent endometrium at the onset of implantation. *Methods Mol Biol*. (2011) 763:83–94. doi: 10.1007/978-1-61779-191-8_5

38. Connolly DC, Wood EH. Simultaneous measurement of the appearance and disappearance of T-1824 (Evans blue) in blood and tissue after intravenous injection in man. *J Appl Physiol*. (1954) 7:73–83. doi: 10.1152/jappl.1954.7.1.73
39. Faul F, Erdfelder E, Lang AG, Buchner A. G*Power 3: a flexible statistical power analysis program for the social, behavioral, and biomedical sciences. *Behav Res Methods*. (2007) 39:175–91. doi: 10.3758/BF03193146
40. Casadevall A, Pirofski LA. The damage-response framework of microbial pathogenesis. *Nat Rev Microbiol*. (2003) 1:17–24. doi: 10.1038/nrmicro732
41. Hagberg H, Wennerholm UB, Savman K. Sequelae of chorioamnionitis. *Curr Opin Infect Dis*. (2002) 15:301–6. doi: 10.1097/00001432-200206000-00014
42. Lee I, Neil JJ, Huettner PC, Smyser CD, Rogers CE, Shimony JS, et al. The impact of prenatal and neonatal infection on neurodevelopmental outcomes in very preterm infants. *J Perinatol*. (2014) 34:741–7. doi: 10.1038/jp.2014.79
43. Voisin l, Breuillé D, Ruot B, Rallière C, Rambourdin F, Dalle M, et al. Cytokine modulation by PX differentially affects specific acute phase proteins during sepsis in rats. *Am J Physiol*. (1998) 275:R1412–9. doi: 10.1152/ajpregu.1998.275.5.R1412
44. Gibson RL, Truog WE, Henderson WR Jr, Redding GJ. Group B streptococcal sepsis in piglets: effect of combined pentoxifylline and indomethacin pretreatment. *Pediatr Res*. (1992) 31:222–7. doi: 10.1203/00006450-199203000-00006
45. Chalmeh A, Rahmani Shahraki A, Heidari SM, Badiei K, Pourjafar M, Nazifi S, et al. The comparative efficacy of tyloxapol versus pentoxifylline against induced acute phase response in an ovine experimental endotoxemia model. *Inflammopharmacology*. (2016) 24:59–64. doi: 10.1007/s10787-015-0257-9
46. Dong J, Yuan X, Xie W. Pentoxifylline exerts anti-inflammatory effects on cerebral ischemia reperfusion-induced injury in a rat model via the p38 mitogen-activated protein kinase signaling pathway. *Mol Med Rep*. (2018) 17:1141–7. doi: 10.3892/mmr.2017.7953
47. Dilek M, Kumral A, Okyay E, Ozbal S, Tugyan K, Tuzun F, et al. Protective effects of pentoxifylline on lipopolysaccharide-induced white matter injury in a rat model of periventricular leukomalacia. *J Matern Fetal Neonatal Med*. (2013) 26:1865–71. doi: 10.3109/14767058.2013.798290
48. D'Hellencourt CL, Diaw L, Cornillet P, Guenounou M. Differential regulation of TNFα, IL-1β, IL-6, IL-8, TNFβ, and IL-10 by pentoxifylline. *Int J Immunopharmacol*. (1996) 18:739–48. doi: 10.1016/S0192-0561(97)85556-7
49. Yee SB, Ganey PE, Roth RA. The role of Kupffer cells and TNF-α in monocrotaline and bacterial lipopolysaccharide-induced liver injury. *Toxicol Sci*. (2003) 71:124–32. doi: 10.1093/toxsci/71.1.124
50. Levy O, Sisson RB, Kenyon J, Eichenwald E, Macone AB, Goldmann D. Enhancement of neonatal innate defense: effects of adding an N-terminal recombinant fragment of bactericidal/permeability-increasing protein on growth and tumor necrosis factor-inducing activity of gram-negative bacteria tested in neonatal cord blood *ex vivo*. *Infect Immun*. (2000) 68:5120–5. doi: 10.1128/IAI.68.9.5120-5125.2000
51. Kaplanski G, Marin V, Montero-Julian F, Mantovani A, Farnarier C. IL-6: a regulator of the transition from neutrophil to monocyte recruitment during inflammation. *Trends Immunol*. (2003) 24:25–9. doi: 10.1016/S1471-4906(02)00013-3
52. Wasan KM, Vadiei K, Luke DR, Keyhani A, White RA, McQueen TJ, et al. Antifungal activity of HWA-138 and amphotericin B in experimental systemic candidiasis. *Antimicrob Agents Chemother*. (1991) 35:2046–8. doi: 10.1128/AAC.35.10.2046
53. Visser CE, Brouwer-Steenbergen JJ, Struijk G, Krediet RT, Beelen RH. Production of IL-1 beta and TNF-alpha by peritoneal macrophages depends on the bacterial species and the inoculum. *Adv Perit Dial*. (1997) 13:201–4.
54. Sjöstedt A, North RJ, Conlan JW. The requirement of tumour necrosis factor-alpha and interferon-gamma for the expression of protective immunity to secondary murine tularaemia depends on the size of the challenge inoculum. *Microbiology*. (1996) 142:1369–74. doi: 10.1099/13500872-142-6-1369
55. Nassif X, Mathison JC, Wolfson E, Koziol JA, Ulevitch RJ, So M. Tumour necrosis factor alpha antibody protects against lethal meningococcaemia. *Mol Microbiol*. (1992) 6:591–7. doi: 10.1111/j.1365-2958.1992.tb01505.x
56. Havell EA, Sehgal PB. Tumor necrosis factor-independent IL-6 production during murine listeriosis. *J Immunol*. (1991) 146:756–61.
57. Louie A, Baltch AL, Franke MA, Ritz WJ, Smith RP, Singh JK, et al. Effect of pentoxifylline on the course of systemic Candida albicans infection in mice. *J Antimicrob Chemother*. (1996) 37:943–54. doi: 10.1093/jac/37.5.943
58. Lai JCY, Svedin P, Ek CJ, Mottahedin A, Wand X, Levy O, et al. Vancomycin is protective in a neonatal mouse model of *Staphylococcus epidermidis*-potentiated hypoxic-ischemic brain injury. *Antimicrob Agents Chemother*. (2020) 64:e02003–19. doi: 10.1128/AAC.02003-19
59. Klein SL, Marriott I, Fish EN. Sex-based differences in immune function and responses to vaccination. *Trans R Soc Trop Med Hyg*. (2015) 109:9–15. doi: 10.1093/trstmh/tru167
60. Gubbels Bupp MR, Jorgensen TN. Androgen-induced immunosuppression. *Front Immunol*. (2018). 9:794. doi: 10.3389/fimmu.2018.00794
61. Adkins B, Leclerc C, Marshall-Clarke S. Neonatal adaptive immunity comes with age. *Nat Rev Immunol*. (2004) 4:553–64. doi: 10.1038/nri1394
62. Aghai ZH, Kode A, Saslow JG, Nakhla T, Farhath S, Stahl GE, et al. Azithromycin suppresses activation of nuclear factor-kappa B and synthesis of pro-inflammatory cytokines in tracheal aspirate cells from premature infants. *Pediatr Res*. (2007) 62:483–8. doi: 10.1203/PDR.0b013e318142582d

Conflict of Interest: OL is a named inventor on patents relating to the anti-infective bactericidal/permeability-increasing protein, human *in vitro* systems that model age-specific immunity, and vaccine adjuvants.

The remaining authors declare that the research was conducted in the absence of any commercial or financial relationships that could be construed as a potential conflict of interest.

frontiers in Immunology

ORIGINAL RESEARCH
published: 30 September 2020
doi: 10.3389/fimmu.2020.565484

Prenatal Endotoxin Exposure Induces Fetal and Neonatal Renal Inflammation via Innate and Th1 Immune Activation in Preterm Pigs

*Tik Muk[1], Ping-Ping Jiang[1,2], Allan Stensballe[3], Kerstin Skovgaard[4], Per Torp Sangild[1,5] and Duc Ninh Nguyen[1]**

[1] Section for Comparative Paediatrics and Nutrition, Department of Veterinary and Animal Sciences, University of Copenhagen, Copenhagen, Denmark, [2] School of Public Health, Sun Yat-sen University, Guangzhou, China, [3] Department of Health Science and Technology, Aalborg University, Aalborg, Denmark, [4] Department of Biotechnology and Biomedicine, Technical University of Denmark, Copenhagen, Denmark, [5] Department of Paediatrics, Odense University Hospital, Odense, Denmark

OPEN ACCESS

Edited by:
Laurel J. Gershwin, University of California, Davis, United States

Reviewed by:
Lulu Shao, University of Pittsburgh, United States
Friederike Ebner, Free University of Berlin, Germany

***Correspondence:**
Duc Ninh Nguyen
dnn@sund.ku.dk

Specialty section:
This article was submitted to Comparative Immunology, a section of the journal Frontiers in Immunology

Received: *25 May 2020*
Accepted: *31 August 2020*
Published: *30 September 2020*

Citation:
Muk T, Jiang P-P, Stensballe A, Skovgaard K, Sangild PT and Nguyen DN (2020) Prenatal Endotoxin Exposure Induces Fetal and Neonatal Renal Inflammation via Innate and Th1 Immune Activation in Preterm Pigs. Front. Immunol. 11:565484. doi: 10.3389/fimmu.2020.565484

Chorioamnionitis (CA) predisposes to preterm birth and affects the fetal mucosal surfaces (i.e., gut, lungs, and skin) via intra-amniotic (IA) inflammation, thereby accentuating the proinflammatory status in newborn preterm infants. It is not known if CA may affect more distant organs, such as the kidneys, before and after preterm birth. Using preterm pigs as a model for preterm infants, we investigated the impact of CA on fetal and neonatal renal status and underlying mechanisms. Fetal pigs received an IA dose of lipopolysaccharide (LPS), were delivered preterm by cesarean section 3 days later (90% gestation), and compared with controls (CON) at birth and at postnatal day 5. Plasma proteome and inflammatory targets in kidney tissues were evaluated. IA LPS-exposed pigs showed inflammation of fetal membranes, higher fetal plasma creatinine, and neonatal urinary microalbumin levels, indicating renal dysfunction. At birth, plasma proteomics revealed LPS effects on proteins associated with renal inflammation (up-regulated LRG1, down-regulated ICA, and ACE). Kidney tissues of LPS pigs at birth also showed increased levels of kidney injury markers (*LRG1*, *KIM1*, *NGLA*, *HIF1A*, and *CASP3*), elevated molecular traits related to innate immune activation (infiltrated MPO^+ cells, complement molecules, oxidative stress, *TLR2*, *TLR4, S100A9*, *LTF*, and *LYZ*), and Th1 responses ($CD3^+$ cells, ratios of *IFNG/IL4*, and *TBET/GATA3*). Unlike in plasma, innate and adaptive immune responses in kidney tissues of LPS pigs persisted to postnatal day 5. We conclude that prenatal endotoxin exposure induces fetal and postnatal renal inflammation in preterm pigs with both innate and adaptive immune activation, partly explaining the potential increased risks of kidney injury in preterm infants born with CA.

Keywords: intrauterine bacterial infection, chorioamnionitis, plasma proteomics, renal inflammation, acute kidney injury, immune activation

INTRODUCTION

Preterm birth (before 37 weeks of gestation, 15 million cases per year, and ∼10% of all pregnancies) is a global health problem and a leading cause of infant mortality and morbidity (1, 2). A majority of preterm births (40–70%) are caused by chorioamnionitis (CA, inflammation of the fetal membranes), which is often derived from bacterial infections in the lower genital tract and amniotic fluid (3–5). CA is often associated with multiple neonatal complications after preterm birth, including necrotizing enterocolitis (NEC), bronchopulmonary dysplasia, periventricular leukomalacia, and sepsis, depending on the location, timing, and severity of maternal inflammation (6). Despite these associations, it remains unclear how CA interacts with reduced gestational age at birth (preterm birth) to affect infant organs, both at birth and later.

Due to the limited access to biological samples in infants, animal models are essential to better understand the underlying organ-specific, pathophysiological mechanisms of prenatal insults. Intra-amniotic (IA) administration of lipopolysaccharide (LPS) has been used to induce CA in rhesus macaques, sheep, and mice (7–10). However, the postnatal effects of prenatal insults in these models are largely unknown, partly due to difficulties in rearing preterm animals. Exposure to IA LPS or microbes often elevates levels of immune cells and pro-inflammatory cytokines in the amniotic fluid, which are thought first to interact with fetal mucosal surfaces (e.g., gut, lung, and skin) to evoke local tissue inflammation, and later the inflammatory signals may or may not extend to the circulation and other internal organs (11, 12). In rodents, lambs, and pigs, CA effects on fetal lung and gut inflammation (via neutrophil and/or macrophage infiltration and TLR signaling modulation) (13–19) as well as on fetal acute brain injuries (20, 21) have well been investigated. In contrast, the effects on other internal organs, both at birth and in postnatal periods, remain elusive.

Neonatal kidney inflammation and acute kidney injury (AKI) are under-recognized neonatal conditions with challenging diagnosis due to the lack of reliable diagnostic biomarkers (22). As nephrogenesis mainly occurs in the last trimester of human pregnancy (23) and *extra-uterine* environment seems not optimal for glomerular development (24), preterm infants, especially those born before 28 weeks of gestation, may be at high risks of developing AKI. In fact, ∼50% of preterm infants with extremely low birth weight (<1000 *g*) are diagnosed with early-onset AKI and AKI is also associated with increased mortality (25–29). Neonatal AKI can also be induced by fetal distress and postnatal exposure to hypotension, sepsis, and nephrotoxic medications (25, 26, 28–30). Further, CA has been reported to be associated with renal and electrolyte abnormalities in indomethacin-treated preterm infants (31). Fetal lambs following IA LPS administration have reduced nephron numbers (32, 33), implying possible sub-optimal renal functions in preterm infants born after CA (32, 34).

Preterm pig delivered at 90% gestation has been used as a clinically relevant model for preterm infants to investigate the effects of nutritional, microbial and immuno-modulatory interventions on organ functions and development (35, 36). Similar to preterm infants, preterm pigs possess multiple immaturities (e.g., underdeveloped gut, lungs, brain, and immune and cardiovascular systems) that make them highly susceptible to systemic infection and organ dysfunctions (37). Relative to rodents, the immune system in pigs is more similar to that in humans (38), with more human-like inflammatory responses to immune challenge (39). We have previously established a preterm pig model of CA to study effects of IA LPS on gut and lung injuries (35). In the current study, we hypothesized that IA LPS would also affect more distant organs like the kidneys, both at birth and during the neonatal period after preterm birth. We investigated clinical parameters, plasma markers of inflammation by proteomics, and kidney tissue evaluation of targets related to inflammation and innate and adaptive immune activation.

MATERIALS AND METHODS

Animal Procedures

All animal procedures were approved by the Danish National Committee of Animal Experimentation (license number 2014-15-0201-00418). The animal experiment was conducted at the pig neonatal intensive care unit, the section for comparative pediatrics and nutrition, Copenhagen, Denmark. Three pregnant sows (Large White × Danish Landrace × Duroc) were operated (35) at day 103 of gestation (term at day 117 ± 2), and each fetus received an IA dose of 1 mg LPS/fetus (LPS group, $n = 28$, from *Escherichia coli* 055:B5, Sigma-Aldrich, Copenhagen, Denmark) in the area close to their mouth, or a control treatment (saline injection or no injection, CON group, $n = 26$). 3 days later, preterm piglets were delivered by cesarean section (90% of gestational age). The piglets were randomized according to their sex and birth weight into two subgroups within each treatment group. For each treatment, a fraction of piglets were euthanized right after delivery ($n = 14$ CON, 16 LPS), and the remaining pigs were reared by formula feeding until euthanasia at postnatal day 5 ($n = 12$ for both CON and LPS groups), as previously described (35). The preterm pig study was designed with parenteral nutrition and enteral nutrition using an infant formula to induce multiple clinically relevant complications, including NEC, shortly after birth (35). The study period of 5

Abbreviations: ACE, Angiotensin-converting enzyme; ACE2, Angiotensin I Converting Enzyme 2; AKI, Acute kidney injury; C3, Complement C3; C3, Complement C3; C4, Complement C4; CA, Chorioamnionitis; CA, Carbonic anhydrase 2; CASP3, Caspase 3; CD14, CD14 molecule; CKD, Chronic kidney disease; FDR, False discovery rate; FOXP3, Forkhead box P3; GA, Gestational age; GATA3, transcription factors GATA3; HIF1A, Hypoxia inducible factor 1 subunit alpha; HPRT1, Hypoxanthine-guanine phosphoribosyltransferase; ICA, Carbonic anhydrase inhibitor; IHC, Immunohistochemistry; IL10, Interleukin 10; IL17, Interleukin 17; IL4, Interleukin 4; INFr, Interferon-gamma; KIM-1, Kidney injury molecule-1; LPS, Lipopolysaccharide; LRG1, Leucine-rich alpha-2-glycoprotein 1; LTF, Lactotransferrin; LYZ, Lysozyme; MDA, Malondialdehyde; MS, Mass spectrometry; NGLA, Neutrophil gelatinase-associated lipocalin; RAS, Renin-angiotensin system; RT-qPCR, Reverse transcription quantitative real-time PCR; ROS, Reactive oxygen species; S100A9, S100 Calcium Binding Protein A9; SEM, Standard error of the mean; SOD, Superoxide dismutase; SAA, Serum Amyloid A; TBET, Transcription factors T-bet; TLR, Toll-like receptor; TLR2, Toll-like receptor 2; TLR4, Toll-like receptor 4; TNF-α, Tumor necrosis factor-α.

postnatal days was selected to investigate the postnatal effect of IA LPS when the animals were not severely affected by formula-inducing complications. At euthanasia, the pig was initially anesthetized with an intramuscular injection of Zoletil mix (dose 0.1 ml/kg, including 0.25 mg/kg Zoletil, 0.25 mg/kg Butorphanol, 1.25 mg/kg Xylazin, and 1.25 mg/kg Ketamine), followed by an intracardiac injection of 20% Pentobarbital (Sigma-Aldrich, Copenhagen, Denmark) (35). Serum and urine samples at euthanasia (day 1 and day 5) were used for biochemistry (Advia 1800 Chemistry System. Siemens, Erlangen, Germany), and EDTA-treated plasma was used for proteomics. Kidney and liver tissues were snap-frozen and stored at −80°C for future analyses, and chorioamnion samples were fixed in paraformaldehyde 4% for histology. To balance the effect of litter and sex for treatment comparisons, one pig of each sex from each litter were selected for each treatment group in the validation stage. A random number selection method was used to choose the sample when more than one pig was eligible for each litter, sex and treatment, resulting in nine pigs in each group selected for the further validation analysis. Due to the sample availability, sample numbers may vary according to different sample types.

Proteomic Analysis

The plasma samples were centrifuged at 1,000 × *g* for 5 min and measured in duplicates for protein content using a NanoDrop 2000 Spectrophotometer (Thermo Scientific, United States). The preparation procedures were based on a PVDF membrane-based proteomic sample processing method (MStern blotting) (40). Plasma protein (10 μg) was diluted into saturated urea followed by a reduction by 10 mM TCEP and alkylation by 50 mM chloroacetamide. Immobilon-P PVDF membrane (Millipore; 0.5 mm^2) was incubated with saturated urea for 5 min and transferred to a 96-well, 1.5-ml deep well plate. Samples were incubated with the membrane for 10 min at ambient temperature using a thermomixer for continuous shaking. After incubation, samples were discarded, and the membranes washed with 150 μl, 50-mM ammonium bicarbonate (Ambic). Digestion buffer (100 μl, 5% TFE (v/v), 5% ACN (v/v), Trypsin 1:35 in 50 mM Ambic) was added to each sample and incubated overnight at 37°C in air incubator keeping high humidity. Tryptic peptides were recovered to collection tube followed by extraction of remaining peptides with 150 μl of 40% acetonitrile (ACN, v/v) 0.1% formic acid (FA; v/v). The pooled extracts were dried by vacuum centrifuge and resuspended with loading solvent (2% ACN, 0.1% trifluoroacetic acid, 0.1% FA in Milli-Q water) before loading into the LC-MS system.

The individual serum samples were randomized and sequenced on a hybrid trapped ion mobility spectrometry (TIMS) quadrupole time of flight (QToF) mass spectrometer, i.e., timsTOF in tims-off mode, (Bruker Daltonics, Bremen, Germany) coupled to modified nano-electrospray ion source (CaptiveSpray, Bruker Daltonics) with an applied voltage of 1800 V. Liquid chromatography was performed using a Dionex RSCL Proflow UHPLC (Dionex, Thermo Scientific, Waltham, United States) setup. Each sample was loaded onto a 2-cm reverse-phase C18-material trapping column and separated on a 75 cm analytical column (both from Acclaim PepMap100, Thermo Scientific). The liquid phase consisted of 96% solvent A (0.1% FA) and 4% solvent B (0.1% FA in ACN), at a flow rate of 300 nl/min. The peptides were eluted from the column by increasing to 8% solvent B and subsequently to 30% solvent B on a 35 min ramp gradient and introduced into the mass spectrometer by a Captivespray emitter for electrospray ionization (Bruker; Germany). The mass spectrometer was operated in positive mode with data-dependent acquisition (DDA), alternating between survey spectra and isolation/fragmentation spectra, using the Top20 method. All samples were analyzed in duplicates in a random order.

Tissue Histology

Fixed chorioamnions were embedded in paraffin, sectioned, and stained with hematoxylin and eosin, as previously described (35). Frozen kidney tissues were sectioned and stained for myeloperoxidase (MPO), using rabbit anti-human MPO polyclonal antibody (AO398, Dako, Glostrup, Denmark), followed by anti-rabbit biotin-conjugated secondary antibody (Dako Denmark) and visualized with nickel-DAB. Frozen kidney sections were also stained for CD3, using CD3e-UNLB porcine primary antibody (monoclonal antibody PPT3) followed by Primary Antibody Enhancer, HRP Polymer (All from SouthernBiotech, Birmingham, United Kingdom), and visualized with nickel-DAB (Sigma-Aldrich) (41). Hematoxylin was used as counter-staining. All pictures were captured using Leica MC190 HD and positively stained area fraction in the total tissue area was quantified using ImageJ software (LOCI, University of Wisconsin).

Gene Expressions by qPCR

Transcription of selected genes related to inflammation and innate and adaptive immune pathways in the liver and kidney tissues were determined by real-time RT-qPCR, using predesigned primers (**Supplementary Table 4**). Briefly, total RNA in tissue homogenates was isolated with RNeasy Lipid Tissue Mini Kit (Qiagen, Copenhagen, Denmark). RT-qPCR in kidney tissues was performed using QuantiTect SYBR Green PCR Kit (Qiagen) on a LightCycler 480 (Roche, Hvidovre, Denmark), and relative levels of target genes were normalized to the housekeeping gene HPRT1 (42). Gene expression in liver tissues was analyzed by 96.96 Dynamic Array Integrated Fluidic Circuits (Fluidigm, CA, United States), and relative expressions of target genes were normalized to the most stable reference genes (*GAPDH, HPRT, RPL13A, PPIA, TBP, B2M,* and *TBP1*), as previously described (35).

Complement Proteins and Targets Related to Reactive Oxygen Species

The frozen kidney samples (Day 1: $n = 9$, Day 5: $n = 8$ in control and 9 in LPS) were also homogenized for analyses of superoxide dismutase (SOD) activity (SOD determination kit, Sigma-Aldrich, MO, United States), membrane attacking complex (MAC, C5b-C9, human C5b-9 ELISA kit, BD Biosciences Pharmingen, CA, United States), and peroxidation product malondialdehyde (MDA, MDA assay kit, Sigma-Aldrich).

Western Blot

Renal protein expression level of leucine-rich alpha 2 glycoprotein 1 (LRG1) was analyzed by Western blot, using rabbit anti-human LRG1 polyclonal antibody antibodies (Sigma Aldrich, St. Louis, United States). Total proteins (Day1: $n = 9$, Day5: $n = 8$ in control and 9 in LPS) were extracted and separated by 10% Tricine SDS Gels (30 μg) and then transferred onto PVDF membrane (Millipore, Bedford, MA, United States). After blocking in 5% BSA 1 h at room temperature, the membranes were incubated with primary antibodies (1:1000 dilution) overnight at 4°C. The membranes were then washed twice with PBST, incubated with HRP-conjugated secondary antibody at 1:20000 dilutions for 1 h at room temperature, and visualized by the SuperSignal West Pico PLUS chemiluminescent substrate (Thermo Scientific^{TM}, MA, United States). Mouse anti-porcine GAPDH monoclonal antibody (1:1000, Santa Cruz, CA, United States) was used as a loading control to generate the relative expression level of target protein. The Western blot results were quantified by Image J software (43). The target protein LRG1 level was analyzed by relative quantification and presented as a fold change to the loading control GAPDH.

Data Analysis and Statistics

Mass spectrometry raw files were processed with MaxQuant (v 1.6.2.3) using the Andromeda search engine. Default MaxQuant settings were used using protein oxidation and N-terminal acetylation as variable modifications and carbamidomethyl cysteine as a fixed modification. Label-free quantification was performed using the MaxQuant label-free-quantification (MaxLFQ) algorithm.

Univariate analysis was applied to raw proteomics data (**Supplementary Data Sheet 1**) at each sampling time point using R studio 3.4.1 (R Studio, Boston, MA, United States). Briefly, a linear mixed effect model was fitted to each protein with treatment as the fixed factor, and litter as a random factor, using the lme4 package (44). To control the type *I* error, *p* value tests were further adjusted by false discovery rate (FDR, $\alpha = 0.2$) into *q* values (45). Proteins with a *q* value ≤ 0.10 in any comparisons were chosen for the functional assignment. The protein interaction network analysis of biological processes and signaling pathways were performed using Cytoscape and ClueGO with a *p*-value cut-off $q \leq 0.1$. Dunn's Kruskal–Wallis multiple comparisons test of clinical data and Pearson's correlation test were conducted in R. Results from qPCR, Western blot, and ELISA assays were analyzed by a linear mixed model, as described above, and a *p*-value < 0.05 was regarded as statistically significant. Data were presented as mean ± SEM.

RESULTS

Effects of IA LPS on Amniotic Fluid, Fetal Membranes, Plasma Proteome, and Systemic Endpoints

Intra-amniotic LPS increased the number of infiltrated inflammatory cells in the chorioamnion (**Figure 1A**), similar to our previous report (35). Consistent with our previous report (35), amniotic fluid leukocyte counts and cytokines IL-6, IL-1β, TNF-α, and IL-10 were all highly elevated after IA LPS exposure (all $p < 0.05$, **Supplementary Table 1**).

Mass spectrometry-based plasma proteomics identified and annotated 245 proteins. IA LPS altered levels of 45 proteins at birth and two proteins at postnatal day 5. Analyses of pathway enrichment and protein-to-protein interaction revealed (**Figures 1B,C**) key regulated pathways, including complement and coagulation cascades, platelet activation, and acute phase response, indicating increased acute systemic inflammation in LPS pigs at birth. According to physiological functions, differentially regulated plasma proteins at birth were categorized into five groups: coagulation, acute phase response, protein processing, metabolism, and other functions (**Supplementary Table 2**). Acute-phase response to IA LPS at birth, but not on postnatal day 5, was confirmed by the increased expressions of liver genes. 64 genes in total were validated in transcription level in liver tissues (**Supplementary Table 6**), and eight genes were significantly changed in at birth, including *C3*, *SAA*, *S100A8*, *TRL4,* ITUH4, CXCL10, TTR, and *CD14* (**Figure 1D**); only two genes were significantly changed at postnatal day 5 (**Supplementary Table 6**). Notably, apart from the classical systemic inflammation-related proteins, a group of plasma proteins related to renal functions, including angiotensin-converting enzyme (ACE), carbonic anhydrase 2 (CA2), and LRG1 (**Figure 1E**), were also altered by IA LPS at birth.

Markers of IA-LPS Induced Kidney Inflammation in Plasma, Urine, and Kidney Tissues

As plasma proteomics showed IA LPS-induced changes of markers related to kidney inflammation, including LRG1 and inhibitor of carbonic anhydrase (ICA), these proteins and related targets were further examined in kidney tissues. Plasma LRG1 and renal *LRG1* expression after IA LPS exposure were both elevated at birth ($q < 0.001$ and $p < 0.01$, respectively, **Figures 2A,B**). This result was confirmed by Western blot analysis of LRG1 in kidney tissues ($p < 0.05$, **Figures 2C,D**). At postnatal day 5, the transcription level of LRG1 was significantly decreased in LPS pigs, but no changes were detected at protein level in both plasma and kidney tissues, probably reflecting differences in the post-transcriptional regulation of this gene between the two groups after birth.

Plasma LRG1 levels were also positively correlated with levels of urine Na + and plasma creatinine, a diagnostic marker of AKI ($r = 0.6$ and 0.647, respectively, $p < 0.001$, **Figure 2E** and **Supplementary Figure 1**). Despite lower levels of plasma ICA in LPS vs. CON pigs at birth, renal *ICA* mRNA levels were not altered by fetal LPS exposure (**Figures 2F,G**). However, the expression of *CA2* (carbonic anhydrase 2) in kidney tissues were elevated in LPS pigs at birth ($p < 0.05$, **Figure 2H**). Carbonic anhydrase is abundantly distributed in renal tissues and thought to play a pivotal role to catalyze the hydration–dehydration reaction of CO_2 and bicarbonate reabsorption (46, 47). These

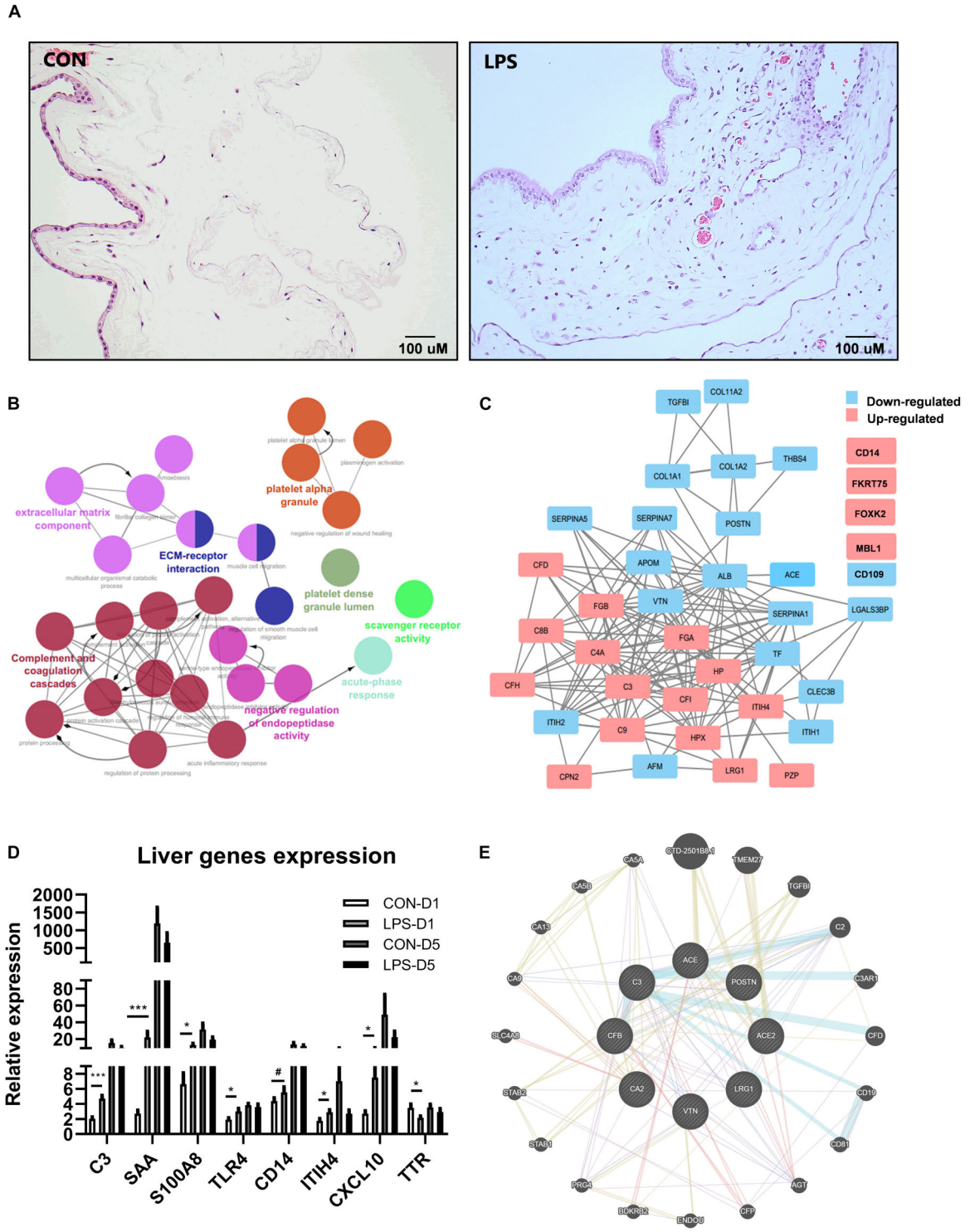

FIGURE 1 | Effects of IA LPS exposure on chorioamnionitis (CA), changes of plasma proteome, and liver acute gene responses in preterm pigs at birth. **(A)** Inflammatory cell infiltration in the chorioamnion. **(B)** Pathway enrichment of differentially regulated proteins in plasma between LPS vs. CON pigs at birth (day 1). Every pathway is labeled according to the color. **(C)** Differentially regulated protein networks in plasma in LPS vs. CON pigs at birth (list of differential expressed proteins in **Supplementary Table 2**). **(D)** Changes of acute response genes in the liver of LPS pigs at birth. $n = 10$ in both groups. **(E)** A subgroup of differentially regulated proteins in plasma showed their functions related to kidney injury. The pathway enrichment was performed by GeneMANIA (84). Color code for **(E)** Blue: pathway interaction; Yellow: shared protein domains; Purple: co-expression; and Red: physical interactions. Width of the edge shows a weighted interaction network where each pair of genes is assigned an association weight (84). Data are presented as mean ± SEM. *, ***$p < 0.05$ and 0.001, respectively. $^{\#}p < 0.1$.

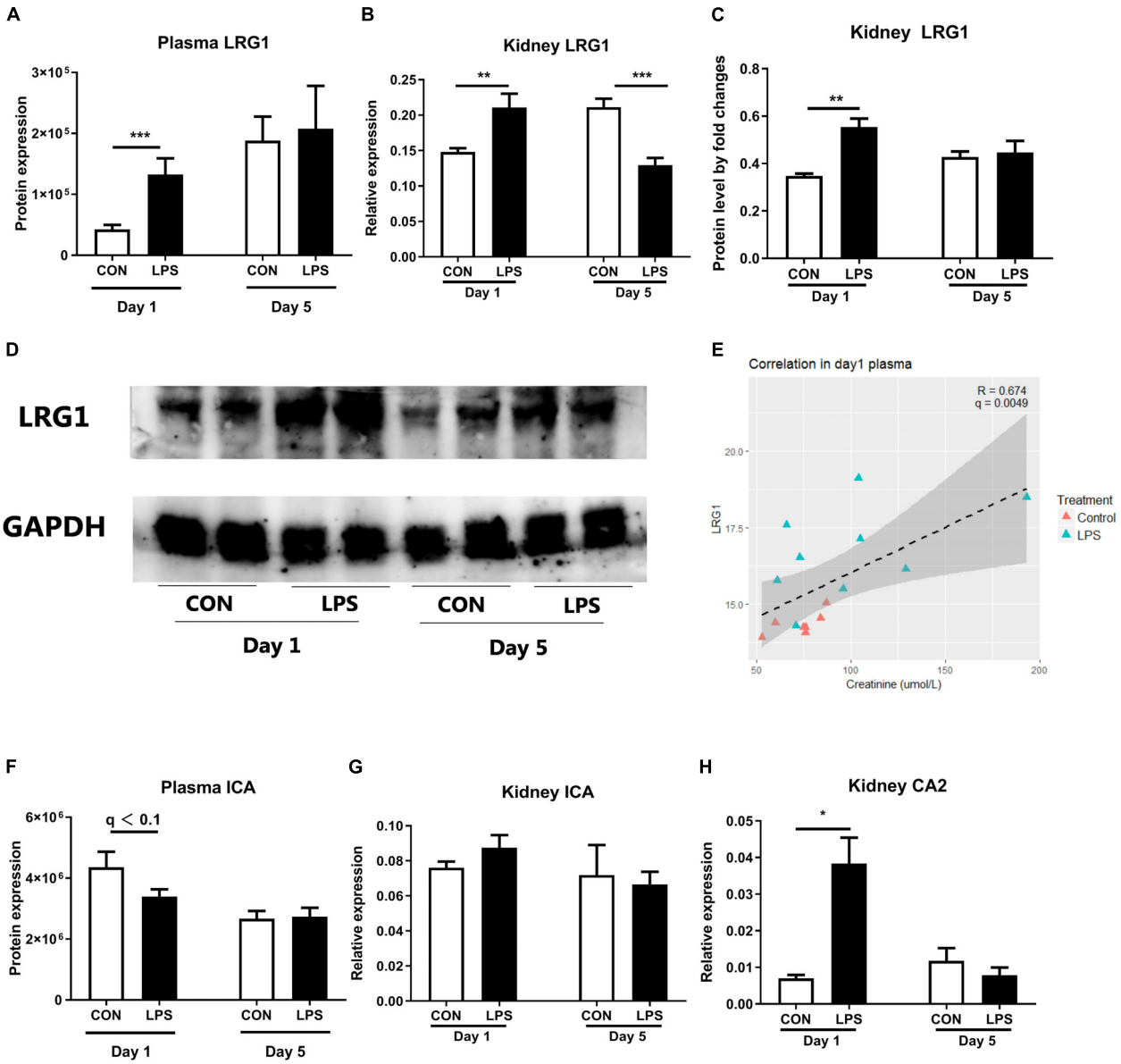

FIGURE 2 | Markers of neonatal acute kidney injury. **(A)** The protein levels of LRG1 in plasma. **(B)** mRNA level of *LRG1* in kidney tissues. **(C,D)** The protein levels of LRG1 in kidney tissues by Western blot and the relative quantification to loading control GAPDH. (Day 1: $n = 9$, Day 5: $n = 8$ in control and 9 in LPS; samples were randomly selected to balance the effect of litter and sex for treatment comparisons; **E)** Correlation of plasma LRG1 levels and plasma creatinine levels. Samples with creatinine levels below detection range were not shown in the figure. Plasma LRG1 is positively correlated with levels of plasma creatinine levels. **(F)** The protein levels of ICA in plasma. **(G,H)** mRNA levels of *ICA* and *CA2* in kidney tissue. Data are presented as mean ± SEM. The Western blot results were quantified by Image J software (43). The target protein LRG1 level was analyzed by relative quantification and presented as a fold change to the loading control GAPDH. *q or $p < 0.05$; **q or $p < 0.01$, and ***q or $p < 0.001$. CA2, LRG1, and ICA, carbonic anhydrase 2, leucine-rich alpha-2-glycoprotein, and inhibitor of carbonic anhydrase.

findings suggest an IA LPS-induced imbalance in renal ICA and CA activity, potentially contributing to kidney inflammation.

Intra-amniotic LPS also altered clinical and biochemical parameters and other kidney injury markers both at birth and postnatal day 5. Relative kidney weight showed no difference at birth but decreased in LPS vs. CON pigs at postnatal day 5 ($p < 0.05$, **Figure 3A**). Plasma creatinine was elevated by LPS exposure only at birth ($p < 0.05$) but not on day 5 (**Figure 3B**). Both the microalbumin levels and the ratio of microalbumin over creatinine in urine were higher on day 5 in LPS vs. CON pigs ($p < 0.05$, **Figures 3C,D**). The renal pathological score and glomerular sizes were unavailable due to a lack of high-quality formalin fixation tissue in the current study. Other markers of kidney injury (48, 49) (kidney injury molecule-1, *KIM-1*, and neutrophil gelatinase-associated lipocalin, *NGLA*), hypoxia, and apoptosis (*HIF1A* and *CASP3*) were also evaluated

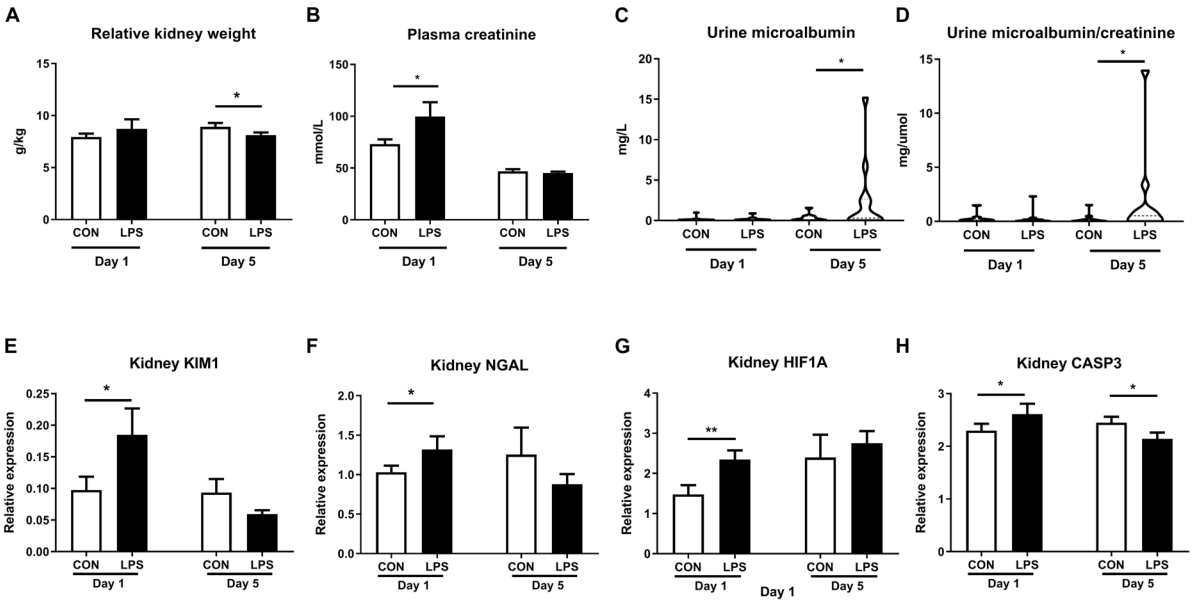

FIGURE 3 | Effects of IA LPS on biochemical parameters and renal injury, hypoxia, and apoptosis markers. **(A)** Relative kidney weight, **(B)** Plasma creatinine, **(C)** Urinary microalbumin, **(D)** Urinary microalbumin/creatinine. **(E,F)** Renal expressions of two biomarkers for acute kidney injury *KIM1* and *NGLA*. **(G,H)** Renal expressions of hypoxia and apoptosis markers *HIF1A* and *CASP3*. Data are presented as mean ± SEM. *$p < 0.05$ and **$p < 0.01$. Serum samples: Day 1: $n = 8$ in control and 10 in LPS, Day 5: $n = 13$ in control and 15 in LPS; Urine samples: Day 1: $n = 11$, Day 5: $n = 10$ in control and 12 in LPS. KIM1, NGLA, HIF1A, and CASP3: kidney injury molecule-1, neutrophil gelatinase-associated lipocalin, hypoxia-inducible factor 1- alpha, and caspase 3.

with consistently higher levels in LPS vs. CON pigs at birth ($p < 0.05$, **Figures 3E–H**). These biochemical and qPCR data further confirmed renal inflammation in LPS pigs at birth, while differences in kidney weight and urine microalbumin potentially indicate renal IA LPS effects persisting until postnatal day 5.

IA LPS Stimulates Renal Innate Immune Activation

Next, we sought to examine innate immune responses in kidney tissues modulated by IA LPS. The area of infiltrated MPO^+ cells (a marker of macrophages and/or neutrophils) was highly elevated both at birth and postnatal day 5 in LPS vs. CON pigs ($p < 0.001$ and 0.01, respectively, **Figures 4A,B**). The same trend was observed for the expression levels of *TLR2* and *TLR4* (all $p < 0.05$ except 0.07 for *TLR2* on day 5, **Figures 4C,D**). mRNA levels of the neutrophil and/or macrophage components *LTF* (product of the secondary granules of neutrophils), *S100A9* (an inflammation marker released by neutrophils and macrophages), and *LYZ* (a marker presented in all three types of human neutrophil granules) were also higher in LPS vs. CON pigs at birth (all $p < 0.05$, **Figures 4E–G**). These data indicate that IA LPS stimulated innate inflammatory responses in kidney tissues both at birth and postnatal day 5 via infiltration of neutrophils and/or macrophages.

IA LPS Activates the Fetal and Postnatal Renal Complement System

As IA LPS-induced kidney effects were strongly associated with innate immune activation, we next assessed the status of the renal complement system, a crucial component of the innate immunity. Plasma proteomics data at birth revealed increased levels of C3, C4, and CFB in LPS vs. CON pigs (all $q < 0.01$, **Figures 5A–C**). In kidney tissues, the mRNA levels of *C3* were elevated in LPS vs. CON pigs on day 5 ($p < 0.01$, **Figure 5D**). To verify the actions of the complement system, the final complement product, membrane attacking complex (MAC) C5b-C9 was determined with higher levels in both plasma and kidneys at birth and also higher levels in the kidneys at postnatal day 5 in LPS vs. CON pigs (all $p < 0.05$, **Figures 5E,F**).

IA LPS Alters the Renal ACE System and Increases Renal Oxidative Stress

As plasma proteomics revealed lower levels of ACEs in LPS vs. CON pigs at birth ($q < 0.1$, **Figure 6A**), we also sought to determine IA LPS effects on status of the renal ACE system and its role in the production of oxidative stress. ACEs are key components in the renin-angiotensin system (RAS) that modulates blood pressure, reactive oxygen species (ROS), and renal status (50). Especially, angiotensin II is damaging to renal tubules via ROS generation and inflammation and may contribute to glomerular injury and proteinuria (51, 52), while ACE2 functions to degrade angiotensin II, thereby decreasing ROS generation (50). Our data showed no IA LPS effects on *ACE* levels but *ACE2* levels were lower in the kidneys of LPS vs. CON pigs, both at birth and postnatal day 5 ($p < 0.05$, **Figures 6B,C**). LPS pigs at birth also showed increased oxidative stress with decreased renal levels of SOD activity and increased renal levels of MDA, relative to CON pigs ($p < 0.01$ and 0.05, **Figures 6D,E**).

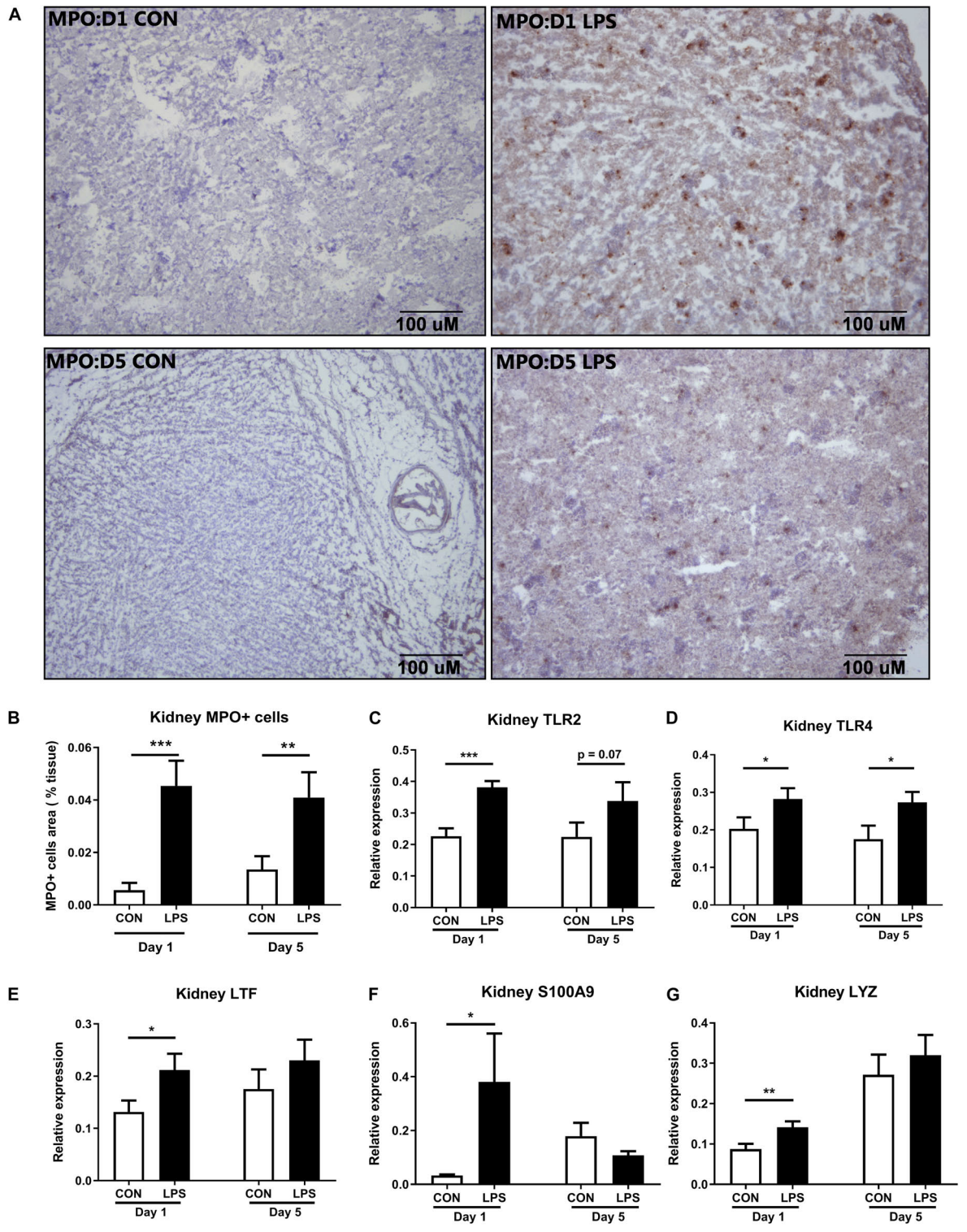

FIGURE 4 | Kidney innate immune response at birth and postnatal day 5 following IA LPS exposure. **(A,B)** MPO^+ stained cells (brown) in the frozen kidney, **(C–G)** mRNA levels of toll-like receptors (*TLR2* and *TLR4*) and neutrophil/macrophage components (*LTF*, *S100A9,* and *LYZ*) in kidney tissues. Data are presented as mean ± SEM. $^*p < 0.05$ and $^{**}p < 0.01$. Day 1: both $n = 9$, Day 5: $n = 8$ in control and 9 in LPS. The scale bars in **(A)** represent 100 μm. LTF, lactoferrin; TLR, toll-like receptor; and LYZ, lysozyme.

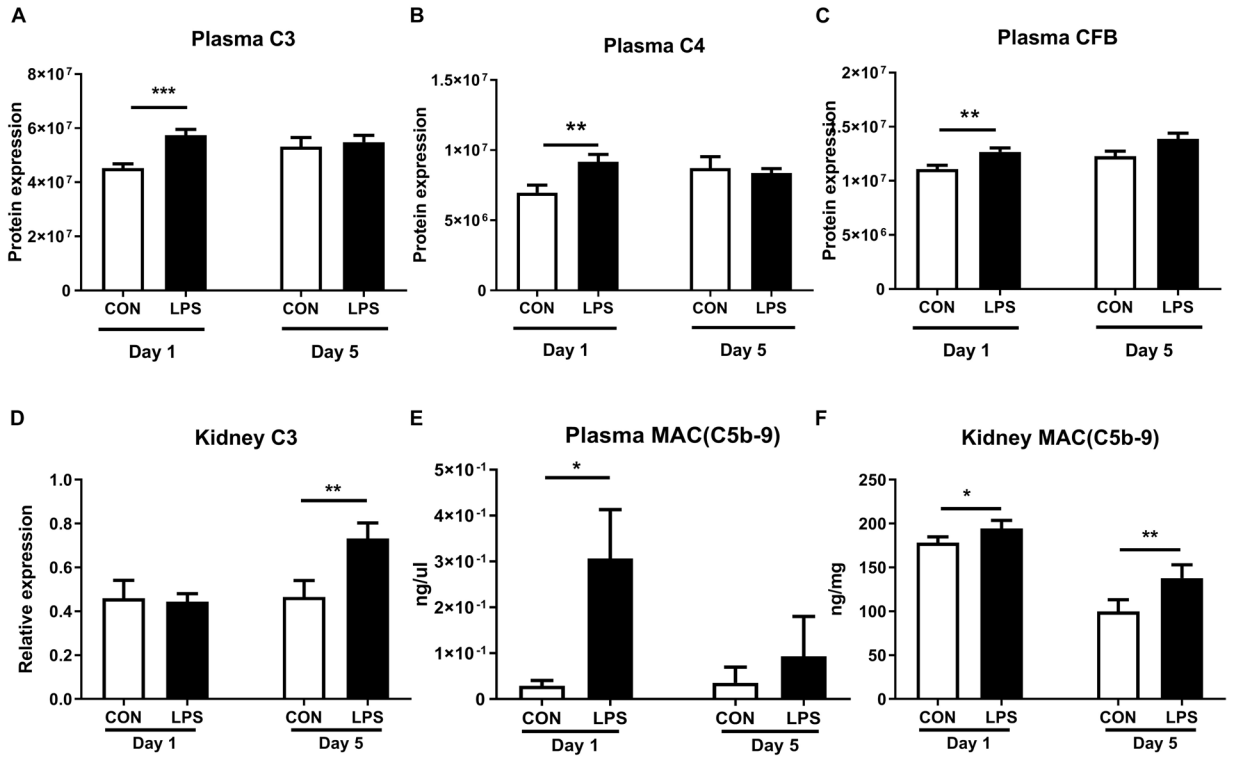

FIGURE 5 | Kidney complement activation induced by IA LPS. **(A–D)** Protein levels of C3, C4, CFB in plasma, and mRNA levels of *C3* in kidneys. **(E,F)** Membrane attacking complex (MAC and C5b-9) in plasma and kidneys. Data are presented as mean ± SEM. **q* or $p < 0.05$; ***q* or $p < 0.01$, and ****q* or $p < 0.001$.

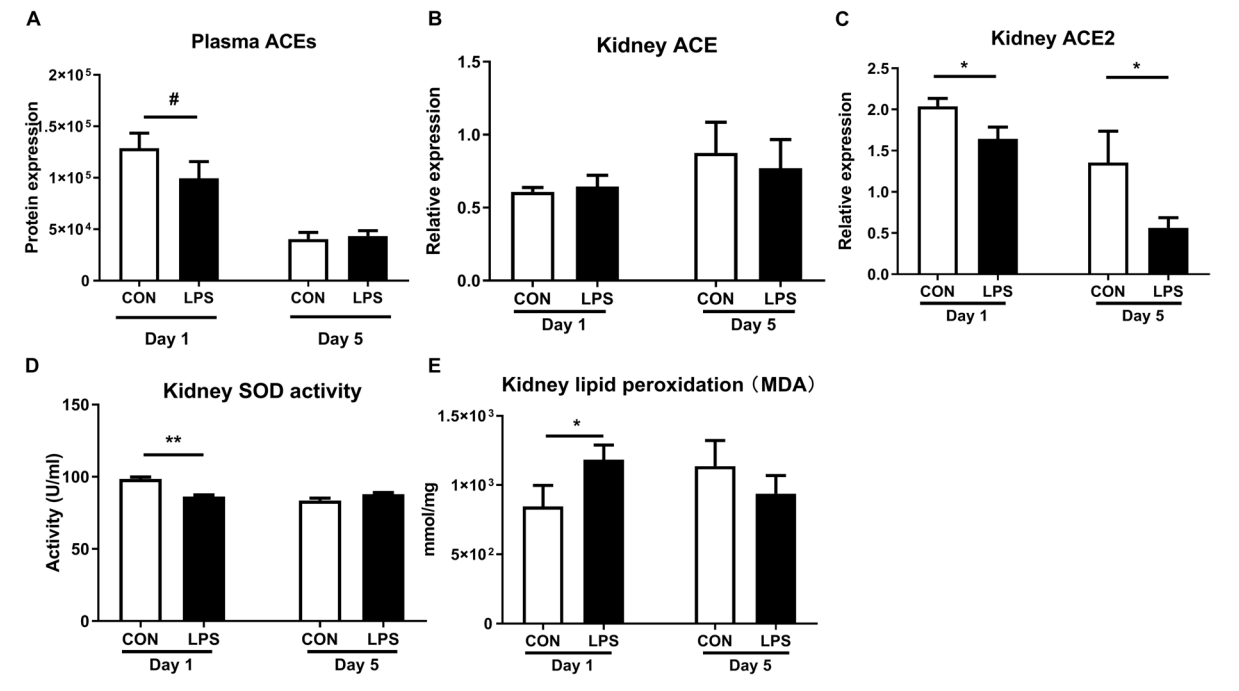

FIGURE 6 | Effects of IA LPS on the renal renin-angiotensin system and generation of reactive oxygen species. **(A)** Protein levels of ACEs in plasma. **(B,C)** mRNA levels of *ACE* and *ACE2* in kidney tissues. **(D)** SOD activity in kidney tissue. **(E)** Lipid peroxidation (malondialdehyde, MDA) level in kidney tissue. Data are presented as mean ± SEM. **q* or $p < 0.05$ and ***q* or $p < 0.01$. ACE, angiotensin-converting enzyme; SOD, superoxide dismutase.

These data suggest that IA LPS elevated ROS activity in kidney tissues with potential involvement of the renal ACE system.

IA LPS Stimulates Renal Adaptive Immune Activation

Likewise, the renal adaptive immune responses were also modulated by IA LPS exposure. The density of renal $CD3^+$ cells (T cells) was significantly up-regulated in LPS pigs both at birth and postnatal day 5 ($P < 0.01$ and 0.001, **Figure 7A**). At birth, the kidneys of LPS pigs showed increased Th1 responses, with higher mRNA levels of Th1-polarizing cytokines, ratio of Th1/Th2 cytokines (*IFNG*, ratio of *IFNG*/*IL4*), Th1 transcription factor (*TBET*), and ratio of Th1/Th2 transcription factors (*TBET/GATA3*), as well as decreased mRNA levels of Th2 transcription factor (*GATA3*, all $p < 0.05$, **Figures 7B–G**). At postnatal day 5, LPS pigs had lower renal mRNA levels of Th2-polarizing cytokines (*IL4, IL10*) and marker of regulatory T cells (*FOXP3* expression, all $p < 0.05$, **Figures 7C,H,I**). *IL17* expression was also reduced in LPS vs. CON pigs on day 5 ($p < 0.05$, **Figure 7J**). These data indicate increased fetal and postnatal renal inflammation in LPS vs. CON pigs with the activation of both innate and Th1-mediated immunity. In contrast to the systemic acute phase response (as assessed by plasma proteomics and liver gene expression above), the renal effects of IA LPS exposure persisted in the postnatal period, at least until day 5.

DISCUSSION

Preterm infants born with CA are often at increased risk of developing neonatal morbidities and organ injuries, including renal inflammation and AKI (21% of hospitalized neonates) (53). Due to the disruption of natural fetal nephrogenesis at a crucial developmental time point, the kidney size and nephron number are reduced in surviving premature infants (54). Fetal insults, including CA that is often accompanied with preterm birth, elicit inflammation in multiple organs and may further worsen the renal outcomes. Early management of kidney inflammation may ameliorate growth failure and suboptimal neurodevelopmental outcomes for preterm infants (55, 56), but reliable diagnostic markers for neonatal kidney diseases are lacking, and underlying mechanisms of the diseases are poorly understood. In the current study with preterm pigs, we demonstrated for the first time that CA, induced by IA LPS exposure, resulted in renal inflammation both at birth and 5 days after preterm birth with the involvement of innate and adaptive immune activation. Our data imply that prenatal insults may play a critical role in determining neonatal kidney outcomes and may explain the high incidence of AKI in preterm infants (46, 57–60), although reduced gestational age at birth is also a risk factor (61).

First, we demonstrated that prenatal IA LPS induced CA-like responses in the fetal membranes, marked systemic immune responses at birth, and altered plasma levels of markers related to kidney injuries, including LRG1, ACE, and ICA. Via evaluation of biochemical parameters, together with analyses of endpoints related to inflammatory pathways in kidney tissues, we showed that IA LPS exposure resulted in renal inflammation not only at birth but also in the neonatal period after preterm birth. Considering that IA LPS-induced lung and gut inflammation mainly occurs at birth (35), our data indicate that the preterm kidneys are relatively sensitive to prenatal endotoxin exposure. This is noteworthy also from the perspective that mucosal surfaces in the gut, lungs, and skin have more direct contact with endotoxin and inflammatory molecules in the amniotic sac following IA LPS or IA inflammation. Conversely, IA inflammation may affect systemic organs, such as kidneys, more gradually and for a longer time, following the translocation of inflammatory signals across the immature gut, lung, and skin barriers. Based on our results, **Figure 8** was suggested to illustrate possible mechanisms whereby prenatal insults may lead to fetal and neonatal kidney inflammation in preterm neonates.

At birth, IA LPS-exposed preterm pigs had elevated levels of plasma creatinine, a commonly used diagnostic marker for AKI (62) and also increased renal transcription levels of two well-known kidney injury markers (*KIM1* and *NGAL*) (63–65). The renal injury in these pigs seemed to persist to postnatal day 5 when urinary levels of microalbumin and the ratio of microalbumin/creatinine were elevated, together with decreased relative kidney weight. The mechanisms may include strong infiltrations of macrophages and/or neutrophils (MPO^+ cells) with elevated expression levels of *TRL2* and *TRL4* in kidney tissues both at birth and postnatal day 5. This was further supported by elevated expression levels of the neutrophil and/or macrophage components *LTF*, *S100A9* and *LYZ* in LPS pigs at birth. As prenatal inflammation is often associated with hypoxia-ischemia (HI) and apoptosis in internal organs (66), we also validated the corresponding markers and found elevated expressions of *HIF1A* and *CASP3* in the kidneys of LPS vs. CON pigs at birth.

Mucosal surfaces, like skin, gut, and lungs, may adapt more rapidly to fetal endotoxin exposure than the kidneys, consistent with the need of epithelia to tolerate the abrupt changes from a relatively sterile *in utero* environment to a microbes-rich environment *ex utero*. In the kidneys, an IA LPS-induced innate inflammatory response via neutrophil/macrophage activation was further potentiated by Th1 adaptive immune responses, i.e., dramatically elevated levels of infiltrated $CD3^+$ T cells, expression of *IFNG* (Th1 cytokine), *TBET* (Th1 transcription factor), and ratios of *IFNG/IL4* and *TBET/GATA3*, together with decreased expression levels of *GATA3* (Th2 transcription factor) at birth. Although these Th1 markers were not different between LPS and CON pigs on day 5, LPS pigs showed lower expression levels of anti-inflammatory genes, including *IL4, IL10* (Th2 cytokines), and *FOXP3* (regulatory T cell transcription factor). Likewise, the reduced *FOXP3* and *IL10* levels further demonstrate reduced regulatory T cell population in postnatal day 5. Thus, the adaptive immune responses may also last at least until day 5, probably via the action of other Th1 cytokines or Th1-enhanced activities of neutrophils/macrophages.

On the other hand, RAS, regulated by ACE molecules, may also be involved in IA LPS-induced renal inflammation as plasma ACEs were down-regulated at birth in LPS pigs and the renal mRNA level of *ACE2* was down-regulated at both time points.

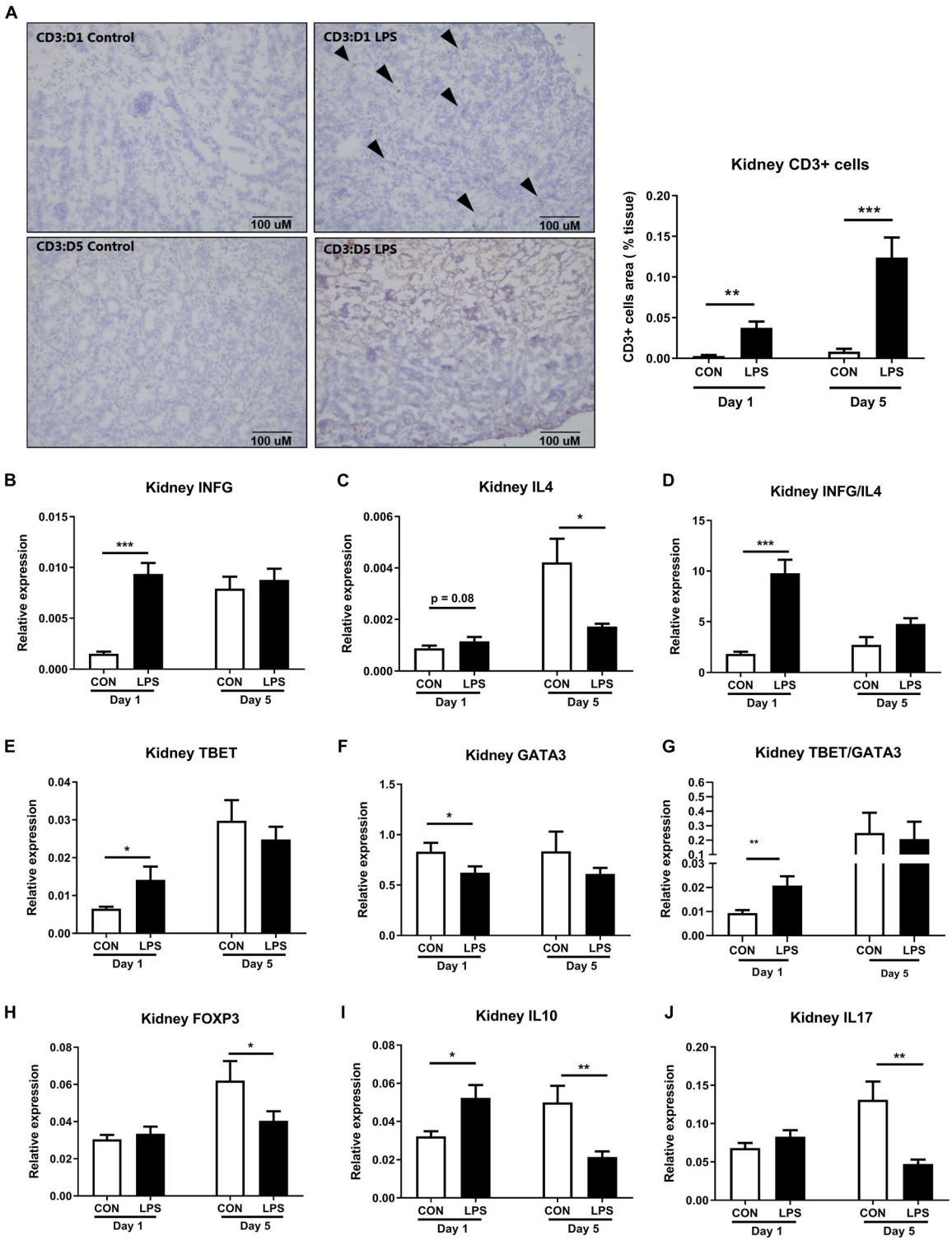

FIGURE 7 | Kidney adaptive immune responses both at birth and postnatal day 5 following IA LPS exposure. **(A)** The density of renal $CD3^+$ cells (T cells). **(B–J)** mRNA levels of Th1-polarizing cytokine *IFNG*, Th2-polarizing cytokines *IL4* and *IL10*, the ratio of Th1/Th2 cytokines *IFNG/IL4*, Th1 transcription factor *TBET*, Th2 transcription factor *GATA3*, the ratio of Th1/Th2 transcription factors *TBET/GATA3*, markers of Treg *FOXP3*, and marker of Th17 *IL17*. Data are presented as mean ± SEM. $^*p < 0.05$; $^{**}p < 0.01$, and $^{***}p < 0.001$. The scale bars in **(A)** represent 100 μm.

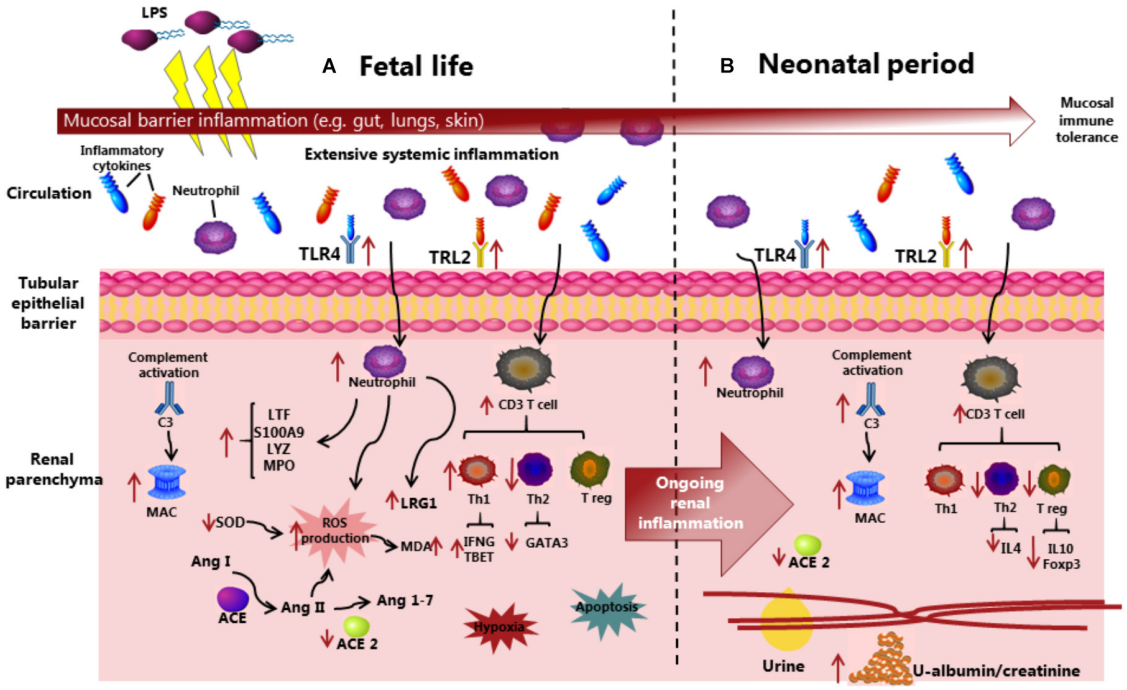

FIGURE 8 | Overview of the suggested mechanisms that IA LPS induces fetal and neonatal acute kidney injury before and after preterm birth. Compared with control pigs, LPS preterm pigs showed compromised kidney function, increased immune cell infiltration with complement system activation and production of reactive oxygen species, and increased level of hypoxia and apoptosis in the kidneys. The inflammatory state in kidney tissues is persistent from fetal to neonatal periods, in contrast with the acute mucosal inflammatory response in the gut and lungs being attenuated at postnatal day 5. ACE, Angiotensin-converting enzyme; Ang, Angiotensin; C3, Complement protein 3; LPS, Lipopolysaccharides; LRG1, Leucine-rich alpha-2-glycoprotein 1; MAC, Membrane attack complex; MDA, Malondialdehyde; MPO, Myeloperoxidase; ROS, Reactive oxygen species; SOD, Superoxidase dismutase; Th, T helper cell; Treg, Regulatory T cell; and TLR, Toll-like receptor.

The balance between ACE and ACE2 controls the production of angiotensin II (ANG II) and angiotensin-(1–7) (ANG-(1–7) (67). Decreased ACE2 level has been reported to cause ANG II accumulation, thereby enhancing ROS and oxidative damage. Consistent with this, we showed IA LPS-induced reduction of SOD enzyme activity (enzyme neutralizing ROS), as well as increased levels of malondialdehyde [MDA, a marker of lipid peroxidation leading to tissue damage (68)] in the kidneys. In LPS pigs, the neutrophil/macrophage and complement activation in kidney tissues may generate vast amounts of ROS while the renal ACE and anti-oxidative systems could be less efficient, potentially leading to increased ROS-induced tissue damage.

The current study results also suggested plasma markers and therapeutic targets of prenatal inflammation and related organ responses including renal inflammation, namely, LRG1 and ICA (increased and decreased by IA LPS, respectively). LRG1 is a neutrophil component and has been reported to play a crucial role in immune responses, cell proliferation and apoptosis, neovascularization, and hypoxia (69–73). LRG1 has been shown to be elevated in the urine of patients with IgA nephropathy and chronic kidney disease (74, 75). In our study, both mRNA and protein levels of LRG1 were increased in the kidneys of LPS pigs at birth and correlated with plasma creatinine, a classical marker of AKI. LRG1 may also play a crucial role in the progression of hypoxia by regulating HIF1A expression (76). As *HIF1A* was also up-regulated by IA LPS in the current study, we speculate that LRG1-mediated hypoxia via HIF-1α activation also contributes to kidney injury and that LRG1 may be a promising diagnostic and therapeutic target of prenatal inflammation and organ responses including neonatal renal inflammation. On the other hand, the ICA is a CA inhibiting protein and pH (acid-base balance) regulating enzyme in multiple cells and tissues (77–79), although in humans it may only be a pseudogene (80). Instead, we found elevated expression of renal carbonic anhydrase II (*CA2*) in LPS pigs at birth and speculated that the imbalance between ICA and CA2 may enhance bicarbonate generation and low tissue pH, contributing to inflammation-related kidney dysfunction.

The nephrogenesis in pig occurs during both intrauterine and extrauterine periods, from day 29 of postconceptional age to postnatal day 21 (81), whereas the nephrogenesis in human completes before gestational week 36. No new nephrons are formed after gestational week 36 over the lifetime in humans (82). We speculate that some postnatal parameters related to inflammation and oxidative stress that were reduced over time may be due to the ongoing extrauterine nephrogenesis in pigs or partly resolved inflammation following fetal acute responses.

In conclusion, prenatal IA LPS exposure induced clear signs of fetal and neonatal kidney inflammation in preterm pigs. In contrast to conditions in the lungs, gut, and liver, the kidney inflammatory effects persisted into the postnatal period,

possibly driven by sustained activation of both innate and adaptive immune cells. Plasma LRG1 may be a new promising diagnostic and therapeutic target for prenatal inflammation and organ responses including neonatal renal inflammation. Preterm infants born after CA may suffer from dysfunctions of multiple organs, including kidneys, that require special care and treatments to prevent further short- and long-term complications.

DATA AVAILABILITY STATEMENT

The datasets presented in this study can be found in online repositories. The names of the repository/repositories and accession number(s) can be found in the article/**Supplementary Material**. The mass spectrometry proteomics data have been deposited to the ProteomeXchange Consortium via the PRIDE (83) partner repository with the dataset identifier PXD016013.

ETHICS STATEMENT

The animal study was reviewed and approved by The Danish National Committee of Animal Experimentation.

AUTHOR CONTRIBUTIONS

TM conceived the study, analyzed the proteomic data, performed tissue analyses, and prepared the manuscript. P-PJ conceived the study, analyzed and interpreted the data, and prepared the manuscript. AS performed the proteomics analysis and protein annotation. PTS conceived the study, interpreted the data, and prepared the manuscript. KS performed the liver gene expression experiment and data analysis. DNN conceived the study, performed the animal experiment, interpreted the data, and prepared the manuscript. All authors drafted the work, revised it critically for important intellectual content, and approved the final version.

FUNDING

This study was supported by the Center of Arla Food for Health (STIMMUNE project, PTS, and DNN) and a scholarship from the Oversea Study Program of Guangzhou Elite Project (TM). The Danish National Mass Spectrometry Platform for Functional Proteomics (PRO-MS; grant no. 5072-00007B); the Obel Family Foundation, and the Svend Andersen Foundation are acknowledged for the funding of infrastructure enabling parts of this study.

ACKNOWLEDGMENTS

We thank Thomas Thymann, Karina Obelizt-Ryom, Jane Poulvsen, and Elin Skytte for assistance in animal experiments.

SUPPLEMENTARY MATERIAL

The Supplementary Material for this article can be found online at: https://www.frontiersin.org/articles/10.3389/fimmu.2020.565484/full#supplementary-material

Supplementary Figure 1 | Correlations between plasma LGR1 levels and biochemical parameters.

Supplementary Table 1 | Amniotic fluid cytokines and infiltrated inflammatory cells in the chorioamnion.

Supplementary Table 2 | Differentially regulated proteins in plasma between LPS and CON pigs at birth (day 1).

Supplementary Table 3 | Differentially regulated proteins in plasma between LPS and CON pigs at postnatal day 5.

Supplementary Table 4 | Primer sequence of selected genes analyzed in kidney tissues.

Supplementary Table 5 | Primer sequences for liver gene analysis.

Supplementary Table 6 | Liver gene expressions.

REFERENCES

1. Strunk T, Inder T, Wang X, Burgner D, Mallard C, Levy O. Infection-induced inflammation and cerebral injury in preterm infants. *Lancet Infect Dis*. (2014) 14:751–62.doi: 10.1016/s1473-3099(14)70710-8
2. Majed B, Bateman DA, Uy N, Lin F. Patent ductus arteriosus is associated with acute kidney injury in the preterm infant. *Pediatr Nephrol*. (2019) 34:1129–39.doi: 10.1007/s00467-019-4194-5
3. Tita AT, Andrews WW. Diagnosis and management of clinical chorioamnionitis. *Clin Perinatol*. (2010) 37:339–54.doi: 10.1016/j.clp.2010.02.003
4. Goldenberg RL, Hauth JC, Andrews WW. Intrauterine infection and preterm delivery. *N Engl J Med*. (2000) 342:1500–7.doi: 10.1056/nejm200005183422007
5. Kim CJ, Romero R, Chaemsaithong P, Chaiyasit N, Yoon BH, Kim YM. Acute chorioamnionitis and funisitis: definition, pathologic features, and clinical significance. *Am J Obstetr Gynecol*. (2015) 213 (4 Suppl.):S29–52.doi: 10.1016/j.ajog.2015.08.040
6. Park HW, Choi YS, Kim KS, Kim SN. Chorioamnionitis and patent ductus arteriosus: a systematic review and meta-analysis. *PLoS One*. (2015) 10:e0138114.doi: 10.1371/journal.pone.0138114
7. Rueda CM, Presicce P, Jackson CM, Miller LA, Kallapur SG, Jobe AH, et al. Lipopolysaccharide-induced chorioamnionitis promotes IL-1-dependent inflammatory FOXP3+ CD4+ T cells in the fetal rhesus macaque. *J Immunol*. (2016) 196:3706–15.doi: 10.4049/jimmunol.1502613
8. Schmidt AF, Kannan PS, Chougnet CA, Danzer SC, Miller LA, Jobe AH, et al. Intra-amniotic LPS causes acute neuroinflammation in preterm rhesus macaques. *J Neuroinflamm*. (2016) 13:238.doi: 10.1186/s12974-016-0706-4
9. Agrawal V, Jaiswal MK, Mallers T, Katara GK, Gilman-Sachs A, Beaman KD, et al. Altered autophagic flux enhances inflammatory responses during inflammation-induced preterm labor. *Sci Rep*. (2015) 5:9410.doi: 10.1038/srep09410
10. Martinez-Lopez DG, Funderburg NT, Cerissi A, Rifaie R, Aviles-Medina L, Llorens-Bonilla BJ, et al. Lipopolysaccharide and soluble CD14 in cord blood plasma are associated with prematurity and chorioamnionitis. *Pediatr Res*. (2013) 75:67.doi: 10.1038/pr.2013.182

11. Kemp MW, Kannan PS, Saito M, Newnham JP, Cox T, Jobe AH, et al. Selective exposure of the fetal lung and skin/amnion (but not gastro-intestinal tract) to LPS elicits acute systemic inflammation in fetal sheep. *PLoS One*. (2013) 8:e63355.doi: 10.1371/journal.pone.0063355
12. Wolfs TG, Kramer BW, Thuijls G, Kemp MW, Saito M, Willems MG, et al. Chorioamnionitis-induced fetal gut injury is mediated by direct gut exposure of inflammatory mediators or by lung inflammation. *Am J Physiol Gastrointest Liver Physiol*. (2014) 306:G382–93.doi: 10.1152/ajpgi.00260.2013
13. Trebichavsky I, Splichal I, Zahradnickova M, Splichalova A, Mori Y. Lipopolysaccharide induces inflammatory cytokines in the pig amnion. *Vet Immunol Immunopathol*. (2002) 87:11–8.
14. Splichal I, Trebichavsky I, Splichalova A, Ditetova L, Zahradnickova M. *Escherichia coli* administered into pig amniotic cavity appear in fetal airways and attract macrophages into fetal lungs. *Physiol Res*. (2002) 51:523–8.
15. Wolfs TG, Kallapur SG, Knox CL, Thuijls G, Nitsos I, Polglase GR, et al. Antenatal ureaplasma infection impairs development of the fetal ovine gut in an IL-1-dependent manner. *Mucosal Immunol*. (2013) 6:547–56.doi: 10.1038/mi.2012.97
16. Nikiforou M, Kemp MW, van Gorp RH, Saito M, Newnham JP, Reynaert NL, et al. Selective IL-1alpha exposure to the fetal gut, lung, and chorioamnion/skin causes intestinal inflammatory and developmental changes in fetal sheep. *Lab Invest*. (2016) 96:69–80.doi: 10.1038/labinvest.2015.127
17. Nikiforou M, Vanderlocht J, Chougnet CA, Jellema RK, Ophelders DR, Joosten M, et al. Prophylactic interleukin-2 treatment prevents fetal gut inflammation and injury in an ovine model of chorioamnionitis. *Inflamm Bowel Dis*. (2015) 21:2026–38.doi: 10.1097/mib.0000000000000455
18. Nikiforou M, Jacobs EM, Kemp MW, Hornef MW, Payne MS, Saito M, et al. Intra-amniotic *Candida albicans* infection induces mucosal injury and inflammation in the ovine fetal intestine. *Sci Rep*. (2016) 6:29806.doi: 10.1038/srep29806
19. Wolfs TG, Buurman WA, Zoer B, Moonen RM, Derikx JP, Thuijls G, et al. Endotoxin induced chorioamnionitis prevents intestinal development during gestation in fetal sheep. *PLoS One*. (2009) 4:e5837.doi: 10.1371/journal.pone.0005837
20. Strackx E, Sparnaaij MA, Vlassaks E, Jellema R, Kuypers E, Vles JS, et al. Lipopolysaccharide-induced chorioamnionitis causes acute inflammatory changes in the ovine central nervous system. *CNS Neurol Disord Drug Targets*. (2015) 14:77–84.
21. Gussenhoven R, Westerlaken RJJ, Ophelders D, Jobe AH, Kemp MW, Kallapur SG, et al. Chorioamnionitis, neuroinflammation, and injury: timing is key in the preterm ovine fetus. *J Neuroinflamm*. (2018) 15:113.doi: 10.1186/s12974-018-1149-x
22. Nada A, Bonachea EM, Askenazi DJ. Acute kidney injury in the fetus and neonate. *Semin Fetal Neonatal Med*. (2017) 22:90–7.doi: 10.1016/j.siny.2016.12.001
23. Gubhaju L, Sutherland MR, Yoder BA, Zulli A, Bertram JF, Black MJ. Is nephrogenesis affected by preterm birth? Studies in a non-human primate model. *Am J Physiol Renal Physiol*. (2009) 297:F1668–77.doi: 10.1152/ajprenal.00163.2009
24. Rodriguez MM, Gomez AH, Abitbol CL, Chandar JJ, Duara S, Zilleruelo GE. Histomorphometric analysis of postnatal glomerulogenesis in extremely preterm infants. *Pediatr Dev Pathol*. (2004) 7:17–25.doi: 10.1007/s10024-003-3029-2
25. Koralkar R, Ambalavanan N, Levitan EB, McGwin G, Goldstein S, Askenazi D. Acute kidney injury reduces survival in very low birth weight infants. *Pediatr Res*. (2011) 69:354–8.doi: 10.1203/PDR.0b013e31820b95ca
26. Cataldi L, Leone R, Moretti U, De Mitri B, Fanos V, Ruggeri L, et al. Potential risk factors for the development of acute renal failure in preterm newborn infants: a case-control study. *Arch Dis Child Fetal Neonatal Ed*. (2005) 90:F514–9.doi: 10.1136/adc.2004.060434
27. Carmody JB, Swanson JR, Rhone ET, Charlton JR. Recognition and reporting of AKI in very low birth weight infants. *Clin J Am Soc Nephrol*. (2014) 9:2036–43.doi: 10.2215/cjn.05190514
28. Gadepalli SK, Selewski DT, Drongowski RA, Mychaliska GB. Acute kidney injury in congenital diaphragmatic hernia requiring extracorporeal life support: an insidious problem. *J Pediatr Surg*. (2011) 46:630–5.doi: 10.1016/j.jpedsurg.2010.11.031
29. Oh SL, Jeon TY, Yoo S-Y, In Sung S, Kim HW, Chang YS, et al. Outcome and risk factors associated with perirenal subcapsular fluid collections in extremely preterm infants with acute kidney injury. *Eur Radiol*. (2019) 29:3847–53.doi: 10.1007/s00330-018-5962-5
30. Askenazi DJ, Ambalavanan N, Goldstein SL. Acute kidney injury in critically ill newborns: what do we know? What do we need to learn? *Pediatr Nephrol*. (2009) 24:265–74.doi: 10.1007/s00467-008-1060-2
31. Itabashi K, Ohno T, Nishida H. Indomethacin responsiveness of patent ductus arteriosus and renal abnormalities in preterm infants treated with indomethacin. *J Pediatr*. (2003) 143:203–7.doi: 10.1067/s0022-3476(03)00303-2
32. Galinsky R, Polglase GR, Hooper SB, Black MJ, Moss TJ. The consequences of chorioamnionitis: preterm birth and effects on development. *J Pregnancy*. (2013) 2013:412831.doi: 10.1155/2013/412831
33. Galinsky R, Moss TJ, Gubhaju L, Hooper SB, Black MJ, Polglase GR. Effect of intra-amniotic lipopolysaccharide on nephron number in preterm fetal sheep. *Am J Physiol Renal Physiol*. (2011) 301:F280–5.doi: 10.1152/ajprenal.00066.2011
34. Brenner BM, Garcia DL, Anderson S. Glomeruli and blood pressure. Less of one, more the other? *Am J Hypertens*. (1988) 1(4 Pt 1):335–47.
35. Nguyen DN, Thymann T, Goericke-Pesch SK, Ren S, Wei W, Skovgaard K, et al. Prenatal intra-amniotic endotoxin induces fetal gut and lung immune responses and postnatal systemic inflammation in preterm pigs. *Am J Pathol*. (2018) 188:2629–43.doi: 10.1016/j.ajpath.2018.07.020
36. Sangild PT, Ney DM, Sigalet DL, Vegge A, Burrin D. Animal models of gastrointestinal and liver diseases. Animal models of infant short bowel syndrome: translational relevance and challenges. *Am J Physiol Gastrointest Liver Physiol*. (2014) 307:G1147–68.doi: 10.1152/ajpgi.00088.2014
37. Ewer AK, Al-Salti W, Coney AM, Marshall JM, Ramani P, Booth IW. The role of platelet activating factor in a neonatal piglet model of necrotising enterocolitis. *Gut*. (2004) 53:207–13.
38. Schook L, Beattie C, Beever J, Donovan S, Jamison R, Zuckermann F, et al. Swine in biomedical research: creating the building blocks of animal models. *Anim Biotechnol*. (2005) 16:183–90.
39. Dawson HD, Smith AD, Chen C, Urban JF Jr. An in-depth comparison of the porcine, murine and human inflammasomes; lessons from the porcine genome and transcriptome. *Vet Microbiol*. (2017) 202:2–15.doi: 10.1016/j.vetmic.2016.05.013
40. Berger ST, Ahmed S, Muntel J, Cuevas Polo N, Bachur R, Kentsis A, et al. MStern blotting-high throughput polyvinylidene fluoride (PVDF) membrane-based proteomic sample preparation for 96-well plates. *Mol Cell Proteomics*. (2015) 14:2814–23.doi: 10.1074/mcp.O115.049650
41. Khan NR, Khan AN, Bashir S, Khan AA, Suleman BA, Chaudhry S. Diagnostic utility of p63 (Ab-1) and (Ab-4) tumor markers in the squamous cell carcinomas of head and neck. *Asian Pac J Cancer Prev*. (2012) 13:975–8.doi: 10.7314/apjcp.2012.13.3.975
42. Wang S, Wang B, He H, Sun A, Guo C. A new set of reference housekeeping genes for the normalization RT-qPCR data from the intestine of piglets during weaning. *PLoS One*. (2018) 13:e0204583.doi: 10.1371/journal.pone.0204583
43. Rueden CT, Schindelin J, Hiner MC, DeZonia BE, Walter AE, Arena ET, et al. ImageJ2: imageJ for the next generation of scientific image data. *BMC Bioinformatics*. (2017) 18:529.doi: 10.1186/s12859-017-1934-z
44. Bates D, Maechler M, Bolker B, Walker S. Fitting linear mixed-effects models using lme4. *J Stat Softw*. (2015) 67:1–48.
45. Pollard KS, Gilbert HN, Ge Y, Taylor S, Dudoit S. *multtest: Resampling-Based Multiple Hypothesis Testing*. vol R package version 2.16.0. (2005).
46. Dobyan DC, Bulger RE. Renal carbonic anhydrase. *Am J Physiol*. (1982) 243:F311–24.doi: 10.1152/ajprenal.1982.243.4.F311
47. DuBose TD Jr. Carbonic anhydrase-dependent bicarbonate transport in the kidney. *Ann N Y Acad Sci*. (1984) 429:528–37.
48. Han WK, Bailly V, Abichandani R, Thadhani R, Bonventre JV. Kidney injury molecule-1 (KIM-1): a novel biomarker for human renal proximal tubule injury. *Kidney Int*. (2002) 62:237–44. doi: 10.1046/j.1523-1755.2002.00433.x
49. Mishra J, Dent C, Tarabishi R, Mitsnefes MM, Ma Q, Kelly C, et al. Neutrophil gelatinase-associated lipocalin (NGAL) as a biomarker for acute renal injury

after cardiac surgery. *Lancet*. (2005) 365:1231–8.doi: 10.1016/s0140-6736(05)74811-x
50. Danilczyk U, Penninger JM. Angiotensin-converting enzyme II in the heart and the kidney. *Circ Res*. (2006) 98:463–71.doi: 10.1161/01.RES.0000205761.22353.5f
51. Oudit GY, Herzenberg AM, Kassiri Z, Wong D, Reich H, Khokha R, et al. Loss of angiotensin-converting enzyme-2 leads to the late development of angiotensin II-dependent glomerulosclerosis. *Am J Pathol*. (2006) 168:1808–20.doi: 10.2353/ajpath.2006.051091
52. Peters H, Border WA, Noble NA. Angiotensin II blockade and low-protein diet produce additive therapeutic effects in experimental glomerulonephritis. *Kidney Int*. (2000) 57:1493–501.doi: 10.1046/j.1523-1755.2000.00994.x
53. Kallapur SG, Presicce P, Rueda CM, Jobe AH, Chougnet CA. Fetal immune response to chorioamnionitis. *Semin Reprod Med*. (2014) 32:56–67.doi: 10.1055/s-0033-1361823
54. Stritzke A, Thomas S, Amin H, Fusch C, Lodha A. Renal consequences of preterm birth. *Mol Cell Pediatr*. (2017) 4:2.doi: 10.1186/s40348-016-0068-0
55. Nagaraj N, Berwal PK, Srinivas A, Berwal A. A study of acute kidney injury in hospitalized preterm neonates in NICU. *J Neonatal Perinatal Med*. (2016) 9:417–21.doi: 10.3233/npm-161614
56. Daga A, Dapaah-Siakwan F, Rajbhandari S, Arevalo C, Salvador A. Diagnosis and risk factors of acute kidney injury in very low birth weight infants. *Pediatr Neonatol*. (2017) 58:258–63.doi: 10.1016/j.pedneo.2016.08.002
57. Lee CC, Chan OW, Lai MY, Hsu KH, Wu TW, Lim WH, et al. Incidence and outcomes of acute kidney injury in extremely-low-birth-weight infants. *PLoS One*. (2017) 12:e0187764.doi: 10.1371/journal.pone.0187764
58. Bonsante F, Ramful D, Binquet C, Samperiz S, Daniel S, Gouyon JB, et al. Low renal oxygen saturation at near-infrared spectroscopy on the first day of life is associated with developing acute kidney injury in very preterm infants. *Neonatology*. (2019) 115:198–204.doi: 10.1159/000494462
59. Elmas AT, Tabel Y, Ozdemir R. Risk factors and mortality rate in premature babies with acute kidney injury. *J Clin Lab Anal*. (2018) 32:e22441.doi: 10.1002/jcla.22441
60. Ladeiras R, Flor-de-Lima F, Soares H, Oliveira B, Guimaraes H. Acute kidney injury in preterm neonates with </= 30 weeks of gestational age and its risk factors. *Minerva Pediatr*. (2018) 71:404–14.doi: 10.23736/s0026-4946.18.04964-2
61. Mackenzie HS, Brenner BM. Fewer nephrons at birth: a missing link in the etiology of essential hypertension? *Am J Kidney Dis*. (1995) 26:91–8.
62. Khwaja A. KDIGO clinical practice guidelines for acute kidney injury. *Nephron Clin Pract*. (2012) 120:c179–84.doi: 10.1159/000339789
63. Breidthardt T, Christ-Crain M, Stolz D, Bingisser R, Drexler B, Klima T, et al. A combined cardiorenal assessment for the prediction of acute kidney injury in lower respiratory tract infections. *Am J Med*. (2012) 125:168–75.doi: 10.1016/j.amjmed.2011.07.010
64. Biezeveld MH, van Mierlo G, Lutter R, Kuipers IM, Dekker T, Hack CE, et al. Sustained activation of neutrophils in the course of Kawasaki disease: an association with matrix metalloproteinases. *Clin Exp Immunol*. (2005) 141:183–8.doi: 10.1111/j.1365-2249.2005.02829.x
65. Yin C, Wang N. Kidney injury molecule-1 in kidney disease. *Renal Fail*. (2016) 38:1567–73.doi: 10.1080/0886022x.2016.1193816
66. Glass HC, Bonifacio SL, Chau V, Glidden D, Poskitt K, Barkovich AJ, et al. Recurrent postnatal infections are associated with progressive white matter injury in premature infants. *Pediatrics*. (2008) 122:299–305.doi: 10.1542/peds.2007-2184
67. Chappel MC, Ferrario CM. ACE and ACE2: their role to balance the expression of angiotensin II and angiotensin-(1-7). *Kidney Int*. (2006) 70:8–10.doi: 10.1038/sj.ki.5000321
68. Nam TG. Lipid peroxidation and its toxicological implications. *Toxicol Res*. (2011) 27:1–6.doi: 10.5487/tr.2011.27.1.001
69. Serada S, Fujimoto M, Terabe F, Iijima H, Shinzaki S, Matsuzaki S, et al. Serum leucine-rich alpha-2 glycoprotein is a disease activity biomarker in ulcerative colitis. *Inflamm Bowel Dis*. (2012) 18:2169–79. doi: 10.1002/ibd.22936
70. Lynch J, Fay J, Meehan M, Bryan K, Watters KM, Murphy DM, et al. MiRNA-335 suppresses neuroblastoma cell invasiveness by direct targeting of multiple genes from the non-canonical TGF-beta signalling pathway. *Carcinogenesis*. (2012) 33:976–85.doi: 10.1093/carcin/bgs114
71. Zhong D, Zhao S, He G, Li J, Lang Y, Ye W, et al. Stable knockdown of LRG1 by RNA interference inhibits growth and promotes apoptosis of glioblastoma cells in vitro and in vivo. *Tumour Biol*. (2015) 36:4271–8.doi: 10.1007/s13277-015-3065-3
72. Furukawa K, Kawamoto K, Eguchi H, Tanemura M, Tanida T, Tomimaru Y, et al. Clinicopathological significance of leucine-rich alpha2-glycoprotein-1 in sera of patients with pancreatic cancer. *Pancreas*. (2015) 44:93–8.doi: 10.1097/mpa.0000000000000205
73. Zhang J, Zhu L, Fang J, Ge Z, Li X. LRG1 modulates epithelial-mesenchymal transition and angiogenesis in colorectal cancer via HIF-1alpha activation. *J Exp Clin Cancer Res*. (2016) 35:29.doi: 10.1186/s13046-016-0306-2
74. Lee H, Fujimoto M, Ohkawara T, Honda H, Serada S, Terada Y, et al. Leucine rich alpha-2 glycoprotein is a potential urinary biomarker for renal tubular injury. *Biochem Biophys Res Commun*. (2018) 498:1045–51.doi: 10.1016/j.bbrc.2018.03.111
75. Maixnerova D, Reily C, Bian Q, Neprasova M, Novak J, Tesar V. Markers for the progression of IgA nephropathy. *J Nephrol*. (2016) 29:535–41.doi: 10.1007/s40620-016-0299-0
76. Pagtalunan ME, Olson JL, Meyer TW. Contribution of angiotensin II to late renal injury after acute ischemia. *J Am Soc Nephrol*. (2000) 11:1278–86.
77. Supuran CT. Carbonic anhydrase inhibitors and their potential in a range of therapeutic areas. *Expert Opin Ther Pat*. (2018) 28:709–12.doi: 10.1080/13543776.2018.1523897
78. Gocer H, Topal F, Topal M, Kucuk M, Teke D, Gulcin I, et al. Acetylcholinesterase and carbonic anhydrase isoenzymes I and II inhibition profiles of taxifolin. *J Enzyme Inhib Med Chem*. (2016) 31:441–7.doi: 10.3109/14756366.2015.1036051
79. Kocyigit UM, Aslan ON, Gulcin I, Temel Y, Ceylan M. Synthesis and carbonic anhydrase inhibition of novel 2-(4-(Aryl)thiazole-2-yl)-3a,4,7,7a-tetrahydro-1H-4,7-methanoisoindole-1,3(2H)-di one Derivatives. *Arch Pharm*. (2016) 349:955–63.doi: 10.1002/ardp.201600092
80. Eckenroth BE, Mason AB, McDevitt ME, Lambert LA, Everse SJ. The structure and evolution of the murine inhibitor of carbonic anhydrase: a member of the transferrin superfamily. *Protein Sci*. (2010) 19:1616–26.doi: 10.1002/pro.439
81. Friis C. Postnatal development of the pig kidney: ultrastucure of the glomerulus and the proximal tubule. *J Anat*. (1980) 130(Pt 3):513–26.
82. Hinchliffe SA, Sargent PH, Howard CV, Chan YF, van Velzen D. Human intrauterine renal growth expressed in absolute number of glomeruli assessed by the disector method and Cavalieri principle. *Lab Invest*. (1991) 64:777–84.
83. Perez-Riverol Y, Csordas A, Bai J, Bernal-Llinares M, Hewapathirana S, Kundu DJ, et al. The PRIDE database and related tools and resources in 2019: improving support for quantification data. *Nucleic Acids Res*. (2019) 47:D442–50.doi: 10.1093/nar/gky1106
84. Warde-Farley D, Donaldson SL, Comes O, Zuberi K, Badrawi R, Chao P, et al. The GeneMANIA prediction server: biological network integration for gene prioritization and predicting gene function. *Nucleic Acids Res*. (2010) 38:W214–20.doi: 10.1093/nar/gkq537

Conflict of Interest: The authors declare that the research was conducted in the absence of any commercial or financial relationships that could be construed as a potential conflict of interest.

frontiers in Immunology

ORIGINAL RESEARCH
published: 08 October 2020
doi: 10.3389/fimmu.2020.565862

Early Protein Markers of Necrotizing Enterocolitis in Plasma of Preterm Pigs Exposed to Antibiotics

Yan-Nan Jiang[1†], Tik Muk[2†], Allan Stensballe[3], Duc Ninh Nguyen[2], Per Torp Sangild[2,4] and Ping-Ping Jiang[1,2]*

[1] School of Public Health, Sun Yat-sen University, Guangzhou, China, [2] Department of Veterinary and Animal Sciences, Section for Comparative Paediatrics and Nutrition, University of Copenhagen, Frederiksberg, Denmark, [3] Department of Health Science and Technology, Aalborg University, Aalborg, Denmark, [4] Department of Neonatology, Rigshospitalet, Copenhagen, Denmark

OPEN ACCESS

Edited by:
Anastasia N. Vlasova, The Ohio State University, United States

Reviewed by:
Janet Elizabeth Berrington, Newcastle upon Tyne Hospitals NHS Foundation Trust, United Kingdom
Husheem Michael, The Ohio State University, United States

***Correspondence:**
Ping-Ping Jiang
jiangpp3@mail.sysu.edu.cn

[†] *These authors share first authorship*

Specialty section:
This article was submitted to Comparative Immunology, a section of the journal Frontiers in Immunology

Received: *26 May 2020*
Accepted: *25 August 2020*
Published: *08 October 2020*

Citation:
Jiang Y-N, Muk T, Stensballe A, Nguyen DN, Sangild PT and Jiang P-P (2020) Early Protein Markers of Necrotizing Enterocolitis in Plasma of Preterm Pigs Exposed to Antibiotics. Front. Immunol. 11:565862. doi: 10.3389/fimmu.2020.565862

Background: Most hospitalized preterm infants receive antibiotics in the first days of life to prevent or treat infections. Short-term, early antibiotic treatment may also prevent the microbiota-dependent gut inflammatory disorder, necrotizing enterocolitis (NEC). It remains a challenge to predict NEC, and a few early blood diagnostic markers exist. Using preterm pigs as model for infants, blood parameters and plasma proteins affected by early progression of NEC were profiled in preterm pigs subjected to oral, systemic, or no antibiotics after preterm birth.

Methods: Preterm newborn pigs were treated with saline (CON) or antibiotics (ampicillin, gentamicin, and metronidazole) given enterally (ENT) or parenterally (PAR), and fed formula for 4 days to induce variable microbiome-dependent sensitivities to NEC. The gut was collected for macroscopic scoring of NEC lesions and blood for hematology, blood biochemistry, and LC/MS-based plasma proteomics. Statistical modeling was applied to detect plasma proteins affected by NEC and/or antibiotics.

Results: Analyzed across different antibiotic regimens, NEC progression was associated with altered blood parameters and abundance of 89 plasma proteins that were functionally involved in extracellular membrane destruction, lipid metabolism, coagulopathy, and acute phase response. Large NEC-related changes were observed in abundance of RBP4, FGA, AHSG, C5, PTPRG, and A-1-antichymotrypsin 2, indicating potential serving as early markers of NEC. Conversely, antibiotic treatment, independent of NEC, affected only 4 proteins with main differences found between ENT and CON pigs.

Conclusion: Early postnatal development of NEC lesions is associated with marked plasma protein changes that may be used for early NEC diagnosis.

Keywords: necrotizing enterocolitis (NEC), antibiotics, proteomics, ECM, lipid metabolism, immunity

INTRODUCTION

Necrotizing enterocolitis (NEC) is a common gastrointestinal tract (GIT) disease with high mortality in preterm infants (1). Besides the gut symptoms, such as elevated permeability, immune cell infiltration, and tissue inflammatory response (1), NEC is closely related to systemic inflammation, potentially leading to injury of organs distant to the GIT, such as the brain and lungs (2). NEC-associated systemic inflammation includes changes in blood cell composition, such as leukopenia, monocytopenia, thrombocytopenia, and/or suppression of erythropoiesis, (3) and in plasma levels of pro-inflammatory cytokines (IL-6 and IL-8) (4) and multiple immune-related proteins, such as C-reactive protein (CRP), procalcitonin, and serum amyloid-A (SAA). All these are potential markers for NEC (5), but it remains difficult to differentiate NEC from systemic inflammatory conditions, like sepsis, which may be associated with NEC or occur independently. There is a need to better understand how gut inflammatory conditions may affect plasma proteins that could serve to predict NEC early, thus allowing timely NEC prevention and treatment (6).

The gut bacterial colonization in early life is involved in NEC. Dyscolonization with a few (pathogenic) strains may predispose to both NEC and systemic infections (7). Early antibiotic treatment, commonly used to treat or prevent sepsis and infection (8), affects the gut microbiome, and a less diverse gut microbiome is associated with NEC in preterm infants (9). Prolonged antibiotic treatment increases the incidence of NEC and sepsis (10, 11), but short-term systemic antibiotic treatment, given to about 90% of very preterm infants, is recently shown to be associated with less NEC in a survey from 13 NICUs across the world (12). This supports findings from previous studies demonstrating protection against NEC after prophylactic enteral antibiotics in infants (13) and preterm pigs (6, 14). In these studies, the enteral antibiotic treatment reduced gut bacterial load and diversity, and prevented structural and functional damage, hypoxic stress, and immune-related DNA methylation changes in the small intestinal tissue (6, 15). As reported earlier, NEC lesions observed in such preterm formula-fed pigs on day 5 of life are generally evident by macroscopic tissue inspection without any previous clinical signs of NEC, e.g., abdominal distention, bloody stools, apnea or lethargy, hence, representing the early phase of clinical NEC (6). Of note, the enteral antibiotic treatment also affected the systemic innate immunity (16), indicating that the antibiotic treatment may affect systemic parameters including plasma proteins, independent of the NEC effects. Among different biofluids available for disease biomarkers, blood remains the sample of choice due to its easy availability and its potential to reflect pathophysiological changes in a variety of organs.

On this background, we hypothesize that early postnatal progression of NEC, as detected in preterm pigs fed formula, induces plasma proteome changes reflecting systemic effects of early NEC. Considering the variable, but frequent, use of antibiotic treatment for preterm infants immediately after birth, and the critical role of the gut microbiome in NEC, preterm newborn pigs were exposed to either no antibiotics, systemic or enteral antibiotics in clinically relevant doses, creating a range of antibiotic-dependent NEC sensitivities. NEC-related systemic responses in these pigs were assessed by hematology, blood biochemistry, and plasma protein profile by mass spectrometry (MS)-based proteomics. Gene expression of selected plasma proteins affected by NEC or the antibiotic treatment was assessed in the liver and small intestinal tissue.

MATERIALS AND METHODS

Animal Procedure and Antibiotic Treatment

Delivery, rearing, feeding, and antibiotic treatment were carried out as previously described (6). In brief, 47 preterm pigs were delivered from three sows (Large White × Danish Landrace × Duroc) by cesarean section on day 106 (90–92%) of gestation (day 1). After being fitted with umbilical arterial catheters (infant feeding tube 4F; Portex, Kent, UK) and orogastric feeding tubes (6F Portex), these pigs were reared in temperature- and oxygen-regulated incubators. A group of pigs was given antibiotics through the umbilical catheter (PAR, $n = 17$), the other 15 pigs received antibiotics via the orogastric tube (ENT, $n = 15$), and the remaining pigs received saline, serving as untreated controls (CON, $n = 15$). The antibiotics used were ampicillin (30 mg/kg BW, 3 times daily), gentamicin (2.5 mg/kg BW, twice daily), and metronidazole (10 mg/kg BW, 3 times daily), specifically formulated for enteral and parenteral use. The antibiotic treatment started immediately after the enteral feeding started on day 1 until the euthanasia on day 5. All pigs were given both parenteral nutrition (4 mL/kg/h in the first 24 h, gradually increasing to 6–8 mL/kg/h) and minimal enteral nutrition (3 mL/kg every 3 h) on days 1 and 2, before being shifted to full enteral feeding (15 mL/kg every 3 h) on day 3 until the end of the experiment on day 5. Formulations of both parenteral and enteral nutrition are provided as **Supplementary Table 1**.

On day 5, under anesthesia, all pigs were euthanized by an overdose of pentobarbital after blood sampling through an intracardiac puncture. Whole blood was collected for cell counting, and EDTA-treated plasma was saved for blood biochemistry and proteomic analysis. As previously described (14), each pig was given an oral bolus (15 mL/kg BW) of a solution containing 5% lactulose and 5% mannitol 3 h before the planned euthanasia, and a urine sample was collected via cystocentesis at euthanasia. Prior to the oral bolus, individual pigs randomly underwent a 2 to 4 h fasting period, and received the last enteral feeding 60 min before the urine collection following euthanasia. Intestinal permeability was assessed by the urinary ratio of lactulose and mannitol. The GIT of each piglet was collected, and five regions, namely, the stomach, proximal, middle, and distal small intestines, and colon, were separately evaluated for macroscopic NEC severity using a validated NEC scoring system as follows: (1) absence of macroscopic hemorrhage, edema, or mucosal abnormality; (2) local hyperemia; (3) hyperemia, extensive edema and local hemorrhage; (4) extensive hemorrhage; (5) local necrosis and

pneumatosis intestinalis; and (6) extensive transmural necrosis and pneumatosis intestinalis (14). The maximal NEC score across these five regions was recorded as the NEC score of the pig to indicate the overall NEC severity.

Blood cell counting was conducted on an Advia 2120i Hematology System (Siemens, Munich, Germany). Plasma biochemistry was analyzed using Advia 1800 Chemistry systems (Siemens, Erlangen, Germany). The study was approved by the Danish National Committee of Animal Experimentation (no. 2014-15-0201-00418).

LC/MS-Based Plasma Proteomics

The preparation of a protein sample was performed using a filter-aided protocol, as previously described (17). Briefly, protein concentration in the plasma samples was determined on a NanoDrop Spectrophotometer (Thermo Scientific, Waltham, MA, USA). Plasma sample containing 100 μg protein was transferred onto an Amicon Ultra centrifugal filter (10 kDa, 0.5 mL, Millipore, Søborg, Denmark), and mixed with a buffer containing sodium deoxycholate (5%) and triethylammonium bicarbonate (50 mmol/L, pH 8.0). Protein was reduced by TCEP solution [0.01 mol/L, 1:50 (v/v)], alkylated by chloroacetamide [0.5 mol/L, 1:50 (v/v)], and digested by trypsin (Promega, 1 μg/100 μg protein, 37°C overnight) inside the spin filter with a centrifuge step (14,000 × g for 15 min) in between. Tryptic peptides were recovered by another step of centrifugation and purified by phase extraction using ethyl acetate acidified by trifluoroacetic acid (1%, v/v). Vacuum-dried peptides were suspended in a solution of 2% acetonitrile, 0.1% formic acid, and 0.1% trifluoroacetic acid, and applied onto a Dionex RSLC UPLC System (Thermo Scientific) coupled to a Q-Exactive HF Hybrid Quadrupole-Orbitrap Mass Spectrometer (Thermo Scientific). Five micrograms of peptide was injected onto a 2 cm reverse-phase C18 material-trapping column and separated on a 50-cm analytical column (Acclaim PepMap100, 75 μm ID, 100 Å, Thermo Scientific) with both columns kept at 40°C. Elution gradient at a constant flow rate of 300 nl/min started with a mixture of water (97.9%) and acetonitrile (2%) containing 0.1% formic acid, then increased to 30% acetonitrile in 225 min. Mass spectrometric data were obtained in positive ionization mode in a data-dependent acquisition (DDA) fashion with survey spectra and isolation/fragmentation spectra alternating using a Top12 method. Selected peptides were excluded from reanalysis for 30 s.

Protein annotation and quantification based on mass spectra of peptides were carried out using MaxQuant (1.5.2.8) (18) against the Uniprot reference database with isoforms (*Sus scrofa*, UP000008227, last modified 2016-08-02). Detection of at least two unique peptides per protein and protein being present in at least 70% of the samples in each group were required for protein annotation and quantification. Protein abundance data were normalized and two-based logarithm transformed using the Perseus software (version 1.2.0.17) (19), then aligned with protein identities and grouping information, such as treatment, litter (sow), NEC score, and sex, and exported into R (version 3.4.1) (20) integrated with R Studio (version 3.1.18) (21) for data analysis. The MS proteomics data are available at the ProteomeXchange Consortium (http://www.proteomexchange.org/) with the data set identifier PXD015938.

RT-qPCR of Hepatic and Distal Small Intestinal Genes

To balance the effect of litter and sex for treatment comparisons, one pig of each sex from each litter was selected for each treatment group. A random number selection method was used to choose the sample when more than one pig was eligible for each litter, sex, and treatment. Two more pigs (one male and one female) were randomly selected from any two treatment groups with eligible candidates, resulting in total 24 pigs selected ($n = 8$ in each group) for the RT-qPCR analysis. The NEC scores of the selected pigs were not significantly different from those of the entire groups (χ^2 test, $P = 0.90$). Transcription of selected genes in the liver and distal small intestine was determined by RT-qPCR, using predesigned primers (sequences listed in **Supplementary Table 3**). Briefly, total RNA in the tissue homogenate was isolated with RNeasy Lipid Tissue Mini Kit (Qiagen, Copenhagen, Denmark). RT-qPCR was performed using QuantiTect SYBR Green PCR Kit (Qiagen) on a LightCycler 480 (Roche, Hvidovre, Denmark). Levels of target gene were normalized to that of the housekeeping gene, HPRT1 (22), before further statistical analysis.

Data Analysis

Univariate analysis was applied to hematologcial, blood biochemical, and proteomic data. A linear mixed-effect model with the antibiotic treatment (CON, PAR, and ENT), NEC score in continuous mode, and sex of the pig as fixed-effect factors, while litter (sow) being a random-effect factor, was fitted to each parameter (hematology, blood biochemistry, and proteomics) using the nlme package (23). Variance Inflation Factor (VIF) of the model was tested by the *vif* function to evaluate the possible colinearity of treatment and NEC score. A VIF larger than 2.5 indicated existence of colinearity, and the model would be rejected. The effect of treatment or NEC was tested by comparing this model with another model without treatment or NEC score as factor, respectively. The difference between the treatment levels was tested in a pairwise fashion by the Tukey *post hoc* test (package multcomp). The regression coefficient of NEC severity was used to show the effect of NEC severity on each parameter. To control the type I error of analysis of the proteomics data, the *P*-value obtained was further adjusted by false discovery rate (FDR, $\alpha = 0.2$) into q-value using the multtest package (24). Proteins with a value of $q \leq 0.10$ in any comparisons between the treatment groups were selected for functional assignment.

To explore associations between proteins revealed by the proteomic analysis, their abundance was applied to Spearman correlation analysis in pairwise fashion. Correlations with the absolute value of Spearman's r <0.7 were manually clustered and imported into AutoAnnotate (Version 1.3.3) (25) based on Cytoscape (Version 3.8.0) (26) to generate a protein correlation network.

Results from RT-qPCR were analyzed using Student's *t*-test, and a two-tailed $P < 0.05$ was considered as statistically significant.

RESULTS

Clinical Data, Hematology, and Blood Biochemistry

A total of 47 pigs out of the initial 64 pigs were included in this study, while 17 pigs dying within the first 2 days from immaturity-related complications (respiratory distress and immaturity of lungs) were excluded. Hematological and plasma biochemical parameters of the pigs included for the proteomic analysis are listed in **Table 1**, and NEC scores of each treatment group are listed in **Supplementary Table 2** and **Supplementary Figure 1**. NEC severity of the small intestine and colon was scored according to their NEC lesions, and representative images are displayed in **Figure 1**. Lower NEC scores were found in ENT pigs, relative to both PAR and CON pigs (two-tailed *t*-test, $P < 0.05$). PAR pigs also had lower NEC score than CON pigs ($P < 0.05$). Regardless of NEC, significantly lower monocyte numbers (absolute counts or relative percentage, both $P < 0.05$) found in the antibiotic groups (PAR or ENT), had no significant difference between the two groups. ENT pigs had the lowest number of neutrophils ($P < 0.05$, ENT vs. CON). The antibiotic treatment tended to reduce levels of total plasma protein (PAR vs. CON, $P < 0.05$; ENT vs. CON, $P = 0.08$) and albumin (PAR vs. CON, $P = 0.05$).

NEC severity, as indicated by NEC scores, negatively affected the numbers of immune cells (total white blood cells, neutrophils, lymphocytes, and monocytes) (**Table 1**). Conversely, blood biochemical parameters reflecting liver (dys)functions increased with increasing NEC score (ALP, ALT, bilirubin, AST, and GGT, all Ps < 0.05). Furthermore, NEC severity scores negatively affected the cholesterol, carbamide and calcium levels (all Ps < 0.05) (**Table 1**). Intestinal permeability, as indicated by the ratio of urinary levels of lactulose over mannitol, increased with increasing NEC severity ($P < 0.01$) (**Table 1**).

Plasma Proteomics

In total, 303 plasma proteins were successfully annotated. Information of proteins with differential abundance, including UniProt ID, gene name, protein name, and abundance in each antibiotic treatment group or regression coefficient of NEC severity, is listed in functional groups in **Table 2**. None of the statistical models, testing the effect of the antibiotic treatment and NEC, had a VIF above 2.5 indicating that keeping both treatment and NEC severity in these models does not inflate the variance; thus, testing the effect of both factors is reliable. Results showed that 90 proteins were significantly affected ($q \leq 0.10$) by either the antibiotic treatment or NEC. Among the differential proteins, only four proteins, namely, serpin, a6 and a8, angiotensinogen, and complement factor I (CFI), were significantly affected by the antibiotic treatment, with changes mainly observed between ENT and untreated control pigs ($q \leq 0.10$), except for CFI (ENT vs. PAR, $q = 0.08$). In contrast, increasing NEC score was associated with changed abundance of 89 plasma proteins. These proteins are involved in several biological processes, including extracellular matrix (ECM) homeostasis, lipid metabolism, coagulopathy, innate immunity, and cytoskeleton. Direction of change in protein levels is summarized in **Figure 2**.

Among the ECM-related proteins, all 11 proteins showed decreased abundance with increasing NEC severity. Multiple apolipoproteins, including APOA4, APOC2, APOE, APOD, APOC3, ApoN, and proteins related to lipoprotein metabolism (PON1, SAA, RBP4, Transthyretin, PCKS9, PAF-AH, and PLTP) were affected in abundance in response to increasing NEC score. As the NEC score increased, antithrombin III (SERPINC1), PROS1, and factor V decreased, while fibrinogen-α-chain, histidine-rich glycoprotein (HRG), and hyaluronan-binding protein 2 (FSAP), all involved in inflammation-related coagulopathy, showed increased abundance. Abundance of "positive" acute phase proteins, including angiotensinogen, ceruloplasmin, inter-α-trypsin inhibitor, heavy chain H4 (ITI heavy chain H4), lipopolysaccharide-binding protein (LBP), and α-1-antichymotrypsin 2, increased with increasing NEC severity, while "negative" acute phase proteins, including α-2-HS-glycoprotein, albumin, protein AMBP, carboxypeptidase-N-catalytic chain (CPN), ITI heavy chain H2, and transferrin, decreased. Plasma C2, C3, C5a, C6, CFI, and C1inh increased as NEC severity increased, while plasma C1r, C4a, α-, β-, and γ-subunits of C8, CD55, and vitronectin all decreased.

Multiple correlations were found among the three major protein clusters relating to acute phase response, complement response, and coagulopathy (**Figure 3**, all Spearman's $r \geq 0.7$), which, together, constituted the systemic inflammation pertaining to NEC. Besides, correlations were also found between proteins involved in lipid metabolism and the aforementioned three protein clusters (**Figure 3**, all Spearman's $r \geq 0.7$), indicating potential interplays between systemic inflammation and lipid metabolism in NEC.

Gene Expression

As shown in **Figure 4**, transcription of selected genes related to lipid metabolism was tested in the liver. For easier visualization, pigs were grouped into three groups according to their NEC score. Liver PON1 levels tend to decrease in the severe NEC group ($P < 0.05$) (**Figure 4A**). However, transcription levels of PSCK9, HRG, and PROS1 showed no significant differences among groups with different NEC severity (**Figures 4B–D**).

Plasma Abundance and Liver Transcription of CBG

Plasma levels of CBG were significantly higher in the antibiotic-treated groups (both $P < 0.05$) (**Figure 5A**), while limited effect related to NEC severity was observed (**Figure 5C**). In contrast to its plasma level, transcription level in the liver of CBG was lower in the antibiotic-treated groups (both $P < 0.05$) (**Figure 5B**), while no effect of NEC was observed (**Figure 5D**).

DISCUSSION

Using preterm pigs as a model for preterm infants, with or without clinically relevant antibiotic treatments, multiple hematological and plasma proteomic markers were affected by NEC severity. In contrast, the antibiotic treatment itself affected

TABLE 1 | Hematology and blood biochemistry.

	Abundance[a] by treatment			*P*-value			NEC severity	
	CON	PAR	ENT	PAR- CON	ENT- CON	ENT- PAR	Coefficient[b]	*P*-value
HEMATOLOGY								
WBC (10^9/L)	2.3 ± 0.4	2.2 ± 0.2	2.2 ± 0.2	0.54	0.17	0.56	−0.31	<0.01
Neutrophils (10^9/L)	0.80 ± 0.21	0.72 ± 0.09	0.59 ± 0.06	0.63	0.04	0.13	−0.13	0.02
Lymphocytes (10^9/L)	1.31 ± 0.14	1.38 ± 0.12	1.54 ± 0.12	0.94	0.97	1	−0.16	0.01
Monocytes (10^9/L)	0.11 ± 0.03	0.06 ± 0.01	0.06 ± 0.01	0.01	<0.01	0.28	−0.02	0.01
Basophils (10^9/L)	0.01 ± 0.00	0.01 ± 0.00	0.01 ± 0.00	0.72	0.20	0.52	<0.01	0.46
Eosinophils (10^9/L)	0.02 ± 0.00	0.01 ± 0.00	0.01 ± 0.00	0.38	0.26	0.88	<0.01	0.78
Neutrophils (%)	31.4 ± 3.6	31.0 ± 2.6	26.3 ± 2.0	0.97	0.27	0.11	−0.69	0.54
Lymphocytes (%)	61.0 ± 4.0	63.5 ± 2.5	68.6 ± 2.3	0.95	0.10	0.10	0.77	0.52
Monocytes (%)	4.5 ± 0.6	3.0 ± 0.3	2.7 ± 0.5	0.03	0.02	0.82	−0.10	0.63
Basophils (%)	0.5 ± 0.1	0.4 ± 0.1	0.3 ± 0.0	0.95	0.97	1	0.05	0.16
Eosinophils (%)	0.6 ± 0.2	0.4 ± 0.1	0.4 ± 0.1	0.53	0.74	0.98	0.04	0.43
Erythrocytes (10^{12}/L)	4.0 ± 0.2	4.0 ± 0.2	4.0 ± 0.2	0.79	0.77	0.99	−0.06	0.38
Hemoglobin (mmol/L)	4.9 ± 0.2	4.9 ± 0.2	4.9 ± 0.2	0.77	0.80	1	−0.06	0.49
Hematocrit (%)	26.4 ± 1.2	26.2 ± 1.0	26.5 ± 1.1	0.72	0.82	1	−0.32	0.51
MCV (fl)	65.4 ± 0.9	66.0 ± 0.5	66.7 ± 0.6	0.80	0.69	0.95	−0.12	0.66
MCHC (g/dl)	18.5 ± 0.1	18.6 ± 0.1	18.4 ± 0.1	0.88	0.71	0.35	−0.01	0.77
Thrombocytes (10^9/L)	137.2 ± 15.2	124.9 ± 18.7	106.9 ± 18.3	0.96	0.34	0.36	−11.4	0.11
MPV (fl)	8.5 ± 0.4	8.1 ± 0.3	8.3 ± 0.2	0.35	0.38	0.98	−0.17	0.20
MPC (g/dl)	209.6 ± 4.2	213.4 ± 4.1	217.3 ± 4.2	0.93	0.19	0.22	2.5	0.16
BLOOD BIOCHEMICAL PARAMETERS								
Total protein, g/L	29.5 ± 0.7	27.6 ± 0.5	27.5 ± 0.4	0.03	0.08	1	0.01	0.97
Albumin, g/L	12.5 ± 0.4	11.6 ± 0.3	11.6 ± 0.2	0.05	0.15	0.99	<0.01	0.93
ALT, U/L	19.9 ± 1.5	20.2 ± 1.9	17.5 ± 0.6	0.77	0.94	0.96	1.4	0.01
AST, U/L	46.1 ± 10.8	93.8 ± 36.2	55.6 ± 30.1	0.19	0.38	0.99	22.8	0.03
ALP, 10^3 U/L	3.1 ± 0.3	2.8 ± 0.2	2.6 ± 0.3	0.89	0.95	1	0.16	0.10
GGT, U/L	26.9 ± 4.1	25.9 ± 4.0	21.7 ± 2.2	0.86	0.45	0.70	3.3	0.01
Bilirubin, μmol/L	2.0 ± 0.7	1.1 ± 0.4	0.5 ± 0.1	0.47	0.87	0.87	0.62	<0.01
Total cholesterol, mmol/L	2.4 ± 0.1	2.4 ± 0.2	2.6 ± 0.1	0.79	0.55	0.86	−0.14	<0.01
Urea, mmol/L	10.3 ± 0.7	10.1 ± 0.7	10.0 ± 1.0	0.43	0.08	0.48	−0.69	0.03
Creatinine, μmol/L	56.0 ± 3.5	56.2 ± 3.0	47.0 ± 1.6	0.95	0.19	0.08	0.05	0.88
Creatine kinase, U/L	166.1 ± 33.4	317.2 ± 95.3	224.4 ± 109.8	0.25	0.47	0.98	48.2	0.15
Iron, μmol/L	6.3 ± 1.0	5.3 ± 0.5	8.0 ± 0.9	0.87	0.57	0.28	−0.25	0.53
Ionized phosphate, mmol/L	1.2 ± 0.1	1.4 ± 0.2	1.2 ± 0.1	0.19	0.30	1	0.14	0.01
Ca, mmol/L	3.0 ± 0.0	3.0 ± 0.0	3.0 ± 0.0	0.44	0.70	0.97	−0.03	0.03
Mg, mmol/L	0.9 ± 0.0	0.9 ± 0.0	0.9 ± 0.0	0.38	0.54	1	0.02	0.28
Na, mmol/L	158.1 ± 1.4	157.9 ± 1.1	161.0 ± 2.0	0.96	0.67	0.47	−0.30	0.70
K, mmol/L	4.5 ± 0.1	4.9 ± 0.5	5.6 ± 1.3	0.84	0.23	0.42	0.46	0.22
INTESTINAL PERMEABILITY								
Lactulose/mannitol ratio (10^{-2})	8.8 ± 3.3	9.5 ± 2.7	3.8 ± 1.3	0.55	<0.01	0.01	−2.4	0.02

[a]Data are shown as mean ± SEM. [b]Regression coefficient from the linear mixed-effect model indicating the effect of NEC severity. CON, no antibiotic treatment; PAR, parenteral antibiotics administered; ENT, enteral antibiotics administered.

WBC, total leukocytes; MCV, mean corpuscular volume; MCHC, mean corpuscular hemoglobin concentration; MPV, mean platelet volume; MPC, mean platelet component; ALP, alkaline phosphatase; ALT, alanine transaminase; AST, aspartate aminotransferase; GGT, γ-glutamyltransferase.

much fewer parameters. Due to the fact that the antibiotics, as a treatment for NEC, had a significant effect on NEC scores ($P < 0.001$, linear mixed-effect model, **Supplementary Table 1** and **Supplementary Figure 1**), it is difficult, pathophysiologically, to fully separate the effects of NEC from that of the antibiotic treatment. However, by using NEC scores as continuous data, our statistical analyses showed that NEC severity, not the antibiotic treatment, was the key factor driving changes to plasma proteins. Besides, bacteremia, the presence of bacteria in the blood, may itself trigger changes in plasma proteins (27). In our previous

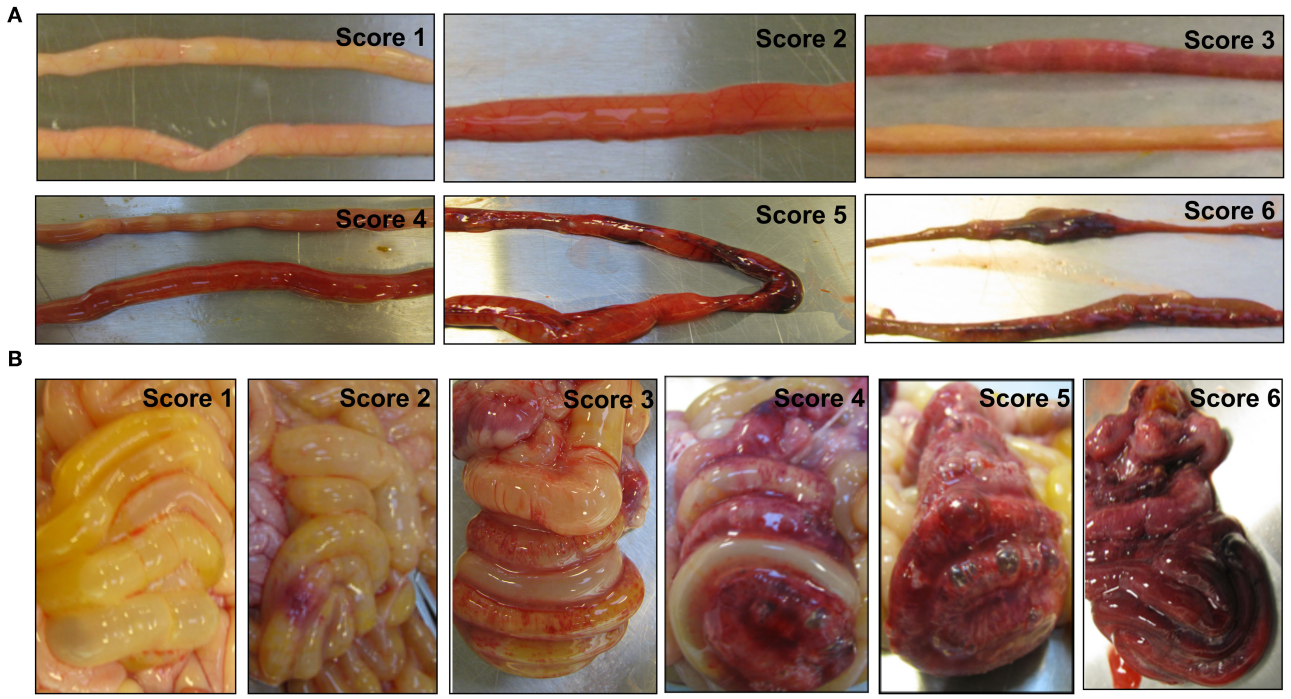

FIGURE 1 | Representative images of the small intestine **(A)** and the colon **(B)** with or without necrotizing enterocolitis (NEC) lesions. The macroscopic NEC severity was evaluated using a scoring system as follows: 1, absence of macroscopic hemorrhage, edema, or mucosal abnormality; 2, local hyperemia; 3, hyperemia, extensive edema, and local hemorrhage; 4, extensive hemorrhage; 5, local necrosis and pneumatosis intestinalis; and 6, extensive transmural necrosis and pneumatosis intestinalis.

publication on the same set of pigs, bacteremia, detected by blood-agar culture, was documented in CON (9 out of 17) and PAR (2 out of 16) pigs, but was absent in all ENT pigs at euthanasia (16), indicating that NEC in 5 day-old preterm pigs is generally associated with bacteremia. Consequently, it is not possible in this study, like in studies on infants, to separate the plasma proteome effects of NEC lesions in the gut from the effects of NEC-associated systemic inflammation following bacterial translocation. This is similar to the situation in preterm infants with NEC where systemic effects are inevitably the combined result of variable gut lesions, antibiotics treatment, and systemic bacteremia, making it difficult to identify NEC-specific systemic biomarkers.

Among the hematological parameters, absolute cell numbers of neutrophils, lymphocytes, and monocytes, but not their relative proportions, decreased with increasing NEC severity, shown as negative regression coefficients, confirming the observations in infants (3), although no eosinophilia or thrombocytopenia was observed in the pigs. These responses may be partly related to the altered levels of the liver function-related enzymes (ALT, AST, and GGT), representing a joint systemic inflammatory response associated with NEC. Increment in the intestinal permeability found here may have initiated this systemic inflammation by allowing bacteria and their toxins to enter into the circulation. This is underscored by our previous finding of the presence of bacteria in the blood of CON and PAR pigs showing NEC lesions and absence of systemic bacteria in ENT pigs, which were essentially NEC free (16). This bacteremia would, in turn, cause changes in various blood parameters. The observed NEC-associated changes in the blood parameters, including the plasma proteins, may, therefore, be the combined response to microbiota-dependent NEC lesions in the gut and their associated systemic effects in the blood and organs distant to the gut, e.g., liver or kidney.

Disruption of the intestinal ECM, together with intestinal inflammation and immune cell infiltration, is closely associated with NEC pathogenesis (28). Disturbed ECM homeostasis was indicated by a change of a matrix metalloproteinase (MMP-2), an MMP-activating thioredoxin (QSOX1) (29), a product of MMP-mediated cleavage (COL6A3), integrin-α2 and vitronectin (connecting ECM and epithelial cells) and cadherin-11, a cell-adhesion protein. The majority of ECM-associated proteins in plasma were decreased in abundance with increasing NEC severity. However, such proteins may change differently in plasma and in the gut tissue during NEC as intestinal expression of MMP-2,−9, TIMP-1,−2 were reported being elevated in human NEC (30), contrasting our findings in plasma. Similarly, desmoglein-2, a component of desmosome and associated with perturbed epithelial barrier function, increased with increasing NEC severity, but was reduced in the intestinal tissue of patients with IBD (31). In NEC, elevated intestinal expression of ECM-associated proteins, especially MMP-2, −9

TABLE 2 | Proteins with differential abundance by NEC or the antibiotic treatment.

Uniprot ID	Gene	Protein	Abundance[a] by treatment			q-value			NEC severity	
			CON	PAR	ENT	PAR- CON	ENT- CON	ENT- PAR	Coefficient[b]	q-value
PROTEINS AFFECTED BY ANTIBIOTICS TREATMENT										
F1RG45	AGT	Angiotensinogen preproprotein	29.2 ± 0.2	29.4 ± 0.2	29.5 ± 0.2	0.77	0.08	0.99	0.32	<0.01
CBG	Serpina6	Corticosteroid-binding globulin	26.7 ± 0.1	26.9 ± 0.2	27.3 ± 0.1	0.97	0.08	0.12	0.07	0.18
F1S133	CFI	Complement factor I	28.1 ± 0.1	27.9 ± 0.1	28.3 ± 0.1	0.86	0.39	0.06	0.05	0.10
F1SCD0	LOC100153899	Serpin A3-8	32.9 ± 0.2	33.2 ± 0.2	33.2 ± 0.1	0.45	0.06	0.99	0.23	<0.01
PROTEINS AFFECTED BY NEC										
EXTRACELLULAR MATRIX HOMEOSTASIS										
F1RFU7	CDH11	Cadherin-11 isoform X1	22.6 ± 0.2	22.8 ± 0.2	23.0 ± 0.1	0.97	0.98	0.99	−0.19	0.05
F1S021	COL5A1	Collagen α-1(V) chain	24.4 ± 0.1	24.7 ± 0.2	24.9 ± 0.2	0.97	0.98	0.99	−0.21	0.02
I3LUR7	COL6A3	Collagen type VI α 3 chain	26.6 ± 0.1	26.9 ± 0.1	27.1 ± 0.1	0.97	0.96	0.99	−0.12	0.05
F1RTT3	COL9A1	Collagen α-1(V) chain	22.8 ± 0.2	23.0 ± 0.3	23.3 ± 0.2	0.97	0.98	0.99	−0.26	0.02
F1S902	COMP	Cartilage oligomeric matrix protein	24.3 ± 0.1	24.2 ± 0.1	24.6 ± 0.1	0.97	0.98	0.99	−0.14	0.02
I3LC64	ECM1	Extracellular matrix protein 1	25.3 ± 0.2	25.3 ± 0.2	25.3 ± 0.2	0.97	0.78	0.99	−0.20	0.02
F1SQL2	EFEMP1	EGF containing fibulin extracellular matrix protein 1	23.2 ± 0.1	23.5 ± 0.1	23.5 ± 0.1	0.97	0.98	0.99	−0.12	0.06
F1SMF4	ITGA2	Integrin subunit α-2	22.4 ± 0.1	22.8 ± 0.2	23.1 ± 0.1	0.97	0.96	0.99	0.16	0.03
F1RF11	MMP2	72 kDa type IV collagenase	22.9 ± 0.2	23.4 ± 0.2	23.8 ± 0.1	0.87	0.51	0.99	−0.17	0.06
F1S682	QSOX1	Sulfhydryl oxidase	28.1 ± 0.1	28.1 ± 0.1	28.2 ± 0.1	0.97	0.98	0.99	−0.06	0.10
VTNC	VTN	Vitronectin	25.5 ± 0.3	25.8 ± 0.4	26.5 ± 0.2	0.97	0.98	0.99	−0.27	0.06
LIPID METABOLISM										
APOA4	SAA2	Serum amyloid A protein	32.0 ± 0.1	32.3 ± 0.1	32.5 ± 0.1	0.64	0.59	0.99	−0.10	0.01
D3Y264	APOA4	Apolipoprotein A-IV	28.4 ± 0.2	28.9 ± 0.2	28.7 ± 0.2	0.89	0.98	0.99	−0.24	0.01
APOC3	APOC2	Apolipoprotein C-II	31.4 ± 0.2	31.4 ± 0.2	31.9 ± 0.1	0.97	0.98	0.99	−0.26	<0.01
F1SQX9_	APOC3	Apolipoprotein C-III	29.3 ± 0.2	29.3 ± 0.2	29.5 ± 0.2	0.97	0.98	0.99	−0.26	0.01
APOE	APOD	Apolipoprotein D	30.4 ± 0.1	30.3 ± 0.1	30.6 ± 0.1	0.97	0.98	0.99	−0.09	0.09
Q68RU1	APOE	Apolipoprotein E	24.6 ± 0.4	24.6 ± 0.3	24.8 ± 0.3	0.97	0.75	0.99	0.30	0.07
Q4Z8N7	ApoN	Ovarian and testicular apolipoprotein N	24.9 ± 0.2	25.3 ± 0.2	25.6 ± 0.1	0.97	0.98	0.99	−0.20	0.02
I3LGB2	PAF-AH	Platelet-activating factor acetylhydrolase	24.7 ± 0.1	24.6 ± 0.2	24.8 ± 0.1	0.97	0.98	0.99	−0.19	0.01
F1SC57	PCSK9	Proprotein convertase subtilisin/kexin type 9	24.2 ± 0.1	24.2 ± 0.1	24.3 ± 0.2	0.97	0.98	0.99	−0.11	0.06
F1SFA1	PLTP	Phospholipid transfer protein	24.8 ± 0.1	24.9 ± 0.2	25.2 ± 0.1	0.97	0.98	0.99	−0.16	0.03
RET4	PON1	Paraoxonase 1	27.2 ± 0.1	26.9 ± 0.2	27.4 ± 0.1	0.42	0.97	0.99	−0.19	0.01
F1S9B9	RBP4	Retinol-binding protein 4	23.4 ± 0.6	23.7 ± 0.9	21.6 ± 0.9	0.97	0.98	0.99	0.84	0.03
TTHY	TTR	Transthyretin	31.9 ± 0.1	32.0 ± 0.1	32.1 ± 0.1	0.97	0.98	0.99	−0.08	0.06
COAGULOPATHY										
FA5	F5	Coagulation factor V	27.9 ± 0.2	27.9 ± 0.2	28.2 ± 0.1	0.97	0.98	0.99	−0.22	<0.01
FIBA	FGA	Fibrinogen-α-chain	28.5 ± 0.6	28.2 ± 0.6	27.0 ± 0.4	0.97	0.98	0.99	0.62	0.02
F1S5J5	HABP2	Hyaluronan binding protein 2	23.4 ± 0.1	23.3 ± 0.1	23.5 ± 0.1	0.97	0.43	0.99	0.08	0.10
F1SFI5	HRG	Histidine-rich glycoprotein	31.0 ± 0.2	31.4 ± 0.1	31.2 ± 0.1	0.51	0.43	0.99	0.13	0.08
F1SK70	PROS1	Vitamin K-dependent protein S isoform 2 preproprotein	27.9 ± 0.1	28.0 ± 0.0	28.2 ± 0.1	0.97	0.66	0.99	−0.05	0.06
F2Z5E2	SERPINC1	Antithrombin III	31.7 ± 0.1	31.7 ± 0.1	31.9 ± 0.1	0.97	0.96	0.99	−0.13	<0.01
ACUTE PHASE RESPONSE										
F1RG45	AGT	Angiotensinogen preproprotein	29.2 ± 0.2	29.4 ± 0.2	29.5 ± 0.2	0.77	0.08	0.99	0.32	<0.01
FETUA	AHSG	A-2-HS-glycoprotein	34.4 ± 0.3	33.8 ± 0.4	34.2 ± 0.4	0.57	0.30	0.99	−0.53	0.01
ALBU	ALB	Serum albumin	34.9 ± 0.2	34.5 ± 0.2	34.9 ± 0.2	0.28	0.35	0.99	−0.30	<0.01
AMBP	AMBP	Protein AMBP	28.4 ± 0.2	27.8 ± 0.2	28.4 ± 0.2	0.13	0.62	0.99	−0.20	0.03

(Continued)

TABLE 2 | Continued

Uniprot ID	Gene	Protein	Abundance[a] by treatment			q-value			NEC severity	
			CON	PAR	ENT	PAR- CON	ENT- CON	ENT- PAR	Coefficient[b]	q-value
F1SKB1	CP	Ceruloplasmin	30.2 ± 0.2	29.5 ± 0.1	29.5 ± 0.1	0.13	0.35	0.99	0.12	0.07
F1S8V7	CPN1	Carboxypeptidase N catalytic chain	25.7 ± 0.2	25.6 ± 0.1	25.7 ± 0.2	0.80	0.98	0.99	−0.11	0.09
F1SH96	ITIH1	Inter-α-trypsin inhibitor heavy chain H1	28.2 ± 0.1	28.2 ± 0.1	28.6 ± 0.1	0.97	0.98	0.99	−0.18	<0.01
ITIH1	ITIH1	Inter-α-trypsin inhibitor heavy chain H1	29.0 ± 0.2	28.6 ± 0.2	29.1 ± 0.1	0.13	0.30	0.99	−0.24	<0.01
ITIH2	ITIH2	Inter-α-trypsin inhibitor heavy chain H2	31.1 ± 0.1	31.1 ± 0.1	31.4 ± 0.1	0.97	0.98	0.99	−0.17	<0.01
F1SH92	ITIH4	Inter-α-trypsin inhibitor heavy chain H4	31.9 ± 0.2	31.6 ± 0.1	31.5 ± 0.1	0.76	0.98	0.99	0.12	0.03
I3L5U6	LBP	Lipopolysaccharide binding protein	25.5 ± 0.2	24.8 ± 0.2	24.7 ± 0.2	0.68	0.98	0.99	0.21	0.02
F1SN68	ORM1	A-1-acid glycoprotein	34.9 ± 0.1	34.8 ± 0.1	34.9 ± 0.1	0.97	0.83	0.99	−0.09	0.05
Q9GMA6	SERPINA3-2	A-1-antichymotrypsin 2	30.5 ± 0.2	30.9 ± 0.2	30.7 ± 0.2	0.41	0.17	0.99	0.28	<0.01
TRFE	TF	Serotransferrin	34.4 ± 0.2	34.3 ± 0.1	34.5 ± 0.2	0.97	0.98	0.99	−0.16	0.06
COMPLEMENT SYSTEM										
F1SLV6	MASP1	Complement component MASP3	26.4 ± 0.2	26.0 ± 0.1	26.2 ± 0.2	0.47	0.31	0.99	−0.17	0.03
F1RQW7	C1R	Complement c1r	23.4 ± 0.3	22.9 ± 0.3	22.3 ± 0.2	0.97	0.98	0.99	0.37	<0.01
F1SBS4	C2	Complement C2	24.8 ± 0.7	25.5 ± 0.5	25.2 ± 0.6	0.82	0.35	0.99	0.71	0.01
I3LTB8	C3	Complement C3	26.1 ± 0.7	25.2 ± 0.9	24.2 ± 0.9	0.97	0.98	0.99	0.86	0.03
F1RQW2	C3	Complement C3	30.7 ± 0.1	30.5 ± 0.1	30.5 ± 0.1	0.71	0.43	0.99	−0.09	0.10
F1SME1	C4A	Complement C4-A isoform 1 preproprotein	28.2 ± 0.1	28.0 ± 0.2	27.9 ± 0.2	0.97	0.96	0.99	0.23	<0.01
F1SMI8	C5	Complement C5a anaphylatoxin	21.9 ± 0.5	20.6 ± 0.5	20.5 ± 0.4	0.97	0.98	0.99	0.48	0.01
F1S788	C6	Complement C6	26.3 ± 0.1	26.6 ± 0.1	26.7 ± 0.1	0.97	0.98	0.99	−0.18	<0.01
F1S790	C8A	Complement C8 α chain	26.9 ± 0.1	26.8 ± 0.1	27.2 ± 0.1	0.73	0.98	0.99	−0.16	<0.01
A0SEH3	C8B	Complement C8 β chain	25.8 ± 0.1	25.6 ± 0.1	25.7 ± 0.1	0.51	0.31	0.99	−0.15	0.01
F1S0J0	C8G	Complement component C8G	22.4 ± 0.1	22.5 ± 0.1	22.5 ± 0.1	0.97	0.98	0.99	−0.13	0.03
F1S133	CD55	Complement decay-accelerating factor	28.1 ± 0.1	27.9 ± 0.1	28.3 ± 0.1	0.86	0.39	0.06	0.05	0.10
D5L7X4	CFI	Complement factor I	22.4 ± 0.2	22.6 ± 0.2	23.0 ± 0.2	0.97	0.98	0.99	−0.18	0.09
F1SJW8	SERPING1	Plasma protease C1 inhibitor	29.3 ± 0.3	29.8 ± 0.2	29.7 ± 0.2	0.45	0.21	0.99	0.28	0.01
INNATE IMMUNITY										
F1SGT4	CD44	CD44 molecule	25.2 ± 0.1	25.2 ± 0.2	25.3 ± 0.2	0.97	0.84	0.99	−0.18	0.01
OSTP	SPP1	Osteopontin	24.3 ± 0.2	24.4 ± 0.2	24.2 ± 0.2	0.97	0.97	0.99	0.21	0.04
CYTOSKELETON										
I3L6D7	DSG2	Desmoglein 2	21.7 ± 0.3	21.9 ± 0.2	21.8 ± 0.3	0.95	0.46	<0.01	0.28	0.02
GELS	GSN	Gelsolin	29.7 ± 0.2	29.8 ± 0.2	30.0 ± 0.1	0.97	0.98	0.99	−0.20	0.01
F1RK02	LCP1	Lymphocyte cytosolic protein 1	22.3 ± 0.2	22.5 ± 0.2	22.5 ± 0.2	0.97	0.48	0.99	0.17	0.08
F1RFY1	PFN1	Profilin	21.9 ± 0.2	21.9 ± 0.3	21.6 ± 0.3	0.97	0.98	0.99	0.28	0.01
OTHERS										
F1RUM1	AFM	Afamin	28.8 ± 0.1	28.6 ± 0.1	28.8 ± 0.1	0.63	0.51	0.99	−0.17	0.01
FETA	AFP	A-fetoprotein	34.2 ± 0.1	34.0 ± 0.1	34.2 ± 0.1	0.35	0.51	0.99	−0.08	0.06
AMPN	ANPEP	Aminopeptidase N	21.6 ± 0.3	21.9 ± 0.2	21.9 ± 0.2	0.89	0.24	0.99	0.27	0.01
F1SBE4	B4GALT5	β-1,4-galactosyltransferase 5	23.0 ± 0.1	23.2 ± 0.1	23.2 ± 0.1	0.45	0.21	0.99	0.12	0.02
B9UJD6	C1QTNF3	C1q and tumor necrosis factor related protein 3 isoform b	22.0 ± 0.1	22.0 ± 0.2	22.2 ± 0.2	0.97	0.97	0.99	−0.24	0.01
I3LRD3	CENPE	Kinesin-like protein	24.8 ± 0.3	24.7 ± 0.3	25.1 ± 0.3	0.97	0.98	0.99	−0.27	0.08
F1SC70	CTSA	Carboxypeptidase	23.2 ± 0.1	23.3 ± 0.2	23.7 ± 0.2	0.97	0.17	0.99	0.11	0.09

(Continued)

TABLE 2 | Continued

Uniprot ID	Gene	Protein	Abundance[a] by treatment			q-value			NEC severity	
			CON	PAR	ENT	PAR- CON	ENT- CON	ENT- PAR	Coefficient[b]	q-value
F1SPE9	DNAJC13	Dnaj heat shock protein family (Hsp40) member C13	27.5 ± 0.3	27.9 ± 0.3	27.9 ± 0.3	0.76	0.21	0.99	0.40	0.01
I3LK59	ENO1	A-enolase isoform 1	21.7 ± 0.4	21.7 ± 0.5	21.7 ± 0.4	0.97	0.96	0.99	0.38	0.07
F1S715	FUCA2	A-L-fucosidase	25.1 ± 0.2	25.2 ± 0.2	25.6 ± 0.1	0.97	0.17	0.99	0.11	0.09
I3LN42	GC	Vitamin D-binding protein	32.0 ± 0.1	32.0 ± 0.1	32.1 ± 0.1	0.97	0.76	0.99	−0.13	0.02
F1S4I1	GOLM1	Golgi membrane protein 1	24.9 ± 0.4	25.0 ± 0.5	24.4 ± 0.3	0.97	0.98	0.99	0.41	0.03
GPX5	GPX5	Epididymal secretory glutathione peroxidase	25.3 ± 0.2	25.3 ± 0.1	25.6 ± 0.1	0.97	0.98	0.99	−0.17	0.03
F1SBR6	HIPK1	Homeodomain interacting protein kinase 1	22.3 ± 0.1	22.4 ± 0.1	22.5 ± 0.2	0.97	0.98	0.99	−0.13	0.05
F1SJL1	IGDCC4	Immunoglobulin superfamily DCC subclass member 4	22.4 ± 0.2	22.7 ± 0.1	22.6 ± 0.1	0.97	0.98	0.99	−0.18	0.01
F1SCC6	LOC100153899	Serpin A3-8	32.3 ± 0.3	31.1 ± 0.3	30.6 ± 0.3	0.48	0.89	0.99	0.46	<0.01
F1SCD0	LOC100153899	Serpin A3-8	32.9 ± 0.2	33.2 ± 0.2	33.2 ± 0.1	0.45	0.06	0.99	0.23	<0.01
F1SCC9	LOC106504545	Serpin A3-8	29.7 ± 0.4	30.4 ± 0.2	30.3 ± 0.2	0.97	0.98	0.99	−0.33	0.01
F1SCC7	LOC396684	Serpin A3-5	31.5 ± 0.2	31.2 ± 0.2	31.0 ± 0.2	0.97	0.98	0.99	0.33	<0.01
F1RLC4	LOX	Protein-lysine 6-oxidase	23.4 ± 0.1	23.5 ± 0.1	23.5 ± 0.1	0.97	0.89	0.99	0.10	0.07
F1S7K2	LRG1	Leucine rich α-2-glycoprotein 1	27.0 ± 0.2	26.6 ± 0.2	26.5 ± 0.2	0.97	0.98	0.99	0.25	<0.01
I3L5Z3	PRG4	Proteoglycan 4	23.4 ± 0.5	22.7 ± 0.4	22.4 ± 0.3	0.97	0.98	0.99	0.36	0.06
F1SGH0	PTPRG	Protein tyrosine phosphatase, receptor type G	22.5 ± 0.4	23.3 ± 0.3	22.4 ± 0.5	0.41	0.76	0.99	0.46	0.01
F1SCD1	SERPINA3-2	A-1-antichymotrypsin 2	27.0 ± 0.7	26.3 ± 0.6	26.6 ± 0.6	0.97	0.65	0.99	−0.61	0.06
TFR1	TFRC	Transferrin receptor protein 1	23.6 ± 0.3	23.9 ± 0.3	24.0 ± 0.3	0.90	0.30	0.99	0.35	0.01

[a]*Data are 2-based logarithm transformed and shown as mean ± SEM. CON, no antibiotic treatment; PAR, parenteral antibiotics administered; ENT, enteral antibiotics administered.*
[b]*Regression coefficient from the linear mixed-effect model indicating the effect of NEC severity.*

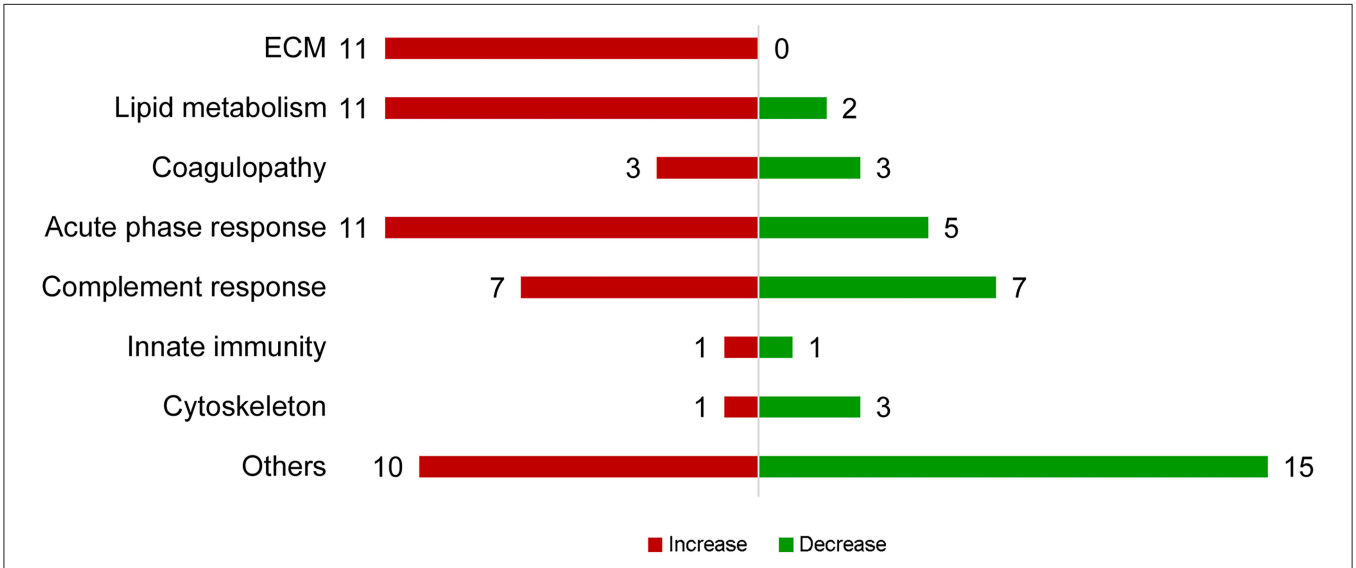

FIGURE 2 | Summary of proteins with abundance changing with NEC severity. Proteins with increasing abundance are in red, decreasing ones in green.

and TIMP-1,−2, facilitates the recruitment of immune cells to cross the endothelial and epithelial layers and reach the infection sites. However, inflammation associated with systemic infection and NEC alters the expression of ECM proteins in other organs, too. Similar transcriptional changes of the above proteins have been found in septic rats (32). Thus, it is difficult to attribute changes in such plasma proteins found here to any specific organ due to the ubiquitous expression of these proteins. They may

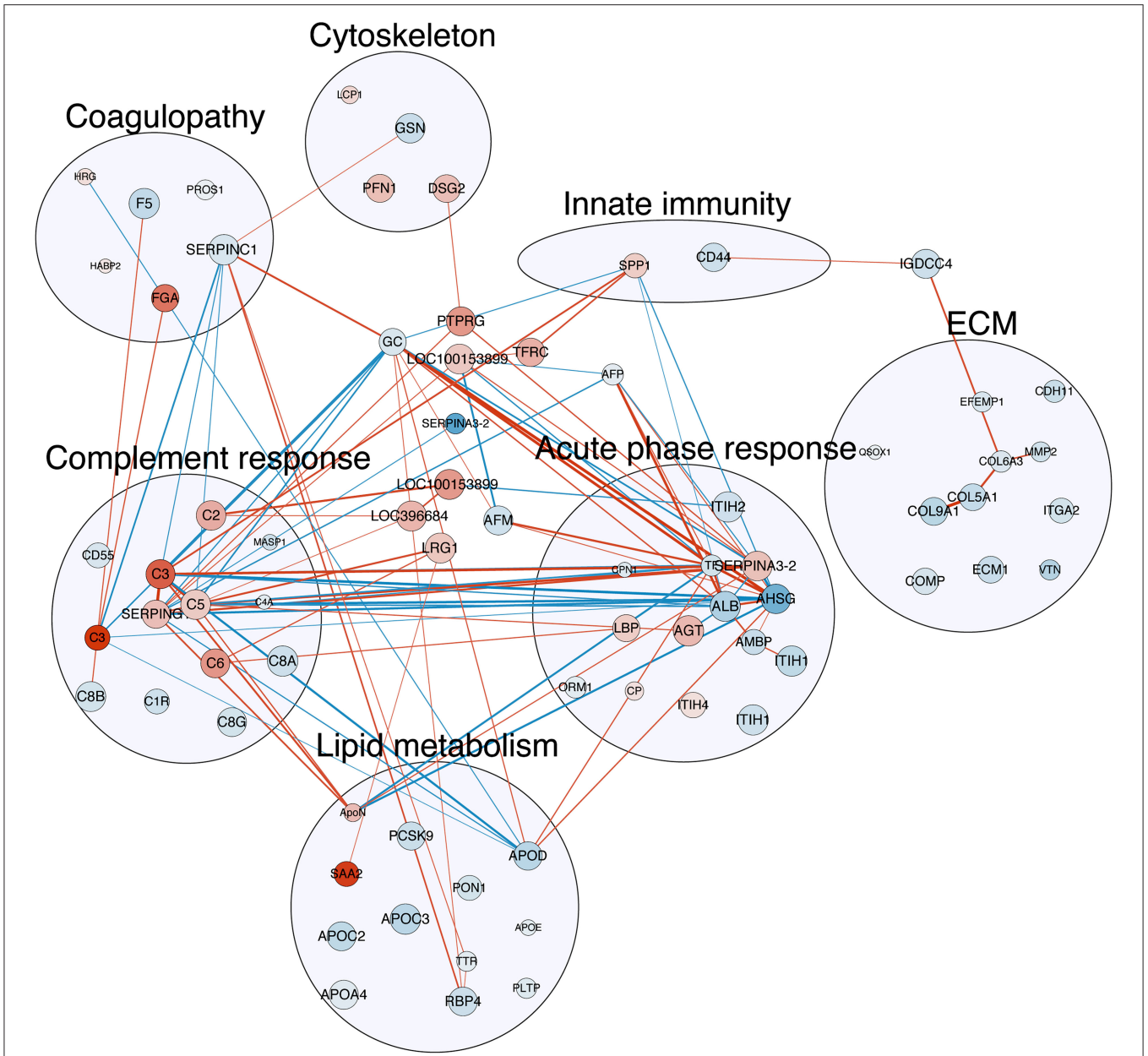

FIGURE 3 | Correlation map of detected plasma proteins with differential abundance with NEC severity. The nodes in red are proteins with increasing abundance with NEC severity, while those in blue are with decreasing abundance. The size of the nodes indicates the q-value of the effect of NEC severity reversely, i.e., the larger the node, the smaller the q-value. The edge (line) in red shows a positive correlation between the two proteins, while those in blue show negative correlation. The width of the edge shows the absolute value of the Spearman's *r*. All correlations listed here are with Spearman's $r \geq 0.7$. Refer to **Table 2** for full protein names.

also show an age-related regulation as elevated (not reduced) serum levels of MMP-9 and TIMP-1, as well as reduced MMP-9/TIMP-1 ratio, were observed in adult sepsis (33). While these plasma proteins are of use in early NEC detection, more research is clearly required to examine their utility in differentiating NEC from sepsis.

Altered lipid metabolism and lipoprotein composition are notable in adult infection and inflammation (34), and in neonatal sepsis (35). In neonatal sepsis, plasma levels of total cholesterol, total triglyceride, lipoprotein-a, high-density lipoprotein (HDL), and apolipoprotein A and B are generally reduced, relative to healthy controls (35). HDL composition changes in endotoxemia, and levels of apolipoproteins, such as the main HDL apolipoproteins, apo-A1 and A2, change (35). Similar to the reduced level of ApoA1 and A2 reported in sepsis, plasma levels of ApoC2, C3, and ApoD decreased with increasing NEC severity. A decreased level of PON1, a hydrolytic enzyme associated with HDL (36), was also observed,

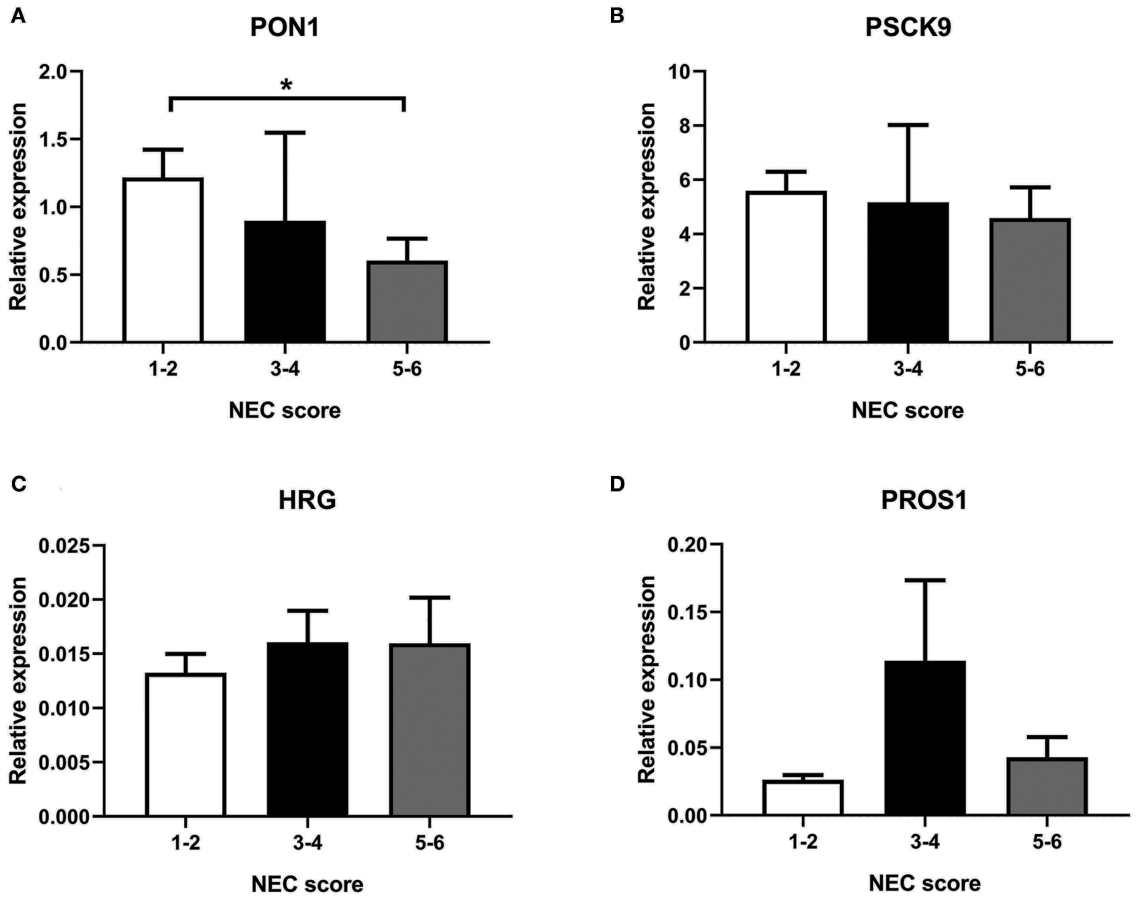

FIGURE 4 | Transcription in the liver of selected genes, **(A)** PON1, **(B)** PSCK9, **(C)** HRG, and **(D)** PROS1. NEC score: 1–2, no-NEC; 3–4, mild NEC; 5–6, severe NEC. Data are presented as mean ± SEM. *$P < 0.05$.

in agreement with a previous report of infected humans (37). PCKS9, binding to LDLR on the liver and increasing the LDL levels in the circulation (38), decreased in abundance when NEC progressed. Platelet-activating factor acetylhydrolase (PAF-AH) degrades PAF, which is involved in NEC pathogenesis (39). In line with our findings, a lower plasma level of PAF-AH was found in NEC patients (40) and endotoxemic rats (39), while increasing activity of plasma PAF-AH or oral feeding of exogenous PAF-AH protects against NEC (41). Combined, these findings suggest a perturbed lipid metabolism during NEC, either as a cause or a consequence of NEC. However, levels of lipoproteins and other lipid metabolism-related parameters are affected by the regimen of parenteral nutrition. Unlike our pigs, which received parenteral nutrition with identical regimens, regimens of parenteral nutrition for human patients vary profoundly among patients and among clinics, thus the utility of lipid metabolism-related plasma proteins as markers of human NEC requires further investigation.

Coagulopathy, a common systemic feature of NEC (42), is characterized by enhanced coagulation and impaired fibrinolysis (43). Among the proteins observed in this study, antithrombin III from the liver inactivates thrombin and coagulant factors, while PROS1 inhibits coagulation as a cofactor in the inactivation of Factors Va and VIIIa (44). Similar to our findings in NEC, plasma levels of antithrombin III and PROS1 decreased in septic neonates (45). Decreased plasma levels of these two proteins, together with increased levels of fibrinogen-α-chain, may reflect enhanced coagulation in NEC. However, Factor V involved in coagulation showed decreasing abundance, while HABP2, enhancing fibrinolysis, increased moderately with NEC progression. HRG showed an increasing plasma level as NEC increased, but it reportedly decreased in septic mice (46). Some of these affected proteins changed in a different direction for NEC and sepsis (e.g., HRG), but more studies are required to identify NEC- and sepsis-specific biomarkers.

Multiple acute phase proteins, including complement components, were affected by NEC, and in prospective infant studies, plasma inter-α-trypsin inhibitor levels decreased in NEC patients (47). In this study, ITIH1 and ITIH2 (two heavy chains of inter-α-trypsin inhibitor) decreased in abundance, while ITIH4 increased. Most "positive" acute phase proteins increase when NEC progresses, while several "negative" regulators

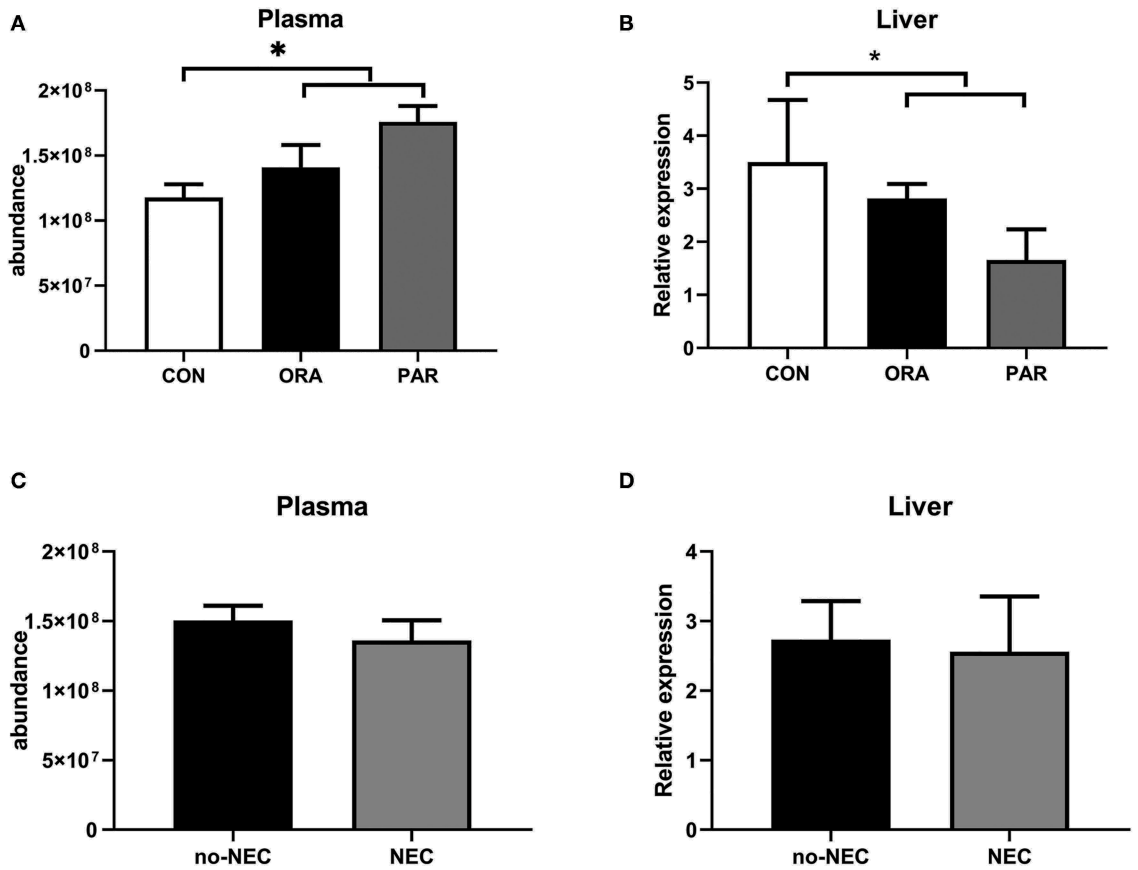

FIGURE 5 | Plasma abundance and transcription levels in the liver of CBG by the antibiotic treatment group **(A,B)** and by the presence of NEC **(C,D)**. Data are presented as mean ± SEM. *$P < 0.05$. CON, no antibiotic treatment; PAR, parenteral antibiotics administered; ENT, enteral antibiotics administered.

decrease. Detected complement proteins include components from all three major pathways, namely, the classical, alternative, and lectin pathways, and components of the early (C1q, C2, C4a, MASP1), middle (C3, C5a), and late (C6, C8) complement response, together with a receptor (CR1) and inhibitors (CFI, CD55). Among these proteins, AHSG, C3, and C5 were found with a relatively large regression coefficient of NEC. Combined, the complement response, such as increased abundance of C2, C3, C5a, decreased negative regulators, CR1 and CD55, suggests a possibility to detect the early NEC by changes in the complement cascade. A comprehensive study is required to investigate the actions of the complement system in NEC progression to ascertain any potential utility in NEC prediction or detection. Besides, more research is required to show if they are indeed among the earliest systemic signs of NEC progression, when clinical signs are unclear.

Besides the effect to kill or suppress microbes, antibiotics may have both local and systemic anti-inflammatory and vasomodulatory effects (6, 48). Our analyses showed that antibiotics altered blood hematology and biochemistry, such as monocyte counts and albumin levels, with similar effects from the two administration routes (PAR or ENT). Multiple proteins were affected by the antibiotic treatment alone, although corticosteroid-binding globulin (CBG) was also affected by NEC. Levels of CBG, the main cortisol-transporting protein in plasma, decreased during infection and sepsis (49). Lower plasma levels of CBG were found by us in preterm piglets with sepsis (50). In contrast, NEC lesions had limited effect on plasma CBG levels in this study. Similar trends of change at transcription level were found in the liver of these pigs, suggesting that at least part of the systemic CBG change in this study originated from liver effects. The proteomic analyzing technology adopted here can only detect the level of total CBG with no differentiation of the high- or low-affinity types. It is of interest to determine the NEC-related plasma level of high-affinity CBG (haCBG), and its relation to cortisol, as bioactive glucocorticoid levels may play a role in NEC progression and repair.

CONCLUSION

In preterm pigs, presence of NEC lesions was associated with numerous systemic plasma protein effects that may be the targets for developing new early biomarkers of NEC. Proteins with large NEC-related changes in abundance (large regression coefficient) were RBP4, FGA, AHSG, C3, C4A, PTPRG, and α-1-antichymotrypsin 2. More research is required to verify their

possible utility in indicating NEC in clinical conditions with varying gestational age, antibiotics usage, and feeding regimen, and in differentiating NEC from the conditions inducing systemic effects, but not related to gut complications, including bacteremia and sepsis.

DATA AVAILABILITY STATEMENT

The datasets presented in this study can be found in online repositories. The names of the repository/repositories and accession number(s) can be found in the article/**Supplementary Material**.

ETHICS STATEMENT

The animal study was reviewed and approved by The Danish National Committee of Animal Experimentation.

AUTHOR CONTRIBUTIONS

Y-NJ contributed to the data analysis and prepared the initial draft. TM conducted the follow-up validation works and contributed to data interpretation. AS conducted the proteomics analysis. DN participated in the animal experiment, prepared the proteomics samples, and contributed to result interpretation. PS conceived the experimental design, contributed to result interpretation, and manuscript preparation. P-PJ contributed to the experimental design, sample processing, data analysis, result interpretation, and manuscript preparation. All authors contributed to the article and approved the submitted version.

FUNDING

This study was sponsored by the Innovation Fund Denmark (the NEOMUNE and NEOCOL projects), The Danish National Mass Spectrometry Platform for Functional Proteomics (PRO-MS; grant no. 5072-00007B), the Obelske Family Foundation, and the Svend Andersen Foundation for the analyzing platform. TM was supported with a scholarship from the Guangzhou Elite Overseas Study Programme. P-PJ was supported by a start-up fund by the Sun Yat-sen University.

SUPPLEMENTARY MATERIAL

The Supplementary Material for this article can be found online at: https://www.frontiersin.org/articles/10.3389/fimmu.2020.565862/full#supplementary-material

Supplementary Figure 1 | NEC scores in the treatment groups.

Supplementary Table 1 | Macronutrient and mineral content of the parenteral nutrition and formula used.

Supplementary Table 2 | NEC scores in the treatment groups. CON, no antibiotic treatment; PAR, parenteral antibiotics administered; ENT, enteral antibiotics administered.

Supplementary Table 3 | Primer sequence of selected genes.

REFERENCES

1. Neu J, Walker WA. Necrotizing enterocolitis. *N Engl J Med.* (2011) 364:255–64. doi: 10.1056/NEJMra1005408
2. Hintz SR, Kendrick DE, Stoll BJ, Vohr BR, Fanaroff AA, Donovan EF, et al. Neurodevelopmental and growth outcomes of extremely low birth weight infants after necrotizing enterocolitis. *Pediatrics.* (2005) 115:696–703. doi: 10.1542/peds.2004-0569
3. Maheshwari A. Immunologic and hematological abnormalities in necrotizing enterocolitis. *Clin Perinatol.* (2015) 42:567–85. doi: 10.1016/j.clp.2015.04.014
4. Müller M, Paul T, Seeliger S. Necrotizing enterocolitis in premature infants and newborns. *J Neonatal Perinatal Med.* (2016) 9:233–42. doi: 10.3233/NPM-16915130
5. Stewart CJ, Nelson A, Treumann A, Skeath T, Cummings SP, Embleton ND, et al. Metabolomic and proteomic analysis of serum from preterm infants with necrotising entercolitis and late-onset sepsis. *Pediatr Res.* (2015) 79:425. doi: 10.1038/pr.2015.235
6. Birck MM, Nguyen DN, Cilieborg MS, Kamal SS, Nielsen DS, Damborg P, et al. Enteral but not parenteral antibiotics enhance gut function and prevent necrotizing enterocolitis in formula-fed newborn preterm pigs. *Am J Physiol Gastrointest Liver Physiol.* (2016) 310:G323–33. doi: 10.1152/ajpgi.00392.2015
7. Denning N-L, Prince JM. Neonatal intestinal dysbiosis in necrotizing enterocolitis. *Mol Med.* (2018) 24:4. doi: 10.1186/s10020-018-0002-0
8. Lodha A, Furlan AD, Whyte H, Moore AM. Prophylactic antibiotics in the prevention of catheter-associated bloodstream bacterial infection in preterm neonates: a systematic review. *J Perinatol.* (2008) 28:526. doi: 10.1038/jp.2008.31
9. Stewart CJ, Embleton ND, Marrs ECL, Smith DP, Nelson A, Abdulkadir B, et al. Temporal bacterial and metabolic development of the preterm gut reveals specific signatures in health and disease. *Microbiome.* (2016) 4:67. doi: 10.1186/s40168-016-0216-8
10. Cantey JB, Pyle AK, Wozniak PS, Hynan LS, Sánchez PJ. Early antibiotic exposure and adverse outcomes in preterm, very low birth weight infants. *J Pediatr.* (2018) 203:62–7. doi: 10.1016/j.jpeds.2018.07.036
11. Esaiassen E, Fjalstad JW, Juvet LK, van den Anker JN, Klingenberg C. Antibiotic exposure in neonates and early adverse outcomes: a systematic review and meta-analysis. *J Antimicrob Chemother.* (2017) 72:1858–70. doi: 10.1093/jac/dkx088
12. Li Y, Shen RL, Ayede AI, Berrington J, Bloomfield FH, Busari OO, et al. Early use of antibiotics is associated with a lower incidence of necrotizing enterocolitis in preterm, very low birth weight infants: The NEOMUNE-NeoNutriNet cohort study. *J Pediatr.* (in press). doi: 10.1016/j.jpeds.2020.06.032
13. Bury R, Tudehope D. Enteral antibiotics for preventing necrotizing enterocolitis in low birthweight or preterm infants. *Cochrane Database Syst Rev.* (2001) 2001:CD000405. doi: 10.1002/14651858.CD000405
14. Jensen ML, Thymann T, Cilieborg MS, Lykke M, Mølbak L, Jensen BB, et al. Antibiotics modulate intestinal immunity and prevent necrotizing enterocolitis in preterm neonatal piglets. *Am J Physiol Gastrointest Liver Physiol.* (2014) 306:G59–71. doi: 10.1152/ajpgi.00213.2013
15. Pan X, Gong D, Nguyen DN, Zhang X, Hu Q, Lu H, et al. Early microbial colonization affects DNA methylation of genes related to intestinal immunity and metabolism in preterm pigs. *DNA Res.* (2018) 25:287–96. doi: 10.1093/dnares/dsy001
16. Nguyen DN, Fuglsang E, Jiang P, Birck MM, Pan X, Kamal SBS, et al. Oral antibiotics increase blood neutrophil maturation and reduce bacteremia and necrotizing enterocolitis in the immediate postnatal period of preterm pigs. *Innate Immun.* (2016) 22:51–62. doi: 10.1177/1753425915615195
17. León IR, Schwämmle V, Jensen ON, Sprenger RR. Quantitative assessment of in-solution digestion efficiency identifies optimal protocols for unbiased protein analysis. *Mol Cell Proteomics.* (2013) 12:2992–3005. doi: 10.1074/mcp.M112.025585

18. Cox J, Mann M. MaxQuant enables high peptide identification rates, individualized p.p.b.-range mass accuracies and proteome-wide protein quantification. *Nat Biotechnol.* (2008) 26:1367. doi: 10.1038/nbt.1511
19. Tyanova S, Temu T, Sinitcyn P, Carlson A, Hein MY, Geiger T, et al. The Perseus computational platform for comprehensive analysis of (prote)omics data. *Nat Methods.* (2016) 13:731. doi: 10.1038/nmeth.3901
20. R CoreTeam. *R. A Language and Environment for Statistical Computing.* R Foundation for Statistical Computing, Vienna. (2013).
21. RStudioTeam. *R Studio: Integrated Development for R.* Boston, MA: RStudio, Inc. (2012).
22. Silver N, Best S, Jiang J, Thein SL. Selection of housekeeping genes for gene expression studies in human reticulocytes using real-time PCR. *BMC Mol Biol.* (2006) 7:33. doi: 10.1186/1471-2199-7-33
23. Pinheiro J, Bates D, DebRoy S, Sarkar D, Team RC. *nlme: Linear and Nonlinear Mixed Effects Models*. R package version 3.1–141. (2019). Available online at: https://CRAN.R-project.org/package=nlme
24. Pollard KS, Dudoit S, van der Laan MJ. Multiple testing procedures: R multtest package and applications to genomics. In Gentleman R, Carey V, Huber W, Irizarry R, Dudoit S editors, *Bioinformatics and Computational Biology Solutions Using R and Bioconductor*. (2005). pp. 251–72.
25. Kucera M, Isserlin R, Arkhangorodsky A, Bader G. AutoAnnotate: a Cytoscape app for summarizing networks with semantic annotations. *F1000Res.* (2016) 5:1717. doi: 10.12688/f1000research.9090.1
26. Shannon P, Markiel A, Ozier O, Baliga NS, Wang JT, Ramage D, et al. Cytoscape: a software environment for integrated models of biomolecular interaction networks. *Genome Res.* (2003) 13:2498–504. doi: 10.1101/gr.1239303
27. Kuusela P, Saraswat M, Joenväärä S, Kaartinen J, Järvinen A, Renkonen R. Changes in plasma protein levels as an early indication of a bloodstream infection. *PLoS ONE.* (2017) 12:e0172987. doi: 10.1371/journal.pone.0172987
28. Martin CR, Bellomy M, Allred EN, Fichorova RN, Leviton A. Systemic inflammation associated with severe intestinal injury in extremely low gestational age newborns. *Fetal Pediatr Pathol.* (2013) 32:222–34. doi: 10.3109/15513815.2012.721477
29. Bonnans C, Chou J, Werb Z. Remodelling the extracellular matrix in development and disease. *Nat Rev Mol Cell Biol.* (2014) 15:786–801. doi: 10.1038/nrm3904
30. Pender SLF, Braegger C, Günther U, Monteleone G, Meuli M, Schuppan D, et al. Matrix metalloproteinases in necrotising enterocolitis. *Pediatr Res.* (2003) 54:160–4. doi: 10.1203/01.PDR.0000072326.23442.C3
31. Sumagin R, Parkos CA. Epithelial adhesion molecules and the regulation of intestinal homeostasis during neutrophil transepithelial migration. *Tissue Barr.* (2014) 3:e969100. doi: 10.4161/21688362.2014.969100
32. Maitra SR, Jacob A, Zhou M, Wang P. Modulation of matrix metalloproteinase-9 and tissue inhibitor of matrix metalloproteinase-1 in sepsis. *Int J Clin Exp Med.* (2010) 3:180–5.
33. Lorente L, Martín MM, Labarta L, Díaz C, Solé-Violán J, Blanquer J, et al. Matrix metalloproteinase-9,−10, and tissue inhibitor of matrix metalloproteinases-1 blood levels as biomarkers of severity and mortality in sepsis. *Crit Care.* (2009) 13:R158. doi: 10.1186/cc8211
34. Pirillo A, Catapano AL, Norata GD. HDL in infectious diseases and sepsis. In: von Eckardstein A, Kardassis D, editors. *High Density Lipoproteins: From Biological Understanding to Clinical Exploitation.* Cham: Springer International Publishing (2015) p. 483–508.
35. Yildiz B, Ucar B, Akşit A, Aydogdu SD, Colak O, Colak E. Diagnostic values of lipid and lipoprotein levels in late onset neonatal sepsis. *Scand J Infect Dis.* (2009) 41:263–7. doi: 10.1080/00365540902767056
36. Devarajan A, Shih D, Reddy ST. Inflammation, infection, cancer and all that…the role of paraoxonases. *Adv Exp Med Biol.* (2014) 824:33–41. doi: 10.1007/978-3-319-07320-0_5
37. Camps J, Iftimie S, García-Heredia A, Castro A, Joven J. Paraoxonases and infectious diseases. *Clin Biochem.* (2017) 50:804–11. doi: 10.1016/j.clinbiochem.2017.04.016
38. Paciullo F, Fallarino F, Bianconi V, Mannarino MR, Sahebkar A, Pirro M. PCSK9 at the crossroad of cholesterol metabolism and immune function during infections. *J Cell Physiol.* (2017) 232:2330–8. doi: 10.1002/jcp.25767
39. Howard KM, Olson MS. The expression and localization of plasma platelet-activating factor acetylhydrolase in endotoxemic rats. *J Biol Chem.* (2000) 275:19891–6. doi: 10.1074/jbc.M001462200
40. Caplan MS, Sun X-M, Hsueh W, Hageman JR. Role of platelet activating factor and tumor necrosis factor-alpha in neonatal necrotizing enterocolitis. *J Pediatr.* (1990) 116:960–4. doi: 10.1016/S0022-3476(05)80661-4
41. Caplan MS, Simon D, Jilling T. The role of PAF, TLR, and the inflammatory response in neonatal necrotizing enterocolitis. *Semin Pediatr Surg.* (2005) 14:145–51. doi: 10.1053/j.sempedsurg.2005.05.002
42. Giuliani S, Tan Y-W, Zheng D, Petropoulou E, Sohail A, Bradley S, et al. Coagulation gene expression profiling in infants with necrotizing enterocolitis. *J Pediatric Gastroenterol Nutr.* (2016) 63:e169–75. doi: 10.1097/MPG.0000000000001215
43. Semeraro N, Ammollo C, Semeraro F, Colucci M. Coagulopathy of acute sepsis. *Semin Thromb Hemost.* (2015) 41:650–8. doi: 10.1055/s-0035-1556730
44. Castoldi E, Hackeng TM. Regulation of coagulation by protein S. *Curr Opin Hematol.* (2008) 15:529–36. doi: 10.1097/MOH.0b013e328309ec97
45. El Beshlawy A, Alaraby I, Abou Hussein H, Abou-Elew HH, Mohamed Abdel Kader MSE. Study of protein C. protein S, and antithrombin III in newborns with sepsis. *Pediatr Crit Care Med.* (2010) 11:52–9. doi: 10.1097/PCC.0b013e3181c59032
46. Kosuke K, Hidenori W, Shuji M, Shiro H, Masahiro N, Hiroshi M. Decrease in histidine-rich glycoprotein as a novel biomarker to predict sepsis among systemic inflammatory response syndrome. *Crit Care Med.* (2018) 46:570–6. doi: 10.1097/CCM.0000000000002947
47. Shah BA, Migliori A, Kurihara I, Sharma S, Lim Y-P, Padbury J. Blood level of inter-alpha inhibitor proteins distinguishes necrotizing enterocolitis from spontaneous intestinal perforation. *J Pediatr.* (2017) 180:135–40.e1. doi: 10.1016/j.jpeds.2016.09.016
48. Mencarelli A, Distrutti E, Renga B, Cipriani S, Palladino G, Booth C, et al. Development of non-antibiotic macrolide that corrects inflammation-driven immune dysfunction in models of inflammatory bowel diseases and arthritis. *Eur J Pharmacol.* (2011) 665:29–39. doi: 10.1016/j.ejphar.2011.04.036
49. Bae YJ, Kratzsch J. Corticosteroid-binding globulin: modulating mechanisms of bioavailability of cortisol and its clinical implications. *Best Pract Res Clin Endocrinol Metab.* (2015) 29:761–72. doi: 10.1016/j.beem.2015.09.001
50. Muk T, Stensballe A, Pankratova S, Nguyen DN, Brunse A, Sangild PT, et al. Rapid proteome changes in plasma and cerebrospinal fluid following bacterial infection in preterm newborn pigs. *Front Immunol.* (2019) 10:2651. doi: 10.3389/fimmu.2019.02651

Conflict of Interest: The authors declare that the research was conducted in the absence of any commercial or financial relationships that could be construed as a potential conflict of interest.

frontiers in Immunology

ORIGINAL RESEARCH
published: 28 October 2020
doi: 10.3389/fimmu.2020.568978

Protective Intranasal Immunization Against Influenza Virus in Infant Mice Is Dependent on IL-6

Elizabeth Ann Bonney[1], Kendall Krebs[1], Jihye Kim[2], Kirtika Prakash[1], Blake L. Torrance[3], Laura Haynes[3] and Mercedes Rincon[4,5]*

[1] Department of Obstetrics, Gynecology and Reproductive Sciences, Larner College of Medicine, University of Vermont, Burlington, VT, United States, [2] Division of Medical Oncology, Department of Medicine, University of Colorado, Anschutz Medical Campus, Aurora, CO, United States, [3] Department of Immunology, University of Connecticut Center on Aging, Farmington, CT, United States, [4] Division of Immunobiology, Department of Medicine, Larner College of Medicine, University of Vermont, Burlington, VT, United States, [5] Department of Immunology and Microbiology, University of Colorado Anschutz Medical Campus, Aurora, CO, United States

Respiratory diseases adversely affect infants and are the focus of efforts to develop vaccinations and other modalities to prevent disease. The infant immune system differs from that of older children and adults in many ways that are as yet ill understood. We have used a C57BL/6 mouse model of infection with a laboratory- adapted strain of influenza (PR8) to delineate the importance of the cytokine IL-6 in the innate response to primary infection and in the development of protective immunity in adult mice. Herein, we used this same model in infant (14 days of age) mice to determine the effect of IL-6 deficiency. Infant wild type mice are more susceptible than older mice to infection, similar to the findings in humans. IL-6 is expressed in the lung in the early response to PR8 infection. While intramuscular immunization does not protect against lethal challenge, intranasal administration of heat inactivated virus is protective and correlates with expression of IL-6 in the lung, activation of lung CD8 cells, and development of an influenza-specific antibody response. In IL-6 deficient mice, this response is abrogated, and deficient mice are not protected against lethal challenge. These studies support the importance of the role of the tissue environment in infant immunity, and further suggest that IL-6 may be helpful in the generation of protective immune responses in infants.

Keywords: infant, influenza, mouse, vaccination, lung

OPEN ACCESS

Edited by:
Per T. Sangild, University of Copenhagen, Denmark

Reviewed by:
Egídio Torrado, University of Minho, Portugal
Gunnveig Grødeland, University of Oslo, Norway

****Correspondence:***
Elizabeth Ann Bonney
elizabeth.bonney@med.uvm.edu

Specialty section:
This article was submitted to Vaccines and Molecular Therapeutics, a section of the journal Frontiers in Immunology

Received: *02 June 2020*
Accepted: *05 October 2020*
Published: *28 October 2020*

Citation:
Bonney EA, Krebs K, Kim J, Prakash K, Torrance BL, Haynes L and Rincon M (2020) Protective Intranasal Immunization Against Influenza Virus in Infant Mice Is Dependent on IL-6. Front. Immunol. 11:568978. doi: 10.3389/fimmu.2020.568978

INTRODUCTION

Respiratory tract inflammatory and infectious disease in infant children represents a significant burden to the healthcare system (1, 2). A particular example is influenza virus infection, for which there is evidence of increased incidence of disease severity in infants, as compared to adults in humans and animal models (3, 4). Classic theory suggests that adaptive immunity, predominantly the T cell immune response, is altered in infants in order to support self-tolerance, maternal

tolerance, and tolerance to new developmental or environmental antigen (5–7). More recent thinking about infant immunity considers the possibility of distinct populations of T cells present in the infant, but not in the adult, that display a "tolerance" phenotype (8). Alternative models suggest that T cells in neonates/infants are not inherently tolerant, but that tissue specific signals can affect T cell activation and effector function by limiting or supporting the access to productive antigenic signals (9–17).

The role of the tissue environment (independently of the immune cells) in which specific immune responses occur could also be an important factor that affects the immune response in neonates/infants (10, 18). Specifically, for influenza virus and other respiratory infections, the epithelium of the respiratory tract provides a unique environment that can tune adaptive immune responses. Lung epithelial cells are a major source of type I IFN which plays a critical role in antiviral responses (19). In addition, lung epithelial cells can produce a variety of inflammatory cytokines (e.g., IL-6) that can influence the course of T cell responses (19). Lung epithelial cells in infants differ from those in adults in humans (20–23) and animals (24). The potential effect of lung epithelial cells in the immune responses of infants is a recent area of inquiry, and could be a significant determining factor in their apparent altered immune response during influenza virus infection.

Although intramuscular administration of a polyvalent formulation of chemically inactivated or disrupted influenza virus is the most common type of vaccine for seasonal influenza both in adults and children (25), intranasal administration of a live attenuated influenza virus (LAIV) in the respiratory tract is also utilized as a method of vaccination (26). However, this formulation is restricted to children more than 2 years of age and adults (27, 28) because of reports of increased risk of reactive airway disease (29, 30) and increased concern over the presence of underlying asthma in young vaccine recipients (31, 32). The factors underlying the relatively lower effectiveness of recent intranasal vaccination with live attenuated virus compared to intramuscular administration of inactivated virus in some flu seasons (33–35) remain incompletely understood. Together, these issues elevate the question of whether there might be novel specific mechanisms or alternative approaches to enhance influenza vaccination in the very young. Similar to the response to respiratory virus infection, lung epithelium could also play a key role in determining the type and strength of the immune response that intranasal immunizations can trigger.

Interleukin 6 (IL-6) is a member of a family of cytokines that play an important role in both innate and adaptive immune responses (36). In addition, IL-6 is important in the processes of tissue regeneration and inhibition of apoptosis (37). IL-6 is produced by innate immune cells such macrophages, but it is also produced by a variety of cell types (e.g. epithelial cells, endothelial cells, astrocytes) upon exposure to insults (36). For example, we and others have shown that IL-6 is produced by lung epithelial cells in response to viral infection or allergens (38, 39). In adult mice, IL-6 can enhance T-cell mediated antibody response against i.m. influenza immunization (40) and there is evidence supporting the importance of IL-6 in the early response to influenza infection (41). However, the specific importance of IL-6 in infant immunity to influenza is less clear (42).

Here, we have performed gene expression profiling studies comparing lung epithelial cells from infant and adult mice and the results have revealed a compromised expression of IL-6 and related signaling pathways in infant lung epithelial cells. Using a heat-inactivated influenza virus, as a surrogate for current attenuated virus formulations, we show that i.m. administration in infant mice does not provide protection, while intranasal administration does. However, such protection induced by i.n. immunization is dependent on IL-6. Thus, these studies underline the relevance of the tissue environment for the efficacy of vaccinations in infants, and they bring to light potential mechanisms related to differences in infant and adult lung epithelium that could influence the efficacy of immunizations. Our results could be relevant for future improvement of vaccines for young children.

MATERIAL AND METHODS

Mice

C57BL/6J (wild type, WT obtained from Jackson Laboratory) or IL-6 KO mice (43) were housed under specific pathogen free, AAALAC-approved conditions using a 12-h light cycle and were given food (normal Chow) and water ad libitum. IL-6 KO mice used in these studies were backcrossed over 12 generation with C57Bl/6J. Females of both strains and 8-24 weeks of age mated freely with same strain males and littered without interference. Thirteen to fourteen days after birth, while still nursing, mothers and infant mice moved to a biosafety room, where they acclimated for 12–24 h before infection or immunization of the pups.

Influenza Virus Infections and Immunizations

These studies utilized Puerto Rico A/PR/8/34 H1N1 influenza A (PR8) (41). Intranasal and intramuscular immunizations utilized heat inactivated PR8 influenza virus (iPR8). Inactivation was performed by incubation at 56 degrees for 30 min. This method of inactivation allows production of a virus that enters cells, since it does not fully denature the HA protein of the virus, but which does not replicate since the virus polymerase is made inactive at this and lower temperatures (44, 45). iPR8 (5×10^5 EIU) in 15–20 or 50 µl PBS was used for intranasal or intramuscular immunizations, respectively. The average weight was 5.9+/–0.15 g at 14–16 days of life and this was not statistically different from any experimental group (**Supplementary Figure S1**). In two experimental cohorts, mice were euthanized three weeks after immunization to collect tissues for *in vitro* examination of the immune response to immunization.

For lethal challenge in juvenile mice (day 35–48 of life) we used 6×10^3 EIU PR8 given intranasally in 50 µl of PBS. For the batch of PR8 virus used in these studies, 10^4 EIU corresponded to 2 LD50 when initially tested in adult mice (8–10 weeks of age). For juvenile mice between 30–45 days of age, we found

6 x 10^3 EIU PR8, could be equivalent to the 2 LD50 in adult mice (**Supplementary Table I**). Female mice weighed 16±1gram and males weighed 20±1gram at the time of challenge. Mice underwent inhalant anesthesia (1.5 L/min O2, 2% isoflurane) in a chamber connected to an isoflurane vaporizer to receive intranasal immunizations or infections with live virus. Infected mice were weighed every 24–48 h. Mice reaching below 70% of starting weight were euthanized consistent with stipulations of our animal use protocol (University of Vermont IACUC# 13-029). Therefore "survival" in these studies indicates mice who did not fall below this threshold. Though males of each group at challenge were heavier than same strain females, the weights of WT and IL6KO females and those of WT and IL6KO males were comparable (**Supplementary Figure S2**). To account for male and female weight differences, males were challenged with higher doses. **Supplementary Figure S3** shows a representative sample of the weight of WT females who were challenged with virus.

Determination of Influenza Viral Load in Tissues

Lungs from assayed mice were freshly harvested and frozen in liquid nitrogen. RNA was isolated from whole lung tissue homogenized in TRIzol reagent (Invitrogen Life Technologies). cDNA was synthesized using iScript cDNA synthesis kit (Bio-Rad Laboratories), using the manufacturer's protocol. Viral loads in harvested whole lungs were determined by real-time RT-PCR for the PR8 viral acid polymerase (PA) gene by comparison to a standard titration of viral PA copies run on the same PCR assay, with 20ng of cDNA used per reaction. The following primers and probe were used to amplify and quantitate the PR8 PA gene: forward primer, 5′-CGGTCCAAATTCCTGCTGA-3′; reverse primer, 5′- CATTGGGTTCCTTCCATCCA-3′; probe, 5′-6-FAM-CCAAGTCATGAAGGAGAGGGAATACCGCT-3′ (Integrated DNA Technologies) (41).

Cytokine Gene Expression

In alternate RNA isolation protocols, the Qiagen RNeasy Mini kit (PN 74104) was utilized as recommended by the manufacturer. cDNA was synthesized as above. Relative mRNA levels were determined by qRT-PCR using Assays–on–Demand TaqMan Gene Expression Assays (FAM-MGB, ThermoFisher Scientific https://www.thermofisher.com) for IL-6(Mm00446190), CCL2 (Mm00441242), γIFN(Mm01168134), IL-10(Mm01288386), TNF (Mm00443258), TGFB1 (Mm01337605), and Beta-2 microglobulin (Mm00437762). Values reported are those obtained after normalization to β2–microglobulin and analyzed by the comparative delta CT method. In addition, serum cytokines were quantified using a Luminex ® xMAP® multiplex platform, combined with a customized Milliplex™ mouse chemokine/cytokine panel from Millipore™.

Analysis of Anti-Influenza Virus Specific Antibodies in Serum by ELISA

Influenza-specific antibody levels in serum samples were determined by ELISA, as previously described (40). ELISA plates were coated with inactive influenza PR8 virus (10^7 EIU/ml) in sodium bicarbonate buffer, washed, blocked (1% BSA/PBS solution) and incubated with 2-fold serial dilutions of serum overnight. Plates were washed and incubated with HRP-conjugated goat anti-mouse total IgG (SouthernBiotech) for 45 min at room temperature. Plates were then washed and developed using TMB Sureblue substrate and development was stopped with TMB stop solution (ThermoFisher). Plates were read at 450 nm in a plate reader.

Flow Cytometry Analyses of Lungs

Whole lungs harvested from immunized mice were used to prepare single cell suspensions using the gentle MACS™ (Miltenyi Biotech) tissue dissociation system. Red cells were removed with Geyes lysis medium and the resulting cell suspensions were washed in Iscove's Modified Dulbecco's medium with 5% FBS. Cell suspensions were stained with antibodies to CD45 (CD45.2, clone 104, PerCP-Cy™ 5.5), CD8(CD8α clone 53–6.7, Pacific Blue™) CD4 (clone GK1.5, R-phycoerythrin) and CD44 (clone IM7 fluorescein isothiocyanate) and were run on an LSRII (BD Biosciences). The gating scheme for these studies is shown in **Supplementary Figure S5**.

Lung Epithelial Cell Gene Expression Analysis

Four samples, each consisting of pooled epithelial cells from the lungs of three male pups or three female pups aged 14 days (total eight pups samples), or epithelial cells from four individual male and four female adult (eight weeks) lungs (eight adult samples total) were used to isolate RNA and examined by array transcriptome profiling. Mice were euthanized by cervical dislocation. Lungs were removed under sterile conditions into 1X PBS and cut up into very small pieces. Tissues were transferred to MACS C-tubes (purple tubes) for homogenization using the gentle MACS™ (Miltenyi Biotech) tissue dissociation system. Red cells were removed by treatment with Geye's solution, and this was followed by resuspension in DMEM/F12+ 5% FBS. The resulting cell suspension was incubated in a cell culture plate at 37C degrees and 5% CO2. Afterwards, nonadherent epithelial cells were removed by slowly rocking the plate back and forth and gently removing the supernatant. This was centrifuged, resuspended and washed in MACS™ buffer and then incubated with anti-CD45 (Miltenyi) beads to remove CD45 + cells by passing the incubated solution on a magnetized LS column (Miltenyi). Purity was checked by flow cytometry for CD45 (less than 5 %) and histochemical identification of keratin + cells. Transcriptome profiling was done using the Affymextrix GeneChip system (Mouse Gene 2.0 ST Array). Chip quality was verified, and scan data was analyzed using RMA (46). Analysis of array data was performed using Partek Genomics Suite® 6.6. Beta Analysis. We report comparisons between groups using the number of probe sets that pass an FDR of 0.05, or a binary filter ($p<0.05$ and 2x fold change).

Functional Analysis

We used GSEA (Gene Set Enrichment Analysis) and pathway analysis, an approach that offers an unbiased global search for genes that are coordinately regulated in predefined pathways (47) rather than interrogating expression differences of single genes. Gene set analysis was performed using the GSEA software (48)

version 4.0.3 obtained from https://www.gsea-msigdb.org/gsea/downloads.jsp. The gene sets database was compiled from the Kyoto Encyclopedia of Genes and Genomes (KEGG) database http://www.kegg.jp/ (47). The KEGG gene sets database contains 210 mouse pathways that include metabolism, genetic information processing, environmental information processing, cellular processes, and human diseases. One hundred eight-eight gene sets passed the gene set size filter criteria (min, 10; max, 500). *P* values for the gene sets were computed by permuting the gene sets 1,000 times in this study.

Additional Statistical Analysis

Viral load, cytokine levels, and antibody level were compared using one-way ANOVA or nonparametric analysis as appropriate. Due to small numbers, most normality testing used the Shapiro-Wilk test. Survival analysis with threshold being weight below 70% of starting (point at which we were compelled to euthanize mice) was performed using the log-rank (Mantel-Cox) test. Data shown represents survival analysis of combined data of percentage of initial weight over time from challenge from over 8 cohorts of mice that received immunization and or challenge as indicated. Means± SEM or Median with range are reported, depending on the hypothesis test used. For hypothesis testing, significance was set at $p<0.05$.

RESULTS

High Mortality to Sublethal Dose of Influenza Virus in Infant Mice

Similar to humans, infection with a sublethal dose of influenza virus in adult mice leads through a period of sickness during the peak of virus replication, and eventual recovery upon virus clearance from the lung. Several lines of evidence suggest that children less than five years of age are more susceptible to seasonal influenza virus infection (3, 49) and this led us to first investigate the age-related susceptibility of infant mice to influenza. We performed viral infection in mice 10–44 days old with different doses of PR8 influenza virus. Because the size of the lungs is determined by the body size of the mouse, we used different doses to normalize by weight. As we have shown (41), nearly all young adult (~5 weeks of age) mice survived infection with a sublethal dose of influenza (**Figure 1** and **Supplementary Table 1**). When we infected 24-day-old mice with same viral dose/weight ratio, we observed a small fraction of mortality (**Figure 1** and **Supplementary Table 1**). In contrast, infection of 10 day or 14–16-day-old mice with a comparative viral dose/weight ratio caused ~75% mortality (**Figure 1** and **Supplementary Table 1**). Thus, when corrected for body size, infants are highly susceptible to an otherwise sublethal dose of PR8 virus infection.

Intranasal, but Not Intramuscular, Immunization With Inactive Influenza Virus Provides Protection in Infant Mice

Because very young children, like infant mice examined above, are more susceptible to death with influenza virus, there has been pressure to identify the most appropriate and efficacious way to immunize them against influenza. However, existing practical, clinical, and biologic limitations on the type of influenza vaccine that is currently provided to very young children make this issue a subject of intense investigation. We therefore used our mouse model above to determine a route and format of immunization that could protect infant mice against lethal infection. Because most children only receive an intramuscular injection of influenza vaccine, often with minor benefit (50), we compared

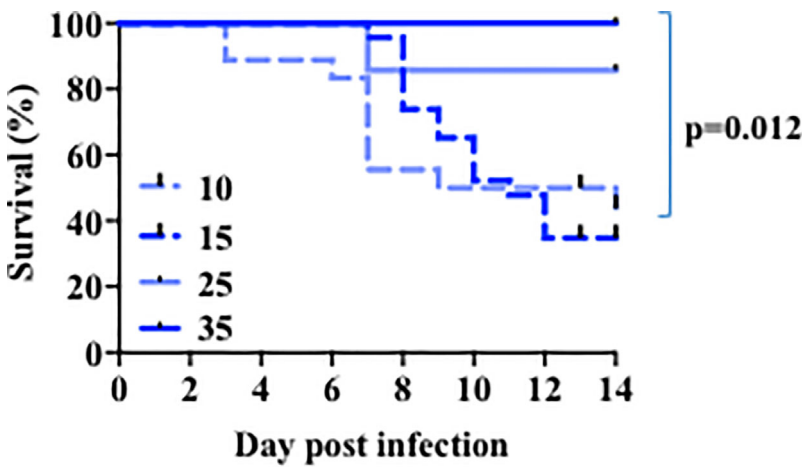

FIGURE 1 | Age-related susceptibility to a sublethal dose of PR8 influenza virus. The 10 days-old mice group (n=18) received 140-200 EIU (~30 EIU per gram of weight) of live PR8 influenza virus, the 15 days-old mice group (n=23) received 200 EIU (~30 EIU per gram of weight), the 25 days-old mice group (n=7) received 300–900 EIU (~30 EIU per gram of weight), the 35 days-old mice group (n=6) received 3000 EIU (~ 200 EIU per gram of weight). Survival was followed. Solid lines, older mice. Dotted lines, infant mice. p value, comparison of curves for day 15 and 35 by Mantel-Cox test. Analysis is of total data obtained from 12 independent cohorts of mice.

both intramuscular (i.m.) and intra-nasal (i.n.) modes of vaccination. Two-week-old mice were immunized with heat-inactivated PR8 virus (5×10^5 EIU/mouse) through i.m. or i.n. administration. As a control, we also included a group of infant mice that received no immunization. Three weeks post-immunization, mice were challenged with a lethal dose of influenza PR8 virus. The mice were observed for weight loss and clinical signs of severe illness as parameters to determine mortality. Mortality in mice immunized by i.m. administration was comparable to the mortality of mice that received no immunization (**Figure 2**), indicating that i.m. immunization does not provide protection from a lethal dose of PR8 virus. In contrast, relative to i.m. immunized and unimmunized mice, those mice immunized through i.n. administration of the same inactive PR8 influenza virus have better survival to the infection with the lethal dose of influenza virus (**Figure 2**). Thus, i.n. administration of the inactive virus provides superior protection in infant mice to influenza virus infection.

Gene Expression Profile Analysis Reveals the Attenuation of IL-6 Gene Expression in Lung Epithelial Cells for Infant Relative to Adult Mice

The increased protection obtained through an intranasal administration of iPR8 relative to the lack of protection with the intramuscular administration suggests that there is some specific component in the lung which supports the immune response. In addition, the fact that infants are more susceptible than adult mice to primary influenza infection (**Figure 1**), suggested that there may be tissue specific differences, the adaptive immune response notwithstanding, that are critical for resolution of infection in infant as compared to older mice. Lung epithelial cells are capable of producing a number of cytokines in response to different insults (e.g. viral infection) (19). To investigate the presence of potential underlining differences between infant and adult lung epithelial cells we performed microarray analyses. We used RNA from lung epithelial cells freshly isolated from naïve infant (2 weeks-old mice) and adult (8 weeks-old mice) mouse lungs. Each pup sample (eight total, four male and four female) included pooled lung epithelial cell RNA preparation from 3 pups, while each adult sample (eight total, four male and four female) contained RNA from a single adult.

Analyses of the microarray results revealed that the number of probe sets that pass an FDR of 0.05 as being differentially expressed in infant versus adult epithelial cells was 7,334. Those passing a binary filter (FDR <0.05 and 2x fold change) were 724. Gene Set Enrichment Analysis and the KEGG database were used to determine pathways that were significantly differently expressed in infant versus adult cells using a criterion of p-value (<0.05) and NES (> |1.5|).

We focused further attention on those immune-related pathways that might be relevant to influenza and that were significantly of lower expression in infant cells as compared to adult. Several pathways were identified. One of the pathways markedly (p= 0.0004) lower in infants was the "cytosolic DNA-sensing pathway" that includes host genes involved in sensing bacteria and viruses such as members of the inflammasome pathway, RIG pathway, type I IFN, chemokines, NF-kB and some cytokines (**Figure 3A** and **Supplementary Figure S6A**). Within-pathway analysis defined a cluster of genes with lower expression in epithelial cells from the lungs of infants relative to adult mice (**Figure 3A**, **Supplementary Figure S6A**). Interestingly, IL-6 was the gene most significantly lower in lung epithelial cells from infants (**Figure 3A**, **Supplementary Figure S6A**). Upon binding to its receptor, IL-6 activates the Jak/Stat pathway leading to the activation of Stat3 (51). The KEGG "Jak/Stat pathway" was also substantially under-expressed in lung epithelial cells from infants relative to adult mice (**Figure 3B**, **Supplementary Figure S6B**). This

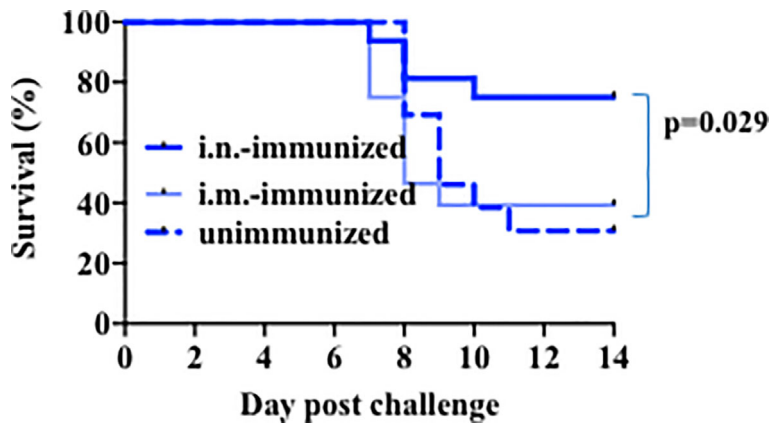

FIGURE 2 | Intranasal immunization with heat inactivated virus protects infant mice against lethal challenge. Mice aged 14–17 days of life were immunized intranasally (Bold Dk blue, n=16) or intramuscularly (Lt blue, n=28) with 5×10^5 EIU heat inactivated PR8 virus, or left unimmunized (dotted lines, n=13). Three weeks later, all mice received a lethal dose of live virus. Y axis: Survival. Mantel-Cox (log-rank) analysis was used to compare unimmunized to i.n.-immunized mice. Significance was set at p<0.05. Analysis is of total data obtained from 8 independent cohorts of mice receiving immunization and or challenge.

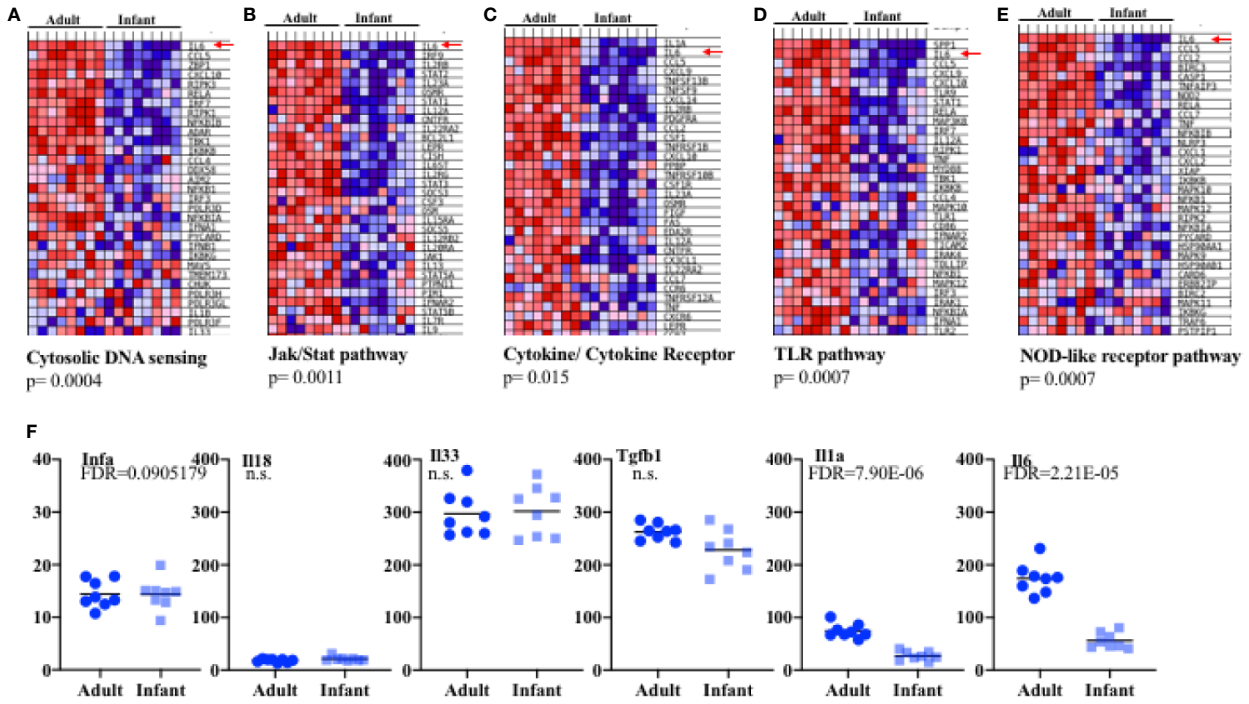

FIGURE 3 | Expression profiling in epithelial cells from infant and adult mice reveals IL-6 deficiency at baseline. Four samples each consisting of pooled epithelial cells from the lungs of three male pups or three female pups aged 14 days (total eight pups samples) or epithelial cells from four individual male and four female adult (8 weeks) lungs (eight adult samples total) were used to isolate RNA and examined by array transcriptome profiling. Gene Set Enrichment Analysis (eight total pools per group) revealed significant differences in expression in pathways relevant to innate immunity. **(A–E)** Shown are heat maps for the most highly differentially expressed genes within the various pathways. Red-up regulated, blue down regulated. Red Arrows: IL-6. *P* values for the gene sets were computed by permuting the gene sets 1,000 times. **(F)** Transformed RMA data for specific genes in infant versus adult epithelial cell pools. Each symbol refers to a pool of 3 mice. FDR, fold discovery rate (reflecting comparison of groups of pools with modification for multiple comparison testing as part of the array analysis) was calculated using Partek Suites Genomics® 6.6 Beta Analysis.

pathway includes genes for cytokines, cytokine receptors, transcription factors, kinases etc. Among them, IL-6 was on the top of the cluster of genes that were significantly lower in epithelial cells from infants (**Figure 3B**, **Supplementary Figure S6B**). The "Cytokine-cytokine receptor interaction" pathway, containing a number of genes for cytokines/chemokines and their receptors, was also observed to be significantly decreased and IL-6 together with IL-1 were the genes with the lowest expression in infant lung epithelial cells relative to the expression found in adult mice (**Figure 3C**, **Supplementary Figure S6C**). Two other innate immune pathways were identified to be significantly lower in infants. One was the "TLR signaling pathway" that includes pattern recognition receptors responsible for detecting microbial pathogens and generating innate immune responses including molecules such as type I IFN, NF-kB, and inflammatory cytokines (**Figure 3D**, **Supplementary Figure S6D**). Another was the NOD-like receptor (NLR) signaling pathway that includes intracellular NLR family members, cytokines regulated by this pathway, caspases, NF-kB, and others (**Figure 3E**, **Supplementary Figure S6E**). Of interest, among all the different genes included in these two pathways, IL-6 was identified as the gene most reduced in lung epithelial cells in infants (**Figures 3D, E**, **Supplementary Figures S6D, E**). Additional comparative modeling for specific cytokines known to be produced by lung epithelial cells further demonstrated selectively reduced expression of IL-6 in infant cells (**Figure 3F**). We did not observe significant differences in the expression of innate cytokine genes well-known to be expressed in epithelial cells (e.g., IFNa, IFNb, IL-33, IL-18, **Figures 3C, F**, **Supplementary Figure S6C**). We have previously shown a constitutive expression of IL-6 (high levels of IL-6 mRNA) in lung epithelial cells isolated from adult wildtype mice under physiological conditions prior to any exposure or insult (38), while no expression was detected in resident leukocytes ($CD45^+$ cells) (38). The results here show that IL-6 gene expression in lung epithelial cells is regulated during development and its expression is attenuated in infants.

Protection of Infant Mice by Intranasal Immunization With Inactive Influenza Virus Requires IL-6

Administration of IL-6 has been shown to enhance the effectiveness of a subcutaneous inactive influenza virus vaccine in adult mice (40). IL-6 derived from lung epithelial cells could therefore contribute to the protective effect of intranasal vaccines. Since the basal levels of IL-6 gene expression in lung epithelial cells in infants was significantly lower when compared to adults, we examined whether i.n. administration of the

inactive influenza virus vaccine could upregulate IL-6 expression. Two-week-old mice were administered with an i.n. dose of inactive PR8 virus and the lung was harvested 2 days post-immunization for cytokine expression. Relative to the levels in lung from non-immunized mice, higher levels of IL-6 expression were present in lungs from i.n.-immunized mice (**Figure 4A**). In contrast, we did not observe an increase in other cytokines, such as TGFβ, in lungs from immunized infants (**Figure 4B**). Thus, i.n. administration of an inactive influenza virus selectively induced IL-6 expression, suggesting that local production of IL-6 in the lung could contribute to the protective effect of i.n. administration relative to i.m. administration.

We next investigated the contribution of IL-6 to the protective effect of i.n. immunization with inactive influenza. IL-6-deficient infants (2 weeks-old) were i.n.-immunized with inactive PR8 virus as described above for wildtype mice, or mice were left with no immunization. Three weeks post-immunization, both immunized and non-immunized mice were challenged with a lethal dose of PR8 virus. Intranasal immunization in IL-6-deficient mice resulted in mortality similar to that observed in unimmunized mice (**Figures 4C, D**) with more than 50% of mice dying by 10 days after challenge. This was true for both females (**Figure 4C**) and males (**Figure 4D**). In contrast to WT female mice (**Figure 2**) and WT male mice (**Figure 4D**), i.n. administration of inactive PR8 fails to provide protection in IL-6 KO mice, suggesting that the success of an i.n. immunization with inactive virus relies significantly on IL-6 production in the lung.

Lack of IL-6 Does Not Cause an Exuberant Systemic Immune Response to Influenza Virus Infection

The results above show that i.n.-immunized IL-6 KO infants experience significant mortality in response to a lethal dose of PR8 influenza virus, while immunized WT infants are significantly protected. The ultimate increased mortality in IL-6-defficient mice could be due to an early-post-challenge exuberant and dysregulated innate response, leading to systemic tissue damage and death. Conversely, our findings could be explained by an insufficiency in the adaptive and protective immune response generated by immunization. To attempt to differentiate between these two possibilities, we investigated the systemic and local immune responses after viral challenge. WT and IL-6 KO mice were intranasally immunized with an inactive PR8 virus as described above. Three weeks post-immunization, mice were infected with a lethal dose of PR8 virus and lungs and serum were harvested 6 days post-infection. Lung viral loads in WT and IL6KO mice were similar (**Supplementary Figure S4**), suggesting that there were not significant differences in the initial ability to undergo infectious challenge. The levels of soluble ICAM in serum, a marker of systemic inflammatory response, endothelial

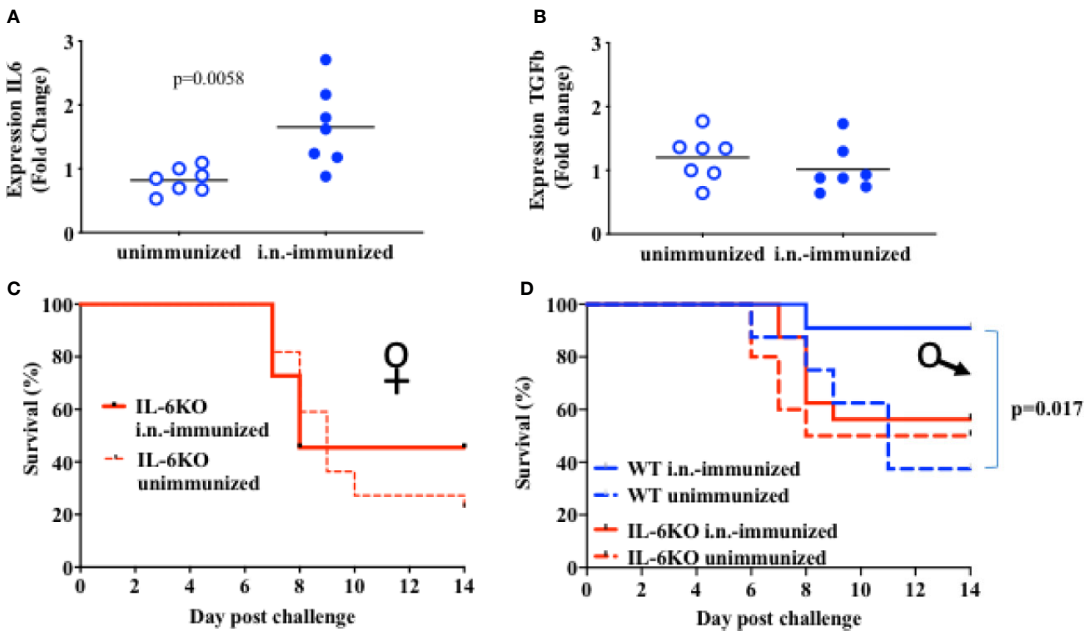

FIGURE 4 | IL-6 is necessary for protective response to an i.n. administration of heat inactivated influenza virus. **(A, B)**: On day 16 of life mice received 5 × 10^5 EIU of heat-inactivated virus intranasally (Dk blue) or not (Lt blue). At 2 days after immunization, lungs were harvested and whole lung was used to extract RNA that was later assayed for RNA expression of IL-6 **(A)** and for TGFb **(B)** by QPCR. Each symbol represents one mouse. Shown is fold-change relative to unimmunized mice in a single experiment. The t-test was used to test for significant differences between groups. **(C, D)**: Mice aged 14–17 days of life were i.n.-immunized (bold) with 5 × 10^5 EIU heat inactivated virus or left unimmunized (dashed). Three weeks later, all mice received a lethal dose of live virus. Y Axis, survival. X axis, day post challenge. **(C)** IL-6KO Female mice; i.n.-immunized, n = 11; unimmunized, n = 22. **(D)** Male mice; IL-6KO (red) i.n.-immunized, n = 16; unimmunized, n = 10. WT males (blue) i.n. immunized n = 11, unimmunized, n = 8). Shown is Mantel-Cox (log-rank) analysis of total data using % initial weight as noted in methods from 5 independent cohorts of mice receiving immunization and or challenge. Significance was set at $p < 0.05$.

cell activation and acute respiratory distress (52, 53), were comparable between WT and IL-6 KO mice (**Figure 5A**). In addition, there was no difference in weight loss between WT and IL-6 KO mice at this early time point of the infection (**Figure 5B**). Since it has been reported that IL-6 deficiency could affect macrophage recruitment by affecting chemokine expression (54), we examined CCL2, important for monocyte trafficking, but no difference was found between WT and IL-6 KO mice (**Figure 5C**). Further, analysis of cytokine expression in the lungs revealed no difference in inflammatory markers such TNF (**Figure 5D**). However, the analysis of IFNγ, a product of the adaptive immune response (CD4 and CD8 T cells), showed a trend toward reduced expression in immunized IL-6 KO mice after the lethal infection with influenza virus (**Figure 5E**). Thus, these results suggest that the death of immunized IL-6 KO infants in response to influenza virus is not caused by an enhanced early pathogenic and dysregulated innate immune response, but they instead suggest an impaired memory T cell response.

IL-6 Is Required for Intranasal Immunization With Inactive Influenza Virus to Sustain Memory T Cell Response in Infant Mice

To investigate whether, in infants, IL-6 is required for an intranasal vaccine to trigger an efficient adaptive memory immune response, 2-week-old WT and IL-6 KO mice were immunized intranasally with inactive influenza virus as described above. Three weeks post-immunization, lungs from immunized mice were harvested and processed, and different T cell populations in lung cell homogenate were examined by flow cytometry analysis. Leukocytes were first gated from other cell populations in the lung using CD45 as a pan leukocyte marker (**Supplementary Figure S5**). We examined the presence of CD8 and CD4 cells within the CD45 cell population. No significant difference in the percentage of CD8 cells could be detected between WT and IL-6 KO i.n.-immunized mice (**Figure 6A**). Similarly, no significant difference in the presence of CD4 cells was found between WT and IL-6 KO mice (**Figure 6B**). However, when we examined the presence of memory CD8 cells using $CD44^{high}$ as marker, the frequency of memory cells was markedly reduced in lungs from immunized IL-6 KO infants relative to WT infants (**Figure 6C**). Similar results were obtained for CD4 cells. The frequency of CD4 $CD44^{high}$ cells was significantly lower in IL-6 KO infants relative to WT mice (**Figure 6D**). Thus, during intranasal influenza immunization of infants, IL-6 does not seem to promote the recruitment of lymphocytes, but is important in a sustained memory T cell response.

IL-6 has been shown to promote antibody production indirectly by acting on CD8 and CD4 T cells and supporting their IL-21 production. IL-21 in turn acts on B cells to promote

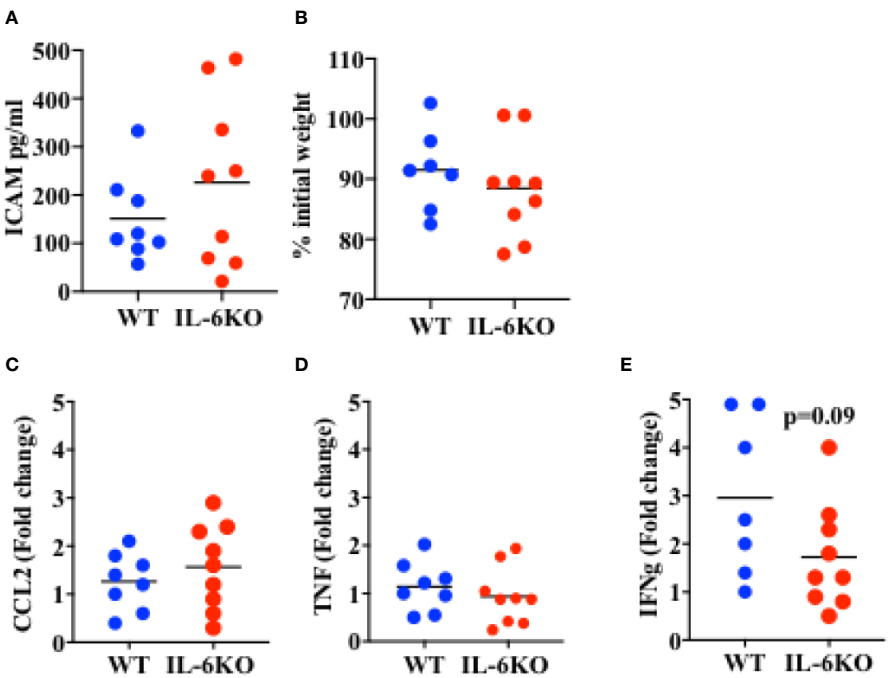

FIGURE 5 | Response to a lethal dose of influenza in i.n. immunized WT and IL-6KO mice. Mice received intranasal immunization with inactive virus on day 14 of life. Three weeks later, mice were weighed and given a lethal dose PR8 virus. Six days after challenge mice were euthanized and tissues harvested for analysis. **(A)** Serum ICAM was analyzed by Luminex™. **(B)** Weight of mice, 6 days post-infection. Shown is the % relative to the initial weight prior to infection. **(C–E)** Whole lung relative mRNA expression for CCL2 **(C)**, TNF **(D)** and IFNg **(E)** determined by real time RT-PCR. Values show fold induction relative to a WT. Each dot represents a mouse. One experiment is shown. Bars indicate mean for group. Comparison utilized the t test, with significance set at $p < 0.05$.

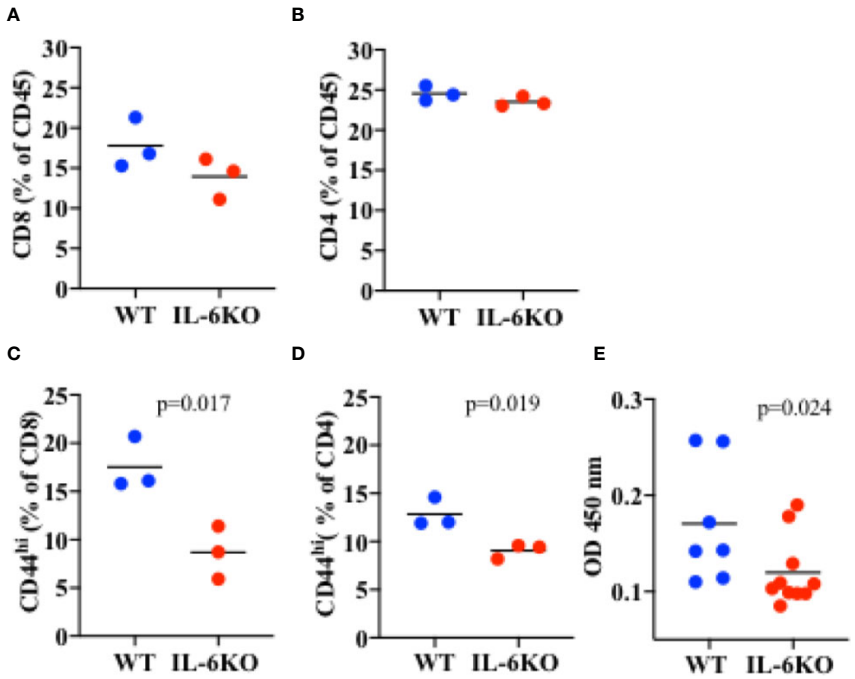

FIGURE 6 | Lower frequency of memory CD8 and CD4 cells in the lungs of i.n. immunized IL-6 KO mice. Mice (n = 3) received intranasal immunization with inactive virus on day 14 of life. Three weeks later, lungs were extracted and analyzed by flow cytometry. **(A)** Cells were gated for CD45 first. % of CD8 cells within the CD45+ population is showed. **(B)** Cells were gated for CD45 first. % of CD4 cells within the CD45+ population is showed. **(C)** Cells were gated for CD45 first, and then for CD8 cells. % of $CD44^{high}$ within CD8 cells is shown. **(D)** Cells were gated for CD45 first, and then for CD4 cells. % of $CD44^{high}$ within CD4 cells is shown. p value is determined by t test. **(E)** PR8-specific IgG antibody titer in serum determined by ELISA. p value is calculated using the Mann-Whitney test, with significance set at $p < 0.05$. One experiment is shown.

antibody production, primarily IgG (40, 55). We therefore also examined the presence of influenza-specific IgG in the serum of WT and IL-6 KO infants 3 weeks post-immunization. The levels of PR8-specific IgG were reduced in immunized IL-6 KO infants compared with WT mice (**Figure 6E**). Thus, during i.n. immunization of infants, IL-6 plays an important role in sustaining effective T and B cell adaptive memory.

DISCUSSION

Infant immunity remains an important area of focus due to significant existing morbidity related to infectious disease. Influenza infection remains a major challenge among infections in children under five years of age (56). While historically it is believed to be due to an inappropriate T/B cell immune response, pathology and resolution of primary influenza virus infection is not dependent on the adaptive immunity but requires innate immunity (57). Another potential difference between children and adults is dose of the virus to which they are environmentally exposed relative to lung size (again, determined by body size). However, in our studies here we show that even when influenza viral dose is normalized to body weight (reflecting lung size), infant mice are more susceptible to sublethal dose than adult mice. Therefore, an increased virus dose/lung size ratio does not seem to be the main cause for the enhanced sensitivity to influenza virus response in infants. This disparity seems to be a developmental issue. Here, our Microarray studies have revealed a different gene expression profile in epithelial cells from the lungs of adult and infant mice prior to exposure to any infection or other type of insult.

The view that infant immune cells are inherently deficient contrasts with the view that, given the appropriate environment infant immune cells can behave similarly to adult (11, 13–15, 58). While it is generally believed that the deficient response of very young children to influenza infection is due to antigen inexperience in T or B cells, the difference in the immune response could also be determined by cells other than immune cells that contribute to shape the adaptive immune response mediated by T or B cells.

For instance, epithelial cells (as well as endothelial cells) can produce cytokines and other factors that can modulate the type or strength of CD4 and CD8 cell mediated immune responses. Lung epithelial cells are the main cell target of influenza virus, as they express high levels of sialic acid on the cell surface to which influenza binds, subsequently enters, and replicates (19). However, lung epithelial cells can also orchestrate the innate anti-viral immune response. Influenza virus replication induces expression and production of type I IFN that acts as an anti-

viral factor (39). Furthermore, lung epithelial cells are known to be able to produce different inflammatory cytokines (e.g. IL-33, IL-1, IL-6) that can then have an effect on the adaptive immune response (19). Under physiologic conditions (not during exposure to an insult) lung epithelial cells from adult mice express high levels of IL-6 mRNA in contrast to the relative absence during of IL-6 expression in lung resident macrophages (38). IL-6 production and secretion by mouse and human lung epithelial cells is triggered during infection with influenza virus and other viruses such coronavirus (39, 59, 60). IL-6 plays a pivotal role in dictating the types of CD4 and CD8 cell responses. Further, IL-6 has been shown to promote differentiation of CD4 cells into Th2 and Tfh cells that can then, by secreting IL-21 and IL-4, enhance isotype switching and antibody production in B cells (40, 61, 62). In influenza virus infection, IL-6 triggers IL-21 production by CD4 cells and IL-21 is essential for virus antibody response (40). In addition, we have also shown that IL-6 makes CD8 cells to become helpers of B cells through induction of IL-21. During influenza virus, CD8 cells in the lung but not in lymph nodes produce IL-21 and this effect requires IL-6 (55). Thus, the difference in IL-6 production by lung epithelial cells between infant and adults could account for the difference in T and B cell responses to influenza virus in the lung.

In this study, our gene profile analyses revealed marked differences the expression of immune regulators in lung epithelial cells from infants as compared to adult mice. Our pathway analysis has revealed IL-6 as a highly selective gene that is lower in pre-weanling epithelial cells. Interestingly, expression of other cytokines that play a role in antiviral immune responses (e.g. type I IFN), regulation of the adaptive immune response (e.g. IL-33) or the innate immune response (e.g. IL-18) was not different between infants and adult mice, further highlighting the potential significance of the differential expression of IL-6 that we observed. The evidence pointing to IL-6 expression in lung epithelial cells as being developmentally regulated could have a major impact on the understanding of childhood immune responses to pathogenic influenza viruses, but also to other respiratory viruses e.g., those producing SARS.

Since our gene expression profiling reveals a marked reduction (more than 3-fold lower) in the IL-6 expression in lung epithelial cells from infants relative to adult mice, it is possible that the lower IL-6 levels in the lungs could be responsible for the increased susceptibility. In this regard, adult mice lacking IL-6 or IL-6R die in response to sublethal dose of influenza virus in part due to the reduced number of neutrophils in the lung to mediate virus clearance (41). In addition, IL-6 can ameliorate acute lung injury in influenza virus infection in mice by promoting tissue repair (63). In humans, the systemic treatment with tocilizumab, the blocking anti-IL-6R antibody approved for treatment of rheumatoid arthritis, has also been shown to increase the risk to respiratory virus infection (64). Therefore, although exaggerated levels of IL-6 have been observed in adult patients with acute respiratory distress syndrome due to massive lung tissue damage (65, 66), IL-6 also likely provides protection from infections with influenza virus and other respiratory viruses (66).

Current influenza vaccination formulations include a live attenuated virus given intranasally, and an inactivated virus administered *via* intramuscular injection (26). Each has variable protection, depending on the formulation, the year of production, and the population vaccinated (27). In addition, the live-attenuated vaccine is not approved for very young children less than 2 years of age. Thus, this population remains at high risk every season. Here we show that a vaccine with inactive influenza virus provides protection to ~15 day-old mice when administered intranasally, suggesting a potential alternative option of vaccination for this highly susceptible population of infant children. Interestingly, our data also show that the protective effect of the intranasal immunization with the inactive influenza virus in infant mice is dependent on IL-6 since it fails to provide protection in IL-6 deficient mice. In contrast to i.n. administration, intramuscular administration of the inactive influenza virus did not provide protection in infant mice, stressing the importance of the intranasal route over the intramuscular route at this dose. The induction of IL-6 by the i.n. vaccine with the inactive virus suggested that this IL-6 may come from lung epithelial cells, although future studies will be needed to further demonstrate that this is the case. Using a commercially formulated multivalent vaccine for the 2012/2013 season, it has been reported that i.m. vaccination produced a protective response in infant mice (67). It is possible that the mix of influenza virus strains (H3N2 in addition to H1N1) in that particular seasonal vaccine could trigger a stronger immune response. However, correlating with our studies in infants, i.m. administration of inactive influenza virus in adult mice also induces a limited antibody response (40). The superior efficacy of the inactive virus vaccine when administered i.n. further reinforces the relevance of the environment where the immune response takes place. Most approved antiviral vaccines are based on their ability to induce antibody production. There is evidence that LAIV may trigger some T cell mediated protection (68, 69) although it has not been fully demonstrated. Intriguingly, here we show a reduction in the frequency of activated CD4 and CD8 cells in the lung in immunized IL-6 deficient mice relative to WT mice. Thus, it is possible that the lower efficacy of our inactive influenza viral vaccine in the IL-6 deficient mice could be due to impaired memory CD4/CD8 T cell response and the subsequent antibody response.

This investigation posits that vaccination of the infant can generate a protective response against lethal challenge if the correct environment is achieved. Our studies are in keeping with previous studies suggesting that immunization of infants against differing antigens, depending on the right source and format can lead to T cell activation in the relevant tissue and/or systemic antibody production (70). The critical role played by IL-6 in these studies when taken in context are consistent with the idea that environment matters in the development of infant immunity. Further understanding and the ability to harness specific tissue environments may aid in developing strategies for protection of the very young.

DATA AVAILABILITY STATEMENT

The raw data supporting the conclusions of this article will be made available by the authors, without undue reservation.

ETHICS STATEMENT

The animal study was reviewed and approved by University of Vermont Institutional Animal Care and Use Committee.

AUTHOR CONTRIBUTIONS

EB designed and helped perform experiments, managed, analyzed, and interpreted the data, and wrote/edited the figures and manuscript. JK helped do gene expression analysis studies. BT helped perform experiments, as did KP and KK. LH provided PR8 and helped with data analysis and editing. MR helped perform experiments, analyzed, and interpreted the data, and wrote and edited the manuscript. All authors contributed to the article and approved the submitted version.

FUNDING

Support for this work came from NIH P30GM118228 to the Vermont Center for Immunology and Infectious Disease, P30GM103532 to the Vermont Lung Center, the University of Vermont College of Medicine New Research Initiative Program, the UVM Flow Cytometry and Cell Sorting Facility, and the Department of Obstetrics, Gynecology and Reproductive Sciences. MR was also supported by NIH R56 AI116255 and R01 AI051454. LH and BT are supported by the University of Connecticut Center on Aging. JK is supported by the University of Colorado Cancer Center Bioinformatics/Biostatistics Shared Resources, supported by NIH P30CA046934. Research reported herein was also supported by an Institutional Development Award (IDeA) from the National Institute of General Medical Sciences of the National Institutes of Health under grant number P20GM103449, The Vermont Genetics Network.

ACKNOWLEDGMENTS

We are grateful for discussions with Matt Poynter and Cory Teuscher in the Vermont Center for Immunology and Infectious Disease, and with James DeGregori, Department of Biochemistry and Molecular Genetics, University of Colorado Anschutz Medical Campus. Thanks goes to Emily Giddings for technical support.

SUPPLEMENTARY MATERIAL

The Supplementary Material for this article can be found online at: https://www.frontiersin.org/articles/10.3389/fimmu.2020.568978/full#supplementary-material

REFERENCES

1. Scheltema NM, Gentile A, Lucion F, Nokes DJ, Munywoki PK, Madhi SA, et al. Global respiratory syncytial virus-associated mortality in young children (RSV GOLD): a retrospective case series. *Lancet Glob Health* (2017) 5:e984–91. doi: 10.1016/s2214-109x(17)30344-3
2. Liao X, Hu Z, Liu W, Lu Y, Chen D, Chen M, et al. New Epidemiological and Clinical Signatures of 18 Pathogens from Respiratory Tract Infections Based on a 5-Year Study. *PloS One* (2015) 10:e0138684. doi: 10.1371/journal.pone.0138684
3. Blanton L, Dugan VG, Abd Elal AI, Alabi N, Barnes J, Brammer L, et al. Update: Influenza Activity - United States, September 30, 2018-February 2, 2019. *MMWR Morb Mortal Wkly Rep* (2019) 68:125–34. doi: 10.15585/mmwr.mm6806a1
4. Fike AJ, Kumova OK, Tardif VJ, Carey AJ. Neonatal influenza-specific effector CTLs retain elevated CD31 levels at the site of infection and have decreased IFN-gamma production. *J Leukoc Biol* (2019) 105:539–49. doi: 10.1002/jlb.4a0518-191r
5. Lederberg J. Genes and antibodies. *Sci (New York NY)* (1959) 129:1649–53. doi: 10.1126/science.129.3364.1649
6. Mold JE, Michaelsson J, Burt TD, Muench MO, Beckerman KP, Busch MP, et al. Maternal alloantigens promote the development of tolerogenic fetal regulatory T cells in utero. *Sci (New York NY)* (2008) 322:1562–5. doi: 10.1126/science.1164511
7. Ohtsuka Y. Food intolerance and mucosal inflammation. *Pediatr Int* (2015) 57:22–9. doi: 10.1111/ped.12546
8. Mold JE, Venkatasubrahmanyam S, Burt TD, Michaelsson J, Rivera JM, Galkina SA, et al. Fetal and adult hematopoietic stem cells give rise to distinct T cell lineages in humans. *Sci (New York NY)* (2010) 330:1695–9. doi: 10.1126/science.1196509
9. Ridge JP, Fuchs EJ, Matzinger P. Neonatal tolerance revisited: turning on newborn T cells with dendritic cells.[see comment]. *Sci (New York NY)* (1996) 271:1723–6. doi: 10.1126/science.271.5256.1723
10. Matzinger P. Friendly and dangerous signals: is the tissue in control? *Nat Immunol* (2007) 8:11–3. doi: 10.1038/ni0107-11
11. Fadel SA, Cowell LG, Cao S, Ozaki DA, Kepler TB, Steeber DA, et al. Neonate-primed CD8+ memory cells rival adult-primed memory cells in antigen-driven expansion and anti-viral protection. *Int Immunol* (2006) 18:249–57. doi: 10.1093/intimm/dxh360
12. Sinnott BD, Park B, Boer MC, Lewinsohn DA, Lancioni CL. Direct TLR-2 Costimulation Unmasks the Proinflammatory Potential of Neonatal CD4+ T Cells. *J Immunol* (2016) 197:68–77. doi: 10.4049/jimmunol.1501297
13. Forsthuber T, Yip HC, Lehmann PV. Induction of TH1 and TH2 immunity in neonatal mice. *Sci (New York NY)* (1997) 271:1728–30. doi: 10.1126/science.271.5256.1728
14. Arulanandam BP, Mittler JN, Lee WT, O'Toole M, Metzger DW. Neonatal administration of IL-12 enhances the protective efficacy of antiviral vaccines. *J Immunol* (2000) 164:3698–704. doi: 10.4049/jimmunol.164.7.3698
15. Kollmann TR, Kampmann B, Mazmanian SK, Marchant A, Levy O. Protecting the Newborn and Young Infant from Infectious Diseases: Lessons from Immune Ontogeny. *Immunity* (2017) 46:350–63. doi: 10.1016/j.immuni.2017.03.009
16. Huygens A, Lecomte S, Tackoen M, Olislagers V, Delmarcelle Y, Burny W, et al. Functional Exhaustion Limits CD4+ and CD8+ T-Cell Responses to Congenital Cytomegalovirus Infection. *J Infect Dis* (2015) 212:484–94. doi: 10.1093/infdis/jiv071
17. Debock I, Flamand V. Unbalanced Neonatal CD4(+) T-Cell Immunity. *Front Immunol* (2014) 5:393. doi: 10.3389/fimmu.2014.00393
18. Cohn M. Giving Context to Non-self-marker Theories of Immune Responsiveness. *Scand J Immunol* (2017) 86:124–9. doi: 10.1111/sji.12579

19. Denney L, Ho L-P. The role of respiratory epithelium in host defence against influenza virus infection. *BioMed J* (2018) 41:218–33. doi: 10.1016/j.bj.2018.08.004
20. Chilvers MA, Rutman A, O'Callaghan C. Functional analysis of cilia and ciliated epithelial ultrastructure in healthy children and young adults. *Thorax* (2003) 58:333–8. doi: 10.1136/thorax.58.4.333
21. Smith LS, Zimmerman JJ, Martin TR. Mechanisms of acute respiratory distress syndrome in children and adults: a review and suggestions for future research. *Pediatr Crit Care Med* (2013) 14:631–43. doi: 10.1097/PCC.0b013e318291753f
22. Mariani TJ. Update on Molecular Biology of Lung Development–Transcriptomics. *Clin Perinatol* (2015) 42:685–95. doi: 10.1016/j.clp.2015.08.001
23. Wang Q, Bhattacharya S, Mereness JA, Anderson C, Lillis JA, Misra RS, et al. A novel in vitro model of primary human pediatric lung epithelial cells. *Pediatr Res* (2020) 87:511–7. doi: 10.1038/s41390-019-0340-9
24. Clay CC, Reader JR, Gerriets JE, Wang TT, Harrod KS, Miller LA. Enhanced viral replication and modulated innate immune responses in infant airway epithelium following H1N1 infection. *J Virol* (2014) 88:7412–25. doi: 10.1128/jvi.00188-14
25. Agarkhedkar S, Chhatwal J, Kompithra RZ, Lalwani SK, Narayan A, Muninarayanaswam V, et al. Immunogenicity and safety of an intramuscular split-virion quadrivalent inactivated influenza vaccine in individuals aged >/= 6 months in India. *Hum Vaccines Immunother* (2019) 15:973–7. doi: 10.1080/21645515.2019.1565259
26. Valdin HL, Begue RE. Influenza vaccines effectiveness 2013-14 through 2015-16, a test-negative study in children. *Vaccine* (2017) 35:4088–93. doi: 10.1016/j.vaccine.2017.06.050
27. Grohskopf LA, Sokolow LZ, Broder KR, Walter EB, Fry AM, Jernigan DB. Prevention and Control of Seasonal Influenza with Vaccines: Recommendations of the Advisory Committee on Immunization Practices-United States, 2018-19 Influenza Season. *MMWR Recomm Rep* (2018) 67:1–20. doi: 10.15585/mmwr.rr6703a1
28. COMMITTEE ON INFECTIOUS DISEASES. Recommendations for Prevention and Control of Influenza in Children, 2019-2020. *Pediatrics* (2019) 144(4):e20192478. doi: 10.1542/peds.2019-2478
29. Bergen R, Black S, Shinefield H, Lewis E, Ray P, Hansen J, et al. Safety of cold-adapted live attenuated influenza vaccine in a large cohort of children and adolescents. *Pediatr Infect Dis J* (2004) 23:138–44. doi: 10.1097/01.inf.0000109392.96411.4f
30. Belshe RB, Edwards KM, Vesikari T, Black SV, Walker RE, Hultquist M, et al. Live attenuated versus inactivated influenza vaccine in infants and young children. *N Engl J Med* (2007) 356:685–96. doi: 10.1056/NEJMoa065368
31. Caspard H, Steffey A, Mallory RM, Ambrose CS. Evaluation of the safety of live attenuated influenza vaccine (LAIV) in children and adolescents with asthma and high-risk conditions: a population-based prospective cohort study conducted in England with the Clinical Practice Research Datalink. *BMJ Open* (2018) 8:e023118. doi: 10.1136/bmjopen-2018-023118
32. Turner PJ, Fleming L, Saglani S, Southern J, Andrews NJ, Miller E. Safety of live attenuated influenza vaccine (LAIV) in children with moderate to severe asthma. *J Allergy Clin Immunol* (2020) 145:1157–1164.e1156. doi: 10.1016/j.jaci.2019.12.010
33. Poehling KA, Caspard H, Peters TR, Belongia EA, Congeni B, Gaglani M, et al. 2015-2016 Vaccine Effectiveness of Live Attenuated and Inactivated Influenza Vaccines in Children in the United States. *Clin Infect Dis an Off Publ Infect Dis Soc America* (2018) 66:665–72. doi: 10.1093/cid/cix869
34. Mandelboim M, Glatman-Freedman A, Drori Y, Sherbany H, Pando R, Sefty H, et al. Ineffectiveness of the 2014-2015 H3N2 influenza vaccine. *Oncotarget* (2016) 7:1185–92. doi: 10.18632/oncotarget.6746
35. Grohskopf LA, Sokolow LZ, Fry AM, Walter EB, Jernigan DB. Update: ACIP Recommendations for the Use of Quadrivalent Live Attenuated Influenza Vaccine (LAIV4) - United States, 2018-19 Influenza Season. *MMWR Morb Mortal Wkly Rep* (2018) 67:643–5. doi: 10.15585/mmwr.mm6722a5
36. Rincon M. Interleukin-6: from an inflammatory marker to a target for inflammatory diseases. *Trends Immunol* (2012) 33:571–7. doi: 10.1016/j.it.2012.07.003
37. Rose-John S. Interleukin-6 Family Cytokines. *Cold Spring Harb Perspect Biol* (2018) 10. doi: 10.1101/cshperspect.a028415
38. Neveu WA, Bernardo E, Allard JL, Nagaleekar V, Wargo MJ, Davis RJ, et al. Fungal Allergen {beta}-glucans Trigger p38 MAPK-mediated IL-6 Translation in Lung Epithelial Cells. *Am J Respir Cell Mol Biol* (2011) 45(6):1133–41. doi: 10.1165/rcmb.2011-0054OC
39. Matsukura S, Kokubu F, Noda H, Tokunaga H, Adachi M. Expression of IL-6, IL-8, and RANTES on human bronchial epithelial cells, NCI-H292, induced by influenza virus A. *J Allergy Clin Immunol* (1996) 98:1080–7. doi: 10.1016/s0091-6749(96)80195-3
40. Dienz O, Eaton SM, Bond JP, Neveu W, Moquin D, Noubade R, et al. The induction of antibody production by IL-6 is indirectly mediated by IL-21 produced by CD4+ T cells. *J Exp Med* (2009) 206:69–78. doi: 10.1084/jem.20081571
41. Dienz O, Rud JG, Eaton SM, Lanthier PA, Burg E, Drew A, et al. Essential role of IL-6 in protection against H1N1 influenza virus by promoting neutrophil survival in the lung. *Mucosal Immunol* (2012) 5:258–66. doi: 10.1038/mi.2012.2
42. Yang J, Sakai J, Siddiqui S, Lee RC, Ireland DDC, Verthelyi D, et al. IL-6 Impairs Vaccine Responses in Neonatal Mice. *Front Immunol* (2018) 9:3049. doi: 10.3389/fimmu.2018.03049
43. Poli V, Balena R, Fattori E, Markatos A, Yamamoto M, Tanaka H, et al. Interleukin-6 deficient mice are protected from bone loss caused by estrogen depletion. *EMBO J* (1994) 13:1189–96. doi: 10.1002/j.1460-2075.1994.tb06368.x
44. Scholtissek C, Rott R. Effect of temperature on the multiplication of an Influenza virus. *J Gen Virol* (1969) 5:283–90. doi: 10.1099/0022-1317-5-2-283
45. Jonges M, Liu WM, van der Vries E, Jacobi R, Pronk I, Boog C, et al. Influenza virus inactivation for studies of antigenicity and phenotypic neuraminidase inhibitor resistance profiling. *J Clin Microbiol* (2010) 48:928–40. doi: 10.1128/jcm.02045-09
46. Irizarry RA, Bolstad BM, Collin F, Cope LM, Hobbs B, Speed TP. Summaries of Affymetrix GeneChip probe level data. *Nucleic Acids Res* (2003) 31:e15. doi: 10.1093/nar/gng015
47. Kanehisa M, Goto S, Furumichi M, Tanabe M, Hirakawa M. KEGG for representation and analysis of molecular networks involving diseases and drugs. *Nucleic Acids Res* (2010) 38:D355–360. doi: 10.1093/nar/gkp896
48. Subramanian A, Tamayo P, Mootha VK, Mukherjee S, Ebert BL, Gillette MA, et al. Gene set enrichment analysis: a knowledge-based approach for interpreting genome-wide expression profiles. *Proc Natl Acad Sci U States America* (2005) 102:15545–50. doi: 10.1073/pnas.0506580102
49. Preaud E, Durand L, Macabeo B, Farkas N, Sloesen B, Palache A, et al. Annual public health and economic benefits of seasonal influenza vaccination: a European estimate. *BMC Public Health* (2014) 14:813. doi: 10.1186/1471-2458-14-813
50. Shinjoh M, Sugaya N, Yamaguchi Y, Iibuchi N, Kamimaki I, Goto A, et al. Inactivated influenza vaccine effectiveness and an analysis of repeated vaccination for children during the 2016/17 season. *Vaccine* (2018) 36:5510–8. doi: 10.1016/j.vaccine.2018.07.065
51. Heinrich PC, Behrmann I, Haan S, Hermanns HM, Muller-Newen G, Schaper F. Principles of interleukin (IL)-6-type cytokine signalling and its regulation. *Biochem J* (2003) 374:1–20. doi: 10.1042/bj20030407
52. Marchesi S, Lupattelli G, Lombardini R, Sensini A, Siepi D, Mannarino M, et al. Acute inflammatory state during influenza infection and endothelial function. *Atherosclerosis* (2005) 178:345–50. doi: 10.1016/j.atherosclerosis.2004.08.036
53. Briassoulis G, Papassotiriou I, Mavrikiou M, Lazaropoulou C, Margeli A. Longitudinal course and clinical significance of TGF-beta1, sL- and sE-Selectins and sICAM-1 levels during severe acute stress in children. *Clin Biochem* (2007) 40:299–304. doi: 10.1016/j.clinbiochem.2006.11.015
54. Romano M, Sironi M, Toniatti C, Polentarutti N, Fruscella P, Ghezzi P, et al. Role of IL-6 and its soluble receptor in induction of chemokines and leukocyte recruitment. *Immunity* (1997) 6:315–25. doi: 10.1016/s1074-7613(00)80334-9
55. Yang R, Masters AR, Fortner KA, Champagne DP, Yanguas-Casas N, Silberger DJ, et al. IL-6 promotes the differentiation of a subset of naive CD8+ T cells into IL-21-producing B helper CD8+ T cells. *J Exp Med* (2016) 213:2281–91. doi: 10.1084/jem.20160417
56. Misra RS, Nayak JL. The Importance of Vaccinating Children and Pregnant Women against Influenza Virus Infection. *Pathogens* (2019) 8:265. doi: 10.3390/pathogens8040265

57. Eichelberger M, Allan W, Zijlstra M, Jaenisch R, Doherty PC. Clearance of influenza virus respiratory infection in mice lacking class I major histocompatibility complex-restricted CD8+ T cells. *J Exp Med* (1991) 174:875–80. doi: 10.1084/jem.174.4.875
58. Schwartz DH, Hurwitz JL, Greenspan NS, Doherty PC. Priming of virus-immune memory T cells in newborn mice. *Infect Immun* (1984) 43:202–5. doi: 10.1128/IAI.43.1.202-205.1984
59. Liu S, Yan R, Chen B, Pan Q, Chen Y, Hong J, et al. Influenza Virus-Induced Robust Expression of SOCS3 Contributes to Excessive Production of IL-6. *Front Immunol* (2019) 10:1843. doi: 10.3389/fimmu.2019.01843
60. Yoshikawa T, Hill T, Li K, Peters CJ, Tseng CT. Severe acute respiratory syndrome (SARS) coronavirus-induced lung epithelial cytokines exacerbate SARS pathogenesis by modulating intrinsic functions of monocyte-derived macrophages and dendritic cells. *J Virol* (2009) 83:3039–48. doi: 10.1128/jvi.01792-08
61. Carbone G, Wilson A, Diehl SA, Bunn J, Cooper SM, Rincon M. Interleukin-6 receptor blockade selectively reduces IL-21 production by CD4 T cells and IgG4 autoantibodies in rheumatoid arthritis. *Int J Biol Sci* (2013) 9:279–88. doi: 10.7150/ijbs.5996
62. Diehl S, Chow CW, Weiss L, Palmetshofer A, Twardzik T, Rounds L, et al. Induction of NFATc2 expression by interleukin 6 promotes T helper type 2 differentiation. *J Exp Med* (2002) 196:39–49. doi: 10.1084/jem.20020026
63. Yang ML, Wang CT, Yang SJ, Leu CH, Chen SH, Wu CL, et al. IL-6 ameliorates acute lung injury in influenza virus infection. *Sci Rep* (2017) 7:43829. doi: 10.1038/srep43829
64. Lang VR, Englbrecht M, Rech J, Nüsslein H, Manger K, Schuch F, et al. Risk of infections in rheumatoid arthritis patients treated with tocilizumab. *Rheumatol (Oxford)* (2012) 51:852–7. doi: 10.1093/rheumatology/ker223
65. Wu W, Shi Y, Gao H, Liang W, Sheng J, Li L. Immune derangement occurs in patients with H7N9 avian influenza. *Crit Care* (2014) 18:R43. doi: 10.1186/cc13788
66. Velazquez-Salinas L, Verdugo-Rodriguez A, Rodriguez LL, Borca MV. The Role of Interleukin 6 During Viral Infections. *Front Microbiol* (2019) 10:1057. doi: 10.3389/fmicb.2019.01057
67. McDonald JU, Zhong Z, Groves HT, Tregoning JS. Inflammatory responses to influenza vaccination at the extremes of age. *Immunology* (2017) 151:451–63. doi: 10.1111/imm.12742
68. Lartey S, Zhou F, Brokstad KA, Mohn KG, Slettevoll SA, Pathirana RD, et al. Live-Attenuated Influenza Vaccine Induces Tonsillar Follicular T Helper Cell Responses That Correlate With Antibody Induction. *J Infect Dis* (2020) 221:21–32. doi: 10.1093/infdis/jiz321
69. Mohn KG, Brokstad KA, Islam S, Oftung F, Tøndel C, Aarstad HJ, et al. Early Induction of Cross-Reactive CD8+ T-Cell Responses in Tonsils After Live-Attenuated Influenza Vaccination in Children. *J Infect Dis* (2020) 221:1528–37. doi: 10.1093/infdis/jiz583
70. Bot A, Bot S, Garcia-Sastre A, Bona C. DNA immunization of newborn mice with a plasmid-expressing nucleoprotein of influenza virus. *Viral Immunol* (1996) 9:207–10. doi: 10.1089/vim.1996.9.207

Conflict of Interest: The authors declare that the research was conducted in the absence of any commercial or financial relationships that could be construed as a potential conflict of interest.

frontiers in Immunology

ORIGINAL RESEARCH
published: 23 April 2021
doi: 10.3389/fimmu.2021.592731

Immune Response of Indian Preterm Infants to Pentavalent Vaccine Varies With Component Antigens and Gestational Age

*Archana Kulkarni-Munje[1], Nandini Malshe[2], Sonali Palkar[2], Aniket Amlekar[1], Sanjay Lalwani[2], Akhilesh Chandra Mishra[1] and Vidya Arankalle[1]**

[1] Department of Communicable Diseases, Interactive Research School for Health Affairs, Bharati Vidyapeeth (Deemed To Be University) University, Pune, India, [2] Department of Paediatrics, Bharati Vidyapeeth (Deemed To Be University) University Medical College, Pune, India

OPEN ACCESS

Edited by:
Andrew Currie,
Murdoch University,
Australia

Reviewed by:
Srinivasa Reddy Bonam,
Institut National de la Santé et de la Recherche Médicale (INSERM), France
Rym Ben-Othman,
University of Western Australia,
Australia

***Correspondence:**
Vidya Arankalle
varankalle@yahoo.com

Specialty section:
This article was submitted to Vaccines and Molecular Therapeutics, a section of the journal Frontiers in Immunology

Received: 07 August 2020
Accepted: 31 March 2021
Published: 23 April 2021

Citation:
Kulkarni-Munje A, Malshe N, Palkar S, Amlekar A, Lalwani S, Mishra AC and Arankalle V (2021) Immune Response of Indian Preterm Infants to Pentavalent Vaccine Varies With Component Antigens and Gestational Age. Front. Immunol. 12:592731. doi: 10.3389/fimmu.2021.592731

Childhood vaccination plays critical role in protecting infants from several dreaded diseases. Of the global 15 million preterm (PT) infants with compromised immune system born annually, India contributes to >3.5 million. Generation of adequate vaccine-induced immune response needs to be ensured of their protection. Immune response of Indian PT (n = 113) and full-term (FT, n = 80) infants to pentavalent vaccine administered as per the national recommendation was studied. Antibody titers against component antigens of pentavalent vaccine, immune cells profiling (T and B cells, monocytes and dendritic cells) and plasma cytokines were determined pre- and post-vaccination. Additionally, cell-mediated recall immune responses to pentavalent antigens were evaluated after short time antigenic exposure to infant PBMCs. Irrespective of gestational age (GA), all the infants developed adequate antibody response against tetanus, diphtheria, and protective but lower antibody levels for *Haemophilus influenzae* type-b and hepatitis B in preterm infants. Lower (~74%) protective antibody response to pertussis was independent of gestational age. PT-infants exhibited lower frequencies of CD4 T cells/dendritic cells/monocytes, increased plasma IL-10 levels and lower proliferation of central and effector memory T cells than in term-infants. Proliferative central memory response of FT-infants without anti-pertussis antibodies suggests protection from subsequent infection. Responder/non-responder PT-infants lacked immunological memory and could be infected with *Bordetella*. For hepatitis B, the recall response was gestational age-dependent and antibody status-independent. Humoral/cellular immune responses of PT-infants were dependent on the type of the immunogen. Preterm infants born before 32 weeks of gestation may need an extra dose of pentavalent vaccine for long lived robust immune response.

Keywords: preterm birth, immune response, pentavalent vaccine, recall immune responses, immunological memory

INTRODUCTION

The introduction of universal immunization program for infants has drastically reduced the dreaded diseases-associated mortality and morbidity in children. However, due to poor vaccination coverage, deaths continue to occur in the developing countries. Approximately 17,000 children from around the world under the age of five succumb daily, mostly to vaccine preventable diseases (VPD) (1). Globally, an estimated 14.9 million infants are born preterm, i.e., before 37 weeks of pregnancy. The risk of infection in preterm (PT) infants increases nine-fold when compared to their full term (FT) counterparts (2–5) and correlates inversely with gestational age (6); furthermore, PT infants face an increased risk of VPDs emphasizing importance of vaccination (7, 8). It is generally recommended that the preterm infants should be vaccinated using the same schedules as those usually recommended for full-term infants with the only exception of birth dose of hepatitis B vaccine, to be administered to babies weighing > 2000 g (9, 10). In view of premature immunity and introduction of more and more immunogens at/around one time, it is of utmost importance to verify if the preterm babies generate satisfactory immune response to all the vaccine components. Immunization of preterm infants from Poland and Spain with a 13-valent pneumococcal conjugate vaccine at the ages of 2, 3, 4 and 12 months led to lower but acceptable antibody levels (11). Based on the response to Haemophilus influenzae type b (Hib) vaccine, schedule modification (12) and need for boosters (13) were recommended in Japan and Poland, respectively. In Bangladesh, hepatitis B vaccine (Hep-B) generated protective, but, <100 mIU/ml anti-HBs titers in 26.4% Preterm infants (14). While revisiting data on immune response of preterm infants from different countries to hexavalent DTPa-HBV-IPV/Hib vaccine (>1600 preterm infants including 596 with GA ≤32 weeks, and 127 with GA <29 infants), excellent seropositivity against diphtheria (98.7%), tetanus (100%) and pertussis (92.4%) was recorded. However, for hepatitis B and Hib, seropositivity rates and antibody concentrations appeared to be lower (15). Based on the studies reported from Italy, it was surmised that though the administration of hexavalent vaccine leads to high seroprotection rates in preterm infants, lower antibody titers against HBV, Hib, poliovirus serotype 1, and pertussis) seem to have been associated with lower gestational age (16).

Under universal Immunization Program, Government of India offers a large number of free vaccines to its infants that are administered at recommended ages of the infants (17). To avoid multiple injections and enhance coverage, several combination vaccines are being introduced. India contributes to >3.5 million preterm births annually and thus protection of these infants against VPDs remains a top priority. Though immune response of full term (FT) infants is widely reported for the newly introduced vaccines (18–20), studies in preterm infants are restricted to BCG and hepatitis B (21–24). This study examines for the first time, antibody and cellular responses of PT infants to the pentavalent vaccine (Diphtheria and Tetanus Toxoids, *B. pertussis* (whole cell), hepatitis B and *Haemophilus influenza* Type b Conjugate) in comparison with their FT counterparts.

Abbreviations: PT, Preterm; FT, Full-term; GA, Gestation age; VPD, Vaccine preventable diseases; CBA, Cytometric bead array; mDC, Myeloid dendritic cells; pDC, Plasmacytoid dendritic cells; BPD, Bronchopulmonary dysplasia ; RDS, Respiratory distress syndrome; GM-CSF, Granulocyte-macrophage colony-stimulating factor; BCG, Bacille Calmette-Guérin; GMT, Geometric mean titer; PRP, Polyribosylribitol phosphate; IQR, Interquartile range; MFI, Mean fluorescence intensity; RBC, Red blood cells; HiB, Haemophilus influenzae type B; NRBC, Nucleated RBC; HBsAg, Hepatitis B surface antigen; LF, Limits of flocculation; IOU, International opacity units; IU, International unit; PBMC, Peripheral blood mononuclear cells; BCMA, B cell maturation antigen.

MATERIALS AND METHODS

Sample Size

In the absence of data in preterm infants from India, the sample size for the study was calculated based on 10% inferiority (Sealed Enveloped Ltd. 2012. Power calculator for continuous outcome non-inferiority. Available from: https://www.sealedenvelope.com/power/continuous-noninferior/trial). At a significance level (alpha) of 5%, 90% power (1-beta), standard deviation of outcome = 2 and non-inferiority limit, d = 1, 69 samples were needed in each group. Considering 15% drop outs, 80 subjects/group were required.

Study Population

The study was conducted during 2017 to 2018. **Figure 1** provides details of recruitment and follow up of study participants. After requesting 256 parents, 193 infants attending the pediatric department of Bharati hospital Pune for vaccination and

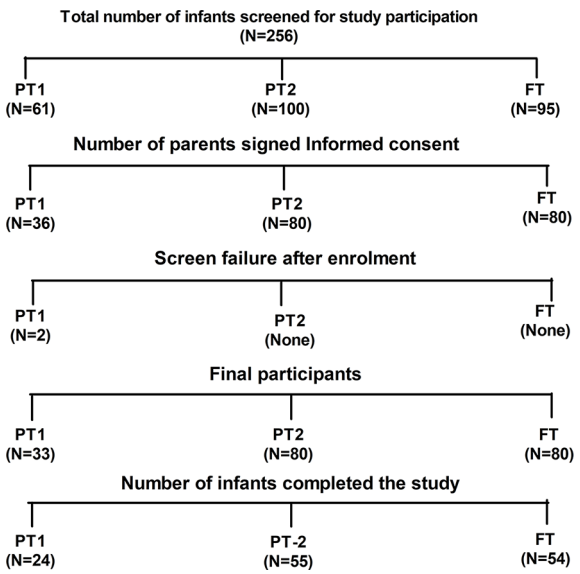

FIGURE 1 | Study participant disposition. Out of 256 screened infants, parents of 193 infants gave informed consent for participation in the study. Two preterm infants from PT1 group were failed two meet inclusion criteria hence excluded from the study. Finally, 133 infants were able to complete the study.

routine checkup could be included. Among these, 33 were very preterm (gestation age [GA], 28–32 WK, PT1), 80 were moderate to late preterm (GA, 32–36 WK, PT2) and 80 were full term infants with >37 weeks of gestation (FT). All infants were born to HBsAg and HIV negative mothers. Exclusion criteria included past or current receipt of immunoglobulins, known suspected congenital or acquired immunodeficiency, chronic administration (defined as >14 days) of immunosuppressant or other Immune modifying drugs since birth (prednisone or equivalent for >0.5 mg/kg/day, inhaled or topical steroids were allowed). The study was approved by the institutional human ethics committee. After obtaining a written informed consent from the parents, demographic and baseline characteristics of the participants were recorded. HBV vaccine birth dose was given to the infants weighing ≥ than 2000 g. National immunization schedule for pentavalent vaccine was followed (17, 25). At the age of 6 weeks, first dose of pentavalent vaccine [DTwP-HBV-HIB vaccine, Biological E Ltd., India, (For details please refer supplementary information)] was administered. The subsequent doses of the same vaccine were given at 10th and 14th week of age. At the end of the follow up, blood samples could be collected from 54 (FT), 24 (PT1) and 55 (PT2) infants (**Figure 1**).

Sample Collection and Processing

After written informed consent from parents, 1 to 3 ml venous blood (in majority, 1–1.5 ml) was collected from the infants in EDTA, at two time points. 1] Before the administration of first dose of pentavalent vaccine and, 2] One month after the last dose of pentavalent vaccine. For multiparameter flow cytometry analyses, whole blood was used within 3 h of collection and from remaining blood, PBMCs and plasma were separated by Ficoll hypaque density gradient method and cryopreserved at −196°C and −80°C, respectively, for recall response study and cytokine profiling.

Multi-Parameter Flow Cytometry Analyses for Immune Cell Quantitation

The whole blood was incubated with flurochrome conjugated antibodies (CD3, CD8, CD4, CD19, CD27, and IgD) in one tube and CD3, CD19, CD56, CD14, CD11C, CD1C, HLA- DR, and CD123 (please refer **Supplementary Table 1** for dye, manufacturer and clone of each antibody) in another tube for 30 min in dark at room temperature. After RBC lysis by 1× FACs lysis buffer (Cat no-349202 BD, Biosciences) and wash (FACS Buffer- PBS with 2% BSA), the stained cells were stored at 4°C in fixative (3% paraformaldehyde in PBS) till acquisition on Navios Flow cytometer (Beckman Coulter, Brea, Cal) using Navios acquisition software; acquisition was performed within 24 h of staining procedure. Gating strategy is depicted in **Figures 2A, B**. Total 100,000 events were recorded. After lymphocyte gate identification, lymphocyte population was segregated depending on CD3 expression and then CD3 positive cells were further discriminated on the basis of CD4 and CD8 expression to identify CD4T cells (CD3+CD4+) and CD8 T cell (CD3+CD4+) frequencies. CD3 negative population was separated

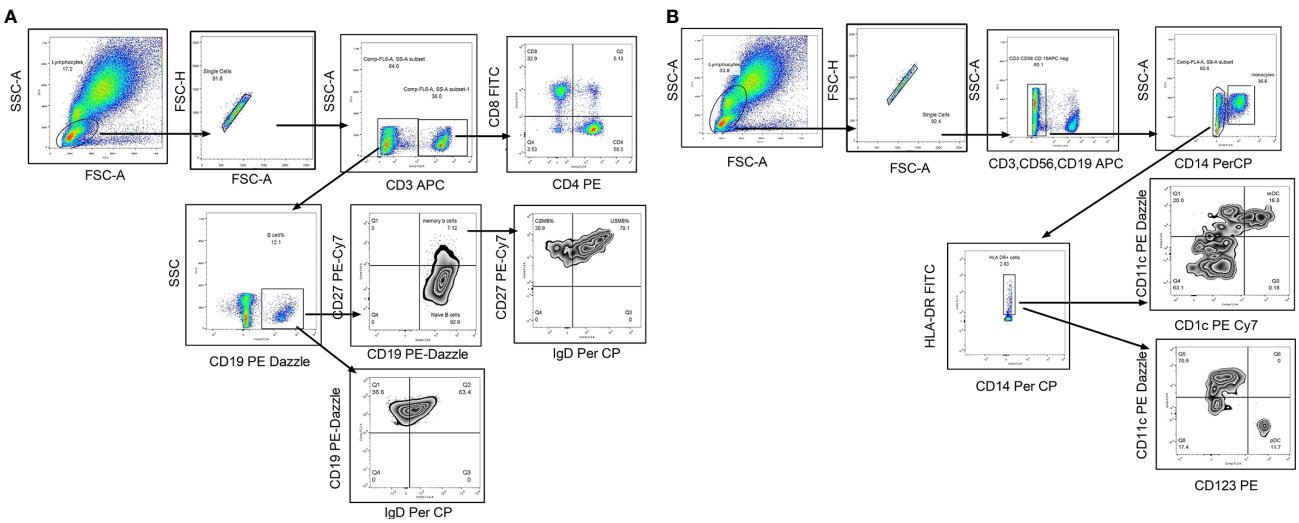

FIGURE 2 | Flow cytometry gating strategy to identify lymphocyte subsets. Representative flowcytometry dot plots from the PBMCs of one of the study participants. **(A)** Gating strategy used to identify T cells and B cell subsets. The lymphocytes were live gated during acquisition using the side and forward scatter dot plot display. Lymphocyte population was further discriminated on the basis of CD3 expression. CD3 positive population was used to identify CD4 and CD8 T cells. Whereas CD3 negative population was used to identify B cells and its subsets such as memory B cells and class switched/unswitched B cells, class switched memory B cells (CSMB) and unswitched memory B cells (USMB). **(B)** Gating strategy used to identify antigen presenting cells (mDC, pDC and Monocytes).During acquisition, with the help of side and forward scatter, cells of lymphomonocyte gate were identified and the cells from this population were further distinguished on the basis of absence of lineage markers (CD3, CD19 and CD56). Lineage negative population was further discriminated as CD14+ and CD14- population to identify monocyte population. CD14 negative population was again distinguished on the basis of HLA-DR expression. Both positive (CD11c and CD1C) population from HLA-DR positive cells was identified as myeloid Dendritic Cells (mDC). Plasmacytoid dendritic cells (pDC) were identified as HLA-DR+CD11C−CD123 + cells. In infants with high NRBC (nucleated RBC) count, contour plot was used to identify lymphocyte gate for further analyses.

on the basis of CD19 expression to identify B cell population (CD3−CD19+) that was categorized in memory B cells (CD3−CD19+CD27+) depending on their CD27 expression. To identify the class switched population, IgD based negative gating strategy was used. Class switched B cells were identified as CD3−CD19+IgD− and unswitched B cells as CD3−CD19+IgD+ whereas class switched memory B cells as CD3−CD19+CD27+IgD− and unswitched memory B cells as CD3−CD19+CD27+IgD+ cells (**Figure 2A**). The monocyte population (CD3−CD14+) was discriminated using CD14 expression on CD3 negative population. CD11c and CD1C expression on HLA-DR + CD3−CD56−CD19− cells was considered for detecting myeloid dendritic cell frequency whereas the plasmacytoid dendritic cells were identified as CD3−CD56−CD19− CD123+ HLA-DR +CD11 C− cells. The immune cell frequencies were expressed in proportion to total lymphocyte population (**Figure 2B**). The flow cytometry data were analyzed by using Flow Jo version7, Tree star.

Plasma Cytokine Profiling by Cytometric Bead Array Analysis

Cytokine analysis was done using the Human CBA flex kits by simultaneous detection of IFN-γ, IL-2, IL-4, IL-5, IL-6, IL-10, IL-13, IL-12p70, IL-17, TNF-α, and IL-21 (BD Biosciences, San Jose, California). Employing thawed aliquots of plasma, CBA analysis was performed as per the manufacturer's instructions. The samples were acquired on the same day on FACS Fusion machine by using FACS Diva software (version 3.0) FCAP Array Software (BD Biosciences, San Jose, CA, USA) was used to build standard curves and to calculate cytokine levels in plasma.

Serology

The antibody (IgG) titers against all the components of pentavalent vaccine were determined by ELISA following instructions of the manufacturers. The anti-HBs levels were determined using TNO certified Anti-surase quantitative ELISA kits by General Biologicals Corporation, Taiwan. For determination of IgG antibody levels for Diphtheria, Tetanus, and *Haemophilus influenzae* b, EN ISO 9001:2000 certified kits from DeMeditec, Germany were used while for pertussis, kits from Euroimmune (Perkin Elmer company-EN ISO 9001, EN ISO 13485/CMDCAS) were used. The IgG antibody cut-off considered for protection was ≥0.01 IU/ml for diphtheria (26) and tetanus (27), ≥10 mIU/ml for hepatitis B (28) and ≥0.15 μg/ml for Hib (29). For long term protection against HiB, the cut-off of ≥1.0 μg/ml was considered. For pertussis, which has no recognized serological correlate of protection, IgG level >22 U/ml for whole cell, was considered as vaccine response (30).

Recall Immune Response

The individual components of the pentavalent formulation were kindly provided by the Serum Institute of India, Pvt. Ltd. (SIIPL, Pune, India). Based on antibody titers against component antigens of pentavalent vaccine, ten representative samples including responders and non-responders against each of the antigen from all study groups (PT1, PT2 and FT) were selected (the details about antibody titers are provided in **Supplementary Table 2**). PBMCs of these samples obtained at post vaccination visits were revived and rested overnight at 37°C in 5% CO2 incubator. Next day, after live cell count by trypan blue, cells were washed with complete media (10% RPMI) and approximately 0.3×10^6 cells were exposed to each of component antigens separately [(tetanus toxoid (3.3 LF/ml), diphtheria toxoid (2.4 LF/ml, PRP of Hib, 1 μg/ml), HBsAg (1 μg/ml) and the whole cell of pertussis (0.18 IOU/ml) for 6 h. A pre-stimulation period of 2 h was included before the addition of 10 μg/ml Brefeldin A(B7651; Sigma-Aldrich, St. Louis, USA) and anti-human CD107a (Degranulation marker) APC-Cy7. To check constitutive cellular frequency and their phenotypic and functional profile, cells without any stimulation were used as negative control. Anti-CD3 and anti-CD28 stimulation was used as positive control. After 6 h, the cells were kept overnight at 4°C followed by staining procedure as follows. Cells were washed with 1× PBS twice and stained by live/dead stain followed by surface staining for following markers. (CD3, CD4, CD8, CD45 RA, CD62L, CCR7, CD19, CD27, CD138, HLA-DR, CD11C, CD1C, CD80, CD86, CD300a, CD154, CD269, CD40, IgD, CD123, CD56, and CD14) Following fixation by 3% paraformaldehyde and thorough washing by FACS Buffer (1× PBS-EDTA with 2%BSA), cells were permeabilized by BD FACS Perm-II (Cat no-340973; BD Biosciences) and stained for intracellular markers (IFN-γ, TNF-α, and IL-2). Cells were acquired on FACS Fusion (BD, Biosciences). Approximately, lymphocyte gated 50,000 thousand events were acquired. Data were analyzed by Flow Jo tree star (version 7.6.5). Gating strategy for recall immune responses is denoted in **Supplementary Figure 1**. (**Supplementary Information** is provided for manufacturer, dye and clone of each antibody in **Supplementary Table 3**)

To assess the comparative efficacy of pentavalent vaccination in term and preterm infants, PBMCs exposed to short term antigenic stimuli with component pentavalent vaccine immunogens were analyzed for memory profile and functionality of B cells, T cells and dendritic cells. The memory profile comprised central (CD3+CD4+CD45RA-CD62L+CCR7+) and effector memory T cells (CD3+CD4+CD45RA−CD62L−CCR7−) and their ability to secrete cytokines such as IFN-γ, TNF-α and IL-2; CD107a expression was used as a marker for CD8 T cell-mediated cytotoxicity. In case of B cells, memory B cells (CD3−CD19+CD27+), plasma cell frequency (CD3−CD19+CD138+) and B cell maturation antigen expression (BCMA-CD269) density was determined. Myeloid (Lineage negative-HLA-DR+CD11C+CD1C+) and plasmacytoid DCs (Lineage negative-HLA-DR+CD11C-CD123+) were analyzed for up regulation of maturation markers such as CD80 and CD86.

The upsurge of 1.5 fold in cellular frequency and phenotypic and functional markers of immune cells after stimulation of respective antigens as compared to constitutive expression obtained in the PBMCs without any stimulation was considered as a positive response.

Statistical Analysis

The data were analyzed using Graph pad prism (version 5). The nonparametric *Mann Whitey U test* was employed to compare the differences in immune cell subset frequencies and plasma cytokine levels between the groups. Student's T test was used to compare antibody titers among the groups. Wilcoxon signed-rank test is employed to determine difference between immune cell subsets at baseline and after follow up visits. Spearman

correlation is used to assess the bivariate correlation in between the parameters using SPSS. Multivariate and univariate analysis were performed using R programing.

RESULTS

Demographic details of 193 infants enrolled in the study are summarized in **Table 1**. Out of the total 193 infants recruited, 33 were very preterm [PT-1 (GA, 28–32 WK)], 80 were moderate preterm [PT-2(GA, 32–36 WK)] and 80 were full term [FT (GA, >37 WK)]. The study included 24, 55 and 54 follow up samples from PT1, PT2 and FT infant study groups, respectively. Overall, male gender was predominant in the preterm groups as compared to the term group. We did not observe any significant difference in age of infants at which pentavalent vaccination was administered. (One way ANOVA; at enrolment- p = 0.0807 and follow up visit- p=0.0984) (**Table 1**).

Antibody Titers Prior to the First Dose of Pentavalent Vaccine (at 6 to 10 Weeks Age)

This time point reflects maternal transfer of antibodies (**Table 2**). In India, a birth dose is mandatory for hepatitis B and administration of this dose to preterm/term infants is deferred till the attainment of 2000g body weight. Therefore, immune response to hepatitis B component of pentavalent vaccine is considered separately.

Tetanus, Pertussis, Diphtheria, and HiB

In accordance with the mandatory immunization of pregnant women with tetanus toxoid during the third trimester, all the infants (except one from the PT-1 group) were circulative protective anti-tetanus antibodies (≥0.1 IU/ml) at the time of vaccination. In contrast, very few infants exhibited protective levels of anti-Pertussis toxin IgG antibodies (>22U/ml); none in PT1, 6.25% in PT2 and 5% in the FT groups suggestive of lack of these antibodies in the mothers. For diphtheria and HiB, respective antibodies were present in 87.9%, 92.5%, 97.5% and 81.81%, 70%, 72.5% infants in PT1, PT2 and FT categories, respectively. Of note, none of the infants from PT1 group circulated anti-Dtx-IgG antibodies at protective levels of ≥0.1 IU/ml while only 17.6% and 25% of the PT2 and FT infants exhibited such antibodies. For HiB, protective antibody positivity (1ug/ml) was recorded in 6.1% to 16.2% infants from the three infant groups.

Figure 3 depicts comparisons of antibody levels against the pentavalent antigens among the three study groups examined. The levels of anti-Ttx, anti-Dtx and anti-PT antibodies were significantly lower in PT1 than the PT2 infants (p = 0.0003, <0.0001 and <0.0001, respectively) while levels of anti-PRP antibodies were comparable (**Figure 3**).

Antibody Titers 1 Month Post-Pentavalent Immunization (at 20 to 24 Weeks Age)

For tetanus, all the PT1/PT2 and FT infants exhibited anti-Ttx antibodies at the level of ≥0.1 IU/ml. Though 100% seroconversion was recorded for diphtheria in all the groups, lower antibody levels (<0.1IU/ml) were noted in 91.7% of PT1 infants as against comparable levels in PT2 (98.2%) and FT infants (98.1%). For HiB, 95.8% to 100% infants from different groups developed antibodies at ≥0.15 μg/ml level. However, almost half of the PT1 infants (54.2%) did not induce antibodies at ≥1 μg/ml as against 80 and 90.7% in PT2 and FT groups. For pertussis, 26% to 28% infants from all the groups lacked adequate antibodies at >22U/ml. Clearly, immune response to pertussis was suboptimal in all the immunized infants. Post-immunization anti-DTx, anti-TTx and anti-Pertussis (PT) antibody titers were comparable in all the groups examined. For HiB, the respective antibody titers were significantly lower in PT1 infants than in the PT2 and FT groups (p = 0.01–0.001) while no difference was noted among PT2 and FT infants (p >0.05) (**Table 2** and **Figure 3**).

Due to varied proportion of maternal antibody positives, we compared fold rise in antibody titers among maternal Ab positives and negatives in different study groups at 1 month post-immunization (**Table 3**). Immunization in the presence of high tittered maternal antibodies did not result in boosting effect as evidenced by post-immunization titers. For HiB, a significant proportion (31.8%, 68.2–75.9%) of Ab-positives did not induce desired antibody response while for pertussis and Hepatitis B, the response was independent of maternal antibody positivity. Whether such infants continue to circulate high antibody titers till receiving booster dose by 15th or 18th months of age in future remains an open question.

TABLE 1 | Demographic characteristics of study groups.

Parameter	PT1 (28–32 weeks)	PT2 (32–36 weeks)	FT (>36 weeks)
Number recruited	33	80	80
Number followed up	24	55	54
Gestation age (weeks)	30.4	34.1	37.9
*Age at enrolment (mean weeks ± SD	10.2 ± 2.85	6.5 ± 1.94	6.4 ± 1.2
*Age at follow up (mean weeks ± SD	24 ± 1.4	20 ± 2.48	20 ± 2.5
M/F	22/11	64/16	36/44
Birth weight (kg) (mean weeks ± SD	1.02 ± 0.34	1.69 ± 0.43	2.9 ± 0.36

Age difference among the groups was not significant (one-way ANOVA; at enrolment, 0.0807 and follow up visit, p = 0.0984)
Age at enrolment, before first dose of pentavalent vaccine.
Age at follow up, 1 month after last dose of pentavalent vaccine.

TABLE 2 | Pre and post pentavalent vaccination antibody titres against tetanus, diphtheria toxoid, *Haemophilus influenza* B and *Bordetella pertussis*.

Name of antibody	Baseline			Post pentavalent vaccination		
	PT1 (n=33)	PT2 (n=80)	FT (n=80)	PT1 (n=24)	PT2 (n=55)	FT (n=54)
Anti-Tetanus- IgG						
% Seroprotection and 95% CI (≥0.01 IU/ml)	100 (100–100)	100 (100–100)	100 (100–100)	100 (100–100)	100 (100–100)	100 (100–100)
% Seroprotection and 95% CI (≥0.1 IU/ml)	93.93 (89.91–100)	100 (100–100)	100 (100–100)	100 (100–100)	100 (100–100)	100 (100–100)
GMT	1.56	2.71	3.57	1.44	1.47	1.82
Anti-Diphtheria-IgG						
% Seroprotection and 95% CI (≥0.01 IU/ml)	87.87 (76–99.75)	92.5 (86.23–98.76)	97.5 (94.07–100.92)	100 (100–100)	100 (100–100)	100 (100–100)
% Seroprotection and 95% CI (≥0.1 IU/ml)	0	18.75 (9.47–28.02)	25 (15.51–34.48)	91.66 (81.6–100)	98.18 (95–100)	98.14 (95.19–100)
GMT	0.02	0.04	0.05	0.53	0.65	0.70
Anti PRP-IgG						
% Seroprotection and 95% CI (≥0.15 μg/ml)	81.81 (67.78–95.85)	70 (59.1–80.89)	72.5 (62.71–82.28)	95.83 (88.56–100)	100 (100–100)	98.14 (95.19–100)
% Seroprotection and 95% CI (≥1 μg/ml)	6.06 (0–14.74)	12.5 (4.63–20.36)	16.25 (8.16–24.33)	54.16 (36.03–72.3)	80 (70.49–89.5)	90.74 (84.38–97.09)
GMT	0.21	0.32	0.35	1.58	4.20	7.71
Anti-Pertussis-IgG						
% Seroprotection and 95% CI (>20 U/ml)	0 (0–0)	6.25 (0.49–12)	5 (0.22–9.77)	75 (59.23–90.76)	72.72 (62.14–83.31)	74.07 (64.47–83.67)
GMT	0.050	0.67	0.16	29.23	25.64	30.28

GMT, geometric mean titer; 95% CI, 95% confidence interval.

Hepatitis B

Anti-HBs Levels Prior to Pentavalent Vaccine Administration

Maternal antibodies were detected in 57.7%, 70.7%, and 80% PT1, PT2 and FT infants prior to pentavalent immunization while 6.6% to 15% circulated protective anti-HBs levels. In PT2 infants receiving birth dose prior to pentavalent vaccine, 31/38 (81.57%) were anti-HBs positive while 30/42 (71.4%) without the birth dose circulated these antibodies (p>0.1). In FT and PT1 groups, 5/80 and 33/33 infants, respectively, did not receive the birth dose and hence such a comparison was not possible. Protective anti-HBs levels were independent of birth dose. Pre-immunization anti-HBs titers were comparable in all the groups with or without birth dose of the vaccine (**Table 4** and **Figure 4**).

Anti-HBs Levels Post-Pentavalent Vaccine Immunization

One-month post-pentavalent immunization, 91.7% to 100% infants from all the three groups seroconverted to anti-HBs, 88.8% to 100% with protective antibody levels (GMT, 253.8–306.8). ~8% PT infants lacked protective levels of anti-HBs antibodies. Post-immunization anti-HBs titers did not vary significantly when the infant groups were compared with respect to the receipt of the birth dose (PT2 p = 0.45 and FT p = 0.15). Overall, FT infants developed higher antibody levels than the PT1 (p = 0.02) and PT2 (p = 0.005) infants (**Table 4**, **Figure 4**).

The serological results demonstrated clear differences in the immunogen-specific antibody positivity rates and proportions with protective titers in the infant groups examined. To understand basis for such differences, we examined circulating immune cells, cytokines and recall immune responses to immunogens of pentavalent vaccine.

Enumeration of Circulating Immune Cells

The median frequency of immune cells (%) and the interquartile ranges (IQR) are summarized in **Table 5**.

Prior to Pentavalent Vaccine Administration

The preterm infants showed lower frequency of CD4 cells (PT-1, 10.6%; PT2, 12.9%) when compared to the FT infants (15.5%, p <0.0001 and 0.008, respectively). The proportion of CD8 T cells was higher in PT1 infants (17.5%) than in the PT2 (10.86%, p <0.0001) and FT infants (12.11%; p = 0.01). CD4/CD8 ratio was equal to 1 or above in 33.3% PT1, 52.5% PT2 and 83.8% FT infants (**Figures 5A–C**). Additionally, PT1 infants were armed with lower number of antigen-presenting cells such as dendritic cells and monocytes. The proportions of both subsets of dendritic cells, myeloid dendritic cells and plasmacytoid dendritic cells were lower in the PT1 group than in PT2 (p = 0.0009 and 0.0057) and FT (p = 0.0035 and 0.0014) infants. Similarly, lower monocyte frequencies were recorded in the PT1 infants when compared to PT2 (p=0.004) and FT (0.0007) categories (**Figures 5D–F**).

Post-Pentavalent Vaccination

At this time, the CD4 and CD8 frequencies were similar to enrolment i.e. lower CD4 and higher CD8 proportions in PT1 infants as compared to PT2 and term groups resulting in lower CD4/CD8 ratio in the PT1 infants. In contrast to pre-vaccination, the frequencies of monocytes and mDC at post-

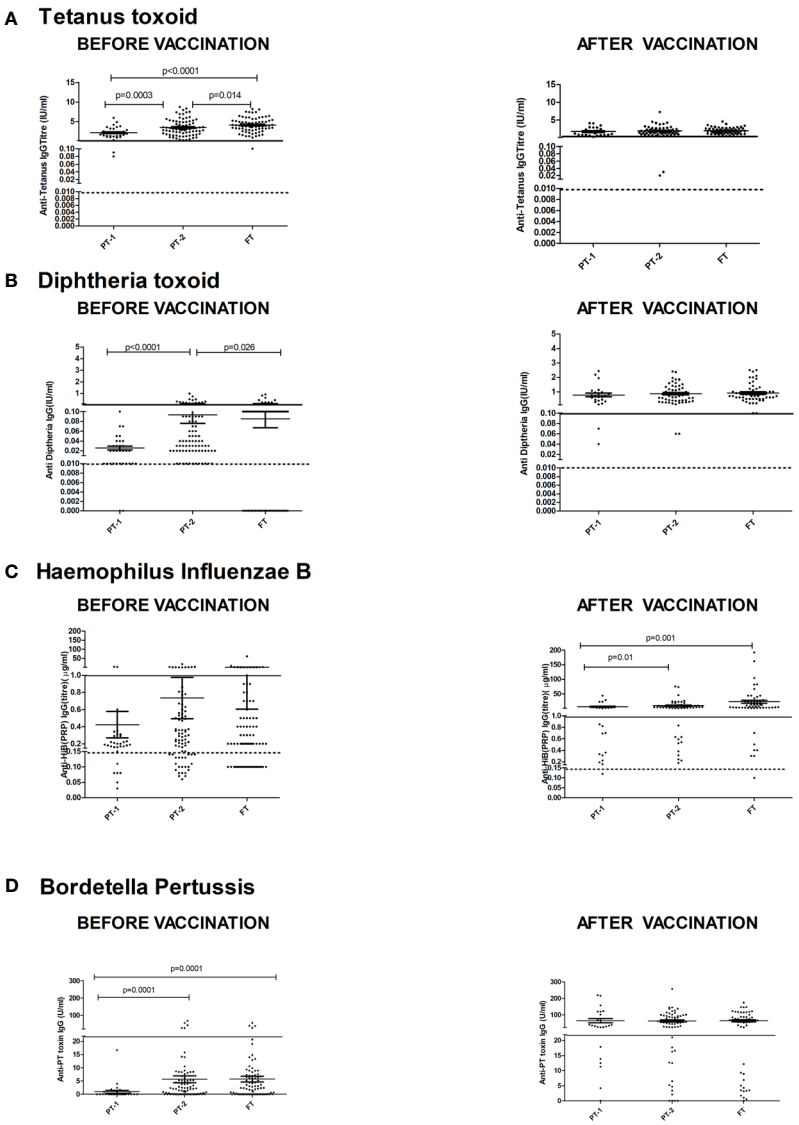

FIGURE 3 | Antibody titers against component antigens of pentavalent vaccine. The vertical scatter dot plots present antibody titers against **(A)** Tetanus (anti-Ttx), **(B)** Diphtheria (anti-Dtx) toxoids, **(C)** anti-PRP (HiB), **(D)** anti-Pertussis toxin (*Bordetella*) before (at baseline) and after pentavalent vaccination. Dotted lines in the graph indicate seroprotective antibody titers. Error bars- Mean with SEM.

TABLE 3 | Fold rise in antibody titres in presence and absence of maternal antibody (MT-Ab).

Immunogen	Infants with MT-Ab			Infants without MT-Ab		
	Number with ≥ 4fold rise in titers/Total Number with MT-Ab (%)			Number of infants seroconverting to protective levels/total number without MT-Ab (%)		
	PT1	PT2	FT	PT1	PT2	FT
Tetanus Toxoid	2/22 (9.1)	2/55 (3.6)	0/54	0/0	0/0	0/0
Diphtheria Toxoid	18/19 (94.7)	49/55 (89.1)	46/54 (85.2)	03/03 (100)	0/0	0/0
Hib (PRP)	15/22 (68.2)	41/55 (74.5)	41/54 (75.9)	0/0	0/0	0/0
Whole cell Pertussis	8/10 (80)	31/39 (79.5)	23/32 (71.9)	9/13 (69.2)	13/16 (81.2)	8/33 (24)
Hepatitis B surface antigen	12/13 (92.3)	36/39 (92.4)	33/36 (91.7)	9/9 (100)	11/14 (78.6)	36/36 (100)

Except for a small proportion of PT1 (2/22) and PT2 (2/55) infants, 4fold rise in anti-TT titers was not recorded post-immunization. It would be necessary to determine dynamics of these antibodies till boosted by an additional dose in 15th to 18th month.
MT-Ab, maternal antibody.

TABLE 4 | Anti-HBs IgG titres in all study groups categorized on the basis of HBV birth dose administration.

Parameter	Pre-pentavalent vaccination			Post-pentavalent vaccination		
Birth status (No)	**PT1 (33)**	**PT2 (80)**	**FT (80)**	**PT1 (24)**	**PT2 (55)**	**FT (54)**
	Irrespective of birth dose					
Anti-HBs+ve	19 (57.7%)	59 (73.7%)	55 (68.7%)	24(100%)	44 (97.8%)	54(100%)
>10mIU/ml	2(6.06%)	6 (7.5%)	12 (15%)	22 (91.7%)	40 (88.8%)	54(100%)
GMT	0.31	2.68	0.52	253.8	275.9	306.8
	Birth dose administered					
Number	**0**	**39**	**75**	**0**	**28**	**50**
Anti-HBs+ve	–	33(94.2%)	51 (68%)	–	27 (96.42%)	50(100%)
>10 mIU/ml	–	4 (10.25%)	11 (14.6%)	–	26(92.85%)	50(100%)
GMT	–	1.86	0.53	–	157.4	312.72
	No birth dose					
Number	**33**	**41**	**5**	**24**	**27**	**4**
Anti-HBs+ve	19 (57.7%)	29 (70.73%)	4 (80%)	22 (91.7%)	27 (100%)	4 (100%)
>10mIU/ml	2(6.06%)	2(4.87%)	1(20%)	22(91.7%)	24(88.88%)	4(100%)
GMT	0.31	2.14	1.09	122.4	130.98	306.76

GMT, geometric mean Titer.
Values in bold represent total number of infants in the corresponding categories.

vaccination time point were comparable among all the three groups. However, pDC frequencies continued to be lower in the PT1 infants than in PT2 (p=0.01) and FT (p=0.03) infants.

Plasma Cytokine Profiles Pre- and Post-Pentavalent Vaccination

For this, 18, 36, and 33 paired serum samples, respectively, from PT1, PT2 and FT infants obtained pre and post pentavalent vaccination were tested. Among the Th-1 cytokines, TNF-α levels were significantly higher in term infants when compared to PT1 infants (p = 0.03) at enrolment visit. In contrast, the levels of IL-10, a Th-2 cytokine were higher in very preterm infants as compared to term infants (p = 0.001) and moderate preterm infants (p = 0.014) (**Figure 6**). Post-vaccination, IL-10 levels continued to be higher in very preterm infants than in the moderate preterm infants (**Figures 6A, B**). Marginal differences without any statistical significance were observed for the other cytokines tested at both the time points. With age, IL-21 and TNF-α level increased in the PT-2 and term infants while IL-4 increase was seen in the term infants (**Figure 6C**).

Correlation Analyses

Next, we evaluated relationship of antibody titers against vaccine component antigens with variables such as gestational age and several immune cells/cytokines present in PT1/PT2/FT infants at the time of vaccination (**Table 6**). Of the immune cell parameters evaluated, univariate analysis revealed significant association of only few with antibody response. Gestation age was identified as a significant variable influencing antibody response to tetanus, diphtheria, pertussis and HBsAg, but not to HiB. For HiB and HBsAg, only single parameter was significant and hence multivariate analysis was not possible.

Anti-tetanus response was significantly associated with CD4, CD8, monocyte and pDC frequencies, but, multivariate analysis identified gestation age as the only predictor for antibody titers. In case of diphtheria toxoid, univariate analysis showed significant associations of humoral response with CD4, unswitched memory B cells, dendritic cells (mDC and pDC) and monocyte frequencies, however, multivariate analysis revealed a strong association with pDC only. For pertussis with compromised seroprotective titers in all the study groups, a significant association with gestation age, monocyte, and plasma levels of IL-6, IL-10, and IL-2 was found in univariate analysis, but plasma IL-6 levels emerged to be the significant parameter in multivariate analysis (**Table 6**).

Recall Immune Responses to Constituent Immunogens of Pentavalent Vaccine

To understand the comparative response of term and preterm infants to pathogen exposure, infant PBMCs from immunized infants were stimulated with component antigens of pentavalent vaccine. Live/dead staining of PBMCs demonstrated approximately 90% viability (median, 92.36; IQR, 85.47–96.32). Memory profile and functionality of B cells, T cells and dendritic cells was determined (**Figure 7**). None of the infants from all the study groups exhibited any modulation when the PBMCs were stimulated with tetanus or diphtheria. For the remaining three immunogens, birth status-specific alterations were noted. As against significant rise (>1.5-fold) of all the indicated markers in the FT group, the response of both PT1 and PT2 was much lower. PT1 documented an increase of 2.06 fold (*Bordetella*: central memory CD8 T cells, CD300a MFI) and 2.35-fold (HiB: TNF-α, and IFN-γ bifunctional central memory CD8 T cells). In the PT2 infants, central memory CD8T cells (CD300a MFI) increased 2.2 fold with pertussis and 1.02-fold, increased, central memory CD8 T cells (TNF-α MFI) and BCMA+ plasma cells raised 1.5-fold with HBsAg while central memory CD8 T cells (CD300a MFI) increased 2.33 fold for HiB. Overall, there was a prompt proliferation of central memory T cell compartment with Th1 cytokine secretion in term infants as compared to preterm infants. Immune cells of term infants showed highest

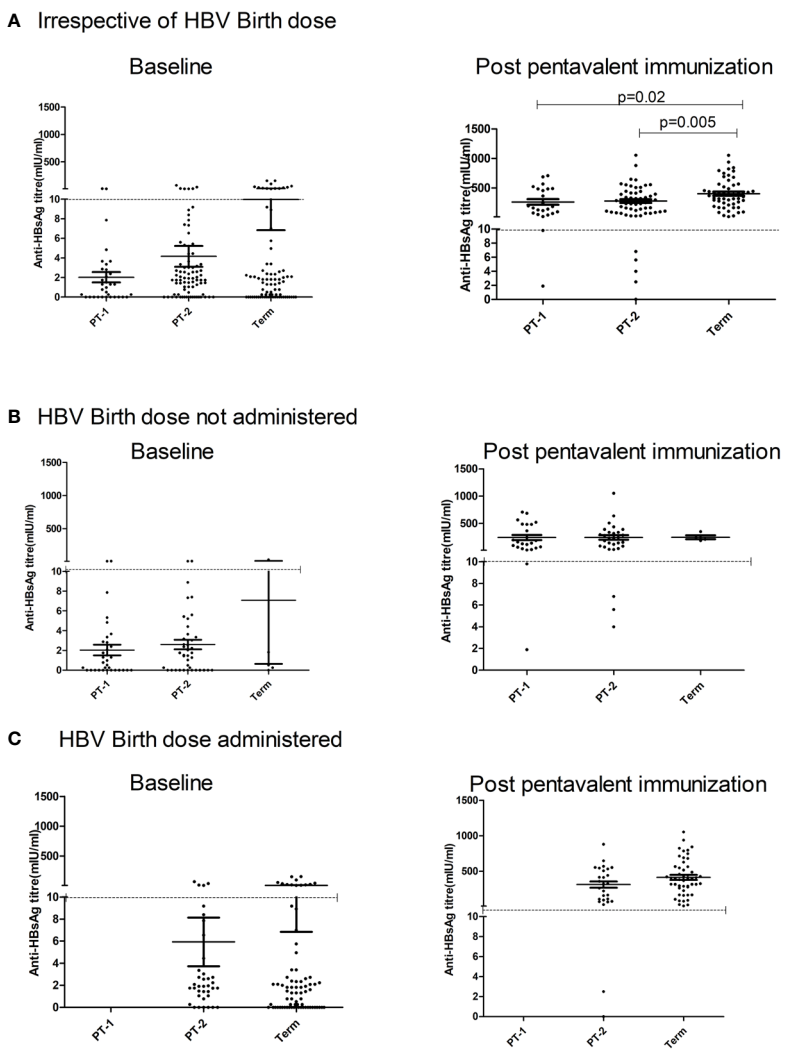

FIGURE 4 | Effect of administration of Hepatitis B Vaccine dose at birth on anti-HBs titers at pre and post pentavalent vaccination. Hepatitis B vaccine birth dose is administered to infants weighing ≥ 2000 g. Pre (baseline) and post-pentavalent vaccination anti-HBs titers are depicted with respect to the administration of birth dose: **(A)** (Irrespective of birth dose), **(B)** (no birth dose administered) and **(C)** (birth dose administered). The vertical scatter dot plots in the figure represent the antibody titers against HBsAg at pre and post pentavalent visits. Dotted line in the graph indicates the seroprotective antibody titers. Error bars- Mean with SEM.

capability to respond to the component immunogens, particularly inactivated whole cell of *Bordetella*, HBsAg and PRP moiety of *Hemophilus influenzae* B, suggestive of robust immunological memory development.

DISCUSSION

The primary aim of our study was to assess if the current national recommendations for pentavalent immunization of preterm infants are appropriate and ensure adequate immune response. For this, we first compared our results among FT infants with recent Indian studies (18). Post-pentavalent vaccination antibody positivity for tetanus, diphtheria, HiB and hepatitis B was similar to previous reports (18, 20, 24). In contrast, seroconversion rate against pertussis was alarmingly lower (74.1%). In view of the growing number of pertussis infections globally, this is indeed a matter of concern and additional studies are needed to assess if this is an isolated observation or a national concern. We would like to point out here that percent seroconversion to PT was found to vary from >95% (18, 20) to ~70% (31, 32). The vaccine administered during this study was provided by the government of India under the national universal immunization program (17).

Though we did not collect blood samples from the mothers, infant samples collected at ~6 weeks of age do reflect maternal antibody pattern in relation to the pentavalent antigens. Positivity rates were comparable to previously reported studies

TABLE 5 | Lymphocyte proportions of immune cells in all study groups at baseline and after pentavalent vaccination.

Type of immune cell	Enrolment			Post pentavalent vaccination		
	PT1 (N=33)	PT2 (N=80)	FT (N=80)	PT1 (N=24)	PT2 (N=55)	FT (N=54)
CD4% (median and IQR)	10.65 ± 5.97 (5.76–13.68)	12.94 ± 7.88 (5.94–17.93)	15.54 ± 7.88 (10.2–19.2)	12.19 ± 5.558 (8.54–15.85)	16.89 ± 7.7 (10.5–20.93)	18.99 ± 6.86 (12.9–25.43)
CD8% (median and IQR)	17.42 ± 10.27 (7.30–27.5)	10.86 ± 8.33 (4.84–13.6)	12.11 ± 7.14 (7.31–15.1)	19.98 ± 8.19 (16.95–24.38)	12.57 ± 6.07 (8.22–17.35)	15.49 ± 6.33 (11.65–18.35)
B cell % (median and IQR)	17.5 ± 9.93 (8.6–25.55)	16.73 ± 8.70 (8.95–23.5)	18.94 ± 10.23 (10.6–24.3)	18.23 ± 7.90 (11.15–25.95)	20.87 ± 8.83 (14.85–28.03)	22.63 ± 8.61 (15.83–27.45)
Class switched B cells % (median and IQR)	25.15 ± 14.53 (14.63–30.93)	25.73 ± 13.91 (14.8–32.9)	19.92 ± 11.95 (8.75–29.8)	28.48 ± 9.501 (20.7–35.1)	32.8 ± 15.38 (25.3–39.03)	29.82 ± 8.32 (24.73–34.38)
Unswitched B cell% (median and IQR)	73.07 ± 16.15 (63.35–82.95)	73.75 ± 14.37 (66.4–85.2)	79.86 ± 11.97 (70.2–91.25)	69.15 ± 9.824 (60.48–77.7)	65.88 ± 15.19 (60.5–73.23)	70.18 ± 8.32 (65.63–75.27)
Memory B cell% (median and IQR)	11.27 ± 15.17 (3.10–9.28)	9.86 ± 13.83 (3.63–8.63)	10.07 ± 10.33 (3.9–10.6)	13.98 ± 12.66 (6.063–15.08)	14.68 ± 16.57 (5.03–15.98)	8.03 ± 3.61 (5.17–10.3)
Class switched memory B cell % (median and IQR)	34.26 ± 22.91 (16.6–55.7)	32.42 ± 20.58 (14.6–44.9)	28.79 ± 17.97 (12.25–42.95)	38.37 ± 22.23 (18.05–52.7)	46.09 ± 22.26 (32.08–64.35)	49.79 ± 15.24 (38.68–61.2)
Unswitched memory B cells % (median and IQR)	64.17 ± 22.34 (43.75–79.98)	66.98 ± 20.37 (54.8–83.8)	71.21 ± 17.97 (57.05–87.75)	59.95 ± 20.82 (47.3–73.3)	53.01 ± 21.55 (35.65–67.58)	50.52 ± 14.74 (38.8–61.33)
Myeloid dendritic cells (mDC)% (median and IQR)	0.20 ± 0.12 (0.09–0.27)	0.35 ± 0.24 (0.19–0.47)	0.33 ± 0.22 (0.16–0.44)	0.30 ± 0.19 (0.17–0.47)	0.32 ± 0.19 (0.185–0.44)	0.32 ± 0.21 (0.18–0.44)
Plasmacytoid dendritic cells (pDC)% (median and IQR)	0.11 ± 0.09 (0.05–0.17)	0.2 ± 0.15 (0.09–0.26)	0.2 ± 0.14 (0.1–0.26)	0.11 ± 0.06 (0.05–0.17)	0.19 ± 0.19 (0.09–0.24)	0.15 ± 0.09 (0.08–0.19)
Monocytes % (median and IQR)	5.5 ± 3.82 (2.5–6.79)	7.75 ± 4.0 (4.77–10.4)	8.34 ± 4.24 (5.06–11.1)	7.4 ± 3.8 (5.033–10.63)	7.0 ± 3.4 (4.58–8.57)	6.26 ± 3.09 (3.58–9.28)

conducted during 2006 to 2009 (18, 20). Next, post-immunization antibody titers against the vaccine components were compared in relation to the gestational age. Different categories did not differ in mounting protective antibody response against tetanus and diphtheria. Though induction of anti-HiB antibodies at ≥0.15 ug/ml level was comparable in all the infants, the proportion of infants developing ≥1 ug/ml levels was lower preterm infants. Over 50% of the PT1 infants and 20% of the PT2 infants did not develop desired antibody levels and hence could be susceptible later. Of concern, suboptimal antibody response against pertussis was independent of gestational age (72–74%) and could be related to the vaccine response in general.

For hepatitis B, excellent and comparable (97.8–100%) anti-HBs positivity was observed in all the three groups, approximately 8% (PT1) and 11% (PT2) infants without protective anti-HBs levels. Nonetheless, FT infants with better developed immune system induced higher anti-HBs titers than the PT1 (p=0.02) and PT2 (p=0.005) infants. Administration of birth dose to the PT2 infants did not significantly influence antibody positivity/titers. Comparable anti-HBs response in full term, normal weight and underweight Indian infants was documented after receiving hepatitis B vaccine at birth and pentavalent vaccination as per recommended schedule (33). The data suggests that rather than birth weight, gestational age plays crucial role in deciding immune response.

Another important issue is the presence and titers of maternal antibodies in relation to birth status and effect on the development of antibody response post-vaccination. For tetanus, Diphtheria and HiB, almost all the infants were born to mothers with respective antibodies. For hepatitis B, rise in titers was independent of maternal antibody positivity (**Table 3**). In contrast, significantly lesser FT infants without maternal anti-pertussis antibodies (8/33, 24.2%) developed ≥4-fold higher titers than those with these antibodies (23/32, 71.9%, p<0.001). High anti-TT titers reflect mandatory immunization of pregnant women with TT. Except for a small proportion of PT1 (2/22) and PT2 (2/55) infants, 4 fold rise in anti-TT titers was not recorded post-immunization. Clearly, maternal antibodies did interfere with boosting effect. In fact, a drop was evident. It would be necessary to determine dynamics of these antibodies till receipt of the booster dose at 15 to 18 months age. Following a tetanus booster at 15 months, comparable humoral and cellular responses were recorded in FT and PT infants. At 15 months, premature infants exhibited lower levels of anti-tetanus antibodies, those born at a gestational age of < 32 weeks with lowest levels (34).

Taken together, our study revealed that as compared to the FT group Indian preterm infants develop adequate antibody response against tetanus and diphtheria, lower titers against HiB and HBsAg while suboptimal anti-pertussis response was independent of gestational age. To understand the basis for such differential responses, we determined relationship of gestation age with proportion of circulating immune cells and cytokines at pre- vaccination. Similar to an earlier observation, all the preterm infants exhibited lower frequency of CD4 and higher CD8 cells at the age of 6 to 8 weeks (35).

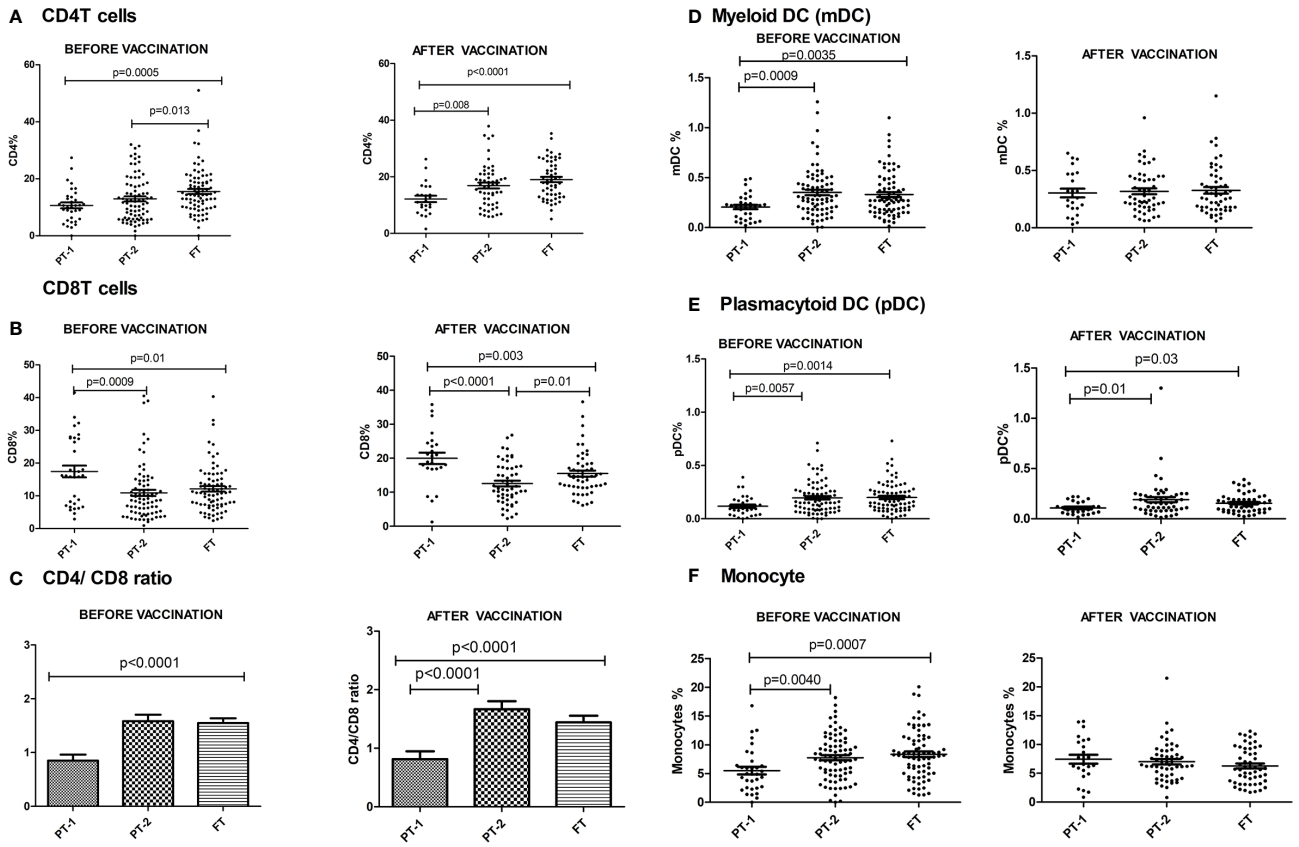

FIGURE 5 | Frequency of major Immune cells in PT1, PT2 and FT infant groups prior to (at baseline) and one month post-pentavalent vaccination. The vertical scatter dot plots represent frequencies of different immune cells before and after pentavalent vaccination: **(A)** CD4 T cells, **(B)** CD8 T cells, **(C)** CD4/CD8 T cell ratio **(D)** Myeloid dendritic cells, **(E)** Plasmacytoid Dendritic Cells and **(F)** monocytes. Error bars- Mean with SEM.

Additionally, the PT1 infants were armed with lower number of antigen-presenting cells such as dendritic cells and monocytes. At this time, lower TNF-α and raised IL-10 levels characterized PT1 infants.

Three months later, PT1 infants continued to have lower CD4 cells and pDCs and, higher CD8 cells as well as IL-10 levels while the other parameters returned to levels similar to other infants. CD8 cells from cord blood of preterm infants were shown to be highly activated and hyper-responsive to inflammatory stimuli *in vitro* (36). Activation of T-cell–mediated immunity, particularly CD8 T cells, takes place during the first postnatal days in preterm infants with RDS (respiratory distress syndrome) and this activation is associated with development of bronchopulmonary dysplasia (BPD) (37). Pathogenesis of BPD is multifactorial (38). In the preterm infants, priming of adaptive immunity leading to augmented inflammatory response may be one of the factors contributing to the pathogenesis of BPD and other chronic complications. Indeed, history of RDS (Respiratory distress syndrome) in our infant series was gestational age-driven; as against 23.5% moderate preterm and 1.2% of FT infants, majority of the very preemies (70%) suffered from RDS (data not shown).

To identify parameters influencing immune response to individual components of pentavalent vaccine, multiple regression analysis was done. In univariate analysis, a significant association of GA with antibody response was found for all the antigens except HiB. Importantly, GA was identified as a significant independent variable influencing response to tetanus ($p = 0.0005$) and to a lesser degree for pertussis ($p = 0.054$) and diphtheria ($p = 0.06$). Though the response to tetanus was universal, GA did influence titers, increasing with GA.

Frequency of pDCs emerged to be the single independent variable positively impacting humoral response to diphtheria. It is pertinent to note that recombinant granulocyte-macrophage colony-stimulating factor (GM-CSF) could improve immune response to the diphtheria component in a multivalent vaccine (39). GM-CSF and IL-3 were able to efficiently promote pDC survival (40). A significant and direct correlation between the number of pDCs and the development of protective humoral immune response to measles vaccine at 3 months post-vaccination is noteworthy (41).

Pertussis component of the vaccine leading to suboptimal antibody response across all the infant groups is of special

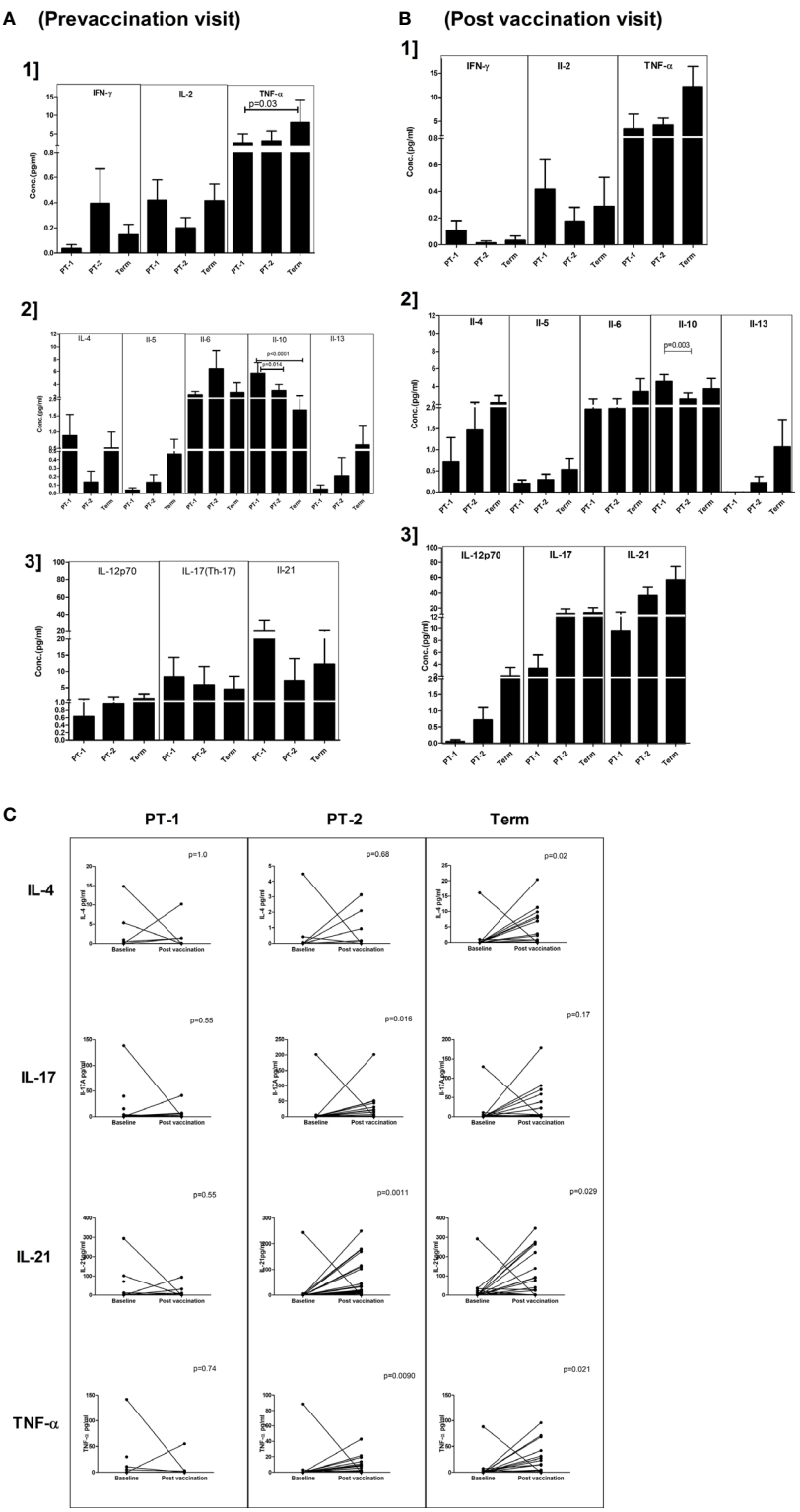

FIGURE 6 | Plasma cytokine levels in PT1, PT2 and FT infants prior to **(A)** and post-**(B)** pentavalent vaccination. The vertical column bar graphs represent A1] Th1 cytokines (IFN-γ, IL-2, TNF-α), A2] Th2 cytokines (IL-4, IL-5, IL-6, IL-10, IL-13) and A3] Th17 and miscellaneous cytokines before vaccination; B1, B2, and B3 plots present respective cytokines at post-pentavalent vaccination. **(C)** The line graphs denote the changes in plasma IL-4, IL-17, IL-21, and TNF-α levels in all the infant groups before and after pentavalent vaccination. Error bars- Mean with SEM.

TABLE 6 | Multivariate analysis to identify independent variables influencing antibody response to the pentavalent vaccine components*.

Immunogen	Variable	Univariate (p value)	Multivariate (p value)
Tetanus toxoid	Birth status	<0.001	0.0005
	CD4%	0.048	0.2
	CD8%	0.045	0.2
	pDC%	0.028	0.2
	Monocyte%	0.025	0.15
Diphtheria toxoid	Birth status	0.046	0.06
	CD4%	0.049	0.09
	Unswitched memory B cells%	0.042	0.16
	mDC%	0.002	0.2
	pDC%	0.007	0.03
	Monocyte%	0.04	0.6
***B. pertussis* (Whole cell)**	Birth status	0.049	0.054
	Monocyte%	0.01	0.055
	IL-2 (pg/ml)	0.02	0.055
	IL-6 (pg/ml)	<0.001	0.001
	IL-10 (pg/ml)	0.04	0.8
HiB(PRP)	mDC%	0.025	NA
HBsAg	Birth status	0.034	NA

**Parameters with significant influence on antibody titers in univariate analysis were included for multivariate analysis. NA, Not Applicable.*

significance. In addition to IL-6 as the most significant independent factor (p=0.001), GA, monocytes and IL-2 seem to be impacting the antibody response as well (p = 0.054–0.055). Cytokine regulation and co-stimulatory molecules are pivotal to the immunological switch from innate to adaptive immunity. IL-6 was shown to contribute to the generation of *B. pertussis*-specific IL-17 responses (42). Studies have suggested that *B. pertussis* infection skews the host immune response toward the expansion of Th17 cells (43, 44). Further, IL-17 promoted macrophage killing of *B. pertussis* while depletion of IL-17 led to reduction in the efficacy of *B. pertussis* whole-cell vaccine (45). In mice, efficient clearance of *B. pertussis* and vaccine-induced immunity against the pathogen were shown to be IL-6 dependent (46). Despite identifying role of IL-6 in generating adequate anti-pertussis antibody response, the question of less efficacy of the vaccine even in term infants remains unanswered. It is indeed intriguing that despite lower frequency of CD4 and higher CD8 cells in the PT infants and lower number of antigen-presenting cells such as dendritic cells and monocytes in the PT1 infants, anti-pertussis antibody titers were comparable with the FT infants. Additional studies are needed to confirm this observation and to identify factors for the GA-independent immune response to pertussis. Whether BCG immunization selectively helped preterm infants in attaining anti-pertussis antibody titers similar to FT infants need to be examined.

We next attempted to evaluate if antibody negative infants will be able to mount cellular immunity responses if exposed to the respective pathogens. For this, recall responses were studied in 10 infants from each group. Data revealed that immunologic memory was not just a function of GA, but, varied with different immunogens. T cell or B cell subset proliferation was not seen for tetanus and diphtheria with high antibody response by all the infants and HiB with adequate protective antibodies.

Proliferation of central memory compartment of CD4 and CD8 T cells with polyfunctional response in FT infants with or without anti-pertussis antibodies revealed that these infants are likely to be protected following exposure to the pathogen. On the contrary, non-responders as well as responders from PT1 and PT2 groups were unable to develop immunological memory as indicated by the absence of proliferating memory T cells. Clearly, PT infants with immature immune system lacked efficient cellular response that could affect subsequent protection from *Bordetella*.

For hepatitis B component, the recall response was gestation age dependent and not influenced by the presence or absence of protective antibody levels. All FT infants mounted efficient antibody as we as cellular immunity in terms of memory CD8 T cells with TNF-α production. PT2 infants with or without protective antibody levels could induce similar responses. On the other hand, irrespective of the antibody status, very preemies were unable to induce rise in memory T cells. On exposure, these infants may be susceptible to the virus.

India being a TB-endemic country, BCG (live attenuated Bacille Calmette-Guérin) at birth is mandatory (17). BCG is a known immunomodulator and shown to reduce overall neonatal mortality as a non-specific beneficial effect (47, 48). In our study, all the FT infants received BCG at birth while the preterm infants were immunized with BCG after 34 weeks of gestation (34–20 weeks). Except for 4 infants receiving BCG and pentavalent vaccine simultaneously, the gap between these vaccinations was 1 to 4 weeks. In PT infants, proportions of mDCs, pDCs and monocytes before pentavalent vaccination were independent of timing of BCG administration (data not shown). Of note, in Gambia, administration of BCG to newborns at the time of priming markedly increased the cellular and Ab responses to the hepatitis B vaccine (at birth), but had only a limited influence on the cytokine response to tetanus toxoid and no effect on the Ab responses to tetanus and diphtheria toxoids (at 2 months age) (49).

In summary, our data provides comparative antibody response of Indian infants classified according to gestational age, to the component immunogens of the pentavalent vaccine.

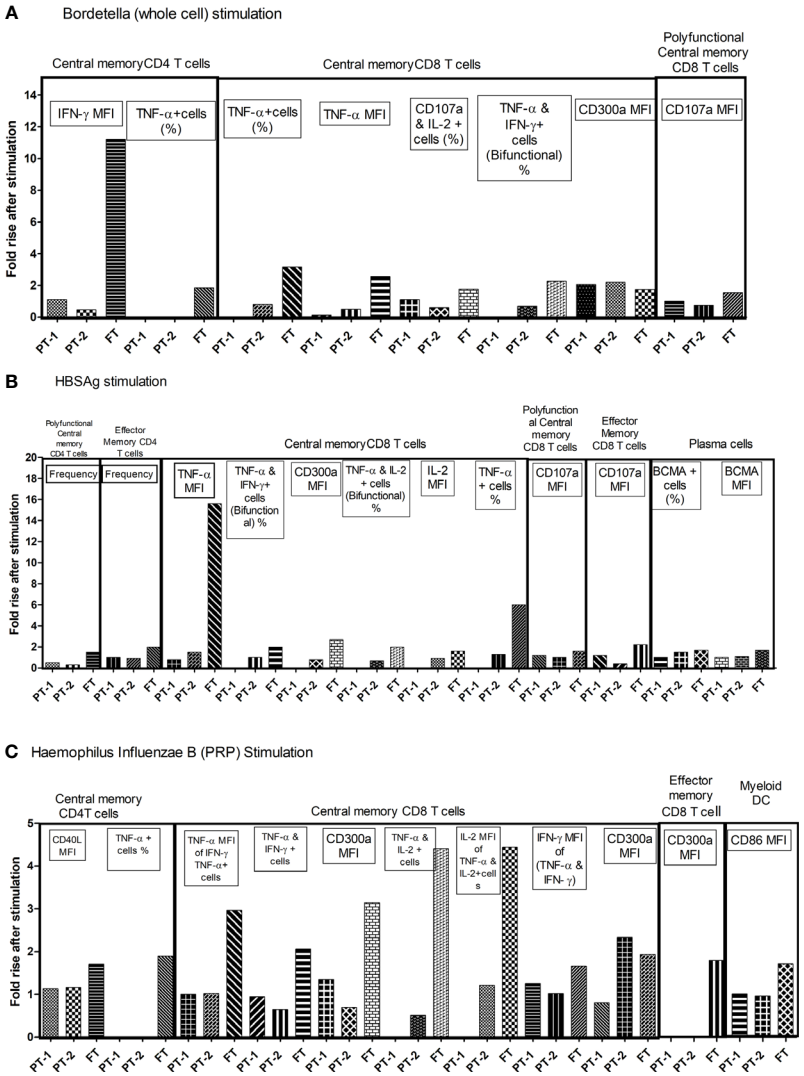

FIGURE 7 | Fold changes in functional parameters of immune cells following individual pentavalent component antigenic stimulation of cultured PBMCs. Bar diagrams in the figure exhibit the fold rise in frequency of immune cells and expression of different markers after short term exposure to **(A)** Bordetella (Whole cell) **(B)** HBsAg **(C)** Haemophilus Influenzae B (PRP) in all study groups. The major memory T cell types are mentioned above the lines. Fold rise in relevant parameters are shown in boxes. In recall response analyses, PBMCs of infants without any stimulation were used as controls. The cellular frequency and their phenotypic and functional characteristics obtained in unstimulated PBMCs were considered as baseline values to estimate fold changes induced by stimulation with component antigens of pentavalent vaccine. [Concentration of antigens used for stimulation-(Tetanus toxoid (3.3 LF/ml), Diphtheria toxoid (2.4 LF/ml, PRP of Hib, 1 μg/ml), HBs Ag (1 μg/ml) and the whole cell of pertussis (0.18 IOU/ml); Incubation time, 6 h]. As against significant rise (>1.5 fold) of all the indicated markers in the FT group, PT1 documented 2.06 fold (Bordetella: central memory CD8 T cells, CD300a MFI) and 2.35 fold (HiB: TNF-α, and IFN-γ bifunctional central memory CD8 T cells). In PT2 infants, 2.2 fold (Bordetella: central memory CD8 T cells, CD300a MFI), 1.5 fold (HBsAg: central memory CD8 T cells, TNF-α MFI, and BCMA+ plasma cells) and 2.33 fold (HiB: central memory CD8 T cells, CD300a MFI).

In view of the changing maternal antibody positivity and concentrations, such studies are essential at predefined intervals or whenever necessary. It is satisfying to note that irrespective of gestational age, all the preterm infants developed adequate antibody response against tetanus, diphtheria and, protective but lower antibody levels for HiB and hepatitis B as compared to their full-term counterparts. Suboptimal response to pertussis in all the infant groups emerged as a major concern. In addition to generating data on the relationship of circulating immune cells and cytokines with GA, the results revealed that both humoral and cellular immune responses of preterm infants were dependent on the type of the immunogen. Preterm infants born before 32 weeks of gestation may need an extra dose of pentavalent vaccine for long lived robust immune response. A further follow up till the receipt of booster dose is necessary to identify the window of susceptibility to these pathogens. For policy makers, our observations need to be extended to a large cohort representing different parts of the country.

DATA AVAILABILITY STATEMENT

The raw data supporting the conclusions of this article will be made available by the authors, without undue reservation.

ETHICS STATEMENT

The studies involving human participants were reviewed and approved by the institutional human ethics committee, Bharati Vidyapeeth (Deemed to be) University, Pune. Written informed consent to participate in this study was provided by the participants' legal guardian/next of kin.

AUTHOR CONTRIBUTIONS

VA conceptualized the study, reviewed results and analyses, and finalized the manuscript. AK-M planned and performed the work, analyzed the data, and wrote the manuscript. AM reviewed the results and contributed to the manuscript. NM, SP, and SL were responsible for subject recruitment, collection of relevant clinical information, and follow-up. AA performed parts of the experiments and provided help to AK-M. All authors contributed to the article and approved the submitted version.

FUNDING

The study was funded by the Department of Health Research, Government of India under Grant in Aids Scheme Inter-Sectoral Convergence and Coordination for Promotion and Guidance on Health Research with the main objective on research studies with emphasis on public health (grant R.11012/03/2017-HR).

ACKNOWLEDGMENTS

The authors are indebted to all the participant infants and their parents. The authors thank Dr. Anjali Kelkar, Department of Pathology, Bharati Hospital and Dr. Madhuri Thakar, National AIDS Research Institute, Pune for providing flow cytometry facilities. The authors would like to thank Serum Institute of India Pvt. Ltd (SIIPL) for providing the component antigens of pentavalent vaccine. Thanks are due to Tushar Bhosale, Rahul Patil and the staff of Pediatric Department, Bharati Hospital.

SUPPLEMENTARY MATERIAL

The Supplementary Material for this article can be found online at: https://www.frontiersin.org/articles/10.3389/fimmu.2021.592731/full#supplementary-material

REFERENCES

1. UNICEF. *Levels & Trends in Child Mortality, Report 2014* (2014). Available at: http://www.who.int/maternal_child_adolescent/documents/levels_trends_child_mortality_2014/en/.
2. Stoll BJ, Hansen NI, Bell EF, Shankaran S, Laptook AR, Walsh MC, et al. Neonatal Outcomes of Extremely Preterm Infants From the NICHD Neonatal Research Network. *Pediatrics* (2010) 126:443–56. doi: 10.1542/peds.2009-2959
3. Stoll BJ, Hansen NI, Adams-Chapman I, Fanaroff AA, Hintz SR, Vohr B, et al. Neurodevelopmental and Growth Impairment Among Extremely Low-Birth-Weight Infants With Neonatal Infection. *J Am Med Assoc* (2004) 292:2357–65. doi: 10.1001/jama.292.19.2357
4. Hornik CP, Fort P, Clark RH, Watt K, Benjamin DK, Smith PB, et al. Early and Late Onset Sepsis in Very-Low-Birth-Weight Infants From a Large Group of Neonatal Intensive Care Units. *Early Hum Dev* (2012) 88:S69–74. doi: 10.1016/S0378-3782(12)70019-1
5. Kent A, Makwana A, Sheppard CL, Collins S, Fry NK, Heath PT, et al. Invasive Pneumococcal Disease in UK Children <1 Year of Age in the Post-13-Valent Pneumococcal Conjugate Vaccine Era: What are the Risks Now? *Clin Infect Dis* (2019) 69:84–90. doi: 10.1093/cid/ciy842
6. Malloy MH. Changes in Infant Mortality Among Extremely Preterm Infants: US Vital Statistics Data 1990 vs 2000 vs 2010. *J Perinatol* (2015) 35:885–90. doi: 10.1038/jp.2015.91
7. Bonhoeffer J, Siegrist CA, Heath PT. Immunisation of Premature Infants. *Arch Dis Child* (2006) 91:929–35. doi: 10.1136/adc.2005.086306
8. Steiner L, Diesner SC, Voitl P. Risk of Infection in the First Year of Life in Preterm Children: An Austrian Observational Study. *PLoS One* (2019) 14: e0224766 1-11. doi: 10.1371/journal.pone.0224766
9. Watterberg K, Benitz W, Hand I, Eichenwald E, Poindexter B, Stewart DL, et al. Elimination of Perinatal Hepatitis B: Providing the First Vaccine Dose Within 24 Hours of Birth. *Pediatrics* (2017) 140:e20171870 1-7. doi: 10.1542/peds.2017-1870
10. Gagneur A, Pinquier D, Quach C. Immunization of Preterm Infants. *Hum Vaccines Immunother* (2015) 11:2556–63. doi: 10.1080/21645515.2015.1074358
11. Martinón-Torres F, Czajka H, Center KJ, Wysocki J, Majda-Stanislawska E, Omeñaca F, et al. 13-Valent Pneumococcal Conjugate Vaccine (PCV13) in Preterm Versus Term Infants. *Pediatrics* (2015) 135:e876–86. doi: 10.1542/peds.2014-2941
12. Tsuda K, Iwasaki S, Horiguchi H, Mori M, Nishimaki S, Seki K, et al. Immune Response to Haemophilus Influenzae Type B Conjugate Vaccine in Preterm Infants. *Pediatr Int* (2012) 54:64–7. doi: 10.1111/j.1442-200X.2011.03505.x
13. Szynczewska E, Chlebna-Sokół D. Immunogenicity and Safety of Heptavalent Conjugate Vaccine Against Streptococcus Pneumoniae in Pre-Term Polish Infants. *Vaccine* (2011) 29:7107–13. doi: 10.1016/j.vaccine.2011.06.124
14. Mollah AH, Naher N, Rahman S, Chowdhury AM. Antibody Titre Against 3 Doses of Hepatitis B Vaccine Among Preterm and Term Babies. *Mymensingh Med J* (2012) 21:109–13.
15. Omeñaca F, Vázquez L, Garcia-Corbeira P, Mesaros N, Hanssens L, Dolhain J, et al. Immunization of Preterm Infants With GSK's Hexavalent Combined Diphtheria-Tetanus-Acellular Pertussis-Hepatitis B-Inactivated Poliovirus-Haemophilus Influenzae Type B Conjugate Vaccine: A Review of Safety and Immunogenicity. *Vaccine* (2018) 36:986–96. doi: 10.1016/j.vaccine.2018.01.005
16. Chiappini E, Petrolini C, Caffarelli C, Calvani M, Cardinale F, Duse M, et al. Hexavalent Vaccines in Preterm Infants: An Update by Italian Society of Pediatric Allergy and Immunology Jointly With the Italian Society of Neonatology. *Ital J Pediatr* (2019) 45:1–14. doi: 10.1186/s13052-019-0742-7
17. National Health Portal. *Universal Immunisation Programme*. Gov India (2018). Government of India. Available at: https://www.nhp.gov.in/universal-immunisation-programme_pg.
18. Sharma HJ, Yadav S, Lalwani SK, Kapre SV, Jadhav SS, Chakravarty A, et al. Immunogenicity and Safety of an Indigenously Manufactured Reconstituted Pentavalent (Dtwp-HBV+Hib) Vaccine in Comparison With a Foreign Competitor Following Primary and Booster Immunization in Indian Children. *Hum Vaccin* (2011) 7:451–7. doi: 10.4161/hv.7.4.14208

19. Rao R, Dhingra MS, Bavdekar S, Behera N, Daga SR, Dutta AK, et al. A Comparison of Immunogenicity and Safety of Indigenously Developed Liquid (Dtwphb-Hib) Pentavalent Combination Vaccine (Shan 5) With Easyfive (Liq) and Tritanrixhb + Hiberix (Lyo) in Indian Infants Administered According to the EPI Schedule. *Hum Vaccin* (2009) 5:425–9. doi: 10.4161/hv.5.6.7816
20. Sharma H, Yadav S, Lalwani S, Gupta V, Kapre S, Jadhav S, et al. A Phase III Randomized, Controlled Study to Assess the Immunogenicity and Tolerability of Dtpw-HBV-Hib, a Liquid Pentavalent Vaccine in Indian Infants. *Vaccine* (2011) 29:2359–64. doi: 10.1016/j.vaccine.2011.01.054
21. Thayyil-Sudhan S, Kumar A, Singh M, Paul VK, Deorari AK. Safety and Effectiveness of BCG Vaccination in Preterm Babies. *Arch Dis Child Fetal Neonatal Ed* (1999) 81:F64–6. doi: 10.1136/fn.81.1.F64
22. Arora NK, Ganguly S, Agadi SN, Irshad M, Kohli R, Deo M, et al. Hepatitis B Immunization in Low Birthweight Infants: do They Need an Additional Dose? *Acta Paediatr Int J Paediatr* (2002) 91:995–1001. doi: 10.1080/080352502760272722
23. Bhave S, Bhise S, Chavan SC, Naik SS, Pusapati RVLN, Bavdekar A, et al. Hepatitis B Vaccination in Premature and Low Birth Weight (LBW) Babies. *Indian Pediatr* (2002) 39:625–31.
24. Sood A, Singh D, Mehta S, Midha V, Kumar R. Response to Hepatitis B Vaccine in Preterm Babies. *Indian J Gastroenterol* (2002) 21:52–4.
25. Balasubramanian S, Shah A, Pemde HK, Chatterjee P, Shivananda S, Guduru VK, et al. Indian Academy of Pediatrics (IAP) Advisory Committee on Vaccines and Immunization Practices (ACVIP) Recommended Immunization Schedule (2018-19) and Update on Immunization for Children Aged 0 Through 18 Years. *Indian Pediatr* (2018) 55:1066–74. doi: 10.1007/s13312-018-1444-8
26. WHO position paper on Diphtheria vaccine. *Wkly Epidemiol Rec*. World Health Organization (2006). pp. 24–32.
27. WHO Position Paper on tetanus vaccines. *Wkly Epidemiol Rec*, World Health Organization Vol. 81. (2006). pp. 198–208.
28. WHO position paper on Hepatitis B vaccines. *Wkly Epidemiol Rec*, World Health Organization Vol. 79. (2004). pp. 255–63.
29. Kayhty H, Peltola H, Karanko V, Makela PH. The Protective Level of Serum Antibodies to the Capsular Polysaccharide of Haemophilus Influenzae Type B. *J Infect Dis* (1983) 147:1100. doi: 10.1093/infdis/147.6.1100
30. World Health Organization. Position Paper on Pertussis Vaccines. *Wkly Epidemiol Rec* (2005) 80:31–9.
31. Gandhi DJ, Dhaded SM, Ravi MD, Dubey AP, Kundu R, Lalwani SK, et al. Safety, Immune Lot-to-Lot Consistency and non-Inferiority of a Fully Liquid Pentavalent Dtwp-Hepb-Hib Vaccine in Healthy Indian Toddlers and Infants. *Hum Vaccines Immunother* (2016) 12:946–54. doi: 10.1080/21645515.2015.1100779
32. Sil A, Ravi MD, Patnaik BN, Dhingra MS, Dupuy M, Gandhi DJ, et al. Effect of Prophylactic or Therapeutic Administration of Paracetamol on Immune Response to Dtwp-Hepb-Hib Combination Vaccine in Indian Infants. *Vaccine* (2017) 35:2999–3006. doi: 10.1016/j.vaccine.2017.03.009
33. Verma C, Faridi MMA, Narang M, Kaur IR. Anti-Hbs Titers Following Pentavalent Immunization (Dtwp-HBV-Hib) in Term Normal Weight vs Low Birthweight Infants. *Indian Pediatr* (2018) 55:395–9. doi: 10.1007/s13312-018-1280-x
34. Perin MCAA, Schlindwein CF, de Moraes-Pinto MI, Simão-Gurge RM, de Mello Almada Mimica AF, Goulart AL, et al. Immune Response to Tetanus Booster in Infants Aged 15 Months Born Prematurely With Very Low Birth Weight. *Vaccine* (2012) 30:6521–6. doi: 10.1016/j.vaccine.2012.08.056
35. Peoples JD, Cheung S, Nesin M, Lin H, Francesca Tatad AM, Hoang D, et al. Neonatal Cord Blood Subsets and Cytokine Response to Bacterial Antigens. *Am J Perinatol* (2009) 26:647–57. doi: 10.1055/s-0029-1220788
36. Scheible KM, Emo J, Yang H, Holden-Wiltse J, Straw A, Huyck H, et al. Developmentally Determined Reduction in CD31 During Gestation is Associated With CD8+ T Cell Effector Differentiation in Preterm Infants. *Clin Immunol* (2015) 161:65–74. doi: 10.1016/j.clim.2015.07.003
37. Turunen R, Vaarala O, Nupponen I, Kajantie E, Siitonen S, Lano A, et al. Activation of T Cells in Preterm Infants With Respiratory Distress Syndrome. *Neonatology* (2009) 96:248–58. doi: 10.1159/000220764
38. Hwang JS, Rehan VK. Recent Advances in Bronchopulmonary Dysplasia: Pathophysiology, Prevention, and Treatment. *Lung* (2018) 196:129–38. doi: 10.1007/s00408-018-0084-z
39. Grasse M, Meryk A, Miggitsch C, Grubeck-Loebenstein B. GM-CSF Improves the Immune Response to the Diphtheria-Component in a Multivalent Vaccine. *Vaccine* (2018) 36:4672–80. doi: 10.1016/j.vaccine.2018.06.033
40. Ghirelli C, Zollinger R, Soumelis V. Systematic Cytokine Receptor Profiling Reveals GM-CSF as a Novel TLR-Independent Activator of Human Plasmacytoid Predendritic Cells. *Blood* (2010) 115:5037–40. doi: 10.1182/blood-2010-01-266932
41. García-León ML, Bonifaz LC, Espinosa-Torres B, Hernández-Pérez B, Cardiel-Marmolejo L, Santos-Preciado JI, et al. A Correlation of Measles Specific Antibodies and the Number of Plasmacytoid Dendritic Cells is Observed After Measles Vaccination in 9 Month Old Infants. *Hum Vaccines Immunother* (2015) 11:1762–9. doi: 10.1080/21645515.2015.1032488
42. Bettelli E, Carrier Y, Gao W, Korn T, Strom TB, Oukka M, et al. Reciprocal Developmental Pathways for the Generation of Pathogenic Effector TH17 and Regulatory T Cells. *Nature* (2006) 441:235–8. doi: 10.1038/nature04753
43. Harrington LE, Hatton RD, Mangan PR, Turner H, Murphy TL, Murphy KM, et al. Interleukin 17-Producing CD4+ Effector T Cells Develop Via a Lineage Distinct From the T Helper Type 1 and 2 Lineages. *Nat Immunol* (2005) 6:1123–32. doi: 10.1038/ni1254
44. Park H, Li Z, Yang XO, Chang SH, Nurieva R, Wang YH, et al. A Distinct Lineage of CD4 T Cells Regulates Tissue Inflammation by Producing Interleukin 17. *Nat Immunol* (2005) 6:1133–41. doi: 10.1038/ni1261
45. Higgins SC, Jarnicki AG, Lavelle EC, Mills KHG. TLR4 Mediates Vaccine-Induced Protective Cellular Immunity to Bordetella Pertussis : Role of IL-17-Producing T Cells. *J Immunol* (2006) 177:7980–9. doi: 10.4049/jimmunol.177.11.7980
46. Zhang X, Goel T, Goodfield LL, Muse SJ, Harvill ET. Decreased Leukocyte Accumulation and Delayed Bordetella Pertussis Clearance in IL-6 –/– Mice. *J Immunol* (2011) 186:4895–904. doi: 10.4049/jimmunol.1000594
47. Brook B, Harbeson DJ, Shannon CP, Cai B, He D, Ben-Othman R, et al. BCG Vaccination-Induced Emergency Granulopoiesis Provides Rapid Protection From Neonatal Sepsis. *Sci Transl Med* (2020) 12:eaax4517. doi: 10.1126/SCITRANSLMED.AAX4517
48. Bassat Q, Moncunill G, Dobaño C. Making Sense of Emerging Evidence on the non-Specific Effects of the BCG Vaccine on Malaria Risk and Neonatal Mortality. *BMJ Glob Heal* (2020) 5:e002301. doi: 10.1136/bmjgh-2020-002301
49. Ota MOC, Vekemans J, Schlegel-Haueter SE, Fielding K, Sanneh M, Kidd M, et al. Influence of Mycobacterium Bovis Bacillus Calmette-Guérin on Antibody and Cytokine Responses to Human Neonatal Vaccination. *J Immunol* (2002) 168:919–25. doi: 10.4049/jimmunol.168.2.919

Conflict of Interest: The authors declare that the research was conducted in the absence of any commercial or financial relationships that could be construed as a potential conflict of interest.

frontiers in Immunology

ORIGINAL RESEARCH
published: 27 May 2021
doi: 10.3389/fimmu.2021.578700

Plasma Adenosine Deaminase (ADA)-1 and -2 Demonstrate Robust Ontogeny Across the First Four Months of Human Life

Oludare A. Odumade[1,2,3†], Alec L. Plotkin[1†], Jensen Pak[1], Olubukola T. Idoko[1,4,5], Matthew A. Pettengill[1,6], Tobias R. Kollmann[7], Al Ozonoff[1,2], Beate Kampmann[4,5], Ofer Levy[1,2,8] and Kinga K. Smolen[1,2*] on behalf of the EPIC Consortium*

[1] Precision Vaccines Program, Division of Infectious Diseases, Boston Children's Hospital, Boston, MA, United States, [2] Department of Pediatrics, Harvard Medical School, Boston, MA, United States, [3] Division of Medicine Critical Care, Boston Children's Hospital, Boston, MA, United States, [4] Vaccines & Immunity Theme, Medical Research Council Unit The Gambia at the London School of Hygiene and Tropical Medicine, Banjul, Gambia, [5] The Vaccine Centre, Faculty of Infectious and Tropical Diseases, London School of Hygiene and Tropical Medicine, London, United Kingdom, [6] Department of Pathology, Anatomy, and Cell Biology, Thomas Jefferson University, Philadelphia, PA, United States, [7] Telethon Kids Institute, University of Western Australia, Perth, WA, Australia, [8] Broad Institute of MIT & Harvard, Cambridge, MA, United States

OPEN ACCESS

Edited by:
Per T. Sangild, University of Copenhagen, Denmark

Reviewed by:
Raghavan Chinnadurai, Mercer University, United States
Jason Michael Springer, University of Kansas Medical Center Research Institute, United States

***Correspondence:**
Kinga K. Smolen
kinga.smolen@childrens.harvard.edu
Oludare A. Odumade
oludare.odumade@childrens.harvard.edu

†These authors share first authorship

Specialty section:
This article was submitted to Vaccines and Molecular Therapeutics, a section of the journal Frontiers in Immunology

Received: *01 July 2020*
Accepted: *11 May 2021*
Published: *27 May 2021*

Citation:
Odumade OA, Plotkin AL, Pak J, Idoko OT, Pettengill MA, Kollmann TR, Ozonoff A, Kampmann B, Levy O and Smolen KK (2021) Plasma Adenosine Deaminase (ADA)-1 and -2 Demonstrate Robust Ontogeny Across the First Four Months of Human Life. Front. Immunol. 12:578700. doi: 10.3389/fimmu.2021.578700

Background: Human adenosine deaminases (ADAs) modulate the immune response: ADA1 *via* metabolizing adenosine, a purine metabolite that inhibits pro-inflammatory and Th1 cytokine production, and the multi-functional ADA2, by enhancing T-cell proliferation and monocyte differentiation. Newborns are relatively deficient in ADA1 resulting in elevated plasma adenosine concentrations and a Th2/anti-inflammatory bias compared to adults. Despite the growing recognition of the role of ADAs in immune regulation, little is known about the ontogeny of ADA concentrations.

Methods: In a subgroup of the EPIC002-study, clinical data and plasma samples were collected from 540 Gambian infants at four time-points: day of birth; first week of life; one month of age; and four months of age. Concentrations of total extracellular ADA, ADA1, and ADA2 were measured by chromogenic assay and evaluated in relation to clinical data. Plasma cytokines/chemokine were measured across the first week of life and correlated to ADA concentrations.

Results: ADA2 demonstrated a steady rise across the first months of life, while ADA1 concentration significantly decreased 0.79-fold across the first week then increased 1.4-fold by four months of life. Males demonstrated significantly higher concentrations of ADA2 (1.1-fold) than females at four months; newborns with early-term (37 to <39 weeks) and late-term (≥41 weeks) gestational age demonstrated significantly higher ADA1 at birth (1.1-fold), and those born to mothers with advanced maternal age (≥35 years) had lower plasma concentrations of ADA2 at one month (0.93-fold). Plasma ADA1 concentrations were positively correlated with plasma CXCL8 during the first week of life, while ADA2 concentrations correlated positively with TNFα, IFNγ and CXCL10, and negatively with IL-6 and CXCL8.

Conclusions: The ratio of plasma ADA2/ADA1 concentration increased during the first week of life, after which both ADA1 and ADA2 increased across the first four months of life suggesting a gradual development of Th1/Th2 balanced immunity. Furthermore, ADA1 and ADA2 were positively correlated with cytokines/chemokines during the first week of life. Overall, ADA isoforms demonstrate robust ontogeny in newborns and infants but further mechanistic studies are needed to clarify their roles in early life immune development and the correlations with sex, gestational age, and maternal age that were observed.

Keywords: adenosine, adenosine deaminase, ontogeny, sex differences, cytokines, chemokines, biomarkers

INTRODUCTION

Early life demonstrates unique immunologic challenges and adaptations related to the transition from an intra-uterine environment and progressive responses to extra-uterine environmental cues (1). This dynamic landscape necessitates age-dependent changes in cellular and soluble factors that shape immunity and that have yet to be fully characterized (1–7). Given that infancy is the time of receipt of most vaccines coupled with the heavy burden of early life infection, and a period of profound changes in the immune system, a better understanding of immune ontogeny in human newborns is essential.

Among the soluble immunoregulatory proteins of human plasma are adenosine deaminases (ADAs) -1 and -2. ADA1 (41kDa) is encoded by the *ADA* gene on chromosome 20q13.12 (OMIM 608958 or Entrez Gene ID 100) and is produced by all cells (8, 9). While the intracellular role of ADA1 has been established, this enzyme also has extracellular roles (10–13), including formation by ADA1 (or ecto-ADA) of a ternary complex with CD26 and A2a receptors bridging two different cells as a co-stimulatory molecule that impacts T-cell proliferation (14, 15). ADA1 converts adenosine, an endogenous purine metabolite that acts *via* leukocyte purine receptors to suppress pro-inflammatory and Th1-polarizing responses, to inosine, which is immunologically inert (16–19). ADA1 also has roles in enhancing T-helper 2 (Th2) immunity *via* adenosine receptors (20). ADA1 deficiency impairs thymocyte development and B-lymphocyte immunoglobulin production (21) resulting in severe combined immunodeficiency (22).

ADA2 has a higher *Km* for adenosine (23, 24) and is thereby less enzymatically active than ADA1. While residual ADA2 activity ADA2 can be measured in patients with ADA1 deficiency (23, 25), its important roles in immunity has previously been under-appreciated. ADA2 (57kDa) is encoded by the *CECR1* (*ADA2)* gene on chromosome 22q11.1 (OMIM 607575 or Entrez Gene ID 51816) and is produced by activated monocytes, macrophages, and dendritic cells (DCs) (8, 9). Independent of its enzymatic activity, ADA2 modulates immunity *via* binding cognate receptors on immune cells (14, 26, 27). ADA2 also induces monocyte differentiation to macrophages in T-cell co-cultures (14). ADA2-deficient cells are unable to differentiate into M2/pro-resolution macrophages (24, 28, 29) suggesting that ADA2 directs differentiation of macrophages towards an anti-inflammatory phenotype. First described in 2014 (30, 31), ADA2 deficiency (DADA2) presents with heterogeneous manifestations of which vascular inflammation is predominant (32–52). Patients with ADA2 deficiency and vasculitis often have missense mutations with at least 3% residual activity, whereas complete loss of function was associated with pure red cells aplasia and bone marrow failure (39). ADA2 binds to neutrophils, monocytes, NK cells, and B cells (27), and patients with ADA2 deficiency can present with inflammatory conditions and altered distribution of immune cell subsets and immunoglobulin levels (32, 35, 39–41, 47, 50, 51). Overall, ADA2 is a protein of relevance to the human immune system whose expression in early life has been incompletely characterized.

We have previously demonstrated that adenosine inhibits TLR-induced production of TNFα but not IL-6 and that pre-incubation of cord blood mononuclear cells with recombinant ADA1 (rADA1) enhances TLR-mediated TNFα production (16). Moreover, in a small cohort (n = 4-12 per group), newborns exhibit lower plasma concentrations of extracellular ADA1 compared to adults, resulting in elevated newborn plasma adenosine concentrations and a Th2/anti-inflammatory bias (3, 16). However, these studies did not evaluate plasma ADA concentrations within the first month of life, nor did they assess whether plasma concentrations of these enzymes correlate with plasma cytokine and chemokine concentrations. Thus, how ADA1, ADA2, and total ADA change during the first week of life and subsequent months of life, when the immune system of neonates and infants undergo dramatic immunologic changes, are most susceptible to infection, and receive the greatest number of vaccines, is still unknown.

Partnering as international collaborators *via* the Expanded Program on Immunization Consortium (EPIC), we conducted the EPIC002 study, a prospective study to characterize immunologic biomarkers in newborn infants followed across a four-month period (53). We measured ADA1 and ADA2 in infant plasma to determine age-dependent changes in early life. We presented higher resolution data on ontogeny of not only total

Abbreviations: ADA, adenosine deaminase; cGAS, cyclic guanosine monophosphate–adenosine monophosphate; CXCL, chemokine (C-X-C motif) ligand; DOL, Day of Life; EPIC, Expanded Program on Immunization Consortium; EHNA, Erythro-9-(2-hydroxy-3-nonyl) adenine; GT, Gene therapy; HIPC, Human Immune Project Consortium; HSCT, Hematopoietic stem cell transplantation; Ig, immunoglobulin; IL, Interleukin; IP, IFNγ-Inducible Protein; kDa, Kilo Daltons; NK, Natural Killer; rADA, recombinant ADA; STING, stimulator of interferon genes; and Th, T-helper.

ADA, but also ADA1 and ADA2 during the first week of human life in a large cohort of infants (N = 540 participants). We investigated the ontogenic patterns in plasma ADA1 and ADA2 concentrations across five Gambian ethnic sub-groups. We explored whether demographic factors such as sex, gestational age, and maternal age were associated with distinct ADA concentrations in infant plasma. Finally, we assessed whether plasma ADA1, ADA2, and total ADA correlated with plasma concentrations of cytokines and chemokines during the first week of life. Overall, our study revealed that these immune-regulatory proteins demonstrate robust changes across the first week and months of life and correlate with plasma cytokine and chemokine concentrations, suggesting a functional role for ADAs in human immune ontogeny.

METHODS

Study Design and Sample Collection

The Expanded Program on Immunization Consortium (EPIC) study 002 (EPIC002) clinical protocol has been previously described (53), and the study is registered on clinicaltrials.gov as NCT03246230. The study's primary goal was to assess vaccine immunogenicity in newborns in 4 different vaccine groups (no vaccines at birth (i.e., delayed immunization), Hepatitis B vaccine (HBV) alone at birth, BCG alone at birth, and both (HBV and BCG) at birth; with n = 180 per group).

In brief, mothers and their newborns were consented and enrolled at time of delivery at the Medical Research Council (MRC) Unit at the London School of Hygiene and Tropical Medicine in The Gambia. Mothers were enrolled only if they were above the age of 18 years old, HIV-negative, had no history of tuberculosis (TB) diagnosis in the mother or family member in the past six weeks prior to enrollment using an electronic case report form (eCRF) and were Hepatitis B-negative; additional maternal exclusion criteria included severe pre-eclampsia and/or physician assessment of high-risk pregnancy such as recurrent early neonatal death. Newborns were included only if gestational age >36weeks (as determined by Ballard scoring), if Apgar scores at 5th minute >8, if birth weight >2.5 kilograms (kg). Infants with macrosomia (birth weight >4kg) with existing risk factors such as major known congenital malformation or abnormal exam as determined by physician assessment at birth were also excluded.

Peripheral blood samples were collected using sterile sodium heparin tubes (Becton Dickinson) from infants at four time points. The first sample, Visit 1, was collected within the first 24 hours of life (Day of Life (DOL)0); Visit 2 sample was collected at either DOL1, DOL3, or DOL7; Visit 3 sample was collected at DOL30 and finally Visit 4 sample was collected at DOL128. Visit 3 and Visit 4 were collected in only 540 of the 720 maternal-newborn pairs enrolled, specifically, only in the HepB, BCG, HepB plus BCG at birth groups, per protocol (53) due to limitations in cost. Hence only the 540 infants for whom plasma biosamples were available for ADA assay at all timepoints (i.e., Visits 1 thru 4) were included in the ADA ontogeny sub-analysis that is the focus of this report. Plasma samples were processed for analysis as we have previously described (4). All plasma samples were stored at -80°C until use. Local and International (collaborator) Ethics and/or IRB committees approved the clinical protocols.

Adenosine Deaminase Assay Methods

Reagents

Adenosine Deaminase Assay Kit, including: ADA Assay reagent kits [cat. # DZ117A], ADA calibrator [cat. # DZ117A-Cal], and Quality Controls [cat. # DZ117A-Con] (Diazyme Laboratories, Poway, CA, USA) and Erythro-9-(2-hydroxy-3-nonyl) adenine (EHNA) [cat. # 1261] (Tocris Bioscience, Bristol, UK).

ADA Chromogenic Assay

ADA1 and ADA2 concentrations in plasma samples were measured with an ADA Assay Kit per the manufacturer's instructions (Diazyme Laboratories, Poway, CA, USA), run in duplicate with or without EHNA (20 μM) on a 384 well plate. ADA2 is not EHNA sensitive, and thus activity in EHNA-containing wells was considered to reflect ADA2 activity. ADA1 concentration was calculated by subtracting ADA2 concentration from total ADA concentration.

ADA Chromogenic Assay Analysis

The plate was read on an Infinite M Plex (Tecan, Mannedorf, Switzerland), programmed to run a kinetic cycle at 37°C with absorbance readings at 550nm performed every 5 minutes over 1 hour.

Cytokine/Chemokine Methods

Reagents

Dulbecco's phosphate-buffered saline (dPBS, cat 14190), Corning CellBIND® 384 well plates (cat # CLS3764), and Milliplex Human Cytokine/Chemokine MAGNETIC BEAD Premixed 41 Plex Kit. (Millipore HCYTMAG-60K-PX41).

Cytokine/Chemokine Assay

Plasma was diluted 1:2 in dPBS prior to use. Diluted plasma samples and the Milliplex 41-plex kit manufacturer provided standards and quality controls were then assayed and results were obtained with a Flexmap 3D system with Luminex *xPONENT* software (both from Luminex Corp.; Austin, TX, USA). Cytokine concentrations were determined using Milliplex Analyst software (version 5.1.0.0).

Statistical Methods

For the analysis of ADAs, the change in absorbance between individual time points was calculated and averaged over all time points to obtain the rate of absorbance change for each sample. The rates were averaged between duplicates. Each plate was converted to concentration in units per liter (U/L) using a log-standard curve, and plates with randomized samples were normalized to the overall mean and standard distribution using a universal standard sample. ADA1 concentration was imputed by subtracting the concentration of ADA2 from the total ADA concentration measured for each sample.

Observations were $\log_{10}$-transformed to generate a data set of approximate normality, and fold-change calculated in relation to DOL0 (Visit 1). Longitudinal statistical comparisons employed ANOVA for non-repeated measurements with post-hoc analysis

using Welch's t-test. Gaussian-distributed data was modeled with generalized estimating equations (GEE), using an identity link function and exchangeable covariance structure for longitudinal comparisons with repeated measures. GEE significance was calculated from the Wald statistic after performing deviance analysis against a null model (54). Comparisons between demographic and physiological variables like biological sex, heart rate, and gestational or maternal age were analyzed using untransformed data (U/L) and rank sum Wilcoxon and Kruskal-Wallis tests (55) to allow for comparison with previously published data (3, 56–60) and hospital-based tests on absolute plasma ADA1, ADA2, and total ADA concentrations. For tables and graphs presenting absolute activity concentrations, the median and the interquartile range (IQR) were used for descriptive statistics (61).

For cytokine/chemokine analysis, the *xPONENT* software files were processed using the *drLumi* R package. The standard curves were fitted using a 4-parameter logistic, 5-parameter logistic, and exponential function by the *drLumi*::scluminex() function. The best-fit curve was used for each cytokine. The lower and upper limits of detection were set as the lowest and highest concentration of the standard curve, respectively. Analytes whose concentration could not be estimated were imputed to either the lower (LLOQ) or upper (ULOQ) limit of quantification for that plate/analyte. Samples that had all analytes below the lower limit of detection were excluded from the final analysis. The raw cytokine or chemokine values were then $\log_{10}$-transformed to achieve a Gaussian distribution. ComBat (62) (sva R package) was then used to further normalize across plates based on plate-specific biases as determined by PCA plots. Correlation coefficients between analytes and ADA concentrations during the first week of life were calculated using Spearman's rho, p-values were determined by R function cor.test, and adjusted using the Holm-Bonferroni method.

Clinical metadata was evaluated based on potential interactions with adenosine and ADAs and biomarkers in general. For example, inhibition of TNFα by adenosine is thought to be cardio-protective both for ischemic heart disease and congestive heart failure (63–66). Gestational age (GA) correlates with biomarkers such as hemoglobin and iron (67–70) and advanced maternal age, defined as age ≥35 years old, can be associated with high-risk pregnancy and inflammatory states like pre-eclampsia (71–73), where ADAs may be altered (74). Thus, variables such as heart rate, gestational age, and maternal age were first analyzed as continuous variables (data not shown) prior to categorization. Definition of categories:

1) *Maternal age* categories were based on standard age group of mother in the Morbidity and Mortality Weekly Report by the United States Center for Disease Control or other Demographic and Health Surveys (75).
2) *Gestational age* (GA) is categorized based on the American College of Obstetricians and Gynecologists (76).

a. Early term: 37 0/7 weeks through 38 6/7 weeks,
b. Full term: 39 0/7 weeks through 40 6/7 weeks,
c. Late term: 41 0/7 weeks through 41 6/7 weeks.

Statistical analyses employed R version 3.6.3, using package versions ggpubr_0.3.0 and gee_4.13-20, for ANOVA/Wilcoxon/Kruskal-Wallis tests and GEE, respectively. Significant p-values depicted as *= p<0.05, ** = p<0.01, *** = p<0.001; **** = p<0.0001; ns = not significant.

RESULTS

Baseline Characterization of Study Participants

540 Gambia mother-newborn pairs enrolled in the EPIC002 cohort were followed for 128 days and were included in our analysis. As shown in **Table 1**, the majority of mothers (30.7%) were 25-29 years old, followed by age 20-24 years old (22.2%) and then age 30-34 (19.1%). A few preterm newborns (n=4, 0.7%), defined as <37 weeks gestation, were enrolled but the majority (87.2%) of newborns were early term (≥37 weeks to <39 weeks gestation) or full term (≥39 weeks to <41 weeks gestation). Participants were recruited from 2 sites (**Figure 1**), and the Mandinka, Jola, and Fula groups made up the majority of ethnic sub-groups (78.2%). There was an approximately equal ratio of male and female newborns enrolled (49.1% female, 50.9% male) and the average birth-weight was 3.2 kg. Initiation of breastfeeding was 87.5% at delivery and continued after the first day of life (>98%) until four months of age for infants in this cohort.

Ontogenic Changes in ADA1, ADA2, and Total ADA Across the First Four Months of Life

We measured the concentrations of plasma ADA1, ADA2, and total ADA during the first week in the Gambian cohort.

TABLE 1 | Characteristics of EPIC002 study participants.

Characteristics	Frequency (N)	Percent (%)
Sex of the newborn:		
Female/Male	265/275	49.1/50.9
Birth weight (kg)		
Avg (± SEM)	3.163 ± 0.017	
Maternal age (years)[a]:		
15 - 19	23	4.3
20 - 24	120	22.2
25 - 29	166	30.7
30 - 34	103	19.1
35 - 39	89	16.5
40 – 45	39	7.2
Gestational age (based on Ballard scoring):		
Preterm (<37 weeks)	4	0.7
Early term (≥37 – <39 weeks)	132	24.4
Full term (≥39 – <41 weeks)	339	62.8
Late term (≥41 weeks)	65	12
Newborn ethnic sub-group:		
Mandinka	269	49.8
Jola	83	15.4
Fula	70	13
Wolof	50	9.3
Serahule	22	4.1
Others	46	8.5
Frequency of breastfeeding		
Visit 1 (Yes/No)	454/65	87.5/12.5
Visit 2 (Yes/No)	519/6	98.9/1.1
Visit 3 (Yes/No)	520/6	98.9/1.1
Visit 4 (Yes/No)	510/5	99.0/1.0

[a]*In EPIC002, all maternal participants are age 18 and above.*

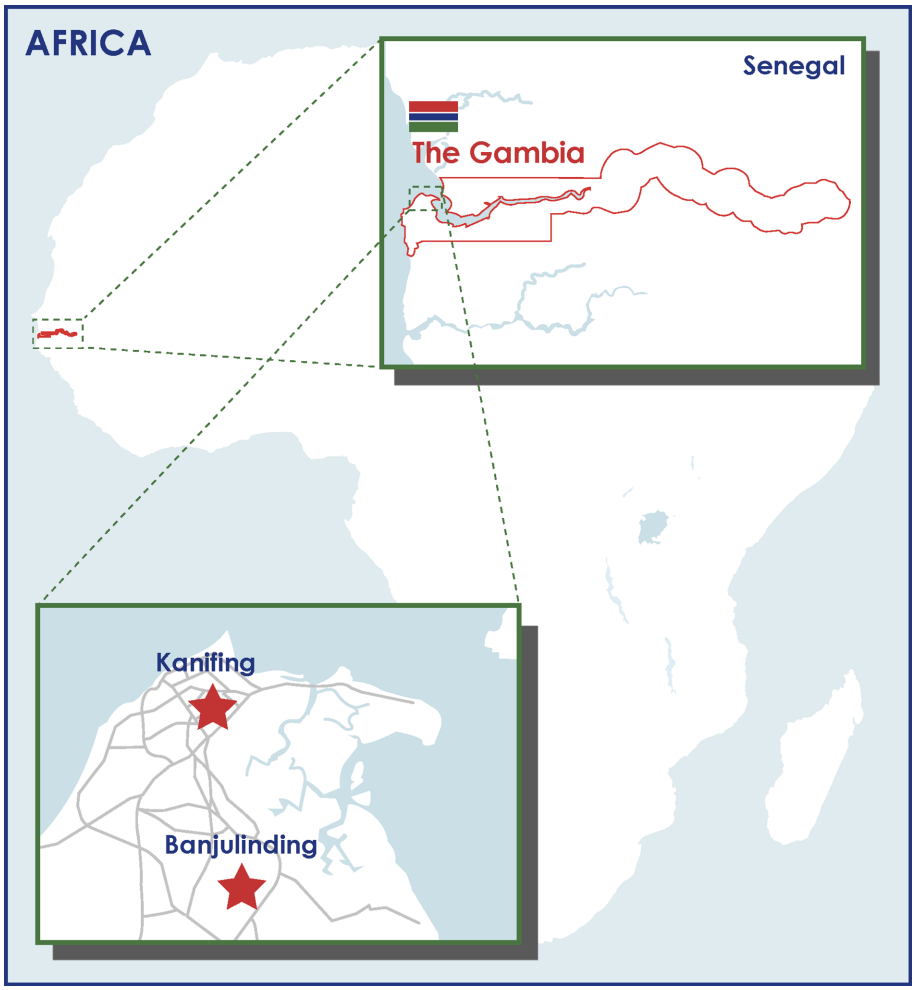

FIGURE 1 | Geographical distribution of the two recruitment sites for the EPIC002 study in The Gambia.

There was a significant fold change ($p \leq 0.0001$) decrease in ADA1, and an increase in ADA2 and total ADA (**Figure 2**). Specifically, while plasma concentrations of ADA1 decreased by 23% (from 4U/L at DOL0 to 3.1U/L at DOL7), concentrations of both ADA2 (from 2.6U/L at DOL0 to 4U/L at DOL7), and total ADA (from 6.7 U/L at DOL0 to 7.5U/L at DOL7), increased by 54% and 12%, respectively, across the first week of life (n =168-173 per group) ($p<0.01$). However, there was no significant difference in total ADA from DOL3 to DOL7.

Next, we investigated ADA isoforms beyond the first week of life by measuring the relative ADA concentration (**Figure 3A**) and the fold change compared to DOL0 (**Figure 3B**) of ADA1, ADA2, and total ADA during the first four months. Interestingly, the concentration of all ADA subtypes (total ADA, ADA1, and ADA2) increased over the first four months of life consistent with an overall increase in plasma ADA concentrations with age ($p<0.0001$) (n = 491-511) (**Figure 3**). Since total ADA is defined as the sum of ADA1 and ADA2, we explored the ratio of ADA2 relative to ADA1 concentration across time. From DOL3, the ratio of ADA2/ADA1 increased ($p<0.0001$), suggesting that elevated ADA2 activity may contribute to the total ADA measured (**Supplementary Figure 1**).

Association of Extracellular Plasma ADAs Concentration and Demographic Factors

First, we explored associations between ADA concentrations and physical exam findings at birth to look for confounders. No significant differences were observed in concentrations of ADA1, ADA2, or total ADA based on respiratory rate, heart rate, weight, length, head circumference, or temperature at birth (data not shown). No difference in ADA concentrations after the first week of life were noted in The Gambian ethnic sub-groups (**Supplemental Figure 2**).

Sex-based differences were observed in plasma concentrations of ADA2 and total ADA, but not ADA1. At 4 months of life, males demonstrated 11% higher median plasma ADA2 concentrations (9.8 U/L *vs.* 8.8 U/L) and 8.5% higher total

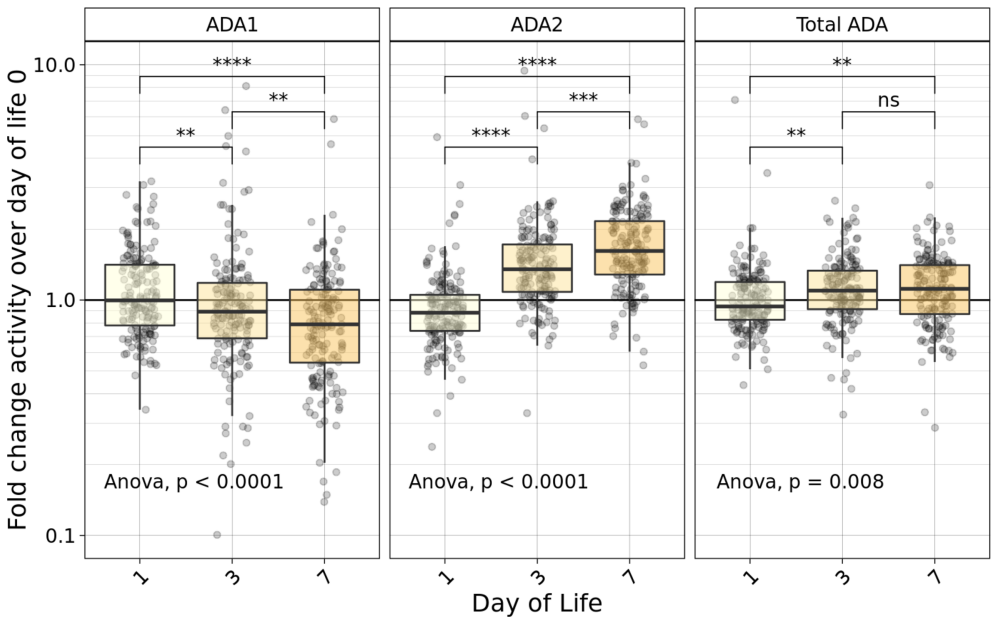

FIGURE 2 | Fold-change relative to DOL0 of ADA concentrations measured in plasma during the first week of life varied based on type of ADA measured. Fold-change of ADA1 (left), ADA2 (middle) and Total ADA (right) plasma concentrations relative to the day of life (DOL) 0 in the Gambian cohort demonstrated an increase in relative plasma ADA2 and total ADA, as well as a decrease in ADA1 across the first week of life (n =168-173/group). Statistical analyses employed ANOVA followed by Welch's t-test for pairwise comparisons. Significant p-values depicted as **p<0.01, ***p<0.001; ****p<0.0001; ns, not significant.

ADA (15.4 U/L *vs.* 14.2 U/L), whereas ADA1 was 3.7% higher (5.6 U/L *vs.* 5.4 U/L) (**Figure 4**). This pattern was significant for ADA2 (p=0.02) and total ADA (p=0.004) (n =254-260 per group). Furthermore, sex-specific differences in ADA concentrations were not observed in the first 30 days of life but only noted at four months of age (**Supplementary Figure 3**).

Plasma ADA1 concentrations were elevated in early term (4.3 U/L) (p<0.05) and late term newborns (4.3 U/L) (p<0.05) compared to full term (3.9 U/L), exhibiting a 10% increase (**Figure 5A**) (n=64-321 per group). At 1 week of life and then 4 months of life, when ADA2 becomes more prominent (**Supplemental Figure 1**), early gestation age was also associated with increased ADA2 and total ADA (but not ADA1) (**Supplemental Figure 4**). Our study was not designed to assess any possible effects of prematurity (GA <37 weeks) on ADA concentrations for which sample size was low (n=4).

Advanced maternal age, defined as age ≥35 years old, can be associated with high-risk pregnancy and inflammatory states like pre-eclampsia. Accordingly, we assessed whether advanced maternal age (n=124-126) was associated with differences in neonatal plasma ADA1 and ADA2 concentrations. We observed lower ADA2 concentrations in infants born to mothers of advanced maternal age, at DOL3 (3.4U/L *vs.* 4U/L) (p=0.02), 1 month (5.1U/L *vs.* 5.4U/L) (p=0.01), and 4 months of life (8.5U/L *vs.* 9.7U/L) (p=0.03) (**Figure 5B**). A similar observation of lower total ADA concentration in newborns of women ≥35 years of age was significant at DOL3 (p=0.006) and demonstrated strong trends at 1- and 4- months (p = 0.06 and 0.07, respectively) (**Supplementary Figure 5**).

Correlation With Plasma Cytokines or Chemokines and ADA Subtypes

We measured plasma concentrations of several cytokines, including IFNγ, TNFα, and IL-6, as well as chemokines such as CXCL8 and CXCL10 at DOL0, 1, 3, and 7. Robust rho values were observed for the correlation between Th1-polarizing cytokines: CXCL10 (aka IP-10) with IFNγ (r=0.58) and TNFα (r=0.55), as well as IFNγ with TNFα (r=0.51) (p<0.0001). As expected, total ADA correlated with the concentration of ADA1 (r=0.71) and ADA2 (r=0.59) (p<0.0001). In assessing correlations between plasma ADAs and cytokines or chemokines, we noted that total ADA was significantly correlated with CXCL10 (r=0.21) and TNFα (r=0.15) (p<0.0001) during the first week of life (**Figure 6**) but not with IFNγ, IL-6, or CXCL8. ADA1 correlated positively with CXCL8 (r=0.24) (p<0.0001) and IL-6 (r=0.09)(p<0.05), while ADA2 correlated positively with CXCL10 (r=0.27), IFN-γ (r=0.18), and TNFα (r=0.15) (p<0.0001, but negatively with IL-6 (r=-0.21) and CXCL8 (r=-0.29) (p<0.0001).

DISCUSSION

To our knowledge, our study is the first that has explored the ontogeny of plasma ADA1, ADA2, and total ADA across the first week of human life. We characterized changes in plasma ADA1, ADA2, and total ADA over the first four months of life and defined novel correlations with sex, gestational age, and maternal age. We observed significant positive correlations between

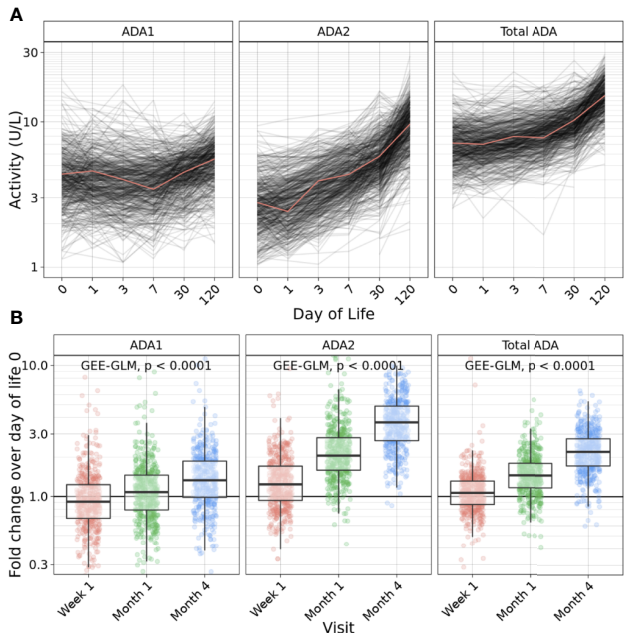

FIGURE 3 | Plasma ADA concentrations increased across the first four months of life. **(A)** Concentration of ADA1 (left), ADA2 (middle) and Total ADA (right) during the first 128 days of life in the Gambian cohort showed an increase of ADA1, ADA2 and total ADA concentrations across the first four months of life (n = 540 participants). **(B)** Log_{10} fold-change of ADA1 (left), ADA2 (middle) and Total ADA (right) relative to day of life (DOL) 0 in the Gambian cohort demonstrated an increase of ADA1, ADA2 and total ADA concentrations during the first four months of life (n = 491-511) (p<0.0001). Statistical analyses fit a GEE-GLM to log_{10} (activity) with Visit as a predictor variable, using Gaussian distribution, identity link function, and exchangeable covariance structure. Deviance analysis was conducted by comparing GEE to a null model, and p-values were found using the Wald statistic.

plasma concentrations of ADA2 and those of CXCL10, IFNγ, and TNFα; in addition to negative correlations with IL-6 and CXCL8.

In depth characterization of the distinct immune ontogeny of human newborns is important to inform development of better agents and approaches to prevent, diagnose, or treat infection in early life (6, 20). We recently demonstrated that dynamic age-dependent molecular and cellular changes occur in the first week of life using a systems biology approach (4). Building on our previous work that suggested total ADA increases over the first year of life (3), we presented higher resolution data on ontogeny of total ADA, ADA1, and ADA2 during the *first week of life* in 540 participants. We observed that there is an initial decrease in ADA1 while ADA2 increased, which may suggest distinct functional roles for these proteins in the first week of life. Of note, ADA1 acts as both an ecto-enzyme and as an intracellular enzyme (10–13, 21), whereas ADA2 can bind cognate leukocyte receptors to re-shape immune polarization (14, 26, 27, 41). Intriguingly, a recent study posted to *bioRxiv* suggests that ADA2 has a role as a lysosomal DNase that degrades ligands for the cytosolic pattern recognition receptors cGAS/STING thereby limiting production of interferons (77), possibly explaining how ADA2 deficiency results in hyper-inflammation.

The plasma concentration of ADA2, and thus total ADA, transiently decreased from day of life (DOL) 0 to DOL1 likely reflecting dynamic perinatal changes. Indeed, plasma concentrations of some proteins, such as hemoglobin, are increased at delivery and decrease before reaching homeostatic levels (67–69, 78, 79). Consistent with these, when human B-cell subsets are isolated from healthy children and stimulated *ex-vivo* with oligodeoxynucleotide-2006 (ODN2006), CD40Ligand, or anti-Ig, ADA2 transcript decreased between time 0 (baseline) and Day 1, but increased again at Day 6 close to the baseline levels at time 0 (41). Interestingly, a small group of neonates in this cohort were hospitalized for a variety of suspected or confirmed diagnoses including early or late onset sepsis, pneumonia, omphalitis and impetigo (n=54); however, inclusion or exclusion of the hospitalized neonates did not change the robust and significant ontogenic patterns demonstrated during the first week of life or during the first four months of life (data not shown). In our infant cohort, after

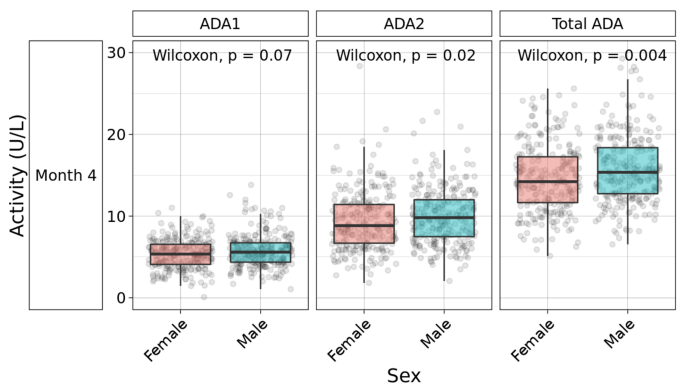

Isoform	Sex	Median conc. (U/L)	IQR (U/L)	n
ADA1	Female	5.4	2.5	254
ADA1	Male	5.6	2.4	260
ADA2	Female	8.8	4.7	255
ADA2	Male	9.8	4.5	260
Total ADA	Female	14.2	5.6	255
Total ADA	Male	15.4	5.6	260

FIGURE 4 | Males exhibited higher plasma ADA2 concentrations at four months of age. Measurement of plasma ADA1, ADA2, and Total ADA in biosamples in the Gambian cohort demonstrated greater concentrations of ADA1 (p=0.07), ADA2 (p=0.02) and Total ADA (p=0.004) in males than females during the first four months of life (n =254-260 per group). Statistical analyses employed Wilcoxon rank sum test.

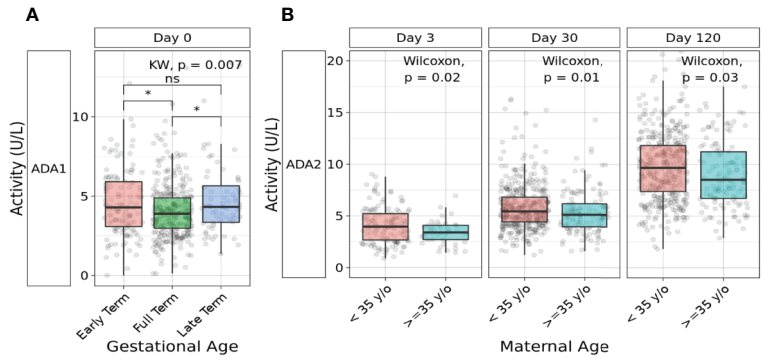

Gestational Age	Median ADA1 conc. (U/L)	IQR (U/L)	n
Early Term (≥37wks; <39wks GA)	4.3	2.8	133
Full Term (≥39wks; <41wks GA)	3.9	1.9	321
Late Term (≥41wks GA)	4.3	2.3	64

Visit	Maternal Age	Median ADA2 conc. (U/L)	IQR (U/L)	n
Day 3	<35 y/o	4.0	2.5	131
Day 3	≥ 35 y/o	3.4	1.4	42
Day 30	<35 y/o	5.4	2.4	400
Day 30	≥ 35 y/o	5.1	2.2	126
Day 120	<35 y/o	9.7	4.4	391
Day 120	≥ 35 y/o	8.5	4.5	124

FIGURE 5 | Association of gestational age and maternal age with plasma ADA concentrations. **(A)** Both early and late gestational age were associated with higher neonatal plasma concentrations of ADA1. Plasma concentrations of ADA1 at Day 0 in the Gambian cohort were significantly elevated in both early and late-term versus to full-term newborns (n = 133 early-term, n = 321 full-term, n = 64 late-term)(*p<0.05; ns, not significant). Statistical analyses employed Kruskal-Wallis and Wilcoxon for post-hoc. **(B)** Greater maternal age was associated with lower ADA2 concentrations during the first four months of life. Concentrations of plasma ADA2 in the Gambian cohort were significantly elevated at Day of Life 3 (p=0.02), 1 month (p=0.01), and 4 months (p=0.03) (n = 131- 400 infants of mothers <35 years of age, n = 42-126 infants of mothers ≥35 years of age). Statistical analyses employed Wilcoxon rank sum test.

the first week of life, activity of ADA1, ADA2, and total ADA increased through the first four months of life consistent with our prior studies (3).

We examined whether a number of demographic features correlated with plasma ADA concentrations. Ethnicity can impact plasma biomarkers (80, 81) and ethnicity, language, and geography have been associated with genetic diversity in African populations (82). The concentration of ADA isoenzymes in the different ethnic sub-groups in our Gambian cohort, including Mandinka, Jola, Fula, Wolof, and Serahule were consistent throughout, suggesting conservation of the ontogeny of plasma ADA expression in these ethnic sub-groups. Given the geographic size of The Gambia and similarity in the Gambian ethnic sub-groups, we cannot draw final conclusions on the impact of ethnicity on ADA concentrations.

Sex also impacts the immune system (83) and male sex is associated with gestational complications such as failure to progress during labor (84), as well as infant susceptibility to infection and mortality (85). Furthermore, while males demonstrate increased susceptibility to a range of infections (86–89), there is an interaction between sex and age (90, 91). A small study of elderly individuals with and without stroke noted that females with a history of stroke had relatively higher plasma concentrations of ADA1 and a higher ratio of plasma ADA1/ADA2 (92). Of note, genetic polymorphisms of ADA genes associated with longevity in males but not females, though this study did not evaluate plasma ADA concentrations (93). Little is known regarding sex-based differences in ADA expression in early life. Our Gambian infant study demonstrated similar plasma concentrations of ADAs for males and females at birth with significantly elevated concentrations of ADA2 and total ADA in males by four months of life. A study of American school-aged children (mean ~8 years of age) did not reveal any significant difference in plasma ADA2 concentration based on sex (94). Further studies focusing on the phase beyond the first four months of life and before age 2 years will be important to delineate the ontogeny of sex-dependent differences in ADA2 and assess potential correlations with immunity, health, and disease given the clinical relevance of ADA2 and inflammation (32–52).

Several risk factors for infection and poor outcome including impaired neurological development have been defined for infants born between late pre-term (≥34 weeks and <37 weeks of gestation) and early term (≥37 week to <39 weeks gestation) (95, 96). Furthermore, gestational age (GA) correlates with neonatal plasma biomarkers such as hemoglobin and iron at birth (67–70). We assessed whether plasma concentrations of ADAs may correlate with GA, although by definition, we did not include any infant below 36 weeks gestation. We observed significantly elevated ADA2 and total ADA in the early term compared to full-term infants. The functional relevance of these correlations is at present unclear. Our study is limited as we did not enroll premature neonates (<36 weeks) and our patient population was not powered to study neonatal conditions

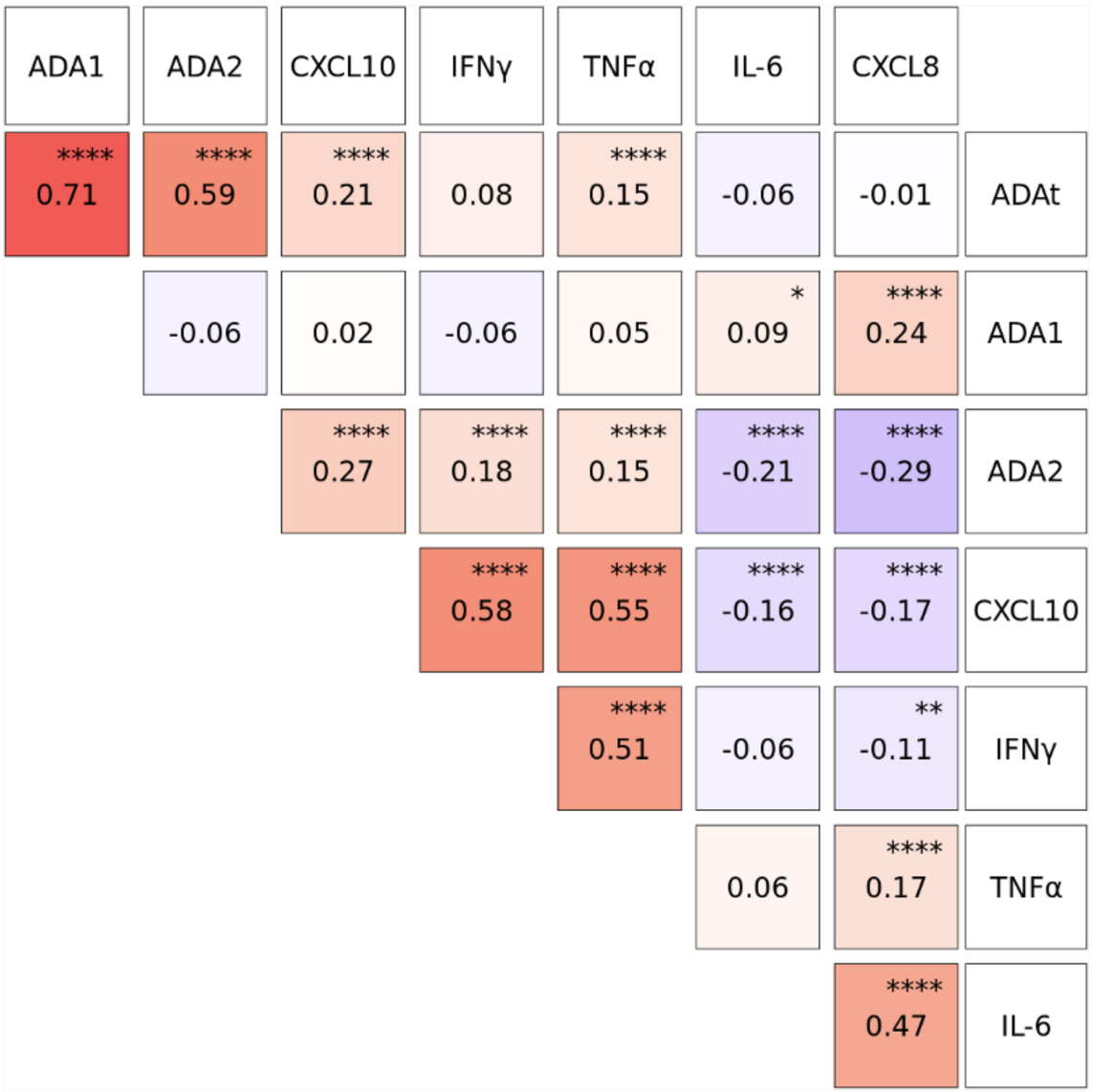

FIGURE 6 | Plasma concentrations of CXCL10, IFNγ and TNFα were positively correlated with Total ADA (ADAt) and ADA2 during the first week of life. Log_{10}-transformed plasma cytokine and chemokine concentration were pooled from Visit 1 and Visit 2 during the first week of life (n= 1027-1044 based on Visit 1 and Visit 2). Correlation coefficients between analytes were calculated using Spearman's rho and plotted using the GGally package in R. Total ADA (ADAt) and ADA2, but not ADA1, were positively correlated (red) with CXCL10, IFNγ and TNFα. ADA1 was positively correlated (red) with IL-6 and CXCL8 while ADA2 was negatively correlated (blue) with IL-6 and CXCL8. P-values were determined by R function cor.test, and adjusted using the Holm-Bonferroni method. Significant p-values depicted as *p<0.05, **p<0.01, ****p<0.0001.

(e.g. jaundice) that may impact the expression of ADAs. Future studies should characterize ADA concentrations in the premature population in relation to immunologic parameters and infection to provide further insight into the functional consequences of ADA expression in early life.

During the first two years of life, there is a gradual switch from a predominantly Th2-polarizing cytokine response toward a more balanced Th1/Th2 response (5). We previously showed that supplementing *in vitro* cultures of neonatal umbilical cord blood mononuclear cells with recombinant ADA1 enhanced TLR-mediated TNFα production (16). Moreover, addition of ADA to cultures of monocyte-derived DCs in IL-4 and GM-CSF medium enhanced DC production of TNFα, IL-6, and CXCL8 (97). To assess whether these previous *in vitro* studies may have relevance *in vivo*, we examined whether plasma concentrations of ADAs correlated with plasma cytokine or chemokine concentrations during the first week of life. Total ADA correlated with CXCL10 and TNFα but not with IFNγ or CXCL8. In assessing each of the ADAs individually, plasma ADA1 weakly correlated with plasma IL-6 and moderately

with CXCL8 while ADA2 correlated positively with TNFα, IFNγ, and the IFN-inducible protein CXCL10, and negatively with IL-6 and CXCL8. Consistent with our observations, *in vitro* studies have demonstrated that stimulation of human PBMCs with IL-12, IL-18 or IFNγ, and TNFα induced expression of ADA2 (94) but not ADA1 (98). While information regarding the impact of ADA2 deficiency (DADA2) on plasma cytokines or chemokine concentrations is limited, observation of increased IL-6 plasma concentrations in a patient with ADA2-deficiency due to a missense mutation (47) is consistent with the negative correlation between ADA2 and IL-6 we observed in our infant cohort. Of note, the report on the ADA2-deficient patient after treatment with HSCT demonstrated normalization of both ADA2 and IL-6 concentrations, suggesting a close interplay between these proteins (47). Overall, there appears to be coordinated expression of ADA and cytokines, such that the cytokines induce ADAs that counter-regulate them (i.e. a potential feed-back loop).

Finally, we observed a decrease in plasma ADA2 concentrations in infants born to women ≥ 35 years of age, which significantly dropped relative to the plasma concentration in infants born to women < 35 years of age; by 6% at 1 month and by 12% at 4 months of life. This is notable as advanced maternal age is related to adverse outcomes including spontaneous abortions, preterm birth, and perinatal morbidity (71–73). Indeed, increased total ADA has been noted in maternal and umbilical cord plasma in women with pre-eclampsia (99, 100), and a genetic polymorphism of ADA1 resulting in lower ADA was associated with a maternal age-dependent lower risk for recurrent spontaneous abortions (101). While statistically significant, it is unclear if the differences observed are due to association versus a causal relationship. These observations provide a rationale for future studies to determine if the balance between ADA1 and ADA2 is relevant to maternal and perinatal health including perinatal morbidity and mortality.

Overall, our observations may have translational relevance as several of the recently described patients with ADA2 deficiency (DADA2) were diagnosed during the first two months of life after presenting with fever and/or anemia (30, 33, 39, 50). Total ADA, ADA1, and ADA2 have been explored as biomarkers (56–60, 94, 102, 103) and ADA1, as well as ADA receptor agonists/antagonists, are studied as possible vaccine adjuvants or disease-modifying drugs (20). In HIV infection, ADA1 concentration is decreased, addition of exogenous ADA1 enhances germinal center formation (102, 104), and co-immunization with HIV-1 envelope protein and plasmid-encoded ADA1 enhanced humoral immunity (105). Characterizing baseline ADA concentrations in a target population may inform translational efforts to modulate ADA-deficient states *via* administration of recombinant ADA, HSCT, or gene therapy (21, 106, 107). Moreover, baseline plasma ADA1, but not ADA2 measurements are also affected by hemolysis (98), highlighting the importance of measuring ADA1 separately from ADA2.

Our study features several strengths, including (a) a robust sample size, (b) rigorous clinical data capture, (c) a quantitative high throughput ADA assay platform that minimizes batch effects, and (d) a highly statistically significant novel observation of ontogeny-driven changes in ADA1, ADA2, and total ADA. As with all studies, our work also has some important limitations. Due to sample volume and field processing limitations, we did not measure ADA receptors, ectonucleotidases, nor the adenosine metabolite, whose half-life is fleeting. It will also be important to determine if the ADA ontogeny trajectory observed in neonates in The Gambia is generalizable to neonates in other geographic locations. Within the constraints of conducting large-scale international human neonatal studies, we described the ontogeny of ADA2 as well as total ADA and ADA1 and correlated these concentrations with those of key cytokines and chemokines. Given growing literature regarding its clinical relevance, our findings highlight the need for further study of ADA2, its mechanisms of action, genotypic variants, and associated clinical phenotypes.

In conclusion, plasma concentrations of ADAs demonstrated marked ontogenic changes across the first week and months after birth that correlated with plasma cytokine and chemokine concentrations, raising the possibility that these immunomodulatory proteins are functionally related to innate immune polarization during infancy. Given the increasing evidence of the relevance of ADA1 and ADA2 in immunity, these proteins should be further characterized as biomarkers for early life immune ontogeny as well as during responses to immune perturbation such as vaccination or infection.

DATA AVAILABILITY STATEMENT

The datasets presented in this study can be found in online repositories. The names of the repository/repositories and accession number(s) can be found below: Per NIH/NIAID guidelines, study data including plasma ADA, cytokine, and chemokine concentrations data have been publicly archived on ImmPort (https://www.immport.org/shared/home) under accession number SDY1539.

ETHICS STATEMENT

The studies involving human participants were reviewed and approved by The Gambia Government/Medical Research Council Unit The Gambia Joint Ethics Committee and The Boston Children's Hospital Institutional Review Board. The patients/participants provided their written informed consent to participate in this study.

AUTHOR CONTRIBUTIONS

Manuscript was drafted by OO, KS, and AP. OL, BK, and TK designed the EPIC study. AO provided expert input on study design and statistical analyses; the members of EPIC listed below assisted with sample processing, clinical data capture, data quality control, and database management. MP developed and validated the ADA assay used and helped edit the manuscript. OI and JP provided support in conducting the ADA assays. Ol provided support to the *Precision Vaccines Program* Data

Management Core, led by AO, for quality assurance of the clinical and biomarker data. All authors contributed to the article and approved the submitted version.

The Expanded Program on Immunization (EPIC) Consortium consists of the following member (in addition to the main authors) listed alphabetically: Nelly Amenyogbe, Asimenia Angelidou, Winnie Bao, Rym Ben-Othman Tue B. Bennike, Morten Bjerregaard-Andersen, Ryan R. Brinkman, Byron Brook, Kendyll Burnell, Bing Cai, Abhinav Checkervarty, Virginia Chen, Mitchell Cooney, Momoudou Cox, Alansana Darboe, Bhavjinder K. Dhillon, Tida Dibassey, Joann Diray-Arce, Reza Falsafi, Benoit Fatou, Rebecca Ford, Freddy Francis, Christian N Golding, Robert E.W. Hancock, Danny J Harbeson, Daniel He, Samuel H. Hinshaw, Joe Huang, Abdulazeez Imam, Wendy Kirarock, Ken Kraft, Kristina Lindberg Larsen, Amy H. Lee, Aaron Liu, Mark Liu, Mehrnoush Malek, Arnaud Marchant, Geraldine Masiria, John Paul Matlam, Kerry McEnaney, Sebastiano Montante, Elena Morrocchi, Jorjoh Ndure, Jainaba Njie-Jobe, Edward Parker, William S. Pomat, Shun Rao, Peter C. Richmond, Elishia Roberts, Gerard Saleu, Lilica Sanca, Guzman Sanchez-Schmitz, Frederik Schaltz-Buchholzer, Casey P Shannon, Amrit Singh, Maren Smith, Hanno Steen, Julia Strandmark, Scott J Tebbutt, Anita H.J. van den Biggelaar, Simon van Haren, Natallia Varankovich, Sofia Vignolo, Diana Vo, Oghenebrume Wariri.

FUNDING

This work was supported by funds from the National Institute of Health (NIH), National Institute of Allergy and Infectious Disease (NIAID) division as part of the Human Immunology Project Consortium (U19AI118608) to OL, and funds from the Boston Children's Global Health Program and an NIH Loan Repayment Program award, the National Institute on Minority Health and Health Disparities (NIMHD) to OO. The *Precision Vaccines Program* is supported in part by the Department of Pediatrics and Chief Scientific Officer of Boston Children's Hospital. The content is solely the responsibility of the authors and does not necessarily represent the official views of the National Institutes of Health or Boston Children's Hospital.

ACKNOWLEDGMENTS

We thank all study participants and their families, our colleagues at the Medical Research Council Unit at London School of Hygiene and Tropical Medicine in The Gambia and the field team data collectors. We also thank *Precision Vaccines Program Coordinators* Diana Vo, Bianca Dy, and Maimouna Murphy for their administrative support, as well as BCH Medical Library staff members for assistance with literature review. The authors acknowledge the support of the Global Health Program at Boston Children's Hospital, Harvard Medical School, Boston, MA, USA. We thank Kristin Johnson of Boston Children's Hospital for artwork in **Figure 1**.

SUPPLEMENTARY MATERIAL

The Supplementary Material for this article can be found online at: https://www.frontiersin.org/articles/10.3389/fimmu.2021.578700/full#supplementary-material

REFERENCES

1. Kollmann TR, Kampmann B, Mazmanian SK, Marchant A, Levy O. Protecting the Newborn and Young Infant From Infectious Diseases: Lessons From Immune Ontogeny. *Immunity* (2017) 46(3):350–63. doi: 10.1016/j.immuni.2017.03.009
2. Pettengill MA, van Haren SD, Levy O. Soluble Mediators Regulating Immunity in Early Life. *Front Immunol* (2014) 5:457. doi: 10.3389/fimmu.2014.00457
3. Pettengill M, Robson S, Tresenriter M, Millan JL, Usheva A, Bingham T, et al. Soluble Ecto-5'-Nucleotidase (5'-Nt), Alkaline Phosphatase, and Adenosine Deaminase (ADA1) Activities in Neonatal Blood Favor Elevated Extracellular Adenosine. *J Biol Chem* (2013) 288(38):27315–26. doi: 10.1074/jbc.M113.484212
4. Lee AH, Shannon CP, Amenyogbe N, Bennike TB, Diray-Arce J, Idoko OT, et al. Dynamic Molecular Changes During the First Week of Human Life Follow a Robust Developmental Trajectory. *Nat Commun* (2019) 10 (1):1092. doi: 10.1038/s41467-019-08794-x
5. Kollmann TR, Levy O, Montgomery RR, Goriely S. Innate Immune Function by Toll-like Receptors: Distinct Responses in Newborns and the Elderly. *Immunity* (2012) 37(5):771–83. doi: 10.1016/j.immuni.2012.10.014
6. Dowling DJ, Levy O. Ontogeny of Early Life Immunity. *Trends Immunol* (2014) 35(7):299–310. doi: 10.1016/j.it.2014.04.007
7. Burl S, Townend J, Njie-Jobe J, Cox M, Adetifa UJ, Touray E, et al. Age-Dependent Maturation of Toll-like Receptor-Mediated Cytokine Responses in Gambian Infants. *PloS One* (2011) 6(4):e18185. doi: 10.1371/journal.pone.0018185
8. Meyts I, Aksentijevich I. Deficiency of Adenosine Deaminase 2 (Dada2): Updates on the Phenotype, Genetics, Pathogenesis, and Treatment. *J Clin Immunol* (2018) 38(5):569–78. doi: 10.1007/s10875-018-0525-8
9. Moens L, Hershfield M, Arts K, Aksentijevich I, Meyts I. Human Adenosine Deaminase 2 Deficiency: A Multi-Faceted Inborn Error of Immunity. *Immunol Rev* (2019) 287(1):62–72. doi: 10.1111/imr.12722
10. Bielat K, Tritsch GL. Ecto-Enzyme Activity of Human Erythrocyte Adenosine Deaminase. *Mol Cell Biochem* (1989) 86(2):135–42. doi: 10.1007/BF00222613
11. Hashikawa T, Hooker SW, Maj JG, Knott-Craig CJ, Takedachi M, Murakami S, et al. Regulation of Adenosine Receptor Engagement by Ecto-Adenosine Deaminase. *FASEB J* (2004) 18(1):131–3. doi: 10.1096/fj.03-0011fje
12. Pacheco R, Martinez-Navio JM, Lejeune M, Climent N, Oliva H, Gatell JM, et al. Cd26, Adenosine Deaminase, and Adenosine Receptors Mediate Costimulatory Signals in the Immunological Synapse. *Proc Natl Acad Sci USA* (2005) 102(27):9583–8. doi: 10.1073/pnas.0501050102
13. Yegutkin GG, Henttinen T, Samburski SS, Spychala J, Jalkanen S. The Evidence for Two Opposite, ATP-Generating and ATP-Consuming, Extracellular Pathways on Endothelial and Lymphoid Cells. *Biochem J* (2002) 367(Pt 1):121–8. doi: 10.1042/bj20020439
14. Zavialov AV, Gracia E, Glaichenhaus N, Franco R, Zavialov AV, Lauvau G. Human Adenosine Deaminase 2 Induces Differentiation of Monocytes Into Macrophages and Stimulates Proliferation of T Helper Cells and Macrophages. *J Leukoc Biol* (2010) 88(2):279–90. doi: 10.1189/jlb.1109764
15. Moreno E, Canet J, Gracia E, Lluís C, Mallol J, Canela EI, et al. Molecular Evidence of Adenosine Deaminase Linking Adenosine A(2A) Receptor and CD26 Proteins. *Front Pharmacol* (2018) 9:106. doi: 10.3389/fphar.2018.00106
16. Levy O, Coughlin M, Cronstein BN, Roy RM, Desai A, Wessels MR. The Adenosine System Selectively Inhibits TLR-Mediated Tnf-Alpha Production in the Human Newborn. *J Immunol* (2006) 177(3):1956–66. doi: 10.4049/jimmunol.177.3.1956

17. Chen JF, Eltzschig HK, Fredholm BB. Adenosine Receptors as Drug Targets–What Are the Challenges? *Nat Rev Drug Discovery* (2013) 12 (4):265–86. doi: 10.1038/nrd3955
18. Bouma MG, Jeunhomme TM, Boyle DL, Dentener MA, Voitenok NN, van den Wildenberg FA, et al. Adenosine Inhibits Neutrophil Degranulation in Activated Human Whole Blood: Involvement of Adenosine A2 and A3 Receptors. *J Immunol* (1997) 158(11):5400–8.
19. Borea PA, Gessi S, Merighi S, Vincenzi F, Varani K. Pharmacology of Adenosine Receptors: The State of the Art. *Physiol Rev* (2018) 98(3):1591–625. doi: 10.1152/physrev.00049.2017
20. Hasko G, Antonioli L, Cronstein BN. Adenosine Metabolism, Immunity and Joint Health. *Biochem Pharmacol* (2018) 151:307–13. doi: 10.1016/j.bcp.2018.02.002
21. Flinn AM, Gennery AR. Adenosine Deaminase Deficiency: A Review. *Orphanet J Rare Dis* (2018) 13(1):65. doi: 10.1186/s13023-018-0807-5
22. Giblett ER, Anderson JE, Cohen F, Pollara B, Meuwissen HJ. Adenosine-Deaminase Deficiency in Two Patients With Severely Impaired Cellular Immunity. *Lancet* (1972) 2(7786):1067–9. doi: 10.1016/S0140-6736(72)92345-8
23. Schrader WP, Pollara B, Meuwissen HJ. Characterization of the Residual Adenosine Deaminating Activity in the Spleen of a Patient With Combined Immunodeficiency Disease and Adenosine Deaminase Deficiency. *Proc Natl Acad Sci USA* (1978) 75(1):446–50. doi: 10.1073/pnas.75.1.446
24. Zuckerman SH, Olson JM, Douglas SD. Adenosine Deaminase Activity During In Vitro Culture of Human Peripheral Blood Monocytes and Pulmonary Alveolar Macrophages. *Exp Cell Res* (1980) 129(2):281–7. doi: 10.1016/0014-4827(80)90494-2
25. Ratech H, Hirschhorn R. Serum Adenosine Deaminase in Normals and in a Patient With Adenosine Deaminase Deficient-Severe Combined Immunodeficiency. *Clin Chim Acta* (1981) 115(3):341–7. doi: 10.1016/0009-8981(81)90247-3
26. Zavialov AV, Engström A. Human ADA2 Belongs to a New Family of Growth Factors With Adenosine Deaminase Activity. *Biochem J* (2005) 391 (Pt 1):51–7. doi: 10.1042/BJ20050683
27. Kaljas Y, Liu C, Skaldin M, Wu C, Zhou Q, Lu Y, et al. Human Adenosine Deaminases ADA1 and ADA2 Bind to Different Subsets of Immune Cells. *Cell Mol Life Sci* (2017) 74(3):555–70. doi: 10.1007/s00018-016-2357-0
28. Ungerer JP, Oosthuizen HM, Bissbort SH, Vermaak WJ. Serum Adenosine Deaminase: Isoenzymes and Diagnostic Application. *Clin Chem* (1992) 38 (7):1322–6. doi: 10.1093/clinchem/38.7.1322
29. Fischer D, Van der Weyden MB, Snyderman R, Kelley WN. A Role for Adenosine Deaminase in Human Monocyte Maturation. *J Clin Invest* (1976) 58(2):399–407. doi: 10.1172/JCI108484
30. Navon Elkan P, Pierce SB, Segel R, Walsh T, Barash J, Padeh S, et al. Mutant Adenosine Deaminase 2 in a Polyarteritis Nodosa Vasculopathy. *N Engl J Med* (2014) 370(10):921–31. doi: 10.1056/NEJMoa1307362
31. Zhou Q, Yang D, Ombrello AK, Zavialov AV, Toro C, Zavialov AV, et al. Early-Onset Stroke and Vasculopathy Associated With Mutations in ADA2. *N Engl J Med* (2014) 370(10):911–20. doi: 10.1056/NEJMoa1307361
32. Batu ED, Karadag O, Taskiran EZ, Kalyoncu U, Aksentijevich I, Alikasifoglu M, et al. A Case Series of Adenosine Deaminase 2-Deficient Patients Emphasizing Treatment and Genotype-Phenotype Correlations. *J Rheumatol* (2015) 42(8):1532–4. doi: 10.3899/jrheum.150024
33. Belot A, Wassmer E, Twilt M, Lega JC, Zeef LA, Oojageer A, et al. Mutations in CECR1 Associated With a Neutrophil Signature in Peripheral Blood. *Pediatr Rheumatol Online J* (2014) 12:44. doi: 10.1186/1546-0096-12-44
34. Bras J, Guerreiro R, Santo GC. Mutant ADA2 in Vasculopathies. *N Engl J Med* (2014) 371(5):478–80. doi: 10.1056/NEJMc1405506
35. Ekinci RMK, Balcı S, Bisgin A, Sasmaz I, Leblebisatan G, Incecik F, et al. A Homozygote Novel L451W Mutation in CECR1 Gene Causes Deficiency of Adenosine Deaminase 2 in a Pediatric Patient Representing With Chronic Lymphoproliferation and Cytopenia. *Pediatr Hematol Oncol* (2019) 36 (6):376–81. doi: 10.1080/08880018.2019.1621973
36. Ganhão S, Loureiro GB, Oliveira DR, Dos-Reis-Maia R, Aguiar F, Quental R, et al. Two Cases of ADA2 Deficiency Presenting as Childhood Polyarteritis Nodosa: Novel ADA2 Variant, Atypical Cns Manifestations, and Literature Review. *Clin Rheumatol* (2020) 39(12):3853–60. doi: 10.1007/s10067-020-05210-4
37. Garg N, Kasapcopur O, Foster J2nd, Barut K, Tekin A, Kızılkılıç O, et al. Novel Adenosine Deaminase 2 Mutations in a Child With a Fatal Vasculopathy. *Eur J Pediatr* (2014) 173(6):827–30. doi: 10.1007/s00431-014-2320-8
38. Gonzalez Santiago TM, Zavialov A, Saarela J, Seppanen M, Reed AM, Abraham RS, et al. Dermatologic Features of ADA2 Deficiency in Cutaneous Polyarteritis Nodosa. *JAMA Dermatol* (2015) 151(11):1230–4. doi: 10.1001/jamadermatol.2015.1635
39. Lee PY, Kellner ES, Huang Y, Furutani E, Huang Z, Bainter W, et al. Genotype and Functional Correlates of Disease Phenotype in Deficiency of Adenosine Deaminase 2 (DADa2). *J Allergy Clin Immunol* (2020) 145 (6):1664–72.e10. doi: 10.1016/j.jaci.2019.12.908
40. Saettini F, Fazio G, Corti P, Quadri M, Bugarin C, Gaipa G, et al. Two Siblings Presenting With Novel ADA2 Variants, Lymphoproliferation, Persistence of Large Granular Lymphocytes, and T-Cell Perturbations. *Clin Immunol* (2020) 218:108525. doi: 10.1016/j.clim.2020.108525
41. Schena F, Penco F, Volpi S, Pastorino C, Caorsi R, Kalli F, et al. Dysregulation in B-Cell Responses and T Follicular Helper Cell Function in ADA2 Deficiency Patients. *Eur J Immunol* (2020) 51(1):206–19. doi: 10.1002/eji.202048549
42. Schepp J, Bulashevska A, Mannhardt-Laakmann W, Cao H, Yang F, Seidl M, et al. Deficiency of Adenosine Deaminase 2 Causes Antibody Deficiency. *J Clin Immunol* (2016) 36(3):179–86. doi: 10.1007/s10875-016-0245-x
43. Schnappauf O, Sampaio Moura N, Aksentijevich I, Stoffels M, Ombrello AK, Hoffmann P, et al. Sequence-Based Screening of Patients With Idiopathic Polyarteritis Nodosa, Granulomatosis With Polyangiitis, and Microscopic Polyangiitis for Deleterious Genetic Variants in ADA2. *Arthritis Rheumatol* (2020) 73(3):512–9. doi: 10.1002/art.41549
44. Schnappauf O, Zhou Q, Moura NS, Ombrello AK, Michael DG, Deuitch N, et al. Deficiency of Adenosine Deaminase 2 (DADA2): Hidden Variants, Reduced Penetrance, and Unusual Inheritance. *J Clin Immunol* (2020) 40 (6):917–26. doi: 10.1007/s10875-020-00817-3
45. Springer JM, Gierer SA, Jiang H, Kleiner D, Deuitch N, Ombrello AK, et al. Deficiency of Adenosine Deaminase 2 in Adult Siblings: Many Years of a Misdiagnosed Disease With Severe Consequences. *Front Immunol* (2018) 9 (1361). doi: 10.3389/fimmu.2018.01361
46. Tanatar A, Karadağ ŞG, Sözeri B, Sönmez HE, Çakan M, Kendir Demirkol Y, et al. Ada2 Deficiency: Case Series of Five Patients With Varying Phenotypes. *J Clin Immunol* (2020) 40(2):253–8. doi: 10.1007/s10875-019-00734-0
47. Van Eyck LJr., Hershfield MS, Pombal D, Kelly SJ, Ganson NJ, Moens L, et al. Hematopoietic Stem Cell Transplantation Rescues the Immunologic Phenotype and Prevents Vasculopathy in Patients With Adenosine Deaminase 2 Deficiency. *J Allergy Clin Immunol* (2015) 135(1):283–7.e5. doi: 10.1016/j.jaci.2014.10.010
48. Van Eyck L, Liston A, Wouters C. Mutant ADA2 in Vasculopathies. *N Engl J Med* (2014) 371(5):480. doi: 10.1056/NEJMc1405506
49. van Montfrans J, Zavialov A, Zhou Q. Mutant ADA2 in Vasculopathies. *N Engl J Med* (2014) 371(5):478. doi: 10.1056/NEJMc1405506
50. Van Montfrans JM, Hartman EA, Braun KP, Hennekam EA, Hak EA, Nederkoorn PJ, et al. Phenotypic Variability in Patients With ADA2 Deficiency Due to Identical Homozygous R169Q Mutations. *Rheumatol (Oxford)* (2016) 55(5):902–10. doi: 10.1186/1546-0096-13-S1-O7
51. van Well GTJ, Kant B, van Nistelrooij A, Sirma Ekmekci S, Henriet SV, Hoppenreijs E, et al. Phenotypic Variability Including Behçet's Disease-Like Manifestations in DADA2 Patients Due to a Homozygous C.973-2A>G Splice Site Mutation. *Clin Exp Rheumatol* (2019) 37 Suppl 121(6):142–6.
52. Westendorp WF, Nederkoorn PJ, Aksentijevich I, Hak AE, Lichtenbelt KD, Braun KP. Unexplained Early-Onset Lacunar Stroke and Inflammatory Skin Lesions: Consider ADA2 Deficiency. *Neurology* (2015) 84(20):2092–3. doi: 10.1212/WNL.0000000000001581
53. Idoko OT, Smolen KK, Wariri O, Imam A, Shannon CP, Dibassey T, et al. Clinical Protocol for a Longitudinal Cohort Study Employing Systems Biology to Identify Markers of Vaccine Immunogenicity in Newborn Infants in The Gambia and Papua New Guinea. *Front Pediatr* (2020) 8:197. doi: 10.3389/fped.2020.00197
54. Højsgaard S, Halekoh U, Yan J. The R Package Geepack for Generalized Estimating Equations. *J Stat Software* (2005) 15(2):11. doi: 10.18637/jss.v015.i02

55. Berry KJ, Mielke PWJr. Exact and Monte Carlo Resampling Procedures for the Wilcoxon-Mann-Whitney and Kruskal-Wallis Tests. *Percept Mot Skills* (2000) 91(3 Pt 1):749–54. doi: 10.2466/pms.2000.91.3.749
56. Conesa-Buendia FM, Llamas-Granda P, Atencio P, Cabello A, Gorgolas M, Largo R, et al. Adenosine Deaminase as a Biomarker of Tenofovir Mediated Inflammation in Naive HIV Patients. *Int J Mol Sci* (2020) 21(10):3590. doi: 10.3390/ijms21103590
57. Ebrahimi-Rad M, Khatami S, Ansari S, Jalylfar S, Valadbeigi S, Saghiri R. Adenosine Deaminase 1 as a Biomarker for Diagnosis and Monitoring of Patients With Acute Lymphoblastic Leukemia. *J Med Biochem* (2018) 37 (2):128–33. doi: 10.1515/jomb-2017-0042
58. Kelgandre DC, Pathak J, Patel S, Ingale P, Swain N. Adenosine Deaminase - a Novel Diagnostic and Prognostic Biomarker for Oral Squamous Cell Carcinoma. *Asian Pac J Cancer Prev* (2016) 17(4):1865–8. doi: 10.7314/APJCP.2016.17.4.1865
59. Li R, Wang J, Wang X, Wang M. Pleural Effusion Adenosine Deaminase: A Candidate Biomarker to Discriminate Between Gram-negative and Gram-positive Bacterial Infections of the Pleural Space. *Clinics (Sao Paulo)* (2016) 71(5):271–5. doi: 10.6061/clinics/2016(05)05
60. Michot JM, Madec Y, Bulifon S, Thorette-Tcherniak C, Fortineau N, Noel N, et al. Adenosine Deaminase is a Useful Biomarker to Diagnose Pleural Tuberculosis in Low to Medium Prevalence Settings. *Diagn Microbiol Infect Dis* (2016) 84(3):215–20. doi: 10.1016/j.diagmicrobio.2015.11.007
61. Vogel RM. The Geometric Mean? *Commun Stat - Theory Methods* (2020) 1–13. doi: 10.1080/03610926.2020.1743313
62. Johnson WE, Li C, Rabinovic A. Adjusting Batch Effects in Microarray Expression Data Using Empirical Bayes Methods. *Biostatistics* (2007) 8 (1):118–27. doi: 10.1093/biostatistics/kxj037
63. Kitakaze M, Hori M, Takashima S, Sato H, Inoue M, Kamada T. Ischemic Preconditioning Increases Adenosine Release and 5'-Nucleotidase Activity During Myocardial Ischemia and Reperfusion in Dogs. Implications for Myocardial Salvage. *Circulation* (1993) 87(1):208–15. doi: 10.1161/01.CIR.87.1.208
64. Kinugawa T, Fujita M, Ogino K, Kato M, Osaki S, Igawa O, et al. Catabolism of Adenine Nucleotides Favors Adenosine Production Following Exercise in Patients With Chronic Heart Failure. *J Card Fail* (2006) 12(9):720–5. doi: 10.1016/j.cardfail.2006.08.215
65. Khodadadi I, Vahedi MS, Abdi M, Daneshkhah N, Rahbari R, Menbari S, et al. Evaluation of Adenosine Deaminase (ADA) Isoenzymes Activity and Tumor Necrosis Factor-α (Tnfα) Concentration in Chronic Heart Failure. *Excli J* (2014) 13:58–66.
66. Asakura M, Asanuma H, Kim J, Liao Y, Nakamaru K, Fujita M, et al. Impact of Adenosine Receptor Signaling and Metabolism on Pathophysiology in Patients With Chronic Heart Failure. *Hypertens Res* (2007) 30(9):781–7. doi: 10.1291/hypres.30.781
67. Bizzarro MJ, Colson E, Ehrenkranz RA. Differential Diagnosis and Management of Anemia in the Newborn. *Pediatr Clinics North Am* (2004) 51(4):1087–107. doi: 10.1016/j.pcl.2004.03.006
68. Forestier F, Daffos F, Galactèros F, Bardakjian J, Rainaut M, Beuzard Y. Hematological Values of 163 Normal Fetuses Between 18 and 30 Weeks of Gestation. *Pediatr Res* (1986) 20(4):342–6. doi: 10.1203/00006450-198604000-00017
69. Zaizov R, Matoth Y. Red Cell Values on the First Postnatal Day During the Last 16 Weeks of Gestation. *Am J Hematol* (1976) 1(2):275–8. doi: 10.1002/ajh.2830010211
70. Zhang JY, Wang J, Lu Q, Tan M, Wei R, Lash G. Iron Stores At Birth in a Full Term Normal Birth Weight Birth Cohort With a Low Level of Inflammation. *Biosci Rep* (2020) 40(12):BSR20202853. doi: 10.1042/BSR20202853
71. Cleary-Goldman J, Malone FD, Vidaver J, Ball RH, Nyberg DA, Comstock CH, et al. Impact of Maternal Age on Obstetric Outcome. *Obstet Gynecol* (2005) 105(5 Pt 1):983–90. doi: 10.1097/01.AOG.0000158118.75532.51
72. Sheen JJ, Wright JD, Goffman D, Kern-Goldberger AR, Booker W, Siddiq Z, et al. Maternal Age and Risk for Adverse Outcomes. *Am J Obstet Gynecol* (2018) 219(4):390.e1– e15. doi: 10.1016/j.ajog.2018.08.034
73. Waldenstrom U, Cnattingius S, Vixner L, Norman M. Advanced Maternal Age Increases the Risk of Very Preterm Birth, Irrespective of Parity: A Population-Based Register Study. *BJOG* (2017) 124(8):1235–44. doi: 10.1111/1471-0528.14368
74. Jadhav AA, Jain A. Adenosine Deaminase Activity in Normal Pregnancy and Pregnancy Associated Disorders. *Arch Physiol Biochem* (2013) 119(2):88–91. doi: 10.3109/13813455.2013.777078
75. Blanc AK, Winfrey W, Ross J. New Findings for Maternal Mortality Age Patterns: Aggregated Results for 38 Countries. *PloS One* (2013) 8(4):e59864. doi: 10.1371/journal.pone.0059864
76. Acog Committee Opinion No 579: Definition of Term Pregnancy. *Obstet Gynecol* (2013) 122(5):1139–40. doi: 10.1097/01.AOG.0000437385.88715.4a
77. Greiner-Tollersrud OK, Boehler V, Bartok E, Krausz M, Polyzou A, Schepp J, et al. ADA2 Is a Lysosomal Dnase Regulating the Type-I Interferon Response. *bioRxiv* (2020). doi: 10.1101/2020.06.21.162990
78. Gairdner D, Marks J, Roscoe JD. Blood Formation in Infancy. *Arch Dis Childhood* (1952) 27(133):214. doi: 10.1136/adc.27.133.214
79. Matoth Y, Zaizov R, Varsano I. Postnatal Changes in Some Red Cell Parameters. *Acta Paediatrica* (1971) 60(3):317–23. doi: 10.1111/j.1651-2227.1971.tb06663.x
80. Forouhi NG, Sattar N. Cvd Risk Factors and Ethnicity–A Homogeneous Relationship? *Atheroscler Suppl* (2006) 7(1):11–9. doi: 10.1016/j.atherosclerosissup.2006.01.003
81. Corbo RM, Scacchi R, Cossu G, Brega A, Scozzari R. Genetic Studies on the Senegal Population. II. Polymorphisms of the Plasma Proteins F13A, F13b, ORM1, Ahsg, C6, C7, and APOC2. *Hum Biol* (1994) 66(5):885–903.
82. Tishkoff SA, Reed FA, Friedlaender FR, Ehret C, Ranciaro A, Froment A, et al. The Genetic Structure and History of Africans and African Americans. *Science* (2009) 324(5930):1035–44. doi: 10.1126/science.1172257
83. Klein SL, Flanagan KL. Sex Differences in Immune Responses. *Nat Rev Immunol* (2016) 16(10):626–38. doi: 10.1038/nri.2016.90
84. Lorente-Pozo S, Parra-Llorca A, Torres B, Torres-Cuevas I, Nunez-Ramiro A, Cernada M, et al. Influence of Sex on Gestational Complications, Fetal-to-Neonatal Transition, and Postnatal Adaptation. *Front Pediatr* (2018) 6:63. doi: 10.3389/fped.2018.00063
85. Zhao D, Zou L, Lei X, Zhang Y. Gender Differences in Infant Mortality and Neonatal Morbidity in Mixed-Gender Twins. *Sci Rep* (2017) 7(1):8736. doi: 10.1038/s41598-017-08951-6
86. Fischer J, Jung N, Robinson N, Lehmann C. Sex Differences in Immune Responses to Infectious Diseases. *Infection* (2015) 43(4):399–403. doi: 10.1007/s15010-015-0791-9
87. Gebhard C, Regitz-Zagrosek V, Neuhauser HK, Morgan R, Klein SL. Impact of Sex and Gender on COVID-19 Outcomes in Europe. *Biol Sex Differ* (2020) 11(1):29. doi: 10.1186/s13293-020-00304-9
88. Ghosh S, Klein RS. Sex Drives Dimorphic Immune Responses to Viral Infections. *J Immunol* (2017) 198(5):1782–90. doi: 10.4049/jimmunol.1601166
89. Jaillon S, Berthenet K, Garlanda C. Sexual Dimorphism in Innate Immunity. *Clin Rev Allergy Immunol* (2019) 56(3):308–21. doi: 10.1007/s12016-017-8648-x
90. Dehingia N, Raj A. Sex Differences in COVID-19 Case Fatality: Do We Know Enough? *Lancet Global Health* (2021) 9(1):e14–15. doi: 10.1016/S2214-109X(20)30464-2
91. Eshima N, Tokumaru O, Hara S, Bacal K, Korematsu S, Karukaya S, et al. Age-Specific Sex-Related Differences in Infections: A Statistical Analysis of National Surveillance Data in Japan. *PloS One* (2012) 7(7):e42261. doi: 10.1371/journal.pone.0042261
92. Tavilani H, Sheikh N, Vaisi-raygani A, Setarehbadi R. Sex Differences in Adenosine Deaminase Activity of Stroke Patients. *Clin Chem Lab Med* (2008) 46(4):506–9. doi: 10.1515/CCLM.2008.108
93. Napolioni V, Lucarini N. Gender-Specific Association of ADA Genetic Polymorphism With Human Longevity. *Biogerontology* (2010) 11(4):457–62. doi: 10.1007/s10522-010-9266-7
94. Lee PY, Schulert GS, Canna SW, Huang Y, Sundel J, Li Y, et al. Adenosine Deaminase 2 as a Biomarker of Macrophage Activation Syndrome in Systemic Juvenile Idiopathic Arthritis. *Ann Rheum Dis* (2020) 79(2):225–31. doi: 10.1136/annrheumdis-2019-216030
95. Natarajan G, Shankaran S. Short- and Long-Term Outcomes of Moderate and Late Preterm Infants. *Am J Perinatol* (2016) 33(3):305–17. doi: 10.1055/s-0035-1571150
96. Spong CY, Mercer BM, D'Alton M, Kilpatrick S, Blackwell S, Saade G. Timing of Indicated Late-Preterm and Early-Term Birth. *Obstet Gynecol* (2011) 118(2 Pt 1):323–33. doi: 10.1097/AOG.0b013e3182255999

97. Casanova V, Naval-Macabuhay I, Massanella M, Rodríguez-García M, Blanco J, Gatell JM, et al. Adenosine Deaminase Enhances the Immunogenicity of Human Dendritic Cells From Healthy and HIV-Infected Individuals. *PloS One* (2012) 7 (12):e51287. doi: 10.1371/journal.pone.0051287
98. Lee PY, Huang Z, Hershfield MS, Nigrovic PA. Analysis of Peripheral Blood ADA1 and ADA2 Levels in Children and Adults. Response to: 'Total Adenosine Deaminase Highly Correlated With Adenosine Deaminase 2 Activity in Serum' by Gao et al. *Ann Rheum Dis* (2020). doi: 10.1136/annrheumdis-2020-217055
99. Kafkasli A, Karabulut AB, Atmaca R, Laurini R. Clinical Correlation Between Adenosine Deaminase Activity and Pre-Eclampsia Severity. *J Int Med Res* (2006) 34(3):247–55. doi: 10.1177/147323000603400303
100. Karabulut AB, Kafkasli A, Burak F, Gozukara EM. Maternal and Fetal Plasma Adenosine Deaminase, Xanthine Oxidase and Malondialdehyde Levels in Pre-Eclampsia. *Cell Biochem Funct* (2005) 23(4):279–83. doi: 10.1002/cbf.1152
101. Nunes DP, Spegiorin LC, Mattos CC, Oliani AH, Vaz-Oliani DC, Mattos LC. The ADA*2 Allele of the Adenosine Deaminase Gene (20q13.11) and Recurrent Spontaneous Abortions: An Age-Dependent Association. *Clinics (Sao Paulo)* (2011) 66(11):1929–33. doi: 10.1590/S1807-59322011001100013
102. Passos DF, Bernardes VM, da Silva JLG, Schetinger MRC, Leal DBR. Adenosine Signaling and Adenosine Deaminase Regulation of Immune Responses: Impact on the Immunopathogenesis of HIV Infection. *Purinergic Signal* (2018) 14(4):309–20. doi: 10.1007/s11302-018-9619-2
103. Polachini CR, Spanevello RM, Casali EA, Zanini D, Pereira LB, Martins CC, et al. Alterations in the Cholinesterase and Adenosine Deaminase Activities and Inflammation Biomarker Levels in Patients With Multiple Sclerosis. *Neuroscience* (2014) 266:266–74. doi: 10.1016/j.neuroscience.2014.01.048
104. Tardif V, Muir R, Cubas R, Chakhtoura M, Wilkinson P, Metcalf T, et al. Adenosine Deaminase-1 Delineates Human Follicular Helper T Cell Function and Is Altered With Hiv. *Nat Commun* (2019) 10(1):823. doi: 10.1038/s41467-019-08801-1
105. Gary E, O'Connor M, Chakhtoura M, Tardif V, Kumova OK, Malherbe DC, et al. Adenosine Deaminase-1 Enhances Germinal Center Formation and Functional Antibody Responses to HIV-1 Envelope DNA and Protein Vaccines. *Vaccine* (2020) 38(22):3821–31. doi: 10.1016/j.vaccine.2020.03.047
106. Whitmore KV, Gaspar HB. Adenosine Deaminase Deficiency - More Than Just an Immunodeficiency. *Front Immunol* (2016) 7:314. doi: 10.3389/fimmu.2016.00314
107. Sauer AV, Brigida I, Carriglio N, Aiuti A. Autoimmune Dysregulation and Purine Metabolism in Adenosine Deaminase Deficiency. *Front Immunol* (2012) 3:265. doi: 10.3389/fimmu.2012.00265

Conflict of Interest: OL is a named inventor on several patents related to microphysiologic platforms that model human immunity *in vitro*, anti-infective proteins, and vaccine adjuvants.

The remaining authors declare that the research was conducted in the absence of any commercial or financial relationships that could be construed as a potential conflict of interest.

Advantages of publishing in Frontiers

OPEN ACCESS
Articles are free to read for greatest visibility and readership

FAST PUBLICATION
Around 90 days from submission to decision

HIGH QUALITY PEER-REVIEW
Rigorous, collaborative, and constructive peer-review

TRANSPARENT PEER-REVIEW
Editors and reviewers acknowledged by name on published articles

Frontiers
Avenue du Tribunal-Fédéral 34
1005 Lausanne | Switzerland

Visit us: www.frontiersin.org
Contact us: frontiersin.org/about/contact

REPRODUCIBILITY OF RESEARCH
Support open data and methods to enhance research reproducibility

DIGITAL PUBLISHING
Articles designed for optimal readership across devices

FOLLOW US
@frontiersin

IMPACT METRICS
Advanced article metrics track visibility across digital media

EXTENSIVE PROMOTION
Marketing and promotion of impactful research

LOOP RESEARCH NETWORK
Our network increases your article's readership